INFORMATION TO USERS

This manuscript has been reproduced from the microfilm master. UMI films the text directly from the original or copy submitted. Thus, some thesis and dissertation copies are in typewriter face, while others may be from any type of computer printer.

The quality of this reproduction is dependent upon the quality of the copy submitted. Broken or indistinct print, colored or poor quality illustrations and photographs, print bleedthrough, substandard margins, and improper alignment can adversely affect reproduction.

In the unlikely event that the author did not send UMI a complete manuscript and there are missing pages, these will be noted. Also, if unauthorized copyright material had to be removed, a note will indicate the deletion.

Oversize materials (e.g., maps, drawings, charts) are reproduced by sectioning the original, beginning at the upper left-hand corner and continuing from left to right in equal sections with small overlaps. Each original is also photographed in one exposure and is included in reduced form at the back of the book.

Photographs included in the original manuscript have been reproduced xerographically in this copy. Higher quality 6" x 9" black and white photographic prints are available for any photographs or illustrations appearing in this copy for an additional charge. Contact UMI directly to order.

UMI®

Bell & Howell Information and Learning
300 North Zeeb Road, Ann Arbor, MI 48106-1346 USA
800-521-0600



Université d'Ottawa · University of Ottawa

HYDROGEOCHEMISTRY OF GROUND AND SURFACE WATERS ASSOCIATED WITH MASSIVE SULPHIDE DEPOSITS, BATHURST MINING CAMP, NEW BRUNSWICK: HALFMILE LAKE AND RESTIGOUCHE DEPOSITS

by

Matthew I. Leybourne

A thesis submitted to the School of Graduate Studies and Research

in partial fulfillment of the requirements

for the degree of Ph.D. in Earth Sciences

OTTAWA-CARLETON GEOSCIENCE CENTRE

AND

UNIVERSITY OF OTTAWA

OTTAWA, CANADA

© Matthew Iain Leybourne, Ottawa, Canada, 1998

National Library of Canada
Acquisitions and Bibliographic Services
395 Wellington Street
Ottawa ON K1A 0N4
Canada

Bibliothèque nationale du Canada
Acquisitions et services bibliographiques
395, rue Wellington
Ottawa ON K1A 0N4
Canada

Your file Votre référence

Our file Notre référence

The author has granted a non-exclusive licence allowing the National Library of Canada to reproduce, loan, distribute or sell copies of this thesis in microform, paper or electronic formats.

The author retains ownership of the copyright in this thesis. Neither the thesis nor substantial extracts from it may be printed or otherwise reproduced without the author's permission.

L'auteur a accordé une licence non exclusive permettant à la Bibliothèque nationale du Canada de reproduire, prêter, distribuer ou vendre des copies de cette thèse sous la forme de microfiche/film, de reproduction sur papier ou sur format électronique.

L'auteur conserve la propriété du droit d'auteur qui protège cette thèse. Ni la thèse ni des extraits substantiels de celle-ci ne doivent être imprimés ou autrement reproduits sans son autorisation.

0-612-38844-1

Canada

Abstract

A deposit-scale study of hydrochemical processes has been conducted at the Halfmile Lake and Restigouche massive (Zn-Pb-Cu-Ag) sulphide deposits, Bathurst Mining Camp (BMC), New Brunswick, Canada. Both the Halfmile Lake and Restigouche deposits are hosted in a deformed sequence of Ordovician (465 Ma) felsic volcanic rocks with similar topography and climate. Groundwater flow is dominated by fracture-flow. The two deposits differ in that the Halfmile Lake deposit is steeply dipping with steep structures whereas the Restigouche deposit is closer to surface with shallower structures. Deposit lithology, geometry and structure play a fundamental role in determining the hydrology which in turn controls the composition of the groundwaters.

Groundwaters were collected using flow-through bailers and a straddle-packer system that permits recovery of groundwaters from a discrete depth interval. In fracture-controlled rocks, straddle-packer groundwater compositions are more depth representative than bailer groundwaters. At the Halfmile Lake deposit, groundwaters were collected at depths up to 760 m and are characterized by low total dissolved solids (TDS; < 230 mg/L) and compositions which range from Ca-HCO_3 to Na-HCO_3. In contrast, groundwaters at the Restigouche deposit are compositionally variable and range from low TDS (< 300 mg/L), shallow Ca-HCO_3- and Ca-SO_4-type groundwaters to higher TDS (up to 2660 mg/L) Na-HCO_3Cl and Na-Cl groundwaters. Saline Na-Ca-Cl waters with up to 22,000 mg/L TDS occur in the deepest part of the Restigouche deposit.

Geochemical modelling and stable isotopic compositions indicate that shallow Ca-HCO_3 groundwaters are produced by modern meteoric recharge and the major solutes are controlled by dissolution of fracture and vein carbonate and silicate hydrolysis. The Ca-SO_4 groundwaters reflect oxidation of the sulphide minerals by modern recharge waters. Deeper brackish to saline groundwaters from the Restigouche, Heath Steele, Brunswick #12, Stratmat Main Zone, and Willett deposits have heavier oxygen and deuterium isotopic compositions than

shallow groundwaters indicating older recharge under warmer climates. Carbon isotopic compositions of dissolved inorganic carbon (DIC) range from -15 to -5‰ $\delta^{13}C_{DIC}$ for most ground and surface waters. Mass balance modelling indicates that recharging groundwaters initially possess $\delta^{13}C_{DIC}$ values of -18 to -20‰ due to equilibration with soil zone CO_2 and the $\delta^{13}C_{DIC}$ evolves to heavier compositions due to dissolution of fracture zone carbonate minerals (-5 to -6‰ $\delta^{13}C_{PDB}$). The carbon isotopic compositions of the saline waters from the Restigouche deposit are relatively heavy (+12‰ $\delta^{13}C_{DIC}$) and suggest methanogenic fractionation of DIC. The Br/Cl ratios of shallow groundwaters are greater than that of modern seawater and similar to local host rocks, whereas saline waters have Br/Cl lower than seawater suggesting either that the saline waters have interacted with non-marine evaporites, or more likely, that Br and Cl were differentially released during water-rock reaction, consistent with B, Sr and Nd isotopic compositions.

Interaction between oxygenated recharge waters at the Restigouche and Stratmat Main Zone deposits has resulted in elevated levels of metals (e.g., up to 4000 µg/L Pb and 5300 µg/L Zn) which, based on geochemical modelling and borehole geophysics (self-potential anomalies), are produced by sulphide oxidation. At low pH, sulphide-associated metals occur primarily as free ions but at pH above 7.5, carbonate and bicarbonate complexes are more important. Although neutral aqueous metal species are important at high pH, metal transport is generally restricted due to adsorption onto Fe-oxyhydroxides. Chloride-metal complexes are significant only for the saline groundwaters from the Restigouche deposit and enhances Zn and Fe solubility. The Pb isotopic composition of ground and surface waters proximal to the Restigouche deposit support dissolution of galena as the primary source of dissolved Pb.

Surface waters collected from the Halfmile Lake and Restigouche deposit primarily represent groundwater discharge based on the compositional and stable isotopic similarity with shallow groundwaters. Geochemical and isotopic modelling indicates that the major solute compositions are controlled primarily by the underlying lithologies and dissolution of

carbonate. Sulphide-associated metals decrease systematically away from sulphide mineralization due to adsorption onto Fe-oxyhydroxides formed by changing pH and Eh conditions. The rare earth elements (REE) are fractionated (light REE-depleted) compared to deeper groundwaters at the Halfmile Lake deposit, and surface waters at both the Halfmile Lake and Restigouche deposits are characterized by negative Ce anomalies. Seeps and shallow groundwaters have flat LREE patterns indicating that the development of negative Ce anomalies occurs rapidly as groundwaters reach the surface environment.

Although sulphide-associated metals (Zn, Cd, Pb, Cu, Fe) in surface waters at the Halfmile Lake and Restigouche deposits are low compared to streams draining other deposits and mine tailings, anomalously high values (with respect to local background) occur proximal to the Restigouche massive sulphides. The Halfmile Lake deposit is deeper and surface water anomalies are therefore more subtle because of limited penetration of O_2-rich recharge waters and restricted metal mobility, although SO_4 and Zn contents are highest closest to the deposit. The generally neutral pH values in the BMC results in more subtle base metal anomalies in surface waters which indicates that detailed sampling is required for hydrogeochemistry to be an effective exploration tool in the BMC. Groundwaters have higher base metal abundances and display greater contrast between anomalous and background compositions such that groundwaters have potential in better outlining mineralized targets during a drilling program.

Acknowledgements

Robin Adair of Noranda Exploration are thanked for access to the Halfmile Lake property and access to drilling logs and maps. Rory Kempster and Robin Adair collected water samples from three sites at the Halfmile Lake deposit over the winter of 94-95 in order to monitor annual variations in surface water chemistry. Chris Lochnar and Ahmed Hussein are thanked for several days assistance in the field during the summer of 1994. Craig Scott assisted for part of the 1995 field season.

Dave Lentz and Jan Peter are thanked for discussions regarding the geology and alteration style in the Bathurst Camp. Jan is especially thanked for years of computer technical support, without which my Macintoshes would be far less-robust and useful tools than they are currently. Jonathon Mwenifumbo is thanked for access to his borehole geophysical data for the Halfmile Lake, Restigouche, and Stratmat Main Zone deposits, and for permission to include some of the data in this thesis. Hazen Russel helped with the draped geology images and Dave Garson with 3D modelling of faults at the Halfmile Lake deposit.

Gilles St. Jean, Wendy Apti, and Natalie Morriset are thanked for their patient instruction in the stable isotope laboratory at the University of Ottawa. Peter Belanger (Geological Survey of Canada) is thanked for overseeing the chemical analyses and Conrad Gregoire for the B isotope measurements. Technicians R. Forcani and K. Lalonde of the GSC Instrument Development Section are thanked for their efforts in constructing, trouble-shooting, and timely repair of the straddle-packer system. Brian Cousens at Carleton University introduced me to the joys of radiogenic isotope preparation and analysis, and assisted me with all the radiogenic analyses described in this thesis.

At Heath Steele Mines, I would like to thank Art Hamilton for permission to sample in the mine and Jerry Sonier, John Creamer and Caroline Stothart for help underground. Brian Corbett is thanked for taking me underground at the Brunswick #12 mine.

Dan Boyle is thanked for discussions on hydrochemistry, for the straddle-packer system

design and instruction, and for reading much of the thesis. Dan Boyle, Eion Cameron, Ian Clark, Brian Cousens and Wayne Nesbitt are thanked for comments on the thesis.

On a more personal note, heartfelt thanks to Beth McClennaghan and Jan Peter for their constant encouragement and enthusiasm, for key papers directed my way, their old sofa, and delicious home-made cookies.

I thank my parents for all their support and encouragement throughout my academic career. Thanks to Shona (and Nemo) for joy and laughter and candle-lit dinners.

Field work for this research was funded by the EXTECH-II program at the Geological Survey of Canada. The GSC also provided most of the analytical facilities. Isotopic analyses were funded by an NSERC grant to Wayne Goodfellow. Personal financial support was provided by Ontario Graduate Scholarships and scholarships from the University of Ottawa.

Finally, this project would not have been possible without the support and encouragement of my supervisor, Wayne Goodfellow. I would like to thank Wayne for giving me the opportunity to undertake this project and for allowing me the freedom to explore areas outside the original mandate of the project.

Statement of Contribution

Major and trace elements of waters and stream sediments were analyzed at the Geological Survey of Canada (GSC), under the supervision of Peter Belanger and Conrad Gregoire. The rare earth elements in a subset of the waters were analyzed by Judy Vaive at the GSC. Stable isotopes were analyzed by the author at the University of Ottawa. Radiogenic isotopes were analyzed at Carleton University by the author with assistance from Brian Cousens. Analysis of P, I, and Br was carried out by the author using the ICP-MS facilities at the GSC.

All field work was carried out by the author. Five weeks of field assistance during the summer of 1995 was provided by Craig Scott. The packer system was designed by Dan Boyle and built in the workshop of the Geological Survey of Canada.

Table of Contents

Abstract ii
Acknowledgements v
Statement of Contribution vii
Table of Contents viii
List of Tables xvii
List of Figures xix
Appendices xxx

CHAPTER 1. INTRODUCTION
1.1 Introduction and Justification 1
1.2 Study Areas 4
1.2.1 Halfmile Lake 5
1.2.2 Restigouche 5
1.2.3 Regional waters, mines, and other occurrences 5
1.3 Organization of the Thesis 6

CHAPTER 2. REGIONAL GEOLOGY AND GEOLOGY OF HALFMILE LAKE AND RESTIGOUCHE DEPOSITS, BATHURST MINING CAMP, NEW BRUNSWICK
2.1 Introduction 10
2.2 Regional Geology 10
2.2.1 Miramichi Group 11
2.2.2 Tetagouche Group 12
2.2.3 Fournier Group 14
2.2.4 Tectonic setting of the Tetagouche Group 14
2.3 Massive Sulphide Deposits in the Bathurst Mining Camp 15
2.3.1 Deposit characteristics and stratigraphic relationships 15
2.3.2 Genesis of VMS deposits in the Bathurst Camp 17
1.4 Halfmile Lake Massive Sulphide Deposit 17
2.4.1 Geology 18
2.4.2 Structure, metamorphism, and lithogeochemistry 20
2.4.3 Depositional setting of the massive sulphides 21
2.4.4 Surficial geology 21

2.5 Restigouche Massive Sulphide Deposit 21
2.5.1 Geology 22
2.5.2 Structure 23
2.5.3 Surficial geology 24
2.6 Other VMS Deposits in the Bathurst Mining Camp 24
2.6.1 Wedge Deposit 24
2.6.2 Willet Deposit 25
2.6.3 Stratmat Main Zone Deposit 26
2.6.4 Heath Steele Deposit 26
2.6.5 Brunswick #12 Deposit 27
2.7 Geochemistry of Halfmile Lake and Restigouche Deposit Lithologies 28

CHAPTER 3. FIELD AND ANALYTICAL METHODS
3.1 Field Methods 48
3.2 Straddle Packer System 49
3.3 Analytical Methods 51
3.3.1 Inductively Coupled Plasma Mass Spectrometry (ICP-MS) 51
3.3.2 Inductively Coupled Plasma Emission Spectroscopy (ICP-ES) 52
3.3.3 Ion chromatography 53
3.3.4 Stable isotopes 53
3.3.5 Radiogenic isotopes 54
3.3.6 Scanning electron microscopy (SEM) 56
3.3.7 Whole rock and bulk stream sediment geochemistry 56
3.3.8 X-Ray diffraction (XRD) analysis 57
3.4 Data Manipulation 57

CHAPTER 4. PHYSICAL HYDROLOGY OF THE HALFMILE LAKE AND RESTIGOUCHE Zn-Pb MASSIVE SULPHIDE DEPOSITS, BATHURST MINING CAMP, NEW BRUNSWICK
4.1 Introduction 68
4.2 Geomorphology and Land Use 69
4.2.1 Preglacial climate 69
4.2.2 Present day climate 70
4.3 Hydrogeology of the Halfmile Lake deposit 71

4.3.1 Surface water environment 71
4.3.2 Groundwater environment 72
4.4 Hydrogeology of the Restigouche deposit 75
4.4.1 Surface water environment 75
4.4.2 Groundwater environment 76
4.5 Geophysical Evidence 77
4.5.1 Halfmile Lake deposit 77
4.5.2 Restigouche deposit 79
4.6 Fracture Zone Mineralogy 80
4.7 Characteristics of Groundwater Flow 81
4.8 Saline Waters at the Restigouche Deposit 82

CHAPTER 5. HYDROCHEMISTRY OF SURFACE WATERS AT THE HALFMILE LAKE AND RESTIGOUCHE Zn-Pb-Cu DEPOSITS, BATHURST MINING CAMP, NEW BRUNSWICK
5.1 Introduction 99
5.2 Halfmile Lake Deposit Surface Waters 101
5.2.1 Major cations and anions 101
5.2.2 Trace elements 105
5.2.3 Statistical Analysis 107
5.2.4 Geochemical modelling 108
5.2.5 Temporal variations 110
5.3 Restigouche Deposit Surface Waters 110
5.2.1 Major cations and anions 110
5.2.2 Trace elements 115
5.2.3 Statistical Analysis 118
5.2.4 Geochemical modelling 118
5.4 Discussion 120
5.4.1 Comparison between Halfmile Lake and Restigouche deposit surface waters . 120
5.4.2 Comparison with world average river and previous studies in the BMC 122
5.4.3 Comparison with host lithologies 123
5.4.4 Comparison with precipitation 124
5.4.5 Source control on major solute variations 127
5.4.6 Modelling of water-rock reactions 132

5.4.7 Trace element variations 134
5.5 Summary 138

CHAPTER SIX: GEOCHEMISTRY OF STREAM SEDIMENT MINERALOGY AT THE HALFMILE LAKE AND RESTIGOUCHE DEPOSITS, BATHURST MINING CAMP, NEW BRUNSWICK
6.1 Introduction 197
6.2 Stream Sediments at the Halfmile Lake Deposit 198
6.2.1 Major and trace element geochemistry 198
6.2.2 Comparison to host lithologies 199
6.3 Stream Sediments at the Restigouche Deposit 200
6.3.1 Major and trace element geochemistry 201
6.3.2 Comparison to host lithologies 202
6.4 Discussion 203
6.4.1 Element fractionation 203
6.4.2 Relationship to bedrock geology 206
6.5 Summary 208

CHAPTER SEVEN: HYDROCHEMISTRY OF GROUNDWATERS AT THE HALFMILE LAKE, RESTIGOUCHE, HEATH STEELE, BRUNSWICK #12. WEDGE, AND WILLETT Zn-Pb-Ag DEPOSITS, BATHURST MINING CAMP, NEW BRUNSWICK
7.1 Introduction 229
7.2 Hydrochemistry of Groundwaters at the Halfmile Lake Deposit 231
7.2.1 Major cations and anions 231
7.2.2 Trace elements 232
7.2.3 Downhole variations 233
7.2.4 Statistical analysis 235
7.2.5 Geochemical modelling 236
7.2.6 Comparison with surface waters 238
7.3 Hydrochemistry of Groundwaters at the Restigouche Deposit 239
7.3.1 Major cations and anions 240
7.3.2 Trace elements 241
7.3.3 High salinity waters (MM-88-02) 242
7.3.4 Downhole variations 244

7.3.5 Statistical analysis 246
7.3.6 Geochemical modelling 247
7.3.7 Comparison with surface waters 250
7.4 Groundwaters at Heath Steele, Brunswick #12, Willett and Wedge Deposits . . . 251
7.4.1 Heath Steele deposit 252
7.4.2 Brunswick #12 deposit 253
7.4.3 Willett deposit 254
7.4.4 Wedge deposit 254
7.4.5 Geochemical modelling 255
7.5 Discussion 256
7.5.1 Halfmile Lake deposit versus Restigouche deposit groundwaters 256
7.5.2 How representative of the true groundwater chemistry are the bailer and packer sampling methods? 258
7.5.3 Origin of low TDS groundwaters at the Halfmile Lake deposit 260
7.5.4 Controls on groundwater major element chemistry 264
7.5.5 Groundwater mixing 272
7.5.6 Origin of saline waters at the Restigouche and Brunswick #12 deposits 276
7.5.7 Sulphide oxidation and sources of metals in BMC groundwaters 280
7.5.8 Base metal loads in BMC groundwaters 285
7.5.9 Adsorption and controls over the fate of trace metals in BMC groundwaters . . 291
7.5.10 Arsenic in BMC groundwaters 297
7.5.11 Mo and U in Halfmile Lake and Restigouche deposit groundwaters 301
7.6 Summary 303

CHAPTER EIGHT: HYDROGEOCHEMICAL AND GEOPHYSICAL EVIDENCE FOR IN SITU OXIDATION OF AN UNDISTURBED MASSIVE SULPHIDE DEPOSIT, STRATMAT MAIN ZONE, NEW BRUNSWICK

8.1 Introduction 372
8.2 Results 373
8.2.1 Downhole geophysics 373
8.2.2 Groundwater geochemistry 374
8.2.3 Mineralogy of suspended sediments and host rocks 376
8.2.4 Geochemical modelling 377
8.3 Discussion 378

8.3.1 Geophysical evidence for sulphide oxidation 378
8.3.2 Hydrogeochemical evidence for sulphide oxidation 379
8.3.3 Generation of SP anomalies 383
8.4 Summary 387

CHAPTER NINE: BULK SUSPENDED MATTER MINERALOGY AND CHEMISTRY, HALFMILE LAKE AND RESTIGOUCHE DEPOSITS, BATHURST MINING CAMP, NEW BRUNSWICK
9.1 Introduction 399
9.2 Mineralogy of Groundwater Suspended Sediments 401
9.3 Geochemistry of Groundwater Suspended Sediments 403
9.3.1 Halfmile Lake deposit 403
9.3.2 Restigouche deposit 406
9.4 Discussion 408
9.4.1 Mineralogy 408
9.4.2 Fractionation between whole rocks, waters, and suspended sediments 409
9.4.3 Size distribution of suspended sediments 412
9.4.4 Hydromorphic and detrital components 413
9.4.5 Environmental implications 416
9.5 Summary 417

CHAPTER TEN: RARE EARTH ELEMENTS (REE) IN GROUNDWATERS, SURFACE WATERS AND STREAM SEDIMENTS ASSOCIATED WITH MASSIVE SULPHIDE DEPOSITS, BATHURST MINING CAMP, NEW BRUNSWICK
10.1 Introduction 432
10.2 REE in Bathurst Mining Camp Waters 434
10.3 REE in Halfmile Lake Deposit Waters and Sediments 435
10.3.1 Surface waters 435
10.3.2 Groundwaters 438
10.3.3 Stream sediments 440
10.3.4 REE in host metavolcanic and metasedimentary rocks 442
10.4 REE in Restigouche Deposit Waters and Sediments 442
10.4.1 Surface waters 442
10.4.2 Groundwaters 445

10.4.3 Stream sediments 446
10.4.4 REE in host metavolcanic and metasedimentary rocks 447
10.5 REE in Other Waters in the BMC 448
10.6 REE in Suspended Sediments 449
10.7 Discussion 451
10.7.1 Origin of the REE in BMC groundwaters 451
10.7.2 Origin of the REE in BMC surface waters 456
10.7.3 Association of REE with suspended matter 458
10.7.4 Origin of low TDS groundwaters at the Halfmile Lake deposit 460
10.8 Summary 460

CHAPTER ELEVEN. STABLE ISOTOPE GEOCHEMISTRY OF GROUND AND SURFACE WATERS AT THE HALFMILE LAKE AND RESTIGOUCHE DEPOSITS, BATHURST MINING CAMP, NEW BRUNSWICK
11.1 Introduction 507
11.2 $\delta^{18}O$ and δD of Precipitation 508
11.3 $\delta^{18}O$ and δD of Halfmile Lake Deposit Waters 511
11.4 $\delta^{18}O$ and δD of Restigouche Deposit Waters 512
11.5 $\delta^{18}O$ and δD of Groundwaters from the Heath Steele, Brunswick #12, Wedge, Willett, and Stratmat Main Zone Deposits 515
11.6 $\delta^{13}C$ of DIC in Ground and Surface Waters 516
11.7 Stable Isotopes of Carbonate 518
11.7.1 Carbonate morphology and paragenesis 518
11.7.2 Geochemistry of BMC carbonates 519
11.7.3 Stable isotopic composition of carbonate minerals and graphite 519
11.7.4 Estimate of temperature and $\delta^{13}C$ of the carbonate-forming fluid 521
11.8 Boron Isotopes 522
11.9 Discussion 523
11.9.1 $\delta^{18}O$ and δD relationships between precipitation, surface and ground waters 523
11.9.2 Flow path of groundwaters and age constraints 525
11.9.3 Spatial distribution of stable isotopes 527
11.9.4 Origin of antithetical patterns in borehole HN87-8 528
11.9.5 Carbon isotopes of DIC 529
11.9.6 Carbon isotopes of DIC in MM-88-02 waters 532

11.9.6 Carbon isotopes of vein and fracture carbonate and graphite 536
11.9.7 Constraints on groundwater origin based on $\delta^{11}B$ 537
11.10 Summary 541

CHAPTER TWELVE: RADIOGENIC ISOTOPES IN GROUND AND SURFACE WATERS, BATHURST MINING CAMP, NEW BRUNSWICK: APPLICATIONS TO WATER-ROCK REACTION AND MINERAL EXPLORATION STUDIES
12.1 Introduction 568
12.2 Results 570
12.2.1 Sr isotopes in BMC waters 570
12.2.2 Sr isotopes of host lithologies 573
12.2.3 Pb isotopes in BMC waters 574
12.2.4 Pb isotopes of host lithologies 577
12.2.5 Nd isotopes in BMC waters 579
12.2.6 Nd isotopes of host lithologies 580
12.3 Discussion 581
12.3.1 Sr isotopes 581
12.3.2 Pb isotopes 588
10.3.3 Pb isotopes in mineral exploration 592
12.3.4 Pb isotopes in environmental applications 598
12.3.5 Nd isotopes 598
12.4 Summary 601

CHAPTER THIRTEEN: EXPLORATION HYDROGEOCHEMISTRY IN THE BATHURST MINING CAMP, NEW BRUNSWICK: HALFMILE LAKE AND RESTIGOUCHE DEPOSITS
13.1 Introduction 611
13.2 Results from the Halfmile Lake Deposit 613
13.2.1 Surface waters 613
13.2.2 Stream sediments 614
13.2.3 Groundwaters and suspended sediments 615
13.3 Results from the Restigouche Deposit 617
13.3.1 Surface waters 617
13.3.2 Stream sediments 618

13.3.3 Groundwaters and suspended sediments 620
13.4 Geochemistry of Mine Waters 622
13.5 Discussion 622
13.5.1 Surface waters at the Restigouche and Halfmile Lake deposits 622
13.5.2 BMC surface waters compared to other studies 626
13.5.3 Surface waters in Mineral Exploration 627
13.5.4 Groundwaters in Mineral Exploration 633
13.5.5 Saline waters from the Restigouche deposit 634
13.5.6 Stream sediments 635
13.5.7 Suspended sediments in VMS exploration 637
13.6 Summary 638

CHAPTER FOURTEEN: CONCLUSIONS 677

BIBLIOGRAPHY 687

List of Tables

Table 2.1 Whole rock and trace element geochemical data for Halfmile Lake and Restigoche 29

Table 3.1 Analytical detection limits and QA/QC results 59
Table 3.2 Comparision between speciation results for selected Restigouche deposit groundwaters: PHREEQC versus EQ3NR 60
Table 3.3 Comparision between saturation indices results for selected Restigouche deposit groundwaters: PHREEQC versus EQ3NR 62

Table 4.1 Water table depths in boreholes 84

Table 5.1 Precipitation data 125

Table 6.1 Pearson product moment correlation between sediments and surface waters from the Halfmile Lake deposit 209
Table 6.2 Pearson product moment correlation between sediments and surface waters from the Restigouche deposit 210

Table 7.1 As speciation results for groundwaters 369

Table 8.1 Geochemical results for Stratmat Main Zone deposit borehole S61-19 388

Table 9.1 Mineralogy of the Bathhurst Mining Camp (BMC) groundwater suspended sediments 418
Table 9.2 Geochemical analysis of suspended sediment 419

Table 10.1 REE contents and ratios for Halfmile Lake deposit surface waters 462
Table 10.2 REE contents and ratios for Halfmile Lake deposit groundwaters 463
Table 10.3 REE contents and ratios for Halfmile Lake deposit stream sediments 465
Table 10.4 REE contents and ratios for Halfmile Lake deposit whole rocks 466
Table 10.5 REE contents and ratios for Restigouche deposit surface waters 467
Table 10.6 REE contents and ratios for Restigouche deposit groundwaters 469

Table 10.7 REE contents and ratios for Restigouche deposit stream sediments 470
Table 10.8 REE contents and ratios for Restigouche deposit whole rocks 472
Table 10.9 REE contents and ratios for mine waters 473
Table 10.10 REE contents and ratios for suspended sediments 474

Table 11.1 Table isotope data for BMC precipitation 508
Table 11.2 Oxygen and hydrogen stable isotope data for Halfmile Lake deposit waters . 543
Table 11.3 Oxygen and hydrogen stable isotope data for Restigouche deposit waters .. 544
Table 11.4 Oxygen and hydrogen stable isotope data for mine waters 545
Table 11.5 Carbon isotope values of DIC in surface and groundwaters 546
Table 11.6 Carbon and oxygen isotope data for fracture and vein carbonate 547
Table 11.7 Elemental and isotopic composition of boron in BMC waters 548
Table 11.8 Mass balance calculations for carbon isotopic compositions of BMC waters . 549

Table 12.1 Pb and Sr isotopic and abundance results for waters, rocks and carbonate from the BMC 571
Table 12.2 Pb isotopes in galena from the BMC (Thorpe et al. unpublished data) 575
Table 12.3 Nd isotopic and abundance results for BMC waters 579
Table 12.4 Nd isotopic and abundance results for Restigouche deposit whole rocks and carbonate 581

Table 13.1 Anomalous and background values for sulphide-associated elements in waters and sediments 641

List of Figures

Figure 1.1 Simplified geological map of the Bathurst Mining Camp 9

Figure 2.1 Simplified geology map of the Bathurst Mining Camp; locations of study . . 36
Figure 2.2 Representative stratigraphic columns for the Bathurst Mining Camp 37
Figure 2.3 A) General lithological map of the Halfmile Lake deposit. B) Geological cross-section A-A' through the Halfmile Lake deposit 38
Figure 2.4 Perspective view from the east of the Halfmile Lake deposit geology draped on the digital elevation model (DEM) 39
Figure 2.5 A) General geological map of the Restigoche deposit. B) Geological cross-section B-B' through the Restigoche deposit 40
Figure 2.6 Perspective view from the south of the Restigouche deposit geology draped on the digital elevation model (DEM) 41
Figure 2.7 General geological map of the Wedge deposit area 42
Figure 2.8 General geological map of the Willet deposit area 43
Figure 2.9 General geological map of the Stratmat Main Zone deposit area 44
Figure 2.10 Composition of Halfmile Lake deposit lithologies normalised to average unaltered Halfmile Lake lithology 45
Figure 2.11 Composition of Restigouche deposit lithologies normalised to average unaltered Restigouche deposit lithology 46
Figure 2.12 Discrimination diagram showing variation in the samples analysed in this study 47

Figure 3.1 Plots showing the charge balance between cations (TZ^+) and anions (TZ^-) . 63
Figure 3.2 Downhole variation plots of selected parameters for borehole MM-89-106 from the Restigoche deposit 64
Figure 3.3 Packer system 65
Figure 3.4 Plot of sampling iteration vs electrical conductivity for borehole B-80-7 . . . 66
Figure 3.5 Comparison of trace element analytical results for total nebulization ICP-MS and Chelation IPC-MS 67

Figure 4.1 Digital Elevation Model (DEM) of the Halfmile Lake deposit showing the major streams 85

Figure 4.2 Digital Elevation Model (DEM) of the Restigouche deposit showing the major streams 86
Figure 4.3 Field shots of the Restigouche deposit study area 87
Figure 4.4 A) Discharge for Upalquitch River for the years 1918-1933, 1943-1993. B) Discharge for ten year period 1984-1993. C) Monthly precipitation for the years 1984-1993 88
Figure 4.5 A) Discharge for the Nepisiguit River (at Nepisiguit Falls) for the years 1921-1993. B) Discharge for ten year period 1984-1993. C) Monthly precipitation for the years 1984-1993 89
Figure 4.6 Map showing streams sampled in the Halfmile Lake deposit - interpreted shallow groundwater flow 90
Figure 4.7 A) Location of boreholes investigated from the Halfmile Lake deposit. B) Depth to water table 91
Figure 4.8 Three dimensional models of major faults at the Halfmile Lake deposit. A) Perspective looking southwest. B) Perspective looking down plunge 92
Figure 4.9 Map showing stream sampled at the Restigouche deposit - interpreted shallow groundwater flow 93
Figure 4.10 A) Location of boreholes investigated at the Restigouche deposit. B) Depth to water table 94
Figure 4.11 Downhole geophysical profiles for boreholes HN94-63 and HN 94-65 from the Halfmile Lake deposit 95
Figure 4.12 Downhole geophysical profiles for the boreholes B80-07 and MM-88-02 from the Restigouche deposit 96
Figure 4.13 Secondary SEM images of fracture zone minerals from the Restigouche deposit 97
Figure 4.14 Secondary SEM images of fracture zone minerals from the Restigouche deposit 98

Figure 5.1 Location of Halfmile Lake deposit surface waters 139
Figure 5.2 Modified Piper plot for surface waters from the Halfmile Lake deposit 142
Figure 5.3 Plots of the major anions, cations, and field parameters for Halfmile Lake deposit surface waters 143
Figure 5.4 Spatial distribution of major cations, anions and field parameters in Halfmile Lake deposit surface waters 145

Figure 5.5 Plots of trace elements in Halfmile Lake deposit surface waters 150
Figure 5.6 Spatial distribution of trace elements in Halfmile Lake deposit surface waters 152
Figure 5.7 Plots of vectors based on Principle Component Analysis of Halfmile Lake deposit surface waters 159
Figure 5.8 Principle component plots of Halfmile Lake deposit surface water data showing variation in the first four factors 160
Figure 5.9 Plots of selected mineral saturation indices (SI) for Halfmile Lake deposit surface waters 161
Figure 5.10 Diagram showing the Halfmile Lake surface waters with respect to the stability of the metastable Fe hydroxides 162
Figure 5.11 Halfmile Lake deposit monitoring sites through time for selected elements . 163
Figure 5.12 Locations of surface waters from the Restigouche deposits 165
Figure 5.13 Modified Piper plot for surface waters from the Restigouche deposit 169
Figure 5.14 Plots of the major cations, anions and field parameters for Restigouche deposit surface waters 170
Figure 5.15 Spatial distribution of major cations, anions and field parameters in Restigouche deposit surface waters 172
Figure 5.16 Plots of trace elements in Restigouche deposit surface waters versus total dissolved solids (TDS) 177
Figure 5.17 Spatial distribution of trace elements in Restigouche deposit surface waters 179
Figure 5.18 Diagram showing the Restigouche surface waters with respect to the stability of the metastable Fe hydroxides 184
Figure 5.19 Plots of vectors based on Principle Component Analysis of Restigouche deposit surface waters 185
Figure 5.20 Principle component plots of Restigouche deposit surface water data showing variation in the first four factors 186
Figure 5.21 Plots of selected mineral saturation indices (SI) for Restigouche deposit surface waters 187
Figure 5.22 Plots of speciation of selected elements versus Ph for Restigouche deposit surface waters 188
Figure 5.23 Halfmile Lake deposit surface waters normalised to world average river water 189
Figure 5.24 Restigouche deposit surface waters normalised to world average

river water 190
Figure 5.25 Variation diagrams comparing surface waters from the Halfmile Lake and Restigouche deposits with data collected from the BMC in 1965 191
Figure 5.26 Trace element contents of Halfmile Lake deposit surface waters normalised to average unaltered Halfmile Lake lithology 192
Figure 5.27 Restigouche deposit surface waters normalised to average unaltered felsic lithologies from the Restigouche deposit 193
Figure 5.28 Plots showing the major cation ratios of Halfmile Lake deposit surface waters compared to those of host rocks and local stream sediments 194
Figure 5.29 Plots showing the major cation ratios of Restigouche deposit surface waters compared to those of host rocks and local stream sediments 195
Figure 5.30 Plots of major cations for the Restigouche deposit surface waters, showing relative variation of Ca, Na, and Mg vs total dissolved solids (TDS) 196

Figure 6.1 Proportional circle maps of selected major and trace elements of stream sediments from the Halfmile Lake deposit 211
Figure 6.2 Halfmile Lake deposit stream sediments normalised to average unaltered felsic rocks from the deposit 217
Figure 6.3 Proportional circle maps of selected major and trace elements of stream sediments from the Restigouche deposit 218
Figure 6.4 Restigouche deposit stream sediments normalised to average unaltered felsic rocks from the deposit 224
Figure 6.5 Surface waters normalised to corresponding stream sediments for selected samples from the Halfmile Lake and Restigouche deposits 226
Figure 6.6 Selected stream sediments and average unaltered lithologies from the Halfmile Lake and Restigouche deposits, normalised to average upper continental crust 228

Figure 7.1 Location of boreholes sampled for groundwaters from the Halfmile Lake deposit 306
Figure 7.2 Modified Piper plot for groundwaters from the Halfmile Lake deposit 307
Figure 7.3 Plots of pH, Eh, anions and cations versus TDS for Halfmile Lake deposit groundwaters 308
Figure 7.4 Downhole variation for field parameters, anions and cations for borehole

HN87-8 from the Halfmile Lake deposit 313
Figure 7.5 Downhole variation for field parameters, anions and cations for boreholes HN94-50, HN94-51, HN94-65, and HN94-65 from the Halfmile Lake deposit . . . 315
Figure 7.6 Diagram showing the stability of metastable Fe hydroxides 317
Figure 7.7 Principle component plots of Halfmile Lake groundwaters, showing variation in the first four factors 318
Figure 7.8 Principle component plots of Halfmile Lake groundwaters, showing variation in the first four factors and subdivided by water type 319
Figure 7.9 Plots showing mineral stabilities 320
Figure 7.10 Plots of selected mineral saturation indices for Halfmile Lake deposit groundwaters 321
Figure 7.11 pH variation showing the distribution of mineral speciation in the Halfmile Lake deposit groundwaters 322
Figure 7.12 Representative Halfmile Lake deposit groundwaters normalised to average surface water composition based on water type 324
Figure 7.13 Location of boreholes sampled for groundwaters at the Restigouche deposit 325
Figure 7.14 Modified Piper plot for groundwaters from the Restigouche deposit 326
Figure 7.15 Plots of pH, Eh, anions and cations versus TDS for Restigouche deposit groundwaters 327
Figure 7.16 Sodium, Magnesium, potassium and bicarbonate plotted against chloride for Restigouche deposit groundwaters 331
Figure 7.17 Plots of selected elements and TDS versus pH and Eh for Restigouche deposit groundwaters 332
Figure 7.18 Downhole variation profiles for field parameters, anions and cations in groundwaters from borehole MM-89-106 334
Figure 7.19 Downhole variation profiles for field parameters, anions and cations in groundwaters from borehole B-80-7 336
Figure 7.20 Downhole variation profiles for field parameters, anions and cations in groundwaters from boreholes MM-88-01, MM-88-06, MM-80-07, EH-1 338
Figure 7.21 Relationship between the conductivity of groundwater in borehole MM-80-02 and sampling interval 340
Figure 7.22 Principle component plots of Restigouche deposit groundwaters showing variation in the first four factors 341

Figure 7.23 Principle component plots of Restigouche deposit groundwaters showing variation in the first four factors. Samples are subdivided by water type 342
Figure 7.24 Plots of selected mineral saturation indices for Restigouche deposit groundwaters 343
Figure 7.25 Speciation variation diagrams showing the distribution of Fe species 344
Figure 7.26 Diagram showing the stability of metastable Fe hydroxides relative to the Restigouche deposit groundwaters 346
Figure 7.27 Plots showing mineral stabilities for the systems 347
Figure 7.28 Restigouche deposit groundwaters normalised to average surface water composition based on water type 348
Figure 7.29 Location of the Brunswick #12, Heath Steele, Wedge and Willett deposits . 349
Figure 7.30 Modified Piper plot for the groundwaters from the Brunswick #12, Heath Steele, Wedge and Willett deposits 350
Figure 7.31 Plots of field parameters, anions and cations for groundwaters from the Brunswick #12, Heath Steele, Wedge and Willett deposits 351
Figure 7.32 Plots of Fe and Mn vs Eh, Mn, Al, and Zn vs pH for groundwaters from the Brunswick #12, Heath Steele, Wedge and Willett deposits 355
Figure 7.33 Diagram showing the stability of metastable Fe hydroxides relative to the groundwaters from the Brunswick #12, Heath Steele, Wedge and Willett deposits . . 356
Figure 7.34 Na and SO_4 vs Cl for Halfmile Lake and Restigouche deposit groundwaters and waters from the Bathhurst Mining Camp (BMC) mines 357
Figure 7.35 Ca and Mg versus Cl for Halfmile Lake and Restigouche deposit groundwaters and waters from the Bathhurst Mining Camp (BMC) mines 358
Figure 7.36 Mo and Pb versus Cl for Halfmile Lake and Restigouche deposit groundwaters and waters from the Bathhurst Mining Camp (BMC) mines 359
Figure 7.37 Plot of pH versus total metal load for all the groundwaters in the present study 360
Figure 7.38 Br vs Cl contents for Bathhurst Mining Camp ground and surface waters . 361
Figure 7.39 Br/Cl vs Br and Cl contents for Bathhurst Mining Camp (BMC) ground and surface waters 362
Figure 7.40 Molar ratios of Na/Cl and Ca/Mg vs Br/Cl for Bathhurst Mining Camp (BMC) ground and surface waters 363
Figure 7.41 Molar ratios of Na/Ca vs Br/Cl for Bathhurst Mining Camp (BMC) ground and surface waters 364

Figure 7.42 Sulfate versus trace metals in groundwaters from the Halfmile Lake and Restigouche deposit 365
Figure 7.43 Absorption of Pb, Zn, Ca, SO_4 onto surface of $Fe(OH)_{3(ppd)}$ as a function of pH 366
Figure 7.44 Geochemical modelling results showing absorption and speciation for selected species from borehole MM-88-02 from the Restigouche deposit 367
Figure 7.45 Plots of arsenic plotted against pH, Eh, SO_4, Fe, and Pb 368
Figure 7.46 Eh-pH stability diagram for As species 369
Figure 7.47 Reaction path model of As speciation for various samples 370
Figure 7.48 Plots of pH, Eh, Cl and sulphate versus U content of Bathhurst Mining Camp (BMC) ground and surface waters 371

Figure 8.1 Location of the Stratmat Main Zone deposit 389
Figure 8.2 Gamma ray, resistivity, self-potential (SP), tempature, and tempature gradient logs in a BQ hole through Stratmat Main Zone deposit 390
Figure 8.3 Modified Piper plot for groundwaters from the Stratmat Main Zone deposit . 391
Figure 8.4 Downhole variation profiles of the field parameters, anions and cations for borehole S61-19 from the Stratmat Main Zone deposit 392
Figure 8.5 Selected speciation and mineral saturation indices (SI) for groundwaters from borehole S61-19 from the Stratmat Main Zone deposit 394
Figure 8.6 Stable isotopic composition of the borehole S61-19 from the Stratmat Main Zone deposit plotted versus depth 395
Figure 8.7 Downhole variation profiles of selected variables for borehole S61-19 from the Stratmat Main Zone deposit, extended to show the variation through the ore zone 396
Figure 8.8 Diagram showing the stability of metastable Fe hydroxides 397
Figure 8.9 A) Modification of the generalised model of SP anomolies about massive sulphide ore bodies. B) Schematic model of oxidation of massive sulfides at the Stratmat Main Zone deposit and development of the SP anomaly 398

Figure 9.1 XRD patterns for suspended sediment samples from Halfmile Lake deposit groundwaters 421
Figure 9.2 Secondary SEM images of suspended sediments from Halfmile Lake deposit groundwaters 422

Figure 9.3 XRD patterns for suspended sediment samples from Restigouche deposit groundwaters 423
Figure 9.4 Secondary SEM images of suspended sediments from Restigouche deposit groundwaters 424
Figure 9.5 Secondary SEM images of suspended sediments from Restigouche deposit groundwaters 425
Figure 9.6 Secondary SEM images of suspended sediments from Restigouche deposit groundwaters 426
Figure 9.7 XRD patterns for suspended sediment samples from Restigouche deposit groundwaters distal from the main ore body 427
Figure 9.8 Trace and major element contents of Halfmile Lake and Restigouche deposit borehole suspended sediments normalised to average unaltered felsic lithologies . . . 428
Figure 9.9 Trace element contents of Halfmile Lake and Restigouche deposit borehole groundwaters normalised to the corresponding suspended sediments 429
Figure 9.10 A) Plot of Fe/Ti vs Al/(Al+Fe+Mn). B) Plot of TiO_2 vs Th. Suspended sediments from the Halfmile Lake and Restigouche deposits. 430
Figure 9.11 A) Gossans and B) Massive sulphides normalized to unaltered felsic rocks 431

Figure 10.1 La/Ce and Ce/Ce* vs pH for ground and surface waters 475
Figure 10.2 ΣREE, La, Gd, Yb vs pH for ground and surface waters 476
Figure 10.3 La/Ce, Gd/Yb, La/Yb, Sm/Nd vs Nd for ground and surface waters 477
Figure 10.4 La/Ce and ΣREE vs Cl for ground and surface waters 478
Figure 10.5 Plots of Ce and Eu anomalies for ground and surface waters 479
Figure 10.6 ΣREE and Ce anomaly vs total Fe for ground and surface waters 480
Figure 10.7 REE in Halfmile Lake deposit surface waters normalized to NASC 481
Figure 10.8 Proportional circle maps of REE in Halfmile Lake deposit surface waters . . 482
Figure 10.9 Variations in REE in Halfmile Lake deposit surface waters 484
Figure 10.10 REE in Halfmile Lake deposit groundwaters normalized to NASC 485
Figure 10.11 Variations in REE in Halfmile Lake deposit groundwaters 486
Figure 10.12 REE in Halfmile Lake deposit stream sediments normalized to NASC . . . 487
Figure 10.13 Proportional circle maps of REE in Halfmile Lake deposit stream sediments 488
Figure 10.14 REE in Halfmile Lake deposit lithologies normalized to NASC 490
Figure 10.15 REE in Restigouche deposit surface waters normalized to NASC 491

Figure 10.16 Proportional circle maps of REE in Restigouche deposit surface waters . . 493
Figure 10.17 Variations in REE for Restigouche deposit surface waters 495
Figure 10.18 REE in Restigouche deposit groundwaters normalized to NASC 496
Figure 10.19 Variations in REE in Restigouche deposit groundwaters 497
Figure 10.20 REE in Restigouche deposit stream sediments normalized to NASC 498
Figure 10.21 Proportional circle maps of REE in Restigouche deposit stream sediments 501
Figure 10.22 REE in Restigouche deposit lithologies normalized to NASC 503
Figure 10.23 REE in Mine and other waters normalized to NASC 504
Figure 10.24 REE in Halfmile Lake and Restigouche deposit suspended sediments normalized to NASC 505
Figure 10.25 Groundwater REE contents normalized to the REE content of the coexisting suspended sediment 506

Figure 11.1 A) Study area and IAEA Truro and St Agathe station locations. B) $\delta^{18}O$ vs δD for precipitation 550
Figure 11.2 Plots showing the variation in $\delta^{18}O$, δD, temperature and precipitation amount for St Agathe and Truro IAEA stations 551
Figure 11.3 Monthly mean weighted averages of $\delta^{18}O$ and δD for precipitation from the study area, Truro and St Agathe 552
Figure 11.4 $\delta^{18}O$ vs δD for Halfmile Lake deposit waters 553
Figure 11.5 Histograms of $\delta^{18}O$ for Halfmile Lake and Restigouche deposit ground and surface waters and mine waters 554
Figure 11.6 Cl vs $\delta^{18}O$ for ground and surface waters from the Halfmile Lake deposit . 555
Figure 11.7 $\delta^{18}O$, δD and Cl vs depth for boreholes HN87-8 and HN94-55, Halfmile Lake deposit 556
Figure 11.8 $\delta^{18}O$ vs δD for ground and surface waters from the Restigouche deposit . . 557
Figure 11.9 Cl vs $\delta^{18}O$ for ground and surface waters from the Restigouche deposit . . 558
Figure 11.10 $\delta^{18}O$ vs δD and Cl vs $\delta^{18}O$ for groundwaters from Brunswick #12, Heath Steele, Stratmat Main Zone, Wedge and Willett deposits 559
Figure 11.11 $\delta^{18}O$ vs $\delta^{13}C$ for ground and surface waters 560
Figure 11.12 Plots of $1/HCO_3$ and HCO_3/SO_4 vs $\delta^{13}C$ for ground and surface waters . 561
Figure 11.13 Plots of pH vs $\delta^{13}C$, pH vs HCO_3, Ca+Mg vs $\delta^{13}C$ and SO_4 vs $\delta^{13}C$ for ground and surface waters 562

Figure 11.14 SEM photomicrographs of vein and vug carbonate from the Restigouche deposit 563
Figure 11.15 $\delta^{13}C$ vs $\delta^{18}O$ for carbonate from the Restigouche and Halfmile Lake deposits 564
Figure 11.16 Calculated temperature vs $\delta^{18}O$ and $\delta^{13}C$ for Restigouche and Halfmile Lake deposit carbonate 565
Figure 11.17 B vs Cl and B/Cl vs Cl for ground and surface waters from the BMC . . . 566
Figure 11.18 $\delta^{11}B$ vs B and Cl for ground and surface waters from the BMC 567

Figure 12.1 $^{87}Sr/^{86}Sr$ vs Rb/Sr and $^{87}Sr/^{86}Sr$ vs 1/Sr for Restigouche deposit ground and surface waters, mine waters and host rocks 604
Figure 12.2 Ca vs Sr, $\delta^{18}O$ vs $^{87}Sr/^{86}Sr$, $^{87}Sr/^{86}Sr$ vs Ca/Na, and $^{87}Sr/^{86}Sr$ vs 1000Sr/Ca or Restigouche deposit ground and surface waters, mine waters and host rocks 605
Figure 12.3 Stacey Kramer Pb evolution curves showing Pb isotopic compositions of Restigouche ground and surface waters, mine waters and host rocks 606
Figure 12.4 $^{207}Pb/^{204}Pb$ vs $^{206}Pb/^{204}Pb$ and $^{208}Pb/^{204}Pb$ vs $^{206}Pb/^{204}Pb$ for Restigouche ground and surface waters, mine waters and host rocks 607
Figure 12.5 $^{206}Pb/^{204}Pb$ vs 1/Pb and $^{206}Pb/^{204}Pb$ vs U/Pb for Restigouche ground and surface waters, mine waters and host rocks 608
Figure 12.6 $^{143}Nd/^{144}Nd$ vs $^{147}Sm/^{144}Nd$ and $^{87}Sr/^{86}Sr$ for Restigouche ground and surface waters, mine waters and host rocks 609
Figure 12.7 Chondrite-normalized REE profiles for groundwaters and whole rocks determined for Nd isotopic composition 610

Figure 13.1 Cumulative probability plots for sulphide-associated elements in Halfmile Lake deposit surface waters 642
Figure 13.2 Proportional circle plots for sulphide-associated elements in Halfmile Lake deposit surface waters 643
Figure 13.3 Cumulative probability plots for sulphide-associated elements in Halfmile Lake deposit stream sediments 646
Figure 13.4 Proportional circle plots for sulphide-associated elements in Halfmile Lake deposit stream sediments 647
Figure 13.5 Cumulative probability plots for sulphide-associated elements in Halfmile

Lake deposit groundwaters 650
Figure 13.6 Proportional circle plots for sulphide-associated elements in Halfmile Lake deposit groundwaters 651
Figure 13.7 Cumulative probability plots for sulphide-associated elements in Restigouche deposit surface waters 655
Figure 13.8 Surface water profiles along Charlotte Brook for selected chemical parameters 656
Figure 13.9 Proportional circle plots for sulphide-associated elements in Restigouche deposit surface waters 658
Figure 13.10 Cumulative probability plots for sulphide-associated elements in Restigouche deposit stream sediments 662
Figure 13.11 Stream sediment profiles along Charlotte Brook for selected chemical parameters 663
Figure 13.12 Proportional circle plots for sulphide-associated elements in Restigouche deposit stream sediments 666
Figure 13.13 Cumulative probability plots for sulphide-associated elements in Restigouche deposit groundwaters 670
Figure 13.14 Proportional circle plots for sulphide-associated elements in Restigouche deposit groundwaters 671
Figure 13.15 Cross-sectional proportional circle plots of metals in Restigouche deposit groundwaters 675

Appendices

Appendices are on the CD-ROM as Microsoft Excel and Adobe Acrobat files.

APPENDIX A. HALFMILE LAKE DEPOSIT

A.1.1 Geochemical results for Halfmile Lake deposit surface waters A11

A.1.2 Summary statistics for Halfmile Lake deposit surface waters A12

A.1.3 Pearson Product Moment correlation matrix for Halfmile Lake deposit surface waters A13

A.1.4 Selected mineral saturation indices for Halfmile Lake deposit surface waters . . . A14

A.1.5 Calculated aqueous species for cations from selected Halfmile Lake deposit surface waters A15

A.2.1 Geochemistry of stream sediments from the Halfmile Lake deposit A21

A.2.2 Summary statistics for stream sediments from the Halfmile Lake deposit A22

A.2.3 Pearson Product Moment correlation matrix for stream sediments from the Halfmile Lake deposit A23

A.2.4 Percent differences for the < 63 μm and 63-125 μm size fractions of Halfmile Lake deposit stream sediments A24

A.3.1 Halfmile Lake deposit groundwater compositions A31

A.3.2 Summary statistics for Halfmile Lake deposit groundwaters A32

A.3.3 Pearson Product Moment correlation matrix for Halfmile Lake deposit groundwaters A33

A.3.4 Principal Components Analysis for Halfmile Lake deposit groundwaters A34

A.3.5 Selected mineral saturation indices for Halfmile Lake deposit groundwaters A35

A.3.5 Calculated aqueous species for cations in selected Halfmile Lake deposit groundwaters A36

APPENDIX B. RESTIGOUCHE DEPOSIT

B.1.1 Geochemical results for Restigouche deposit surface waters B11

B.1.2 Summary statistics for Restigouche deposit surface waters B12

B.1.3 Pearson Product Moment correlation matrix for Restigouche deposit surface waters B13

B.1.4 Selected mineral saturation indices for Restigouche deposit surface waters B14

B.1.5 Calculated aqueous species for cations from selected Restigouche deposit surface waters B15

B.2.1 Geochemistry of stream sediments from the Restigouche deposit B21

B.2.2 Summary statistics for stream sediments from the Restigouche deposit B22

B.2.3 Pearson Product Moment correlation matrix for stream sediments from the Restigouche deposit B23

B.3.1 Geochemistry of Restigouche deposit groundwaters B31

B.3.2 Summary statistics for Restigouche deposit groundwaters B32

B.3.3 Pearson Product Moment correlation matrix for Restigouche deposit groundwaters B33

B.3.4 Principal Components Analysis for Restigouche deposit groundwaters B34

B.3.5 Selected mineral saturation indices for Restigouche deposit groundwaters B35

B.3.5 Calculated aqueous species for cations in selected Restigouche deposit groundwaters B36

APPENDIX C. Mine and Other Waters

C.1.1 Geochemistry of groundwaters from Brunswick #12, Heath Steele, Wedge and Willett deposits C11

C.1.2 Summary statistics for groundwaters from Brunswick #12, Heath Steele, Wedge and Willett deposits C12

C.1.3 Selected mineral saturation indices for mine waters C13

C.1.4 Calculated aqueous species for cations in mine waters C14

CHAPTER ONE:
INTRODUCTION

1.1 Introduction and Justification

In recent years there has been increased appreciation of the importance of understanding the processes and pathways of water-rock interactions around abandoned mine sites and tailings impoundments and of the impacts of mining on the environment (e.g. Curtis and Walker, 1994; Goodyear et al., 1996; Pratt et al., 1996; Thornton, 1996; Wayne et al., 1996). There has also been considerable research into the mechanisms and processes of massive sulphide oxidation, typically under laboratory or mine tailings conditions (e.g. Al et al., 1994; Bigham et al., 1990; Blowes et al., 1990; Nicholson, 1994; Ritchie, 1994). There have been relatively few detailed studies of water-rock interaction around undisturbed massive sulphide deposits. There have also been very few detailed studies which have focussed on ground and surface water compositions in small catchment basins in order to unravel water-rock reactions and to understand the hydrological connection between the surface and subsurface environments.

The utility of ground and surface water hydrogeochemistry as a mineral exploration tool has been recognized for some time (e.g. Boyle et al., 1971; Cameron, 1977; Goodfellow, 1983; Miller et al., 1982; Runnells and Lahermo, 1984). However, despite considerable interest in hydrogeochemical methods for uranium exploration during the 1970's and 1980's (e.g. Earle and Drever, 1983; Toulhoat and Beaucaire, 1991), and recent reviews (Giblin, 1994; Taufen, 1997), there are comparatively few detailed studies in the literature, although there has been an increase in interest in recent years (e.g. Cidu et al., 1995; Grimes et al., 1995; Ruijin et al., 1994; Wang et al., 1995). Unfortunately, many of these studies have made little attempt to understand the processes and pathways of metal dispersion away from mineralization. Historically, one of the major limitations in the application of hydrogeochemical methods to mineral exploration has been the low solubility and abundance of pathfinder metals in natural waters (Runnells and Lahermo, 1984). This disadvantage has largely been resolved through

the development and application of inductively-coupled plasma mass spectrometry (ICP-MS) to the routine analysis of waters which now permit detection limits at the ppt level (e.g. Hall et al., 1995b; Stetzenbach et al., 1994). These techniques are now sufficiently rapid that large numbers of samples can be analyzed for a wide range of elements to allow better geochemical modelling and understanding of metal speciation and mobility.

One of the problems faced by the mineral exploration industry is the interpretation of geochemical anomalies found by more traditional stream sediment, soil and till geochemical methods (Goodfellow, 1983). The mineral exploration industry would benefit, therefore, from an increased understanding of metal dispersion in the secondary environment in order to improve the recognition of massive sulphide-associated anomalies from false anomalies. Several massive sulphide deposits in the BMC were discovered using stream sediment geochemical methods (e.g., the Restigouche deposit) but apart from work in the 1960's during regional stream sediment sampling (Boyle et al. unpublished data; Boyle et al. 1966) there have been no studies of the composition of surface waters associated with undisturbed deposits in the BMC. There is even less known about the composition of groundwaters, the depth of penetration of oxygenated recharge waters and the effective depth of natural oxidation of massive sulphides in the BMC.

Although ground and surface water hydrogeochemistry has great potential for mineral exploration, there is also increasing recognition that environmental guidelines for mining activities need to be placed in a proper geological context and that there needs to be much better baseline geochemical data (Maest, 1996). Although there are numerous studies in the literature related to the impacts of past mining activities on the surface environment, there is a paucity of undisturbed natural analog sites that allow characterization of pre-mining impact of ore bodies on the natural environment (Maest, 1996).

With the above problems in mind, the objectives of this research areas follows:

1) to characterize the composition of ground and surface waters in the BMC and the compositional variation in ground and surface waters in small catchment basins,

2) to determine the sources of waters and dissolved metals associated with undisturbed massive sulphide deposits in the BMC,

3) to better understand natural water-sulphide interaction and how metals are mobilized and transported in groundwater and surface water environments,

4) to demonstrate the utility of hydrogeochemical methods in mineral exploration in a mature mining camp like the BMC and to improve the methodology, and

5) to establish the background values of trace metals in the BMC in order to better understand natural metal variations produced by leaching of unmineralized rocks and naturally oxidizing massive sulphide deposits.

In order to meet the objectives of this study and address the issued identified above, ground and surface waters were collected from several massive sulphide deposits in the Bathurst Mining Camp, northern New Brunswick, Canada (Fig. 1.1). Emphasis was placed on two deposits, the Halfmile Lake and Restigouche deposits. The Halfmile Lake and Restigouche deposits are well suited for this type of study because they are the same age, are hosted in similar lithologies and exist under the same climatic and physiographic regime as several past and active producing mines in the Bathurst Mining Camp. In addition, both deposits are being studied under the multi-disciplinary research initiative, EXTECH-II (Goodfellow, 1995; Goodfellow and participants, 1996). Both the Halfmile Lake and Restigouche deposits are Zn-Pb deposits with minor contents of Ag, Cu and lesser Au. These two deposits were chosen on the basis of access, availability of exploration drill holes likely to be open for sampling of deep groundwaters, contrasts in deposit geometry, and the large number of complementary geological, geophysical, rock geochemical and quaternary studies at these deposits. Groundwaters were also collected in less detail at a number of other deposits in the Bathurst Camp, as it became obvious during the second field season that groundwaters from the Halfmile Lake and Restigouche deposits were radically different. It was therefore necessary to test if one or both of Halfmile Lake and Restigouche were anomalous from a hydrogeochemical standpoint. Groundwaters were also collected from two active mines in the BMC, the Heath

Steele and Brunswick #12 deposits.

Surface waters were collected from streams, springs and seeps around both the Halfmile Lake and Restigouche deposits in order to understand metal dispersion in the surface environment. Groundwaters were sampled to better understand metal mobilization processes and were collected from exploration boreholes using flow-through bailer and straddle-packer methodologies. The straddle-packer system allowed the sampling of groundwaters from specific depths flowing through known lithologies. Several boreholes sampled for groundwaters were also investigated using downhole geophysical methods allowing inferences to be made on groundwater flow and sulphide oxidation reactions in the subsurface (Mwenifumbo, 1993; Mwenifumbo and Killeen, 1995).

The major, trace and rare earth element compositions of ground and surface waters from the Halfmile Lake and Restigouche deposits are used to interpret the style and extent of water-rock reaction and dispersion away from the massive sulphides. Metal sources are identified through the use of both trace metals and radiogenic isotopes. Stable isotopes and major and trace elements compositions are used to interpret ground and surface water sources as well as mixing relationships and the timing of recharge. Suspended and stream sediments were also analyzed to characterize metal partitioning between the aqueous and solid phases.

1.2 Study Areas

The study areas are located in northern New Brunswick, Canada, south and west of the town of Bathurst (Fig. 1.1). The Bathurst Mining Camp hosts over 30 massive sulphide deposits including the very large Brunswick #12 Zn-Pb deposit as well as several smaller deposits which are either in production (Restigouche, Heath Steele, Caribou deposits), are past producers (Brunswick #6, Wedge, Austin Brook, Murray Brook deposits), or are presently uneconomic because of either small size, low grade, or complex structure (e.g. Halfmile Lake deposit)

1.2.1 Halfmile Lake deposit

The Halfmile Lake deposit is an undeveloped Zn-Pb-Cu deposits and one of the larger undisturbed deposits in the Bathurst Camp (Adair, 1992). The property is located 66 km northwest of Newcastle and 70 km southwest of Bathurst. Good access is provided by logging roads. The Halfmile Lake deposit is the focus of many geochemical, geophysical and surficial studies (e.g. Adair, 1992; Parkhill and Doiron, 1995) which, combined with its size and undisturbed nature, made it a good choice for this hydrogeochemical study.

1.2.2 Restigouche deposit

The Restigouche deposit is located in the Portage Lakes and Upsalquitch Lake area, approximately 75 km west of Bathurst. Access to the property is for the most part very good along old logging roads and roads utilized during exploration programs. The Restigouche deposit provides a good contrast to the Halfmile Lake deposit for this hydrogeochemical study in that it occurs in rocks of similar age and tectonic affinity with similar physiography, yet with different deposit geometry and structure. The Restigouche deposit crops out as a small gossan near Charlotte Brook. Unlike the Halfmile Lake deposit which is steeply dipping and overturned, the Restigouche deposit dips shallowly at 25° and is right side up.

The Restigouche deposit is drained by several streams that facilitate the study of hydromorphic dispersion of metals in surface waters. The main stream in the area, Charlotte Brook, runs perpendicular to the deposit and crosses mineralization just below the gossan outcrop. A small stream (herein referred to as North stream) runs parallel to the deposit, just east of the ore body.

1.2.3 Other deposits sampled

A limited number of samples were collected at other sites to provide reference from other mineral deposits in the BMC. Where possible, surface waters were also sampled at a more regional scale around the Halfmile Lake and Restigouche deposits. In addition, groundwaters

were collected from the two presently active mines in the Bathurst Camp, the Heath Steele and Brunswick #12 mines (Fig. 1.1). In addition, Fe-precipitating groundwaters were collected from the Wedge deposit, a currently inactive, past producer of base metals (primarily Cu). The Willett deposit, a recent discovery, was also sampled. This deposit is located 35 km southwest of Bathurst (Fig. 1.1). Groundwaters from the Stratmat Main Zone deposit were collected to test some borehole geophysical anomalies (Mwenifumbo, 1991; Mwenifumbo, 1993). The Stratmat Main Zone deposit is located near and to the north of Heath Steele Mines (Fig. 1.1).

1.3 Organization of the Thesis

This thesis was organized to facilitate publishing of material during and after completion, without the constraints imposed by following a strict paper format. Each of the main chapters (Four to Thirteen) is intended to stand alone with the exception that the geology and analytical methods are not discussed in each chapter as this would result in unnecessary duplication. Thus each chapter has an introduction, presentation of the main results, detailed discussion of those results, and a summary section.

Chapters Two and Three present the background geological and analytical information pertinent to the presentation and discussion of results that follow. Chapter Two presents a brief synthesis of the geology of the Bathurst Mining Camp as well as a more detailed discussion of the local geology around the Halfmile Lake and Restigouche deposits. In this study a small number of whole rock samples were analyzed for major and trace element composition and fracture zone mineralogy to complement published and company geochemical data. Chapter Three presents a brief discussion of the analytical methods used in this study as well as a more detailed description of the field sampling methods used. Chapter Four presents background hydrological information which allows the hydrogeochemical data to be placed in context and to improve interpretation of the chemical data. Chapter Five presents the results and discussion of the major and trace element hydrogeochemistry of surface waters collected from the Halfmile Lake and Restigouche deposits. To complement the surface water chemistry, stream sediments

were also collected at the same sites as the surface waters. These data are presented and discussed in Chapter Six. Chapter Seven presents the major and trace element geochemistry of groundwaters collected from the Halfmile Lake, Restigouche, Heath Steele, Brunswick #12, Willett, and Wedge deposits. The composition of groundwaters from the Stratmat Main Zone deposit are presented and discussed in Chapter Eight. These waters are not included in Chapter Seven because they were collected to explain self-potential anomalies detected by downhole geophysical surveys. Chapter Nine presents the results of the mineralogy and chemical composition of particles suspended in groundwater of groundwater suspended sediments. These results complement the groundwater chemistry in much the same way as the stream sediments complement the surface water chemistry. The results of detailed analyses of the rare earth elements in a subset of ground and surface waters as well as stream sediments, suspended sediments and the host lithologies are presented in Chapter Ten. The stable isotopic compositions of the ground and surface waters are presented in Chapter Eleven and the radiogenic isotopic data are discussed in Chapter Twelve. Chapter Thirteen is a synthesis of the potential application of hydrogeochemistry in the exploration for massive sulphide deposits in the Bathurst Mining Camp, and by extension, in mineral belts elsewhere. This chapter draws on material discussed throughout the thesis.

Some of the material presented in the thesis has been published or has been submitted or is in review. Initial results from the Halfmile Lake deposit were published in Current Research published by the New Brunswick Department of Natural Resources and Energy, Minerals and Energy Division (Leybourne et al., 1995a). Preliminary results from the Restigouche deposit were published in the Geological Survey of Canada's Current Research (Leybourne et al., 1996a). In addition, some of the results have been presented at various meetings over the course of the thesis (Leybourne et al., 1995b; Leybourne et al., 1995c; Leybourne et al., 1996b; Leybourne et al., 1996c; Leybourne et al., 1997b; Leybourne et al., 1997c; Leybourne et al., 1997d; Leybourne et al., 1997e; Leybourne et al., 1997f). To date, three papers have been submitted to refereed journals.

1) The REE geochemistry of ground and surface waters is in review at Applied Geochemistry (Leybourne et al., submitted-b). All the water samples were collected by Leybourne during the summers of 1994-1996. The rationale for investigating the REE in these waters and writing of the manuscript was by Leybourne. Goodfellow and Boyle revised the manuscript and Hall organized the analytical work.

2) Some of the results of the geochemistry of the groundwaters at the Halfmile Lake and Restigouche deposits has been accepted with minor revisions by The Journal of Exploration Geochemistry (Leybourne et al., submitted-a). All the water samples were collected by Leybourne during the summers of 1994-1996. The manuscript was written by Leybourne, with input from Goodfellow and Boyle.

3) Chapter Eight represents a paper which has been submitted to Chemical Geology (Leybourne et al., submitted-c). The sampling the groundwaters in borehole ST61-19 was suggested by Mwenifumbo, who also organized the collection of the borehole geophysical data. Sampling and manuscript writing was by Leybourne, with input from Mwenifumbo, Goodfellow and Boyle.

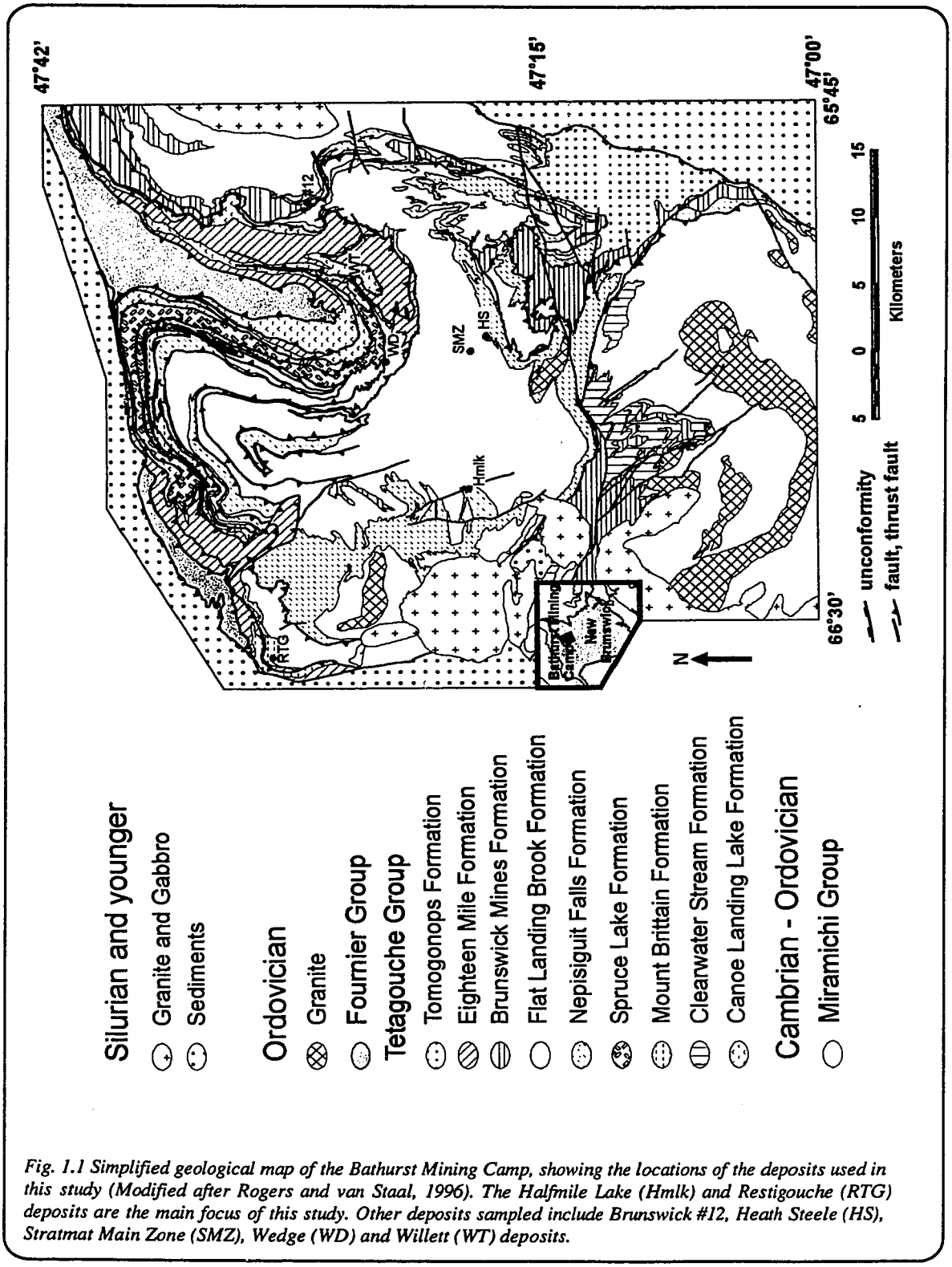


Fig. 1.1 Simplified geological map of the Bathurst Mining Camp, showing the locations of the deposits used in this study (Modified after Rogers and van Staal, 1996). The Halfmile Lake (Hmlk) and Restigouche (RTG) deposits are the main focus of this study. Other deposits sampled include Brunswick #12, Heath Steele (HS), Stratmat Main Zone (SMZ), Wedge (WD) and Willett (WT) deposits.

CHAPTER TWO:
REGIONAL GEOLOGY AND GEOLOGY OF THE HALFMILE LAKE AND RESTIGOUCHE DEPOSITS, BATHURST MINING CAMP, NEW BRUNSWICK

2.1 Introduction

It is well established that one of the primary controls on the chemistry and hydrology of ground and surface waters is the physical and chemical properties of the underlying bedrock. This chapter is a synthesis of information previously published about the regional geology and structure of the Bathurst Mining Camp, and of the two deposits investigated in detail in this study. This material lays the groundwork for interpretations of surface waters and groundwaters as a function of water-rock reactions and fluid evolution from the deposit into streams. In addition to published data on the two main deposits investigated in this study, a limited number of sulphide and host lithologies from the Halfmile Lake and Restigouche deposits were analyzed for major, trace and rare earth elements, and the data is presented in this chapter.

2.2 Regional Geology

The northern Appalachians have been subdivided into five tectono-stratigraphic zones (Williams, 1979). The Bathurst Mining Camp (BMC), part of the northern Miramichi Highlands (Fig. 2.1), includes rocks assigned to the Gander Zone and Dunnage Zone (McCutcheon et al., 1993). The Bathurst Camp is overlain to the west by Upper Ordovician to Silurian flysch and Siluro-Devonian shallow marine volcanic and sedimentary rocks and to the east by Silurian turbidites and terrestrial Carboniferous rocks of the New Brunswick Platform. The Bathurst Camp has been further subdivided into three main groups, the Cambro-Ordovician Miramichi Group, the Middle to Late Ordovician Tetagouche Group, and the Middle to Late Ordovician Fournier Group (van Staal and Fyffe, 1991b; van Staal et al.,

1992). In the northern Miramichi Highlands, the Miramichi Group is equivalent to the Gander Zone and the Tetagouche and Fournier groups are equivalents to the Dunnage Zone (McCutcheon et al., 1993). Cambro-Ordovician quartzose turbidites of the lower Tetagouche group have previously been assumed to be correlative with the Gander Zone of Newfoundland (Rast et al., 1976), although the Gander Zone in Newfoundland does not have the thick sequence of Middle Ordovician volcanic rocks (Rast et al., 1976). More recent work has defined the Gander Zone in New Brunswick as the Miramichi Group, the lower siliciclastic part of the former Tetagouche Group, and the Dunnage Zone of Newfoundland is represented by the volcanic and sedimentary rocks that overlie the Miramichi Group (van Staal and Fyffe, 1991a).

2.2.1 Miramichi Group

The Miramichi Group is interpreted to represent a flysch apron on the margin of the Avalon continent (van Staal and Fyffe, 1991b). The Miramichi Group has been subdivided into the Chain of Rocks Formation composed mostly of quartzite and siltstone and the overlying Knights Brook Formation (Fig. 2.2) which contains a greater proportion of graphitic slate than the lower formation (McCutcheon et al., 1993). The Knights Brook slate is typically pyrite-rich and is interbedded with medium to thinly bedded sandstones (van Staal et al., 1992). Age determinations to date indicate that the Miramichi Group is older than Late Argenigan, consistent with Lower Ordovician fossils in correlative rocks to the southwest (Fyffe et al., 1983).

Fyffe et al. (1996) suggested that the Patrick Brook Formation, previously assigned to the Tetagouche Group, should be reassigned to the Miramichi Group. The Patrick Brook Formation is composed of dark grey to black shale, argillite, quartzite and quartz wacke. Sandstones are epiclastic to volcaniclastic with interbedded shales. The sandstones are both epiclastic and volcaniclastic in origin, the latter with common relict vitreous black to smoky quartz phenocrysts, that are interpreted to represent turbidites deposited on an outer continental

slope (Rice and van Staal, 1992). Wilson (1993) has assigned wackes and siltstones near the Halfmile Lake deposit to the Nepisiguit Falls Formation based on lithological similarities with rocks at Heath Steele, although De Roo and van Staal (De Roo and van Staal, 1991) placed these units within the Patrick Brook Formation.

2.2.2 Tetagouche Group

The Tetagouche Group is the primary host of the volcanogenic massive sulphide (VMS) deposits in the BMC (van Staal et al., 1992). In the BMC, the Tetagouche Group is also referred to as the Bathurst Subzone of the Dunnage Zone (van Staal and Fyffe, 1991b). In a broad sense, volcanic rocks of the Tetagouche Group diminish in volume to the south, where siliciclastic metasedimentary rocks predominate (van Staal, 1987). The Tetagouche Group is subdivided into a number of formations (McCutcheon et al., 1993; van Staal et al., 1992) including the Vallée Lourdes, Spruce Lake, Nepisiguit Falls, Flat Landing Brook, Canoe Landing Lake, Brunswick Mines and Eighteen Mile formations. Recent mapping around the Restigouche Deposit has identified a new unit, referred to as the Mount Brittain volcanic suite (Gower, 1996).

The oldest unit is the Vallée Lourdes Formation which comprises limestone, calcareous phyllite and conglomerate. These rocks disconformably overlie Miramichi Group rocks. The Vallée Lourdes Formation has been dated on the basis of brachiopod and conodont fossils and is estimated to be middle Argenigan to earliest Llanvirnian in age. Wilson (1993) subdivided the Nepisiguit Falls Formation into a sedimentary and a volcanic member, with the latter typically volumetrically dominant. The two members locally grade into each other and are commonly intercalated, indicative of subaqueous deposition. The Nepisiguit Falls Formation has been described in detail by Lentz and Goodfellow (Lentz and Goodfellow, 1992b). The volcanic units include those described as quartz-feldspar augen schist (QFAS) or quartz-feldspar porphyry (QFP), quartz augen schist (QAS), and fine grained quartz-feldspar crystal tuff (CT). This formation also includes the metamorphosed equivalents of siltstone,

mudstone, and metalliferous sedimentary rocks. van Staal et al. (1992) separated the Nepisiguit Falls Formation from the Patrick Brook Formation on the basis of the absence of black shale in the former. Chlorite-rich metasedimentary rocks and iron formations occur near the upper part of the Nepisiguit Falls Formation stratigraphy and constitute the "Brunswick Horizon".

The Flat Landing Brook Formation is characterized by aphyric and feldspar-phyric felsic flows and rhyolite to rhyodacite domes, autobrecciated rhyolite of local extent and minor pyroclastic units (van Staal et al., 1992). Intercalated metasedimentary rocks are less common and include grey to green siltstone, shale, feldspathic wacke or sandstone, and volcaniclastic wackes (Wilson 1993). Hematitic and manganiferous shale and chert also occurs in the Flat Landing Brook Formation. Mafic flows and gabbroic bodies also occur within the Flat Landing Brook Formation. The Flat Landing Brook Formation yields a volcanic zircon U-Pb ages of 466±5.3 Ma (Rogers et al., in press; Sullivan and van Staal, 1990).

The Canoe Landing Lake Formation is comprised of massive to pillowed basalt, with lesser interbedded red hematitic shale and chert. There are two mafic suites in the Canoe Landing Lake Formation. One suite comprises more primitive alkali basalts with high Cr (> 200 ppm) and a second suite which comprises tholeiitic pillow flows with intercalated alkali basalt flows (McCutcheon et al., 1993).

Eighteen Mile Formation rocks are dominated by thinly bedded to laminated feldspathic wackes and shales which young upwards to black shale. The Eighteen Mile Formation also hosts alkalic volcanic rocks ranging from basalt to comendite in composition.

The Mount Brittain Formation is comprised of feldspar-phyric dacitic flows overlain by felsic feldspar crystal-lithic tuff. This formation is interpreted to conformably overlie the Patrick Brook Formation near the Restigouche deposit.

Recent reinterpretation of the geology of the Bathurst Mining Camp suggests that the Tetagouche Group occurs as repeated stratigraphic sequences in a series of at east four major thrust sheets (McCutcheon, 1997). Representative stratigraphic columns of these nappes is shown in Figure 2.2. A full description of the geology of each nappe has recently been

presented by McCutcheon et al. (1997).

2.2.3 Fournier Group

This allochthonous group has been subdivided into the Sormany Formation and Millstream formations (McCutcheon, 1997). The Sormany Formation is older and is made up of pillow basalts and gabbroic rocks dominated by MORB (mid-ocean ridge basalt) compositions with lesser transitional basalts (McCutcheon, 1997). These have been interpreted to have formed in a back-arc basin (van Staal et al., 1991) or an ensialic rift, similar to the present day Gulf of California (Paktunc, 1990). The Sormany Formation is conformably overlain by the Millstream Formation which is dominated by lithic and feldspathic wackes and slate and only minor limestone and mafic volcanic rocks. A zone of blueschist facies rocks 70 km in length marks the contact between the Tetagouche and Fournier groups.

2.2.4 Tectonic setting of the Tetagouche Group

Various tectonic models have been proposed for the Tetagouche Group. Early models postulated that the Tetagouche Group formed in an island arc setting (Pajari et al., 1977), although later geochemical data and recognition of the large volume of explosive felsic volcanic rocks within the Tetagouche Group required modification of the models to include the involvement of continental crust. Harley (1977) suggested that the Tetagouche Group formed during extension in continental crust and presented a collapsed cauldron model to account for the lithological association and distribution of sulphide deposits.

However, recent work has resulted in a general consensus that the Tetagouche Group was formed in an ensialic back-arc basin (van Staal, 1987). The mafic-dominated Fournier Group is more consistent with formation in an oceanic back-arc basin (Whitehead and Goodfellow, 1978). A model involving back-arc spreading in a continental convergent margin setting followed by development of an ocean basin through seafloor spreading is consistent with the lithogeochemistry and age-relationships between the Tetagouche and Fournier groups.

Blueschists that occur between the Fournier Group and the Eighteen Mile Formation suggest that the ocean (back-arc) basin closed in the Late Ordovician, due to northwest facing subduction (van Staal, 1987). A Late Ordovician age is consistent with $^{40}Ar/^{39}Ar$ ages on crossite and phengite from the blueschists (447 ± 6 Ma; (van Staal, 1990) and that Fournier Group rocks are unconformably overlain by conglomerates of the Early Silurian Chaleur Group (McCutcheon et al., 1993).

2.3 Massive Sulphide Deposits in the Bathurst Mining Camp

2.3.1 Deposit characteristics and stratigraphic relationships

The Bathurst-Newcastle mining district contains about 100 known base-metal occurrences, and 37 of these have defined tonnages (McCutcheon, 1992; Rose and Johnson, 1990). Most of the discoveries were made prior to 1970, and most of these were made between 1952 and 1960. The first major VMS deposit discovered was the Brunswick #6 deposit, in 1952. That discovery was closely followed by the Brunswick #12, Key Anacon and Nigadoo deposits in 1953, Heath Steele in 1954, the Caribou, Halfmile Lake, and Chester deposits in 1955, and the Wedge, Murray Brook, Stratmat, Captain, Devil's Elbow and Armstrong Brook deposits in 1956.

The Bathurst Camp VMS deposits are spatially associated with Tetagouche Group rocks (Fig. 2.2). The deposits have been subdivided by van Staal et al. (1992) into three groups on the basis of inferred stratigraphic and geological relationships: A) Brunswick type; these deposits are all hosted by Nepisiguit Falls rock and range in age from 471 ± 3 to 469 ± 2 Ma and are associated with the laterally extensive Algoma-type iron formation (Peter and Goodfellow, 1996). Important examples include the Brunswick #12, Brunswick #6, Austin Brook, Flat landing Brook, and Heath Steele deposits. B) Caribou type; these deposits are hosted by thinly bedded to laminated feldspathic wackes and black shales of the Eighteen Mile Formation near the contact with the Spruce Lake Formation. They are interpreted to be slightly younger than type A deposits. In addition to Caribou, examples of this deposit type include the

Nepisiguit A, B, C, Nine Mile Brook, Canoe Landing Lake and Wedge deposits. There are no extensive iron-formations associated with these deposits. C) Halfmile Lake type; these deposits are hosted by epiclastic sandstones, dark shales and felsic volcanics and includes the Halfmile Lake, Chester, Murray Brook, and Key Anacon deposits. There are no major iron-formations associated with these deposits (van Staal et al. 1992; Peter pers. comm. 1996).

However, this subdivision is disputed by others. For example, McCutcheon et al. (1993) subdivided the deposits into four types. These workers placed Halfmile Lake, FAB and the Heath Steele ore bodies in their Group 1, the oldest deposits hosted within Nepisiguit Falls rocks, close to the contact with the Patrick Brook Formation. Their group 2 deposits are essentially the same as Group A of van Staal et al. (1992) except for Heath Steele. Group 3 deposits include Stratmat, Louvicourt, Coulee, Taylor Brook Road and Consolidated Morrison and these deposits are hosted by the Flat Landing Brook Formation. Group 4 of McCutcheon et al. (1993) is the same as Group C of van Staal et al. (1992). Wilson (1993) placed the Halfmile Lake and Heath Steele deposits in the same group as the Brunswick horizon deposits. Recent mapping and lithogeochemical work on the felsic volcanic and intrusive rocks in the camp (Rogers and van Staal, 1995) will likely result in further re-interpretation of the stratigraphic position of the deposits. There is some suggestion that Groups A and C of van Staal et al. (1992) and Groups 1, 2 and 3 of McCutcheon et al. (1993) may all be time equivalents, hosted by different volcano-sedimentary facies (Rogers pers. comm. 1995). Regardless, these classification schemes are likely to be oversimplifications, although all of the major ore deposits are associated with felsic volcanic rocks in the lower parts of the Tetagouche Group (McCutcheon, 1997).

General features of the VMS deposits within the Bathurst Camp include: 1) the massive-sulphide deposits are fine-grained, layered, stratiform lenses that are pyrite-rich, barite-poor, and texturally complex, 2) pyrite, sphalerite, galena, chalcopyrite and pyrrhotite constitute more than 95% of the sulphides present, and arsenopyrite, marcasite, tetrahedrite, and bournonite are only minor constituents, 3) layering results from variations in mineral

abundances, grain sizes, or both and is best developed in zinc-lead-rich portions of the lenses, 4) disseminated mineralization, mainly pyrite, underlies most of the lenses but is generally absent in hanging-wall rocks, 5) many of the stratiform sulphide deposits are overlain by, or have laterally equivalent oxide (± carbonate and silicate) iron-formation, and 6) some of the stratiform deposits are underlain by discordant stockwork zones containing pyrrhotite, pyrite and chalcopyrite (McAllister, 1960).

2.3.2 Genesis of VMS deposits in the Bathurst Camp

The consensus view at the present time is that the VMS deposits in the Bathurst Camp are syngenetic (McAllister, 1960; Stanton, 1959; Stanton, 1960), although de Roo et al. (1991) and Dechow (1960) have suggested that the Heath Steele Deposit is epigenetic. In addition, it is generally accepted that the massive sulphides were deposited at or near the seafloor either from a bottom-hugging brine similar to the Atlantis II deep in the Red Sea Rift (Scholten et al., 1991; Zierenberg and Shanks, 1988), or by precipitation from a buoyant plume, similar to hydrothermal venting processes at modern mid-ocean ridges and back-arc basins (Baker et al., 1994; Feely et al., 1994; Fouquet et al., 1991a; Fouquet et al., 1991b). Fluid inclusion evidence suggests that hydrothermal fluids which formed the BMC massive sulphide deposits were most likely buoyant (J.M. Peter, pers. comm.), contrary to McCutcheon et al. (1993) who suggested a brine-pool model.

Goodfellow and Peter (Goodfellow and Peter, 1996) favour a model whereby hydrothermal venting of Cl-complexed metals occurred into H_2S-rich anoxic bottom waters. The H_2S was produced by bacterial reduction of seawater SO_4^{2-} under closed to partially closed conditions. Closed conditions permits the Raleigh fractionation necessary to generate the range and heavy S-isotopic values of Bathurst Camp sulphide minerals.

2.4 Halfmile Lake Massive Sulphide Deposit

The Halfmile Lake Pb-Zn deposit is one of the primary deposits studied in this

hydrogeochemical program. It is a moderately large, as yet undeveloped, massive sulphide deposit of approximately 26 million tonnes of iron and base metal sulphides; approximately 8-10 million tons is ore grade, dominantly Zn-Pb. Late in 1995, the decision was made by Noranda Exploration to put on hold plans to develop the Halfmile Lake deposit.

The deposit is generally subdivided into three sub-zones; the Upper AB zone, the Lower AB zone (which both constitute the Halfmile Lake South deposit), and the Halfmile Lake North zone (Fig. 2.3). The Lower AB is the largest in terms of tonnage with 7,782,000 tonnes grading 10.50% Zn, 3.66% Pb, 0.09% Cu, and 44 g/t Ag. The ore body crops out at the Upper AB zone, which is estimated to contain 866,000 tonnes grading 8.94% Zn, 3.23% Pb, 0.46% Cu, and 53 g/t Ag. The Halfmile Lake North zone is slightly larger at 1,150,000 tonnes but only grades 4.6% Zn, 0.88% Pb, 0.47% Cu, and 8 g/t Ag (Adair, 1992).

2.4.1 Geology

The regional geology has been most recently mapped by Wilson (1993). The detailed geology of the Halfmile Lake deposit was mapped initially by Harley (1977; Harley, 1979) and more recently by Adair (Adair, 1992). The rocks in the study area occur primarily within the Tetagouche Group (Adair, 1992; Wilson, 1993) (Figs. 2.3, 2.4). There is some disagreement as to whether Patrick Brook rocks occur in the Halfmile Lake area. Wilson (1993) included rocks west and south of Little Bald Mountain in the Patrick Brook Formation based on the dark grey to black colour of the quartzites and quartz wackes. These rocks were considered to be Miramichi Group rocks by De Roo et al. (1991) and van Staal et al. (1992). Metasedimentary rocks near Halfmile Lake were assigned to the Patrick Brook Formation by De Roo et al. (1991), based on dark colours. However, Wilson (1993) contends that these rocks are green in colour and therefore should be assigned to the Nepisiguit Falls Formation.

Quartz-feldspar porphyry rocks include feldspar and quartz-phyric felsic domes and subvolcanic intrusions. Contacts with surrounding rocks have been observed to be discordant and chill margins have also been observed (Adair, 1992). Combined with the occurrence of

host-rock xenoliths, contact relations support the interpretation of these rocks as intrusive. Harley (1977) interpreted these rocks as porphyritic felsic tuffs. In the QFP, phenocryst content varies from 5 - 50% by volume and phenocrysts consist of variable proportions of quartz, albite and K-feldspar (Harley, 1977). The matrix is composed of quartz, feldspar, chlorite and sericite.

Felsic volcanic rocks were interpreted by Adair (1992) to be primarily pyroclastic in origin based on bedding, compositional layering and presence of felsic fragments. The pyroclastic units range from crystal-rich to crystal-poor pyroclastic rocks and are typically medium to thinly bedded. Felsic lava-flows are the least common and are typically massive and homogeneous (Adair, 1992).

Sedimentary rocks occur interbedded with volcanic rocks and are typically fine-grained and volumetrically minor compared to felsic volcanic and intrusive rocks although the proportion of sedimentary rocks increases to the southwest (Adair, 1992) (Fig. 2.3). These rocks consist of mudstones, siltstones and lesser wackes and very minor coarse-grained sandstone. The sediments are largely volcaniclastic with well-developed bedding in some units, and graded bedding is locally evident.

The sulphides occur as seafloor massive sulphides (2 - 4 m thick on average but up to 75 m thick) with a well-developed stringer or stockwork zone (3 - 150 m in thickness) (Adair, 1992). Stockwork sulphides are composed dominantly of pyrrhotite and chalcopyrite veins and impregnations with associated quartz and lesser carbonate. The stringer zone is best developed in fine-grained mudstones and siltstones in the stratigraphic footwall and is overlain by breccia-matrix sulphides. The boundary with the stratigraphically overlying massive sulphides is marked by a sharp increase in sulphides. The seafloor massive sulphides are composed of breccia-matrix sulphides and layered sulphides with interbedded black argillite and chert (Adair, 1992). There is no oxide or carbonate iron formation at Halfmile Lake. The dominant sulphide minerals are pyrrhotite, chalcopyrite, pyrite, sphalerite, and galena in the breccia-matrix sulphides, and pyrite, pyrrhotite, sphalerite and galena in the layered sulphides. Pyrite-

pyrrhotite layers are interbedded on a scale of 0.3 mm to 1 cm with sphalerite-galena layers (Adair 1992).

2.4.2 Structure, metamorphism and lithogeochemistry

The Halfmile Lake deposit is structurally complex. The deposit shows evidence of at least three phases of deformation (Adair, 1992) and perhaps as many as five (De Roo and van Staal, 1991). The stratigraphy is overturned and steeply dipping to the north and northwest.

Drill core, geophysical, satellite and surface geological data suggests that there were two major episodes of faulting (Adair, 1992). Dip-slip faults are relatively easy to correlate between drill holes and are subparallel to or at low angles to S_1/S_0 (penetrative foliation and bedding). These faults have been interpreted to be axial planar to F_1 (Adair, 1992). The F_1 folds are large scale, with amplitudes in the kilometers range and are manifested by an overturned anticlinal axis to the north and an overturned synclinal axis to the south. F_2 (second generation) folds are much smaller scale (2 cm to 2 m), observable in drill core and outcrop as open to tight isoclinal folds (Adair, 1992). A broad open fold which plunges steeply to the north and alters the strike of the stratigraphy from E-W to NE-SW marks F_3. A second set of major faults post-dates F_3 and cuts the deposit from NW to SE.

The rocks of the Halfmile Lake deposit have been metamorphosed to lower greenschist facies (Adair, 1992). The main silicate minerals associated with metamorphism are chlorite and, more proximal to sulphides, development of pervasive muscovite. Carbonate alteration occurs mainly in the stratigraphic hanging wall (structural footwall) and locally in the stratigraphic footwall at Halfmile Lake North (Adair, 1992). Visual examination of core from drill holes that were sampled using the packer system indicates, however, that the volume percentage of carbonate at Halfmile Lake is less than at Restigouche.

The felsic volcanic rocks at Halfmile Lake generally classify as subalkaline dacites and rhyolites, although some samples of Adair (1992) are classified as alkaline on Nb/Y discrimination diagrams.

2.4.3 Depositional setting of the massive sulphides

Harley (1977) interpreted the depositional setting of the deposit to be a sea-floor sedimentary basin. The massive sulphides were interpreted to have been deposited in deeper water in the more distal portions of the basin (Harley, 1977). Adair (1992) suggested a similar depositional setting, although he suggested that the QFP units were the heat source for the hydrothermal system, whereas, Harley (1977) preferred a model where the heat source was derived by rapid burial and over-pressuring of felsic pyroclastic units emplaced as hot density flows. Adair (1992) considered the black argillite and chert which overly the massive sulphides to represent an exhalative unit equivalent to chlorite iron-formation elsewhere in the camp.

2.4.4 Surficial geology

The Halfmile Lake deposit is generally covered by a thin layer of till, typically < 2 m in thickness (Parkhill and Doiron, 1995). Glacial transport across the deposit is generally eastward, based on striations and pebble and boulder lithology mapping (Parkhill and Doiron, 1995). Regional striations trend between 80 and 100° and those found on Halfmile Lake vary from 81 to 93°. Although boulder erratics derived from the Mount Elizabeth complex 25-30 km to the west have been recovered in the area, glacial dispersion is typically short (< 2 km) with > 90% of pebbles in basal till representing local bedrock (Parkhill and Doiron, 1995).

2.5 Restigouche Massive Sulphide Deposit

The Restigouche massive sulphide deposit is the second deposit studied as part of the EXTECH-II hydrogeochemical program. The deposit is 5 km west of the Murray Brook property, some 75 km west of Bathurst (Fig. 2.1). The property was purchased from Marshall Minerals by East-West Caribou Mining in 1995. Over the 1996-1997 winter, open-pit operations were initiated at the Restigouche Deposit, and as of November 1997, open pit mining activities were underway. The open pitting of this deposit followed the hydrogeochemical study of the deposit.

2.5.1 Geology

The area of the Restigouche deposit has been mapped previously (Skinner, 1956; Clark, 1957; Boyle, 1969; Helmstaedt, 1970; Michener and Booth, 1972; Davidson, 1976; Rankin, 1982) and more recently by Gower (1996). The base of the sequence consists of Miramichi Group rocks which are dominantly metasedimentary rocks of the Chain of Rocks, Knights Brook, and Patrick Brook formations exposed in the southern and south-eastern portion of the study area (Figs. 2.5, 2.6) (Gower, 1996). These rocks are overlain by felsic volcanic rocks of the Nepisiguit Falls and Mount Brittain formations which are in turn overlain by mafic volcanic and sedimentary rocks of the Eighteen Mile Formation. The Tetagouche Group rocks hosting the Restigouche Deposit are in fault contact to the north with Late Ordovician - Early Silurian mafic volcanic rocks, and to the west with Late Silurian to Early Devonian conglomerate, sandstone, and intercalated volcanics (Simpsons Field, Bryant Point, Benjamin, and Greys Gulch formations) (Gower, 1996).

The Restigouche Deposit is hosted by a package of felsic volcanic rocks now referred to as the Mount Brittain volcanic suite (Gower, 1996; McCutcheon, 1997). Barrie (1982) recognized that two major felsic units occurred in the area of the Restigouche Deposit, a southern felsic unit which hosts the Restigouche deposit and a northern unit which hosts the C4 and C5 mineralized zones. Mapping by Gower (1996) indicates that these units are the same, repeated due to thrust faulting. The Mount Brittain volcanic suite consists of grey to greenish grey feldspar lithic tuffs. The contact between the Mount Brittain volcanic suite and the Patrick Brook Formation is conformable in this area (Gower, 1996).

Three major sedimentary units cross the Restigouche property (south to north): 1) sandstones, argillites, and local pockets of graphitic argillite, 2) siltstones, graphitic and mafic tuff, and 3) ferruginous and graphitic argillites. The general stratigraphy for the Restigouche deposit is as follows: banded argillite to siltstone in sharp contact and intercalated with feldspar crystal and lapilli tuff, grading upwards to coarse pyroclastic lithic tuff, lithic lapilli and fragmental units intercalated with massive and disseminated sulfides (Barrie, 1982). The

massive pyritic sulfides are in sharp contact with overlying massive rhyolite tuff grading upwards to lapilli and lithic tuffs and crystal tuff. The ore zone crops out on the south side of Charlotte Brook in a small gossan pit.

The Restigouche deposit is a volcanogenic Pb-Zn-Ag-(Cu-Au) massive sulphide deposit, is elongate and composed of a series of four vertically contiguous lenses up to 40 m thick and two satellite lenses in the hanging wall (Burns and Westoll, 1989). The major sulphide minerals are pyrite, marcasite, galena, sphalerite, and minor chalcopyrite; accessory minerals are enargite, tennantite and cassiterite. There is a stringer zone, indicating that the massive sulphides are not displaced from the feeder system. The deposit is cut by a northeast trending mafic dyke swarm that in places appears to infill fault zones. Quartz and carbonate veins are common in both the footwall and hanging wall units.

Drilling by Marshall Minerals, especially Hole MM-88-02 (extension) found a stringer zone, despite the 1982 report suggesting that the deposit was not situated over a seafloor vent. For example, in MM-88-02, massive sulphides were recovered from 66.6 m to 78.85 m and stringer zone mineralization occurred from 183.6 m to 259 5 m which contained 2-10% sulphides.

There are several minor occurrences in the area of the Restigouche deposit. The C4 and C5 occurrences are situated on top of a hill about 1 km to the northwest of the main Restigouche deposit. Based on similar stratigraphy, these small Cu-rich zones have been interpreted to represent thrust repetition of the Restigouche mineralized horizon (Gower, 1996). Because of their elevation, any gossan developed on these deposits has been removed during glaciation (Parkhill, 1997).

2.5.2 Structure

On a regional scale the deposit lies on the northern limb of an overturned F_1 (where F_x refers to the generation of fold structures) anticline and on the western limb of an open F_3 anticline. Lithologies strike ENE-WSW and dip northerly at about 45°. Minor F_2 kink folds are

not apparent. The long axis of the deposit, which is subparallel to both the dip direction and the F_3 fold axis, strikes at about 325°. On cross-sections the deposit is seen to have an apparent dip to the west of up to 30°. To the west of the deposit a steeper dip of about 45-50° is indicated by the attitudes of the contact between the hanging wall sequence and footwall stringer zone, and of the hanging wall sulphide lenses (Westoll, 1990).

2.5.3 Surficial geology

Based on exploration soil geochemical surveys, there is a strong copper anomaly associated with the C5 zone, but only a minor anomaly over the Restigouche deposit where it outcrops. The copper anomaly associated with the C5 zone extends to the northwest and southeast and is interpreted to be due to fluid migration of copper along a fault or fracture (Westoll, 1990). Zinc in soils is apparently not effective at delineating the Restigouche deposit, although there is a significant downstream dispersion (see Chapter Thirteen). Hanging wall felsic units are much lower in disseminated sulphide contents compared to the felsic units hosting the massive sulphides, and this is reflected in the soil geochemistry. Soil cover is thin, typically < 1 m in thickness and is composed primarily of a thin 0.25 m veneer of sand and humus overlying sand and gravel.

2.6 Other VMS Deposits in the Bathurst Mining Camp Utilized in this Study

2.6.1 Wedge Deposit

Two samples were collected from the Wedge Deposit in 1995; one sample from a seep in a sulphide-rich debris pile and the other from an artesian borehole.

The Wedge Deposit was discovered in 1957 based on an EM survey carried out over a gossan on the property (McCutcheon, 1997; Walker and McCutcheon, 1996). A shaft was sunk in 1959 and the deposit went into production between 1962 and 1968, during which time 1.5035 Mt of ore (0.65% Pb, 1.61% Zn, 2.88% Cu, and 20.6 g/t Ag) was extracted (McCutcheon, 1997; Walker and McCutcheon, 1996). The Wedge deposit differs from the

Halfmile Lake and Restigouche deposits in that it has an extensive copper zone with a minor Pb-Zn zone (Walker and McCutcheon, 1996). The deposit area is bounded to the south by the Nepisiguit River and to the north and east by Forty Mile Brook . A diamond drill hole, sunk in the 1950's is presently artesian and has flowed since it was emplaced. This hole has consistently produced Fe-rich waters for many years (Belland, 1991). As a consequence, the drill collar is no longer visible having been buried in thick accumulations of Fe-oxyhydroxides. The southern face of the deposit is characterized by Fe-stained debris, sulphide boulders and a debris pile adjacent to the Nepisiguit River.

The Wedge deposit is hosted by volcanic rocks of the Nepisiguit Falls Formation (Fig. 2.7). The lower part of the Nepisiguit Falls Formation in this area is conformable and locally intercalated with the older Spruce Lake Formation (McCutcheon, 1997; Walker and McCutcheon, 1996). Both formations are thrusted over younger sediments and minor volcanic rocks of the Brunswick Mines Formation (Walker and McCutcheon, 1996).

2.6.2 Willet Deposit

This deposit (Fig. 2.8) was chosen as a minor follow-up site because of its recent discovery and therefore the good access and recent drill holes. This deposit differs from the Halfmile Lake and Restigouche deposits in that it occurs in flat to gently rolling hills. Groundwater seeping from the outcrop of the ore zone were sampled in 1995, and additional groundwater samples were collected with a pressure-bailer system in 1996.

Initial discovery of the deposit was made in 1975 on the basis of high-grade massive sulphide boulders, although confirmation was not made until 1994 based on trenching and drilling (Parkhill and Doiron, 1995). The geology around the deposit was mapped by van Staal (1994; Fig. 2.8). However, reinterpretation of the geology indicates that the deposit is hosted by Nepisiguit Falls sedimentary units (Rogers, pers. comm).

2.6.3 Stratmat Main Zone Deposit

The Stratmat Main Zone deposit was sampled using the packer system during the summer of 1996. This site was chosen to explain the large self potential anomalies in borehole S61-19 in the vicinity of the massive sulphides (81-89 m depth).

The geology of the deposit has been described by Hamilton (Hamilton, 1992). The Stratmat Main Zone was discovered between 1954 and 1956 by follow-up drilling of EM and soil geochemical anomalies. The massive and disseminated sulphides are hosted by argillaceous to cherty sedimentary rocks and dacitic volcanic tuffs and cross-cut by gabbroic units (Deveaux et al., 1988) (Fig. 2.9). The deposit has variable dip (45 to 70°) to the southeast, plunges to the east and massive sulphides display distinct metal zonation with a copper zone and a lead-zinc zone (Deveaux et al., 1988). The Stratmat Main Zone deposit had reserves (as of 1988) of approximately 835,000 tonnes as a grade of 2.68% Pb, 6.39% Zn, 0.28% Cu and 69.48 g/tonne Ag. The copper zone has 175,000 tonnes at 2.79% Cu, with minor Pb, Zn and Ag (Deveaux et al., 1988).

2.6.4 Heath Steele Deposit

Groundwaters were sampled from various depths in the B and C zones of the Heath Steele deposit in 1995 in order to provide information on the composition of groundwaters flowing into an active mine in the Bathurst Camp, and to characterize changes in groundwater chemistry with depth in this deposit.

The Heath Steele deposit was discovered in 1953 during an airborne electromagnetic survey (Hamilton and Wilson, 1997). Diamond drilling in 1954 resulted in the delineation of the A, B, C, D, and E zones. The deposit was put into operation between 1957 and 58, and 1962 and 1983. During the shut-down, stockpiled gossan was processed to recover the gold and silver. In 1989, Heath Steele was reopened, and apart from a brief period of closure in 1993-94, is still in production (Hamilton and Wilson, 1997). The different ore zones at Heath Steele are all hosted by volcaniclastic and felsic pyroclastic rocks of the Nepisiguit Falls Formation. Footwall units are mainly siltstones and quartz wackes and the hanging wall units consist of

quartz-feldspar porphyry that is overlain by rhyolites of the Flat Landing Brook Formation (Hamilton, 1992; Hamilton and Wilson, 1997). The deposit generally strikes east-west and dips steeply to the north.

The principle massive sulphides minerals are pyrite, pyrrhotite, sphalerite, galena, chalcopyrite, arsenopyrite, tetrahedrite and sulfosalts.

2.6.5 Brunswick #12

Groundwater flow is very restricted in the Brunswick #12 mine. Only a couple of groundwater samples were able to collected from the 1000 m-level, along an exploration drift away from the main ore zone and mining activity. One of the waters is the most saline water collected to date in the BMC. Although the exploration drift and the holes drilled were all but dry by 1995, drilling water flow was greater during earlier times and thick salt pans formed over puddles along the exploration drift (Corbett pers. comm. 1996).

The Brunswick #12 deposit has been the focus of considerable research since its discovery in 1953 (e.g. Goodfellow, 1975; Goodfellow and Peter, 1996; LeBlanc, 1989; Lentz and Goodfellow, 1992a; Lentz and Goodfellow, 1993a; Lentz and Goodfellow, 1993b; Lentz and Goodfellow, 1996; Luff et al., 1992; Smith, 1985; van Staal and Luff, 1990; van Staal and Williams, 1986). Mining operations began in 1964 and continues to the present with as little as 10 years of production left. Between 1964 and 1996, production totalled 82,277,000 t of ore grading 8.82% Zn, 3.51% Pb, 0.33% Cu, and 99.0 g/t Ag (Luff et al., 1992; Luff et al., 1997). The deposit is hosted in the upper parts of the Nepisiguit Falls Formation and consists of massive pyrite with minor sphalerite and galena and banded pyrite-sphalerite-galena with lesser amounts of chalcopyrite and pyrrhotite (Luff et al., 1992; Luff et al., 1997).

2.7 Geochemistry of Halfmile Lake and Restigouche Deposit Lithologies

In order to better understand water-rock reactions at the Halfmile Lake and Restigouche deposits, a limited number of samples of the host lithologies were analyzed (Table 2.1). At the

Restigouche deposit, samples were selected of unaltered to highly altered felsic volcanic rocks and massive sulphide intersected in holes through the orebody that were sampled for groundwater. At the Halfmile Lake deposit, samples of representative altered and unaltered lithologies were selected from borehole HN94-65 (Table 2.1). A large database of whole rock geochemistry exists (Adair, unpublished data).

A full description of the geochemistry and petrology of the host rocks is outside the scope of this thesis. Excellent discussions of the geochemistry of the felsic and mafic host rocks are given by Lentz (1996), Rogers and van Staal (1995) and Rogers et al. (in press). Least altered felsic rocks from both deposits were averaged to provide a normalizing value for waters and sediments in subsequent chapters. Most of the rocks analyzed in this study have very flat patterns, normalized to average unaltered felsic rocks, with the exception of mafic rocks, massive sulphides, and rocks with extensive carbonate alteration (Figs. 2.10, 2.11). The lithologies at both deposits show a bimodal distribution between dacitic to rhyolitic units and mafic tholeiitic dykes and flows (Fig. 2.12). The felsic rocks at the Halfmile Lake deposit are from the Flat Landing Brook and Nepisiguit Falls formations, and fall within compositional fields for these formations (Fig. 2.12). The Restigouche deposit felsic volcanic rocks have been assigned to the Mount Brittain Formation (Gower, 1996), and those analyzed in this study plot within the Nepisiguit Falls and extend into the Spruce Lake formation fields (Fig. 2.12). Mafic dykes at the Restigouche deposit are early Silurian (Lentz, pers. comm. 1998).

The massive sulphides are characterized by the elevated contents of Zn, Pb, Cu, Ag, Cd, In, Mo, Sn, and Tl compared to unaltered host lithologies (Table 2.1). Cobalt and Ni are not characteristic of either the Halfmile Lake or Restigouche deposit. Mafic volcanic rocks typically have higher Co and Ni than massive sulphides (Table 2.1).

Table 2.1 Whole rock major and trace element geochemical data for Halfmile Lake and Restigouche deposit host lithologies

Sample#	ML95-320-1 *	ML95-321-1	ML95-322-1 *	ML95-323-1	ML95-324-1	ML95-325-1 *	ML95-326-1	ML95-326-1I	ML95-328-1 *	ML95-329-1 *
Hole	HN94-65	HN94-65	HN94-65	HN94-65	HN94-65	HN94-65	HN94-65	HN94-65	HN94-65	HN94-65
Deposit	HMLK	HMLK	HMLK	HMLK	HMLK	HMLK	HMLK	HMLK	HMLK	HMLK
SiO_2	69.70	75.10	73.90	47.70	51.40	67.00	73.80	67.40	59.40	67.90
TiO_2	0.38	0.26	0.26	0.83	1.10	0.29	0.25	0.24	1.23	0.59
Al_2O_3	16.20	13.20	12.40	14.40	15.00	11.70	11.90	10.40	14.40	15.80
$Fe_2O_3^T$	2.70	1.60	2.20	11.00	9.70	7.00	3.00	8.70	10.30	2.60
Fe_2O_3	1.80	1.10		0.90	0.50	0.60	0.30	1.00	1.20	0.80
FeO	0.80	0.50		9.10	8.30	5.80	2.50	6.90	8.20	1.60
MnO	0.01	0.01	0.01	0.23	0.17	0.08	0.02	0.12	0.07	0.01
MgO	1.20	0.84	1.27	14.22	12.14	5.52	1.82	6.66	5.57	2.28
CaO	0.12	0.15	0.29	1.75	0.22	0.23	0.13	0.59	0.47	0.19
Na_2O	2.20	2.90	0.10	0.00	1.60	0.10	1.00	0.00	0.10	0.10
K_2O	5.48	4.04	5.76	2.25	2.75	3.78	5.26	2.17	3.56	5.93
H_2O^T	2.50	1.40	2.00	7.30	5.70	3.60	1.80	4.10	5.20	3.10
CO_2^T	0.10	0.10	0.20	1.40	0.20	0.10	0.10	0.40	0.10	0.10
P_2O_5	0.10	0.11	0.13	0.07	0.08	0.12	0.10	0.12	0.30	0.19
S^T	0.02	0.01	0.89	0.02	0.12	0.66	0.05	0.02	0.02	0.02
LOI										
Total	100.60	99.70	99.60	100.20	99.30	99.50	99.10	100.10	99.80	98.60
F	471	425	827	1988	2041	917	639	996	1017	896
Cl			173	128	151	151			184	
S	645	85		269	1044	5254	521	304	139	86
Ag	0.2	0.7	0.4	1	0.7	0.4	0.2	0.1	0.7	0.2
Ba	1000	900	1100	380	360	830	1200	290	850	840
Be	2.7	2	2.1	2.3	1.6	2.6	1.4	1.5	1.6	2.8
Bi				0.9	0.5	0.6				
Cd					1.2					
Co				37	41	16	5	16	23	6
Cr	12	11	11	290	370	14		12	24	26
Cs	1.1	0.7	9.1	3.1	4.8	2.7	1.6	2.4	5.3	6.9
Cu	19			19	12	80				
Ga	23	16	16	24	22	22	15	21	19	24
Hf	6.5	4.8	4.4	1.4	1.7	4.9	4.4	4.3	4.6	5.8
In	0.07	0.1		0.06				0.06	0.08	0.05
Mo	0.4	0.2	3.7	1.1	0.4	2.6	1.4	1.1	0.3	1.1
Nb	14	11	11	4.8	6.7	8.6	9.8	9.8	11	15
Ni				58	65					13
Pb	38	14	14	49	350	19	8	13	4	3
Rb	190	130	190	66	100	120	140	85	99	210
Sc	5.7	4.5	4.7	27	33	5.4	4.1	5	25	7.1
Sn	6.9	42	4.8	2.3	0.7	8.7	2.1	3.3	35	7.8
Sr	41	42	35	15	20	19	32	12	63	31
Ta	0.8	0.7	0.6	0.3		0.6	0.7	0.5	0.6	0.7
Th	22	16	16	0.4	0.38	16	15	15	7.7	15
Tl	0.68	0.48	1.2	0.37	0.59	0.57	0.56	0.35	0.53	0.7
U	5.9	3.9	6.3	0.34	0.33	4.6	4.4	4.2	2.5	5.1
V	16	18	15	190	210	20	11	28	220	38
Y	54	39	41	24	25	29	34	33	32	43
Zn	120	17	29	86	520	48	22	45	45	20
Zr	250	170	160	56	71	180	160	170	170	210

HMLK, Halfmile Lake deposit; RSTG, Retsigouche deposit

* Samples used to calculate average unaltered felsic composition for each deposit

Major elements in weight %, trace elements in ppm

Sample#	ML95-330-1	ML95-331-1	ML95-332-1 *	ML95-333-1	ML95-334-1	ML95-335-1	ML95-336-1	ML95-338-1 *	ML95-339-1 *	ML95-341-1 *
Hole	HN94-65	HN94-65	HN94-65	HN94-65	HN94-65	HN94-65	HN94-65	HN94-65	HN94-65	HN94-65
Deposit	HMLK	HMLK	HMLK	HMLK	HMLK	HMLK	HMLK	HMLK	HMLK	HMLK
SiO_2	80.80	62.50	72.90	69.30	52.10	50.80	50.20	74.70	62.30	73.40
TiO_2	0.12	1.20	0.52	0.50	1.18	1.91	1.16	0.28	0.73	0.29
Al_2O_3	9.00	14.40	11.40	15.10	17.30	15.90	16.50	11.40	12.80	13.50
$Fe_2O_3^T$	2.20	7.60	3.90	2.70	12.80	13.30	9.00	3.90	11.60	2.30
Fe_2O_3	0.00	1.00	0.80	0.60	1.00	1.40	0.60	0.70		0.30
FeO	2.00	6.00	2.80	1.90	10.60	10.70	7.60	2.90		1.80
MnO	0.01	0.09	0.03	0.02	0.15	0.17	0.16	0.04	0.03	0.01
MgO	1.43	3.92	2.87	1.18	7.86	6.15	7.54	3.54	2.24	1.13
CaO	0.02	1.37	0.30	0.34	0.63	2.49	3.37	0.13	0.17	0.57
Na_2O	0.00	2.20	0.10	2.70	0.00	1.40	3.90	0.00	0.08	2.10
K_2O	4.61	3.36	4.57	5.43	1.97	2.40	0.96	3.25	3.59	4.34
H_2O^T	1.60	3.30	2.50	1.70	6.90	5.00	4.40	3.00		1.80
CO_2^T	0.10	0.90	0.20	0.20	0.50	1.80	2.50	0.10	0.10	0.40
P_2O_5	0.06	0.33	0.15	0.14	0.15	0.25	0.13	0.14	0.07	0.13
S^T	0.01	0.00	0.01	0.02	0.03	0.02	0.02	0.02	5.93	0.03
LOI									6.40	
Total	99.80	100.40	99.10	99.10	100.40	100.30	99.00	100.20	99.80	99.80
F	396	881	960	343	1089	568	1032	1043	436	847
Cl	104	111	144							140
S	129	116	59	170	228	316	238	190		253
Ag	0.1	0.6	0.3	0.3	0.8	0.5	0.3	0.5	0.2	0.2
Ba	1200	840	800	1100	380	740	210	490	380	530
Be	1.2	1.4	1.6	2.4	2	1.6	1	1.8	2.4	2.3
Bi					2.3		0.7		0.6	
Cd					0.3		0.6			
Co		16	7	5	35	41	28		23	
Cr			11		200	110	200	13	59	
Cs	2.3	1.5	4.6	1.9	4	1.3	0.8	2.1	6.7	2.2
Cu							30		50	
Ga	8.1	20	18	21	20	19	17	15	18	17
Hf	2.1	5.5	7.1	10	4.4	4.7	3.7	5.3	6.7	5.2
In		0.05		0.05	0.22	0.06	0.1		0.06	
Mo	1.3	1.2	1.4	2.5	0.9	0.5	0.5	0.7	0.8	0.4
Nb	4.3	13	15	20	8.1	15	7.8	8.9	17	11
Ni					27	45	26		50	
Pb	48	10	10	6	99	10	10	6	34	8
Rb	140	89	160	160	68	68	29	140	0	150
Sc	1.9	25	9.1	9.1	37	32	36	4.2	12	4.9
Sn	1.6	3.4	3.2	6.7	5.3	2.2	1.1	3.5	3.1	4.3
Sr	16	55	20	64	32	90	95	9	24	31
Ta	0.4	0.6	0.7	1.1	0.4	0.7	0.4	0.6	0.6	0.7
Th	5.8	9.7	15	28	3.6	6.3	3.3	12	13	17
Tl	0.57	0.43	0.62	0.68	0.31	0.32	0.14	0.54	0.62	0.49
U	1.8	2.6	3.7	7.2	1	1.7	0.87	4	3.2	5
V	8	200	48	40	260	300	250	25	98	20
Y	12	43	39	62	30	44	25	32	52	44
Zn	19	13	27	5	170	77	170	21	65	16
Zr	72	210	280	400	150	190	140	190	230	190

Sample#	ML95-342-1 *	ML95-343-1	ML95-344-1	ML95-345-1	ML95-346-1	ML95-347-1	ML95-348-1	ML95-349-1	ML95-358-1	ML95-235 *
Hole	HN94-65	HN94-65	HN94-65	HN94-65	HN94-65	HN94-65	HN94-65	HN94-65	HN94-65	MM-88-02
Deposit	HMLK	HMLK	HMLK	HMLK	HMLK	HMLK	HMLK	HMLK	HMLK	RSTG
SiO_2	71.20	74.30	68.00	39.50	80.10	73.50	23.60	10.00	10.50	69.40
TiO_2	0.29	0.24	0.63	1.46	0.21	0.30	0.23	0.13	0.62	0.30
Al_2O_3	13.00	11.10	15.80	11.40	10.30	13.60	11.60	3.06	9.32	16.20
$Fe_2O_3^T$	2.90	2.80	4.00	11.50	1.50	2.00	27.70	37.20	62.00	2.50
Fe_2O_3	0.20	0.30	0.00	0.50	0.00	0.00				1.50
FeO	2.40	2.20	3.60	9.90	1.40	2.10				0.90
MnO	0.05	0.07	0.06	0.24	0.03	0.03	0.37	0.11	0.08	0.02
MgO	1.57	1.50	3.63	5.88	1.00	1.22	14.20	2.72	2.73	1.24
CaO	1.10	2.08	0.18	14.54	0.64	0.12	2.76	1.41	0.11	0.00
Na_2O	2.40	4.00	0.00	2.00	0.30	1.80	0.05	0.03	0.05	0.80
K_2O	5.00	0.98	4.22	0.08	3.38	4.38			1.01	4.47
H_2O^T	1.60	1.40	3.50	4.00	1.60	1.80				3.90
CO_2^T	0.90	1.60	0.10	10.30	0.50	0.10	3.70	1.20	0.20	0.10
P_2O_5	0.13	0.09	0.18	0.15	0.15	0.12	0.06	0.04	0.03	0.10
S^T	0.02	0.01	0.49	0.25	0.28	0.50	13.30	34.90	26.50	0.02
LOI							14.20	21.10	11.20	
Total	99.90	99.80	100.40	100.20	99.90	99.60	98.90	106.80	113.70	98.90
F	429	432	965	926	734	798	2036	147	510	871
Cl	138		138	172	123	262				185
S	194	88	4234	1881	2646	4578				274
Ag	0.2	0.9	0.4	0.4	0.5	0.3	8.2	86	1	1.2
Ba	1400	270	490	23	550	790	20		120	430
Be	1.2	1.1	2	0.9	1.6	2.5	0.5			2.8
Bi	0.5	0.9	1.2				1.3	1.9	12	
Cd							19	190	0.3	
Co			9	37			5		21	
Cr	12		30	130		10	28	19	58	14
Cs	1.9	0.71	3.2	0.33	1.6	2.5	0.29	0.08	0.58	5.9
Cu			45	39	18		790	84	4500	51
Ga	13	11	21	16	12	19	19	5.3	12	24
Hf	5.4	3.6	7.3	3.1	3.2	5.9	3.3	1.2	4.8	9.6
In	0.06		0.07	0.08	0.07		3.6	22	0.55	0.1
Mo	0.7	0.2	1.2	0.8	0.4	1.3	2	12	1.7	
Nb	12	11	17	7.5	6.7	12	5.3	2.7	13	19
Ni			15	32			28		18	
Pb	13	62	32	8	29	21	2000	60000	170	1400
Rb	99	31	160	3.2	170	170	1.8	0.48	36	220
Sc	4.6	3.6	8.9	36	2.9	5.2	6.9	2.7	9	13
Sn	4.7	9.8	7.2	1.7	3.3	6.9	61	340	40	9.9
Sr	54	90	14	280	17	18	32			4
Ta	0.6	0.9	0.8	0.4	0.4	1.1	0.6	0.2	2.7	0.7
Th	18	13	18	1.2	8.4	19	4.6	2.4	9.9	26
Tl	0.52	0.15	0.69	0.05	1	1	0.55	4	0.6	4.5
U	5.2	4.1	5.2	0.37	3.4	5.7	1.5	4.5	2.2	5.6
V	11	15	62	300	16	24	65	22	59	15
Y	49	49	56	32	17	39	14	6.2	25	54
Zn	22	26	57	59	66	22	10000	99000	490	160
Zr	190	150	270	120	120	210	110	48	160	330

Sample#	ML95-237 *	ML95-240	ML95-241	ML95-250	ML95-253	ML95-255	ML95-256	ML95-258	ML95-259	ML95-260 *
Hole	MM-88-02	MM-88-02	MM-88-02	MM-88-02	MM-88-02	MM-88-02	MM-88-02	MM-88-02	MM-88-02	MM-88-02
Deposit	RSTG	RSTG	RSTG	RSTG	RSTG	RSTG	RSTG	RSTG	RSTG	RSTG
SiO_2	65.10	27.20	66.90	12.90	46.60	23.30	71.00	64.50	64.90	68.70
TiO_2	0.68	1.87	0.62	0.05	1.77	0.04	0.42	0.09	0.64	0.49
Al_2O_3	16.50	15.20	14.40	3.71	13.30	1.61	11.90	12.30	9.70	14.50
$Fe_2O_3^T$	4.70	14.50	3.80	36.10	11.30	45.10	4.90	3.00	12.60	7.00
Fe_2O_3	1.00	2.70	1.30		2.60		0.00	0.00	0.60	0.40
FeO	3.30	10.60	2.20		7.90		4.90	3.00	10.80	5.90
MnO	0.01	0.76	0.08	0.62	0.15	0.15	0.09	0.14	0.18	0.07
MgO	1.85	5.69	2.12	3.54	5.47	2.47	1.84	2.11	4.27	2.93
CaO	0.19	12.45	1.26	0.43	9.24	1.21	0.19	3.76	0.55	0.14
Na_2O	0.00	0.00	0.00		2.50	0.06	1.40	6.60	0.00	0.00
K_2O	6.99	0.20	6.07		0.29	0.28	2.38	0.03	0.93	2.82
H_2O^T	3.00	6.00	2.60		2.30		1.70	0.40	3.40	3.40
CO_2^T	0.10	17.30	1.60	3.00	7.50	6.80	4.00	6.70	4.00	0.20
P_2O_5	0.28	0.21	0.23	0.02	0.18	0.01	0.10	0.08	0.08	0.13
S^T	0.40	0.02	0.14	32.10	0.13	31.90	0.19	0.04	0.15	0.02
LOI		22.00		21.80		24.00				
Total	99.30	100.20	99.60	107.50	99.90	115.20	100.10	99.80	100.10	99.70
F	1354	523	1141	131	390	81	773	123	509	957
Cl	163	257			219			237	190	
S	3392	141	1269		1199		1894	435	1414	166
Ag	0.9	0.7	0.2	59	0.6	4.3	0.4	0.2	0.4	1.9
Ba	770	22	690		140	30	240	15	130	220
Be	4.1	1.7	3.6		0.8		1.4		0.6	1.6
Bi	0.9		0.6	130	0.6	11				
Cd	0.7	1.6		320	0.3	54				
Co		22	7	29	40	51			5	
Cr	13	43	15	15	46	15	15		47	18
Cs	6.5	0.63	7.4	0.1	1.8	0.4	3.5	0.12	1.4	2.8
Cu	35	18		3300	24	6400	20	17	25	
Ga	26	19	23	6.3	19	2.4	18	5.7	16	20
Hf	14	4.7	11	1.1	3.5	0.56	5.4	1.3	6	6.5
In	0.08	0.13	0.07	8	0.11	11	0.1	0.1	0.14	0.24
Mo	2.1	0.3	1	1.6	0.7	0.9	1.5	0.2	1.4	1.3
Nb	26	6.9	21	1.7	6.2	1.1	11	2.5	13	13
Ni	11	19			10				14	
Pb	59	97	10	27000	38	420	10	5	10	
Rb	310	9.6	250	1	6	14	130	1.4	45	120
Sc	15	38	13	2.9	35	1.9	7.7	4.8	8.2	10
Sn	26	4.7	4.8	8.2	8.6	4.6	7.6	0.8	14	27
Sr	18	31	50	13	240	54	56	360	21	18
Ta	1.1	0.7	0.9		0.3		0.8		0.8	0.7
Th	24	3.3	20	2.2	2.6	1.2	15	3.2	11	17
Ti	6.4	0.5	7.8	3.9	0.06	0.51	1.2	0.04	0.26	0.56
U	5.7	6	5.2	0.87	0.63	0.54	4.5	0.78	2.5	4.5
V	29	240	33	9	260		29		47	36
Y	63	38	56	7	36	3.3	36	12	32	42
Zn	110	240	53	119000	170	16000	84	23	240	190
Zr	650	150	520	45	130	23	220	51	260	260

Sample#	ML95-262	ML95-263 *	ML95-264	ML95-265 *	ML95-266 *	ML95-269	ML95-273a	ML95-273b	ML95-274	ML95-276
Hole	MM-88-02	MM-88-02	MM-88-02	MM-88-02	MM-88-02	MM-88-02	MM-88-02	MM-88-02	MM-89-106	MM-89-106
Deposit	RSTG	RSTG	RSTG	RSTG	RSTG	RSTG	RSTG	RSTG	RSTG	RSTG
SiO_2	71.10	66.30	50.30	57.50	65.00	65.10	59.00	64.40	79.10	22.30
TiO_2	0.44	0.68	1.72	0.67	0.39	0.55	0.56	0.12	0.30	0.10
Al_2O_3	9.30	14.00	13.70	16.30	16.50	14.30	20.20	18.90	12.50	4.60
$Fe_2O_3^T$	4.00	5.60	12.00	7.40	4.10	4.90	3.00	0.70	0.80	9.70
Fe_2O_3	0.20	0.50	3.40	1.10	1.10	0.10	1.10	0.10	0.80	
FeO	3.40	4.60	7.80	5.60	2.70	4.30	1.70	0.50	0.00	
MnO	0.17	0.06	0.24	0.06	0.04	0.06	0.03	0.02	0.04	1.10
MgO	2.07	2.23	6.72	4.34	2.71	1.89	1.32	0.65	0.47	8.91
CaO	3.24	1.91	8.23	1.35	1.43	1.39	1.31	1.32	0.11	20.13
Na_2O	0.00	3.50	4.60	1.60	2.10	1.00	3.00	9.60	0.00	0.00
K_2O	2.42	1.38	0.13	6.65	3.75	4.68	7.15	1.30	2.41	1.16
H_2O^T	1.60	2.50	2.90	3.10	2.90	2.30	2.20	0.40	3.10	1.10
CO_2^T	5.50	1.40	0.30	0.90	0.70	2.80	1.40	1.80	0.10	31.30
P_2O_5	0.11	0.13	0.18	0.19	0.25	0.19	0.36	0.13	0.15	0.09
S^T	0.07	0.04	0.12	0.04	0.03	0.63	0.03	0.02	0.02	0.02
LOI										30.40
Total	99.60	99.30	100.30	99.50	99.60	99.30	99.30	99.40	99.20	100.50
F	726	551	463	964	1027	1021	1245	290	825	280
Cl	186	123	441	165	105	216	149	142		586
S	620	308	1174	445	255	5645	242	154	95	252
Ag	0.5	0.7	0.2	0.3	0.3	1.5	0.5	0.3	0.3	1.1
Ba	300	290	88	830	990	930	1200	660	590	250
Be	1.6	2.2	0.8	3.1	3.9	3.2	3	1.1	2.3	0.8
Bi			0.6			1.7				1.1
Cd										
Co	9	8	41	8		11	6			
Cr	30	45	66	29		16	11			
Cs	2.9	2.2	0.92	12	7.9	7.1	6.7	0.81	4.2	1.9
Cu	14	15	14			26				37
Ga	12	19	19	25	29	23	30	12	18	7.6
Hf	4.2	6.4	4.3	10	8.4	9.8	13	3.1	6.9	2.6
In	0.07	0.05	0.11	0.11	0.12	0.05	0.14	0.06		0.13
Mo	0.4	0.4	0.6	1.5	0.5	2.6	0.5		1.5	1
Nb	11	16	6.1	23	20	22	28	7.5	15	5.6
Ni	17	11	11	11						
Pb	8	18	5	7	17	14	10			4
Rb	100	67	3.9	170	160	160	210	32	90	44
Sc	8.6	12	44	22	10	18	15	3.5	8.2	3.5
Sn	3	4.4	1.7	5.7	7.6	4.9	9.4	2.9	6.6	4.2
Sr	99	80	170	46	64	58	80	180	180	50
Ta	0.6	0.6	0.4	1.3	1.1	1	1.5	0.4	0.9	0.3
Th	9.7	14	2.6	22	31	24	44	7.8	24	9.1
Tl	0.49	0.27	0.06	0.82	0.7	0.91	0.96	0.17	0.45	0.2
U	2.5	2.9	0.66	5.9	6.2	4.2	8.7	1.8	4.8	2.6
V	42	63	260	40	10	23	12		9	6
Y	29	36	38	78	71	63	97	31	49	55
Zn	30	57	80	65	47	31	49		6	
Zr	170	260	140	440	360	440	540	110	290	88

Sample#	ML95-277 *	ML95-278	ML95-279 *	ML95-280	ML95-283	ML95-284	ML95-285	ML95-297	ML95-298	ML95-299
Hole	MM-89-106	MM-89-106	MM-89-106	MM-89-106	MM-89-106	MM-89-106	MM-89-106	MM-88-16	MM-88-16	MM-88-16
Deposit	RSTG	RSTG	RSTG	RSTG	RSTG	RSTG	RSTG	RSTG	RSTG	RSTG
SiO_2	68.30	57.60	79.00	52.60	46.40	58.00	68.00	4.00	2.80	3.90
TiO_2	0.29	0.39	0.23	0.67	0.83	0.91	0.92			
Al_2O_3	13.30	15.10	10.60	22.90	26.30	17.60	16.90	0.38	0.33	0.33
$Fe_2O_3^T$	5.00	4.00	1.20	6.20	6.80	6.80	1.90	34.10	47.40	46.00
Fe_2O_3	4.30	0.70	0.30	2.60	1.50	0.60	0.10			
FeO	0.60	3.00	0.80	3.20	4.70	5.50	1.60			
MnO	0.09	0.12	0.02	0.06	0.07	0.12	0.06	0.17	0.09	0.17
MgO	1.07	3.05	0.48	1.73	2.58	3.05	1.07	1.16	0.61	2.08
CaO	2.40	4.56	0.70	0.95	1.44	2.82	1.33	2.43	1.07	3.07
Na_2O	0.50	0.10	2.60	0.90	0.00	1.00	0.00	0.08	0.05	0.03
K_2O	3.07	4.27	2.14	9.50	8.76	3.39	2.28	0.07		
H_2O^T	3.40	2.70	1.00	3.40	4.50	3.80	4.60			
CO_2^T	2.10	7.40	0.80	1.00	1.90	2.40	2.20	3.80	2.00	7.50
P_2O_5	0.54	0.15	0.22	0.43	0.37	0.12	0.20	0.01	0.01	
S^T	0.00	0.05	0.09	0.04	0.02	0.01	0.16	36.90	44.60	38.50
LOI								21.00	27.20	26.40
Total	100.00	99.10	98.90	99.90	99.50	99.40	99.40	111.20	112.80	111.70
F	1486	1487	1105	1713	2092	927	826			
Cl	108	184	252	161	128		304			
S	68	517	718	336	185	145	1260			
Ag	0.3	0.9	0.1	0.3	1.2	1	0.4	340	96	63
Ba	680	770	460	1500	1300	530	380			
Be	2.8	3	1.5	4.8	5.6	2.6	2.6			
Bi	0.5		0.5		6.9		0.6		3.8	69
Cd		0.2						380	200	230
Co				6	23	14	15	6		6
Cr		21		18	61	55	54	12	11	12
Cs	6	6.4	2.5	12	14	3.7	4.4	0.05	0.23	0.08
Cu	10	11				18	29	1700	4100	3500
Ga	20	23	14	45	37	25	20	1	3.9	3.6
Hf	6.8	8.8	5.5	18	10	9.1	8.2	0.19	0.15	0.29
In	0.11	0.13		0.2	0.24	0.1	0.07	0.42	0.56	2.3
Mo	0.4	18	0.5	0.8	2.2	0.4	4.9	1.6	18	46
Nb	16	18	12	33	28	21	21	0.15	0.13	0.14
Ni		73			32	13	19			
Pb	38	6	55	7	610	7	38	166000	59000	28000
Rb	120	160	80	330	310	150	89	0.5	0.27	0.27
Sc	8.3	10	5.6	23	23	15	14	0.7		
Sn	5.8	8.2	8.7	14	14	4.2	4.3	350	79	56
Sr	45	74	48	93	64	81	50	35	10	38
Ta	0.5	1	0.7	1.4	1.3	1	0.7			
Th	26	28	20	53	25	18	19	0.06	0.06	0.06
Tl	0.52	0.74	0.49	1.6	1.4	0.78	0.76	6.9	24	9.5
U	5.4	5.3	4.2	11	5.6	4.2	5.5	0.15	3	7.7
V	5	12		60	110	95	76		6	6
Y	84	58	54	97	52	58	51	3.8	1.1	1.8
Zn	110	25	31	150	110	69	130	112000	75000	70000
Zr	280	370	240	770	430	380	360	9.1	7.2	14

Sample#	ML95-300	ML95-321	ML95-322	ML95-324	ML95-371
Hole	MM-88-16	B-80-7	B-80-7	B-80-7	B-80-7
Deposit	RSTG	RSTG	RSTG	RSTG	RSTG
SiO_2	6.30	3.80	2.10	47.00	8.00
TiO_2			0.02	0.02	0.18
Al_2O_3		0.22	0.55	0.52	3.55
$Fe_2O_3^T$	42.70	46.70	42.00	26.20	52.40
Fe_2O_3					
FeO					
MnO	0.17	0.04	0.11	0.03	0.14
MgO	2.27	0.25	0.54	0.48	3.23
CaO	2.27	0.45	1.12	0.88	0.23
Na_2O	0.03	0.03	0.07	0.03	0.03
K_2O			0.07		
H_2O^T					
CO_2^T	9.00	0.90	1.80	1.40	1.00
P_2O_5	*0.10*	*0.01*	*0.06*	*0.01*	*0.04*
S^T	33.70	44.50	40.80	23.60	32.60
LOI	25.50	27.00	23.20	15.00	16.50
Total	110.40	112.70	111.90	107.20	111.30
F					581
Cl					
S					
Ag	40	100	170	36	39
Ba					
Be					
Bi	41				56
Cd	210	160	110	64	150
Co	7		6		120
Cr		12	13	11	22
Cs		0.04	0.48	0.05	0.04
Cu	420	1200	2800	1400	1800
Ga	1.1	1.2	2.7	1.5	8.9
Hf	0.25	0.08	0.26	0.2	2.1
In	1.8				35
Mo	4.5	11	37	0.9	4.3
Nb	0.49	0.18	0.48	0.58	3.7
Ni			48		
Pb	60000	79000	174000	29000	23000
Rb	0.62	0.16	0.75	0.86	0.29
Sc	0.5	0.5		0.6	3
Sn	12	48	60	21	550
Sr	72	12	64	12	
Ta					0.2
Th	0.16	0.08	0.32	0.38	3
Tl	4.8	4.3	71	2.2	1.6
U	1.9	1.5	5.9	0.63	2.4
V			19	5	21
Y	4	0.85	1.7	2.5	8.5
Zn	76000	77000	50000	40000	74000
Zr	12	3.7	11	8.2	78

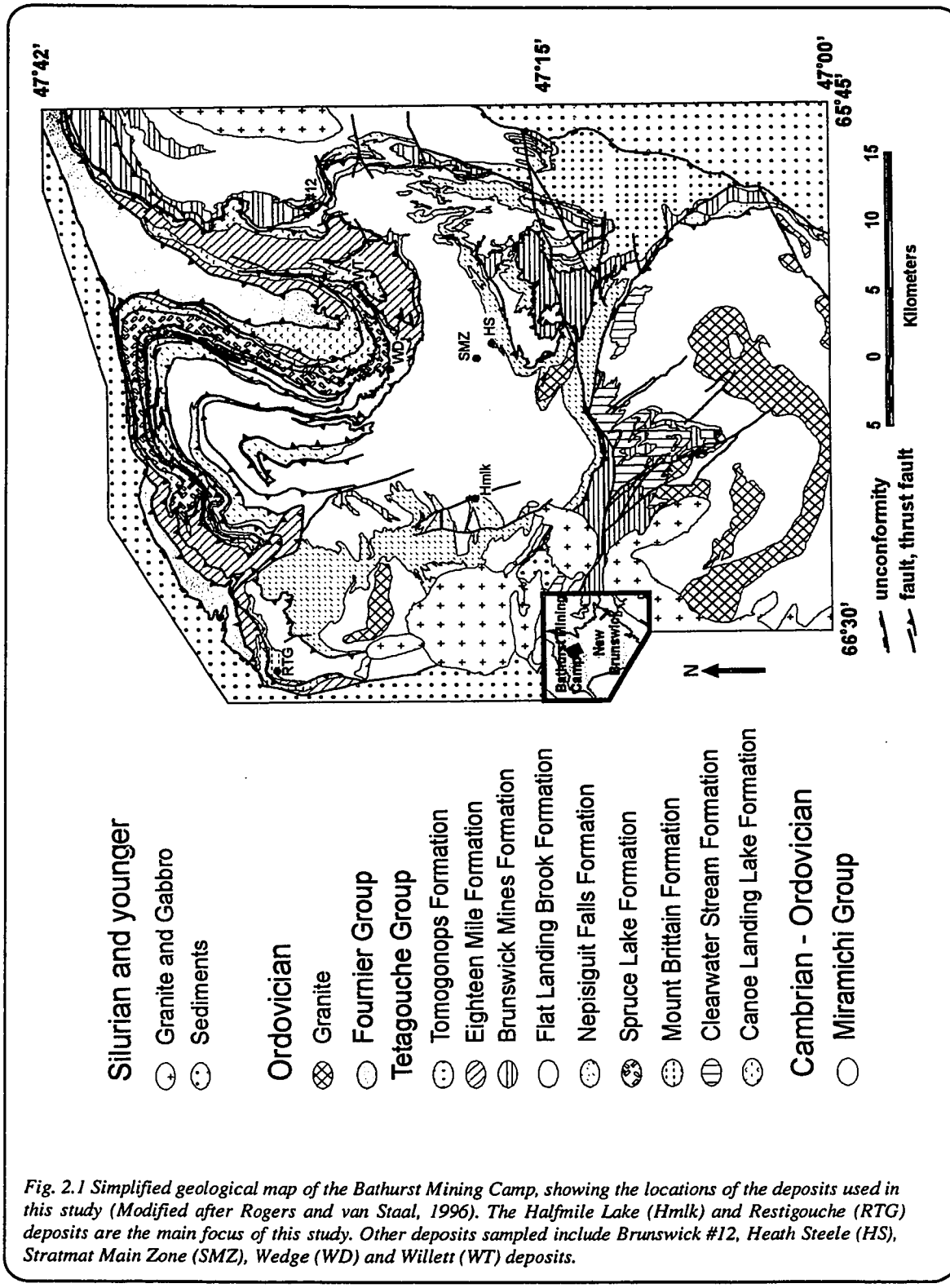


Fig. 2.1 Simplified geological map of the Bathurst Mining Camp, showing the locations of the deposits used in this study (Modified after Rogers and van Staal, 1996). The Halfmile Lake (Hmlk) and Restigouche (RTG) deposits are the main focus of this study. Other deposits sampled include Brunswick #12, Heath Steele (HS), Stratmat Main Zone (SMZ), Wedge (WD) and Willett (WT) deposits.

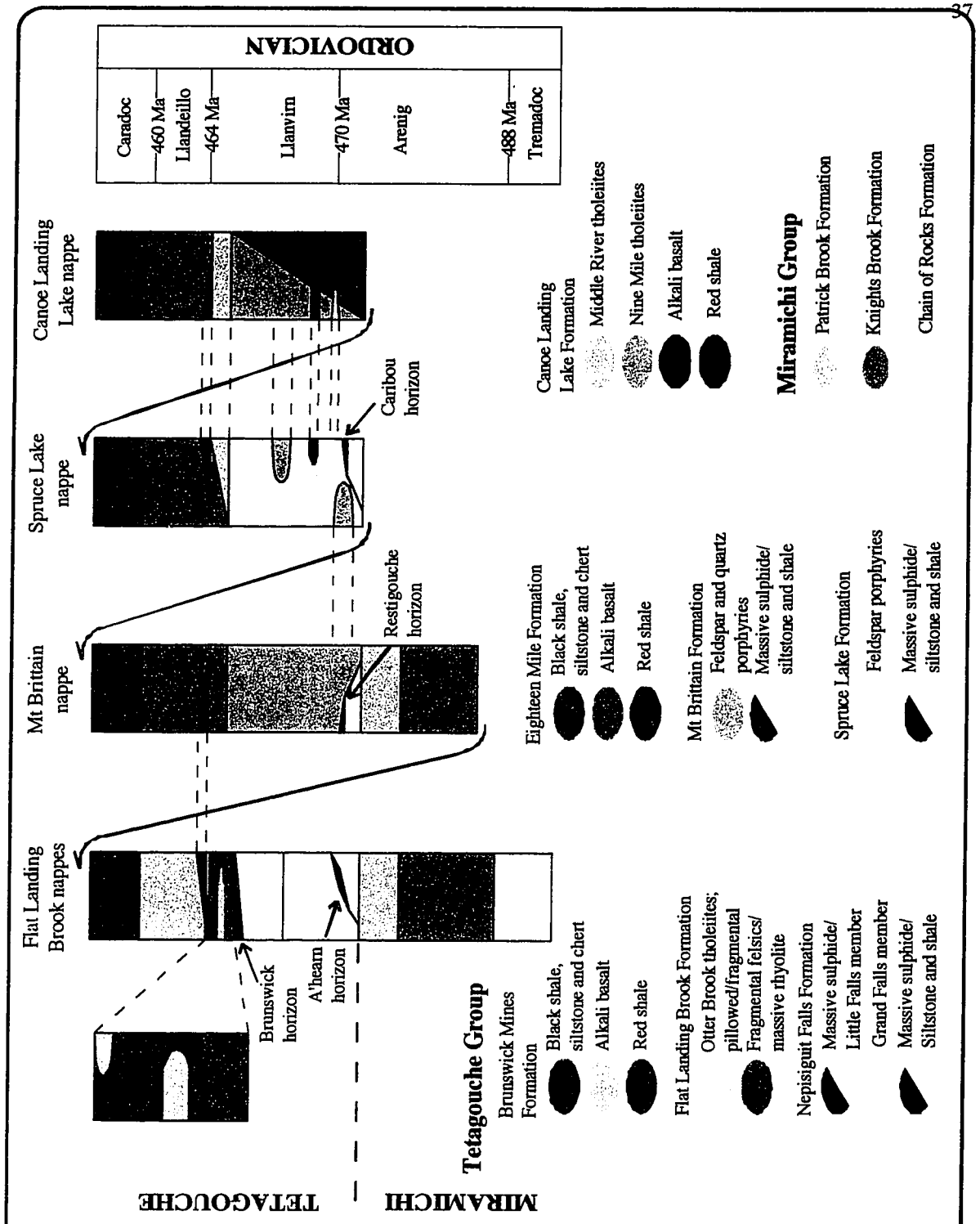
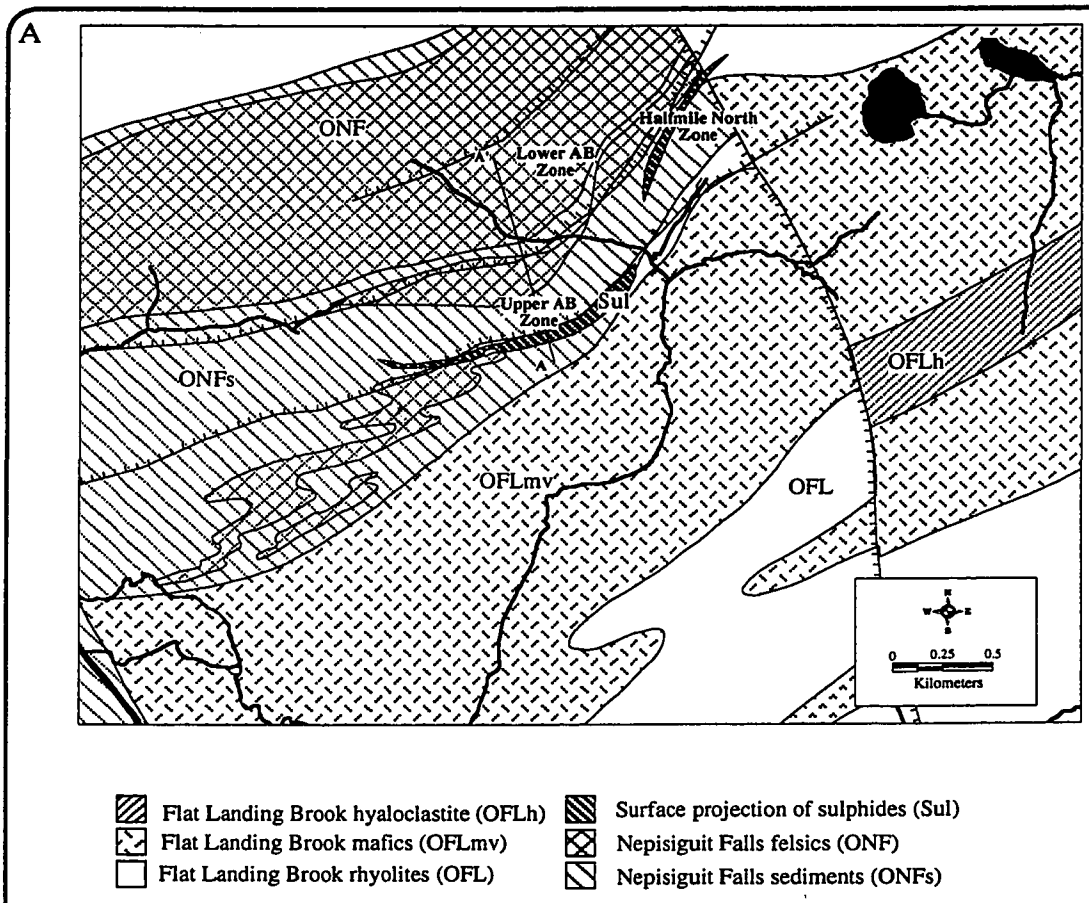


Fig. 2.2 Respresentative stratigraphic columns for the Bathurst Mining Camp (after Rogers and van Staal, unpublished).



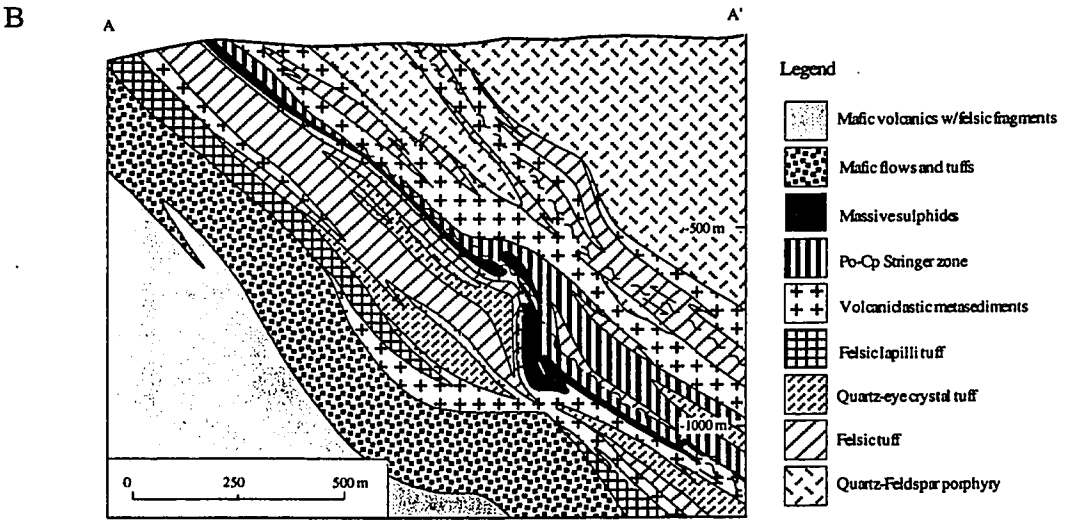


Fig. 2.3 A) General geological map of the Halfmile Lake deposit (after Wilson, 1993). B) Geological cross-section A-A' through the Halfmile Lake deposit (after Adair, 1992).

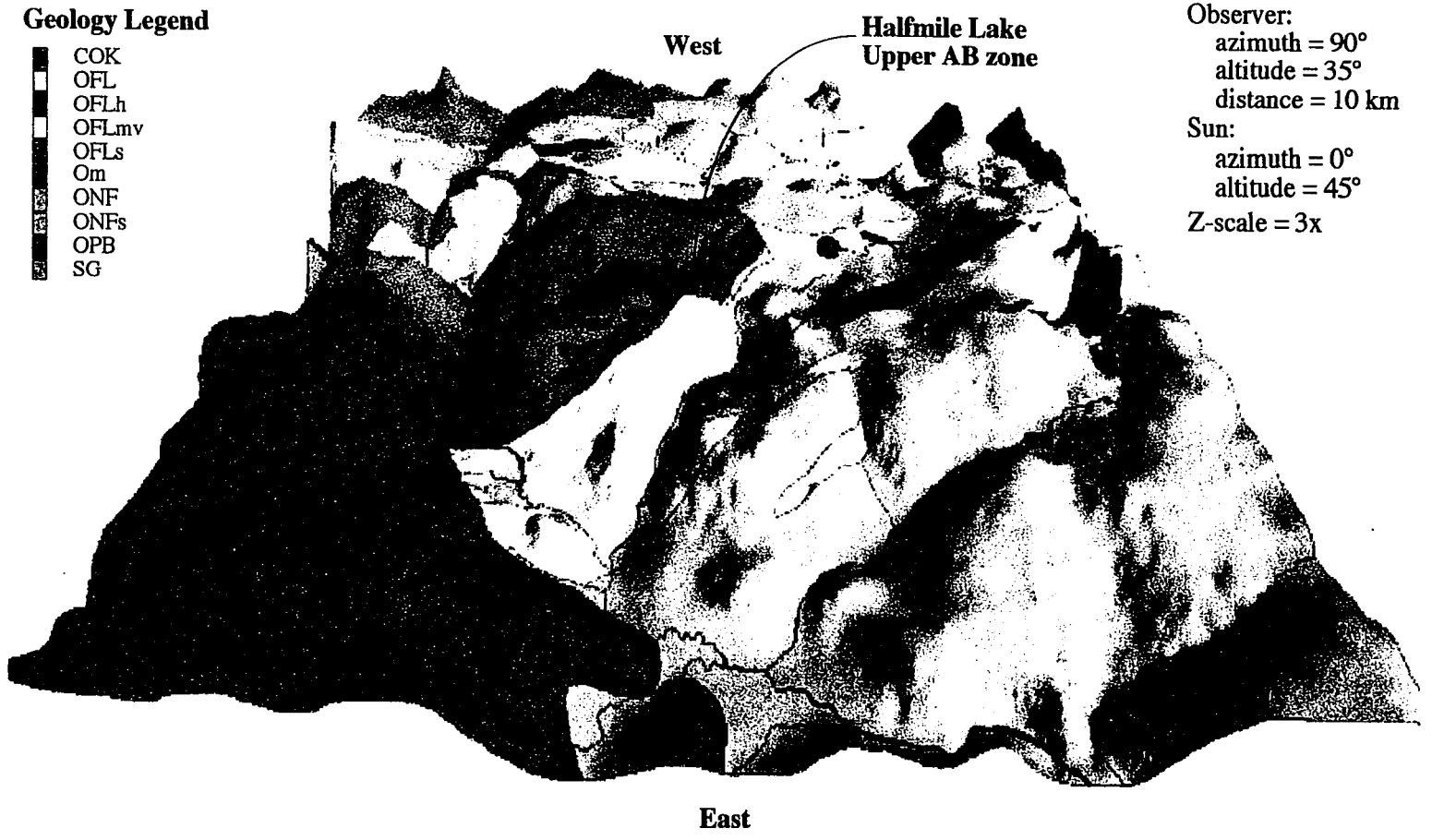
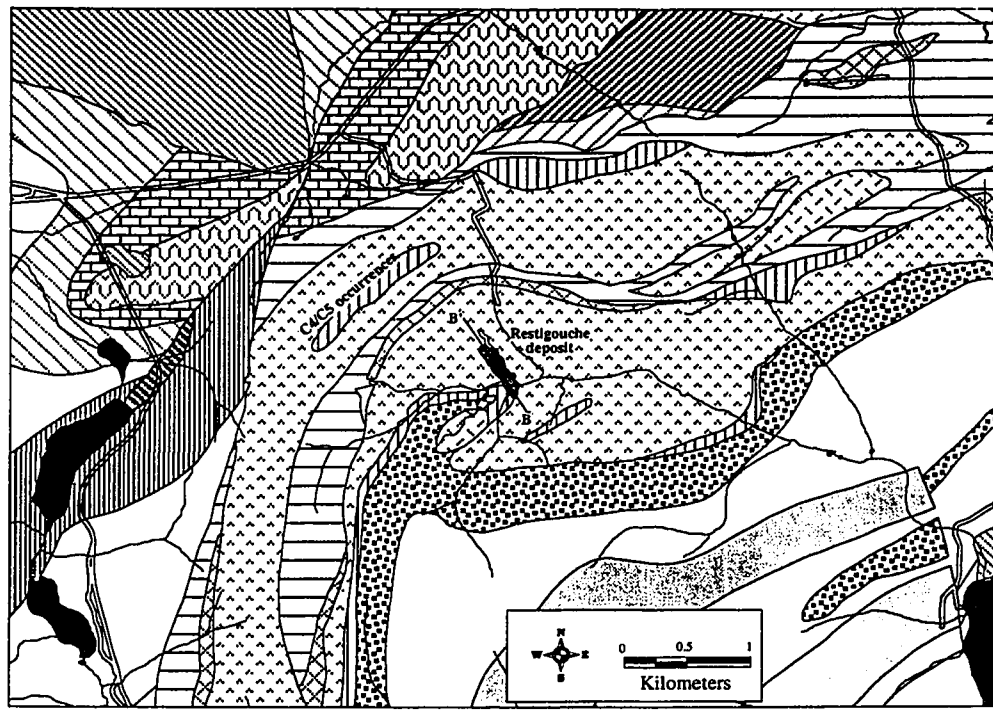


Fig. 2.4 Perspective view from the east of the Halfmile Lake deposit geology draped on the digital elevation model (see Fig. 4.1 in Chapter Four). Geology: COK, Knight Brooks Fm.; OPB, Patrick Brook Fm.; OFL, Flat Landing Brook rhyolites; OFLh, Flat Landing Brook hyaloclastites; OFLmv, Flat Landing Brook mafic volcanics; Om, mafic intrusives; ONF, Nepisiguit Falls felsics; ONFs, Nepisiguit Fals sediments; SG, granites.

A



Mount Brittain F. dacite (OMB)
Mount Brittain F. tuffs (OMBt)
Patrick Brook F. (OPB)
Knights Brook F. (COK)
Chain of Rocks F. (COC)
Simpsons Field F. (SSF)
Sormany F. basalts (OSAb)
Mafic intrusives (Om)
Boucher Brook sediments (OBBs)
Boucher Brook basalts (OBBb)
Tobique Group (DTb)
Greys Gulch F. (SDGGs)
Budworm City F. (SBC)
Mafic intrusives (SDm)
LaPlante F. (SLP)

B

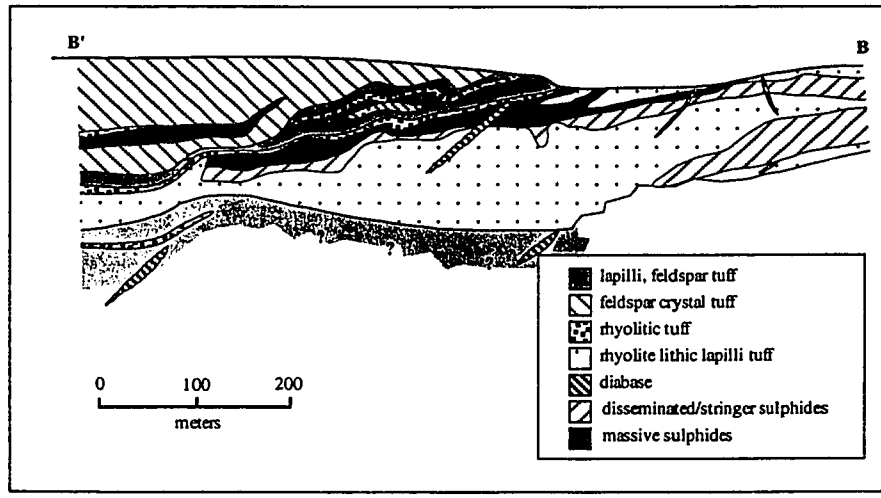


Fig. 2.5 A) General geological map of the Restigouche deposit (after Gower, 1995). B) Geological cross-section B-B' through the Restigouche deposit (after Barrie, 1982).

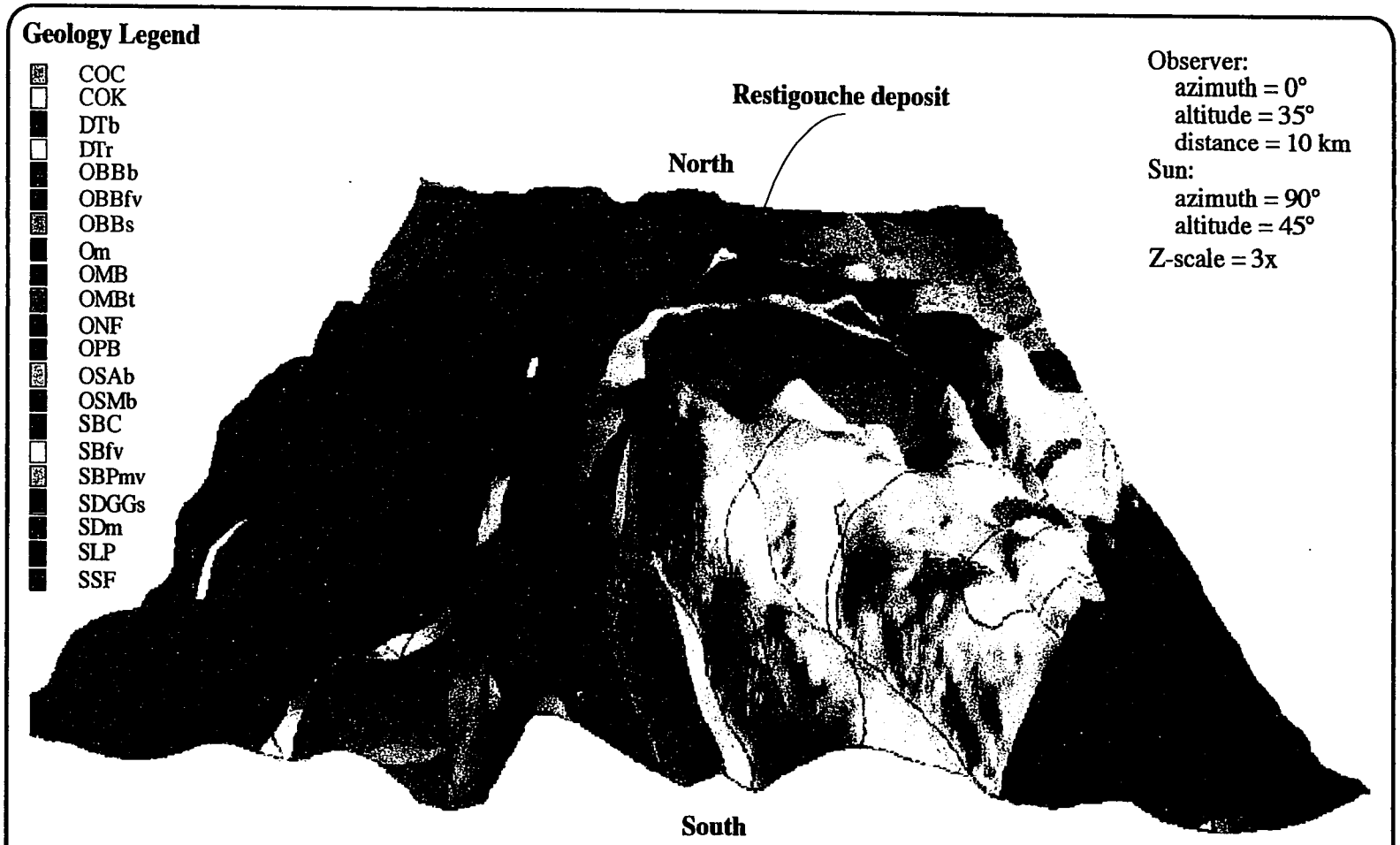
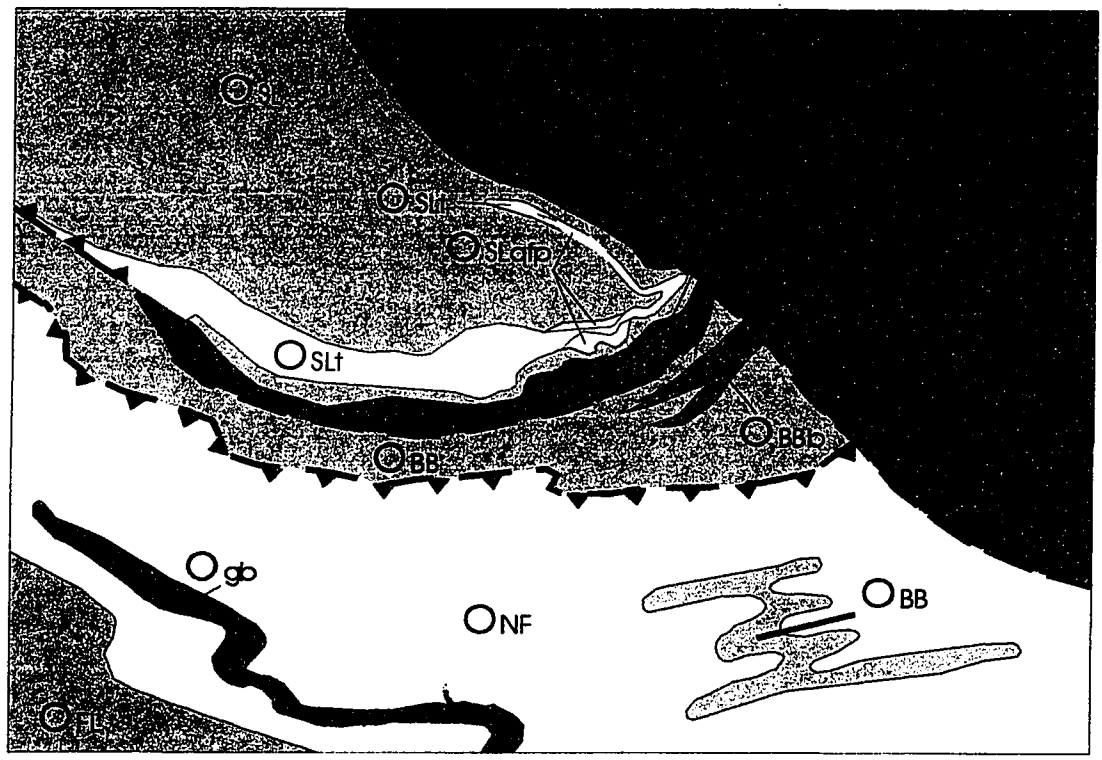


Fig. 2.6 Perspective view from the south of the Restigouche deposit geology draped on the digital elevation model (see Fig. 4.2 in Chapter Four). Geology: COC, Chain of Rocks Fm.; COK, Knight Brooks Fm.; OPB, Patrick Brook Fm.; DTb, DTr, Tobique Group; OBBb, 18 Mile Brook basalts; OBBfv, 18 Mile Brook felsic volcanics; OBBs, 18 Mile Brook sediments; Om, mafic intrusives; OMB, Mount Brittain dacite; OMBt, Mt Brittain tuff; ONF. Nepisiguit Falls Fm.; OSAb, Sormany Fm.; SBC, Budworm City Fm.; SBPmv, Bryant Point Fm.; SBfv, Benjamin Fm.; SDGGs, Greys Gulch Fm.; SDm, mafic intrusives; SLP, LaPlante Fm.; SSF, Simpsons Filed Fm.



WEDGE GEOLOGY

- gb Mafic intrusion
- FL Flat Landing Brook ryholite
- BB Brunswick Mines sediments
- BBb Brunswick Mines basalts
- NF Nepisiguit Falls Formation tuffs

Spruce Lake Formation

- SL Aphyric to fine feldspar phyric rhyolite
- SLfp Fine- to coares-feldspar phyric rhyolite
- SLf Felsic ash tuffs and interbedded epiclastic rocks
- SLqfp Quartz feldspar phyric epiclastic rocks

- Tectonic melange

Fig. 2.7 General geological map of the Wedge deposit area after Walker (1996) and Rogers (1998 pers. comm.). Contour intreval is 20 m.



Fig. 2.8 General geological map of the Willett deposit area. Geology: OCrs,Conoe Landing Lake shale/chert; OBm, Brunswick Mines tholeiitic basalts; OF, Flat Landing Brook rhyolite; ONF, Nepisiguit Falls sediments; OFif, massive sulphides and iron formation; OBBvb2, Beresford alkali basalt; OCNvb, Nine Mile tholeiite; OCCvb, Canoe Landing Lake alkali basalt; OBBvb1, Brunswick Mines alkali basalt; OB, Eighteen Mile tholeiitic basalt; SDp, granite. After van Staal (1994) and Rogers (1998 pers. comm.). Contour intreval is 20 m.

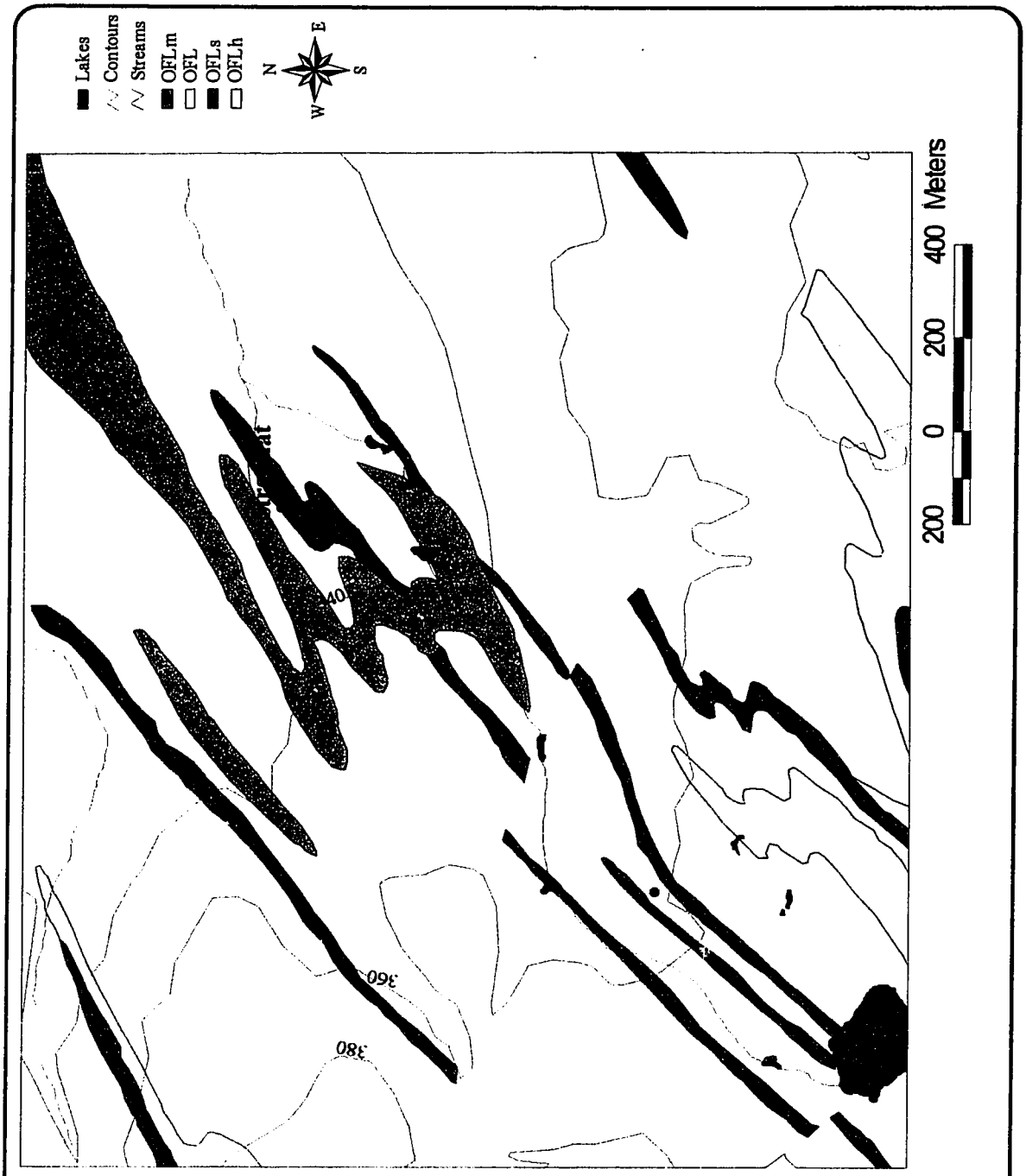


Fig. 2.9 General geological map of the Stratmat Main Zone deposit area. Geology: OFLm, Flat Landing Brook mafic volcanics; OFL, Flat Landing Brook rhyolite; OFLs, Flat Landing Brook sediments; OFLh, Flat Landing Brook hyaloclastites. After Wilson (1993). Contour intreval is 20 m.

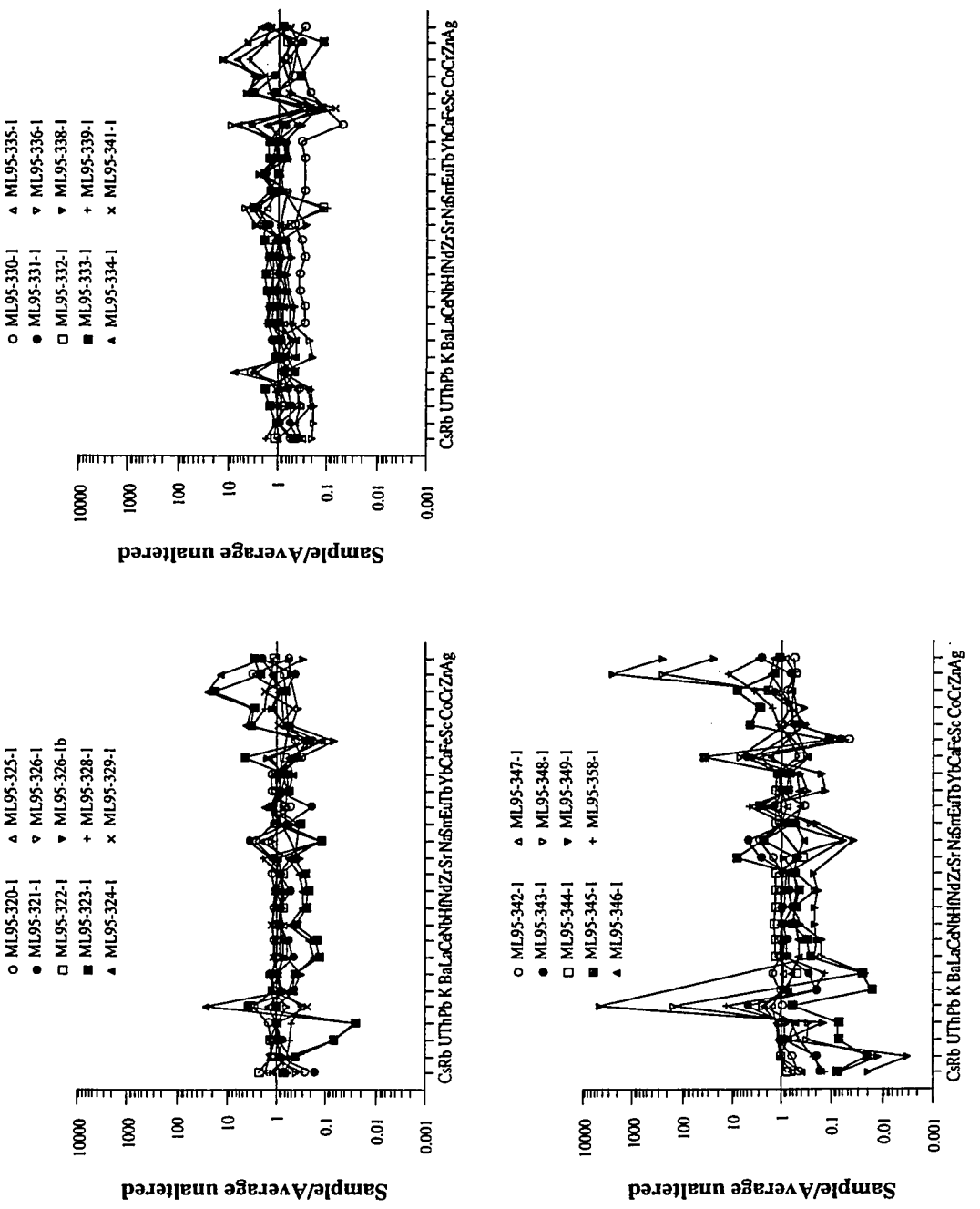


Fig. 2.10 Composition of Halfmile Lake deposit lithologies normalized to average unaltered Halfmile Lake lithology. Data from Table 2.1.

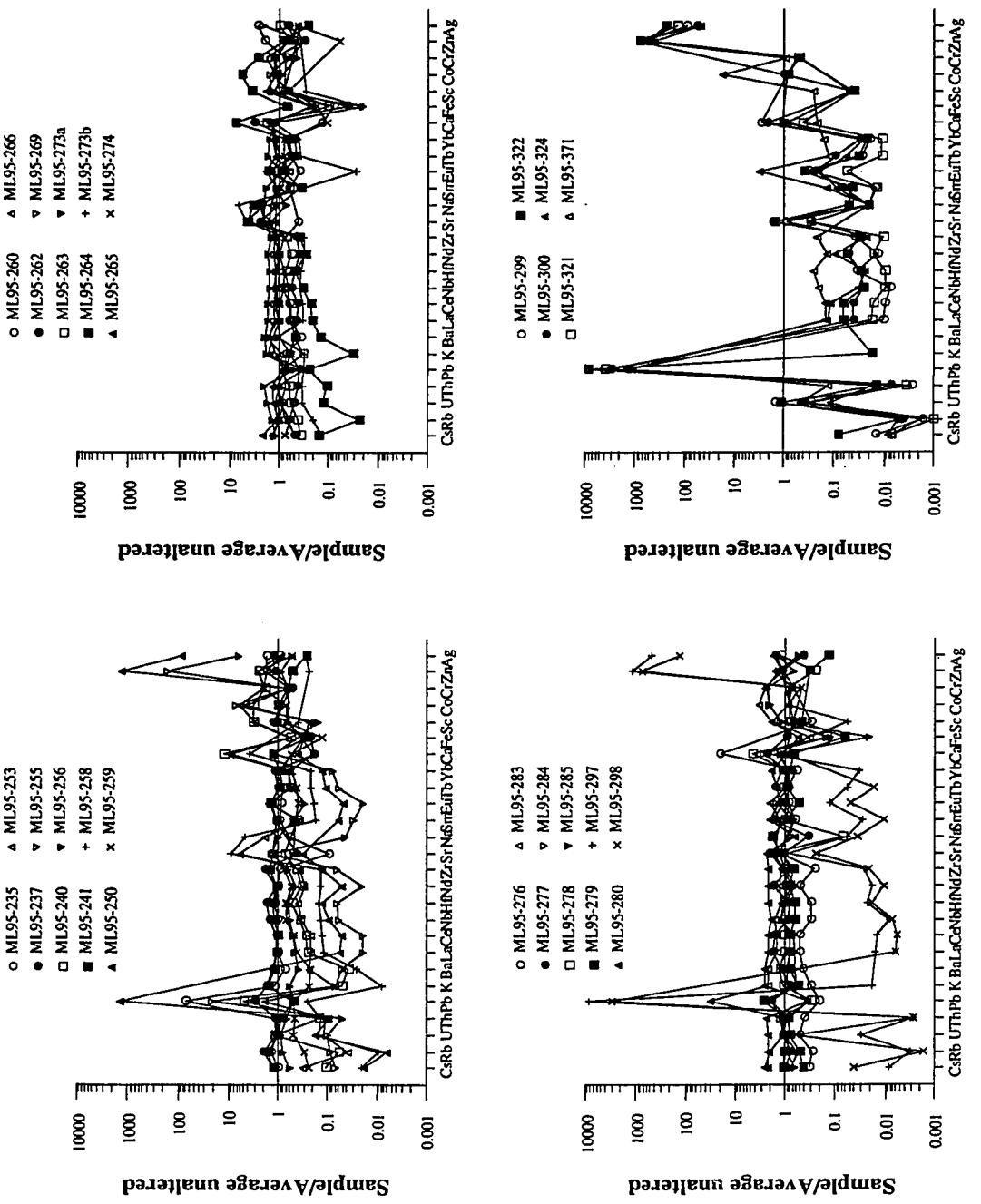


Fig. 2.11 Composition of Restigouche deposit lithologies normalized to average unaltered Restigouche deposit lithology. Data from Table 2.1.

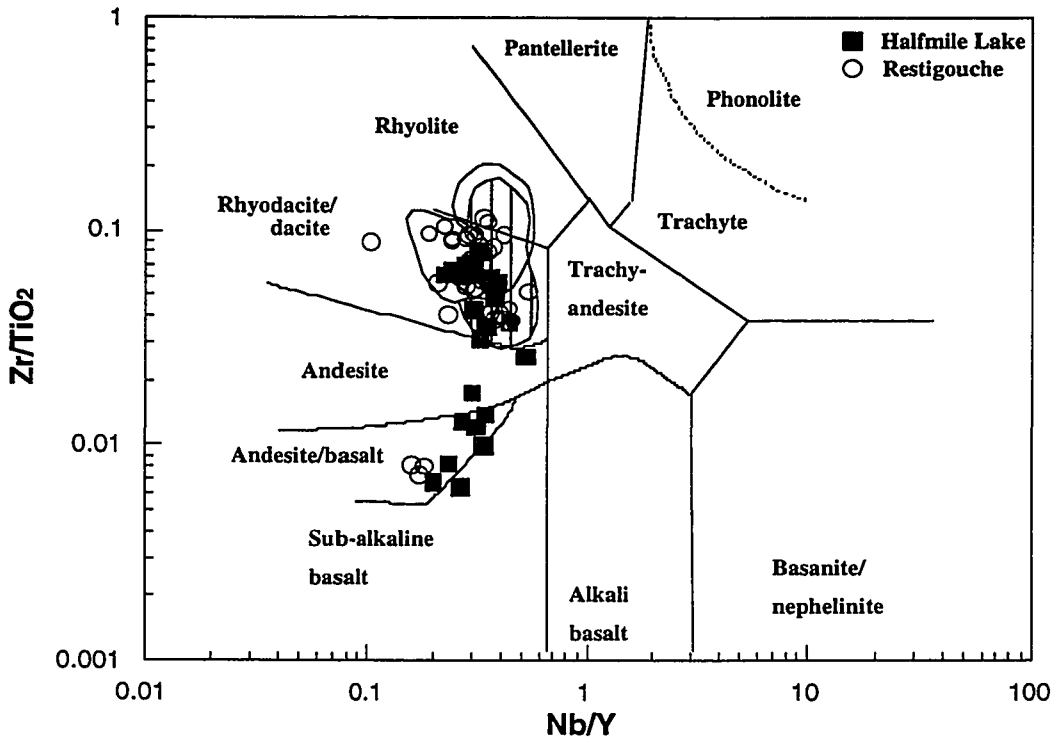


Fig. 2.12 Discrimination diagram showing the variation in the samples analyzed in this study from the Halfmile Lake and Restigouche deposits. Fields also shown for Spruce Lake (stippled), Flat Landing Broom (open), and Nepisiguit Falls (striped) felsic volcanic rocks (After Rogers, in press). The mafic rocks analyzed in this study are tholeiitic dykes. Boucher Brook mafic volcanic rocks are typically alkalic.

CHAPTER THREE:
FIELD AND ANALYTICAL METHODS

3.1 Field Methods

Surface water samples were collected during the summer of 1994 from streams, springs and seeps draining the Halfmile Lake deposit. Surface water samples were similarly collected in the area of the Restigouche deposit during the summer of 1995. Control samples were taken at roughly two week intervals during the summer field seasons and less often during the winter of 1994-95 from the Halfmile Lake deposit. At each site three samples were collected in one 125 ml sample bottle and two 60 ml sample bottles. One 60 ml bottle was acidified upon return to base camp with analytical grade nitric acid from Seastar Chemicals (Table 1.1 for composition of nitric acid). Samples from the Halfmile Lake deposit were collected sporadically over the winters of 1994-95 and 1995-96 by Rory Kempster (Noranda Exploration), following the same procedures but using 0.45 μm acrodiscs and syringes for sampling. Samples were typically collected every 100 to 200 meters along streams except near deposits where the sample density was increased.

Borehole waters that were collected during the summer of 1994 were sampled using a flow-through bailer system. The bailer is composed of PVC and holds a volume of approximately one litre. Samples were collected at regular intervals (generally 50 m) except where core logs indicated the presence of massive and stringer sulfides, in which case the sample depth was reduced accordingly. At each sample station, three samples were generally collected in one 125 ml sample bottle and two 60 ml sample bottles. One 60 ml bottle was acidified upon return to base camp with analytical grade nitric acid from Seastar Chemicals.

Water samples were measured in situ for pH, Eh, conductivity, temperature and dissolved oxygen (DO). The pH was commonly very slow to come to equilibrium due to low electrical conductivities for surface waters at Halfmile Lake and Restigouche. For borehole samples, temperature, DO and Eh were analyzed as quickly as possible after bringing the sample to

surface in order to minimize pressure and temperature induced changes in these parameters. All samples were filtered in situ through 0.45 μm sterile filters in a Nalgene 500 ml filter holder with an attached hand pump. For some boreholes, the suspended load was so high that several filter papers were required to filter 500 ml. The filter holder and filters were washed with approximately 50 ml of sample prior to filtering the collected sample and the filtering apparatus was cleaned with distilled water between samples. All samples were refrigerated at base camp prior to transport back to Ottawa for chemical analysis. High salinity waters from Restigouche exsolved gases during sample collection.

In order to determine QA/QC (quality assurance/quality control) for laboratory analyses, every batch of 20 samples contained one replicate sample and a field standard collected from a single site at the end of the field season. Replicates include both surface waters and groundwaters, and for most elements the average percent difference between the replicate pairs is less than one percent. Larger differences are present for Cu (27%), Pb (8.5%), and Zn (5.3%), although differences are minor for higher TDS waters. The field standards used were surface waters from Charlotte Brook (1995 field season) and the Upper/Lower AB stream (1994, 1996 field seasons). Thus, the standards were close to detection for most trace metals, and the standard deviations are higher than for the major cations and anions (Table 3.1). Another useful check on the data is a comparison of the sum of the cations with the sum of the anions which are < 10% difference for all samples, with most < 5 % (Fig. 3.1). Notable exceptions are low pH groundwaters from the Heath Steele and Wedge deposits which require the inclusion of Fe, Al, and Zn to achieve electrical balance.

3.2 Straddle Packer System

Borehole waters from the Halfmile Lake and Restigouche deposits were collected during the summer of 1995 using the flow-through bailer and a high-pressure mini-packer system. The bailer system is useful in that it allows rapid sampling of borehole waters. However, the degree to which a bailer sample approximates the groundwaters flowing through bedrock at the depth

recovered is highly dependent on flow regime and distribution of hydraulic heads. In sedimentary aquifers where flow is pore-dominated, the bailer method gives good results (e.g. Grimes et al., 1995). However, in crystalline rocks where groundwater flow is fracture-dominated, results derived by bailing are more equivocal and it is less clear that recovered samples represent groundwater flow at the indicated depth (see discussion in Chapter Seven).

The results indicate that the downhole composition of groundwaters is generally poorly represented by the bailer system (Fig. 3.2). In most cases, the composition of groundwaters collected by bailer generally increased in TDS with depth, but typically the magnitude of the variations were poorly represented. Although a bailer system is effective in sampling zones with the highest hydraulic conductivity, in most boreholes, and particularly at Halfmile Lake, the bailer samples represent the shallow groundwater system.

To eliminate the problem of flow within a borehole a straddle packer and dedicated winch system was designed by D.R. Boyle and constructed at the Geological Survey of Canada workshops (Fig. 3.3). The straddle-packer system consists of two packers, spaced 1.5 m apart which are inflated using N_2 gas. The packed-off zone is sampled using N_2 gas through a sampling head located above the packers. Water flowing through the packed-off zone enters the sample head through a uni-directional one psi cracking-valve and is then recovered from the sample head by forcing N_2 gas into the chamber. Several samples are taken at different time intervals dependant on the hydraulic conductivity of the zone being developed until the electrical conductivity of the recovered water reaches a steady state (Fig. 3.4). Zones to be developed are selected based on analysis of fracture and fault patterns and densities in drill core. Groundwater flows through a 45 μm in-line filter prior to passage through the cracking valve to avoid clogging of the cracking valve, although this was still a common problem, especially at shallow depth.

The straddle-packer proved useful in recovering groundwater from discrete zones within boreholes. However, there are some limitations to the system. The system uses high-pressure poly-ethylene tubing for sample recovery. As this tubing is used for successive samples, there

is no mechanism to "decontaminate" it between samples. Therefore, there is the risk of cross-contamination. However, because many iterations are required to reach a steady-state in terms of conductivity, cross-contamination is unlikely to be significant. Secondly, field measurements are likely to be somewhat in error due to the time for sample return and resulting changes in temperature and pressure.

In general, the packer system worked well at the Restigouche deposit but poorly at the Halfmile Lake deposit where relatively few good samples were recovered by this method. The most likely explanation for poor performance at the Halfmile Lake deposit is that the bedrock is more unstable, resulting in common caving of side walls and cross-flow during the packer operation.

3.3 Analytical Methods

3.3.1 Inductively Coupled Plasma Mass Spectrometry (ICP-MS)

Trace elements in waters were analyzed by ICP-MS using a Perkin-Elmer Sciex ELAN 5000 ICP mass spectrometer at the Analytical Chemistry Laboratories, Geological Survey of Canada. The system is equipped with an autosampler and a flow-injection system for on-line dilution and addition of internal standards. All results were corrected for blanks, and saline waters are diluted prior to analysis. Elements analyzed by this method and the detection limits are given in Table 3.1.

Bromine, I, and P were measured by ICP-MS manually on a sub-set of samples. Samples were injected into the mass spectrometer and blanks were run after every sample and results were blank-corrected. A standard was also run every 20 samples. Only the most saline waters had detectable Br by ion chromatography (waters from borehole MM-88-02 from the Restigouche deposit and sample MLW95-492 from the Brunswick #12 deposit). For these samples, there is close agreement between the ICP-MS and ion chromatography data for Br.

Rare earth elements (REE) and selected trace elements were determined by ICP-MS following pre-concentration by chelation, using a method developed by Gwendy Hall at the

Geological Survey of Canada (Hall et al., 1995b). Pre-concentration was carried out on a CC-1 chelating resin of macroporous iminodiacetate that preferentially retains free ionic REE and transition metals relative to the alkali and alkaline-earth elements. As a result, this method does not measure REE or transition metals associated with colloids < 0.45 μm, i.e., colloids that are small enough to pass through the filter paper used in this study. The chelation ICP-MS technique allows determination of all 14 REE as well as Al, Ti, V, Mn, Fe, Co, Ni, Cu, Zn, Y, Cd, In, Pb, and U to very low detection limits (as low as 1 ng/l using 5x pre-concentration; Table 3.1). For the REE, the following isotopes were measured in order to minimize the effects of isobaric interferences: ^{139}La, ^{140}Ce, ^{141}Pr, ^{146}Nd, ^{149}Sm, ^{151}Eu, ^{157}Gd, ^{159}Tb, ^{163}Dy, ^{165}Ho, ^{166}Er, ^{169}Tm, ^{172}Yb, and ^{175}Lu.

Several elements were analyzed by both ICP-MS techniques; total nebulization which measures total concentration (dissolved and colloidal) and chelation ICP-MS which measures only dissolved concentrations. For the common elements (Fe, Mn, Al, Cu, Pb, Zn, Co, Cd) for which both techniques gave acceptable detection limits there is very high correlation (Fig. 3.5). This correlation in part results from the fact that although the chelation technique should not allow colloidally bound elements to be included in the analysis, in practice, acidification of the sample most likely strips most metals bound to colloids.

3.3.2 Inductively Coupled Plasma Emmision Spectroscopy (ICP-ES)

The remainder of the cations were determined in the same lab on a Perkin-Elmer Optima 3000 ICP emission spectrometer equipped with an autosampler. ICP-ES uses an argon plasma flame operating at a temperature of between 6000 - 10,000 K. The sample solution is introduced as an aerosol into the plasma where it dissociates producing atomic and ionic spectral lines which are detected by photomultipliers. Comparison between sample spectral lines and calibration lines allows conversion from line intensity to elemental concentrations. Elements analyzed by this method and the detection limits are given in Table 3.1.

3.3.3 Ion chromatography

Ion chromatography was used to determine the concentrations of the major anions in the ground and surface waters, i.e., nitrate, nitrite, fluoride, phosphate, sulphate, chloride and bromide. These anions were analyzed on a Dionex Series 4500I Ion Chromatograph fitted with an IonPac AS4A-SC (4mm) column at the Analytical Chemistry Laboratories, Geological Survey of Canada. The technique involves chromatography of 5 ml of sample solution with concentrations determined by peak profile areas. The limits of detection for all anions is 50 µg/L (Table 3.1). All waters had PO_4^{2-} values below detection and most waters were below detection for Br.

3.3.4 Stable isotopes

Stable isotopes were analyzed at the stable isotope laboratory of the Geology Department, University of Ottawa. For deuterium analyses, 3 µl of sample was trapped by liquid nitrogen under vacuum (< 10 mT) in pyrex breakseals with 100 mg of zinc. Samples were baked at 500°C for 30 minutes before analysis on a Micromass 602E mass spectrometer. Two standards were run for every eight unknowns and the data reduced by linear regression to account for variations in oxidation of zinc and changes in the reference gas. Reproducibility is typically better than ± 2 ‰.

Oxygen isotopes were analyzed on a VG Isogas Sira 12 mass spectrometer, using 1 ml sample aliquots. Samples were equilibrated with CO_2 gas for 6 hours prior to analysis. However, for samples with salinities > 10 ‰ TDS (total dissolved solids), equilibration times were increased to 36-48 hours to allow for the greater hydration sheath of ions in high salinity solutions. During a typical analytical run, 16-17 samples were run with three or four standards and the data corrected by linear regression on the standards. Reproducibility is typically better than ± 0.5 ‰. Oxygen and deuterium data are presented in standard δ notation:

$$\delta^{18}O = \left(\frac{(^{18}O/^{16}O)_{Sample}}{(^{18}O/^{16}O)_{VSMOW}} - 1 \right) \cdot 1000$$

where VSMOW is Vienna standard mean ocean water, the accepted standard for stable oxygen and hydrogen isotopes (Craig 1961).

Boron isotopes were determined by Conrad Gregoire at the Analytical Chemistry Laboratories of the Geological Survey of Canada using ICP-MS. The precision for Boron isotopes at the 2σ level was 0.3% during analysis of the samples reported here (see Chapter Eleven). Ratios were converted to $\delta^{11}B$ notation relative to the standard NBS SRM 951 which has a $^{11}B/^{10}B$ ratio equal to 4.044 (Spivack and Edmond, 1987):

$$\delta^{11}B = \left(\frac{^{11}B/^{10}B_{sample}}{^{11}B/^{10}B_{NBS\ 951}} - 1 \right) \cdot 1000$$

Carbon isotopes were analyzed on the dissolved inorganic carbon (DIC) for a subset of waters, primarily from the Restigouche Deposit. Samples were preserved in the field using HgCl and stored refrigerated. The $\delta^{13}C$ was measured by converting the DIC to CO_2 with 100% phosphoric acid (H_3PO_4) followed by cryogenic separation and analysis by mass spectrometry on a VG Isogas Sira 12 mass spectrometer. Calcite, dolomite and siderite were also measured on fracture zone and stockwork carbonate from the Restigouche deposit. Carbonate was micro-drilled from veins and fractures, and analyzed using a similar technique as for DIC. Calcite was equilibrated with orthophosphoric at 25°C for two hours, dolomite-ankerite was equilibrated at 50°C for two days and siderite-magnetite was equilibrated for four days at the same temperature. The $\delta^{13}C$ of both DIC and carbonate are reported relative to the international standard Vienna-PDB (VPDB):

$$\delta^{13}C = \left(\frac{^{13}C/^{112}C_{sample}}{^{13}C/^{12}C_{VPDB}} - 1 \right) \cdot 1000$$

3.3.5 Radiogenic isotopes

Waters and whole rocks were analyzed for Pb and Sr isotopes at Carleton University using

the procedures described by Cousens (1996). Sample aliquots of ground and surface waters were decanted into Teflon bombs and evaporated under clean laboratory conditions to achieve the required Pb and Sr concentrations (1 ng Pb and 10 ng Sr). For Nd, only a few samples had sufficient Nd and sample volume to attempt analysis. Two samples of carbonate vein were also analyzed. Carbonate was separated from silicate minerals by dissolution in HCl. Rocks were crushed to < 200 mesh in an agate mill. Between 100 and 300 mg of powder were then dissolved in 8N HNO_3 and 6N HCl. The residue was taken up in 1N HBr for Pb and 2.5 N HCl for Sr.

Lead was separated in Bio-Rad 10-ml polyethylene columns and Dowex AG1-8X anion resin, using 1N HBr to elute other elements and 6N HCl to elute Pb. The effluent was collected for subsequent Sr separation. The basic procedure for isolation of Pb involves:

1) addition of 0.6 ml of Dowex AG1-8X anion resin,

2) columns are rinsed with 2 x 2 ml 6N HCl to strip out any contaminant Pb, 1 x 1 ml of doubly distilled deionized water to prevent reaction between HCl and Hbr, and 2 x 2 ml 1N HBr to equilibrate the column,

3) sample is added to the column,

4) 2 x 2 ml HBr to remove other elements (collected for Sr separation),

5) 1 x 0.5 ml doubly distilled deionized water

6) the Pb is stripped out with 5 ml 6N HCl. The collected sample was then dried and the above process repeated using half the volumes of reagents.

Total procedural blanks for Pb are < 150 pg. Samples are loaded onto single Re filaments with H_3PO_4 and silica gel, and were run at filament temperatures of 1250-1350°C. Analysis of USGS Standard BCR-1 yields $^{206}Pb/^{204}Pb$ = 18.818, $^{207}Pb/^{204}Pb$ = 15.429, and $^{208}Pb/^{204}Pb$ = 36.502 ± 0.048 (2 s.d.), based on 25 runs between Sept. 1992 and Sept. 1994. The fractionation correction, based on the value of Todt et al. (1984), is + 0.13%/amu.

Strontium was separated chromatographically in Bio-Rad 12-ml borosilicate glass columns and Dowex AG-50 cation resin. The resin was pre-cleaned with 6N HCl. Sr was taken into solution after drying with 1.5 ml of 2.5N HCl were added to the columns. Fifteen ml of 2.5N HCl were then added to wash other elements through after which the Sr was collected in 6 ml of 2.5N HCl.

The rare earth elements were separated chromatographically in the same columns as Sr. However, the REE have a greater affinity for the resin. The REE were collected by washing the columns with 3 ml of 6N HCl after collection of the Sr, followed by collection of 9 ml of 6N HCl. The resulting solution was dried and the REE taken up in 0.26 N HCl. Neodymium was separated from the rest of the REE by ion chromatography using columns with 2 cm high beds of HDEHP (di(2-ethylhexyl) orthophosporic acid) coated Teflon powder (Richard et al., 1976).

3.3.6 Scanning electron microscopy (SEM)

Polished thin sections and grain mounts were analyzed using a Cambridge S-200 scanning electron microscope (SEM) equipped with an energy dispersive x-ray (EDS) detection system (Link Analytical AN10 analyzer) to allow semi-quantitative determinations of the clay minerals. The SEM was run at 20 kV at working distances of 15 to 30 mm, in both secondary and backscatter modes. Sections of filter paper with suspended sediments were analyzed by SEM. All samples were mounted on discs and carbon coated.

3.3.7 Whole rock and bulk stream sediment geochemistry

Stream sediments were collected from the same sites as surface water samples at the Halfmile Lake and Restigouche deposits. Samples of silt and sand were collected from the active centre of streams, placed in paper bags and dried on return to base camp. Where there was insufficient sediment in the active centre of the stream, sediment was collected from beneath boulders and trapped in the root network of moss. Stream sediments from the Halfmile Lake deposit were sieved to < 63 μm and 63-125 μm fractions. For the Halfmile Lake samples both of these size fractions were analyzed by ICP-MS and ICP-ES for the major and trace elements and REE in order to determine if there are any differences related to grain size. Although there are some differences between the two size fractions, mean differences for all samples are generally less than 10% (see Chapter Six). The data presented in Chapters Six and

Ten represent the averages of the two size fractions. Stream sediments from Restigouche were sieved to < 125 μm and analyzed by the same methods.

Sediments trapped on the filter papers used to filter borehole waters were also analyzed by ICP-MS for a selected suite of samples and, where there was sufficient material, by ICP-ES. Most filter papers did not contain sufficient material for analysis.

Representative rocks from drill core from both the Halfmile Lake and Restigouche deposits were analyzed by XRF and ICP-MS to complement published data and data provided by Robin Adair at Noranda Exploration.

3.3.8 X-ray diffraction (XRD) analysis

Selected suspended sediment samples were analyzed by XRD on a Phillips PW1830 diffractometer, at the University of Ottawa. Filter residue samples were ground between glass plates prior to loading on a zero background quartz plate as an acetate slurry. Samples were run at a scan rate of 1.5 s/step in steps of 0.04θ.

3.4 Data Manipulation

Geochemical data were displayed, analyzed, and interpreted using geochemical modelling, statistical, and GIS software. Geochemical modelling was used to investigate element speciation and to calculate mineral saturation as a function of ground and surface water evolution. The software packages EQ3NR (Wolery, 1992a) and PHREEQC (Parkhurst, 1995) were used for speciation and mineral saturation calculations. These programs use different databases and as a result it was found that they produced somewhat different results (e.g., Tables 3.2, 3.3). Although the database used by PHREEQC (WATEQ4F) has a more limited suite of included elements, this database was considered to be more up to date and internally consistent than the EQ3NR databases and therefore the PHREEQC results were used more extensively. Examination of the main EQ3NR database shows that this database is incomplete or out of date for many species. The software packages NETPATH (Plummer et al., 1995) and

The Geochemist's Workbench (Bethke, 1994) were used to investigate groundwater reaction pathways, mixing, and adsorption processes. The uses and abuses of geochemical modelling have been presented in detail elsewhere (Bethke, 1996; Carmichael and Eugster, 1987; Melchior and Bassett, 1990).

Statistical manipulation of the data, including correlation coefficients, factor analysis, cluster analysis and principal component analysis were carried out using the software DataDesk. In some calculations, obvious outliers were removed from the statistical database. For example, sample MLW95-300 was taken from a small seep flowing into the small gossan pit where the Restigouche ore body crops out. This water sample had two orders of magnitude higher concentrations of most trace elements compared to the other surface water samples from the Restigouche deposit, and therefore skewed correlation and factor analysis calculations. As a result, it was not included in the main statistical analysis for Restigouche surface waters.

Geochemical data is treated differently from most other types of data because geochemical data is considered as parts of a whole, e.g., ppm, weight % (Rollinson, 1993). As a consequence, geochemical data is commonly mistreated. The arithmetic mean is the most commonly used summary statistic but the problem with it is that it assumes that the data is normally or log-normally distributed (Rollinson, 1993). The data generated from this study is typically not normally or log-normally distributed.

Spatial relationships of surface waters and stream sediments were investigated using the GIS software package MapInfo. For maps showing geochemical anomalies, data that was below detection was included with a value set to half the detection limit. For maps showing spatial variation as a function of lithology, data that was below detection was typically excluded from the data set. The use of GIS in geological applications has recently been reviewed by Bonham-Carter (1993).

Table 3.1 Analytical detection limits and QA/QC results

Medium	Water			Bulk rock/stream sediment		HNO_3	Water	Water
Method	ICP-ES	ICP-MS	Ion chrom.	ICP-ES	ICP-MS		Replicates[1]	Field std[2]
unit	ppb	ppb	ppb	wt%	ppm	ppb		ppb
HCO_3							0.16	560
SO_4			50				0.40	50
Cl			50				0.48	130
NO_2			50					
NO_3			50					
F			50				8.31	
PO_4	1.1		50					
Br	0.54		50	0.01				
Si	3.3			0.5		<2	0.10	51.7
Ti	0.4 (0.05)			0.02		<0.05		
Al	5.5	0.5 (2)		0.2		<0.5	4.09	2.9
Fe	1.9	3 (5)		0.06		<0.5	1.61	2.6
Mn	0.2	0.2 (0.1)		0.01		<0.05	0.62	0.26
Mg	1.1			0.04		<0.09	0.21	26.3
Ca	2.8			0.01		0.5	0.24	92.4
Na	12.1			0.03		<2	0.29	196
K	12			0.05		<2	0.29	10.5
Ag		0.2			0.1	<0.005		
As	12	1				<0.1	2.24	
B	9.5					≤6	2.94	
Ba	0.6	0.5		0.003		≤0.08	0.96	0.39
Be	0.1	1				<0.005		
Bi		0.2			0.5	<0.005		
Cd	0.3	0.5 (0.005)			0.2	<0.005		
Co	3.1	0.2 (0.005)				<0.05	0.29	
Cr	29	2		0.02		0.016		
Cs		0.2			0.02	<0.005		
Cu	0.4	0.5 (0.05)				≤0.05	27.05	0.66
Ga		0.2			0.1	<0.1		
Hg		0.2				<0.1		
In		0.2 (0.001)			0.05	<0.005		
Li	0.6					<0.01		
Mo		0.5			0.2	≤0.02	0.61	
Ni	1.6	1 (0.1)				≤0.1		
Pb	9.4	0.2 (0.005)			2	0.005	8.54	0.07
Rb		0.2			0.05	<0.005	0.96	0.03
Sb		0.2				<0.01	3.40	
Sc	0.3					<0.005		
Se	23.8	2					33.33	
Sr	0.2					<0.005	0.11	0.51
Tl		0.2			0.02	<0.005		
U		0.2 (0.001)			0.02	<0.005	2.78	
V	1	0.2 (0.01)				<0.005		
Zn	0.32	2 (0.1)				<0.06	5.30	1.05
Hf					0.05	<0.005		
Nb					0.05	<0.005		
Sn					0.5	<0.01		
Ta					0.2	<0.005		
Th					0.02	<0.01		
Y		0.002			0.02	<0.005		
Zr					0.5	<0.005		
La		0.005			0.1	<0.005		
Ce		0.005			0.1	<0.005		
Pr		0.001			0.02	<0.005		
Nd		0.001			0.1	<0.005		
Sm		0.001			0.02	<0.005		
Eu		0.001			0.02	<0.005		
Gd		0.001			0.02	<0.005		
Tb		0.002			0.02	<0.005		
Dy		0.001			0.02	<0.005		
Ho		0.001			0.02	<0.005		
Er		0.001			0.02	<0.005		
Tm		0.001			0.02	<0.005		
Yb		0.001			0.05	<0.005		
Lu		0.001			0.02	<0.005		

Numbers in parentheses indicate chelation ICP-MS
HNO_3 analysis from Seastar Chemicals
[1] average difference between replicate pairs
[2] standard deviation of field standards

Table 3.2 Comparison between speciation results for selected Restigouche deposit groundwaters: PHREEQC versus EQ3NR

Sample#	MLW95-561 B-80-15	MLW95-365 EH-1	MLW95-606 MM-88-02	MLW95-364 MM-88-06	MLW95-508 MM-89-106	MLW95-561 B-80-15	MLW95-365 EH-1	MLW95-606 MM-88-02	MLW95-364 MM-88-06	MLW95-508 MM-89-106
			PHREEQC					EQ3NR		
$HAlO_{3,aq}$						5.40	7.84	6.28	25.24	
$Al(OH)_3^*$	0.70	68.81		2.53			22.65		4.36	
$Al(OH)_3$	2.30	6.70	0.79	4.28						
$Al(OH)_4^-$	96.95	8.34	99.13	92.57	99.98					
Al^{+3}		2.03					20.53			
$Al_{13}O_4(OH)_{24}^{+7}$						73.08				
AlF^{+2}									2.46	
AlF_2^+				0.44		0.53			15.30	
AlF_3				0.11					3.45	
AlO2-						20.27		91.65	48.56	99.36
$AlOH^{+2}$		13.29					45.90			
$AlSO_4^+$		0.83					2.20			
$NaAlO_{2,aq}$								1.80		
Ba^{+2}	89.62	93.79	98.62	84.01	89.23	99.97	100.00	97.76	99.98	96.83
BaCl+								2.22		
$BaCO_3$			0.20		9.08					2.67
$BaHCO_3^+$	1.68		1.18	0.80	1.68					
$BaSO_4$	8.61	6.11		15.17						
Ca^{+2}	93.74	97.34	97.77	92.11	73.72	96.46	98.60	96.98	95.94	86.02
$CaCl_2$								1.95		
$CaCO_3$	0.32		0.65		24.31					12.06
CaF^+										
$CaHCO_3^+$	2.34	0.14	1.55	1.17	1.85	1.60		0.51		1.53
$CaPO_4^-$										
$CaSO_4$	3.59	2.53		6.62		1.78	1.38		3.29	
$Cd(CO_3)_2^{-2}$					1.25	100.00	100.00		100.00	100.00
$Cd(OH)_2$					0.26					
Cd^{+2}	88.96	95.93		83.66	12.83					
$CdBr^+$										
$CdCl^+$	0.26	0.14		4.81	39.87					
$CdCl_2$					5.41					
$CdCl_3^-$					0.11					
$CdCO_3$	0.15				2.01					
CdF^+										
$CdHCO_3^+$	5.50	0.33		2.63	0.80					
$CdOH^+$	0.17				2.28					
CdOHCl					35.16					
$CdSO_4$	4.92	3.60		8.69						
$Cu(CO_3)_2^{-2}$	0.12				0.27					42.63
$Cu(OH)_2$	43.37	0.81		2.28	98.06					
Cu^+	1.53	0.84		84.30		0.85			89.23	
Cu^{+2}	4.14	88.90		0.83		6.71	96.22		1.93	
$CuCl_2^-$				9.64	0.52				2.14	1.21
$CuCl_3^{-2}$										
$CuCO_3$	45.69	1.62		2.38	1.09	85.74			5.75	48.96
$CuCO_3(OH)_2^{-2}$										3.85
$CuHCO_3^+$	4.06	4.88		0.41						
$CuOH^+$	0.93	0.59				6.34	3.00			2.85
$CuSO_4$	0.16	2.36								
$Fe(OH)_2^+$	7.82				0.12	3.48				
$Fe(OH)_3$	22.54				33.89	33.98				61.13
$Fe(OH)_4^-$	0.46				65.98					38.79
Fe^{+2}	53.78		62.91	84.65		33.40	96.63	73.15	70.76	
$FeCl^+$			21.86					4.95		
$FeCO_3$	2.65		5.96	1.09		2.54		3.81	1.26	
$FeHCO_3^+$	10.52		7.84	8.41		25.38	0.95	17.47	24.48	
$FeOH^+$	0.38		1.33	0.31						
$FeSO_4$	1.83			5.42		0.81	1.79		3.21	
K^+	99.86	99.91	100.00	99.75	100.00	99.85	99.90	99.62	99.72	99.94
KSO_4^-	0.14			0.25						
Mg^{+2}	93.35	96.92	98.14	91.09	81.92	95.72	97.96	90.67	94.43	89.90
$MgCl^+$								8.71		1.51
$MgCO_3$	0.18		0.37		15.39					6.93
MgF^+	0.13			0.11		0.89			0.68	

Table 3.2 Comparison between speciation results for selected Restigouche deposit groundwaters: PHREEQC versus EQ3NR

Sample#	MLW95-561 B-80-15	MLW95-365 EH-1	MLW95-606 MM-88-02	MLW95-364 MM-88-06	MLW95-508 MM-89-106	MLW95-561 B-80-15	MLW95-365 EH-1	MLW95-606 MM-88-02	MLW95-364 MM-88-06	MLW95-508 MM-89-106
$MgHCO_3^+$	2.14	0.12	1.43	1.06	1.88	1.55				1.63
$MgOH^+$					0.64					
$MgPO_4^-$					0.11					
$MgSO_4$	4.19	2.95		7.69		2.61	2.02		4.78	
Mn^{+2}	72.86	96.78	38.88	83.47	5.88	91.86	97.77	84.67	93.23	18.81
$MnCl^+$			39.87	0.20	0.78			12.03		
$MnCl_2$			4.38							
$MnCl_3^-$			0.30							
$MnCO_3$	11.89	0	12.19	3.55	91.98	4.31		2.72	1.02	79.76
$MnHCO_3^+$	12.71	0.94	4.31	7.39	1.03	1.01				
$MnOH^+$					0.32					0.63
$MnSO_4$	2.48	2.24		5.35		2.73	2.21		5.15	
Na^+	99.79	99.93	99.92	99.76	99.52	99.55	99.91	97.31	99.60	99.07
$NaCl_{(aq)}$								2.54		
$NaCO_3^-$					0.36					
$NaHCO_3$	0.11				0.11					
$NaSO_4^-$				0.18						
$Pb(CO_3)_3^{-2}$			0.78	0.11	32.58					
$Pb(OH)_2$					0.67					
Pb^{+2}		81.13	1.14	8.65		99.92	99.97		98.73	64.65
$PbCl^+$			11.44	0.21					1.25	32.25
$PbCl_2$			4.57							3.03
$PbCl_3^-$			0.91							
$PbCl_4^{-2}$			0.11							
$PbCO_3$		4.78	78.39	80.49	65.86					
$PbHCO_3^+$		7.06	1.13	6.83						
$PbOH^+$		1.05	1.49	1.94	0.80					
$PbSO_4$		5.93		1.75						
Rb^+	100.00	100.00	100.00	100.00	100.00	99.98	100.00	98.60	99.98	99.77
$RbCl_{(aq)}$								1.40		
Sr^{+2}	93.58	97.37	97.89	92.10	86.52	96.99	97.72	95.78	94.60	94.87
$SrCl^+$								4.19		
$SrCO_3$	0.12		0.25		10.87					4.20
$SrHCO_3^+$	2.80	0.16	1.87	1.40	2.60					
$SrSO_4$	3.50	2.47		6.47		2.96	2.28		5.37	
$Zn(CO_3)_3^{-2}$	1.03		1.84		61.60					
$Zn(OH)_2$	0.36		1.56	0.12	21.39					
$Zn(OH)_3^-$					0.14					5.33
Zn^{+2}	57.13	95.63	27.70	74.95	0.37	96.26	99.93	87.64	98.16	63.16
$ZnCl^+$			18.77	0.12				5.73		
$ZnCl_2$			4.95					1.48		
$ZnCl_3^-$			1.40							
$ZnCl_4^{-2}$			0.18					3.04		
$ZnCO_3$	23.41	0	21.82	8.00	14.64					
$ZnHCO_3^+$	14.07	1.32	4.34	9.38		3.09		0.89	1.44	2.17
$ZnOH^+$	1.40		2.03	0.94	0.87			0.80		28.47
ZnOHCl			15.42		0.86					
$ZnSO_4$	2.57	2.91		6.33						
AsO_4^{-3}					0.54					
$As(OH)_{3(aq)}$								43.22		
AsO_3^-								1.62		
AsO_3F^{-2}						97.38				
$H_4AsO_3^-$			2.74					1.36		
$H_3AsO_4^-$	20.37		2.24	32.90	0.27					
H_3AsO_3			68.56	1.13						
$HAsO_{3(aq)}$								51.60		
$HAsO_3F^-$						2.62				
$HAsO_4^{-2}$	79.62		26.45	65.96	99.20			2.13		99.26

Table 3.3 Comparison between saturation indices results for selected Restigouche deposit groundwaters: PHREEQC versus EQ3NR

Species	MLW95-561 B-80-15	MLW95-365 EH-1	MLW95-606 MM-88-02	MLW95-364 MM-88-06	MLW95-508 MM-89-106	MLW95-561 B-80-15	MLW95-365 EH-1	MLW95-606 MM-88-02	MLW95-364 MM-88-06	MLW95-508 MM-89-106
			PHREEQC					EQ3NR		
Albite	-3.93	-6.45	-1.81	-4.91	-3.20	-0.18	-3.01	2.29	-0.76	1.16
Alunite	-4.01	-2.09	-15.06	-6.14		-3.42	-2.47		-4.36	
Analcime	-5.11		-2.88	-5.96	-3.93	-0.74	-3.47	1.77	-1.20	0.93
Anglesite		-3.63	-9.96	-3.70		-3.41	-3.39		-2.57	
Anhydrite	-2.56	-3.51	-5.30	-2.51	-6.49	-2.72	-3.69		-2.67	-6.76
Annite	6.45			6.09	-2.24	-2.81		1.82	-2.29	
Anorthite	-2.99		-3.84	-6.60	-5.38	-3.55		-3.35	-6.36	-4.62
Aragonite	-0.55	-4.12	0.66	-1.36	0.64	-0.81	-5.07	0.37	-1.67	0.53
Barite	-0.42	-0.53	-1.13	0.20	-2.43	-0.08	-0.22		0.56	-2.22
Beidellite	1.15	-1.41	-1.44	-2.24	-4.97	6.46	3.07	4.60	3.83	1.42
Boehmite	1.11	0.24	-0.15	-0.17	-1.23	2.30	1.12	1.66	1.42	0.65
Calcite	-0.41	-3.98	0.80	-1.22	0.78	-0.67	-4.92	0.52	-1.53	0.68
Celestite	-3.18	-3.90	-4.31	-2.82	-5.72	-4.12	-4.87		-3.78	-6.78
Cerrusite		-2.87	-2.63	-1.19	-3.04	0.24	-3.02		0.18	0.92
Chalcedony	-0.58	-0.57	-0.68	-0.70	-1.02	0.26	0.27	0.08	0.14	-0.20
Chamosite-7A						-0.10		1.01	-0.80	
Chlorite14A	-4.95		2.05		5.46	-5.88		2.00		5.87
Cristobalite	-0.54	-0.54	-0.65	-0.66	-0.98	-0.52	-0.52	-0.71	-0.64	-0.99
Cuprite	-3.82	-6.45		-1.13	-5.47	-3.77	-6.69		-0.48	-2.93
Diaspore	2.81	1.94	1.55	1.53	0.48	2.73	1.55	2.10	1.85	1.08
Diopside	-5.36	-13.10	-1.72	-7.11	0.20	-6.92		-3.49		-1.39
Dolomite	-0.90		1.61	-2.42	1.59	-0.45		2.03	-2.05	2.37
$Fe(OH)_{3a}$	1.86		-1.61	-0.44	0.70	0.01		-3.55	-2.25	-5.22
Fluorite	-1.98			-2.27	-3.73	-2.37			-2.67	
Gibbsite	1.58	0.71	0.32	0.30	-0.75	2.21	1.02	1.56	1.33	0.55
Goethite	7.75		4.29	5.45	6.59	5.34	-2.54	1.78	3.07	0.11
Gypsum	-2.34	-3.29	-5.09	-2.29	-6.28	-2.39	-3.36		-2.35	-6.44
Halite			-2.89		-4.59			-2.89		-4.55
Hematite	17.51		10.59	12.91	15.19	11.60	-4.15	4.49	7.07	1.14
Illite	0.22	-3.51	-1.37	-3.33	-4.35	5.58	1.14	5.14	2.96	2.51
Jarosite-K	-5.02					-7.46				
K-Feldspar						2.06	-0.37	2.84	0.81	1.56
Kaolinite	3.70	1.95	0.95	0.89	-1.86	6.11	3.74	4.46	4.10	1.87
Kmica	6.34	2.48	4.23	2.14	0.57	8.00	3.20	7.50	5.00	4.20
Laumontite	0.01	-5.58	-1.08	-3.84	-3.27	2.94	-3.27	2.76	-0.11	0.93
Magnesite	-1.07	-4.69	0.23	-1.78	0.23	-1.50	-5.80	-0.22	-2.25	-0.03
Magnetite	19.04		13.25	14.86	14.19	9.45		3.62	5.51	-7.58
Melanterite	-6.94		-10.47	-5.66	-16.57	-6.90			-5.46	
Montmorillonite-Ca	1.55	-1.11	-1.47	-2.01	-4.99	5.41	1.52	4.55	3.09	2.40
Phlogopite	-9.78	-23.58	-3.46	-13.53	-1.04	-4.44		2.18		4.94
Pyrophyllite	5.86	4.12	2.91	2.82	-0.58	5.43	3.07	3.41	3.18	0.26
Quartz	-0.15	-0.15	-0.25	-0.27	-0.59	0.55	0.55	0.37	0.43	0.08
Rhodochrosite	-0.01	-4.38	-0.83	-0.65	0.29	-0.77	-5.90	-1.58	-1.50	-0.16
Sepiolite	-5.57	-13.35	-1.97	-7.33	-0.34			-2.63		1.09
Siderite	-0.23		0.23	0.20	-4.73	-1.18		-0.55	-0.64	
SiO_{2a}	-1.41	-1.41	-1.52	-1.54	-1.86	-0.86	-0.86	-1.05	-0.98	-1.33
Smithsonite	-1.75	-4.32	-0.79	-1.31	-2.77	-2.11	-5.53	-1.06	-1.83	-0.77
Strontianite	-2.51	-5.84	0.31	-3.01	0.07	-1.22	-5.25	1.51	-1.78	1.50
Talc	-4.05	-15.72	1.43	-6.64	4.02	-3.66		1.44	-6.24	4.35
Tremolite	-10.17	-37.31	2.60	-16.25	9.03			-3.63		3.50
Witherite	-3.80	-6.52	-0.55	-4.04	-0.68	1.12	-2.30	4.24	0.86	4.37

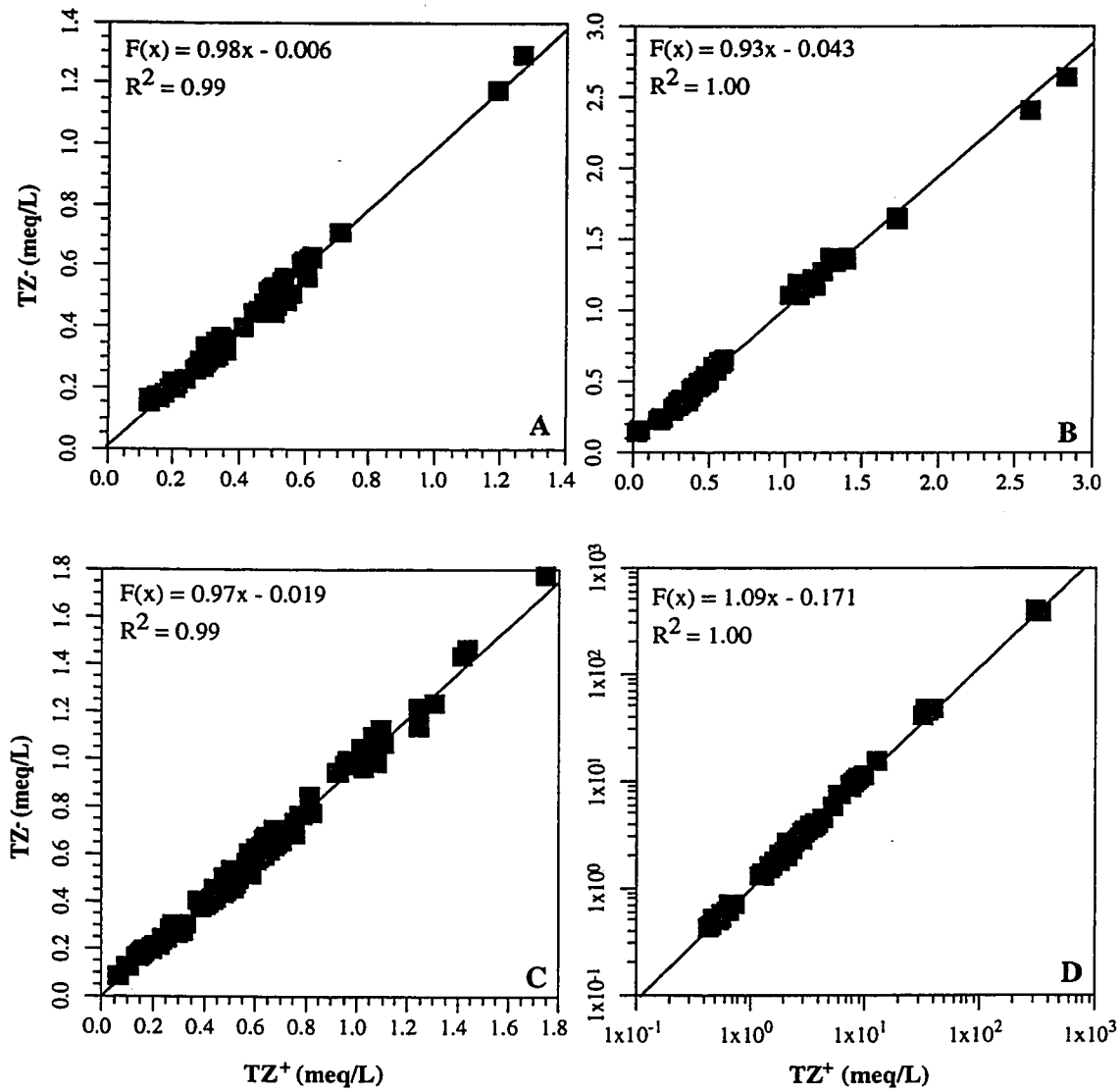


Fig. 3.1 Plots showing the charge balance between cations (TZ^+) and anions (TZ^-) for A) Halfmile Lake deposit surface waters, B) Halfmile Lake deposit groundwaters, C) Restigouche deposit surface waters, and D) Restigouche deposit groundwaters.

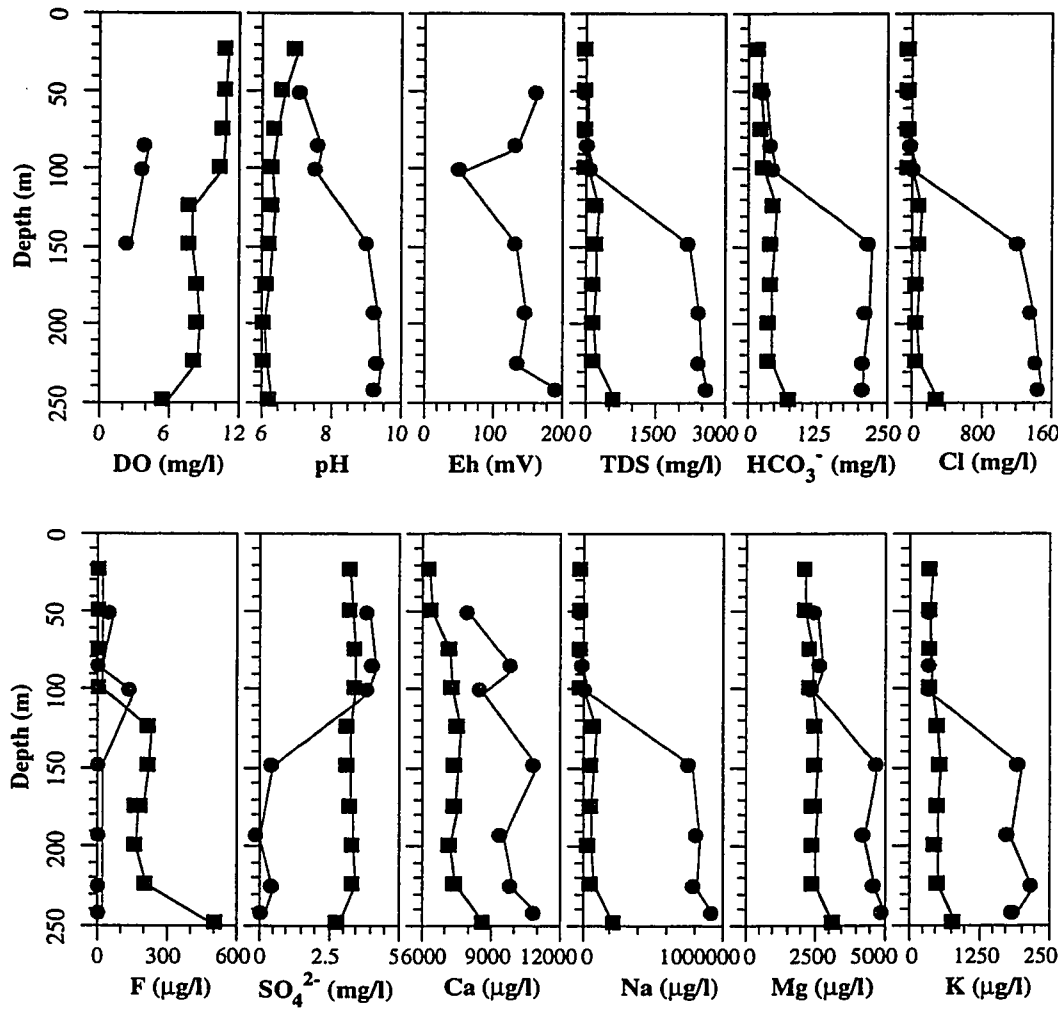


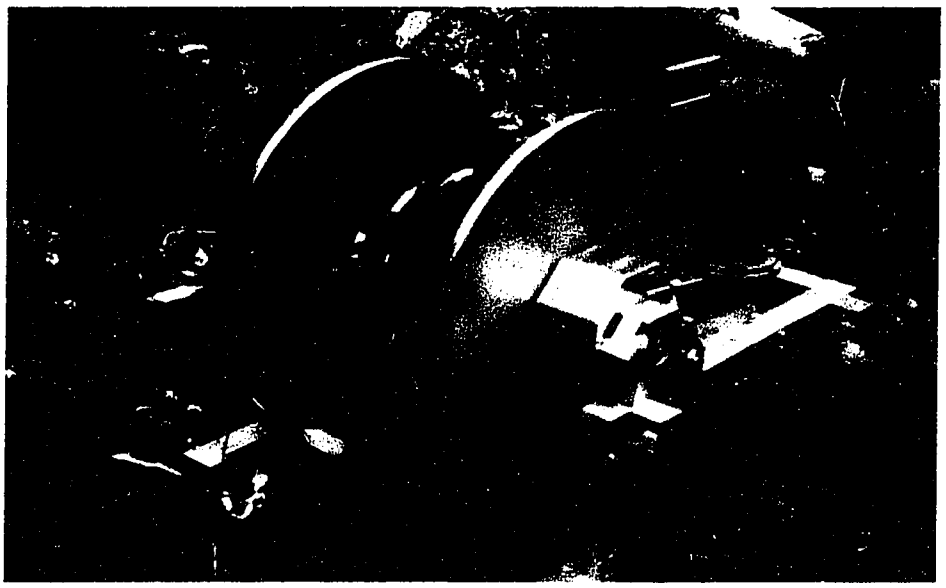
Fig. 3.2 Downhole variation plots of selected parameters for borehole MM-89-106 from the Restigouche deposit. Squares are bailer samples, circles are packer samples. These plots illustrate the differences between samples collected using the bailer system and those using the packer system. In this case, the bailer samples indicated that there were significant chemical changes downhole, but did not reflect the full magnitide of those changes. See Chapter Seven for more detail.



A



B



C

Fig. 3.3 A) Top packer prior to lowering into borehole. Once the system is inplace nitrogen gas is used to infalte the packer (black section). B) Sample chamber. connected to the top of the top packer with a 1 psi uni-directional cracking valve at the base of the chamber to prevent return flow to the sampled zone. C) Winch apparatus with nitrogen tank in the background.

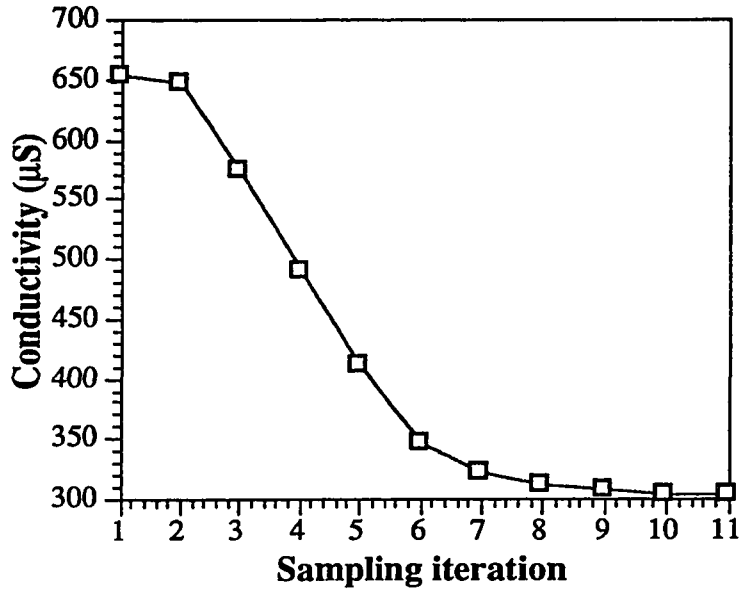


Fig. 3.4 Plot of sampling iteration vs electrical conductivity for borehole B-80-7. Samples for analysis are taken after the conductivity reaches a steady state which is assumed to represent groundwater flowing at the packed-off depth.

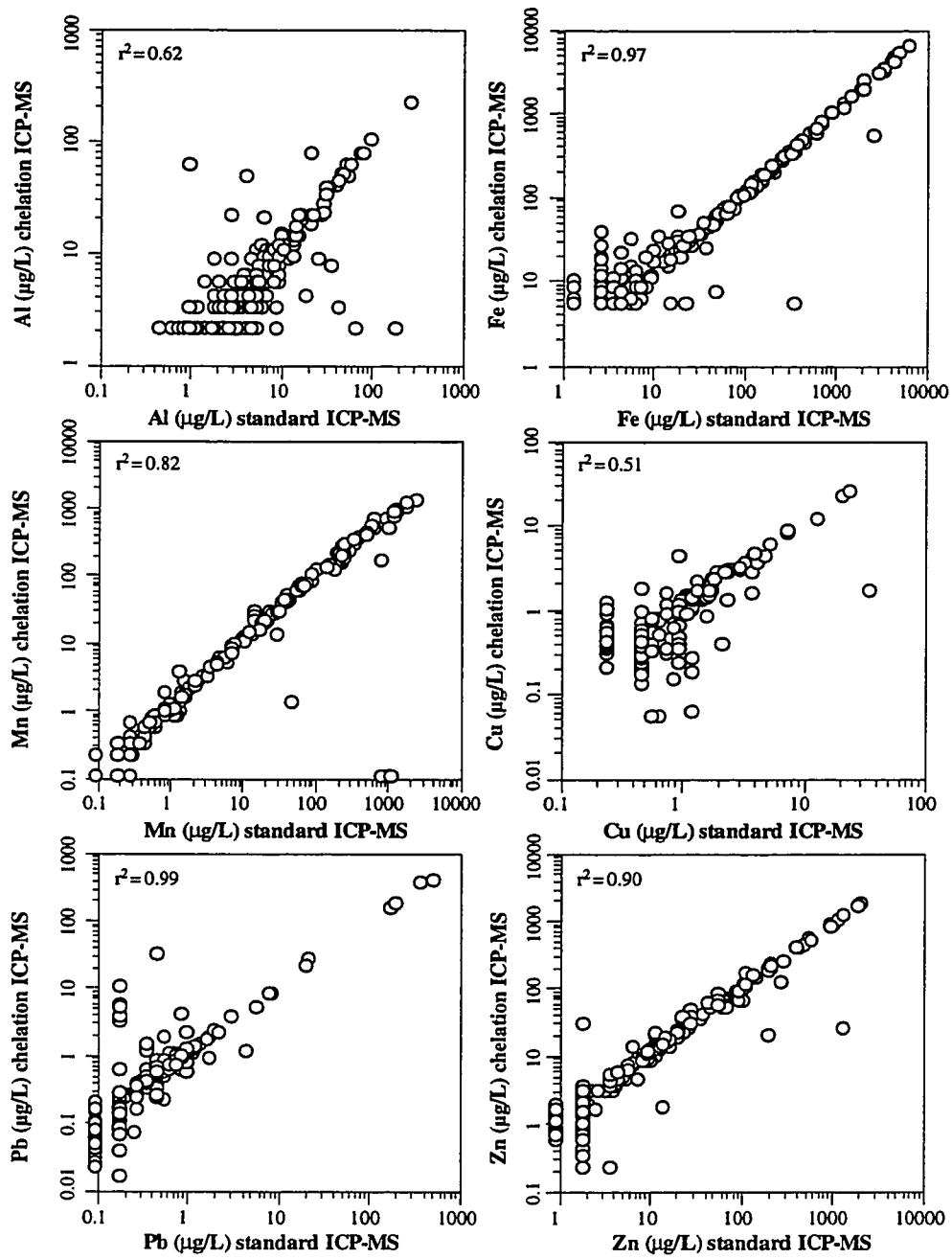


Fig. 3.5 Comparison of trace element analytical results for total nebulization ICP-MS and Chelation ICP-MS. There is very good correlation for Fe, Mn, and Zn. Pb and Cu generally correlate well. Al shows the poorest correlation.

CHAPTER FOUR:
PHYSICAL HYDROLOGY AND FRACTURE ZONE MINERALOGY OF THE HALFMILE LAKE AND RESTIGOUCHE Zn-Pb MASSIVE SULPHIDE DEPOSITS, BATHURST MINING CAMP, NEW BRUNSWICK

4.1 Introduction

This study is primarily focussed on the hydrogeochemistry of ground and surface waters which are interacting with undisturbed (at the time of sampling) massive sulphide deposits in the Bathurst Mining Camp (BMC) of northern New Brunswick. The background geology of the study areas was described in Chapter Two. This chapter presents a brief description of the present ground and surface water flow conditions based on the limited data available such as topography, borehole geophysics, direct observations of drill core, and the response of the straddle-packer during groundwater sampling (see Chapter Three for sampling methodology). The only viable approach (Memon, 1995) to interpret the subsurface hydrology and groundwater flow at the Halfmile Lake and Restigouche deposits is to utilize field observations of locations of springs, artesian boreholes, and water levels in boreholes. Scanning electron microscope (SEM) data was collected for fracture zone samples from drill core in several boreholes intersecting the Restigouche deposit in order to characterize the mineral assemblage with which groundwaters might be in contact.

The geology of the Halfmile Lake and Restigouche deposits is similar. Both deposits are hosted in an Ordovician volcanic-volcaniclastic sequence which is interpreted to have been formed in a continental back-arc basin (van Staal et al., 1992). Host rocks are dominantly felsic in composition, although younger mafic volcanic rocks and derived metasedimentary rocks are present in both areas, and mafic dykes are common in the footwall to the Restigouche deposit. The mineralogy of the massive sulphide deposits are similar in that both are dominated by pyrite, sphalerite and galena, with variable chalcopyrite (and pyrrhotite at the Halfmile Lake deposit) in footwall sulphide stringer zones.

4.2 Geomorphology and Landuse

The Halfmile Lake catchment area is dominated by steep sided slopes (Fig. 4.1). Topographically, the Restigouche deposit study area is similar to the Halfmile Lake deposit with slightly more subdued relief and a more extensive drainage system (Figs. 4.2, 4.3). Both study areas show evidence of glaciation during the Late Wisconsonian and are variably covered by a thin veneer of basal till over weathered bedrock (Parkhill and Doiron, 1995). Till cover thickens in the valleys at both deposits but is generally only 1-2 meters thick. Hill tops and ridges commonly have bedrock exposures with little or no till cover (Parkhill and Doiron, 1995). Evidence from till geochemistry, glacial stria, and pebble lithologies indicates that the dominant ice-flow direction at both the Halfmile Lake and Restigouche deposits was dominantly west to east (Parkhill and Doiron, 1995). Later ice movement was to the northeast (Parkhill, 1997). Glacial transport is generally limited to about 0.5 km, although boulder erratics at the Halfmile Lake deposit originate 23 - 30 km to the west (Parkhill and Doiron, 1995).

4.2.1 Preglacial climate

Gossans represent the weathered remnants of massive sulphide oxidation (Boyle, 1996). In the BMC, many of the massive sulphide deposits, including the Halfmile Lake and Restigouche deposits, have gossans capping the surface expressions of the ore deposits. At the Halfmile Lake deposit, the gossan outcrops on the Upper AB zone, a topographic high point at this deposit (Fig. 4.1). In contrast, a small gossan is present at the Restigouche deposit on the south side of Charlotte Brook, and is situated in a topographic low in the lee of Mt Brittain (Figs. 4.2, 4.3). As well as being economically important (Boyle, 1996), the gossans provide good evidence for the preglacial weathering conditions in the BMC. Symons et al. (1996) presented paleomagnetic data from gossans from the Murray Brook and Heath Steele deposits, and concluded that they were produced by weathering in a temperate climate sometime between 1-3 Ma BP. Their calculations suggest that gossans as large as the Murray Brook gossan

deposit require on the order of one Ma to form. Bedrock at both the Halfmile Lake and Restigouche deposits is typically fractured and extensively weathered in the uppermost 50 m or so, with extensive Fe-oxide formation along fracture surfaces. Much of this weathering is interpreted to be preglacial in origin.

4.2.2 Present-day climate

The Wisconsonian ice sheet is interpreted to have retreated from most of New Brunswick by about 12.4 to 12.1 ka BP, although highlands in the Northwest may have had ice sheets until as late as 11.5 ka BP (Cwynar et al., 1994). Cwynar et al. (1994) suggested that boreal forest ecosystems were not established in central New Brunswick until after the Younger Dryas (11 to 10 ka BP) (Cwynar et al., 1994; Wilson et al., 1993).

Precipitation and river discharge data for several sites in northern New Brunswick are available from Environment Canada (Canada, 1991). Precipitation records (monthly values) are incomplete but date back to 1967 for the Upsalquitch Lake station (Fig. 4.4) and to 1928 for the Nepisiguit Falls station (Fig. 4.5). Discharge data for these stations (daily and mean monthly records) are somewhat more complete with almost continuous records to 1918 for the Upsalquitch River (except for the years 1933-1943) and to 1921 for the Nepisiguit Falls station. For both the Upsalquitch and Nepisiguit rivers, there is a strong increase in discharge typically beginning in late April and reaching a maximum in May (Figs. 4.4, 4.5). In many of the yearly cycles, there is a smaller peak in discharge in October/November. Less commonly, a smaller peak can be observed, generally occurring in July (Figs. 4.4B, 4.5B). The significance of this data is that, as will be shown in subsequent chapters, the surface waters collected in this study very closely approximate base flow conditions, based on the geochemical (Chapter Five) and stable isotopic (Chapter Eleven) similarity between shallow groundwaters and surface waters. The oxygen and deuterium stable isotopic composition of surface waters and shallow groundwaters strongly indicates that recharge is dominated by winter precipitation released in the spring as snow melt. This is supported by the discharge data for Upsalquitch and

Nepisiguit river hydrometric stations. Only the monthly data for the last ten years of records are shown for the precipitation data (Figs. 4.4C, 4.5C), but the full data sets show the same relationships. Essentially, the precipitation records show that there is not a marked seasonal effect in the monthly amounts of precipitation. Peaks occur in different months in different years and there is no apparent consistency in terms of timing of maximum monthly precipitation. This is also shown by the IAEA (International Atomic Energy Agency) stable isotope monitoring stations at St Agathe, Quebec and Truro, Nova Scotia (see Fig. 11.2, Chapter Eleven). For the Upsalquitch Lake precipitation station, the average annual temperature, based on mean monthly averages for the years 1967 to 1993, is 6.3°C, with a monthly average ranging between -13.8 and 23.1°C. For the Nepisiguit Falls station, the mean annual temperature for the years 1928 to 1993 is 9.9°C, with a monthly mean temperature ranging from -9.6 to 28.9°C. The Nepisiguit Falls station is closer to the ocean and at lower elevation, accounting for the differences in temperatures for the two stations.

At the time of sampling, both deposits were essentially undisturbed with the exception of exploration drilling at both deposits since the 1950's. The primary landuse is logging for wood pulp. Both deposits are forested and are dominated by boreal forest type vegetation including black and red spruce, jack pine, balsam fir and birch. Alders are common in swampy areas of valley bottoms. Subsequent to sampling in 1996, the Restigouche deposit was put into production as an open pit operation.

4.3 Hydrogeology of the Halfmile Lake Deposit

4.3.1 Surface water environment

The digital elevation model (DEM) of the Halfmile Lake deposit study area was calculated based on provincial topography data regridded in ARCINFO at a contour interval of 10 meters. The DEM shows the generally steep sided valleys (Fig. 4.1). The main streams sampled at the Halfmile Lake deposit include the Upper/Lower AB, Halfmile North, Northeast tributary, North tributary and West tributary streams. All these streams ultimately drain into the

Northwest Miramichi River which flows from northwest to southeast to the south of the study area (Fig. 4.1). The Upper/Lower AB stream is fed by seeps at a break in slope and runs west to east. This stream runs parallel to the strike of the main ore body which crops out at the Upper AB zone and dips steeply to the north. Boreholes drilled in the Lower AB zone intersect the main ore zone at depths up to 1000 meters. Boreholes drilled close to the Upper/Lower AB stream are typically capped as they are artesian in the spring and early summer, indicating that the stream represents a zone of discharge. The Halfmile North stream drains the southwest slope of the Halfmile North zone. This zone is an extension of the main ore body as the strike changes from east-west to a northeast trend (Adair, 1992). This stream is approximately coincident with the surface projection of a major fault (Fig. 4.6). The northeast tributary drains more mafic lithologies and flows from the northeast. The Upper/Lower AB, Halfmile North, and Northeast tributary streams merge to form what is here referred to as the North tributary stream. This stream flows to the south and eventually joins the Northwest Miramichi River, one of the major salmon fishing rivers on the east coast of Canada. The final stream sampled is the West tributary which flows to the west away from the Upper and Lower AB zones. The saddle between the Upper and Lower AB hills therefore represents a groundwater divide. The West tributary eventually flows into the Northwest Miramichi River.

Within the study area, most shallow groundwater flow is interpreted to be directed towards the Upper/Lower AB stream from the Upper and Lower AB streams, and to the Halfmile North stream from the Halfmile North deposit.

4.3.2 Groundwater environment

The Upper/Lower AB stream runs between the Upper and Lower AB deposits and marks the discharge site for shallow groundwaters draining the north side of the Upper AB and the south slope of the Lower AB hills (Fig. 4.1). Boreholes located near the bottom of the valley, close to the stream are typically capped as they are artesian in the spring and early summer. For example, sample MLW94-100 was sampled from an artesian BQ hole adjacent to the

Upper/Lower AB stream.

During the 1994 field season, a number of boreholes were tested to determine the depth to which they were open. Caving and collapse of boreholes is common at the Halfmile Lake deposit, and as a result, a relatively small number of holes were open to sufficient depth to warrant sampling by bailer and packer sampling methods. As part of the testing, water levels in the boreholes was determined with an electronic probe. Drilling by Noranda Exploration (1987 to 1996 drilling) was focussed on to Lower AB zone and a possible extension of the orebody to the west. Drilling and delineation of the shallow Upper AB zone of the deposit was done in the 1950's to early 1970's, and most of these boreholes have caved in. As a result, most of the holes sampled in this study are from the top of the Lower AB zone, extending south to the Upper/Lower AB stream valley (Fig. 4.7). Water table depths in boreholes at the top of the Lower AB zone are on the order of 20 meters below ground level. Boreholes towards the Upper/Lower AB stream show generally decreasing depths to the water table (6 - 11 meters), although the decrease is not uniform with decreasing collar elevation. This is most likely a result of fracture dominated flow conditions. Fracture-dominated flow can be highly variable over short distances resulting in upward and downward gradients (Sen, 1995). Boreholes close to the Upper/Lower AB stream have the shallowest depths to water table. Boreholes HB80-1, HN88-14, and the artesian borehole have water levels at or above surface (artesian on Fig. 4.7B). Borehole HN87-8 is close to the top of the Lower AB hill, yet has a relatively shallow water table (10.8 meters). This borehole intersects a major fault. Geochemical data (Chapters Seven and Ten) suggests that there may be rapid recharge to depth as well as upward gradients in this hole.

Visual examination of drill core for several of the boreholes sampled using the straddle packer indicates that the upper 50 to 100 m or so of bedrock is commonly highly fractured. These fractures are the most likely pathway for the bulk of the shallow groundwater flow. Fracture surfaces typically have Fe-oxide staining and carbonate minerals (±feldspar) and the rocks are weathered near the surface. Typically, below 150 m depth, the bedrock increases in

competence, and at greater depths, bedrock is commonly massive over core lengths of several meters to tens of meters. These observations are generally consistent with observations made by drilling crews during borehole emplacement. Some of the logs include geotechnical information, including water loss or return data. In general, in the upper parts of the holes, drilling water (mainly surface water from the Upper/Lower AB stream) was lost to bedrock, whereas with increasing depth, most holes for which there is data indicate water return.

The Halfmile Lake deposit has several major faults that lie parallel to the main lithologies. Based on drilling logs, an attempt was made using 3D visualization software to reconstruct these faults in three dimensions (Fig. 4.8). Most of the drill hole information is available as part of the EXTECH-II project. Using the software program LYNX, and based on fault density information in the drilling logs, five major faults were modelled and interpolated through the Upper and Lower AB zones of the Halfmile Lake deposit (Fig. 4.8). The modelling was not wildly successful due to inconsistencies in the fault information recorded by various geologists who logged the holes during drilling. However, Figure 4.8 gives a general impression of the geometry of major structures through the Upper and Lower AB zones.

Some of the boreholes at the Halfmile Lake deposit were sampled using the straddle-packer system. Although the straddle-packer system used in this study was not designed to measure hydraulic conductivities, a relative sense of groundwater flow is obtained based on how the system responds, i.e., the length of time required to develop a zone for sampling (see Chapter Three for a description of the methodology). In general, the packer response was much slower than at the Restigouche deposit. At the Halfmile Lake deposit, several days to a week was required to develop a zone to the point that groundwater electrical conductivity had levelled sufficiently to warrant groundwater sampling (Chapter Three). The packer response data would suggest that groundwater flow at the Halfmile Lake deposit is generally much slower than at the Restigouche deposit. However, observation of drill core showed that below 100 to 150 meters depth, zones of fractures considered likely to yield groundwaters were generally thin, and therefore hard to isolate with the packer apparatus. A curious observation is that whereas at

the Restigouche deposit the packer system worked extremely well, for the most part, at the Halfmile Lake deposit it proved very difficult to successfully sample groundwaters with the system. Failure of the packers was common, and a whole packer set was lost in one hole due to caving. It would seem that the very faulted nature of the deposit means that the ground is much more unstable than the Restigouche deposit, such that boreholes at the Halfmile Lake deposit are less conducive to this style of sampling.

4.4 Restigouche deposit

4.4.1 Surface waters

A DEM of the Restigouche deposit area was calculated in the same manner as for the Halfmile Lake deposit (Fig. 4.2). The study areas is characterized by 200-300 meters relief with steep sided valleys (Fig. 4.2). The main stream crossing the Restigouche deposit is Charlotte Brook which flows west to east and drains into the southeast Upsalquitch River. Charlotte Brook crosses the main ore zone of the Restigouche deposit close to its surface expression. Several smaller, fourth order, streams flow from the north and south into Charlotte Brook (Fig. 4.2). Other streams included in this study flow to the east and west of the deposit and drain into the Upsalquitch and Portage Brook rivers, respectively. Within the study area, most shallow groundwater flow is interpreted to be directed towards Charlotte Brook and its tributaries (Fig. 4.9).

Most of the streams sampled flowed throughout the summers of 1995 and 1996. A notable exception was the North stream which dried up by mid summer in the section adjacent to the main Restigouche ore body, although flow continued closer to the headwaters of this stream where it is fed by seeps, some of which flow through transported gossan. Two boreholes were sampled beside the North stream (boreholes MM-89-102 and MM-89-106; Fig. 4.10). Both these holes had water tables at slightly lower elevation than the adjacent stream bed. This would suggest that groundwater gradients are downward on the west side of the stream, consistent with the observation that this stream was mostly dry towards the latter part of the

1995 field season.

The Mt Fowler east stream bifurcates into two channels around a high knoll of land from which Fe-rich waters seep, indicating direct contribution from mineralized waters to the surface environment. Similarly, Fe-rich sediments in streams draining towards Portage Lakes suggest sulphide mineralization in the subsurface west of the main Restigouche deposit.

4.4.2 Groundwaters

A smaller number of boreholes was investigated at the Restigouche deposit compared to the Halfmile Lake deposit. Although the ground at the Restigouche deposit appears to be more stable than at the Halfmile Lake deposit, many of the boreholes drilled by Marshall Minerals in 1988 were not cased and are no longer evident at surface. However, several holes were sampled in a north-south transect through the main ore zone (boreholes B-80-7, MM-88-01, EH-1, MM-88-02, MM-88-06, and MM-88-07) and into hanging wall units south of the gossan (boreholes MM-89-100 and B-80-15). In addition, several boreholes east of the deposit (MM-89-102, MM-89-106, MM-89-107) and west of the deposit (MM-89-104 and MM-89-109) were sampled by bailer and/or straddle-packer. There is a small deposit (C4/C5 zone) one km to the northwest of the Restigouche ore body. Two artesian boreholes were found and sampled at this deposit.

Based on the water table levels in the holes close to the main ore zone, shallow groundwater flow is north to south, towards Charlotte Brook. Borehole MM-88-07 has the shallowest water table (2.5 meters below surface), and water table depths increase to the north with the deepest water table level observed in borehole B-80-7 (20 m below surface) which intersect massive sulphide mineralization close to its northern extent (Fig. 4.10). These data suggest that the immediate deposit area is a zone of recharge. Water table levels decrease to the east of the ore zone towards the North stream, indicating shallow groundwater flow to the south and southeast over the deposit (Fig. 4.9). An environmental report prepared in preparation of open pit operations at the Restigouche deposit suggested that average hydraulic conductivity in the

shallow bedrock aquifer are on the order of 1.5 x 10^{-4} cm/s (Group, 1996), and that groundwaters flowing through the deposit discharged at Charlotte Brook. However, as discussed in Chapters Five and Seven, there is evidence to indicate that the area in which Charlotte Brook crosses the deposit may be a losing (recharge) reach, based on geochemistry of stream waters and shallow groundwaters from boreholes MM-88-07 and MM-88-06.

Two boreholes were sampled in hanging wall units south of the gossan (boreholes B-80-15 and MM-89-100; Fig. 4.10). Both boreholes have similar water tables (6.5 to 7 m below surface), although shallow groundwater flow is interpreted to be to the north towards Charlotte Brook (Fig. 4.9). The shallowest groundwater samples from both these boreholes are compositionally similar ($CaHCO_3$-type waters) with a slight increase in TDS and trace metal values from borehole MM-89-100 to borehole B-80-15, consistent with this interpretation (see Chapter Seven).

Visual examination of drill core was undertaken in order to identify zones suitable for groundwater sampling with the straddle packer system. The depth to which bedrock is significantly fractured is less than was the case for the Halfmile Lake deposit. As with the Halfmile Lake deposit, carbonate minerals have been weathered from the upper parts of the bedrock and Fe-oxides coat fracture surface to depths of 30 to 60 meters. For example, borehole MM-88-02 core is variably broken with intense Fe-oxide alteration along fractures to a depth of around 60 m.

In general, the straddle-packer system worked very well at the Restigouche deposit. Packer response to groundwater flow indicated that hydraulic conductivities may be generally higher than is the case for the Halfmile Lake deposit. This was the case for both shallow groundwaters and deeper, more saline, waters. The fact that saline waters dominated borehole MM-88-02 suggests that fractures transmitting these waters were overpressured.

4.5 Geophysical Evidence

4.5.1 Halfmile Lake deposit

As part of the EXTECH-II program, several boreholes at both the Halfmile Lake and Restigouche deposits were studied using downhole geophysical techniques by the borehole geophysics group at the Geological Survey of Canada (Mwenifumbo and Killeen, 1995). Two boreholes were logged at the Halfmile Lake deposit, boreholes HN94-63 and HN94-65 (Fig. 4.11; locations shown in Fig. 4.7). Borehole geophysical parameters of interest to hydrogeology include density, temperature, and temperature gradient logs (Mwenifumbo, 1993). For borehole HN94-63, temperature was not measured. However, based on the density and acoustic velocity logs (Fig. 4.11), there appears to be a few zones of anomalous density below 100 meters depth (logging was initiated at 60 meters). Density maxima between 510 and 550 meters and between 615 and 645 meters depth coincide with massive sulphide mineralization. There are several density minima at 130, 247, 285, and 589 meters depth. These are interpreted to represent fractures along which groundwaters may be flowing. Two groundwater samples were recovered from 400 and 450 meters depth in this borehole, and these $NaHCO_3$ waters are the highest TDS waters recovered to date from the Halfmile Lake deposit (226 mg/L total dissolved solids; Chapter Seven). These waters may originate from the apparent fracture set at 589 meters depth.

Borehole HN94-65 was logged for density as well as temperature (Fig. 4.11). This borehole differs from borehole HN94-63 in that there are no apparent density minima below 150 meters depth. Increases in density coincide with massive sulphide mineralization, however. Borehole HN94-65 was logged from close to surface, and it is apparent from both the density and temperature gradient logs that the upper 100 meters is heavily fractured, as noted previously based on drill core observation. Based on the density and temperature gradient data there is little evidence for deeper groundwater flow, with the exception of a temperature gradient anomaly at 225 meters depth. Sample MLW95-608 was collected using the straddle packer from 223 meters depth, coincident with the observation of fracturing at this depth in drill core. This groundwater has higher TDS (95 mg/L) than any of the bailer waters recovered from the full depth of the borehole (all < 55 mg/L TDS; Chapter Seven). The lack of

perturbations in the downhole geochemical profiles (bailer samples) at this depth for this borehole indicates that the fractures at 223-225 meters do not have a high hydraulic gradient; this is supported by the packer response.

4.5.2 Restigouche deposit

Boreholes B-80-7 and MM-88-02 were logged at the Restigouche deposit. Both boreholes penetrate massive sulphide mineralization (Fig. 4.12; Fig. 4.10 for borehole locations). Although only separated by about 300 meters, groundwaters recovered from both boreholes (bailer and straddle-packer) are very different (Chapter Seven).

Borehole MM-88-02 is the deepest hole drilled at the Restigouche deposit (600 metres depth). The hole is dominated by felsic and dacitic volcanic rocks in the upper parts of the hole, and by felsic volcanic rocks with cross-cutting mafic dykes at greater depth (Fig. 4.12). Density logs indicate extensive fractures to a depth of around 50 meters. Below that depth, density maxima are coincident with massive sulphide mineralization (67-76 meters) and mafic dykes at greater depth (Fig. 4.12). The only density minima of any note below the massive sulphides occurs at 251 meters depth. The temperature gradient log also shows an anomaly at this depth. In addition, the temperature gradient log is very irregular below 500 meters depth (Fig. 4.12). Saline waters with TDS values up to 22,000 mg/L were recovered from this hole, far in excess of TDS values for all groundwaters from the Halfmile Lake deposit. Based on the temperature gradient log, it is interpreted that these saline waters are flowing along fractures in the deeper parts of the borehole, below 500 meters depth. The density and temperature gradient anomaly at 251 metres was sampled with the straddle packer, and saline waters were also recovered from this zone. Therefore, these fluids may be flowing at depth as shallow as 250 meters. However, the fact that these waters dominate the hydrology of the hole (bailer samples were uniformly saline in composition) indicates that the fractures transmitting these fluids are over-pressured, and the fluids may have originated at depth but flowed upwards and outwards along more shallow fractures subsequent to drilling of the borehole.

Borehole B-80-7 was drilled to a depth of 240 meters and was logged for density and temperature (Fig. 4.12). Logging was started at 25 meters depth, and there are only minor anomalies in the density log at the top of the hole. Visual examination of drill core indicates that the bedrock is very fractured to a depth of 35 meters, below which the rock is more competent. The density logs suggest only one major fracture set at around 172 meters depth within the massive sulphides. There is a large associated temperature gradient anomaly at this depth (Fig. 4.12), indicating significant groundwater flow in which case the groundwater is not interacting significantly with the massive sulphides. A packer sample was collected from 173 meters depth and shows no anomalous values of Fe, Zn, or Pb (Chapter Seven). There are smaller temperature gradient anomalies below the massive sulphides, consistent with the observation of fault zones in drill core, and with relatively rapid groundwater flow, based on packer response.

4.6 Fracture Zone Mineralogy

Scanning electron microscopy was carried out on grain mounts of fracture zone material from the Restigouche deposit in order to better understand the relationships between groundwater flow along fractures and water-rock reactions. Essentially there was very little variation observed in the mineralogy of fracture gouge material (Figs. 4.13, 4.14). The dominant fracture minerals are illite (± sericite), quartz, minor albite, rare sulphides, chlorite/smectite and carbonate minerals (ferroan dolomite primarily). It is somewhat difficult to constrain the timing and age of alteration along fractures, given that the observed fracture zone mineralogy is very similar to the assemblage imparted by hydrothermal alteration during formation of the ore deposits during the Ordovician. To fully determine the paragenesis would require a detailed stable isotope study of the fracture minerals, outside the scope of this thesis.

Carbonate associated with the main Restigouche ore body occurs predominantly as massive veins and less commonly infilling pore spaces and coating fractures (See Chapter Eleven). SEM analysis indicates that discrete idiomorphic crystals are also present within a K-silicate matrix in fault and fracture gouge material (Fig. 4.14). K-silicates (illite, sericite) have

morphologies that ranges from fine grained fibrous (Fig. 4.13B), to platy and blocky (Figs, 4.13, 4.14). Kaolinite is less common and is present as platy and blocky, commonly equant, crystals (Fig. 4.13C).

4.7 Characteristics of Groundwater Flow

The bedrock at both the Halfmile Lake and Restigouche deposits consists predominantly of metamorphosed felsic volcanic rocks, intrusive equivalents and sediments derived from the felsic volcanics. Mafic volcanic rocks and derived sediments are also locally significant. In both study areas there are no aquifers in the true sense of the word. Groundwater flow is dominated by flow along fractures and faults, with the exception of the uppermost 50 - 150 m of bedrock where bedrock is typically broken so that groundwater flow more closely approximates flow in a porous medium. At greater depths at both the Halfmile Lake and Restigouche deposits, visual examination of drill core, as well as downhole geophysical logging, indicates that fractures are less common with increasing depth. This relationship of intense fracturing close to surface but significantly more competent rock at greater depth has been observed in other crystalline "aquifers", e.g., at the Strip Mine, Sweden (Nordstrom et al., 1989c) and southwest New Brunswick (Bottomley, 1984). One of the consequences of groundwater flow in this type of medium is that groundwater compositions can be highly variable over short vertical and horizontal distances (Nordstrom et al., 1989a; Sen, 1995). This is certainly the case at the Halfmile Lake and Restigouche deposits (Chapter Seven).

Based on the response of the packer, in terms of water recovery times, some of these deeper fractures are acting as conduits for groundwater flow. In the case of the Restigouche deposit, the deeper waters typically have much higher TDS values than shallow groundwaters. In contrast, at the Halfmile Lake deposit, no high TDS groundwaters were recovered, regardless of the depth of sampling (see Chapter Seven). This fundamental difference between the two deposits is interpreted to reflect the steeper structures present at the Halfmile Lake deposit (Fig. 4.8) that may have caused the flushing of saline fluids by more deeply circulating meteoric

waters.

4.8 Saline Waters at the Restigouche Deposit

One of the most critical questions regarding saline waters is how they have been preserved over time in their present location. One possible answer is that pockets of saline water in the BMC in areas of low hydraulic conductivity are effectively decoupled from active groundwater flow systems because of their density (Bottomley et al 1994).

In order to fully address the question of the cause of the low salinities observed at the Halfmile Lake deposit, it is important to establish how representative the different groundwater sampling techniques used in this study are of the true groundwater compositions. The success of the flow-through bailer in fracture-flow dominated systems is highly dependent on the variations in hydraulic gradients and hydraulic conductivities with depth. For example, high salinity waters were recovered throughout borehole MM-88-02 using the bailer system, and this was confirmed by the packer sampling, at least to as shallow as 185 m. This suggests that either high salinity waters dominate the hole or that discrete fractures which are transmitting the saline fluids have sufficiently high head to prevent contribution from low TDS shallow groundwaters into the hole. High hydraulic head would allow saline waters to flow along more shallow fractures, displacing shallow, low-TDS groundwaters. This is suggested for sample MLW96-669 (47 m depth), where the packer was in place for a greater number of sampling intervals than other groundwaters taken from the hole. The electrical conductivities of the waters in this zone levelled off at around 15-16,000 μS/cm. This conductivity may represent the true value for groundwaters at this depth, or more likely, it represent a function of mixing between shallow groundwaters and saline waters travelling along fractures which originate below the packers. In contrast to borehole MM-88-02, bailer samples from borehole MM-89-106 showed an increase in salinity with depth with waters less than 125 m depth having low TDS contents and groundwaters below this depth showing increasing TDS. However, although the bailer samples indicated progressive change with increasing depth, the magnitude

of the change was suppressed due to mixing within the open borehole, and smaller contrasts in head between deep and shallow waters than was the case in borehole MM-88-02. Straddle-packer groundwaters from borehole MM-89-106 indicate that groundwaters flowing near the bottom of the hole have salinities in excess of 2,500 mg/L, compared to 660 mg/L in the deepest bailer groundwater.

Table 4.1 Water table depths in boreholes

Borehole	Easting	Northing	Depth open	Water Table
		Halfmile Lake deposit		
Artesian bore	702744	5242989		
HB79-2	702365	5243049	576	4
HB80-1	702302	5243179	740	0
HB80-2	702275	5243537	284	20
HB81-3	702218	5243651	54.5	19
HB81-5	702275	5243614	390	18
HK75-1A	702246	5243363	226	6
HK79-6	702415	5243125	86	3.5
HN87-10	702519	5243185	119	9
HN87-8	702387	5243472	1000	10.8
HN88-14	702652	5242953	capped	Artesian
HN88-15	702718	5243402	418	11
HN88-17	702342	5243250	204	11
HN92-33	702477	5243112	219	10.3
HN92-40	702099	5242768	420	nm
HN92-34A	702202	5243663	19	18
HN93-51	702523	5243132	560	nm
HN93-53	701811	5242995	420	9
HN94-50	702502	5243232	470	10
HN94-55	702544	5243270	551	6.6
HN94-63	702319	5243219	284	10
HN94-65	702383	5243180	681	2
HN94-79	702402	5242908	150	nm
HN94-82	702227	5243008	500	nm
HT55-43	702281	5242508	82	32.3
HT79-12	702250	5243665	545	19
		Restigouche deposit		
B80-07	684278	5263642	240	20
B80-15	684622	5263213	110	7
C4-borehole	683700	5264463	unknown	artesian
C5-borehole	683288	5264187	unknown	0
EH-1	684388	5263492	78	11.3
MM-88-01	684389	5263481	155	10.8
MM-88-02	684397	5263442	559	14
MM-88-06	684450	5263404	66	10
MM-88-07	684451	5263377	58	2.5
MM-89-100	684639	5263043	110	6.5
MM-89-102	684341	5263927	110	4
MM-89-104	683704	5263169	210	nm
MM-89-106	684663	5263494	254	4
MM-89-107	684832	5263599	235	43
MM-89-109	683690	5263074	unknown	0

nm, not measured



Fig. 4.4 Digital elevation model (DEM) of the Halfmile Lake deposit showing the major streams. The main deposit crops out at the Upper AB zone (as a gossan) and dips steeply to the north (Lower AB) and northwest (Halfmile North).



Fig. 4.2 Digital elevation model of the Restigouche deposit showing the main streams. Stream names are informal. "G" indicates location of gossan outcrop.

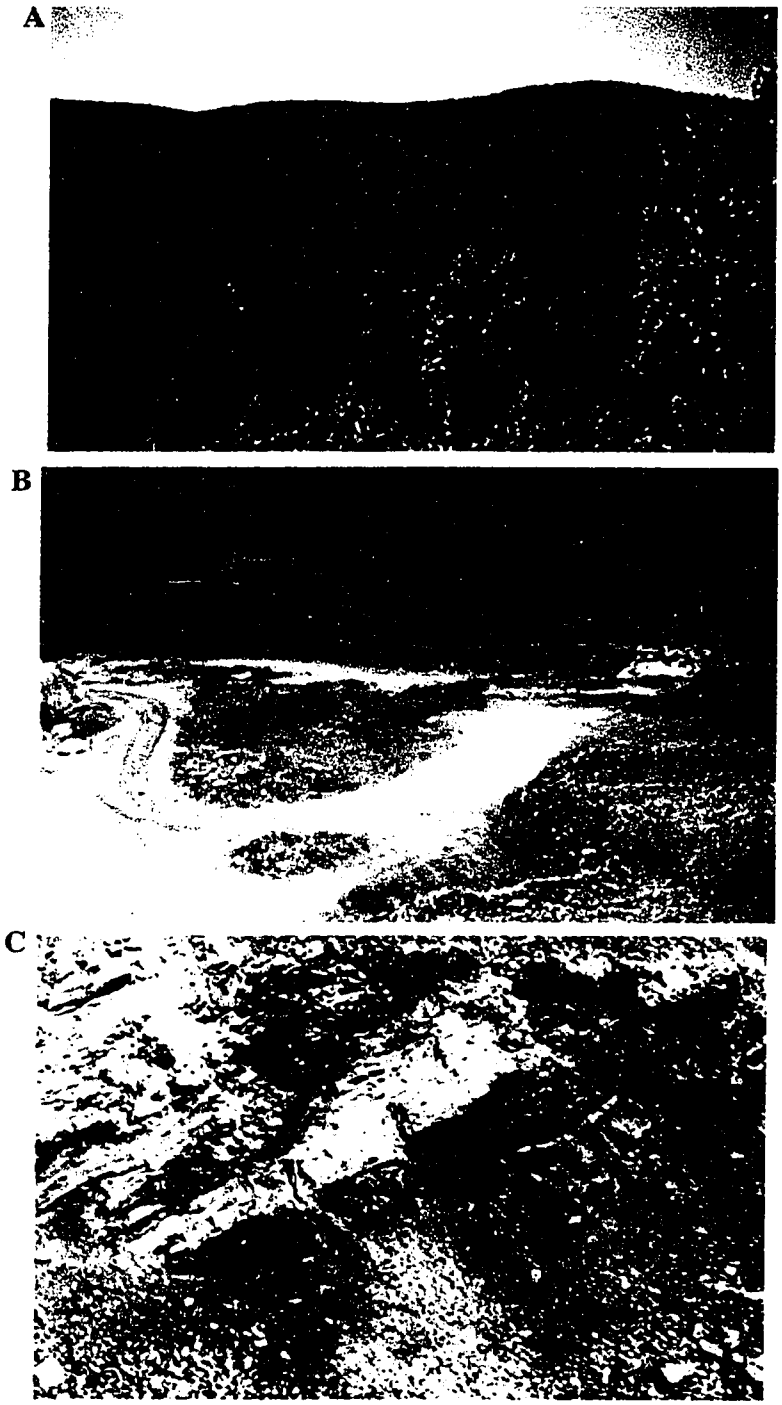


Fig. 4.3 A) View looking south over Charlotte Brook to Mt Vroom, Restigouche deposit. B) Restigouche deposit during open pit operations, with gossan pit in the background. Charlotte Brook has been diverted. C). Gossan at the Restigouche deposit (photo by D.R. Boyle).

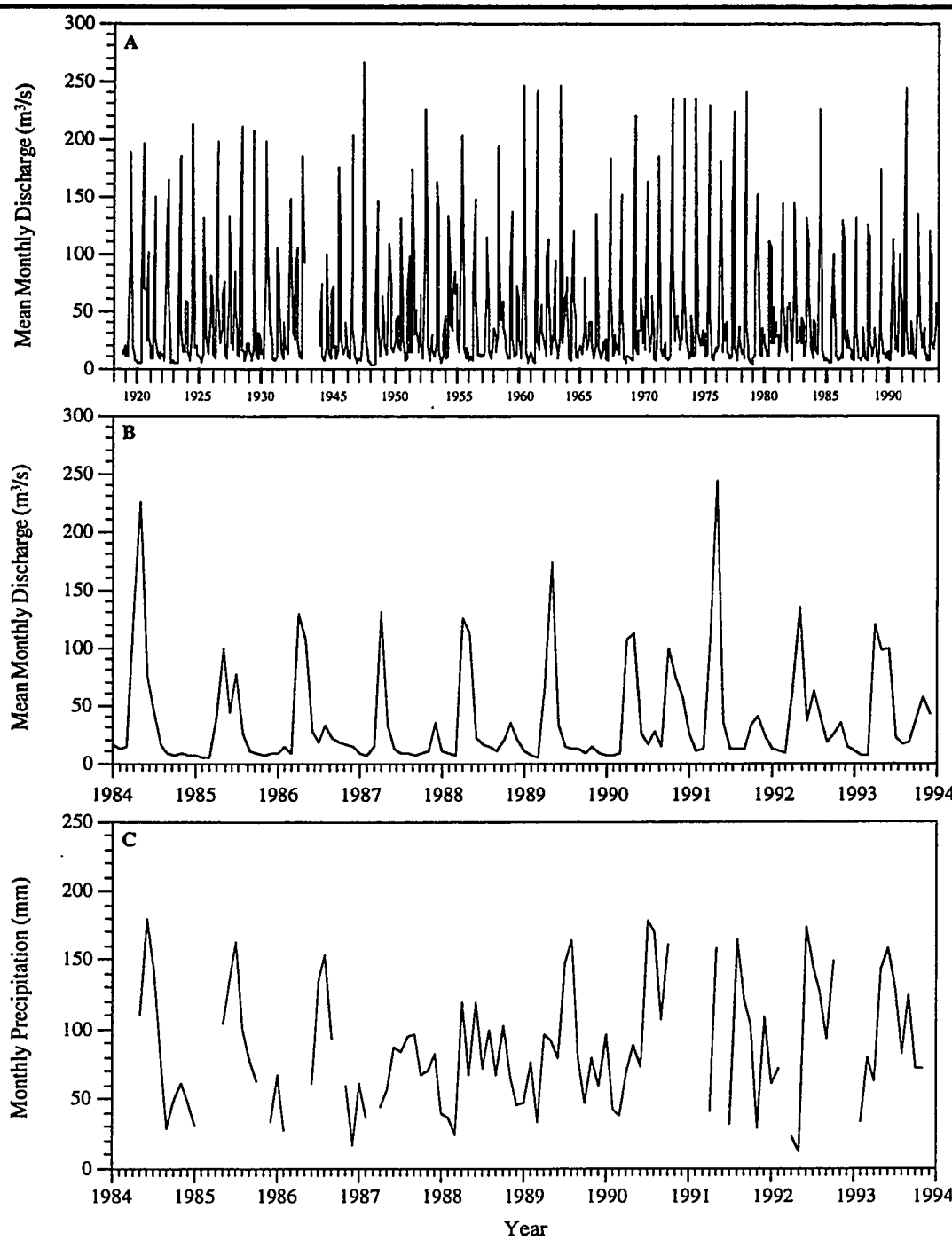


Fig. 4.4 A) Discharge for Upsalquitch River for the years 1918-1933, 1943-1993. B) Discharge for ten year period 1984-1993. Note peak discharge is in May. C) Monthly precipitation (Upsalquitch Lake station) for the years 1984-1993. Data from Environment Canada.

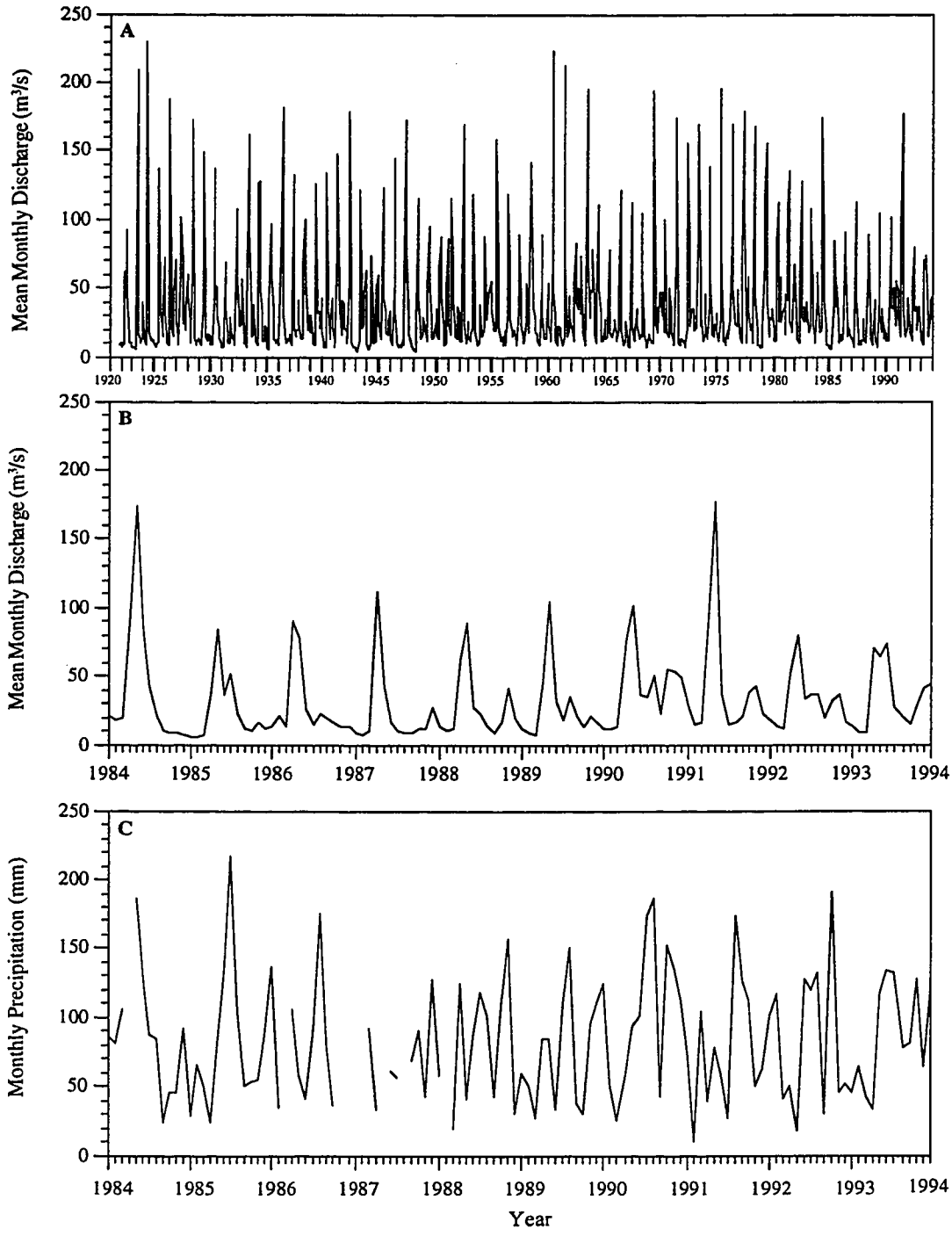


Fig. 4.5 A) Discharge for Nepisiguit River (at Nepisiguit Falls) for the years 1921-1993. B) Discharge for ten year period 1984-1993. Note peak discharge is in May. C) Monthly precipitation for the years 1984-1993. Data from Environment Canada.

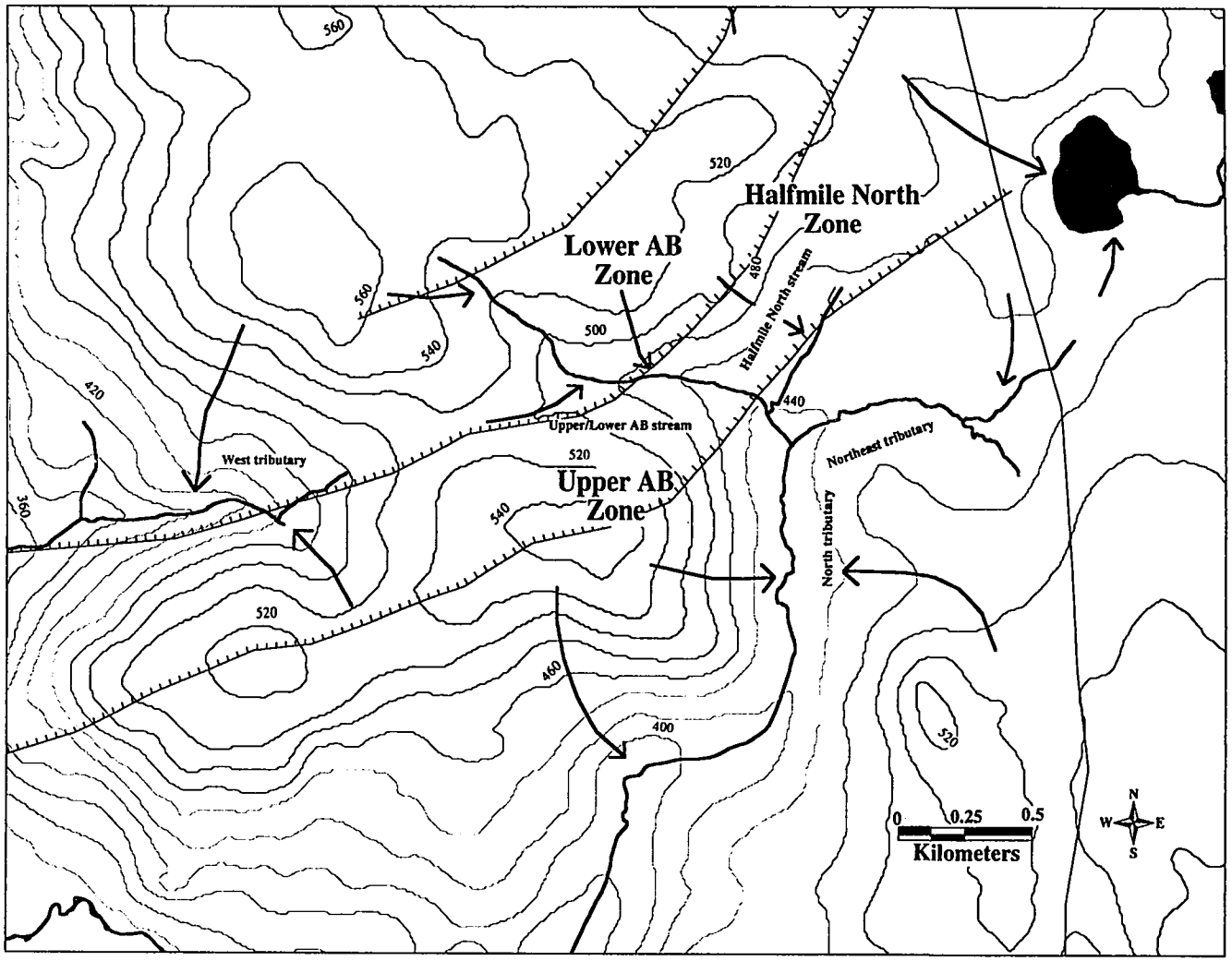


Fig. 4.6 Map showing streams sampled at the Halfmile Lake deposit, with interpreted shallow groundwater flow (arrows). Contours are in 20 m intervals. Hatched lines are faults (after Adair, 1992).

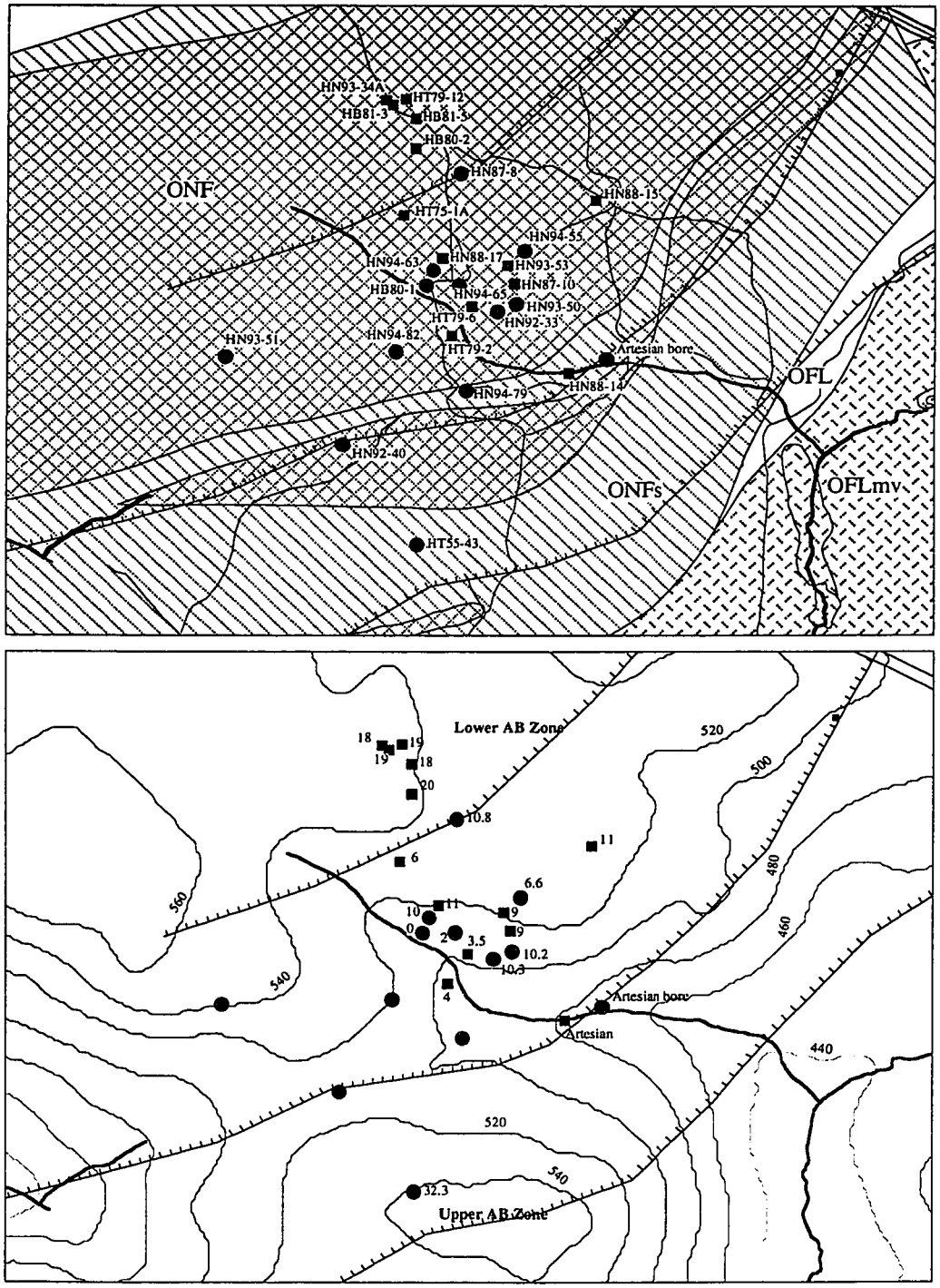


Fig. 4.7 A) Location of boreholes investigated from the Halfmile Lake deposit. Circles are boreholes which were sampled for groundwaters, squares not sampled. B) Depth to water table (metres). Contours are in 20 m intervals.

Geology: ONF, Nepisiguit Falls felsic volcanics; ONFs, Nepisiguit Falls sedimentary rocks; OFL, Flat Landing Brook felsic volcanics; OFLmv, Flat Landing Brook mafic volcanics. Hatched lines are faults after Adair (1992).

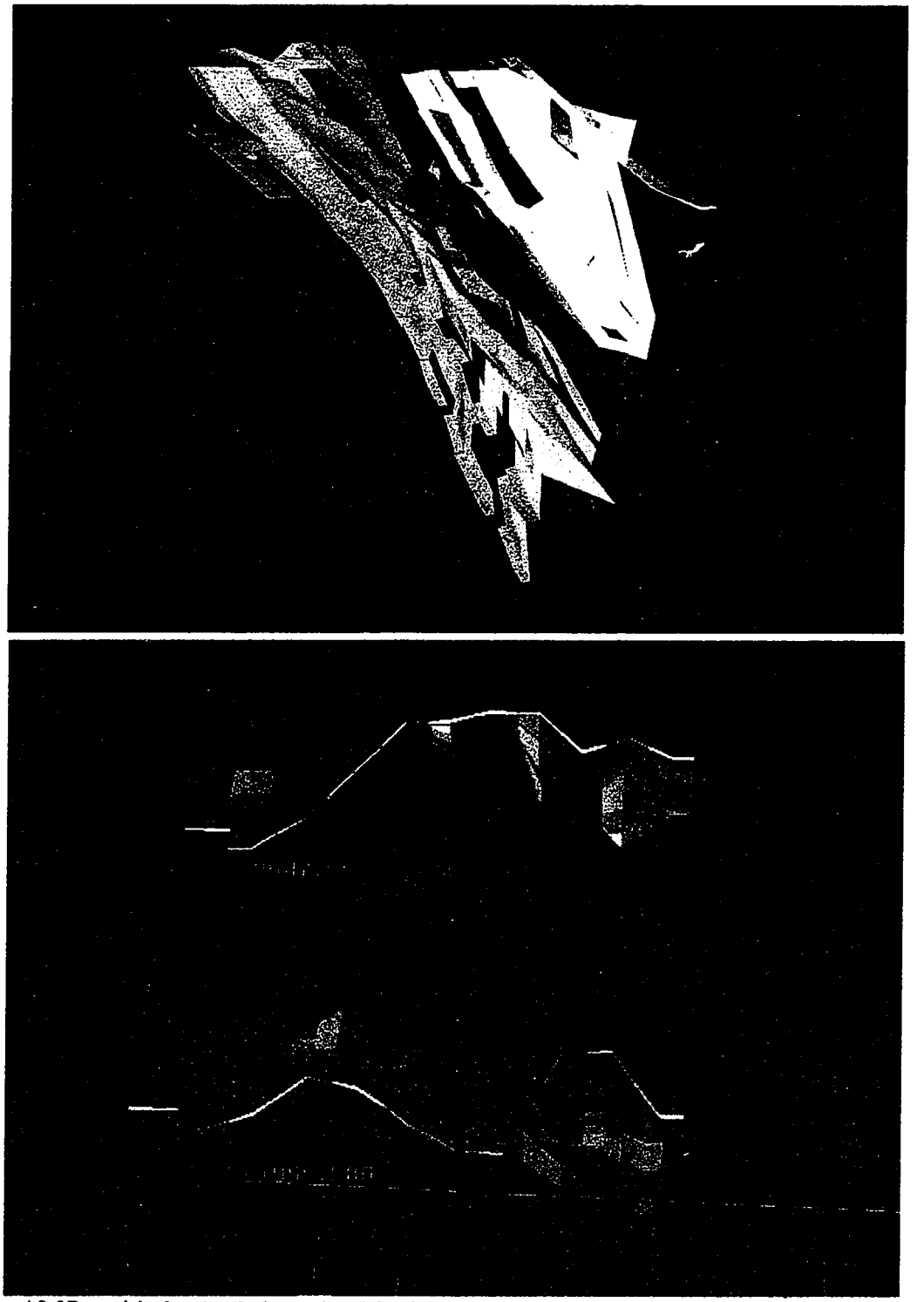


Fig. 4.8 3D model of major faults at the Halfmile Lake deposit. A) Perspective looking southwest. B) Perspective looking down plunge. Fault interpolation based on logs from exploration drill holes.

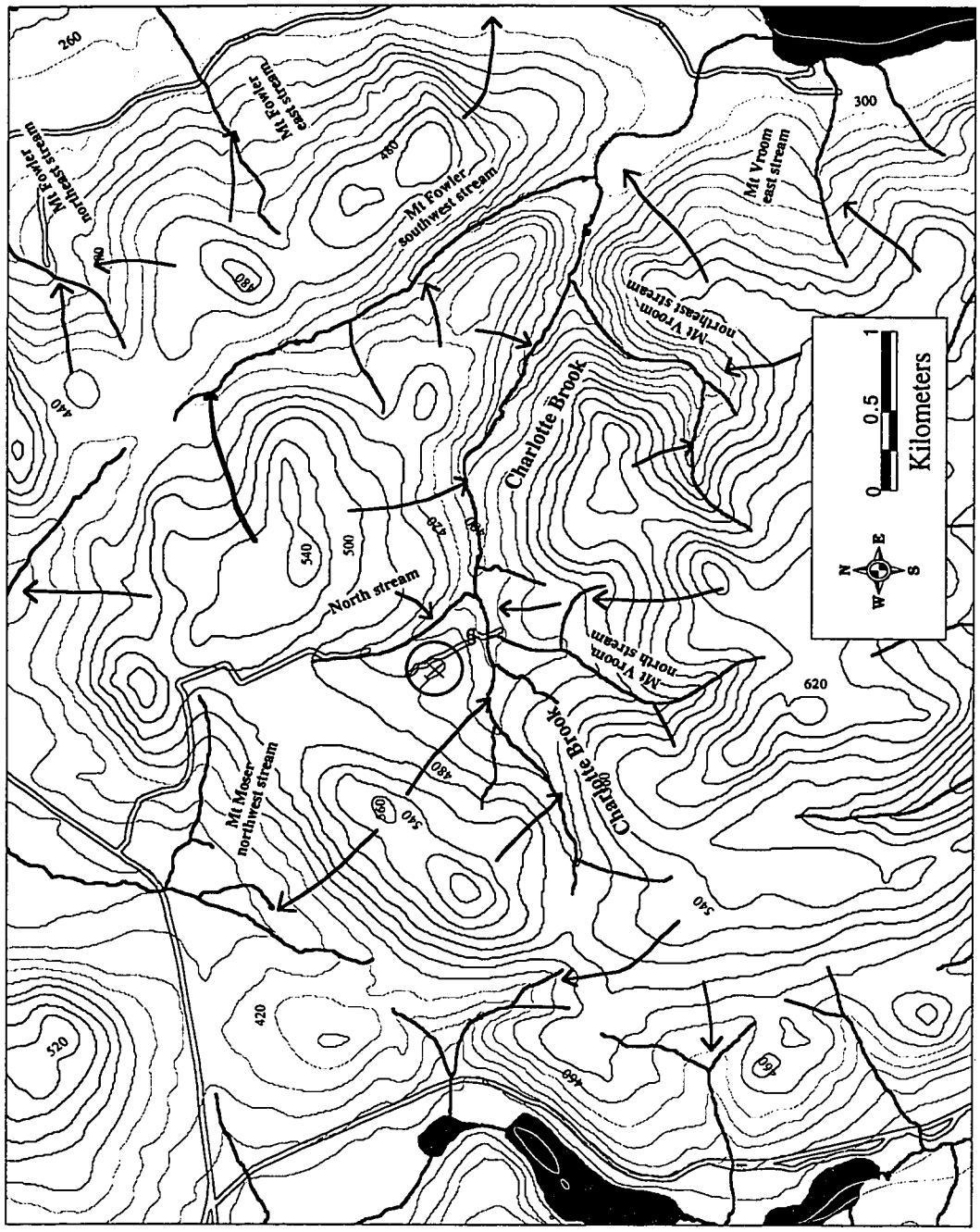


Fig. 4.9 Map showing stream sampled at the Restigouche deposit, with interpreted shallow groundwater flow (arrows). Contours are in 20 meter intervals.

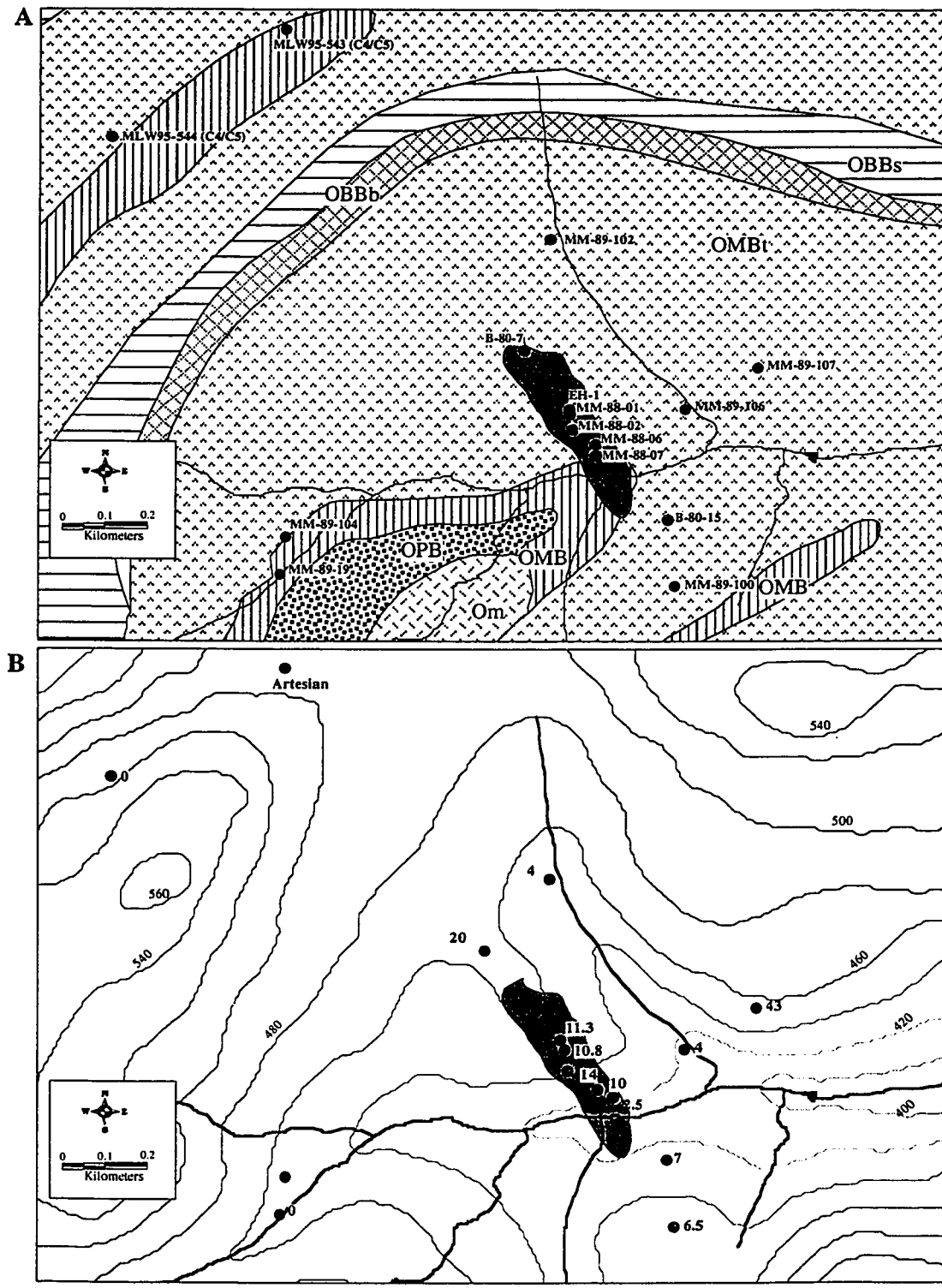


Fig. 4.10 A) Location of boreholes investigated at the Restigouche deposit. Contourinterval is 20 m. Geology: OBBs, Boucher Brook sedimentary rocks; OBBb, Boucher Brook mafic volcanics; OMBt, Mount Brittain felsic Tuffs; OMB, Mount Brittain rhyolite; OPB, Patrick Brook sedimentary rocks; Om, mafic intrusives. B) Depth to water table (metres). Shaded area is surface projection of sulfides.

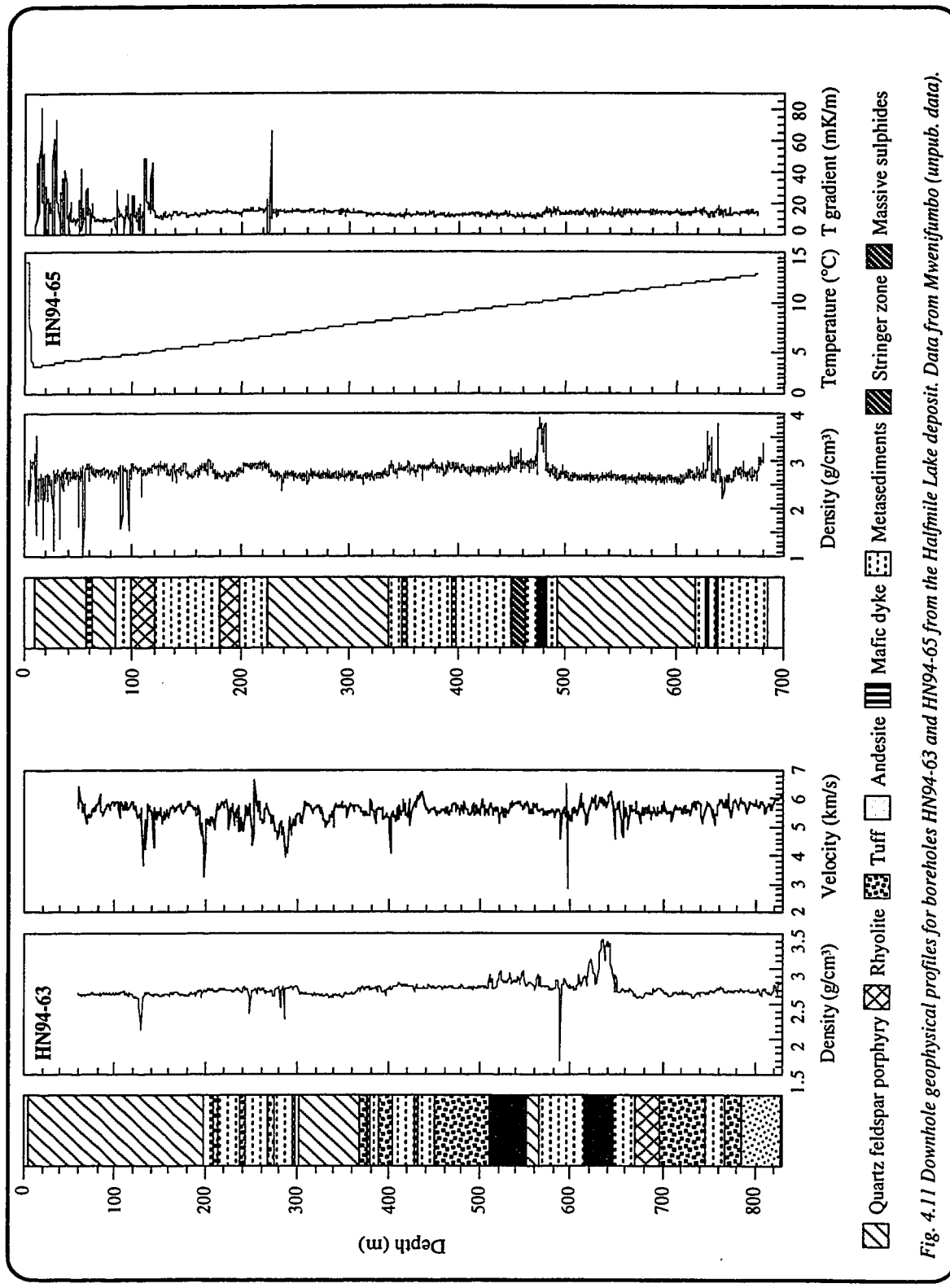


Fig. 4.11 Downhole geophysical profiles for boreholes HN94-63 and HN94-65 from the Halfmile Lake deposit. Data from Mwenifumbo (unpub. data).

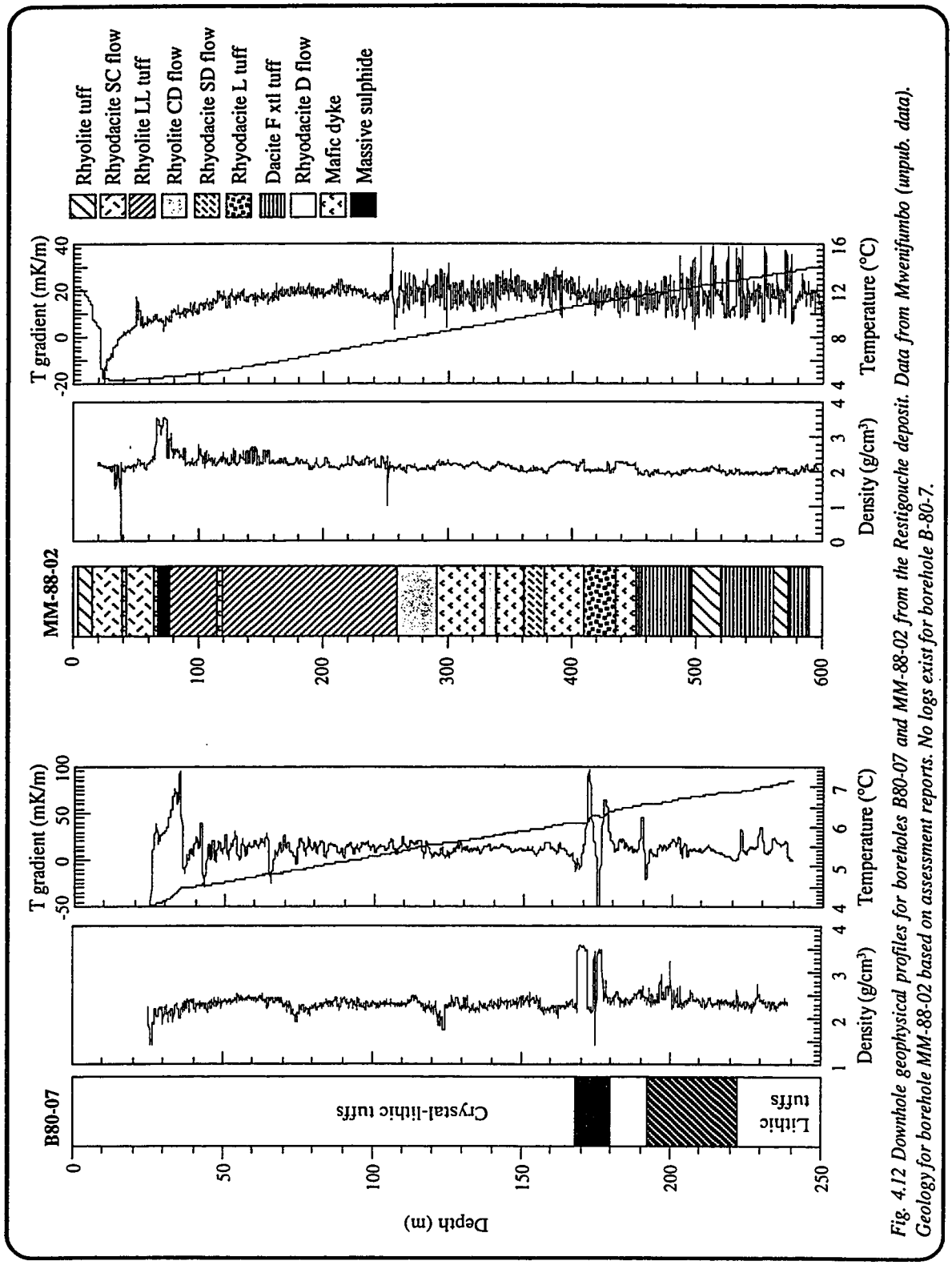


Fig. 4.12 Downhole geophysical profiles for boreholes B80-07 and MM-88-02 from the Restigouche deposit. Data from Mwenifumbo (unpub. data). Geology for borehole MM-88-02 based on assessment reports. No logs exist for borehole B-80-7.

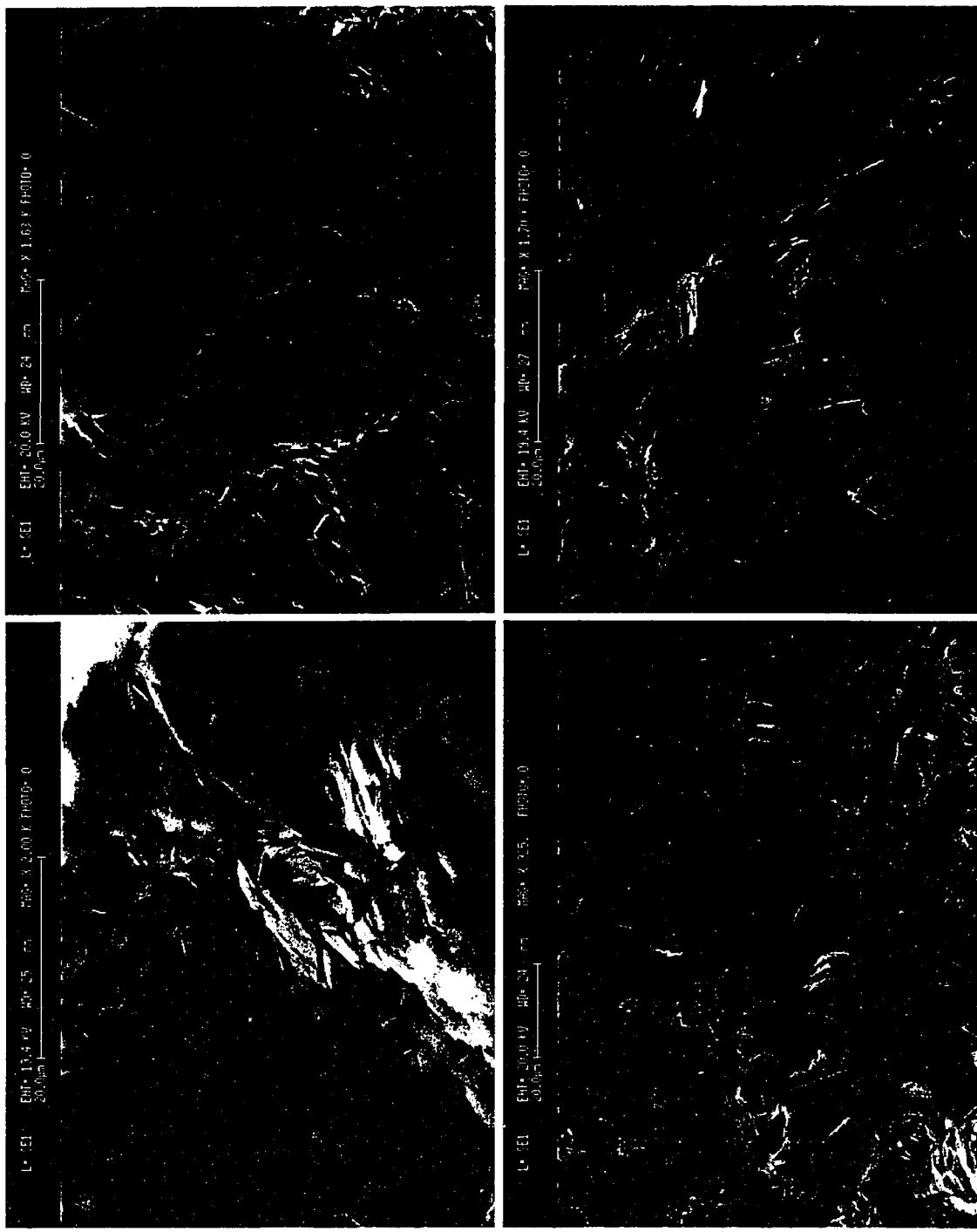


Fig. 4.13 Secondary SEM images of fracture zone minerals from the Restigouche deposit. A) Sample ML95-226, illite (sericite?) sheets. Borehole MM-88-01. B) Sample ML95-236, Ko = kaolinite, K = illite. Illite present as plate and fibrous forms. C) Sample ML95-236, equant kaolinite plates. D) Minor quartz (Q) with platy illite. Borehole MM-88-02.

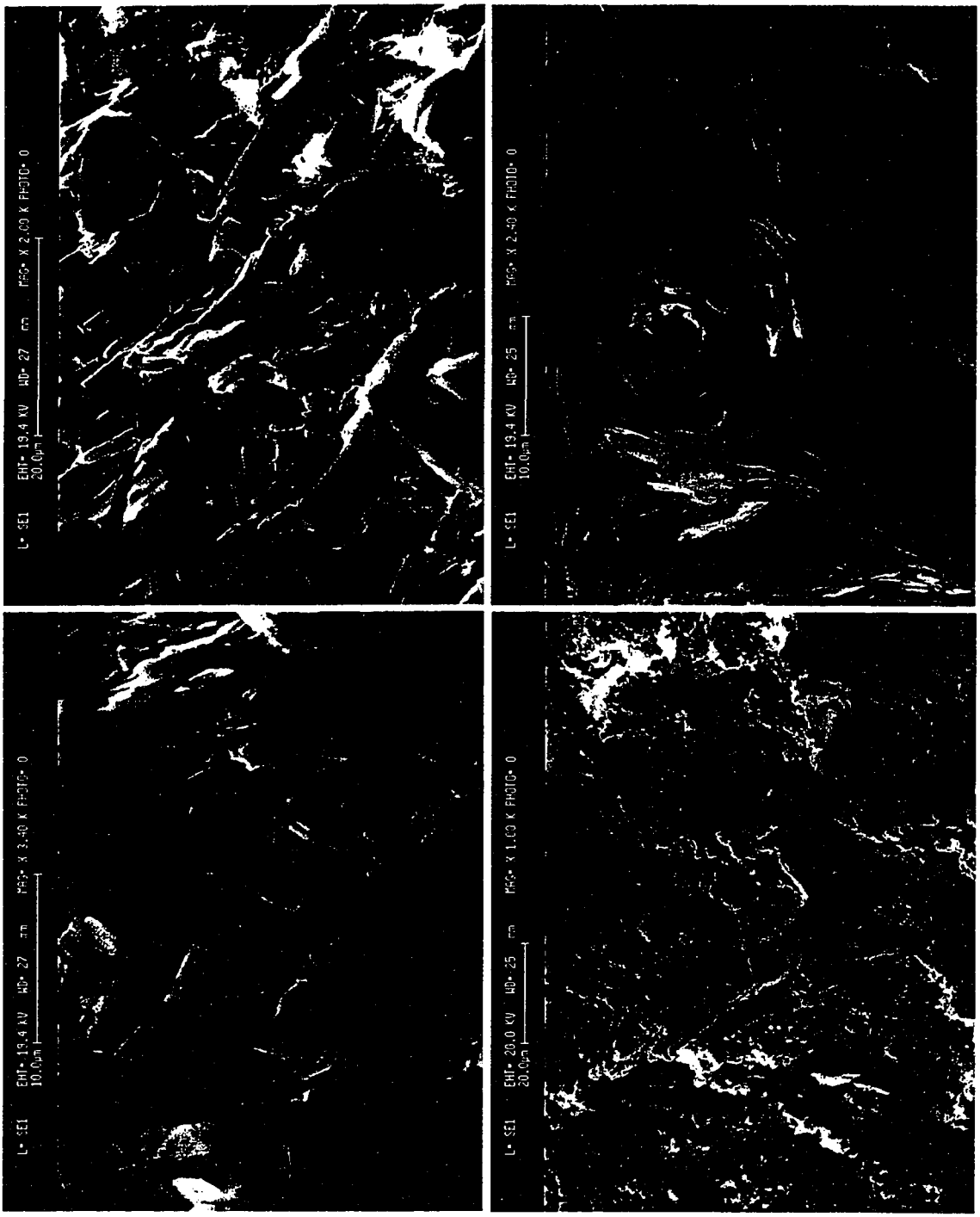


Fig. 4.14 Secondary SEM images of fracture zone minerals from the Restigouche deposit. A) Sample ML95-237, platy and blocky illite (sericite?). B) Sample ML95-237, platy illite, with minor Fe and Mg peaks. C) Sample ML95-239, Fe and Al oxides. D) Sample ML95-261, Carbonate crystal (c) in matrix of platy illite. Borehole MM-88-02.

CHAPTER FIVE:
HYDROCHEMISTRY OF SURFACE WATERS AT THE HALFMILE LAKE AND RESTIGOUCHE Zn-Pb-Cu DEPOSITS, BATHURST MINING CAMP, NEW BRUNSWICK

5.1 Introduction

Unlike studies of large rivers which provide important information on fluxes of upper crustal material to the oceans and on global erosion processes because they represent the chemical integration of the large diversity of lithologies that comprise continental crust, detailed studies of small catchment basins can also provide insight into local variations based on restricted variation in lithologies, soil and till compositions, and the effects of precipitation and topography. For example, Stallard and Edmond (1983) in a study of the Amazon River basin noted that substrate lithology and erosional regime were the most important controls on river composition. For this study, the small spatial extent effectively limits significant variations in erosional regimes, allowing a better examination of the effects of lithology on stream chemistry. Another important reason to undertake a detailed study of the surface waters in the Bathurst Mining Camp is the dearth of hydrogeochemical data for Northern New Brunswick. In fact, this is the first detailed examination of surface water chemistry in the Bathurst Mining Camp. Previous studies have been restricted to National Geochemical Reconnaissance (NGR) regional surveys of stream sediment chemistry where pH, F, and U concentrations of surface waters were also collected. Boyle et al. (1966) in 1965 and 1966 collected a suite of water samples from the Bathurst Mining Camp which were analyzed for the major anions, cations and selected trace metals (pH, alkalinity, Ca, Mg, Fe, Al, Mn, Cu, Zn, K, SO_4, Cl, F, NO_3 and Si). Catchment basin scale studies are also important in increasing understanding of water-sulphide interaction with respect to the oxidation and transport of massive sulphide minerals in exploration and environmental geochemistry.

In order to better understand water-rock interactions in the very near-surface environment

(soil/till zone and shallow groundwater systems), surface waters were collected from small streams, seeps and springs that occur at the Halfmile Lake and Restigouche deposits. This chapter focuses on the major and trace element chemistry of these surface waters. Stable isotopic (Chapter Eleven), radiogenic isotopic (Chapter Twelve), and rare earth element (Chapter Ten) data are discussed elsewhere. These results have important implications for exploration geochemistry (Chapter Thirteen) and for establishing baseline chemical inputs by ore deposits to the surface water environment under natural conditions. For example, the streams draining the Halfmile Lake deposit are tributaries to the Northwest Miramichi River, one of the major salmon fishing rivers on the East Coast of Canada. It is important, therefore, to establish the natural impacts of massive sulphide degradation at the Halfmile Lake deposit on this important resource in order to mitigate the potential effects of future mine development. The important questions addressed in this chapter are: 1) what parameters most influence the chemical composition of surface waters at the Halfmile Lake and Restigouche deposits; 2) what are the natural metal loads in small streams draining different lithologies at these deposits; and 3) what is the influence of the deeply buried and steeply dipping Halfmile Lake orebody compared to the shallowly dipping, near-surface Restigouche deposit on the distance of metal transport. Given that there are a large number of base metal occurrences in the Bathurst Mining Camp (Chapter Two), can the Halfmile Lake and Restigouche deposits, which were sampled prior to mining activity, be used as analogues to understand the effects of future mining activities on the local environment. This kind of data is of added significance for the Restigouche deposit as open pit operation was initiated in the past year.

Both the Restigouche and Halfmile Lake catchment basins have been mapped in detail by the mining industry, Geological Survey of Canada (GSC), and New Brunswick Department of Natural Resources (NBDNR) and drilled extensively, thereby providing excellent geological control to interpret the hydrogeochemistry. Gaillardet et al. (1997) noted that there has been very few studies in which the detailed trace element systematics of major rivers have been reported. This is certainly the case for small catchment studies (e.g., Billett et al., 1996). This

study makes use of recent advances in analytical techniques (e.g. Hall et al., 1995a; Stetzenbach et al., 1994) and presents trace element data based on standard total nebulization ICP-MS as well as chelation ICP-MS on a subset of the waters. This latter technique allows determination of many trace metals to the ppt level (Chapter Three).

The rationale for this study is different from most catchment and hydrogeochemistry studies. This study attempts to determine the impact the Halfmile Lake and Restigouche massive sulphide deposits have on the local stream chemistry, and to identify the major sources of solutes in surface waters. Therefore, a large number of samples were collected over a small area, rather than a single sample at the mouth of a stream as is more typical. Surface waters were collected, as much as possible, during base-flow conditions in order to minimize variations in stream-water composition caused by rain-storm events. Many studies have shown that different chemical attributes respond differently due to increased storm discharge (e.g. Caissie et al., 1996). The very similar $\delta^{18}O$ and δD between the surface waters and shallow groundwaters from both the Halfmile Lake and Restigouche deposits (Chapter Eleven) indicates that base-flow conditions were closely approximated during sampling.

5.2 Halfmile Lake Deposit Surface Waters

5.2.1 Major cations and anions

The Halfmile Lake deposit is characterized by steep hills (typical relief is on the order of 100 m) with generally poorly developed soils. Streams range from rock and pebble bottoms in steeper flowing areas to swampy wetlands. Streams at the Halfmile Lake deposit are typically surrounded by vegetation with the exception of more exposed swampy areas, and the waters are typically clear with little or no obvious suspended sediment; discolouration by high organic matter contents is rare. The bedrock geology consists primarily of metamorphosed felsic volcanic and volcaniclastic sedimentary rocks and, in the eastern part of the study area, of metamorphosed mafic to intermediate volcanic rocks (Adair, 1992; Wilson, 1993). There are no evaporite or carbonate lithologies in the study area although there is small amounts of

carbonate veining associated with the massive sulphide deposits (Adair, 1992).

Surface waters at the Halfmile Lake deposit are dominantly $CaHCO_3$-type waters although there is a slight trend towards more Na- and K-rich compositions (Fig. 5.2). The trend is seen mainly in the headwaters of the Upper/Lower AB stream and in the West tributary, and is unrelated to increasing concentration of total dissolved solids (TDS), represented primarily by high K (Fig. 5.3). Anions in surface waters at the Halfmile Lake deposit are dominated by HCO_3 with a very slight trend to increasing SO_4 for waters from the Upper/Lower AB and West tributary streams (Fig. 5.2). The dominance of HCO_3 is also evident from the very strong correlation between HCO_3 and TDS ($r^2 = 0.94$).

All surface waters typically have very low contents of total dissolved solids (TDS). TDS values are all < 110 mg/L, with most samples ranging from 14 - 60 mg/L and one sample from the Northeast tributary with 106 mg/L TDS (Appendix A.1.1). The small range in TDS is consistent with the small area of the catchment and limited range in rock types represented within the catchment (see Chapter Two). Waters draining from the Halfmile North zone (Fig. 5.3) have higher TDS than those from the Upper/Lower AB stream, although the latter waters have higher Mn and Fe contents. Surface waters show a restricted range in oxidation state (generally ranging from 150 - 350 mV with dissolved oxygen contents typically between 8 and 12 mg/L).

The Upper/Lower AB stream flows between the Upper and Lower AB zones of the Halfmile Lake deposit (Fig. 5.1) and more or less runs parallel to the strike of the deposit. The headwaters are fed by seeps (samples MLW94-185, MLW94-186, and MLW94-187). Total dissolved solids in this stream are low, ranging from 14.2 mg/L in a seep at the headwaters to 30.6 mg/L further downstream (Fig. 5.4). Compared to the other streams at the Halfmile Lake deposit, HCO_3 contents are low (6.61 - 14.99 mg/L). Given the low TDS contents of these waters, Upper/Lower AB waters are relatively elevated in SO_4 and K and to a lesser extent Si (Figs. 5.3, 5.4). The seeps at the headwaters to this stream have very low sulphate contents. Compared to the Halfmile North stream, Upper/Lower AB waters have much lower Ca but

higher Mg, Na, K and Si. The three spring/seep samples near the stream's headwaters have the lowest TDS values for this stream and have the lowest contents of all solutes with the exception of K and Cl. These waters are coincident with a fault and may be transmitting rapidly recharged waters through the quartz-feldspar porphyry felsic volcanic rocks.

The Halfmile North stream runs parallel to and down-gradient from the strike of the Halfmile North ore body and flows across different lithologies than the Upper/Lower AB stream (Fig. 5.1). Despite close proximity and similar elevations (see Fig. 4.1), these two streams have strikingly different compositions. Halfmile North stream waters have significantly higher TDS values than the Upper/Lower AB stream (Figs. 5.2, 5.3, 5.4) with all samples between 38 and 51 mg/L TDS (with the exception of sample MLW94-146 which has 25.3 mg/L TDS). The Halfmile North stream is characterized by moderately high HCO_3 and Ca contents, elevated SO_4 and low Na, Mg, Si, K, and Cl contents (Figs. 5.3, 5.4).

Three samples downstream from where the Halfmile North and Upper/Lower AB streams merge were also taken; two from the main course and one at a seep away from the main course. Sample MLW94-123 was sampled just downstream from the confluence. This sample has low TDS (26.69 mg/L) and plots closest to the Upper/Lower AB stream samples. In contrast, samples MLW94-151 and MLW94-152 (seep) typically plot closer to the Halfmile North stream samples. These two samples have higher Mg contents than Halfmile North waters (Fig. 5.3).

The Northeast tributary stream is compositionally most similar to the Halfmile North stream. Both streams have similar TDS values although the Northeast tributary is on average slightly higher in TDS and ranges up to 59.1 mg/L with the exception of a seep which has 106 mg/L TDS (Appendix A.1.1). The Northeast tributary waters are all $CaHCO_3$ waters which plot close to the Ca and HCO_3 apices on a Piper plot (Fig. 5.2). These waters have the highest concentrations of HCO_3, pH, Ca, Mg, Na and low SO_4, Eh and K compared to most of the other streams (Figs. 5.3, 5.4). This stream also has the lowest Na/Mg and K/Ca ratios at the Halfmile Lake deposit and moderate Ca/Mg ratios. There is little variation in most chemical

parameters along the length of the stream with the obvious exception of the higher TDS seep (sample MLW94-228) and three other samples of seeps and small tributaries which have somewhat lower major ion contents (samples MLW94-216, MLW94-221, MLW94-223; Appendix A.1.1). Sample MLW94-228 has anomalously high nitrate (1084 mg/L NO_3) and was sampled from a seep within the root-zone of a large tree. This water is also anomalously high in TDS and HCO_3, and low in temperature compared to other samples from this stream.

The North tributary stream represents the confluence of the three previous streams and this is evident from the geochemistry (Fig. 5.3). Several geochemical parameters diminish with distance downstream suggesting dilution from non-mineralized base-flow and/or attenuation through precipitation/adsorption reactions. For example, for the major cations and anions, Cl and K decrease or are lower downstream than the other tributaries (except Halfmile North for K) whereas Ca and HCO_3 increase slightly downstream and Si, Mg, and Na show little variation along this tributary (Fig. 5.4). The fact that TDS only varies slightly downstream (all samples from the main course of the stream are between 40 and 44 mg/L TDS; samples from a seep and a small tributary have 22 - 28 mg/L TDS) suggests that some of the variation in other elements is due to reactions within the stream system as opposed to major changes in the chemical composition of base flow waters.

The West tributary drains the Upper and Lower AB zones to the west and ultimately flows to the Northwest Miramichi River (Fig. 5.1). These waters are among the freshest observed at the Halfmile Lake deposit (Fig. 5.2) with TDS values ranging from 15.3 to 19.6 mg/L and are similar to waters from the Upper/Lower AB stream in that they have proportionately higher SO_4 contents although the dominant anion is HCO_3 (Fig. 5.4). Similarly, although the dominant cation is Ca, these waters have proportionately higher K and Mg compared to the other streams with the exception of the Upper/Lower AB stream.

Other streams sampled near the Halfmile Lake deposit include the Northwest Miramichi River upstream of its confluence with the North tributary, and streams draining Mt Venning south of the northwest Miramichi River (Fig. 5.1). A sample was also collected from the

surface of Halfmile Lake (Fig. 5.1). The northwest Miramichi River and Mt Venning waters are $CaHCO_3$-type waters of moderate TDS, with the exception of sample MLW96-705, which has very low TDS (18.2 mg/L) but moderately elevated sulphate and classifies as a $CaHCO_3SO_4$ water (Fig. 5.2). Geochemically these waters are most similar to the least concentrated Northeast tributary waters (Fig. 5.3). The northwest Miramichi River sample has the highest Si contents for Halfmile Lake deposit surface waters and has high K, Na and Fe.

The sample from the surface of Halfmile Lake was difficult to filter due to high suspended sediment load, consisting primarily of organic matter. This sample is $CaHCO_3$ in composition and has one of the highest Ca/Na and $HCO_3/(SO_4+Cl)$ ratios of all the Halfmile Lake deposit samples (Fig. 5.2).

5.2.2 Trace elements

Analysis and interpretation of trace element contents in natural waters is difficult due to low detection limits, particularly for surface waters in crystalline rock terrains. Most trace elements are below the detection limit for the standard ICP-MS analytical technique (Appendix A.1.1). Only Fe, Al, Mn, Ba, Rb, Sr, and Zn have contents typically greater than the detection limits with Pb and Cu commonly below detection. The base metals are more readily detectable by chelation ICP-MS which allows lower detection limits (Table 3.1). A subset of the Halfmile Lake deposit surface water samples was analyzed using this technique (Appendix A.1.1). The discussion in this chapter does not emphasize the base metals (Zn, Pb, Cu, Co, Cd) as these are discussed fully in Chapter Thirteen in relation to geochemical exploration.

Several areas of anomalous Fe and Mn occur along the Upper/Lower AB stream, the most obvious associated with sample MLW94-110, the artesian borehole with Fe-(Mn) oxyhydroxide-rich water (discussed in Chapter Seven). Overall, this stream has the highest contents of Fe and Mn (Figs. 5.5, 5.6). The seeps at the headwaters of the stream contain variable contents of these elements and sample MLW94-187 from a seep with an organic-matter rich substrate has the highest contents of both elements. The Upper/Lower AB stream

also has elevated contents of Ba and Rb compared to the other streams, but has lower Sr, indicating that Sr is controlled by phases different from those affecting than Ba and Rb. There is only minor variation in these elements along the length of the stream (Fig. 5.6). Aluminum and Ti are variable with the highest contents at the headwater seeps and at the lower end of the stream. The Al contents are not obviously controlled by pH as this stream has the lowest pH values but moderate Al contents. Uranium contents are highest in the Halfmile Lake deposit study area at the headwater seeps and overall in the Upper/Lower AB stream.

The Halfmile North stream, in contrast to the Upper/Lower AB stream, has very low Fe (mostly below detection) and Mn contents. Similarly, Ti (mostly below detection) and Al abundances are very low, coincident with higher pH (lab; Appendix A.1.1). One sample near the top of the stream has the highest Al content along this stream and the lowest pH (lab). The Halfmile North stream in contrast to the Upper/Lower AB stream has the highest Sr contents in the study area, coincident with the high Ca (Fig. 5.4), but typically has low Ba and Rb (Figs. 5.5, 5.6). The high U and Y values most likely reflect the largely felsic lithologies over which this stream flows.

The Northeast tributary stream is characterized by low contents of Ba, Rb, U, and moderate Sr given the generally high TDS values (Fig. 5.5). In contrast, Al and V contents are generally high along this stream.

As with the major cations and anions, the upper parts of the North tributary have trace element contents that in general reflect the contributions of the Upper/Lower AB, Halfmile North and Northeast tributary streams. However, Fe contents are low for a 500 m section of the stream downstream from the confluence of these three streams. Rubidium, Al, Sr, and Y contents are also lower in this section of stream, although Ba and PO_4 do not show a depletion to the same extent.

The West tributary stream is most similar to the Upper/Lower AB stream in most trace elements. Iron and Mn contents are low, as are Sr and U. Rubidium values are moderately elevated in some of the waters, similar to the Upper/Lower AB stream.

5.2.3 Statistical analysis

Statistical analysis is useful in highlightling relationships not necessarily evident from graphical representation, in particular where dealing with large data sets and large numbers of variables. For Halfmile Lake deposit surface waters, statistical analysis is complicated by the fact that the majority of the variables are not normally or log-normally distributed. Most of the more common statistical functions have an inherent assumption of a normal distribution; the lack of normal distribution is a common problem in geochemistry (Rollinson, 1993). With that caveat, several different methods were used to analyze the data statistically; cluster analysis, principal component analysis and correlation analysis.

Cluster analysis was performed on the data after calculating correlation coefficients using Pearson-Product Moment Correlation. The relationships between the chemical variables were measured using complete linkage cluster analysis, which showed five groups of element associations:

Group 1	Group 2	Group 3	Group 4	Group 5
Sr, Ca, HCO_3, TDS, pH	Na, Mg, Si, Cl,	Zn, SO_4, Eh	Ba, K, Rb	Mn, Al, Pb, Cu, Fe

Several of these groupings are clearly evident in element-element diagrams and the proportional circle maps (Figs. 5.4, 5.6). However, the strength of the correlation is more easily quantified using statistical analysis. The association of elements by cluster analysis is also shown by the PCA (Fig. 5.7), with a few exceptions.

Principal components analysis (PCA) is very successful at delineating the different groups of surface water samples based on the chemical variables and thus by stream segment. Although this analysis primarily reflects differences in the stream segments evident from the proportional circle maps, it allows these differences to be reflected in a small number of

diagrams (Figs. 5.7, 5.8). The PCA for the Halfmile Lake deposit surface waters yields generally similar results as the cluster analysis of sample variables. The PCA indicates that 82% of the variation between samples can be explained by six factors. Factor 1 (30.5%) is dominated by strong correlation between TDS, HCO_3, Mg, Ca, Sr and Na and, to a lesser extent, Cl. Factor 2 (19.5%) is dominated by correlations between Si, Al, Na, Ba, Mn, Mg, K and Rb. Eh and SO_4 are moderately correlated with each other. Factor 3 (12.4%) is dominated by correlations by Fe, Zn, and Mn and by correlations between dissolved oxygen (DO), Si and pH. Factor 4 (8.5%) shows moderate correlations between Eh, K, and Ba. Factor 5 accounts for only 5.9% of the variation and is dominated by pH and SO_4, whereas, factor 6 (5.3%) is a dominated by DO. On eigenvector variation diagrams (Fig. 5.7), the elements accounted for by these factors tend to cluster together.

5.2.4 Geochemical modelling

Element speciation and mineral saturation indices were modelled for a selected group of Halfmile Lake deposit surface waters with PHREEQC using the WATEQ4F database. The samples selected for speciation and mineral saturation calculations were those which had been analyzed for trace metals and REE by chelation ICP-MS, providing a more complete dataset. These waters were also analyzed for Br and PO_4 by ICP-MS (see Chapter Three). Saturation indices for selected minerals are presented in Appendix A.1.4 and the results of the speciation calculations for the major cations, trace metals and phosphate are presented in Appendix A.1.5. Note that the contribution of metal-humate speciation was not considered in these calculations. Dissolved organic carbon (DOC) was not measured as part of this study. It is likely that DOC contents are relatively minor in the waters studied given that a) base flow waters were sampled, b) surface waters were typically clear at the time of sampling (i.e., no discolouration by organic acids), and C) cation-anion balances are typically very good (Chapter Three). Viers et al. (1997) have shown that much or all of Fe, Al, Pb and Cu are associated with organic ligands in organic-rich waters from Cameroon.

Halfmile Lake deposit surface waters are well below saturation for all carbonate minerals (Fig. 5.9). Surface waters from the Upper/Lower AB and West tributary streams have lower P_{CO2} and $SI_{Calcite}$ (SI = saturation index) at an equivalent pH value than waters from the other streams (Fig. 5.9). With increasing pH, Halfmile Lake deposit surface waters show increasing $SI_{Calcite}$ but are well below values shown for Restigouche deposit surface waters. Solution pH exerts a dominant control over the saturation of Fe-oxide and hydroxide species, and there is a strong positive correlation between pH and $SI_{Fe(OH)3}$ (Fig. 5.9). Surface waters at pH > 7 are supersaturated with respect to amorphous Fe-oxyhydroxides. There is no correlation between dissolved Fe contents and $SI_{Fe(OH)3}$ (Fig. 5.9). In contrast, there is a strong positive correlation between $SI_{Kaolinite}$ and dissolved Al contents. All surface waters are supersaturated with respect to kaolinite and gibbsite (Appendix A.1.4; Fig. 5.9), and $SI_{Kaolinite}$ values decrease with increasing pH.

Elemental speciation results show that for the alkali and alkali-earth elements (Ca, Mg, Na, K, Rb, Sr, Ba), greater than 98% are present as free ions (Appendix A.1.5). Sulphate complexes are significant only for the divalent cations Ca, Mg, and Ba, with Ba showing the greater preference for sulphate complexes (up to 1.7% of Ba is present as $BaSO_{4(aq)}$). Cadmium and Mn are also present dominantly as divalent free ions. Aluminum speciation is highly dependent on pH, but Al is complexed almost exclusively by hydroxide. Iron speciation is variable. All surface waters, based on pH and Eh, plot in the Fe^{3+} stability field (Fig. 5.10) and PHREEQC speciation results suggest that most surface waters are dominated by Fe^{2+} species with the free ion the most prevalent species. For several waters, $Fe(OH)_3$ is an important species comprising up to 70% of total Fe in sample MLW94-122 (Appendix A.1.5). Copper in most waters occurs as Cu^{2+} ions or complexes with Cu^{2+} although surface waters with low Eh have Cu^{+} contents of up to 25% of the total Cu present. Whereas Zn is present primarily as Zn^{2+} (> 87%) and $ZnHCO_3^{+}$, Pb speciation is more variable. Lead is variably complexed as $PbCO_{3(aq)}$ (up to 73%), as free Pb^{2+} ions (up to 75%), and as $PbHCO_3^{+}$ (<15%). Solution pH is the overriding control over Pb speciation with the free ion dominant at

lower pH.

5.2.5 Temporal variations

Three sites were sampled over the course of the study and, where logistically possible, during the fall, winter and spring (Appendix A.1.7). During summer sampling at both the Halfmile Lake and Restigouche deposits, there was generally minor variations in most elements for the three monitoring sites (Fig. 5.11). However, larger variations occur for some elements during the spring and in the fall (Fig. 5.11). Aluminum contents peaked for the Upper/Lower AB stream and seep sites in May and October. In comparison, the Halfmile North stream showed very little variation in Al content. For all three sampling sites, HCO_3 contents fell in May and October although the magnitude of variation was small for the seep monitoring site. For the Upper/Lower AB stream site, the decrease in HCO_3 likely reflected a decrease in pH which would account for the coincident increase in Al. Both Mg and Ca decrease with HCO_3 in May and October. During the 1994 field season, Mg contents increased for the Upper/Lower AB and Halfmile North sites but Ca contents decreased for the latter site.

5.3 Restigouche Deposit Surface Waters

5.3.1 Major cations and anions

As with the Halfmile Lake deposit, the Restigouche deposit is characterized by steep-sided hills although there is somewhat greater relief the Restigouche deposit (Chapter Four; Fig. 4.2). The area surrounding the Restigouche deposit has a more extensive network of streams than at the Halfmile Lake deposit and as a result more surface water samples were collected (Fig. 5.12; Appendix B.1.1). The main stream sampled in this study is Charlotte Brook which crosses the Restigouche ore body close to where it outcrops. Several streams drain different lithologies into Charlotte Brook and provide important contrasts. In addition, several streams to the east of the deposit, tributaries to the Southeast Upsalquitch River and Upsalquitch Lake, and streams to the north and west draining away from the Restigouche deposit area were also

sampled (Fig. 5.12).

The overall variation in Restigouche deposit surface waters is primarily controlled by HCO_3 abundance (Figs. 5.13, 5.14). There is a very strong correlation between HCO_3 and TDS content (r^2 = 0.954) whereas sulphate does not vary coherently with TDS (r^2 = 0.239). Chloride shows more scatter than HCO_3 but generally increases with increasing TDS. Eh and pH display almost antithetical trends compared to TDS and pH values increase sharply at low TDS contents from values as low as 5 to > 7. Above TDS contents of around 30 - 40 mg/L, the increase in pH is less than at low TDS (Fig. 5.14). In contrast, Eh values decrease sharply at low TDS contents. Silica shows a scattered pattern but in general Si contents increase with increasing TDS.

Calcium is very strongly correlated with TDS (r^2 = 0.964) and with HCO_3 (r^2 = 0.977; Figs. 5.14, 5.15). The notable exception is a seep in the gossan which has very low Ca (sample MLW95-300). At TDS contents below 70 mg/L, Mg displays a strong correlation with TDS (r^2 = 0.964). However, at higher TDS values, Mg contents do not increase with increasing TDS. Both Na and K show generally positive correlations with TDS.

The surface water compositions in Charlotte Brook are different upstream and downstream from the deposit (Fig. 5.15). Waters from Charlotte Brook are $CaHCO_3$ in composition with moderate TDS values of 41.41 to 82.60 mg/L. The highest TDS sample is from a small stream fed by seeps that enters Charlotte Brook upstream from the main ore body (Fig. 5.12). TDS contents are typically slightly higher upstream from the deposit with the exception of the sample from the headwaters to this stream and two adjacent seeps. Charlotte Brook waters have relatively low SO_4 contents (Figs. 5.14, 5.15), even immediately downstream from the deposit. Groundwaters recovered from shallow boreholes close to the stream (boreholes MM-88-06 and MM-88-07; Fig. 7.13) have very elevated sulphate contents due to the oxidation of Restigouche deposit massive sulphides (see Chapter Seven for discussion). In contrast, waters in Charlotte Brook immediately downstream from the deposit typically have elevated Cl contents compared to waters upstream from the deposit. Very saline waters were recovered

from borehole MM-88-02 which intersects the Restigouche ore body (see Chapter Seven). Charlotte Brook waters have uniform pH with most ranging from pH 7 to 7.5. In contrast, Eh shows a sharp decrease with increasing TDS (Fig. 5.14). However, pH and Eh values are generally lower upstream of the deposit (Fig. 7.15E, F).

Both Ca and Mg are strongly correlated with TDS in Charlotte Brook waters, and values are similar to other waters at the Restigouche deposit at the same TDS value (Fig. 5.14). In contrast, Charlotte Brook waters have lower K contents than the North Stream and Mt Fowler southwest streams which flow into Charlotte Brook. Waters upstream from the Restigouche ore body typically have higher Ca and Mg and lower Na compared to those downstream from the ore body.

The most distinctive feature of Mt Fowler east stream was the observation of significant Fe-oxyhydroxide accumulation on the stream bed. These Fe-oxyhydroxides increased in abundance up to sample sites MLW96-664 and MLW96-665 (Fig. 5.12E). At these sites, seeps are inferred to be flowing in the stream bed; Fe-rich precipitates are abundant about and downstream of these locations and rarely upstream of these locations. Mt Fowler east waters are moderately sulphate-rich (7.91 to 15.50 mg/L) with very low Na contents (most are < 1 mg/L Na). They range in composition from $CaHCO_3$ to $CaHCO_3SO_4$-type waters (Fig. 5.13). The two samples closest to where the seeps are inferred to come to surface have lower Eh and pH values than the other samples along this stream, consistent with the Fe-oxyhydroxide precipitation.

The Mt Fowler northeast stream drains similar lithologies to the Mt Fowler east stream. However, TDS values in these waters are higher ranging from 74 to 115.5 mg/L although sulphate contents are lower than in the Mt Fowler east waters. Chloride, pH and Na are also elevated in the Mt Fowler northeast waters. With increasing TDS, these waters show a trend of decreasing Mg and K, but increasing Ca (Fig. 5.14).

The Mt Fowler southwest stream waters are characterized by $CaHCO_3$ compositions with lower TDS contents (49 - 54 mg/L) than the other two stream draining Mt Fowler. These

waters are characterized by elevated K and have sulphate contents that are higher than for Charlotte Brook but lower than Mt Fowler east and northeast streams. Although this stream crosses three lithologic boundaries, there are few obvious changes in stream composition from the headwaters to the confluence with Charlotte Brook (Fig. 5.15).

Mt Moser northwest stream flows to the north away from the Restigouche deposit and down gradient from the C4 and C5 deposits (see Chapter Seven). Sample MLW96-650 was collected from a stream fed by a seep to the east of the primary stream sampled, and sample MLW96-709 was sampled from a stream draining a large swamp to the west of the main stream (Fig. 5.12). All these waters are $CaHCO_3$-type waters (Fig. 5.13) with TDS values ranging from 22.2 to 53.85 mg/L. The seep to the east has a TDS value of 142.93 mg/L and sample MLW96-709 to the west has a TDS value of 78.28 mg/L. Sample MLW96-650 differs from the other waters in that it has very elevated Ca, HCO_3 and Si contents but very low K, low Cl/TDS and SO_4/TDS. The waters from the main stream sampled at Mt Moser are characterized by low Si and Na and uniform K contents.

The waters collected from Mt Vroom east and southeast streams differ from most of the other streams on the basis of the very high SO_4/HCO_3 ratios. These waters are classified as Ca-SO_4- to Ca-SO_4-HCO_3-type waters (Fig. 5.13) and are characterized by low TDS contents (11.54 to 17.22 mg/L), with the exception of sample MLW96-641 (47.24 mg/L TDS), and uniformly low HCO_3 contents (Fig. 5.15). Sample MLW96-641 was collected from a seep in the stream bed.

Mt Vroom north waters are $CaHCO_3$-type waters with the exception of sample MLW96-661 from the headwaters to this stream. This sample has very low TDS, low pH and high SO_4/HCO_3. Waters from this stream are characterized by generally low TDS (12 - 42.42 mg/L), Cl (< 0.5 mg/L), and SO_4 (2.13 - 4.30 mg/L; Fig. 7.14). At a given TDS value, these waters have elevated Si and Na and low K compared to the other Restigouche deposit surface waters. The samples closest to the headwaters have the lowest TDS, Ca, Mg, Na, K and HCO_3 values along the stream (Fig. 5.15).

Mt Vroom northeast waters are somewhat transitional between Mt Vroom north and Mt Vroom northeast waters in that they have intermediate SO_4/HCO_3 ratios (Fig. 5.13). These waters, as with the other water draining Mt Vroom, have very low TDS values (8.71 to 21.38 mg/L). Given the very low TDS, Na and Si are slightly elevated compared to other low TDS waters. Both Eh and pH show rapid decreases and increases, respectively, with increasing TDS (Fig. 5.14). There are no coherent trends downstream along the Mt Vroom northeast stream. Unlike the Mt Vroom east stream, no Fe-oxides were observed in the stream bed.

On a plot of K versus TDS two trends are evident; one trend shows increasing K with little increase in HCO_3 whereas the other trend shows more rapid increase in HCO_3 compared to K (Fig. 5.14). The first trend is dominated by waters from the North stream which runs parallel to and east of the main ore zone (Fig. 5.14) and is intimately associated with potassic alteration around the ore body (Lentz and Goodfellow, 1996; Lentz and Gregoire, 1995). This interpretation is consistent with the dominance of K-clays along fractures. Most grain mounts of fracture/fault zone material (see Chapter Four) are dominated by illitic/sericitic minerals. Near the headwaters of this stream, transported gossan material is common. Samples MLW94-289 and MLW96-714 are seep samples that flowed through the gossan at the time of sampling. Sample MLW95-715 is from the main stream course and numerous gossan pebbles were observed in the stream bed at this location. North stream waters have low TDS values (34.8 to 41.44 mg/L) but have SO_4 contents greater than Charlotte Brook. Despite the elevated SO_4, these waters classify as $CaHCO_3$-type waters.

Several seeps occurring away from streams, including two had significant associated Fe-oxyhydroxides were sampled. Sample MLW95-300 seeped through the gossan on the south bank of Charlotte Brook. This sample was collected at the beginning of the 1995 field season; the seep dried up within two weeks of sampling. This sample is characterized by very low pH (2.87) and high SO_4 (71.1 mg/L), and low cation contents. Sample MLW95-345 is a very low-flow seep associated with deep red oxyhydroxide staining and is located northwest of the Restigouche deposit and southeast of the C4/C5 deposits (Fig. 5.12). Sample MLW95-434

was collected from a seep fed stream downslope from the previous sample. The latter water has low TDS and is similar in composition to stream waters from the North stream. In contrast, sample MLW95-345 has high TDS (94.69 mg/L) and moderately high SO_4 (14.00 mg/L) and Cl (1.00 mg/L).

Samples collected from small streams west of the Restigouche deposit (samples MLW96-710 to MLW96-713; Fig. 5.12) have a wide range in TDS (26.61 to 114.97 mg/L). Sample MLW95-713 has the highest TDS and flows over very different lithologies than the other three samples (Fig. 7.12).

Samples were also collected from Simpsons Brook, the Southeast Upsalquitch River and the Second Portage Lake. These samples were taken from higher order rivers (second order) and this is reflected in the higher TDS values for these waters. These waters are all $CaHCO_3$ waters with generally high pH (7.44 to 7.68).

5.3.2 Trace elements

As with the major species, many trace elements in Charlotte Brook waters show major differences upstream and downstream from the deposit (Fig. 5.17). Iron contents of Charlotte Brook waters are elevated in the headwaters although Fe is below detection in the two seeps adjacent to the stream at the headwaters (Fig. 5.15A). Dissolved Fe contents are low in Charlotte Brook waters further downstream but increase again in the vicinity of the main Restigouche ore body. Immediately downstream from the deposit, Fe contents are as high as 90 µg/L and decrease with increasing distance downstream. Manganese displays a pattern similar to Fe with the highest values in the headwaters and adjacent to the ore body. Downstream from the deposit, Al shows very little variation ranging from 3.3 to 5.2 µg/L. Upstream from the deposit, Al values are lower, generally < 3 µg/L. Barium and Sr contents are fairly uniform along the stream, although Sr contents are slightly higher downstream of the deposit and Ba contents slightly lower. Although all Restigouche deposit surface waters show a strong positive correlation between Sr and TDS, the higher TDS waters from Charlotte Brook

have slightly lower Sr than the lower TDS waters (Fig. 5.16). The waters show a trend of increasing U with increasing TDS. Nickel and PO_4 contents are generally low throughout the stream with the exception of samples at the headwaters which are elevated in these elements. Bromide values are high and Br/Cl low downstream from the deposit (Fig. 5.17).

The two samples along Mt Fowler east stream taken closest to where the Fe-oxides are thickest have the lowest Eh and pH values along this stream. These two samples plot well into the Fe^{2+} stability field (Fig. 5.18). In addition, samples MLW95-665 and MLW96-665 have elevated Fe contents relative to the other waters along this stream and contain the highest values in the study area (Fig. 5.16). The samples with the low Eh and pH have U contents that are among the highest values for all surface waters from the Restigouche deposit. There are differences in the composition of the two tributaries along this stream. The northern tributary (samples MLW96-665 and MLW95-667) have lower Sr and higher Rb than the southern tributary (samples MLW96-664, MLW96-666, and MLW96-668). Nickel contents in the Fe-rich waters are elevated but PO_4 contents are higher in the other waters along this stream.

Iron contents are low along the length of Mt Fowler northeast stream whereas, Mn contents increase downstream (Fig. 5.15A, B). Mt Fowler northeast waters are distinctive in having very elevated Sr contents compared to other surface waters from the Restigouche deposit (Fig. 5.16). Barium contents are higher than Charlotte Brook waters but lower than waters from Mt Fowler east stream, and Ba varies little along the length of the stream except at the headwaters where a higher TDS sample has lower Ba. Rubidium and Ni values are uniformly low along this stream, again in contrast to the Mt Fowler east stream.

Mt Fowler southwest stream has the only surface waters with consistently detectable F in the Restigouche deposit study area (Appendix B.1.1). Although Mn contents are moderately high, there are no consistent trends along the stream. Iron and Al differ in that they generally decrease downstream with the exception of samples closest to the confluence with Charlotte Brook (Fig. 5.17). Both Sr and U contents are somewhat elevated at the TDS values of these waters but show little variation along the stream.

Mt Moser northwest waters have generally low Fe contents and variable Mn contents. Surface waters in this area have higher Ba contents than surface waters elsewhere at a similar TDS value (Fig. 5.16). Both Sr and U contents are strongly correlated with TDS for these waters and increase downstream.

Mt Vroom east and southeast waters are characterized by generally elevated Fe and Mn contents, particularly given the very low TDS values (Figs. 5.16, 5.17A, B). All the waters plot in the Fe^{2+} stability field (Fig. 5.18). These waters have generally elevated Al contents (6 - 34 μg/L), which is consistent with the low pH values (Fig. 5.16). Barium, Sr, PO_4, and U contents are very low with the exception of seep sample MLW96-641 which has higher Ba and Sr than the other waters from this stream. This stream drains older metasedimentary rocks and is notable for having elevated Ni contents (Fig. 5.17I).

Mt Vroom north stream is characterized by low Fe (mostly below detection) and Mn contents. As with the Mt Vroom east stream, Al contents are typically elevated especially in the upper reaches and are coincident with low pH. Dissolved phosphate contents are variable, but increase with increasing TDS. Barium, Rb, Sr, and U contents are low although Sr contents are greater closer to the confluence with Charlotte Brook.

Waters from Mt Vroom northeast stream show the same general characteristics as the other two Mt Vroom streams such as low Fe (most are below detection), Mn, Ba, Rb, Sr and U, and elevated Al and Ni. Sample MLW95-467 is anomalous in that it has higher Al and Mn contents than the other waters along this stream. As discussed in later chapters, this sample is also slightly anomalous in Pb (Chapter Thirteen) and the dissolved Pb has a Pb-isotopic signature similar to galena from the Bathurst Mining Camp (Chapter Twelve). Manganese contents decrease in the waters downstream from this sample (Fig. 5.17B).

Most of the waters in North stream are below the detection limit for Fe. However, several samples at the top of the stream near the transported gossan have detectable Fe. Manganese contents are also elevated for these waters (Figs. 5.16, 5.17). Waters in this stream have variable, though commonly elevated, values of Al and PO_4 as well as elevated Ba and to a

lesser extent Rb.

The three seep samples are anomalous in the trace elements Fe, Mn, Al, Ba and Rb. Sample MLW95-300 has a very high PO_4, but the other two samples are very low. The samples recovered from west of the Restigouche deposit typically have elevated Fe and Mn contents as well as elevated Sr, Ba, and Rb.

5.3.3 Statistical analysis

As with the surface waters from the Halfmile Lake deposit, statistical analysis involved calculation of summary statistics (Appendix B.1.2), and correlation coefficients (Appendix B.1.3), and principal components analysis (PCA; Figs. 5.19, 5.20). More samples were collected over a larger area at the Restigouche deposit compared to the Halfmile Lake deposit. As a result, many elements in Restigouche deposit surface waters are normally or log-normally distributed. Significant inter-element correlations are shown by the Pearson Product Moment correlations (Appendix B.1.3) and PCA vectors (Fig. 5.19). The PCA suggests that six factors account for most of the variation in the Restigouche deposit surface water data. TDS, Ca, HCO_3, Sr, pH, and Cl typically cluster and have strong positive covariations. These elements are controlled by carbonate dissolution and rock weathering for Cl. Although Mg, Si and Na show strong correlations with TDS, they typically cluster together (Fig. 5.19) and are related to silicate weathering. Iron, Mn, SO_4 and Al tend to plot closely and for most factors DO and Eh are strongly correlated. The different stream consistently plot coherently based on PCA (Fig. 5.20). The streams draining Mt Vroom tend to plot close to each other as do the streams draining Mt Fowler.

5.3.4 Geochemical modelling

Element speciation and mineral saturation indices were modelled for a selected group of Restigouche deposit surface waters with PHREEQC using the WATEQ4F database. The samples selected for speciation and mineral saturation calculations were those which had been

analyzed for trace metals and REE by chelation ICP-MS. Saturation indices for selected minerals are presented in Appendix B.1.4 and the results of the speciation calculations for the major cations, trace metals and phosphate are presented in Appendix B.1.5.

Based on PHREEQC calculations, none of the surface waters at the Restigouche deposit are saturated with respect to carbonate minerals (Fig. 5.21), although seep sample MLW95-345 has a $SI_{Siderite}$ value of -0.06 and is essentially at siderite saturation. Surface waters with the highest pH values approach saturation with respect to calcite. Water pH is the dominant control of Fe-oxide solubility and most surface waters are saturated to strongly supersaturated with respect to hematite, goethite and magnetite. However, the stabilization of these minerals is kinetically inhibited compared to amorphous Fe-oxyhydroxides. Many of the higher pH waters from Charlotte Brook and Mt Fowler SW stream are supersaturated with respect to $Fe(OH)_{3(aq)}$ whereas lower pH surface waters are undersaturated (Fig. 5.21). Surface waters from Mt Vroom east and Mt Fowler east streams are strongly undersaturated with respect to Fe-oxyhydroxides. In the case of the Mt Vroom east streams, these waters were associated with ferricrete ledges and adjacent to sample MLW96-641 there is good evidence for amorphous Fe-oxyhydroxide precipitates. Samples MLW96-663, MLW96-664 and MLW96-665 from Mt Fowler east stream were associated with thick accumulations of Fe-oxyhydroxides on the stream bed. That these waters all have $Fe(OH)_3$ saturation indices below saturation indicates either that these waters are not related to those that precipitated the Fe-oxyhydroxides or that Fe-oxyhydroxides had already precipitated from solution prior to sampling. This latter is the most like given that oxidation of Fe from ferrous to ferric iron and subsequent precipitation as oxides is an acid producing reaction accounting for the moderately low pH values of these waters. Although "dissolved" Fe contents do not control $Fe(OH)_3$ saturation, there is a positive correlation between Fe content and $SI_{Fe(OH)3}$ for waters which are saturated to supersaturated (Fig. 5.21). This may be an artifact of very fine particles of $Fe(OH)_3$ having passed through the filter during sampling which may also influence the data for Al and Al-mineral saturation. There is a strong positive correlation between Al contents and the degree of supersaturation of

kaolinite. Experimental work has shown that the main phases controlling Al in natural aqueous systems (gibbsite, kaolinite, pyrophyllite) have minimum solubility at a pH of 6 to 7. Restigouche deposit surface waters reach a maxima for $SI_{Kaolinite}$ at pH 6 (Fig. 5.21). All the waters are undersaturated with respect to amorphous silica but are uniformly close to quartz saturation (SI_{Quartz} varies from -0.07 to -0.46; Appendix B.1.4).

Element speciation results show the following characteristics. The major cations occur primarily as free ions. Greater than 95% and 94% of calcium and magnesium, respectively, occur as free ions, and Na and K are essentially present only as free ions. Sample MLW95-300 with very low pH and high sulphate content is the exception. In this sample, complexes with sulphate account for 9% of the Ca, 10.6% of the Mg, 0.36% of the K and 0.25% of the Na in this sample. For all other waters, CO_3, HCO_3 and SO_4 complexes typically comprise less than 2% of the Ca and Mg speciation and Sr and Ba show essentially identical results to Ca and Mg. The speciation of Pb, Zn, PO_4, Cu, Fe and Al is more complex and highly dependent on solution pH and to a lesser extent redox condition. For example, Pb is present in surface waters with pH values < 6 primarily as Pb^{2+} whereas at pH values > 6, $PbCO_{3(aq)}$ is the dominant species (Fig. 5.22). Sample MLW95-300 also has 22% of its Pb load complexed as $PbSO_{4(aq)}$. Zinc shows similar behaviour to Pb except that the point at which $ZnCO_{3(aq)}$ is the more dominant Zn species over Zn^{2+} is shifted to higher pH (Fig. 5.22).

5.4 Discussion

5.4.1 Comparison between Halfmile Lake and Restigouche deposit surface waters

Surface waters at the Restigouche differ from those at the Halfmile Lake deposit in a number of important ways. Surface waters at the Restigouche deposit are proportionally more Mg and Ca-rich and Na-poor compared to those from the Halfmile Lake deposit when viewed on a piper plot (cf, Figs. 5.2, 5.13). This may be a reflection of the greater amount of carbonates within the Restigouche deposit host rocks compared to the Halfmile Lake deposit

but is more likely a combination of factors that include the host rocks, the fracture zone mineralogy and pre-glacial and modern weathering histories. Surface waters at Restigouche are proportionally enriched in HCO_3 compared to SO_4 and Cl relative to the Halfmile Lake deposit waters. Average unaltered host rocks from the Restigouche deposit have higher Ca, Fe, Na and lower K compared to average unaltered Halfmile Lake lithologies (see Table 2.1).

Restigouche deposit surface waters are more variable in pH and Eh than those from the Halfmile Lake deposit (Fig. 5.18). Restigouche deposit surface waters commonly have lower pH values, a function primarily of differences in lithology and Fe-oxyhydroxide precipitation. Surface waters at the Restigouche deposit adjacent to the main ore body have relatively high pH values (Charlotte Brook; Fig. 5.15). Thus, the trend to lower pH values at the Restigouche deposit is not the result of closer proximity of the Restigouche ore body to surface compared to the Halfmile Lake deposit. The surface waters at the Restigouche deposit that uniformly have the lower pH values are from streams draining the older metasedimentary rocks (Miramichi Group) in the southern part of the study area (Fig. 5.15). Some of these waters are associated with Fe-oxide and oxyhydroxide precipitates (Mt Vroom east and Mt Fowler east streams). Although Fe-oxyhydroxide precipitation is an acid producing reaction, this factor is probably controlling the low pH of a few waters only (e.g., samples MLW96-664 and MLW96-665 from Mt Fowler east stream and samples MLW96-710 and MLW96-711 from west of the deposit). The lack of significant Fe-oxides along the Mt Vroom north and northeast streams suggests that the low pH values in waters draining the older metasediments is mostly controlled by the lithology. No significant Fe-oxides were observed associated with streams at the Halfmile Lake deposit with the exception of the area adjacent to an artesian borehole (Sample MLW94-100; Chapter Seven). The lack of major Fe-oxyhydroxides at the Halfmile Lake deposit is reflected in the low Fe_2O_3 contents of stream sediments. At the Restigouche deposit, stream sediments range up to 54 weight% Fe_2O_3 whereas Halfmile Lake deposit stream sediments have a maximum of 7 weight % Fe_2O_3 (see Chapter Six).

5.4.2 Comparison with world average river and previous studies in the BMC

A subset of the Halfmile Lake and Restigouche deposit surface waters were compared to world average river (WAR) compositions (Figs. 5.23, 5.24) using data from Berner and Berner (1987). Although there are systematic differences in surface water composition between the Halfmile Lake and Restigouche deposits, these surface waters compared to WAR show several features in common. Surface waters from both deposits are strongly depleted in Cl compared to WAR by an order of magnitude. In contrast, HCO_3 contents are similar to (Halfmile Lake deposit) or greater than (Restigouche deposit) WAR. Because the primary control over sulphate compositions is proximity to oxidizing sulphide minerals in the BMC waters (see below), this anion shows more variation compared to WAR. Restigouche deposit surface waters have generally elevated sulphate compared to Halfmile Lake deposit waters and WAR, a function of the more shallow nature of the Restigouche deposit and the possible occurrence of mineralization to the east and west of the deposit (Chapter Thirteen). Compared to WAR, cations are generally lower in abundance and surface waters are relatively depleted in K and enriched in Ba.

There have been few detailed hydrogeochemical studies published on the Bathurst Mining Camp. Boyle et al. (1966) analyzed over 3,500 stream sediments and waters from the BMC during the 1960's. These waters, however, were determined only for pH, temperature and total heavy metals. A subset of 250 samples from the BMC but east of the Restigouche deposit area and northeast of the Halfmile Lake deposit area and extending towards Bathurst were analyzed for a more complete suite of elements. In general, the waters analyzed by Boyle et al. (1966) have higher Na and Cl contents than Halfmile Lake and Restigouche deposit surface waters (Fig. 5.25). This is possibly due to sampling of generally larger streams in the 1966 study, resulting in more integrated chemical signatures from larger catchments. Furthermore, the streams sampled by Boyle et al. (1966) are located closer to the coast than those sampled in this study. There may be a greater influence of marine aerosols on waters collected in 1966. This interpretation is consistent with much lower Na/Cl_{molar} of the 1966 waters compared to

those from the Halfmile Lake and Restigouche deposits. The Na/Cl_{molar} of surface waters in the study of Boyle et al. (1966) approach the seawater value of 0.85. As with the data in this study, the 1966 data indicates that the TDS contents of surface waters in the BMC are controlled primarily by Ca and HCO_3 (Fig. 5.25). The 1966 data has uniformly higher Al, Zn and Cu values than surface waters from the Halfmile Lake and Restigouche deposits. This is in part a function of much lower detection limits possible with modern ICP-MS analytical methods. Some of the elevated SO_4 and Zn values in the 1966 data set are from Middle River downstream from the Brunswick #12 deposit. These samples were collected soon after that deposit went into production.

5.4.3 Comparison with host lithologies

Studies of large river basins (Dupré et al., 1996; Gaillardet et al., 1995; Gaillardet et al., 1997; Négrel et al., 1993; Stallard and Edmond, 1983) have looked at element-source relationships by normalizing to average upper continental crust. Although this may be an appropriate approach for large catchments which integrate disparate rock types, it is less appropriate for studies of small catchments. A better approach is to normalize water compositions to the local lithologies. A representative subset of Halfmile Lake deposit surface waters were normalized to average unaltered felsic lithologies from the deposit (Fig. 5.26) and a subset of Restigouche deposit surface waters were normalized to the average unaltered composition of felsic and dacitic rocks from the Restigouche deposit (Chapter Two; Fig. 5.27). The order of the elements in these plots is based on a monotonic decrease in elemental abundance in continental crust normalized to chondritic abundances (Hofmann, 1988). There are several striking features of host lithology-normalized surface water compositions. Elemental abundances are highly variable compared to average unaltered host rocks. Compared to surrounding elements, K, Ba, Sr, Na and Ca are elevated and Fe and the REE are depleted. There is also a general increase in REE with increasing element compatibility (the REE are discussed more fully in Chapter Ten). The low Fe contents are interpreted to reflect removal of

Fe by formation of Fe (± Mn) oxyhydroxides. Patterns for surface waters from the Restigouche deposit are generally very similar to those from the Halfmile Lake deposit although the former tend to show greater relative enrichments in Pb and Co (Figs. 5.26, 5.27).

The BMC surface waters were also normalized to average upper continental crust (not shown) and essentially the same patterns are evident. Most of the lithologies in the Halfmile Lake and Restigouche deposits have very flat patterns close to unity when normalized to average upper crust, with minor exceptions. Strontium, Na, and Ca show particularly strong depletions in unaltered Halfmile Lake and Restigouche rocks compared to average upper continental crust. The positive anomalies in these elements in the surface waters are therefore more subdued normalized to upper continental crust. The patterns observed for the surface waters are not an artifact of inheritance from the host rocks but rather related to processes of speciation and element mobility in the surface environment. The element variations seen in the surface waters compared to upper continental crust are more extreme than those seen in a similar study of surface waters from the Congo River basin by Dupré et al. (1996), which showed similar but more subdued continental crust-normalized patterns. The differences in degree of enrichment or depletion may be an artifact of comparing large rivers (Congo River basin) which represent regionally integrated samples with smaller stream from local catchments where variations in geology, climate and topography are reflected by surface waters and shallow ground waters on a smaller scale.

5.4.4 Comparison with precipitation

A limited number of precipitation samples were collected during the course of this study. Of the six precipitation samples recovered, two have been rejected from further consideration because it was obvious at the time of recovery that the intensity of the storms had resulted in small amounts of sediment being splashed into the collector. Elevated TDS for these two samples are consistent with this interpretation. For the other four samples (Table 5.1), the following generalizations can be made.

Table 5.1 Precipitation data

Sample #	MLW95-304	MLW95-524	MLW96-670	MLW96-672
Deposit	Restigouche	Restigouche	Restigouche	Halfmile Lake
pH	4.92	4.67	5.02	4.38
mg/L				
SO_4	1.00	1.69	0.55	1.70
Cl	<0.05	0.16	<0.05	0.12
µg/L				
NO_3	632	779	339	1648
Al	14	9.6	3.3	10
Fe	35		3	10
Mn	10	8.3	1.4	2.6
Mg	24	34	21	17
Ca	230	130	39	45
Na	150	100	475	137
K	87	140		30
Ba	5.7	7.4	1.1	7.1
Sr	0.9	0.5	5	

Total dissolved solid contents are very low (1-2 mg/L) with Cl ranging from less than detection to 0.16 mg/L and SO_4 ranging from 0.5 to 1.7 mg/L. Precipitation pH values are low (4.38 to 5.02) and therefore there is no HCO_3 alkalinity.

Consideration must be given to precipitation as a source of solutes for the surface waters from both deposits. From the comparison between the limited precipitation data and the surface waters with the lowest TDS values, it is clear that precipitation is not a major source of solutes. For example, in a study on the Miramichi River system, Caissie et al. (1996) inferred, based on storm hydrograph separation, that precipitation was a major source of sulphate. Although some of the surface waters at the Halfmile Lake have low sulphate contents similar to precipitation (Fig. 7.3), the sulphate contents at both the Halfmile Lake and Restigouche deposits are for the most part well in excess of values for local precipitation (Figs. 7.3, 7.13). Samples were not collected for sulphur isotope determination but given that the waters were collected proximal to oxidizing massive sulphide deposits, the elevated SO_4 contents of many

of the surface waters are interpreted to be due primarily to sulphide oxidation.

There are several possible explanations to account for the high Cl contents of the surface waters at both the Halfmile Lake and Restigouche deposits compared to precipitation. Although evaporation is commonly an important process for producing high Cl in natural waters, it is unlikely that evaporation is a very significant process for the surface waters in this study. In Chapter Eleven, it is shown that the $\delta^{18}O_{V\text{-}SMOW}$ and $\delta D_{V\text{-}SMOW}$ contents of surface waters from both deposits overlap those of shallow groundwaters and plot above the meteoric water line. Evaporation preferentially fractionates oxygen relative to deuterium, producing trends with shallow slopes away from the meteoric water line. It is more difficult to assess the effects of evapotranspiration in concentrating solutes in the surface waters as this is isotopically non-fractionating. However, Cl is a conservative element and is expected to increase where evapotranspiration processes are important (Billett et al., 1996). There is little apparent relationship between Cl content and distance downstream at the Halfmile Lake and Restigouche deposits (Figs. 5.4, 5.15). Chloride contents of surface waters from Charlotte Brook at the Restigouche deposit are higher downstream from the Restigouche ore body compared to upstream of the ore body. However, this is interpreted to be due to the influence of saline waters recovered proximal to the deposit (Chapter Seven), an interpretation that is supported by the spatial distribution of Br/Cl_{molar} ratios (Fig. 5.17J). Charlotte Brook waters immediately downstream from the deposit have very low Br/Cl_{molar} relative to other surface waters and the saline waters recovered from borehole MM-88-02 have the lowest Br/Cl_{molar} of all waters in this study (Chapter Seven). Most surface waters have Br/Cl_{molar} considerably greater than the seawater value of 0.00154 indicating that marine derived aerosols are not the primary origin of surface water Cl salinity and that higher Cl abundance is not caused by concentration by evapotranspiration.

Typically, Cl in stream waters is assumed to be derived entirely from precipitation due to the general lack of easily solubilized Cl-bearing phases in most geological environments (e.g. Gaillardet et al., 1997; Viers et al., 1997). Although this is a common assumption in the

hydrogeochemical literature, it is commonly not substantiated by rock compositions. From the data presented in Chapter Two, it is clear that, at least for the BMC, the host rocks are in fact the most likely source of Cl. Chloride contents in the host rocks at the Halfmile Lake and Restigouche deposits range from less than detection (100 ppm Cl) to 586 ppm (Table 2.2). Chloride contents of stream sediments are typically higher than the host lithologies (Chapter Six). Thus, the elevated Cl contents of the surface waters over those of local precipitation are interpreted to be produced primarily by rock weathering. Note that compared to average unaltered host lithologies, Cl is the element most preferentially incorporated into the aqueous phase (assuming an average rock Cl content of 150 ppm; Figs. 5.26, 5.27), consistent with this interpretation.

The precipitation data (Table 5.1) suggests that for the study areas most of the NO_3 originates from precipitation unlike Cl. However, nitrate is a minor constituent of surface waters from the Halfmile Lake and Restigouche deposits (Appendices A.1.1 and B.1.1). Only sixteen of 147 surface water samples from the Restigouche deposit have NO_3 values greater than the detection limit (50 μg/L) and only one of these has $NO_3 > 400$ μg/L. At the Halfmile Lake deposit, only three samples have NO_3 values greater than detection, ranging from 52 to 1084 μg/L. This suggests that a) the primary source of nitrate in the surface waters is due to precipitation input, and b) that the surface waters primarily reflect base flow. Nitrate is reduced in the soil zone and shallow groundwater system by denitrifying bacteria. If the surface waters had a significant component of storm event water, nitrate levels would be expected to be uniformly higher. The similarity in stable isotopic compositions between shallow groundwaters and surface waters also indicates base flow conditions (see Chapter Eleven).

5.4.5 Source control on major solute variations

From the preceding discussion, the primary source of major solutes to the surface waters in the two study areas is interpreted to be the host lithologies. Studies of large drainage basins typically focus on quantifying the relative contributions of silicate, evaporite and carbonate

rocks to river water chemistry (e.g. Gaillardet et al., 1997; Négrel et al., 1993). However, for the Halfmile Lake and Restigouche deposits, there are no known limestone or evaporite units in the study areas. The main lithological controls over stream water chemistry are related, therefore, to differences in silicate lithology and degree of water-rock reactions with those lithologies. A common approach to investigating the influence of lithology on surface water composition is through the use of major ion ratios which are independent of water flux and evaporation (Gaillardet et al., 1997). For the Halfmile Lake deposit, an extensive database of whole rock geochemistry exists (Adair, 1992). This data has been complemented by analyses presented in Chapter Two. Data from the Restigouche deposit is more limited and is presented in Chapter Two. These two data sets allow comparison with the surface waters from both deposits in terms of element ratios (Figs. 5.28, 5.29). Constraints based on a limited number of Sr isotope analyses from the Restigouche deposit are presented in Chapter Twelve.

One of the important features of the Halfmile Lake surface waters is the division between the compositions of waters draining the rocks on the west half of the study area compared to those draining the eastern half (Fig. 5.4). There is an obvious subdivision in rock type with rocks on the western half of the study area dominantly felsic volcanic and felsic volcaniclastic rocks whereas those on the eastern half are more mafic in composition. This general subdivision is reflected in higher TDS, HCO_3 and Ca contents in waters from the North and Northeast tributaries as well as the Halfmile North stream. Felsic rocks have higher K and Na and lower Ca and Mg than mafic rocks (Chapter Two, Table 2.1). The Upper/Lower AB and West tributary streams have higher K/Ca, Na/Mg and lower Ca/Mg than the eastern streams, reflecting interaction with more felsic host rocks. The higher Na and K may also in part reflect sericitic and albitic alteration of footwall (structural hanging wall) lithologies by hydrothermal fluids during formation of the ore deposit (Lentz and Goodfellow, 1994; Lentz and Goodfellow, 1996; Lentz and Gregoire, 1995).

The Northeast and North tributaries have the lowest Na/Mg ratios which may be related to lower Na in hydrothermally altered rocks hosting the ore body and/or higher Mg and lower Na

contents in mafic rocks drained by these streams (Fig. 5.1). The fact that Na and Mg are so well correlated suggests that both elements originated from silicate weathering. There are no known evaporite deposits in the Ordovician sequences in the area. The Mg/Na ratios of the stream waters (0.4 - 0.8) are quite different from precipitation (< 0.2). However, with the exception of the waters from the Halfmile North stream, Ca and Mg are highly correlated with each other and with HCO_3, which is consistent with carbonate weathering given the lack of other Ca-bearing minerals in the host lithologies.

There are no obvious differences between spring/seep and stream compositions at the Halfmile Lake deposit. However, as discussed in Chapter Ten, there are interesting differences in terms of response of dissolved REE contents and the development of large negative Ce anomalies. Significantly, the spring/seep waters at the headwaters of the Upper/Lower AB stream have elevated K (as a proportion of total cations) relative to other waters suggesting that these fluids may be interacting with sericitic (argillic) alteration associated with the orebody.

There is more variation in lithology at the Restigouche deposit compared to the Halfmile Lake deposit. Charlotte Brook and North stream, adjacent to the deposit, primarily drain Ordovician felsic volcanic units of the Mt Brittain Formation (Gower, 1996). Streams draining Mt Vroom in the southern and southeastern part of the study area (Fig. 5.12) flow over older Cambro-Ordovician Miramichi Group metasedimentary rocks. Mt Fowler southwest stream partly flows over these older rocks, but is dominated by waters closer to the headwaters which drain Mt Brittain and Boucher Brook formations. The two streams draining Mt Fowler to the east flow primarily over Boucher Brook Formation sedimentary units (Gower, 1996). Finally, the Mt Moser NW stream drains younger Silurian sedimentary rocks. Some major differences in surface water compositions are evident based on these broad subdivisions of the lithologies over which the streams flow (Fig. 5.15) which are reflected in the PCA (Fig. 5.20).

The Mt Vroom streams are characterized by low TDS and HCO_3, and generally low Cl contents. Sulphate in Mt Vroom east waters are relatively high and may be related to sulphide mineralization in the subsurface (see Chapter Thirteen for further discussion). These streams

also have lower pH values and major cation contents compared to the other streams. Thus, the older metasedimentary rocks that comprise the Miramichi Group are interpreted to be less susceptible to weathering compared to the other lithologies, resulting in much lower solute loads in the associated streams.

Streams draining Mt Fowler have very different characteristics. In these waters (Mt Fowler east and northeast streams and, to a lesser extent, Mt Fowler southwest), TDS contents are elevated and the dominant anion is HCO_3. However, sulphate is typically elevated, especially in Mt Fowler east stream, where high SO_4 contents are associated with extensive Fe-oxides in the stream sediments, interpreted to be produced by sulphide oxidation in the subsurface. All three streams have high Mg and Ca but Mt Fowler east and northeast streams have generally low K contents whereas in the southwest stream K contents are high. Although the east and northeast streams drain mostly Boucher Brook rocks, the northeast stream has Boucher Brook and Sormany Formation mafic volcanic rocks within its catchment. This probably accounts for the high Na contents of waters from the Mt Fowler northeast stream relative to the Mt Fowler east stream.

Charlotte Brook, the main stream in the Restigouche deposit study area, shows the most variation along its length. Charlotte Brook flows over the Restigouche ore body close to where the deposit is exposed at the surface. Thus, surface water upstream from the deposit is commonly compositionally different than surface water downstream from the deposit (Figs. 5.13, 5.14). Shallow groundwaters recovered from boreholes close to Charlotte Brook (borehole MM-88-06 and MM-88-07; see Fig. 7.13) have very elevated base metal and sulphate contents. The SO_4 contents of Charlotte Brook are, however, lower downstream from the deposit than in the headwaters, and lower than North stream which enters Charlotte Brook just downstream from the deposit. In addition, although Charlotte Brook is anomalous in terms of dissolved metal contents (e.g., Pb, Zn; Chapter Thirteen), metal loads are much lower than in shallow groundwaters. There are two explanations for the lower SO_4 content of the stream below the deposit. Firstly, Charlotte Brook is diluted with respect to SO_4 loads because Mt

Vroom north stream with low SO_4 contents enters Charlotte Brook near the ore body. Secondly, it is possible that Charlotte Brook is recharging where it crosses the deposit, such that the influence of the shallow ore body is subdued. This is consistent with water table levels observed in boreholes adjacent to Charlotte Brook (Chapter Four).

Restigouche deposit surface waters have lower pH values than Halfmile Lake deposit surface waters. At lower pH there is a sharp increase with increasing TDS (Fig. 5.14). This is interpreted to be due to rapid equilibration of recharging waters with carbonate and silicate minerals in the soil zone and shallowest groundwater zone. The involvement of silicate minerals in this process is suggested by the positive correlation between Si and TDS for these low-pH surface waters (Fig. 5.14; Appendix B.1.3). In contrast, Halfmile Lake deposit surface waters show no statistically significant correlation between TDS and Si.

Surface waters from both the Halfmile Lake and Restigouche deposits display major cation ratios which illustrate the influence of host lithologies but which also indicate that another end-member is required to explain the compositional variation (Figs. 5.28, 5.29). The host rocks show large variations in Ca/Na, Mg/Ca, and K/Ca reflecting variations in lithology (mafic to felsic volcanic rocks and sediments). These ratios are also affected by alteration, both at the time of ore deposition, and due to weathering. Stream sediments show a much more restricted range in major element ratios compared to the host lithologies. This is in part due to mixing of sources during erosion and the homogenizing effect of chemical weathering. Surface waters are also much more restricted in major element ratios than the host rocks and are shifted to lower Mg/Ca and K/Ca and higher Ca/Na compared to the stream sediments. There are two reasons for this. Firstly, as discussed below, weathering of carbonate minerals is a major control on the Ca, Mg and HCO_3 contents of the surface waters. Thus, on Mg/Ca vs Ca/Na and K/Ca vs Ca/Na plots, the waters trend away from the host lithology array towards carbonate compositions. Carbonate minerals make up only a minor component of the host rocks but have a major influence on stream composition. The shift of the surface waters to higher Ca/Na and lower K/Ca and Mg/Ca compared to the stream sediments (Figs. 5.28, 5.29)

is due to the greater solubility of carbonate minerals compared to silicate minerals. Magnesium, K and Na are contained in chlorite, sericite/illite and albite, respectively, which are more resistant to weathering than carbonate, the primary source of Ca for surface waters at both deposits. Carbonate altered host rocks (i.e. those with elevated CO_2 contents; Table 2.1), plot towards high Ca/Na and low K/Ca which supports the importance of carbonate weathering at both the Halfmile Lake and Restigouche deposits.

5.4.6 Modelling of water-rock reactions

Modelling was carried out using the geochemical modelling code NETPATH (Plummer et al., 1995). NETPATH was used to constrain likely water-rock reactions rather than to quantify specific reaction pathways. The purpose of this exercise was to try and determine 1) plausible sources of the major solutes and 2) the source of high dissolved Ca, the dominant cation in most of the surface waters in this study. Consideration was given to the likely minerals undergoing dissolution to produce the stream water compositions. The activities of Si, Al, Ca, Na, Mg and K indicate that of the major silicates comprising host lithologies, weathering of feldspar to kaolinite is the main silicate hydrolysis reaction. In most activity diagrams, the surface waters plot in the kaolinite stability field. Given the presence of large massive sulphide deposits, high SO_4 in surface waters is more likely related to sulphide oxidation, and this is clearly shown for high-sulphate groundwaters (see Chapter Seven). Therefore, pyrite was included in NETPATH models as the primary source of dissolved sulphate. The surface waters at both the Halfmile Lake and Restigouche deposits are dominantly Ca-HCO_3-type waters (Figs. 5.2, 5.13). However, other than carbonate which is present as cross-cutting veins and coating fractures, there are no Ca-bearing minerals in the host lithologies. Although feldspar is a common phenocrysts and groundmass phase in the host rocks, plagioclase cannot be a major source of Ca for surface waters because microprobe analyses of plagioclase feldspar indicates that the dominant feldspar is albite with compositions greater than Ab_{97} (Rogers et al., in press). Thus, for the purposes of NETPATH modelling, the following minerals were

considered: albite, kaolinite, sericite (with a composition based on sericite compositions reported by Lentz (1995)), dolomite, calcite, goethite, pyrite and K-feldspar; cation exchange involving exchange of Ca for Na was also considered an important process. Mass balance calculations using NETPATH indicate that the Ca contents of the surface waters can be accounted for on the basis of carbonate (calcite and dolomite) dissolution combined with the dissolution of feldspar and pyrite and cation exchange of Ca for Na. Most models suggest that K-silicates (illite, sericite) are precipitated along with goethite and in some models chlorite. Therefore, based on mineralogical evidence which is supported by NETPATH modelling, the majority of the dissolved Ca load in surface waters is interpreted to be due to carbonate dissolution. The volume of carbonate is typically minor but accounts for a disproportionate amount of the major ion budget in the Halfmile Lake Deposit surface waters. Previous studies have suggested that excess Ca reflects incongruent plagioclase dissolution such that the Ca-rich component is preferentially weathered compared to the Na-rich component and/or to minor amounts of vein carbonate (e.g. Mast et al., 1990). The excess Ca in the surface waters is evident by comparing the surface water Ca/Na with that of the local host rocks and stream sediments (Figs. 9.28, 9.29).

Many previous studies of large river basins have used element ratios and inverse modelling approaches to determine mass balance constraints on silicate, carbonate and evaporite end-members (e.g. Gaillardet et al., 1995; Gaillardet et al., 1997). This study of surface waters in a silicate-only terrane highlights the influence of minor minerals in the host rock on elemental budgets. However, note that Sr isotopes on six surface water samples from the Restigouche deposit range from non-radiogenic (MLW96-664) to moderately radiogenic (Chapter Twelve). Although carbonate minerals are also typically non-radiogenic due to the exclusion of Rb from the mineral structure, two carbonate samples analyzed from the veins below the Restigouche deposit vary in composition from non-radiogenic to moderately radiogenic ($^{87}Sr/^{86}Sr$ = 0.708889 to 0.714467) and span much of the range of the surface water compositions at the Restigouche deposit ($^{87}Sr/^{86}Sr$ = 0.708079 to 0.718478; n = 6). This is discussed in greater

detail in Chapter Twelve. Thus, the range in Sr isotopic composition for surface waters and shallow groundwaters can be accounted for by carbonate dissolution although Sr may also be in part derived from K-silicates such as sericite, especially close to the main Restigouche ore deposit.

At the Restigouche deposit, Si contents increase with increasing TDS, consistent with increasing silicate hydrolysis. Although it can be argued that the Ca and Mg contents to a large extent are controlled by carbonate dissolution in the shallow bedrock environment (which is consistent with $\delta^{13}C_{DIC}$ values of shallow groundwaters and surface waters; Chapter Eleven), the increasing Si coupled with increasing Na and, to a lesser extent K, indicates that some silicates are also being weathered. The decrease in Mg at high pH but not in Ca for the Restigouche deposit surface waters (Fig. 5.30) may be due to: 1) dissolution of carbonate is dominated by calcite at the higher TDS waters although this seems unlikely (note however that the waters with the higher TDS and lower Mg but high Ca are away from the Restigouche deposit, which may be where hydrothermal dolomite is concentrated); 2) preferential loss of Mg compared to Ca by cation exchange reactions; and 3) stabilization of secondary Mg-phases. No Mg-secondary phases, however, have been observed or are stable based on geochemical speciation (Appendices A.1.5, B.1.5).

5.4.7 Trace element variations

Most of the discussion of trace element variations at the Halfmile Lake and Restigouche deposits with respect to massive sulphide related metals (Zn, Pb, Cu, Co, Cd etc) is presented in Chapter Thirteen. This section examines the sources of non-ore related trace elements in the surface waters at the two deposits.

At the Halfmile Lake deposit the highest U contents in surface waters are in the Upper/Lower AB stream which are also reflected in the stream sediment data (Chapter Six). This implies that the dominant control on U contents of the surface waters is lithology. The Northeast and North tributaries consistently have the lowest U values which are consistent with

the more mafic underlying lithologies; U is an incompatible element in igneous systems such that abundances typically increase with increasing Si content. For example, mafic and felsic volcanic rocks from the Halfmile Lake analyzed in this study have < 1 ppm and 3-6 ppm U, respectively (see Table 2.1). Also, upper continental crust has greater U contents than the mantle and therefore felsic volcanic rocks are elevated relative to mafic volcanic rocks. Uranium is generally well correlated with Sr at the Restigouche deposit suggesting that carbonate minerals are the host for Sr and U. At the Halfmile Lake deposit, Sr and U do not correlate suggesting other minerals control the variations of these elements. Thus, Sr contents are higher in the stream waters flowing over more mafic lithologies, whereas U contents are generally greater in the Upper/Lower AB stream draining felsic rocks. Potassium and Rb show generally strong correlations with U in Halfmile Lake deposit surface waters, which is consistent with this interpretation. Uranium in stream water and sediments at the Restigouche deposit is very well correlated ($r^2 = 0.796$; Chapter Six). Uranium contents of Restigouche deposit surface waters is strongly negatively correlated with Si/Σ_{anions} which supports the derivation of U from carbonate minerals (Palmer and Edmond, 1993). Palmer and Edmond (1993) showed for rivers in the Amazon basin that this relationship held for waters draining carbonate and silicate terrains but that U was significantly higher for the carbonate terrains. Although the streams at the Restigouche deposit are draining silicate rocks, the relationship between U and Si still holds because the dissolved U contents reflect the weathering of vein and fracture carbonate. In contrast, U in surface waters from the Halfmile Lake deposit does not show the same U versus Si/Σ_{anions} relationship, consistent with U being controlled primarily by weathering of the felsic volcanic rocks.

At the Halfmile Lake deposit, surface waters draining the mafic lithologies on the eastern half of the study area have generally higher V contents than those draining the felsic volcanic rocks whereas Y contents are higher in the Upper/Lower AB stream. Yttrium in felsic volcanic rocks is greater than in the mafic units (Chapter Two; Table 2.2).

Phosphate in surface waters is not well correlated with any other parameter (Appendices

A.1.3, B.1.3). However, low-pH waters at the Restigouche deposit tend to have lower PO_4. Speciation calculations show that PO_4 is primarily complexed as oxyanions (Fig. 5.22) and at low pH is more readily adsorbed to oxide and silicate substrates, especially Fe-oxyhydroxides. Seeps (samples MLW95-300, MLW95-353, and MLW95-424) also have low pH, abundant Fe-oxyhydroxide minerals and relatively low PO_4. At both deposits there is a general relationship of decreasing PO_4 with increasing TDS (Figs. 5.5, 5.16), with the exception of very low TDS waters from the Restigouche deposit. At the Halfmile Lake deposit, the highest phosphate occurs in the West tributary and Upper/Lower AB streams draining the more felsic lithologies, possibly due to weathering of apatite. At the Restigouche deposit, surface waters with the highest PO_4 are primarily from Mt Moser northwest stream. Note also that although Y and PO_4 are not correlated in the surface waters, Restigouche deposit stream sediments show a very strong positive correlation between Y and P_2O_5, suggesting that apatite may be important in controlling aqueous PO_4 abundances.

Iron in Halfmile Lake deposit surface waters does not vary as a function of lithology or proximity to massive sulphide mineralization because the main ore body occurs at depth (Chapter Two). In fact, Fe contents are anomalously low along the north tributary downstream from the confluence of the Upper/Lower AB, Halfmile North and Northeast tributaries. This may be the result of precipitation of Fe-oxides caused by mixing of the different stream waters. However, all Halfmile Lake deposit surface waters based on measured Eh and pH values are stable with respect to ferric Fe (Fig. 5.10). Alternatively, the low Fe contents in the upper parts of the North tributary may be the result of increased base flow from seeps that were not observed during sampling. The Fe contents of the stream sediments are also low compared to the other streams at Halfmile Lake, which does not indicate significant precipitation of Fe-oxyhydroxides.

At the Restigouche deposit, there is more variation in dissolved Fe and some streams have abundant Fe-oxyhydroxides in the steam sediments. Much of this variation is due to more variable Eh and pH conditions for Restigouche deposit surface waters such that they straddle

the Fe^{2+}/Fe^{3+} stability boundary, unlike Halfmile Lake deposit surface waters (Fig. 5.18). For example, the Mt Fowler east stream contains significant Fe-oxyhydroxides (stream sediments have up to 54.3 weight % Fe_2O_3; Chapter Six). The two water samples collected close to where the Fe-rich seeps are inferred to come to surface along the Mt Fowler east stream have the lowest Eh and pH values along the stream and plot in the Fe^{2+} stability field (Fig. 5.18). The interpretation is therefore that reducing Fe-rich waters come to surface at this point at the break in slope and rapidly oxidize upon reaching the surface environment resulting in the precipitation of Fe-oxyhydroxides. Although the formation of Fe-oxyhydroxides is an acid-producing reaction, mixing with waters flowing from further upstream is sufficient to maintain moderate pH levels downstream from samples MLW96-664 and MLW96-665. The critical question is the source of the high Fe and SO_4 values in the stream sediments; these waters have moderate Fe values (338 and 215 μg/L, respectively) compared to the rest of the stream, but base metal contents are low. Given the lack of sulphate minerals in the host rocks to the Halfmile Lake and Restigouche deposits, the most likely explanation for the high sulphate is oxidation of sulphide minerals in the subsurface. This is discussed more fully in Chapter Thirteen. Note that sample MLW96-664 has a Pb isotopic composition which is similar to galena from massive sulphide deposits in the BMC suggesting that the Pb in Mt Fowler east stream, although in low abundance, was derived from sulphide mineralization. This is discussed in detail in Chapter Twelve.

Iron-oxyhydroxides and ferricrete are well developed in the Mt Fowler east and Mt Vroom east streams, respectively. In contrast, Fe-oxyhydroxides and ferricrete are not observed, except very locally, in Charlotte Brook and the North stream adjacent to the main Restigouche deposit. This may be a function of the mineralogy of the Fe-sulphides undergoing oxidation. Pyrrhotite is rare at the main Restigouche ore body. The higher abundance of Fe-oxides for the eastern streams may suggest that they host pyrrhotite which is more reactive than pyrite, galena, or sphalerite (Boyle, 1995). However, stream sediment chemistry (Chapter Six) indicates that the sulphide oxidation responsible for the high sulphate and Fe-oxide rich nature

of the Mt Fowler east stream is unlikely to be only pyrite or pyrrhotite. Stream sediment Zn contents in some of these sediments are comparable to Zn contents in stream sediments downstream from the main Restigouche Deposit in Charlotte Brook (1500 - 1600 ppm; Chapter Six). As noted previously, there is some evidence to suggest that Charlotte Brook is a losing (recharge) reach where it crosses the main Restigouche ore body (Chapter Four), preventing precipitation of significant Fe-oxides in Charlotte Brook.

5.5 Summary

1) Surface waters at the Halfmile Lake and Restigouche deposits are dominated by Ca-HCO_3 compositions. Surface waters at the Restigouche deposit have a greater range in pH and SO_4 contents, reflecting the closer proximity of known, and speculated, mineralization to surface at the Restigouche deposit.

2) Precipitation is interpreted to have little impact on major solute loads. Unlike many studies of surface water composition, elevated Cl contents in surface waters at the Halfmile Lake and Restigouche deposits is interpreted to be the result of rock weathering which is consistent with Cl in host rocks and stream sediments. There is no evidence for evaporative concentration of Cl.

3) Differences in the lithologies over which different streams flow is the dominant control over major and trace element contents. However, Ca (and to a lesser extent Mg) in surface waters is dominantly controlled by dissolution of carbonate minerals, present in veins and coating fractures. This is consistent with Sr and C isotopic data presented elsewhere (Chapters Twelve and Eleven, respectively). There are no other known sources of Ca within the host lithologies.

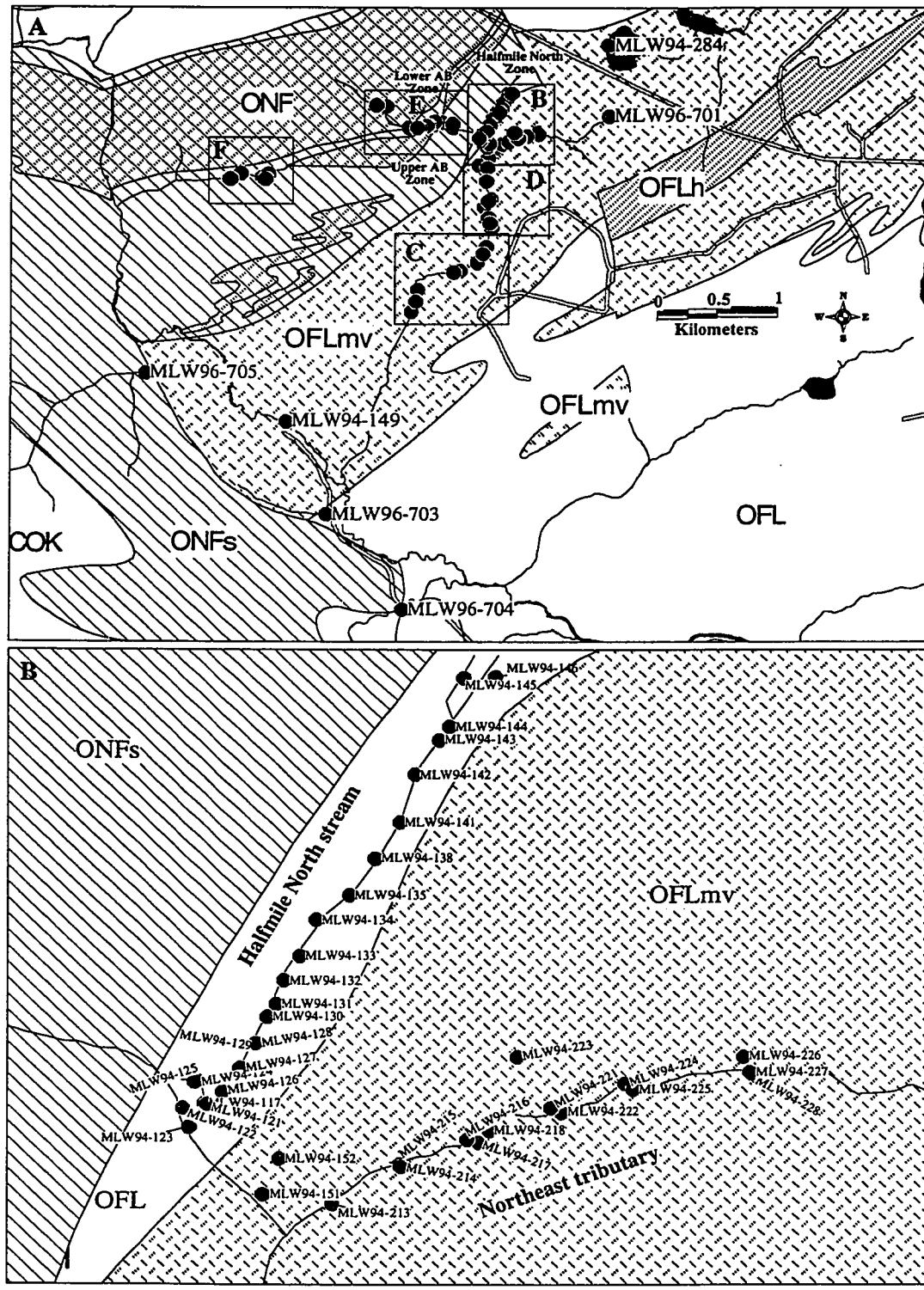


Fig. 5.1 Location of Halfmile Lake deposit surface waters. ONF = Nepisiguit Falls felsic volcanics, ONFs= Nepisiguit Falls sediments, OFLmv = Flat Ladning Brook mafic volcanics, OFL = Flat Landing Brook rhyolite, OFLh = Flat Landing Brook hyaloclastite, COK = Knights Brook Formation.

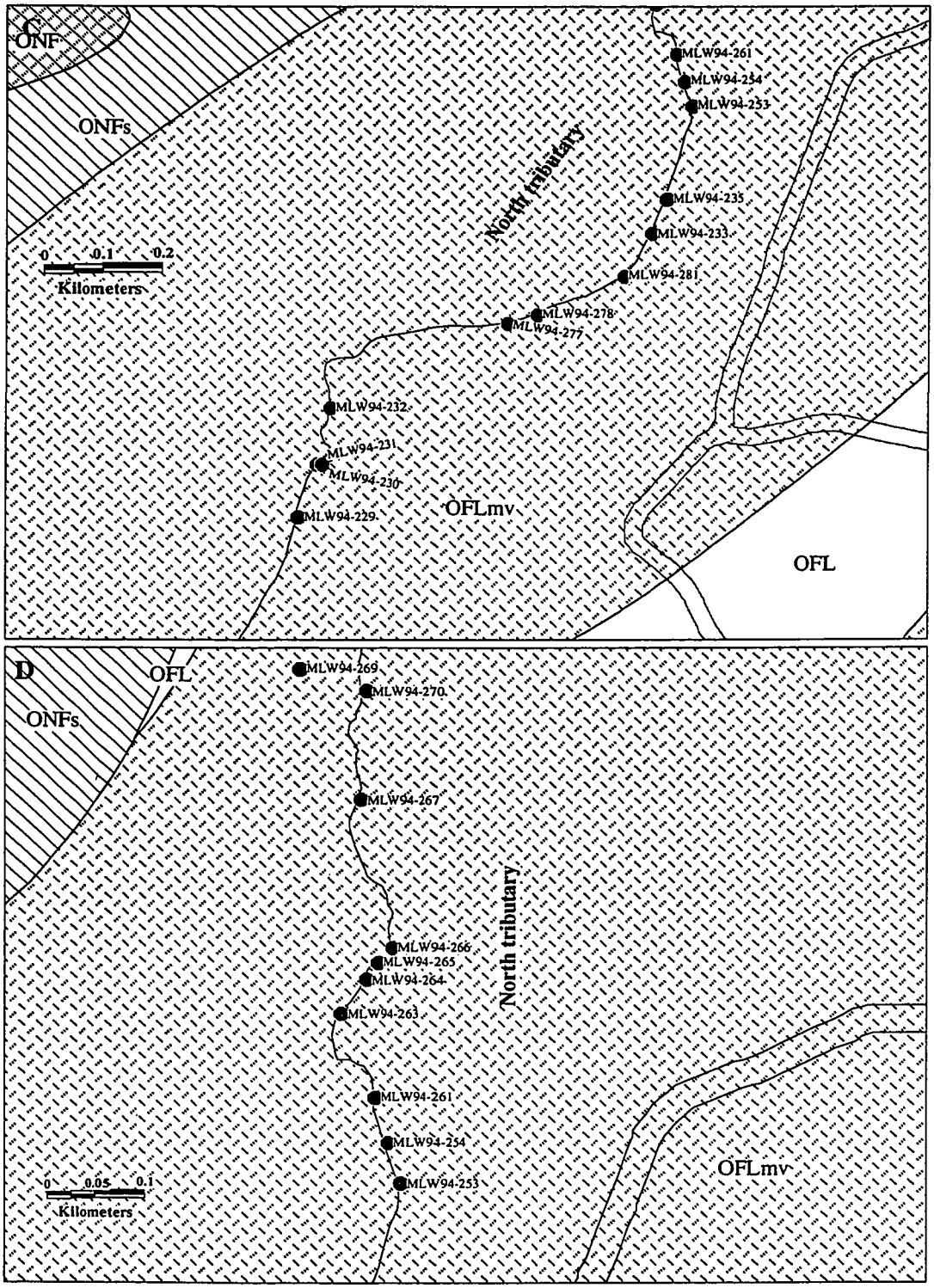


Fig. 5.1 continued.

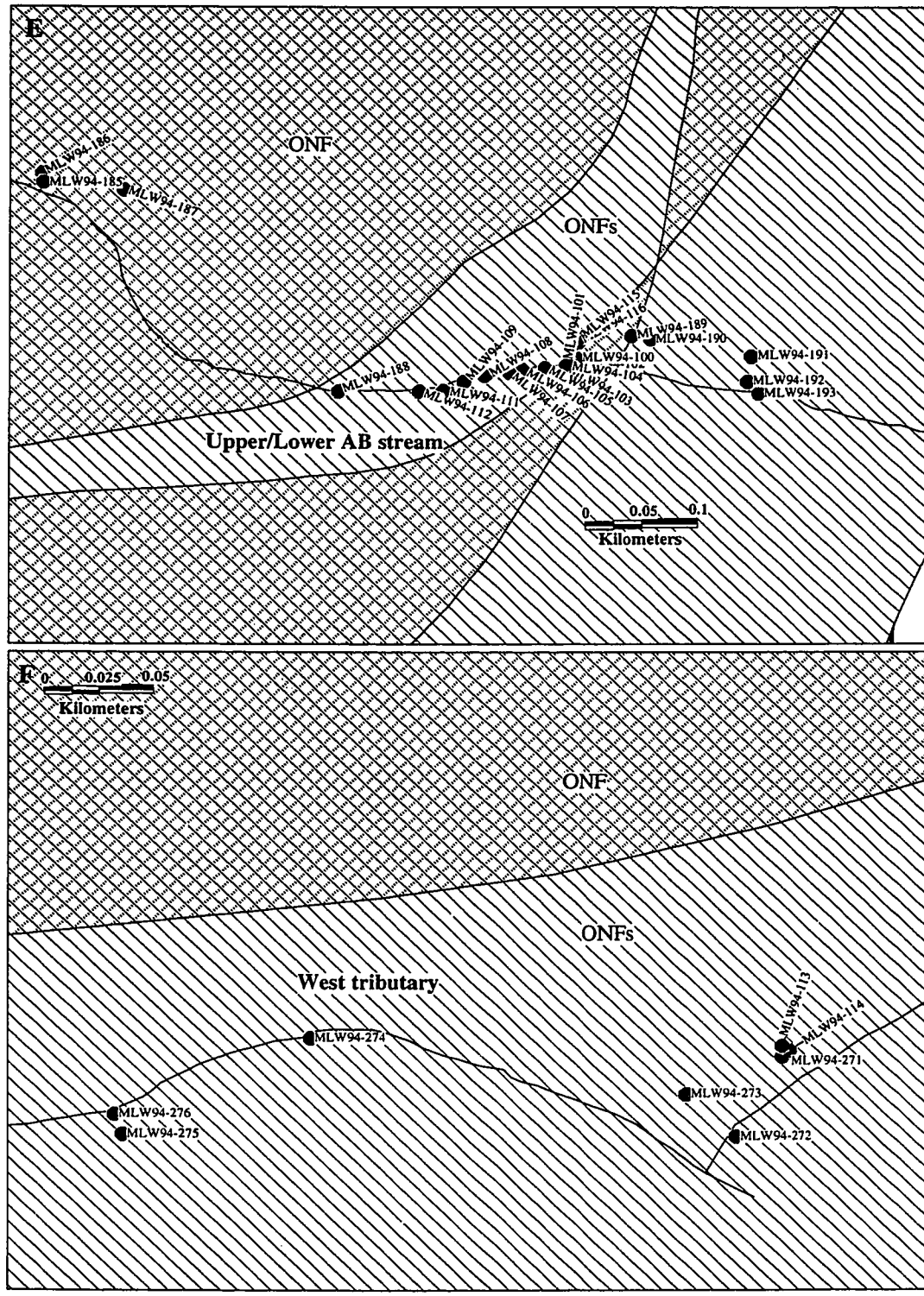


Fig. 5.1 continued.

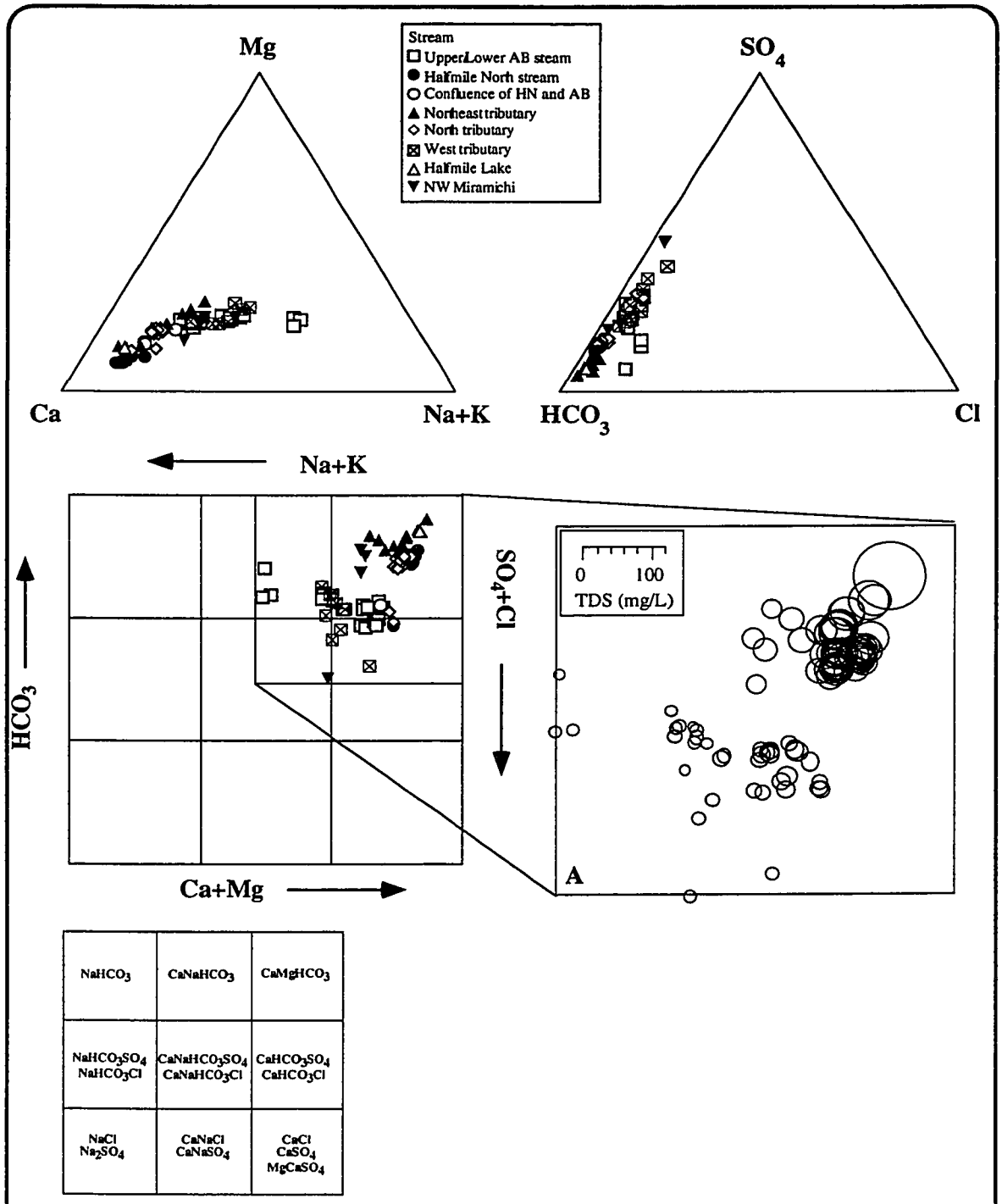


Fig. 5.2 Modified Piper plot for surface waters from the Halfmile Lake deposit. The inset (A) shows the groundwaters proportional to total dissolved solids. Data from Appendix B.1.1.

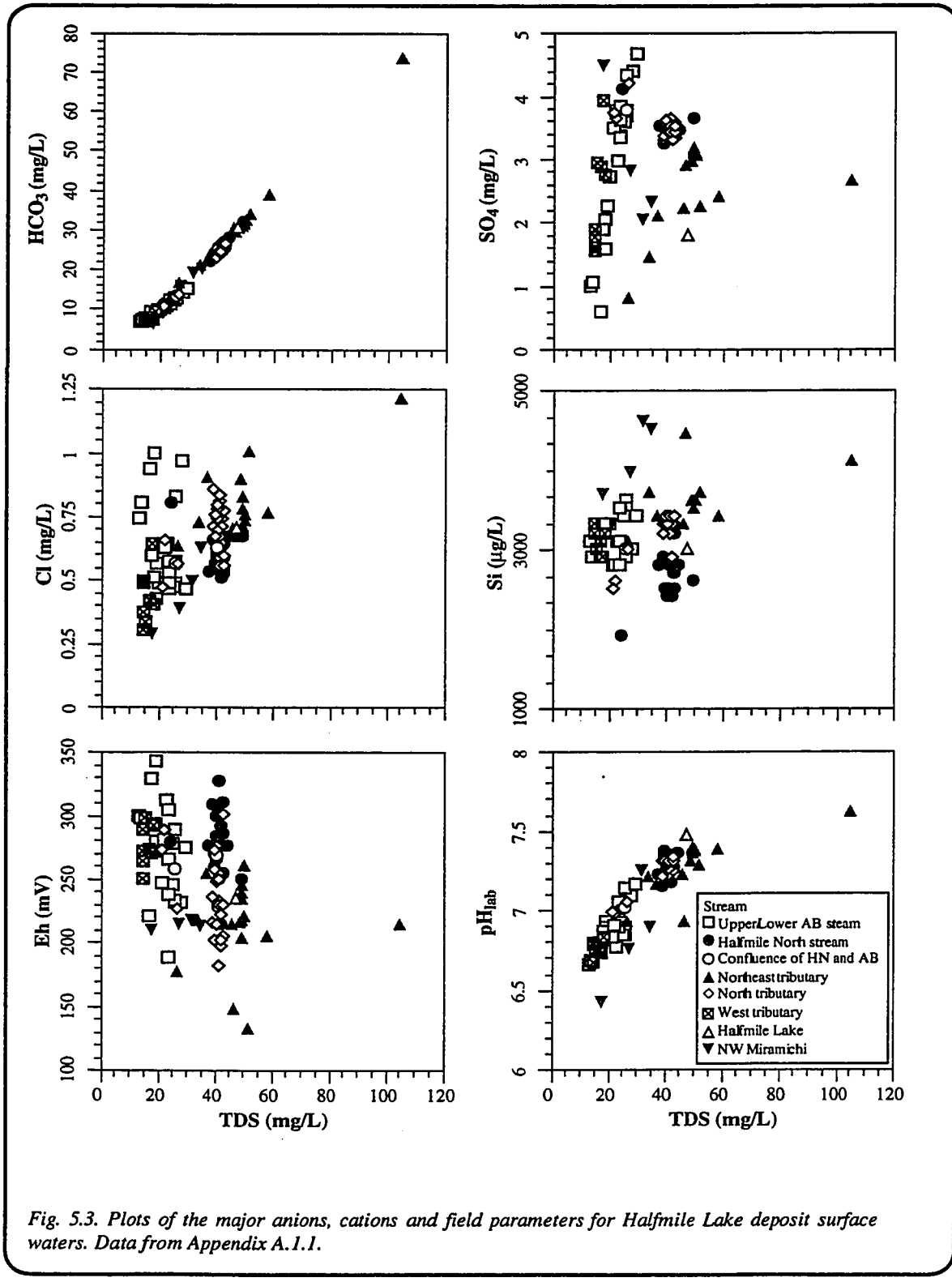


Fig. 5.3. Plots of the major anions, cations and field parameters for Halfmile Lake deposit surface waters. Data from Appendix A.1.1.

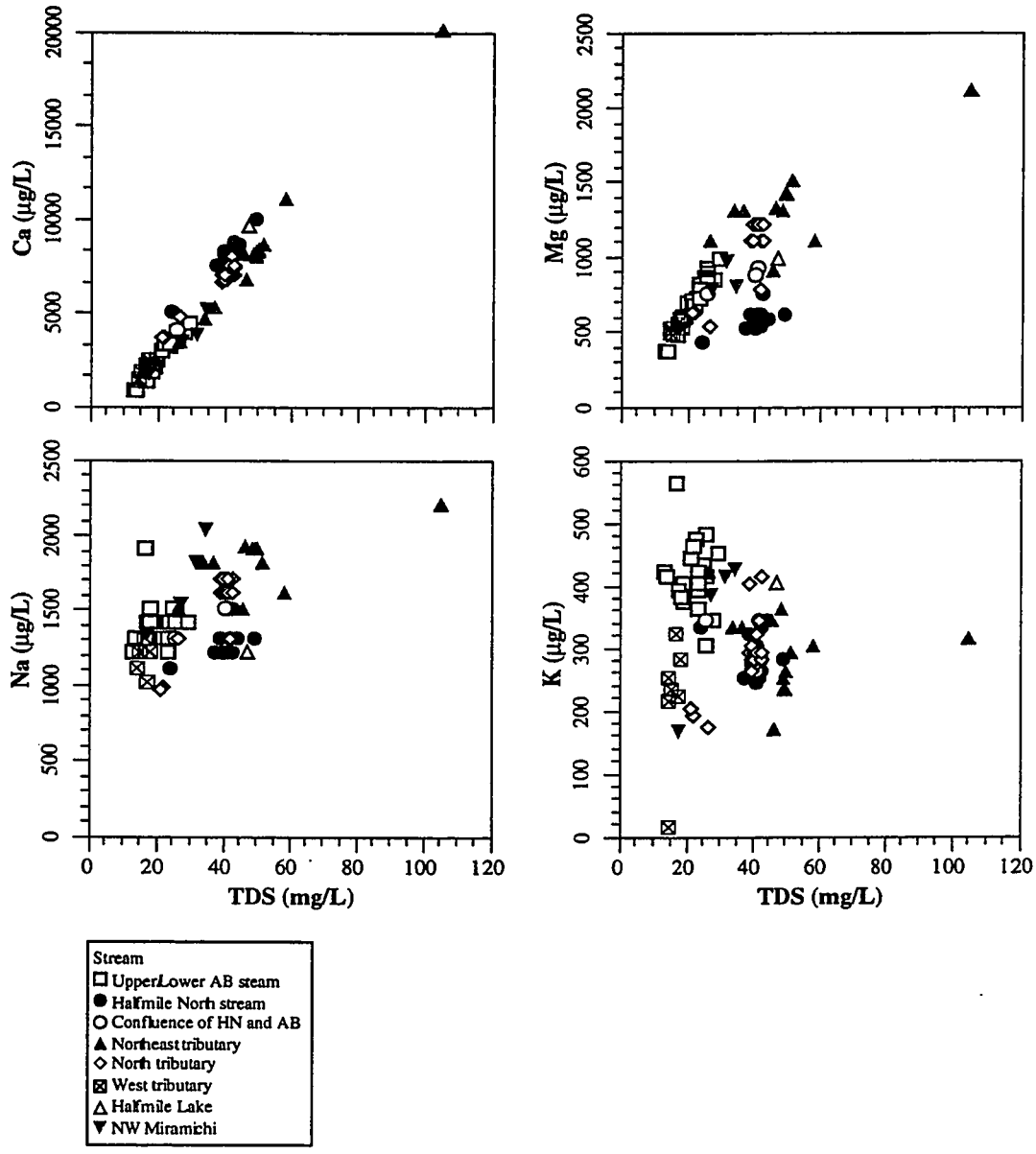


Fig. 5.3. continued.

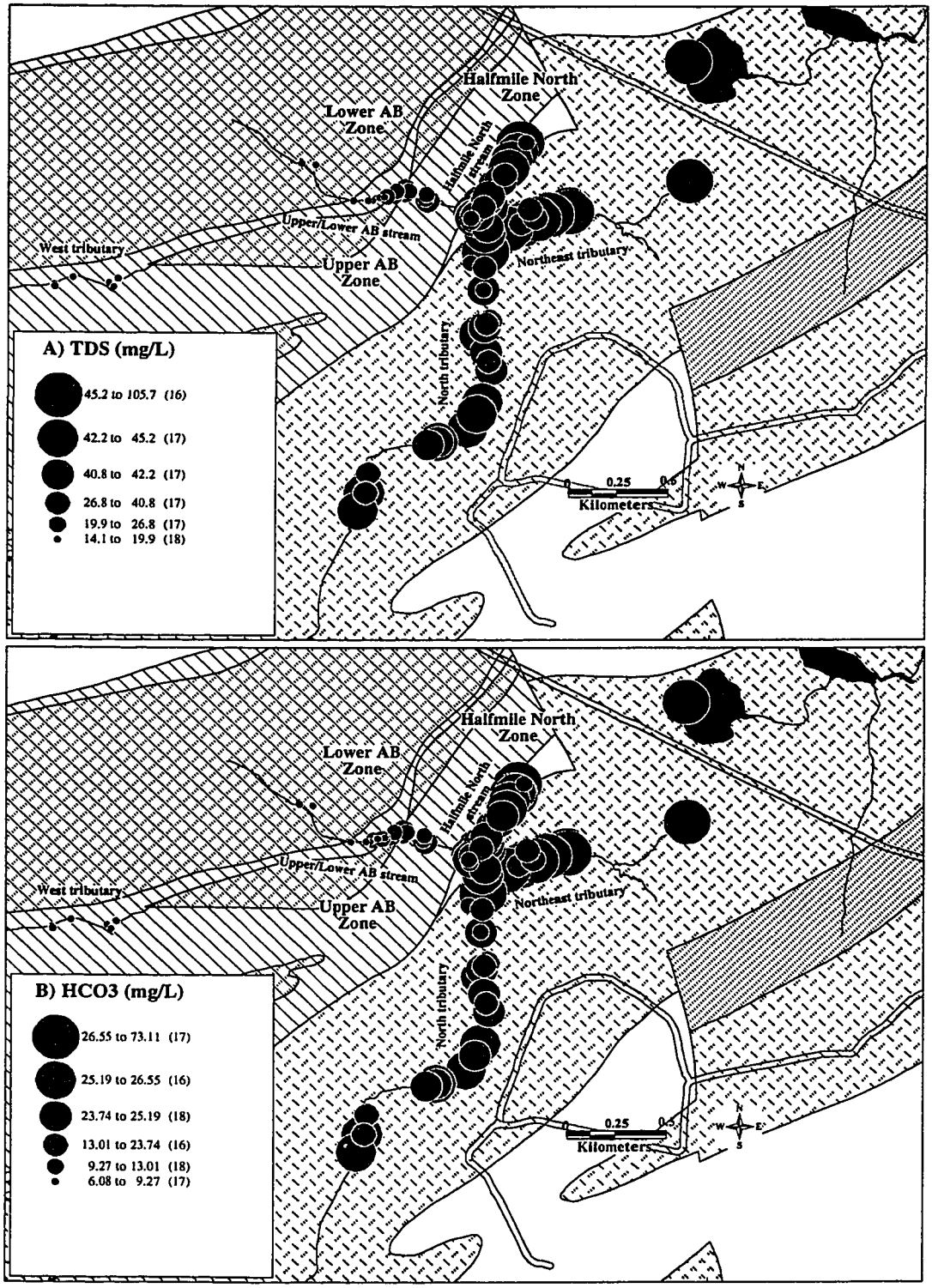


Fig. 5.4 Spatial distribution of major cations, anions, and field parameters in Halfmile Lake deposit surface waters.

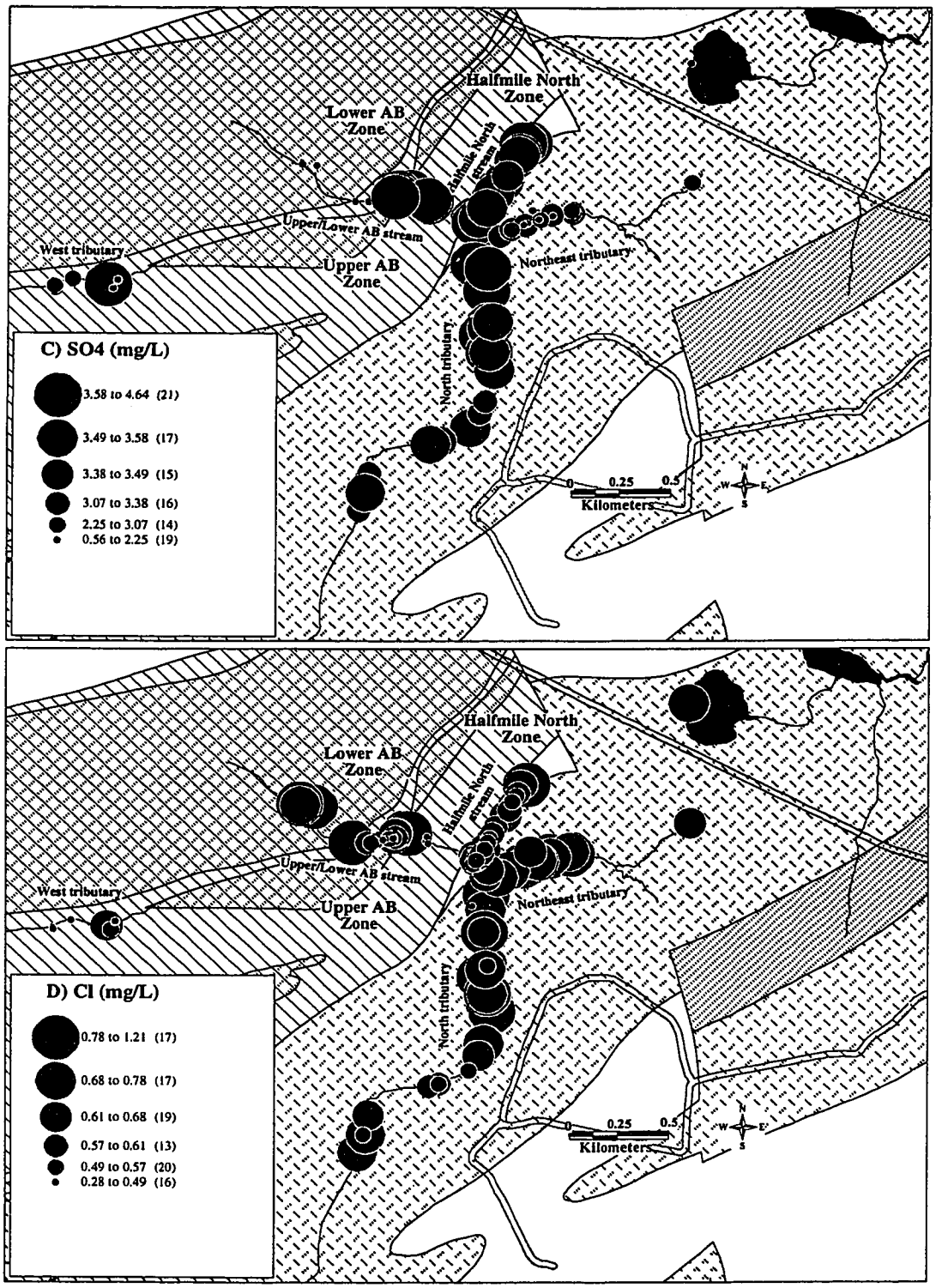


Fig. 5.4 continued.

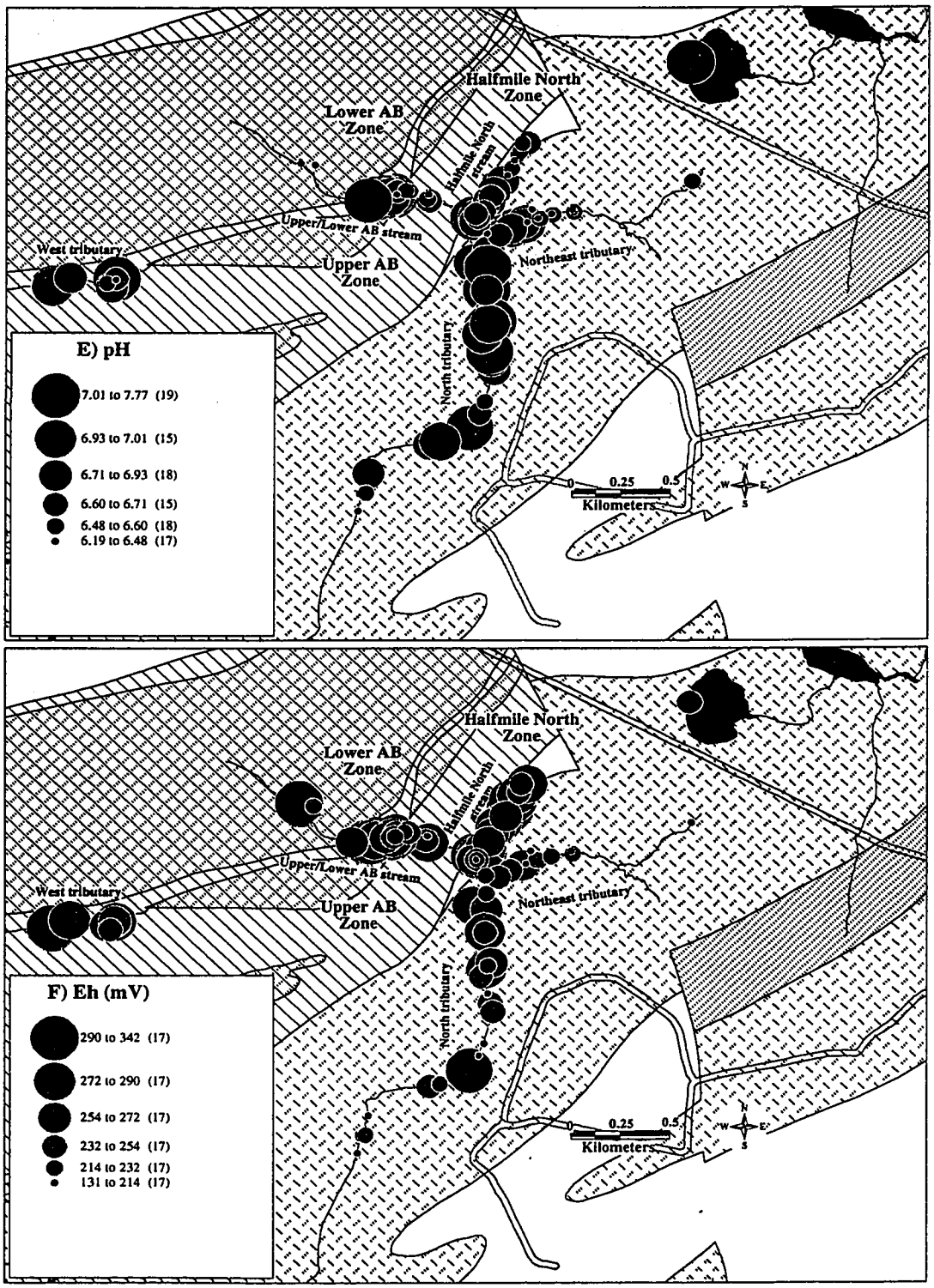


Fig. 5.4 continued.

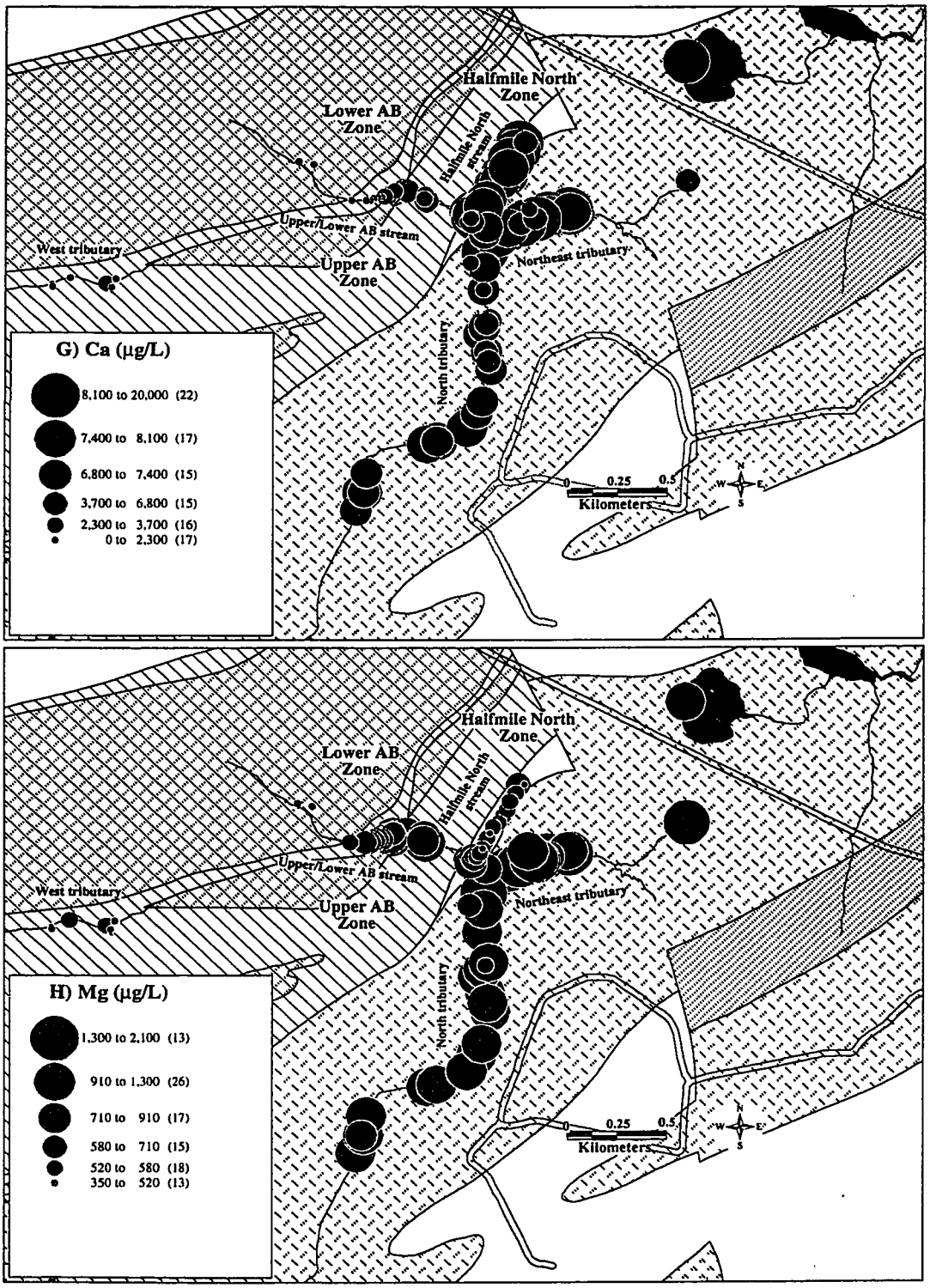


Fig. 5.4 continued.

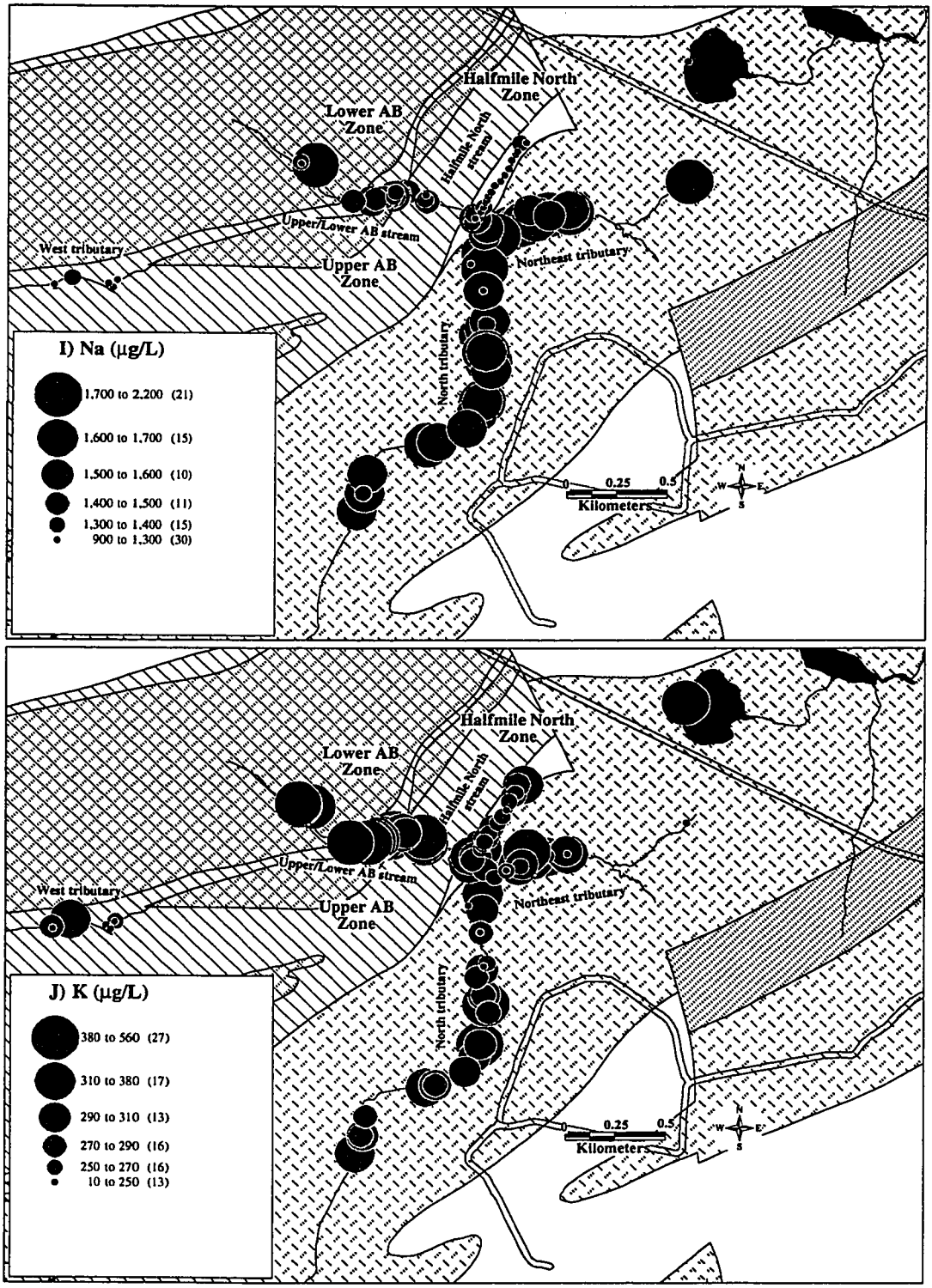


Fig. 5.4 continued.

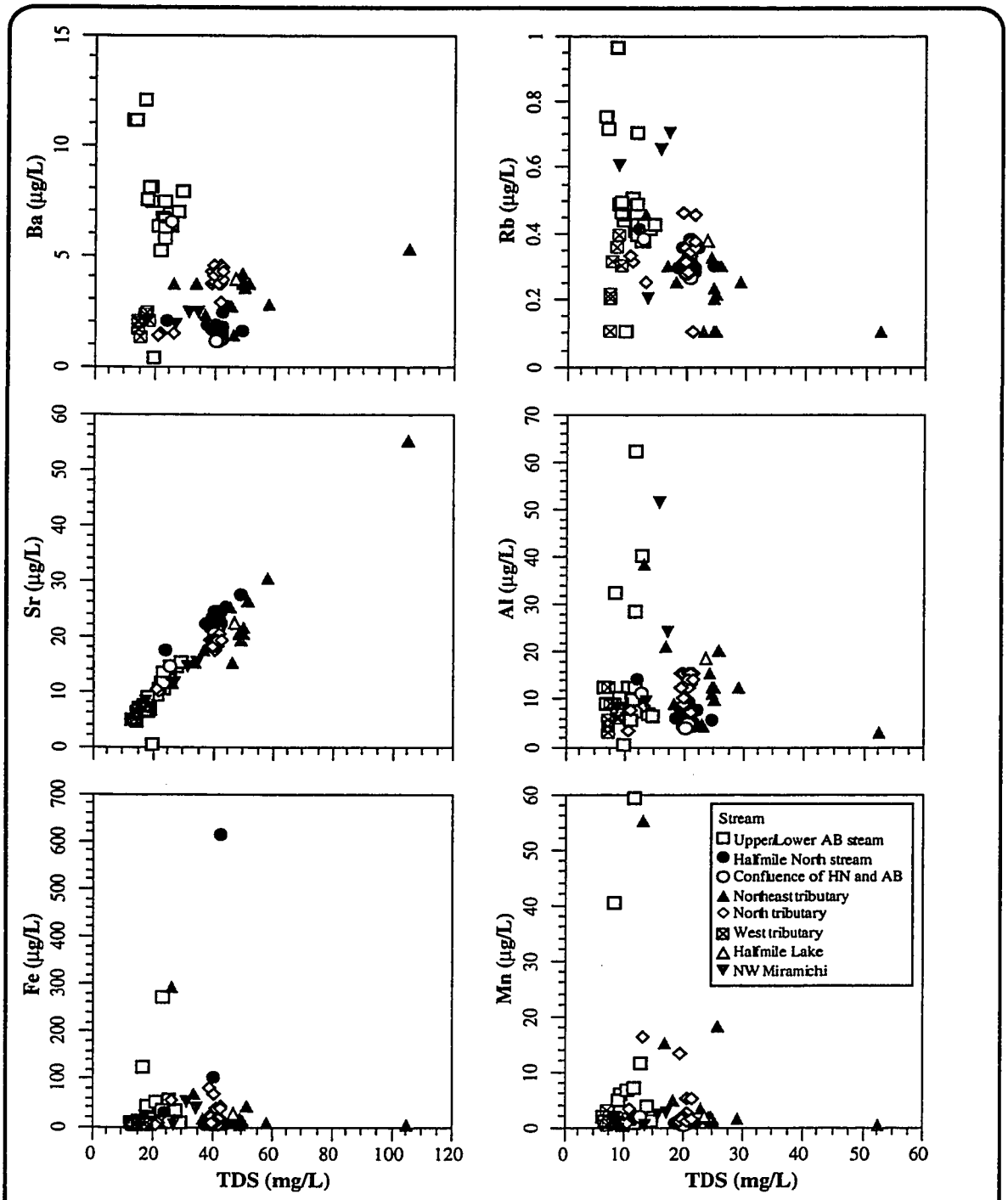


Fig. 5.5 Plots of trace elements in Halfmile Lake deposit surface waters. Data from Appendix A.1.1.

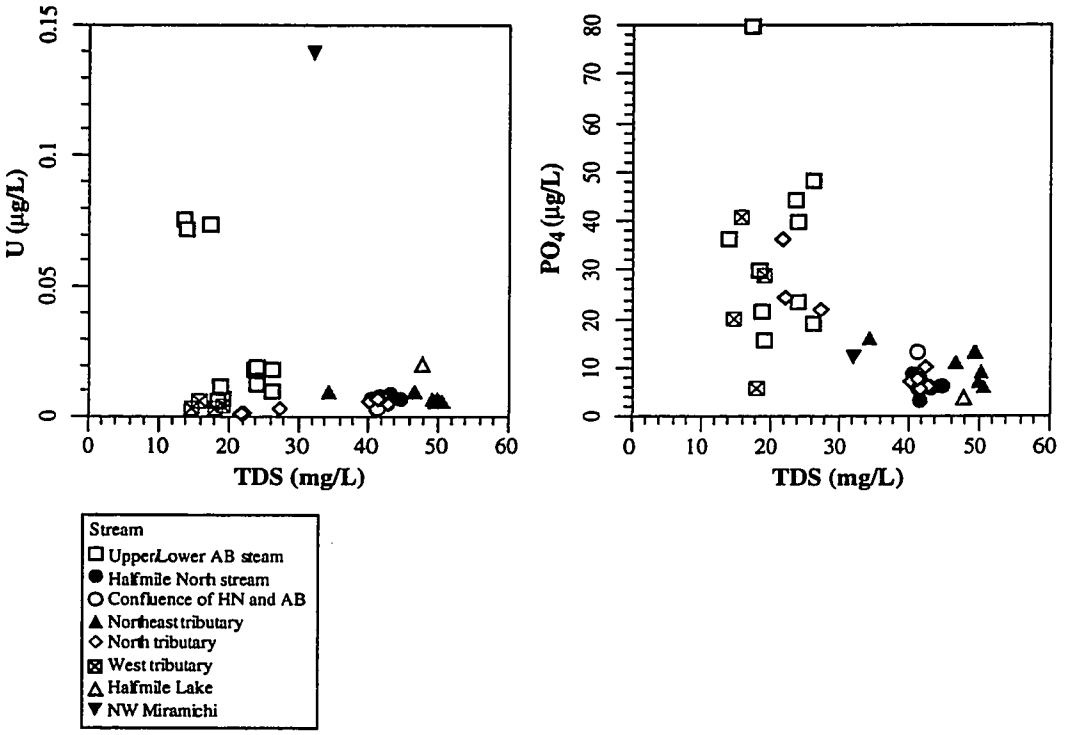


Fig. 5.5 continued.

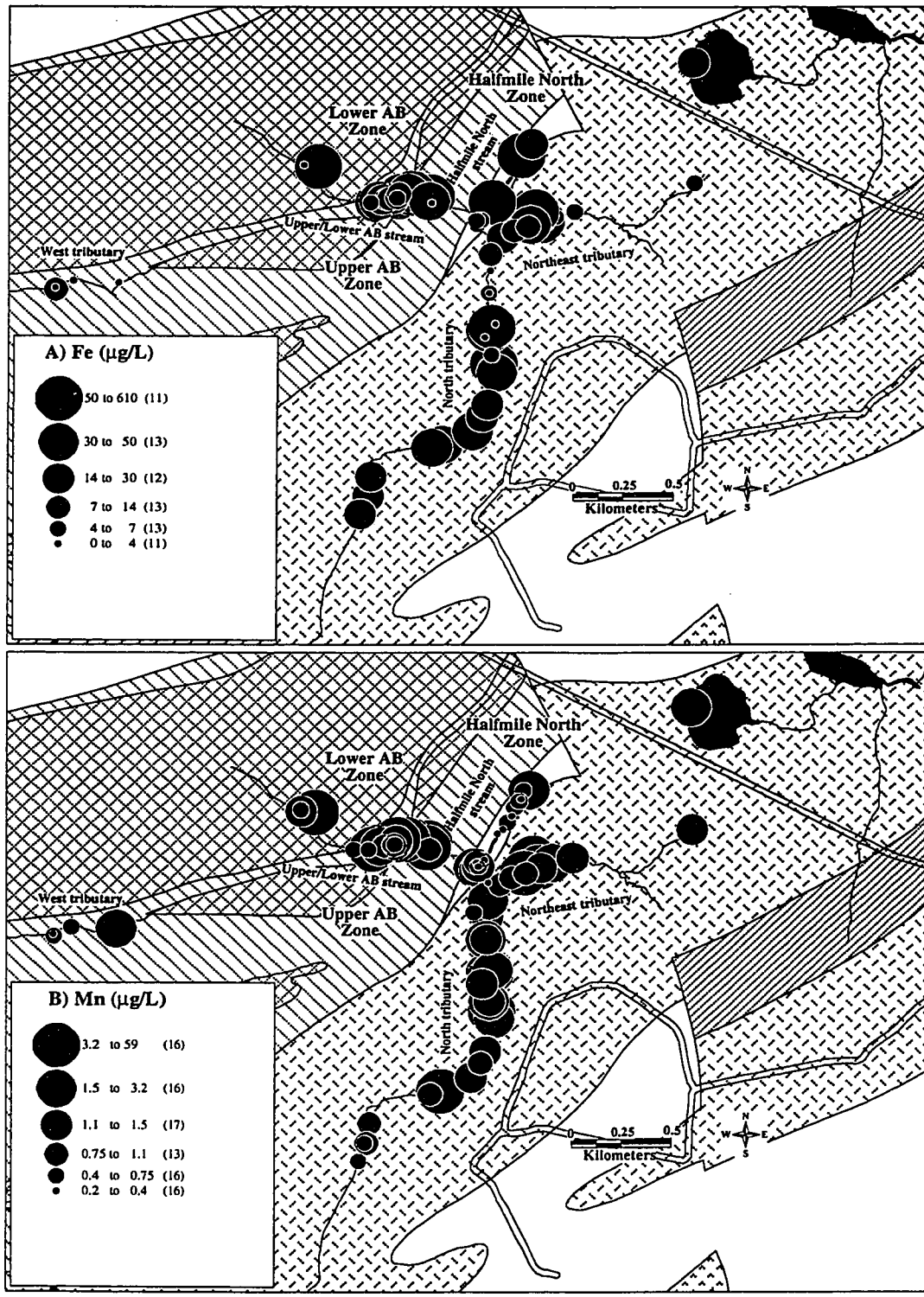


Fig. 5.6 Spatial distribution of trace elements in Halfmile Lake deposit surface waters.

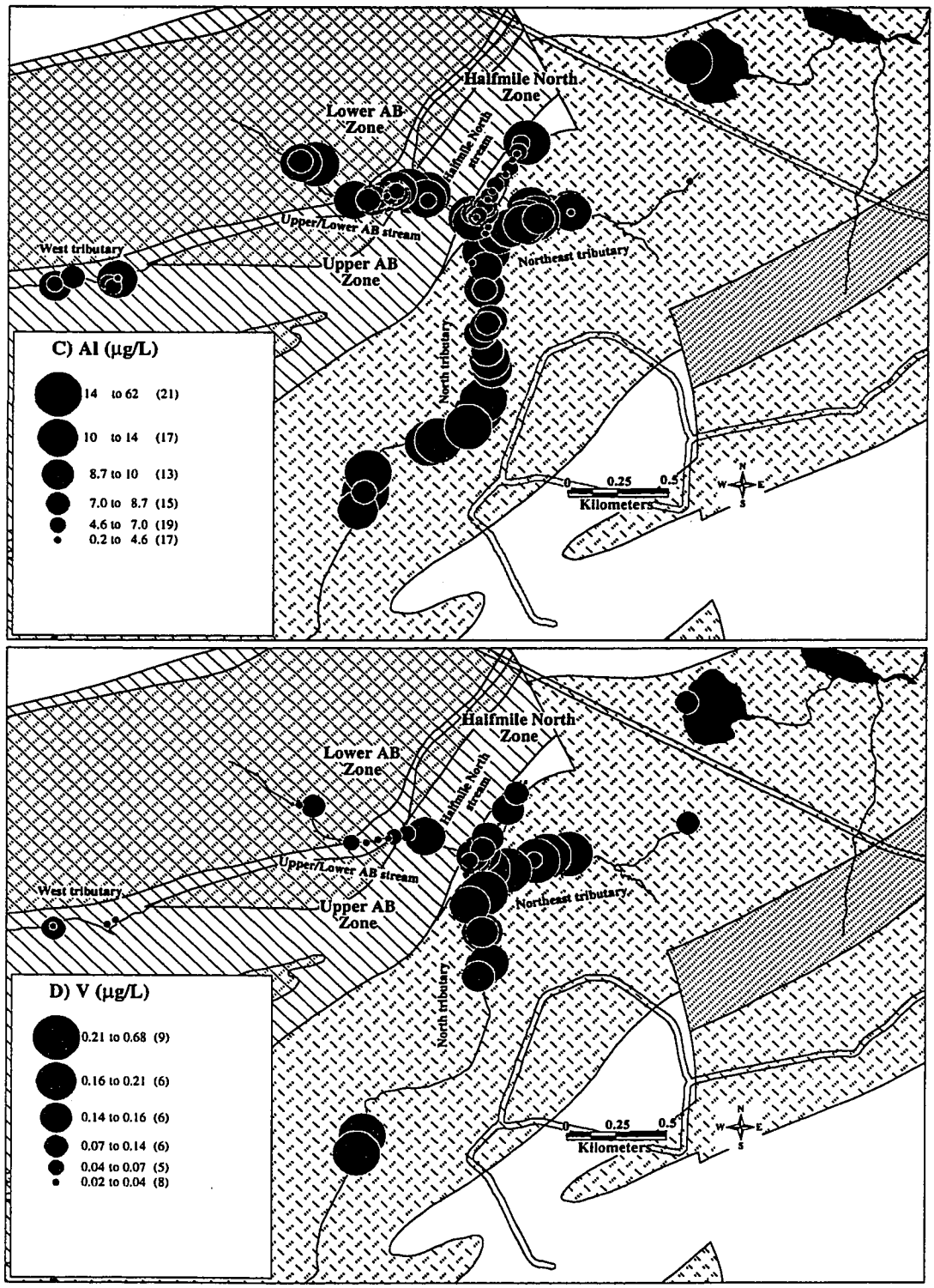


Fig. 5.6 continued.

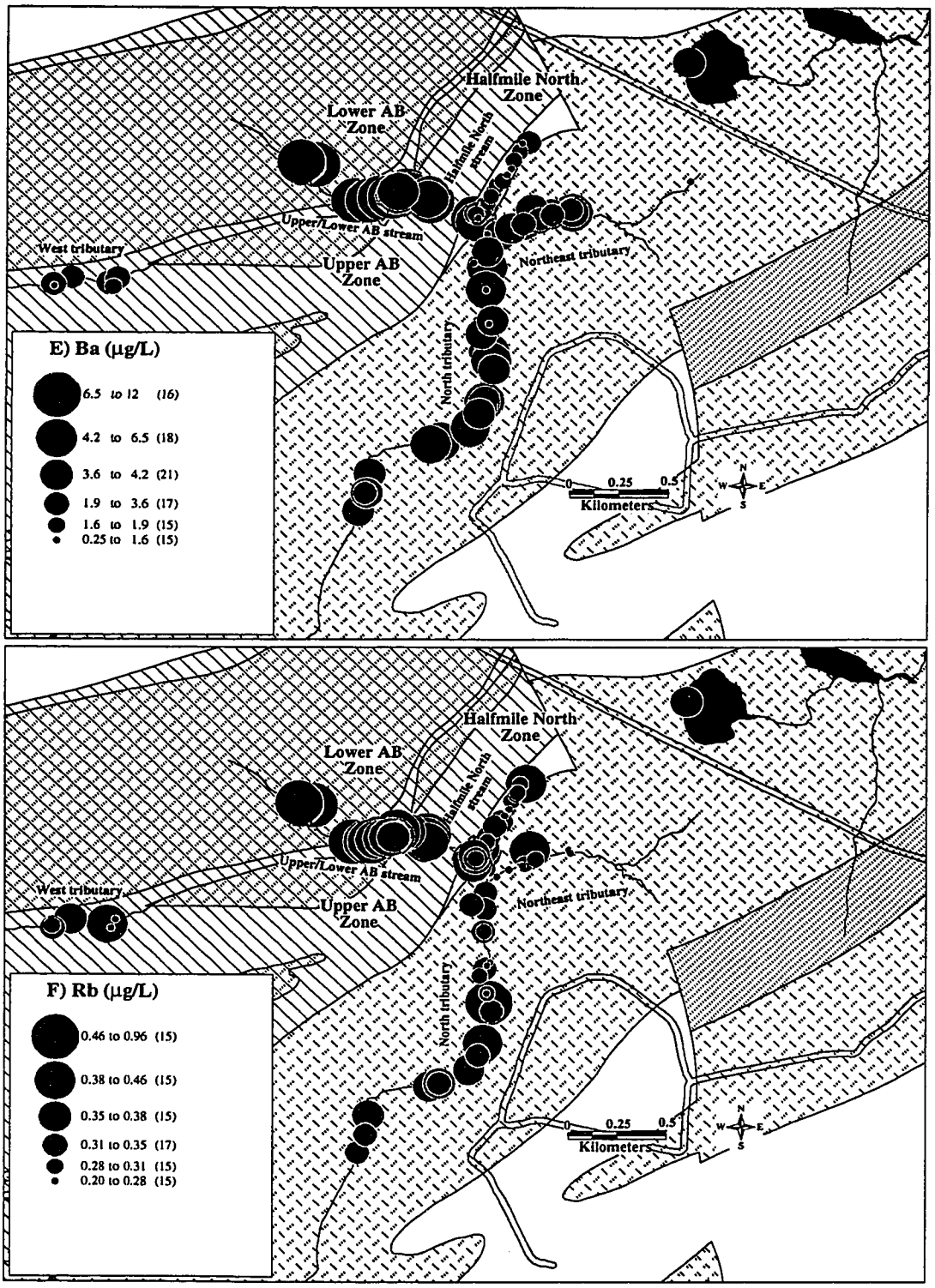


Fig. 5.6 continued.

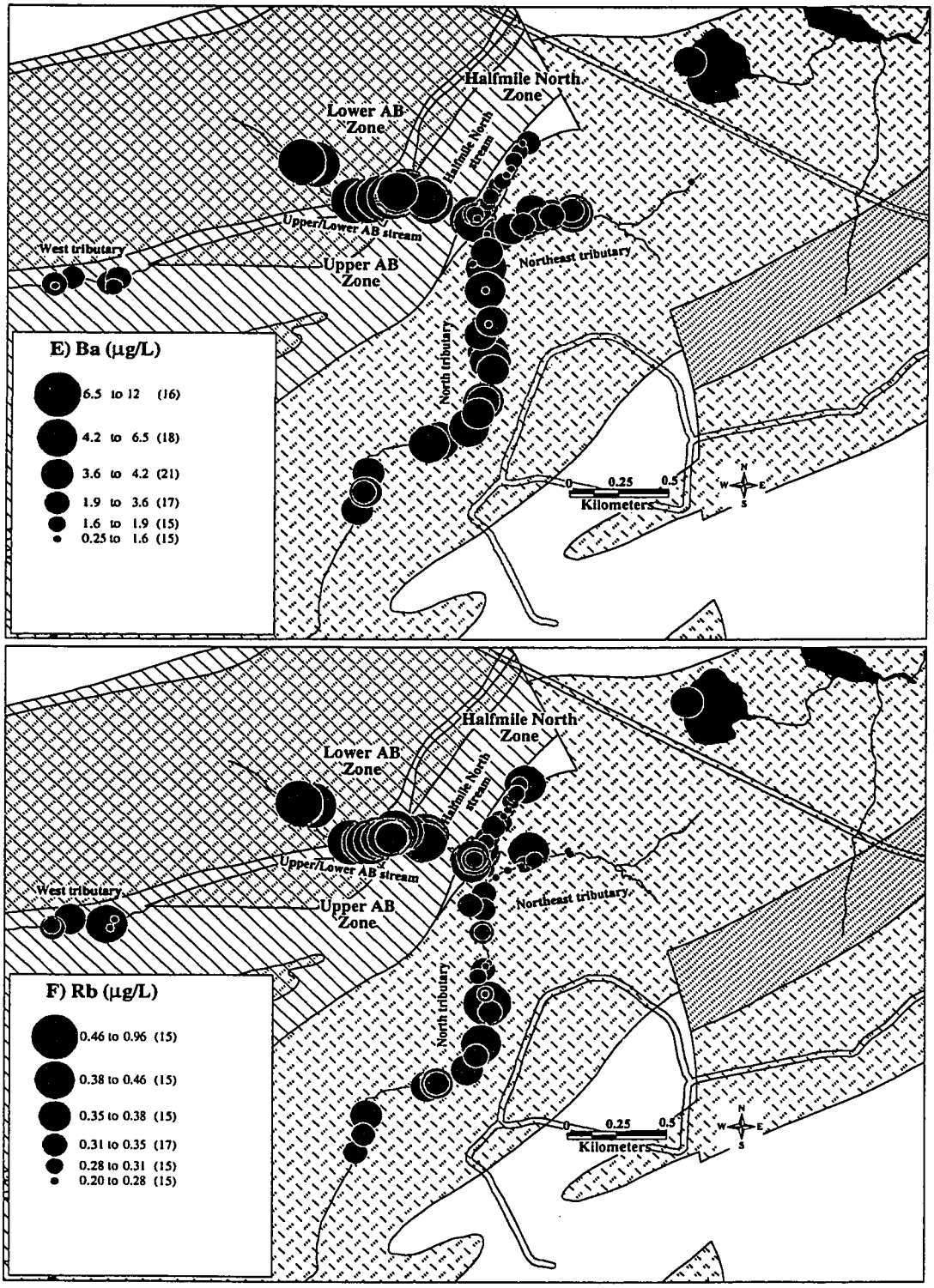


Fig. 5.6 continued.

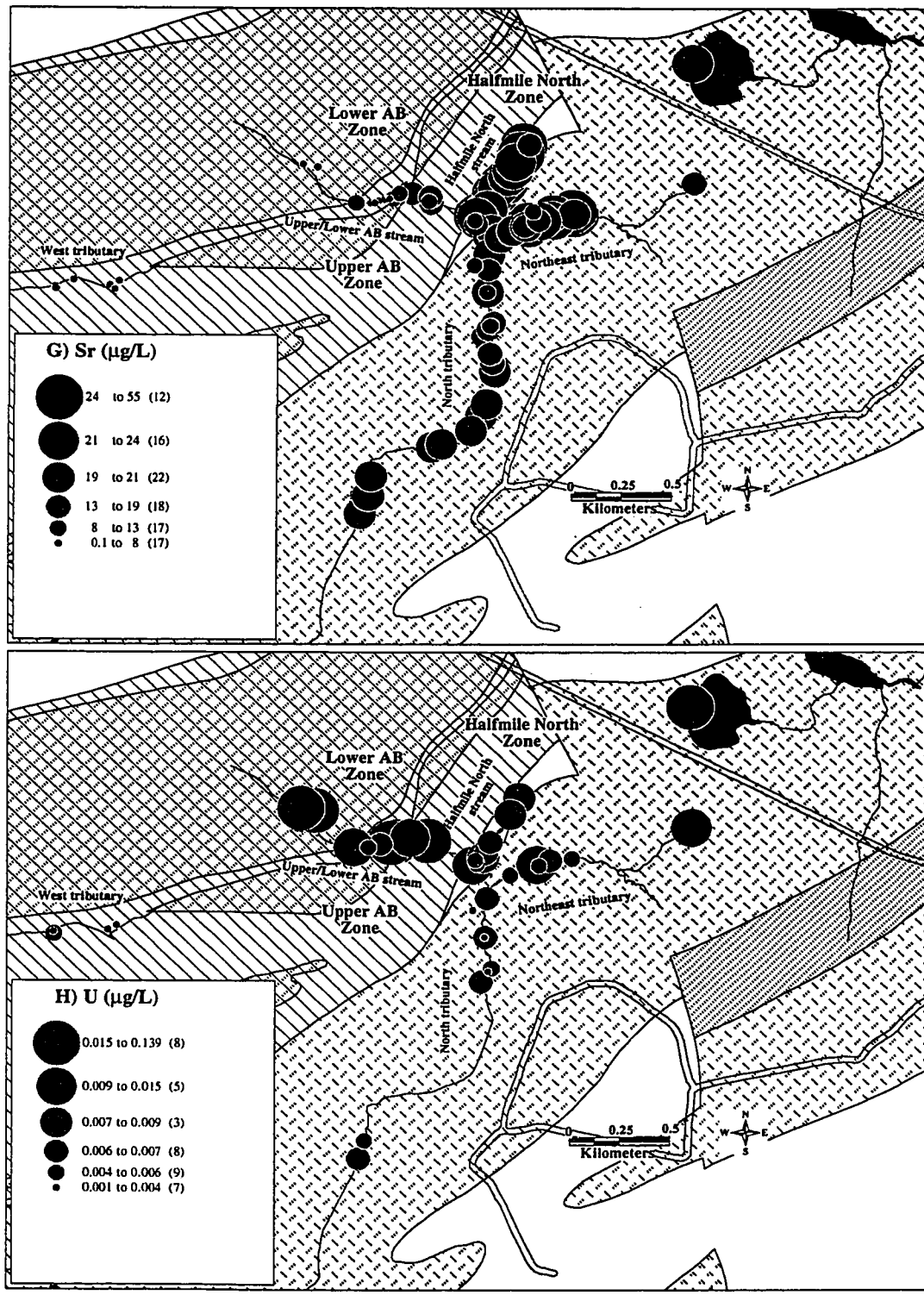


Fig. 5.6 continued.

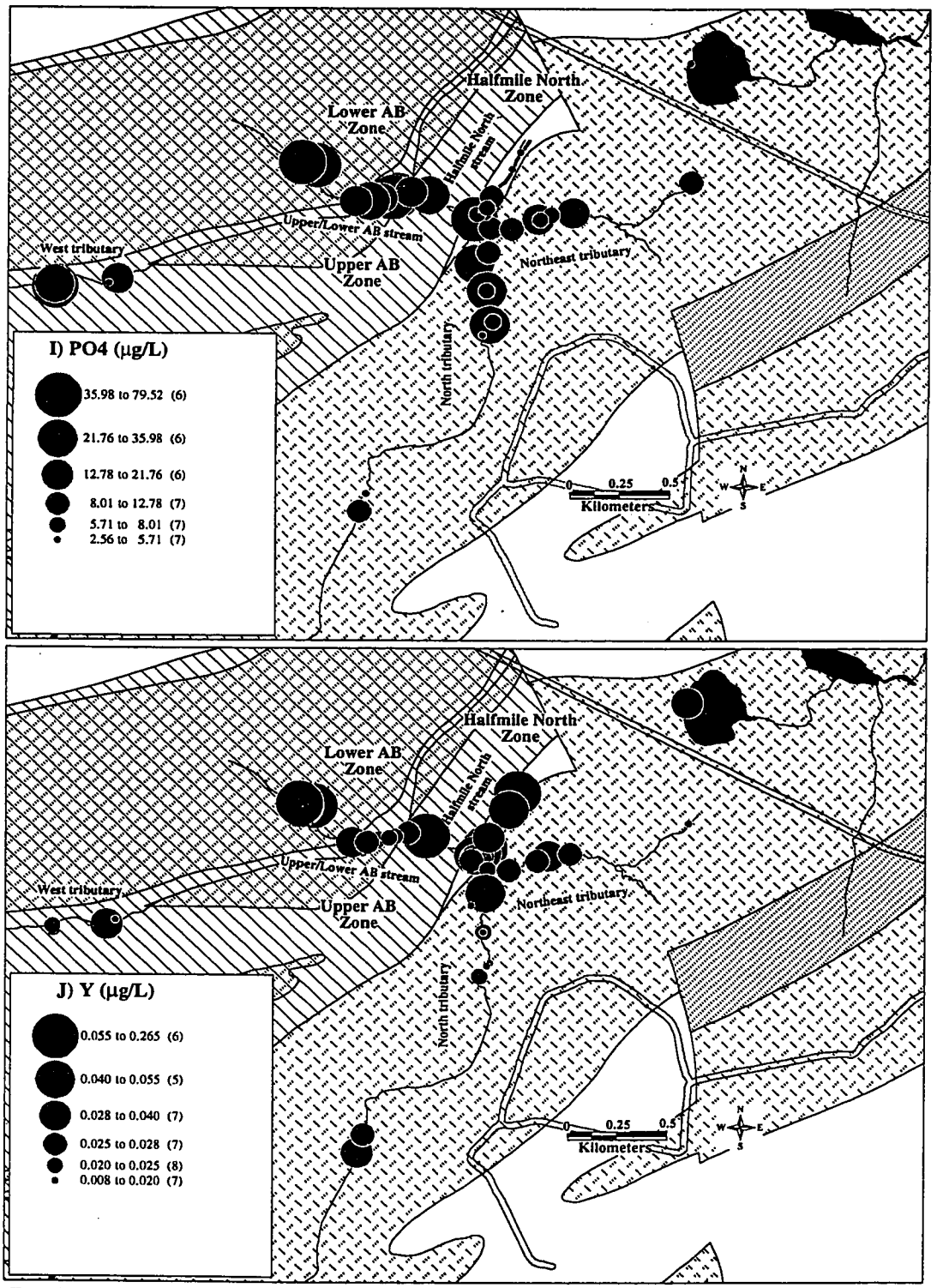


Fig. 5.6 continued.

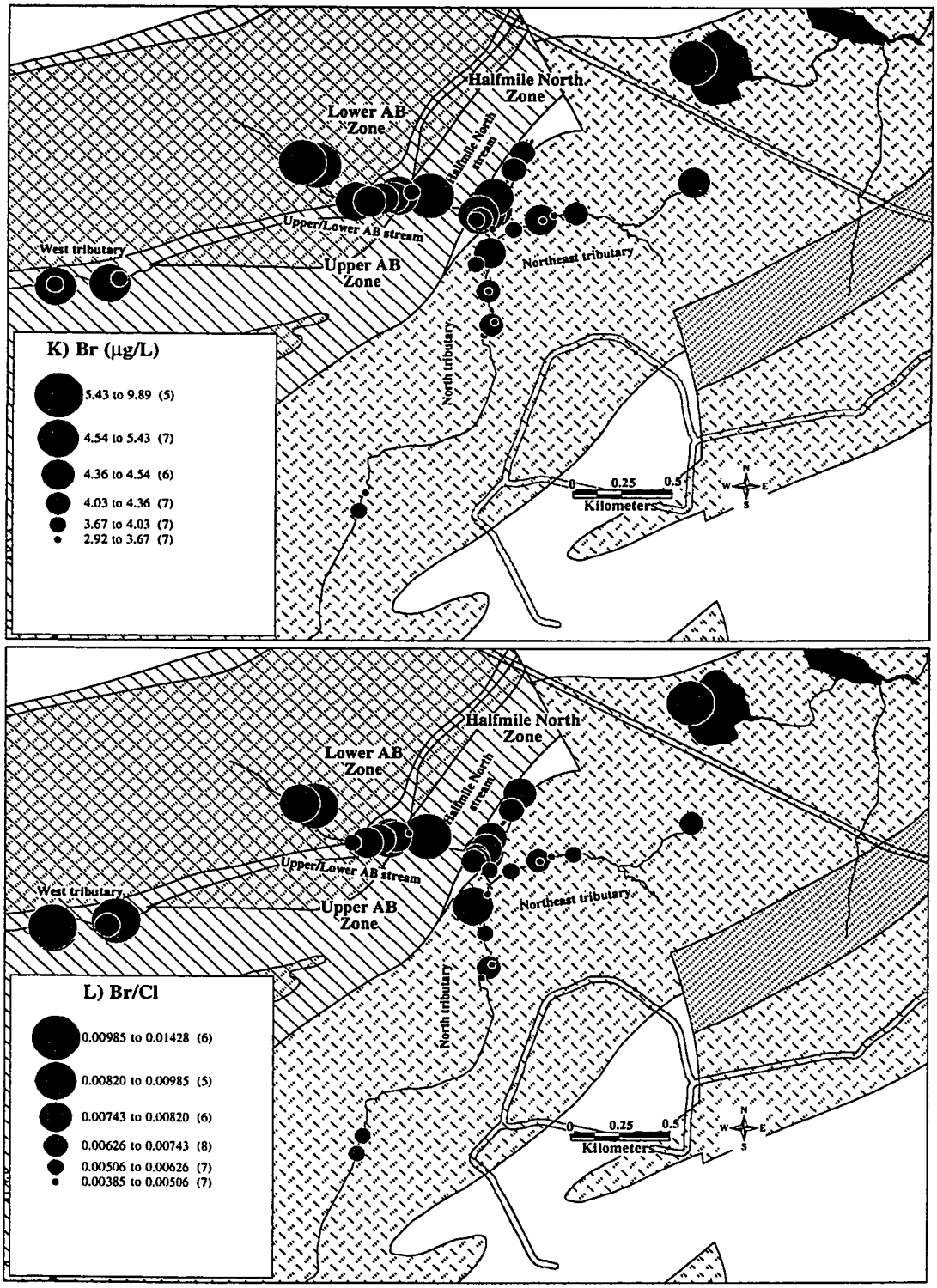


Fig. 5.6 continued.

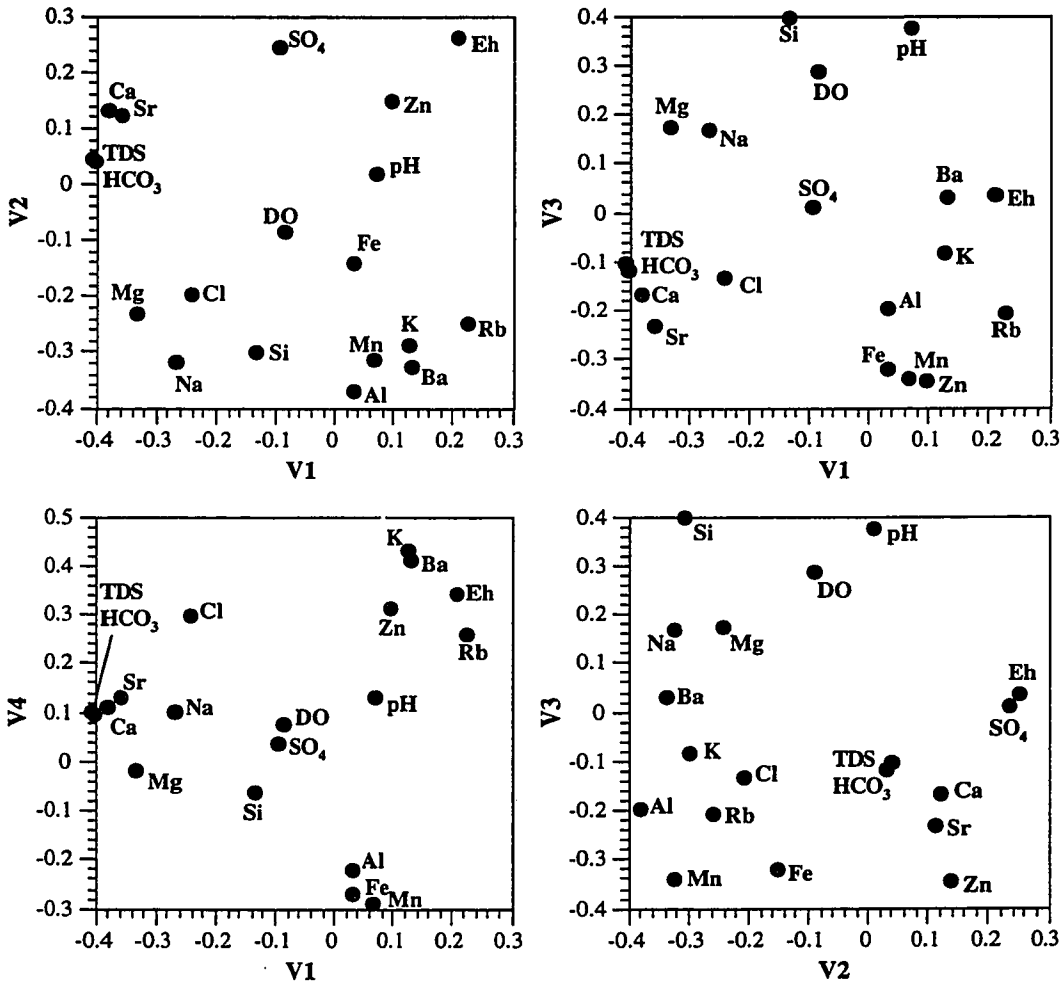


Fig. 5.7 Plots of vectors based on Principal Component Analysis of Halfmile Lake deposit surface waters. Six factors explain 82% of the variance in this data.

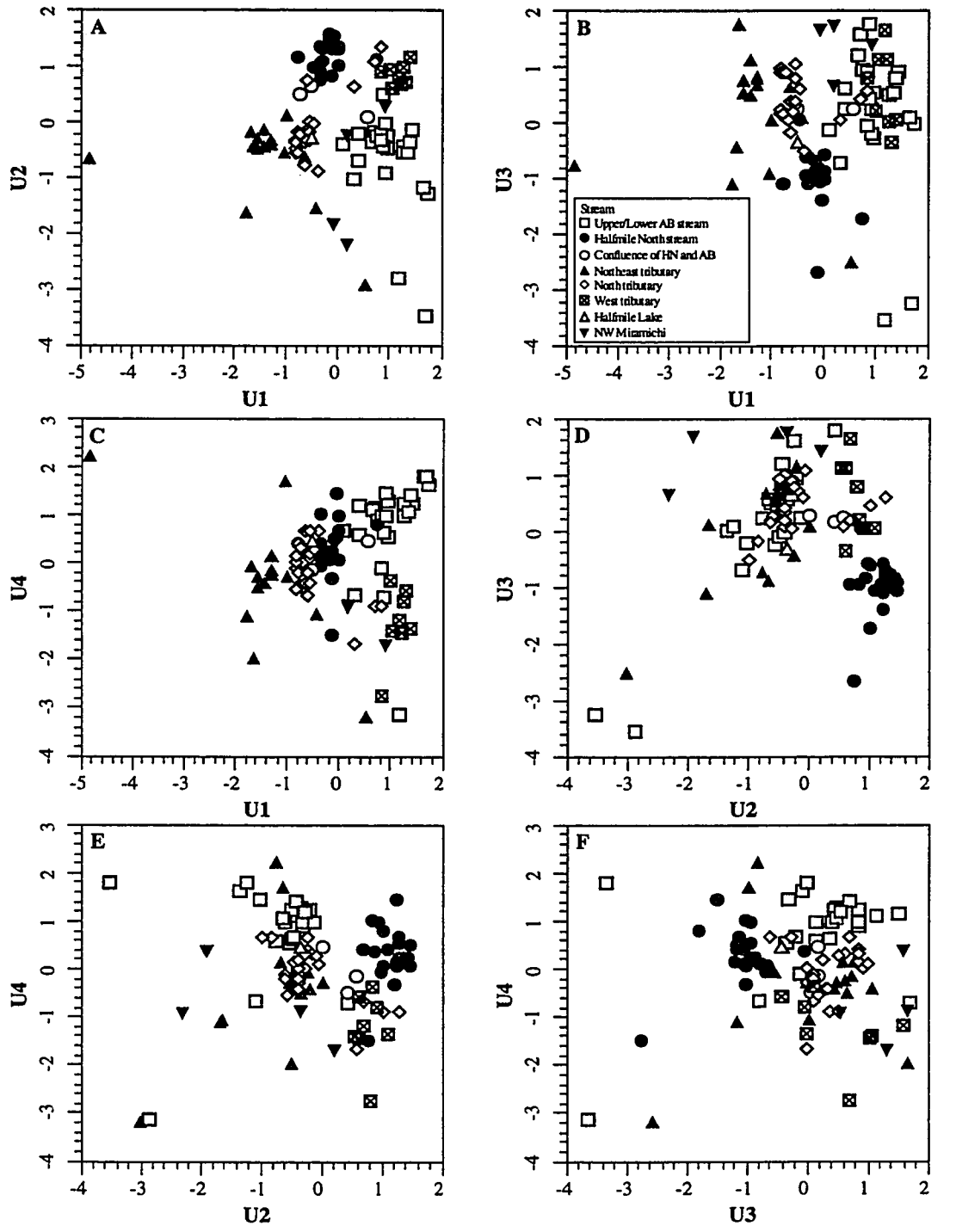


Fig. 5.8 Principal component plots of Halfmile Lake Deposit surface water data, showing variations in the first four factors.

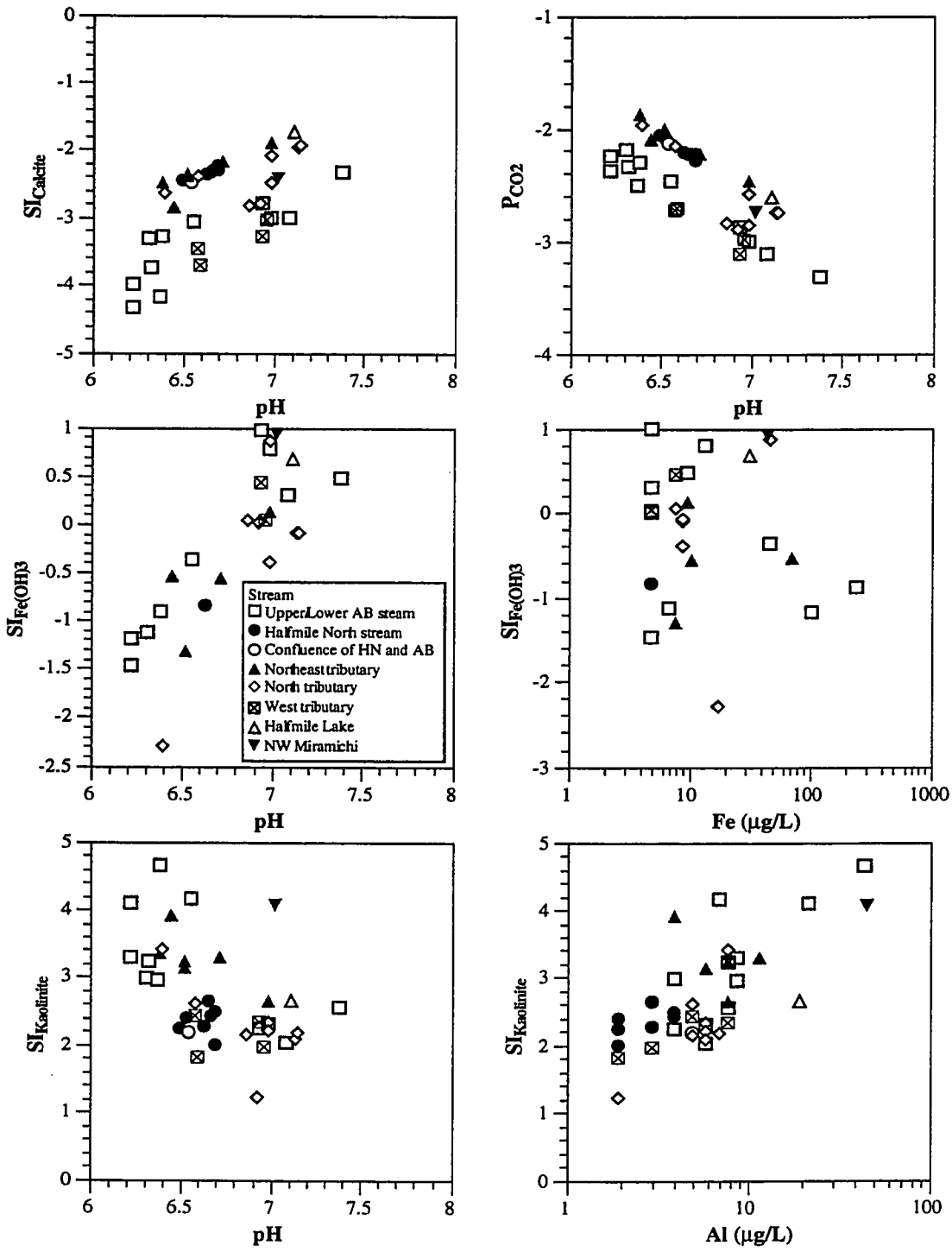


Fig. 5.9 Plots of selected mineral saturation indices (SI) for Halfmile Lake deposit surface waters. Data from Appendix A.1.4.

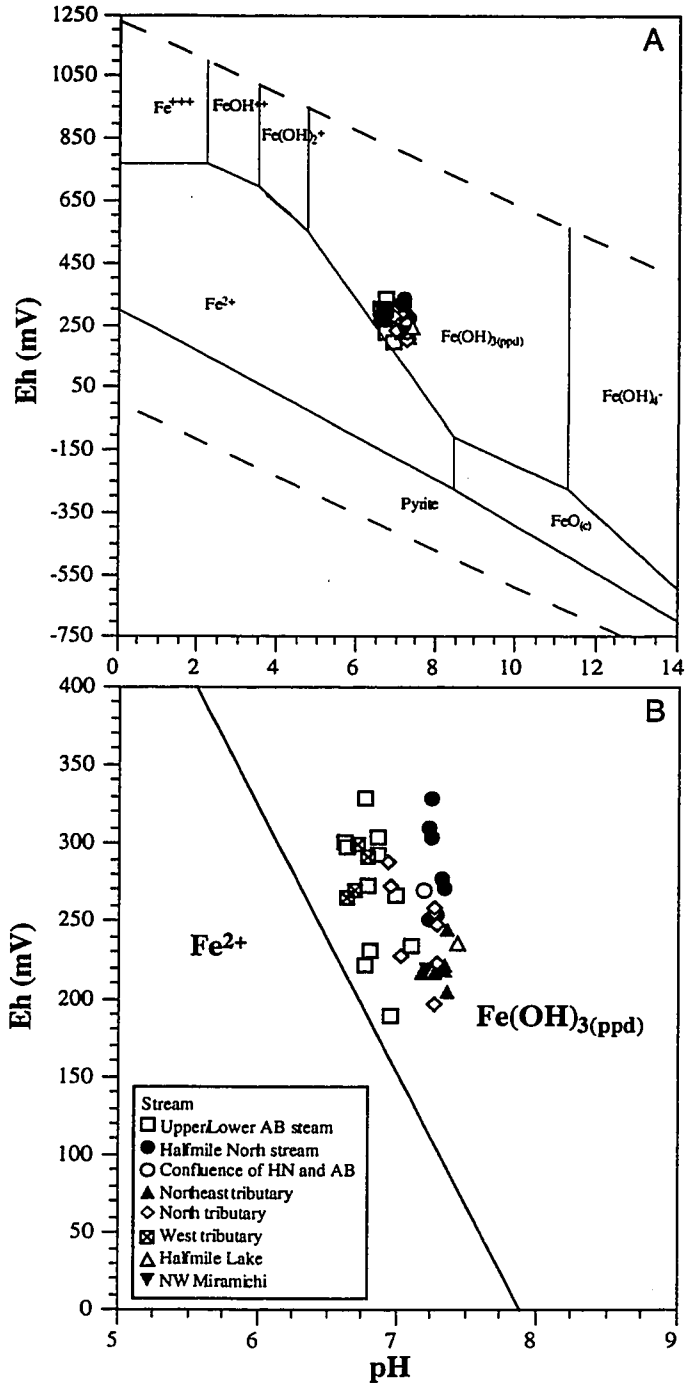


Fig. 5.10 Diagram showing Halfmile Lake deposit surface waters with respect to the stability of metastable Fe hydroxides. The fields were calculated using The Geochemist's Workbench (Bethke, 1994). Conditions are: $[HCO_3] = 10^{-3.5}$, $[SO_4] = 10^{-4.5}$, $[Fe] = 10^{-5.5}$. The formation of hematite, goethite and magnetite were suppressed, reflecting the slow kinetics of formation of these phases compared to amorphous oxide phases.

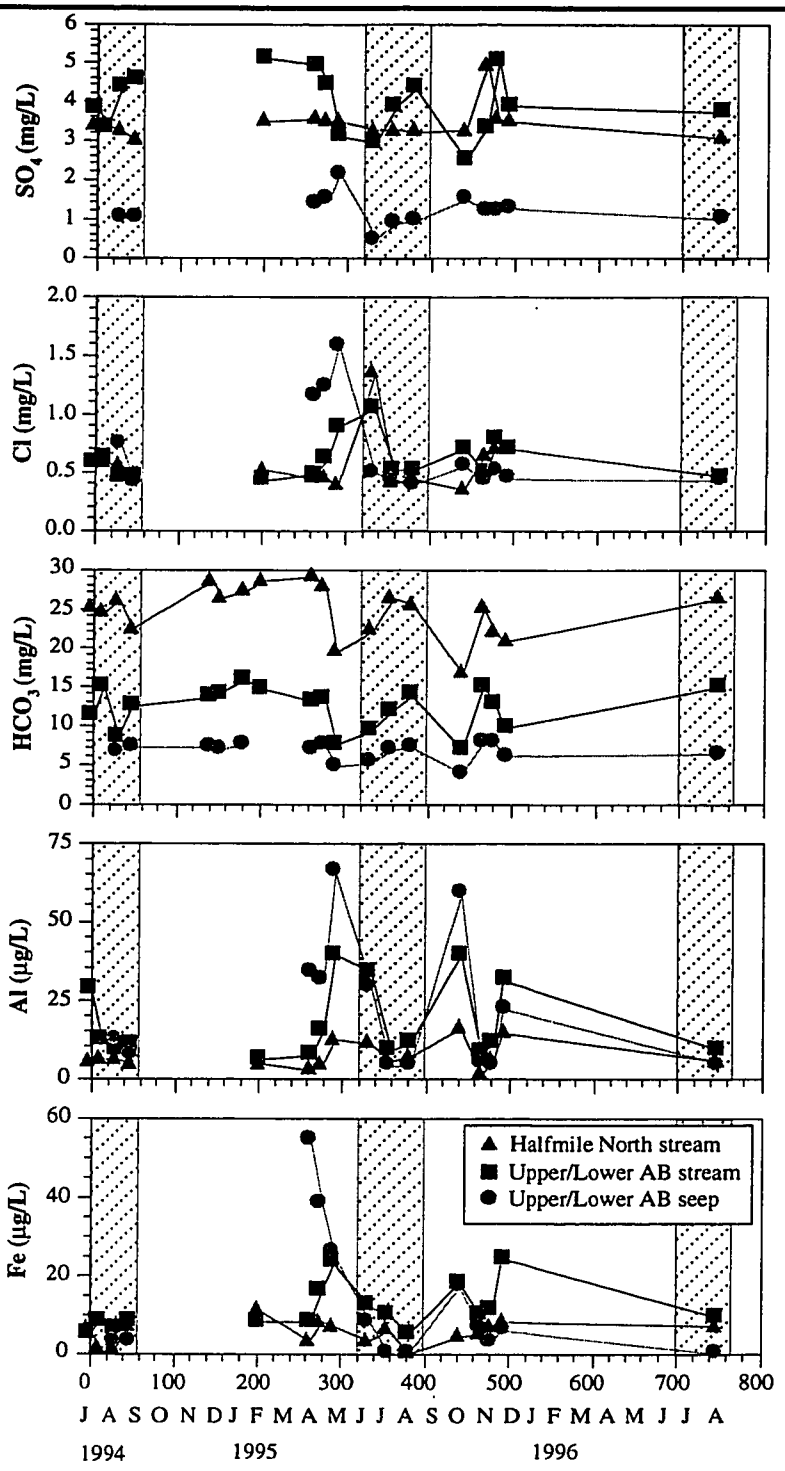


Fig. 5.11 Halfmile Lake deposit monitoring sites through time for selected elements. Shaded regions indicate time when main sampling occurred at the Halfmile Lake and Restigouche deposits.

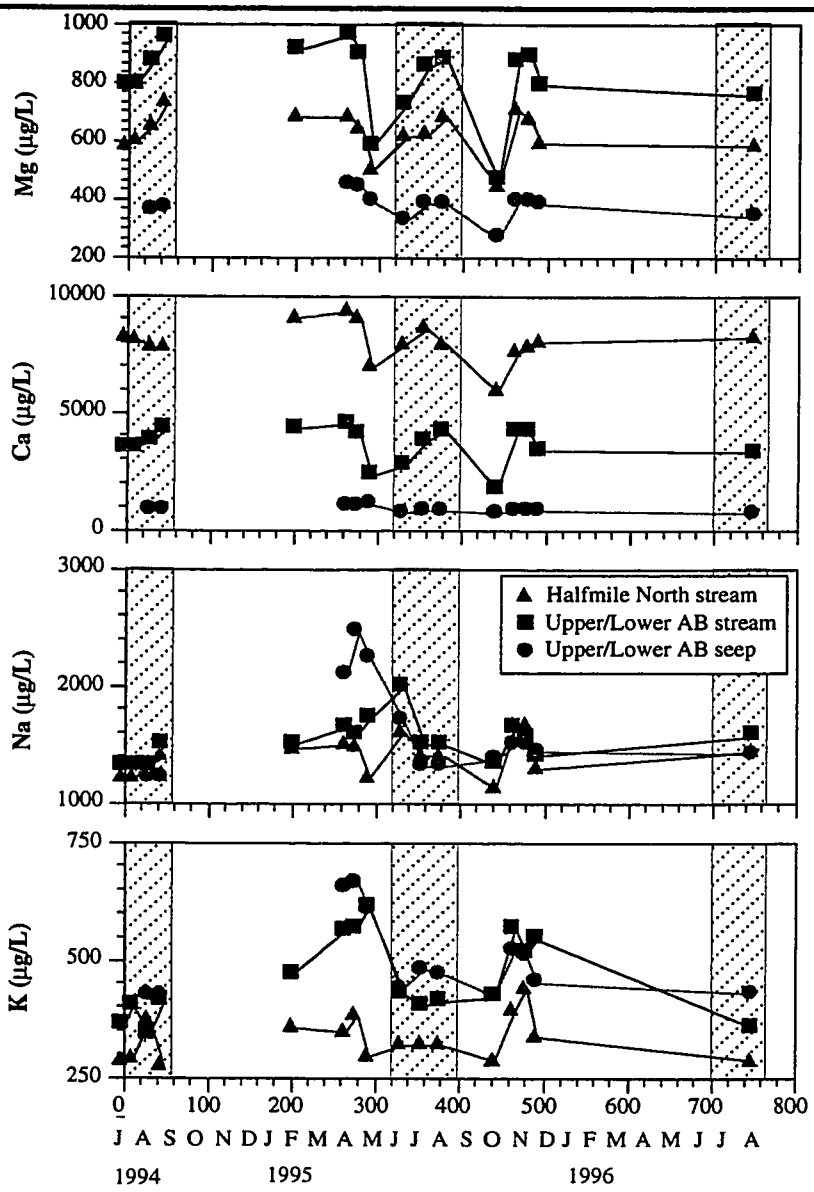


Fig. 5.11 continued.

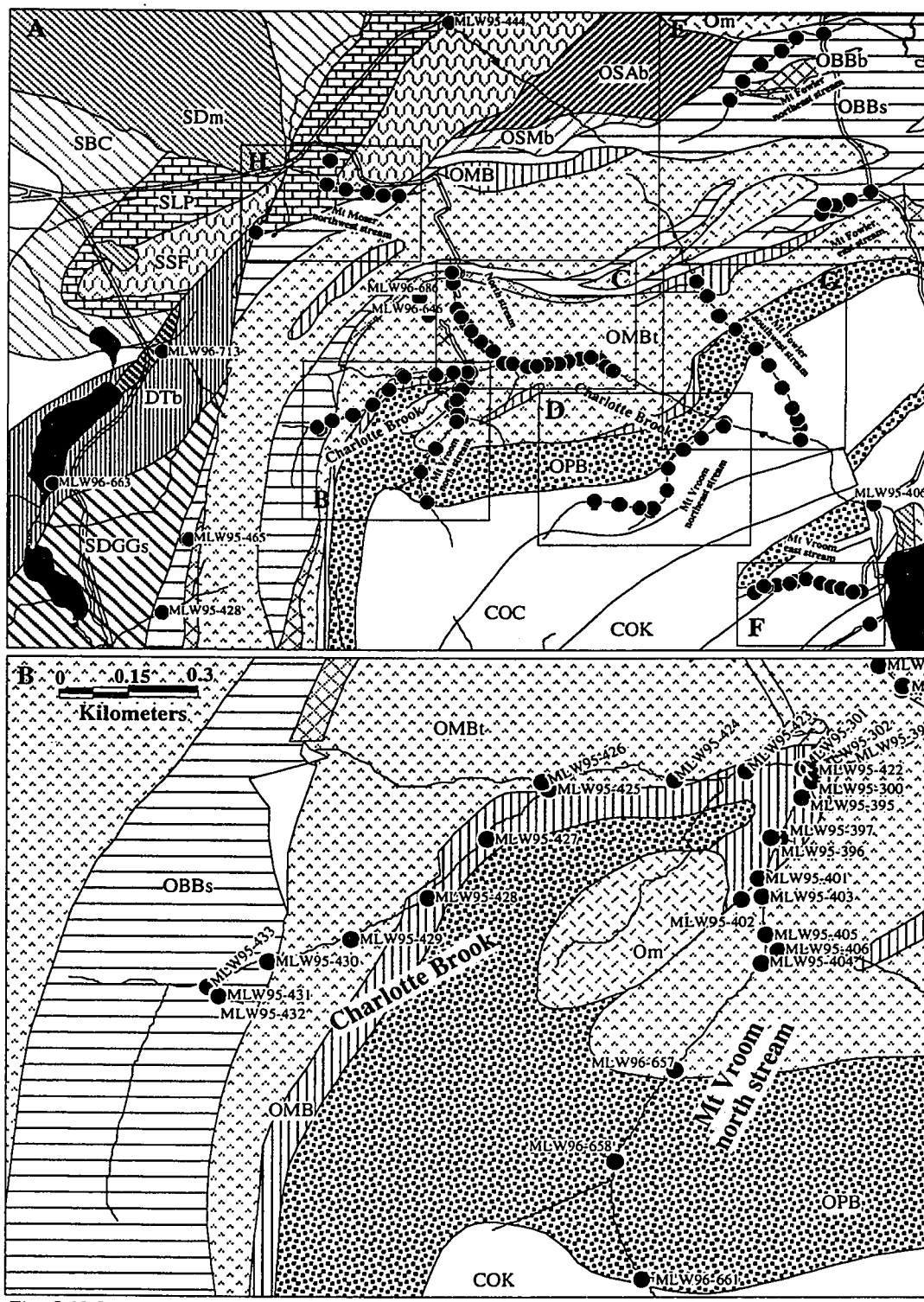


Fig. 5.12 Location of surface waters from the Restigouche deposit. COK, Knights Brook Fm; COC, Chain of Rocks Fm; OPB, Patrick Bk Fm; OMBt, Mt Brittain felsic tuff; OMB, Mt Brittain dacite;

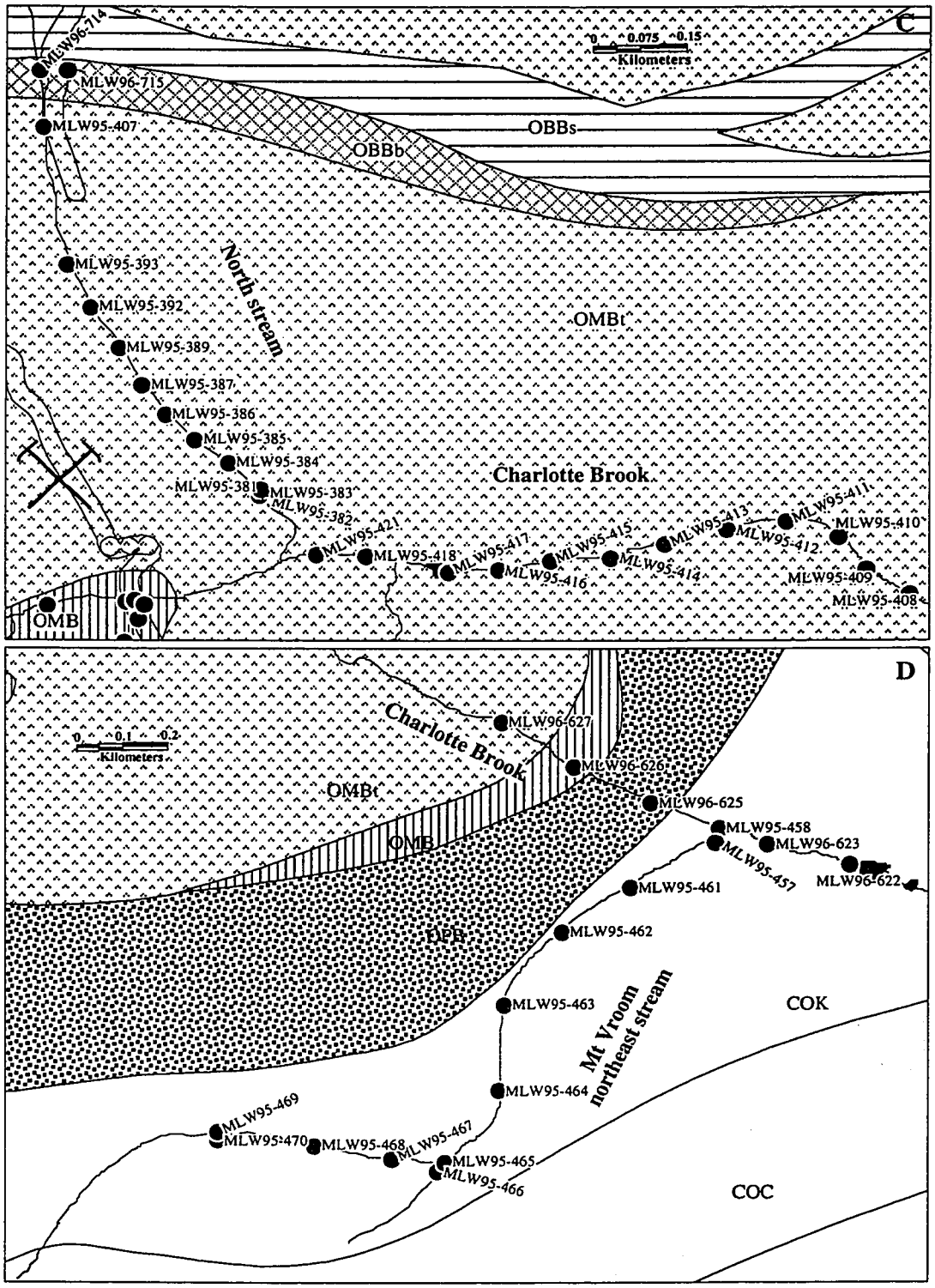


Fig. 5.12 continued.

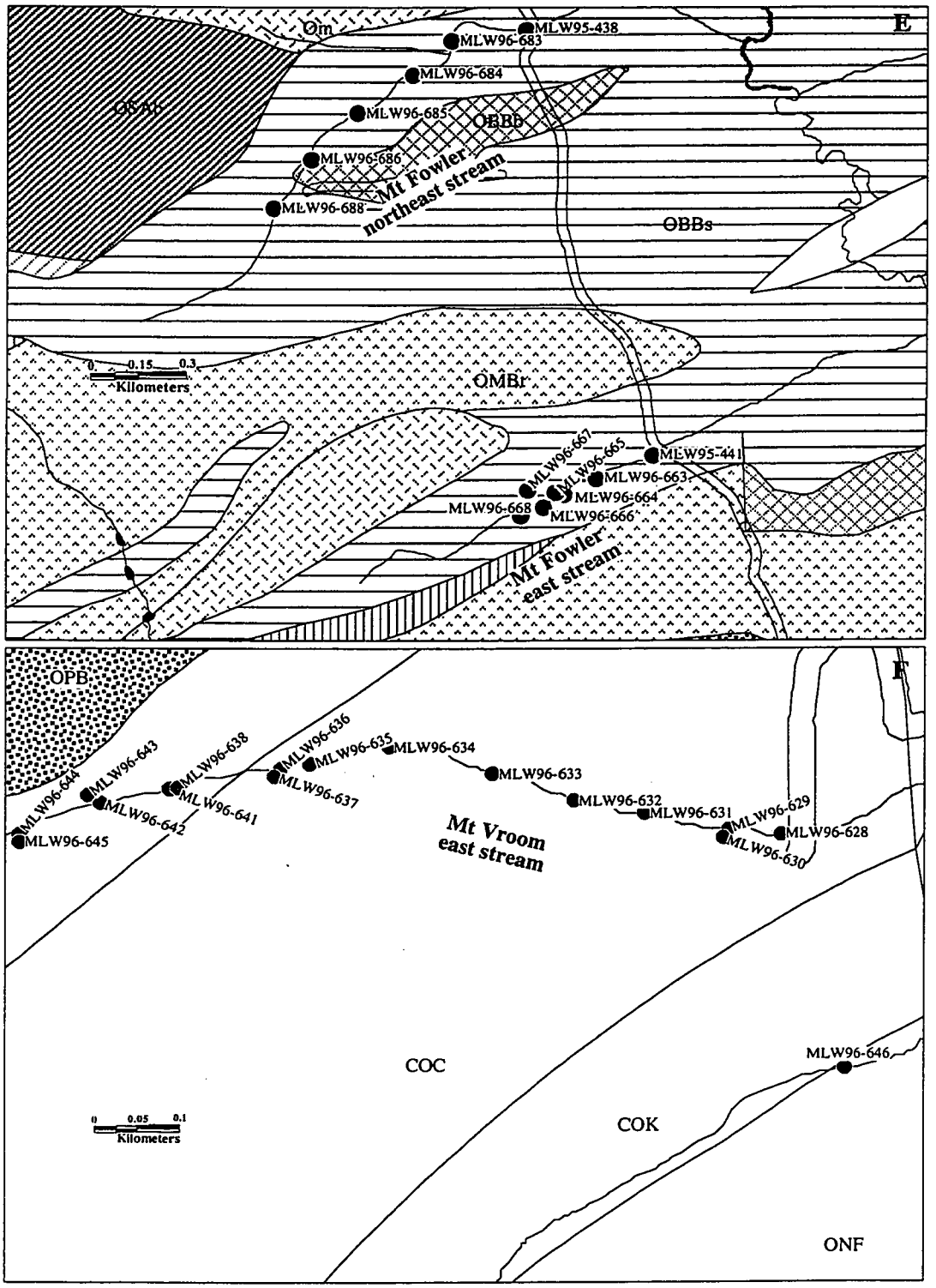


Fig. 5.12 continued.

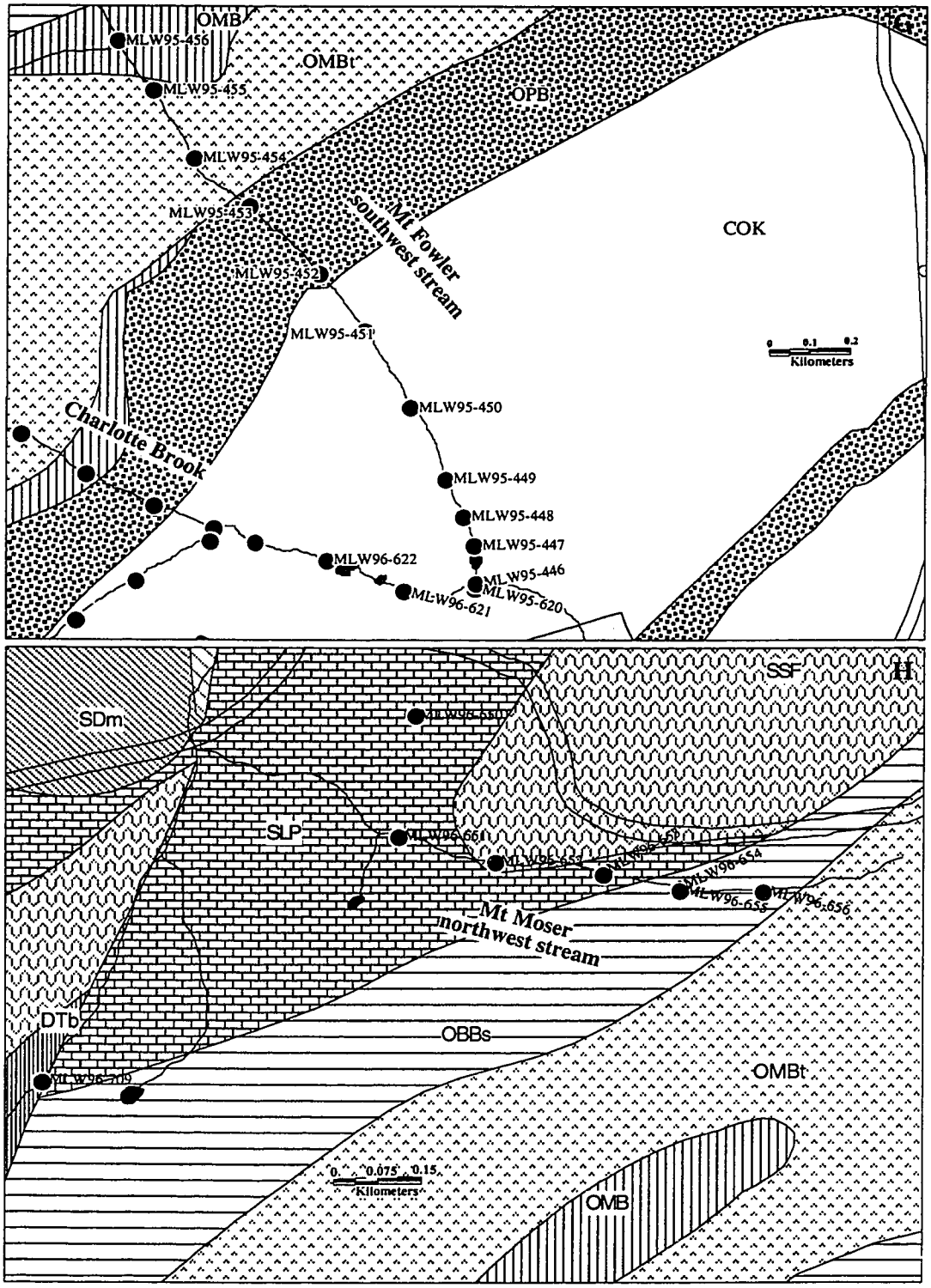


Fig. 5.12 continued.

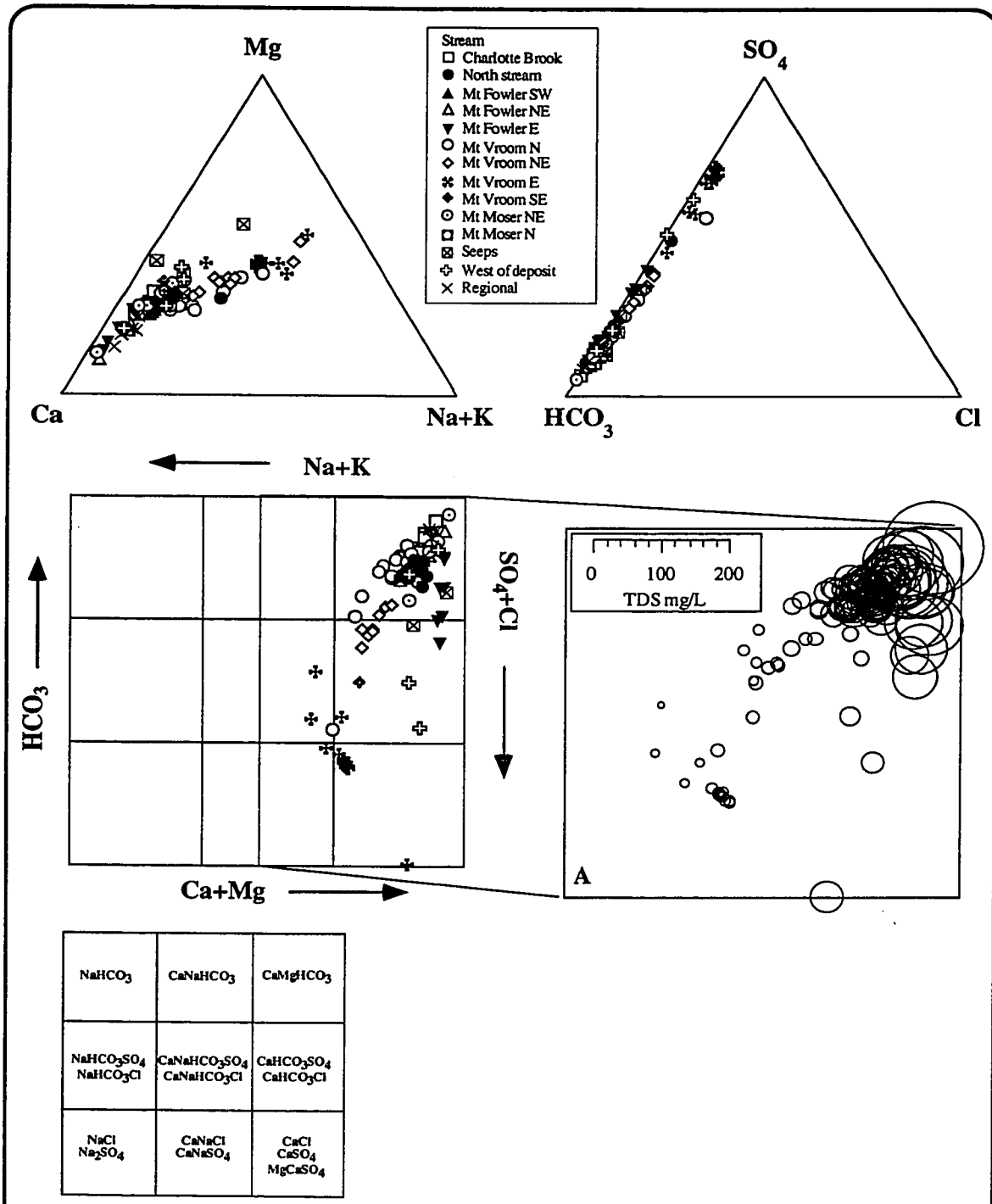


Fig. 5.13 Modified Piper plot for surface waters from the Restigouche deposit. The inset (A) shows the groundwaters proportional to total dissolved solids (TDS). Data from Appendix B.1.

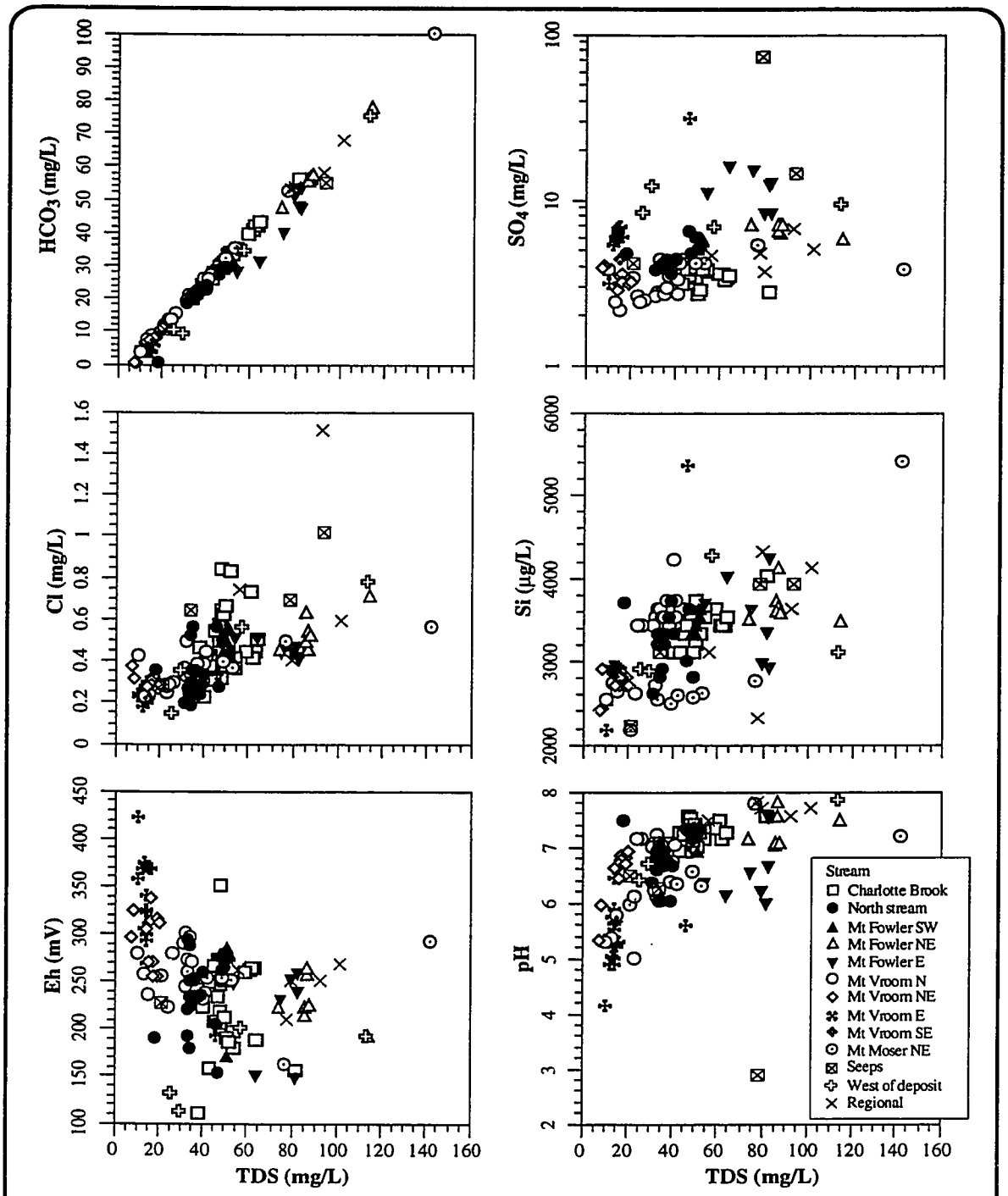


Fig. 5.14 Plots of the major anions, cations and field parameters for Restigouche deposit surface waters. Data from Appendix B.1.1.

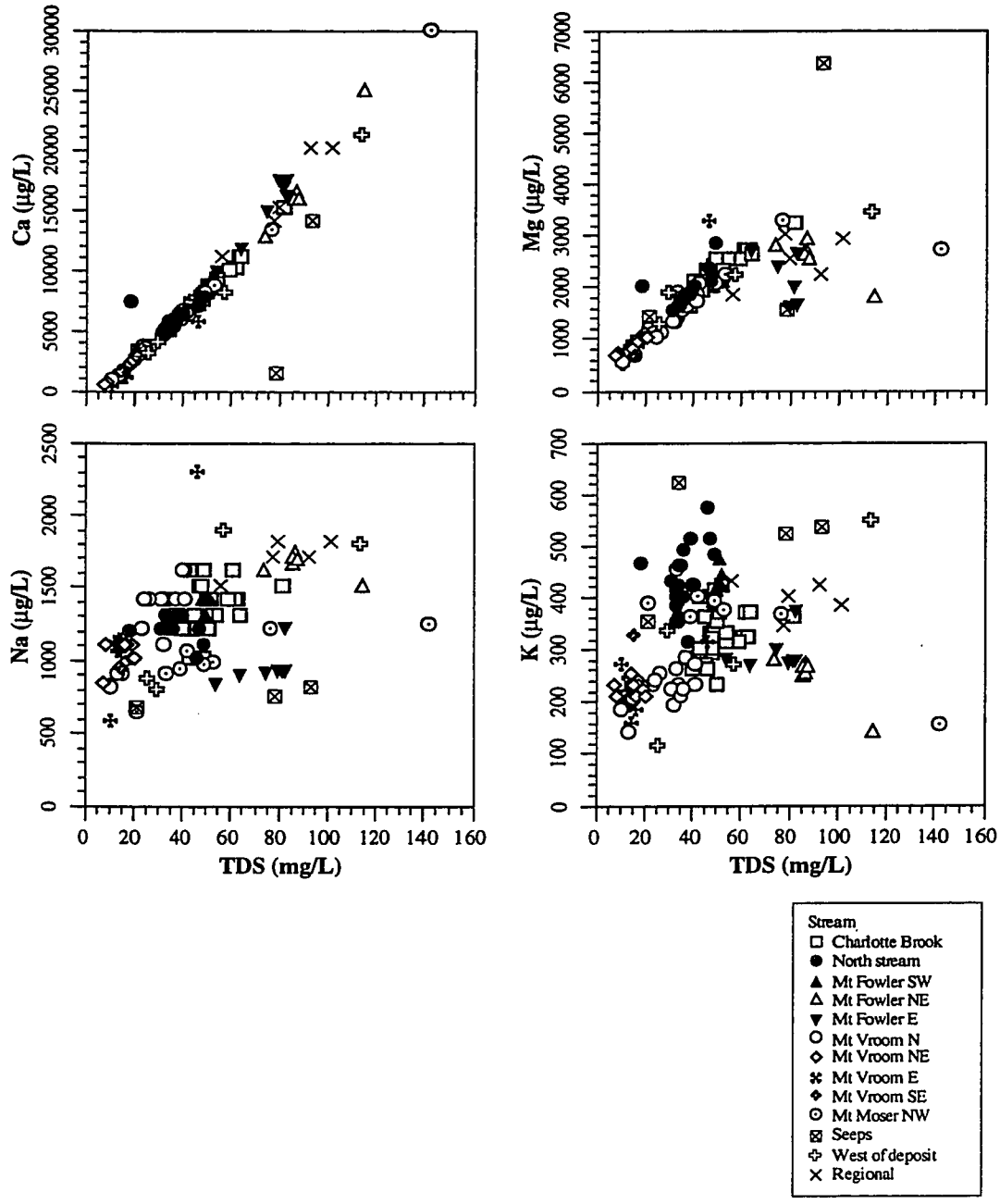


Fig. 5.14 continued.

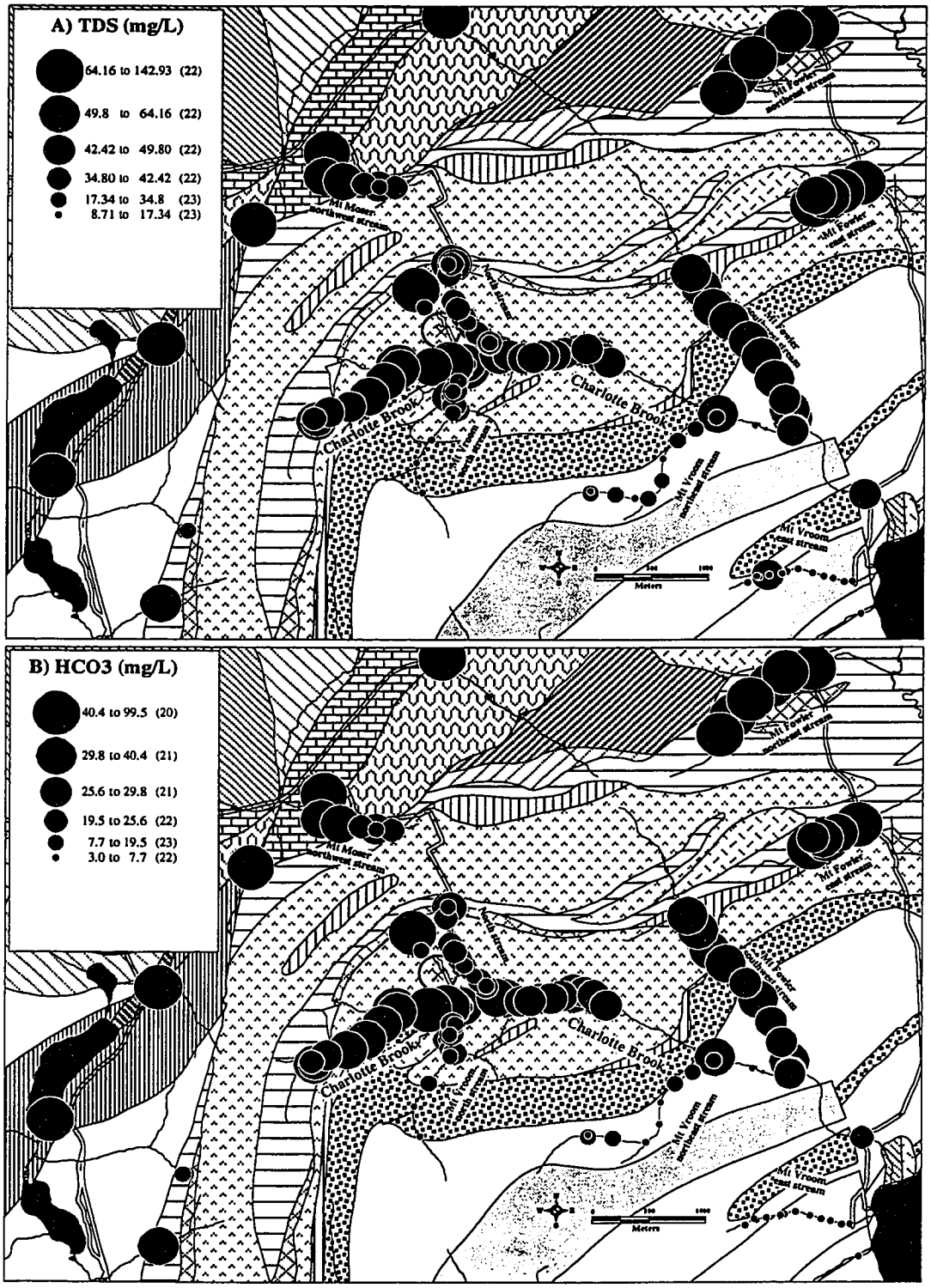


Fig. 5.15 Spatial distribution of major cations, anions and field parameters in Restigouche deposit surface waters.

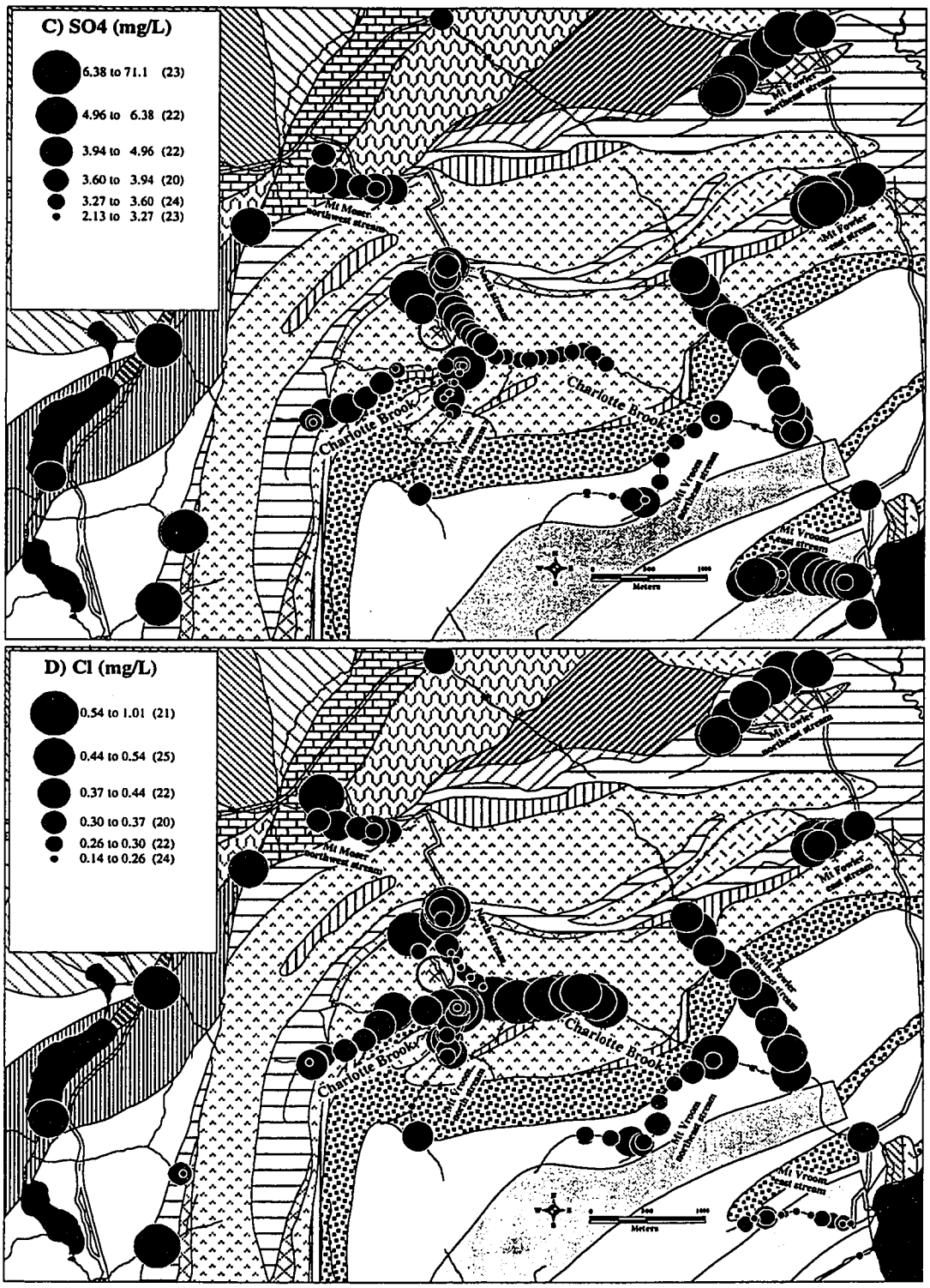


Fig. 5.15 continued.

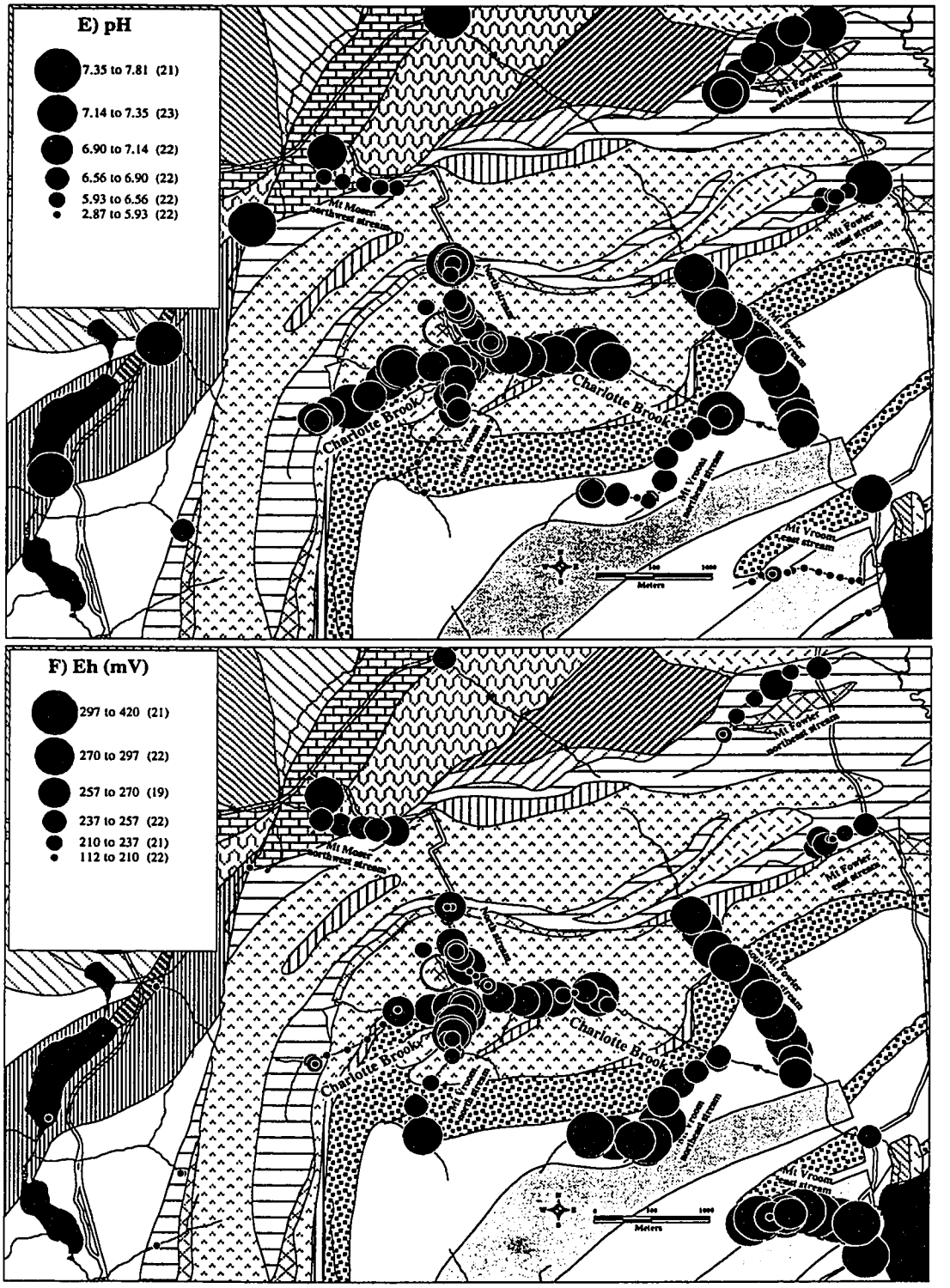


Fig. 5.15 continued.

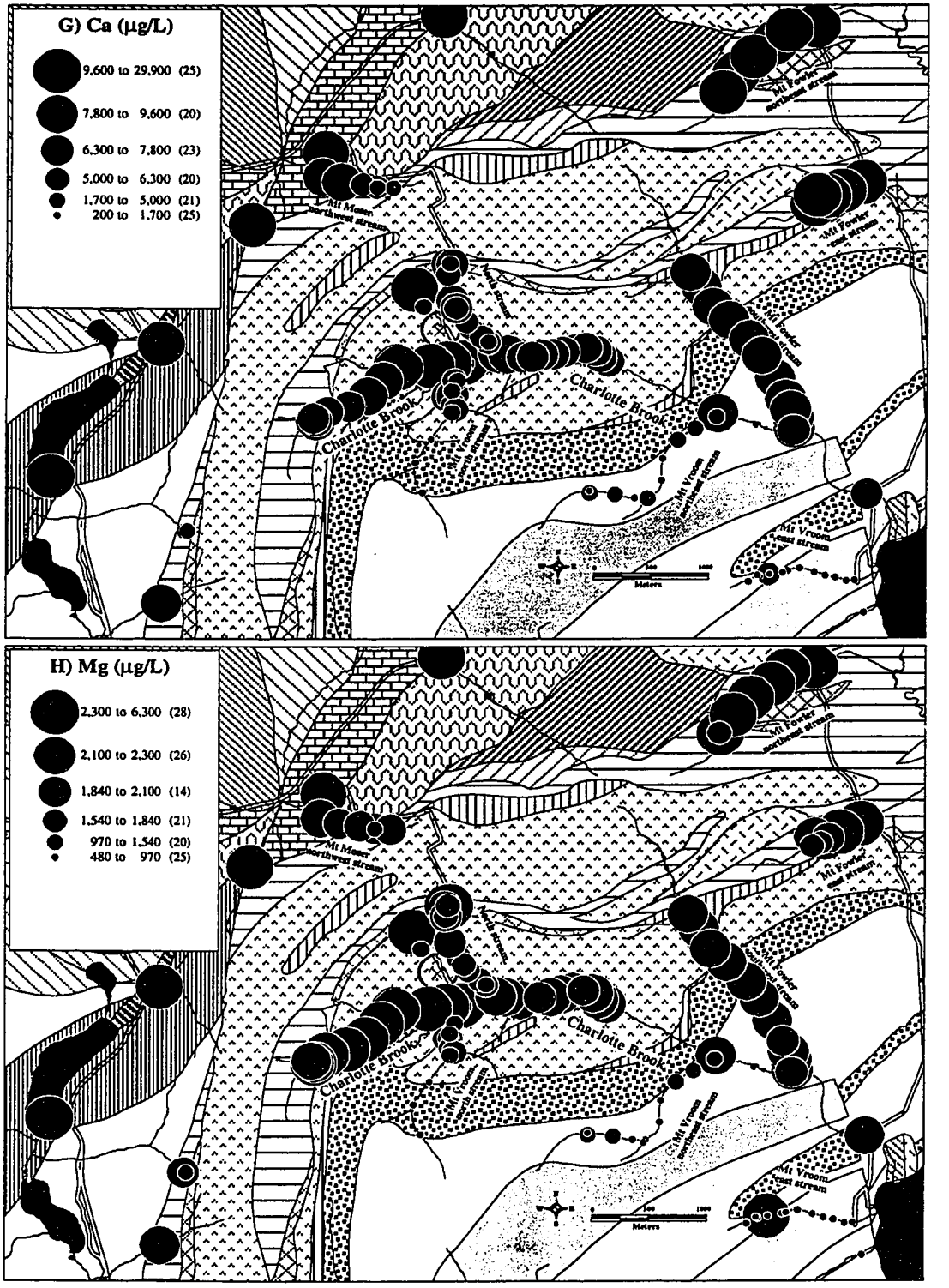


Fig. 5.15 continued.

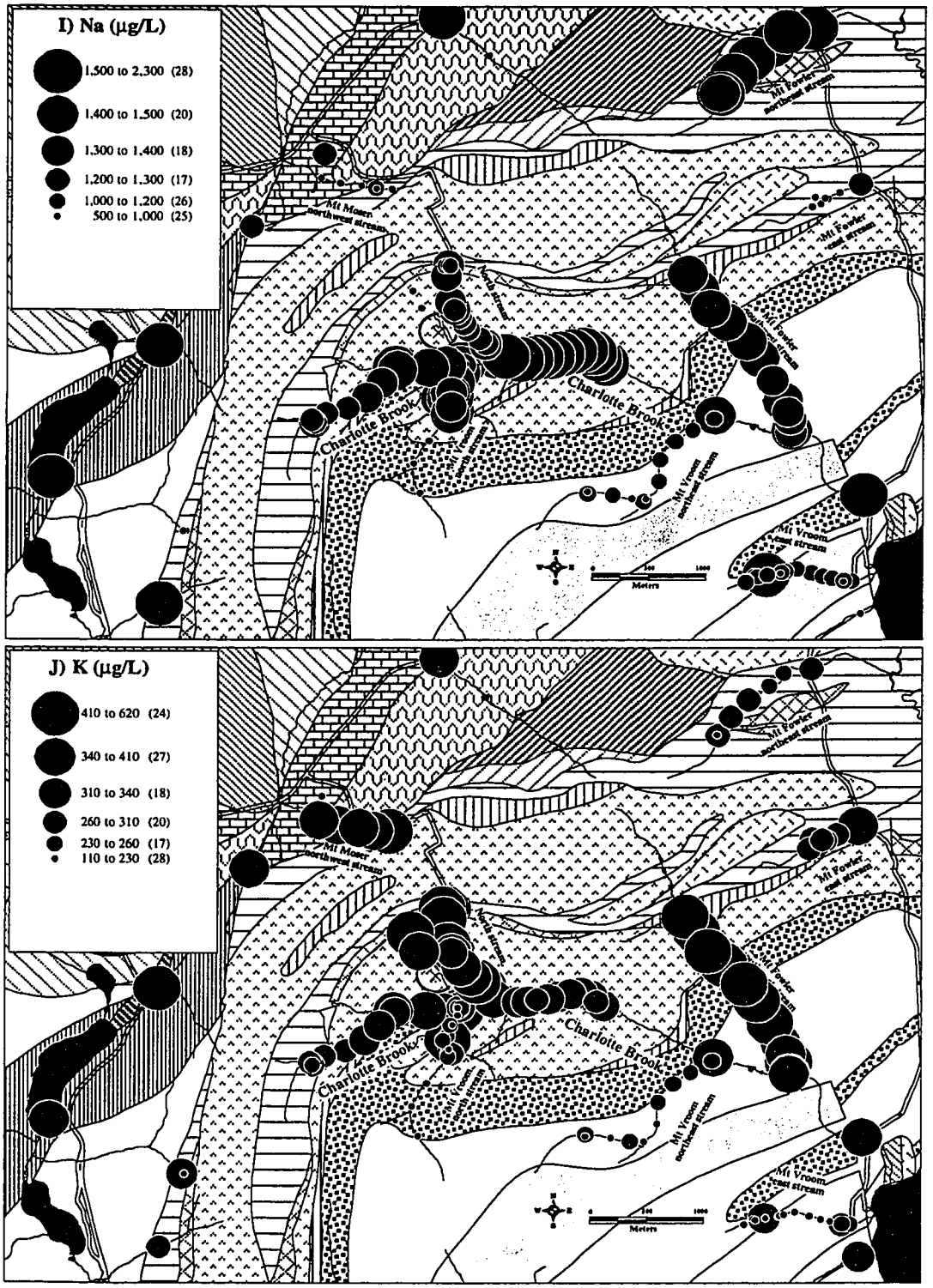


Fig. 5.15 continued.

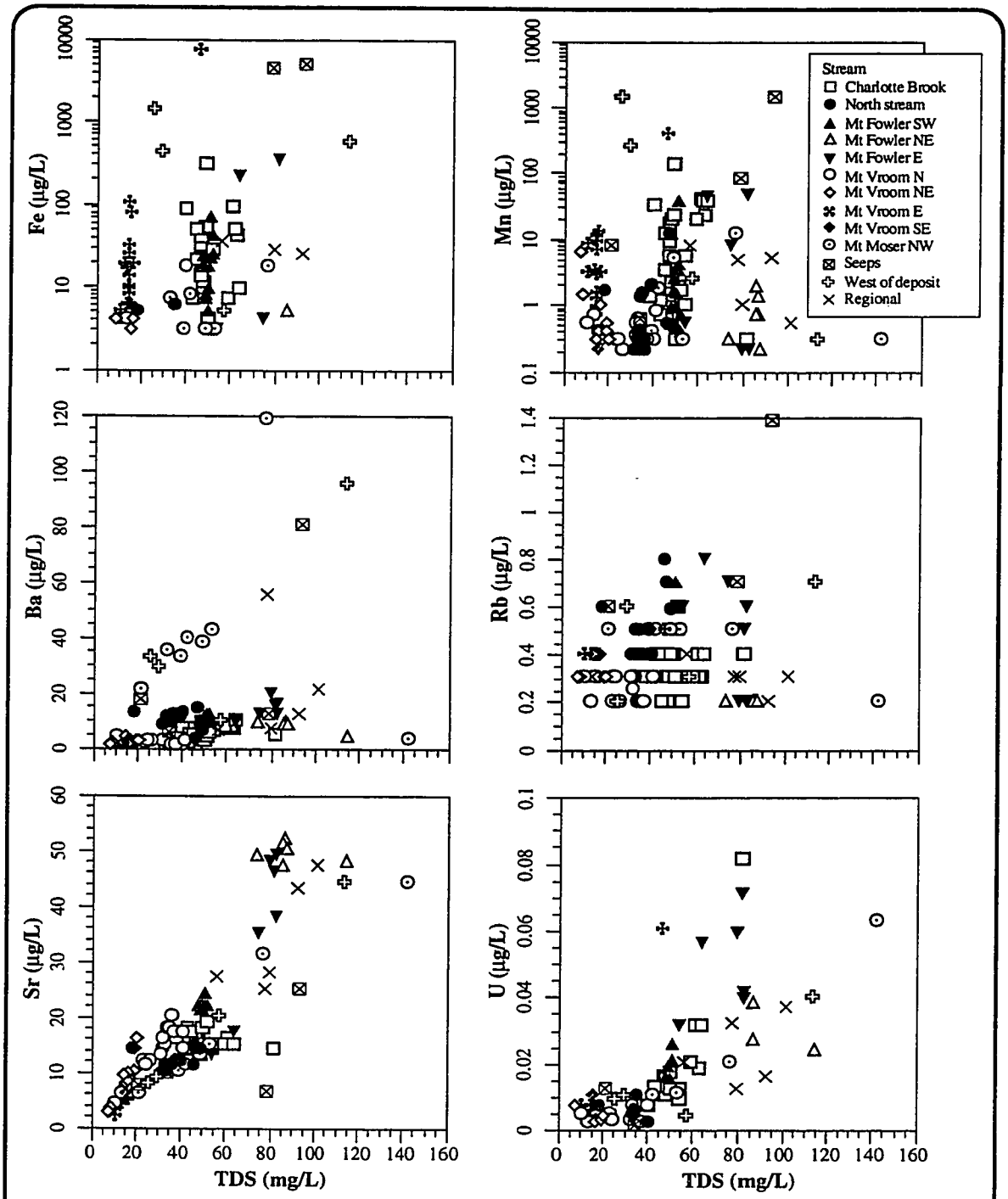


Fig. 5.16 Plots of trace elements in Restigouche deposit surface waters versus TDS. Data from Appendix A.1.1.

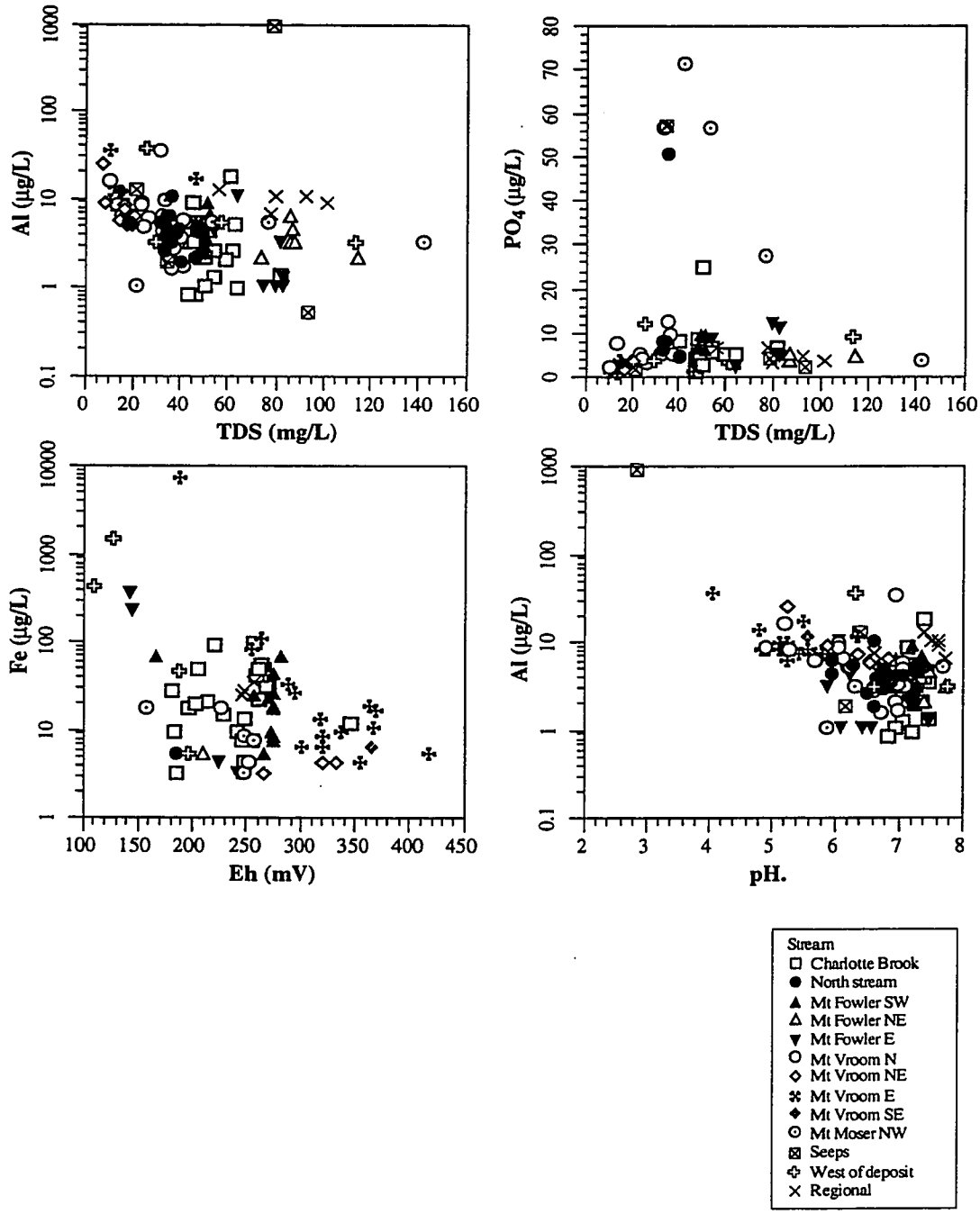


Fig. 5.16 continued.

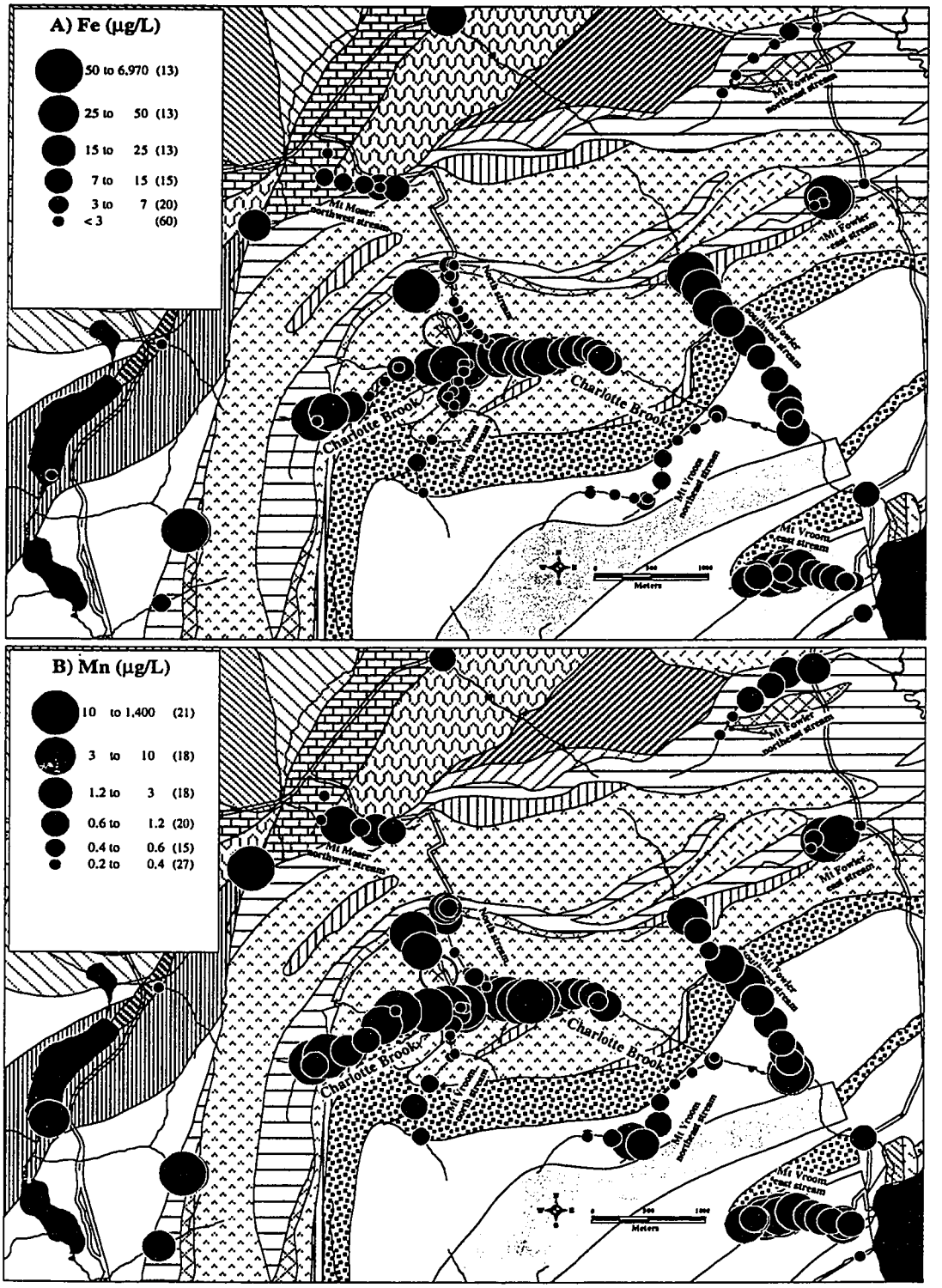


Fig. 5.17 Spatial distribution of trace elements in Restigouche deposit surface waters. Data from Appendix B.1.1.

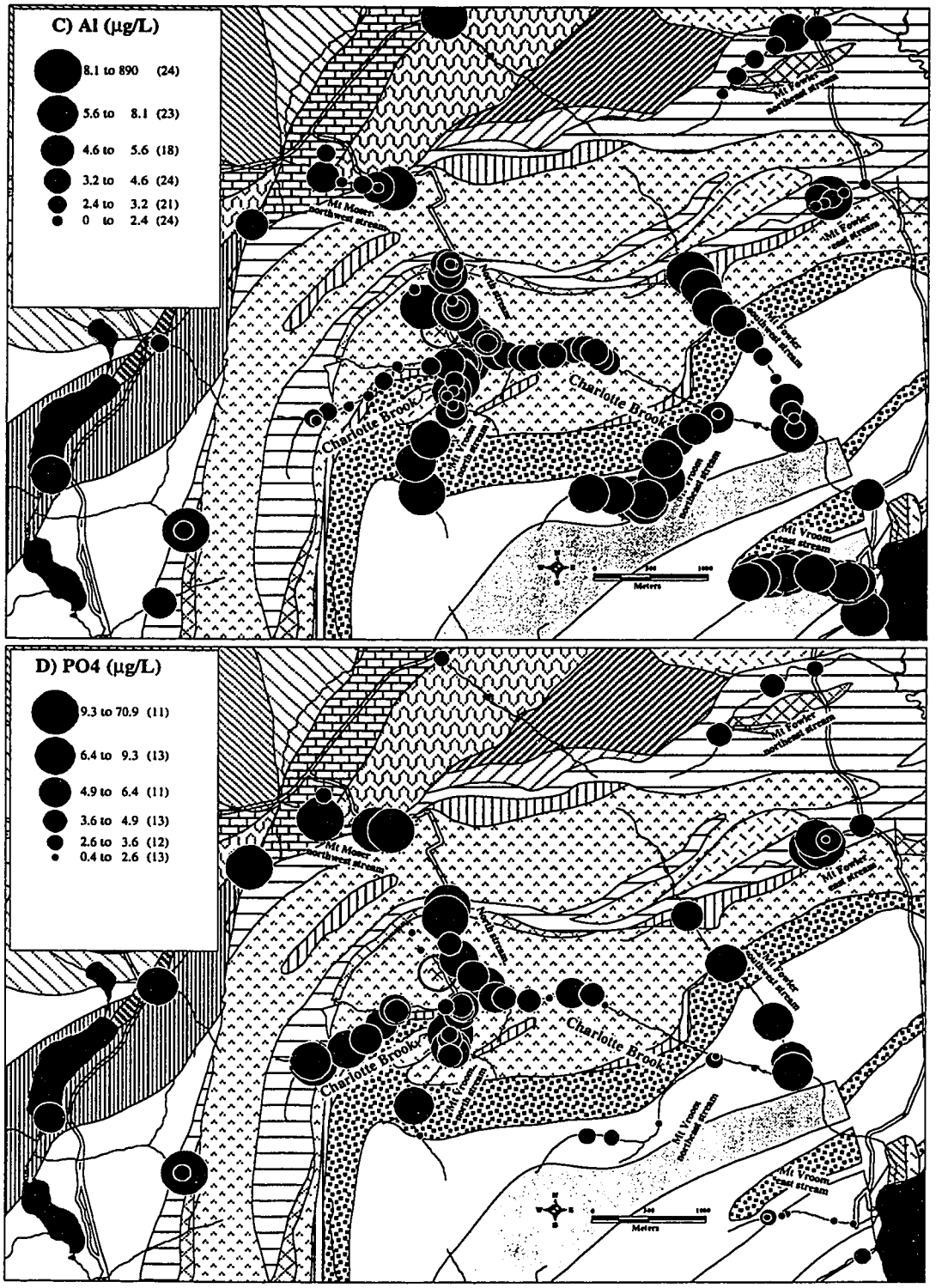


Fig. 5.17 continued.

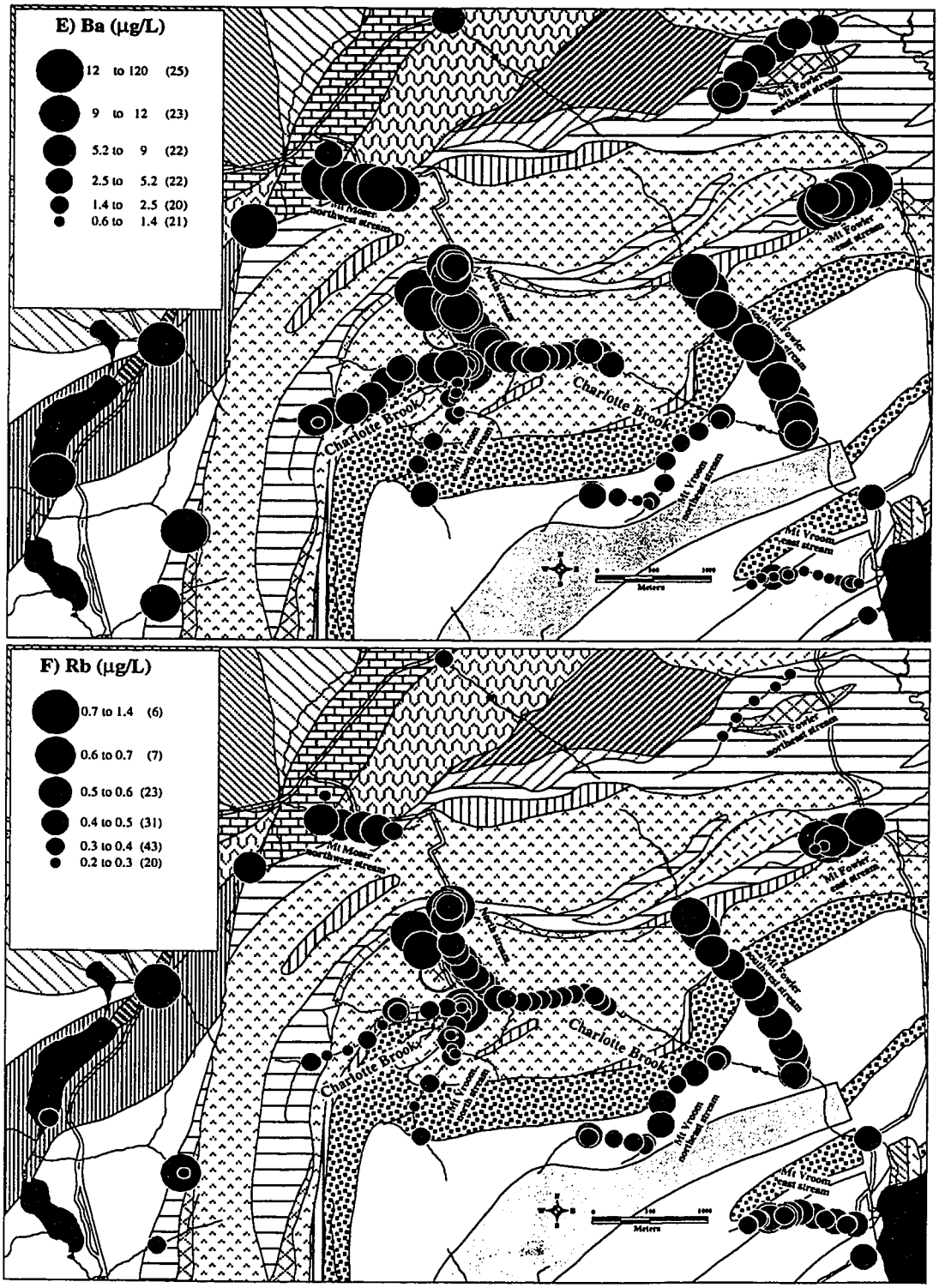


Fig. 5.17 continued.

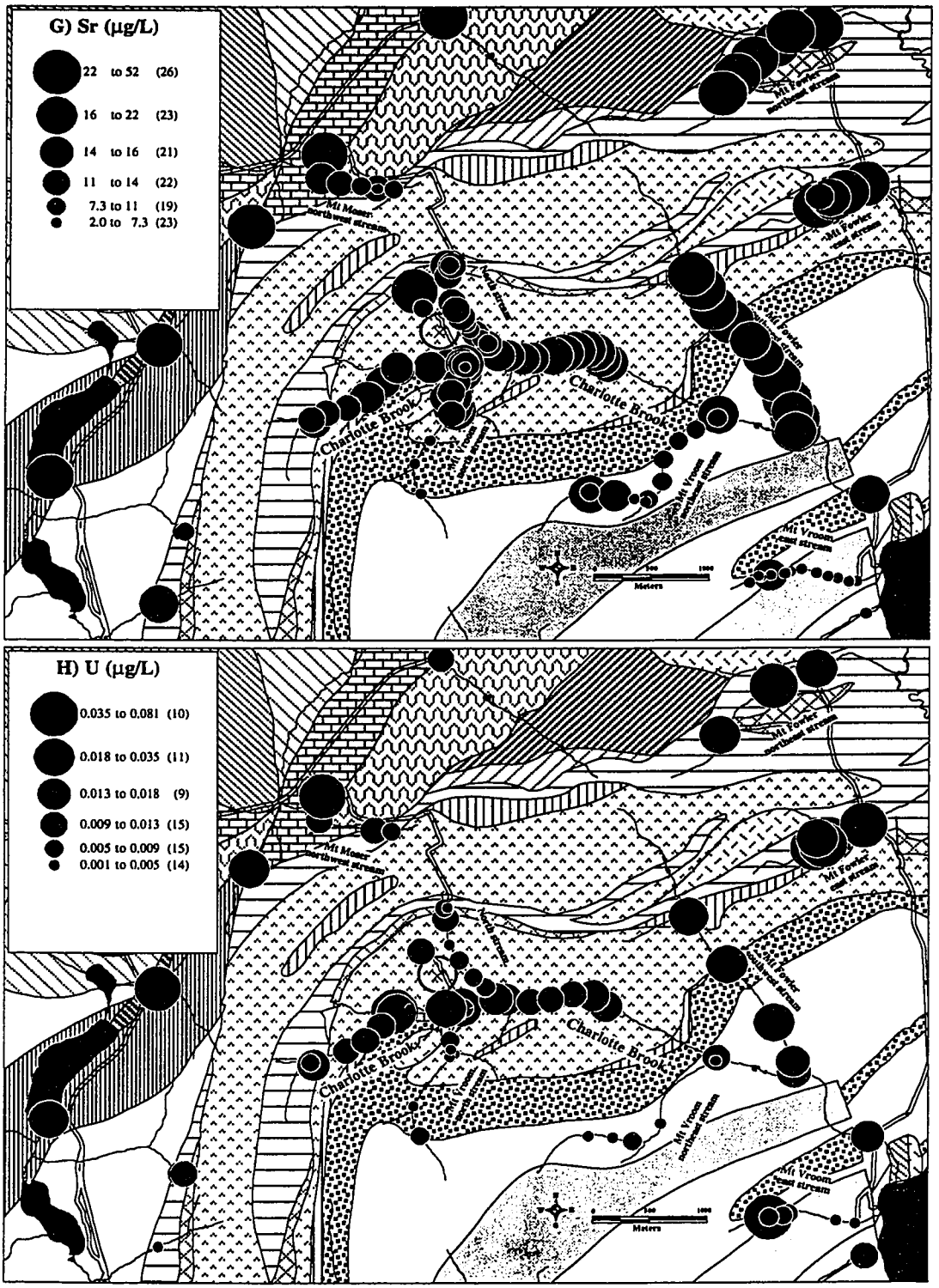


Fig. 5.17 continued.

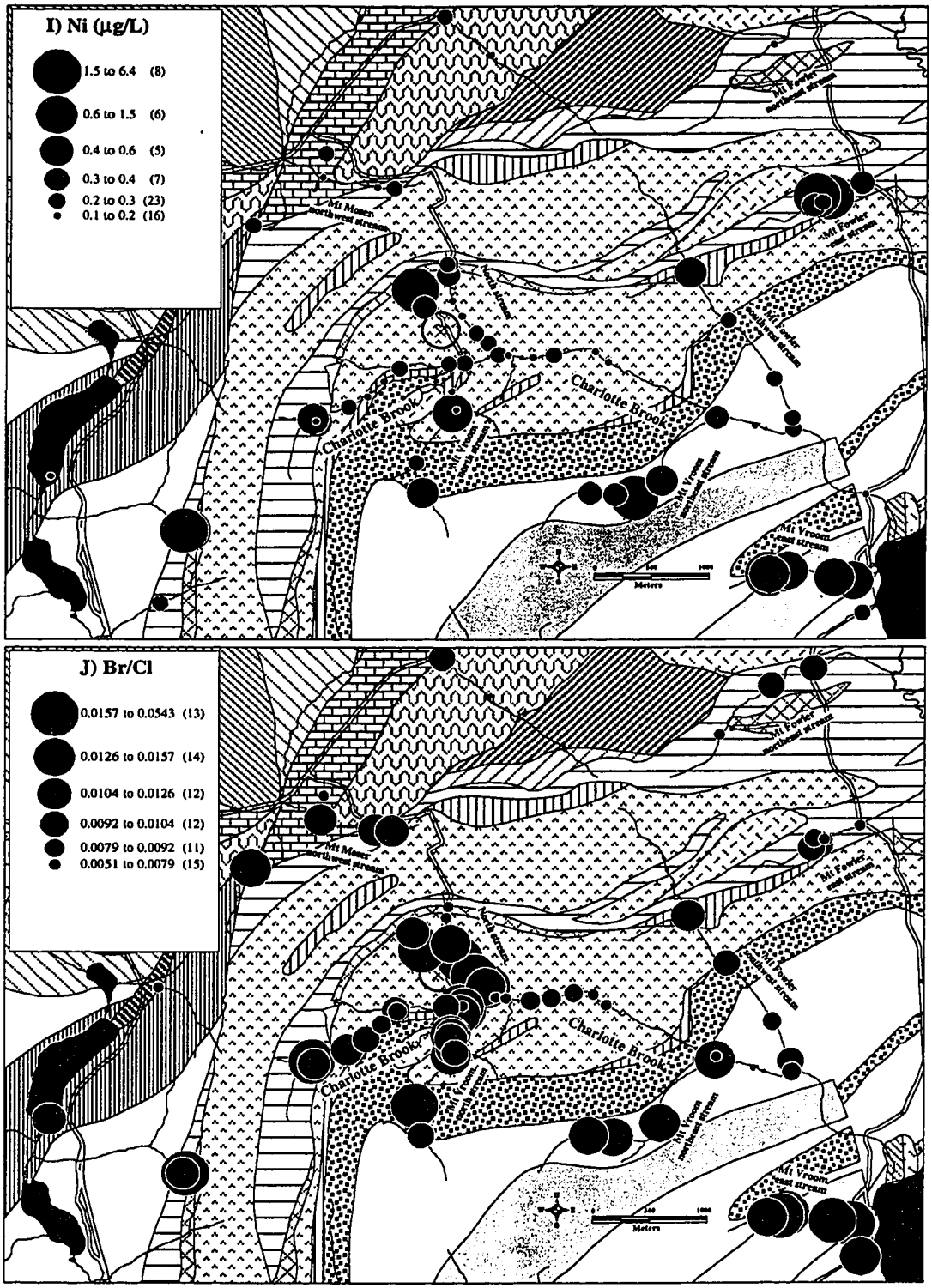


Fig. 5.17 continued.

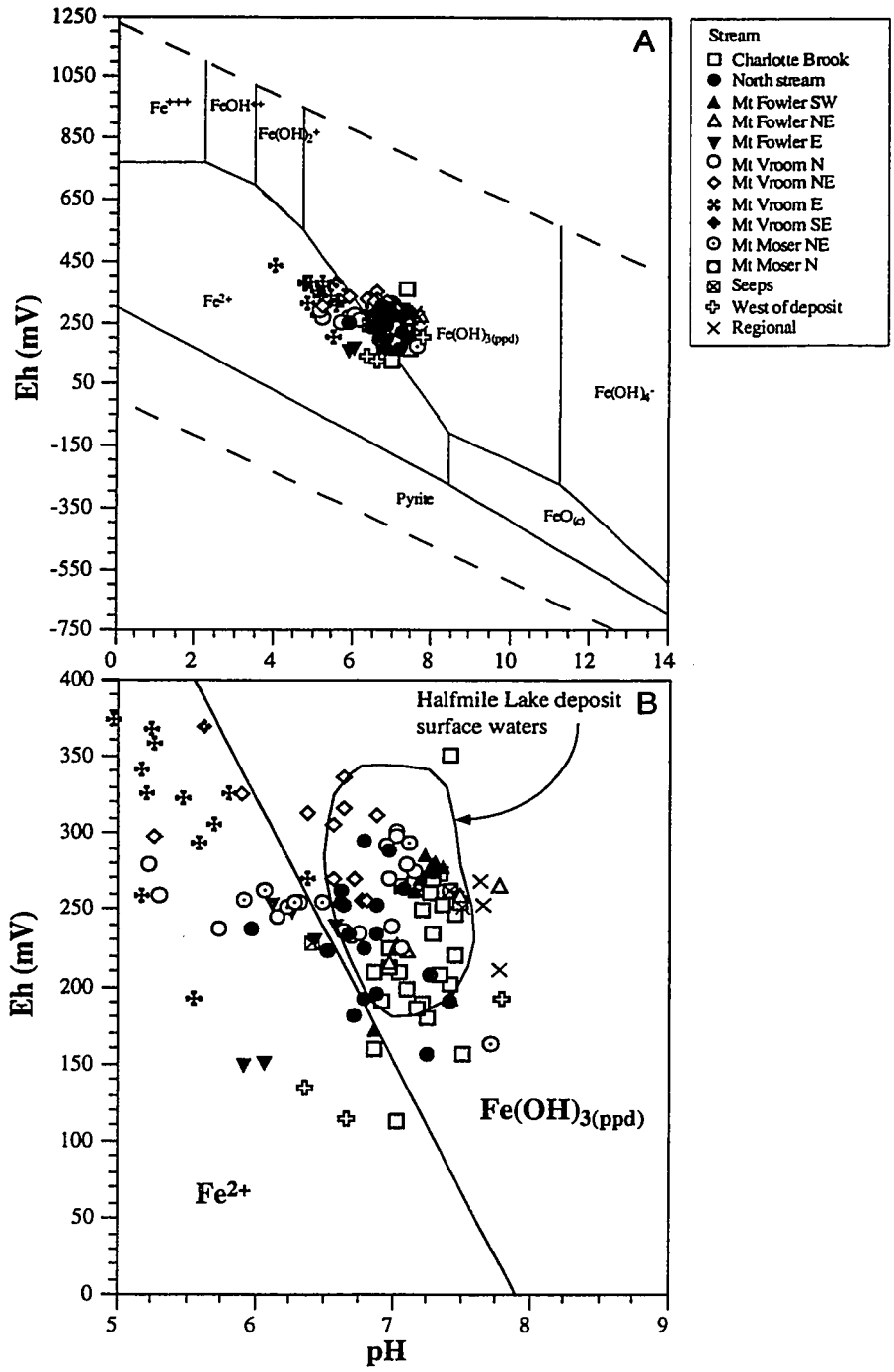


Fig. 5.18 Diagram showing Restigouche deposit suface waters with respect to the stability of metastable Fe hydroxides. The fields were calculated using The Geochemist's Workbench (Bethke, 1994). Conditions are: $[HCO_3] = 10^{-3.5}$, $[SO_4] = 10^{-4.5}$, $[Fe] = 10^{-5.5}$. The formation of hematite, goethite and magnetite were suppressed, reflecting the slow kinetics of formation of these phases compared to amorphous oxide phases.

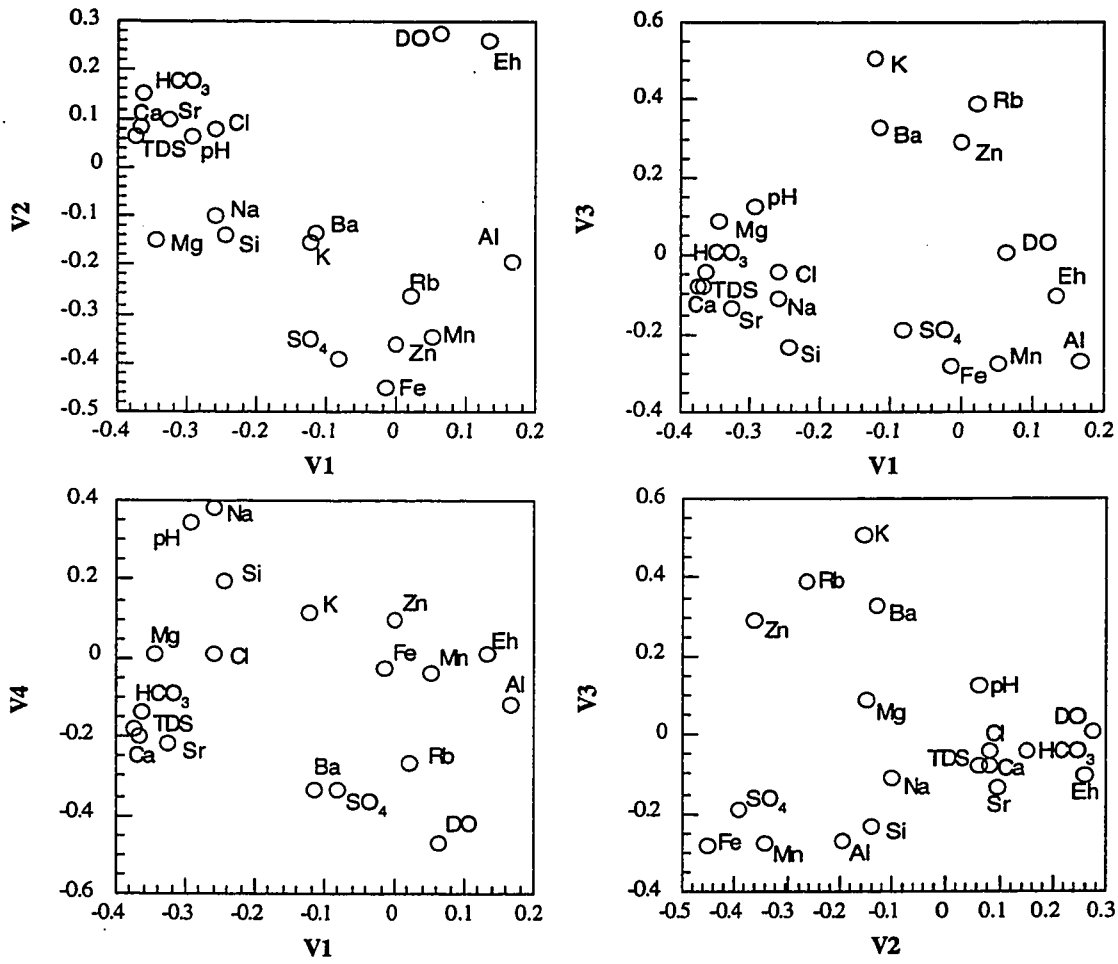


Fig. 5.19 Plots of vectors based on Principal Components Analysis of Restigouche deposit surface waters. Six factors explain 84% of this data set. Vectors for the first four factors are shown.

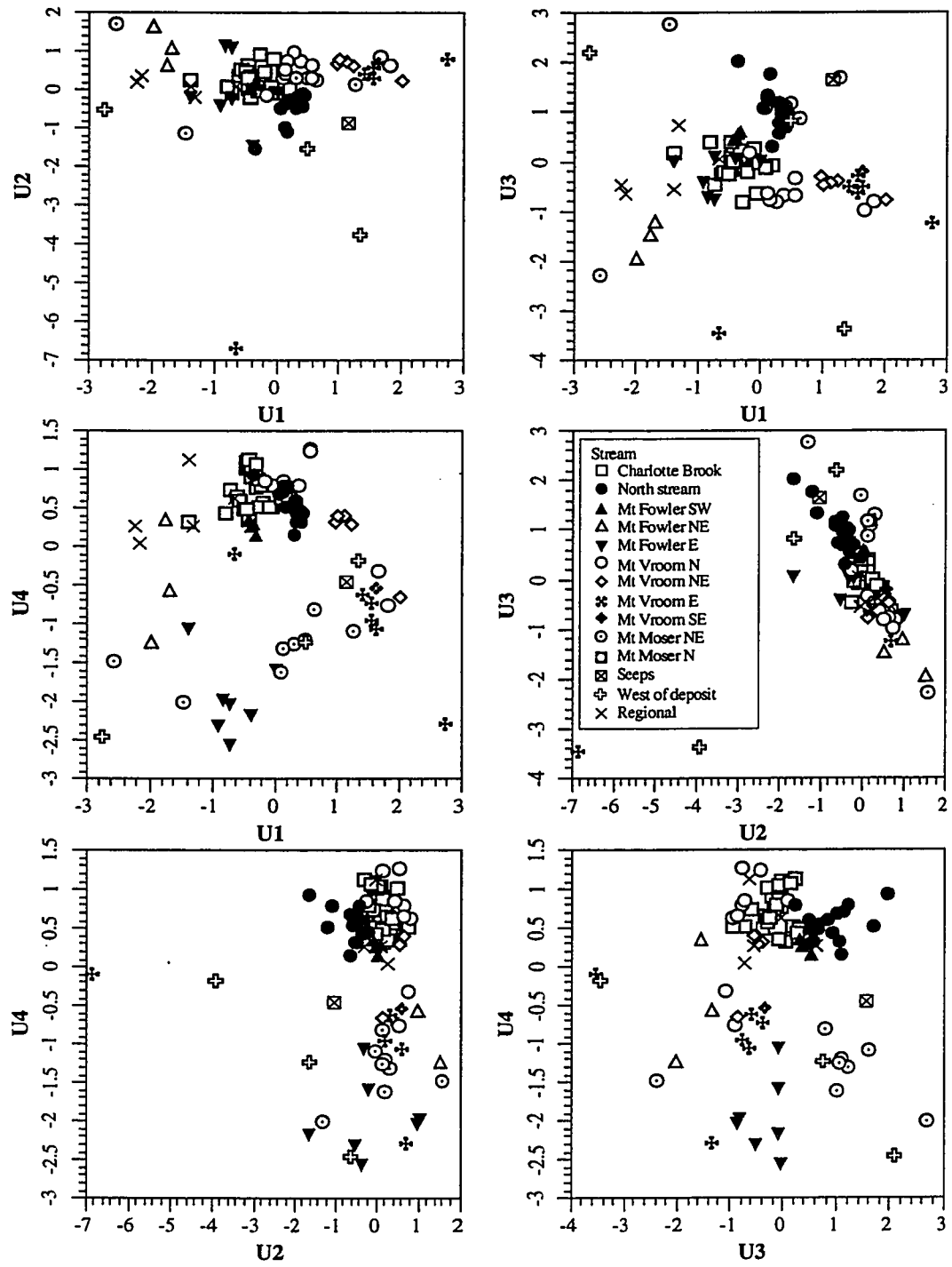


Fig. 5.20 Principal component plots of Restigouche deposit surface water data, showing variations in the first four factors (84% of the variation).

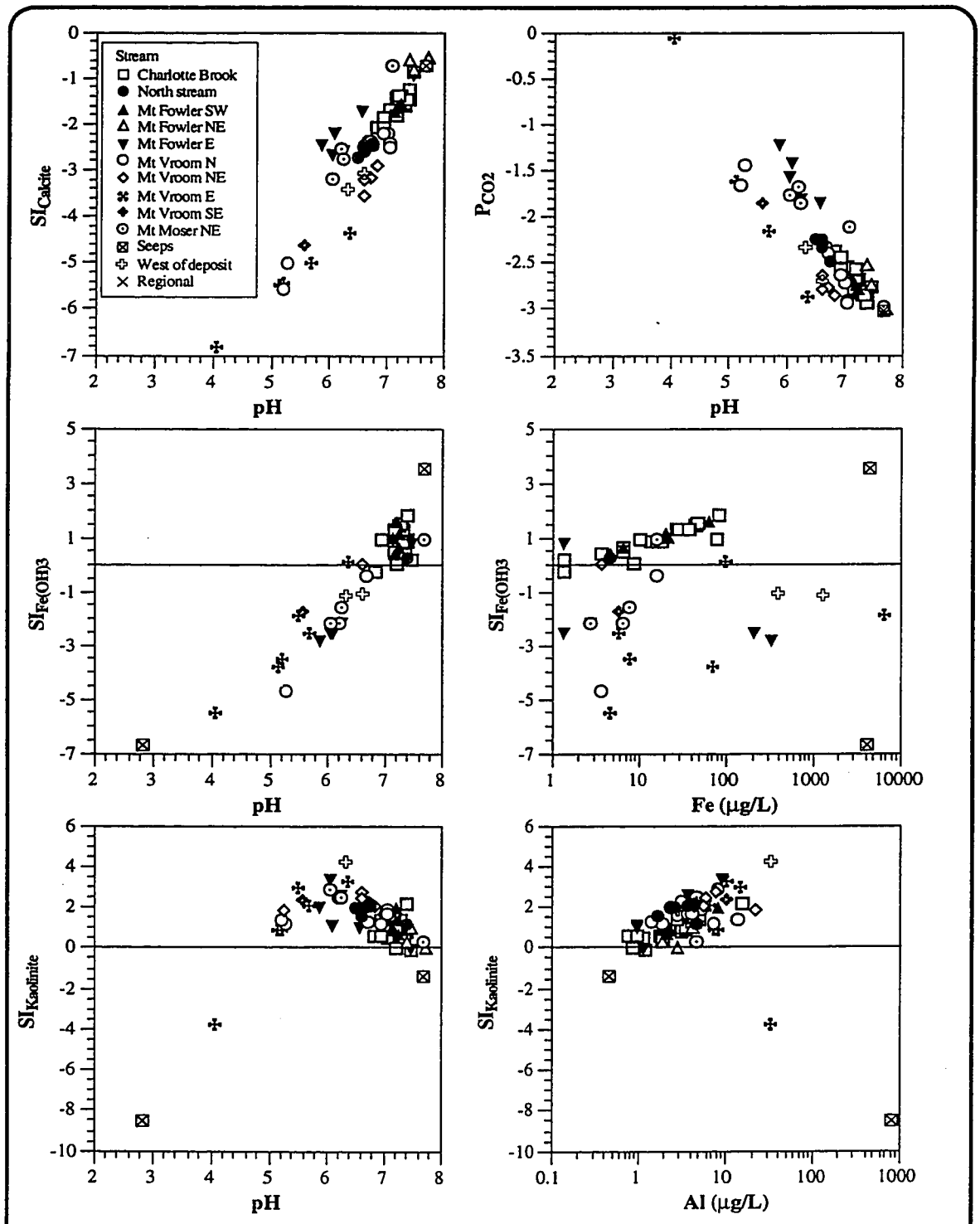


Fig. 5.21 Plots of selected mineral saturation indices (SI) for Restigouche deposit surface waters. Data from Appendix B.1.4.

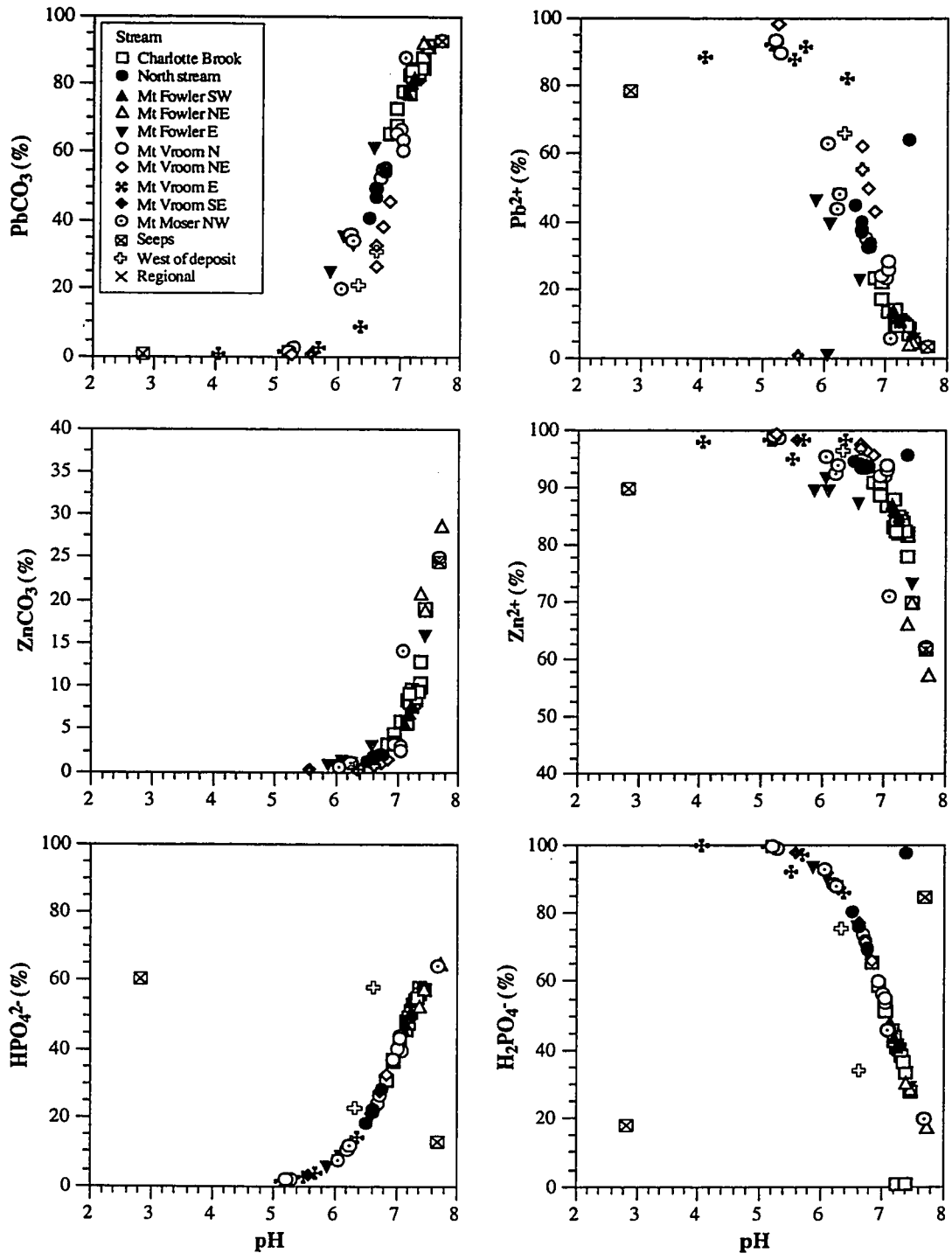


Fig. 5.22 Plots of speciation of selected elements versus pH for Restigouche deposit surface waters. Data from Appendix B.1.5.

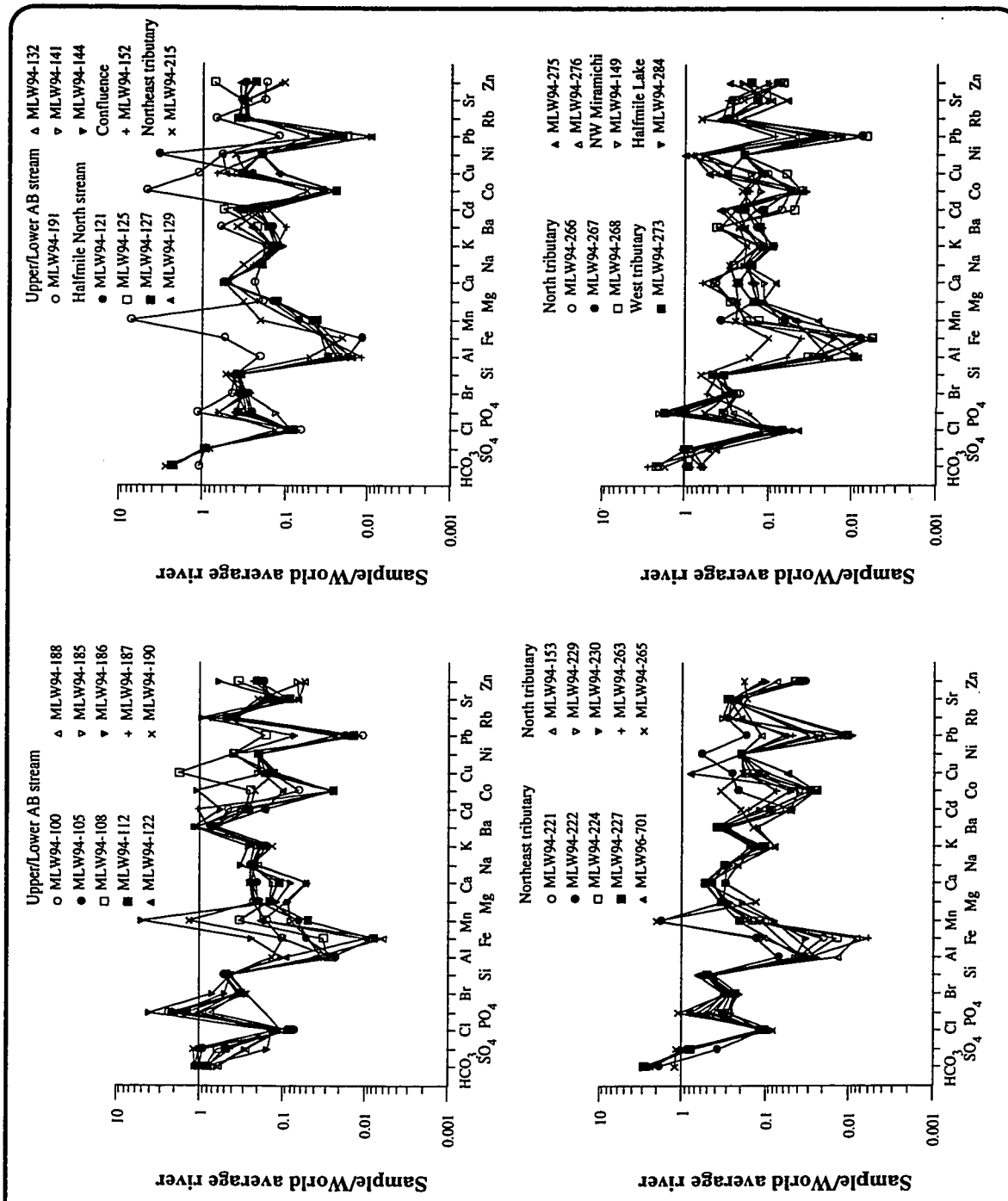


Fig. 5.23 Halfmile Lake deposit surface waters normalized to world average river water. Normalizing values from Berner and Berner (1987). Data from Appendix A.1.1.

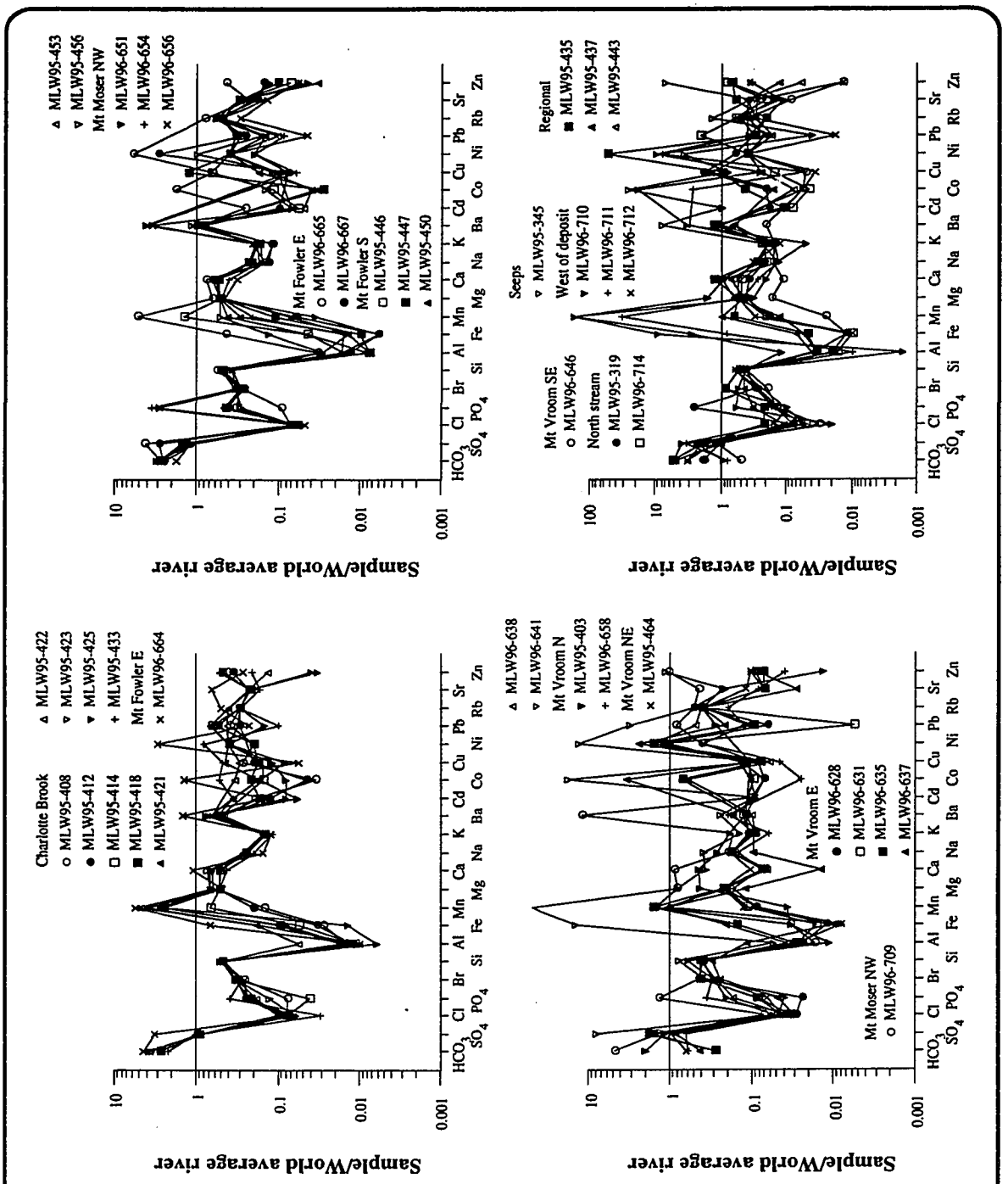


Fig. 5.24 Restigouche deposit surface waters normalized to world average river water. Normalizing values from Berner and Berner (1987). Data from Appendix B.1.1.

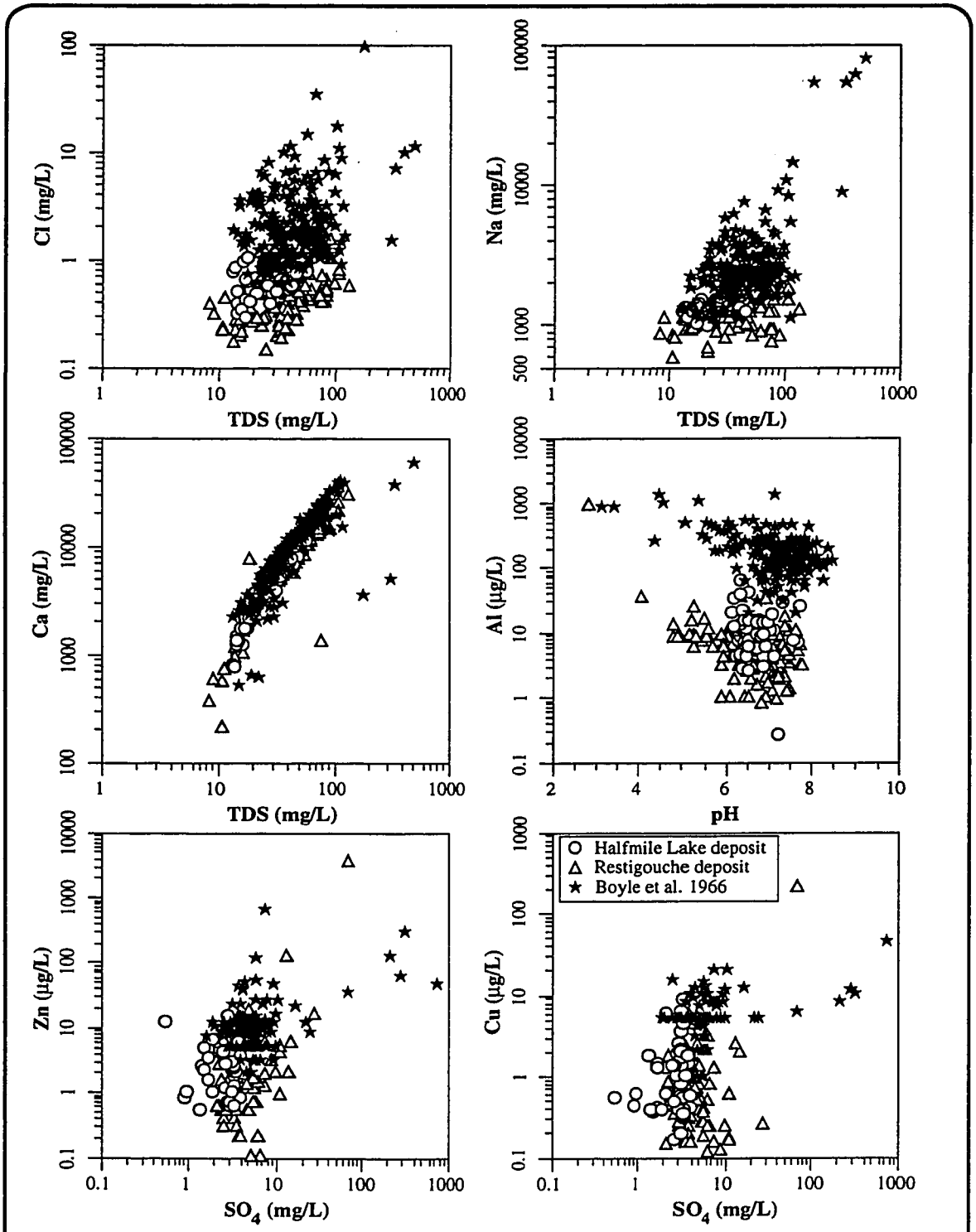


Fig. 5.25 Variation diagrams comparing surface waters from the Halfmile Lake and Restigouche deposits with data collected from the BMC in 1965 (Boyle et al. 1966).

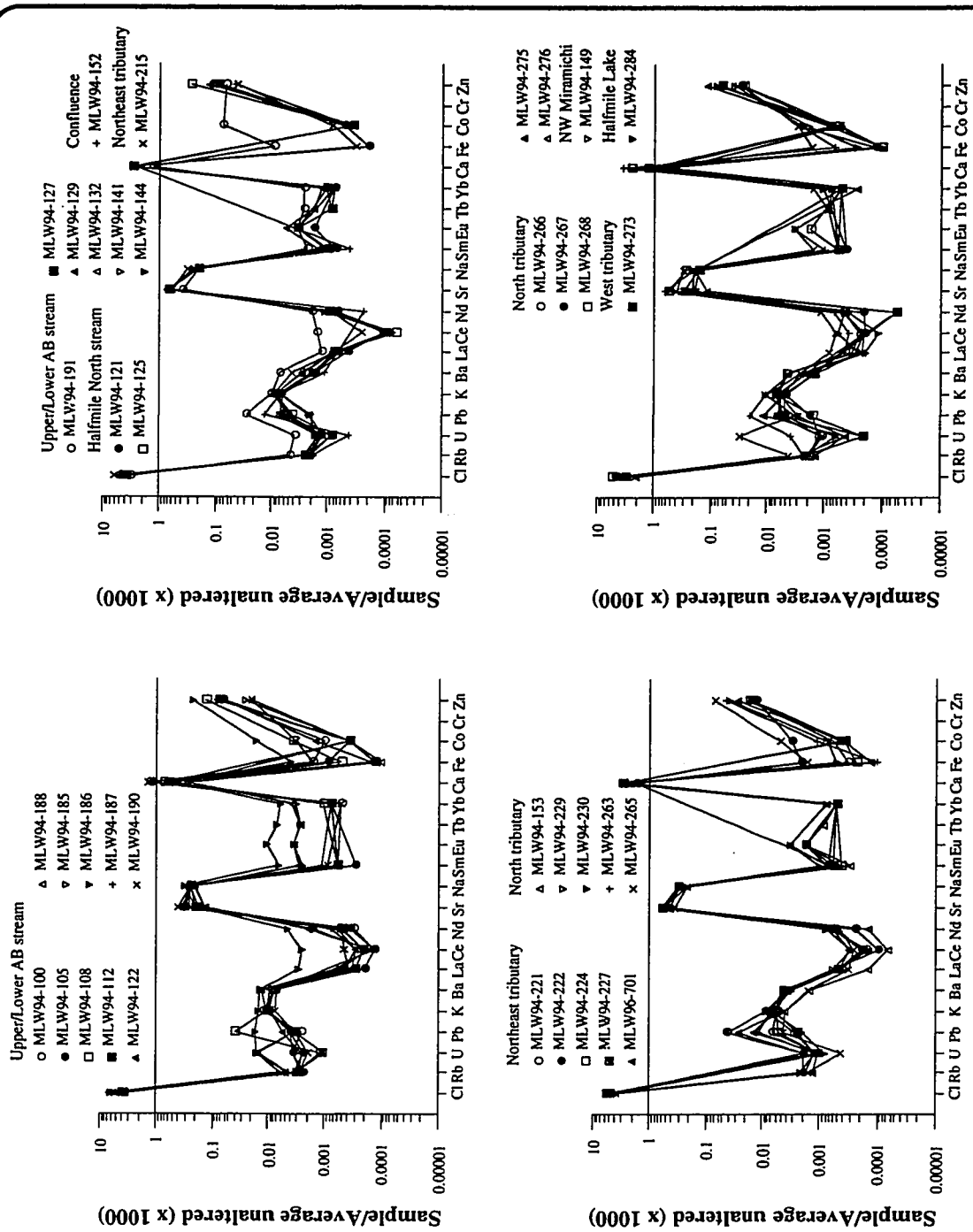


Fig. 5.26 Trace element contents of Halfmile Lake deposit surface waters normalized to average unaltered Halfmile Lake lithology (defined in Chapter Two). Data from Appendix A.1.1.

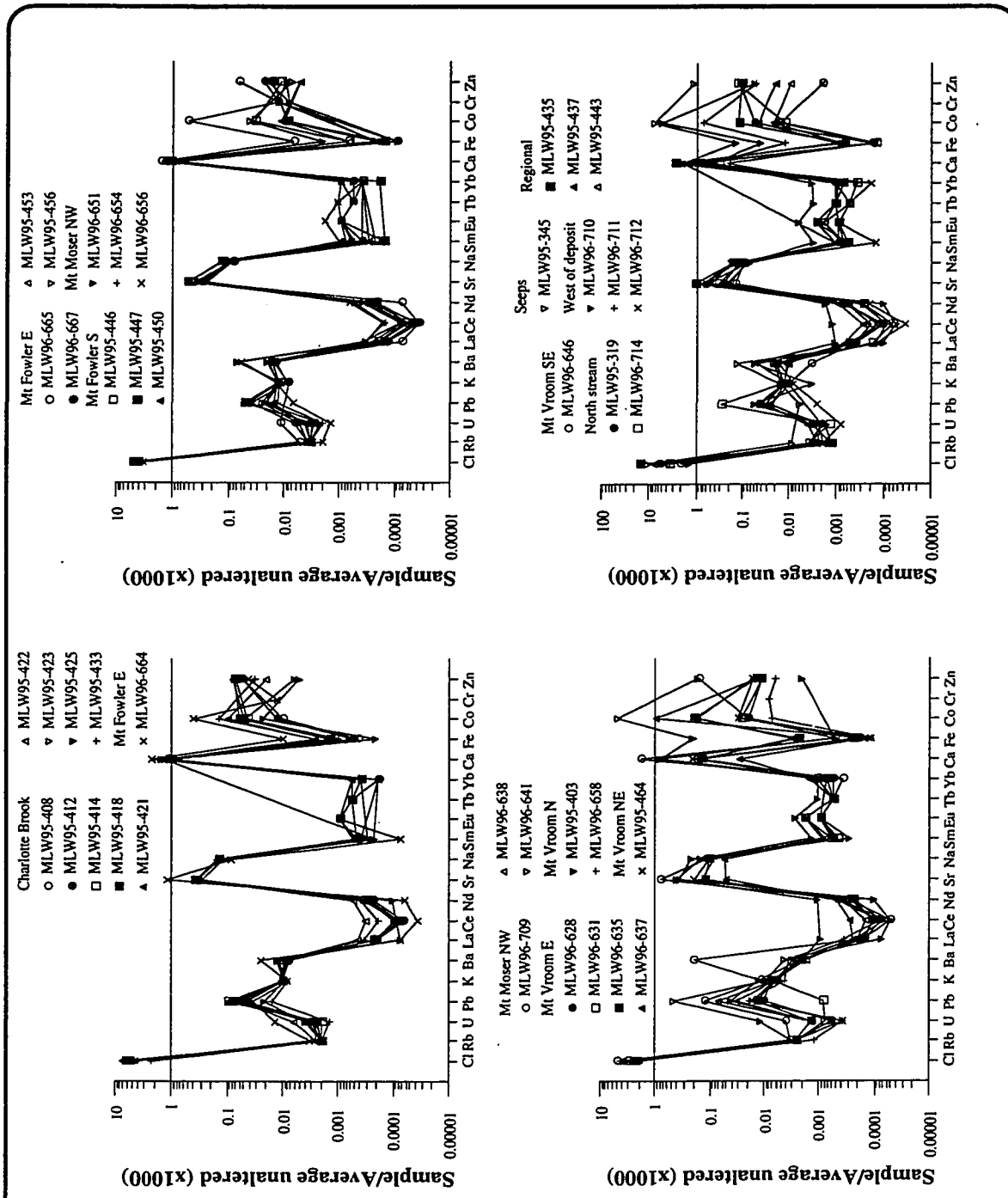


Fig. 5.27 Restigouche deposit surface waters normalized to average unaltered felsic lithologies from the Resiguche deposit. Normalizing values from Chapter Two. Data from Appendix A.1.1.

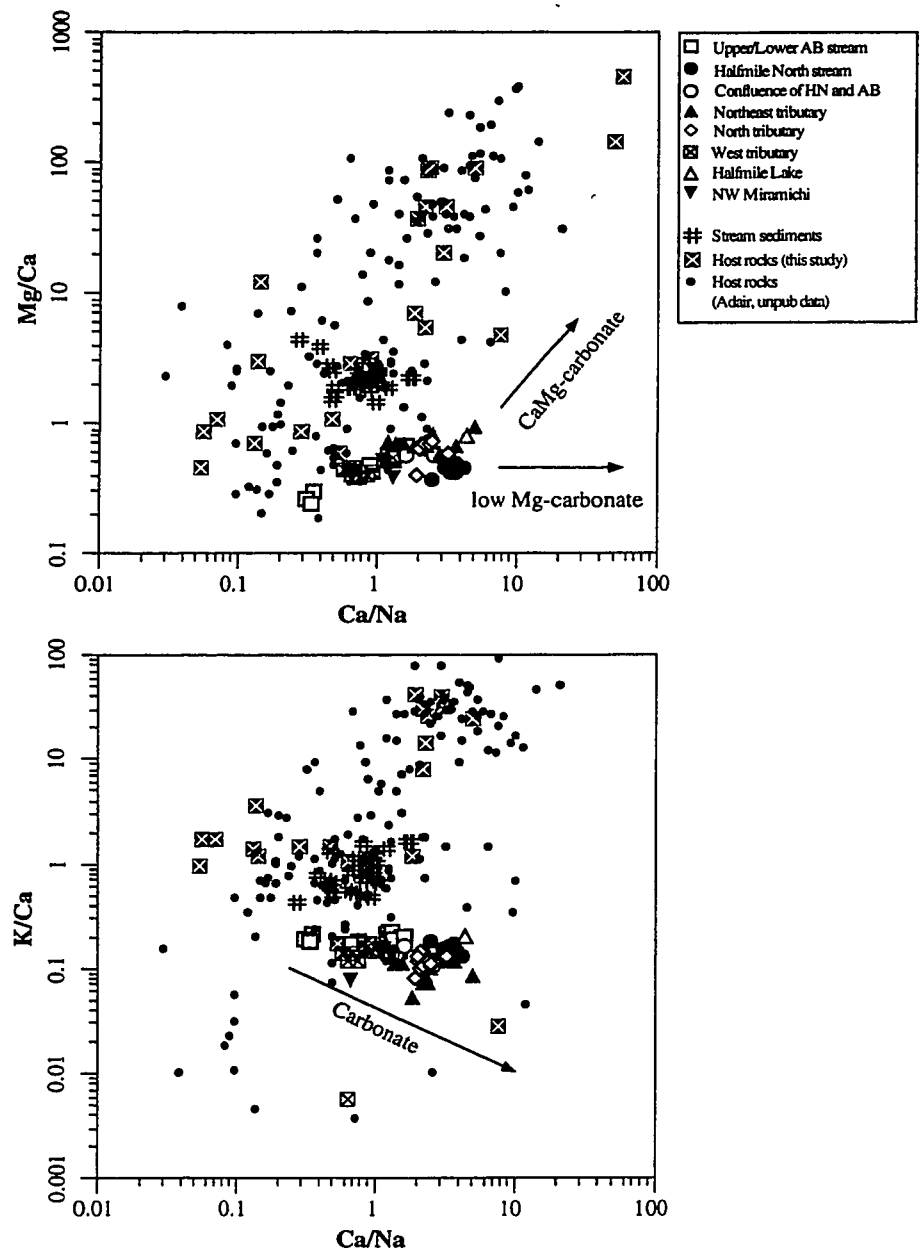


Fig. 5.28 Plots showing the major cation ratios of Halfmile Lake deposit surface waters compared to those of the host rocks (Chapter Two and Adair, unpublished data) and local stream sediments (Chapter Six). Halfmile Lake surface waters are enriched in Ca relative to other cations compared to host lithologies, with the notable exception of carbonate-rich host rocks.

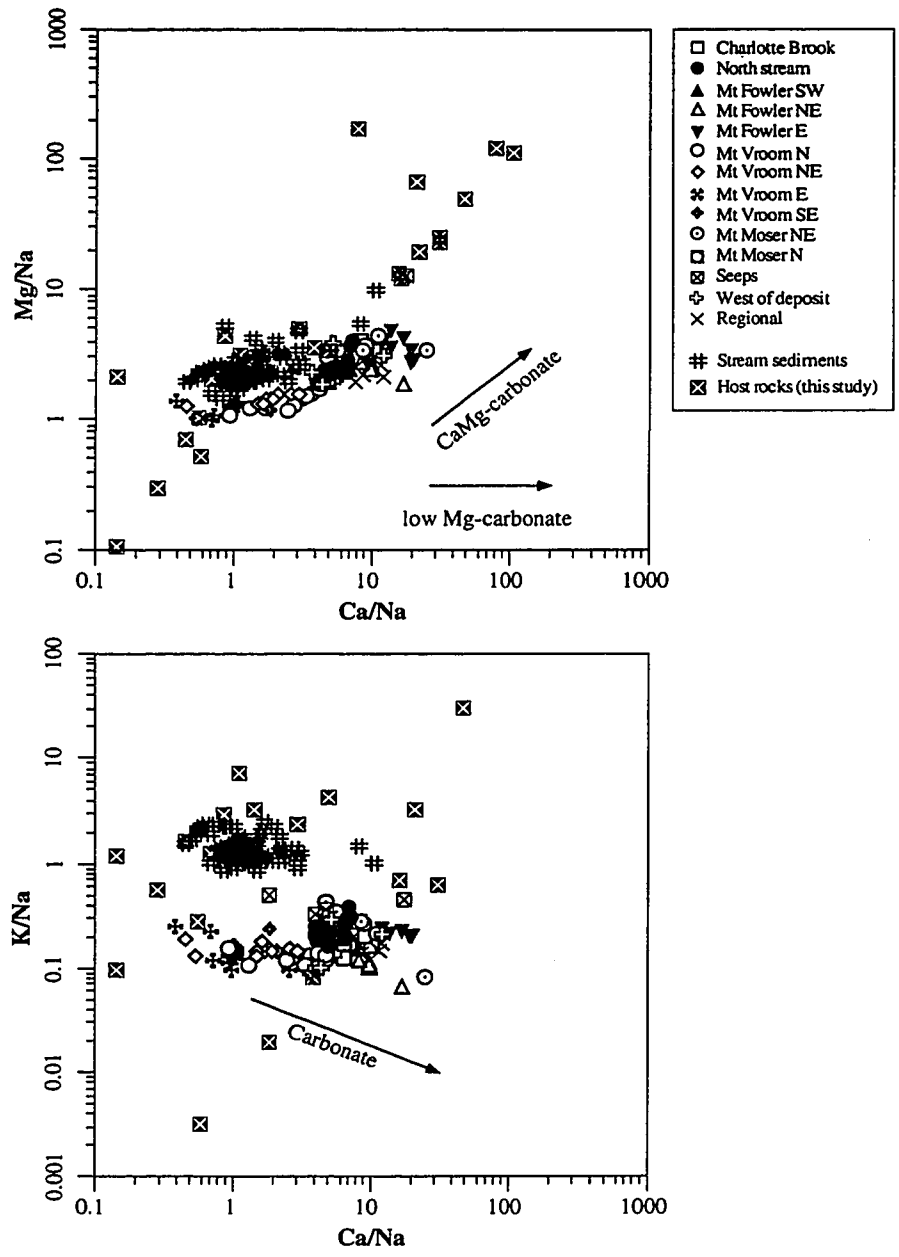


Fig. 5.29 Plots showing the major cation ratios of Restigouche deposit surface waters compared to those of the host rocks (Chapter Two) and local stream sediments (Chapter Six). Restigouche deposit surface waters are relatively enriched in Ca relative to other cations compared to host lithologies, with the notable exception of carbonate-rich host rocks.

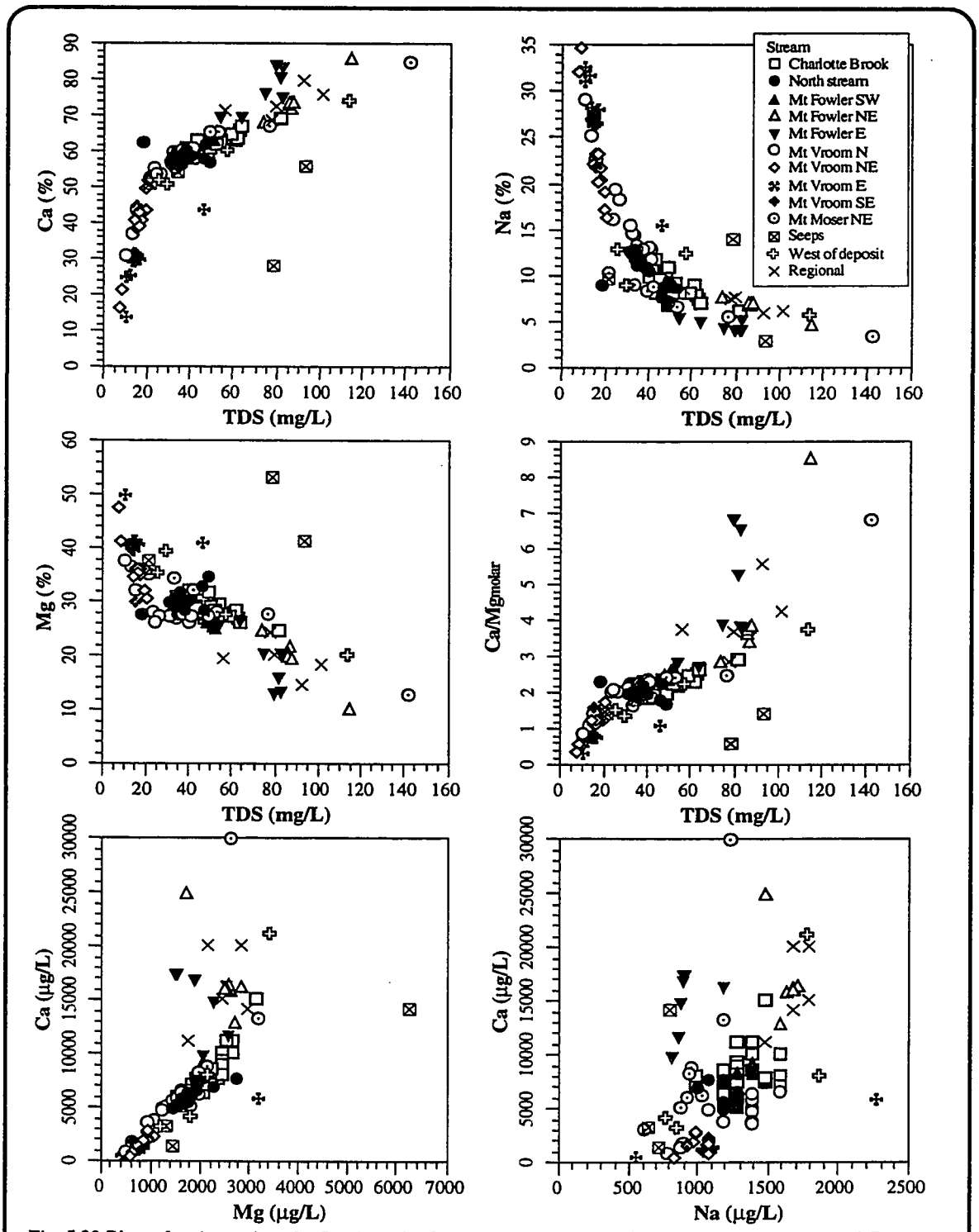


Fig. 5.30 Plots of major cations for Restigouche deposit surface waters, showing relative variation of Ca, Na, and Mg versus TDS. Note also the strong covariation between Ca and Mg for lower TDS waters. Elemental percent data in meq/L.

CHAPTER SIX:
GEOCHEMISTRY OF STREAM SEDIMENTS AT THE HALFMILE LAKE AND RESTIGOUCHE DEPOSITS, BATHURST MINING CAMP, NEW BRUNSWICK

6.1 Introduction

To help understand the relationship between waters and sediments, selected sites were also sampled for stream sediments (see Chapter Three for sampling methodology) and were analyzed for the major, trace and rare earth element geochemistry using ICP-ES and ICP-MS techniques. Studies of large drainage basins have utilized the suspended loads of large rivers in order to understand erosion and weathering processes, and to try to quantify river contributions of elements to the oceans (e.g. Asmerom and Jacobsen, 1993; Dupré et al., 1996; Gaillardet et al., 1995; Gaillardet et al., 1997). However, in the small catchments sampled in this study (Halfmile Lake and Restigouche deposits), suspended sediment loads were minor. Typically, very little suspended material was observed on filter papers after sampling. In this study the stream sediments were determined only for their bulk composition. It is recognized that the analyses therefore represent contributions from erosion (detrital contribution) and from weathering (hydromorphic contribution). A more detailed study involving sequential extraction to better understand element partitioning between the detrital, hydromorphic, and dissolved loads is in progress but is outside the scope of this thesis (Leybourne, Goodfellow and Boyle, unpublished data). The purposes of this chapter are to: 1) present the results of the geochemistry of stream sediments from the Halfmile Lake and Restigouche deposits, 2) examine the relationship between stream sediment composition and the composition of the "dissolved" load (Chapter Five), in order to better understand weathering processes within small catchment basins, and 3) compare the stream sediment compositions with those of the host lithologies to examine relative element partitioning.

This Chapter discusses the major and trace element geochemistry; the rare earth elements are

discussed in Chapter Ten. The full data set is given in Appendices A.2.1 and B.2.1. The application of stream sediment geochemistry in the exploration for massive sulphides in the Bathurst Mining Camp (BMC) is presented in Chapter Thirteen.

6.2 Stream Sediments at the Halfmile Lake Deposit

Stream sediments from the Halfmile Lake deposit were sieved and the < 125 μm and < 63 μm fractions were analyzed by ICP-ES and ICP-MS (Chapter Three). Comparison of the chemical results for the two size fractions shows that variations are generally less than 10% for the major elements. For the base metals there are significant differences whereas for the REE there is very little variation between the size fractions. The differences between the two size fractions varies depending on the element determined (Appendix A.2.4). For example, for the base metals, Cu is very preferentially enriched in the smaller size fraction compared to Pb and Zn. The difference in the Cu contents of the two size fractions ranges from 9 to 80% with a mean difference of 52%. Both Pb and Zn show much smaller inter-fraction variation (Pb = -2 to + 38%, mean = 14%; Zn = -20 to +7%, mean = -1.6). Lead is also preferentially partitioned into the finer size fraction whereas Zn is slightly partitioned into the coarser size fraction.

6.2.1 Major and trace element geochemistry

Stream sediments at the Halfmile Lake deposit show more restricted compositional ranges compared to those from the Restigouche deposit (Appendices A.2.2, B.2.2). Overall, there is minor variation in Fe_2O_3 at the Halfmile Lake deposit (2.68 to 7.70 wt%). The lowest Fe_2O_3 contents occur immediately downstream of the confluence of the Upper/Lower AB, Halfmile North and Northeast tributary streams (< 4. wt%; Fig. 6.1). In this section of the North tributary, Na_2O contents are lower (<1.2 wt%) and K_2O contents are higher (>1.4 wt%) than in the Halfmile North and Northeast tributary streams, but are more similar to values for stream sediments from the Upper/Lower AB stream. This suggests that the Upper/Lower AB stream has the greatest influence on the composition of stream sediments of the North tributary below

the confluence.

The Halfmile North stream has generally elevated phosphate (0.12 to 0.21 wt%), co-incident with elevated Y (31 to 74 ppm). Phosphate contents are also generally elevated in the Upper/Lower AB and West tributary streams (up to 0.40 wt%). The Halfmile North stream has the highest CaO contents (with the exception of the headwater samples; up to 1.75 wt%) and the highest MgO contents in the study area (up to 6.20 wt%; Fig. 6.1). The surface waters from this stream are also characterized by high dissolved Ca contents, but very low Mg (Chapter Five). Stream sediments from the Upper/Lower AB stream are characterized by generally low CaO and MgO contents (< 1.3 and 2.1 wt%, respectively) and moderately high K_2O (≥ 1.8 wt%; Fig. 6.1), which is consistent with the composition of the underlying felsic host rocks.

Barium and Rb abundances are highest in stream sediments from the Upper/Lower AB stream (up to 790 and 130 ppm, respectively) but are also elevated in the North tributary stream below the confluence of the Upper/Lower AB, Halfmile North, and Northeast tributary streams (Fig. 6.1). Uranium contents are also highest along the Upper/Lower AB and West tributary streams (up to 11 ppm; Fig. 6.1). Strontium contents are very low in the Northeast tributary stream (< 50 ppm) and increase somewhat in the North tributary due to addition from the Upper/Lower AB and Halfmile North streams. In the latter stream, Sr increases in abundance downstream (41 - 82 ppm).

Sulphide-related metals are discussed fully in Chapter Thirteen but have generally low contents in stream sediments at the Halfmile Lake deposit (up to 730 ppm Zn, 100 ppm Pb, 2.6 ppm Cd and 3.6 ppm Mo) compared to the Restigouche deposit, with the exception of Cu (up to 1000 ppm). Zinc, Cd, Cu, and Mo are generally anomalous in streams closest to known mineralization (see Chapter Thirteen; Fig. 13.4).

6.2.2 Comparison to host lithologies

Most stream sediments show generally restricted ranges in elemental abundance compared

to average unaltered host felsic volcanic rocks (Fig. 6.2). One sample from the Upper/Lower AB stream is compositionally distinct from the other stream sediments, especially for the REE. This sample represents a seep and the differences in the REE compared to the other stream sediments is due to a change in the redox conditions as the seep exits the subsurface environment (e.g. positive Ce anomalies due to the rapid oxidation of Ce^{3+} to Ce^{4+}; see Chapter Ten). Stream sediments show major differences for some elements compared to the composition of the host rocks. There is a general increase in element abundance from left to right on host lithology-normalized diagrams (Fig. 6.2). Incompatible elements on the left side of the plots are generally relatively depleted compared to the host rocks, whereas, more compatible elements (right side) show a general enrichment in the stream sediments compared to the host rocks. Within this overall trend, there are important relative elemental fractionations. Rubidium, K, Ba and Cs (and for some samples, U) are typically depleted whereas, Na, Ca and Sr are generally enriched in the stream sediments (Fig. 6.2). Metals typically associated with BMC ore deposits (Pb, Zn) are moderately enriched in the stream sediments. Elements which are generally considered to be immobile during weathering fall closest to the composition of the average host rock (e.g. REE, Hf, Zr, Nb). Iron shows some variation but typically falls close to average host rock.

6.3 Stream Sediments at the Restigouche Deposit

Stream sediments from the Restigouche deposit are more variable than those from the Halfmile Lake deposit. At the Restigouche deposit, several streams are characterized by Fe-oxyhydroxide precipitation whereas Fe-oxyhydroxides were not observed in streams draining the Halfmile Lake deposit. Along the Mt Fowler east stream, orange Fe-oxyhydroxides were observed to increase in abundance upstream. At the sites where samples MLW96-664 and MLW96-665 were collected (see Fig. 5.12 for locations), the Fe-oxyhydroxides are the most extensive yet several meters further upstream, the stream bed was essentially free of Fe-oxyhydroxides. Seeps in the stream bed are delivering Fe-rich waters which are rapidly

precipitating Fe-oxyhydroxide minerals upon entering the surface environment. On the Mt Vroom east stream, Fe-rich sediments were observed as ferricrete ledges and Fe-cemented stream sediments and here the Fe-oxides are darker in colour and considerably more indurated. Mt Vroom north stream flows past the gossan outcrop of the main Restigouche deposit before it joins Charlotte Brook. At the site where sample MLW95-302 was collected, ferricrete was observed at the base of the gossan pile at and below the stream surface. Stream sediments with gossan material were observed in the North stream northeast of the main Restigouche ore body.

6.3.1 Major and trace element geochemistry

In general, stream sediments from Charlotte Brook have higher Si, Ti, Ca, Mg, Na and K contents immediately downstream from the deposit compared to sediments upstream from the deposit (Fig. 6.3). Iron contents are only moderately variable along Charlotte Brook but trend to higher contents upstream from the deposit compared to the section immediately downstream from the deposit (Fig. 6.3). The lower reaches of Charlotte Brook have the lowest Fe contents along this stream. Sulphide-related trace elements (Zn, Cd, Pb, Cu, Ag, Bi, In) display distinct anomalies over the Restigouche deposit in Charlotte Brook, with background contents upstream from the deposit and metal contents decrease with increasing distance from the deposit (see Chapter Thirteen). In contrast, other trace elements show no obvious relationship to proximity to the Restigouche deposit (Fig. 6.3).

For the three streams draining Mt Vroom (north, northeast and east streams), there is greater similarity in surface water composition than there is in stream sediment composition, probably in part as a function of the high Fe contents of the Mt Vroom east stream. Although all three streams drain the older Miramichi Group metasedimentary rocks, differences in major and trace elements between these three streams reflect differences in abundance of Fe-oxyhydroxide minerals.

Both the Mt Fowler northeast and Mt Fowler east streams drain Eighteen Mile Formation

metasediments but they differ in stream sediment composition. The northeast stream has higher Si, Al, Mg, Na, and K and generally lower Fe, Mn, and P (Fig. 6.3). The Mt Fowler east stream has high Mo (up to 150 ppm) and Zn (up to 1600 ppm) in the Fe-rich stream sediments. In contrast, Fe-rich stream sediments from Mt Vroom east stream have low Mo (< 9 ppm), suggesting that the style of mineralization is different, consistent with different bedrock lithologies (see Chapter Thirteen).

6.3.2 Comparison to host lithologies

Stream sediments are normalized to average unaltered felsic host lithologies from the Restigouche deposit (Fig. 6.4). Although stream sediments from the Restigouche deposit differ compositionally in many respects to those from the Halfmile Lake deposit there are several similarities compared to local host lithologies. There is a general increase in normalized elemental abundance from left to right on lithology-normalized diagrams (Fig. 6.4). In addition, Rb, Th, and Ba are typically moderately to strongly depleted compared to the host lithologies. Unlike the Halfmile Lake deposit, Cs and U are commonly strongly fractionated from Rb and partitioned strongly into the stream sediment phase. Restigouche deposit stream sediments have much higher average values for Cs (8.3 versus 2.3 ppm) and U (10.6 versus 4.3 ppm) than Halfmile Lake deposit stream sediments (Appendices A.2.2, B.2.2). REE, Hf, Zr, Nb and Sc generally display the least deviation from average rock values. Stream sediments that have very elevated Fe contents (especially sediments from Mt Fowler east and Mt Vroom east streams) have depleted patterns due to dilution by Fe-oxyhydroxides with the exception of elements which tend to adsorb strongly to Fe-oxide surfaces. For example, the Fe-rich sediments from Mt Fowler east stream have very strong positive anomalies for U and Pb, Ba, and Sr compared to other elements in these sediments. Stream sediments from Charlotte Brook downstream of the main Restigouche deposit show very strong positive anomalies for Pb and Zn. Strontium, Fe and Eu typically show moderate positive peaks indicating a relative partitioning of these elements into the sediment phase. Calcium and Na typically show little

relative deviation from average rock values.

6.4 Discussion

6.4.1 Element fractionation

Strontium, Ca and Na are slightly to moderately enriched in the stream sediment phase, suggesting greater mobilization. Strontium is typically more enriched in the stream sediment phase relative to the host rocks than Ca, but Ca is more strongly partitioned into the aqueous phase than Sr (Fig. 6.5). This is consistent with the interpretation that Ca in surface waters and shallow groundwaters is derived primarily from carbonate dissolution at both the Halfmile Lake and Restigouche deposits. Strontium is present in both carbonate and silicate minerals such that it is less readily transferred from the host rocks to the aqueous phase and, therefore, relatively more Sr is fixed in detrital silicate phases in the stream sediments than is the case for Ca. This interpretation is supported by the Sr isotopic compositions of waters and coexisting sediments (Allègre et al., 1996). Sample MLS96-664 from Mt Fowler east stream at the Restigouche deposit and its corresponding water sample (MLW96-664) were analyzed for Sr isotopes. The stream sediment is more radiogenic than the water sample, consistent with a greater contribution of Sr from low Rb/Sr carbonate for the waters and a greater contribution of Sr from high Rb/Sr silicate rocks for the stream sediment (see Chapter Twelve).

For K, Rb and Ba there is significant fractionation between the host rocks, stream sediments and surface waters. These elements are lower in the stream sediments relative to the host rocks (Figs. 6.2, 6.4). Compared to the surface waters, these elements show relative preference for the stream sediment phase in the order Rb $\geq$ Ba $\gg$ K (Fig. 6.5). The most likely explanation is that these elements reside in detrital minerals (K-silicates) eroded from the underlying host rocks.

Iron shows little fractionation between the host rocks and the stream sediments (Fig. 6.2) in stream sediments draining the Halfmile Lake deposit. In contrast, Fe contents of Restigouche stream sediments are much more variable and relatively elevated compared to the host rocks.

The difference in the behaviour of is related to the depth and geometry of the respective sulphide deposits and, therefore, the proximity of massive sulphide deposits to oxidizing shallow groundwaters. At the Restigouche deposit, the main ore body is close to surface and both surface water and shallow groundwater compositions indicate that the deposit is undergoing active oxidation. As a result, stream sediments in Charlotte Brook downstream from the deposit are moderately enriched in Fe compared to the host rocks and are strongly enriched in Zn, Pb and Ag (Fig. 6.4). Similarly, stream sediments from Mt Fowler east and Mt Vroom east streams contain high contents of Fe suggesting strong oxidation of sulphide minerals in the subsurface.

Figure 6.5 shows the relative elemental fractionations between surface waters and corresponding stream sediments. It should be emphasized that on plots where the surface waters are normalized to the corresponding stream sediment, that normalized values are a factor of three too large. Surface water data is in μg/L and stream sediment data in ppm. Thus, discussion of fractionation between the surface waters and stream sediments are referred to in a relative sense. Of all elements for which there is data for both stream sediments and corresponding surface waters, Cl is the most readily partitioned into the fluid phase. Chloride contents of stream sediments were analyzed for stream sediments for which there was sufficient material, primarily at the Restigouche deposit, and contents range from 181 to 1171 ppm. These values are generally higher than those measured ine host lithologies, suggesting that Cl is partitioned into the stream sediment phase (as detrital Cl-bearing sheet silicates) and ultimately into the fluid phase (Fig. 6.5). Calcium, Mg, Na and Sr are all very strongly partitioned into the fluid phase relative to other elements whereas, K, Rb, and Ba are moderately fractionated into the sediment phase, primarily as K-silicate minerals. For most water-sediment pairs, the base metals have a very strong affinity for the sediments phase although Zn shows greater affinity for the aqueous phase compared to Pb, which is consistent with the general immobility of Pb compared to Zn in most natural waters. Given that most of the surface waters have generally neutral pH values (Chapter Five), Al, Fe, and Mn are

generally only sparingly soluble and are strongly partitioned into the sediment phase as secondary oxides, and in primary and secondary silicates for Al (illite, kaolinite, chlorite and sericite).

For Halfmile Lake deposit stream sediments, elements which are relatively partitioned strongly into the aqueous phase are strongly positively correlated (e.g., Ca, C, S, Sr). These elements are negatively correlated with Si and related detrital elements such as Zr, Hf, Nb etc. Uranium and Mo are strongly correlated for Halfmile Lake deposit sediments, suggesting a common source, most likely the felsic volcanic rocks.

Magnesium is strongly correlated with Al, Fe, V, Sc in Halfmile Lake deposit stream sediments. The primary Mg mineral in the host lithologies for Mg, other than dolomite, is chlorite. The lack of correlation between Mg and Ca for the sediments indicates that chlorite is an important phase for Halfmile Lake stream sediments. Although strong correlations are indicated for Mg between Cr and Ni, this is primarily due to outliers and only sediments from the Halfmile North stream actually show a strong correlation between these elements. There is also a strong positive correlation between Mg and Zn for Halfmile Lake deposit stream sediments ($r^2 = 0.524$), especially for the Halfmile North stream. This may be a function of Zn substitution into chlorite or to the greater proximity to surface of the main part of the Halfmile Lake North ore body compared to the Halfmile Lake South orebody (see Chapter Three). In the latter case, the Zn contents of the stream sediments would be produced by adsorption onto mineral surfaces and high Mg from chlorite associated with hydrothermal alteration of the host rocks during mineralization. It was noted in Chapter Five that surface waters from this stream have the highest Zn contents at the Halfmile Lake deposit, whereas dissolved Mg contents are low, suggesting that breakdown of Zn-bearing Mg-silicates or carbonates is not producing higher Zn in the surface waters. For Halfmile Lake stream sediments and surface waters as a whole, dissolved Zn is highly correlated with stream sediment Zn and Mg (Table 6.1).

There are some significant correlations between coexisting stream sediments and waters (Table 6.1). For example, there is a high positive correlation ($r^2 > 0.477$) between elements in

waters and sediments which are likely to be associated with sheet silicates such as illite (e.g., Si, K, Ba and Rb) or are known to form or be strongly adsorbed to colloids (e.g., Y, Fe, U), there are strong positive correlations between the dissolved phase and stream sediments (Table 6.1). In contrast, elements which are strongly partitioned (in a relative sense) into the aqueous phase (carbonate and albite weathering; Chapter Five) compared to the stream sediment phase (Ca, Sr, Na) show very poor correlations ($r^2 < 0.142$) between water and sediment. This suggests that although the surface waters are very low in suspended sediment, some of the K, Al and Fe is present as fine colloids that passed through the 0.45 μm filters and is consistent with Fe-oxide and K-silicate saturation index calculations for surface waters (see Chapter Five).

Stream sediments from streams draining the Restigouche deposit show strong correlation between P_2O_5 and Y, especially for the North stream. There is no correlation between dissolved PO_4 and Y (or REE) for the surface waters, due to the very low solubility of Y under these conditions. It is possible that PO_4 and Y contents of the surface waters are controlled by phosphate minerals in the stream sediments (e.g., apatite). Detrital REE phosphates were observed on filter papers from groundwater sampling (Chapter Nine) and hydrothermal monazite was observed in fracture zone material (Chapter Four).

It was noted previously that Ni, Mo, Co and U were positively correlated with Fe and Mn. This suggests that these elements are probably adsorbed to Fe- and Mn-oxide surfaces during precipitation of these phases in the stream environment. This element association reflects older metasediments southeast of the Restigouche deposit and younger Eighteen Mile formations rocks northeast of the deposit which are distinct from rocks hosting the Restigouche deposit. It is possible, therefore, that groundwaters are oxidizing sulphide mineralization in the subsurface, and that the mineralization is more Ni, Co, and Mo-rich than is the case for the main Restigouche deposit (see Chapter Thirteen for further discussion).

6.4.2 Relationship to bedrock geology

Stream sediments (and suspended sediments; Chapter Nine) represent a mixture of detrital (physical and mechanical erosion) and hydromorphic (chemical weathering). That stream sediments do not merely represent the underlying lithologies is readily demonstrated by the spatial maps of element abundance for both the Halfmile Lake and Restigouche deposits (Figs. 6.2, 6.3).

Dupré et al. (1996) investigated the suspended sediment loads of rivers draining the Congo Basin by comparing the suspended sediment compositions to average upper continental crust (UCC). They noted strong depletions in the suspended sediments relative to UCC for Sr, Na, K and lesser depletions for Ca and Rb. The stream sediments from the Halfmile Lake and Restigouche deposits show similarly strong depletions in these elements normalized to UCC (Fig. 6.6). However, normalized to more local lithologies, the magnitude of these elemental depletions is more subdued (Figs. 6.2, 6.4). This is an important observation because it suggests that studies that try to quantify riverine contributions to the oceans and estimates of global erosion by normalizing to a universal standard may be overestimating or underestimating the contributions. Universal normalization standards such as UCC or N-type MORB are useful in petrogenetic studies for comparative purposes with other studies, but may produce erroneous results when used for modelling purposes. For example, compared to UCC, the Halfmile Lake deposit stream sediments are depleted in Nb and Ta, which would lead to the erroneous assumption that these elements were either fractionated into the fluid phase or were preferentially retained in the bedrock. However, normalized to average local unaltered felsic rocks, these stream sediments display no Nb or Ta anomalies. Using UCC-normalization techniques, Dupré et al (1996) suggested Congo Basin river waters and suspended sediments were depleted in Hf. However, this is most likely an artifact of normalizing to a value (in this case UCC) that did not represent Congo Basin lithologies. Alkali and alkaline-earth elements (i.e., Sr, Na, K, Ba, Cs, Ca and Rb) are variably depleted in both Halfmile Lake and Restigouche deposit stream sediments relative to upper continental crust; however, the magnitude of the depletion is less where values are normalized to local lithologies. For the

purposes of discussion of relative fractionation of elements between different reservoirs in this study, average unaltered felsic rocks from the two study areas are used (Figs. 6.2, 6.4).

6.5 Summary

1) Elements in stream sediments are fractionated relative to unaltered host lithologies in a manner consistent with the relative mobility of elements during weathering. Although stream sediments were only determined for their bulk composition, hydromorphic effects can also be discerned if the hydromorphic component is significant. The stream sediment data therefore acts as a proxy for suspended sediments for small catchment streams at the Halfmile Lake and Restigouche deposits.

2) Many previous studies have normalized suspended sediment loads of rivers to average upper continental crust. Data presented here, however, indicates that stream sediment compositions should be normalized to local host lithologies. Halfmile Lake and Restigouche deposit stream sediments normalized to average upper continental crust show large depletions of Na, Sr and Ca which are much smaller where normalized to host lithologies. Apparent depletions of very immobile elements (e.g., Nb) disappear where normalized to local host rocks. This suggests that studies which that use the normalization to a universal standard such as upper continental crust to make inferences regarding riverine contributions to the oceans and rates of crustal erosion may be erroneous.

3) Comparison of the host rock, stream sediment, and surface water data reveals that different elements are fractionated in a relative sense into these different phases. Rubidium, Ba, and Cs tend to remain in the host rock, probably in secondary mineral phases whereas Sr, Ca and Na are fractionated into the stream sediment phase relative to the host rock phase, and Ca is relatively fractionated into the aqueous phase compared to Sr and Na. Iron shows little fractionation between host rocks and stream sediments at the Halfmile Lake deposit, but at the Restigouche deposit, Fe is variably enriched in stream sediments compared to host rocks due to the contribution of oxidized sulphides in the near-surface environment.

Table 6.1 Pearson product moment correlation between stream sediments and surface waters from the Halfmile Lake deposit

	Si	Ti	Al	Mg	Ca	Na	K	P	S	LFe	LMn	LBa	LCd	LCo	LCu	LNi	LPb	LRb	LSr	LU	LZn	LV	LY
WSi	0.467	-0.074	-0.230	-0.553	-0.242	-0.333	0.295	-0.055	-0.428	-0.122	0.203	0.437	-0.290	-0.293	-0.328	-0.110	-0.075	0.442	-0.471	0.063	-0.799	-0.447	-0.556
WTi	0.351	0.023	-0.150	-0.206	0.158	0.092	-0.099	-0.302	-0.056	-0.096	-0.120	-0.165	-0.310	-0.708	-0.521	-0.422	-0.219	-0.172	-0.296	-0.199	-0.565	0.022	-0.201
WAl	0.597	0.420	0.154	-0.239	-0.087	0.180	0.102	-0.178	-0.463	0.056	0.144	0.130	-0.562	-0.329	-0.534	-0.419	-0.380	0.052	-0.361	-0.144	-0.571	0.096	-0.269
WMg	0.581	0.122	-0.245	-0.357	-0.185	-0.034	0.023	-0.361	-0.236	-0.171	-0.063	0.082	-0.427	-0.487	-0.461	-0.454	-0.291	0.012	-0.594	-0.364	-0.733	-0.086	-0.556
WCa	0.122	0.350	0.036	0.456	0.142	0.576	-0.453	-0.516	0.243	0.106	-0.409	-0.656	-0.077	-0.261	-0.052	-0.469	-0.371	-0.695	-0.110	-0.675	0.237	0.690	0.094
WNa	0.542	0.110	-0.149	-0.307	-0.183	0.003	0.096	-0.347	-0.317	-0.072	-0.054	0.102	-0.455	-0.511	-0.386	-0.411	-0.320	0.043	-0.543	-0.284	-0.710	-0.041	-0.438
WK	-0.206	-0.196	0.059	-0.272	0.000	-0.447	0.477	0.651	-0.484	0.320	0.522	0.640	0.158	0.148	-0.151	0.160	-0.006	0.699	0.187	0.763	-0.171	-0.351	0.125
WP	-0.669	-0.696	-0.602	-0.443	0.371	-0.599	0.001	0.770	0.317	0.118	0.690	0.542	0.597	0.426	0.124	0.232	0.082	0.669	0.359	0.777	-0.086	-0.551	-0.250
WS	-0.146	-0.047	-0.498	0.020	0.217	-0.066	-0.402	0.029	0.343	-0.128	-0.049	-0.204	0.276	0.026	-0.197	-0.446	-0.146	-0.256	-0.017	-0.299	0.148	0.175	-0.106
WLFe	-0.383	0.177	-0.079	0.468	0.744	0.527	-0.585	0.225	0.073	0.538	0.460	-0.344	0.237	0.061	-0.022	-0.220	-0.326	-0.277	0.494	-0.098	0.329	0.513	-0.049
WLMn	0.579	-0.005	-0.069	-0.409	-0.314	-0.110	0.140	-0.325	-0.073	-0.383	-0.140	0.277	-0.521	-0.301	-0.440	-0.489	-0.033	0.095	-0.421	-0.044	-0.745	-0.162	-0.326
WLBa	0.293	-0.107	0.033	-0.471	-0.277	-0.390	0.543	0.202	-0.583	0.088	0.275	0.670	-0.308	-0.256	-0.385	-0.104	-0.104	0.615	-0.294	0.510	-0.703	-0.447	-0.183
WLCd	-0.462	0.082	0.307	0.280	0.060	-0.025	0.105	0.436	-0.121	0.252	0.396	0.097	0.345	0.627	0.414	0.579	0.050	0.295	0.585	0.418	0.559	0.070	0.346
WLCo	0.084	-0.302	-0.515	-0.383	0.234	-0.412	-0.321	-0.154	0.775	-0.708	0.028	-0.105	0.071	-0.029	-0.501	-0.263	0.295	-0.018	-0.068	-0.126	-0.193	-0.422	-0.359
WLCu	0.229	0.383	0.107	0.005	0.278	0.342	-0.119	-0.020	-0.347	0.148	0.008	-0.247	0.079	0.148	0.087	-0.274	-0.262	-0.236	0.318	-0.186	0.215	0.375	0.092
WLNi	-0.042	-0.143	-0.205	-0.221	0.046	-0.344	0.042	0.161	-0.171	-0.272	0.179	-0.145	0.350	0.394	0.356	0.461	0.227	0.390	0.189	0.147	0.002	-0.302	-0.040
WLPb	0.243	0.294	0.155	-0.030	0.220	0.269	0.055	-0.149	-0.372	0.209	0.051	-0.154	-0.135	-0.062	0.073	-0.376	-0.317	-0.126	0.125	-0.176	0.096	0.279	0.082
WLRb	-0.123	-0.027	0.328	-0.143	0.021	-0.209	0.429	0.472	-0.314	0.192	0.280	0.441	-0.087	0.104	-0.162	0.119	0.111	0.536	0.349	0.795	-0.038	-0.235	0.458
WLSr	0.001	0.289	-0.066	0.431	0.238	0.509	-0.513	-0.375	0.296	0.122	-0.336	-0.625	0.032	-0.191	-0.065	-0.521	-0.352	-0.655	-0.040	-0.601	0.298	0.656	0.115
WLU	-0.188	0.083	0.693	0.193	-0.273	0.030	0.702	0.367	-0.831	0.710	0.260	0.694	-0.223	0.031	0.170	0.361	-0.224	0.573	0.236	0.796	0.011	-0.002	0.513
WLZn	-0.591	0.007	0.009	0.439	0.290	0.096	-0.258	0.356	0.187	0.365	0.257	-0.253	0.542	0.560	0.467	0.238	-0.039	-0.206	0.531	0.019	0.822	0.373	0.304
WLV	0.513	0.375	-0.217	0.135	0.106	0.528	-0.524	-0.661	0.456	-0.289	-0.595	-0.675	-0.153	-0.506	-0.378	-0.583	-0.207	-0.710	-0.389	-0.816	-0.135	0.483	-0.320
WLY	0.012	0.617	0.897	0.639	-0.345	0.572	0.391	0.033	-0.716	0.617	-0.057	0.166	-0.388	0.016	0.269	0.442	-0.357	-0.035	0.217	0.335	0.296	0.568	0.633

Sediment data in ppm, water data in µg/L
L = log; W = water

Table 6.2 Pearson Product Moment correlation between stream sediment and surface waters for samples from the Restigouche deposit

	Si	Ti	Al	Mg	Ca	Na	K	C	P	S	Cl	LFe	LMn	LBa	LCd	LCo	LCu	LNi	LPb	LRb	LSr	LU	LV	LY	LZn
WSi	-0.071	-0.037	-0.137	-0.016	0.115	0.026	-0.118	0.006	0.089	-0.090	-0.253	0.082	-0.191	-0.067	0.123	-0.322	-0.405	-0.054	0.023	-0.137	0.029	0.363	-0.022	0.010	0.141
WTi	-0.284	-0.154	0.153	-0.418	-0.268	-0.241	0.004	0.151	0.283	0.075	-0.019	0.014	-0.011	0.022	-0.143	-0.173	-0.098	0.000	-0.090	-0.073	-0.143	0.004	0.267	-0.280	-0.006
WAl	-0.166	-0.203	-0.168	-0.091	-0.246	-0.176	-0.214	0.012	-0.263	0.077	0.286	0.189	0.077	-0.202	-0.188	0.378	-0.011	-0.086	-0.150	-0.147	-0.437	-0.316	-0.307	-0.176	-0.352
WMg	0.057	0.211	0.068	0.047	0.269	0.204	0.072	-0.150	0.196	-0.089	-0.329	-0.070	-0.261	0.144	-0.017	-0.575	-0.413	-0.020	0.109	0.007	0.296	0.507	0.319	0.076	0.221
WCa	0.028	0.262	0.023	0.103	0.550	0.210	0.008	-0.095	0.208	-0.074	-0.248	-0.135	-0.171	0.307	0.121	-0.530	-0.204	0.186	0.031	-0.079	0.464	0.677	0.304	0.042	0.236
WNa	0.252	0.288	0.240	0.118	0.069	0.325	0.225	-0.361	0.016	0.009	-0.429	-0.159	-0.423	-0.234	-0.212	-0.472	-0.386	-0.472	0.304	0.295	0.198	0.009	0.283	0.083	0.034
WK	0.191	0.099	0.147	0.129	0.244	0.291	0.205	-0.298	0.570	-0.078	-0.291	-0.078	-0.241	0.368	-0.021	-0.514	-0.214	-0.171	0.167	0.327	0.272	0.545	0.197	0.642	0.392
WC	0.163	0.380	0.175	0.165	0.539	0.333	0.122	-0.206	0.251	-0.095	-0.277	-0.270	-0.224	0.294	0.040	-0.614	-0.221	0.085	0.109	0.045	0.568	0.600	0.443	0.118	0.242
WP	0.247	0.320	0.362	-0.019	0.129	0.306	0.418	-0.268	0.091	-0.111	-0.030	-0.221	-0.287	0.387	-0.257	-0.373	-0.147	-0.098	-0.060	0.298	0.277	-0.010	0.367	0.125	-0.037
WS	-0.479	-0.305	-0.461	-0.301	-0.052	-0.391	-0.303	0.350	-0.213	-0.011	-0.016	0.527	0.085	-0.004	0.323	0.106	-0.186	0.304	-0.292	-0.430	-0.336	0.345	-0.365	-0.321	-0.013
WCl	0.132	0.251	0.004	0.137	0.382	0.293	0.012	-0.183	0.046	-0.113	-0.211	-0.132	-0.123	0.142	0.116	-0.388	-0.239	-0.158	0.455	-0.005	0.236	0.407	0.182	0.055	0.356
LWFe	-0.469	-0.540	-0.397	-0.471	-0.320	-0.462	-0.406	0.215	-0.059	0.513	-0.206	0.430	0.165	-0.392	0.302	0.087	-0.258	0.083	-0.032	-0.439	-0.577	0.237	-0.444	-0.368	0.022
LWMn	-0.509	-0.410	-0.410	-0.392	-0.329	-0.489	-0.386	0.268	-0.276	-0.068	-0.173	0.513	0.249	-0.244	-0.020	0.108	-0.383	0.114	-0.048	-0.379	-0.488	0.209	-0.260	-0.440	-0.055
LWBa	0.093	0.190	0.171	0.075	0.443	0.268	0.102	-0.155	0.518	-0.118	-0.093	-0.184	-0.130	0.503	0.096	-0.598	-0.132	0.055	0.034	0.098	0.432	0.649	0.329	0.417	0.378
LWCd	0.286	0.309	0.228	0.410	0.059	0.262	-0.008	-0.006	0.223	-0.119	-0.383	-0.329	-0.099	0.079	0.221	-0.247	0.195	-0.163	0.154	0.068	0.185	-0.095	0.074	0.216	0.300
LWCo	-0.703	-0.531	-0.610	-0.354	-0.287	-0.610	-0.549	0.389	-0.372	-0.038	-0.161	0.682	0.319	-0.067	0.196	0.384	-0.193	0.240	-0.235	-0.527	-0.757	0.192	-0.575	-0.595	-0.086
LWCu	0.168	0.067	0.026	-0.096	-0.048	0.094	0.201	-0.104	-0.243	-0.287	-0.418	0.022	-0.159	-0.020	-0.101	-0.116	-0.211	-0.232	0.115	0.322	-0.178	-0.114	-0.008	-0.078	0.055
LWNi	-0.616	-0.588	-0.648	-0.290	-0.302	-0.622	-0.580	0.441	-0.231	0.369	0.211	0.656	0.332	-0.220	0.151	0.660	-0.044	0.310	-0.483	-0.578	-0.685	0.057	-0.686	-0.371	-0.309
LWPb	0.054	0.055	-0.023	0.013	0.118	0.029	0.037	-0.238	-0.009	0.202	-0.361	-0.039	-0.130	-0.052	0.195	-0.373	-0.018	-0.396	0.377	0.175	0.023	0.086	0.000	-0.033	0.282
LWRb	-0.257	-0.380	-0.373	-0.190	-0.114	-0.196	-0.156	0.239	0.234	-0.040	-0.082	0.458	0.061	0.261	0.177	0.157	-0.194	0.201	-0.175	-0.174	-0.336	0.398	-0.479	0.336	0.279
LWSr	0.180	0.329	0.072	0.223	0.556	0.325	0.085	-0.191	0.291	0.001	-0.284	-0.227	-0.321	0.269	0.094	-0.567	-0.216	0.085	0.071	-0.013	0.556	0.568	0.321	0.114	0.209
LWU	-0.331	-0.164	-0.380	-0.136	0.392	-0.113	-0.195	0.096	0.028	-0.102	-0.440	0.310	0.018	0.311	0.251	-0.232	-0.218	0.310	-0.038	-0.257	-0.058	0.768	-0.160	-0.158	0.254
LWV	-0.353	-0.542	-0.285	-0.375	-0.148	-0.264	-0.265	0.263	-0.019	0.343	-0.033	0.135	-0.103	-0.524	-0.076	-0.094	-0.043	-0.224	0.367	-0.238	-0.343	-0.182	-0.175	-0.228	0.163
LWY	-0.102	-0.293	0.017	-0.133	-0.379	-0.129	-0.117	0.005	0.046	0.198	0.318	0.097	-0.048	-0.241	-0.138	0.069	-0.034	-0.430	0.127	-0.060	-0.337	-0.379	-0.333	0.284	0.026
LWZn	-0.094	-0.278	-0.170	-0.073	0.091	-0.091	-0.047	0.023	0.193	0.116	-0.167	0.004	0.146	0.081	0.516	-0.203	0.244	-0.324	0.534	0.024	-0.217	0.080	-0.258	0.240	0.691

Note, sediment major element data converted to ppm
L = log, W = water

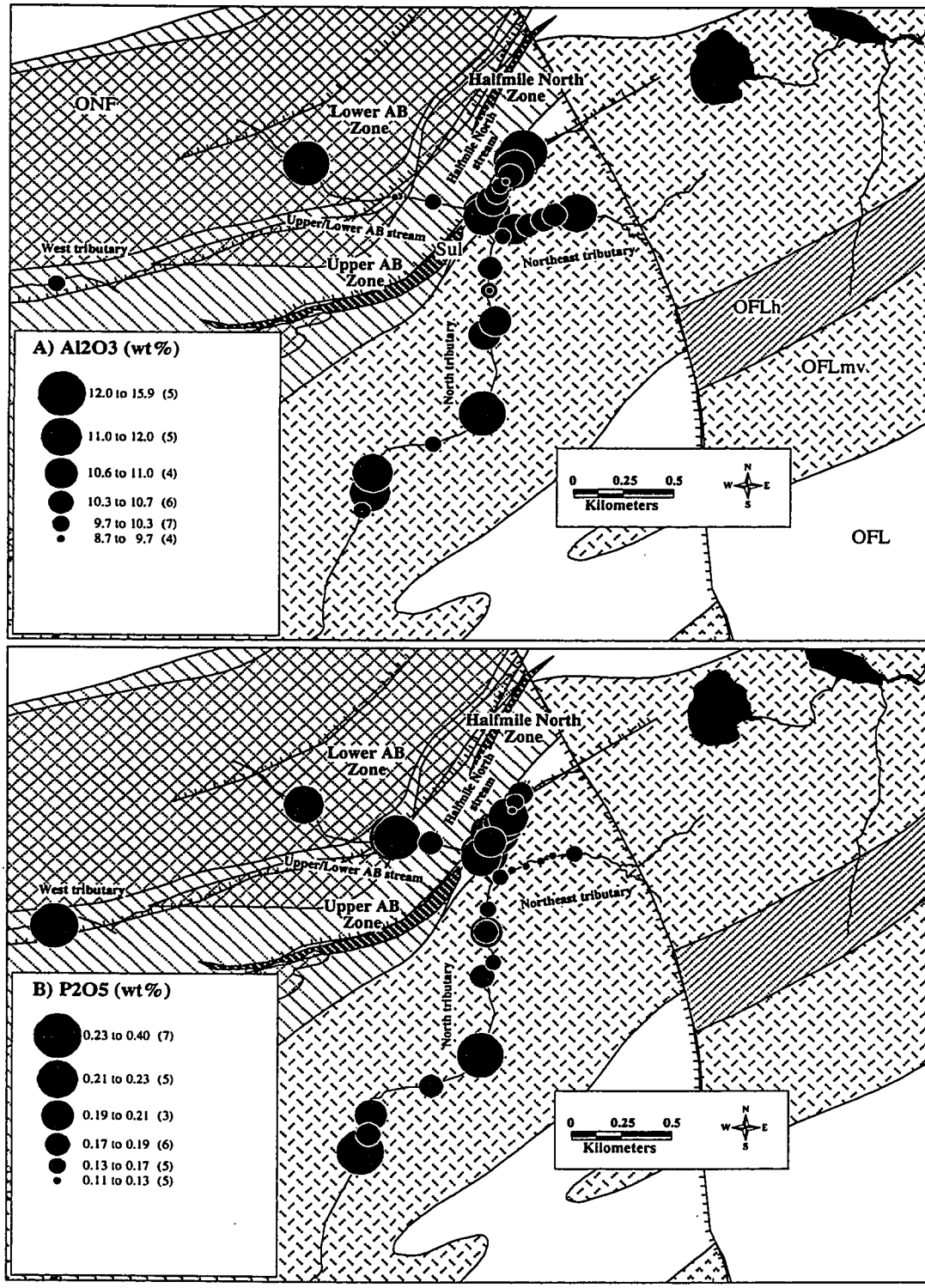


Fig. 6.1 Proportional circle maps of selected major and trace elements of stream sediments from the Halfmile Lake deposit. Geology as in Chapter Two.

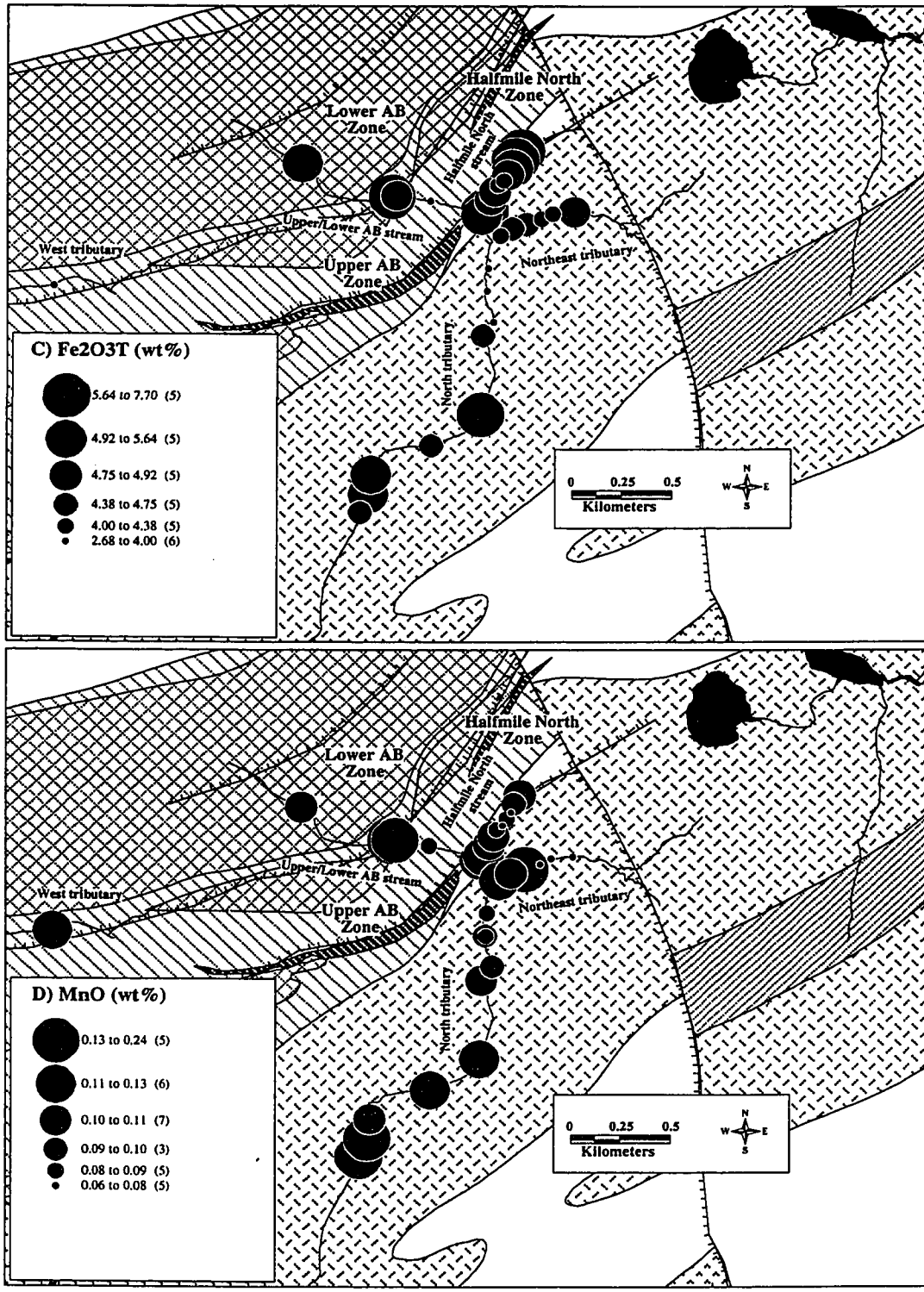


Fig. 6.1 continued.

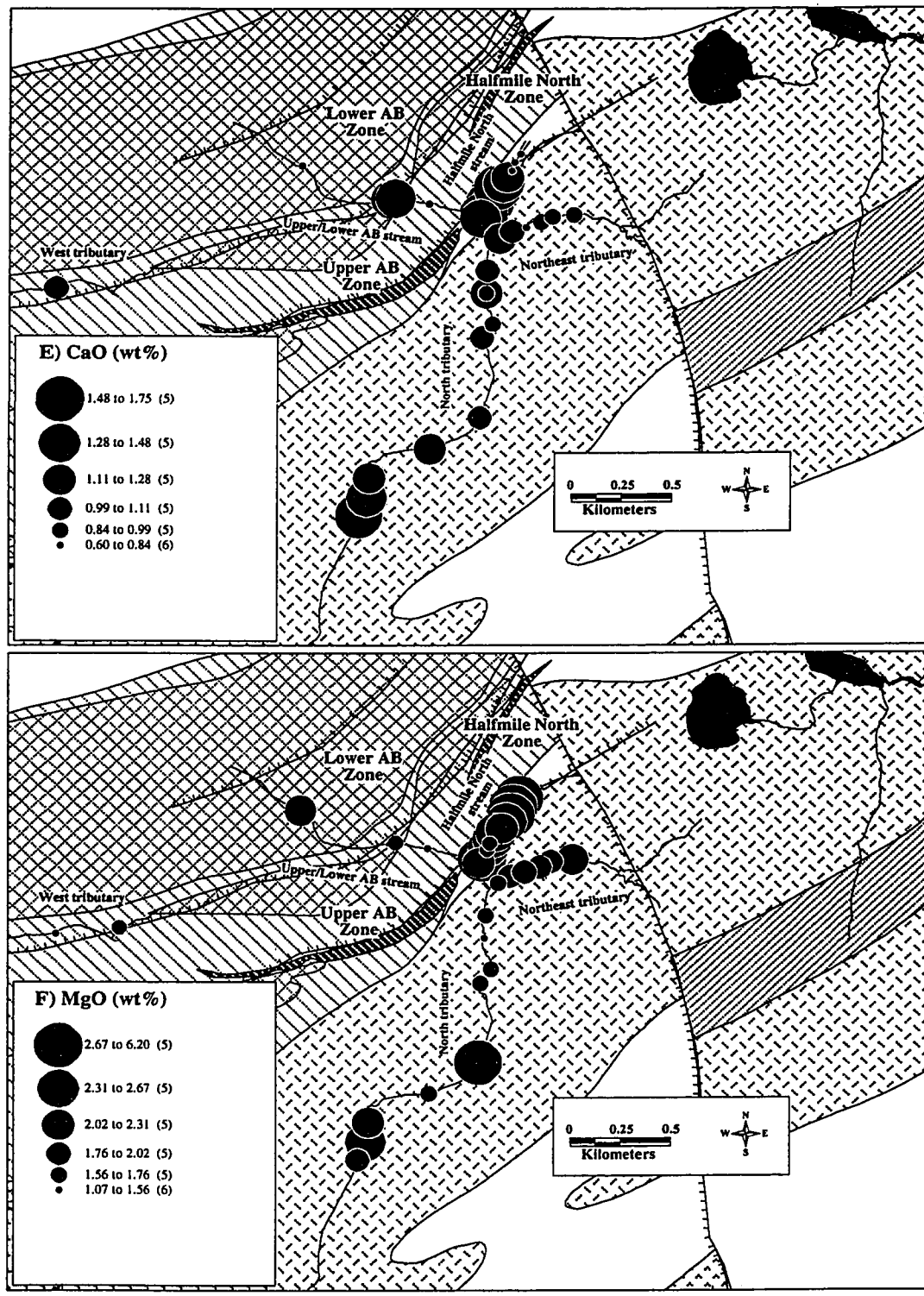


Fig. 6.1 continued.

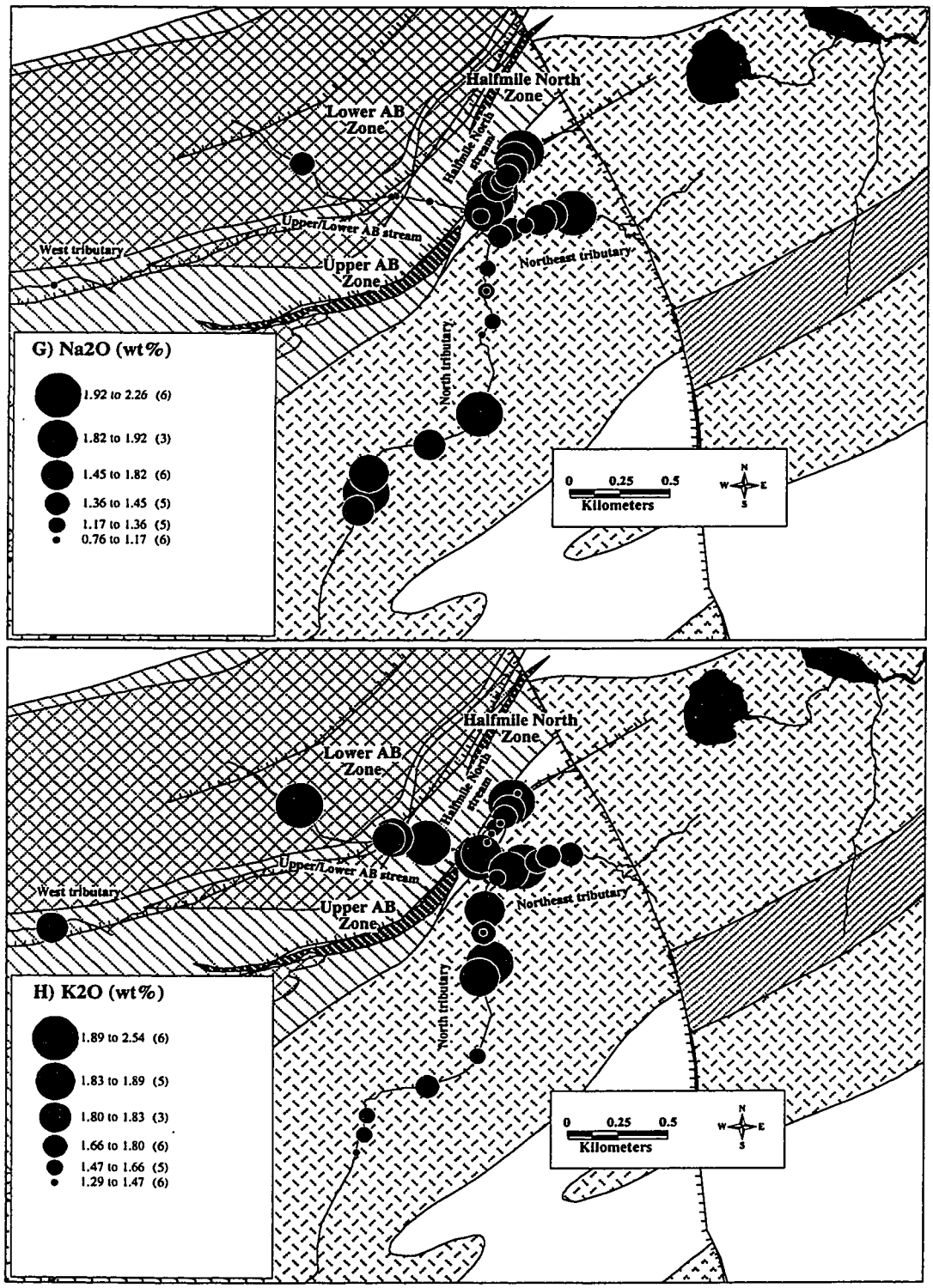


Fig. 6.1 continued.

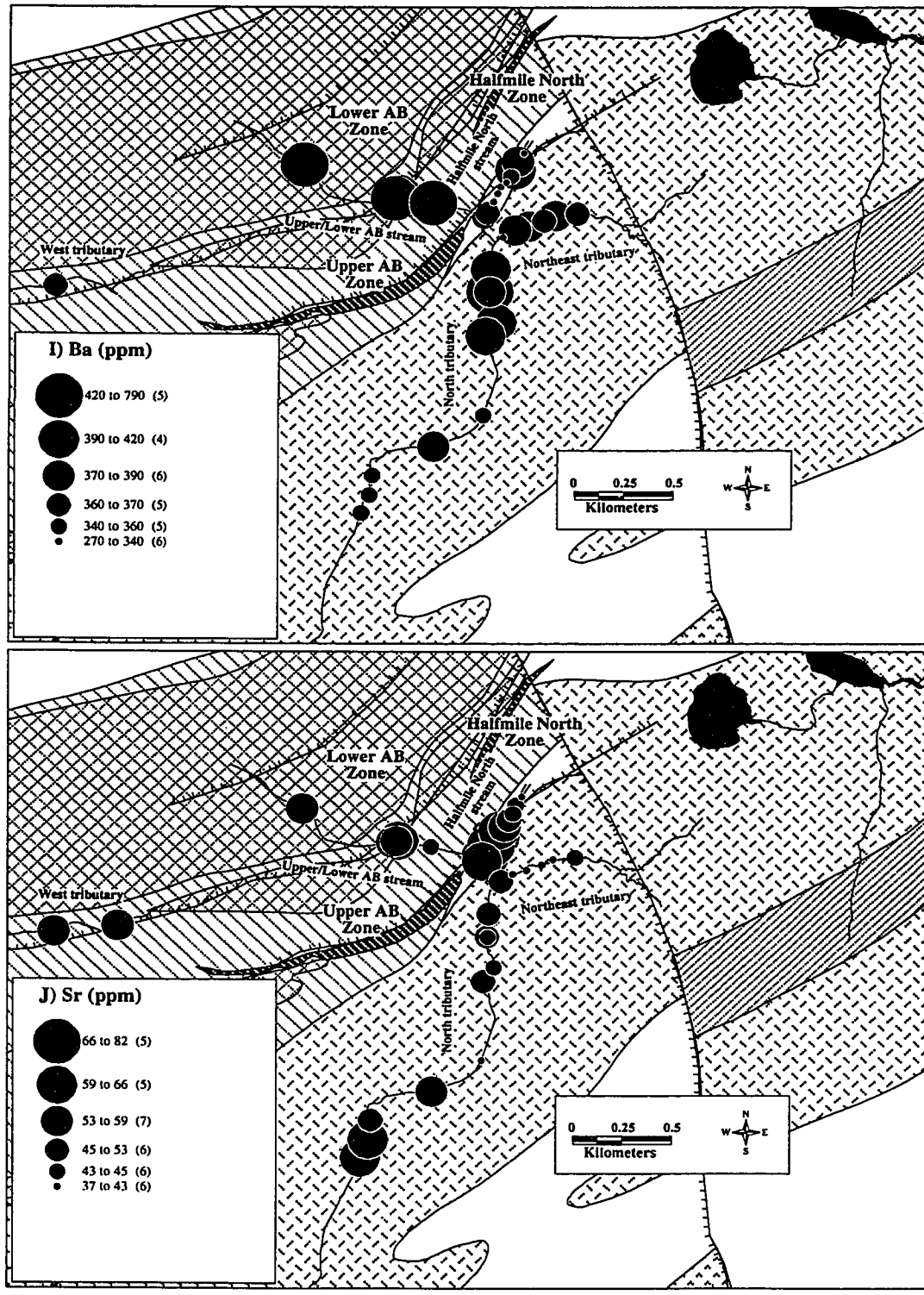


Fig. 6.1 continued.

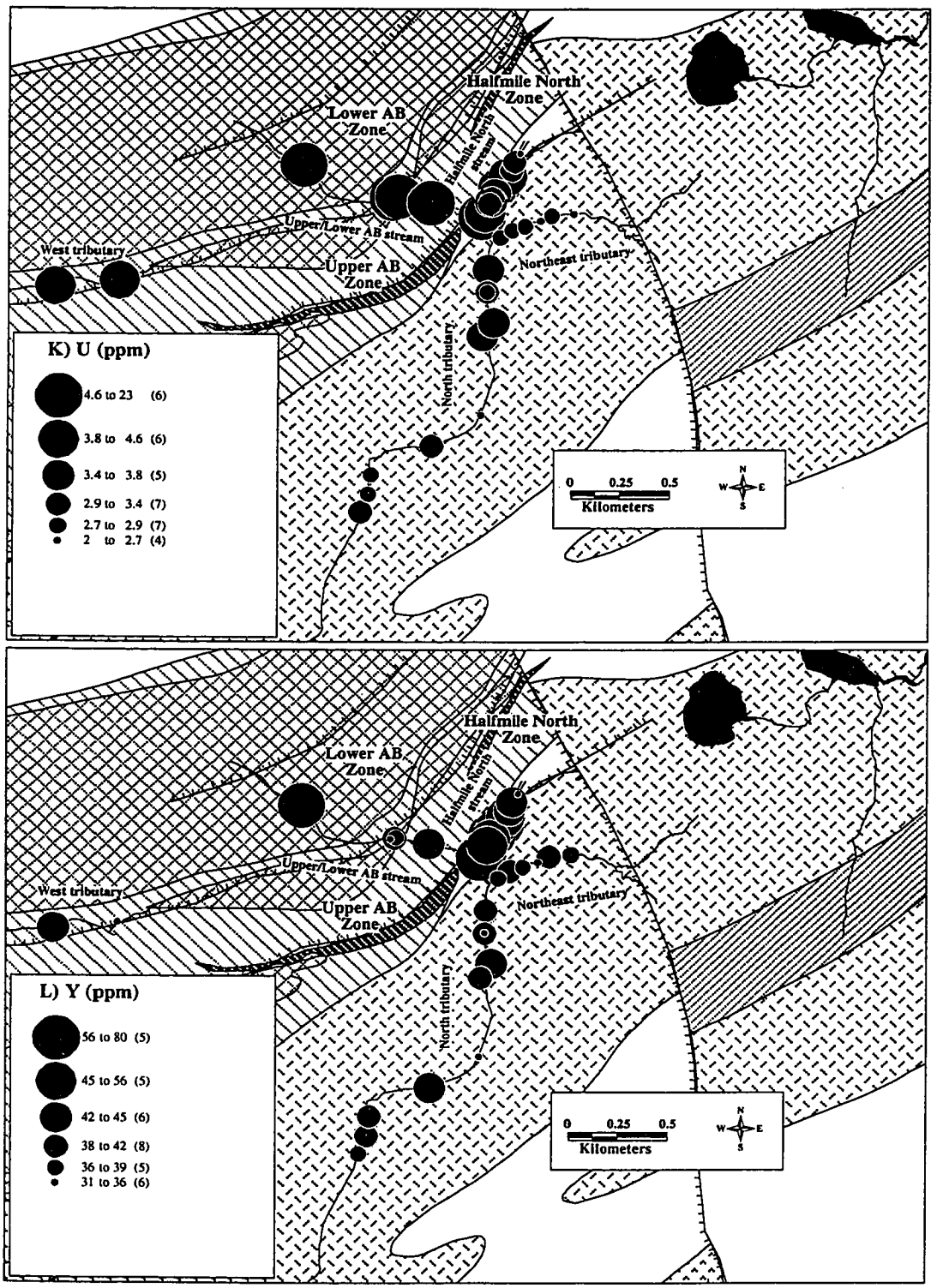


Fig. 6.1 continued.

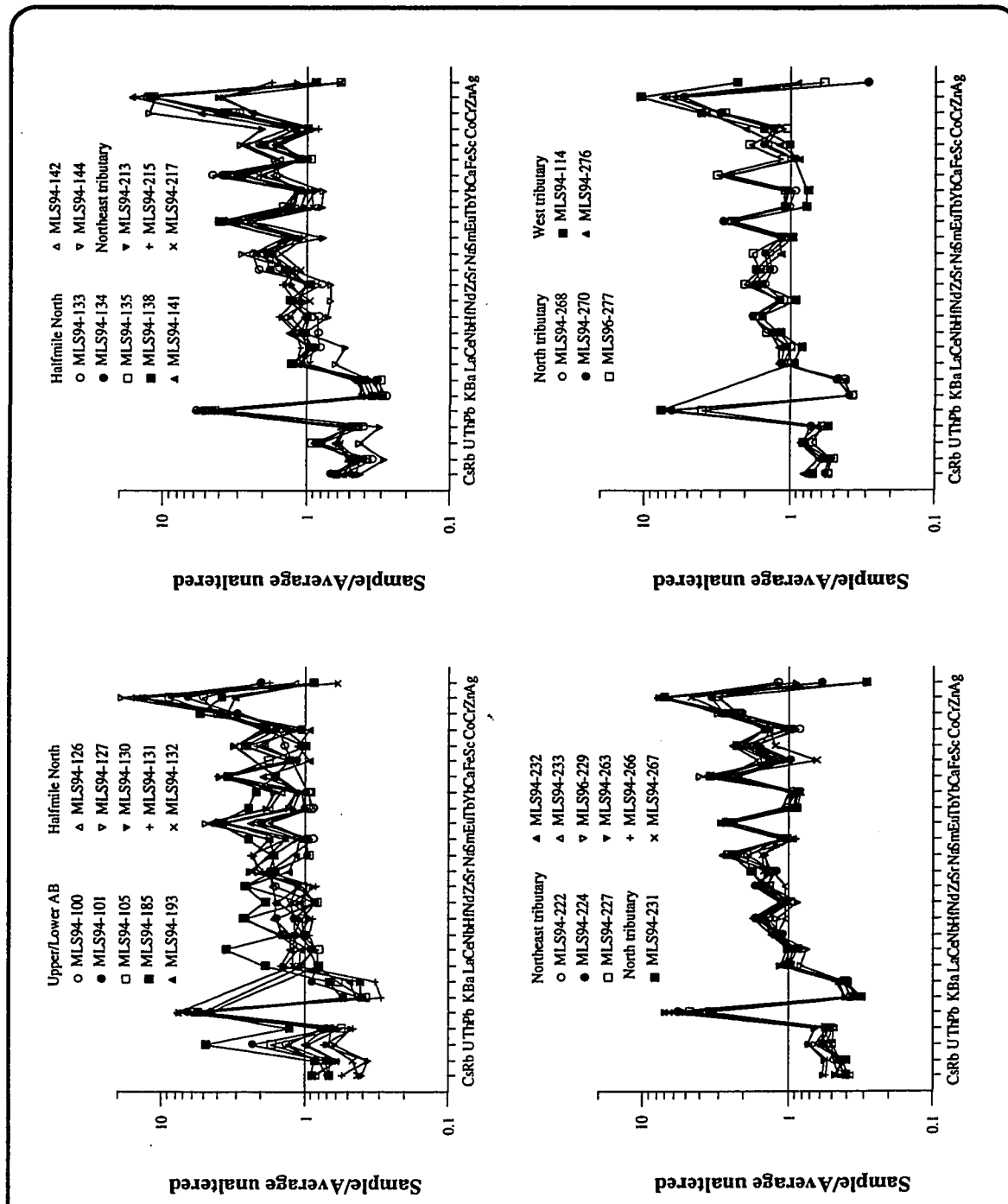


Fig. 6.2 Halfmile Lake deposit stream sediments normalized to average unaltered felsic rocks from the deposit. Normalizing values from Chapter Two. Data from Appendix A.2.1.

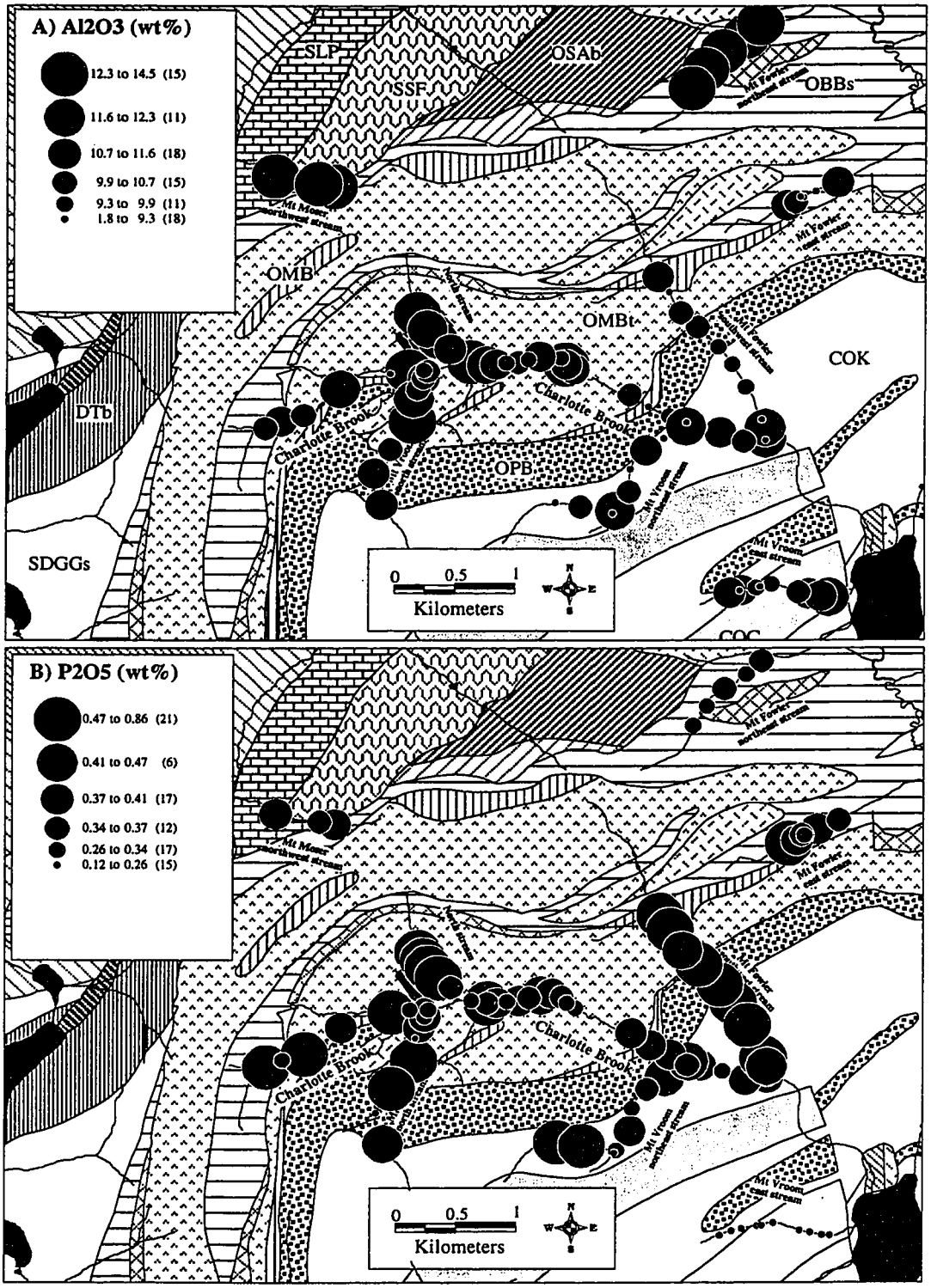


Fig. 6.3 Proportional circle maps of selected major and trace elements of stream sediments from the Restigouche deposit. Geology as in Chapter Two.

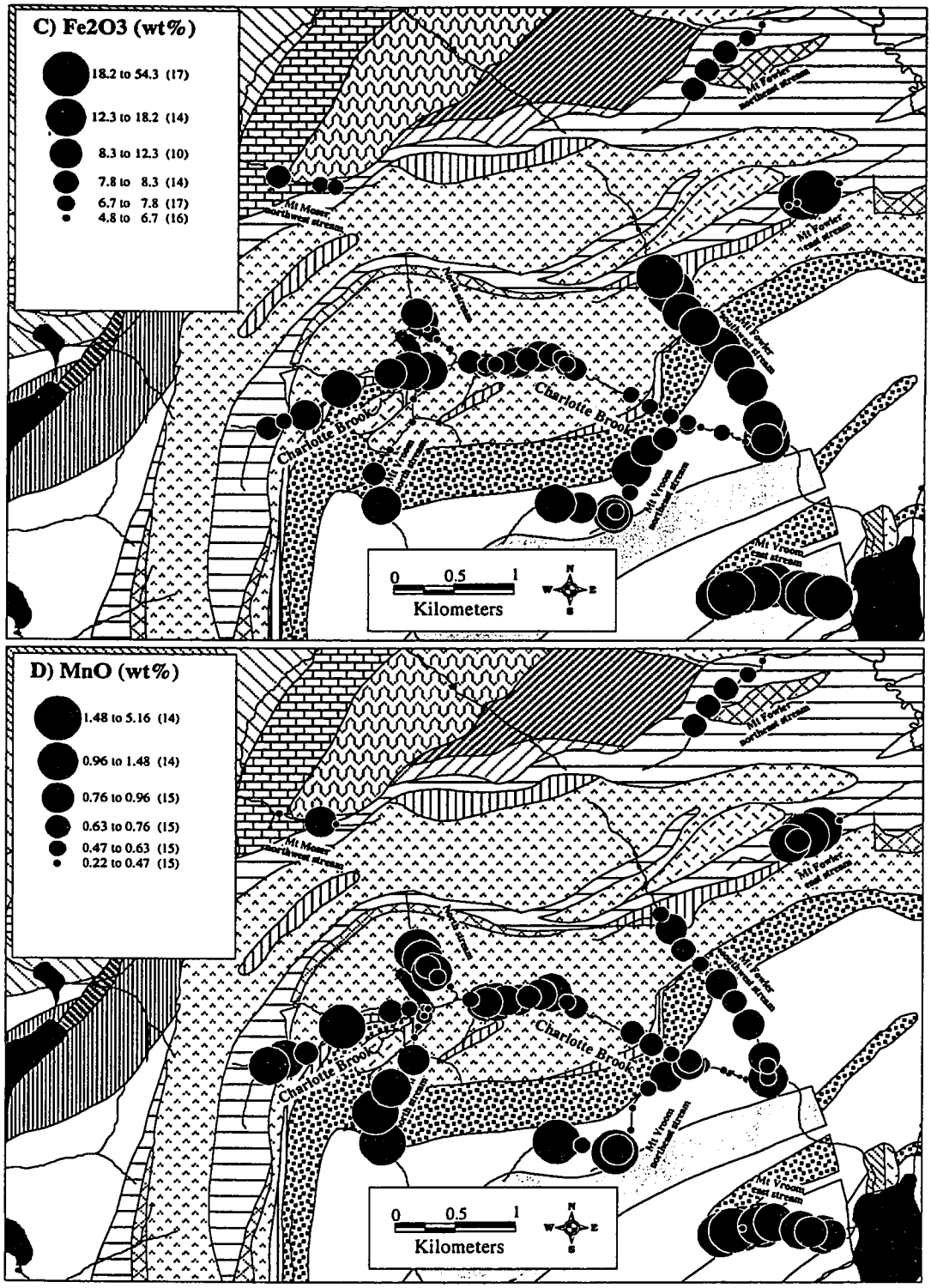


Fig. 6.3 continued.

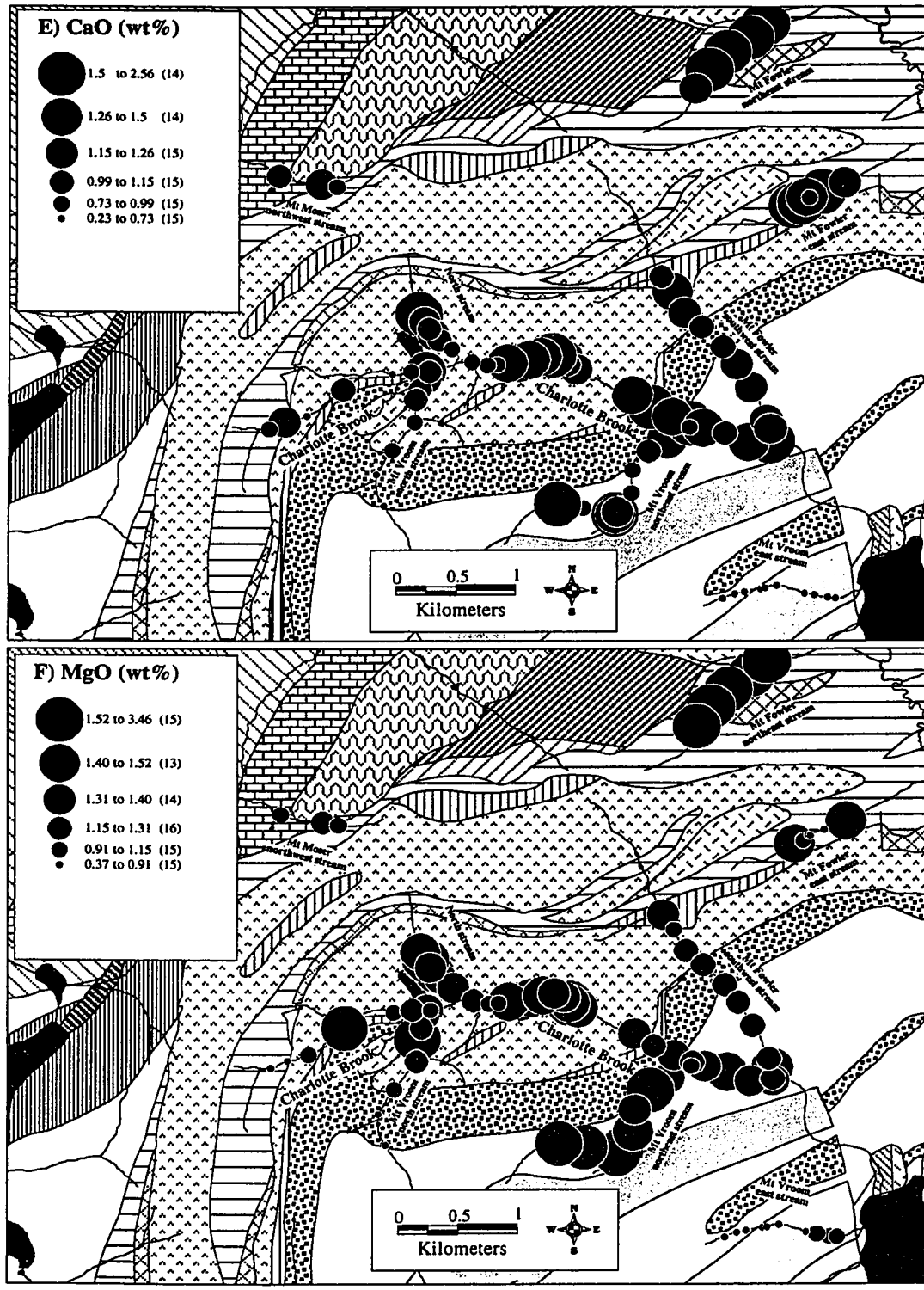


Fig. 6.3 continued.

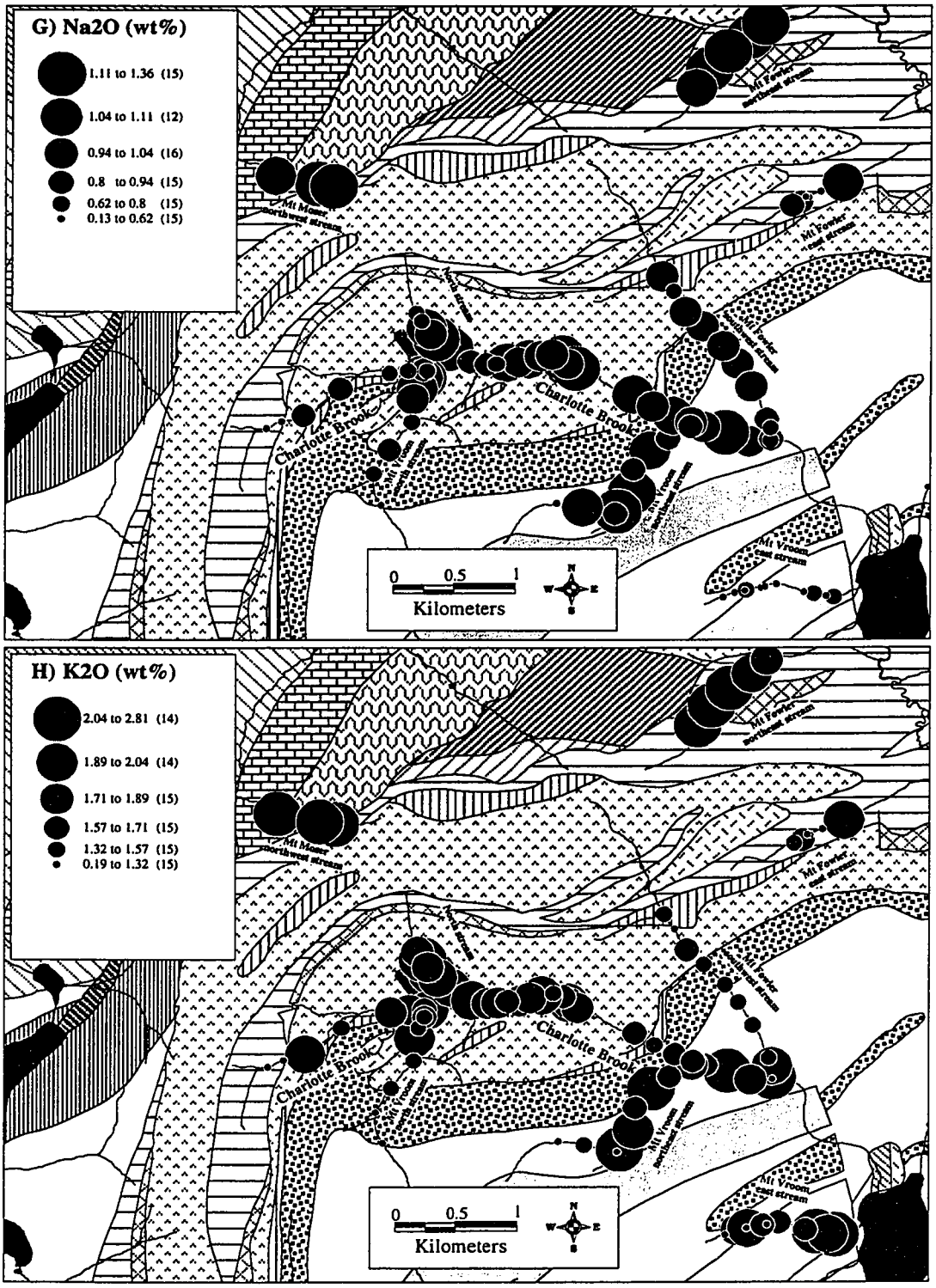


Fig. 6.3 continued.

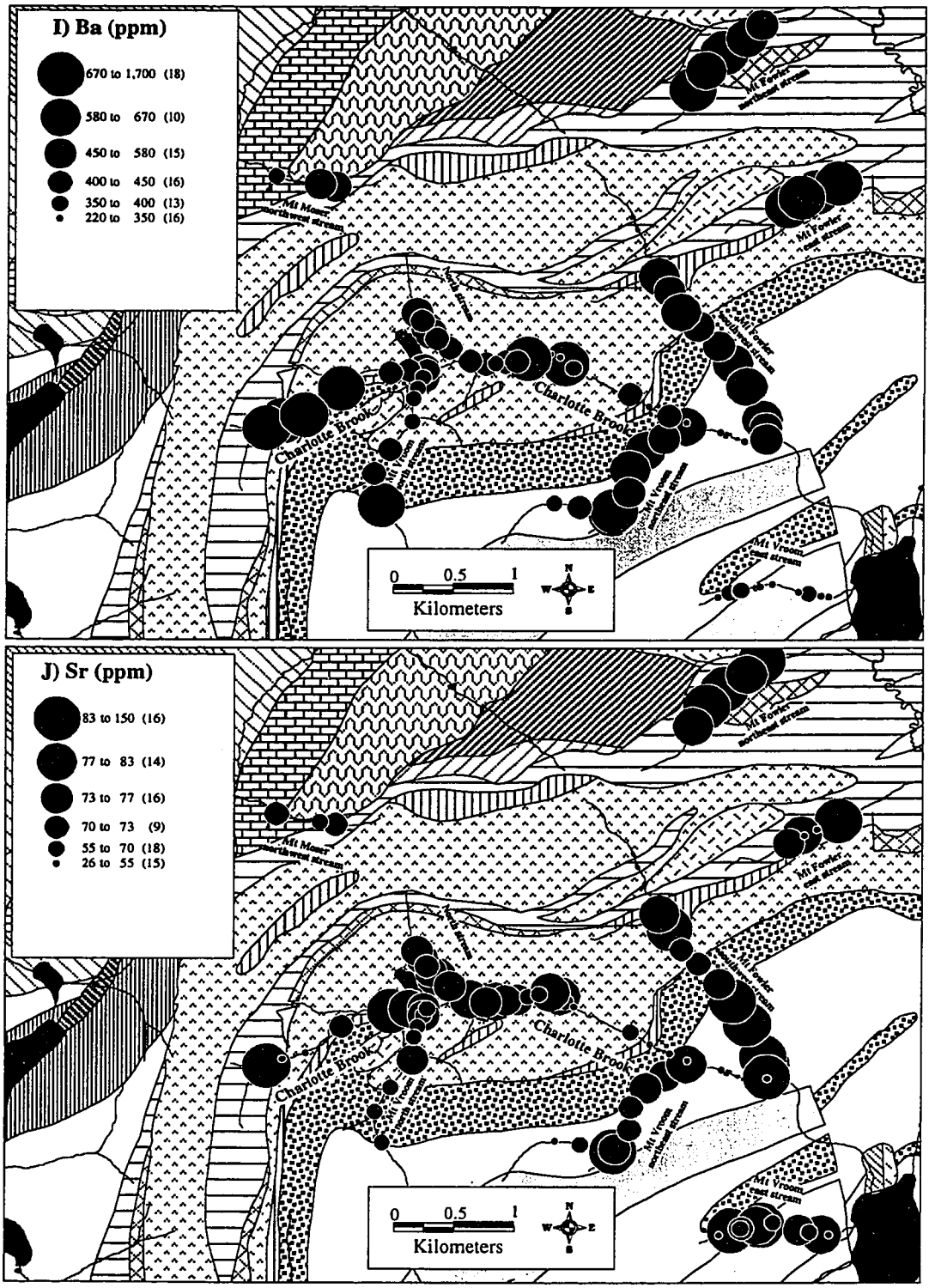


Fig. 6.3 continued.

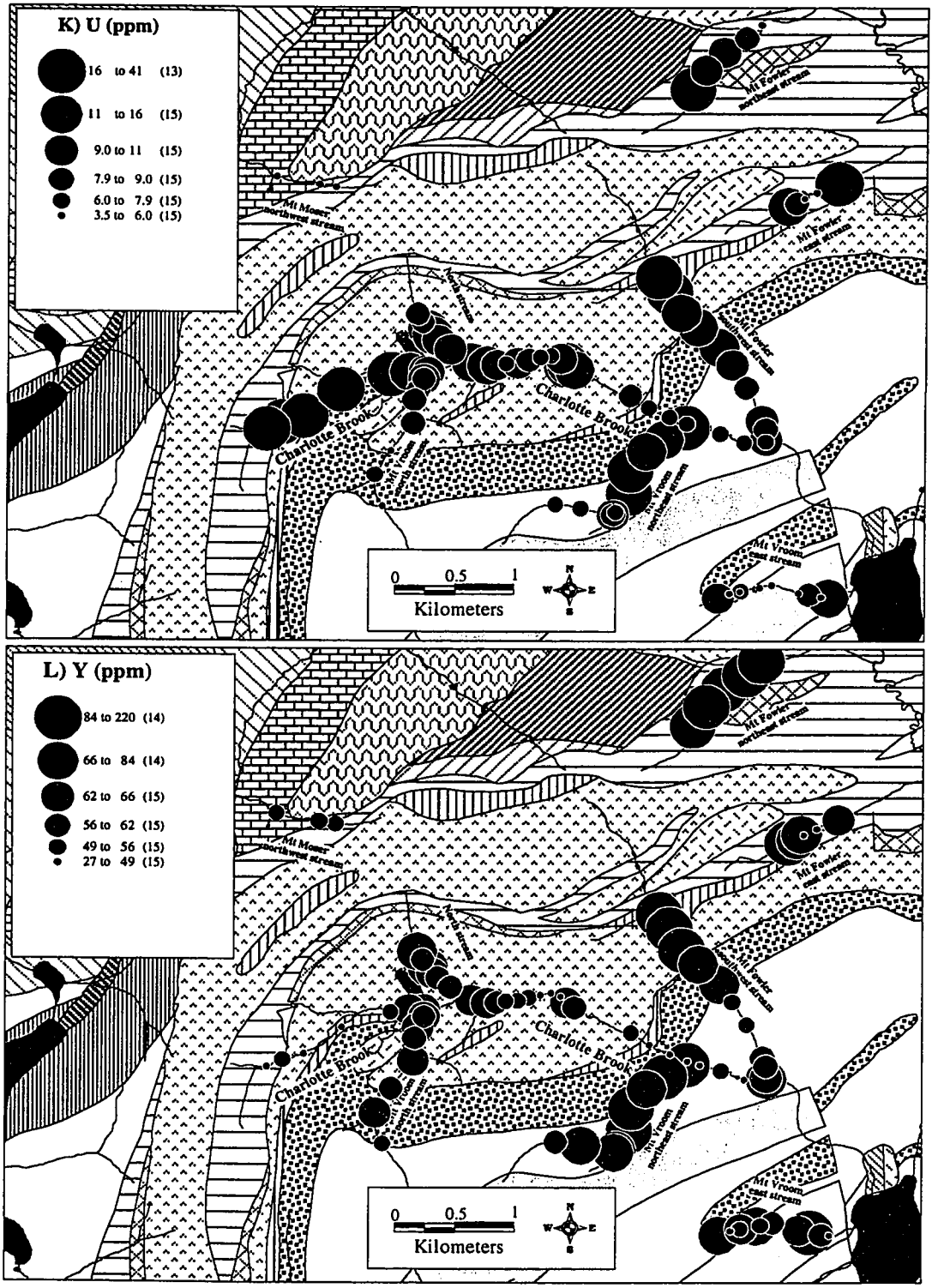


Fig. 6.3 continued.

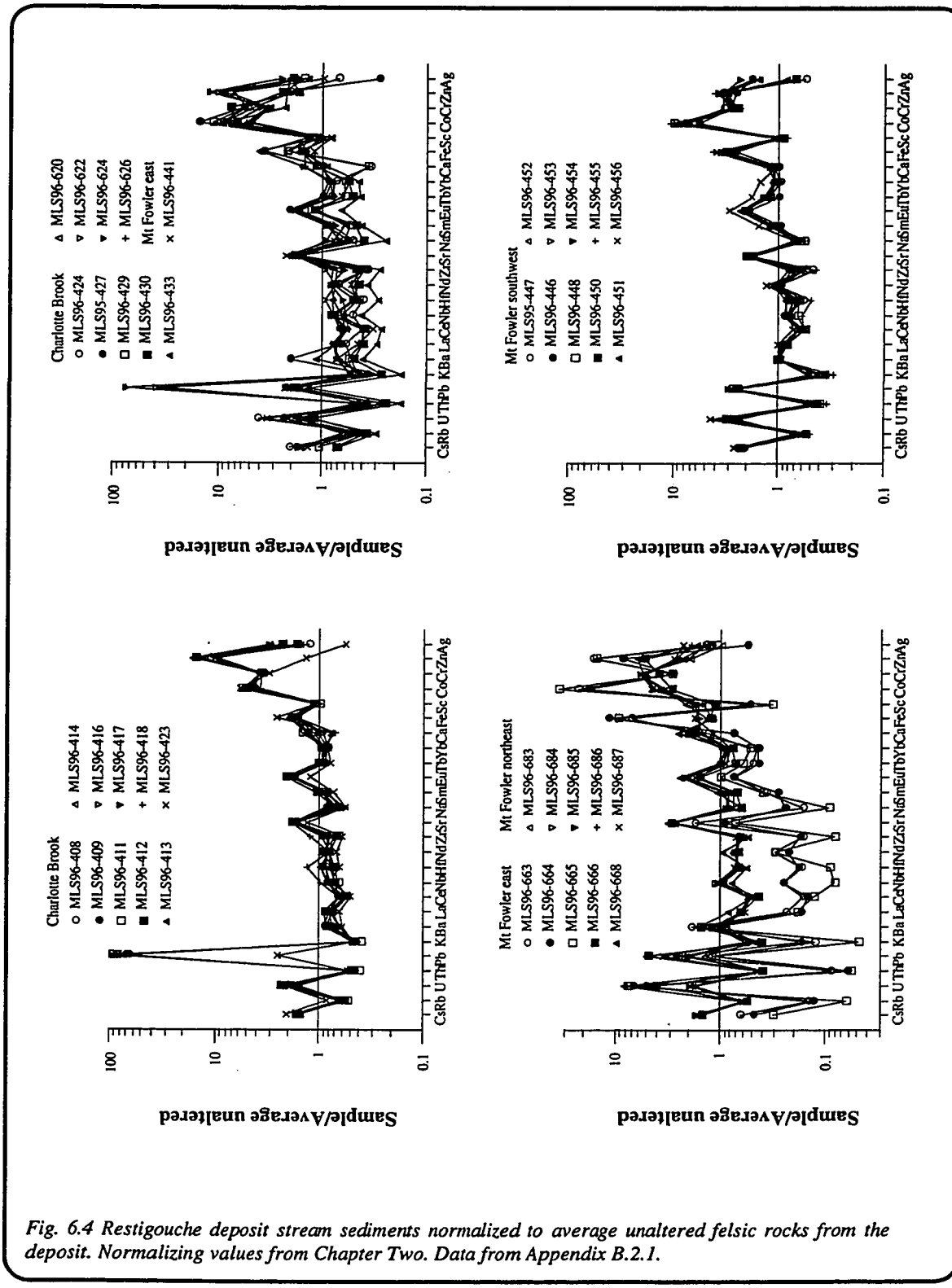


Fig. 6.4 Restigouche deposit stream sediments normalized to average unaltered felsic rocks from the deposit. Normalizing values from Chapter Two. Data from Appendix B.2.1.

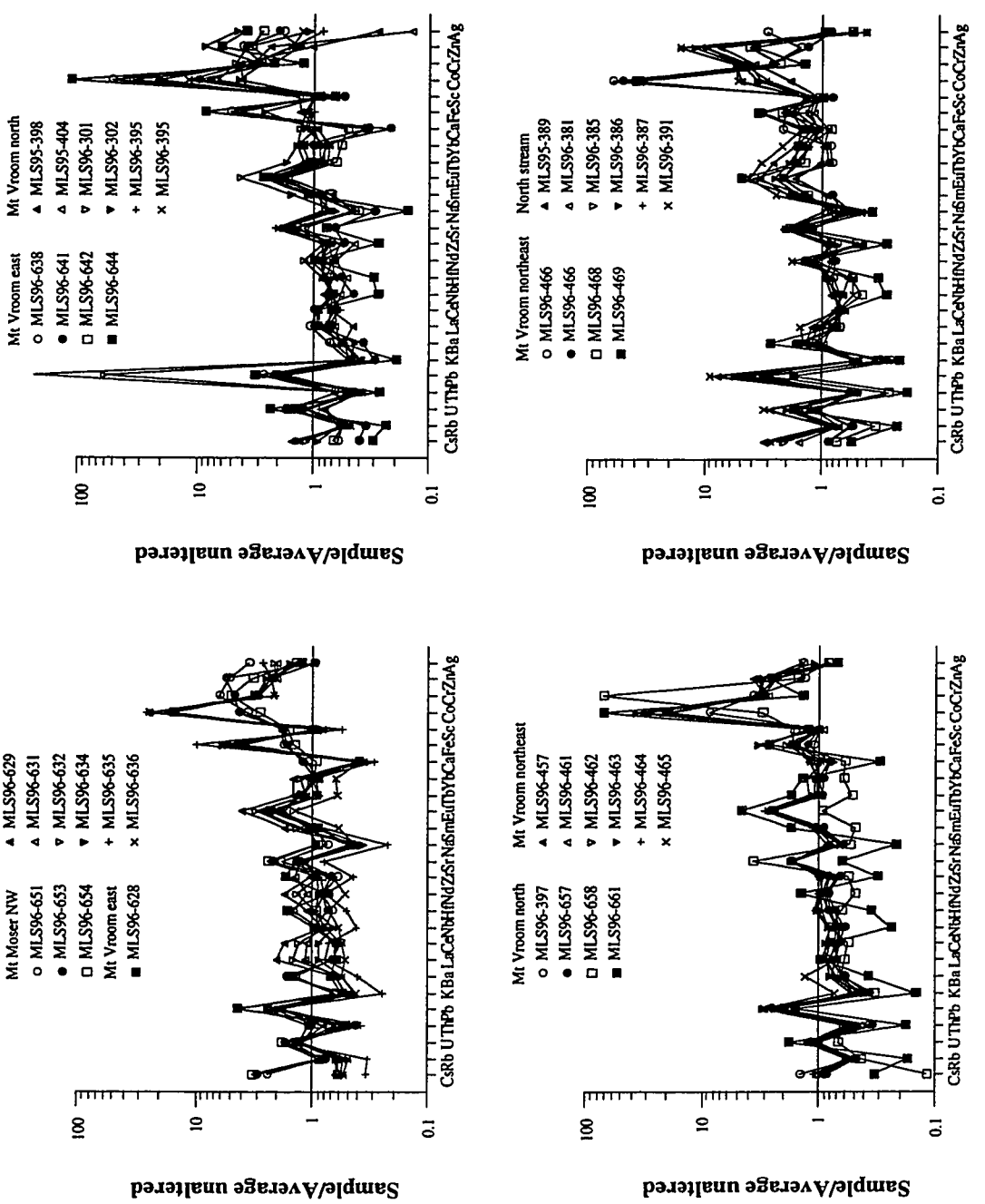


Fig. 6.4 continued.

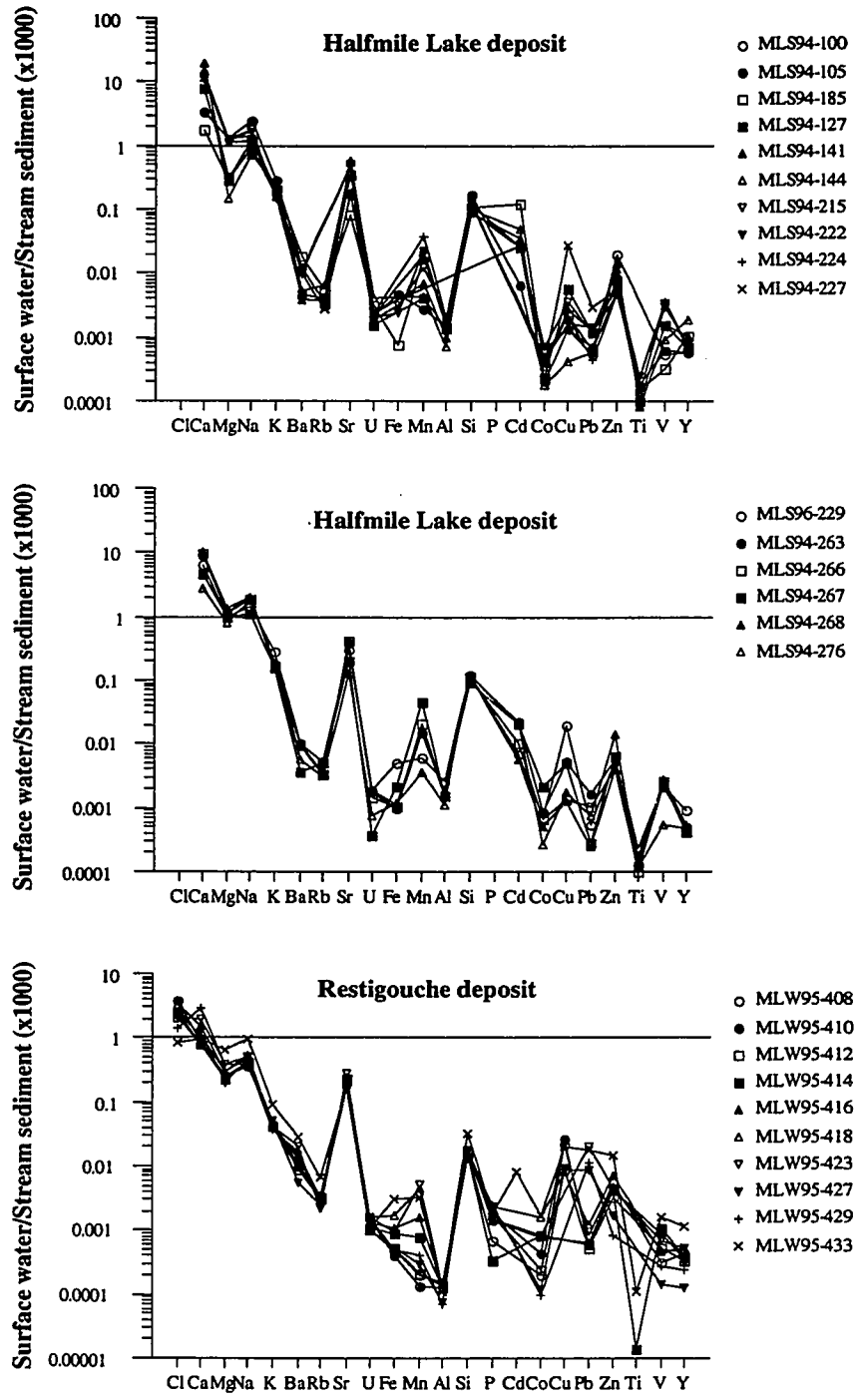


Fig. 6.5 Surface waters normalized to corresponding stream sediments for selected samples from the Halfmile Lake and Restigouche deposits. Water data in µg/L, stream sediment data in ppm.

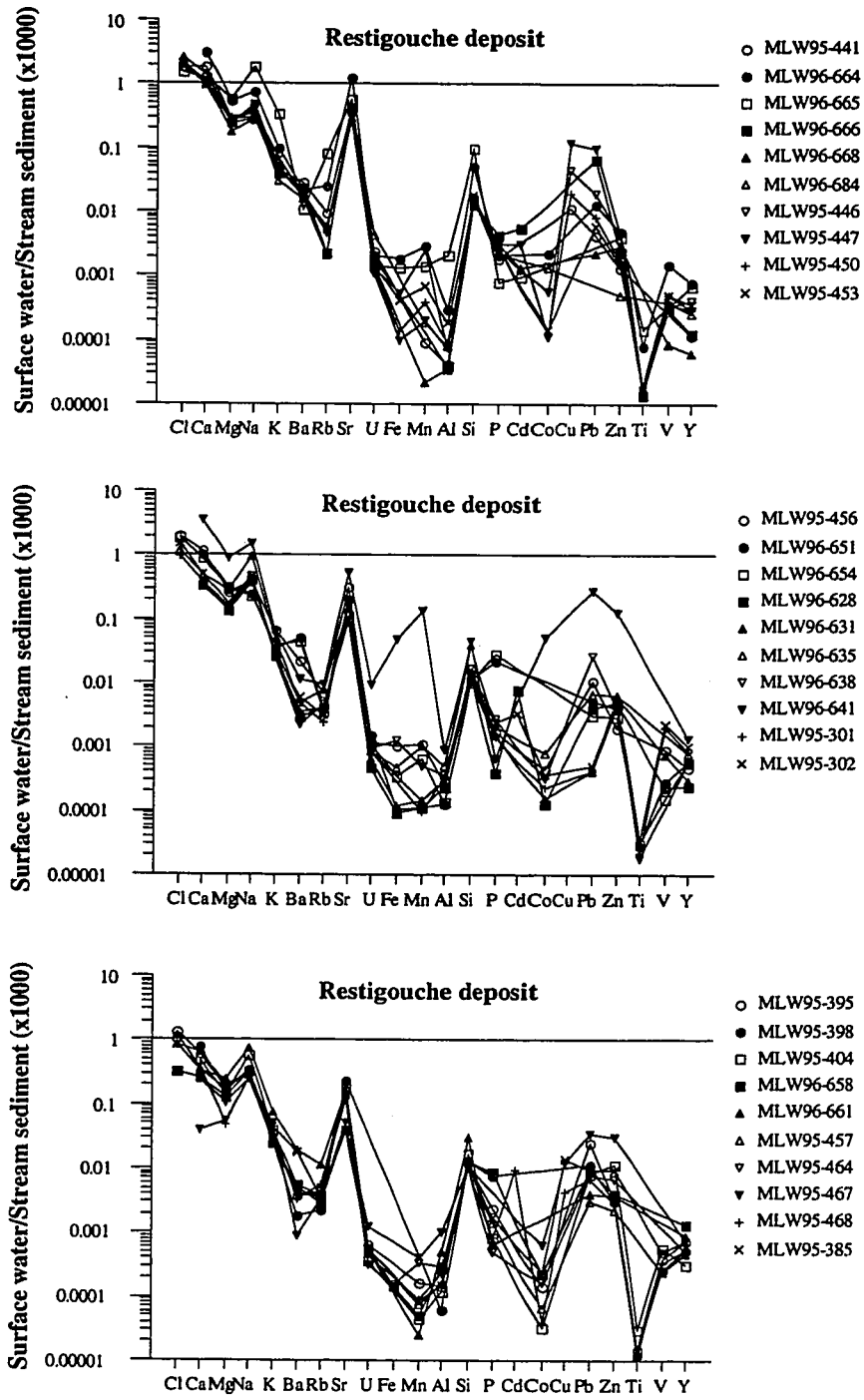


Fig. 6.5 continued.

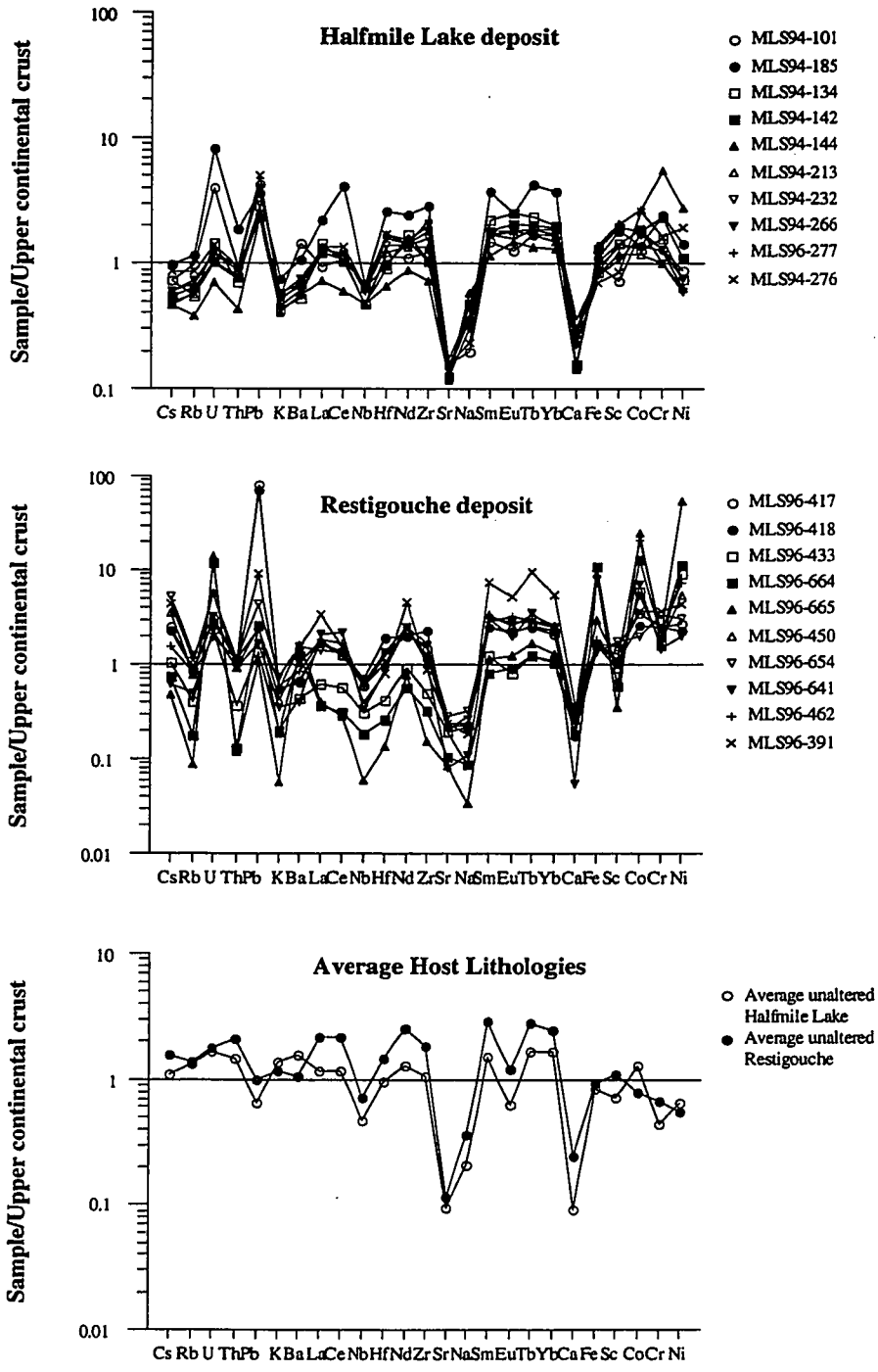


Fig. 6.6 Selected stream sediments and average unaltered lithologies from the Halfmile Lake and Restigouche deposits normalized to average upper continental crust (Taylor and McClennan, 1985).

CHAPTER SEVEN:
HYDROCHEMISTRY OF METALS IN GROUNDWATERS AT THE HALFMILE LAKE, RESTIGOUCHE, HEATH STEELE, BRUNSWICK #12, WEDGE, AND WILLETT DEPOSITS, BATHURST MINING CAMP, NEW BRUNSWICK

7.1 Introduction

This chapter examines the processes controlling the dissolution and transport of metals in groundwaters associated with the Halfmile Lake and Restigouche deposits and other massive sulphide deposits in the Bathurst Mining Camp (BMC). During the course of this study it became apparent that the chemical compositions of the groundwater at the Halfmile Lake and Restigouche deposits were fundamentally different (Leybourne et al., 1995a; Leybourne et al., 1996a; Leybourne et al., 1996b; Leybourne et al., submitted-a; Leybourne et al., submitted-b). This raised the question about the range of compositions and origins of groundwaters in the BMC. To address this question, a limited number of groundwaters were collected from a representative group of deposits in the BMC, including active mines (Heath Steele and Brunswick #12) and other, smaller, deposits (Wedge, Willett and Stratmat Main Zone deposits).

Critical questions addressed in this chapter are: 1) what are the chemical characteristics of groundwaters in the BMC, 2) why are there such large differences in groundwater compositions between the Halfmile Lake and Restigouche deposits, 3) what is the relationship between the deeper saline waters and dilute shallow groundwaters observed at the Restigouche deposit, 4) under what conditions are metals dissolved from sulphide minerals and dispersed in groundwaters, and 5) how are the metals complexed in solution and how does metal solubility and fluid composition change as a function of distance from massive sulphide deposits. These questions will be addressed using a combination of hydrogeochemical methods, geochemical modelling, speciation and solubility calculations, comparisons between the compositions of

groundwaters and bedrock samples and suspended sediments.

The solubility of metals in groundwaters is controlled by a number of factors including pH, redox state, concentration of ligands that complex metals in solution, and the availability of precipitates that can act as surfaces for adsorption-desorption reactions. There has been a lot of experimental work in recent years investigating the role of adsorption in the fixation and transport of metals. Empirical and geochemical modelling methods are used to show the potential significance of adsorption processes for metal dispersion in the BMC.

In recent years, increasing attention has been given to the problems of acid-mine drainage (AMD) and to the processes and pathways by which metals are transported away from active and abandoned mine sites (e.g. Curtis and Walker, 1994; Goodyear et al., 1996; Pratt et al., 1996; Thornton, 1996; Wayne et al., 1996). Less attention, however, has been paid to the impact of undeveloped and shallow ore bodies on the environment and their potential as analogues for AMD sites (Maest, 1996). This latter point is important given the paucity of suitable analogue sites for active and abandoned mines (Maest, 1996). The Halfmile Lake and Restigouche deposits in the Bathurst Mining Camp are well suited for this type of study because they are the same age, hosted in the same lithologies and exist under the same climatic and physiographic regime as several past and actively producing mines in this Camp (e.g. Heath Steele, Brunswick #6, Brunswick #12, Wedge deposits).

In order to meet the objectives of this study, ground and surface waters were collected from the vicinity of the Halfmile Lake and Restigouche Zn-Pb-Cu-Ag massive sulphide deposits (Chapter Two). These deposits were chosen for a number of reasons, including availability of exploration drill holes likely to be open for sampling of groundwaters, contrasts in deposit geometry, and complementary geological, geophysical, lithogeochemical and, quaternary studies. The importance of analogue studies for understanding natural and anthropogenic sulphide oxidation and dispersion of metals away from massive sulphide deposits is shown by the different geochemical responses in the two deposits studied here. The timeliness of this kind of study in the BMC is emphasized by the recent excavation of the Restigouche deposit as

an open pit mine and the ongoing assessments of the Halfmile Lake deposit as an underground operation.

7.2 Hydrochemistry of Groundwaters at the Halfmile Lake deposit

Although over 300 holes have been drilled by various mining companies over the past 40 years, most holes were not accessible for sampling either due to lack of casings in the overburden or to fault-related cave-ins of cored holes. As discussed previously (Chapter Four), collection of groundwaters with the packer system at Halfmile Lake proved to be difficult compared to the Restigouche and Stratmat deposits. Despite these limitations, twelve boreholes and one artesian borehole were sampled by bailer and/or straddle-packer for groundwaters (Fig. 7.1; Appendix A.3.1). Most of the boreholes sampled intersect the Lower AB zone, as this is where drilling has been focussed over the last ten years. Groundwater was recovered from only one borehole on the Upper AB zone because the other holes are not accessible (Fig. 7.1).

7.2.1 Major cations and anions

Halfmile Lake deposit groundwaters have uniformly low total dissolved solids (TDS), ranging from 8.1 to 226.1 mg/L (average TDS = 51.1 mg/L, n = 86). The low TDS contents of these groundwaters was unexpected and will be discussed in detail in a later section. Although conductivities of straddle-packer waters increase with depth, deeper groundwaters at the Halfmile Lake deposit have low TDS values compared to groundwaters from the Restigouche and Stratmat Main Zone deposits (see below and Chapter Eight). Packer waters from boreholes HN93-50 and HN94-65 are significantly elevated in Ca, Mg and Na compared to the bailer waters from the same depth, but lower in K (Appendix A.3.1). Halfmile Lake deposit groundwaters show a weak geochemical evolutionary trend towards the Na+K apex and a weaker trend towards more chloride-rich waters, but are dominantly $CaHCO_3$-type waters (Fig. 7.2). These waters dominate in boreholes HN94-65, HN93-55, HB80-1 and

HN93-51. Waters with higher sulphate contents (Ca-HCO_3-SO_4-, Ca-Na-HCO_3-SO_4-, and Ca-Mg-SO_4-type waters) typically have the lowest TDS contents and occur in boreholes HT55-43, HN93-50, HN92-40 and the artesian borehole. The most evolved groundwaters range from Na-Ca-HCO_3- to Na-HCO_3-type waters, recovered from boreholes HN87-8 (deeper waters, below 500 m), HN92-33, HN94-82, and HN94-63. The groundwaters from borehole HN94-63 have the highest TDS recovered to date from the Halfmile Lake deposit. Unlike the Restigouche deposit, no Na-Cl-type waters have been recovered from this deposit, despite the range in depths sampled (up to 740 m with the flow-through bailer and 450 m with the packer).

As a group the Halfmile Lake deposit groundwaters show very strong correlations between HCO_3 and TDS, highlighting the paucity of waters dominated by sulphate and chloride (Figs. 7.2, 7.3). Sulphate and Cl show much less systematic correlation with TDS except in a few boreholes where Cl and TDS display a high positive correlation (Fig. 7.3). Both pH and Eh are strongly positively and negatively correlated with TDS, respectively. The groundwaters with the lowest pH values are shallow Ca-HCO_3- and Ca-HCO_3-SO_4-type waters. The Na-HCO_3 waters from borehole HN94-63 have the highest pH and HCO_3 contents of all the Halfmile Lake deposit groundwaters (Fig. 7.3). Of the major cations, Ca and Mg generally increase with increasing TDS at low TDS contents, but behave more erratically at higher TDS. Groundwaters in boreholes HB80-1, HN92-40, HN94-79, and HN94-82 have anomalously high Ca (and Mg for borehole HN92-40 waters) and low Na, whereas, groundwaters from borehole HN94-63 show the reverse trend. Potassium shows very scattered TDS relationships, although K contents tend to remain low at higher TDS levels. Boreholes HT55-43 and HN94-63 waters have anomalously low and high Si contents, respectively, although Si is generally less variable relative to TDS.

7.2.2 Trace elements

The abundance of several trace elements and oxides, including NO_2 and NO_3, Be, Bi, Cs, Li, Sc, Se, and Tl is below the detection limit in most Halfmile Lake deposit groundwaters.

For elements above the detection limit, Ba, Rb and Sr typically increase with increasing TDS (Fig. 7.3). However, groundwaters from borehole HN94-63 with the highest TDS contents, have low Ba and Sr, but moderately elevated Rb. These waters also have anomalously low contents of the base metals including Co, Cu, Pb, and Zn. Uranium shows a strong correlation with TDS, with the exception of the waters from borehole HN94-63, which have moderately low U contents.

Base metal contents are generally low. The largest variations in base metal, Fe, and Mn contents occurs in waters with low TDS values. The groundwaters with the highest Pb contents have TDS < 50 mg/L. Most of the groundwaters have Zn contents above detection (detection limit, d.l., = 2 μg/L for total nebulization ICP-MS), and range between 2 and 1090 μg/L. Zinc values measured with chelation ICP-MS show essentially the same range in values (Appendix A.3.1). Molybdenum shows the strongest correlation with TDS of all the base metals and also typically correlates with Al, although different boreholes have different Al/Mo ratios. For examples, borehole HN94-65 has high Al/Mo ratios, whereas, boreholes HN93-55 and HN93-33 have very low Al/Mo ratios. Molybdenum contents vary from 0.76 to 56 μg/L (average = 6.36, n = 75) and most Halfmile Lake deposit groundwaters have Mo values well above detection. The Fe and Mn content varies significantly between boreholes and for each borehole, Mn displays a more restricted range than Fe.

Phosphate ranges from 0.4 to 65 μg/L (average = 14.8 μg/L) and Br ranges from 3.3 to 22 μg/L (average = 7 μg/L). Bromide typically increases with increasing TDS similar to Cl, consistent with the similar conservative behaviour of these elements in natural waters (Fig. 7.3). Phosphate displays unexpected behaviour with high values in dilute groundwaters. For the other groundwaters there is a slight increase in PO_4 with increasing TDS (Fig. 7.3).

7.2.3 Downhole variations

There are no consistent trends with depth between boreholes, although there is a tendency for TDS to increase with depth, and Eh and DO to decrease with depth (Figs. 7.4, 7.5). In

boreholes HN87-8, HN93-50 and HN93-55, Fe contents increase with decreasing Eh whereas in borehole HN94-55 both Eh and Fe decrease in the vicinity of the massive sulfides (Fig. 7.5).

Borehole HN87-8 (Fig. 7.4) is the deepest hole sampled at the Halfmile Lake deposit. The hole is in excess of 1000 m deep, but was blocked below 780 m. In this borehole, TDS, HCO_3, and Cl increase with depth. Calcium is the dominant cation in the upper part of the hole, but Na becomes dominant below a depth of 450 m depth which marks a significant change in groundwater composition (Fig. 7.4). Although TDS only increases from 25 to 50 mg/L between 450 m and 760 m, the composition of the waters is very different above and below 450 m. Below 450 m, REE contents and Y (Fig. 7.4) increase with depth and the REE patterns are very different compared to the shallower waters above 450 m (see Chapter Ten for REE data; Figs. 10.10, 10.11). Below 450 m, Eh values decrease and Fe abundances increase, consistent with a change in the dominant Fe species in these waters (Fig. 7.6). Molybdenum is typically immobile under reducing conditions (see section 7.5.11 below). However, although Eh decreases downhole, conditions are still sufficiently oxidizing that Mo contents increase. Aluminum contents also increase downhole, although pH shows little variation with depth. Base metal contents are generally low in these waters, and Cu, Pb, Cd, and Zn contents decrease slightly with increasing depth, despite increased proximity to massive sulphide mineralization (massive sulphides occur between 900 and 920 m in this hole).

Four other boreholes were sampled systematically with depth using a flow-through bailer (Fig. 7.5). Groundwaters from these boreholes show only minor variations with depth. Typically TDS and Cl increase with depth indicating greater water-rock reaction with depth. Eh and pH generally decrease and increase, respectively, with depth. In borehole HN95-65, lower Eh values at the bottom of the hole coincides with low Fe contents and slight increases in base metals (Fig. 7.5). Overall, base metals are lower than at the Restigouche deposit, and there are only small increases with proximity to massive sulphides. All these boreholes were drilled in the Lower AB zone, where the massive sulphides occur at greater depth compared to the

Halfmile North and Upper AB zones of the Halfmile Lake deposit (Chapter Two).

7.2.4 Statistical analysis

The statistical methods used are described in Chapter Three and summary statistics for the Halfmile Lake deposit groundwaters are presented in Appendix A.3.2. Two main methods have been used to reduce the geochemical data and try to determine the underlying relationships. Pearson Product and Spearman Rank correlations have been calculated for all elements in the Halfmile Lake deposit groundwater dataset. Only the Pearson Product Moment (PPM) data is presented in the Appendices (Appendix A.3.3); the Spearman Rank correlation was used to test the influence of outliers in the data on the PPM results. Principle Components Analysis (PCA) was also carried out on a subset of the data. Because PCA looks at the interrelationships between all variables, rather than pair-wise as in the PPM correlation matrix, variables were chosen for PCA that maximized the number of samples in the analysis. Thus, the PCA analysis was carried out using the field variables DO, pH, and Eh, the anions HCO_3^-, SO_4^{2-}, and Cl^-, and the cations Al, Fe, Mn, Si, Mg, Ca, Na, and K (Appendix A.3.4).

Factor analysis (PCA) suggests that the majority of the geochemical variability (85.8%) of the Halfmile Lake deposit groundwaters can be accounted for by five factors (Appendix A.3.4). The first factor accounts for 44.9% of the variation and includes positive loadings for pH, TDS, HCO_3, Cl, Si, Ca, Na, with lower loadings for SO_4, Mg, and Al. Negative loadings in factor 1 are for Eh and DO. Factor one can best be interpreted as a general bedrock weathering factor. Factor two accounts for 23.7% of the variation and includes strong positive loadings for SO_4, Mn, Mg, and Ca and negative loadings for Al, Na, Cl, and DO. This factor is interpreted to represent the extent of water-rock reaction combined with adsorption processes. Factor three (11.2% of the variation) is strongly positively loaded in K and somewhat negatively loaded in Fe and SO_4. Potassium contents show little variation with increasing TDS in Halfmile Lake deposit groundwaters. The correlation between Fe and SO_4 may be an artifact of outlier data or due to sulphide oxidation. Factor four (6.0%) has positive

loadings for Fe only, and is most likely an Fe-oxide factor. The final factor (4.8%) is strongly loaded for Si only.

The factor loadings represent the relationships between chemical variables for all the groundwaters. The influence of the first four factors on the individual groundwaters can be shown graphically to highlight trends in the dataset (Fig. 7.7). Groundwaters from individual boreholes tend to plot close to one another. The same factor scores for individual groundwaters can also be shown subdivided by water-type (Fig. 7.8). In this case, trends related to groundwater evolution (degree of water-rock reaction) are shown. For example, Na-HCO_3 waters have moderate to high scores in factor 1 but low factor 2 scores. Sulphate-rich waters from borehole HT55-43 at the Upper AB zone have very low factor 1 scores and moderate factor 2, 3 and 4 scores.

7.2.5 Geochemical modelling

Two computer programs to model hydrogeochemical data were used in this study. The purpose of this exercise was to determine the activities of aqueous species for different elements in solution as well as the likely minerals controlling the composition of the groundwaters. Initially the EQ3NR module of EQ3/6 (Wolery, 1992a; Wolery, 1992b) was used to speciate the waters and determine mineral saturation indices. The EQ3NR database includes most trace elements including the REE. However, it was found that much of the thermodynamic data is either incomplete or out of date, especially for the REE. Results proved more consistent using the more widely distributed WATEQ4F database (Ball and Nordstrom, 1991). The program PHREEQC (Parkhurst, 1995) was utilized to execute the WATEQ4F database. Although the results presented below were generated mostly by PHREEQC, reference is made to the EQ3NR data where important. Mineral saturation indices and percentages for cation species accounting for $\geq 0.1\%$ are presented in Appendices A.3.5, A.3.6, based on the PHREEQC data.

The geochemical modelling for Halfmile Lake groundwaters indicates that many Fe and Al

oxyhydroxides and aluminosilicates are supersaturated (Appendix A.3.5). It is possible that much or all of this supersaturation is an artifact of colloids that passed through the filter paper during sample collection. SEM results of suspended and colloidal material trapped on the filter papers (see Chapter Nine for full detaiis) suggests that much of the colloidal material that may have passed the filters is dominated by quartz and aluminosilicates (clays).

Activity diagrams for the major cations suggest that there is little variation in the Halfmile Lake deposit surface waters. Mineral stability is controlled primarily by aluminum oxides and alumina-silicates (e.g., gibbsite and kaolinite; Fig. 7.9). $NaHCO_3$ and $NaCaHCO_3$ waters show the highest K, Ca, and Na activities relative to pH and most data plots close to the gibbsite-kaolinite cotectic, below quartz saturation (Fig. 7.9). Only groundwater MLW96-708 from borehole HN94-63 plots outside of the kaolinite and/or gibbsite stability fields. The composition of this groundwater suggests equilibrium with respect to the higher temperature mineral phases muscovite-prehnite-paragonite. The very low TDS waters from borehole HT55-43 fall within the gibbsite stability field with very low activities of K, Ca, and Na (Fig. 7.9). Mineral saturation indices suggest that these waters are saturated with respect to kaolinite (Fig. 7.10). Only the waters from borehole HN94-63 are saturated with respect to calcite. This groundwater has the highest pH and HCO_3 contents of all the Halfmile Lake deposit groundwaters. All the Halfmile Lake groundwaters are supersaturated with respect to goethite and hematite. However, precipitation of these Fe-oxides is kinetically sluggish, and it is more likely that the stable Fe^{3+} species would be amorphous Fe-hydroxide (e.g., $Fe(OH)_3$; Fig. 7.6). Based on the Eh and pH field measurements for these waters, the dominant Fe species is Fe^{2+} (Fig. 7.11), which is relatively soluble. The $NaHCO_3$ and $NaCaHCO_3$ groundwaters plot in the $Fe(OH)_3$ stability field (Fig. 7.6) and are also the only waters at or near saturation with respect this phase (Fig. 7.10).

Calculations using PHREEQC suggest that for the lower pH groundwaters, Pb occurs primarily as free ions, but that with increasing pH (above pH 7), Pb carbonato and dicarbonato complexes become increasingly dominant (Fig. 7.11). None of the Halfmile Lake deposit

groundwaters have sufficiently low pH values or high sulphate activities for Pb-sulphate complexes to be major components of the Pb speciation in these waters. For Zn, Zn^{2+} is the dominant species at pH values up to at least 8 (Fig. 7.11). For groundwater MLW96-708 from borehole HN94-63, $Zn(CO_3)_2^{2-}$ and $Zn(OH)_2$ species dominate (Fig. 7.11). This latter groundwater has low Zn and Pb contents compared to many of the other groundwaters from this deposit (Fig. 7.3). Cadmium is speciated similarly to Zn; greater than 90% of the Cd in Halfmile Lake deposit groundwaters occurs as free ions, with the exception of groundwater MLW96-708, in which carbonate and hydroxide species dominate. Copper shows a much more complex distribution, similar to Fe in that different groundwaters have variable amounts of Cu in different oxidation states (Garrels and Christ, 1965).

7.2.6 Comparison with surface waters

Groundwaters from the Halfmile Lake deposit are, in many respects, broadly similar to nearby surface waters but with important differences. Groundwaters have typically higher trace element contents and are more reducing compared to surface waters (Fig. 7.6). Most of the groundwaters have Eh-pH values that place them in the Fe^{2+} stability field, whereas, surface waters fall in the $Fe(OH)_3$ field (Fig. 7.6).

Representative groundwaters have been normalized to average Halfmile Lake deposit surface water (Fig. 7.12). Compared to surface waters, groundwaters at the Halfmile Lake deposit have similar pH and Si values, are generally higher in Fe and base metals such as Co, Zn, Cd, and Pb, and are much more enriched in Mn (Fig. 7.12). Copper values are more variable and some groundwaters have lower Cu contents than surface waters. Calcium and magnesium are only moderately enriched compared to surface waters with the exception of Na-rich groundwaters (Ca-Na-HCO_3-, Na-Ca-HCO_3-, Na-HCO_3-type waters) which have lower Ca and Mg than average surface water. Sodium and Cl are generally elevated in the groundwaters, as are K, Ba, and Rb. Strontium typically shows the same behaviour as Ca.

7.3 Hydrochemistry of Groundwaters at the Restigouche Deposit

Boreholes sampled for groundwaters were selected on the basis of access and distribution with respect to the main sulphide deposit. For the packer system, holes were selected that provided a cross section of the sulphide deposit and that were removed from mineralization to provide background compositions. In general, cased holes (NQ) drilled in 1988 and 1989 by Marshall Minerals were open and accessible (MM-88 and MM-89 series holes). Most of the BQ holes (> 90 holes) drilled by Marshall Minerals were uncased and were therefore not accessible for sampling due to caving of unconsolidated overburden and shallow bedrock. In addition, two of the holes drilled between 1980 and 1982 by Billiton were partially to fully open (B-80 series holes). Older holes were generally blocked at or near surface. Of the boreholes sampled using the packer system, three penetrate the massive sulphides (boreholes MM-88-01, MM88-02 and B80-07) and the other two are east of the deposit (MM-89-106 and MM-89-107) and do not intersect massive sulphide mineralization. Additional holes were sampled using the flow-through bailer. Of these, three are in the main ore zone and two intersect massive sulphide mineralization at shallow depth (8.4 - 55.4 m below surface, MM-88-06, and 2 - 51 m below surface, MM-88-07). The third borehole, EH-1, is a large diameter hole drilled for environmental assessment work during the initial mining application by Marshall Minerals. The boreholes in the ore zone form a south-north transect with increasing depth to the north reflecting the northward dip of the Restigouche ore body. The exception is borehole MM-88-02 which was drilled to a depth of 600 m to test a gravity anomaly for potential additional mineralization at depth (Westoll, 1990). Other boreholes sampled include B-80-15 and MM-89-100 which were drilled through hanging wall units to the south of the gossan outcrop, MM-89-104 and MM-89-109 located approximately 1 km to the west (Westoll, 1990), and MM-89-102, a 400 m borehole located to the northeast of the main ore zone (Fig. 7.13B). In addition, two artesian boreholes drilled into the mineralized C4/C5 deposits to the northwest of the Restigouche deposit were also sampled at the surface (Fig. 7.13A).

7.3.1 Major cations and anions

Groundwaters at the Restigouche deposit display a wide variation in geochemistry, spanning a much larger compositional range than groundwaters from the Halfmile Lake deposit (cf Figs. 7.2, 7.14). Shallow, oxidizing groundwaters in contact with the massive sulphides are dominantly Ca-SO_4 to Ca-SO_4-HCO_3 waters (e.g., groundwaters from boreholes MM-88-06, MM-88-07, MM-88-01, and EH-1). These waters typically have TDS contents ranging from 35-55 mg/L in borehole EH-1, and up to 200 mg/L in boreholes MM-88-01 and MM-88-06. Shallow groundwaters recovered from boreholes away from the main ore zone are dominantly Ca-HCO_3 to Ca-Na-HCO_3 waters (Fig. 7.14), with TDS contents ranging from 40 to 320 mg/L. With increasing depth, groundwaters increase in total dissolved solids (up to 3,000 mg/L) and trend towards Na-HCO_3-Cl and ultimately to Na-Cl waters. In the deepest borehole (600 m depth; borehole MM-88-02), Na-(Ca)-Cl waters were recovered with up to 21,000 mg/L TDS. These saline waters have lower Na/Ca than the brackish waters from borehole MM-89-106 (Figs. 7.14, 7.15). Groundwaters also show a strong trend with increasing TDS and Cl contents away from Ca-Mg-dominated compositions to Na-dominated compositions (Fig. 7.14). This relationship is evident from the strong correlation between Na and Cl contents (Fig. 7.16). Both Ca and Mg correlate positively with Cl, but groundwaters with Cl contents > 10 mg/L decrease somewhat in Ca and Mg with further increases in Cl. Five groups of groundwaters are evident from the Ca versus Cl plot (Fig. 7.16). Group 1 groundwaters are characterized by low Ca and low Cl. This group includes waters from boreholes EH-1 and MM-89-107. The second group includes waters from boreholes MM-88-01, MM-89-100, MM-89-104, MM-89-109 and B-80-15 and is characterized by high Ca and low Cl. Groundwaters from boreholes MM-89-102 and MM-89-106 contain moderately high Cl and low Ca. Boreholes MM-89-06 and MM-88-07 waters have intermediate Cl and Ca contents. The high saline waters from borehole MM-88-02 represent a fifth group with very high Cl and Ca. Calcium and Mg are highly correlated for all borehole waters ($r^2 = 0.947$), regardless of concentration, suggesting a common control over the dissolved concentrations.

Potassium contents are greatest in the saline waters and in the lowest Cl waters from boreholes EH-1 and MM-88-01. Waters with Cl contents between 1 and 1000 mg/L show very little variation in K contents. Bicarbonate typically increases with increasing Cl, although the relationship is complex (Fig. 7.16) with variable Cl/HCO_3 ratios. Waters with Cl/HCO_3 include the high-sulphate waters from boreholes MM-88-06, MM-88-07 and MM-89-107. The highest HCO_3 contents were measured in water from borehole MM-89-102. The HCO3 contents in brackish and saline waters display an inverse correlation with Cl. Water from boreholes MM-88-01 and B-80-7 has the most elevated Na and Ca contents for a given Cl value whereas, water from MM-88-07 has the lowest Na/Cl and Ca/Cl ratios for water with TDS < 500 mg/L. The higher TDS groundwaters from borehole MM-89-106 have the lowest Ca/Cl ratios.

The SO_4 content of groundwater is generally highest in the vicinity of the massive sulphides. Boreholes MM-88-06 and MM-88-07 are close to the surface outcrop of the deposit (Fig. 7.13) and have elevated sulphate values (36.3 - 51.2 mg/L; Figs. 7.14, 15). Borehole MM-88-01 is further removed from the outcrop, but still intersects the main sulphide zone and has the highest SO_4 values (38-87 mg/L). The water in this borehole is more O_2-rich than water from boreholes MM-88-06 or MM-88-07 (DO = 4 - 5 mg/L versus < 3 mg/L).

7.3.2 Trace elements

Trace elements display patterns similar to the major cations (Fig. 7.15). In general, the trace metals increase with increasing chloride and TDS content (e.g., Sr, Ba, Li). Potassium and Rb contents are higher in the lowest salinity groundwater from boreholes penetrating hanging wall and footwall alteration zones than in more saline water, and probably originate from illitic clays in the fractures by cation exchange and silicate hydrolysis reactions. Potassium and Rb contents are lowest for groundwaters with Cl contents between 0.7 and 20 mg/L above which contents of both elements increase (Fig. 7.16).

Iron contents are generally low in borehole MM-88-01 (160 - 230 µg/L in bailer waters, <

10 µg/L in packer waters), whereas, the most elevated Fe contents are in groundwaters from boreholes MM-88-06 and MM-88-07 (2000-4600 µg/L) (Fig. 7.15). Groundwaters from boreholes which intersect the massive sulphides also have elevated Mn contents compared to other groundwaters. Zinc contents of waters proximal to the Restigouche ore body are also high, up to 5300 µg/L, particularly in boreholes MM-88-01, MM-88-06 and MM-88-07 which have the highest values. Although groundwaters from borehole MM-88-01 has the highest Fe and Zn contents, Pb contents are highest in groundwaters from borehole MM-88-06 and MM-88-07, with values up to 1400 µg/L (Fig. 7.15) indicating metal fractionation in groundwater. Groundwater from two artesian boreholes which intersect the C4 and C5 sulphide deposits have similar base metal contents as groundwaters from boreholes that intersect the Restigouche massive sulphide deposit.

Boreholes remote from the deposit are low in the base metals and SO_4. The groundwaters from the bottom of borehole MM-89-106 and, to a lesser extent, borehole MM-89-107 show an increase in Cu and Mo and in alkali and alkaline-earth elements which would be expected to be associated with hydrothermal alteration. The core descriptions for these holes noted that the units near the bottom of the holes were correlative with the stringer zone underlying the main ore body, but without major stringer sulphide mineralization.

Phosphate contents range from 1 to 223 µg/L and shows moderately strong correlation with TDS ($r^2 = 0.409$). Groundwaters from boreholes intersecting the massive sulphides have low PO_4 values (< 5 µg/L) compared to other groundwaters (Fig. 7.15). Bromine ranges up to 1280 µg/L, excluding the saline waters which have Br contents up to 10,775 µg/L.

7.3.3 High salinity waters (borehole MM-88-02)

Saline waters from borehole MM-88-02 are classified as NaCl-type waters based on Piper diagram (Fig. 7.14). Based on the classification of Gavrieli et al. (1995), these waters are of Ca-Cl-type. Gavrieli et al. (1995) defined Ca brines on the basis of Na/Cl < 1, and (Cl-Na)/Mg > 1, implying that at least part of the chloride is balanced by Ca. Ca-Cl-type brines also have

$Ca/(SO_4 + HCO_3) > 1$, indicating that there has been relative depletion of sulphate and bicarbonate compared to chloride. Groundwaters from borehole MM-88-02 have Na/Cl ratios that range from 0.70 to 0.78, (Cl-Na)/Mg from 5.65 to 8.68, and $Ca/(SO_4 + HCO_3)$ from 7.76 to 9.24.

Restigouche deposit saline waters differ from saline formation waters and Canadian and Fennoscandian shield brines in that they have no SO_4 and low Br contents. Bromide contents range from 9275 - 10779 µg/L and $Br/Cl_{(molar)}$ ratios are extremely low ($Br/Cl_{(molar)}$ = 0.00031 - 0.00036).

The saline waters have lower TDS than seawater with proportionately lower Cl and Na (Appendix B.3.1) but have considerably lower Mg and higher Ca, producing higher Ca/Mg ratios than seawater. Borehole MM-88-02 groundwaters are also depleted in K and Rb compared to seawater. Barium and Sr, along with Li and Cs are elevated compared to seawater.

The saline waters have low Pb (< 1-2 µg/L) and moderately high Zn and Fe contents. Zinc ranges from 370 to 1700 µg/L (though < 20 µg/L in all bailer groundwaters) and Fe from 1000 to 3000 µg/L. For the packer groundwaters from borehole MM-88-02, there is no obvious explanation for the high Zn and Fe contents, as these groundwaters are from well below the ore zone. These saline waters also have high Cu compared to the other groundwaters (Fig. 7.15) and may indicate that these saline waters have reacted with the mafic dykes which constitute a significant portion of the lower half of the stratigraphy in this hole. This interpretation is consistent with the higher Cr and Ni values for these waters as well (Appendix B.3.1). It is also evident that the K/Cl and Rb/Cl are anomalously low in these waters, compared to other Restigouche groundwaters. Potassium and Rb are elements that are typically depleted in mafic rocks compared to felsic rocks that dominate the stratigraphy at Restigouche (Chapter Two). For example, K/Cl ratios for MM-88-02 waters are the lowest of all groundwaters at Restigouche. The Marshall Minerals assessment report suggested that the mafic dykes were likely intruded along major faults cutting the deposit. These reactivated faults may also have

acted as conduits for saline fluids.

7.3.4 Downhole variations

Borehole MM-89-106 was sampled in detail with both the flow-through bailer and the straddle-packer system. Bailer waters indicate an increase in TDS with depth, however, packer waters below 125 m have considerably higher TDS contents than bailer waters from the same depth (Fig. 7.18). There is, therefore, a sharp break at around 125 m depth separating a shallow groundwater system dominated by $CaHCO_3$ waters (Fig. 7.14) from a deeper system composed of NaCl waters. There are no obvious downhole relationships with lithology. Most of the lithologies close to the deposit are felsic volcanic flow and pyroclastic rocks (Chapter Two). The major anions and cations all show a sharp increase at around 125 m depth, whereas, changes in trace elements are not as consistently tied to water-type. Both Eh and pH also change at 125 m depth. Above this depth, pH is less than 8 (for packer groundwaters), and > 9 below 125 m depth. The Eh decreases with increasing depth to 100 m, and then increases below 125 m depth. Although Eh measurements are semi-quantitative, the downhole variations for Fe are consistent with the Eh results. Iron reaches a maximum where Eh is lowest in the upper part of the hole, and is close to or below detection in the lower part of the hole where Eh is high. At high Eh and pH, Fe^{3+} is stable relative to Fe^{2+}. $Iron^{III}$ is highly insoluble and rapidly precipitates as $Fe(OH)_3$. This change in the behaviour of Fe as a function of Eh and pH is demonstrated by the results of speciation calculations. The waters below 125 m depth have $Fe(OH)_{3(aq)}$ and $Fe(OH)_4^-$ as the dominant Fe species, whereas those from above 125 m depth have significant ferrous Fe species (Fe^{2+}, $FeHCO_3^+$, $FeCO_{3(aq)}$). Other trace metals such as Zn, Co, and Cd show maximum contents coincident with elevated Fe contents and these elements may be controlled by adsorption/desorption reactions with Fe-oxyhydroxides. Metals such as Cu, Mo, As, Ni, Cr, and Al show similar patterns downhole and exhibit sharp increases towards the bottom of the hole (Fig. 7.18). These increases are coincident with a change in the lithology from rhyodacite flows to pyroclastic rocks at the

bottom of the hole that are interpreted as non-mineralized equivalent to the stockwork zone of the main ore body (Westoll, 1990). Zinc and Pb show very different trends downhole. Zinc contents are greatest in the upper part of the hole ranging up to 230 µg/L, decreasing to 13 - 14 µg/L at the bottom of the hole. In contrast, Pb contents are around 0.2 µg/L at the top of the hole and increase to 1.0 to 1.3 µg/L at the bottom of the hole (Fig. 7.18).

Borehole B-80-7 was drilled close to the northern limit of the Restigouche ore body (Fig. 7.13). Consequently, massive sulphides occur at greater depth than in other holes intersecting the ore zone. In contrast to borehole MM-89-106, the packer and bailer data are fairly similar, although no shallow packer groundwaters were collected due to problems with the packer apparatus. The exception is the deepest packer groundwater (223 m depth) which has higher TDS, HCO_3, Cl, Na and K and lower Eh, SO_4, Ca, and Mg contents than the other packer and bailer waters (Fig. 7.19). The sharp change at the bottom of the hole suggests that the more shallow waters are unrelated to the deeper waters. Packer groundwater pH values are lower at the bottom of the hole, and may account for the increase in dissolved Al at the bottom of the hole (Fig. 7.19). In contrast, the sharp increase in Fe and Mn is probably related to a decrease in Eh resulting in greater Fe solubility. The low Eh would be expected to keep metals in solution which could be removed by precipitation of $Fe(OH)_3$ higher in the hole. Zinc, Pb, and Mn increase in these lowermost waters, consistent with this interpretation. Unlike the other holes that penetrate the ore zone (see below), these waters have low base metal contents (Fig. 7.15, 7.19). For example, Zn is below detection in all bailer groundwaters. Either the sulphides are too deep to have undergone extensive oxidation or the waters in the hole are dominated by waters flowing below or well above the ore zone. The most significant zone in terms of potential water flow, based on density and temperature gradient anomalies in the downhole geophysical data (Chapter Four; C.J. Mwenifumbo, unpublished data), occurs at around 175 m depth. Groundwater MLW95-581 was collected with the straddle-packer from this depth, and has low metal contents.

Several boreholes intersect the main ore body at depths of 2 to 51 m (MM-88-07), 8.4 to

55.4 m (MM-88-06) and 63 to 83.25 m (MM-88-01). Borehole EH-1 is located only a few meters from MM-88-01 and does not intersect the ore zone. In borehole MM-88-06, Ba and Sr contents increase downhole, similar to Na and Cl (Fig. 7.20). The most consistent interpretation is that these waters have mixed with a small component of the saline waters recovered from borehole MM-88-02. Borehole MM-88-07 has high Cl and Na, moderate Sr, and lower Ba than the other short boreholes. If these waters have also mixed with the saline waters, Ba has been lost from the system, perhaps due to precipitation of barite. Borehole MM-88-07 waters are saturated with respect to barite ($SI_{barite} = 0.142$). Base metals are highly elevated in boreholes MM-88-06 and MM-88-07 reflecting the positive DO and Eh and lower pH of these waters and the shallow nature of the ore zone which is clearly undergoing extensive oxidation of the sulphide minerals. Borehole MM-88-01 has higher Zn and SO_4 in the bailer groundwaters but much lower Pb and Fe compared to boreholes MM-88-06 and MM-88-07.

There is very little downhole variation in the composition of groundwaters in borehole MM-88-02. Both bailer and straddle-packer groundwaters show consistently high salinity (Appendix B.3.1). One exception is groundwater MLW96-669, a straddle-packer groundwater recovered from 47 m depth. The packer was in place for much longer than other groundwaters collected from the borehole. The conductivity of the waters was initially high, on the same order of magnitude as the deeper groundwaters (40,000 µS/cm; Fig. 7.21). However, the conductivity quickly fell before levelling off at around 15,000 µS/cm. This value is still considerably higher than values for groundwaters in adjacent boreholes.

7.3.5 Statistical analysis

Summary statistics (Appendix B.3.2), Pearson Product Moment correlation (PPM; Appendix B.3.3) and Principal Component Analysis (PCA; Appendix B.3.4) were carried out on the Restigouche deposit groundwaters to try and ascertain some of the interrelationships amongst the major variables. Both the PPM correlation and PCA analyses were run twice using

the field parameters and major anions and cations (pH, Eh, DO, HCO_3, SO_4, Cl, Mg, Ca, Na, and K); one run included the highly saline waters from borehole MM-88-02 and the second run did not. In the first case, the very elevated Cl, Na, Mg, Ca, and K contents of the saline waters skews the analysis and causes biased correlation between Mg, Na, and K with Cl. In the second PCA analysis, only Na is well correlated with Cl. The results will be dealt with more fully in the discussion section. However, it is evident from the PCA (Figs. 7.22, 7.23) that there are no simple relationships between the different groundwaters, and at least 4 or 5 end-member compositions can be derived, not including the highly saline end-member (borehole MM-88-02 waters).

7.3.6 Geochemical modelling

The groundwaters were modelled for speciation and mineral saturation indices (SI) using the EQ3NR and PHREEQC codes, as described for the Halfmile Lake deposit groundwaters (section 7.2.5). In some cases, for major elements which were below detection, levels were set to half the detection limit. For example, the saline waters from borehole MM-88-02 have sulphate contents below detection. These waters had sulphate contents set to 0.025 mg/L based on the observation of barite in suspended sediments in groundwaters from this hole (see Chapter Nine).

The calculated activity of Al in the Restigouche deposit groundwaters is highly variable and greatly depends on solution pH and the speciation code used to calculate the activities (see Chapter Three). According to PHREEQC derived speciation, in higher pH waters, Al is present primarily as $Al(OH)_4^-$, with other hydroxyl forms present in much lower abundance. In contrast, EQ3NR calculations suggest that at high pH (> 7.5), Al occurs primarily as AlO_2^-. At lower pH, the solubility and activity of Al is highly dependent on the activity of F^- in the system; lower pH waters with detectable F have in excess of 80% Al accounted for by F species (i.e. AlF^{2+}, AlF_2^+, $AlF_{3(aq)}$; Appendix B.3.6), according to both speciation programs.

As would be expected, monovalent cations typically occur as free ions in dilute waters.

EQ3NR indicates that Cs, Rb and Na form Cl complexes in the most saline waters from borehole MM-88-02. Cesium also forms Cl complexes in the deeper waters from borehole MM-89-106. The PHREEQC code indicates that Rb only occurs as free ions, and that Na and K form SO_4-complexes for the high-sulphate waters from the main ore zone, and Na forms CO_3 and HCO_3 complexes in the higher pH waters (above a pH of 8.5). However, these sulphate and carbonate complexes are always less than 1% combined of the Na and K species (Appendix B.3.6).

Saturation calculations suggest that the total amount of Pb in borehole MM-89-106 waters may be controlled by Pb and Cl equilibria (Appendix B.3.6). The deepest groundwater from borehole MM-89-107 is saturated with respect to the mineral $(Pb(OH)_2)_3 \cdot PbCl_2$ and with decreasing depth in the hole, the degree of undersaturation with respect to this mineral increases (Appendix B.3.5). The activity of Pb and Cl are not the only critical parameters for the stability of this mineral. For example, the high salinity waters from borehole MM-88-02 have Pb concentrations similar to the deeper waters from MM-89-106, and have Cl activities an order of magnitude greater, yet are very undersaturated with respect to PbCl minerals. However, when the MM-88-02 waters were run through EQ3NR with an increase in pH from the measured values of 7.8 to 8.0 to a value of 9.0, $(Pb(OH)_2)_3 \cdot PbCl_2$ was supersaturated. Even in high sulphate waters associated with the main ore body, Pb occurs primarily as a free ion according to EQ3NR calculations. The activity of $PbSO_{4(aq)}$ is never greater than 10^{-20} mol/L. Although no waters are saturated with respect to anglesite ($PbSO_4$), waters from borehole MM-88-06 and MM-88-07, which have the highest Pb contents, approach saturation with respect to this mineral (e.g. $SI_{angelsite} = -0.833$ in groundwater MLW95-315; Fig. 7.24). As discussed later (Chapter 9), suspended sediments filtered from borehole MM-88-06 and MM-88-07 waters are dominated by Fe and Pb sulphur species.

Restigouche groundwaters show a very strong correlation between $SI_{chlorite}$ and pH (Fig.7.24). The groundwaters with the highest pH, highest Cl, and thus greatest extent of water-rock reaction (boreholes B-80-7, MM-89-102, MM-89-106) are saturated to

supersaturated with respect to chlorite. The most saline waters, from borehole MM-88-02, are saturated with respect to chlorite, but have lower pH than the brackish waters and therefore fall off the trend of the shallower groundwaters.

None of the groundwaters at the Restigouche deposit are saturated with respect to Pb-sulphide, -sulphate, or -carbonate minerals. However, groundwaters intersecting the deposit close to its surface expression (boreholes MM-88-06 and MM-88-07) have high Pb abundances and are closest to saturation with respect to anglesite ($PbSO_4$) and cerussite ($PbCO_3$; Fig. 7.24). There is a strong correlation between $SI_{cerussite}$ and Pb abundance (Fig. 7.24). However, there is no such correlation between $SI_{cerussite}$ and HCO_3 abundance. There is an apparent upper limit of cerussite saturation index that is increasingly negative with increasing HCO_3 abundance (Fig.7.24). The groundwaters with the highest HCO_3 abundances typically have the lowest Pb abundances and in these waters Pb speciation is dominated by carbonate and bicarbonate complexes. Groundwater MLW95-570 from borehole MM-89-102 has, according to PHREEQC speciation, no Pb as free ions. In contrast, high Pb groundwaters with low HCO_3 contents, have variable amounts of Pb present as free ions. Note that although no groundwater is saturated with respect to metal-sulphate minerals, XRD and SEM data from suspended sediments trapped on filter papers for groundwaters from boreholes MM-88-06 and MM-88-07 suggest that Fe-sulphate and anglesite may have precipitated from these waters (Chapter Nine). The only documented occurrence of anglesite in the BMC is in the gossans from the Restigouche deposit (Boyle, pers. comm.). As pH increases, carbonate and Cl complexes of Pb become dominant over free ions (Fig. 7.25). In contrast, at higher pH, carbonate and hydroxide complexes become dominant for Fe and Zn (Fig. 7.26). Restigouche groundwaters straddle the boundary between ferrous and ferric Fe (Fig. 7.26). Groundwaters recovered from within the massive sulphide zone at the Restigouche deposit have high Fe and tend to plot in the Fe^{2+} stability field. Higher pH water have low Fe contents and typically plot in the Fe^{3+} stability field. Groundwaters from borehole MM-88-01 are for the most part reducing with high Fe contents, consistent with Fe speciation dominated by Fe^{2+} (Fig. 7.26).

Fluorine and phosphate form rare complexes with divalent cations, but always in very low abundance (typically « 1% of cation abundance; Appendix B.3.6). Bromide is essentially never complexed at significant levels.

Activity-activity diagrams show that the Restigouche deposit groundwaters are below quartz saturation (Fig. 7.27). However, the very constant value of SiO_2 activity for the waters indicates that Si contents are being controlled by a Si-phase. Most of the groundwaters plot on the gibbsite-kaolinite cotectic, similar to the Halfmile Lake deposit groundwaters. However, Restigouche deposit groundwaters trend to higher Ca, Na, and K activities, with the higher TDS waters plotting in the muscovite and paragonite fields (Fig. 7.27).

7.3.7 Comparison with surface waters

Selected Restigouche deposit groundwaters have been normalized to average surface water from the Restigouche deposit area (Fig. 7.28). Three major groups of waters are shown in figure 7.28 including deep brackish to saline (NaCl) waters, shallow groundwaters recovered away from known mineralization, and shallow groundwaters recovered from within the Restigouche deposit ore zone and from the C4/C5 deposit.

Compared to average surface water, saline and brackish groundwaters are enriched in all elements with the exception of Si, Y, Ti, and Pb (Fig. 7.28A). These high TDS groundwaters have much lower SO_4 contents compared to surface waters.

Groundwaters distal to the deposit are compositionally more similar to average surface water (i.e., groundwaters with $CaHCO_3$ and $CaNaHCO_3$ compositions) but typically have higher Cl, Na, Ba, U, HCO_3, Zn and Cd (Fig. 7.28B). Transition metals Ti, V, Co, Ni, and Cu are generally in lower abundance in these groundwaters compared to average surface water. Iron is variable with some groundwaters having very low Fe contents.

Shallow groundwaters proximal to mineralization are generally SO_4-rich and have moderately to highly elevated base metal (Pb, Zn, Cd) contents compared to surface waters (Fig. 7.28C). Copper contents are close to or lower than average surface water. Some of the

shallow groundwaters are elevated in Cl, Br and Na compared to surface waters. This most likely reflects post-drilling mixing with saline groundwaters from borehole MM-88-02 (see discussion). Groundwaters from the C4/C5 deposits are very Mg-rich compared to other groundwaters and surface waters.

7.4 Groundwaters at Heath Steele, Brunswick #12, Willett and Wedge deposits

Although sampling of waters from the other deposits in the Bathurst Camp was not a major focus of this study, several days were spent at Heath Steele and Brunswick #12 mines in order to get a general idea of the chemistry of groundwaters associated with active mining for comparison with the un-mined Halfmile Lake and Restigouche deposits. Additional groundwaters were collected from the Wedge (past producer of Cu ore) and Willett (small recently discovered occurrence) deposits. One borehole from the Stratmat Main zone deposit was sampled with a straddle-packer system, and these results are discussed in a subsequent chapter (Chapter Eight). Due to time constraints, sample locations were chosen on the basis of known areas of water flow within the two mines. Overall chemical balances are generally good with all groundwaters less than 10% error with the exception of the very low pH waters from the Heath Steele B zone and the groundwater from the Wedge deposit which flows through the waste pile. The very high abundances of Al, Fe, and Zn in these waters requires that these elements be included as cations in the charge balance equation.

Although these waters come from disparate locations (Fig. 7.29) and span a large range in composition (Fig. 7.30), there are a number of features which they share in common. For example, Cl, SO_4, and HCO_3 increase systematically with increasing TDS, with the notable exception of the saline water from the Brunswick #12 deposit, which has low SO_4 and HCO_3 (Fig. 7.31). These trends are mimicked by the major cations Ca, Mg, K, and to a lesser extent Na, and by Sr, and Rb. Barium is more scattered but typically shows decreasing contents with increasing TDS, again with the exception of groundwater MLW95-492 from the Brunswick

#12 deposit. Most of the base metals display scattered relationships with TDS, although there appears to be two broad groups of groundwaters. One group shows increasing Zn, Co, Fe, Mn and to a lesser extent Cu and Pb contents with increasing TDS, whereas the second group has high TDS but no increase in metal loads (Fig. 7.31). There is a relatively strong relationship between Eh and TDS such that Eh values decrease with increasing TDS. Iron, Zn and Mn increase with decreasing pH, and Fe and Mn generally have higher values at lower Eh values (Fig. 7.32).

7.4.1 Heath Steele deposit

A total of sixteen groundwaters were collected from Heath Steele mine, from a range of depths within the B and C zones (Appendix C.1.1). As a general rule, TDS contents increase with increasing depth in the deposit, although the groundwater with the highest TDS (5,330 mg/L; groundwater MLW95-486) is from 450 m depth whereas the deepest waters have TDS values between 1,120-1,820 mg/L. The Heath Steele waters are highly variable in major and trace element composition. With the exception of the three deepest waters and groundwater MLW95-488, all the waters have dominantly $CaSO_4$ to $CaSO_4HCO_3$ compositions. The deepest waters are Na-rich (Appendix C.1). Most of the waters have elevated sulphate contents ranging from 16.7 to 4,572 mg/L. Many of the groundwaters were collected from boreholes or fractures that intersected areas of massive sulphide mineralization (see Appendix C.1.1). The waters with the lowest TDS and SO_4 are closest to the surface with the exception of groundwaters MLW95-487, 488 and 489 from 187 m depth. These waters were collected away from known mineralization and have low SO_4 contents as well as low Fe contents, consistent with the lack of Fe-oxide staining where the waters exited. In contrast, most of the other Heath Steele waters were associated with build up of Fe-oxide precipitates. Low Eh waters associated with significant accumulations of Fe-oxides on drift walls have very elevated Fe contents, up to 650 mg/L (groundwater MLW95-486). Iron contents are also strongly negatively correlated with pH (Fig. 7.32). In addition, base metals reach elevated contents in

the lowest pH waters (Fig. 7.32). Zinc ranges up to 340 mg/L and Co to 2,500 μg/L whereas Pb (35 μg/L) and Cu (860 μg/L) are not as enriched. Aluminum contents are generally low, except in the very low pH waters recovered from the Heath Steele B-zone, where Al contents are up to 12,000 μg/L. The lowest Zn contents occur in shallow groundwaters (< 200 m depth) in the C-zone deposit and in the groundwaters collected from the deepest level in the B-zone deposit (840 m).

7.4.2 Brunswick #12 deposit

The Brunswick #12 deposit is very dry and surface water is pumped into the mine to keep dust levels down. As a consequence, only two groundwaters were collected from the mine along an exploration drift on the 1000 m level. Groundwater MLW95-492 was collected from an angled drill hole near the base of the drift wall. Water flow was almost non-existent, although levels recovered after sampling. Intermittent gas bubbles were also observed. Groundwater MLW95-493 was from an old drill hole in the drift wall which was flowing slowly and had light olive-grey mud precipitated on the wall. A drill hole lower down the wall had a white precipitate but no flow at the time of sampling. Groundwater MLW95-493 has very high NO_3 contents (193 mg/L) suggesting that this groundwater is contaminated by drilling fluids. Both of the Brunswick #12 groundwaters are Na-Cl waters, although MLW95-493 also has high SO_4 whereas groundwater MLW95-492, like the saline waters from the Restigouche deposit, has SO_4 contents lower than detection. Although the two groundwaters were collected along the same exploration drift, they have very different trace element compositions. Groundwater MLW95-492 is characterized by low metal loads with Fe = 6 μg/L, Al = 13 μg/L, and Zn = 22 μg/L. In contrast, groundwater MLW95-493 has much higher metal contents with Fe = 96,000 μg/L, Al = 45,000 μg/L and Zn = 31,000 μg/L. The former groundwater is also characterized by very high Ba (390,000 μg/L) and low Sr (880 μg/L) compared to the latter water (200 and 7,300 μg/L, respectively).

7.4.3 Willett deposit

Three groundwaters were collected from seeps and an artesian drill hole within the massive sulphide outcrop and five groundwaters were collected from two boreholes using the pressure-profiler. Waters from a borehole approximately 100 m northeast of the outcrop of the deposit (borehole 95-10) have the highest TDS levels recorded at the Willett deposit, ranging from 350 to 360 mg/L. In contrast, waters from borehole 95-15 and from the seeps in the sulphide outcrop have lower TDS, ranging from 40 to 120 mg/L (Appendix C.1.1). The presence of higher TDS waters close to surface in borehole 95-10 compared to the other shallow groundwaters sampled suggests upward gradients in the hole. However, trace metal contents decrease systematically downhole. For example, the shallow groundwater (MLW95-716) has the most elevated Fe (175 μg/L), Cu (26 μg/L) and Zn (49 μg/L) contents in the hole, whereas, the deepest groundwater has the lowest Fe (27 μg/L), Cu (1.3 μg/L), and Zn (4 μg/L) and the highest Pb (24 μg/L). Sulphate is also highest where metal contents are highest. The two seeps at the top of the sulphide outcrop have low TDS (40 mg/L) and do not have associated Fe-oxyhydroxide precipitates (Fe < 3 - 380 μg/L), whereas the artesian drill hole water is actively precipitating Fe-oxyhydroxide minerals and has much higher metal contents (Fe = 2800 μg/L, Zn = 1400 μg/L).

7.4.4 Wedge deposit

Two water waters were collected from the Wedge deposit. The Wedge deposit differs from the Halfmile Lake and Restigouche deposits in that it has an extensive copper zone that was mined from 1962 until 1968 (Walker and McCutcheon, 1996). The copper-rich character of this deposit is reflected in the seep (MLW95-482) which has 17,000 μg/L Cu, far greater than any other water in this study. The two waters recovered from the Wedge deposit come from different settings. Seep MLW95-482 was sampled from a seep towards the base of a debris pile close to the Nepisiguit River. Seeps in the debris pile dry up by mid-summer but the large extent of ferricrete development and Fe-Al-sulphate precipitation indicates that the seeps are

important pathways of metal mobility from the Wedge Deposit. Seep MLW95-482 is characterized by low pH (2.33), high sulphate (1331 mg/L) and high metal loads, e.g., Fe (96,000 µg/L), Al (45,000 µg/L), Cu (17,000 µg/L), Ni (190 µg/L), and Zn (31,000 µg/L).

In contrast, groundwater MLW95-491 was collected from an artesian borehole adjacent to the Forty Mile Brook. This hole has consistently produced Fe-rich waters for many years (Belland, 1991). As a consequence, the drill hole collar is no longer visible, having been buried in thick accumulations of Fe-oxyhydroxides. The Fe-oxyhydroxide mound is approximately 50 cm high and 1.5 m in diameter at its top, spreading to 3 m in diameter at the base. Water flow from the top of the mound is steady. The waters flowing from this mound differ from the seep in that the pH is neutral (7.25), TDS is lower (1,200 versus 1,600 mg/L) and metals are lower (e.g., Fe (23,000 µg/L), Cu (2.1 µg/L) and Zn (2,300 µg/L)). Groundwater MLW95-491 is also dominantly a SO_4 water, but the Ca content is higher than the seep water (Fig. 7.26).

7.4.5 Geochemical modelling

Geochemical speciation and mineral saturation calculations were performed on the mine waters using EQ3NR, PHREEQC, and The Geochemist's Workbench. The results presented in the appendices (Appendix C.1.3 and C.1.4) are based on the PHREEQC data.

Results of the geochemical modelling are varied, as expected from the wide range in water chemistry represented by these mine waters. For the seep from the Wedge deposit, measurement of Eh in the field was unsuccessful, so an Eh of 0 mV was assumed in the calculations. This water highlights the sensitivity of the speciation models to pH and Eh. For example, the modelling indicates that the S in this water occurs as HS-. Thus, several sulphide minerals (e.g., pyrite, chalcocite, chalcopyrite, sphalerite) are saturated in this water. The main Fe-oxyhydroxide minerals are all very undersaturated in this water, at odds with the observation of ferricrete formation where the seeps exit. None of the mine waters are saturated with respect to jarosite, despite high sulphate and low pH in some of the Heath Steele and

Wedge deposit waters. This is because the measured Eh values (or assumed, in the case of MLW95-482) are too low, such sulphate activity is too low to stabilize jarosite. In Heath Steele deposit groundwaters MLW95-485 and MLW95-486, jarosite is saturated if the Eh is increased to around 200 mV. Most of the mine waters, with the exception of those with low pH, are saturated or close to saturation with respect to barite and many of the carbonate minerals (calcite, dolomite, and siderite).

7.5 Discussion

7.5.1 Halfmile Lake deposit versus Restigouche deposit groundwaters

Groundwaters from the Restigouche deposits differ from those at the Halfmile Lake deposit in a variety of ways. Restigouche deposit groundwaters trend to much more Na- and Cl-rich compositions (Fig. 7.34). Many of the groundwaters from the other mines are more enriched in Na relative to Cl than groundwaters from the Halfmile Lake and Restigouche deposits. Mine waters also typically have higher SO_4 than other groundwaters, whereas Halfmile Lake deposit groundwaters have generally low SO_4 contents. At Cl contents above 100 mg/L, SO_4 values typically decrease (Fig. 7.34). In general, Restigouche deposit groundwaters are more Ca- and Mg-rich than those from the Halfmile Lake deposit, and groundwaters closest to the Restigouche orebody are much more SO_4-rich than Halfmile Lake deposit groundwaters (Figs. 7.34, 7.35). This reflects the lower degree of water-rock reaction at the Halfmile Lake deposit and the more shallow nature of the Restigouche ore body and therefore the greater degree of sulphide oxidation. The only groundwaters from the Halfmile Lake deposit with SO_4/HCO_3 ratios similar to Restigouche deposit groundwaters are from borehole HT55-43 in the Upper AB zone. This hole penetrates the gossan and is therefore most analogous to the boreholes at the Restigouche deposit (i.e., associated with near-surface sulphides).

Groundwaters at the Halfmile Lake deposit have higher average Al contents than groundwaters at the Restigouche deposit. For example, at the Restigouche deposit all of the groundwaters, with the exception of those from borehole MM-88-01, have low Al (Appendix

B.3.1). Restigouche deposit groundwaters are also very low in Mo compared to those from the Halfmile Lake deposit. At the Restigouche deposit, most of the groundwaters are below or close to the detection limit for Mo, whereas, those from the Halfmile Lake deposit are mostly above detection and range up to 16 µg/L (Fig. 7.36). There are strong correlations between Mo and Al for Halfmile Lake deposit waters ($r^2 = 0.547$) which suggests that these elements are behaving in similar ways and that the low Al and Mo in the Restigouche deposit waters is not a function of analytical error. The difference in the Al contents of the Halfmile Lake and Restigouche deposit groundwaters is most likely due to the generally lower pH of the former. This lower pH also has important implications for REE stability and REE patterns in groundwaters (see Chapter Ten). Groundwaters from the other mines have variable Mo contents and are generally lower than those for the Halfmile Lake deposit (Fig. 7.36).

Groundwaters from the Halfmile Lake and Restigouche deposits have different base metal contents. Restigouche deposit groundwaters generally contain higher base metal contents (Zn + Cu + Pb + Cd + Co) at higher pH values than Halfmile Lake deposit groundwaters (Fig. 7.37). The Wedge deposit seep and the low pH water from the Heath Steele deposit have the highest base metal loads, similar to very elevated values associated with acid mine drainage sites in Colorado, such as the Summitville Mine (Fig. 7.37).

Geochemical modelling with PHREEQC illustrates some of the differences between groundwaters from the Halfmile Lake and Restigouche deposits. Most of the modelled groundwaters from the Halfmile Lake deposit have $SI_{kaolinite} > 0$, i.e., most of these waters are saturated to supersaturated with respect to kaolinite. These waters show a very strong correlation between $SI_{kaolinite}$ and Al content (Fig. 7.10). Many of the groundwaters fall on a line indicating an upper limit to kaolinite supersaturation, presumably due to constraints imposed by another Al-phase. It is most likely that gibbsite is in part controlling Al abundance in these waters. Groundwaters that define the straight line on the $SI_{kaolinite}$-Al diagram (Fig. 7.10), fall on the gibbsite-kaolinite cotectic (Fig. 7.9), whereas, groundwaters that have lower $SI_{kaolinite}$ than the apparent upper limit, plot primarily in the kaolinite stability field. Compared

to pH, Halfmile Lake deposit groundwaters with the lowest $SI_{kaolinite}$ have the highest pH, with the exception of two waters from borehole HN94-65, which plot close to the muscovite stability field (Fig. 7.9).

In contrast, groundwaters from the Restigouche deposit have lower silica activity and therefore tend to plot more in the gibbsite stability field compared to Halfmile Lake deposit groundwaters (Fig. 7.25) and also trend to higher log([K]/[H]), log([Na]/[H]), and $\log([Ca]/[H]^2)$. As a result of both of these factors, there is only a very weak correlation between $SI_{kaolinite}$ and Al abundance (Fig. 7.26). Additionally, $SI_{kaolinite}$ values are generally lower and more groundwaters are undersaturated with respect to kaolinite than is the case for the Halfmile Lake deposit. The Restigouche deposit groundwaters with $SI_{kaolinite} < 0$ are mainly from boreholes B-80-7, MM-89-106 and MM-89-102. These waters plot outside the kaolinite stability field and apparently are stable with respect to muscovite. Compared to Halfmile Lake deposit groundwaters, those from the Restigouche deposit show a strong negative correlation between $SI_{kaolinite}$ and pH (Fig. 7.26).

7.5.2 How representative of the true groundwater chemistry are the bailer and packer sampling methods?

Bottomley et al (1984) noted that sampling of depth-representative groundwaters in low-permeability fractured rock is difficult due to contamination by waters used in drilling the boreholes, mixing within open boreholes by groundwaters entering the hole from different fractures at different depths, and because fractures commonly have low hydraulic conductivities which increases the difficulty and time of sampling. It was hoped in this study that the use of the straddle-packer system would overcome some, or all, of these problems. Work by Bottomley et al. (1984) and Graham and Johnson (1991) suggests that much longer time periods and greater extraction volumes are required to obtain a depth-representative groundwater than was achieved at the Halfmile Lake and Restigouche deposits. The small volumes extracted using the straddle-packer may mean that the measured geochemistry of the

waters do not accurately reflect the true groundwater compositions at the sampled depths. However, conductivities typically reached steady state fairly rapidly at the Restigouche deposit (e.g., Fig. 3.4) and I believe that much of this data is probably a fair representation of the groundwater geochemistry. Certainly the straddle-packer data is likely to be more accurate than the bailer method, as best illustrated by borehole MM-89-106 (Fig. 7.18). However, saline groundwaters collected from borehole MM-88-02 at the Restigouche deposit show only minor differences between bailer and packer-derived groundwaters. The situation at the Halfmile Lake deposit is more equivocal, especially given the many problems experienced with the packer system at that deposit.

In order to fully address the question of the cause of the low salinities observed at the Halfmile Lake deposit, it is important to establish how representative the different groundwater sampling techniques used in this study are of the true groundwater compositions. The success of the flow-through bailer in fracture-flow dominated systems is highly dependent on the variations in hydraulic gradients and hydraulic conductivities with depth. For example, high salinity waters were recovered throughout borehole MM-88-02 using the bailer system, confirmed by the packer sampling, at least at depths > 185 m. This suggests that either high salinity waters dominate the hole or that discrete fractures which are transmitting the saline fluids have sufficiently high head to prevent contribution from low TDS shallow groundwaters (Fig. 7.21). High hydraulic head would allow saline waters to flow along more shallow fractures, displacing shallow, low-TDS groundwaters. This is suggested for groundwater MLW96-669 (47 m depth), where the packer was in place for a greater number of sampling intervals than for other groundwaters taken from this hole (Fig. 7.21). The electrical conductivities of the waters in this zone levelled off at around 15-16,000 μS/cm. This conductivity may represent the true value for groundwaters at this depth, or more likely, it represents a function of mixing between shallow groundwaters and saline waters travelling along fractures which originate below the packers (Fig. 7.21). In contrast to borehole MM-88-02, bailer groundwaters from borehole MM-89-106 showed an increase in salinity with depth

with waters less than 125 m depth having low TDS contents and groundwaters below this depth showing increasing TDS with depth (Fig. 7.18). Although the bailer groundwaters indicated progressive change with increasing depth, the magnitude of the change was suppressed due to mixing within the open borehole, and smaller contrasts in head between deep and shallow waters than was the case in borehole MM-88-02. Straddle-packer groundwaters from borehole MM-89-106 indicate that groundwaters flowing near the bottom of the hole have salinities in excess of 2,500 mg/L, compared to a value of 660 mg/L measured in the deepest bailer groundwater (Fig. 7.18).

Although the straddle-packer system worked well at the Restigouche deposit, it was less successful at the Halfmile Lake deposit. Therefore, most of the groundwaters from the Halfmile Lake deposit were collected using the flow-through bailer. Although a small number of straddle-packer groundwaters were collected from the Halfmile Lake deposit, these groundwaters still have very low TDS values (< 250 mg/L; Appendix A.3.1), although they are generally higher than bailer groundwaters at an equivalent depth. The deepest bailer groundwater from the Halfmile Lake deposit was from 760 m depth. The deepest packer groundwater was from 475 m. This groundwater was lost due to packer failure but the last recorded electrical conductivity for this depth was 340 μS/cm. Thus, although the bailer groundwaters may not be fully representative of the groundwater salinities at the Halfmile Lake deposit, I believe that if saline waters existed at the Halfmile Lake deposit, they would have been observed, even with the flow-through bailer. Saline waters are commonly overpressured, as at the Restigouche deposit (borehole MM-88-02), and therefore should have been sampled if they existed.

7.5.3 Origin of low TDS groundwaters at the Halfmile Lake deposit

Groundwater compositions between the two deposits are distinctly different. Whereas the Halfmile Lake deposit groundwaters are $CaHCO_3$ to $NaHCO_3$ in composition (Fig. 7.2), groundwaters at the Restigouche deposit trend away from these typical compositions to high

salinity NaCl waters (Figs. 7.14, 7.16). Even where groundwaters are similar in terms of water classification (Figs. 7.2, 7.14) between the two deposits, Restigouche deposit groundwaters tend to be higher in TDS, Ca, Na, Cl, HCO_3, SO_4 (Figs. 7.35, 7.36). For Restigouche deposit groundwaters, those shallow groundwaters distal to the deposit are chemically most similar to the groundwaters recovered from the Halfmile Lake deposit. These groundwater regimes are also similar in stable isotope compositions, overlapping local surface water isotopic compositions and indicating modern recharge (Chapter Eleven).

There are a number of possible explanations for the different geochemical signatures for groundwaters at the two ore deposits, and more specifically, why saline waters were not recovered from the Halfmile Lake deposit. These include: 1) saline waters exist at depth in both deposits but have simply not yet been found at Halfmile Lake; 2) saline "zones" are spatially limited such that it is fortuitous that such a zone was encountered at the Restigouche deposit; 3) saline waters are allochthonous and regional flow paths were intersected at the Restigouche deposit but not at the Halfmile Lake deposit; 4) contamination by dilute drilling fluids is more evident at the Halfmile Lake deposit than at the Restigouche deposit; and 5) saline waters are common throughout the BMC, but have been displaced at Halfmile Lake by recharge of young fresh meteoric waters.

1) More than 100 exploration holes have been drilled at the Halfmile Lake deposit since 1987, and many of the holes are > 1000 m in length. If saline waters existed in the subsurface at Halfmile Lake, it seems likely that they would have been intersected by drilling. In contrast, the deepest borehole at the Restigouche deposit is 600 m and most are less than 150 m in depth.

2) The suggestion that such saline zones are spatially limited is inconsistent with similarities in age, topography and geology between the two deposits. In addition, high TDS waters also occur at the Heath Steele and Brunswick #12 deposits.

3) The saline waters at the Restigouche deposit could be allochthonous, possibly from younger sedimentary units to the north and west. The Restigouche deposit is close to the

boundary between the Ordovician rocks of the Tetagouche Group and the overlying Silurian metasedimentary rocks. The Silurian rocks consist of siltstones, sandstones and limestones (McCutcheon, 1997), whereas, there are no equivalent units proximal to the Halfmile Lake deposit. However, the saline waters at the Restigouche deposit are chemically and isotopically closer in affinity to shield-type brines than they are to brines found in sedimentary basins. In addition, the Br/Cl ratios are too low to support derivation from a seawater source, although dissolution of halite could account for the very low Br/Cl (see section 7.5.4).

4) Dilution of the deeper groundwaters by drilling fluid (surface waters were used as a drilling fluid) is inconsistent with low hydraulic conductivities, the fact that the packer groundwaters are not significantly elevated in TDS compared to bailer groundwaters, the composition of groundwaters from more recent holes are similar to those from holes drilled before 1990, and the variation in REE downhole show different waters with depth. In addition, water was typically recovered during drilling below 200 m depth. Some contribution from drilling water, however, cannot be discounted.

5) The preferred interpretation, that saline waters have largely been flushed due to rapid recharge to depth of meteoric waters, is consistent with the low TDS and lower pH of the Halfmile Lake groundwaters compared to those at the Restigouche deposit and with similar stable isotopic compositions in ground and surface waters at the Halfmile Lake deposit. Rapid recharge is also suggested by the positive Eh and moderate to high DO values of deeper groundwaters at the Halfmile Lake deposit. In addition, the variation in REE downhole show different waters with depth (see Chapter Ten). Deeper groundwaters at the Halfmile Lake deposit have REE profiles similar to the host rocks, unlike the shallow groundwaters.

It is suggested, therefore, that the most likely explanation for the gross differences in groundwater geochemistry between the two deposits is due to differences in the physical hydrology and the nature of active groundwater circulation. Steep structures at the Halfmile Lake deposit have allowed recharge waters to penetrate deeper, displacing any saline waters that may have existed. Drilling at the Halfmile Lake commonly required HQ boreholes at

shallow depths, followed by NQ and in some cases, BQ drilling at greater depth due to the presence of faults. In contrast, the shallow and deep groundwater systems are more isolated at the Restigouche deposit due to more shallow, tighter structures. A similar situation to the Restigouche deposit was observed at the Oak Ridge Reservation, Tennessee, where brines were found to occur as shallow as 30 m, although tritium and carbon isotope evidence indicates that the brines are influenced by meteoric waters (Nativ, 1996). However, there are differences in the compositions of packer and bailer waters for many of the boreholes sampled at the Halfmile Lake deposit. Typically, the packer groundwater from a given depth displays higher TDS and somewhat more evolved compositions than the bailer groundwater from similar depth (Appendix A.3.1). This indicates that some dilution due to mixing with shallow groundwaters has occurred.

A further point is that if the water in the holes at the Halfmile Lake deposit were merely shallow groundwater which has travelled down the holes with little subsequent modification, then there should be greater similarity in groundwater composition between holes. However, there are chemical differences in waters in different boreholes, in both absolute concentrations and in element ratios. This suggests that flow is dominated by fracture flow, consistent with the steep structures in the deposit. Previous studies of groundwaters from the Stripa Mine, Sweden, have also noted that groundwater chemistry is highly variable between even closely spaced boreholes (Nordstrom et al., 1989a). Borehole HN87-8 has low concentrations of TDS, particularly near the top of the hole, and consistently plots closest to the origin in trace element-element plots (Fig. 7.2). Similarly, borehole HT55-43 has the lowest TDS values in the study. Both of these holes are from near the summits of the Lower and Upper AB zone hills, respectively. This would strongly suggest that the low conductivities of these borehole waters is due to rapid and recent local recharge at the Upper and Lower AB zones. However, rapid recharge is not consistent with the generally low hydraulic conductivities at the Halfmile Lake deposit encountered with the packer system (Chapter Four). It may be that the low TDS of the Halfmile Lake deposit groundwaters is due in part to transmission of meteoric waters

along major faults and fractures, modified by some water-rock reactions and subsequently variably diluted by shallow groundwaters and/or drilling fluids.

7.5.4 Controls on groundwater major element chemistry

The chemistry of the Halfmile Lake and Restigouche deposit groundwaters reflects a variety of processes including sulphide oxidation, carbonate dissolution and precipitation, silicate hydrolysis and possibly silicate precipitation, oxide formation and adsorption processes. This section considers the sources of the major solutes in the BMC groundwaters in terms of groundwater geochemical evolution and mixing processes. Subsequent sections address sources of base metals by sulphide oxidation and transport of trace metals away from these sources.

The sources of the major solutes of the BMC groundwaters can be constrained to a certain degree on the basis of observed host rock and fracture zone mineralogy and geochemical modelling. Weathering of sericite and chlorite in the host rocks and fractures may be a source for Mg in groundwaters. However, for most waters there is a very strong correlation between Mg and Ca (Figs. 7.3, 7.15), which indicates either that these cations are controlled by common phases or that they are controlled by common secondary processes such as cation exchange. There are very few sources of Ca in the host felsic volcanic and metasedimentary rocks. Plagioclase feldspar is dominated by near end-member albite (Lentz and Goodfellow, 1993c; Rogers et al., in press). SEM and XRD data on fracture zone minerals and suspended sediments (Chapters Two and Nine, respectively) also identified carbonate minerals (calcite and ferroan dolomite; see Chapter Eleven) as a potential source of both Ca and Mg. Dolomite dissolution could therefore account for the coherent behaviour of Ca and Mg. Siderite is also a common carbonate phase in veins associated with the Restigouche deposit. However, most of the groundwaters are oxidizing and close to or within the Fe^{3+} stability field (Figs. 7.6, 7.21) such that ferrous Fe released as a result of siderite dissolution would be expected to be oxidized to ferric Fe and rapidly precipitated as Fe-oxides. Iron is generally poorly correlated with Ca

and Mg (Tables A.3.3, B.3.3).

As the degree of water-rock reaction increases (as measured by conservative tracers, such as Cl), Mg and Ca contents reach a maximum and subsequently decrease (Figs. 7.3, 7.16). This marks the evolution of groundwaters from Ca-HCO_3-dominated recharge waters to Ca-Na-HCO_3 and ultimately Na-HCO_3 compositions. The groundwaters from the Halfmile Lake deposit with the highest TDS (Na-HCO_3 waters from borehole HN94-63; Fig. 7.3) have low Ca and Mg contents relative to most of the other Halfmile Lake deposit groundwaters. Similarly, at the Restigouche deposit, deeper waters from boreholes MM-89-102, MM-89-106, and B-80-7 have high TDS (500 - 2660 mg/L) and have lower Ca and Mg contents than low TDS recharge waters (Fig. 7.15). In contrast to Mg and Ca, Na contents show strong correlation with Cl contents. Exceptions to the decrease in Mg and Ca at high TDS are the groundwaters from borehole MM-88-02 at the Restigouche deposit (Fig. 7.15). These waters (up to 22,000 mg/L TDS) have elevated Ca and Mg compared to all other Restigouche and Halfmile Lake deposit groundwaters, but still have Na » Ca.

The decrease in Ca and Mg in groundwaters with moderately high TDS and Na-HCO_3 and Na-Cl compositions is commonly observed in groundwater geochemical evolution. Two main processes can account for this in the BMC groundwaters; 1) cation exchange, and 2) mineral precipitation. Cation exchange is commonly invoked as a mechanism to explain Ca to Na evolution in groundwaters because Ca has a stronger affinity for exchange sites on clay minerals than Na. NETPATH modelling of BMC groundwater evolution (see below) shows that inclusion of Ca-Na exchange as a process produces realistic models. The most likely phases involved in mineral precipitation reactions include carbonate, sulphate and clay minerals. The more evolved groundwaters from the Restigouche deposit are saturated with respect to chlorite (Appendix B.3.6; Fig. 7.25). It is possible that stabilization of chlorite might account for some of the Mg loss. Chlorite is one of the dominant phases of the host felsic rocks and it is difficult to assess paragenetic relationships. However, SEM analyses of fault and fracture zone minerals (Chapter Two) indicates that Fe-Mg-silicate minerals are common.

Geochemical modelling indicates that none of the Halfmile Lake and Restigouche deposit groundwaters are saturated with respect to Ca and Mg sulphate minerals. Groundwater MLW95-486 from the Heath Steele deposit is saturated with respect to gypsum and anhydrite. Salts were observed on the mine wall where this water exited. Carbonate minerals (calcite, dolomite, siderite) are saturated to supersaturated in most of the higher TDS waters (Figs. 7.10, 7.25, 7.34). Carbonate was observed as a fracture zone mineral (Chapter Two). The carbon isotope composition of fracture carbonate is isotopically similar to massive and vuggy vein carbonate (Chapter Eleven).

Thus, although carbonate precipitation may well account for some of the loss of Mg and Ca, consistent with somewhat lower alkalinity in brackish waters from borehole MM-89-106 and saline waters from borehole MM-88-02 compared to those from borehole MM-89-102, cation exchange may be the dominant process in the evolution from Ca-dominated to Na-dominated groundwater compositions. If this is the case, it implies that the amount of available exchange sites with Na far exceeds the capacity of Ca-rich recharging groundwaters to exhaust them.

The sources of Na are more easily constrained for the shallow groundwaters. The dominant source is weathering of albite with perhaps some contribution from fluid inclusions. However, for reasons argued below, fluid inclusions are unlikely to be a major source of salinity for Restigouche deposit groundwaters. There is a trend of decreasing Na/Cl ratio with increasing total Cl concentration (Fig. 7.16).

It is most likely that the K contents of shallow recharge waters and moderate TDS waters is controlled by sheet K-silicates (primarily illite; Chapter Two). Potassium contents initially increase with increasing TDS but show little change over a broad range in TDS values (Figs. 7.3, 7.15), consistent with buffering of K contents due to formation of illite during alteration of primary silicates. The saline waters from borehole MM-88-02 have elevated K values which may suggest K-feldspar weathering, although if this is the case, the extent must be minor, based on Sr isotopic compositions of these waters (Chapter Twelve). Mine waters show a more coherent trend of increasing K with TDS (Fig. 7.31).

Geochemical modelling was carried out using NETPATH (Plummer et al., 1995) in order to test these sources of the major solutes as well as constrain likely water-rock reactions. NETPATH models were initially constrained by including phases observed in Restigouche and Halfmile Lake deposit drill core (Chapter Two). The minerals which are likely to control the major element chemistry of the groundwaters include albite, K-feldspar, chlorite, sericite, sulphide, calcite, dolomite, and siderite. Only pyrite was included as a source of sulphate. Sericite is variable in composition (Chapter Two), however, a generalized composition was added to the NETPATH code based on published microprobe results of sericite from the BMC (Lentz and Goodfellow, 1993c). Minerals which were allowed to precipitate were partly constrained by observation of fracture zone (Chapter Two) and suspended sediment (Chapter Nine) mineralogy as well as by minerals which were close to or at saturation based on PHREEQC calculations. Minerals allowed to precipitate included Fe-oxides (goethite), kaolinite, gibbsite, sericite, and for the more saline waters, carbonates. Some of the models were additionally constrained by $\delta^{13}C_{DIC}$ data, where available (see Chapter Eleven). The carbon isotopic composition of carbonate sources of CO_2 was constrained by the composition of vein carbonate at the BMC (Chapter eleven) and was set to -5‰ $\delta^{13}C_{VPDB}$.

Although the major cations, HCO_3 and SO_4 are relatively easy to account for, the source of Cl-salinity is more equivocal. Potential sources of Cl in BMC waters include 1) marine aerosols (e.g. Long et al., 1992), 2) evaporation and evapotranspiration of marine derived Cl, 3) dissolution of evaporite deposits, 4) water-rock reaction with Cl-bearing minerals (Kamineni, 1987; Kamineni et al., 1992), and 5) leakage from fluid inclusions (Nordstrom et al., 1989b). Many of these sources can be readily discounted as sources of salinity for groundwaters from the Restigouche and Halfmile Lake deposits on the basis of the geochemical data presented in this chapter and stable isotope data presented later (Chapter Eleven).

Although Cl and Br are likely to be major constituents of precipitation over the BMC (see Chapter Five for precipitation data), the concentrations are low compared to Cl and Br contents

of the groundwaters (and surface waters). In addition, contribution from marine sources would preserve Br/Cl ratios as both these anions are conservative in natural waters. Surface waters and most groundwaters presented in this study have Br/Cl_{molar} ratios much higher than seawater (Figs. 7.38-7.40). In addition, Na/Cl_{molar} ratios are also elevated compared to seawater (Fig. 7.40). Evaporation is readily discounted as a source of increased salinity based on oxygen and deuterium isotopes. As discussed in Chapter Eleven, surface waters and shallow groundwaters from both deposits are very uniform in stable isotopic composition and fall on a local meteoric water line as well as close to, and above, the global meteoric water line (Figs. 11.4, 11.8). Evaporative concentration of Cl and Br would produce waters with stable isotopic compositions which became progressively heavier with a shallower slope than the meteoric water line. Thus, the stable isotope data indicate that both Halfmile Lake and Restigouche deposit groundwaters have undergone little, if any, evaporation during recharge.

Evapotranspiration is a potential source of increased salinity and, because it is, isotopically, a non-fractionating process, cannot be discounted on the basis of stable isotopes. However, it is likely that evapotranspiration would also preserve the Br/Cl ratio of the dominant source (seawater) of these elements during precipitation. As noted above, Br/Cl ratios of most of the waters are inconsistent with a marine origin. In addition, surface waters have Br/Cl greater than seawater and generally greater than local groundwaters (Figs. 7.38-7.41). If concentration by evapotranspiration of marine derived salts was a significant process, surface waters would be expected to have Br/Cl close to seawater, and certainly less than the groundwaters.

Fluid inclusions are unlikely to be significant for the surface waters and shallow groundwaters but are of potential significance for the more saline waters from boreholes MM-89-106 and MM-88-02 from the Restigouche deposit. For example, Nordstrom et al. (1989b) showed that the chemistry of brackish waters at the Stripa mine, Sweden, was consistent with a major contribution of Cl-salinity from leakage of fluid inclusions. Although no Br and Cl analyses are as yet available for fluid inclusions from BMC lithologies, some inferences can be made on the basis of models on the development of the BMC. Peter and Goodfellow (1993)

showed, on the basis of stable isotopic data from iron formation carbonates and carbonate in massive sulphides (also shown by data presented for Restigouche deposit carbonate; Chapter Eleven), that the hydrothermal fluids that formed the BMC ore deposits (and likely responsible for many fluid inclusions) were a mixture of marine and meteoric waters. The present meteoric waters at the Halfmile Lake and Restigouche deposits have Br/Cl > seawater. Hydrothermal or metamorphic fluids that represented mixtures of seawater and meteoric waters would likely have Br/Cl ratios somewhat greater than seawater. However, the more saline waters from the Restigouche deposit (boreholes MM-89-106 and MM-88-02) have Br/Cl_{molar} between 0.00036 and 0.00037, compared to a seawater value of 0.00154 (Figs. 7.38-7.41). Therefore, for these waters, fluid inclusion leakage is unlikely to be a major source of salinity, although a minor contribution cannot discounted.

For the shallow groundwaters and surface waters, the most likely source of Br and Cl salinity is weathering of the host rocks. Although many studies suggest that Cl abundances of silicate rocks are too low to be a source of Cl salinity, Kamineni (Kamineni, 1987; Kamineni et al., 1992) has shown that such a source is consistent with Br and Cl abundances and ratios in saline waters and brines from the Canadian Shield. There are few Br and Cl data available for host lithologies from the BMC. Gower (1996) recently presented geochemical data for host rocks remote from the Restigouche deposit. For samples with both Br and Cl above detection (1 and 100 ppm, respectively), Br/Cl_{molar} ratios range from 0.003 to 0.015. These values are greater than seawater and are similar to most of the shallow groundwaters and surface waters from the BMC.

As a group, the BMC waters trend to lower Br/Cl than host lithologies with increasing water-rock reaction progress (Fig. 7.40). As noted above, the more saline waters typically have Br/Cl_{molar} less than seawater. There appears to be few mechanisms for producing waters with Br/Cl less than seawater. Evaporation of seawater produces no change in Br/Cl ratios until halite saturation is reached, at which point Br/Cl increases as Br is excluded from the halite crystal lattice. Dissolution of halite by meteoric waters is capable of producing waters with

increased salinity and Br/Cl less than seawater. However, such waters would also have Na/Cl_{molar} close to unity (Kesler et al., 1995). For the saline waters from borehole MM-88-02, the Na/Cl_{molar} ratios are less than seawater (0.86) and range from 0.70 to 0.78. If the Cl and Br contents of these waters were produced by halite dissolution, it implies that these groundwaters have subsequently undergone extensive water-silicate reactions to alter the Na/Cl ratios (e.g., by albitization). There are two additional constraints on such a mechanism for producing the Cl and Br salinity of these waters. Firstly, there is no obvious source of evaporites in the area of the Restigouche deposit, and secondly, B isotope data for these saline waters (and those from borehole MM-89-106) suggest a crustal, rather than marine, source for the B (Chapter Eleven). Groundwater MLW95-492 from the Brunswick #12 deposit has Br/Cl and Na/Cl close to seawater (Fig. 7.40), but also has a B concentration and isotopic value which are inconsistent with a marine origin. It is possible to produce crustal B isotopic values from non-marine evaporites, but there is no evidence for non-marine evaporites in northern New Brunswick.

It is unclear, therefore, how to explain the low Br contents and low Br/Cl of the more saline waters from the Restigouche deposit. It is clear from the rare earth element and radiogenic isotope data (Chapter Twelve) that the host lithologies undergo differential weathering. Therefore, an alternative explanation for the low Br/Cl is that Br and Cl are being released to the aqueous phase by water-rock reactions, but that different minerals are contributing these solutes. This would be at odds with the strong linear relationship between Br and Cl observed in mafic and ultramafic rocks, which was interpreted to be the result of equal release of Br and Cl from the host rocks (Kamineni et al., 1992). However, Kamineni et al. (1992) only measured the bulk rock and did not look at the sources of Br and Cl at the mineralogical level. Nevertheless, there is a very strong correlation between Na/Cl and Br/Cl for the BMC ground and surface waters (Fig. 7.40). Sodium is probably more readily released from silicate minerals than Cl but with increasing water-rock reaction, Cl is increasingly preferentially weathered relative to Na, resulting in decreasing Na/Cl with increasing extent of water-rock

reaction (Fig. 7.34A). Additionally, at high degrees of water rocks reaction, albitization of plagioclase may become important, further decreasing Na/Cl and Na/Ca ratios. Similarly, if Br and Cl are released from different minerals at different rates, the Br/Cl ratio will change with different extents of water-rock reaction.

A very interesting observation of the Br/Cl ratios of the BMC shallow groundwaters and surface waters is that many are similar to brines and saline waters from the Canadian Shield (Fig. 7.41). In addition, Canadian Shield brines have very low Na/Ca ratios due to extensive water-rock reaction and albitization of feldspar (Davisson and Criss, 1996). The majority of BMC shallow groundwaters and surface waters also have low Ca/Na ratios, but are $CaHCO_3$-type waters rather than the CaNaCl compositions typical of Canadian Shield brines. Thus, it seems that groundwaters at the two extremes of degree of water-rock reaction have similar Na/Ca and Br/Cl ratios (Fig. 7.41). Moderately saline waters from the Restigouche deposit are more variable in Br/Cl (lower) and Na/Ca (higher) reflecting different stages along an inferred evolutionary pathway.

The range in Na/Ca and Br/Cl are interpreted as follows. As shallow groundwaters are recharged, they are initially dominated by Ca and HCO_3. These waters take on the Br/Cl of the easily soluble portions of the local bedrock and/or regolith. As the degree of water-rock reaction increases, Na contents increase through silicate weathering and/or cation exchange reactions with Ca. Thus, groundwaters evolve to Na-HCO_3 type compositions. As water-rock reaction progresses, Br and Cl are increasingly released by less soluble phases, and the Br/Cl ratio decreases as Cl is preferentially leached from the host lithologies. Concurrently, the Na/Ca ratio continues to increase through dissolution of albite, cation exchange, and precipitation of carbonate minerals. Thus, Br/Cl may eventually decrease from initially whole-rock values to values less than seawater, and Na/Ca may increase to the point where Na contents are two orders of magnitude greater than Ca contents. This type of composition is represented by the deeper waters in borehole MM-89-106 (Fig. 7.41). Ultimately, Ca contents begin to increase as Na is consumed due to albitization-type reactions. Additionally, Br/Cl

ratios eventually increase as the extent of reaction increases, ultimately achieving whole-rock type ratios as the compositions of the waters approaches those of shield brines. Gascoyne et al. (1987) presented data from saline waters associated with plutons in the Canadian Shield. Some of these waters have Br/Cl similar to shield brines but higher Na/Ca. These waters have relatively low salinity (Cl < 900 mg/L) which can be interpreted to represent groundwaters on the increasing Na/Ca and decreasing Br/Cl part of the evolutionary cycle (Fig. 7.41). Higher salinity fluids (Cl up to 25,000 mg/L) from the plutons have slightly higher Na/Ca and lower Br/Cl than shield brines (Gascoyne et al., 1987) and are interpreted to be somewhat more evolved than the groundwaters from borehole MM-88-02. It would seem, therefore, that the Br/Cl systematics of groundwaters may be more complex than previously thought and that the Br/Cl ratio may not be a useful discriminator of marine and non-marine sources of salinity. Note, however, that Bottomley et al. (1994) have suggested, on the basis of B isotopes (see Chapter Eleven for greater discussion), that the Cl and Br salinity of Canadian Shield brines is marine in origin and therefore at odds with the above interpretation. Gascoyne et al (1987) suggested that low Br/Cl and high Na/Ca ratios in saline waters associated with the plutons in the Canadian Shield was the result of mixing between shield-type brines (high Br/Cl, low Na/Ca) produced through water-rock reactions within the plutons with waters (low Br/Cl, high Na/Cl) from nearby (40-50 km distant) sedimentary basins.

7.5.5 Groundwater mixing

Groundwater flow in crystalline rock terranes such as the BMC is dominated by fracture flow (Chapter Four). It is well recognized that sampling of groundwaters in such areas is difficult in terms of collecting depth-representative groundwaters. Mixing of groundwaters is commonly observed, especially where groundwaters are collected from open boreholes. For example, at the Stripa mine, Sweden, Nordstrom et al. (1989a) observed that groundwaters at intermediate depths were mixtures of shallow groundwaters and deeper more saline groundwaters. The degree of mixing was found to be highly fracture-dependent rather than

depth-dependent such that the geochemistry of groundwaters in a borehole varied significantly and erratically in TDS , both horizontally and vertically. Factor analysis was used in this study to investigate potential mixing relationships in BMC groundwaters.

For the Restigouche deposit, Principle Component Analysis (PCA) suggests that mixing relationships cannot be explained by simple two-component mixing. Several possible end-member groundwater compositions can be identified using PCA. One end-member is represented by shallow, low TDS, Ca-HCO_3 waters from the upper parts of boreholes MM-89-106 and MM-89-107 that are unaffected by oxidation of the Restigouche ore body. The second end-member is represented by high-sulphate shallow groundwaters from borehole MM-88-01, where the high sulphate is due to oxidation of sulphide minerals. The majority of the shallow groundwaters can be accounted for by two-component mixing if the first two factors in the PCA are considered. The first two factors account for 77.8% of the variance in the data. Consideration of the third factor (17% of the variance) suggests a third shallow groundwater end-member represented by the waters in boreholes B-80-15 and MM-89-109, both off-axis holes. Considering all three PCA factors, most of the shallow groundwaters could represent three-component mixing. However, the situation is clearly more complicated. A fourth component is indicated by the brackish waters recovered in borehole MM-88-102 and the deeper parts of borehole B-80-7. The highly saline waters in borehole MM-88-02 are distinctly different than any of the above end-members. The deeper waters from borehole MM-89-106 may represent mixing between the borehole MM-89-102 end-member and another end-member represented by a mixture between borehole MM-88-02 waters and the shallow groundwaters (Figs. 7.22, 7.23). Groundwaters at the Restigouche deposit suggest mixing between at least three different end-member compositions. One end-member is represented by the shallow groundwaters and surface waters distal to ore mineralization. The other major end-member is the deeper saline waters recovered from borehole MM-88-02. Stable isotopic and chemical data suggest that the deeper waters in borehole MM-89-106 represent mixing between these two end-members. A third end-member composition is the high SO_4 and base metal waters

recovered close to the surface expression of the ore body that are controlled by sulphide oxidation processes. Note, however, that the ratio of Mg to the other major cations (Mg/(Mg+Ca+K+Na) is lower in the more saline waters from MM-89-106 than the high salinity waters from MM-88-02. Also, the Ca and Mg values for the MM-88-02 waters are too high relative to the Na and K for the MM-88-02 waters for the MM-89-106 saline waters to be simple mixtures. Alternatively, if these waters are mixtures, the mixing is not a recent phenomena, allowing time for modification of the Mg and Ca values. Thus, although the Cl and stable isotopic data suggests that the MM-89-106 saline waters are mixtures between saline (as represented by waters from MM-88-02) and meteoric end-members, if this is so, it is not a recent, drilling-induced mixing given the differences in the major element compositions. There is also clear evidence for modern (drilling-induced) mixing between the high salinity waters in MM-88-02 and shallow groundwaters in MM-88-06 and 07. The Cl contents are very consistent with some cross-flow between these boreholes, as they are down-gradient from MM-88-02.

Figure 7.16 shows the relationship between HCO_3 and Cl for the Restigouche deposit groundwaters. Some of the waters show a sharper increase in Cl compared to HCO_3 than most of the waters. These higher Cl/HCO_3 waters include the high sulphate waters from borehole MM-88-06 and MM-88-07 as well as the bailer and shallow packer waters from borehole MM-89-106. For the high-sulphate waters, the most likely explanation for the elevated Cl contents is leakage of high Cl waters from borehole MM-88-02. These boreholes are upslope from borehole MM-88-02 whereas boreholes MM-88-06 and MM-88-07 are downslope and therefore show a greater influence from the saline waters. The groundwaters from borehole MM-88-07 have higher Cl contents and significantly lower Br/Cl, approaching ratios for the saline waters. Similarly, surface waters in Charlotte Brook downstream from the Restigouche deposit have very low Br/Cl. For the shallow MM-89-106 waters there are two possible explanations. The higher Cl could be due to mixing between the shallow groundwaters and the deeper Cl-rich waters, or mixing due to leakage along shallow fractures from the high Cl

waters in borehole MM-88-02. The collar of borehole MM-89-106 is to the east and slightly south of the collar of borehole MM-88-02. It is conceivable that fluids have travelled laterally away from MM-88-02 along shallow fractures. It was noted that the stream waters immediately adjacent from the deposit had somewhat higher Cl contents than other stream waters, perhaps reflecting an influence from saline groundwaters.

Geochemical and isotopic data suggest that the moderately saline waters may be mixtures between two end-member compositions (e.g. Fig. 11.9). However, there is clearly not a simple mixing relationship because the ratio of Mg to the other major cations (Mg/(Mg+Ca+K+Na) is lower in the more saline waters from MM-89-106 than the high salinity waters from MM-88-02. Also, the Ca and Mg values for the MM-88-02 waters are too high relative to the Na and K for the MM-88-02 and MM-89-106 waters to be simple mixtures. There is also little evidence to support mixing between very saline waters similar to shield brines with the shallow groundwaters at the Restigouche deposit, as a result of drilling induced perturbations to the local hydrology. The shallow groundwaters all have very elevated sulphate and negative carbon isotopes whereas the groundwaters from borehole MM-88-02 have no S and carbon isotopes are very heavy indicative of methanogenesis in the absence of sulphur reducing bacteria (see Chapter Eleven). Alternatively, if these waters are mixtures, the mixing is not a recent phenomena, allowing time for modification of the Mg and Ca values.

The interpretation of the groundwater data at the Restigouche deposit is: 1) shallow local recharge system that is dominated by Ca and HCO_3 produced by dissolution of carbonate coupled with silicate hydrolysis in the soil and upper parts of the weathered bedrock; 2) modified Ca-HCO_3 shallow groundwaters characterized by oxygenated waters flowing through or along the ore horizon. This water mass is actively oxidizing the ore deposit resulting in elevated SO_4 and base metals; 3) a deeper groundwater flow system characterized by elevated Na and Cl concentrations as a result of greater water-rock reaction times and elevated HCO_3 due to dissolution of carbonate in the footwall alteration zone of the ore deposit (as in borehole MM-89-102 and the deeper parts of B-80-7).

Principle component analysis of the Halfmile Lake groundwaters shows no clear mixing relationships between different groundwaters (Figs. 7.7, 7.8). This is because of variable mixing with surface waters, rapid downward penetration of shallow recharge waters along fractures, possible upward gradients in the lower parts of at least some of the boreholes, and perhaps to the greater reliance on bailer groundwaters which reflect mixing within the borehole water column. At the Halfmile Lake deposit, steep structures result in more variable groundwater chemistry between boreholes, whereas at the Restigouche deposit, the structures are more shallow and more conducive to mixing relationships between groundwater flow systems. In some cases there are general downhole trends at the Halfmile Lake deposit, reflecting both in-hole mixing controlled by upward and downward gradients at the bottom and top of these holes respectively and due to cation exchange and water-rock reactions with depth. However, there are no obvious trends between boreholes (i.e., with depth as a whole).

7.5.6 Origin of saline waters at the Restigouche and Brunswick #12 deposits

The most striking difference between the chemistry of groundwaters at the Halfmile Lake deposit compared to the Restigouche deposit is the occurrence of brackish to moderately saline waters at the Restigouche deposit. Similarly, the groundwater collected from 1000 meters depth at the Brunswick #12 deposit (MLW95-492) is the most saline water recovered to date from the Bathurst Mining Camp. In this section, the origin of these unusual waters is considered.

Saline groundwaters occur in a wide variety of geological settings, in particular sedimentary basins and the Canadian and Fennoscandian shields (e.g. Bottomley et al., 1994; Carothers and Kharaka, 1980; Davisson and Criss, 1996; Fritz et al., 1994; Gascoyne et al., 1987; Knauth, 1988; Nativ, 1996; Wilson and Long, 1993). The fundamental questions regarding the origin of these saline waters which remain the focus of much debate in the hydrogeochemical literature include: a) what are the sources of saline waters (specifically, the sources for the different major constituents), b) what are the main processes controlling the

geochemical characteristics of saline waters, and c) how is the movement of saline fluids controlled and to what extent are they isolated, if at all, from the meteoric groundwater regime (e.g. Davisson and Criss, 1996). Nordstrom et al (1989a) suggest that it is possible that each field area for brine waters may have a unique source or a unique combination of sources for its saline groundwaters, seemingly at odds with the findings of Davisson and Criss (1996). Davisson et al. (1996) state that the fact that saline fluids from both sedimentary basins and the Canadian and Fennoscandian shields fall along the same 2:1 Na to Ca relationship indicates that saline and brine fluids originate from crystalline basement at hotter temperatures and subsequently migrate into different, lower temperature, reservoirs. An alternative explanation for Canadian Shield saline waters has been proposed by Bottomley et al. (1994) who suggest that chemical and B-isotopic data are consistent with a marine origin with subsequent modification due to water-rock reactions during groundwater flow from sedimentary basins into shield environments.

As discussed previously with respect to sources of Cl-salinity, there are a number of potential mechanisms to account for the elevated salinities of the groundwaters recovered from borehole MM-88-02 at the Restigouche deposit, as well as the saline water from the Brunswick #12 deposit. These include 1) the waters are very old and the elevated TDS values represent very long periods of water-rock interaction (e.g. Frape et al., 1984), 2) evaporation of fresh water or seawater, 3) seawater incursion, 4) sea salt deposition, 5) leakage of fluid inclusions, and 6) dissolution of halite.

Of the various causes of high salinities in groundwaters, many can be eliminated for the Restigouche deposit groundwaters based on the anion compositions. Any origin that invokes seawater as a precursor or as a source of aerosol salts fails to account for the very low Br contents of the Restigouche groundwaters. Seawater typically has Br contents of around 67 mg/L and $Br/Cl_{(molar)}$ of around 0.00154. In contrast, groundwaters from borehole MM-88-02 have Br contents that range from 9.3 to 10.8 mg/L and $Br/Cl_{(molar)}$ of around 0.00036. Bromine is more geochemically conservative than Cl and it is therefore difficult to decrease the

Br/Cl from a seawater precursor. The high salinity groundwater from Brunswick #12 differs from the Restigouche groundwaters in that it has much higher Br content (129 mg/L) and $Br/Cl_{(molar)}$ slightly greater than seawater (Fig. 7.39). The great difference in Br/Cl between these waters likely requires different origins for these groundwaters and different fluid histories (consistent with the differences in the Sr isotopic compositions; Chapter Twelve). Borehole MM-88-02 waters have much higher Na/Ca and Na/K and have Sr contents two orders of magnitude greater than groundwater MLW95-492. Strontium isotopes (see Chapter Twelve) are consistent with equilibration of the MM-88-02 waters with plagioclase or carbonate whereas groundwater MLW95-492 derived its Sr (and its major cations) through equilibration with a higher Rb/Sr mineral, such as feldspars or micas. Thus, the low Br/Cl of the Restigouche waters indicate that they are unrelated to an ancient seawater precursor, seawater incursion, or deposition of seawater aerosols.

As previously discussed, Br/Cl ratios make a fluid-inclusion origin of salinity unlikely for the saline groundwaters. However, a fluid-inclusion dominated origin cannot be discounted for the Brunswick #12 deposit saline water. Fluid inclusions from host rocks to the Brunswick #12 deposit commonly have saline compositions with daughter crystals (J.M. Peter, unpublished data).

A final possibility is that the high salinities were produced by evaporation of surface waters in a continental setting. Although B-isotopes (Chapter Eleven) indicate that dissolution of marine evaporites is unlikely, dissolution of non-marine evaporite deposits could explain both the crustal B-isotope values and low Br/Cl. Highly saline waters are common in restricted basins in semi-arid climates. Few analyses exist for Br in continental brine waters, however. Waters from Lake Tyrell in Australia have high Br contents and high Br/Cl ratios. Some continental brines from China have low Br and characteristically low Br/Cl ratios (Vengosh et al., 1995). These authors note that the brines are far removed from the influence of marine aerosols, as confirmed by B isotopes. However, for such a mechanism to be viable for the saline waters at the Restigouche deposit implies that all evidence for non-marine evaporites has

subsequently been removed by erosion.

A further difficulty with an origin based on dissolution of evaporites is that evaporation of natural waters typically results in residual brines which are more concentrated in SO_4 and Br (e.g. Frape et al., 1984; Vengosh et al., 1995). In fact, most saline waters and brines from the Canadian Shield are enriched in SO_4 and Br (Frape et al., 1984). Saline waters from the Restigouche and Brunswick #12 deposits have non-detectable SO_4. Groundwaters with such low sulphate contents are rare and there is generally good evidence for extensive sulphate reduction, as there is for the groundwaters from borehole MM-88-02 (see Chapter Eleven). The low sulphate in the Restigouche saline waters is interpreted be the result of sulphate reduction. These waters strongly degassed when brought to surface and the very positive $\delta^{13}C_{DIC}$ values (+12‰; see Chapter Eleven) are consistent with biogenic methanogenesis. Methanogenic bacteria typically only thrive where sulphate-reducing bacteria are no longer dominant due to reduction of the available dissolved sulphate.

For the Restigouche waters in general, there is an overall relationship of increasing HCO_3 with increasing Cl (Fig. 7.16), and for the high salinity waters there is a decrease in HCO_3 with further increases in Cl. These waters are all saturated with respect to carbonate minerals. The decrease in HCO_3 may be related to carbonate precipitation and/or to consumption of CO_2 by methanogenic bacteria (see Chapter Eleven).

One of the most critical questions surrounding the saline waters is how they have been preserved over time in their present location. One answer may be that in the Bathurst Camp there are pockets of saline brine that because of their density and occurrence in areas of low hydraulic gradient are effectively decoupled from the active groundwater flow systems (Bottomley et al 1994). Bottomley et al. (1994) invoked an allochthonous origin for the saline waters and brines from the Canadian Shield. They noted that much of the shield was covered by ocean during the Lower Paleozoic, as shown by salt deposits of that age in the Alberta and Michigan Basins, and in the Hudson Bay region.

Restigouche deposit groundwaters have Na and Cl compositions which plot on or above the

seawater dilution line, unlike deeper groundwaters from the Stripa mine, Sweden, which have Na/Cl ratios below the seawater dilution line. High Na/Cl ratios are considered typical of surface waters and dilute shallow groundwaters, and of groundwaters associated with halite dissolution (Nordstrom et al., 1989a). The deeper packer groundwaters from MM-89-106 and the waters from MM-88-02 have lower Na/Cl ratios, reflecting either loss of Na if derived from halite dissolution or seawater, or derivation from feldspar dissolution. However, the B isotopes (Chapter Eleven) and the Br/Cl ratios (section 7.5.4 above) indicate that a marine origin is highly unlikely for the BMC saline waters. The model proposed by Bottomley et al. (1994), although possible for shield brines, does not hold for the waters in this study. The saline waters from the Restigouche and Brunswick #12 deposits are most consistent with an origin involving recharge of meteoric waters followed by a very long period (millions of years) of water-rock reaction. Very long distances of transport, as implied by previous models (Bottomley et al., 1994; Davisson and Criss, 1996) are not required.

7.5.7 Sulphide oxidation and sources of metals in BMC groundwaters

There are large variations in metal loads of groundwaters within borehole, between boreholes and between deposits in the BMC. This section examines the sources of metals to the groundwater environment and processes of metal transport and precipitation. The dominant potential source of metals is the massive sulphide deposits themselves. For the Restigouche deposit, there is a very clear spatial association, for most boreholes, between groundwater base metal loads and proximity to known mineralization. Metal concentrations and ratios also correlate well with mineralization at depth in boreholes. Groundwaters from the Halfmile Lake deposit are less obviously related to oxidation of massive sulphide minerals.

The most obvious difference in geochemical response to oxidation of the respective massive sulphide deposits is the depth to mineralization and geometry of the deposit. The Restigouche deposit is close to surface, shallow dipping, and therefore proximal to oxygenated recharge waters. In contrast, as discussed previously, the Halfmile Lake deposit is steeply dipping and

the main body of massive sulphide mineralization is at greater depth and therefore further removed from contact with O_2-rich recharge waters.

Mineralization at both the Halfmile Lake and Restigouche deposits is dominated by pyrite-sphalerite-galena-chalcopyrite. Pyrrhotite is a significant sulphide mineral at the Halfmile Lake deposit, but is apparently absent from the Restigouche deposit (Chapter Two). Part of the difference in geochemical response for the two deposits may therefore be related to differences in sulphide mineralogy. Many studies of massive sulphide oxidation have attempted to quantify relative rates of sulphide mineral oxidation. Jambor (1994) compiled many of these studies and there is considerable variation in inferred mineral oxidation rates, reflecting differences in oxidation conditions. Given the different reactivities found in different studies, Jambor (1994) suggested that the main trend in common in these studies was that pyrrhotite was much more reactive than pyrite with galena and sphalerite. Experimental work suggests that pyrrhotite is as much as 1-2 orders of magnitude more reactive than pyrite (Nicholson, 1994). Recently, Boyle (1995) reported on the relative oxidation rates of massive sulphides during the formation of the Murray Brook gossan deposit, east of the Restigouche deposit. He found that the relative oxidation sequence was:

sphalerite > tetrahedrite > chalcopyrite > Bi-Sb sulfosalts > galena > arsenopyrite > pyrite

Pyrrhotite is only present in trace quantities in the Murray Brook massive sulphides and was not included in the reaction sequence (Boyle, 1995).

There are two oxidants that are most important in pyrite oxidation, dissolved O_2 and ferric Fe (Nicholson, 1994). Pyrite oxidation by dissolved oxygen is expressed as:

$$FeS_2 + \tfrac{7}{2} O_2 + H_2O \Rightarrow Fe^{2+} + 2SO_4^{2-} + 2H^+$$

At pH < 8, the intermediate sulphur compounds are not considered important (Nicholson,

1994). At pH values < 3, ferric iron oxidation of pyrite is 1-2 orders of magnitude faster than oxidation by dissolved oxygen (Ritchie, 1994). This reaction can be expressed as:

$$FeS_2 + 14Fe^{3+} + 8H_2O \Rightarrow 15Fe^{2+} + 2SO_4^{2-} + 16H^+$$

The oxidation of pyrrhotite is much less acid producing than that of pyrite and may be expressed as (Nicholson, 1994):

$$Fe_{1-x}S_{(s)} + \left(2 - \tfrac{x}{2}\right)O_2 + xH_2O \Rightarrow (1-x)Fe^{2+} + SO_4^{2-} + 2xH^+$$

where x from 0 to 0.125. By analogy with pyrite, galena and sphalerite oxidation by DO can be expressed as (assuming no Fe in the sphalerite structure):

$$PbS + \tfrac{3}{2}O_2 + H_2O \Rightarrow Pb^{2+} + SO_4^{2-} + 2H^+$$

and

$$ZnS + \tfrac{3}{2}O_2 + H_2O \Rightarrow Zn^{2+} + SO_4^{2-} + 2H^+$$

The greater abundance of pyrrhotite at the Halfmile Lake deposit compared to the Restigouche deposit does not appear to be a significant factor. Other factors such as grain size, deposit depth and geometry, depth of DO penetration and local hydrology are more important. Sulphate and Fe contents of Halfmile Lake deposit groundwaters are generally lower than Restigouche deposit groundwaters (Fig. 7.42).

One of the major factors in controlling the rate of sulphide oxidation is the surface area (Nicholson, 1994). Although many of the recent studies into sulphide oxidation have focussed on acid-mine drainage problems and the oxidation of massive sulphides can be considered somewhat analogous, there are fundamental differences, especially with respect to surface area. It may be important to the base metal loads that the grain size of the Restigouche and Caribou deposits is much smaller than that of the Brunswick, Heath Steele and Halfmile Lake type

deposits. Thus, the closer proximity of the Restigouche deposit to surface combined with finer grain size of the sulphide minerals, is interpreted to result in much greater rates of sulphide oxidation and subsequently higher base metal loads compared to the Halfmile Lake deposit.

The pH of porewaters in mine tailings is buffered by three main reactions, carbonate dissolution, Al and Fe hydroxide dissolution, and silicate hydrolysis (Blowes and Ptacek, 1994). Reaction rates are such that pH is buffered between 6.5 and 7.5 where there is sufficient carbonate minerals, between 4 and 4.3 by Al hydroxides, and less than 2 for silicate hydrolysis. It is obvious from the chemistry of the shallow groundwaters that interact with the Restigouche orebody that the massive sulphides are actively undergoing oxidation. However, the pH is not that low (> 5; Fig. 7.37), and it is likely that the lack of mobility of metals far from the Restigouche deposit is in part because of acid-neutralization reactions. Now that the deposit has been disturbed, this may no longer be true. Blowes and Ptacek (1994) suggested that where porewaters in tailings piles are near-neutral pH, the rate of acid consumption by carbonate dissolution is greater than the rate of acid production by sulphide oxidation. They suggest that in cases such as these, pore-water pH is controlled primarily by carbonate dissolution reactions. The implication for the Restigouche deposit massive sulphides is that either there is sufficient carbonate as gangue and vein phases to compensate for the amount of sulphide oxidized or that the rate of acid production is slow enough to be buffered by silicate and hydroxide dissolution. Elevated Al and Si contents are considered to be good evidence for silicate hydrolysis in mine tailings. The only BMC waters in this study with high Al and Si contents are low pH waters from the Heath Steele and Wedge deposits. Groundwater MLW95-485 (Heath Steele) has values of 12 and 10 mg/L Al and Si, respectively, and groundwater MLW95-482 (Wedge) has values of 45 and 27 mg/L for these elements (Appendix C.2.1). In both of these waters, most Al-silicate minerals are undersaturated according to PHREEQC calculations.

Another important factor in mine tailings is catalysis of sulphide oxidation by bacteria. The bacteria *Thiobacillus ferrooxidans* is known to enhance the rate of pyrite oxidation by 1-2

orders of magnitude, by increasing the rate limiting step of oxidation of ferrous to ferric Fe (Nicholson, 1994). However, *Thiobacillus ferrooxidans* is only important at low pH (< 4), much lower than most of the groundwaters recovered from the Restigouche deposit. In fact, at the Eh-pH conditions of the Restigouche deposit groundwaters, sulphide oxidation is most likely occurring primarily as a result of oxidation by dissolved oxygen.

There is an important distinction between the packer and the bailer data for borehole MM-88-01. The three packer groundwaters are from above the ore zone and from the base of the main ore zone. These waters have lower SO_4 and base metals than the bailer groundwaters, suggesting that the standing water in the borehole was dominated by waters flowing through the upper part of the ore zone.

High Pb in groundwaters from boreholes MM-88-06 and MM-88-07 may in part be due to very fine grained sulphide minerals, i.e., mechanically transported from the actively weathering sulphides. SEM data of suspended sediments from these groundwaters suggests that metal-sulphate minerals are dominant (Chapter Nine). It is possible that the sulphides in these two boreholes are exposed at least some of the time to atmosphere. For borehole MM-88-06, massive sulphides begin at 8.4 m depth and for borehole MM-88-07, at 2 m depth. At the time of sampling of these boreholes, the water table was at 10 and 2 m, respectively. Thus, massive sulphides are at times exposed to atmospheric oxygen. Suspended sediments less than 0.45 μm may account for some of the differences in the Pb contents between these waters and those recovered from borehole MM-88-01 (Chapter Nine). However, if mechanical abrasion were significant, it should be expected that metal abundances would increase with depth due to particle settling as a result of the high specific gravity of sulphide minerals. However, for Pb the reverse is true suggesting that release of trace metals by sulphide oxidation occurs most extensively near the top of the ore zone and decreases with increasing depth (Appendix B.3.1). Regardless, the oxidation of the massive sulphides at the Restigouche deposit takes place primarily below the water table (the same is also true of the Stratmat deposit; see Chapter Eight), whereas, the main zone of sulphide oxidation in tailings piles occurs in the unsaturated

(vadose) zone (Blowes and Ptacek, 1994). The high Pb contents in groundwaters from boreholes MM-88-06 and MM-88-07 compared to borehole MM-88-01 are likely facilitated by the close proximity of the massive sulphides to the surface and availability of dissolved oxygen.

At the Halfmile Lake deposit, Zn is not well correlated with other ore parameters in the groundwaters, but does show somewhat positive correlations with Mg and Ca (Appendix A.3.3). This may indicate that some of the elevated Zn values in groundwaters from the Halfmile Lake deposit are produced by carbonate and/or silicate weathering rather than sulphide oxidation. Some of the highest Zn contents are from groundwaters from borehole HN93-51 from the Lower AB zone. These waters have very low TDS and low SO_4 (Fig. 7.3), consistent with this interpretation.

It was noted in a previous section that there are differences in the metal loads of the groundwaters from the two deposits. Groundwaters from the Halfmile Lake deposit have higher Mo and generally higher Cu than most groundwaters from the Restigouche deposit (Fig. 7.42). However, base metal loads in general are lower (Fig. 7.37). The generally more elevated Cu and Mo are interpreted to reflect the generally lower pH of the Halfmile Lake deposit groundwaters as well as the fact that the deposit is overturned so that stringer-zone sulphides (pyrite-pyrrhotite-chalcopyrite) are closer to surface than massive sulphide mineralization. There is no statistically significant correlation between Mo and Cu contents for Halfmile Lake deposit groundwaters, however.

7.5.8 Base metal loads in BMC groundwaters

Although the geometry and proximity of the Restigouche deposit to surface are conducive to intensive alteration of the massive sulphides, very little evidence is found in the surface waters for this (Chapter Five). It is clear from the chemistry of shallow borehole waters intersecting the Restigouche deposit, that the sulphides are undergoing oxidation (Fig. 7.42). However, comparison with the surface waters would suggest that prior to mining there was very little

direct connection between the shallow groundwater system dominant in the ore zone and the surface environment. The bailer-collected waters suggests that there is a limit to which sulphide-rich waters can dominate the local groundwater geochemistry. In other words, in shallow boreholes, high base metal contents, especially for Pb, indicate extensive massive sulphide oxidation, but in holes where the ore zone is deeper (e.g., borehole B-80-7) other metal-poor groundwaters dominate the hydrology (c.f. Figs. 7.19. 7.20). This has important implications for both exploration using hydrogeochemistry (Chapter Thirteen) and for environmental monitoring.

Trace metals near the sulphide zone are highly elevated but not as elevated as at some deposits (e.g., Red Dog; Fig. 7.37) or from mine tailings (e.g., acid-mine drainage areas in Colorado; Fig. 7.37). This is due to the higher pH of groundwaters interacting with massive sulphides at the Restigouche deposit compared to these other examples, indicating that metals do not stay in solution because they form insoluble complexes, adsorb strongly onto oxides, and co-precipitate. For example, groundwater MLW95-482 from the seep in the waste pile can be compared to the artesian borehole (groundwater MLW95-491) at the Wedge deposit (Appendix C.1.1). The former groundwater has twice the SO_4 content of groundwater MLW95-491 but one to several orders of magnitude greater metal contents because of its very low pH compared to groundwater MLW95-491 (2.33 versus 7.25). Similarly, two groundwaters from the B-zone at Heath Steele have high SO_4 and base metal loads and low pH (Fig. 7.37). In addition, the seep through the gossan at the Restigouche deposit also has low pH and elevated base metal loads (Fig. 7.37). Pb/Zn ratios are higher than most borehole waters due to the fact that the gossan is dominated by Pb because Zn was more mobile during the gossanization process (Boyle, 1995).

The low Fe contents of groundwaters in borehole MM-88-01 is likely also related to the higher oxidation state of these waters, with Fe being precipitated as Fe-oxyhydroxides, consistent with geochemical modelling (Fig. 7.26). At both deposits, the majority of the groundwaters are undersaturated with the main base metal sulphate, sulphide, and carbonate

minerals. None of the waters are close to saturation with respect to sulphide minerals.

Geochemical modelling of the BMC groundwaters allows some inferences to be made as to the speciation of the base metals and how they are being complexed. In general terms, the groundwaters in this study can be subdivided into five broad groups; 1) shallow groundwaters with low TDS, dominated by Ca-HCO_3 and Ca-NaHCO_3 compositions, 2) Ca-SO_4 waters associated with oxidizing massive sulphide minerals, 3) higher TDS waters dominated by Na-HCO_3 compositions, including waters from borehole HN94-63 at the Halfmile Lake deposit and waters from borehole MM-89-102, 4) low pH groundwaters associated with the Wedge and Heath Steele deposits, and 5) brackish to saline waters with high Cl contents.

Shallow groundwaters which are characterized by Ca-HCO_3 and CaNa-HCO_3 compositions include most waters from the Halfmile Lake deposit as well as groundwaters from borehole B-80-15, MM-89-107, MM-89-109, MM-89-100, and B-80-7 from the Restigouche deposit. Most of the waters recovered from the Willett deposit are also of this type. In these groundwaters, base metals (e.g., Pb, Zn, Cu, Cd) are present primarily as free ions. For example, in Halfmile Lake deposit groundwaters, typically greater than 95% of the cadmium occurs as Cd^{2+} with minor amounts of $CdSO_{4(aq)}$, $CdHCO_3^+$, and $CdCl^+$ (Appendix A.3.6). Similar relationships hold for shallow groundwaters from the Restigouche and Willett deposits (Appendices B.3.6, C.1.4). Zinc displays similar behaviour to Cd (generally > 90% occurs as Zn^{2+}), although $ZnCO_{3(aq)}$ and $ZnHCO_3^+$ species are present in amounts as high as 30% of the total Zn (Appendices A.3.6, B.3.6, C.1.4). Lead displays more complex behaviour, according to PHREEQC speciation. Lower pH groundwaters are dominated by free ions (Pb^{2+}), but the contribution of $PbCO_{3(aq)}$ increases rapidly with increasing pH (Figs. 7.11, 7.25). For these low TDS waters, Cl^-, OH^-, and SO_4^{2-} complexes are generally less than a few percent of the total Pb speciation. Copper speciation is more complex because copper may be present in two oxidation states (Cu^{II}, Cu^{I}). Lower pH groundwaters tend to be dominated by free Cu^{2+} ions with lesser amounts of $CuCO_{3(aq)}$. As pH increases, at similar Eh values, Cu^+ species predominate, with the free ion the primary species (Appendices A.3.6, B.3.6).

High sulphate groundwaters associated with oxidation of the Restigouche and C4/C5 massive sulphide deposits (boreholes MM-88-06, MM-88-07, MM-88-01 and C4/C5 groundwaters) have generally low TDS values and are characterized by moderate pH, elevated SO_4^{2-} and high base metal loads (Figs. 7.15; 7.42) relative to HCO_3-rich groundwaters. In general these sulphate-rich waters have similar trace metal speciation to the Ca-HCO_3 and Ca-Na-HCO_3 waters. However, the increased activity of dissolved sulphate results in higher contents of SO_4-complexes with Cd, Zn, Pb, and Fe (see Appendices A.3.6, B.3.6). An extreme example is groundwater MLW95-486 from the Heath Steele deposit. In this high TDS (5330 mg/L), Ca-SO_4 water, 67% of the Zn, 69% of the Cd, 66% of the Fe, and 81% of the Pb occurs as SO_4 complexes (Appendix C.1.4).

Groundwaters dominated by Na-HCO_3 and Na-HCO_3-Cl compositions occur at the Halfmile Lake deposit in borehole HN94-63, the Restigouche deposit in borehole MM-89-102, the Heath Steele deposit (groundwaters MLW95-488 and MLW95-609), and the Willett deposit (groundwaters MLW96-616, MLW96-617). These groundwaters tend to have moderately elevated TDS and are characterized by generally high pH (8 - 10). For Cd, OH^- and Cl^- complexes are increasingly important due to the increased pH and generally elevated Cl compared to the Ca-rich waters. Lead speciation in these waters is dominated by $PbCO_{3(aq)}$, $Pb(CO_3)_2^{2-}$, and $PbOH^-$ complexes. Only minor amounts of Pb occur as free ions in these waters. Whereas $PbCO_{3(aq)}$ complexes generally predominate over $Pb(CO_3)_2^{2-}$, for Zn the reverse is generally the case. Zinc is also strongly complexed as $Zn(OH)_{2(aq)}$ in these waters.

The low pH waters include groundwaters MLW95-482 and MLW95-485 from the Wedge and Heath Steele deposits, respectively (Appendix C.1.3). These two waters have elevated metal and sulphate contents and low pH (Figs. 7.31, 7.38). As a result of the low pH, metal speciation in these waters is very sensitive to Eh due to SO_4-H_2S equilibria. Field measurements of Eh failed for both of these waters. Geochemical modelling assuming an Eh close to zero (as measured in other waters at the same level in the Heath Steele mine) indicates that most of the S is present as S^{2-} and sulphide phases (pyrite, chalcopyrite etc) are therefore

supersaturated (Appendix C.1.3). If the geochemical modelling is carried out using the DO values as the measure of redox equilibria, no sulphide phases are saturated and in both groundwaters, jarosite is stable. Assuming an Eh close to zero, Cd, Cu, Pb, and Zn occur almost exclusively as HS^- and $(HS)_2^{2-}$ species (Appendix C.1.4). However, assuming Eh values consistent with the DO values results in these metals occurring as essentially equal proportions of free ions and sulphate complexes.

Brackish and saline waters occur in boreholes MM-89-106 and MM-8802 at the Restigouche deposit and groundwater MLW95-492 from the Brunswick #12 deposit. In the brackish waters from borehole MM-89-106, Cd is present primarily as Cl- and OHCl-complexes. Free ions constitute between 10 and 20% of the Cd species. In contrast Cu is dominantly complexed as $Cu(OH)_2$. Lead and Zn are present primarily as carbonate complexes dominated by PbCO3 and $Zn(CO_3)_2^{2-}$, respectively. The complex $Zn(OH)_2$ is also present. In contrast, the much higher salinity waters from borehole MM-88-02 have significant amounts of Pb and Zn present as Cl complexes, although carbonate complexes are also present in greater abundance. In the groundwaters from borehole MM-88-02, the most common Zn species is the free ion. The highest salinity groundwater in this study, MLW95-492 from the Brunswick #12 deposit has Cu, Pb, and Zn dominated by Cl, Cl_2, and Cl_3 complexes (Appendix C.1.4).

The saline waters from borehole MM-88-02 at the Restigouche deposit have elevated Zn contents but relatively low Pb contents (Appendix B.3.1; Fig. 7.15). This raises the question as to the origin of the high Zn loads. The shallow boreholes which are proximal to the Restigouche ore body have elevated Zn and Pb concentrations (Fig. 7.42) and correspondingly high SO_4 indicating that the high base metal loads are the product of massive sulphide oxidation. However, there is no obvious relationship between the high Zn contents of the MM-88-02 waters and the known ore body as the highest Zn values are observed in packer-derived samples at depths well below the deposit. There are several possible explanations for the high Zn contents of the saline waters:

1) The deep saline waters have mixed with more shallow groundwaters with high metal

loads from sulphide oxidation. If this is the case, the low Pb contents could be explained by the low solubility of Pb in natural waters; note the sharp decrease in Pb contents with depth and distance from the ore body in the shallow borehole waters (Fig. 7.42). However, if the MM-88-02 waters are mixed waters, the mixing cannot be recent given that the saline waters have no sulphate, in sharp contrast to the shallow groundwaters.

2) The high Zn contents may be unrelated to mineralization. Brines from the Mississippi oil fields contain elevated Zn and Pb concentrations as a result of diagenetic reactions at elevated temperatures (Saunders and Swann, 1990).

3) There may be further mineralization at depth with which these waters have been in contact. Borehole MM-88-02 is the deepest hole drilled to date at the Restigouche deposit. It was drilled to test a gravity anomaly (Westoll, 1990) but further investigation of deeper mineralization was abandoned due to the intersection of thick diabase sills in the hole which were considered adequate to explain the anomalies. If the elevated Zn contents are due to further Zn mineralization, the low Pb contents and lack of sulphate suggests migration of these waters from the source of the zinc.

4) The high Cl nature of these waters may be related to Zn-Cl complexing, increasing the solubility of Zn in these solutions. However, geochemical modelling, as discussed above, suggests that free ions and carbonate complexes are more important in these waters than Cl complexes of Zn (Appendix B.3.6).

Thus, the preferred hypothesis for the high Zn contents in the saline waters is that there is further mineralization at depth. However, the degree to which these saline waters have been transported is unconstrained by the present data. These waters also have moderately high Ni, Cr, Cu and Co contents suggesting either a different ore mineralogy/host lithology or that the high salinities result in greater solubilities for these elements.

The different behaviours of Pb and Zn in the upper and lower waters of borehole MM-89-106 from the Restigouche deposit is probably partly controlled by the activities and speciation of the major anions and by the Eh-pH conditions of the waters. Chen et al. (1996) showed that

the mobility of Pb and Al were greater than Zn in contaminated sediments at high pH. Similarly, Chuan et al. (1996) showed that Pb solubility from soils was greater than Zn at pH 8 under both oxic and anoxic conditions, whereas at lower pH, Zn mobility was much greater than Pb mobility. The higher salinity groundwaters in the lower part of borehole MM-89-106 have higher pH (> 9) than the upper waters (pH < 8), suggesting that Pb is more mobile under these conditions. In addition, the high Cl activity in the lower waters means that 30-36% of the Pb is complexed as $PbCl^+$ or $PbCl_{2(aq)}$ in addition to free Pb^{2+}, whereas, Zn is complexed as Zn^{2+}, $Zn(OH)^+$ and $Zn(OH)_3^-$. In contrast, in the upper parts of the borehole, both metals occur predominantly as free ions (> 95%).

7.5.9 Adsorption and controls over the fate of trace metals in BMC groundwaters

Concentration of trace metals in BMC groundwaters reach highly anomalous values, as discussed above (Fig. 7.42). However, the total concentration of metals does not balance the amount of sulphate in solution. For Fe, much of this is most likely balanced by the formation of Fe-oxyhydroxide minerals (e.g. $Fe(OH)_3$, ferrihydrite, goethite). However, the other base metals are well below saturation for common oxide and sulphate minerals (Appendices A.3.5, B.3.5, C.1.3). The most likely explanation for the lack of sulphate-metal mass balance is loss of metals from solution by adsorption onto Fe-oxyhydroxide and clay minerals. There is no evidence for the presence of sulphate minerals that could otherwise account for the excess sulphate (e.g. barite, gypsum).

Adsorption processes are fundamentally controlled by the surface reactivity of a mineral substrate which in turn is dependent on three surface characteristics; chemical composition, atomic structure, and fine scale morphology (Hochella, 1990). Approaches to studying sorption processes fall into two broad categories; empirical approaches, and those utilizing spectroscopic techniques as attempts to model adsorption in terms of surface complexation. In surface-complexation models, the relationship between any cation or anion sorbed onto a

mineral surface and metal/surface-site complex is explicitly defined, whereas, in macroscopic models, the relationship between adsorption and changes in proton activity are based only on generalized empirical considerations (Davis and Kent, 1990). One of the main objectives of recent work in the field of surface-solution interactions has been to understand the macroscopic observations of trace metal removal from solution by attempting to quantify the possible microscopic subreactions (Honeyman and Leckie, 1986). The fundamental problem with such surface-complexation model approaches is that they are too detailed compared with present knowledge of the chemical reactions occurring in natural aqueous systems (Davis and Kent, 1990).

There are two fundamentally different types of sites for adsorption on oxides and phyllosilicates; those that arise through protonation/deprotonation reactions of surface hydroxyl groups and those that are intrinsic to the mineral as a result of isomorphous substitution in the octahedral (e.g. Fe^{2+} and Mg^{2+} for Al^{3+} in dioctahedral clays or Li^{+} for Mg^{2+} in trioctahedral clays) or tetrahedral layers (e.g. Al^{3+} for Si^{4+}). These two types may be referred to as surface hydroxyl groups (proton-bearing surface functional groups) and siloxane groups (ion-bearing exchange sites) (e.g. Davis and Kent, 1990; Goodman, 1986; Sposito, 1983) and they have different properties that influence adsorption processes.

The Fe-, Ti- and Al- oxides primarily host proton-bearing (hydroxyl) functional groups, whereas the phyllosilicates and Mn-oxides have ion-bearing exchange sites in addition to hydroxyl sites (Davis and Kent, 1990). The surface hydroxyl groups occur in different configurations, i.e., there are a variety of sites that will have different affinities to different metals (Benjamin and Leckie, 1981b). It is most likely that there is a continuous distribution of nonequivalent surface groups, as described by Freundlich models (Benjamin and Leckie, 1981a; Davis and Kent, 1990). However, cation adsorption can usually be successfully modeled using two nonequivalent sites, high (strong) and low (weak) complexation sites (e.g. Benjamin and Leckie, 1981; Davis and Kent, 1990). This is the approach taken by geochemical models of surface complexation, such as PHREEQC and The Geochemists Workbench.

There are two ways in which pH affects the adsorption of trace metals. The pH affects dissociation of the trace metal in solution and the electric potential of the surface (Barrow et al., 1989). In general terms, cations are increasingly adsorbed with increasing pH (Figs. 7.43, 7.44). Solution pH is one of the dominant controls on adsorption and desorption processes on clays and oxide mineral due to competition from protons and ions released by clays and oxides in solution (e.g. Anderson and Christensen, 1988). On oxide surfaces and the edge sites of clay minerals, adsorption of the trace metals has been shown to increase from essentially zero to almost complete adsorption over a very narrow range of pH (Fig. 7.43). This rapid increase in adsorption with increasing pH is referred to as the adsorption edge, and the rapid adsorption occurs in response to both chemical and electrostatic forces (Davis and Kent, 1990). Adsorption of a cation requires that protons are released concurrently (or that hydroxide ions are adsorbed) although Davis and Kent (1990) indicate that the precise stoichiometry of the process is not well understood. Anion adsorption is likewise dependent on pH though with the opposite effect; anion adsorption tends to increase with increasing acidity of the aqueous solution (Davis and Kent, 1990). Anion adsorption results in protonation of the surface (or release of OH^-).

The pH of the aqueous phase also exerts an influence by controlling the chemical form of trace metals in solution (Farrah et al., 1980). For example, Co(II) adsorption on kaolinite and illite was found to occur as the Co^{2+} ion below pH 6 and as the hydroxide ($CoOH^+$) above pH 8. Similarly, Pb(II) on montmorillonite is adsorbed as the Pb^{2+} ion, and Cr on kaolinite, chlorite and illite is adsorbed as Cr(III) below pH 4 and as the hydroxide above pH 6 (Goodman, 1986). The strong correlation between heavy metal adsorption on clays and Fe-oxides and pH of the aqueous solution implies that it is the result of decreased competition with H^+ with increasing pH and because the trace metals have greater affinity for edge surface functional groups (Farrah et al., 1980). However, deprotonization of the clay surface with heavy metal adsorption is not a linear 1:1 or 1:2 relationship, which supports the idea that different forms of the metals are being complexed (Parks, 1990).

Adsorption processes are also controlled by the ionic strength of the solution in contact with the mineral surface and by the ionic strength of the trace metal solute. Increasing ionic strength commonly decreases sorption density (Goodman, 1986; Parks, 1990). In non-specific adsorption, the increasing ionic strength of the solution results in a decrease in adsorption density, whereas, in specific adsorption, ionic strength has only minor effect (Parks, 1990). Davis and Kent (1990) showed that trace metal ions are soft acids that tend to react with the least basic hydroxyl groups on the surface, such that adsorption is largely independent of the ionic strength of the solution, whereas, the hard acids, such as the alkaline earth elements, are strongly dependent on the ionic strength of the solution.

The dominant anionic species in the solution also influences the magnitude and nature of adsorption, because complexing by aqueous ligands can inhibit adsorption densities and change pH dependence (Parks, 1990). Some of the dominant ligands in solutions are only adsorbed weakly or non-specifically (e.g. Cl, CO_3) and they can reduce the activity of the adsorbing trace metal by binding the metal ions in complexes which adsorb less strongly than the free metal ion or its hydroxy complexes (Parks, 1990). The ligands Cl^- and SO_4 inhibit adsorption of Cd(II) on amorphous $Fe(OH)_3$, and carbonate inhibits adsorption of U(VI) onto kaolinite and Fe-oxyhydroxides (Giblin, 1980; Waite et al., 1994).

Kinetic considerations are likely to be significant in natural systems because of the effects of flow of water through the soil and those of mixing between waters of different ionic strength (e.g. river water mixing with ocean water). In soils with a good structure or in highly fractured soils there may be more rapid flow through the soil profile allowing less time for trace metals to interact with and adsorb onto soil particles. In very clay rich soils, where there is lower permeability but high porosity, there is likely to be greater time for adsorption reactions to occur.

Although reaction path modelling of surface complexation on ferrihydrite surfaces indicates that at low pH, SO_4 is preferentially adsorbed due to excess protonation of surface sites (Bethke, 1996), in reality low pH waters will typically be closer to equilibrium with Fe^{2+} than

ferrihydrite resulting in fewer exchange sites for SO_4 to sorb to than at higher pH where ferrihydrite is stable (i.e., above pH ≈ 4; Figs. 7.6, 7.23). For example, the seep at the Wedge deposit (sample MLW95-482) has very low pH and very high Fe contents. However, SO_4 is elevated in this groundwater.

Although adsorption processes are important in terms of understanding metal dispersion away from massive sulphide deposits, the effects of adsorption is difficult to quantify with the present data set. The effects of adsorption on the metal contents of the BMC groundwaters was modelled in a general sense using geochemical modelling software such as The Geochemists Workbench (Bethke, 1994).

The results of this modelling suggest that over the pH range of most of the groundwaters considered in this study, most of the base metals, such as Pb and Zn, are presently adsorbed to Fe-oxyhydroxides. For example, Figure 7.43 shows the results of modelling the adsorption of Pb, Zn, and SO_4 for groundwater MLW95-314 from borehole MM-88-07 at the Restigouche deposit. The adsorption edge for Pb occurs at a lower pH than is the case for Zn indicating that the mobility of Pb is more controlled by Fe-oxyhydroxides than is the case for Zn. This is supported by Zn/Pb ratios which are lower in the suspended sediments than the groundwaters, indicating that Pb is preferentially adsorbed (see Chapter Nine for greater discussion). Zinc and Pb adsorption is also shown for saline waters from borehole MM-88-02 (Fig. 7.44). As with the high sulphate waters, Pb is overwhelmingly present as sorbed species. Zinc is increasingly sorbed at higher pH (Fig. 7.44B). The modelling results also suggest that Pb is preferentially adsorbed to strong (specific) sites on Fe-oxyhydroxide surfaces, whereas, Zn is adsorbed to both weak (non-specific) and strong sites (Fig. 7.44C, D).

An important implication of this modelling is that the dispersion of metals away from the Restigouche deposit was probably strongly limited by adsorption processes due to the circumneutral pH values of the groundwaters. Thus, metal dispersion was likely strongly attenuated due to low mobility of Fe-oxyhydroxides. However, since these groundwaters were collected, the Restigouche deposit has been put into production as an open pit operation. There

is therefore potential for a lowering of the pH of groundwaters interacting with the ore deposit as well as the waste rock generated from the mining. A lowering of groundwater pH would enhance the dispersion of metals away from the deposit into the secondary environment. In the pre-mining state, many of the groundwaters had very elevated metal contents (e.g. Pb in excess of 1000 μg/L; Fig. 7.42).

The fact that there are very high contents of metals in the groundwaters from boreholes MM-88-06, MM-88-07 and to a lesser extent MM-88-01, and high SO_4 and relatively high pH, yet low (though still anomalous) contents in the surface adjacent surface waters of Charlotte Brook (see Chapter Five) indicates that the metals are not being transported very far. There are three possible explanations.

1) The metals are dominantly in the dissolved form, but groundwater flow is downward for these sites, especially MM-88-06 and MM-88-07. In other words, if Charlotte Brook is a losing (recharge) stream in the vicinity of the sulphide outcrop, the influence of sulphide oxidation at the location where the stream crosses the deposit would be minimized. This would also allow a continuous supply of oxygenated surface waters to the shallow groundwater environment to allow enhanced and continued oxidation of the sulphide minerals.

2) The metals are largely bound to colloidal Fe-oxides and clay minerals. The generally circumneutral pH of the Restigouche Deposit groundwaters is consistent with strong adsorption of metals to Fe-oxides and clay minerals (as well as organometallic complexes, although there are no data available in this study to quantify this contribution). The fact that the shallow groundwaters within the ore zone have SO_4 contents in excess of that required to balance the combined metal contents (i.e. $\Sigma_{[Fe + Mn + Zn + Pb + Cu + Co]}$) is strongly suggestive of loss of metals from solution by adsorption onto oxide and silicate surfaces and/or coprecipitation with freshly formed Fe-oxides. Modelling of adsorption is possible using geochemical reaction programs such as The Geochemist's Workbench (Bethke, 1994). For example, for the Pb- and Zn-rich waters from borehole MLW95-314, such modelling suggests that at the measured field pH of 5.34 the main adsorbed species are Ca (0.01% sorbed), Pb

(87%), Zn (21%), and SO_4 (64%). Using the data for this water and allowing the pH to vary from 3 to 7 shows the adsorption edges (isotherms) for these elements (Fig. 7.43).

3) A corollary to point 2 above is that for the high-metal load groundwaters to have limited influence on the surface waters because of metal adsorption onto colloids implies that the colloids are effectively prevented from transport away from their site of formation. The high suspended matter contents on filter papers for these waters (see Chapter Nine) may therefore be due to disturbance during sampling of boreholes MM-88-06 and MM-88-07 with the flow-through bailer.

Adsorption processes have important implications for metal dispersion away from the site of sulphide oxidation for groundwaters compared to surface waters. Groundwaters from the Halfmile Lake deposit have Eh-pH values such that they mainly plot in the Fe^{2+} stability field. In contrast, local surface waters plot in the $Fe(OH)_3$ stability field. As ferrous Fe is much more soluble than ferric oxyhydroxides, given suitable pathways, dispersion in the groundwater environment may be less impeded by adsorption phenomena than dispersion in the surface environment.

7.5.10 Arsenic in BMC groundwaters

Arsenic concentrations vary over a couple of orders of magnitude in the groundwaters sampled from the Bathurst Mining Camp, ranging from below detection (2 μg/L for 1994 samples, 1 μg/L for 1995 and 1996 samples) to 285 μg/L. However, in contrast to the Restigouche deposit, relatively few groundwaters and surface waters at the Halfmile Lake deposit had As contents above detection (Fig. 7.45). For the Restigouche groundwaters, it is not immediately clear what the relationship is between As and other parameters such as Fe, Mn, Eh or DO. However, there is a probable relationship between As concentrations and the Fe-oxyhydroxide suspended sediment content. This would fit with the association between As and Fe oxyhydroxides noted by Sullivan and Aller (1996). All the waters from the Wedge, Halfmile Lake, and Restigouche deposits which have high As were also high in suspended

Fe-oxyhydroxides. This association is probably a function of oxidation of massive sulphides releasing Fe and As from pyrite and/or arsenopyrite. There is clearly an association with respect to As contents at the Restigouche deposits in terms of proximity to massive sulphides and the depth of intersection of the ore body. For example, the groundwaters with the highest As concentrations from the Restigouche deposit are from boreholes MM-88-06 and MM-88-07 (Fig. 7.15). These groundwaters have the highest metal loads, high sulphate concentrations and moderately low pH values compared to the other Restigouche deposit waters. Also note that As contents increase downhole in MM-89-106 (for packer groundwaters), consistent with the observation that the alteration at the bottom of the borehole, although unmineralized, shows similar alteration styles as the footwall to the main ore body (Westoll, 1990). The artesian boreholes from the C4/C5 zones have high Zn contents, moderate sulphate and high As (34 and 43 μg/L respectively). Thus, the As content of the BMC groundwaters appears to be controlled by proximity to sulphide mineral oxidation and to adsorption associated with Fe-oxyhydroxide minerals. Azcue et al. (1995) suggested that the strong correlation between dissolved As contents and dissolved Fe and Mn in porewaters of lake sediments indicated that the dissolved As contents were, at least in part, controlled by sorption/desorption from Fe and Mn oxides.

Some groundwaters were collected in 1995 and 1996 for As speciation (Chapter Three). Problems with the analytical labs at the GSC prevented the analysis of the 1996 sample set. However, twenty-three groundwaters were analyzed for As speciation based on the 1995 groundwaters (Table 7.1).

The mine waters from the Heath Steele deposit (n = 6) are typically more oxidized (lower As^{III}/As^{total}) than high TDS groundwaters from the deeper boreholes at the Restigouche deposit. Borehole MM-89-107 from the Restigouche deposit and borehole HN94-65 from the Halfmile Lake deposit are the most oxidized reflecting the fact that these holes are dominated by low TDS shallow groundwaters. Arsenic in borehole MM-89-104 shows roughly equal proportions of both As species; these groundwaters are bailer groundwaters and thus the

increased degree of oxidation compared to MM-89-106 and B-80-07 may reflect oxygenation in the open standing water column.

Arsenite (As^{III}) is the more stable form of As under reducing conditions. In oxidizing environments As^{V} is most abundant, but is removed from the water column through preferential adsorption onto Fe-oxyhydroxides. In the water column, biological activity increases reduction of As^{V}, accounting for the large offset from thermodynamic equilibrium. The chemical oxidation of As^{III} to As^{V} in the presence of oxygen is typically a slow process at neutral pH values, with equilibrium occurring on the order of weeks to months. In the presence of Fe and Mn oxyhydroxides, oxidation can occur in hours to days.

For borehole MM-89-106 groundwaters, arsenic in the deepest waters is present almost entirely as As^{III}, although they plot in the As^{V} stability field in terms of Eh and pH (Fig. 7.46). Groundwater MLW95-511 (equivalent to groundwater MLW95-512) is compositionally similar to the deeper waters (Fig. 7.18), but the As is more oxidized. This groundwater is close to the transition between the shallow meteoric waters in this hole and more deeper saline waters. The change in As speciation may be related to the proximity of shallower groundwaters (i.e., mixing and/or diffusion between low TDS shallow groundwaters and higher TDS deeper groundwaters). The high-salinity waters from borehole MM-88-02 have low Eh and moderate pH, consistent with predominantly reduced As species. The As contents in these waters are low, and close to detection, however. Similarly, waters from borehole MM-89-104 have Eh and pH values that straddle the As(III)-As(V) boundary on As stability diagrams (Fig. 7.46), consistent with nearly equal amounts of reduced and oxidized As in these waters (Table 7.1).

For Heath Steele deposit waters, five of the six groundwaters plot in As(III) stability fields, and one in the $HAsO_4^{2-}$ field (groundwater MLW95-610). The As in this latter groundwater occurs as As^{V}, consistent with its measured Eh and pH values. Groundwater MLW95-485 has very low pH (3.03), and therefore plots on the $HAsS_2$ stability field, assuming an Eh of 0 (Fig. 7.46). However, the As in this water is dominantly As^{V} (80%; Table 7.1). The kinetics of As oxidation and reduction are sluggish (Bowell et al., 1994). The interpretation of the As

speciation in groundwater MLW95-485 is that the low pH was produced by precipitation of Fe-oxyhydroxides where the water entered the mine workings. Ferrous to ferric iron oxidation is an acid producing reaction. Given that the kinetics of Fe oxidation are rapid at pH > 4.5 (e.g. Millero et al., 1987), it is likely that the rate at which the pH shifted due to Fe-oxyhydroxide precipitation was greater than the rate at which arsenate was reduced to arsenite to reflect the new Eh-pH conditions of the groundwater. Groundwater MLW95-486, from the same mine (though at slightly greater depth) as MLW95-485 had a field pH of 6.56 and As(III) > As(V). Note, however, that the lab pH was 3.33 and the anion sample bottle has Fe-oxyhydroxide precipitates.

For the BMC groundwaters, it appears that there are competing forces with respect to the behaviour of As. Arsenic occurs primarily as oxyanions in natural waters (Figs. 7.47). Therefore, the adsorption behaviour of arsenic is expected to be the reverse of that of cations (as discussed in the previous section). However, in the BMC the primary source of anomalous As is from the oxidation of massive sulphides. Thus, in normal circumstances (i.e., distal from massive sulphide mineralization), As contents are expected to increase as pH increases. However, in an environment where large amounts of As are being released by sulphide oxidation, there is commonly a reduction in pH due to acid production. At lower pH, ferrous Fe-oxyhydroxides become less stable, reducing the surface sites for As adsorption.

Recently, Johannesson et al. (1996c) presented As and Se data of groundwaters from south-central Nevada and Death Valley, California. They suggested that these elements could be used as tracers for regional groundwater flow based on their conservative (Se) and near-conservative (As) behaviour. However, as shown above, As in BMC groundwaters is closely associated with adsorption on Fe-oxyhydroxides (Figs. 7.44, 7.47), and therefore cannot be used as tracers for these waters. Johannesson et al. (1996c) do not account for adsorption as a possible control on As contents in their study.

7.5.11 Mo and U in Halfmile Lake and Restigouche deposit groundwaters

There are some very interesting relationships between the different groundwaters and U and Mo. These elements are commonly believed to behave similarly in natural waters. In oxidizing waters, U and Mo are considered moderately to highly mobile, whereas, in reducing waters, both elements are highly stable. Hodge et al. (1996) attempted recently to show that U, Mo, and Re showed strong correlations with Cl and SO_4 in springs from the southern Great Basin. They interpreted these correlations as indicating that these trace elements were behaving conservatively and that they might therefore be useful tracers for groundwater flow models. These spring waters had previously been shown to be oxidizing throughout their flow paths, which led Hodge et al. (1996) to conclude that the conservative behaviour of U was due to the formation of stable carbonate complexes. However, Waite et al. (1994) presented experimental evidence to suggest that, in the pH range of 5.5 to 8, most U^{VI} was adsorbed to ferrihydrite. With increasing pH, carbonato complexes increase in importance, and U adsorption is reversed. The study of the southern Great Basin groundwaters does not report pH values, although data on these waters has been presented elsewhere and indicates that most of the waters have pH values of around 7 (Hodge et al., 1996; Johannesson et al., 1997). It is therefore interesting that in terms of experimental data, these waters should not be showing conservative behaviour for U, due to adsorption. The authors state that the waters are oxidizing, however there is no data presented to demonstrate that this is the case. Hodge et al. (1996) do note that some of the groundwaters from their study (those from Furnace Creek springs) have anomalously low U contents. The reason for these low U groundwaters is not addressed, but it seems consistent with experimental work to suggest that the cause of the relative U depletion is related to adsorption processes which are not addressed.

The BMC ground and surface waters have variable, though generally low U contents which range from 2 to 4,350 ng/L, with an average of 139 ng/L (n = 207). Similarly, Mo varies from 0.6 to 66 µg/L, with an average of 4.61 µg/L (n = 151). Uranium shows moderate to poor correlations between log(SO_4), pH, Eh, and log(Cl) (Fig. 7.48). If U was controlled primarily by oxidation state and pH of the aqueous phase as well as the activity of carbonate, there

should be a positive correlation between U content and Eh. For the BMC waters as a whole, there is a negative correlation. However, if the concentration of U in these waters is also controlled by adsorption processes, this negative correlation can be accounted for because at higher Eh, Fe-oxyhydroxides are stable (Fe^{III}). As pH increases, TDS and DIC contents generally increase. The combined effects are that at pH < 7 but > 5.5, U in BMC waters will be strongly sorbed. At pH values around 8, adsorption should decrease rapidly (Waite et al., 1994).

Uranium and Mo typically behave similarly in natural waters. However, comparison of U/Mo ratios in the various media analyzed in this study show that the situation is more complex for the BMC. Uranium can be shown to be less mobile compared to Mo in BMC waters by comparing U/Mo ratios in the host rocks with those in stream sediments, suspended sediments, ground waters and surface waters. The host lithologies are dominantly felsic and have U/Mo generally much greater than 1, except for massive sulphides and two mafic rocks with tholeiitic REE patterns (Chapter Ten). The low U/Mo ratios of massive sulphides indicates that these elements were fractionated in the original hydrothermal fluids that formed the deposit. Uranium is excluded from most sulphide minerals (Chapter Twelve), and most of the U in the massive sulphide samples occurs in the gangue minerals. Stream sediments have U/Mo that are typically > 1. At the Halfmile Lake deposit, the U/Mo of stream sediments ranges from 1.31 to 6.39 (mean = 3.93, n = 35) and at the Restigouche deposit, U/Mo range from 0.26 to 7.8 (mean = 2.54, n = 90). Ten samples from the Restigouche deposit have U/Mo < 1, and of these six are associated with Fe-oxide rich sediments or occur proximal to gossans. Three of the samples come from seeps and Charlotte Brook. Suspended sediments from groundwaters at both deposits are highly with respect to U/Mo. However, suspended sediments from borehole HN94-65 have U/Mo that ranges from 0.191 to 0.214, whereas the corresponding groundwaters have ratios of 0.013 to 0.071. This pattern between suspended sediment and corresponding groundwater where the latter has lower U/Mo than the former is also shown for the Restigouche deposit (Chapter Nine). For all waters, where U and Mo are both above

detection, U/Mo ranges from 0.001 to 1.57, with an average of 0.199 (± 0.318, n = 207). Thus, the pattern is one of decreasing U/Mo ratios from the host rocks, to sediments, to waters. This indicates that as waters interact with the host lithologies, Mo is more readily mobilized in these waters relative to U. Additionally, U is preferentially removed from the aqueous phase relative to Mo onto suspended sediments/colloids, and stream sediments where there is a strong hydromorphic component. This is an interesting conclusion given that under the acid conditions under which the Murray Brook Gossan deposit is assumed to have formed, Mo was interpreted to be relatively immobile (Boyle, 1995).

(Gascoyne, 1997) discusses the use of U as an indicator of the redox state of groundwaters in the Canadian Shield. However, as with Hodge et al., the impact of Fe-oxides and adsorption does not seem to have been taken into consideration.

The Mo concentrations of the Halfmile Lake groundwaters provide further evidence that the low TDS waters at Halfmile Lake are not merely drilling fluid (which utilized surface waters) or surface waters filling in the boreholes; all surface waters had Mo contents below detection, whereas the Halfmile Lake groundwaters are high in Mo, even compared to much higher conductivity waters at the Restigouche deposit (Fig. 7.36A).

7.6 Summary

Groundwaters from the Halfmile Lake deposit are dominated by low TDS, Ca-HCO_3 compositions. The highest TDS groundwaters are more evolved $NaHCO_3$-type waters. The Halfmile Lake deposit groundwaters are most likely modern meteoric waters rapidly transmitted to depth along steep structures. Any saline groundwaters that may have existed at the Halfmile Lake deposit have been "flushed" from the system.

Groundwaters from the Restigouche deposit range from shallow Ca-HCO_3 and Ca-SO_4 waters and to high TDS Na-Cl waters with increasing depth. The interpretation of the groundwater data at the Restigouche deposit is: 1) shallow local recharge is dominated by Ca and HCO_3 due to dissolution of carbonate and silicate minerals in the shallow soil zone and

upper parts of the weathered bedrock. There are possibly two end-members here that may reflect different dominant lithologies and different temporal characteristics; 2) a second shallow groundwater system characterized by oxygenated waters flowing through or along the ore horizon. This water mass is actively oxidizing the ore deposit resulting in elevated SO_4 and base metal contents; 3) a deeper groundwater flow system is characterized by elevated Na and Cl concentrations due to greater water-rock reactions and elevated HCO_3^- due to dissolution of carbonate in the footwall alteration zone to the ore deposit (as in boreholes MM-89-102 and the deeper parts of B-80-7); and 4) deeper saline groundwaters occur with no obvious relationships to the shallow groundwater system. Brackish waters from borehole MM-89-106 are not related by mixing to the saline waters in borehole MM-88-02 as shown by differences in element ratios and radiogenic isotopes (Chapter Twelve).

The elevated sulphate and base metal contents of shallow Ca-SO_4-type groundwaters indicate that the massive sulphides are undergoing significant oxidation and releasing metals that are transported hydromorphically. Although base metals are elevated in streams flowing across and adjacent to the deposit, there is little evidence for significant contribution of the high sulphate groundwaters to the surface environment. The lower base metal and sulphate contents of Halfmile Lake groundwaters close to the ore zone is a function of lower dissolved oxygen which is due to the different hydrology of this deposit and greater depth to the ore body compared to the Restigouche deposit. Lower metal contents in groundwaters is reflected by more subdued metal anomalies in stream waters at the Halfmile Lake deposit. These results have important implications for mineral exploration in the Bathurst Mining Camp and elsewhere, and to setting water quality limits for the remediation of AMD sites.

The Br/Cl ratios of the groundwaters vary from values less than seawater in the saline waters to values much greater than seawater for the shallow groundwaters and surface waters. The shallow groundwaters and surface waters have similar Br/Cl values as those measured in brines from the Canadian Shield. This data suggests either that the saline waters have interacted with non-marine evaporites, or more likely, that Br and Cl are differentially released during

water-rock reaction.

The saline waters are interpreted to have been produced by long periods of water-rock reaction. There is no compelling evidence to support a marine origin for these waters. Elevated Cu, Co, Ni, and Cr contents of the saline waters from borehole MM-88-02 suggest that these waters have interacted with mafic rocks. The mafic dikes which cross-cut the Restigouche deposit may have acted as conduits for flow of these water.

The question was posed in the introduction as to what types of groundwater characterize the massive sulphide deposits of the BMC. There is no simple answer to that question. Groundwater flow is dominated by fracture-flow and as such deposit lithologies, geometry and structures play a fundamental role in determining the hydrology which in turn controls the geochemistry of the groundwaters. Proximity of the ore deposit to surface, and therefore to O_2-rich recharge waters, influences sulphide oxidation and therefore groundwater metal contents.

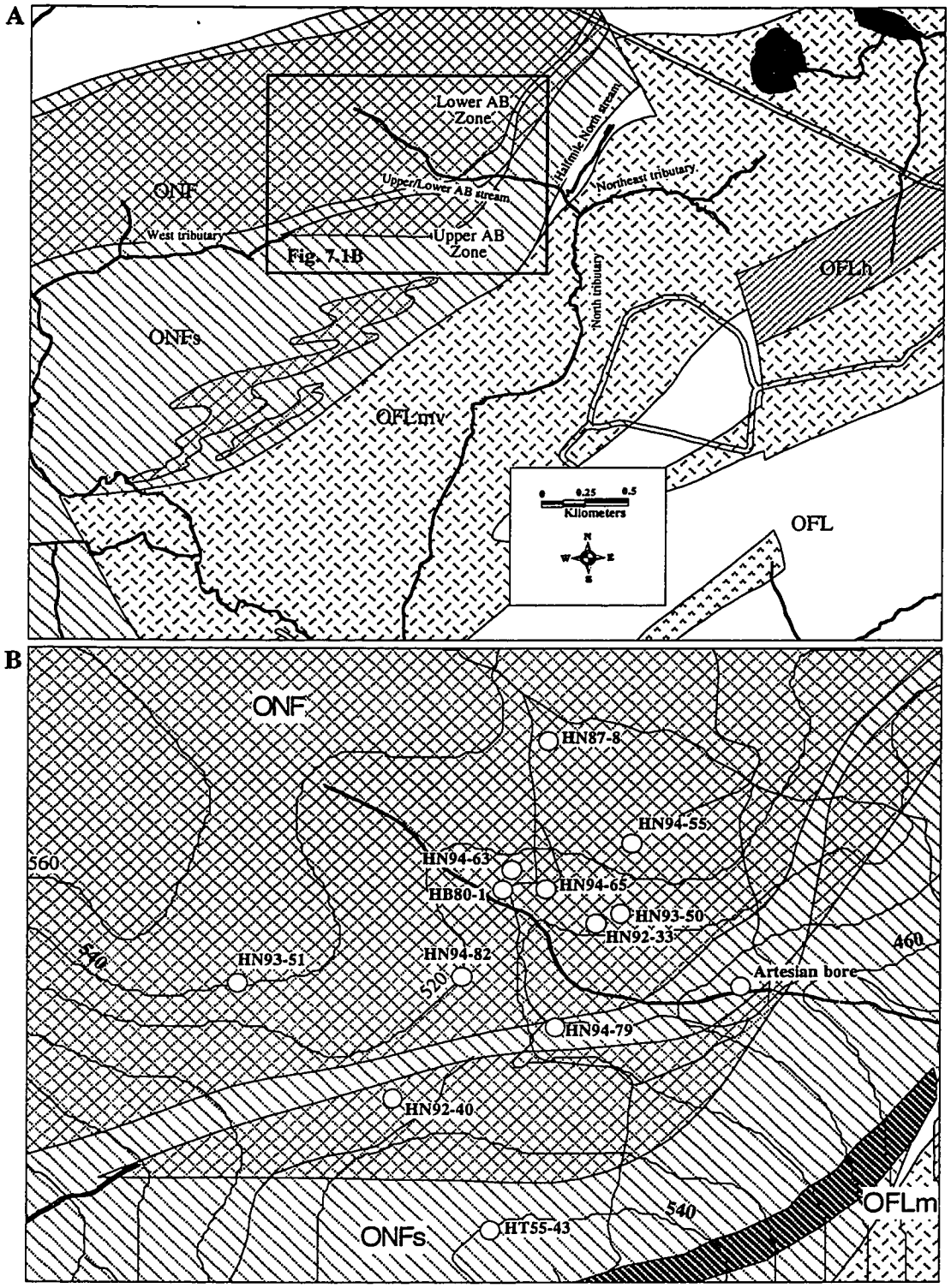


Fig. 7.1 Location of boreholes sampled for groundwaters from the Halfmile Lake deposit. Contours are in 20 m intervals. ONF = Nepisiguit Falls felsic volcanics, ONFs = sediments, OFLmv = Flat Landing Brook mafic volcanics, OFL = Flat Landing Brook rhyolite, OFLh = Flat Landing Brook hyaloclastite, Sul = surface projection of massive sulphides.

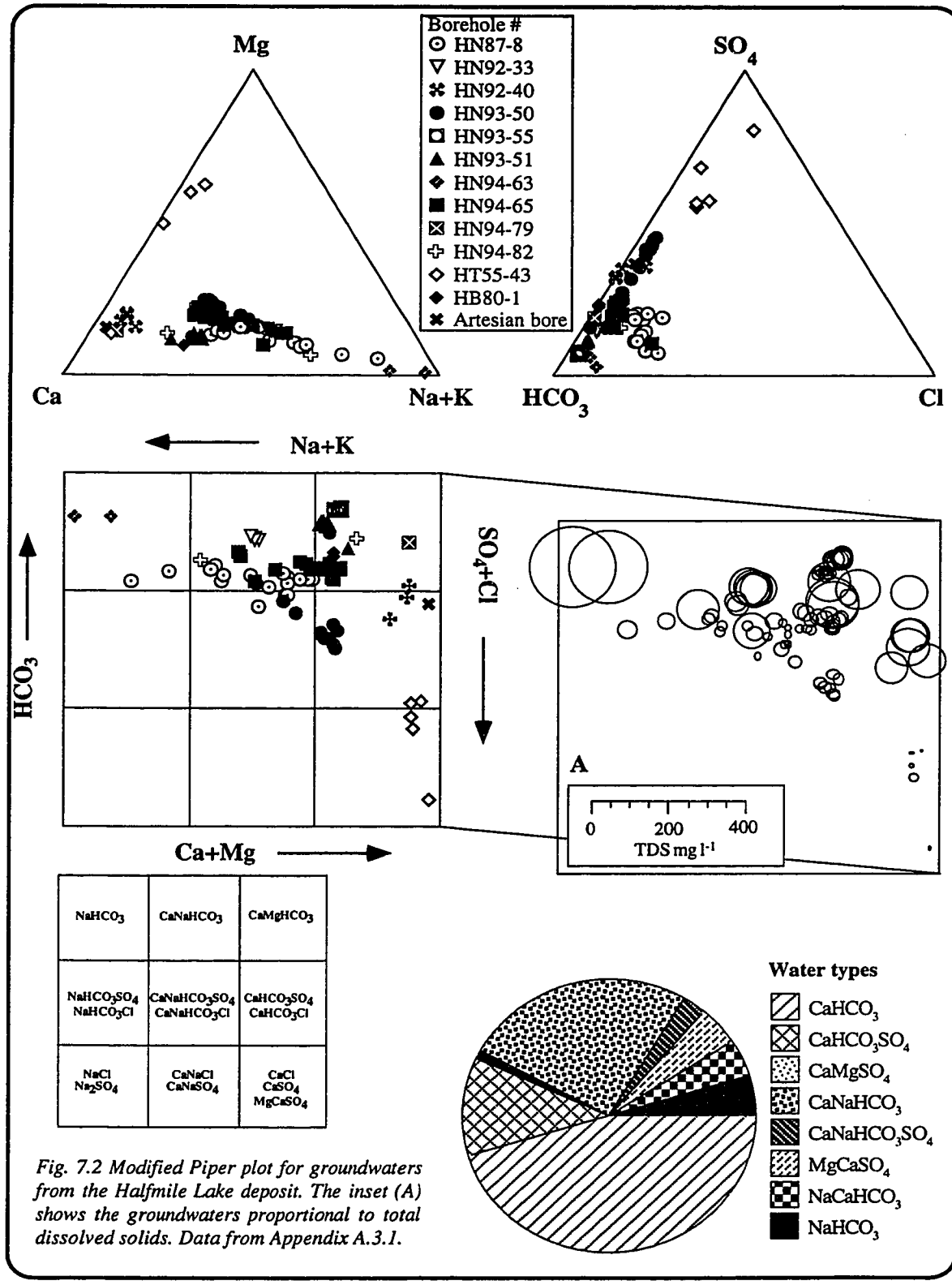


Fig. 7.2 Modified Piper plot for groundwaters from the Halfmile Lake deposit. The inset (A) shows the groundwaters proportional to total dissolved solids. Data from Appendix A.3.1.

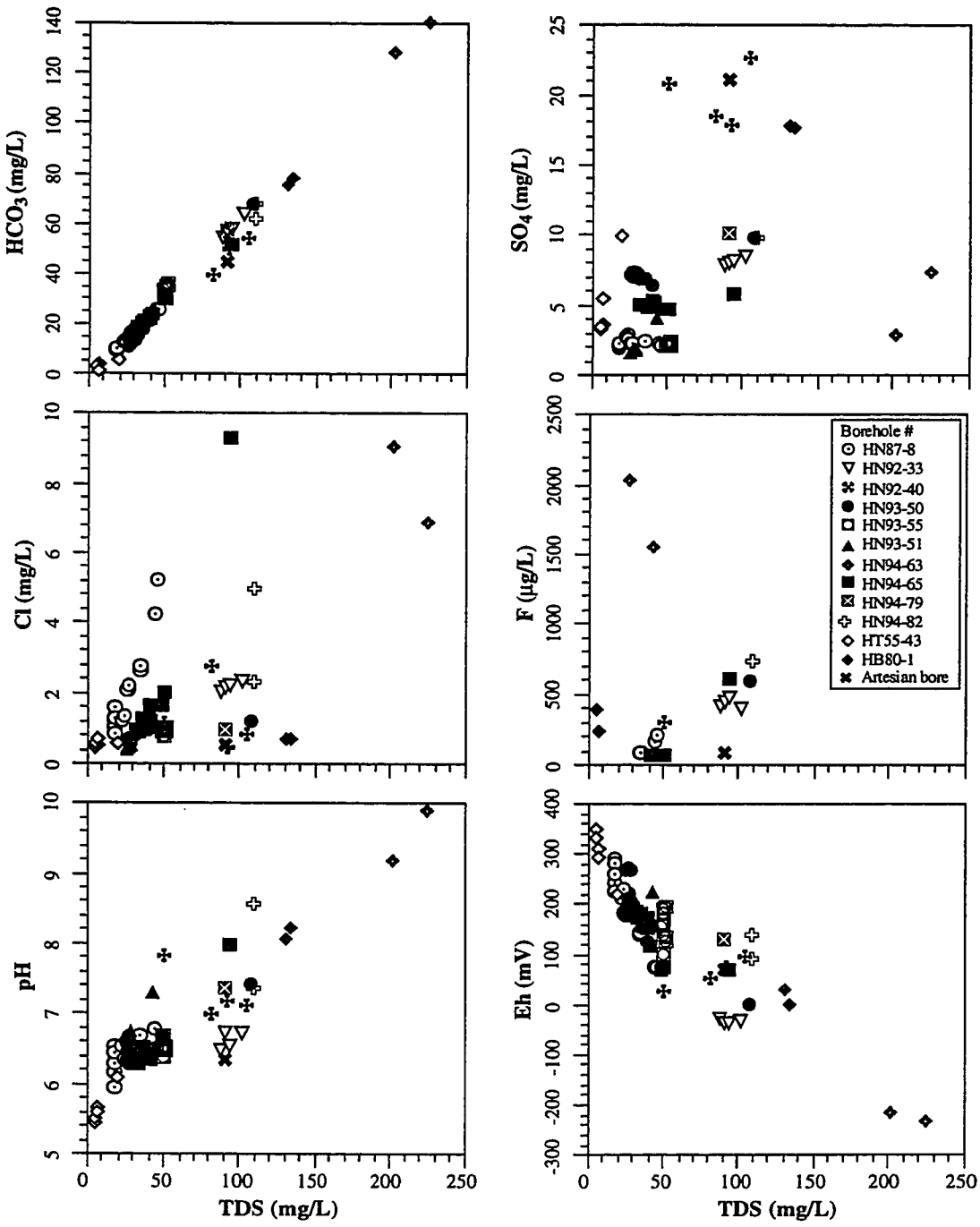


Fig. 7.3 Plots of pH, Eh, anions and cations versus TDS for Halfmile Lake deposit groundwaters. Data from Appendix A.3.1.

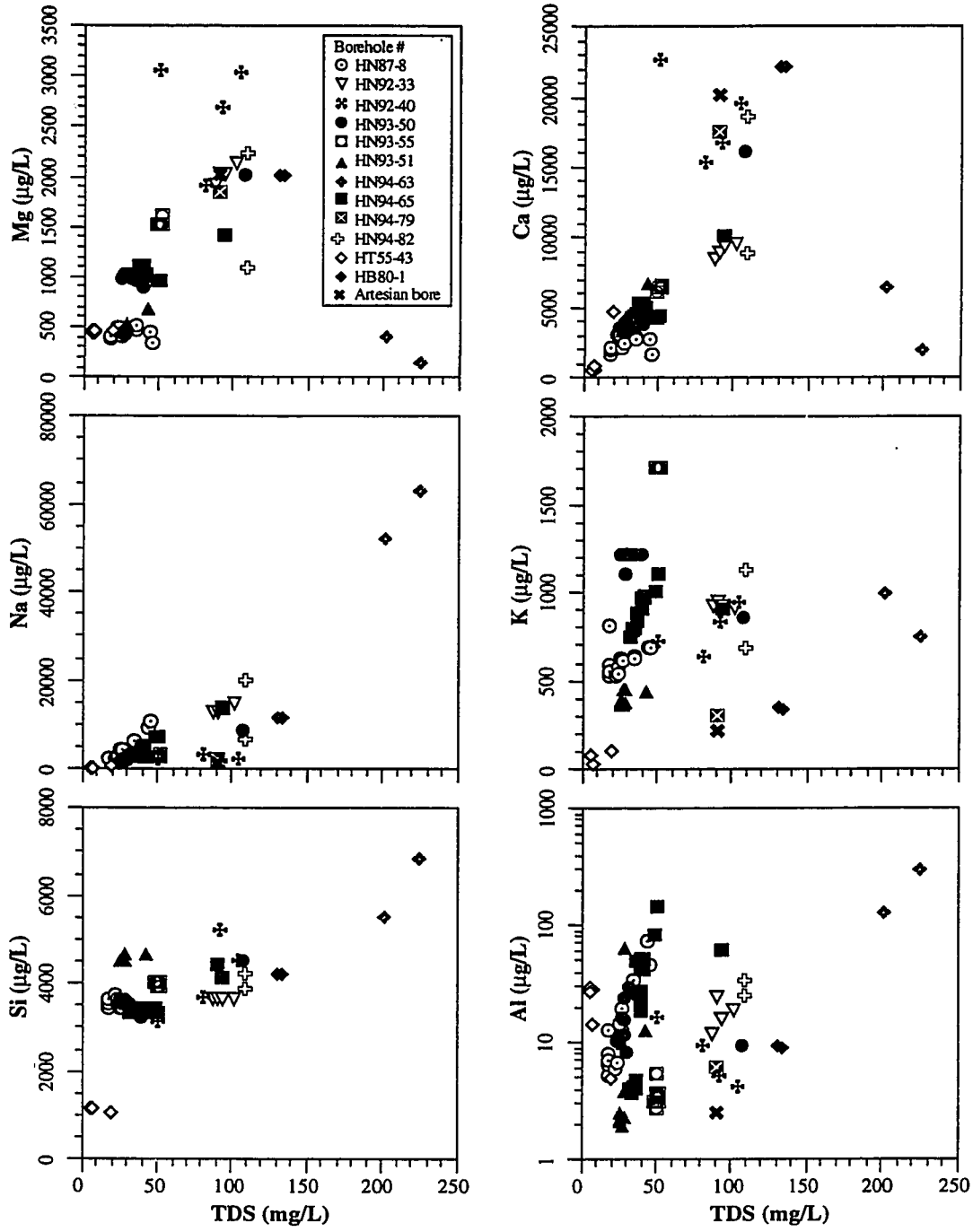


Fig. 7.3 continued.

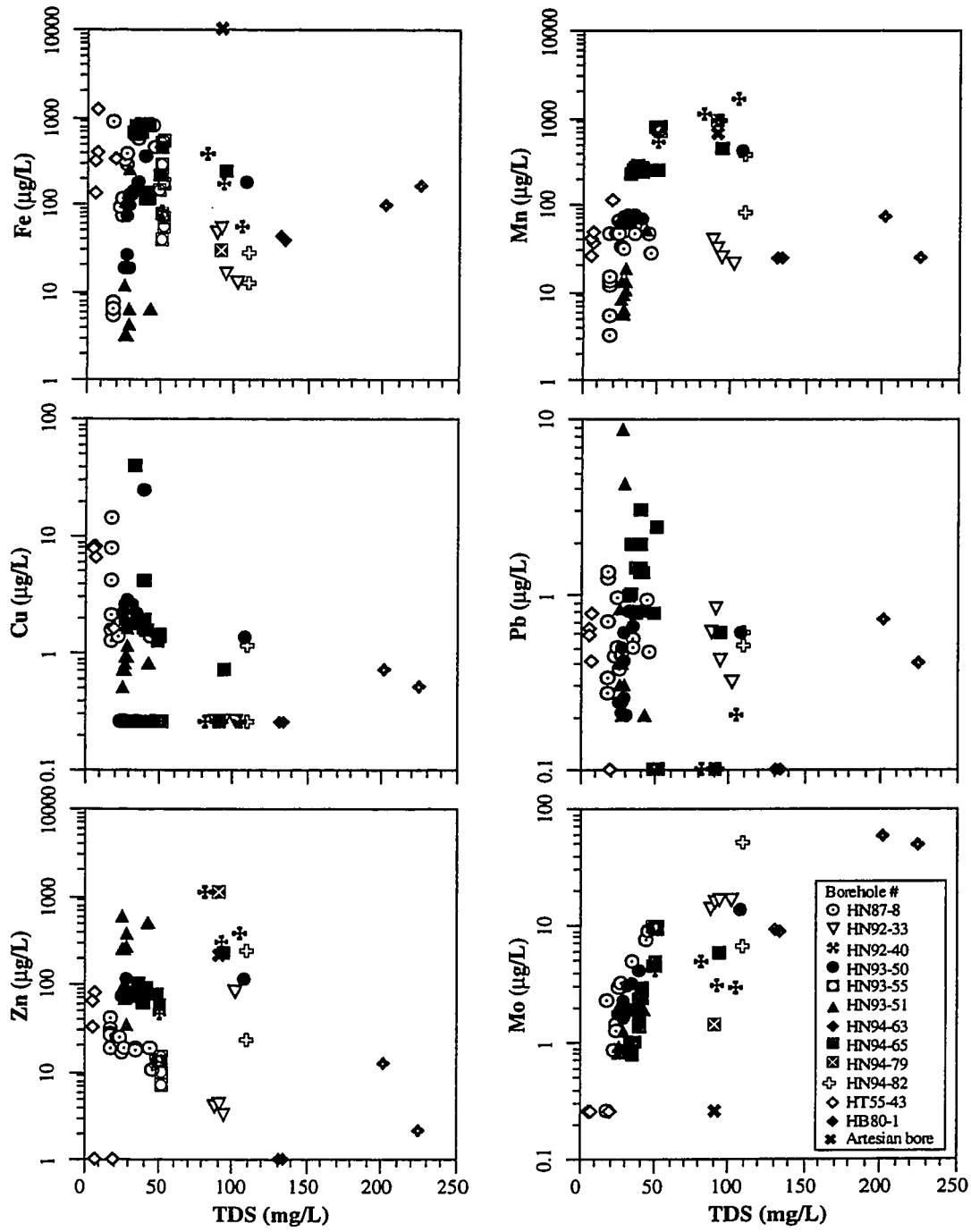


Fig. 7.3 continued.

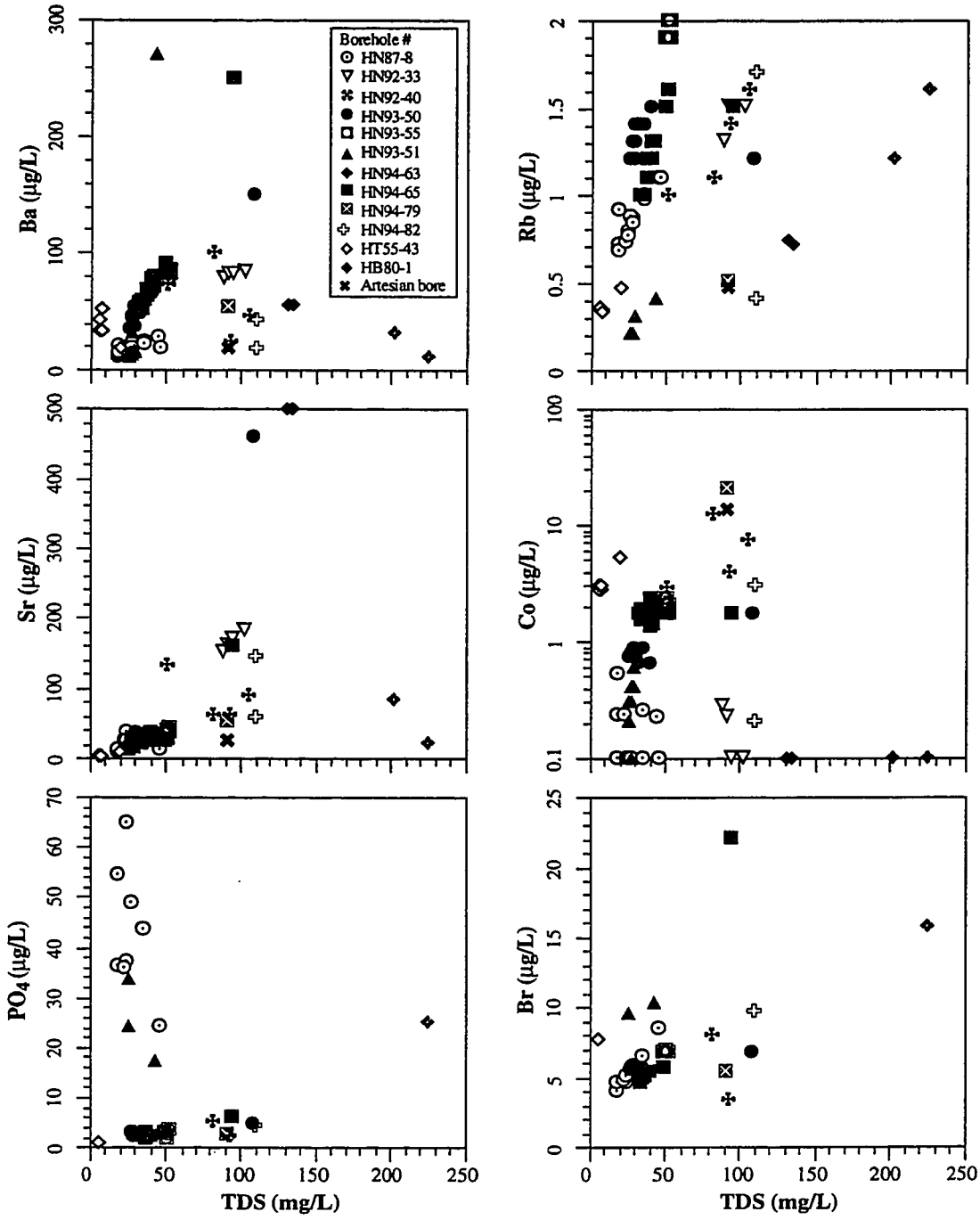


Fig. 7.3 continued.

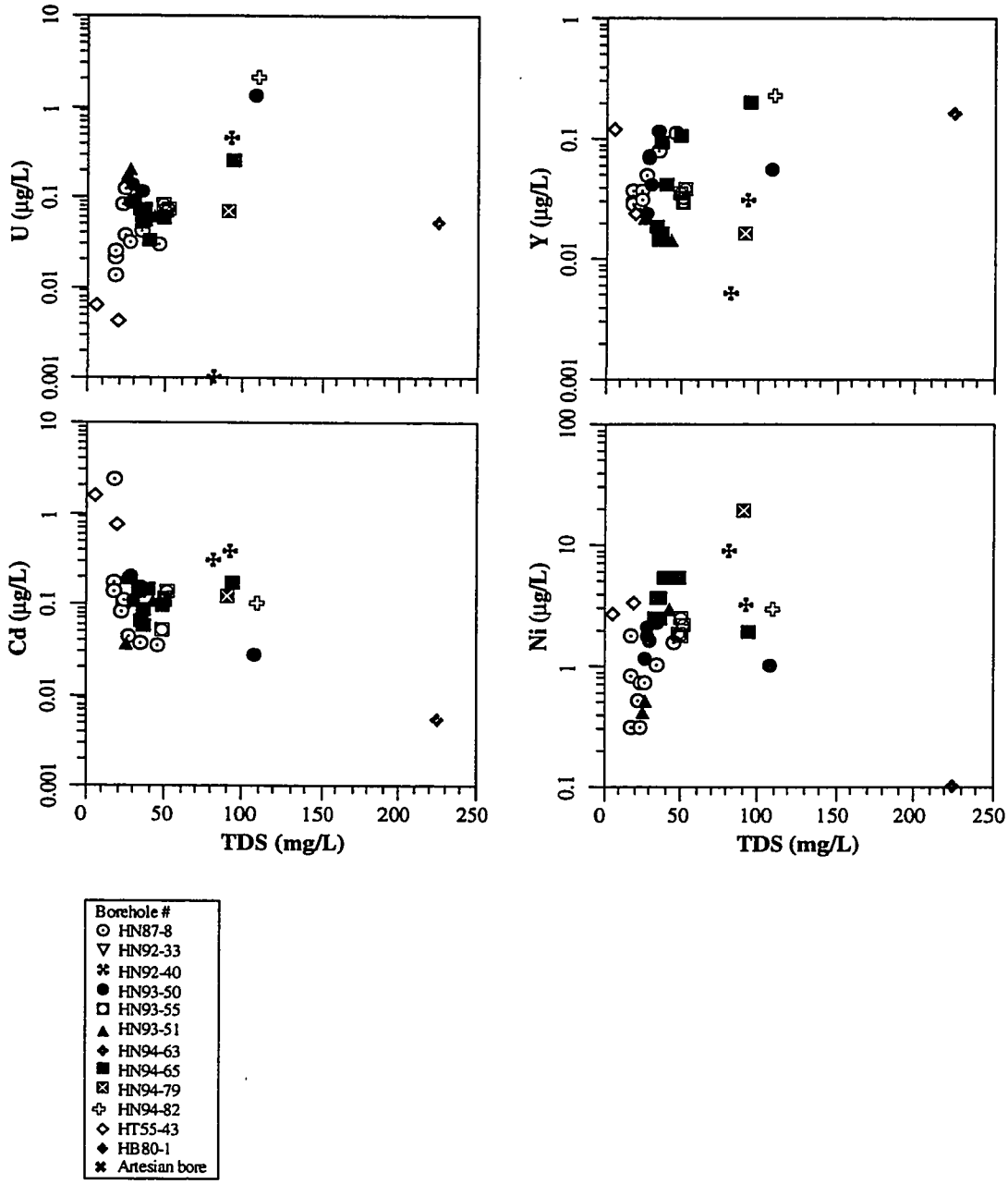


Fig. 7.3 continued.

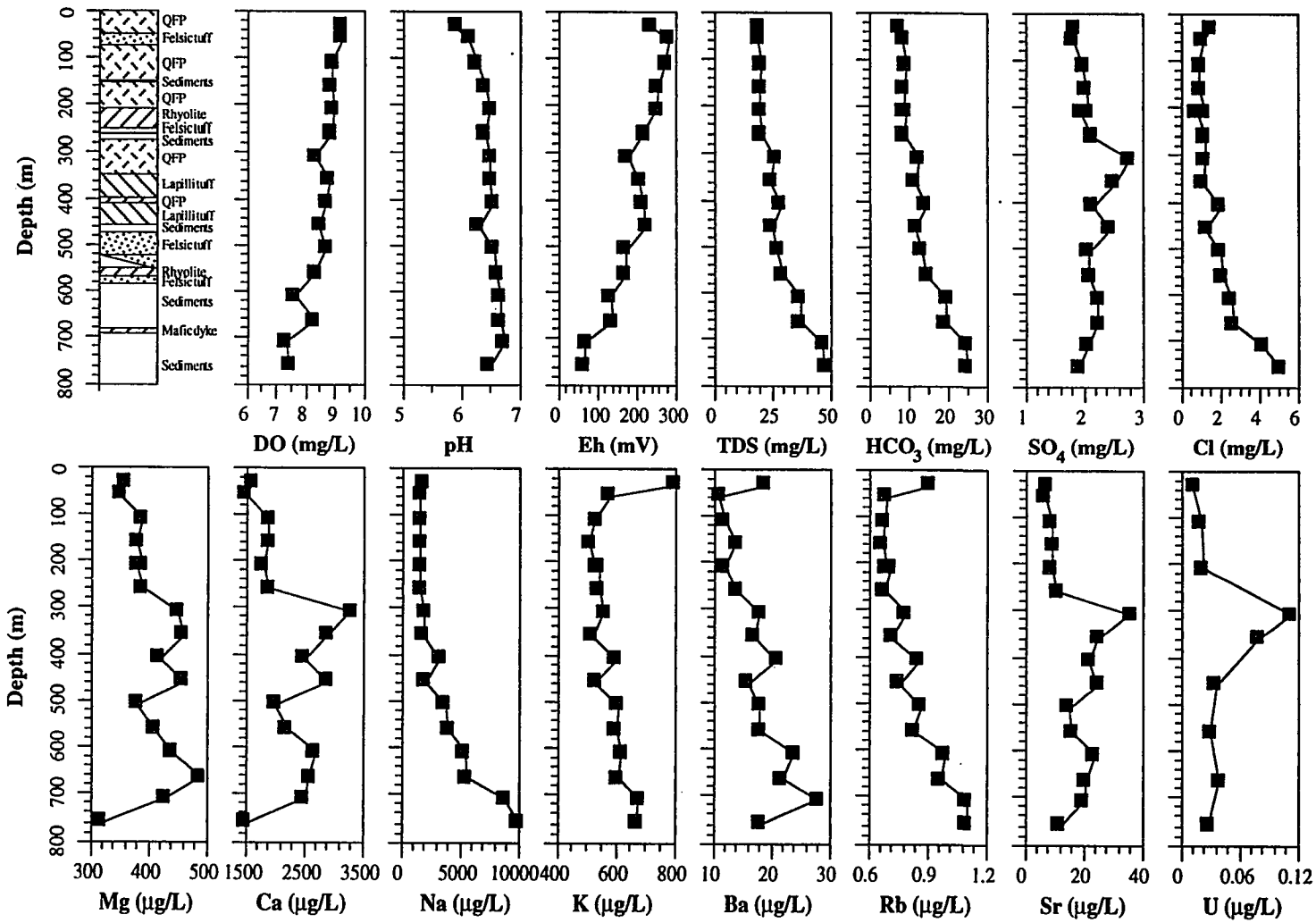


Fig. 7.4 Downhole variation profiles for field parameters, anions and cations for borehole HN87-8 from the Halfmile Lake deposit. See Table A.3.1 for data. Profiles for Cu, Pb and Zn show ICP-MS (square) and chelation ICP-MS (circle) data. All data collected with flow-through bailer.

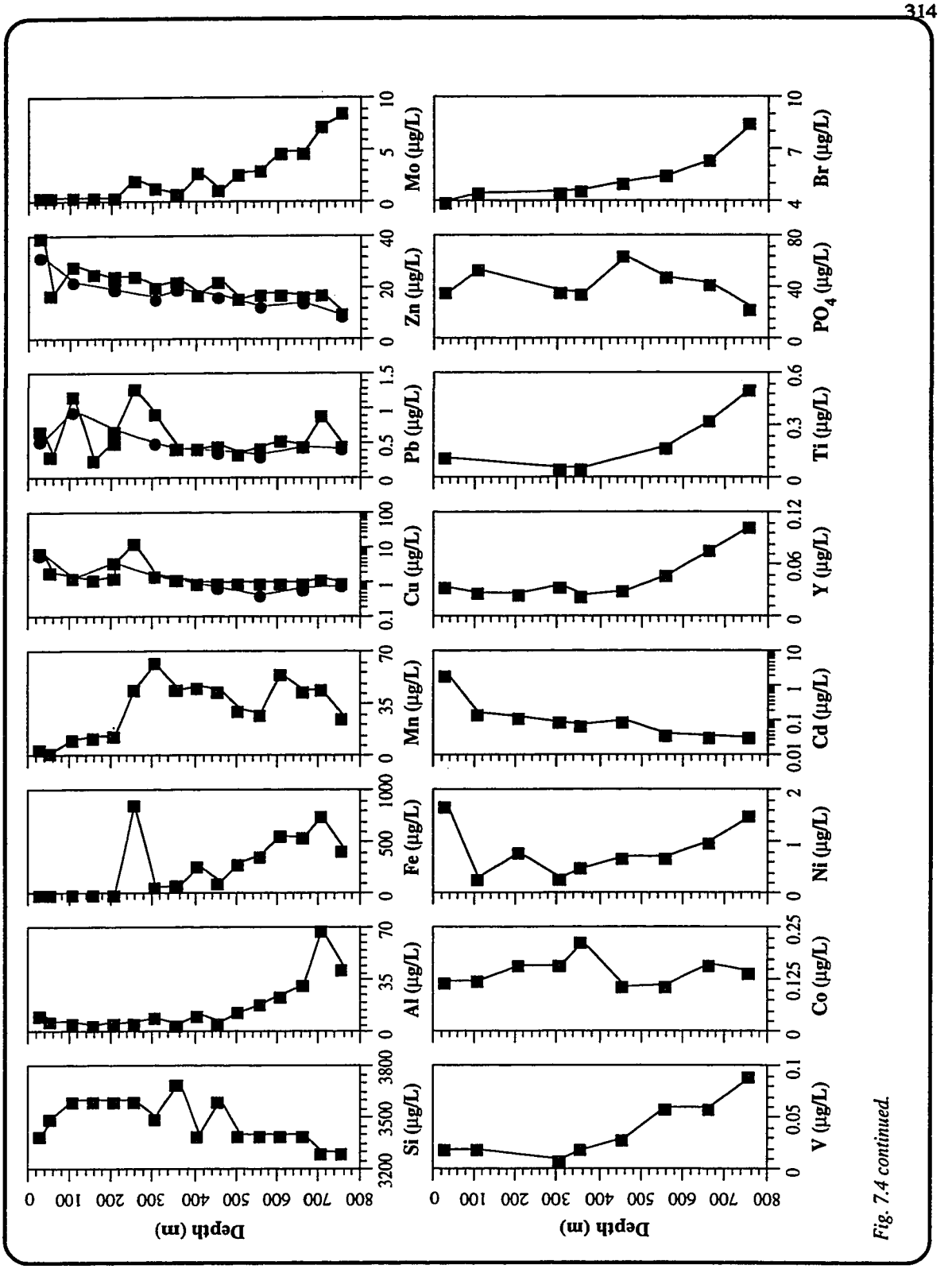


Fig. 7.4 continued.

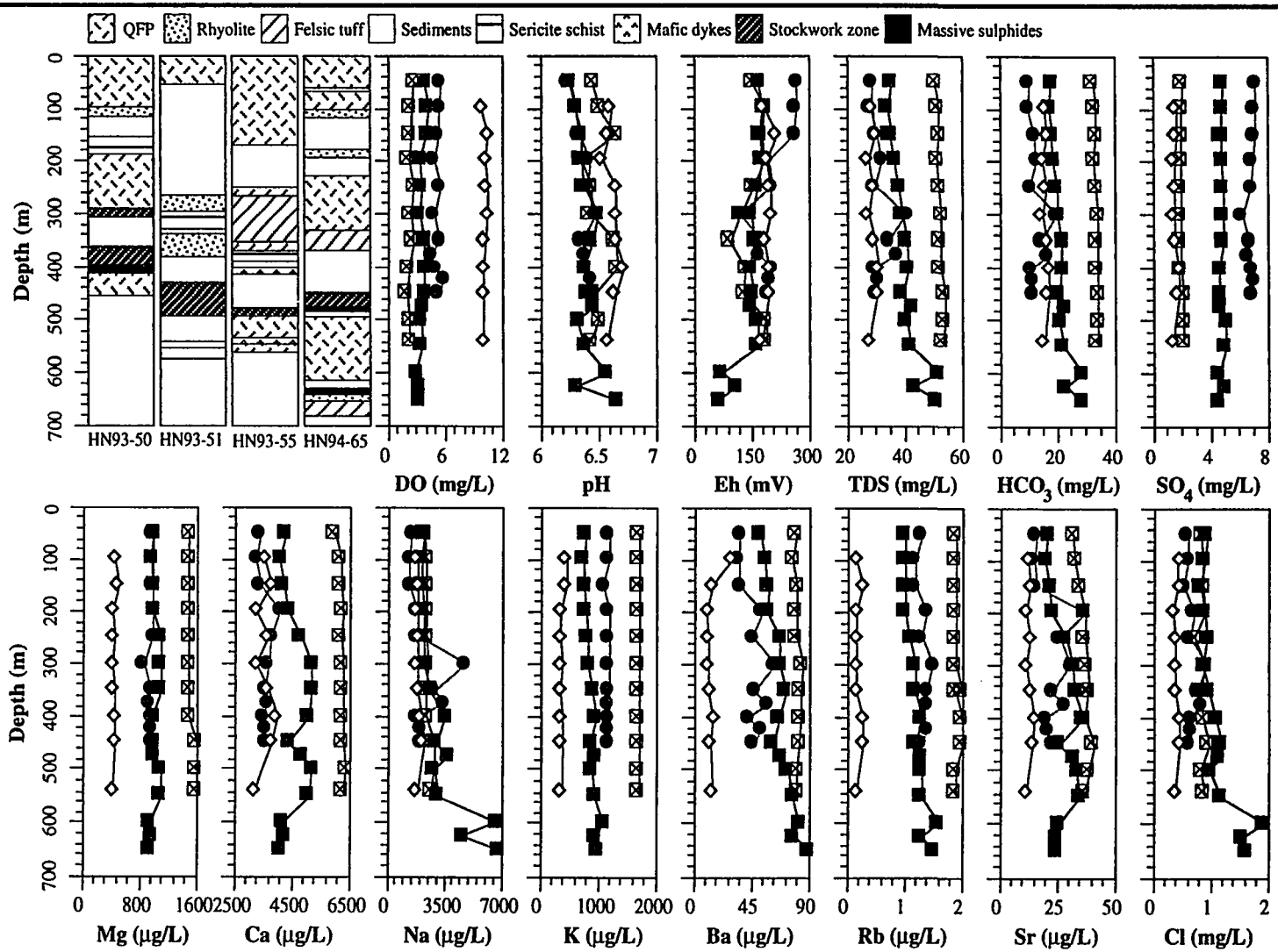


Fig. 7.5 Downhole variation profiles for field parameters, anions and cations for boreholes HN94-50 (solid dots), HN94-51 (diamond), HN94-55 (open square) and HN94-65 (solid square). All samples were collected by flow-through bailer. Data from Table A.3.1.

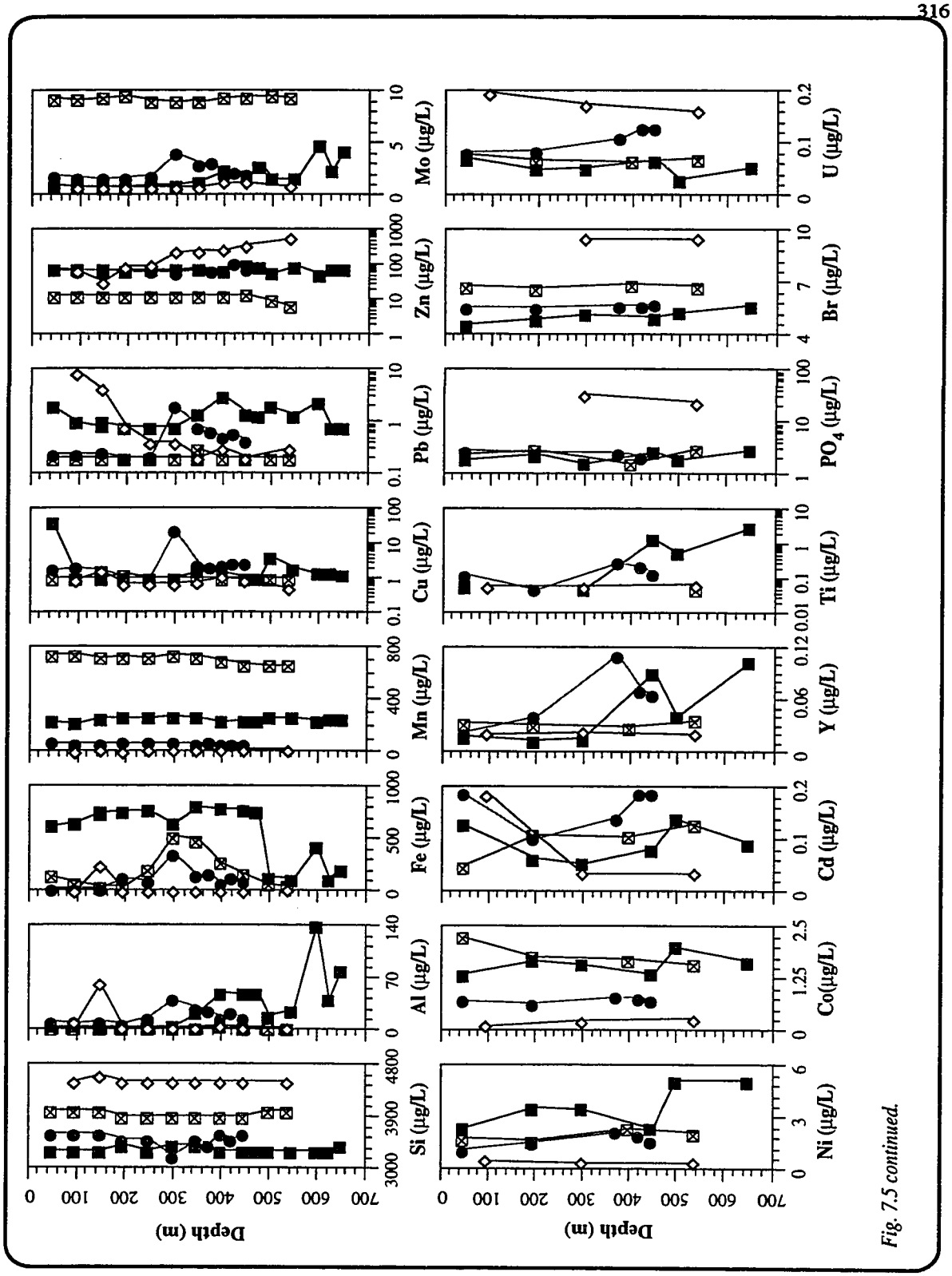


Fig. 7.5 continued.

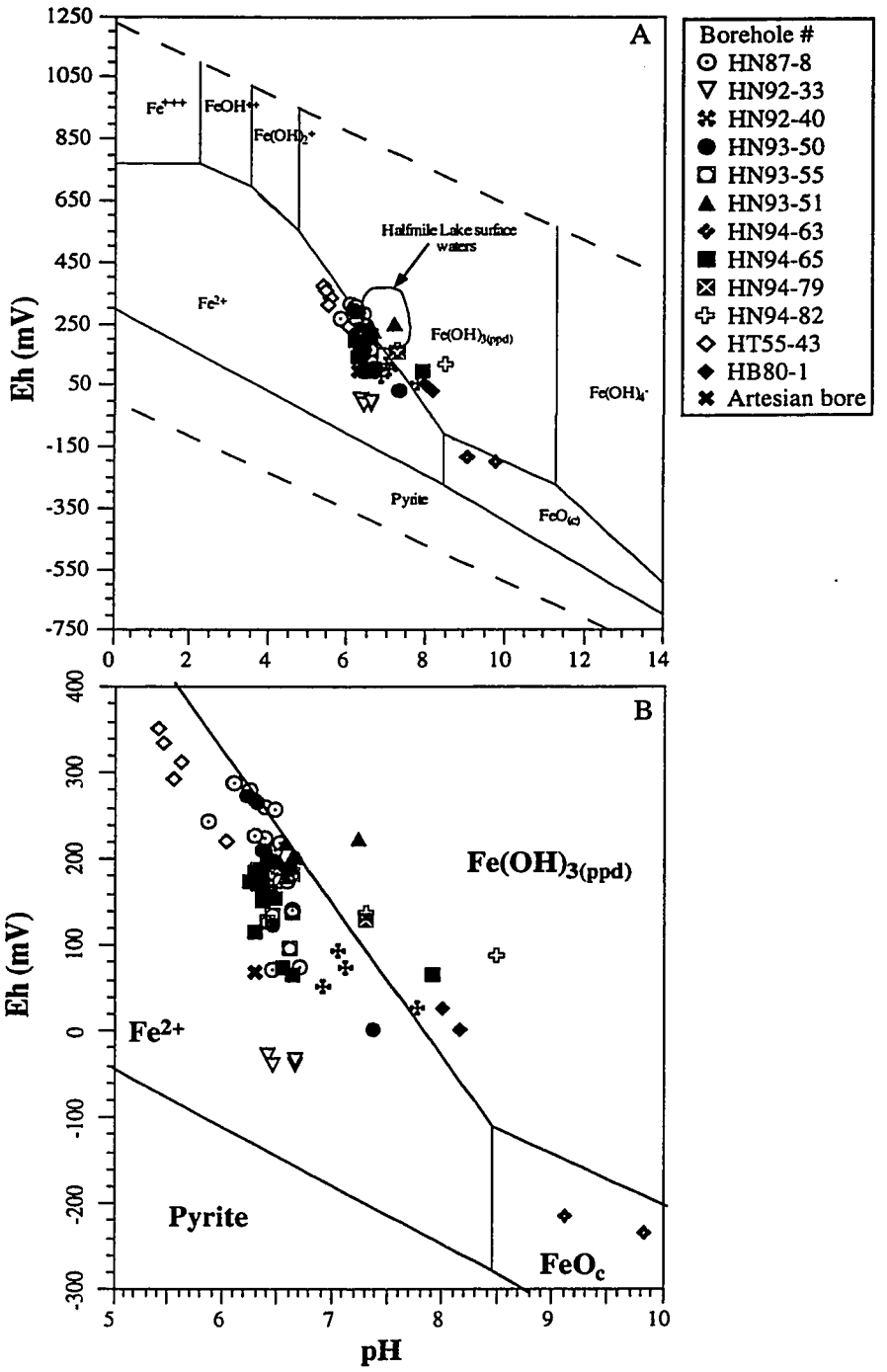


Fig. 7.6 Diagram showing the stability of metastable Fe hydroxides. The fields were calculated using The Geochemist's Workbench (Bethke, 1994). Conditions are: $[HCO_3] = 10^{-3.5}$, $[SO_4] = 10^{-4.5}$, $[Fe] = 10^{-5.5}$. The formation of hematite, goethite and magnetite was suppressed, reflecting the slow kinetics of formation of these phases compared to amorphous oxide phases. Shown in A is the field for Halfmile Lake deposit surface waters (Chapter Five).

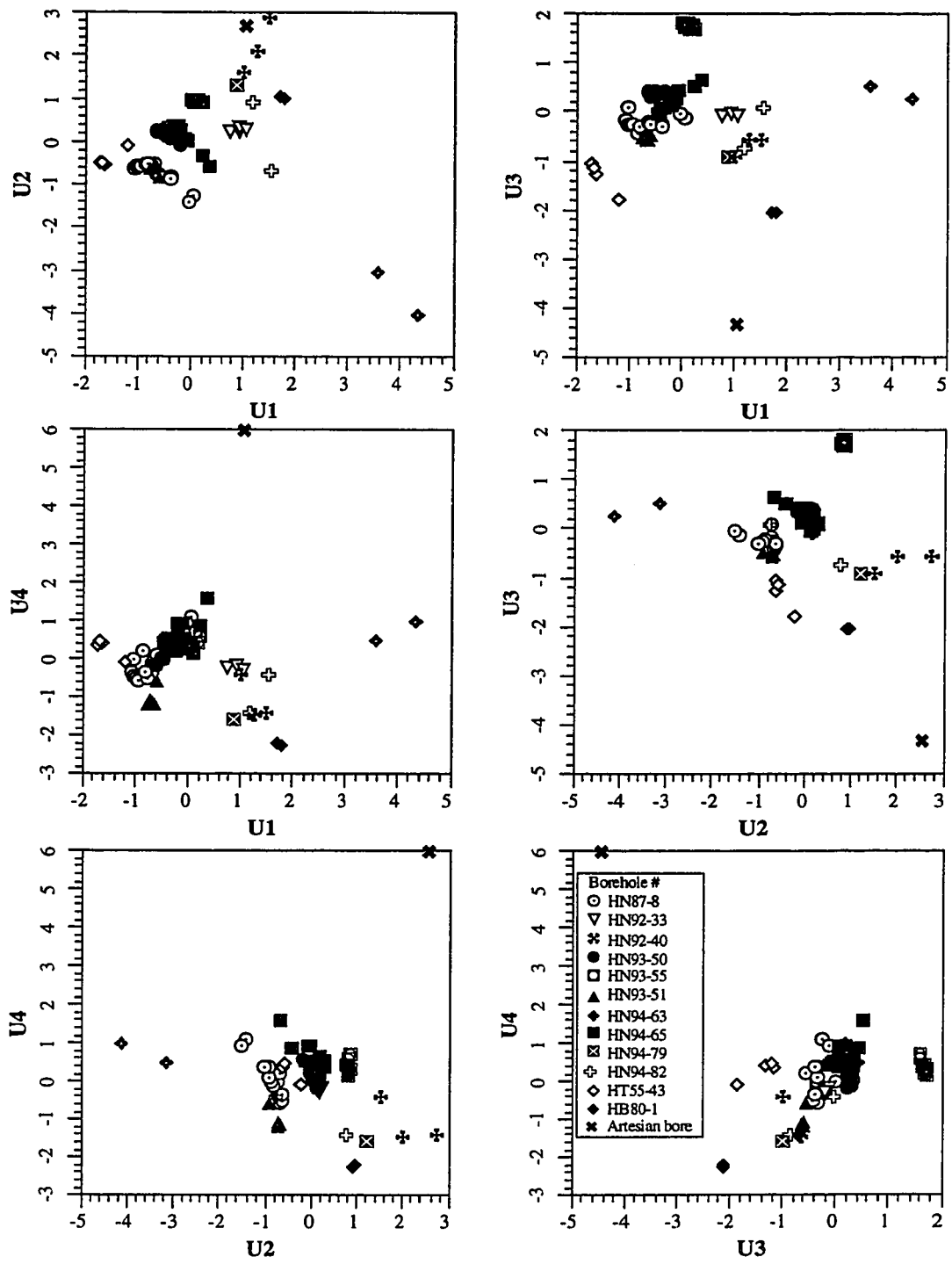


Fig. 7.7 Principle component plots of Halfmile Lake groundwaters, showing the variation in the first four factors (85.8% of the variation). PCA based on pH, Eh, DO, TDS, HCO_3, SO_4, Cl, Si, Al, Fe, Mn, Mg, Ca, Na, K.

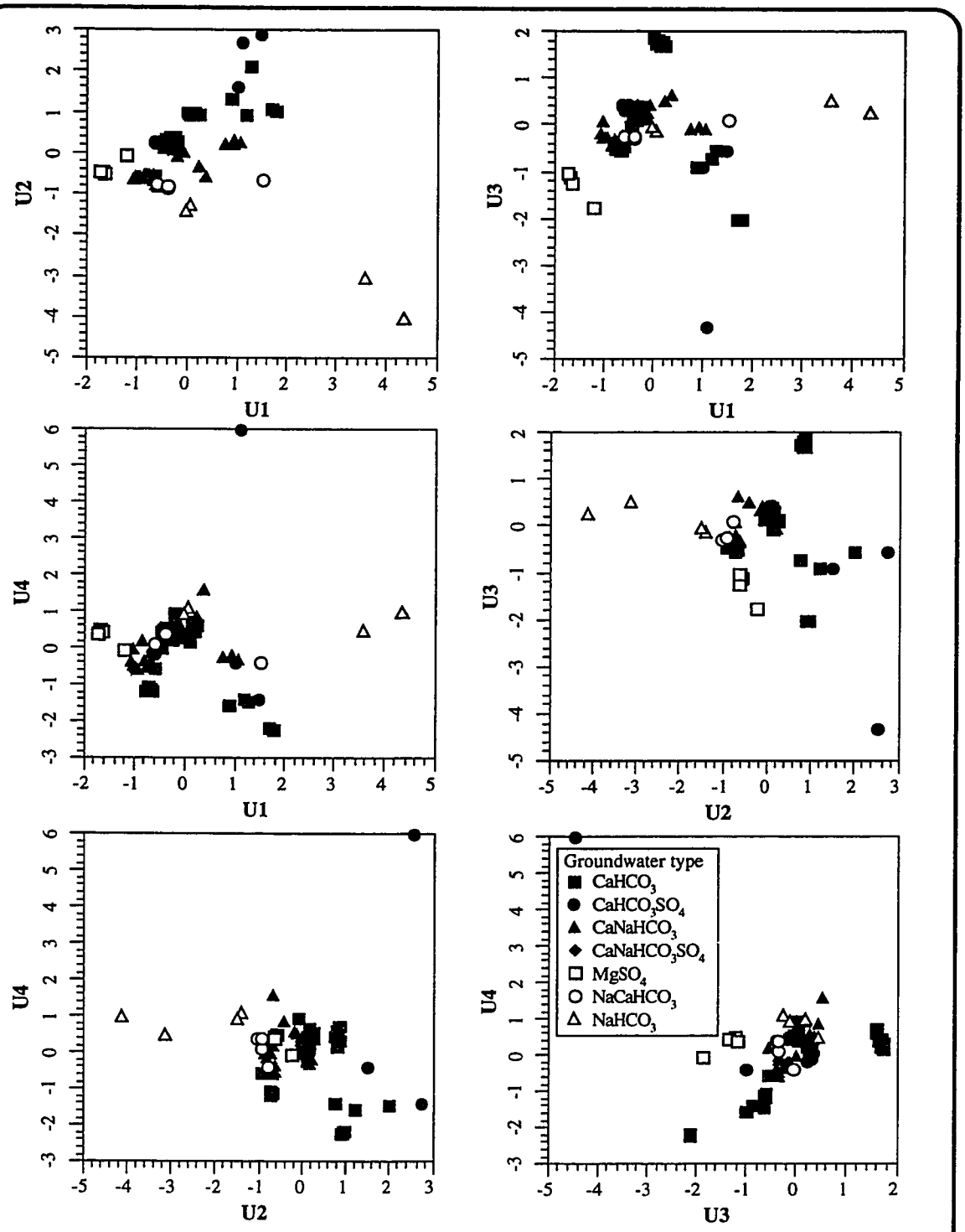


Fig. 7.8 Principle component plots of Halfmile Lake groundwaters, showing the variation in the first four factors (85.8% of the variation) and subdivided by water type. PCA based on pH, Eh, DO, TDS, HCO_3, SO_4, Cl, Si, Al, Fe, Mn, Mg, Ca, Na, K.

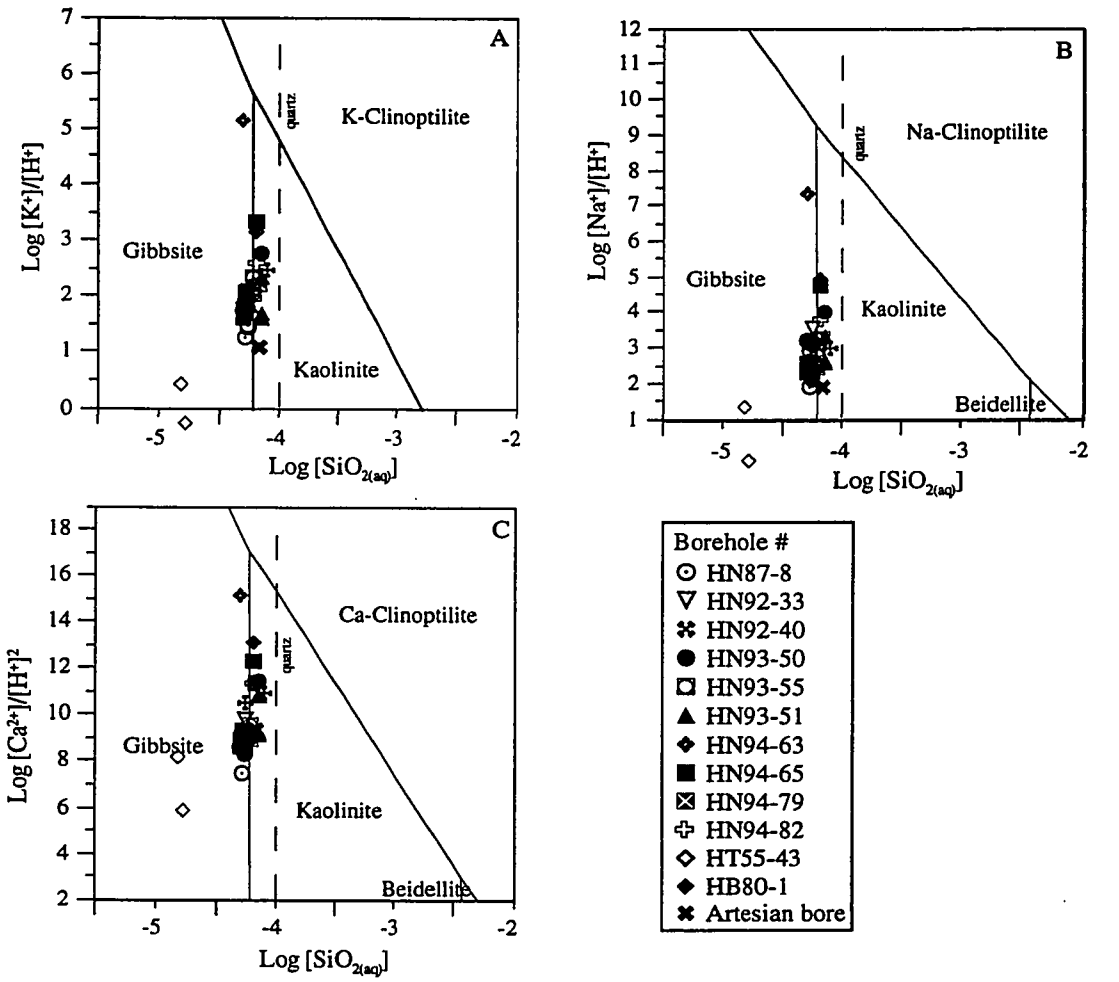


Fig. 7.9 Plots showing mineral stabilities for the systems A) Na_2O—Al_2O_3—SiO_2—H_2O, B) K_2O—Al_2O_3—SiO_2—H_2O, and C) Ca_2O—Al_2O_3—SiO_2—H_2O at 25°C and 1 atmosphere pressure for Halfmile Lake deposit groundwaters. Field boundaries plotted using The Geochemist's Workbench (Bethke, 1994). The dashed line indicates quartz saturation. Plotted data are for Halfmile Lake deposit groundwaters, based on activities calculated from PHREEQC using the WATEQ4F database. Geochemical data is from Table A.3.1.

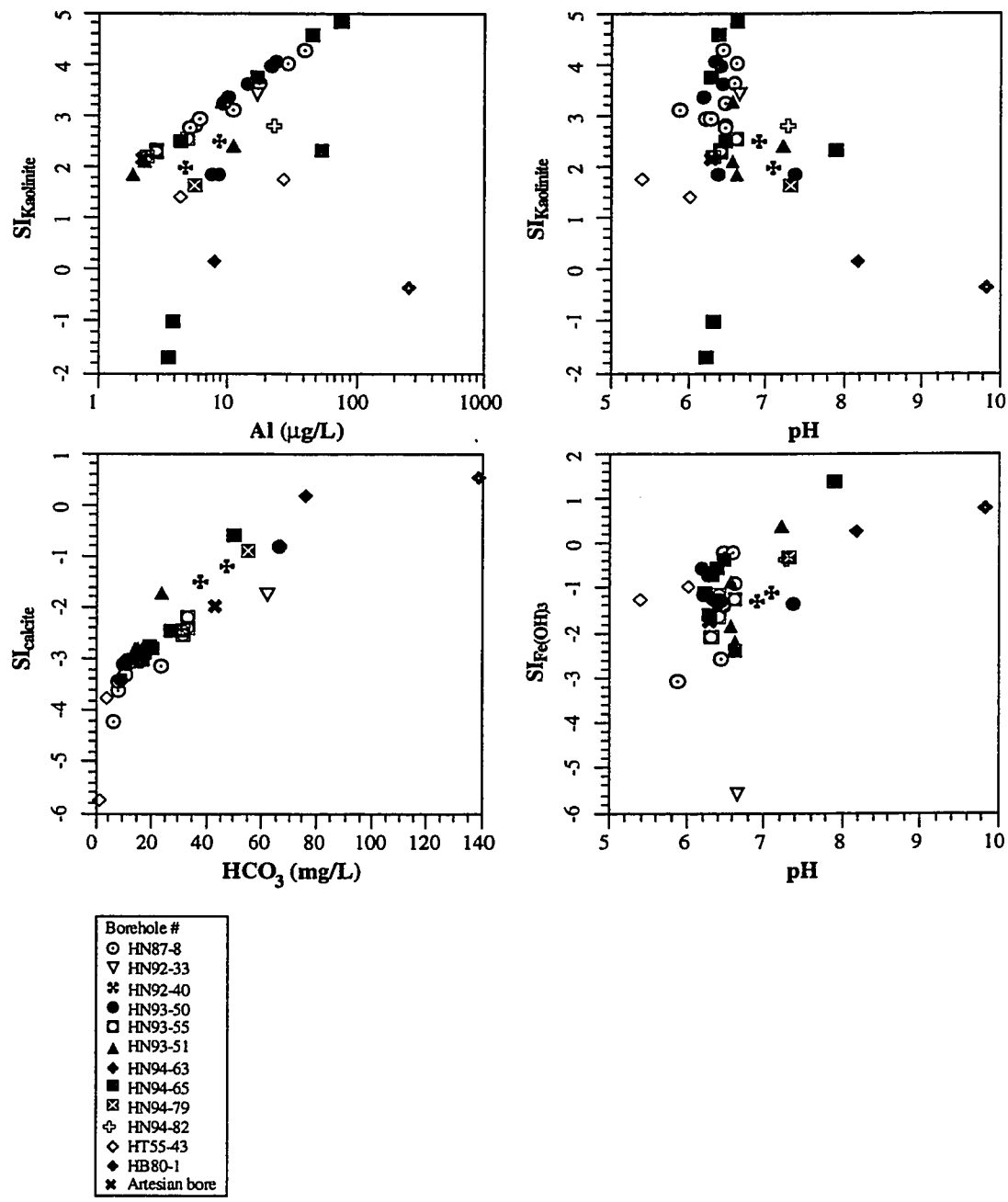


Fig. 7.10. Plots of selected mineral saturation indices for Halfmile Lake deposit groundwaters.

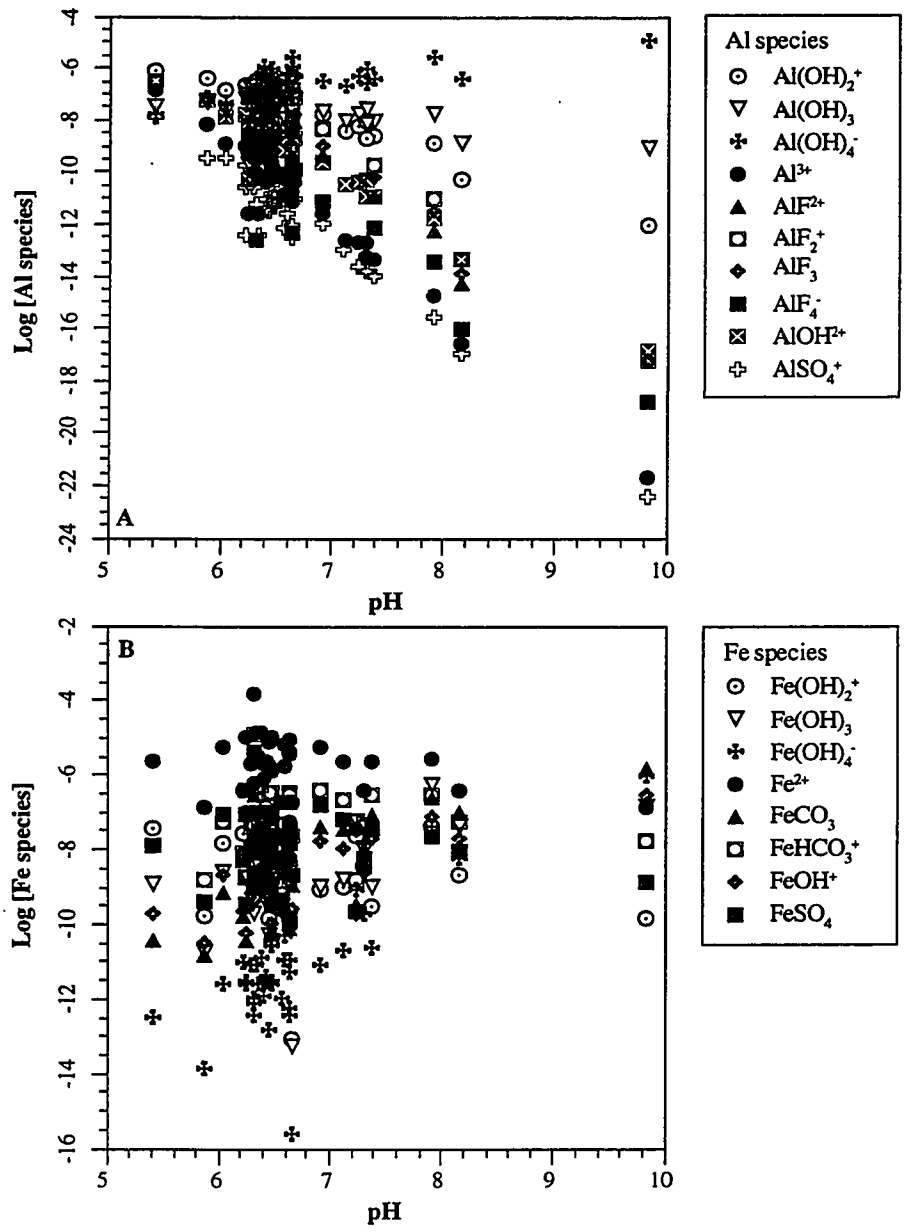


Fig. 7.11 pH variation diagrams showing the distribution of dominant A) Al, B) Fe, C) Pb, and D) Zn species in the Halfmile Lake deposit groundwaters. Speciation calculated with PHREEQC using the WATEQ4F database.

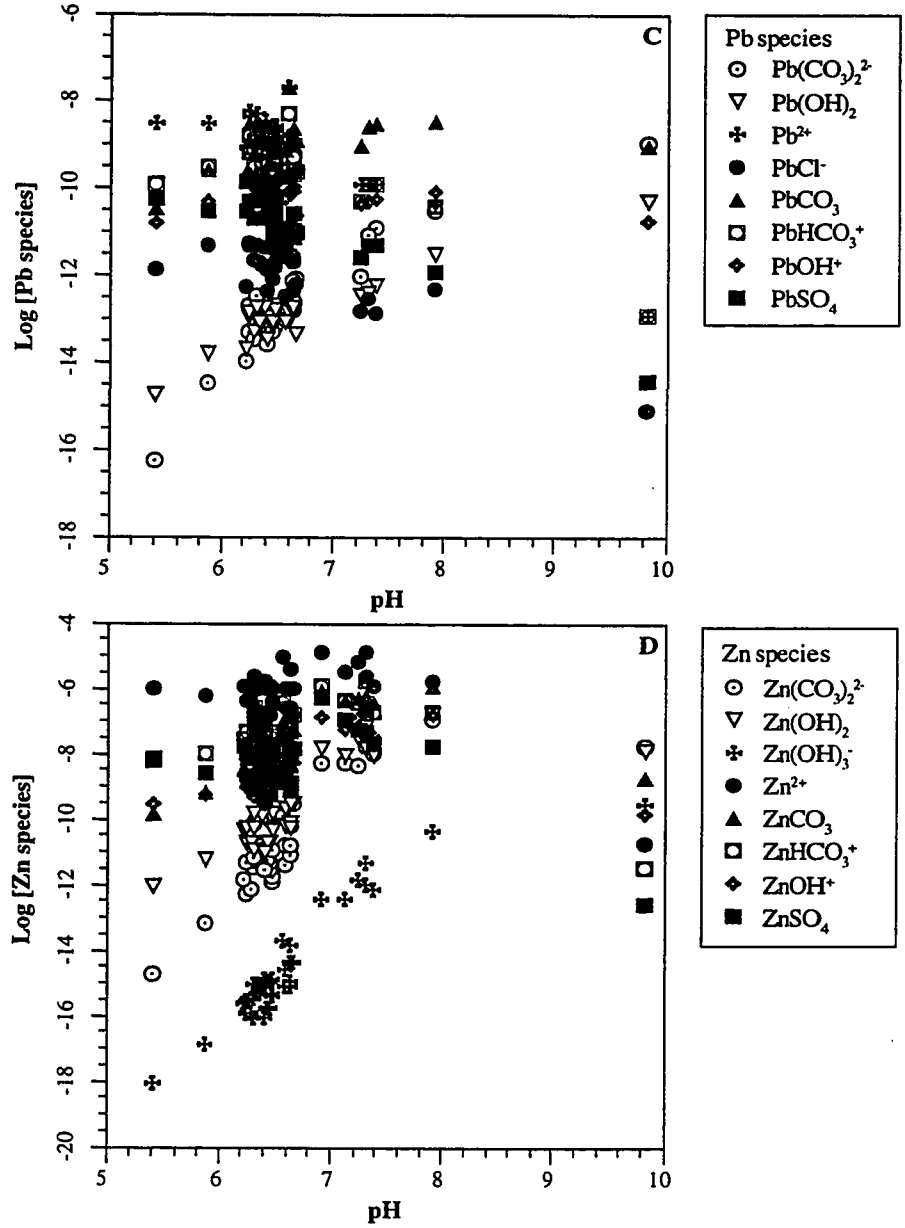


Fig. 7.11 continued.

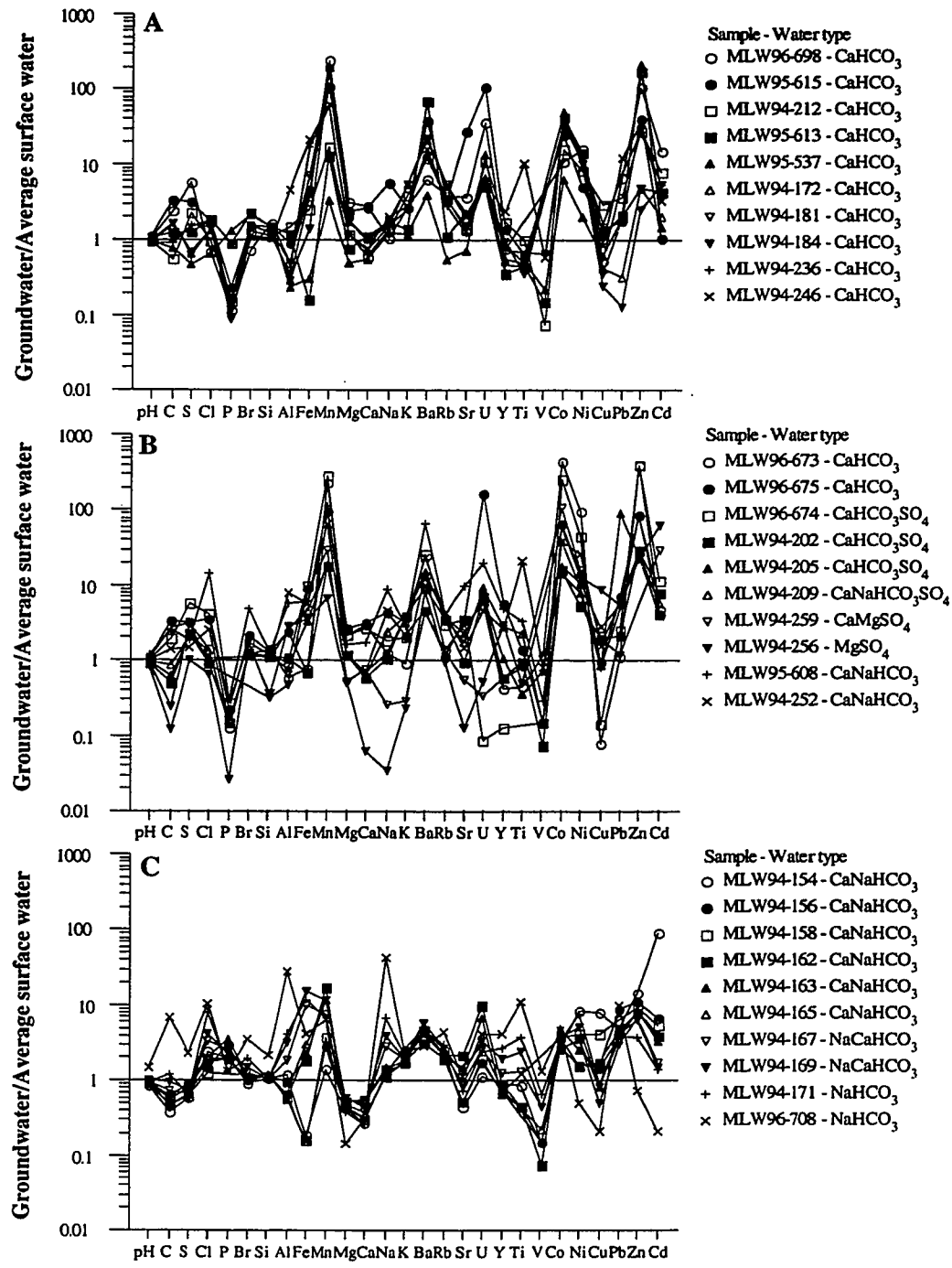


Fig. 7.12 Representative Halfmile Lake deposit groundwaters normalized to average surface water composition, based on water type. Note the different patterns for different water-types. Groundwater data from Table A.3.1.

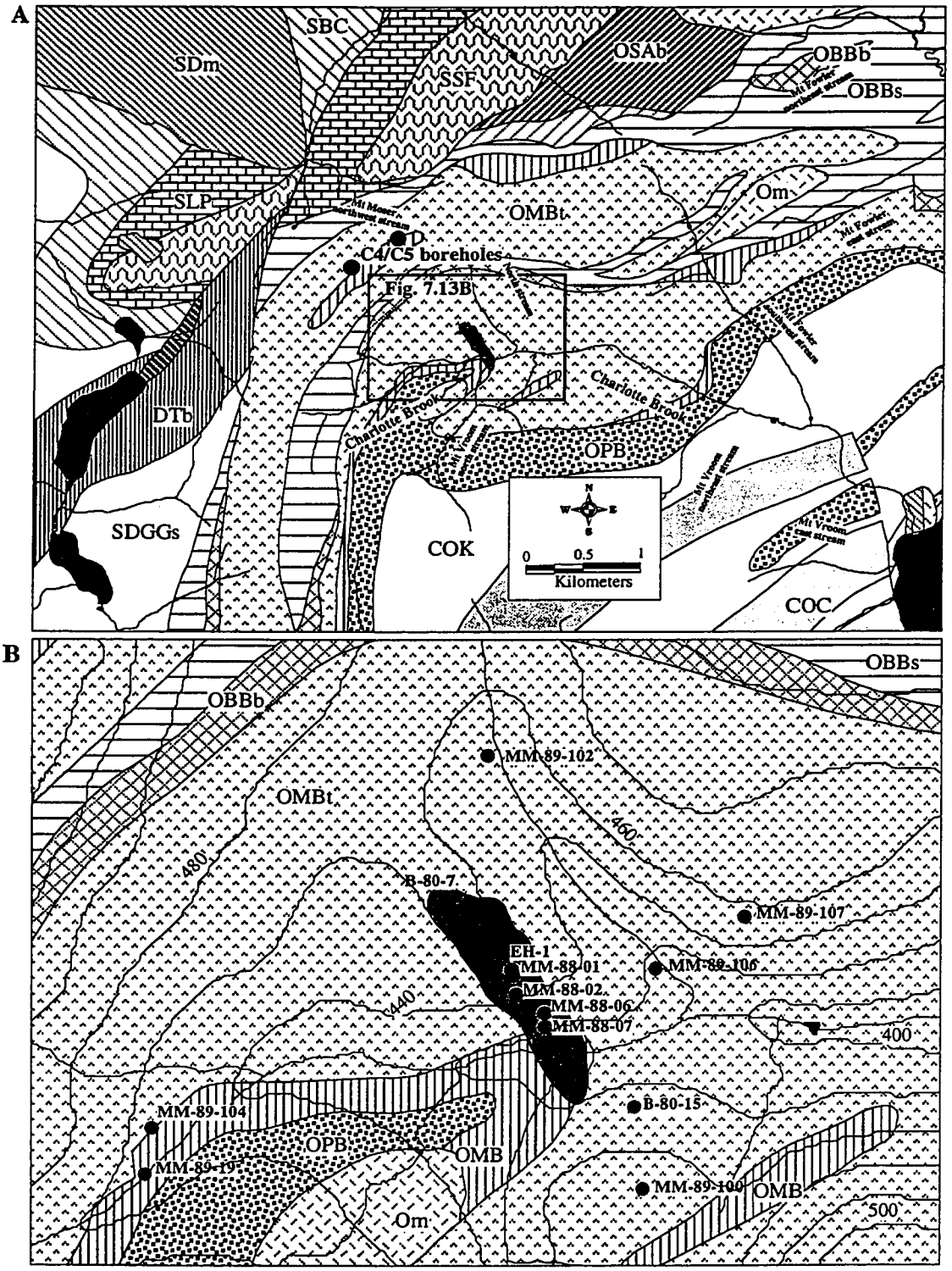


Fig. 7.13 Location of boreholes sampled for groundwaters at the Restigouche deposit. Contour interval is 20 m. Geology as in Chapter Two. Shaded area is the surface projection of the massive sulphides.

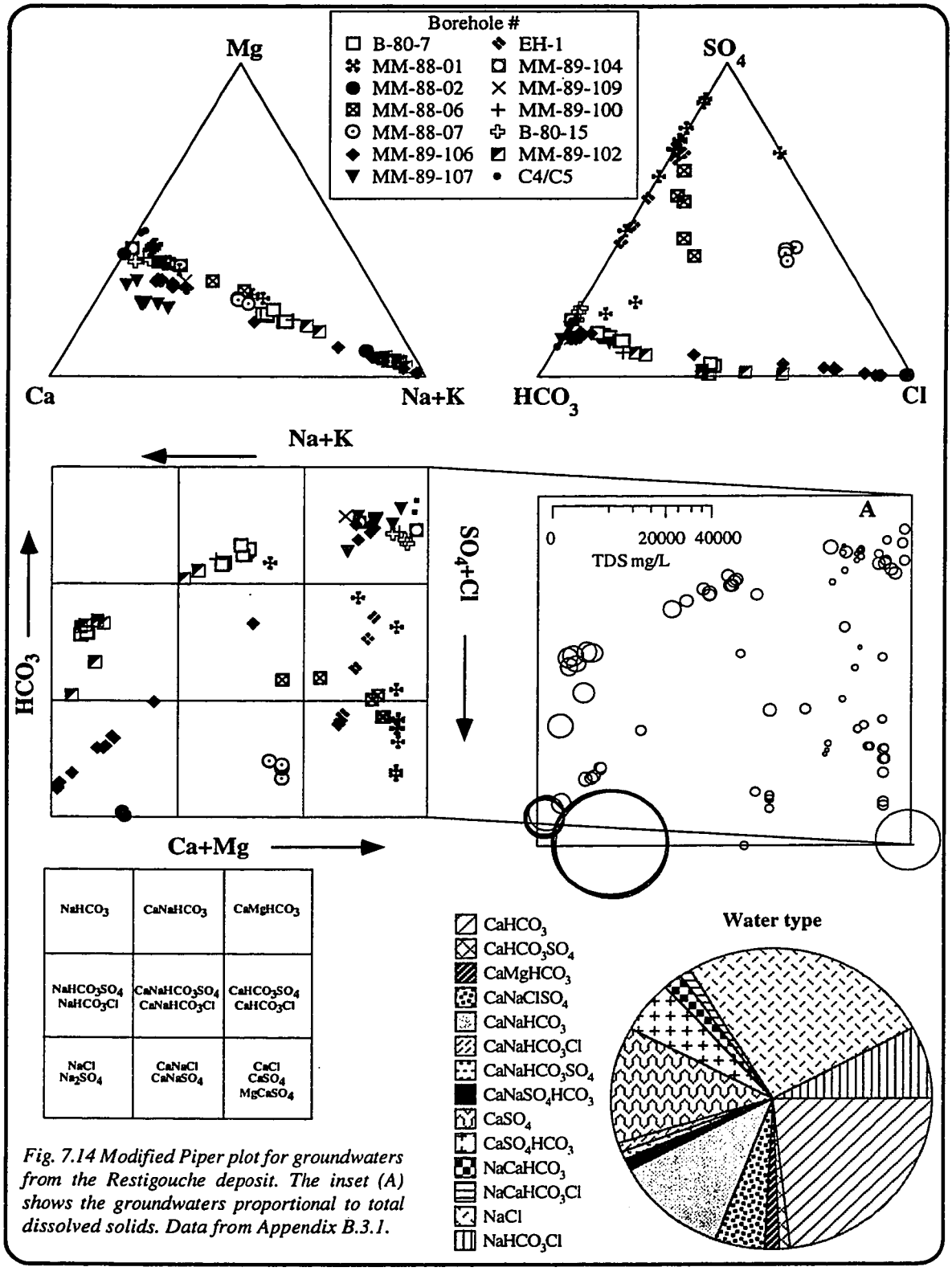


Fig. 7.14 Modified Piper plot for groundwaters from the Restigouche deposit. The inset (A) shows the groundwaters proportional to total dissolved solids. Data from Appendix B.3.1.

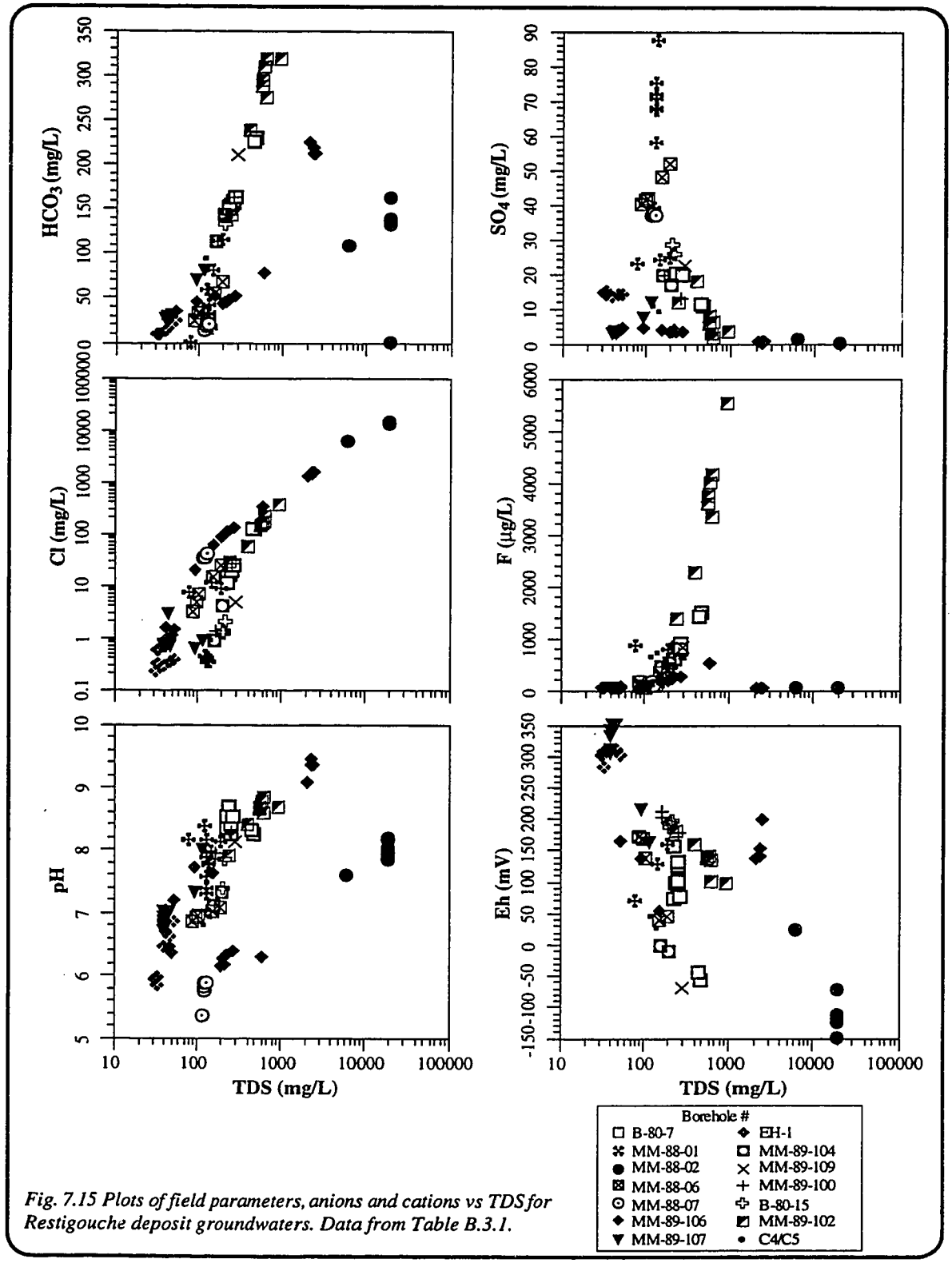


Fig. 7.15 Plots of field parameters, anions and cations vs TDS for Restigouche deposit groundwaters. Data from Table B.3.1.

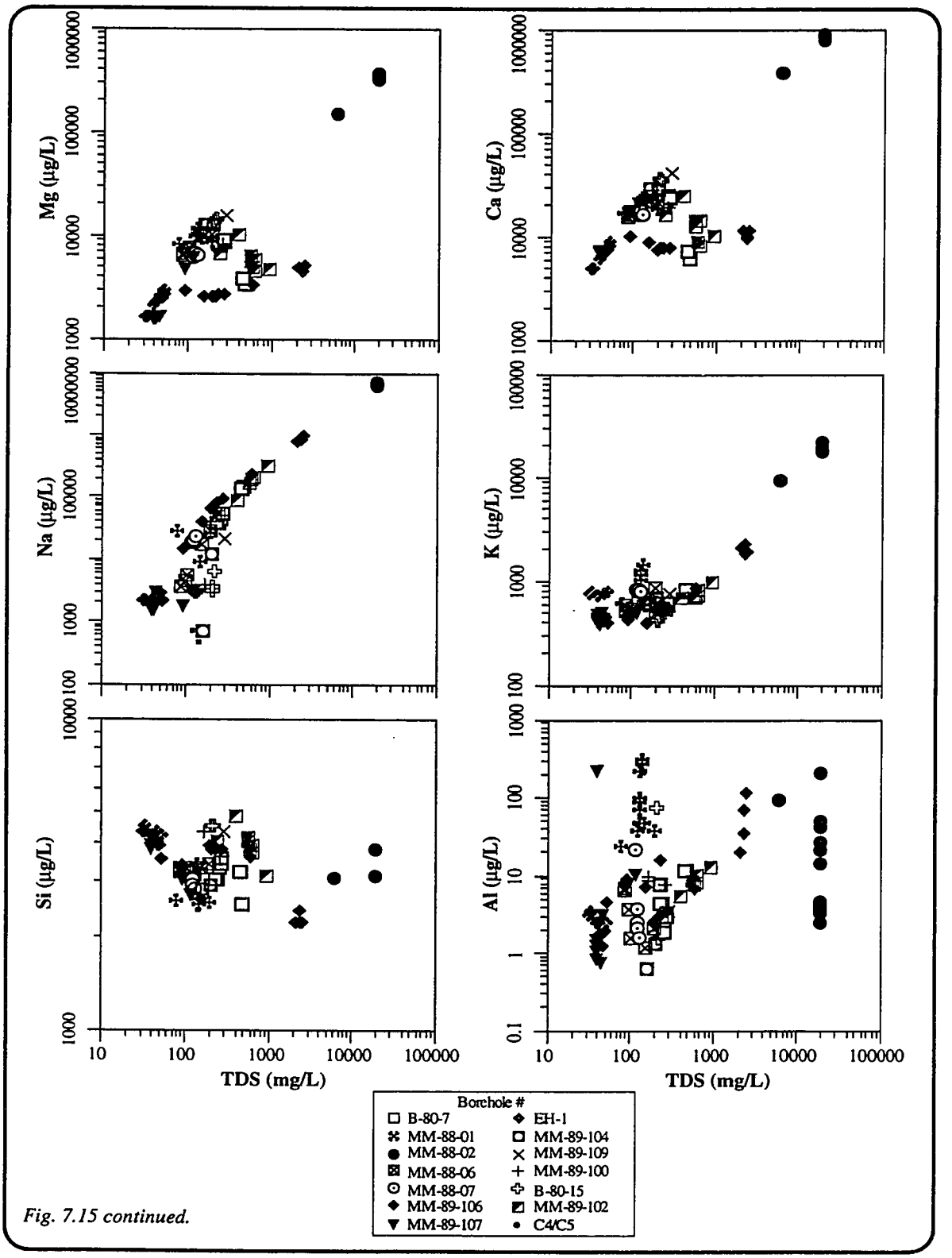


Fig. 7.15 continued.

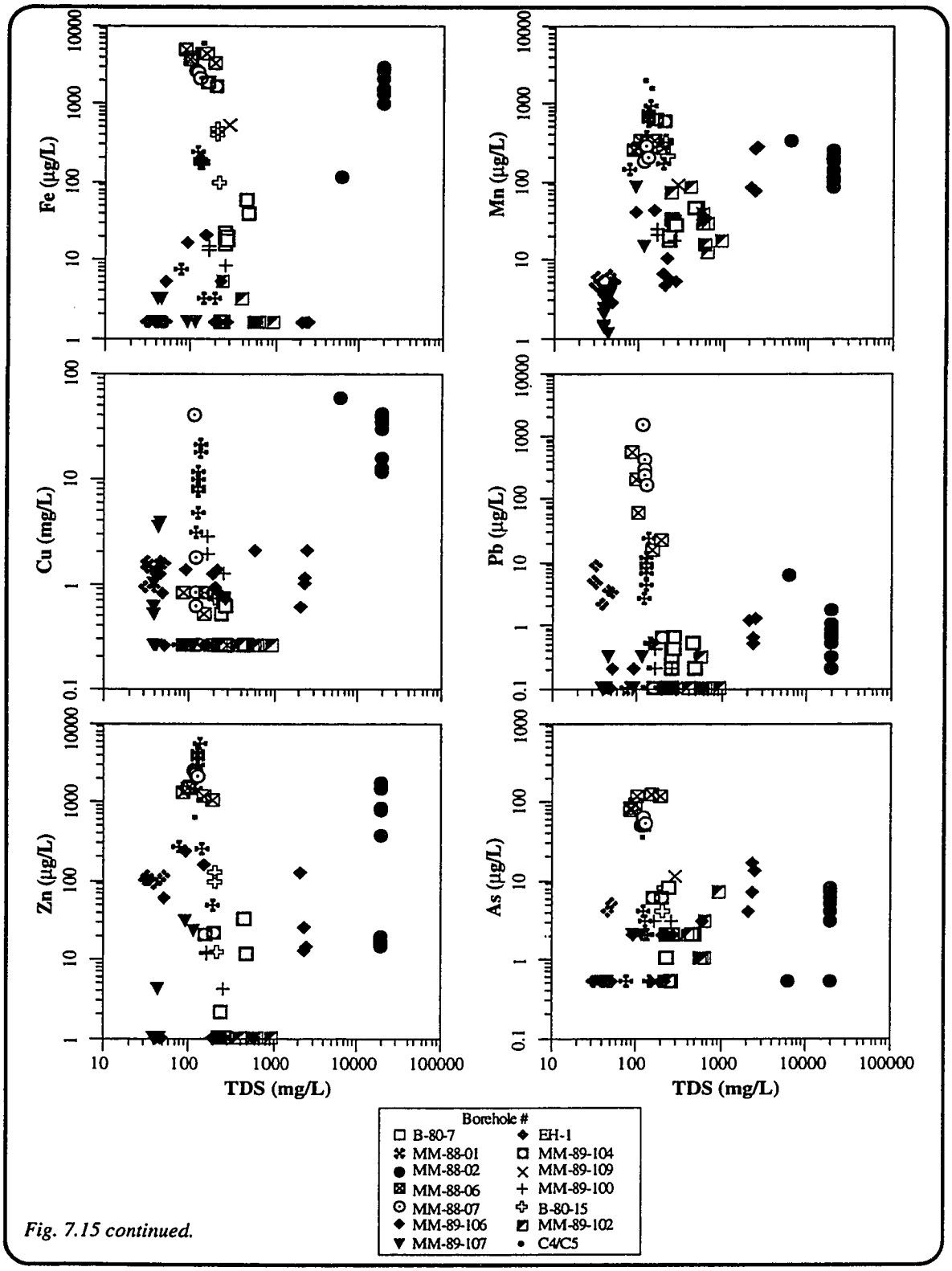


Fig. 7.15 continued.

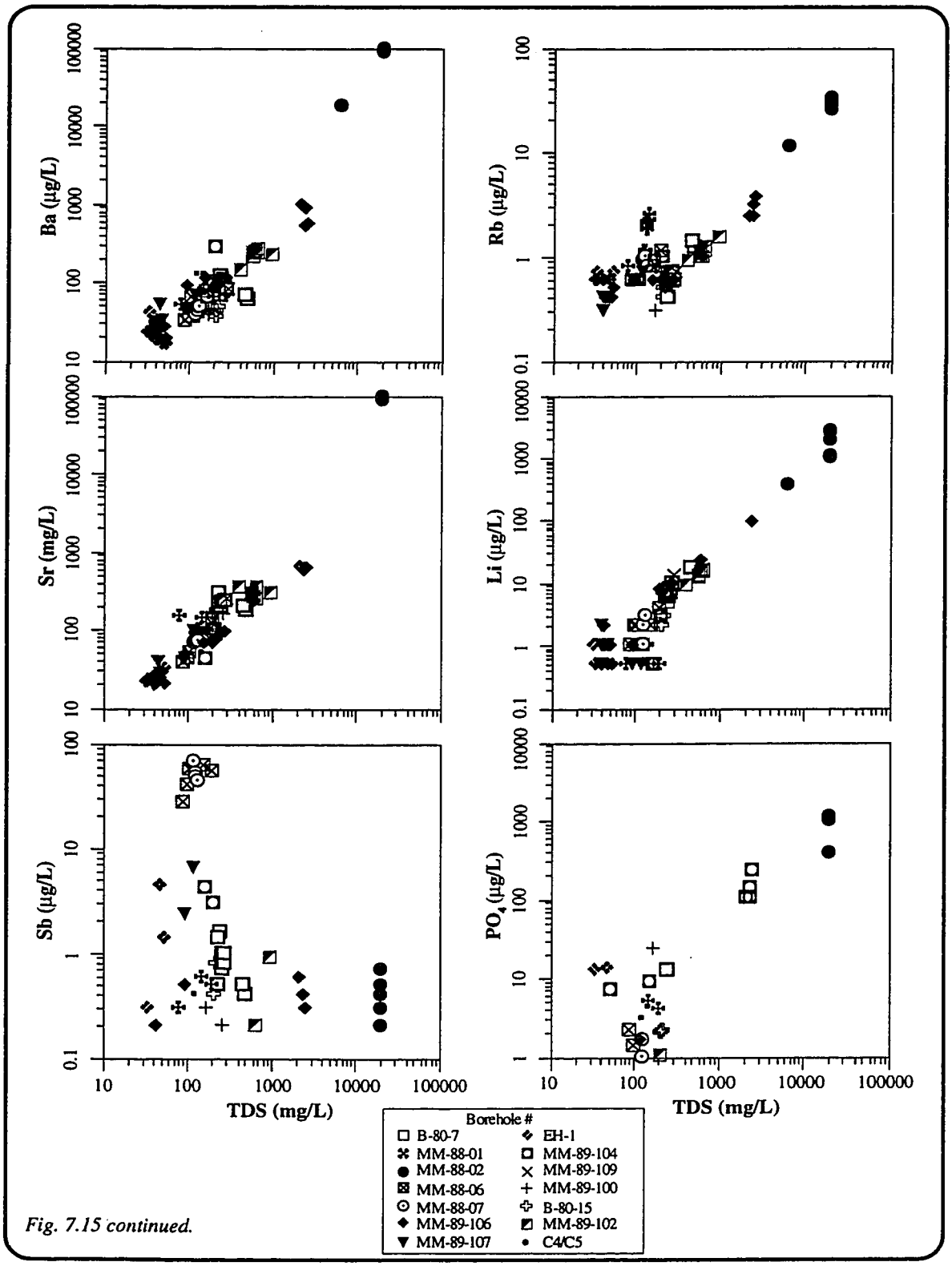


Fig. 7.15 continued.

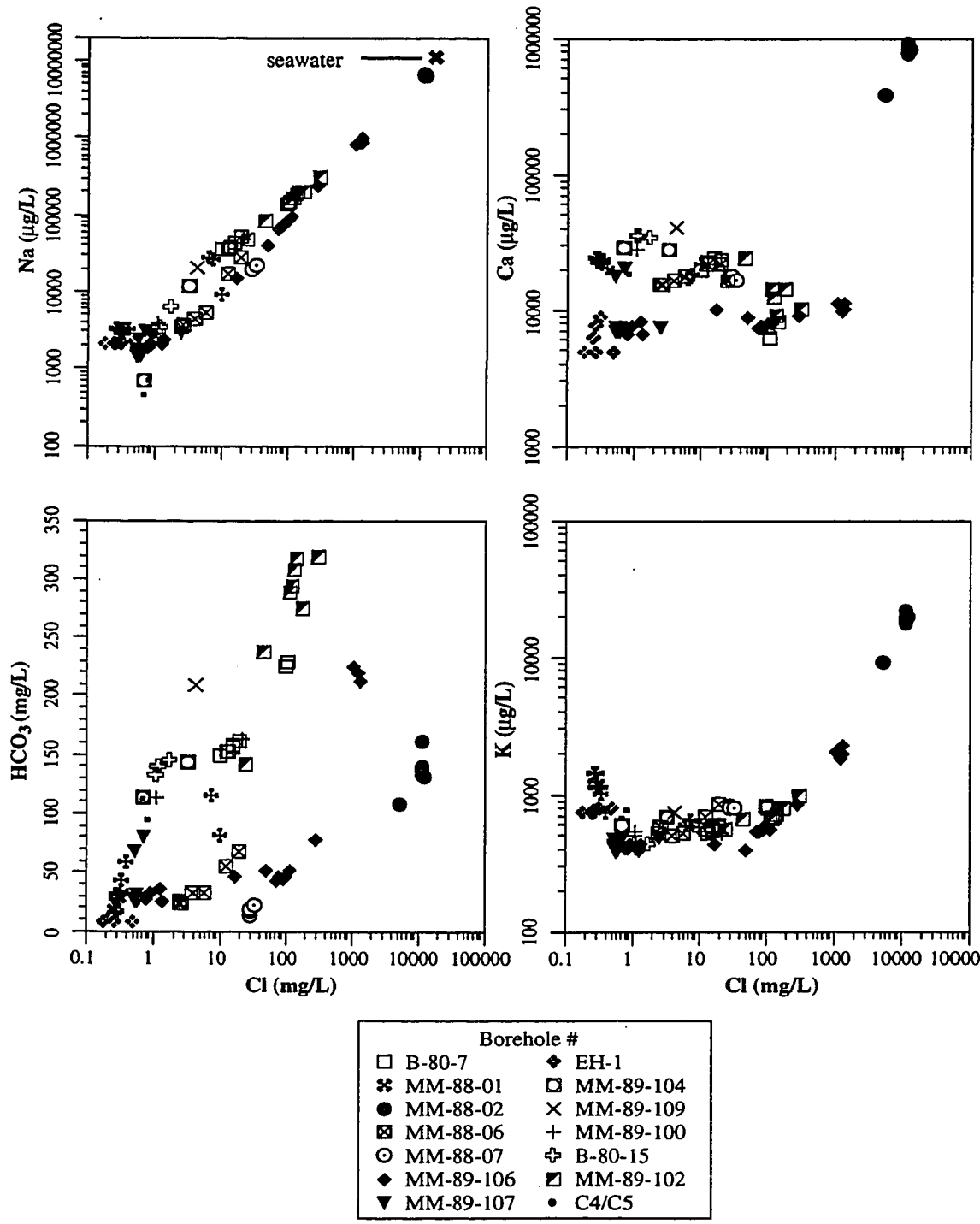


Fig. 7.16 Sodium, magnesium, potassium, and bicarbonate plotted against chloride for Restigouche deposit groundwaters. Data from Table B.3.1.

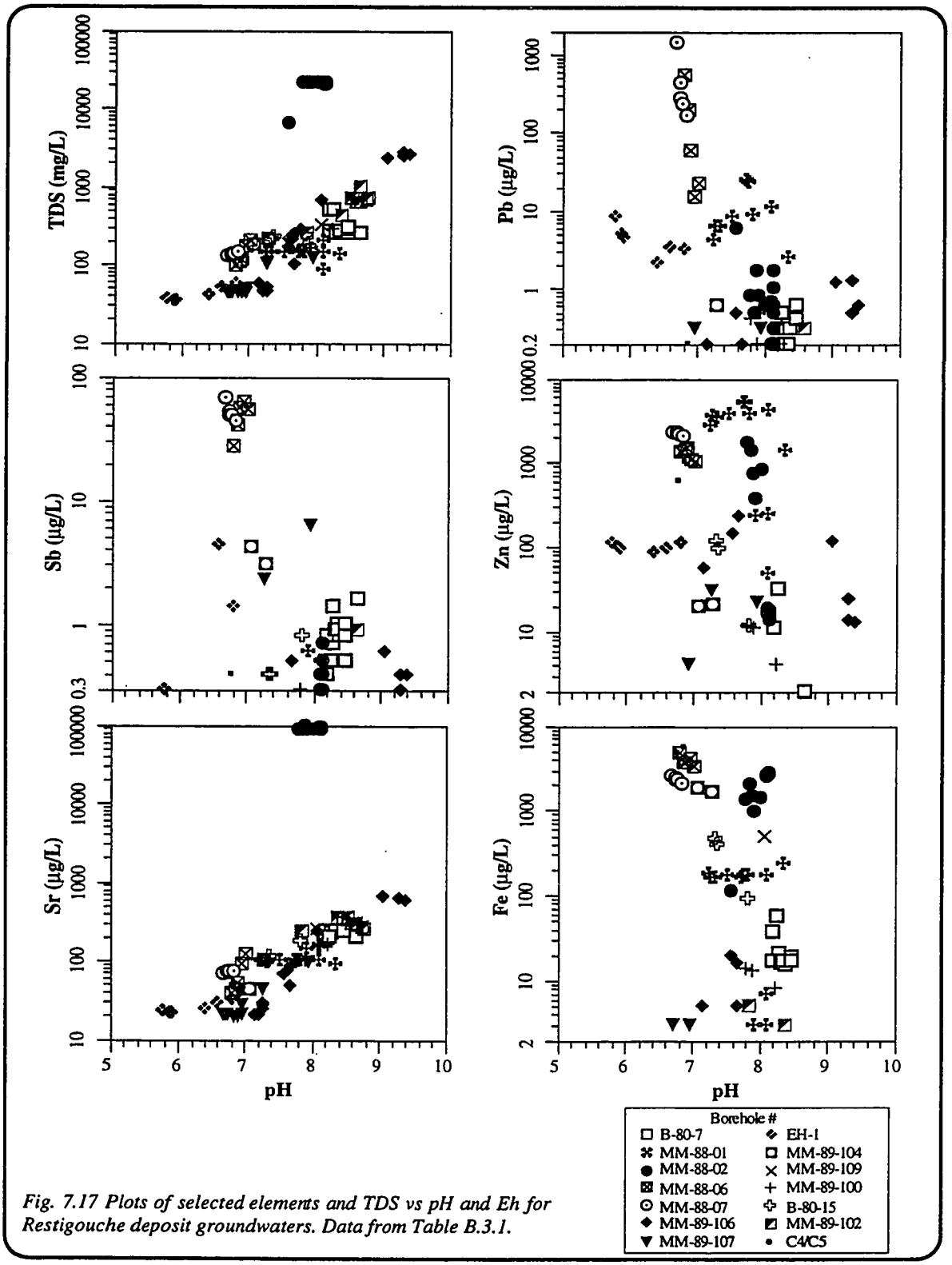


Fig. 7.17 Plots of selected elements and TDS vs pH and Eh for Restigouche deposit groundwaters. Data from Table B.3.1.

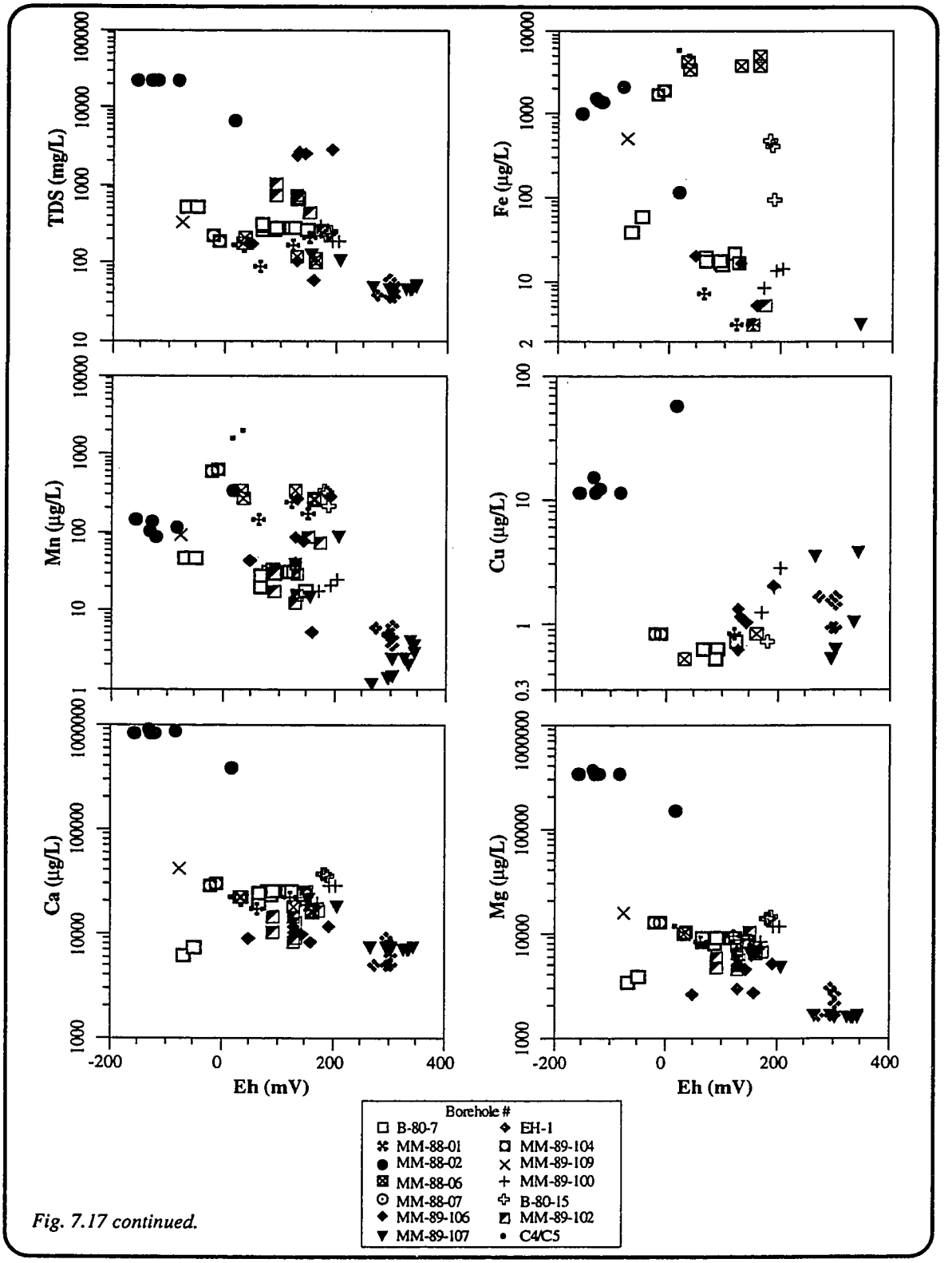


Fig. 7.17 continued.

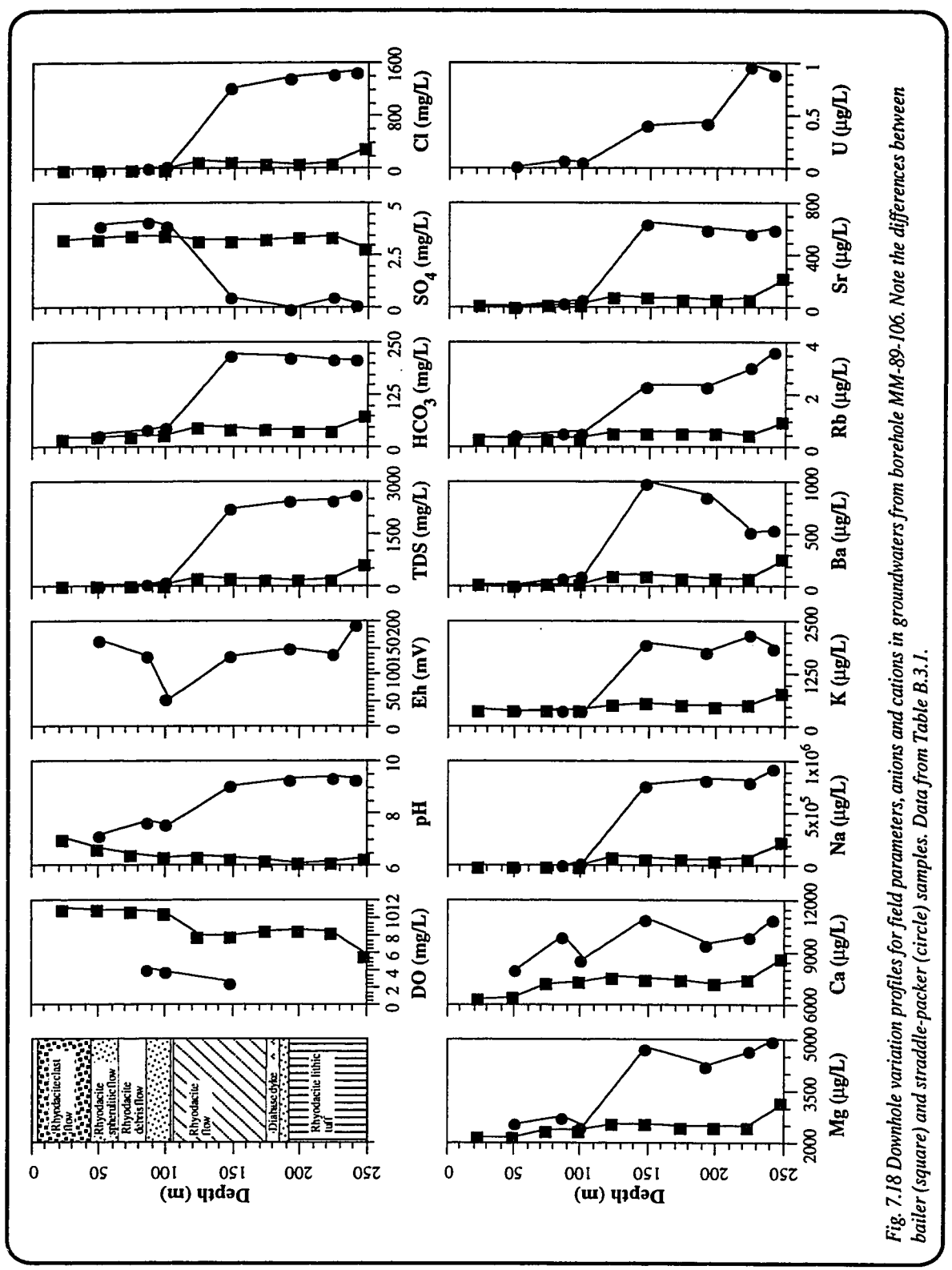


Fig. 7.18 Downhole variation profiles for field parameters, anions and cations in groundwaters from borehole MM-89-106. Note the differences between bailer (square) and straddle-packer (circle) samples. Data from Table B.3.1.

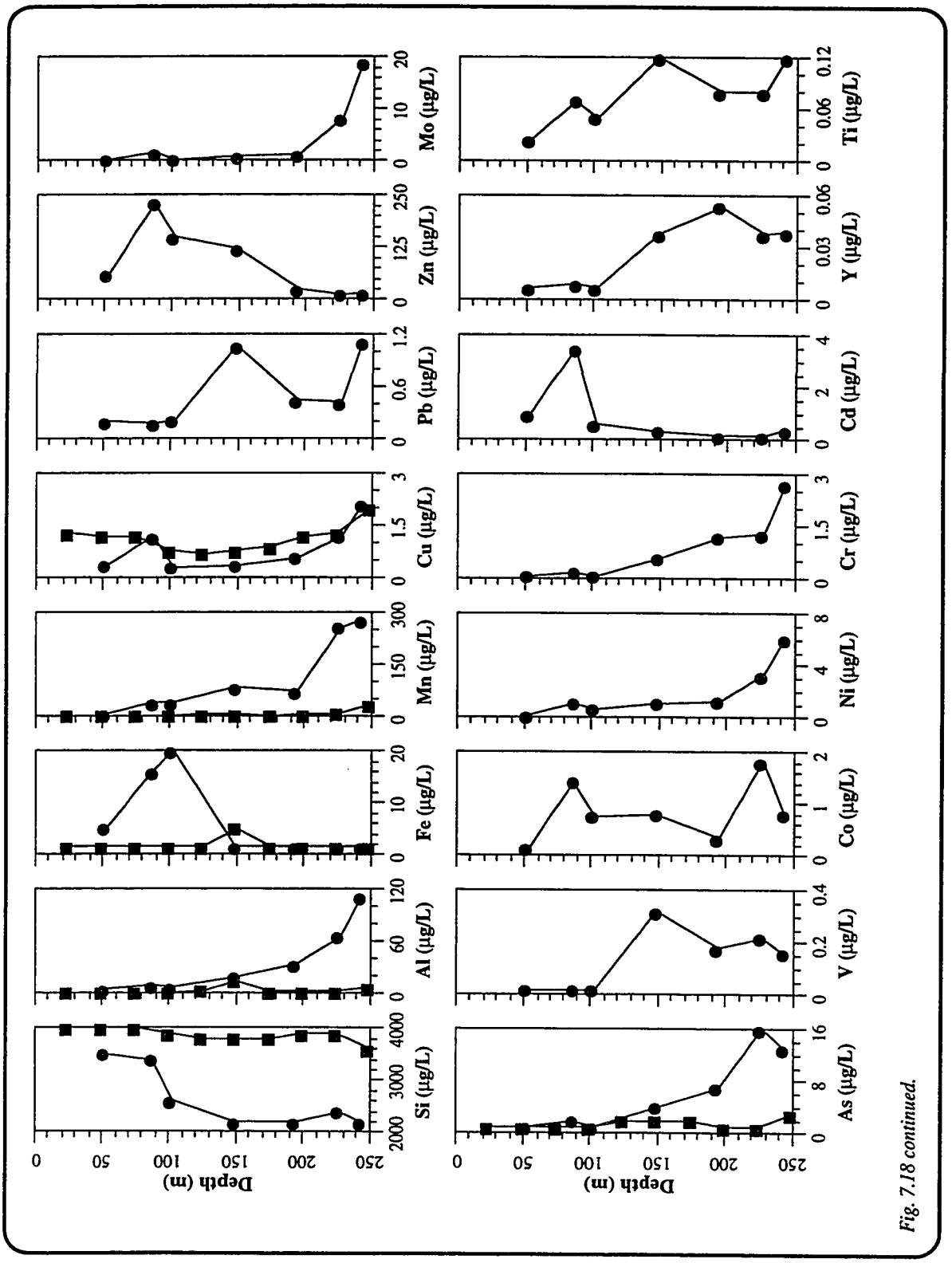


Fig. 7.18 continued.

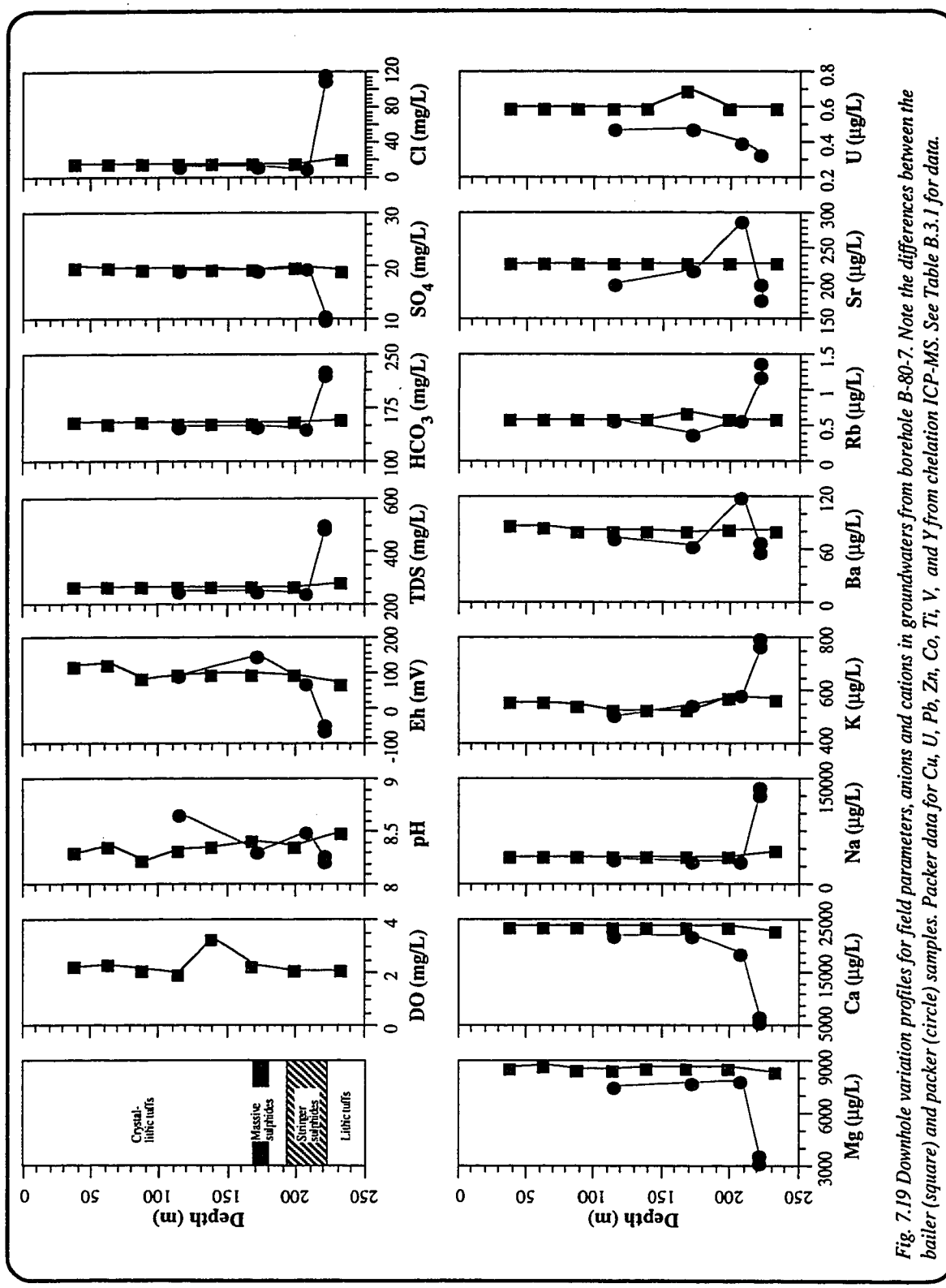


Fig. 7.19 Downhole variation profiles for field parameters, anions and cations in groundwaters from borehole B-80-7. Note the differences between the bailer (square) and packer (circle) samples. Packer data for Cu, U, Pb, Zn, Co, Ti, V, and Y from chelation ICP-MS. See Table B.3.1 for data.

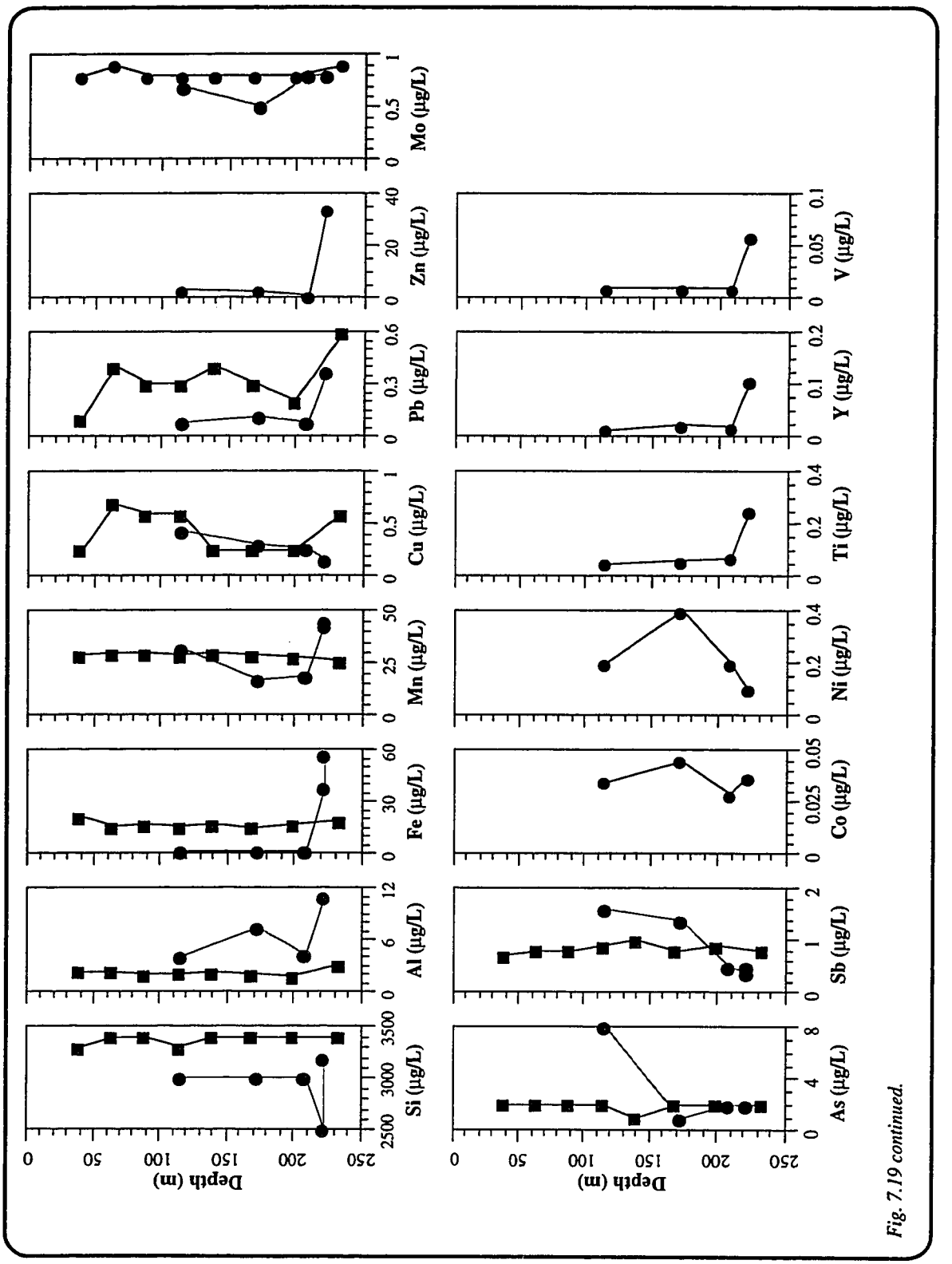


Fig. 7.19 continued.

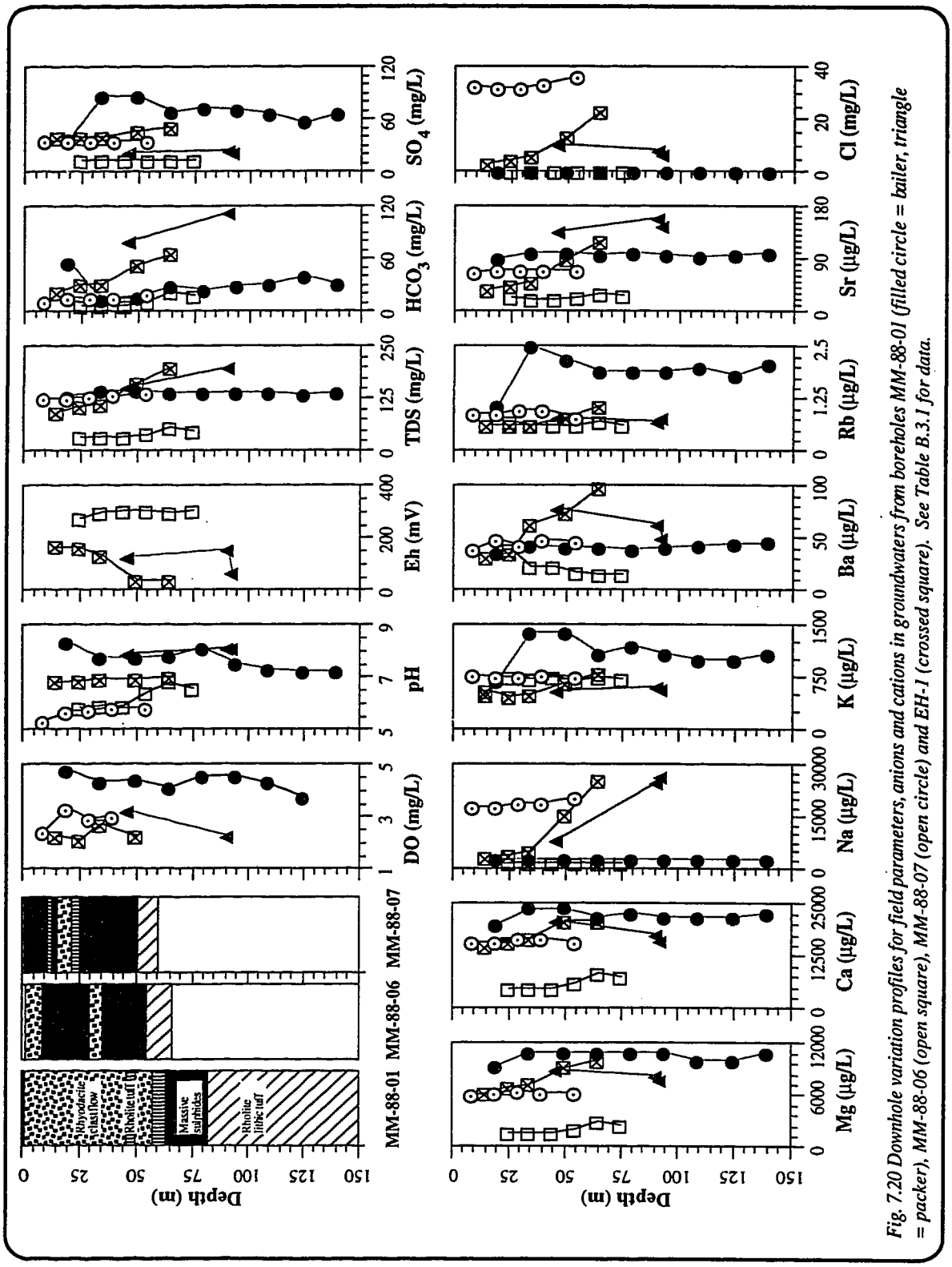


Fig. 7.20 Downhole variation profiles for field parameters, anions and cations in groundwaters from boreholes MM-88-01 (filled circle = bailer, triangle = packer), MM-88-06 (open square), MM-88-07 (open circle) and EH-1 (crossed square). See Table B.3.1 for data.

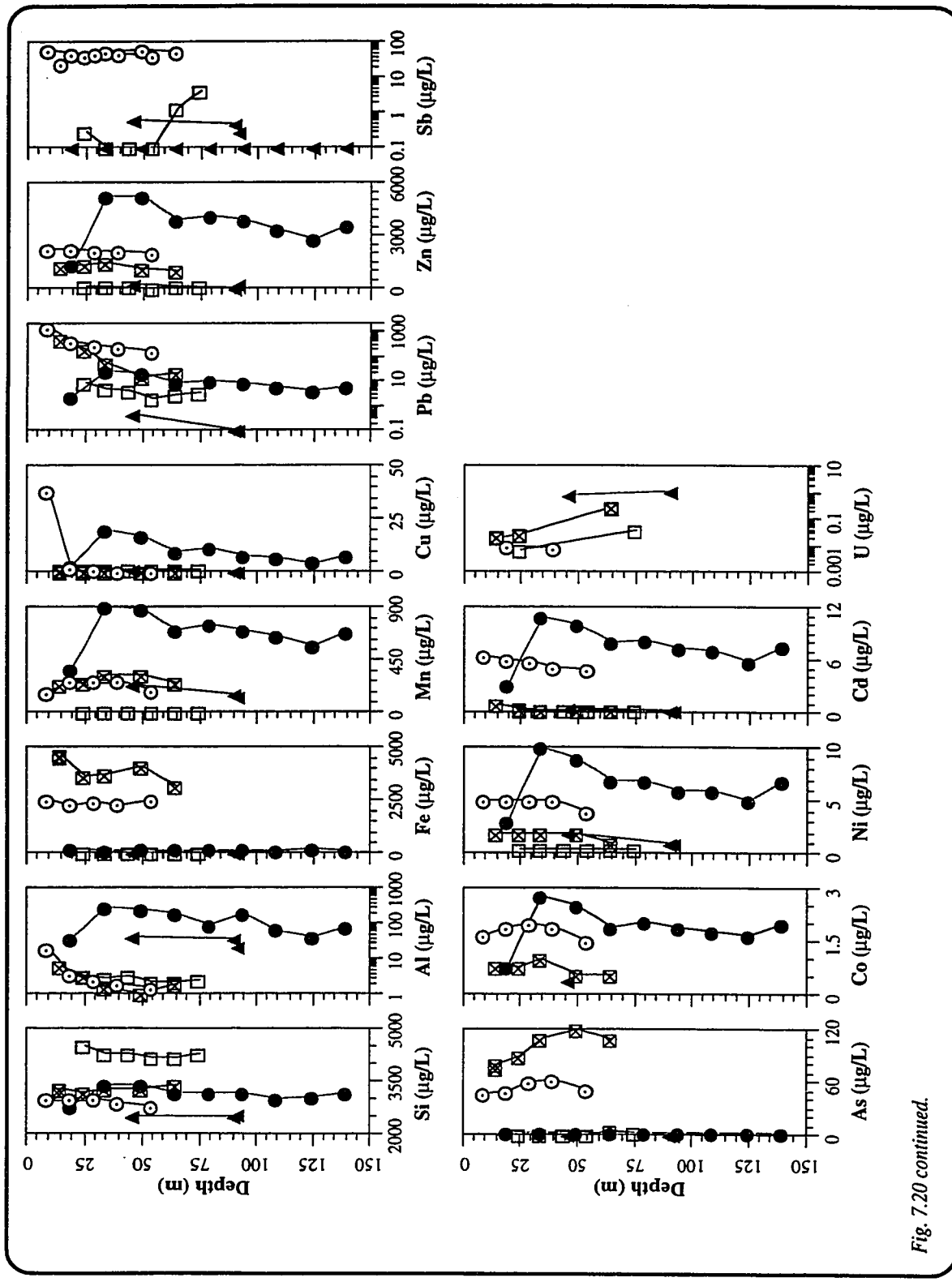


Fig. 7.20 continued.

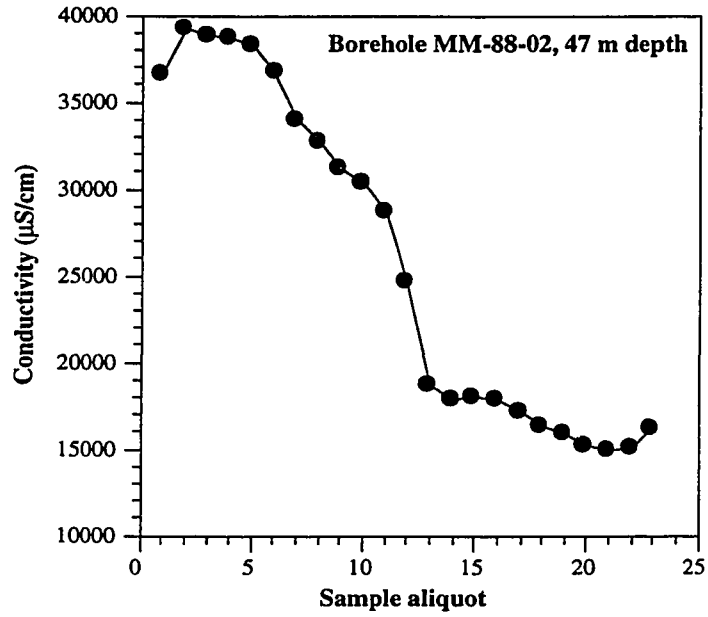
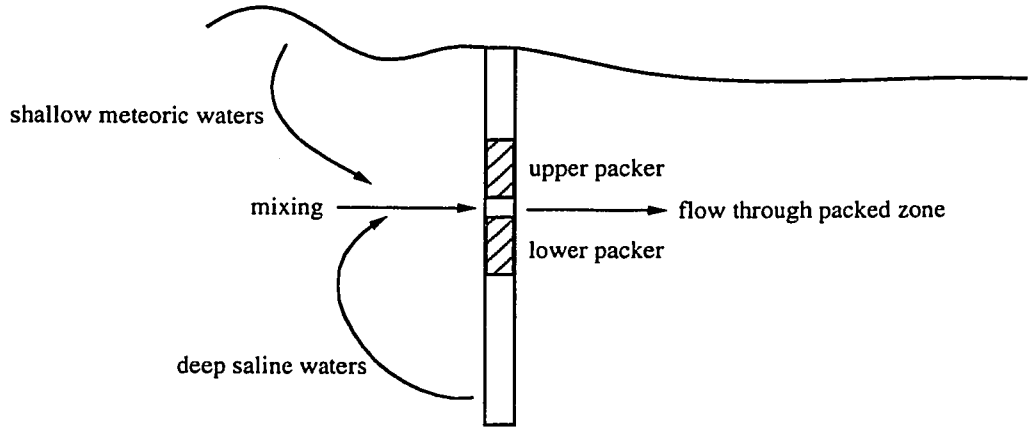


Fig. 7.21 Relationship between conductivity of groundwater in borehole MM-88-02 and sampling interval. The final sample collected is MLW96-669. Note that although this sample was from a shallow depth (47 m), the waters never dropped to values close to those in adjacent holes (e.g. MM-8-01 and MM-88-06). The most likely explanation for the high conductivity is mixing between deeper saline waters and the shallow meteoric waters, as shown below.



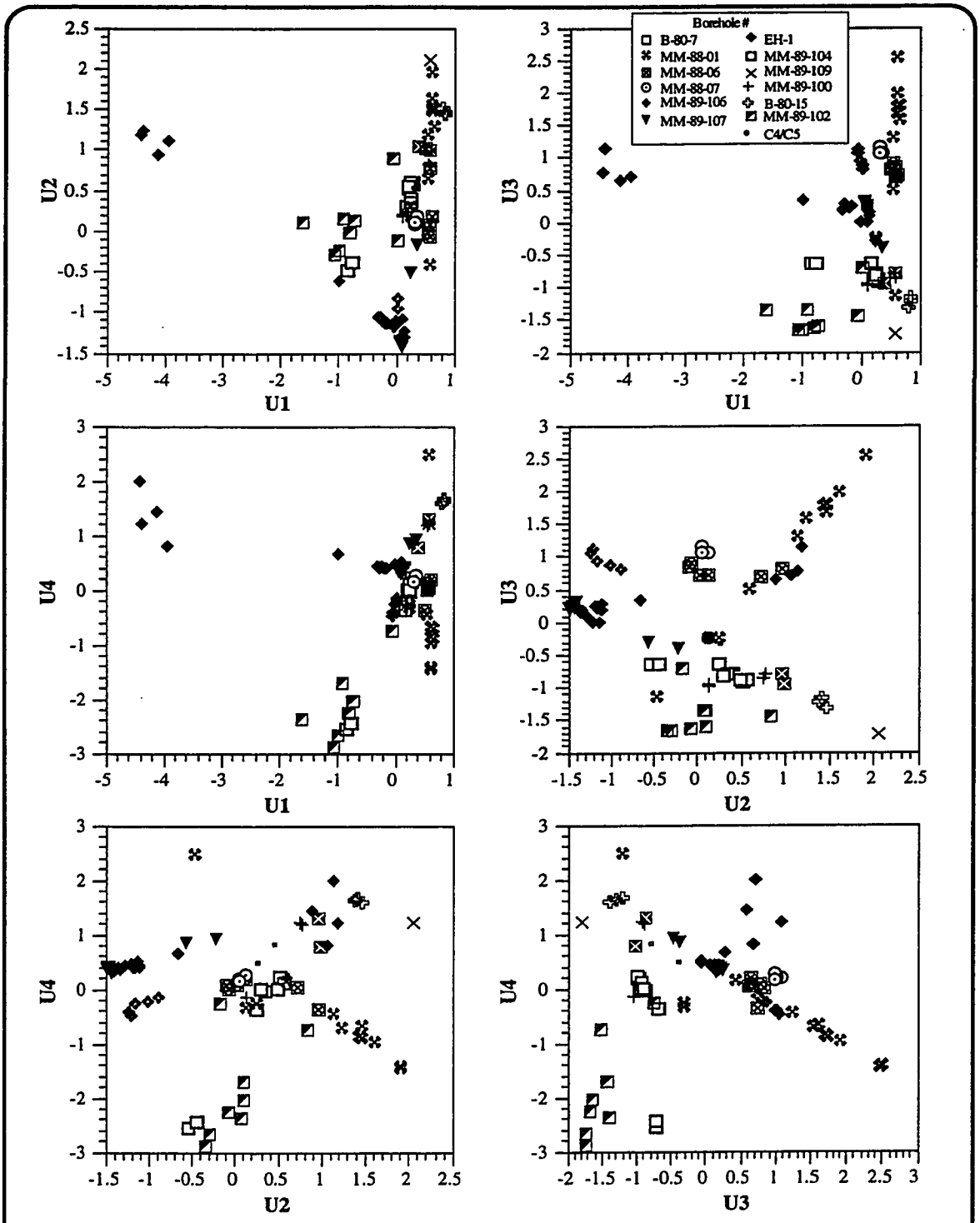


Fig. 7.22 Principle component plots of Restigouche deposit groundwaters, showing the variation in the first four factors (85.8% of the variation). PCA based on pH, Eh, DO, TDS, HCO_3, SO_4, Cl, Si, Al, Fe, Mn, Mg, Ca, Na, K. Groundwaters from borehole MM-88-02 were excluded from the analysis.

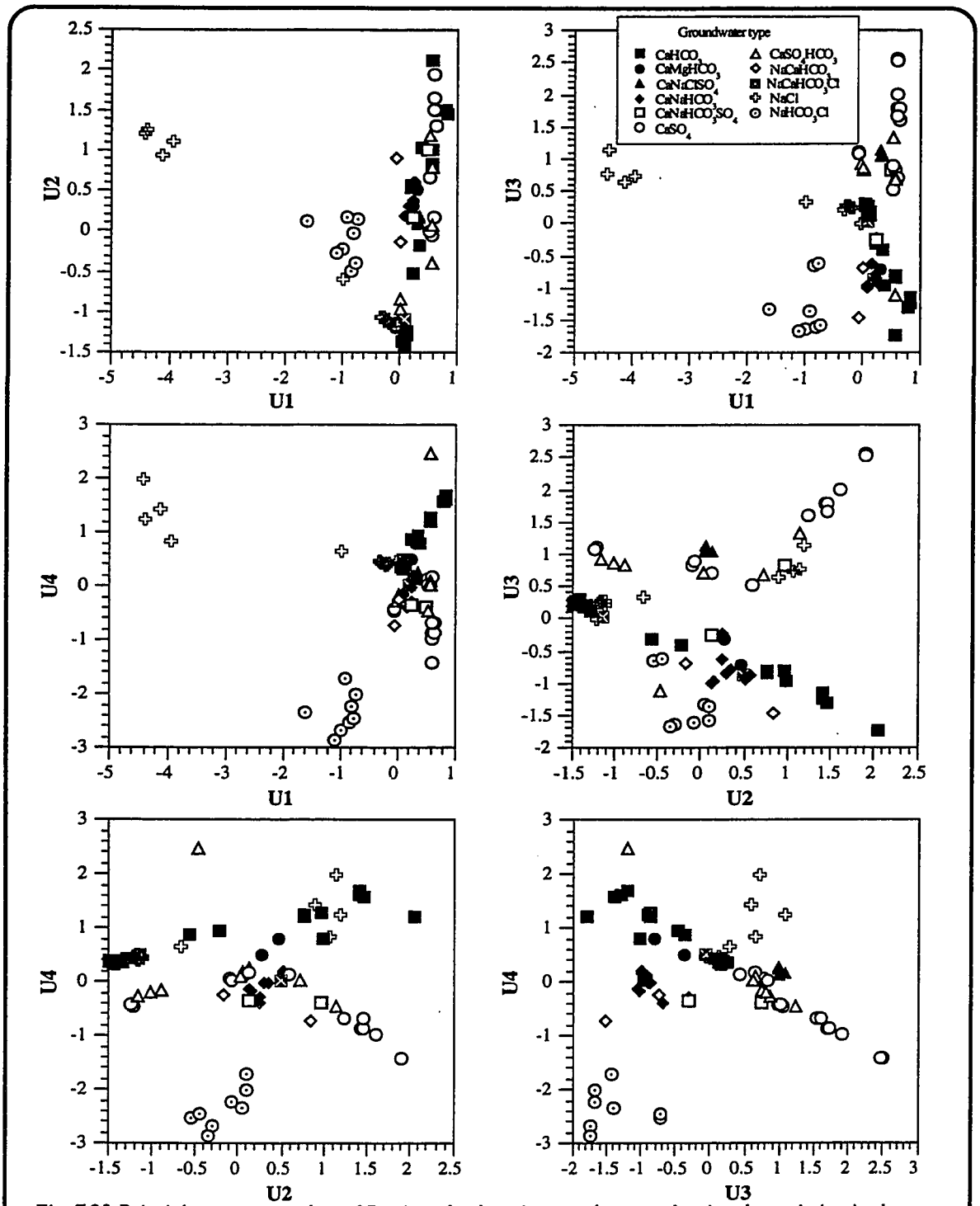


Fig. 7.23 Principle component plots of Restigouche deposit groundwaters, showing the variation in the first four factors (85.8% of the variation). Samples are subdivided by water type. PCA based on pH, Eh, DO, TDS, HCO_3, SO_4, Cl, Si, Al, Fe, Mn, Mg, Ca, Na, K. Groundwaters from borehole MM-88-02 were excluded from the analysis.

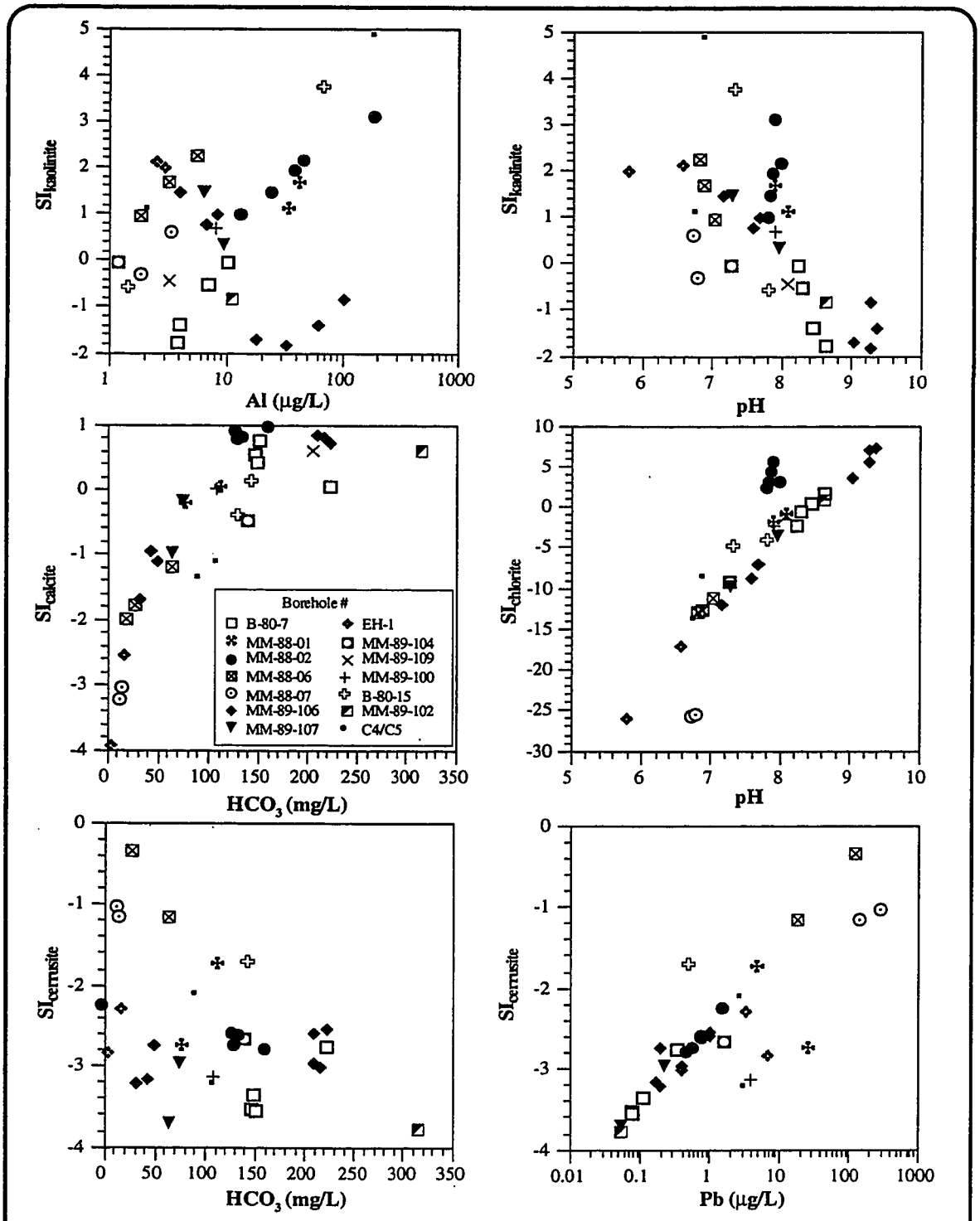


Fig. 7.24 Plots of selected mineral saturation indices for Restigouche deposit groundwaters. Data from Tables B.3.1 and B.3.5.

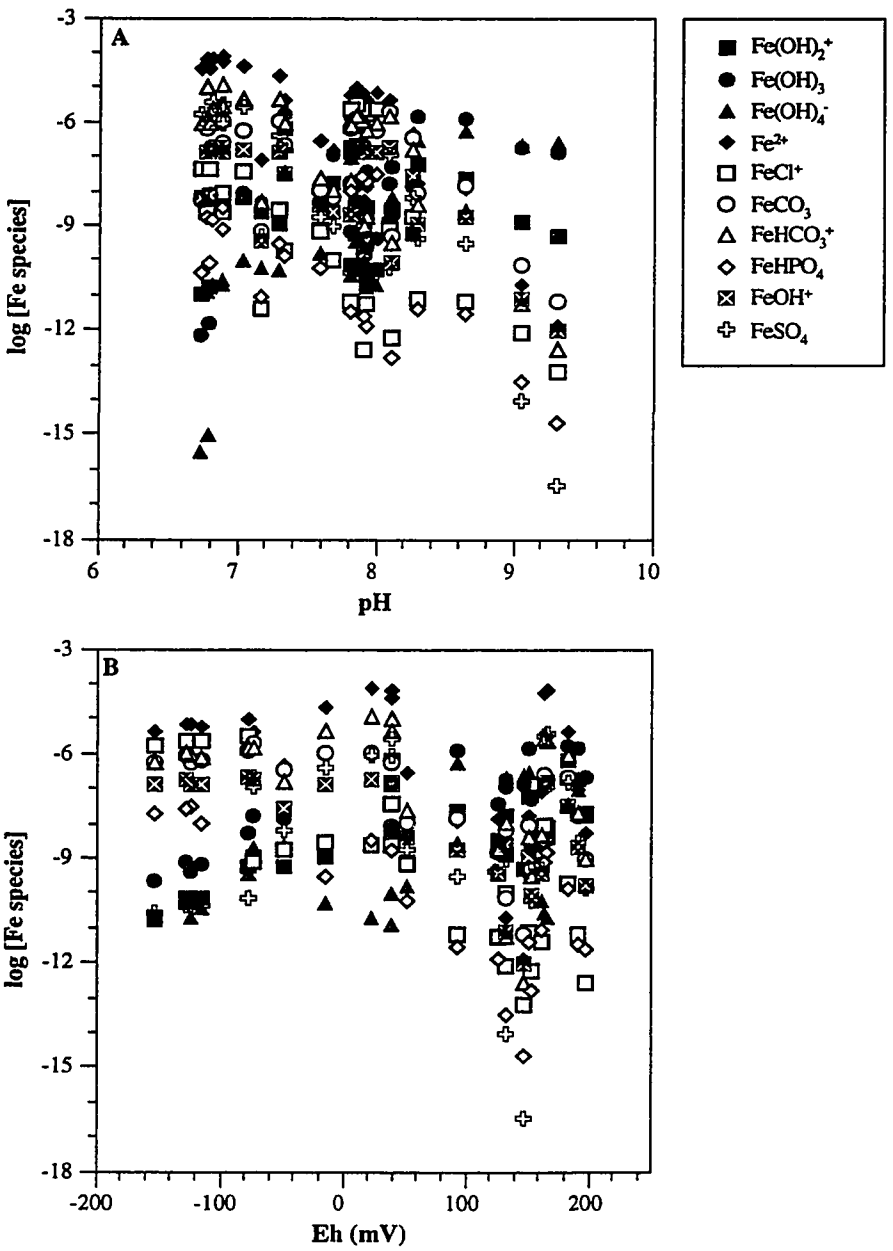


Fig. 7.25 Speciation variation diagrams showing the distribution of Fe species versus pH (A) and Eh (B) and Pb (C) and Zn (D) species versus pH in the Restigouche deposit groundwaters. Speciation calculated using PHREEQC with the WATEQ4F database.

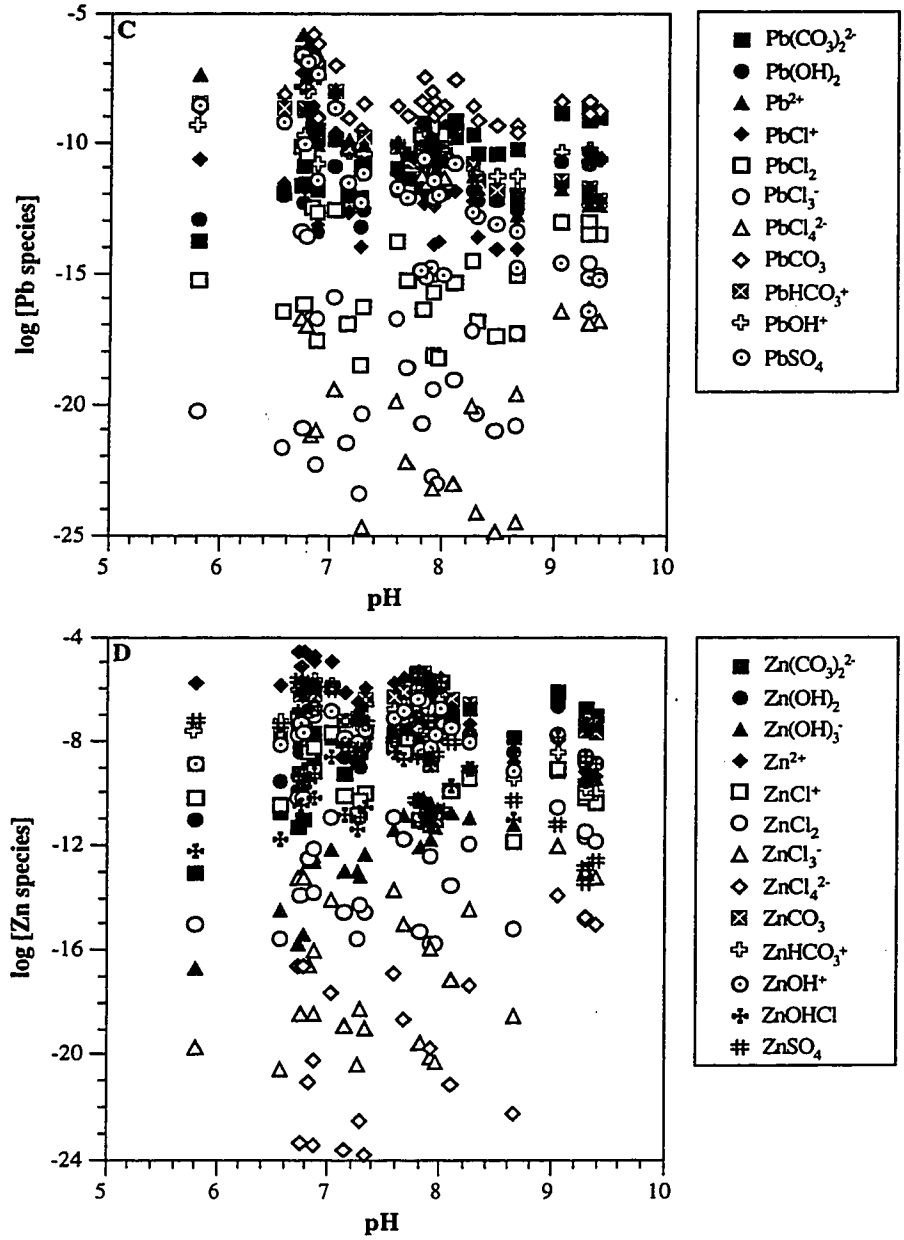


Fig. 7.25 continued.

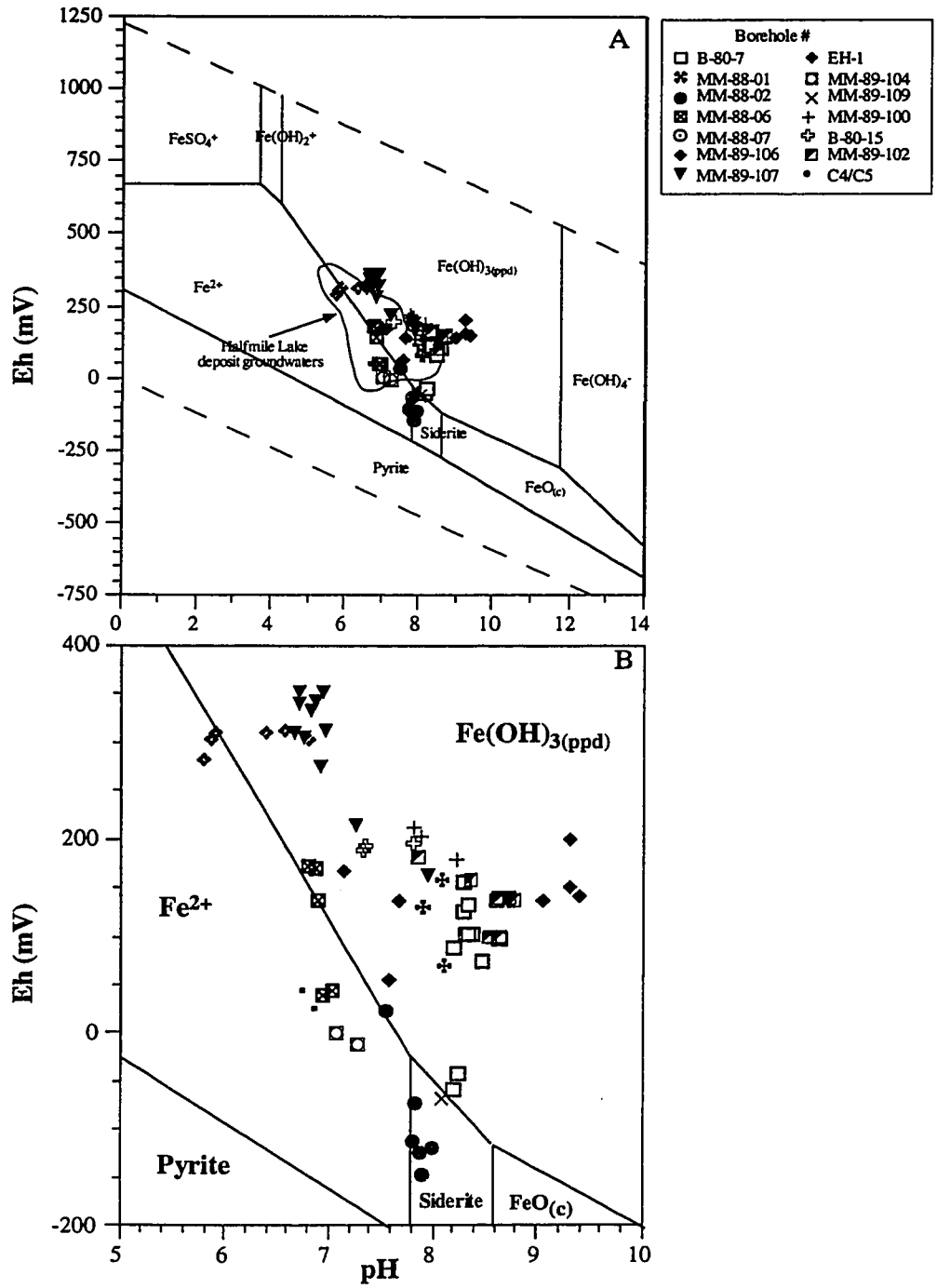


Fig. 7.26 Diagram showing the stability of metastable Fe hydroxides relative to Restigouche deposit groundwaters. The fields were calculated by the Geochemist's Workbench computer program (Bethke, 1994). Conditions are similar to sample MLW96-697 from borehole S61-19. Conditions were: $[HCO_3] = 10^{-3}$, $[SO_4] = 10^{-2.5}$, $[Fe] = 10^{-5}$. The formation of hematite, goethite and magnetite were suppressed, reflecting the slow kinetics of formation of these phases at these groundwater conditions.

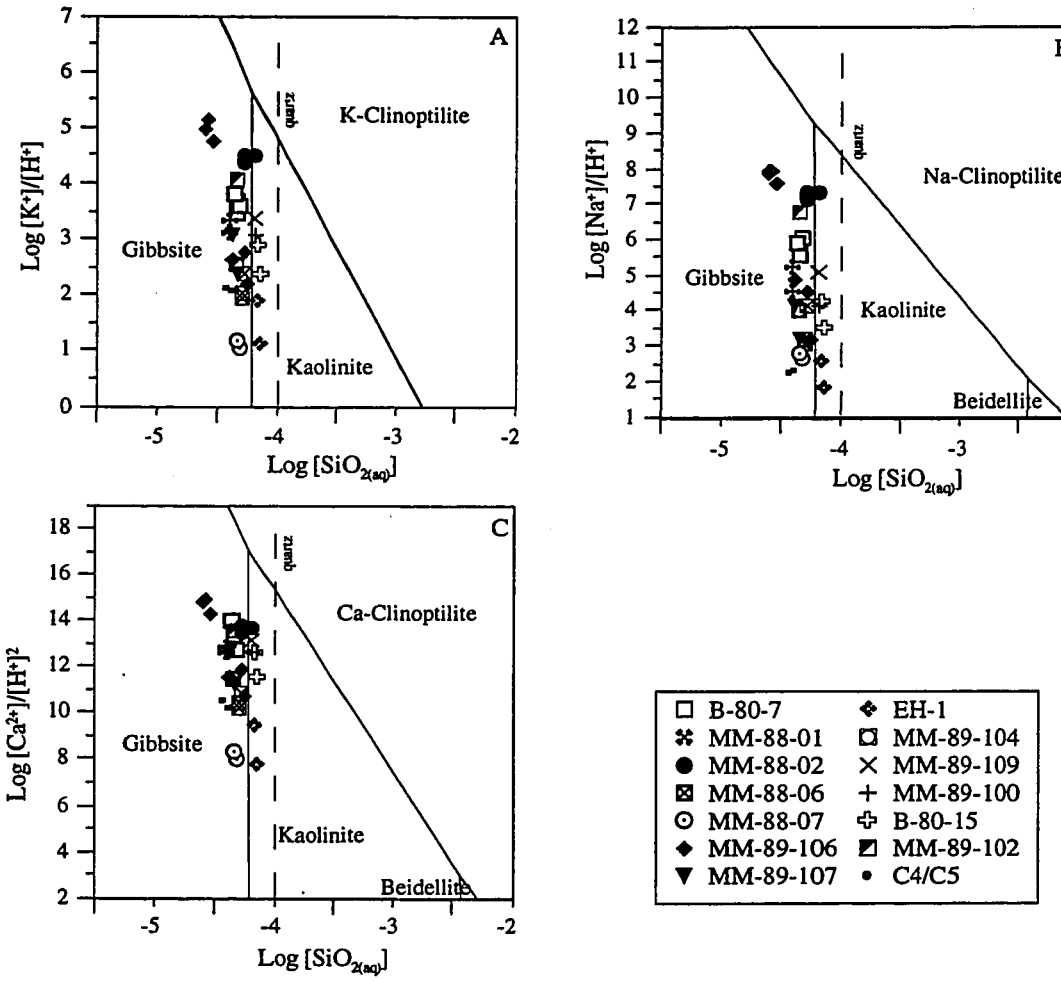


Fig. 7.27 Plots showing mineral stabilities for the systems A) Na_2O—Al_2O_3—SiO_2—H_2O, B) K_2O—Al_2O_3—SiO_2—H_2O, and C) Ca_2O—Al_2O_3—SiO_2—H_2O at 25°C and 1 atmosphere pressure for Restigouche deposit groundwaters. Field boundaries plotted using The Geochemist's Workbench (Bethke, 1994). Dashed line represents quartz saturation. Plotted data are for Restigouche deposit groundwaters, based on activities calculated with PHREEQC using the WATEQ4F database. Geochemical data is from Table B.3.1.

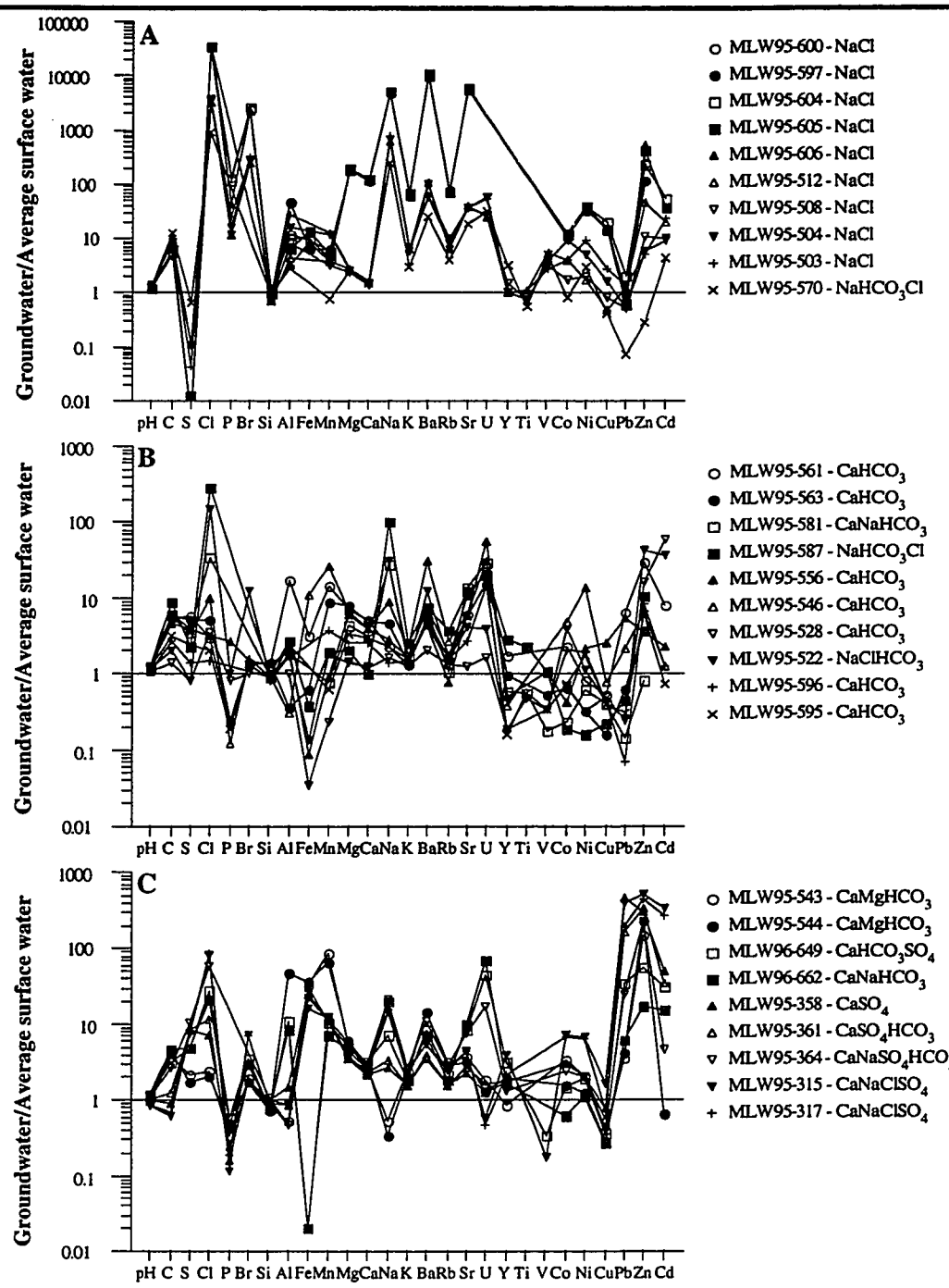


Fig. 7.28 Representative Restigouche deposit groundwaters normalized to average surface water composition. A) Saline waters. B) Shallow groundwaters distal to mineralization. C) Shallow groundwaters proximal to mineralization. Note the different patterns for different water-types. Groundwater data from Table B.3.1.

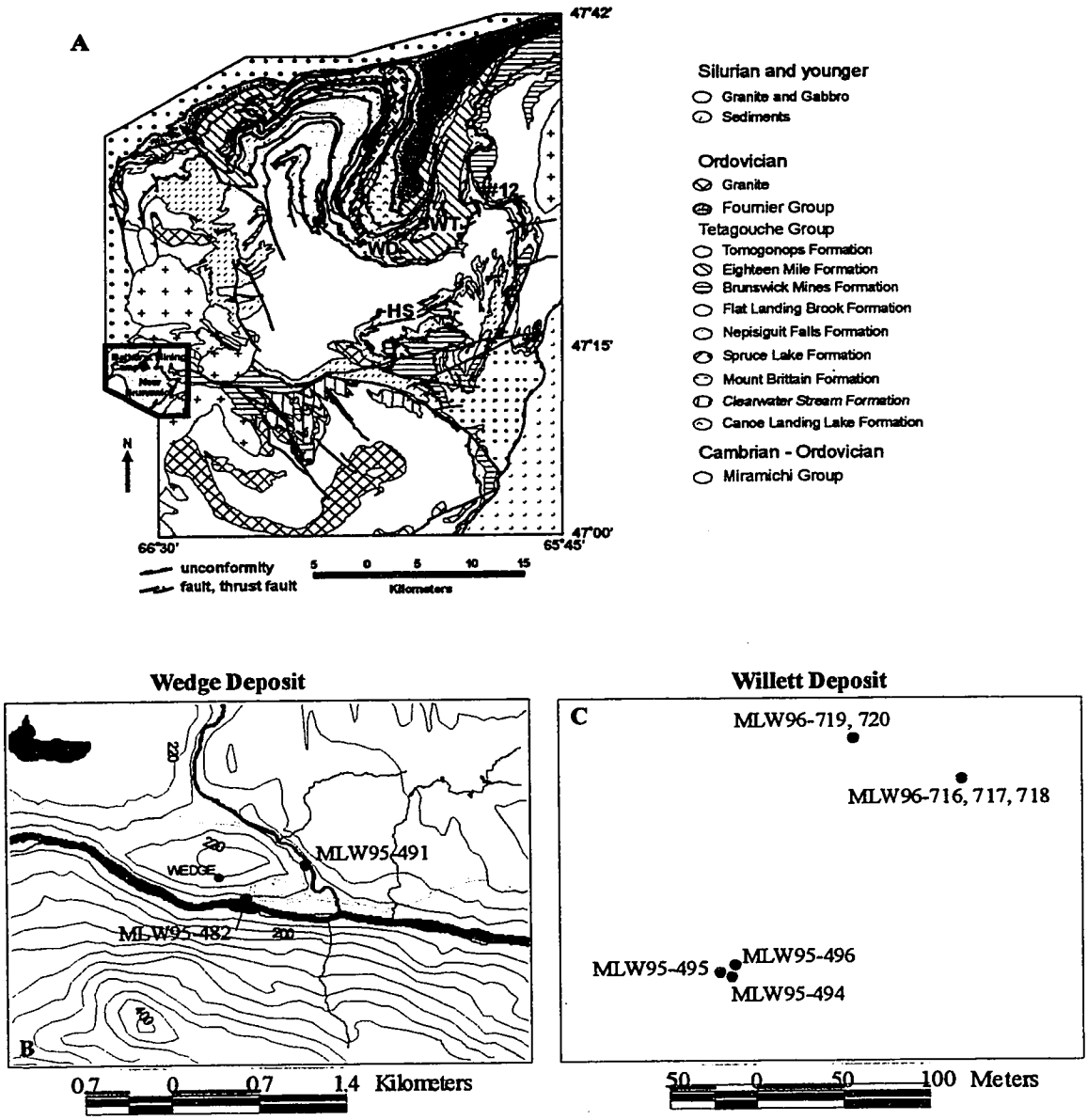


Fig. 7.29 A) Location of the Heath Steele (HS), Wedge (WD), Willett (WT) and Brunswick #12 (#12) deposits. B) Location of samples at the Wedge deposit. Contour intreval is 20 m. C). Location of samples at the Willett deposit.

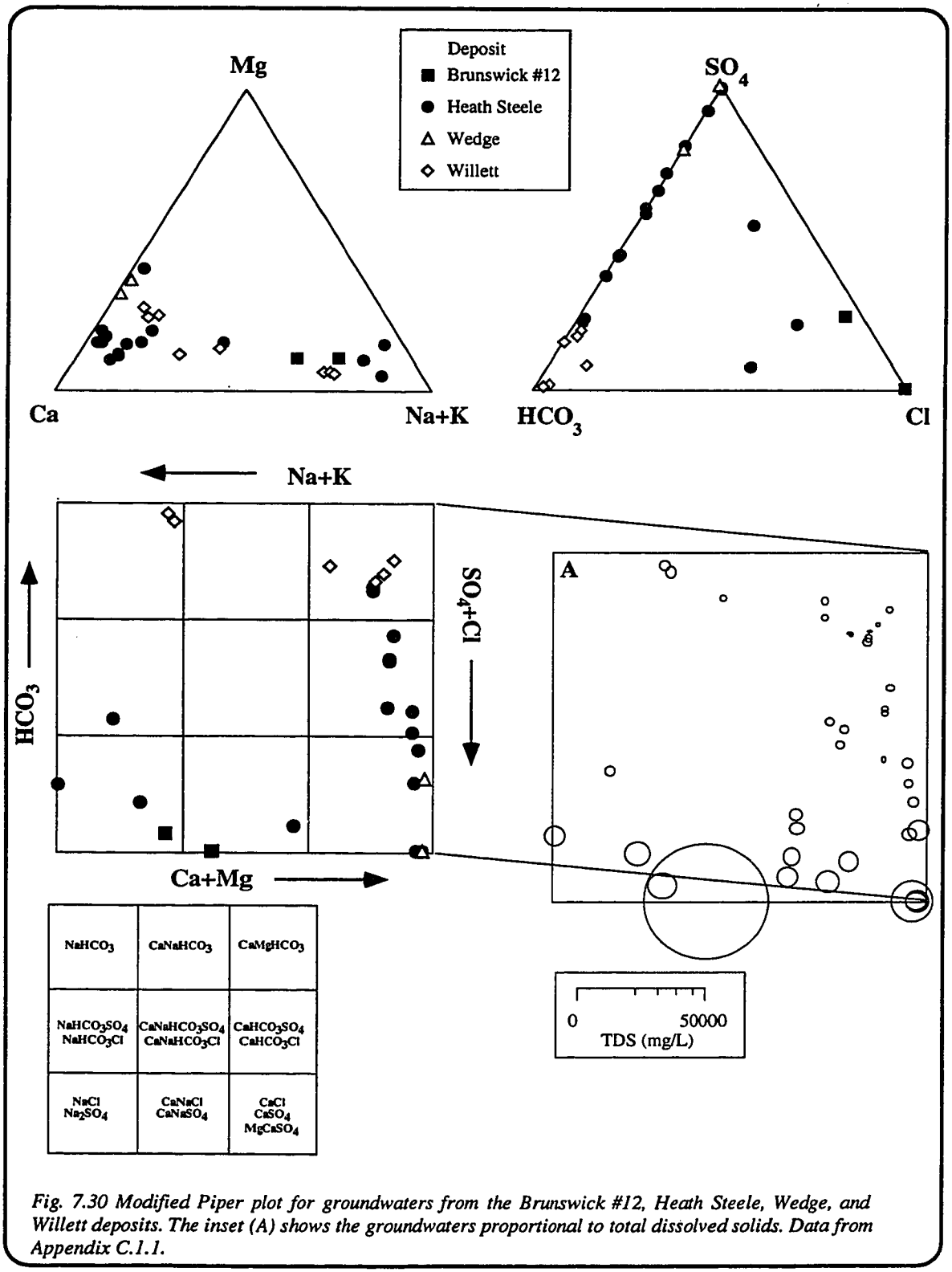


Fig. 7.30 Modified Piper plot for groundwaters from the Brunswick #12, Heath Steele, Wedge, and Willett deposits. The inset (A) shows the groundwaters proportional to total dissolved solids. Data from Appendix C.1.1.

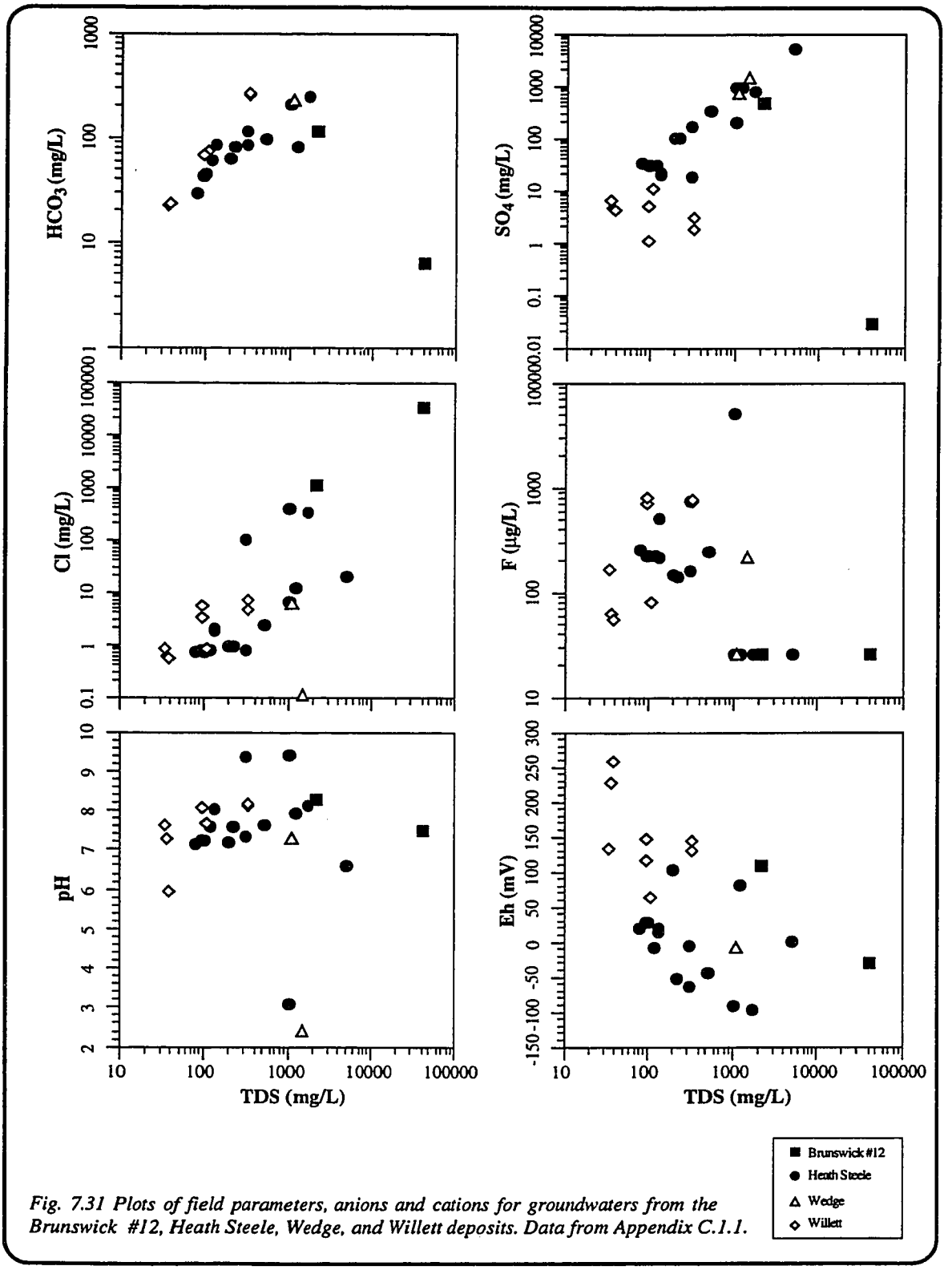


Fig. 7.31 Plots of field parameters, anions and cations for groundwaters from the Brunswick #12, Heath Steele, Wedge, and Willett deposits. Data from Appendix C.1.1.

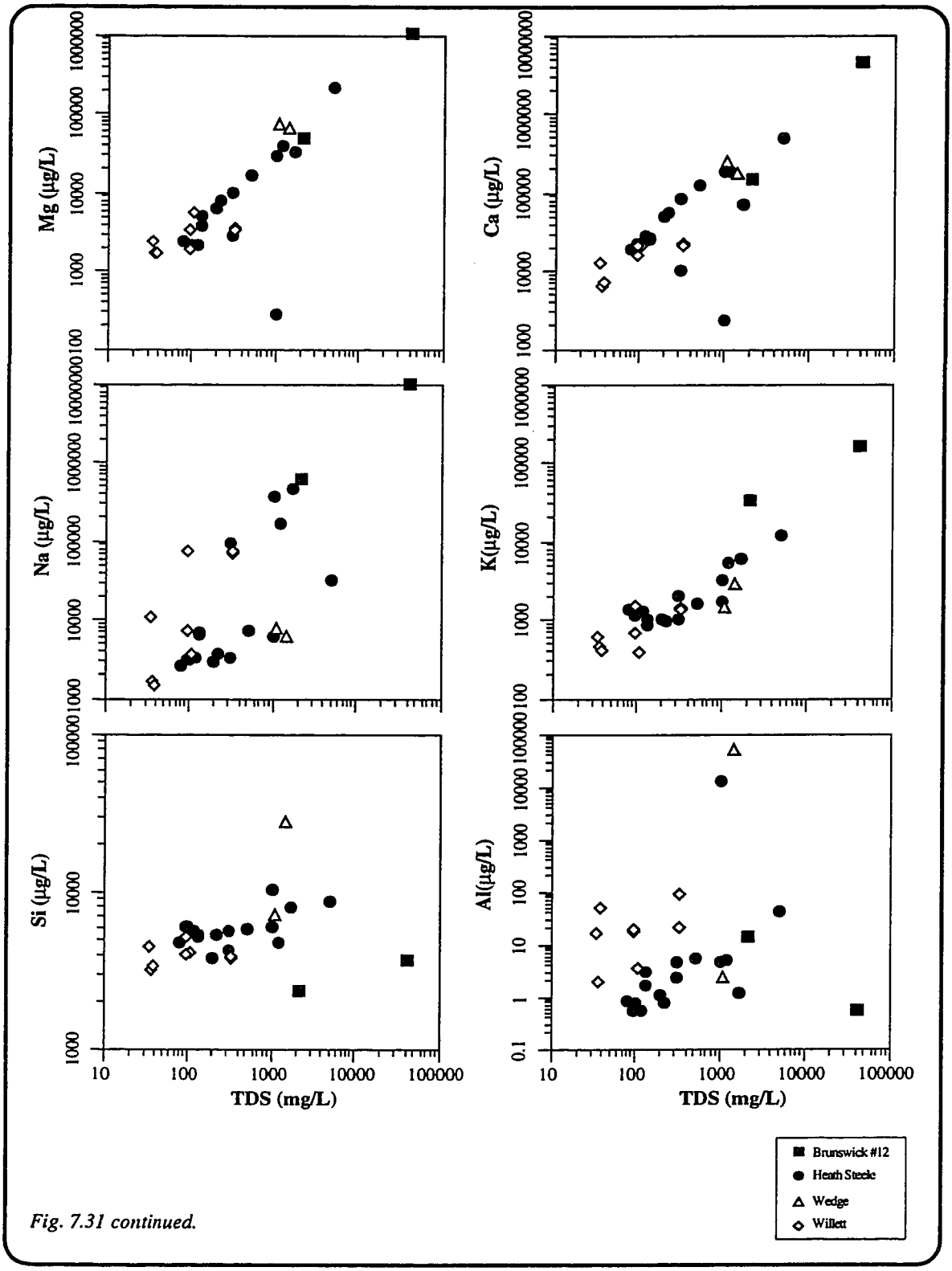


Fig. 7.31 continued.

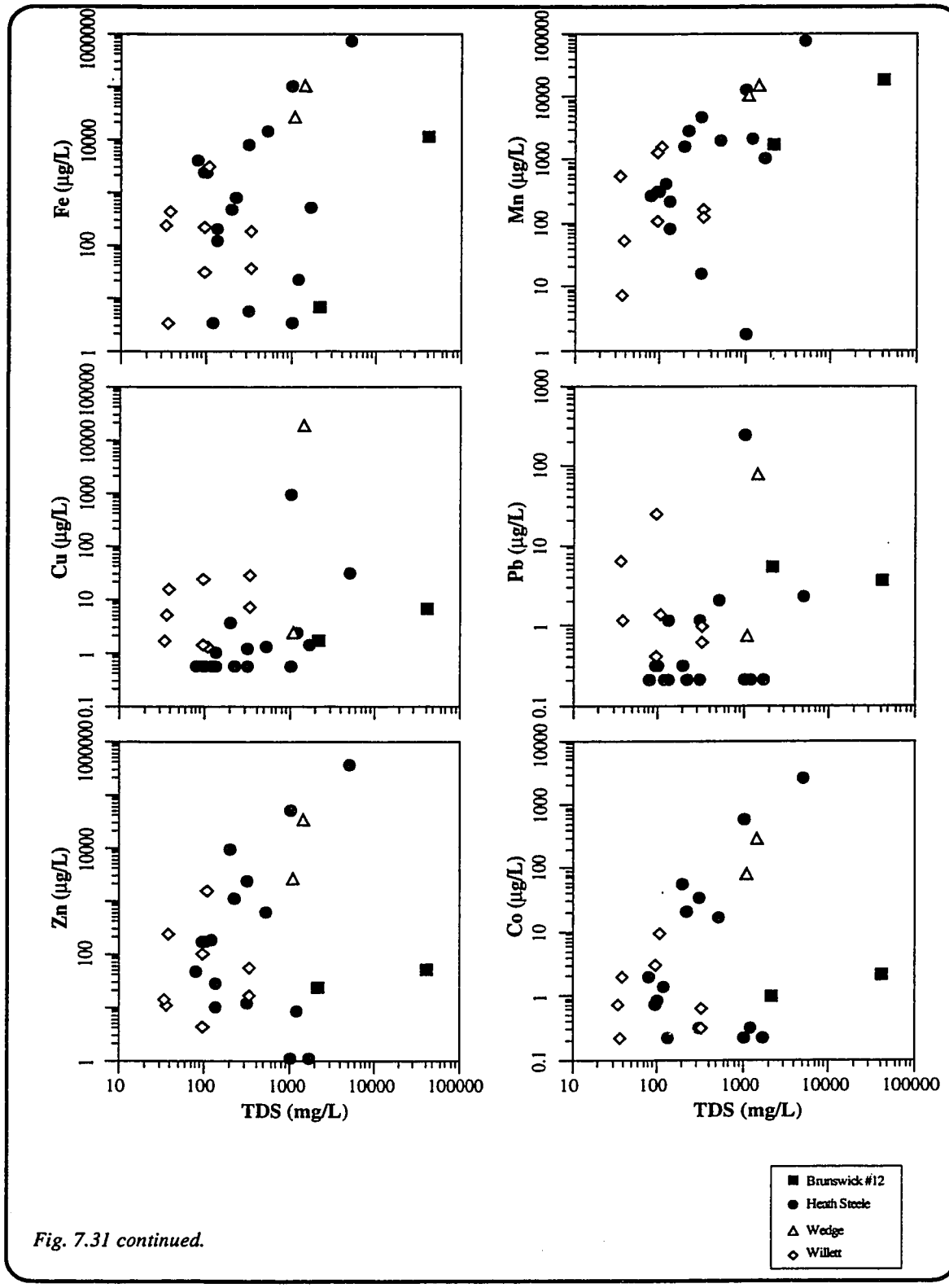


Fig. 7.31 continued.

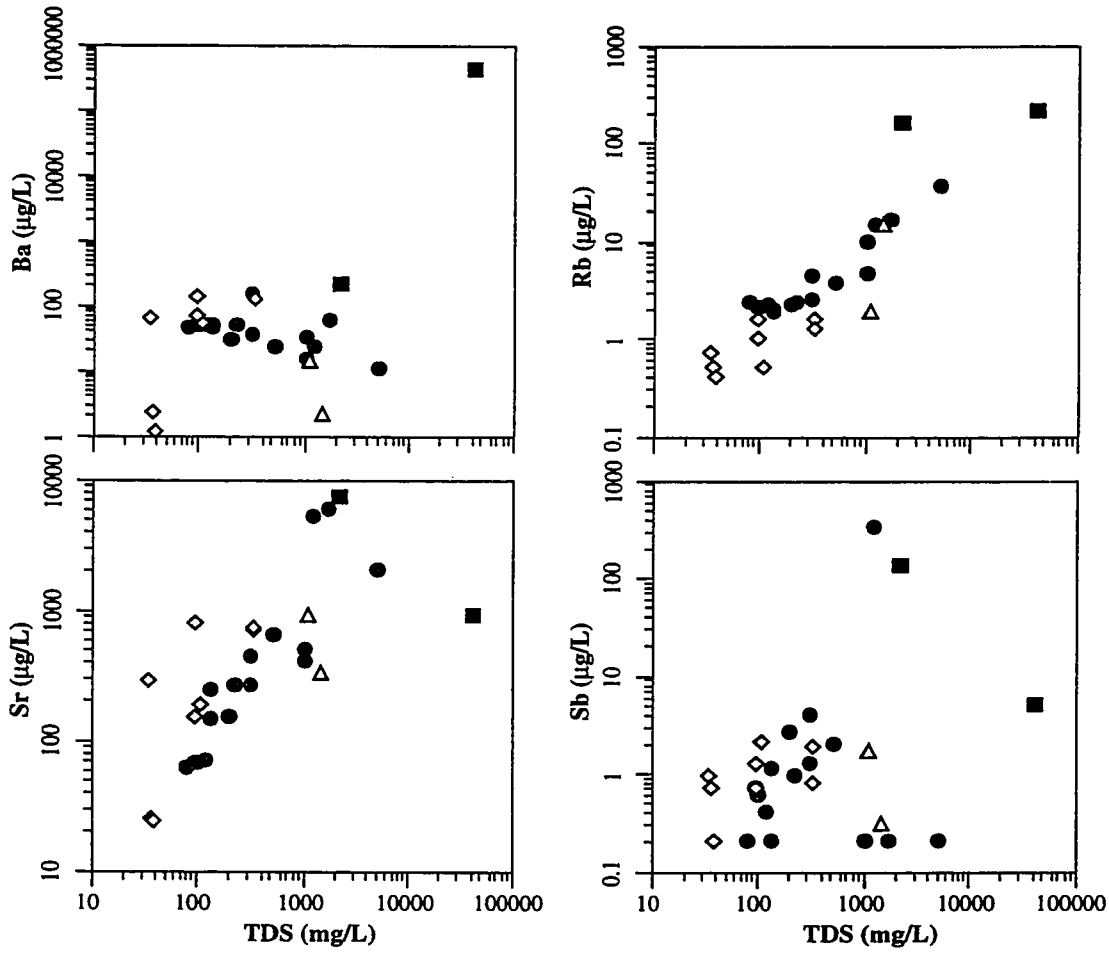


Fig. 7.31 continued.

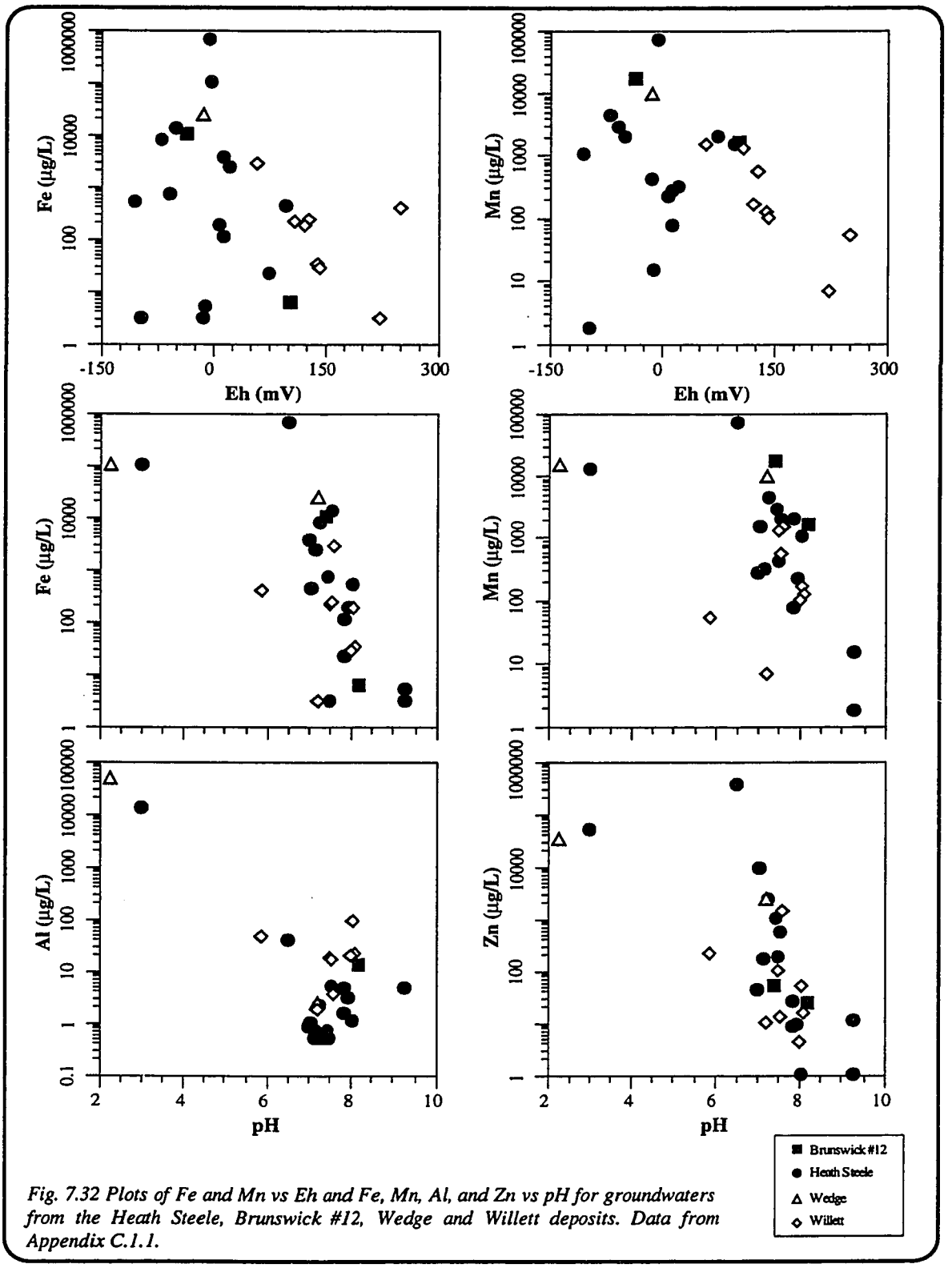


Fig. 7.32 Plots of Fe and Mn vs Eh and Fe, Mn, Al, and Zn vs pH for groundwaters from the Heath Steele, Brunswick #12, Wedge and Willett deposits. Data from Appendix C.1.1.

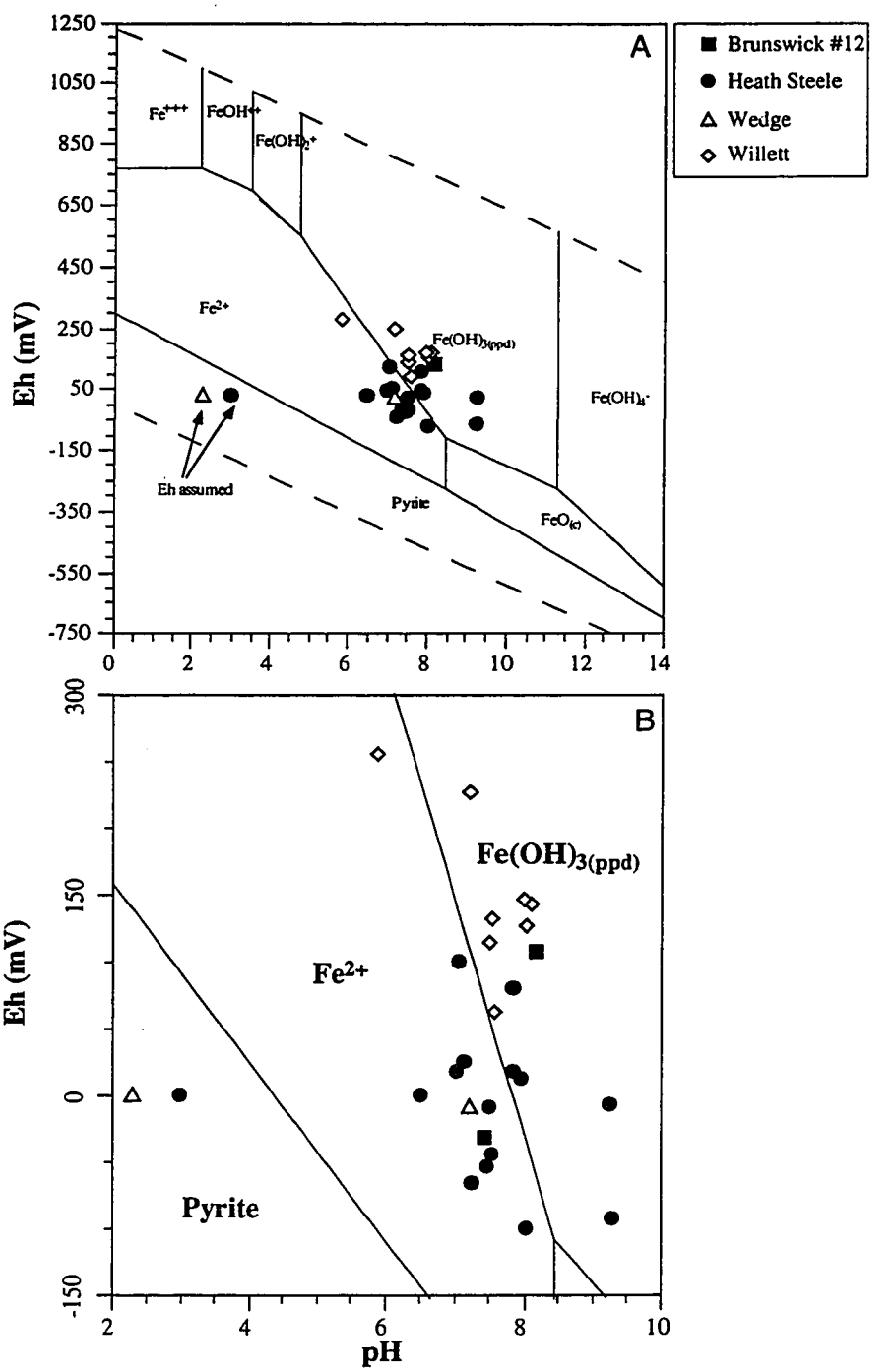


Fig. 7.33 Diagram showing the stability of metastable Fe hydroxides relative to groundwaters from the Heath Steele, Brunswick #12, Wedge, and Willett deposits. The fields were calculated using The Geochemist's Workbench (Bethke, 1994). Conditions are: $[HCO_3] = 10^{-3.5}$, $[SO_4] = 10^{-4.5}$, $[Fe] = 10^{-5.5}$. The formation of hematite, goethite and magnetite was suppressed, reflecting the slow kinetics of formation of these phases compared to amorphous oxide phases.

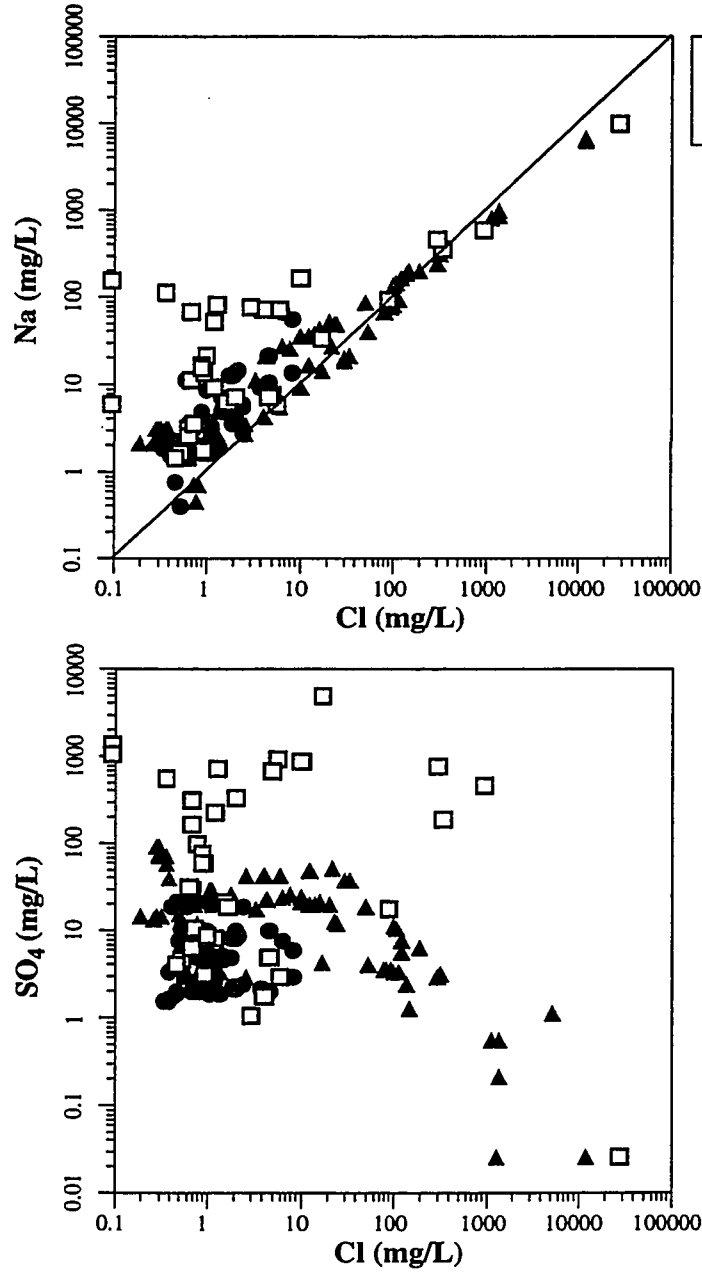


Fig. 7.34 Na and SO_4 versus Cl for Halfmile Lake and Restigouche deposit groundwaters and waters from BMC mines.

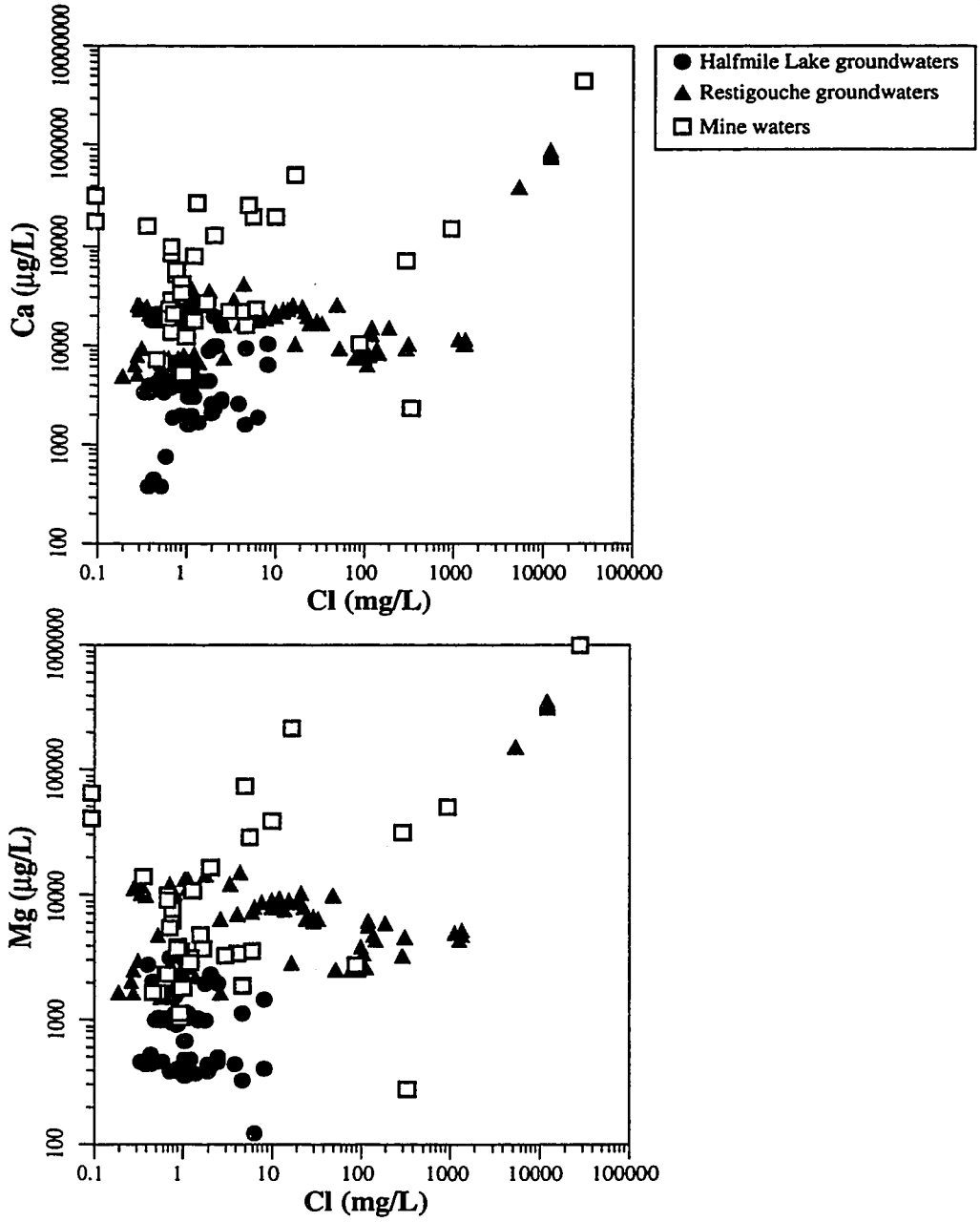


Fig. 7.35 Ca and Mg versus Cl for Halfmile Lake and Restigouche deposit groundwaters and waters from BMC mines.

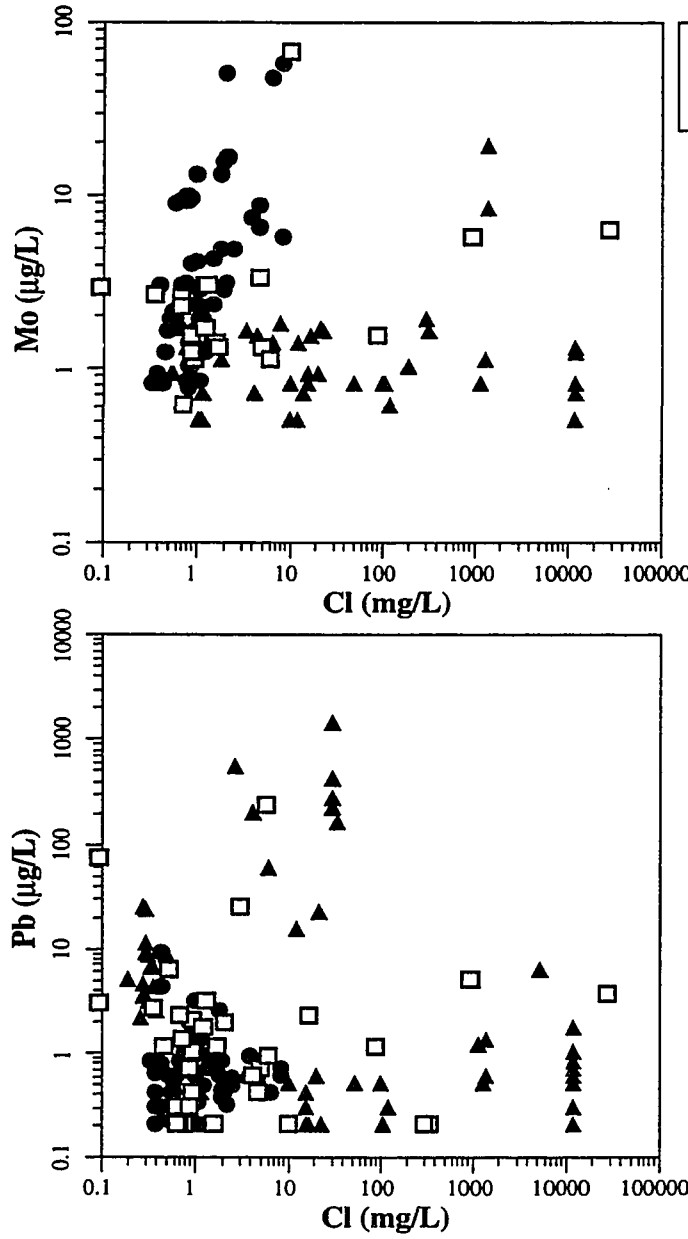


Fig. 7.36 Mo and Pb versus Cl for Halfmile Lake and Restigouche deposit groundwaters and waters from BMC mines.

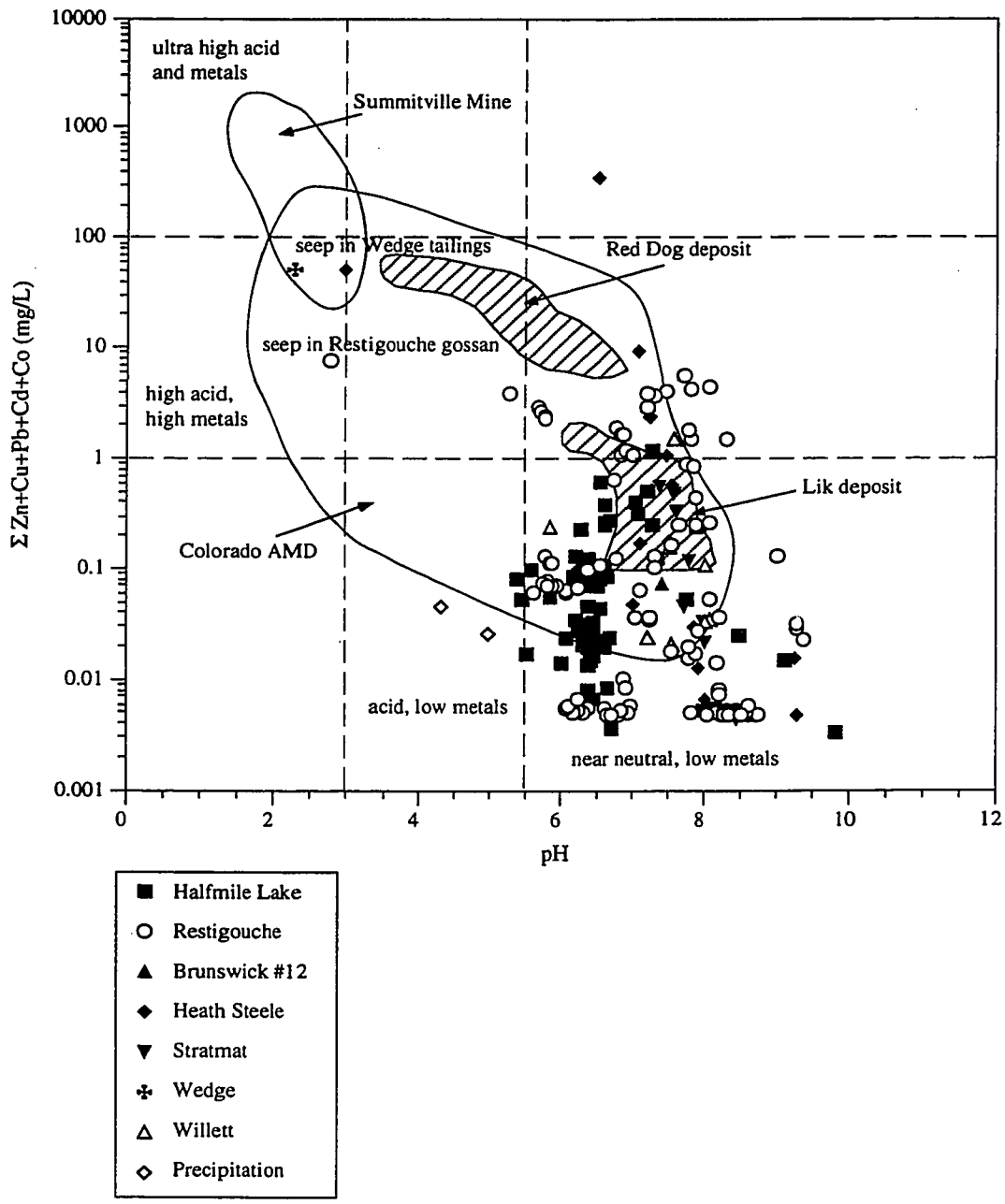


Fig. 7.37 Plot of pH vs total metal load for all the groundwaters in the present study. The majority of the groundwaters have near neutral pH and low to moderate metal loads. Also shown are data for surface waters draining undisturbed deposits (Red Dog, Lik; Kelley and Taylor, 1997) and acid mine drainage (AMD; King, 1994).

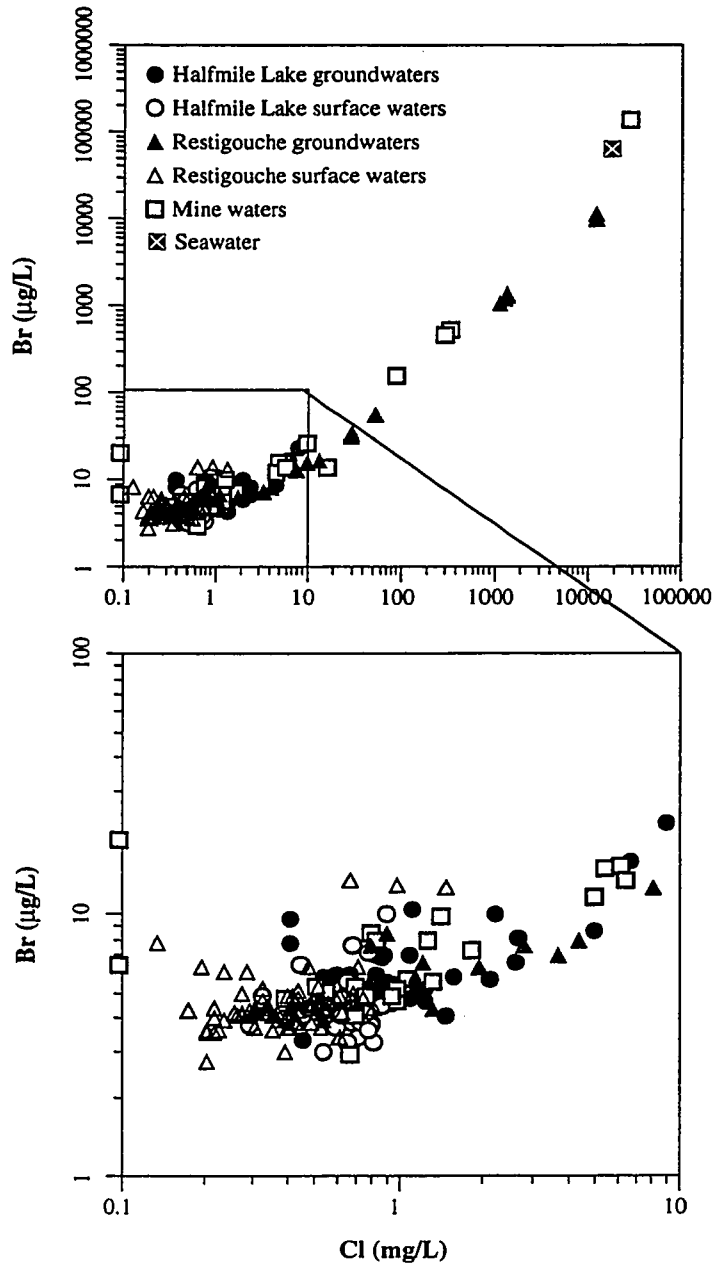


Fig. 7.38 Br vs Cl contents for Bathurst Mining Camp ground and surface waters. Also shown is seawater (Drever, 1988).

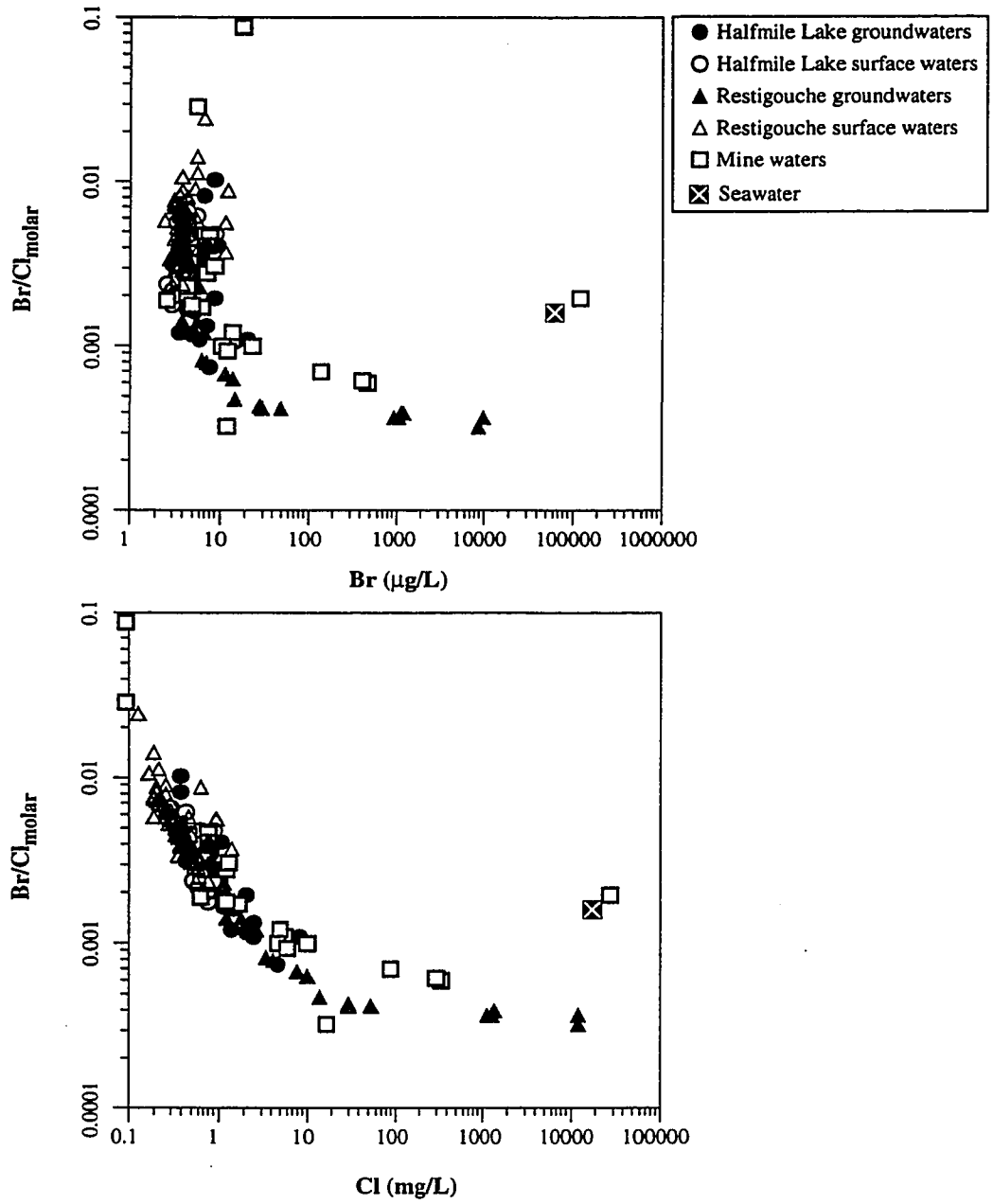


Fig. 7.39 Br/Cl vs Br and Cl contents for Bathurst Mining Camp ground and surface waters. Also shown is seawater (data from Drever, 1988).

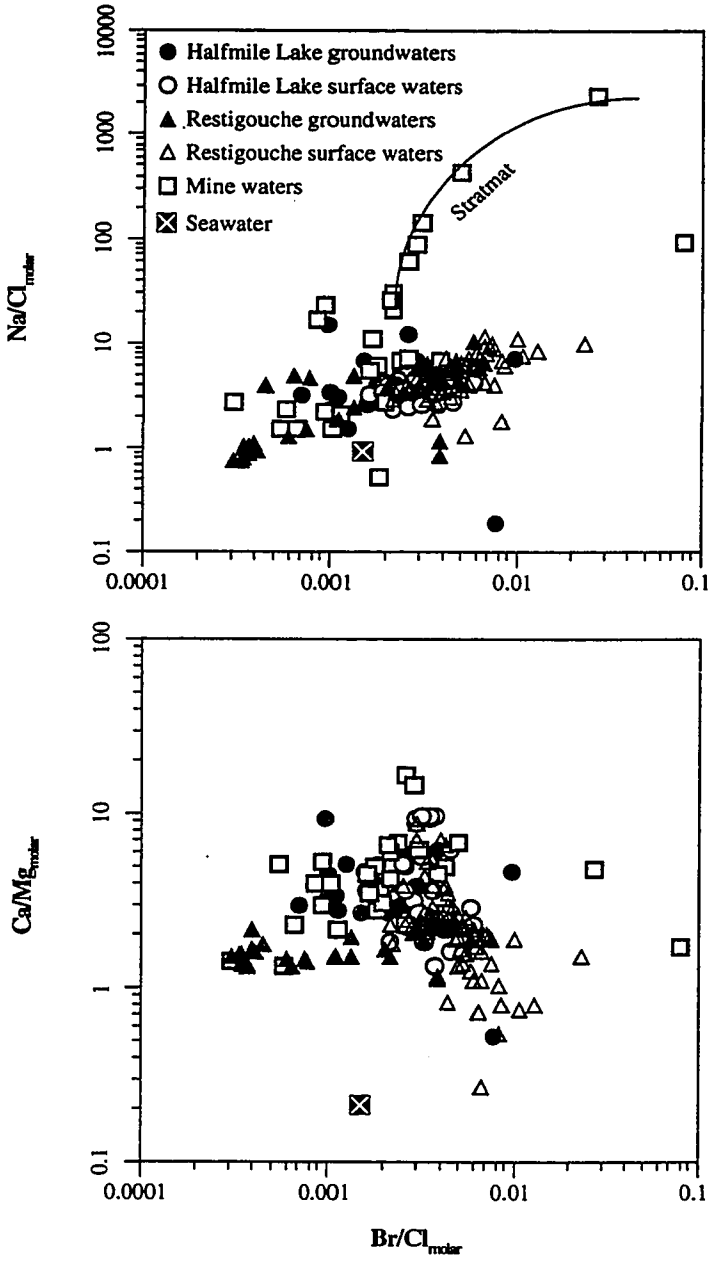


Fig. 7.40 Molar ratios of Na/Cl and Ca/Mg vs Br/Cl for BMC waters. Seawater is shown for comparison. Most of the more saline groundwaters have Br/Cl lass than seawater. Stratmat waters trend to very elevated Na/Cl compositions.

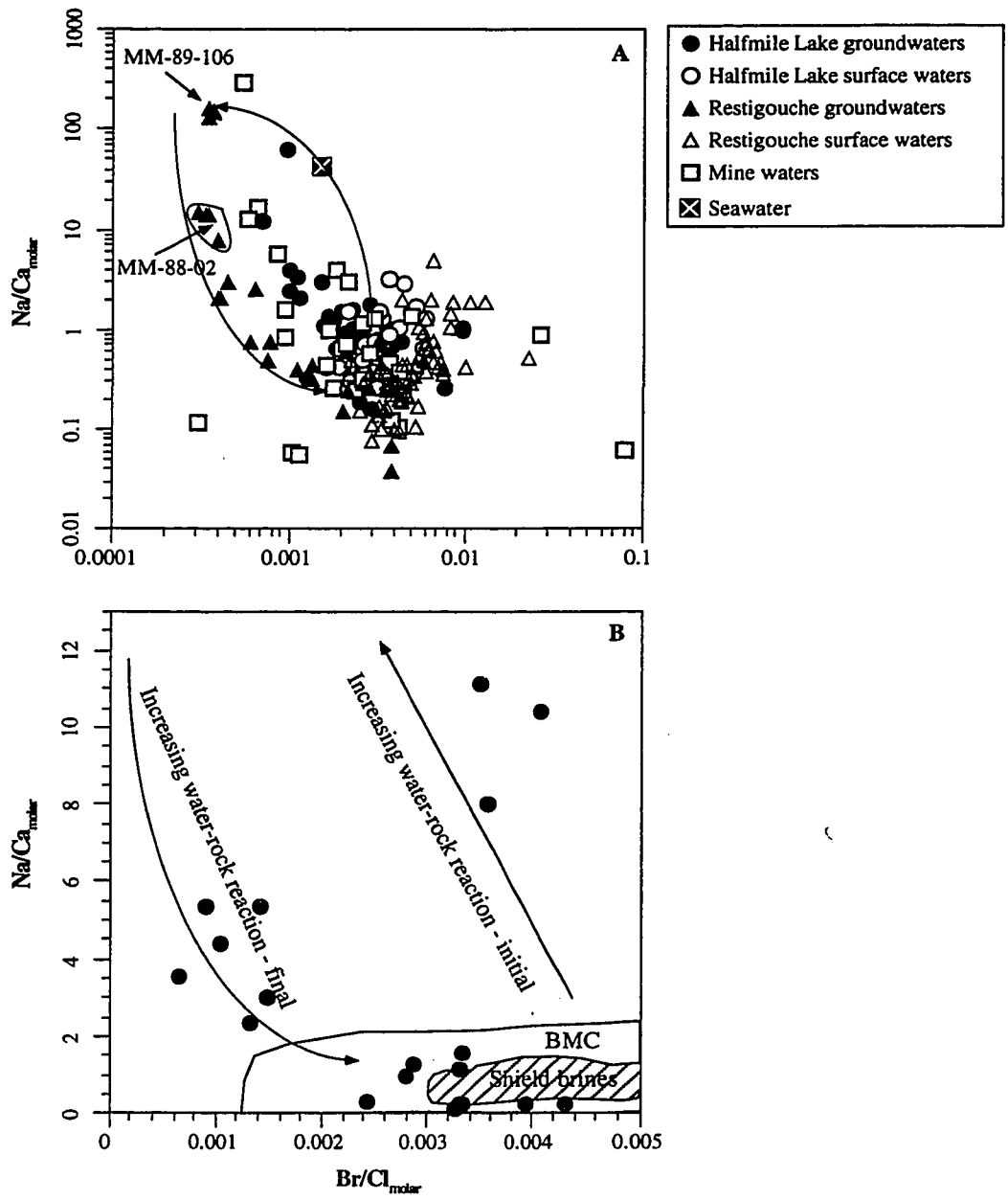


Fig. 7.41 Molar ratios of Na/Ca versus Br/Cl for BMC waters (A) compared to saline waters from plutons in the Canadian Shield (B; Gascoyne et al., 1987). The main feature of this plot is the similarity in Na/Ca and Br/Cl between shallow groundwaters and surface waters (BMC in B) and saline brines from the Canadian Shield. Saline waters from the BMC have higher Na/Ca and lower Br/Cl, but trend towards the shield brine field with increasing water-rock reaction (curve).

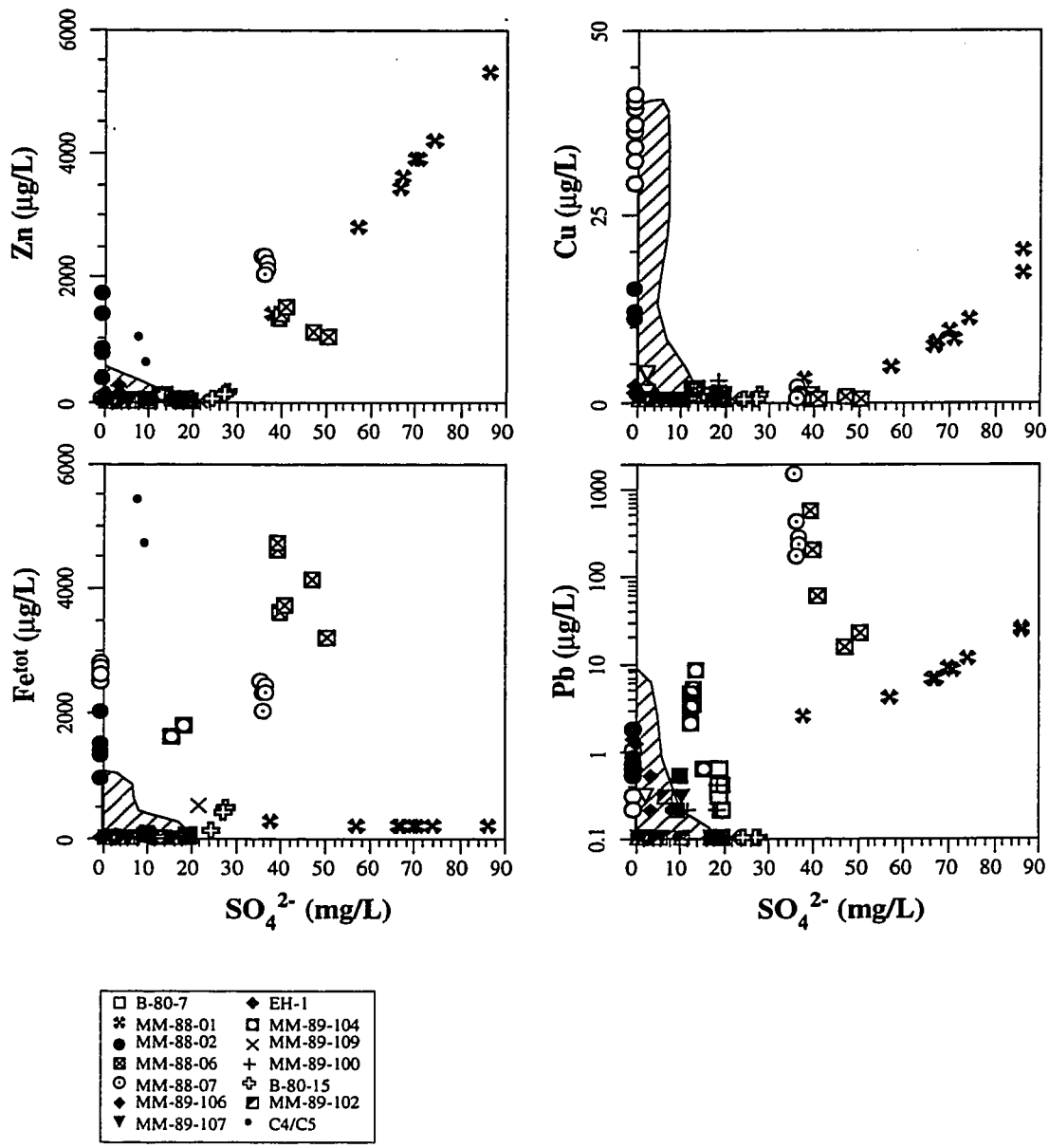


Fig. 7.42 Sulphate versus trace metals in groundwaters from the Restigouche deposit (symbols) and the Halfmile Lake deposit (shaded region). Pb concentrations in Restigouche deposit groundwaters are highest in boreholes closest to where the orebody crops out, but lower in holes where the orebody is intersected at greater depth. The greater mobility of Zn and Cu compared to Pb is indicted by the stronger correlation with dissolved sulphate content.

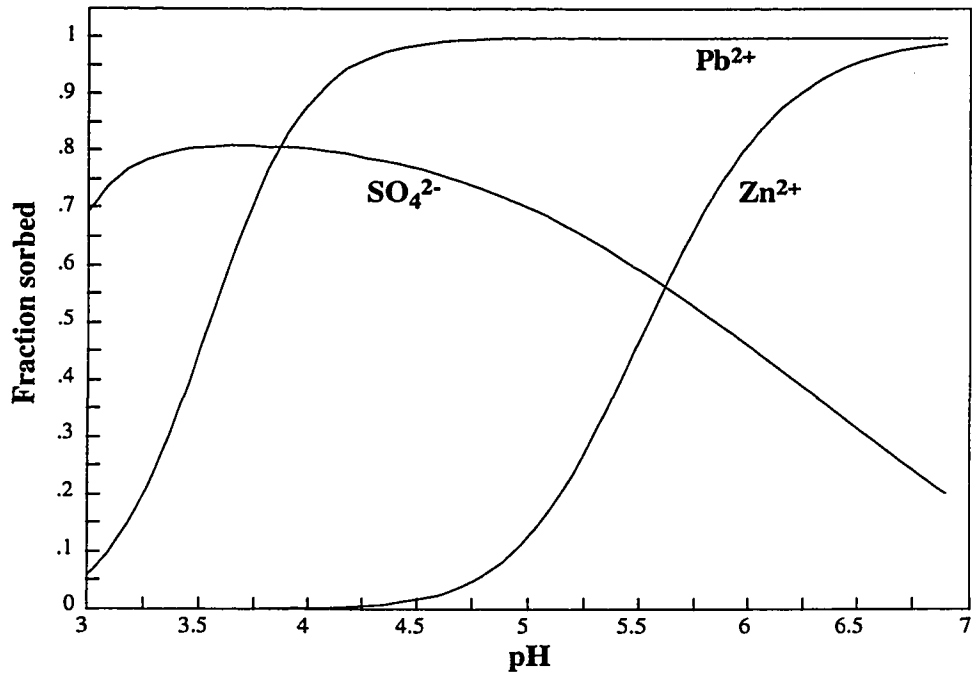


Fig. 7.43 Adsorption of Pb, Zn, Ca and SO_4 onto surface of $Fe(OH)_{3(ppd)}$ as a function of pH using "dissolved" values for sample MLW95-314 from borehole MM-88-07 at the Restigouche Deposit. See Table B.3.1 for analytical details. Reaction path was calculated using The Geochemist's Workbench (Bethke, 1984).

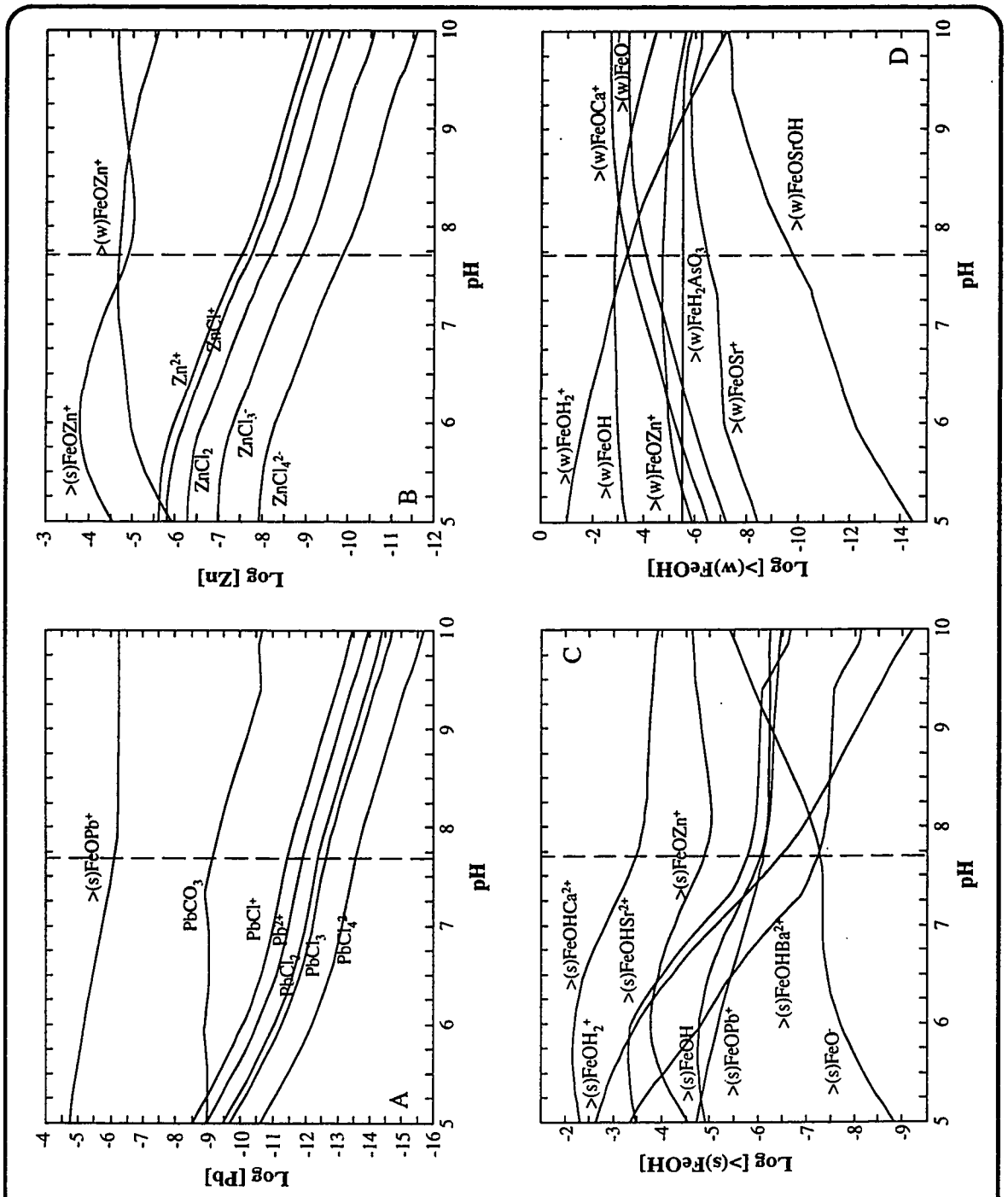


Fig. 7.44 Geochemical modelling results showing adsorption and speciation for selected species from borehole MM-88-02 (sample MLW95-604) from the Restigouche deposit. Dashed line represents pH of the sample. A) Pb speciation, B) Zn speciation, C) major species associated with strong adsorption sites on $Fe(OH)_3$, and D) major species associated with weak adsorption sites on $Fe(OH)_3$. Results calculated using The Geochemists Workbench (Bethke, 1994), with sliding pH from 5 to 10.

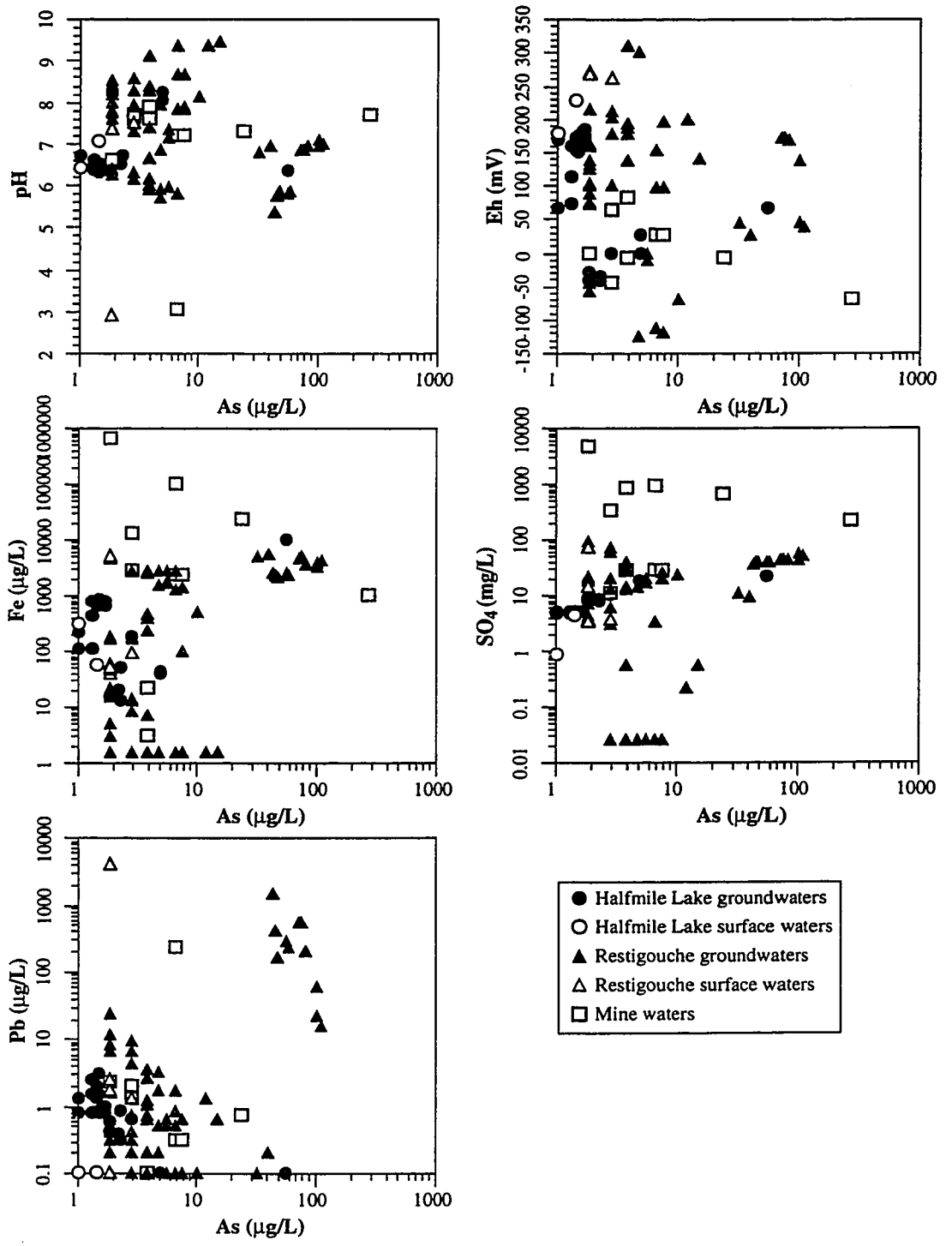


Fig. 7.45 Plots of arsenic plotted against pH, Eh, SO_4, Fe and Pb.

Table 7.1 As speciation results for groundwaters

Sample#	Location		As^{III}	As^{Total}	As^{V}	As^{III}/As^{Total}	pH	Eh(mV)
MLW95-608	Halfmile Lake	HN94-65	<0.2	0.6	0.6	»	7.94	64
MLW95-485	Heath Steele	B-zone	1.1	5.9	4.8	0.2	3.03	0
MLW95-486	Heath Steele	B-zone	1.2	1.5	0.3	0.8	6.56	-2
MLW95-474	Heath Steele	C-zone	0.4	0.6	0.2	0.7	7.31	-67
MLW95-476	Heath Steele	C-zone	0.2	0.3	<0.2	0.7	7.52	-54
MLW95-481	Heath Steele	C-zone	0.3	0.8	0.5	0.4	7.07	17
MLW95-610	Heath Steele	B-zone	<0.2	2.6	2.6	»	7.87	79
MLW95-577	Restigouche	B-80-7	2.1	1.1	<0.2	1.9	8.50	72
MLW95-583	Restigouche	B-80-7	4.5	4.8	0.3	0.9	8.32	156
MLW95-583 rep	Restigouche	B-80-7	5.0	4.9	<0.2	1.0	8.32	156
MLW95-586	Restigouche	B-80-7	1.6	1.0	<0.2	1.6	8.23	-60
MLW95-590	Restigouche	B-80-7	5.6	6.5	0.9	0.9	8.67	95
MLW95-597	Restigouche	MM-88-02	0.3	<0.2	<0.2	«	7.94	-150
MLW95-600	Restigouche	MM-88-02	0.6	0.4	<0.2	1.5	7.79	-120
MLW95-604	Restigouche	MM-88-02	0.2	<0.2	<0.2	«	7.91	-125
MLW95-606	Restigouche	MM-88-02	<0.2	<0.2	<0.2		7.83	-113
MLW95-545	Restigouche	MM-89-104	3.0	5.6	2.6	0.5	7.10	-3
MLW95-546	Restigouche	MM-89-104	2.9	5.8	2.9	0.5	7.31	-13
MLW95-504	Restigouche	MM-89-106	8.4	9.9	1.5	0.8	9.42	140
MLW95-508	Restigouche	MM-89-106	2.9	5.2	2.3	0.6	9.33	150
MLW95-511	Restigouche	MM-89-106	0.4	3.3	2.9	0.1	9.07	136
MLW95-522	Restigouche	MM-89-106	<0.2	0.2	0.2		7.61	54
MLW95-522 rep	Restigouche	MM-89-106	0.3	0.2	<0.2	1.5	7.61	54
MLW95-526	Restigouche	MM-89-106	0.5	0.6	<0.2	0.8	7.71	135
MLW95-593	Restigouche	MM-89-107	0.4	3.2	2.8	0.1	7.98	161

Values in µg/L
Note: As^{V} calculated

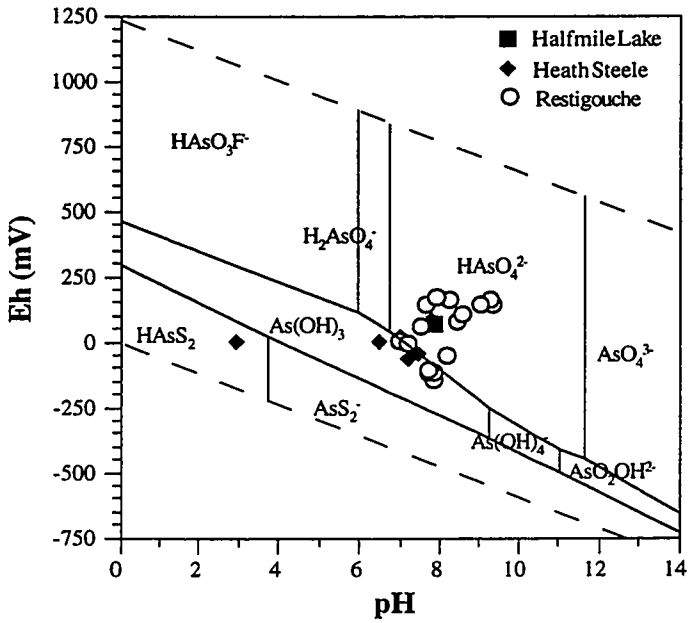


Fig. 7.46 Eh-pH stability diagram for As species. Field boundaries plotted using The Geochemist's Workbench (Bethke, 1994). Conditions are set to 25°C, 1.013 bars, $[SO_4] = 10^{-4}$, $[HCO_3] = 10^{-4}$, $[Fe] = 10^{-5}$, $[As] = 10^{-7}$ and $[F] = 10^{-5}$. Orpiment, scorodite, and realgar were suppressed.

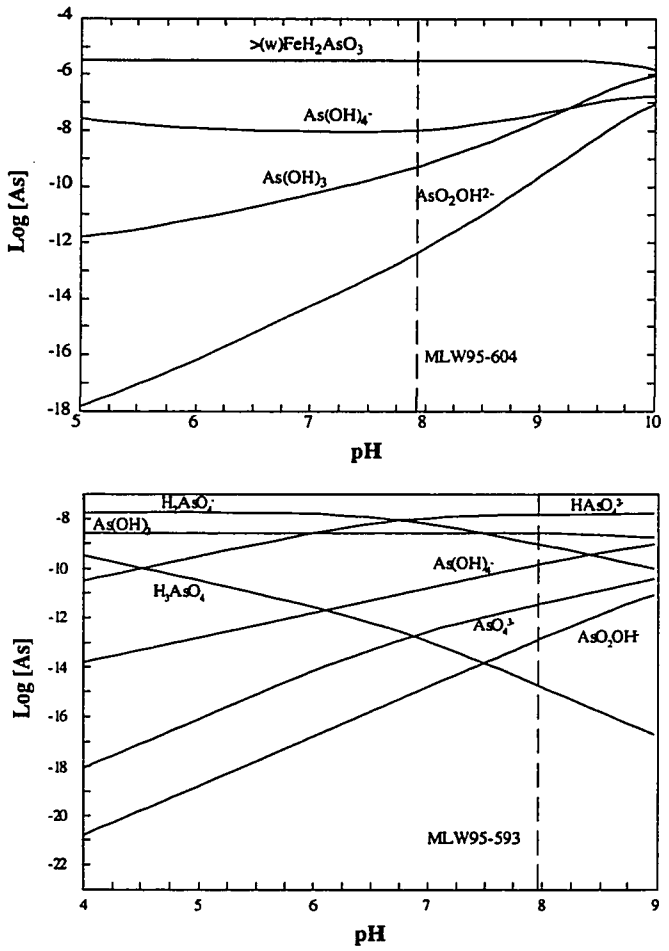


Fig. 7.47 Reaction path model of As speciation for A) sample MLW95-604 including consideration of Fe-oxide adsorption, and B) sample MLW95-593 (borehole MM-89-107) plotted using The Geochemist's Workbench (Bethke, 1994).

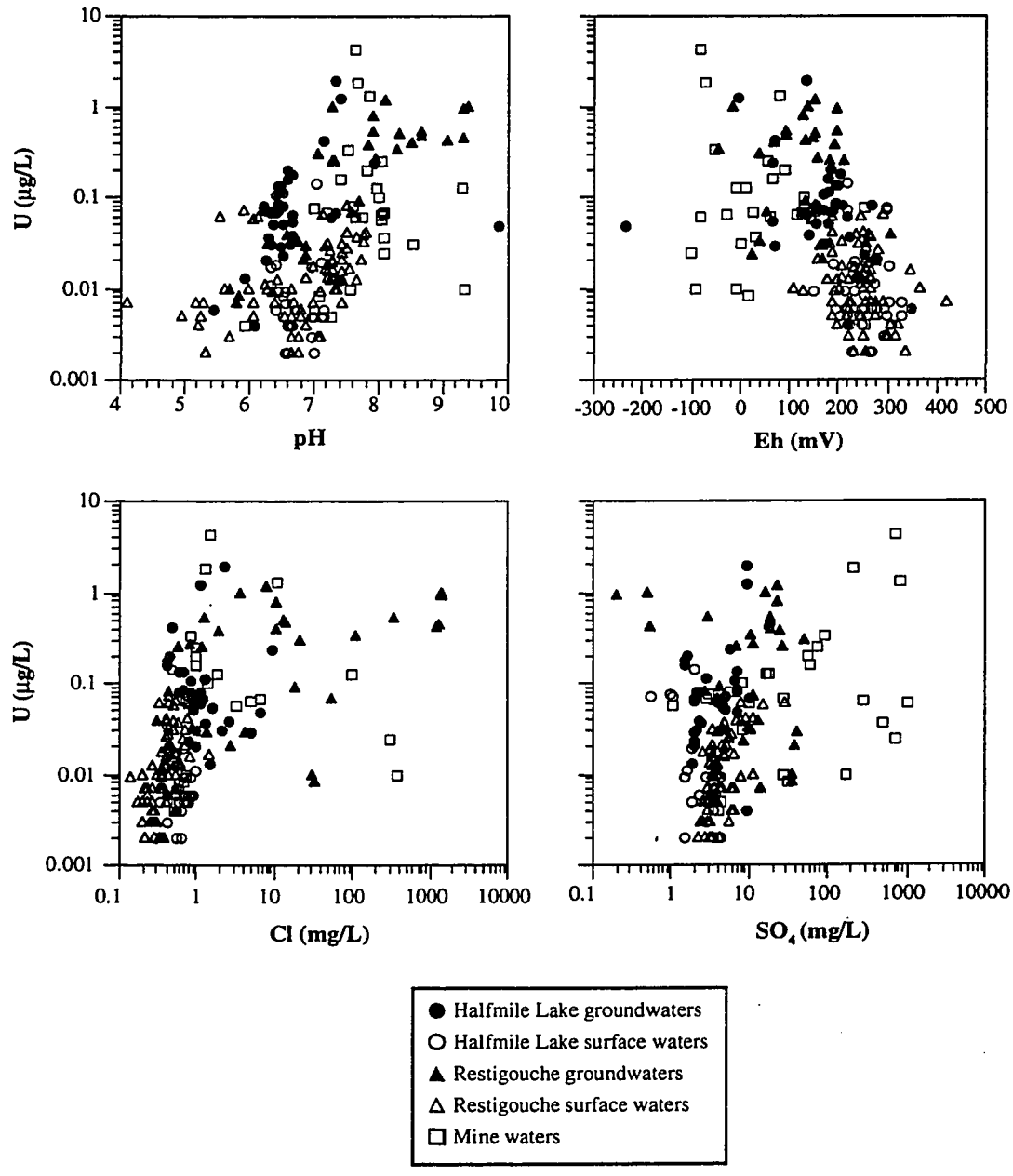


Fig. 7.48 Plots of pH, Eh, Cl, and sulphate versus U content of ground and surface waters from the BMC.

CHAPTER EIGHT:
HYDROGEOCHEMICAL AND GEOPHYSICAL EVIDENCE FOR IN SITU OXIDATION OF AN UNDISTURBED MASSIVE SULPHIDE DEPOSIT BELOW THE WATER TABLE, STRATMAT MAIN ZONE, NEW BRUNSWICK

8.1 Introduction

During downhole geophysical studies at the Stratmat Main Zone VMS deposit (Fig. 8.1), large self-potential (SP) anomalies were observed in several closely spaced exploration drill holes. In one of the boreholes (S61-19), a positive temperature gradient was observed through the massive sulphide zone (Mwenifumbo, 1991; Mwenifumbo, 1993). Mwenifumbo (1991; 1993) speculated that the SP and temperature anomalies were produced by exothermic oxidation of the massive sulphide minerals (Mwenifumbo, 1993).

This deposit presents an excellent opportunity to better understand some of the processes associated with the production of self-potential (SP) and temperature anomalies as well as processes associated with natural oxidation of massive sulphide minerals. Classical descriptions of SP anomalies associated with massive sulphide deposits suggest that the SP anomaly is produced as a result of ohmic potential reductions in groundwaters or pore-waters adjacent to or within an ore body (Kilty, 1984; Sato and Mooney, 1960). In these models, the massive sulphides are not required to undergo oxidation, but act as conductors for the flow of electrons. However, the development of large gossan bodies over weathered massive sulphides indicates that massive sulphides undergo extensive oxidation in the natural environment. Moderate SP anomalies (e.g., 100 - 500 mV) are typically associated with outcropping sulphides and associated gossans (e.g. Andrew, 1980; Blain, 1977; Blain and Brotherton, 1975; Thornber, 1975). Previous investigations of massive sulphide oxidation and the development of self-potential anomalies has focussed mainly on gossans in Australia and South Africa, where part of the orebody occurs above the water table. The hole sampled for

groundwaters at the Stratmat Main Zone deposit was chosen in order to determine if redox reactions between groundwater and massive sulphides were responsible for the large self potential and temperature anomalies (J. Mwenifumbo pers. comm. 1996). This borehole represents a natural laboratory to test ideas about in situ massive sulphide oxidation. Previous studies of sulphide mineral oxidation have focussed on experimental work (Govett et al., 1976; Nicholson, 1994) or acid-mine drainage problems associated with oxidation of sulphide minerals in mine tailings (e.g. Al et al., 1994; Blowes and Ptacek, 1994; Bowell and Bruce, 1995; Goodyear et al., 1996).

In order to test the origin of the SP anomaly, groundwaters from borehole S61-19 were sampled with a straddle-packer system. The straddle-packer design used at the Restigouche and Halfmile Lake deposits was modified to accommodate the small internal diameter of borehole S61-19 and to minimize the sampling interval between packers. The sampling interval was restricted to 60 cm when the packers were fully inflated to allow detailed sampling through the sulphide zone. Low permeabilities between 50 and 80 m in the hole prevented sampling in this interval. A total of ten samples were successfully recovered including six samples adjacent to or within the massive sulphide zone. Field measurements of pH, Eh, dissolved oxygen, and groundwater electrical conductivity all showed that there are significant chemical changes occurring in the vicinity of the massive sulphides.

8.2 Results

8.2.1 Downhole geophysics

Temperature exhibits a steady increase with depth from 3.6 °C at the top of the hole to 5.5 °C at the bottom of the hole (Fig. 8.2). However, the temperature gradient shows that there is some variation in the temperature profile. There is a temperature anomaly associated with the massive sulphides of approximately 0.05°C compared to the host lithologies. The temperature anomaly was calculated by subtracting a local geothermal gradient of 13.7 mK/m from the measured temperature profile (Mwenifumbo, 1993). Geophysical logging in nearby holes

indicates lower temperature gradients through massive sulphides (Mwenifumbo, 1993). Temperature logging of borehole S61-19 was carried out in August 1988 and 1989, and the temperature-depth profiles are essentially identical (Mwenifumbo, 1993). Measured SP is fairly constant throughout the borehole with the exception of a small negative anomaly (approximately 20 mV) at 71.5 to 72 m depth, which corresponds to a small zone of sulphides and a large negative anomaly (< -600 mV) between 84 and 89 m depth, corresponding to the main massive sulphide intersection (Fig. 8.2). Within the main sulphide zone there is an increase in the SP, corresponding to a thin section of altered argillite (Fig. 8.2). There is considerable variation in resistivity, correlating slightly with lithology. The gabbroic dykes have the highest average resistivity (up to 30,000 Ohm-m), and the massive sulphides are highly conductive, with resistivity of < 0.1 Ohm-m. Gamma-ray profiles also reflect lithology with felsic metavolcanic and metasedimentary units showing higher counts per second than the gabbroic units. Massive sulphides have the lowest gamma-ray activity (Fig. 8.2).

8.2.2 Groundwater geochemistry

Ten samples were collected with the straddle-packer in borehole S61-19. Recovery rates were relatively rapid in the ore zone, suggesting groundwater flow throughout the ore zone. In contrast, the borehole was apparently hydrologically tight between 50 - 80 m depth as evidenced by poor water return to the packer system. Within the ore zone, recovery times varied such that apparent hydraulic conductivities were higher in the upper part of the ore zone compared to the lower part.

The groundwaters vary from shallow Ca-HCO_3 and Ca-Na-HCO_3 waters to Ca-SO_4 waters within the ore zone (Table 8.1, Fig. 8.3). The pH of the waters is in general slightly lower in the sulphide zone than above and below the sulphides. Total dissolved solids (TDS) increase downhole from 120 mg/L at the top of the hole, to 1600 mg/L at the base of the massive sulphide zone, and decreases below the sulphide zone (Fig. 8.4). Although the massive sulphides are only approximately 5 m thick (borehole S61-19 is vertical), TDS values increase

from around 200 mg/L at the top of the sulphides and approximately double in TDS value every meter to 89 m depth (Fig. 8.4). The dominant anion in the massive sulphide zone is SO_4^{2-} and the dominant cation is Ca^{2+} with lesser Na^+. Dissolved oxygen (DO) decreased in the vicinity of the massive sulphides, but still exceeded 2 mg/L. The DO values should be treated with caution due to sample recovery times and possible entrainment of atmospheric O_2. Both Eh and pH are higher for the samples at 85 and 86 m depth and decrease in the lower part of the massive sulphides. However, pH values are all above 7, despite the high dissolved SO_4 contents.

Downhole profiles show the following characteristics. The distribution of Fe is controlled by the redox state (Eh) of the groundwaters. Assuming that the DO and Eh values were not excessively perturbed by the sampling method, the Fe^{2+}/Fe^{3+} redox couple is most likely to be dominant in these waters. For example, speciation calculations indicate that essentially all of the Mn occurs in the Mn(II) form, with the majority of the dissolved Mn is present as free ions. The proportion of $MnSO_{4(aq)}$ and $MnCO_{3(aq)}$ increases at the bottom and top of the massive sulphide zone, respectively, but these are still minor components in these waters (Fig. 8.5). Additionally, Mn contents show similar trends as TDS and the major ions (Fig. 8.4). In contrast, Fe contents are lowest at the top of the massive sulphide zone, and highest at the bottom of the sulphides. There is also an increase in Fe in the sample taken immediately above the massive sulphides. Zinc and Cd show very similar downhole trends (Fig. 8.4). Both metals reach maximum concentrations towards the bottom of the ore zone and just above the top of the ore zone. Zinc and Cd are low in the waters from the upper part of the ore zone, despite increasing TDS. Trends for Pb are more equivocal due to the lack of agreement between the two ICP-MS methods. The chelation ICP-MS data suggest that Pb values are highest at the bottom of the ore zone, similar to many other metals such as Sb, Ni, and Mo (Fig. 8.4). Vanadium is highest in the oxidizing waters in the upper part of the ore zone and at the top of the hole. Speciation calculations do not show any systematic variation that would explain the behaviour of V downhole.

At the Restigouche deposit, F contents typically increase with increasing salinity (with the exception of the MM-88-02 waters). In groundwaters from borehole S61-19, F contents, with the exception of one sample, decrease downhole as sulphate increases and F is below detection in the three samples where sulphate contents are highest.

Stable isotopic results are discussed in detail elsewhere (see Chapter Eleven). Briefly, oxygen and hydrogen isotopes show a shift to heavier isotopic compositions from the top to the bottom of the ore zone of approximately 0.35 and 4‰, respectively (Fig. 8.6). The $\delta^{13}C_{DIC}$ values also increase through the ore zone, and are approximately 3‰ heavier at the bottom of the ore zone compared to the top (Figs. 8.6, 8.7).

8.2.3 Mineralogy of suspended sediments and host rock

Unfortunately, core from borehole S61-19 no longer exists. However, drilling logs provide visual estimates of the main ore minerals. The main sulphide mineral is pyrite, with minor sphalerite and chalcopyrite. Limited assays indicate Zn grades up to 5.44%, Pb to 1.31% and Cu to 0.46%. Although no pyrrhotite was noted in the log, nearby diamond drill holes (ST-218 to ST-220) that intersect the same lithologies and presumably the same massive sulphide zone are also dominantly pyrite but pyrrhotite is noted as a minor sulphide mineral. Assays from borehole ST-218 have grades of 6.82% Zn, 2.22% Pb and 0.15% Cu over an interval of 18 m. In borehole ST-220, the grades are lower at 3.70% Zn, 1.47% Pb, and 0.13% Cu, also over an interval of 18 m.

Suspended sediments from two groundwaters from borehole S61-19 (MLW96-695 and MLW96-702) were analyzed by SEM (see Chapter Nine). Sediments on filter papers was sparsely distributed and there was insufficient suspended sediment on the filter papers for ICP-MS or XRD analysis. Sample MLW96-695 from the lower part of the ore zone appears to be dominated by amorphous patches with strong Fe, S, and O peaks in SEM spectra. These patches are interpreted to be Fe-sulphate. However, geochemical modelling indicates that melanterite ($FeSO_4 \cdot 7H_2O$) is well below saturation. This sample has rare silicates, probably

chlorite with surface coatings of Fe-sulphate (peaks of Si, Al, Mg, Fe and S, with minor K and P). In contrast, sample MLW96-702 from immediately below the ore zone is characterized mainly by K-silicates and Mg-Fe silicates, with variable surface coatings of Fe-sulphate.

8.2.4 Geochemical modelling

Goethite and hematite are both supersaturated in all the waters. Due to kinetic factors, any stable Fe species are more likely to be amorphous in character (Nicholson, 1994). However, the magnitude of the saturation index (SI) values for goethite (and hematite) are highest where Fe^{3+} increases due to increasing Eh and where total dissolved Fe contents are lowest (Figs. 8.4, 8.5, 8.8). With the exception of the upper part of the hole, Fe^{2+} species are dominant throughout, with $Fe^{2+}_{(aq)}$, $FeHCO_3^+$, $FeCO_{3(aq)}$, and $FeSO_{4(aq)}$ the main species in decreasing order of abundance. $Fe(OH)_{3(aq)}$ is the dominant species of ferric iron and is present in significant amounts only at the top of the hole and just above the ore zone. The highest Fe contents occur where the Eh is the lowest. At these low Eh values (< -50 mV), Fe^{2+} is the most stable Fe species.

These waters were modelled using two different geochemical modelling programs; PHREEQC (Parkhurst, 1995) and EQ3NR (Wolery, 1992b). The PHREEQC program was used with the WATEQ4F database. These two geochemical modelling programs yielded quite different results for base metal speciation and saturation, although they were closer for the major elements and for Fe speciation.

For Zn, EQ3NR indicates that this metal occurs predominantly as free ions, with only minor HCO_3^- and OH^- complexes. In contrast, PHREEQC modelling indicates that in the low TDS waters in the upper part of the borehole, Zn^{2+} and $ZnCO_{3(aq)}$ species are in approximately equal proportions, whereas in the high sulphate waters at the base of the ore zone, Zn^{2+} and $ZnSO_{4(aq)}$ species dominate. Below the ore zone, $ZnCO_{3(aq)}$ becomes increasingly dominant over the sulphate complex. For Pb, EQ3NR indicates that > 99% of the Pb in these waters occurs as free ions, whereas, PHREEQC indicates that $PbCO_{3(aq)}$ is by far the dominant

species of Pb in solution. Copper speciation also differs between the two software programs. Both programs indicate that Cu^{2+} dominates over Cu^{+} in the upper part of the hole, and that Cu^{+} is the dominant species of copper at the bottom of the ore zone, in the more reducing waters. However, EQ3NR indicates that $CuCO_{3(aq)}$ is the dominant species of Cu^{2+}, whereas, PHREEQC indicates that $Cu(OH)_{2(aq)}$ is generally in much greater abundance than $CuCO_{3(aq)}$.

8.3 Discussion

Based on the field chemistry, and the increase in temperature through the sulphides, two possible explanations were considered for the increase in groundwaters electrical conductivity through the massive sulphide zone. The first possibility is that the sulphide zone is acting as a fortuitous conduit for deeper, warmer, higher TDS fluids or that the massive sulphides are undergoing exothermic oxidation reactions. The anion data very clearly indicates which of these possibilities is the most likely. The SO_4^{2-} contents clearly dominate the anion chemistry increasing from 8.00 mg/L near the top of the hole to in excess of 1000 mg/L within the sulphide zone (Fig. 8.4). If these waters represented deeper saline waters similar to those at Restigouche, Cl^- would be expected to be the dominant anion. In fact, Cl^- contents are low throughout the hole and are lowest where SO_4^{2-} is at a maximum. However, the stable isotope data indicate that the first possibility has some applicability (see below).

8.3.1 Geophysical evidence for sulphide oxidation

Mwenifumbo (1993) suggested that temperature logging in boreholes might be useful in mineral exploration because massive sulphides typically possess low electrical resistivity (Fig. 8.2) and high thermal conductivity. Therefore, in the vicinity of massive sulphides, the local geothermal gradient should become perturbed, with a reduction in the measured thermal gradient. At the Stratmat Main Zone, temperature logging was carried out in five holes proximal to S61-19 (Mwenifumbo, 1993). Through the massive sulphide lenses in these holes, the temperature profiles were flat and the temperature gradients were significantly lower than

the local geothermal gradient. In contrast, the temperature increased in borehole S61-19 through the massive sulphide lenses, coincident with the large negative SP anomaly recorded in this hole (Fig. 8.2). The anomaly has been calculated as about 0.05°C above the local geothermal gradient (Mwenifumbo, 1993).

The explanation for the occurrence of a positive temperature anomaly through the massive sulphides in borehole S61-19, but nearly constant temperatures (almost zero gradients) through the sulphide zones in nearby boreholes ST218, ST219, and ST220 can be related to exothermic oxidation of massive sulphide minerals. Self potential anomalies are also associated with massive sulphide intersections in nearby boreholes, but are smaller in magnitude, without associated increases in temperature. The rate of groundwater recovery with the straddle-packer gives a qualitative sense of relative groundwater flow. Based on straddle-packer data, groundwater flow through the upper part of the massive sulphide zone in borehole ST61-19 is greater than in the lower part of the sulphide zone, and greater than flow immediately above or below the sulphides. Therefore, the positive thermal anomaly through the massive sulphides in borehole S61-19 is here interpreted to be related to groundwater flow. The lower magnitude of SP anomalies and absence of a positive temperature anomalies in boreholes near borehole ST61-19 indicates that there is less groundwater flow through the ore zone in these boreholes.

8.3.2 Hydrogeochemical evidence for sulphide oxidation

Mwenifumbo (1991; 1993) postulated that the SP and temperature anomalies were caused by exothermic redox reactions within the massive sulphides. The alternative is that the sulphides are fortuitously acting as a conduit for warmer fluids. The groundwater field data (pH, Eh, and electrical conductivity) is compatible with either hypothesis. If the higher salinities are the product of exothermic redox reactions then the waters are expected to have high SO_4 as well as high base metal concentrations. If the sulphides are merely acting as a conduit for a deeper (and therefore warmer) higher TDS fluid, the expected chemistry would be more similar to higher TDS fluids recovered at the Restigouche and Brunswick #12 deposits,

i.e. dominated by Na-Ca-Cl compositions (Chapter Seven).

The waters in contact with the ore zone are high-sulphate waters (Fig. 8.4). There are a couple of possible explanations for this; 1) Fe-sulphide minerals (pyrite, pyrrhotite) are not being oxidized and that instead the high sulphate is being produced by dissolution of Ca sulphate minerals, and 2) the high sulphate is produced by sulphide oxidation but the Fe has been removed from solution by precipitation of Fe-bearing oxyhydroxides and/or sulphates. Hematite, goethite, and magnetite are all supersaturated in these waters (Fig. 8.4). In addition, SEM results on suspended sediments in these waters (MLW97-695 and MLW96-702) appear to contain Fe-sulphates (although melanterite [$FeSO_4 \cdot 7H_2O$] is well below saturation based on geochemical modelling). Note that the speciation results for sample MLW96-697 indicates that all the Fe in solution is Fe^{2+} which would explain the undersaturation of melanterite. Other Fe-sulphate minerals such as szomolnokite [$FeSO_4 \cdot H_2O$] and rozenite [$FeSO_4 \cdot 4H_2O$] are not included in either the EQ3NR or PHREEQC databases. Iron sulphate minerals are highly soluble in water (Alpers et al., 1994) so that it is possible that the Fe-sulphate observed by SEM was not saturated in the groundwater but formed on the surface of the filter paper subsequent to sampling. For example, NaCl crystals were observed on the filter papers of samples from borehole MM-88-02 at the Restigouche deposit (Chapter Nine). Although these waters are saline Na-Ca-Cl waters, NaCl is well below saturation, but halite is interpreted to have formed as a result of evaporation on the filter paper surface. It is impossible to determine the Fe-sulphate species from the SEM, but based on the colour of the filter paper residue, the sulphates may be Fe^{III} or mixed Fe^{II}-Fe^{III} species such as copiapite ($Fe^{II}Fe_4^{III}(SO_4)_6(OH)_2 \cdot 20H_2O$) or ferricopiapite ($Fe_5^{III}(SO_4)_6O(OH) \cdot 20H_2O$), both of which form yellow to yellow orange precipitates (Alpers et al., 1994).

The high sulphate and moderate Fe and Zn contents of borehole S61-19 groundwaters as well as the close association of high metals and sulphate with massive sulphides indicates that the massive sulphides are undergoing oxidation. The drilling logs for borehole S61-19 indicate that the primary sulphide is pyrite. Logs from nearby holes (e.g. boreholes ST-218, ST-219,

ST-220) indicate that pyrrhotite is present as a minor constituent, consistent with increased magnetic susceptibility as measured during geophysical logging (Mwenifumbo, pers. comm.). Given that the effective oxidation rate of pyrrhotite is generally 20 - 100 times greater than that of pyrite (Nicholson, 1994), it is possible that the pyrrhotite may be disproportionately involved in the oxidation occurring in borehole S61-19.

The actual mechanism of pyrite (and pyrrhotite) oxidation is important for the interpretation of the SP anomalies at the Stratmat Main Zone deposit. Much of the research on the oxidation of pyrite and pyrrhotite has been carried out at low pH, primarily driven by concerns over acid-mine drainage problems (e.g. Nicholson, 1994) and the importance of gossans in mineral exploration in arid and semi-arid environments (e.g. Andrew, 1980; Blain, 1977; Blain and Brotherton, 1975). At low pH, Fe^{3+} is sufficiently soluble that it is assumed to take a major role in the oxidation of pyrite through the reaction (Garrels and Thompson, 1960):

$$FeS_2 + 14Fe^{3+} + 8H_2O \Rightarrow 15Fe^{2+} + 2SO_4^{2-} + 16H^+ \qquad (8.1)$$

However, at pH > 4, this reaction is commonly assumed to be less important than pyrite oxidation by DO, i.e. (Smith et al., 1968):

$$FeS_2 + \tfrac{7}{2} O_{2(aq)} + H_2O \Rightarrow Fe^{2+} + 2SO_4^{2-} + 2H^+ \qquad (8.2)$$

More recently, Moses and Herman (1991) showed that even at neutral pH, Fe^{3+} could be an important mediator of pyrite oxidation provided that there is a supply of DO to the system. Therefore, regardless of which mechanism is actually involved, both reactions 8.1 and 8.2 require the presence of dissolved oxygen to drive the pyrite oxidation reactions at the pH values observed in borehole S61-19. There are two possible mechanisms to maintain DO in the groundwaters at such a depth below the water table. Either O_2 is supplied to the deeper groundwater by diffusion or by groundwater flow. Given the depth of the sulphide zone in borehole S61-19, it is unlikely that diffusion of O_2 is the primary mechanism. A more likely process to account for the sustainability of pyrite oxidation and the positive DO values recorded in the groundwaters is groundwater flow. The stable isotope data suggest that there is differential groundwater flow with depth in this hole. For example, the $\delta^{18}O_{VSMOW}$,

δD_{VSMOW}, and $\delta^{13}C_{DIC}$ values all become increasingly heavy through the ore zone (Figs. 8.6, 8.7). Although the heavier carbon isotopic values can be explained by increased dissolution of carbonate, the coupled increase in oxygen and deuterium isotope values cannot be easily explained by mineral reactions, unless very low water-rock ratios are assumed. Low water-rock ratios are incompatible with the generally good water recovery with the packer system suggesting moderate hydraulic conductivities. It is most likely that the increased $\delta^{18}O_{VSMOW}$ and δD_{VSMOW} are related to somewhat lower hydraulic conductivities at the base of the ore zone such that waters with the heavier isotopes were recharged under a warmer climate. This suggest that the waters at the base of the ore zone are somewhat older than those above and below these waters. The smooth profile in $\delta^{18}O_{VSMOW}$ with depth may indicate diffusional mixing. The heavier $\delta^{13}C_{DIC}$ are still interpreted to be due to a greater extent of carbonate dissolution as a result of longer (temporally) flow paths. Isotopic mass balance calculations would suggest that on the order of 30-40 mg/L carbonate would be required to dissolve (assuming a carbonate $\delta^{13}C$ value of 0‰) to account for the carbon isotope shift.

The low Fe and high pH is the result of precipitation of Fe(III)-oxyhydroxides or Fe(III)-oxyhydroxysulfates with the pH buffered by carbonate and silicate dissolution. Carbon isotope data also suggest that there is a contribution from carbonate dissolution (Fig. 8.6; see Chapter Eleven for full discussion of carbon isotope systematics).

Although Fe contents are elevated in the lower portion of the ore zone, there is insufficient Fe to compensate for the amount of SO_4^{2-} in the system. This implies that although the speciation calculations indicate that Fe^{2+} species are dominant, especially in the lower part of the ore zone, it is likely that a majority of the Fe released through sulphide oxidation is rapidly reprecipitated as Fe^{3+} oxyhydroxides. This is entirely consistent with the Eh-pH conditions of these waters and their position on an equilibrium Fe speciation diagram (Fig. 8.8). The implication is that the kinetics of Fe oxidation from Fe^{2+} to Fe^{3+} is somewhat more sluggish compared to the oxidation of S^- to SO_4^{2-}.

The base metal (Zn, Pb, Cu) loads in groundwaters in the sulphide zone of borehole S61-19

are lower than would be expected from the amount of dissolved sulphate present in the waters and the proportion of different sulphide minerals. There are three possible explanations; 1) dissolution of a sulphate mineral rather than sulphide minerals, 2) oxidation mainly of pyrite (and pyrrhotite) such that the base metals are under-represented, and 3) oxidation of the massive sulphides coupled with reprecipitation of the base metals as oxide phases. Sulphate minerals are only rare constituents of massive sulphide deposits in the BMC. The latter possibility seems the most likely, although if this is true, the oxides are not being transported, as the colloid contents on filter papers from these waters was minimal compared to waters from boreholes adjacent to the Restigouche deposit. In addition, previous work has shown that sulphide oxidation follows a typical order of reactivity. Recently, Jambor (1994) presented a compilation of previous studies of sulphide mineral reactivity to oxidation. Different studies have reached quite different conclusions. In general, pyrrhotite is considered very reactive. In some studies, sphalerite and galena were found to be more reactive than pyrite, whereas, other studies showed that pyrite was more reactive than base metal sulphides, especially if the pyrite was fine grained (Jambor, 1994). Boswell and Bruce (1995) noted that secondary phases were more abundant along sulphide-gangue interfaces than sulphide-sulphide interfaces. Thus, the lower than expected base metal contents of borehole S61-19 groundwaters may be a combination of preferential dissolution of Fe-sulphides and loss of metals through adsorption and/or coprecipitation with Fe-oxyhydroxide phases.

The increase in Zn, Cd, and Fe contents just above the ore zone is interpreted to be due to upward hydraulic gradients and/or upward diffusion. Thus, if $Fe(OH)_{3(aq)}$ is transported upwards to a region of higher Eh and pH, the net result will be dissolution of the amorphous iron and release of adsorbed metals, consistent with the observed geochemical profiles (Fig. 8.4).

8.3.3 Generation of SP anomalies

Most models to explain development of large SP anomalies associated with massive

sulphide deposits indicate that chemical reactions are a fundamental component (Govett et al., 1976; Kilty, 1984). Although some models suggested that the massive sulphides were intimately involved in the chemical reactions, Sato and Mooney (1960) showed that the massive sulphides primarily act as a conductor for the flow of electrons. The higher SO_4^{2-} values and the strong correlation between Fe species and Eh of borehole S61-19 groundwaters suggests that for the Stratmat Main Zone deposit, the massive sulphides are intimately involved in the production of the SP anomalies. Kilty (1984) suggested that the oxidizing reactions take place in the lower part of the orebody and reduction reactions in the upper part of the orebody. The increase in sulphate contents with depth in the ore zone is certainly consistent with most of the sulphide oxidation taking place at the base of the massive sulphides.

Blain (1975) also suggested that the sulphides were involved in the development of self-potentials associated with gossans. Many previous models of the development of self-potential anomalies have focussed on gossans developed above massive sulphide deposits, primarily in South Africa and Australia (e.g. Andrew, 1980; Blain, 1977; Blain and Brotherton, 1975; Thornber, 1975). However, in this case, the situation is different. Although the Stratmat Main Zone deposit comes to surface, the large chemical and Eh gradients through the ore zone coupled with the large SP anomaly suggest the electrochemical "cell" is more local in origin. Thus, the self-potential anomaly in borehole S61-19 occurs in a borehole where the ore zone and the self-potential "cell" is interpreted to occur well below the water table. In addition, there is a similar variation through the ore zone in groundwater Eh values as has been recorded for gossan deposits where the more oxidized portion of the ore body lies above the water table. In gossans, the reduction part of the redox pair is interpreted to be the reduction of atmospheric oxygen. This may still be occurring towards the top of the ore zone in borehole S61-19; note that the DO values decrease in this region and increase towards the bottom of the ore zone (Fig. 8.4). For example, Blain and co-workers (Andrew, 1980; Blain and Brotherton, 1975) suggested that the cathodic reactions involved reduction of O_2 in the following manner:

$$O_2 + 2H_2O + 4e^- \Rightarrow 4OH^- \qquad (8.3)$$

The production of hydroxide would be counteracted somewhat by the oxidation of ferrous to ferric iron and the precipitation of goethite in the reaction (Andrew, 1980; Blain and Brotherton, 1975):

$$Fe^{2+} \Rightarrow e^- + Fe^{3+} \qquad (8.4)$$

and

$$Fe^{3+} + 3OH^- \Rightarrow FeOOH + H_2O \qquad (8.5)$$

Initially, it is more likely that amorphous ferric oxides would be stable, such as ferrihydrite ($Fe(OH)_3$). The reduction of O_2 is base-producing (or acid-consuming) and may explain the higher pH at the top of the sulphide zone compared to the rest of the sulphide zone (Fig. 8.4). For this reaction to be maintained, there must be a constant supply of $O_{2(aq)}$ to the top of the ore zone

The interpretation of the SP anomalies and groundwater geochemistry in borehole S61-19 is as follows (Fig. 8.9). Sulphide minerals are oxidized primarily at the base of the massive sulphides, releasing Fe^{II} and S^- to solution. The S^- is in turn oxidized to sulphate. The massive sulphides, in addition to undergoing oxidation, act as a conductor for the flow of electrons towards the cathode at the top of the massive sulphides. Cations move upward due to the induced self-potential, towards the cathode, whereas anions flow towards the anode. As Fe^{II} moves upwards through the massive sulphides (along fractures or secondary porosity) it is oxidized to Fe^{III} which is rapidly removed from solution as amorphous Fe-oxides (e.g. $Fe(OH)_3$; Fig. 8.5). Base metals released due to sphalerite, galena and chalcopyrite oxidation have lower contents in the upper part of the ore zone due to upward flow, to adsorption and/or co-precipitation with the Fe^{III}-oxides, perhaps combined with lower rates of sulphide weathering in the upper part of the ore zone. This model is consistent with previous models suggested for the Joma deposit (Bölviken and Logn, 1974) but differs in the fact that the massive sulphides are interpreted to be intimately involved in the redox reactions and the production of the SP anomaly. At the Eh-pH conditions in the lower part of the ore body, SO_4^{2-} is the prevalent anion species and Fe^{2+} is the prevalent Fe species. Ferrous Fe is soluble

and this accounts for the elevated Fe contents of the samples collected from the base of the ore zone (Fig. 8.4).

It is possible that massive sulphides are being oxidized throughout the ore zone, however, the increase in SO_4^{2-} throughout the ore zone to a maximum at the base of the ore zone, indicates that the bulk of the oxidation is taking place at the base of the sulphide zone.

As noted, the stable isotope and packer response data suggest that there is differential flow through the ore zone such that groundwaters at the bottom of the ore zone are probably older waters with longer water-rock reaction times. This is consistent with the increase in major cations (Ca, Na, Mg) through the ore zone indicative of longer periods of carbonate and silicate dissolution. However, pyrite, and to a lesser extent pyrrhotite, oxidation is acid generating (reactions 8.1 and 8.2). Although there is a drop in pH in the ore zone, pH values are still high. This indicates that enhanced carbonate and silicate dissolution is buffering the pH of these groundwaters.

Hovdan and Bølviken (1985) suggested that large negative self potential anomalies recorded by down-hole geophysical measurements were an artifact of differences in the redox state of sulphide porewaters compared to that of the borehole fluid. These workers further suggested that large self potential anomalies adjacent to ore zones would decrease in magnitude with increasing time following cessation of drilling. In borehole 528 from the Tverrfjellet Mine in Norway, Hovdan and Bølviken (1985) showed that negative self potential anomalies adjacent to sulphide lenses disappeared two months after drilling of the borehole. This is an unlikely mechanism to explain the large self potential anomaly in borehole S61-19 at the Stratmat Main Zone deposit. The most obvious objection to the Hovdan and Bølviken (1985) hypothesis is that borehole S61-19 was drilled in 1956, and the SP anomalies were recorded in both 1988 and 1989. Thirty years is sufficient time to remove any vestigial effects of drilling. Additionally, as shown above, the geochemistry of borehole waters, as collected by straddle packer sampling, are entirely consistent with the production of the SP anomaly by coupled sulphide oxidation and Fe reduction in the upper and lower parts of the sulphide body,

respectively.

8.4 Summary

1) Downhole geophysical profiles of borehole S61-19 from the Stratmat Main Zone deposit show large negative self potential anomalies and subtle positive thermal anomalies through the main massive sulphide ore zone. The thermal anomalies are interpreted to be due to greater groundwater flow through the ore zone compared to nearby boreholes.

2) Groundwaters sampled systematically downhole and through the ore zone increase rapidly in TDS in the ore zone and decrease below the ore zone. The dominant anion is SO_4^{2-}, indicating that the primary control over groundwater chemistry is sulphide oxidation.

3) Geochemical profiles of Fe and base metals through the ore zone are consistent with sulphide oxidation, predominantly at the base of the ore zone, with increasing oxidation of Fe^{2+} to Fe^{3+} and precipitation of Fe-oxyhydroxides towards the top of the ore zone. Base metals also decrease toward the top of the ore zone due to diffusion and adsorption onto Fe-oxyhydroxides.

4) The self potential anomaly associated with the ore zone is interpreted to reflect the development of an electrochemical cell driven by oxidation of massive sulphides at the bottom of the ore zone and reduction of dissolved oxygen at the top of the ore zone.

5) Stable isotope and packer response data indicate that there is differential groundwater flow through the ore zone, with groundwaters close to the bottom of the ore zone having been recharged under a slightly warmer climatic regime, consistent with the observation if differential groundwater flow through the ore zone. Carbon isotopes indicate that neutral pH values are maintained due to dissolution of carbonate.

Table 8.1 Geochemical results for Stratmat Main Zone deposit borehole S61-19

Sample#	MLW96-676	MLW96-689	MLW96-690	MLW96-691	MLW96-693	MLW96-694	MLW96-695	MLW96-697	MLW96-702	MLW96-706
Depth (m)	26	41	83.5	85	86	87	88	89	92	103
Water type	$CaHCO_3$	$CaNaHCO_3$	$CaSO_4HCO_3$	$CaSO_4HCO_3$	$CaHCO_3SO_4$	$CaNaSO_4$	$CaSO_4$	$CaSO_4$	$CaNaSO_4$	$CaNaSO_4$
DO (mg/L)	3.77	3.18	3.29	3.28	2.74	2.75	3.03	2.86	3.11	3.43
pH (field)	7.99	8.5	7.42	8.05	7.83	7.66	7.63	7.75	8.07	8.02
Eh (mV)	132	2	63	58	89	-72	-81	-85	29	-30
Cond. (μS/cm)	146	164	257	312	277	588	1356	1757	1022	661
pH (lab)	7.66	7.79	7.53	7.68	7.72	7.87	8.05	7.9	8.02	8.02
mg/L										
TDS	118.95	128.99	189.12	214.47	190.75	438.14	1166.39	1603.65	890.85	564.20
HCO_3	76.16	80.11	73.94	76.13	77.86	90.19	115.74	78.89	97.50	99.38
SO_4	8.00	8.23	58.30	73.20	56.00	212.00	703.00	1032.00	519.00	294.00
Cl	1.36	1.09	1.00	0.96	0.97	1.29	1.44	0.10	0.40	0.72
μg/L										
F	191	297	105	174	126	653				526
PO_4	4.38	5.77	1.05	1.41		8.93	9.32	31.62	14.15	13.48
Br	5.35	5.54	5.10	4.76		7.79	9.69	6.30	4.69	5.19
Si	3827	5491	4319	4513	4272	6056	6994	6993	6329	6325
Al	14	5	2	2	2	2	3	2	2	3
Fe	36	9	47	44	1.5	975	2323	1374	62	288
Mn	28	12	48	45	28	97	245	1155	170	170
Mg	3029	1740	3535	3718	3564	2855	10613	39005	13520	9030
Ca	17002	11867	34478	39654	32512	75922	248895	298526	145570	90719
Na	9070	19978	12745	15451	14760	48790	78533	146841	107730	63384
K	495	489	802	846	813	1035	1174	1301	797	638
As						285				
B	34					17	34	48	37	28
Ba	9.3	3.1	33	34	29	40	39	22	7.5	10
Cd			0.8				0.8			
Co	0.3		0.8	0.4	1.5	0.5	1.3	0.9	0.9	1.1
Cr	0.5	0.2								
Cs							0.2			
Cu	0.6			1			0.9	1.3	0.7	0.6
Mo	3	1.5	1.1	1.2	1.5	1.7	3	2.9	2.6	2.2
Ni	11	2	3	2	2	4	13	12	6	4
Pb			0.4	0.7	0.3					
Rb	0.8	1	1.6	1.7	1.8	2.6	2.8	2.9	2	1.6
Sb	1.8	0.4	76	150	94	360	61	6	3.9	4.1
Se	2									
Sr	149	151	164	181	159	292	463	664	386	272
Tl			0.5	0.7	0.2	0.2	0.2			0.2
U			0.2	0.3	0.2	2.1	5.1			
V	0.2		0.2		0.2					
Zn	12	2	514	218	110	306	436	30	13	26
*										
Al	13	5	2	2	2	3	2	2	3	3
V	0.20	0.12	0.21	0.17	0.29	0.03	0.03	0.01	0.08	0.07
Mn	23.3	10.6	38.4	36.7	23.5	73.9	139.2	445.5	129.4	131.4
Fe	35	8	44	40	5	905	2236	1236	68	285
Co	0.306	0.049	0.664	0.340	1.441	0.379	0.986	0.433	0.843	0.944
Ni	10.1	1.2	1.4	0.6	1.0	1.0	4.5	1.6	0.6	0.7
Cu	0.50	0.18	0.13	0.81	0.07	0.05	0.14	0.06	0.05	0.05
Zn	13.4	2.5	388.8	161.8	104.8	238.6	352.0	42.3	18.4	31.8
Y	0.003	0.002	0.006	0.007	0.007	0.010	0.140	0.022	0.012	0.012
Cd	0.280	0.076	0.831	0.358	0.461	0.403	1.042	0.040	0.036	0.070
Pb	0.149	1.479	0.998	0.946	0.340	0.129	4.323	5.456	0.119	0.428
U	0.100	0.030	0.154	0.247	0.194	1.798	4.349	0.059	0.037	0.065

* Chelation ICP-MS data

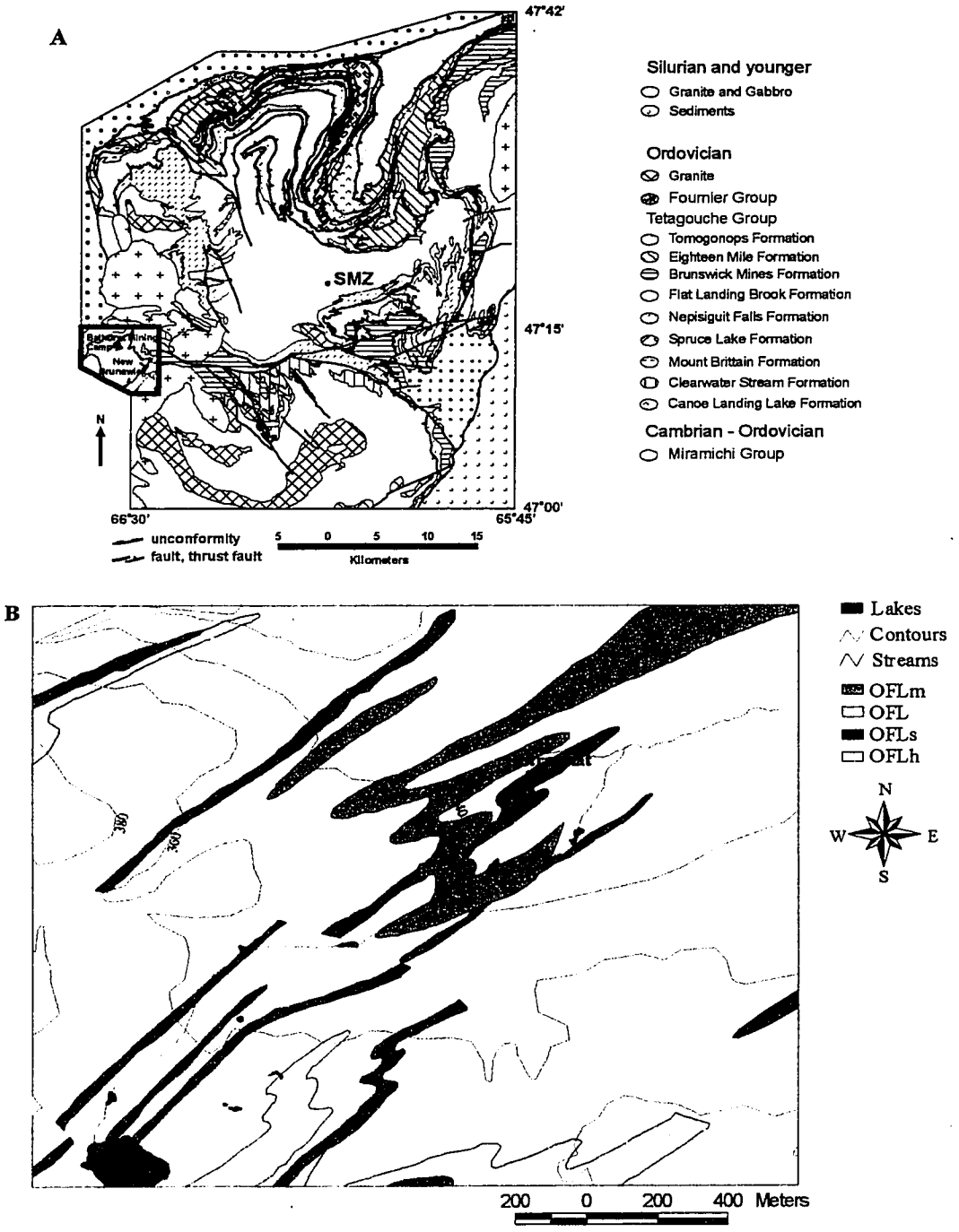


Fig. 8.1 A) Location of the Stratmat Main Zone deposit (SMZ). B) Geology of the Stratmat Main Zone deposit after Wilson (1993). Contour intreval is 20 m.

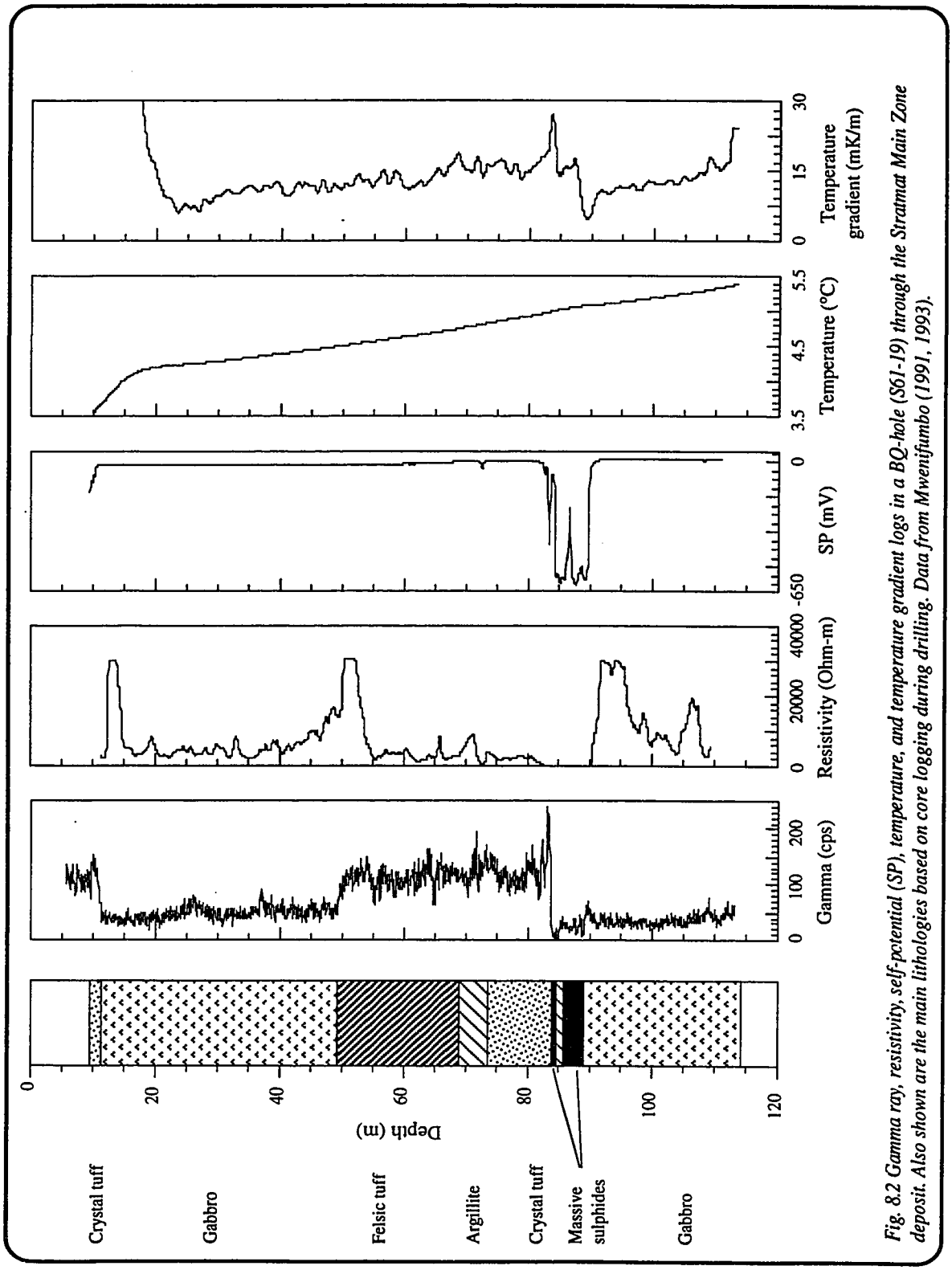


Fig. 8.2 Gamma ray, resistivity, self-potential (SP), temperature, and temperature gradient logs in a BQ-hole (S61-19) through the Stratmat Main Zone deposit. Also shown are the main lithologies based on core logging during drilling. Data from Mwenifumbo (1991, 1993).

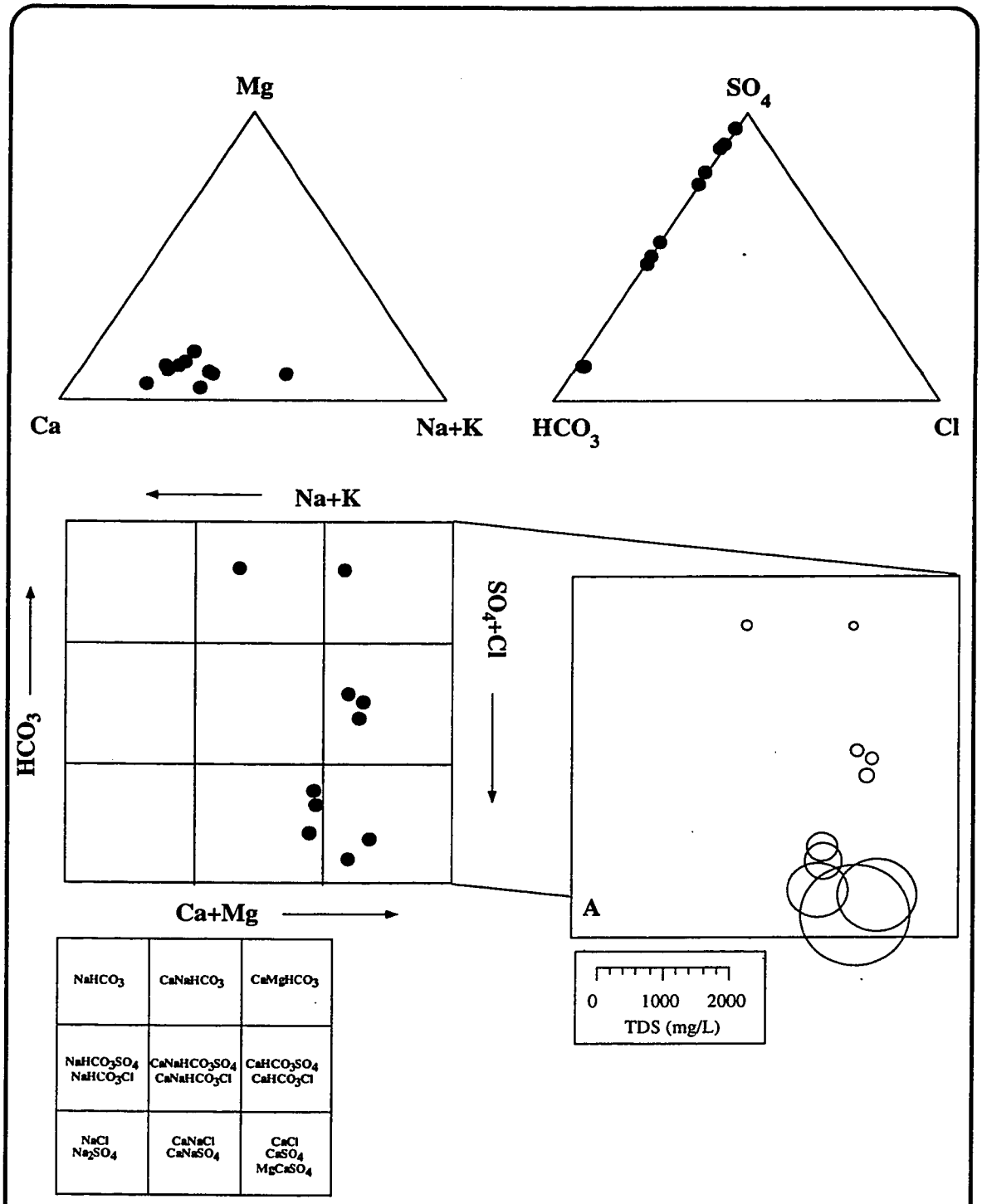


Fig. 8.3 Modified Piper plot for groundwaters from the Stratmat Main Zone deposit. The inset (A) shows the groundwaters proportional to total dissolved solids.

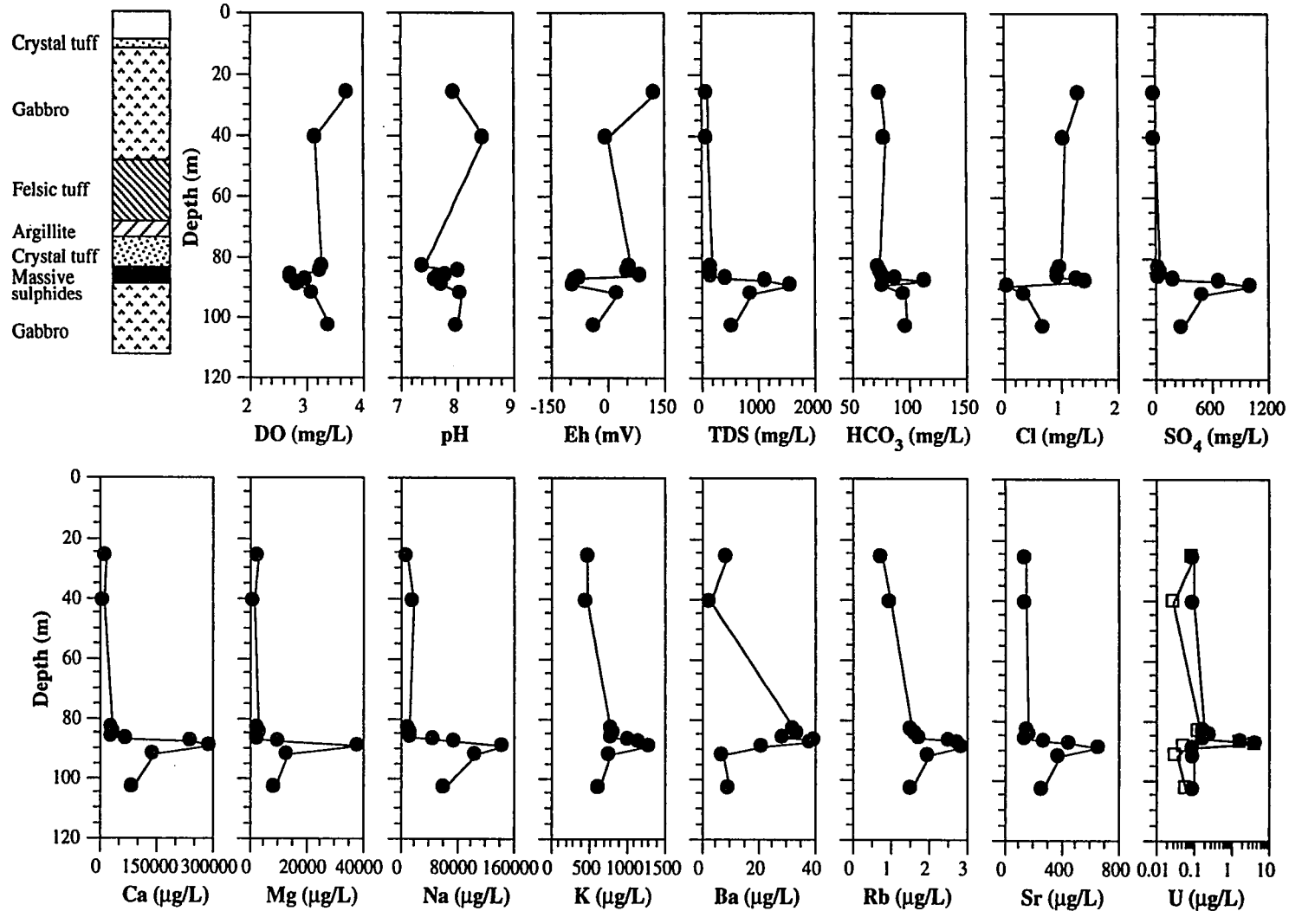


Fig. 8.4 Downhole variation profiles of field parameters, anions and cations for borehole S61-19 from the Stratmat Main Zone deposit. Open squares represent chelation ICP-MS data. Data from Table 8.1.

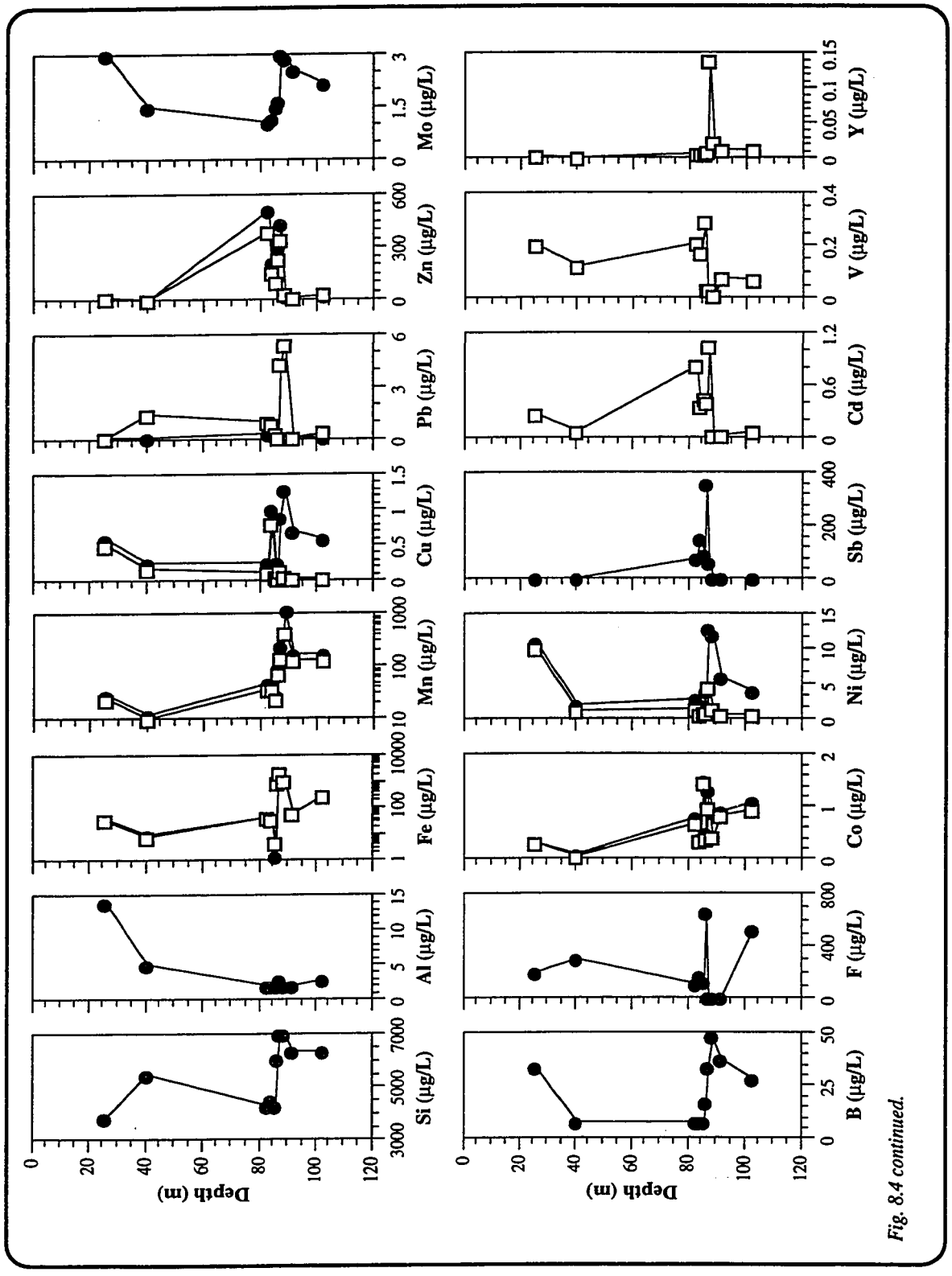


Fig. 8.4 continued.

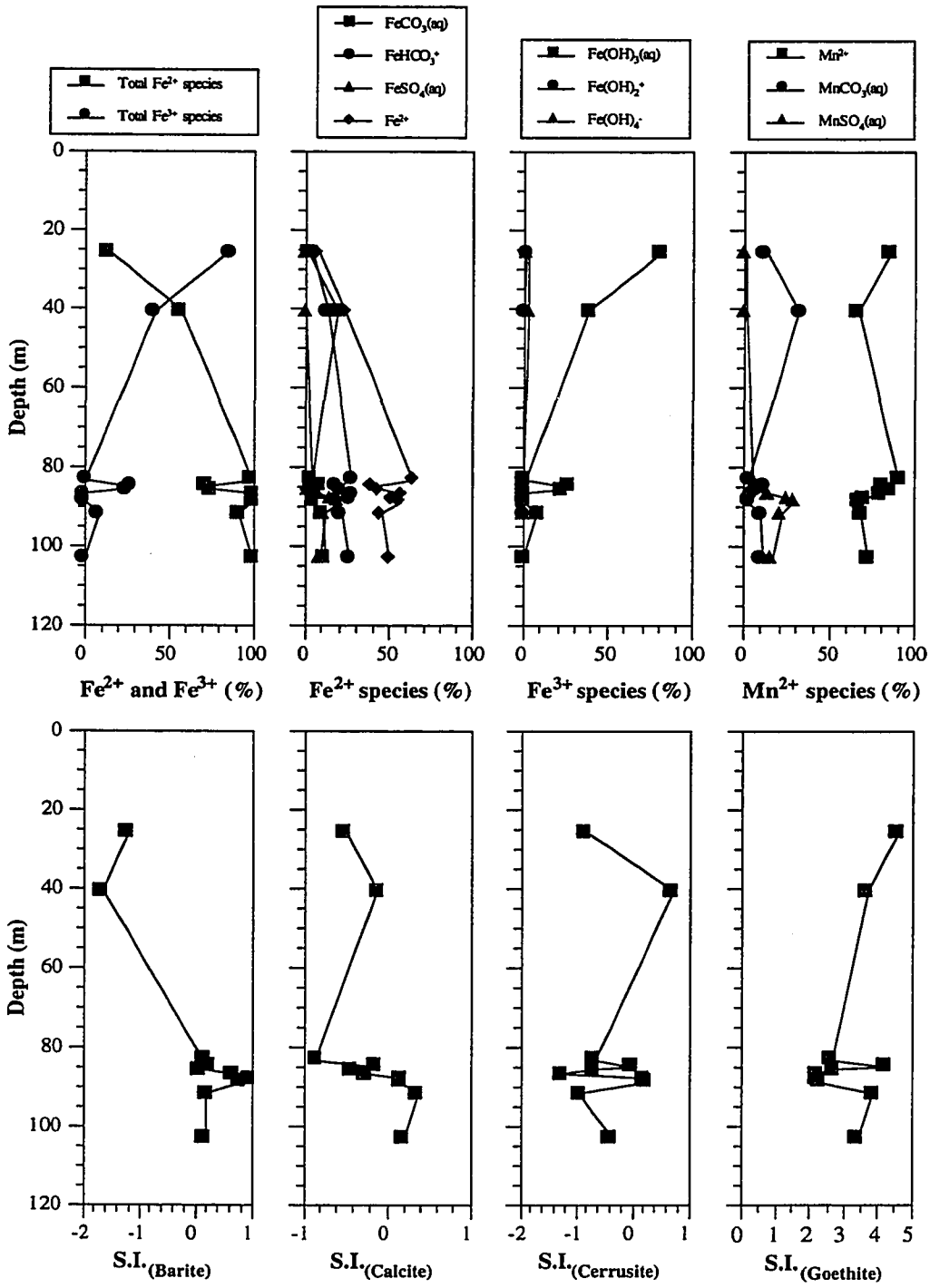


Fig. 8.5 Selected speciation and mineral saturation indices (SI) for groundwaters from borehole S61-19, Stratmat Main Zone. Speciation plotted as percentage of total element content.

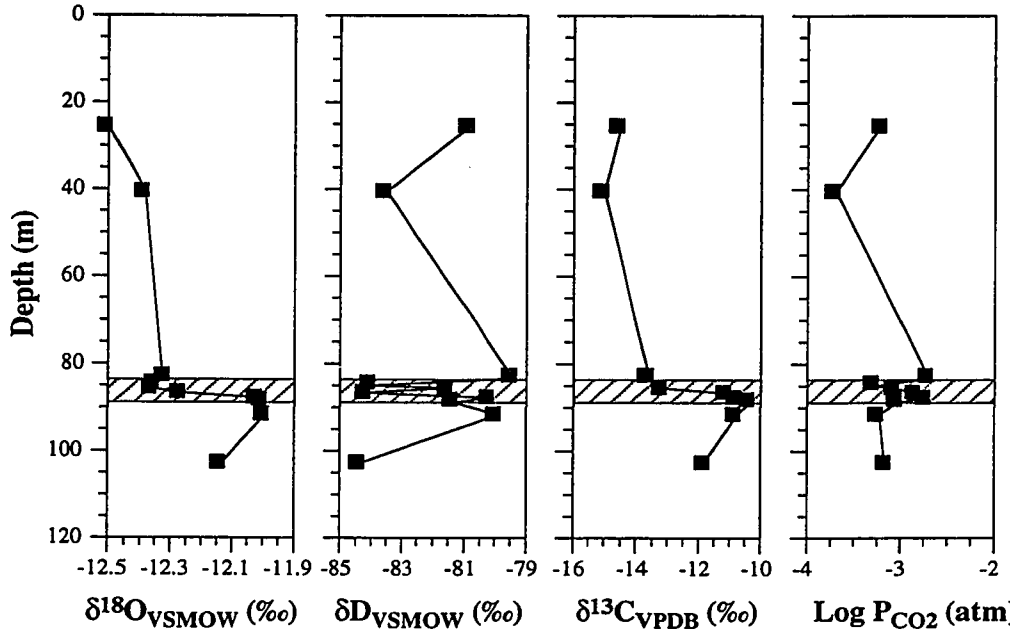


Fig. 8.6 Stable isotopic composition of the Stratmat Main Zone deposit borehole S61-19 waters, plotted versus depth. Also shown is the location of the massive sulphide zone. P_{CO_2} calculated with speciation code EQ3NR (Wolery 1992). Stable isotope data from Tables 11.4, 11.5.

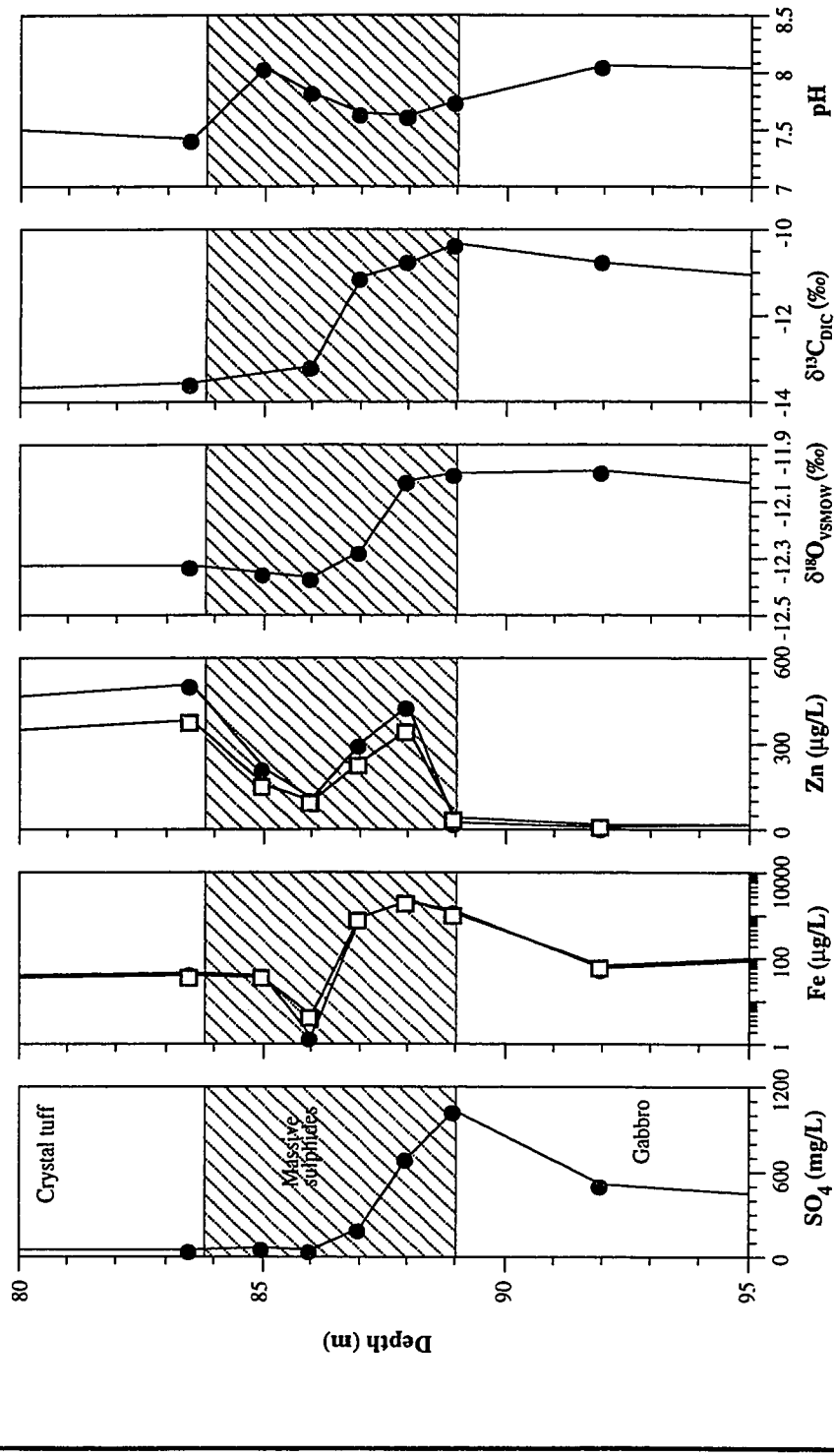


Fig. 8.7 Downhole variation profiles of selected variables for borehole S61-19 from the Stratmat Main Zone deposit, expanded to show the variation through the ore zone. Open squares represent chelation ICP-MS data. Data from Table 8.1.

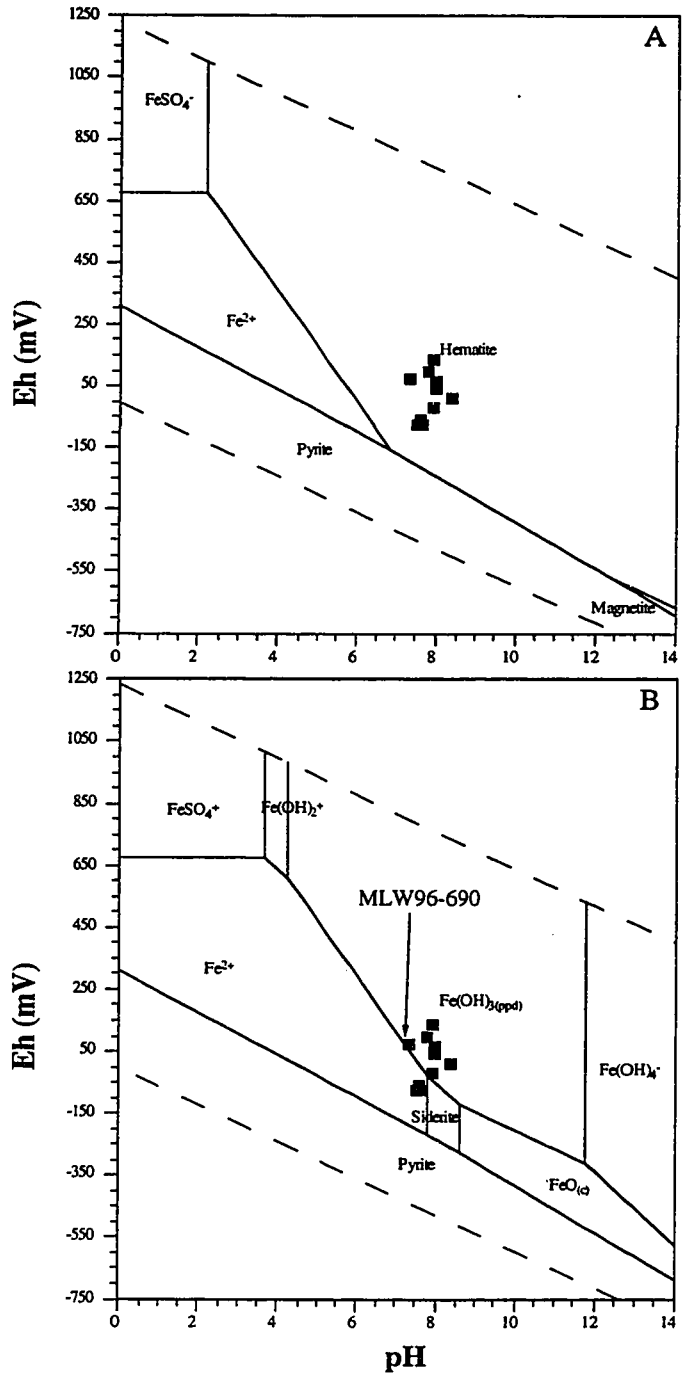


Fig. 8.8 Diagram showing the stability of metastable Fe hydroxides. The fields were calculated by the Geochemist's Workbench computer program (Bethke, 1994). Conditions are similar to sample MLW96-697 from borehole S61-19. Conditions were: $[HCO_3] = 10^{-3}$, $[SO_4] = 10^{-2.5}$, $[Fe] = 10^{-5}$. In (B) the formation of hematite, goethite and magnetite were suppressed, reflecting the slow kinetics of formation of these phases at these groundwater conditions.

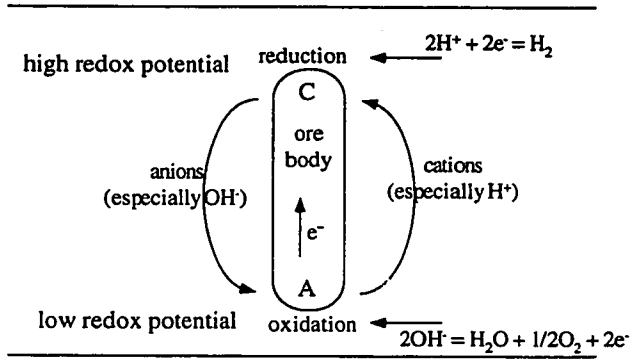


Fig. 8.9A Modification of the generalized model of SP anomalies about massive sulphide ore bodies. A represents the anode and C the cathode. Modified from Bölviken and Logn (1974).

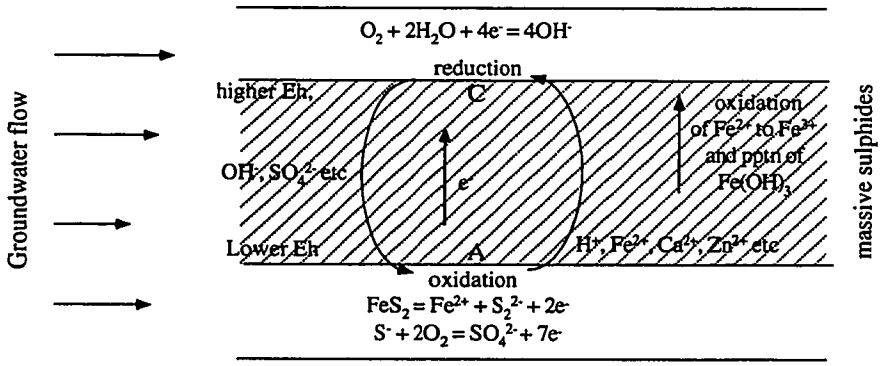


Fig. 8.9B Schematic model of oxidation of massive sulphides at the Stratmat Main Zone deposit and development of the observed SP anomaly. Zn, Pb, Cu released due to base metal sulphide oxidation are adsorbed to Fe-oxyhydroxides as Fe^{II} is oxidized to Fe^{III}. A represents the anode and C the cathode. Shown are the dominant redox reactions that are likely to be occurring. Sulphide mineral oxidation is represented by pyrite, but pyrrhotite, sphalerite, galena etc oxidation may also be taking place. Differential groundwater flow is schematically represented by the arrows on the left of the diagram, based on the packer sampling results.

CHAPTER NINE:
BULK SUSPENDED SEDIMENT MINERALOGY AND CHEMISTRY, HALFMILE LAKE AND RESTIGOUCHE DEPOSITS, BATHURST MINING CAMP, NEW BRUNSWICK

9.1 Introduction

Suspended sediments from groundwater samples were analyzed in order to compare the chemistry of suspended matter with "dissolved" (i.e. < 0.45 μm) matter. Of the groundwaters sampled, a subset of 31 samples was selected on the basis of spatial and downhole distribution, and on the basis of sufficient sediment on the filter paper to be extracted for ICP-MS and ICP-ES analysis.

The processes of adsorption onto clay and oxide surfaces have been the focus of intense research over the last few decades because of the importance of these processes to understanding such effects as sewage sludge disposal, leaching of solutes from landfills, pesticide and fertilizer applications to soils and runoff to water systems, mine tailings and acid mine drainage, and soil and groundwater quality in general (Anderson and Christensen, 1988; Lasaga, 1990). At a more fundamental level, mineral surface-aqueous fluid interactions greatly influence or control most water-rock processes including the movement of solutes through rock, soil and groundwater systems, weathering reactions and diagenesis, and redox reactions such as sulfide precipitation (Eggleston and Stumm, 1993). The fate of trace metals (i.e., As, Sb, Se, Cr, Co, Ni, Cd, Cu, Zn, Pb) in the natural aquatic environment depends critically on adsorption-desorption reactions at particle surfaces (Muller and Sigg, 1992).

The colloidal and suspended fraction of ground and surface waters have received increased attention in recent years as it has been recognized that suspended matter may be important in contaminant and radionuclide transport (Swartz et al., 1997). It has also been increasingly recognized that suspended sediments and colloids complicate the simplistic view that metal distribution can be described in terms of water-rock partitioning (Miekeley et al., 1992a).

Surface reactions between metals in solution with suspended material and between suspended material and the aquifer are fundamental in regulating trace metal transport. In addition, recent studies have shown that there is a strong relationship for some trace metals between metal adsorption onto fine colloids and colloid coagulation onto larger particles (Wen et al., 1997).

Particles and colloids have the potential to concentrate pollutants by sorption. In some cases, such sorption can lead to greater stability and potentially enhance metal mobility if the particles are sufficiently small to migrate through fractured or porous rock (Miekeley et al., 1992a). In the case of groundwaters intimately associated with massive sulphide deposits in the Bathurst Mining Camp (BMC), it is important to assess the possibility of enhanced mobility of certain elements associated with sulphide mineralization that are not normally very mobile in aqueous systems (e.g., Pb). This study is concerned with the complexation and transport of the products of sulphide oxidation. This kind of information has important implications for both exploration and environmental geochemistry of waters associated with massive sulphide deposits and their tailings in the BMC.

The suspended sediments discussed in this chapter represent the residue collected on 0.45 μm filter papers during groundwater sampling. Suspended sediment samples are identified as MLF with the corresponding water sample labelled MLW (Chapter Seven). Most of the samples described here represent groundwaters collected using the flow-through bailer. Bailer waters typically had a greater amount of suspended material compared to packer samples. The packer apparatus included an in-line 45 μm filter to prevent clogging of the cracking valve in the sample head (Chapter Three). In addition, suspended sediment on filters collected during packer sampling tended to decrease with time during development of a zone. Although many recent studies have focussed on the suspended sediment contents of surface waters, streams at the Halfmile Lake and Restigouche deposits typically have insufficiently low suspended sediment loads for routine sampling. Sampling and analytical methods are presented in Chapter Three. The geochemistry of the corresponding groundwaters is discussed in Chapter Seven for Halfmile Lake and Restigouche deposit groundwaters and Chapter Eight for groundwaters

from the Stratmat Main Zone deposit.

9.2 Mineralogy of Groundwater Suspended Sediments

Suspended sediments were analyzed by SEM and XRD (Table 9.1). Filter papers containing suspended sediment analyzed by SEM were mounted directly and carbon coated. Due to insufficient sample size, XRD analyses were performed by grinding the sediment in a mortar and pestle followed by mounting an a zero background silicon disc as a slurry of sediment and acetone. As a result, counts are generally quite low (e.g., Fig. 9.1).

Suspended sediment from the Halfmile Lake deposit is dominated by quartz and aluminosilicate minerals (Table 9.1; Figs. 9.1, 9.2). XRD analyses suggest that quartz is the dominant silicate, although SEM data indicates that K-silicates (illite and sericite) are also common. Chamosite is a common phase in some samples, and kaolinite is also present, although typically in lesser abundance. Accessory phases include albite, pyrite, and Fe-oxides (Table 9.1). Oxides of Fe and Al were only rarely positively identified, but most phases analyzed by SEM indicate an Fe peak, consistent with surface coatings of Fe-oxides on other mineral phases. Standard SEM is poor at resolving Fe- and Al-oxides where they have thicknesses < 5 μm (Coston et al., 1995). The sample from borehole HT55-43 is curious. XRD results suggest that there may be only minor lepidocrocite present (Fig. 9.1). Samples from this borehole were noted to be very Fe-oxide rich during sampling. It may be that the oxides are dominantly amorphous and so were not detected by XRD. Suspended sediments from all Halfmile Lake deposit samples are dominantly < 10 μm in size (Fig. 9.2).

Suspended sediments from Restigouche deposit groundwaters are also dominated by quartz and aluminosilicates (mainly illite-sericite, chamosite and lesser kaolinite; Table 9.1). However, there is greater variety than was the case for the Halfmile Lake deposit. Suspended sediments from boreholes MM-88-06 and MM-88-07 are dominated by Fe, Pb, and Zn sulphides and/or sulphates. XRD data for one sample from each of these boreholes suggest that pyrite is the dominant sulphur phase (Fig. 9.3). However, SEM data shows strong Fe, Pb,

and variable Zn peaks coupled with strong S peaks and variable, though generally smaller, O peaks. This would suggest that at least some of the metals are present as sulphates and perhaps oxides. XRD analysis of sample MLF95-317 yielded peaks which are consistent with anglesite ($PbSO_4$). However, speciation calculations on groundwaters from boreholes MM-88-06 and MM-88-07 indicate that all the waters are below saturation for metal-sulphate minerals in their databases (EQ3NR and PHREEQC), although anglesite comes closest to saturation with $SI_{anglesite}$ as high as -0.833 in sample MLW95-315 (EQ3NR calculation; Chapter Seven). The SEM images of these metal-sulphur species have a more porous, semi-amorphous appearance than is typical of metal sulphides (Fig. 9.4A, B).

Suspended sediments from borehole MM-88-01 are dominated by illite/sericite, according to SEM and XRD data (Table 9.1; Figs. 9.3, 9.4). However, the chemistry of these waters indicate that Al-oxide and/or kaolinite should be abundant. The fact that only small kaolinite peaks were observed by XRD suggests that Al-oxides are common phases in these sediments. As with boreholes MM-88-06 and MM-88-07, suspended sediments from borehole MM-88-01 have metal-sulphur species (Fe, Zn) which may be present as sulphides, sulphate, or both (Fig. 9.4).

Samples from the saline waters in MM-88-02 contain primarily K-silicates and quartz with minor barite (Fig. 9.5). The presence of barite is an interesting observation because the waters contain less than detectable SO_4, and attempts to recover sulphate by precipitation in the field were unsuccessful. Therefore, either the analyses are incorrect, the barite represents disaggregation of wall-rock barite, or very minor amounts of S (below the detection limit of 50 µg/L) in the groundwaters is sufficient to stabilize barite due to the very elevated Ba contents of these waters (≈ 90 mg/L). Halite is another common phase present in SEM and XRD data for suspended sediment from borehole MM-88-02. Although these waters are Na-Cl-type waters, halite is well below saturation. The most likely explanation is that the halite is secondary, due to evaporation on the surface of the filter papers.

Suspended sediments from the boreholes more distal to the Restigouche deposit are

dominated by silicates, consistent with low metal and generally low sulphate contents of the groundwaters. Quartz, sericite, chamosite, and kaolinite with accessory albite and K-feldspar are the dominant phases (Figs. 9.6, 9.7). Sample MLF95-504 from borehole MM-89-106 also has accessory REE phosphate minerals (Fig. 9.6) and NaCl. The latter is most likely due to post-sampling evaporation of this brackish NaCl-type groundwater.

Two samples were analyzed by SEM from borehole S61-19 at the Stratmat Main Zone deposit (Table 9.1). Sample MLF96-695 is from close to the bottom of the massive sulphide zone (see Chapter Eight), whereas sample MLF96-702 is from below the massive sulphides. Chamosite, illite/sericite and quartz occur in both sediments, but sample MLF95-695 is apparently dominated by Fe-sulphate minerals occurring as amorphous mats on the filter paper. The groundwaters from the massive sulphide zone of borehole S61-19 are undersaturated with respect to Fe-sulphates (e.g., melanterite, $FeSO_4 \cdot 7H_2O$). As with the halite in the borehole MM-88-02 suspended sediments, these Fe-sulphate minerals may have formed by evaporation after sampling.

9.3 Geochemistry of Groundwater Suspended Sediments

Thirty-one samples were analyzed for trace and major elements by ICP-MS and ICP-ES (see Chapter Three; Table 9.2). Due to insufficient sample sizes, SiO_2, LOI, P_2O_5, and total S were not determined. The variation in suspended sediment mineralogy is reflected in the chemical composition. A potential source of error is that there is likely, at least for the more saline waters, to have been salt formation due to drying, i.e., high Na in MM-88-02 filter indicates formation of NaCl, consistent with the SEM and XRD data. A single major phase, NaCl, was detected in sample MLF95-605. To evaluate detrital versus hydromorphic components, suspended sediments are compared to least altered felsic rocks from the Halfmile Lake and Restigouche deposits (see Chapter Two, Table 2.2).

9.3.1 Halfmile Lake deposit

Eleven groundwaters from three boreholes had sufficient suspended sediment for geochemical analysis (Table 9.2). Two of the boreholes (HN92-40) and (HN94-65) penetrate the Halfmile South Lower AB massive sulphide deposit whereas borehole HT55-43 was drilled at the top of the Upper AB in the vicinity of the gossan outcrop (see Chapter Seven for borehole locations, Fig. 7.1).

The geochemistry of the suspended sediments from borehole HT55-43 broadly reflects what is expected from gossanized massive sulphides. Total Fe contents are elevated (39.3 to 64.0 weight % as Fe_2O_3). Base metal contents (Zn, Pb, Cd) are generally low compared to the suspended sediments from the other two boreholes, although the HT55-43 sediments have higher Cu contents (690 - 1400 ppm versus a maximum of 490 ppm from the other Halfmile Lake deposit samples). Borehole HT55-43 sediments have generally higher Mn than sediments from borehole HN94-65, consistent with high Fe and suggesting the presence of Mn-oxides. Although XRD data indicate that the main phases in these sediments are quartz and alumino-silicates, Fe-oxides predominate visually. Compared to average unaltered Halfmile Lake felsic lithologies, borehole HT55-43 sediments show depletion in the large ion lithophile elements (LILE) such as Cs, Rb, U and in many of the high field strength elements such as the LREE and to an even greater extent Nb, Hf, and Zr (Fig. 9.8). Conversely, these sediments are highly enriched in Fe, Pb, Co, Zn, Ag, and Eu relative to the host lithologies (Fig. 9.8). Figure 9.9 shows the groundwater normalized to the corresponding suspended sediment. Note that the water samples have been multiplied by 1000 times (major and trace elements in waters are typically at the ppm and ppb level versus weight % and ppm levels for the sediments). Thus, the 1:1 line in Figure 9.9 actually represents 1:1000. There is a variation of about six orders of magnitude in the differences between suspended sediment and the corresponding water. For borehole HT55-43, elements which are relatively fractionated into the solid phase include Al, Fe, Pb, and Cu. Zinc, Mn and K are also fractionated into the solid phase but less strongly. Relative to these metals, Mg, Na, and especially Ca are fractionated into the groundwater. Cadmium exhibits greater affinity for the aqueous phase than Zn (Fig. 9.9).

Borehole HN94-65 suspended sediments are characterized by lower Fe contents, and higher Al, K, and Na than those from borehole HT55-43 (Table 9.2). The higher alkali metals and Al is consistent with significant quantities of silicate minerals identified by XRD and SEM (Table 9.1; Figs. 9.1, 9.2). Zinc and Pb contents are high in these sediments. Indeed, the Zn and Pb contents are considerably higher than any of the stream sediments from the Halfmile Lake deposit (Table 6.1) and the Pb contents are similar to Pb contents of stream sediments immediately downstream from the Restigouche deposit. Zinc contents of the borehole HN94-65 sediments are 2-3 times higher than Zn contents of stream sediments immediately downstream from the Restigouche deposit (Table 6.2). Compared to the host felsic lithologies, borehole HN94-65 suspended sediments have very flat patterns overall, indicating little fractionation (Fig. 9.8). All the suspended sediments have very uniform patterns indicating little difference between samples. However, the suspended sediments are depleted in Cs, Rb, K, and Ba compared to the host rocks and enriched in Eu, Fe, Pb, Co, Zn, and Ag (Fig. 9.8). Zinc and Pb contents are around 100 times host rock values. Compared to the coexisting groundwaters, these sediments show similar relationships as borehole HT55-43 suspended sediments (Fig. 9.9). However, samples from borehole HN94-65 show less fractionation between the groundwater and the suspended sediment in Mn, Ca, Na, K, and Ba, but generally greater fractionation for Pb and Zn.

One suspended sediment sample was analyzed from borehole HN92-40. In many respects this sample is similar to those from borehole HN94-65 in that the Al, K, and Na contents are elevated compared to borehole HT55-43 sediments, and the Fe content is lower. This sediment sample has moderately high Zn and Pb contents, although lower than borehole HN94-65 suspended sediments (Table 9.2). Compared to the host rocks, this sample is generally unfractionated with the exception of elevated Cs, Ca, Sc, Pb, Co, Cr, Zn, and Ag (Fig. 9.8). Compared to the corresponding groundwater, sample MLF96-696 shows greater relative affinity for Al, Fe, Pb and relatively low affinity for Ca, Sr, and Zn (Fig. 9.9).

For suspended sediments at the Halfmile Lake deposit, there is a relationship between

Zn/Pb ratios and proximity to massive sulphides. Although base metal contents are variable with depth in boreholes HT55-43 and HN94-65 (Table 9.2), the Zn/Pb ratios decrease towards the depth at which massive sulphides occur. The lowermost samples from both boreholes have Zn/Pb < 1. Similar relationships exist for proximity to the Restigouche deposit (see below).

9.3.2 Restigouche deposit

Twenty suspended sediments from six boreholes at the Restigouche deposit had sufficient material for geochemical analyses (see Chapter Seven for borehole locations, Fig. 7.13). Four of the boreholes intersect the massive sulphides at the Restigouche deposit. Boreholes MM-88-06 and MM-88-07 are shallow holes that intersect sulphides close to the surface and groundwaters from these holes have very high metal loads (Chapter Seven). Boreholes MM-88-01 and MM-88-02 are deeper holes that intersect the sulphides at greater depth and groundwaters in the latter hole are saline Na-Ca-Cl fluids (Chapter Seven). Boreholes MM-89-106 and MM-89-107 were drilled to the east of the deposit and do not intersect massive sulphide mineralization.

Suspended sediments from boreholes MM-88-06 and MM-88-07, as with the groundwaters, are characterized by high Fe contents and very elevated base metal loads. In this latter respect they are quite different from the high-Fe sediments from borehole HT55-43 at the Halfmile Lake deposit. For example, Pb contents range from 11.1 to 15.3 weight% (Table 9.2). Zinc loads are also high, but are lower than Pb, ranging from 0.89 to 7.7 weight %. Other metals that correlate strongly with Pb and Zn are similarly enriched, including Cd, Tl, and Bi. These sediments also have high Ag contents, up to 140 ppm. Compared to average unaltered host lithologies, suspended sediments from these boreholes are depleted in most terrigenous clastic elements (i.e., LILE, HFSE, and the REE; Fig. 9.8). The sediments are very enriched in Pb, Co, Ag and Zn, and somewhat enriched in Fe. There are some differences between the sediments from these two boreholes. Sediments from borehole MM-88-07 are enriched in U and depleted in Na compared to the host lithologies and the MM-88-06 sediments

(Fig. 9.8). Compared to the corresponding groundwaters these sediments are enriched in Cu, Pb, Zn, and Al (Fig. 9.9).

Sediments from borehole MM-88-01 are different compared to sediments from the more shallow boreholes. These sediments have much lower, though still elevated, base metal loads. Zinc and Pb contents range from 2100 - 3400 ppm and 3500 - 6700 ppm, respectively. These sediments also have unusually high Al_2O_3 contents ranging from 21.00 to 31.40 weight % (Table 9.2). All the other suspended sediments analyzed in this study have < 15 weight % Al_2O_3 and most are < 10 weight %. However, despite the high Al contents, Na, K, Mg, and Ca contents are generally low. This would suggest that the Al occurs primarily as kaolinite or Al-oxide phases. Compared to the host lithologies, borehole MM-88-01 sediments have low concentrations of most elements with the exception of elevated U, Pb, Nb, Fe, Co, and Ag. In addition, these sediments are very LREE depleted (Chapter Ten; Fig. 10.24) and have very large Eu anomalies relative to the host lithologies (Fig. 9.8).

Only one sample from borehole MM-88-02 had sufficient suspended sediment for geochemical analysis. This sediment sample (MLF96-606) is characterized by high Ba (3300 ppm) and Sr (530 ppm) compared to the other sediments. The groundwaters from this borehole also have very high Ba and Sr on the order of 90 ppm (Chapter Seven). Some caution should be placed on the analysis for this sample. The groundwaters have elevated Na and Cl contents but are well below halite saturation (Chapter Seven). Despite this, SEM and XRD analyses detected significant halite on some filter papers from this borehole. This halite is interpreted to be due to evaporation on the surface of the filter after the groundwaters had been processed. Note also that although the groundwaters from this hole had sulphate contents that were below detection and attempts to precipitate $BaSO_4$ in the field were unsuccessful. However, if a small amount of sulphate is added to speciation calculations, borehole MM-88-02 groundwaters are close to saturation with respect to barite (Chapter Seven). Small crystals and rosettes of barite were observed by SEM (Table 9.1; Fig. 9.3). It is unclear if this barite formed prior to sampling, was produced by mechanical erosion of barite from fractures (although none has

been identified at the Restigouche deposit), or formed subsequent to sampling in the same manner as the halite.

Suspended sediments from the two distal boreholes at the Restigouche deposit (boreholes MM-89-106 and MM-89-107) have compositions that closely approximate the host lithologies (Fig. 9.8). These sediments have generally low base metal contents and moderately low Fe contents compared to the sediments from boreholes that intersect the Restigouche deposit. Suspended sediments from borehole MM-89-106 show some differences between bailer and packer samples. As shown in Chapter Seven, the deeper waters from this borehole were more saline where sampled with the packer compared with the flow-through bailer. The suspended sediment from the packer sample is from the bottom of the hole, and shows higher base metal loads than the other sediments from this borehole (Table 9.2). Compared to the host lithologies, suspended sediments from both boreholes have generally flat patterns with slight enrichments in the LREE, Cs, U, and Sr, and strong enrichment in Pb and Co. The only element showing consistent depletion is Ca, probably related to dissolution of carbonate (Fig. 9.8). Compared to the corresponding groundwaters, these sediments show similar relationships to the other suspended sediments. Differences include a stronger partitioning of Mn onto the suspended sediment phase and greater partitioning of Na into the aqueous phase (Fig. 9.9).

9.4 Discussion

9.4.1 Mineralogy

The mineralogy of the suspended sediments is generally consistent with fracture zone and groundmass mineralogy of the host rocks (Chapter Two, Four). Close to the ore deposits, hydrothermal alteration at the time of ore formation produced a silicate alteration mineral assemblage dominated by quartz, sericite, and chlorite. More distal to the deposits, felsic metavolcanic and metasedimentary host rocks are dominated by quartz, feldspar (albite and K-feldspar), sericite, and chlorite (Lentz and Goodfellow, 1993b; Lentz and Goodfellow, 1996).

This raises the question as to whether the suspended sediments represent only disaggregated fracture zone material, or are they controlled in part by the chemistry of the present groundwaters. Degueldre et al. (1996a) suggested that there were three main sources of colloids and suspended sediments in groundwater systems; 1) alteration of host lithology minerals by groundwaters with subsequent suspension, 2) mechanical abrasion or disaggregation of non-cemented particles of aquifer material, and 3) precipitation of minerals directly from the groundwater. The Pb contents of the suspended sediments from boreholes MM-88-06 and MM-88-07 are interesting in this respect. The Pb contents are much higher than assay samples collected during mineral exploration (Westoll, 1990) and are higher than most samples of massive sulphide analyzed in this study (compare Tables 9.2 and 2.2). This suggests that Pb is being released from the host rocks as a product of massive sulphide oxidation (Chapter Seven) and then concentrated in suspension as Pb-sulphates and/or adsorbed onto Fe-oxyhydroxides. In contrast, Zn abundances although high in boreholes MM-88-06 and MM-88-07 suspended sediments are lower than Pb contents (low Zn/Pb ratios), which indicates that Zn is preferentially partitioned into the aqueous phase relative to Pb (Fig. 9.9).

9.4.2 Fractionation between whole rocks, waters, and suspended sediments

No attempt was made to quantify the amount of suspended sediment present. This was because it was recognized that the sampling methodology (especially with respect to the flow-through bailer) might result in dislodging material from borehole walls during raising and lowering of sampling apparatus, and thus biasing the sample. However, this is not believed to affect the results presented here for several reasons. Firstly, it is unlikely that normalizing suspended sediment elemental abundances to the amount of suspended sediment accurately indicates relative fractionations. Miekeley et al. (1992a) used such normalizing techniques to show that U was present predominantly in the dissolved phase, despite high suspended sediment U contents, due to the low suspended sediment abundances of the groundwaters.

However, suspended sediment abundance does not represent the only source and sink of elements in a groundwater system; fractures consist of minerals and oxide coatings that are typically similar mineralogically to the suspended sediment load. For example, the mineralogy of suspended sediments in Halfmile Lake and Restigouche deposit groundwaters are mineralogically very similar to the fracture zone minerals (see Chapter Two). This suggests that additional elemental sources and sites for adsorption/co-precipitation reactions are present that are not "recorded" by a groundwater sample.

Secondly, much of the discussion presented below is based on normalizing waters and sediments to the host rocks and the sediments to the corresponding waters. This means that conclusions regarding element partitioning can be achieved in a relative sense.

In many respects, the suspended sediments are compositionally similar to the host lithologies. For example, normalized to average unaltered felsic host rocks, many of the suspended sediments display flat element patterns, especially for the detrital elements identified previously. The suspended sediments that most closely approximate unaltered host rocks are those more distal to massive sulphides at the Restigouche deposit and from borehole HN94-65 at the Halfmile Lake deposit (Fig. 9.8). Suspended sediments from groundwaters proximal to massive sulphides and gossan show relative depletions in mobile elements (K, Na, Ca, Rb, Cs) and strong to very strong enrichments in relatively immobile hydromorphic elements such as Fe and Pb.

Thus, for some of the suspended sediments there is an apparent fractionation of some elements compared to the host rocks. However, much of this fractionation disappears or is reduced in magnitude if these sediments are normalized to rocks with which they are more spatially related. The low trace element contents and generally lower base metal loads of suspended sediments from borehole HT55-43 (Halfmile Lake deposit) most likely reflects mechanical erosion and transport of previously gossanized and ferruginous material rather than fractionation of elements during weathering of primary felsic volcanic rocks. The suspended sediments from borehole HT55-43 show felsic host-rock normalized element patterns that are

similar to some gossan samples from the Halfmile Lake deposit (Fig. 9.11; D.R. Boyle, unpublished data). Although the suspended sediments from borehole HT55-43 are fractionated compared to the host felsic rocks, they are less fractionated than the gossans. Many of the gossan samples show more fractionated patterns than the suspended sediments (Fig. 9.11A).

Suspended sediments from boreholes MM-88-06 and MM-88-07 at the Restigouche deposit were sampled adjacent to the massive sulphides. Again, compared to the host lithologies (Fig. 9.8), these sediments show very fractionated patterns. However, compared to the massive sulphides there are some similarities (cf Figs. 9.8, and 9.11B). The suspended sediments and massive sulphides show strong depletions in the detrital elements and very strong enrichments in hydromorphic elements. Interestingly, both show less depletion or enrichment in Sr, U, and Eu compared to the host lithologies. The enrichment in Eu in the suspended sediment relative to host rocks is greater than for the massive sulphides. This indicates that Eu is preferentially being mobilized during rock and sulphide weathering, but is strongly adsorbed to the suspended phases. Similarly, U shows relatively little depletion in the massive sulphides compared to the host rocks, whereas the suspended sediment is enriched in U for these boreholes. Compared to the corresponding groundwater, U is apparently strongly partitioned into the suspended sediment phase. Speciation modelling of these groundwaters indicates that between 70 and 85% of the U in the waters is present as U^{6+}. Uranium is highly soluble in the 6+ state but is insoluble in the 4+ state. Previous work has shown that $U^{(VI)}$ has a strong affinity for adsorption to Fe-oxyhydroxides of Halfmile Lake and Restigouche deposit groundwaters. Waite et al. (1994) showed that $U^{(VI)}$ adsorption to ferrihydrite approached 90-100% in the pH range 5-8 for a variety of experimental conditions with variable ionic strength, and U and Fe activities. Strontium is similar to U in that the massive sulphides show little fractionation compared to the host rocks (Fig. 9.11B), but the suspended sediments from borehole MM-88-06 show enrichment (Fig. 9.8). However, unlike U, Sr shows a relatively strong partitioning into the aqueous phase (Fig. 9.9).

Suspended sediments from borehole MM-88-01 cannot easily be related to any of the host

rocks or massive sulphides. These sediments show strong fractionation in many elements compared to the host rocks (Fig. 9.8) and are strongly enriched in Al relative to all the host rocks and other suspended sediments (Table 9.2). These sediments show the strong influence of the aqueous phase compared to that of the host rocks. This is emphasized by the rare earth element systematics of these sediments which display a strong LREE depletion compared to NASC and the host rocks, have strong negative Ce anomalies unlike any of the other suspended sediments, and are similar only to local surface waters (see Chapter Ten for a full treatment of the REE; Figs. 10.24, 10.27).

9.4.3 Size distribution of suspended sediments

There is a functional difference between colloidal material and suspended particles (Degueldre et al., 1996b). Degueldre et al. (1996b) referred to particles < 1000 nm as colloids and particles > 1000 nm as suspended matter. In this study, only material > 450 nm was analyzed due to the filter size chosen. However, based on previous studies (e.g. Degueldre et al., 1996b), the finer grained material observed by SEM is probably a good approximation of the colloids < 450 nm in size that may have passed through the filter and thus influenced the "dissolved" load of the waters (see Chapter Seven). In this study no quantitative analyses of the size distribution of the suspended sediments was attempted. However, it is obvious from the SEM data (Figs. 9.2, 9.4-9.6) that the majority of the suspended sediment in Halfmile Lake and Restigouche deposit groundwaters is between < 1 and 10 μm in size. This size distribution is consistent with previous studies of the > 0.45 μm fraction of groundwaters. For example, Gómez et al. (1992) showed that suspended sediments from groundwaters associated with granites in Spain gave size peaks at 1 and 10 μm. The truly colloidal fraction of these Spanish groundwaters (< 0.45 μm) showed a maxima at 50-100 nm and 350 nm for different waters (Gómez et al., 1992). The mineralogy of these Spanish groundwater suspended sediments was similar to those of BMC groundwaters (Gómez et al., 1992).

In addition, it should be noted that the content of suspended and colloidal material in this

study is somewhat artificial because of the methods used to sample the groundwater. The bailer method probably contributes excess material due to scraping of borehole walls during lowering of the instrument and because a standing water column is sampled. The packer system is much less prone to this as it is in place for a longer period of time and the sampled zone is purged many times (see Chapter Three). Suspended sediment contents of packer samples typically decreased with time. However, the differences in the mineralogy and geochemistry of the suspended sediments are not related to the sampling method. Rather they are the result of differences in groundwater geochemistry, the adjacent lithology and the style and extent of interaction between suspended sediment, groundwater and host rocks.

9.4.4 Hydromorphic and detrital components

Previous work has shown that sediments proximal and distal to massive sulphide deposits (Peter and Goodfellow, 1993; Peter and Goodfellow, 1996) and modern sea-floor hydrothermal vent sites exhibit mixing trends between elements associated with hydrothermal fluids and those associated with clastic derived sediment. Elements have been subdivided into hydrothermal, hydrogenous, and detrital (Peter and Goodfellow, 1993; Peter and Goodfellow, 1996). Peter and Goodfellow (1993) showed that iron formation along the Brunswick Belt showed mixing relationships with respect to Fe/Ti and Al/(Al+Fe+Mn). The ratio Fe/Ti increases with increasing hydrothermal input to the iron formations (Fe/Ti = hydrothermal/detrital), whereas the ratio Al/(Al+Fe+Mn) increases with increasing detrital input [Al/(Al+Fe+Mn) = detrital/(detrital + hydrothermal + hydrogenous)]. The suspended sediment from the Halfmile Lake and Restigouche deposits have been plotted on a similar diagram (Fig. 9.10A). It is very interesting that the BMC suspended sediments fall on a very similar mixing line between hydrothermal and detrital components as the Brunswick Belt iron formations. The suspended sediment data can be best fit with a power-law function:

$$Fe/Ti = 9.864 \cdot \left(\frac{Al}{Al+Fe+Mn}\right)^{-1.0585} \qquad (r^2 = 0.7996)$$

The detrital end-member is represented by least-altered felsic lithologies from the Halfmile Lake and Restigouche deposits (Table 2.2). The suspended sediments with high base metal loads due to proximity to the massive sulphides and/or high Fe due to proximity to gossan, plot closest to the massive sulphide end-member. Samples more distal to the Restigouche deposit (from boreholes MM-89-106 and MM-89-107) plot close to the host lithologies indicating a high detrital component. The exceptions are the suspended sediment from borehole MM-88-01. These sediments have relatively high metal loads (Table 9.2) but have anomalously high Al contents due to formation of Al-oxides ± kaolinite.

The fact that suspended sediments show similar Fe/Ti versus Al/(Al+Fe+Mn) values as hydrothermal sediments suggests that weathering and dissolution of massive sulphides by meteoric groundwaters imparts a similar composition between end-members as ancient products of hydrothermal fluids. Instead of mixing between hydrothermal and detrital components, the relationship for groundwater suspended sediments can be thought of as representing mixing between detrital (host rock-derived) and hydromorphic (sulphide-derived) components. Thus, as massive sulphides are oxidized, Fe and base metals are released to the aqueous phase. If the pH and Eh conditions are favourable, as they will be in most natural groundwaters, Fe and metals will strongly, though variably, partition into the suspended sediment phase relative to the aqueous phase.

This subdivision of suspended sediment elements into hydromorphic and detrital components is also indicated by inter-element correlation and factor analysis. Elements typical of the detrital component (e.g., Ti, K, Al, Ca, Mg, Na, Ga, Nb, Hf, Sc, Rb, Th, Zr) show strong positive inter-element correlations whereas these elements are typically negatively correlated with Fe and base metals. Similarly, hydromorphic elements from massive sulphide/gossan dissolution show strong correlations (e.g., $r^2 = 0.805$ for Zn-Pb, $r^2 = 0.726$ for Ag-Pb, and $r^2 = 0.821$ for Cd-Pb). The strength of the inter-element correlations amongst the hydromorphic elements very much depends on their relative mobility, which is controlled by the pH and Eh conditions, that in turn reflects the affinity for the aqueous phase.

Of particular interest is the Zn/Pb ratios. Whereas Zn/Pb is always > 1 in the Restigouche deposit groundwaters, suspended sediments from boreholes close to the Restigouche ore body have ratios < 1. Similarly, suspended sediments in boreholes HN94-65 and HT55-43 show decreasing Zn/Pb ratios downhole towards the massive sulphides. This relationship between Zn and Pb is consistent with the greater solubility of Zn compared to Pb; Pb is more readily adsorbed (or co-precipitated) with the suspended sediment than Zn. With increasing distance from the deposit, the Zn/Pb ratio is > 1 as Pb is not readily hydromorphically transported away from the immediate area of the deposit.

The Zn/Pb ratios in the suspended sediments closest to the ore body at Restigouche are extremely low. Note that the ratios in MM-88-01 and MM-88-06/07 are all < 1, whereas in suspended sediments from boreholes MM-89-106 and MM-89-107 and boreholes from the Halfmile Lake deposit, the ratios are all > 1. The very low ratios in suspended sediments from boreholes MM-88-06 and MM-88-07 indicate that the suspended sediments are not merely material scraped from the ore body as the bailer was lowered into the borehole. Assay Zn/Pb values given in the Marshall Minerals assessment files are > 1 except in borehole MM-88-06 where leached limonitic gossans were recovered from 8.43 to 13 m below surface and where the Zn/Pb ratios for two assays are « 1. This suggests either that the suspended sediments represent gossan material, or that there is preferential loss of Pb from the water due to formation of anglesite.

Although suspended sediments from both the Halfmile Lake and Restigouche deposits show similar relationships between hydromorphic and detrital components, suspended sediments also display interesting differences. For example, Ti and Th, both detrital (lithological) components show a strong correlation (r^2 = 0.568; Fig. 9.10B). However, suspended sediments from the two deposits define very different Ti/Th trends. These differences in Ti and Th are not evident in the host lithologies. The low TiO_2 and high Th contents of the suspended sediments are more similar to the felsic host rocks than the mafic lithologies at both deposits. It is unclear why there should be such a striking difference in Ti/Th

in the suspended sediments. It is possible that due to the closer proximity of the Restigouche ore body to surface that Th is more mobile in Restigouche deposit groundwaters.

9.4.5 Environmental implications

The results presented in this chapter have important environmental and mineral exploration implications for metal mobility and transport in the groundwater environment. The latter will be discussed in detail in Chapter Thirteen.

Clearly, metals are associated, to a variable degree, with particulate matter in BMC groundwaters. These suspended sediments can be considered "stable" for the pH, Eh and groundwater geochemical conditions under which they were sampled. Under the present conditions, many metals show a strong preference for the suspended phase and are strongly adsorbed. However, perturbations to the present conditions could result in enhanced metal uptake, or more likely, enhanced metal desorption and release to the dissolved phase and potentially to the surface environment. For example, at the time of sampling, the Restigouche deposit was relatively undisturbed. It has been shown (Chapter Seven) that, despite very high metal loads in borehole MM-88-06 and MM-88-07 groundwaters, and the close proximity of these boreholes to Charlotte Brook, metal contents of Charlotte Brook waters are not as high as would be expected. This suggests that groundwater flow under "natural" conditions was away from Charlotte Brook where the stream crosses the deposit (Chapter Seven). The Restigouche deposit has since gone into production as an open-pit operation. Mining and excavation will perturb groundwater flow, increase the exposure of sulphide minerals to atmospheric oxygen, and may result in increased ground and surface water acidity. If this happens, there is the potential for significant release of adsorbed metals (especially Pb) from suspended sediments. Swartz et al. (1997) note that the mobilization and transport of colloids is strongly affected by perturbations in the pH, Eh, ionic strength, and cation chemistry of groundwaters and pore fluids.

9.5 Summary

1) Suspended sediments recovered from Halfmile Lake deposit groundwaters are dominantly quartz and aluminosilicate minerals. Fe-oxyhydroxides are probably present as surface coatings and amorphous Fe-phases. Suspended sediments in groundwaters remote from the main Restigouche ore body are mineralogically similar. However, suspended sediments from boreholes that intersect the Restigouche ore body consist primarily of Fe, Pb, and Zn sulphate minerals.

2) The Halfmile Lake deposit suspended sediments are depleted in the mobile elements Cs, Rb, and K host rocks. Suspended sediments show generally flat patterns normalized to the host lithologies for most other elements but strong enrichments in the hydrothermal suite of elements Pb, Fe, Co, Zn, Ag, and Eu. Iron oxide-rich suspended sediments from borehole HT55-43 which penetrates the gossan are more depleted in most elements than the other sediments.

3) The geochemistry of the suspended sediments from the Restigouche deposit shows similar relationships, although the degree of enrichment in metals associated with massive sulphide mineralization is greater.

4) Compared to coexisting groundwaters suspended sediments are relatively enriched in Al, Fe, Pb, and relatively depleted in Ca, Sr, and Mg. Potassium and Rb are generally more strongly fractionated into the suspended sediment phase than other mobile elements, indicating that their abundance in the groundwaters is controlled by secondary phases.

Table 9.1 Mineralogy of BMC groundwater suspended sediments

Sample#	Borehole	Type	Analysis	Quartz	Silicates	Fe-oxides	Other
					Halfmile Lake deposit		
MLF94-209	HN94-55	bailer	SEM	present	Sericite, chamosite	coatings?	
MLF94-237	HN94-65	bailer	XRD	present	Sericite, chamosite, albite		pyrite
MLF94-238	HN94-65	bailer	XRD	present	Sericite, chamosite, albite		pyrite
MLF94-244	HN94-65	bailer	SEM	present	Sericite, chamosite, kaolinite	present	pyrite
MLF94-250	HN94-65	bailer	SEM	present	Sericite, chamosite, kaolinite	coatings?	pyrite
MLF94-257	HT55-43	bailer	XRD	present	Chamosite, sericite	Lepidicrocite	
MLF96-698	HN96-40	packer	SEM	present	Chamosite, sericite, kaolinite	Fe-Mn coatings	pyrite
					Restigouche deposit		
MLF95-312	MM-88-01	bailer	XRD	present	Sericite, chamosite, kaolinite		pyrite
MLF96-671	MM-88-01	packer	SEM	trace	Sericite, kaolinite		Fe-sulphate, Zn-sulphate, S
MLF95-331	MM-88-02	bailer	SEM	present	Sericite, chamosite?		Barite-minor, rare Ti-oxide
MLF95-326	MM-88-02	bailer	SEM		Sericite, rare chamosite		NaCl, barite, Fe-sulphate/pyrite
MLF95-358	MM-88-06	bailer	SEM		Sericite, kaolinite, albite?	Fe, Pb, Zn oxides?	Pb, S, Fe, Zn with small O peaks =pyrite, galena, sphalerite + sulphates
MLF95-364	MM-88-06	bailer	XRD	present	Sericite, kaolinite, feldspar		pyrite
MLF95-315	MM-88-07	bailer	SEM				Fe, Pb sulphates and/or sulphides
MLF95-317	MM-88-07	bailer	XRD	present	Kaolinite, feldspar, sericite		pyrite, angelsite?
MLF95-332	MM-89-106	bailer	XRD	present	Sericite, chamosite, kaolinite, albite, K-feldspar		
MLF95-341	MM-89-106	bailer	XRD	present	Sericite, chamosite, kaolinite, albite		
MLF95-504	MM-89-106	packer	SEM	present	Kaolinite? Typically with trace K and Fe	coatings?	NaCl, S common, REE phosphates
MLF95-592	MM-89-107	packer	XRD	present	Sericite, kaolinite, chamosite, albite, K-feldspar		
					Stratmat Main Zone deposit		
MLF96-695	S61-19	packer	SEM	rare	Sercite, chamosite, albite		Fe-sulphate, rarely w/trace Zn
MLF96-702	S61-19	packer	SEM	present	Chamosite, sericite	coatings?	

Some sericite is likely illite.

Table 9.2 Geochemical analyses of suspended sediment

Sample#	MLF94-236	MLF94-237	MLF94-238	MLF94-242	MLF94-248	MLF94-249	MLF94-255	MLF94-257	MLF94-258	MLF94-259	MLF96-696	MLF95-307	MLF95-309	MLF95-312	MLF95-313	MLF95-606	MLF95-361
Borehole	HN94-65	HN94-65	HN94-65	HN94-65	HN94-65	HN94-65	HT55-43	HT55-43	HT55-43	HT55-43	HN92-40	MM-88-01	MM-88-01	MM-88-01	MM-88-01	MM-88-02	MM-88-06
Deposit	Halfmile	Halfmile	Halfmile	Halfmile	Halfmile	Halfmile	Halfmile	Halfmile	Halfmile	Halfmile	Halfmile	Restigouche	Restigouche	Restigouche	Restigouche	Restigouche	Restigouche
Type	bailer	bailer	bailer	bailer	bailer	bailer	bailer	bailer	bailer	bailer	packer	bailer	bailer	bailer	bailer	packer	bailer
TiO_2	0.39	0.39	0.43	0.44	0.40	0.44	0.12	0.19	0.30	0.25	0.58	0.05	0.08	0.12	0.12	0.21	0.14
Al_2O_3	9.19	9.50	9.41	9.70	8.64	8.85	2.66	3.77	9.50	6.27	14.00	31.40	26.90	21.00	21.90	11.60	5.08
Fe_2O_3*	12.50	12.70	12.80	12.50	12.90	14.10	64.00	53.80	39.30	43.80	17.50	7.01	9.60	13.40	13.00	6.45	16.80
MnO	0.06	0.06	0.06	0.06	0.05	0.05	0.30	0.23	0.16	0.19	0.52	0.02	0.03	0.05	0.05	0.03	0.05
MgO	1.88	2.01	1.99	2.09	1.93	1.91	0.66	0.89	1.25	1.12	2.06	0.40	0.65	1.13	1.07	1.38	0.76
CaO	0.27	0.28	0.29	0.30	0.31	0.45	0.05	0.06	0.73	0.05	0.63	0.19	0.22	0.29	0.24	1.27	0.21
Na_2O	1.11	1.14	1.15	1.12	1.07	1.38	0.14	0.20	0.31	0.50	1.02	0.52	0.50	0.53	0.53	6.18	0.26
K_2O	1.95	2.01	2.01	2.00	1.80	1.87	0.32	0.46	1.62	1.08	3.17	0.38	0.59	0.94	0.89	4.04	1.17
Ag	15	15	17	13	14	29	4.6	8.0	4.3	6.8	11	9.1	12	9.4	45	22	27
Ba	490	510	510	510	470	500	2400	2500	1100	70	560	110	140	240	190	3300	2700
Be	1.6	1.6	1.6	1.7	2.7	6.3	0.5	0.5	1.1	0.6	11	7.6	7.2	6.2	6.4	8	2.6
Bi	3.6	3.5	3.8	3.5	4.2	5.1	8.7	11	7.3	46	6.1	3.2	4.2	5.8	5.2	2	6.1
Cd	6.4	6.9	6.7	7.1	5.6	6.6	1.1	0.9	0.6	0.8	7.1	4.6	6.5	10	17	1.9	320
Co	30	29	29	37	70	180	60	47	26	57	180	110	100	51	80	15	94
Cr	83	89	95	100	110	190	61	64	70	52	250	91	88	140	110	120	63
Cs	1.5	1.6	1.6	1.6	1.4	1.3	0.36	0.57	1.3	1.1	42	0.8	1.2	2.3	2.2	14	2.2
Cu	380	390	390	400	410	490	1400	1400	690	1800	240	360	480	600	590	110	2200
Ga	14	13	12	13	17	31	5.4	5.7	12	9.2	20	6.1	7.9	10	10	19	14
Hf	5.4	4.8	6.2	5.8	5.2	6.8	1.1	1.7	2.7	2.9	5.7	2.3	2.3	3.3	3	5.4	3.1
In	1.4	1.4	1.4	1.5	1.7	1.7	0.61	0.9	0.45	2	1.9	1	0.94	1.3	1.3	0.71	1.6
Mo	24	23	23	21	21	22	20	15	10	11	50	6.1	6.2	46	16	5.9	32
Nb	11	11	11	12	11	12	3	4.4	6.8	5.6	14	1.8	2.6	7.2	4.3	10	5.3
Ni	39	40	42	44	58	110	130	98	65	69	79	55	55	170	80	30	65
Pb	1400	1500	1500	1500	1600	1500	190	230	120	270	560	3500	4800	6700	6500	230	153000
Rb	80	82	80	88	81	81	16	22	74	53	150	19	29	54	45	160	62
Sc	7.4	7.7	7.7	7.9	7.4	8	3.6	4.5	9.4	6.8	17	6.6	7.2	8.1	8.1	9.5	5.4
Sn	18	16	29	29	16	350	13	44	12	29	54	29	77	16	74	130	39
Sr	26	24	25	25	24	28	24	22	26	20	47	11	15	25	21	530	71
Ta	0.9	0.8	0.5	0.9	0.5	1.2	0.4	0.8	0.6	0.4	1.5	1.0	0.5	3.3	2.8	1.1	0.6
Th	9.5	9.9	9.9	10	9.9	9.7	2.6	3.7	7.7	5.6	13	3.7	5.4	9.1	8.9	21	10
Tl	0.79	0.79	0.79	0.77	0.76	0.85	0.11	0.13	0.46	0.42	1.1	0.83	1.6	2.9	2.7	0.98	46
U	4.7	4.4	4.5	4.4	4.3	4.7	0.86	1.1	2.2	1.8	6.1	65	58	49	50	4.6	6.5
V	47	48	48	49	46	47	22	26	58	41	96			13	5	12	18
Y	27	27	34	35	28	36	7.9	10	19	14	34					48	16
Zn	3800	4000	3900	4000	2800	2700	420	400	340	230	1400	2100	2800	3400	3100	3900	77000
Zr	200	180	230	220	190	250	46	64	89	92	200	69	81	110	95	210	110
U/Mo	0.20	0.19	0.20	0.21	0.20	0.21	0.04	0.07	0.22	0.16	0.12	10.66	9.35	1.07	3.13	0.78	0.20
Zn/Pb	2.71	2.67	2.60	2.67	1.75	1.80	2.21	1.74	2.83	0.85	2.50	0.60	0.58	0.51	0.48	16.96	0.50

Major element in weight %, trace elements in ppm.

Table 9.2 continued

Sample#	MLF95-362	MLF95-364	MLF95-315	MLF95-317	MLF95-318	MLF95-332	MLF95-335	MLF95-336	MLF95-341	MLF95-343	MLF95-508	MLF95-354	MLF95-355	MLF95-592
Borehole	MM-88-06	MM-88-06	MM-88-07	MM-88-07	MM-88-07	MM-89-106	MM-89-106	MM-89-106	MM-89-106	MM-89-106	MM-89-106	MM-89-107	MM-89-107	MM-89-107
Deposit	Restigouche	Restigouche	Restigouche	Restigouche	Restigouche	Restigouche	Restigouche	Restigouche	Restigouche	Restigouche	Restigouche	Restigouche	Restigouche	Restigouche
Type	bailer	bailer	bailer	bailer	bailer	bailer	bailer	bailer	bailer	bailer	packer	bailer	bailer	packer
TiO_2	0.25	0.21	0.05	0.07	0.08	0.40	0.42	0.42	0.39	0.40	0.36	0.37	0.17	0.33
Al_2O_3	7.45	8.14	3.97	3.46	3.63	13.90	14.10	14.00	12.70	13.50	14.50	11.90	6.00	15.40
Fe_2O_3	20.50	22.10	35.60	38.20	37.10	10.30	9.90	10.70	10.00	9.11	6.71	8.12	3.65	4.88
MnO	0.08	0.09	0.01	0.02	0.02	0.69	0.61	0.64	0.56	0.57	0.10	1.17	0.52	0.06
MgO	1.05	1.16	0.35	0.42	0.51	1.29	1.32	1.32	1.25	1.29	1.46	1.05	0.51	1.49
CaO	0.28	0.39	0.12	0.14	0.15	0.40	0.41	0.42	0.41	0.44	0.57	0.53	0.22	0.41
Na_2O	0.28	0.29	0.08	0.08	0.10	1.51	1.56	1.54	1.33	1.51	1.83	1.64	0.93	2.58
K_2O	1.44	1.54	0.26	0.30	0.40	2.64	2.68	2.64	2.52	2.63	2.99	1.86	0.97	2.88
Ag	39	40	99	110	140	2.2	2.0	2.0	13	15	4.7	7.0	7.5	6.9
Ba	220	1400	150	250	310	1100	1100	1100	1100	1200	1300	1300	600	1100
Be	1	1.3	2.1	1.2	1	2.8	2.9	2.9	3.5	3.6	5.3	6.6	5.9	3.9
Bi	7.4	8.4	4.6	5.7	6.1	0.8	0.6	1.1	0.9	1.2	1.8	2.7	1.7	2.1
Cd	280	230	40	47	52	2.9	2.6	2.9	2.7	2.5	9.3	4.6	2	4.8
Co	39	48	13	15	13	50	46	57	64	41	120	170	180	91
Cr	39	48	36	29	30	64	69	73	78	92	180	160	120	23
Cs	2.5	2.7	0.46	0.48	0.76	8.2	8.5	8.8	8.7	9.6	16	9.4	4.5	15
Cu	3100	3000	2000	2500	2600	150	150	160	170	150	180	130	59	55
Ga	16	17	7.8	7.4	8.3	18	20	20	21	22	23	23	13	21
Hf	4.7	3.9	1.4	1.8	2.2	6.6	7	7	6.3	6.8	6	7.9	4	8
In	1.4	1.5	0.9	0.71	0.76	0.16	0.08	0.22	0.14	0.21	0.4	1.1	0.56	0.16
Mo	26	23	32	25	23	6.2	6.2	7.7	10	8.8	7.4	20	12	0.7
Nb	8.1	6.6	3.5	2.2	2.6	13	14	13	14	13	12	15	7.7	15
Ni	37	42	20	16	12	41	44	51	54	47	120	120	95	210
Pb	129000	109000	112000	119000	111000	120	110	110	120	120	430	300	96	110
Rb	71	74	13	14	18	110	110	120	120	120	150	110	57	150
Sc	7.2	7.6	7.8	8.8	9	14	14	14	13	14	16	20	9.4	13
Sn	85	59	62	70	120	7.4	10	8.2	16	12	16	27	30	76
Sr	95	96	10	14	16	80	95	100	93	120	140	110	52	71
Ta	0.7	0.6	0.7	0.5	0.4	0.9	1.0	1.1	0.9	0.8	0.9	1.2	0.9	0.9
Th	12	13	5.5	6.6	6.9	18	19	19	20	21	21	21	9.4	21
Tl	38	32	5.5	5.9	6.7	1.1	1	0.92	1	1	1.1	1.3	0.73	1
U	7.6	8.9	37	35	29	9.2	9.7	9.4	9.3	9.4	7.3	12	3.3	7.4
V	26	27	17	16	17	45	46	45	43	44	57	37	14	27
Y	26	20	24	20	19	59	62	60	59	60	48	68	24	41
Zn	72000	64000	8900	11000	12000	280	270	290	290	300	1600	370	200	800
Zr	190	150	59	74	82	260	260	260	220	240	200	290	160	320
U/Mo	0.29	0.39	1.16	1.40	1.26	1.48	1.56	1.22	0.93	1.07	0.99	0.60	0.28	10.57
Zn/Pb	0.56	0.59	0.08	0.09	0.11	2.33	2.45	2.64	2.42	2.50	3.72	1.23	2.08	7.27

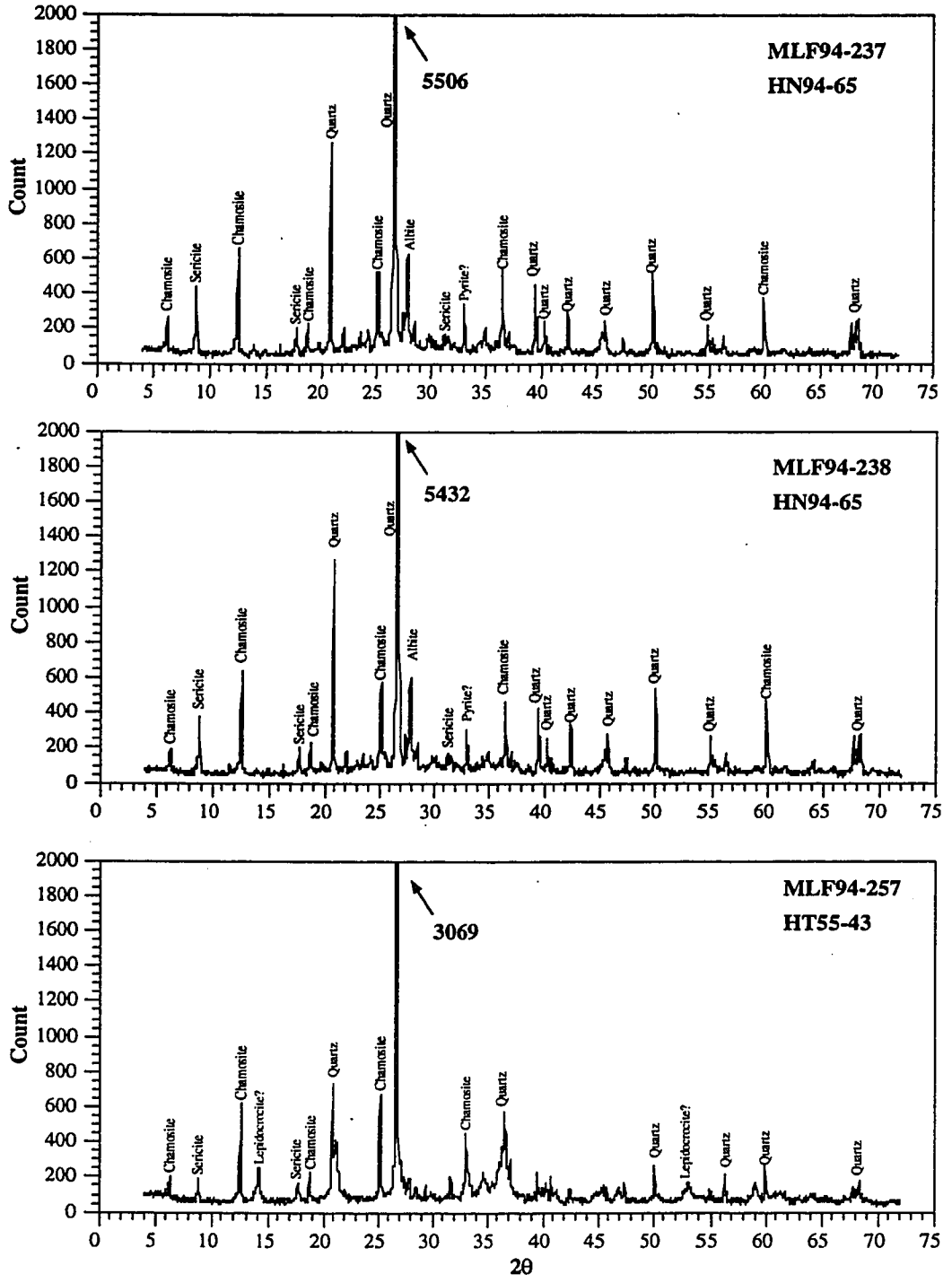


Fig. 9.1 XRD patterns for suspended sediment samples from Halfmile Lake deposit groundwaters.

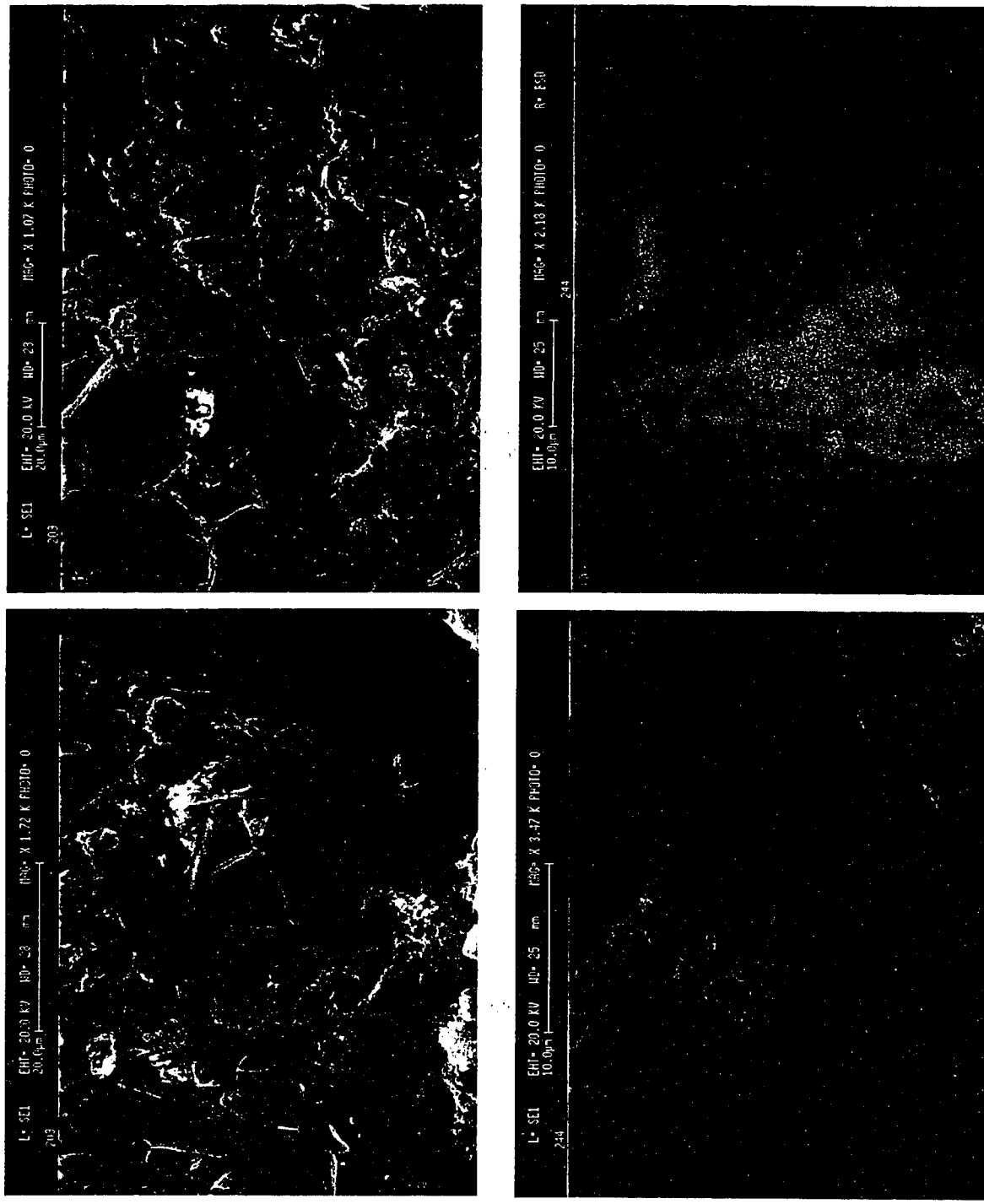


Fig. 9.2 Secondary SEM images of suspended sediments from Halfmile Lake deposit groundwaters. Q = quartz, K = K-silicates, FeO = Fe-oxides, Si = sheet aluminosilicates, Py = pyrite. A, B) Sample MLF94-209, borehole HN93-50. C, D) Sample MLF94-244, borehole HN94-65.

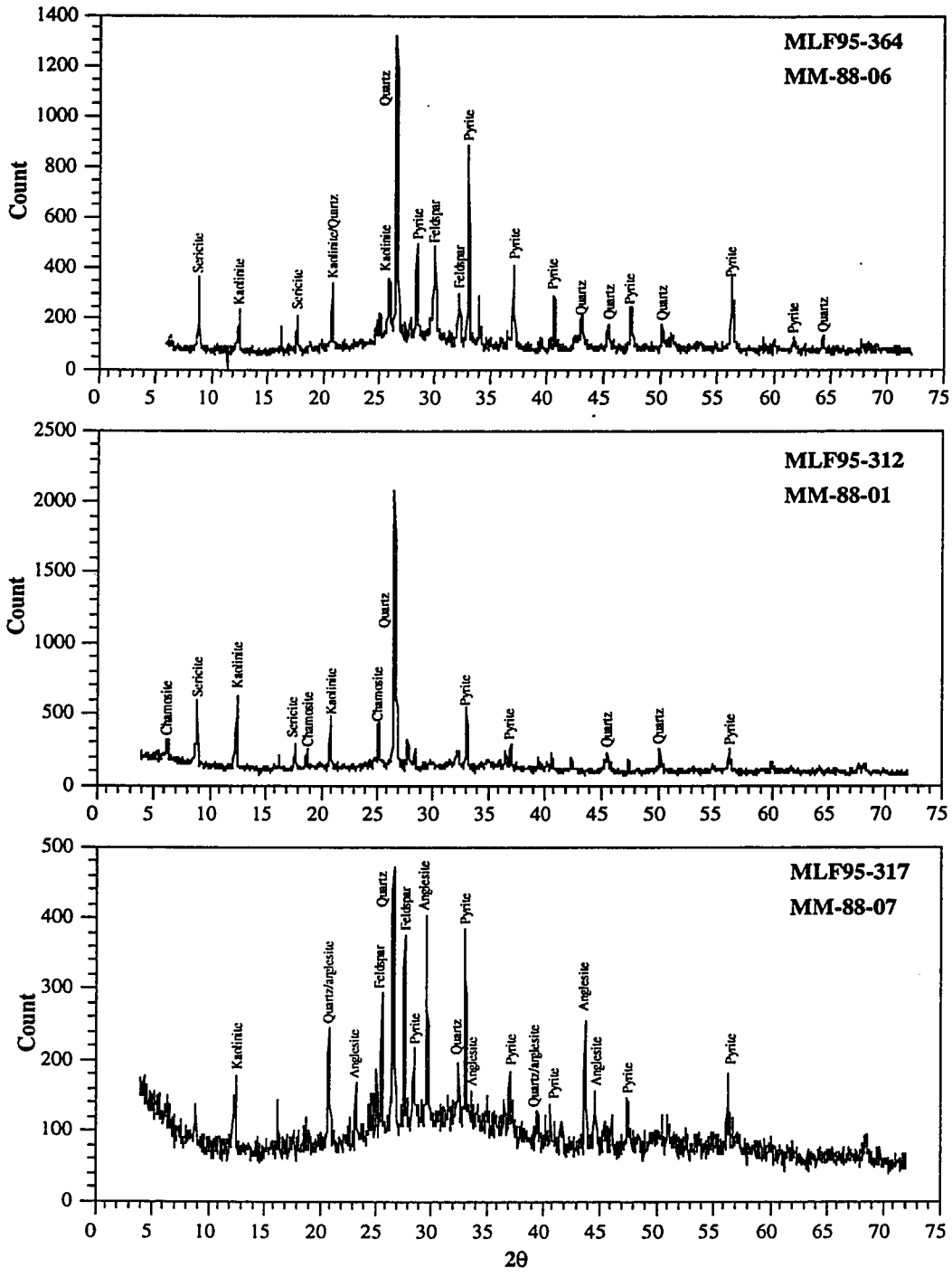


Fig. 9.3 XRD patterns for suspended sediment samples from Restigouche deposit groundwaters.

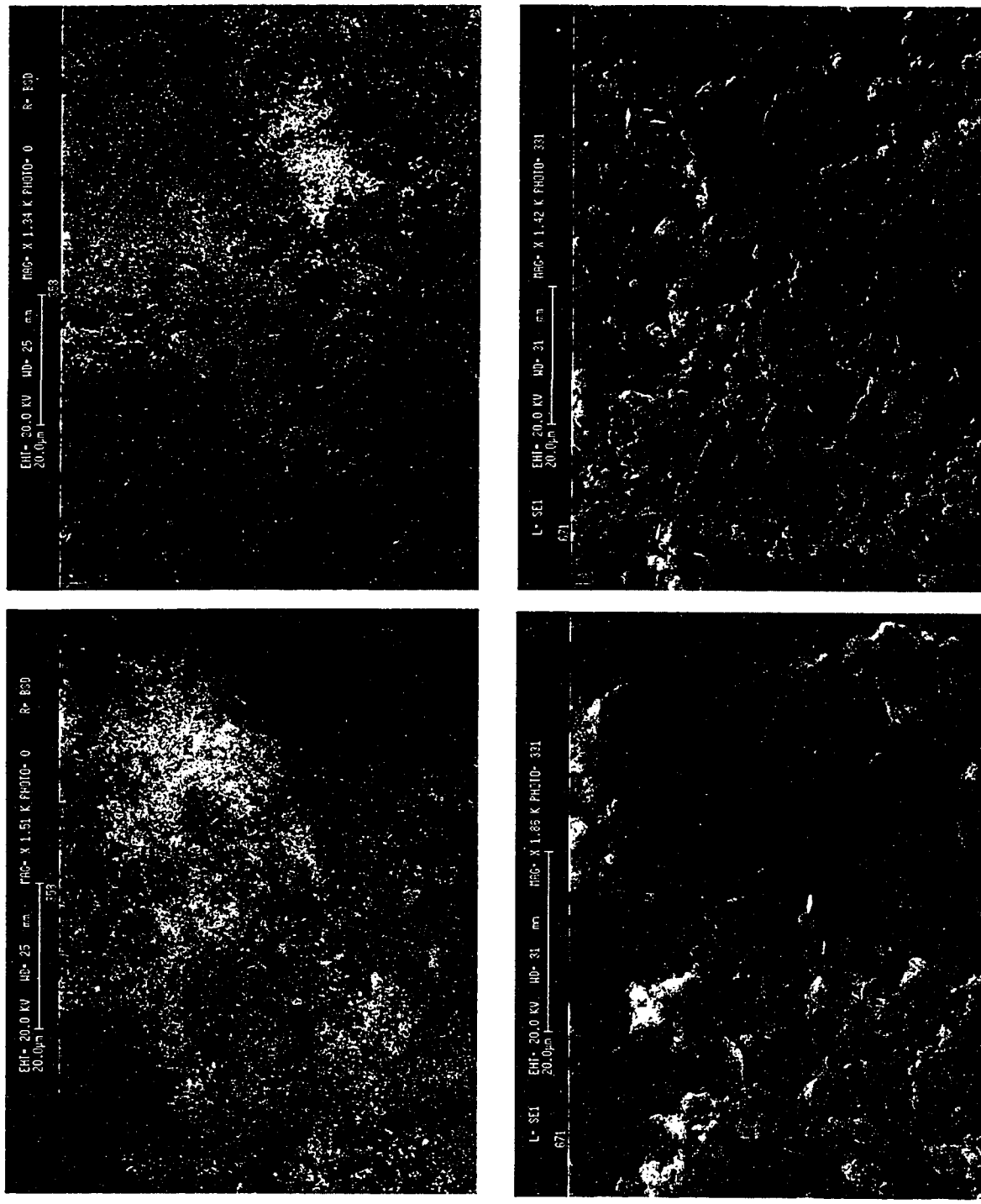


Fig. 9.4 Secondary SEM images of suspended sediments from Restigouche deposit groundwaters. Q = quartz, K = K-silicates, Si = sheet aluminosilicates, S, Fe, Zn, Pb refer to the dominant peaks on the porous sulphates. A, B) Sample MLF95-358, borehole MM-88-06. C, D) Sample MLF96-671, borehole MM-88-01.

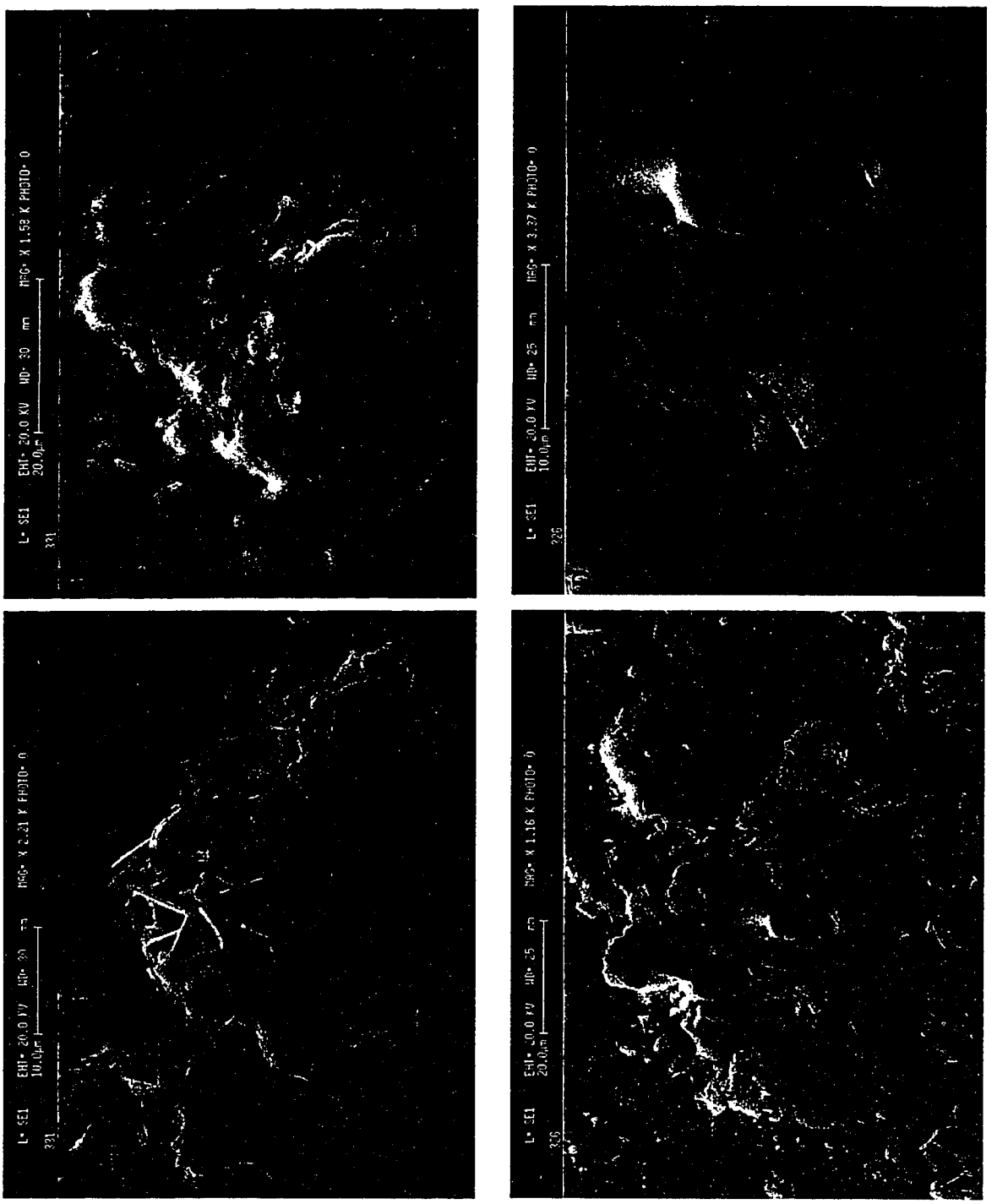


Fig. 9.5 Secondary SEM images of suspended sediments from Restigouche deposit groundwaters. Q = quartz, K = K-silicates, Ko = kaolinite, Ba = barite. A, B) Sample MLF95-331, borehole MM-88-02. C, D) Sample MLF95-326, borehole MM-88-02.

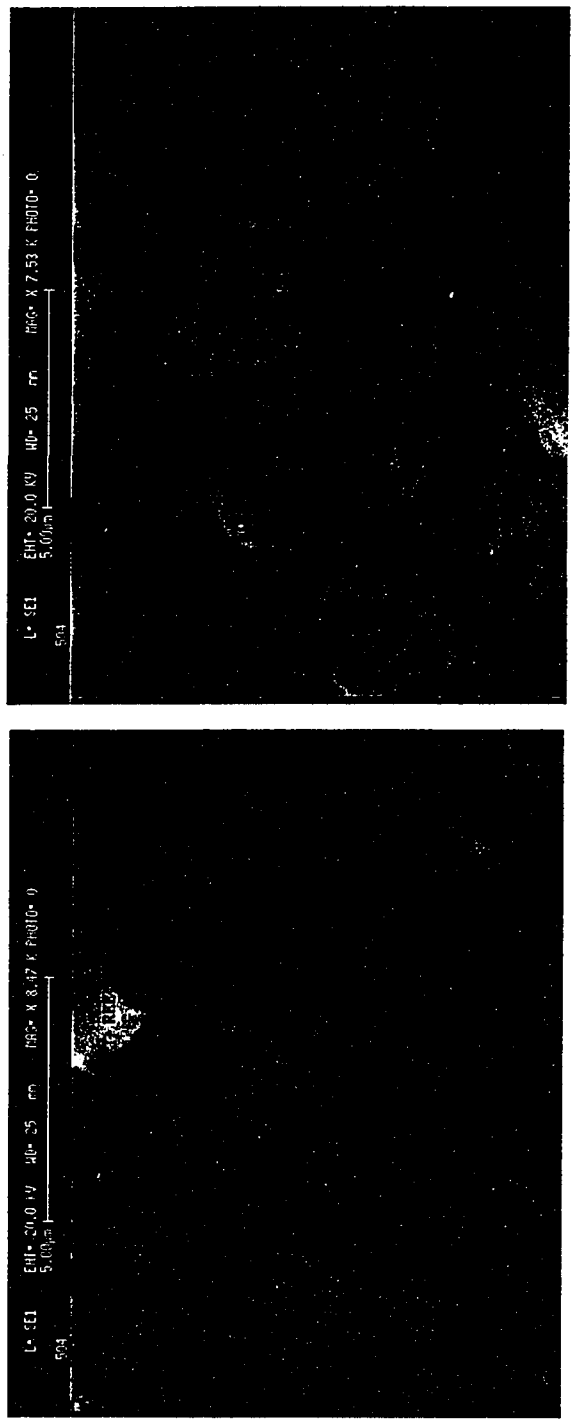


Fig. 9.6 Secondary SEM images of suspended sediments from Restigouche deposit groundwaters. Q = quartz, Si = sheet aluminosilicates, S = sulphur peak, REE = REE-phosphate. A, B) Sample MLF95-504, borehole MM-89-106.

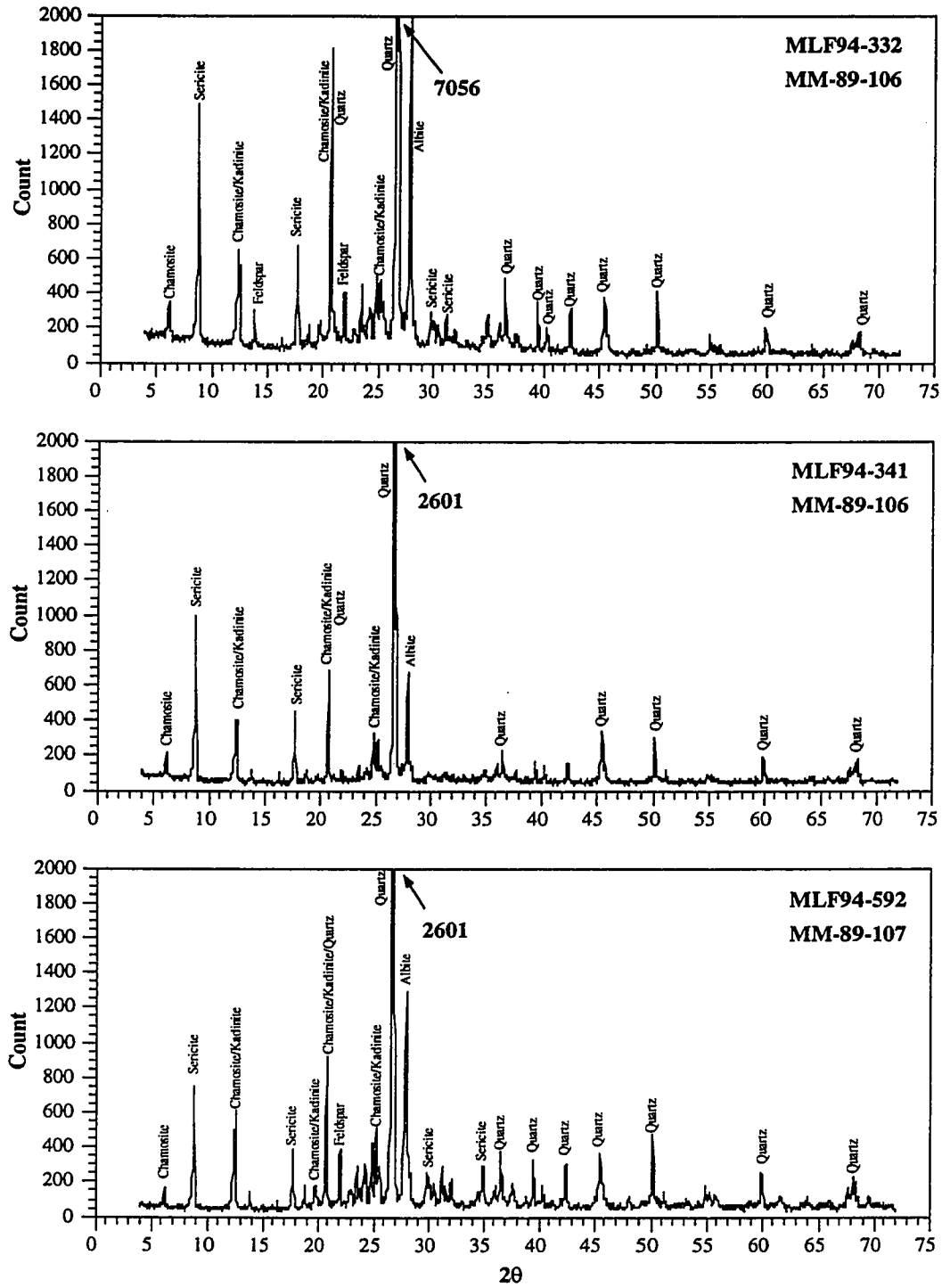


Fig. 9.7 XRD patterns for suspended sediment samples from Restigouche deposit groundwaters, distal from the main ore body.

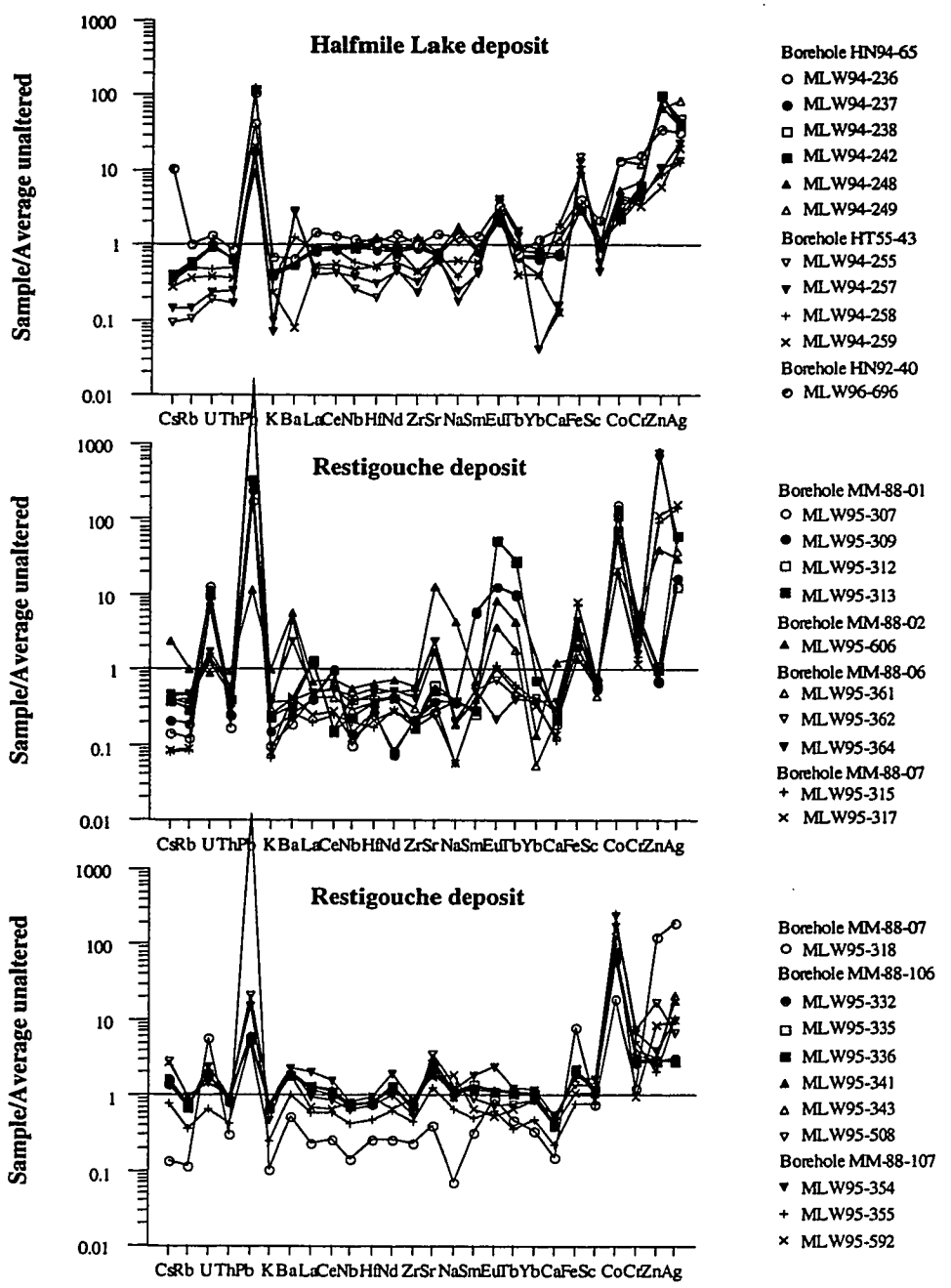


Fig. 9.8 Trace and major element contents of Halfmile Lake and Restigouche deposit borehole suspended sediments normalized to average unaltered felsic lithologies from the same deposit. Normalizing values are given in Chapter Two. Data from Table 9.2.

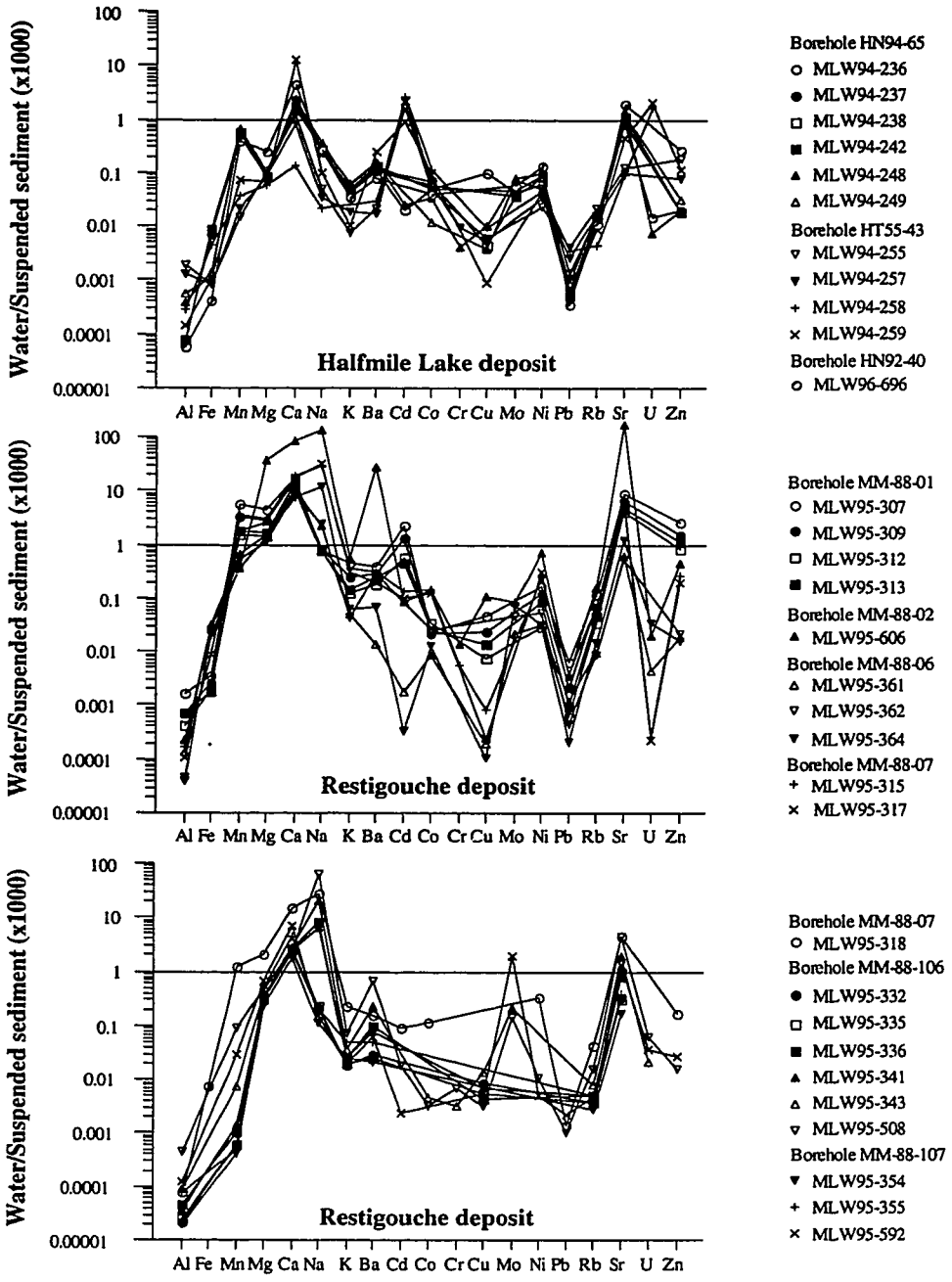


Fig. 9.9 Trace element contents of Halfmile Lake and Restigouche borehole groundwaters normalized to the corresponding suspended sediments.

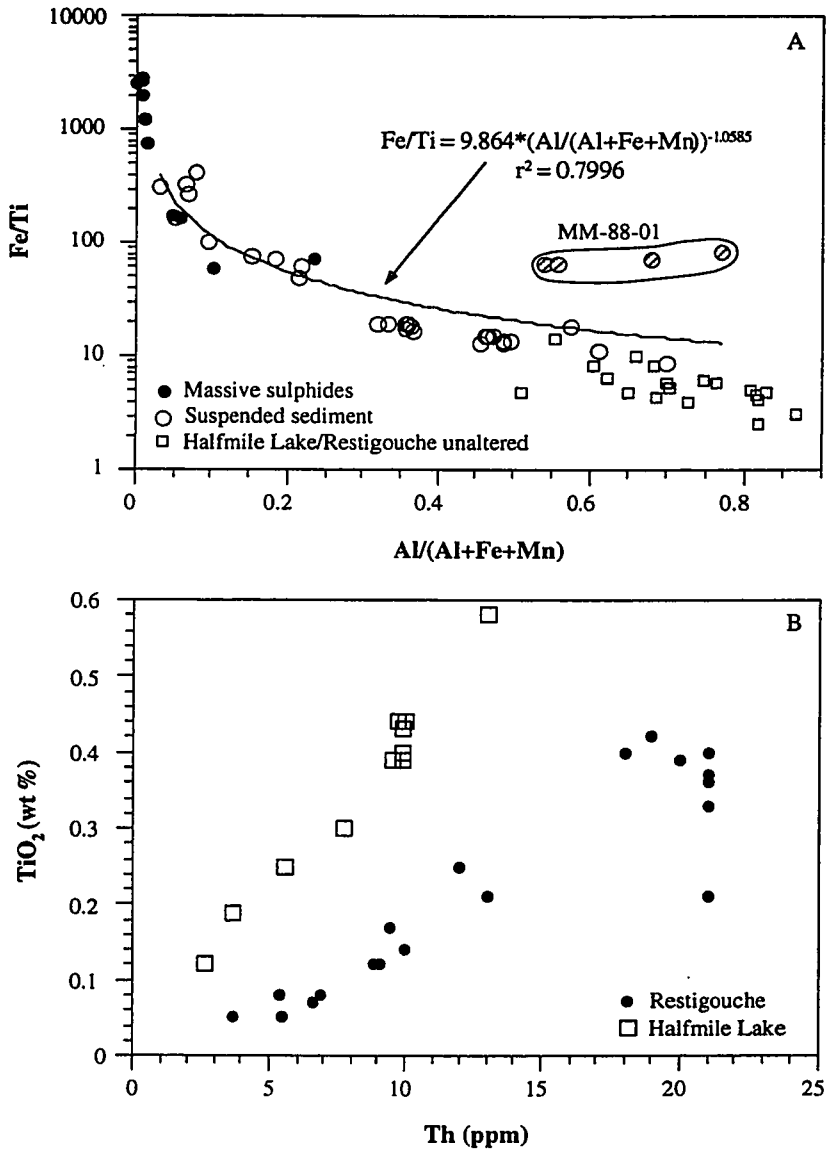


Fig. 9.10 A) Plot of Fe/Ti versus Al/(Al+Fe+Mn) for suspended sediments from Halfmile Lake and Restigouche deposit groundwaters. Also shown are the values for unaltered felsic host rocks and massive sulphide from the Halfmile Lake and Restigouche deposits. The suspended sediment data fit a power law curve. This curve is very similar to a best fit curve through iron formation samples proximal and distal to the Brunswick Belt massive sulphide deposits (Peter and Goodfellow 1993). Host rock and massive sulphide data from Table 2.2 and suspended sediment data from Table 9.2. The suspended sediments from borehole MM-88-01 have high base metal loads (high Fe, Zn) but also have anomalously high Al due to Al-oxides. Thus they do not fit the relationship well.
B) Plot of TiO_2 vs Th showing differences in source material for suspended sediments at the Halfmile Lake and Restigouche deposits.

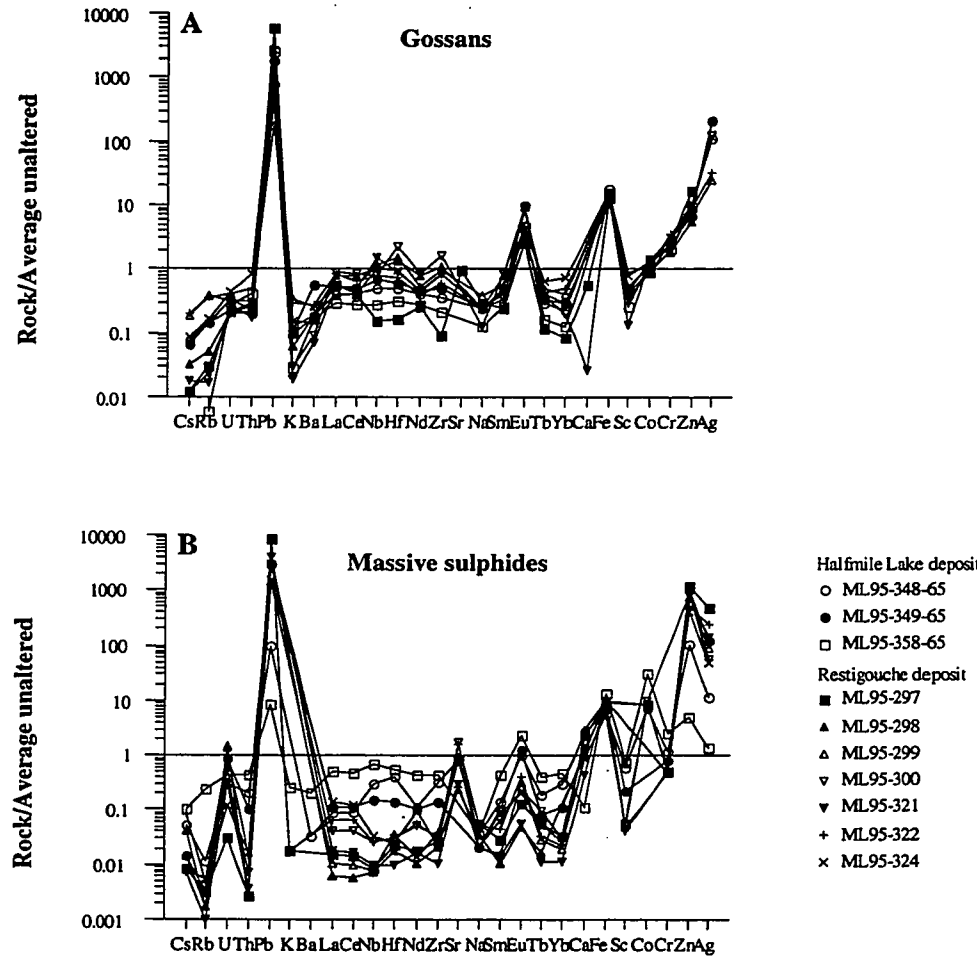


Fig. 9.11 A) Gossans from the Halfmile Lake deposit (D.R. Boyle, unpublished data) normalized to average unaltered Halfmile Lake deposit felsic rocks. B) Halfmile Lake and Restigouche deposit massive sulphides normalized to average unaltered Restigouche deposit felsic rocks. Felsic rock and massive sulphide data from Table 2.2.

CHAPTER TEN:

RARE EARTH ELEMENTS (REE) IN GROUNDWATERS, SURFACE WATERS AND SUSPENDED AND STREAM SEDIMENTS ASSOCIATED WITH MASSIVE SULPHIDE DEPOSITS, BATHURST MINING CAMP, NEW BRUNSWICK

10.1 Introduction

The rare earth elements (REE) are a useful complementary tool in trying to elucidate variations in the chemistry of aqueous systems because of the generally coherent and predictable behaviour of the REE (Byrne and Kim, 1990; Wood, 1990). The coherent behaviour of the REE, combined with their sensitivity to changes in pH, redox conditions and adsorption/desorption reactions, make the REE particularly useful in hydrogeochemical studies. The rare earth elements in aqueous systems are fractionated by a number of processes such as the type of complex formed, which is in large part controlled by the major ion chemistry, cation exchange reactions, adsorption and desorption reactions and transport by colloids (Gosselin et al., 1992). The use of REE as natural tracers requires an understanding of the extent to which these fractionation processes influence ground and surface water compositions. Because the REE typically behave coherently, perturbations from the expected patterns can yield critical information on the types of processes operating within an aqueous system. For example, Ce and Eu in some instances behave differently to the adjacent REE because of their greater sensitivity to changes in oxidation states. Thus, anomalies in these elements have implications regarding the present and/or past redox state of the system. In a recent study, Bau and Dulski (1996) found large positive Gd anomalies in rivers from Germany which were best explained by input of Gd tracers used in MRI (magnetic resonance imaging) from hospitals, whereas rivers from uncontaminated parts of Europe do not show this large anomaly. Recent studies of REE in natural waters have been justified on the grounds that the REE are good analogues for the behaviour of the trivalent actinide elements (Am, Cm, and

Cf) (Johannesson et al., 1996a). This understanding may help to improve prediction models for the movement of these species in groundwaters interacting with nuclear waste containment facilities.

Measurement of REE in aqueous systems has traditionally been hampered by detection limit problems due to typically low concentrations in natural waters. These problems have been alleviated in recent years by the advent of new analytical methods, in particular inductively-coupled plasma mass spectrometry (ICP-MS) (Hall et al., 1995b), and studies of REE in groundwaters and surface waters are now increasingly appearing in the literature. However, many of these studies are regional or global in scope, investigating the rare earth element mass balance between rivers and the oceans (e.g. Elderfield et al., 1990). Elderfield et al. (1990) noted that there was only a narrow range of REE patterns for rivers, independent of bedrock lithology, and suggested that aquatic chemistry rather than local bedrock controlled the distribution of the REE. Hall et al. (1995b) however, studied the REE chemistry of lakes in Newfoundland and found that the REE patterns were very similar to the REE patterns of lake sediments and that both typically reflected local geology. Part of the explanation for this discrepancy is that Elderfield et al. (1990) measured waters from major rivers which likely were more reflective of averaged geology over large drainage systems, rather than the more localized drainage studied by Hall et al. (1995b). The present study provides an opportunity to investigate the more detailed relationships between REE in groundwaters, surface waters, and weathering at the local catchment basin scale. In addition, REE were measured in stream sediments, suspended colloids in groundwaters trapped by the 0.45 μm filters, and host lithologies. These complementary data allow a better understanding of the partitioning of the REE between the dissolved, colloidal and bedrock reservoirs.

Some of the important questions to be addressed in this chapter are therefore: 1) to what extent do the REE contents of stream waters reflect the local lithologies at the catchment basin scale in the Bathurst Mining Camp (BMC), 2) what are the relationships between the REE compositions of groundwaters versus surface waters, 3) how are the REE speciated and

fractionated between waters, sediments and host lithologies, and 4) to what extent are solution/solubility important in controlling aqueous REE distributions? In order to address these questions, the REE were measured by ICP-MS on a subset of the waters collected in this study following pre-concentration and chelation extraction (see Chapter Three for analytical details). The major and trace elements of the surface waters and groundwaters have already been discussed in Chapters Five and Seven, respectively.

10.2 REE in Bathurst Mining Camp Waters

A total of 231 samples from the larger data set were analyzed for the REE; all but the saline waters were preconcentrated and analyzed by chelation-ICP-MS (Chapter Three). The most saline and Fe-rich waters (13 samples in total) were analyzed directly after dilution. In all, 224 samples had some REE above the detection limit, with La, Ce, Pr, Nd, Sm, Gd, Dy, Er and Yb more typically above detection than the other REE. In the following discussion, in order to assess variations in REE patterns between samples, the measured REE are normalized to North American Shale Composite (NASC). NASC-normalized cerium anomalies are expressed as:

$$[Ce/Ce^*]_{NASC} = Ce_{NASC} / \sqrt{(La_{NASC} \cdot Pr_{NASC})} \qquad (10.1)$$

and europium anomalies are expressed as:

$$[Eu/Eu^*]_{NASC} = Eu_{NASC} / \sqrt{(Sm_{NASC} \cdot Gd_{NASC})} \qquad (10.2)$$

Surface waters in the BMC typically have considerably higher La/Ce and lower Ce/Ce* anomalies compared to groundwaters from both the Halfmile Lake and Restigouche deposits and the mine waters. Almost all groundwaters have La/Ce < 1, whereas most surface waters, with the notable exception of some spring and seep waters have La/Ce > 1 (Fig. 10.1A). Restigouche deposit surface waters commonly have lower $[Ce/Ce^*]_{NASC}$ than Halfmile Lake deposit surface waters (Fig. 10.1B). Although there is considerable scatter, in a general sense ΣREE increases with decreasing pH (Fig. 10.2), a typical trend for REE in natural waters

(Elderfield et al., 1990). Total REE concentrations are highly variable, ranging from < 0.005 μg/L to 6,900 μg/L (Fig. 10.2). Although there is a good subdivision between the surface waters and groundwaters with respect to La/Ce, there is almost complete overlap between them in other REE ratios, e.g. La/Yb, Gd/Yb and Sm/Nd (Fig. 10.3). In a very general sense, Gd/Yb and Sm/Nd increase and decrease with increasing Nd, respectively. For waters where Cl < 1 mg/L, La/Ce is highly variable whereas at higher Cl concentrations, La/Ce defines a narrow range and typically less than unity (Fig. 10.4A). Halfmile Lake deposit borehole waters have higher total REE concentrations than Restigouche deposit groundwaters at equivalent Cl concentrations (Fig. 10.4B).

As noted, the surface waters typically have more pronounced negative Ce anomalies than the groundwaters relative to NASC, whereas, groundwaters and surface waters both possess some apparent negative Eu anomalies relative to NASC (Fig. 10.5). At least some of the Eu anomalies are likely to be analytical artifacts as Eu concentrations in many waters are close to or below the detection limit for Eu. Many previous studies have noted the association between Fe contents and total REE, due to adsorption of REE by Fe-Mn colloids (Elderfield et al., 1990). With the exception of Fe-rich waters associated with the Restigouche and Heath Steele ore bodies, there is a trend of increasing Fe with increasing ΣREE (Fig. 10.6A). There is also a trend of increasing Ce/Ce* with increasing Fe content for surface waters from both the Restigouche and Halfmile Lake deposits (Fig. 10.6B).

10.3 REE in Halfmile Lake Deposit Waters and Sediments

10.3.1 Surface waters

The REE contents of surface waters from the Halfmile Lake deposit are generally low, ranging from < 5 to 171 ng/l with two seeps containing 322 (sample MLW94-191) and 709 ng/l (sample MLW94-187) (Table 10.1). The majority of the surface waters have NASC-normalized REE patterns which display increasing slopes from the light REE (LREE) to the middle REE (MREE) and are generally flat from the MREE to the heavy REE (HREE) (Fig.

10.7). There is a slight convexity to the REE patterns; all samples have $[La/Sm]_{NASC} < 1$ and the majority of the waters have $[Gd/Yb]_{NASC} > 1$ ($[La/Sm]_{NASC}$ ranges from 0.19 to 0.84 with an average of 0.52 and $[Gd/Yb]_{NASC}$ ranges from 0.69 to 2.61 with an average of 1.33). This convexity is similar to that displayed by the associated stream sediments (see section 10.3.3). The degree of scatter in REE profiles increases with decreasing REE content reflecting lower analytical precision near the detection limits. With few exceptions, all surface waters have variable but pronounced negative Ce anomalies (Fig. 10.7), with $[Ce/Ce^*]_{NASC}$ as low as 0.08 and up to 2.26 (Figs. 10.8, 10.9). Only rare surface water samples lack negative Ce anomalies, and these are all seep and spring waters, with the exception of one sample from the West tributary which has a positive Ce anomaly. Cerium anomalies are not evident on NASC normalized profiles for some samples due to Ce being below detection (suggesting that these samples would have large negative anomalies if Ce were detectable). Seeps and springs have similar REE profiles to surface waters but differ in that they typically have no negative Ce anomaly. The positive Ce anomaly in sample MLW94-275 from the West tributary is probably real given that the La, Ce and Nd contents in this water are sufficiently above the detection limits. This sample was collected from a small stream entering the West tributary and was likely spring fed a short distance from the collection point.

Several samples show strong negative Eu anomalies. The apparently small number of Eu anomalies reflects the limited number of surface water samples with detectable Eu (Figs. 10.5 and 10.7). Of those with detectable Eu, the seeps from Upper/Lower AB stream (Fig. 10.8A) have the largest negative anomalies. These seeps have relatively high REE contents indicating that the Eu anomalies are real features of these waters rather than analytical artifacts.

There are differences in the REE patterns and REE ratios between the different stream segments (as defined in Chapter Three) which cannot easily be related to variations in the underlying lithologies (Fig. 10.8). The Halfmile North stream has the largest negative Ce anomalies and therefore the largest La/Ce ratios of any of the surface waters at the Halfmile Lake deposit. This is also evident from the spatial distribution of Ce/Ce* (Fig. 10.8B) where

samples from Halfmile North stream and the North tributary stream have the lowest values. In contrast, waters from the Upper/Lower AB and West tributary streams have much higher ratios. Total REE contents also vary between streams, and along streams. The Upper/Lower AB stream has elevated REE contents at the upstream and downstream ends due to REE-enriched seeps (Fig. 10.8A) and REE contents in the middle portion of the stream decrease downstream. This portion of the stream was influenced by an Fe-rich artesian borehole at the time the samples were collected. A decrease in REE contents may be related to adsorption of the REE onto Fe-oxide colloids associated with the borehole waters. However, stream sediments from this portion of the Upper/Lower AB stream are also low (see section 10.3.3 below), suggesting that base-flow dilution is controlling the concentration of the REE. The low REE contents in the upper part of the North tributary stream suggests that there is removal of REE from solution. The three streams which join the North tributary all have more elevated REE concentrations (Fig. 10.8A). The Upper/Lower AB and West tributary streams have the lowest La/Yb and Gd/Yb ratios and are the least depleted in Ce/Ce* (Fig. 10.8).

The sample from the surface of Halfmile Lake (sample MLW94-284) has only a small negative Ce anomaly but has a pronounced convex-up pattern with low $[La/Sm]_{NASC}$, and high $[Gd/Yb]_{NASC}$ and $[La/Yb]_{NASC}$ (Figs. 10.7, 10.8). The sample from the Northwest Miramichi River has relatively high total REE (171 ng/L) and a moderately negative Ce anomaly.

Statistically, the REE are well correlated with one another although the degree of correlation decreases with increasing atomic number, with the exception of Ce. Cerium shows poor correlations with all other REE, consistent with Ce being controlled by different processes. The REE are generally not well correlated with other chemical parameters, although positive correlations exist between ΣREE and Rb and K ($r = 0.433$ and 0.478, respectively), suggesting that elevated REE contents may in part be controlled by lithology or proximity to alteration minerals associated with the Halfmile Lake ore body. The highest correlation ($r = 0.813 - 0.940$) exists between all REE (except Ce) and Y (Table D.2). Conversely, Ce and Ce/Ce* are well correlated with Al, Mn, Fe and Co (e.g. log(Ce) correlations are $r = 0.735$,

0.623, 0.671, and 0.740 for these elements) and are poorly correlated with Y, Rb, and K. The correlation between Eh and the REE is highest for Ce of all the REE; for log(Ce) vs log(Eh), the Pearson Product Moment correlation is r = -0.434 which, given 34 degrees of freedom, is statistically significant at the 95% confidence interval. The positive correlations of Ce with redox sensitive species Fe, Mn and Co indicates that Ce anomalies in surface waters are, at least in part, redox controlled. The correlation between Al and Ce can be explained by the preferential loss of Ce through adsorption onto colloidal material. One of the principal colloids in natural waters is Al-oxides. SEM data of suspended colloids in Halfmile Lake deposit borehole waters suggest that this fraction is dominated by aluminosilicates. Thus, inter-element correlations (e.g. Ce/Ce* vs Gd/Yb) emphasize the fact that Ce is essentially decoupled from the rest of the REE in Halfmile Lake deposit surface waters.

10.3.2 Groundwaters

The most striking feature of the REE patterns of Halfmile Lake deposit groundwaters is that they are in many respects distinct from the associated surface waters (Figs. 10.1, cf 10.7 and 10.10). NASC-normalized REE patterns for Halfmile Lake groundwaters vary very slightly from LREE-enriched to highly LREE depleted with dish-shaped concave-up profiles between the LREE and the MREE (Fig. 10.10). Many samples show a slight upward convexity about the MREE resulting in $[La/Sm]_{NASC} < 1$ and $[Gd/Yb]_{NASC} > 1$ (Figs. 10.10, 10.11). Several samples from boreholes HN94-65 and HT55-43 have relatively flat patterns from La to Eu, with progressive depletion from Gd to Yb. The sample from the top of borehole HT55-43 has the highest REE concentrations (ΣREE = 1816 ng/L) yet waters from this hole have the lowest TDS of all waters from the Halfmile Lake deposit (TDS = 8 to 22 mg/L). This hole is located in the Upper AB zone and intersects the gossan (see Chapter Two). These waters were rich in suspended Fe-oxyhydroxides when sampled (see section 10.7 below), and there is likely an association between high contents of suspended Fe-oxides and high REE contents (cf Fig. 10.6A). Iron contents in these waters are moderately high ranging from 130 to 1200 µg/L. The

Fe and Mn contents of the two samples from HT55-43 which were analyzed by both ICP-MS methods (see Chapter One for methodologies) are Fe = 130 and 132 μg/L, Mn = 25 and 25.7 μg/L for sample MLW94-256 and Fe = 320 and 324 μg/L, Mn = 110 and 116 μg/L for sample MLW94-259 (Table A.4). These values are very similar, despite the differences in analytical technique.

The groundwaters typically lack consistently negative NASC-normalized Ce/Ce* anomalies like the surface waters, and values range from 0.55 to 1.41, and most close to unity (Table 10.2; Fig. 10.1, 10.6, 10.10). The magnitude of the negative Ce anomalies is small compared to the surface waters from the same area; the average $[Ce/Ce^*]_{NASC}$ value is 0.51 for all Halfmile Lake deposit surface waters and 0.95 for all Halfmile Lake deposit borehole waters. Groundwaters waters typically possess small negative Eu anomalies, for samples with detectable Eu (Fig. 10.10).

Despite the overall relative chemical uniformity of Halfmile Lake deposit groundwaters compared to Restigouche deposit groundwaters (Chapter Seven) there are significant variations in REE patterns with depth. For example, borehole HN87-8 shows very consistent changes with depth. In this hole $[La/Sm]_{NASC}$ and $[La/Yb]_{NASC}$ increase systematically with depth from 0.18 to 0.84 and from 0.16 to 1.28, respectively whereas Sm/Nd decreases downhole (Table 10.2; Fig. 10.11). The REE patterns of the three deeper samples are distinct from the shallower samples such that the latter are depleted in the LREE with pronounced dish-shaped concave-up profiles in the LREE. The deeper samples show flatter patterns overall (Fig. 10.10). The change in REE patterns downhole and variations in REE ratios are coincident with an increase in the ΣREE from < 100 ng/L to 170 - 490 ng/L (Table 10.2; Figs. 10.10, 10.11). There is no apparent trend in Ce anomaly with depth, all waters have only slight negative Ce anomalies with $[Ce/Ce^*]_{NASC}$ ranging from 0.71 to 0.96. The downhole trends of increasing total REE, La/Yb and La/Sm and decreasing Sm/Nd observed in HN87-8 are also evident, though less pronounced, in boreholes HN94-50, HN94-65, and HN94-51 (Fig. 10.11A). The concave-up dish pattern evident in the samples < 450 m in depth in borehole HN87-8 is also observed for

all samples from borehole HN94-55 and from the more shallow groundwaters in boreholes HN92-40, HN94-50 and HN94-82 (Fig. 10.10).

The groundwaters at the Halfmile Lake deposit generally show poor correlations with most other elements although there are some exceptions. For example, there are good correlations between total REE and Al and Ti. The correlation of total REE with Eh and Fe is greater than with pH (Fig. 10.6). There is also a moderate correlation between $[La/Yb]_{NASC}$ and ΣREE (Fig. 10.11). Samples with $[La/Yb]_{NASC} > 1$ have higher total REE and tend to have REE patterns more similar to host lithologies.

10.3.3 Stream sediments

Stream sediment samples from the Halfmile Lake deposit were analyzed in two splits; < 63 μm and < 125 μm size fractions (see Chapter Six for discussion of major and trace element variations). For the REE, the differences in abundances between the two size fractions are typically small (3 - 20% variation, mean ranges from 0.001 to 3.3%). The LREE and MREE (La to Ho) are, on average, weakly partitioned into the larger size fraction whereas there is no consistent fractionation of the HREE into either size fraction. The REE profiles shown represent the average for the two size fractions (Fig. 10.12).

The rare earth element patterns for stream sediments from the Halfmile Lake deposit are similar to North American Shale Composite (NASC) with all samples within 0.5 and 5 times NASC (Fig. 10.12). All samples have remarkably uniform profiles although there are some minor variations between streams. For example, samples from the Halfmile North stream typically show a more convex-up pattern centred on the MREE than sediments from the other streams. This is indicated by generally higher $[Gd/Yb]_{NASC}$ and lower $[La/Sm]_{NASC}$ than sediments from other streams. The Halfmile North stream also has the highest total REE contents (Fig. 10.13A; Table 10.3) and the largest $[Ce/Ce^*]_{NASC}$ anomalies (Fig. 10.13B). This is similar to the water data where the Halfmile North stream has the largest "dissolved" load $[Ce/Ce^*]_{NASC}$ anomalies (Fig. 10.8D). The REE contents of Upper/Lower AB stream

sediments are highly variable with elevated contents at the upper and lower ends of the stream reflecting the influence of seeps with elevated REE (cf Figs. 10.8A and 10.13A). This stream segment also has the flattest REE patterns, the lowest La/Yb and the smallest Ce anomalies of all the sediments in streams draining the Halfmile Lake deposit area (Fig. 10.13). The Northeast tributary has the lowest total REE contents overall and moderate $[La/Yb]_{NASC}$ and negative Ce anomalies. The North tributary near the confluence of the other streams is moderate in all parameters reflecting the mixing of sediments from the other three streams (Fig. 10.13). One sample along the middle portions of this stream is anomalously low in all characteristics suggesting either the influx of an unobserved seep/spring or the influence of organic matter; this segment of the stream has numerous swamps.

The positive Ce anomaly in sample MLS94-185 may be related to the development of negative anomalies in surface waters (see discussion). This sample is from a seep with large negative Ce anomalies in the water. Although the other seep waters on the Upper/Lower AB stream do not have negative Ce anomalies, nearby stream waters have large negative anomalies. The high Ce in this stream sediment therefore likely represents preferential removal of Ce, compared to the other REE, from surface waters. However, this must be largely a local effect as most of the stream sediments have small negative Ce anomalies. This would suggest that the loss of Ce through preferential adsorption onto colloidal material or direct exchange with stream sediment material is not, in a bulk chemical sense, progressive along the stream course, but rather restricted to near the point of discharge of groundwaters into streams.

Stream sediment NASC-normalized REE patterns are similar to the host rocks (cf Figs. 10.12 and 10.14); REE abundances for stream sediments and host rocks are also similar. As with many of the host rocks, the sediments are characterized by small negative Eu anomalies, and the largest anomalies are in the sediments from the Upper/Lower AB stream. The stream sediments differ from the host lithologies in that the negative Ce anomalies of the stream sediments is evident in the NASC-normalized plots but absent in whole rock plots (Fig. 10.14).

10.3.4 REE in host metavolcanic and metasedimentary rocks

In this study, a series of samples were selected from borehole HN94-65 (Fig. 10.14). Additional REE data for Halfmile Lake deposit host rocks are available from Adair (1992). The samples analyzed in this study are representative of the major felsic and mafic volcanic lithologies, metasedimentary units and massive sulphides. Most samples have generally flat profiles relative to NASC with essentially no Ce anomalies ($[Ce/Ce^*]_{NASC}$ varies from 0.88 to 1.14; Table 10.4). Samples analyzed in this study exhibit generally negative Eu anomalies (0.103 - 0.693) with the exception of mafic rocks (0.793 to 1.52) and massive sulphides (2.17 - 4.95) which have generally positive Eu anomalies. Some of the sulphide and related argillite lithologies have significant to very large positive Eu anomalies, a typical pattern for massive sulphides due to the redox conditions of the hydrothermal fluids (Klinkhammer et al., 1994a; Klinkhammer et al., 1994b). The most REE depleted samples are the massive sulphides which also show the most extreme depletion in the HREE (Fig. 10.14). The negative Eu anomalies shown by the felsic and sedimentary units are larger than those of the stream sediments. The overall patterns displayed by the metavolcanic and metasedimentary units are similar to the deeper groundwaters at the Halfmile Lake deposit (cf Figs. 10.10 and 10.14). mafic rocks show two different trends. Samples ML95-323-65 and ML95-324-65 have strongly LREE depleted patterns typical of tholeiitic rocks. The other mafic samples have patterns similar to the felsic rocks.

10.4 REE in Restigouche Deposit Waters and Sediments

10.4.1 Surface waters

The surface waters at the Restigouche deposit have generally low abundances of the REE ranging from 3.3 ng/L total REE to 311 ng/L. The average REE content is 124 ng/L, compared to 104 ng/L for Halfmile Lake deposit surface waters. However, if sample MLW95-300 is removed, the average for Restigouche deposit surface waters falls to 87 ng/L. All Restigouche deposit surface waters, normalized to NASC, are LREE depleted with positive slopes from the

LREE to the MREE and flat to downward slopes from the MREE to the HREE (Fig. 10.15). $[La/Sm]_{NASC}$ ranges from 0.089 to 1.488 with an average of 0.498 and $[Gd/Yb]_{NASC}$ ranges from 0.478 to 3.063 with an average of 1.596. Cerium anomalies are ubiquitous for those samples for which Ce is above the detection limit (Fig. 10.15). The Ce/Ce* anomalies are, on average, lower than Halfmile Lake deposit surface waters (Fig. 10.1B) (average = 0.329 at Restigouche deposit vs 0.509 at Halfmile Lake deposit).

The highest REE contents occur in streams near the small gossan outcrop at the confluence of Mt Vroom north and Charlotte Brook streams, suggesting some influence of low pH waters associated with the sulphide outcrop (e.g. the seep in the gossan has a pH of 2.87 and the highest REE contents for Restigouche deposit surface waters; Table 10.5). High REE concentrations are also associated with North stream and with lower pH waters along Mt Vroom SE stream (Fig. 10.16). The highest REE contents in the North stream are adjacent to the main massive sulphide body of the deposit and may reflect greater mobilization of the REE from altered rocks hosting the mineralization. REE concentrations are lower downstream from the Restigouche deposit in Charlotte Brook compared to the Mt Vroom north and North streams indicating dilution after mixing of the different streams; REE concentrations are amongst the lowest in the area in Charlotte Brook upstream from the orebody (Fig. 10.16A). The low REE contents in the upper part of Charlotte Brook are associated with relatively organic-rich stream sediments, suggesting that the REE contents in the waters may in part be controlled by complexation by organic matter. Total REE contents are also very low in Mt Fowler east stream, despite the high TDS values, low pH, and high sulphate concentrations in this stream (Chapter Five). This stream was notable for the very high Fe-oxide loads in the stream sediments suggesting rapid removal of the REE from solution through adsorption processes (see discussion). In contrast, Mt Vroom northeast and Mt Vroom east streams are distinctive in that they have very low TDS contents but have moderately elevated REE abundances (Table 10.1). These elevated REE contents are coincident with low pH and high dissolved Al contents. The Mt Vroom east stream has low pH and high REE and also has the

lowest La/Yb indicating a preferential loss of the LREE relative to the HREE compared to streams with high La/Yb. The Mt Vroom east stream also has the smallest Ce anomalies; the low pH inhibits preferential loss of Ce through adsorption onto inorganic colloids. The Mt Vroom east also has consistently low $[Gd/Yb]_{NASC}$. Most of the surface waters have normalized Gd/Yb > 1 whereas the Mt Vroom east stream has values < 1, suggesting that the convex-up shape is a function of relative REE solubility. However, Mt Vroom northeast stream, which also has high REE and low pH, typically has large negative Ce anomalies and moderate to low La/Yb. It is interesting to note that sample MLW9-467, which has the smallest Ce anomaly along the stream and is thus most like the waters in Mt Vroom east, is also the sample with anomalous non-radiogenic (ore) Pb (see Chapter Twelve). Waters from the upstream end of Mt Vroom north stream share many common characteristics with other Mt Vroom streams including low pH, conductivities, La/Yb, Gd/Yb and high ΣREE (Fig. 10.16).

There appears to be an association between the REE profile and thus fractionation of the LREE from the HREE, relative rare earth element concentrations, pH and sulphide mineral potential. Where sulphides are undergoing oxidation in the subsurface, sulphate will be released resulting in a reduction in pH, which facilitates greater mobilization of the REE and inhibits the preferential removal of the Ce through adsorption onto Fe-oxides. The streams west of the deposit have pH values < 7.00 and have moderate REE contents and low Ce anomalies. These streams also have anomalous base metal contents which may suggest mineralization west of the Restigouche deposit (see Chapter Thirteen for further discussion).

Inter-element correlations are similar to the Halfmile Lake deposit surface waters in that the REE are generally poorly correlated with other chemical parameters, except Y. Cerium has the poorest correlation with Y, reflecting the decoupling of Ce from the rest of the REE. Although the REE are generally poorly correlated with pH, there is a general trend of increasing REE contents with decreasing pH (Fig. 10.17; r = -0.273 for Pearson Product and -0.362 for Spearman Rank correlations, respectively) and with increasing Al (r = 0.681). There is a very strong correlation between $[La/Yb]_{NASC}$ and $[Gd/Yb]_{NASC}$ but only a moderate correlation

between $[La/Sm]_{NASC}$ and $[Gd/Yb]_{NASC}$ (Fig. 10.17). There are good correlations between Ce/Ce* and Mn (Fig. 10.17; r = 0.505 with 48 degrees of freedom), Co (Fig. 10.17; r = 0.551 with 42 degrees of freedom) and with Fe (Fig. 10.6B; r = 0.443 with 31 degrees of freedom) and SO_4^{2-} (r = 0.434 with 48 degrees of freedom).

10.4.2 Groundwaters

In general, Restigouche deposit shallow groundwaters have REE patterns that are variable but more similar to local surface waters than was the case for the Halfmile Lake deposit. As shown in Chapter Seven, the groundwaters from the Restigouche deposit span a very large compositional range in major cations and anions. The range in REE is more restricted, varying from 5.4 ng/L to 240 ng/L with an average of 65.9 ng/L. These values are much lower than for the Halfmile Lake deposit groundwaters despite higher TDS in Restigouche deposit groundwaters (Chapter Seven). Halfmile Lake deposit groundwaters have lower average pH which may be important in accounting for the differences in REE abundance between the two deposits (see discussion).

Compared to NASC, most Restigouche deposit groundwaters display REE patterns with positive slopes from the LREE to the MREE with $[La/Sm]_{NASC}$ ranging from 0.23 to 2.08; the average value is 0.63. REE slopes from the MREE to the HREE are variable but generally flat; $[Gd/Yb]_{NASC}$ ranges from 0.38 to 3.11, with an average slope of 1.25 (Fig. 10.18). Exceptions to the LREE depleted nature of the groundwaters are waters from borehole MM-88-06, and to a lesser extent from borehole MM-88-07, which show concave-up patterns from La to Gd (Fig. 10.18). As with Halfmile Lake deposit groundwaters, Ce anomalies are poorly developed compared to the local surface waters. The $[Ce/Ce^*]_{NASC}$ varies from 0.19 to 1.15 (Table 10.6), with an average of 0.73. However, the low end of the range is found in the two samples from the shallow borehole EH-1. Excluding these two samples gives a range of 0.48 to 1.15 with an average of 0.82, closer to the Halfmile Lake deposit average of 0.95, and considerably higher than the surface water average of 0.33 at the Restigouche deposit. Note

that the two boreholes closest to where sulphides outcrop, MM-88-06 and MM-88-07, have high dissolved sulphate loads, high suspended sediment loads and low Ce anomalies. These samples are also distinct from other Restigouche deposit groundwaters in that they have $[La/Yb]_{NASC}$, $[La/Sm]_{NASC}$ and $[Gd/Yb]_{NASC} > 1$ (Fig. 10.19). A few samples show small negative Eu anomalies (Fig. 10.18).

As a group the Restigouche deposit borehole waters show no correlation with pH (Fig. 10.19). However, the deeper more saline waters show a trend of decreasing REE with increasing pH and this trend is somewhat independent of TDS. The shallow groundwaters show a similar trend, though displaced to lower total REE (Fig. 10.2A, 10.19).

10.4.3 Stream sediments

Stream sediments from the Restigouche deposit show broadly similar REE patterns to those from the Halfmile Lake deposit. Most Restigouche deposit sediments have REE abundances between 0.5 and 5 times NASC, except three samples from Mt Fowler E stream which have LREE abundances < 0.5 times NASC (Fig. 10.20). In detail, however, there are differences between streams and between the two deposits.

Most of the stream sediments have a somewhat more convex-up REE patterns than Halfmile Lake deposit stream sediments. The stream sediments from the Restigouche deposit have identical $[La/Yb]_{NASC}$ (average = 0.95) as Halfmile Lake deposit sediments but have lower $[La/Sm]_{NASC}$ (0.71 versus 0.84) and higher $[Gd/Yb]_{NASC}$ (1.55 versus 1.26). Restigouche deposit stream sediments also typically have more negative Ce (0.73 versus 0.86) and Eu (0.78 versus 0.90) anomalies.

There are some variations between streams. Downstream of the main deposit, Charlotte Brook sediments exhibit very uniform REE patterns, ratios and overall REE abundances (Figs. 10.20, 10.21). An exception is that immediately downstream of the deposit, sediments in Charlotte Brook have lower $[Gd/Yb]_{NASC}$, which then increases downstream (Fig. 10.21). Sediments upstream of the deposit typically have lower REE abundances, higher $[Ce/Ce^*]_{NASC}$

and lower $[La/Yb]_{NASC}$ and $[Gd/Yb]_{NASC}$ (Fig. 10.21).

Generally elevated REE abundances are shown for Mt Fowler SW, Mt Vroom E, and Mt Vroom NE streams. Sediments from Mt Fowler E stream have decreasing LREE abundances upstream to where Fe-rich seeps enter the stream from the stream bed. Further upstream of the seeps, REE abundances are higher and REE patterns more similar to the other sediments. Sediments from Mt Vroom E stream have generally flat to slightly LREE-enriched patterns with minimal convexity in the MREE ($[Gd/Yb]_{NASC}$ is low; Table 10.7). Mt Fowler SW stream sediments have moderately high REE contents but are quite fractionated compared to NASC with low $[Ce/Ce^*]_{NASC}$, high $[Gd/Yb]_{NASC}$ and low $[La/Yb]_{NASC}$ (Fig. 10.21).

10.4.4 REE in host metavolcanic and metasedimentary rocks

A number of samples from borehole MM-88-02 and MM-88-16 that intersect the deposit and borehole MM-89-106 to the east of the deposit were analyzed for their REE content (Table 10.8). Some of the samples were selected to represent altered equivalents of fresh material. Analyzed samples include the host felsic metavolcanic units as well as mafic sills, massive sulphides, and intensely carbonate altered/veined metavolcanic rocks. Less altered felsic metavolcanic rocks typically have higher REE contents than those from the Halfmile Lake deposit. For example, least altered felsic volcanic rocks from the Halfmile Lake deposit have average $\Sigma REE = 182$ ppm, $[La/Yb]_{NASC} = 0.90$, $[Gd/Yb]_{NASC} = 1.02$, $[La/Sm]_{NASC} = 0.91$ and $[Eu/Eu^*]_{NASC} = 0.34$. In contrast, least altered felsic units from the Restigouche deposit have average $\Sigma REE = 336$ ppm, $[La/Yb]_{NASC} = 1.16$, $[Gd/Yb]_{NASC} = 1.24$, $[La/Sm]_{NASC} = 0.88$ and $[Eu/Eu^*]_{NASC} = 0.41$.

Europium anomalies are ubiquitous (average = 0.399) with the exception of highly carbonate altered rocks, mafic sills, and massive sulphides which tend to have positive to highly positive Eu anomalies (Fig. 10.22). Two stringer zone sulphide samples from borehole MM-88-02 have strong negative Eu anomalies, in contrast to the massive sulphide samples. Mafic rocks have LREE depleted patterns and lower overall REE abundances compared to the

felsic volcanic rocks. Massive sulphide samples have the lowest REE abundances (Fig. 10.22).

10.5 REE in Other Waters in the BMC

Waters from the other deposits studied are quite variable in total REE content and REE patterns, reflecting the wide range in major and trace element compositions and location of these waters (Fig. 10.23). Total REE contents vary from < 0.005 μg/L to 690 μg/L. The highest REE contents are from groundwater samples from the Heath Steele deposit (Table 10.9; Fig. 10.2A). The lowest REE contents occur in waters from Stratmat Main Zone borehole S61-19, despite high sulphate contents, and from shallow groundwaters at the Heath Steele deposit (< 100 m depth). Waters of variable, though generally low, pH from deeper in the Heath Steele mine, from Brunswick #12 mine, and from Fe-rich waters at the Wedge deposit have the highest REE abundances (Fig. 10.23).

Waters least enriched in REE display LREE-depleted profiles, with $[La/Sm]_{NASC}$ varying from 0.23 to 15.92. The extreme enrichment of La over Sm occurs in a sample from the ore zone in Stratmat Main Zone deposit borehole S61-19. Removing that sample gives a range of 0.23 to 2.05 with an average of 0.67. The $[Gd/Yb]_{NASC}$ of mine waters varies from 0.61 to 3.97 with an average of 1.51. Some of the waters have negative Ce anomalies, although many samples had non-detectable La or Ce (Table 10.9). For those samples with detectable La, Ce and Pr, the average $[Ce/Ce^*]_{NASC}$ anomaly is 0.84, similar to Restigouche deposit groundwaters. Several waters adjacent to the main ore zone at Heath Steele have strong positive Eu anomalies, similar to anomalies for massive sulphides from the Halfmile Lake and Restigouche deposits. The waters from Stratmat Main Zone deposit borehole ST61-19 have very unusual REE patterns with highly elevated La compared to the other LREE (Fig. 10.23). These waters are dominated by sulphate and for the most part the REE are near or below detection. SEM analyses indicate the presence of either a mixture of quartz and an Al-Fe-sulphate mineral, such as alunite, or a complex intergrowth of an aluminosilicate with Fe-

sulphate. It is likely that this mineralogy is influencing the relative solubilities of the LREE.

10.6 REE in Suspended Sediments

Thirty one samples of filtrate were analyzed by ICP-MS for the trace elements and rare earth element contents (Table 10.10; see Chapter Nine for discussion on major and trace element variations). Of critical importance is the comparison in the shape of the REE profiles in the suspended sediments compared to the waters. For example, one of the points of debate in the recent literature relates to the importance of REE-phosphate species in natural waters (Byrne and Liu, 1996; Johannesson et al., 1996b). It is perhaps important that rare REE phosphate minerals were identified by SEM in one sample of suspended sediment (MLW95-504) (Fig. 9.6). Unfortunately, there was insufficient suspended sediment to carry out P analyses.

The suspended sediment REE profiles are variable, reflecting the variation in mineralogy (Chapter Nine) and in the variation in the REE contents of the groundwaters with which they are associated. The suspended sediments from the Halfmile Lake deposit (three boreholes) show less variation ($[La/Sm]_{NASC}$ ranges from 0.80 to 1.01, $[La/Yb]_{NASC}$ from 0.91 to 2.29 and $[Gd/Yb]_{NASC}$ from 0.77 to 1.74) in the REE profiles and contents than those from the Restigouche deposit ($[La/Sm]_{NASC}$ ranges from 0.29 to 1.01, $[La/Yb]_{NASC}$ from 0.15 to 1.94 and $[Gd/Yb]_{NASC}$ from 1.10 to 2.07). The suspended sediments from the Halfmile Lake deposit have only very minor Eu and Ce anomalies (Eu/Eu* ranges from 0.90 to 1.11, with one sample at 1.84, Ce/Ce* ranges from 0.91 to 0.99). Suspended sediments from the Restigouche deposit are more variable (Eu/Eu* ranges from 0.19 to 0.96, Ce/Ce* ranges from 0.37 to 0.98).

Compared to NASC, suspended sediments from Halfmile Lake deposit borehole HN94-65 have very flat REE profiles with no Ce or Eu anomalies (Fig. 10.24). In contrast, suspended sediments from borehole HT55-43 which penetrates the gossan at the Upper AB zone of the Halfmile Lake deposit has relatively flat patterns from La to Sm and more depleted concave up profiles from Gd to Lu (Fig. 10.24). In both cases, the suspended sediments are similar in

general shape to the corresponding waters. In contrast, waters from boreholes at the Restigouche deposit have REE patterns which show greater differences compared to the corresponding suspended sediment. For example, suspended sediments from borehole MM-88-06 have flat LREE profiles and are slightly HREE depleted compared to the MREE. Waters from this borehole have convex-up REE profiles from the LREE to the MREE and are generally HREE-enriched. Suspended sediments from borehole MM-88-07 display convex-up REE profiles with no Eu or Ce anomalies whereas the corresponding waters have small negative Ce anomalies and, like the waters from borehole MM-88-06, have convex-up LREE profiles and are HREE-enriched. The REE patterns displayed by suspended sediments from borehole MM-89-106 are antithetical to the waters; the sediments have LREE/HREE > 1 and have significant negative Eu anomalies and slight negative Ce anomalies, whereas, the groundwaters are LREE depleted compared to NASC. Suspended sediments from borehole MM-89-107 are similar in pattern to MM-89-106. The REE contents of the groundwaters from this borehole are so close the detection limits that it is difficult to assess their relationship to the suspended sediments. Shallow groundwaters from boreholes EH-1, B-80-1 and MM-88-01 are all similar in that they are LREE-depleted compared to NASC and negative Ce anomalies are developed in some of these waters (Fig. 10.18). The suspended sediments from borehole MM-88-01 are broadly similar in that they also have LREE-depleted profiles, flatter from the MREE to the HREE. In addition, they have strong negative Ce and Eu anomalies.

The suspended sediments from boreholes MM-88-06 and MM-88-07 at the Restigouche deposit have different REE patterns despite many similarities in the chemistries of the waters from these boreholes. The suspended sediments from borehole MM-88-07 have lower La/Yb and La/Sm, higher Gd/Yb, and lower REE abundances than the borehole MM-88-06 sediments. The MM-88-07 sediments also have higher Fe and lower Al, K, Ca, Mg, and base metal contents (Chapter Nine).

For some of the suspended sediments, the corresponding water was also analyzed for the REE (Fig. 10.25). Some water-sediment pairs show relatively flat patterns indicating little

fractionation between the water and the sediment. Flat patterns exist for waters samples with elevated REE from the Halfmile Lake deposit. At lower total REE contents (lower water/sediment) there tends to be greater fractionation of the LREE, though generally less so for La than for Ce, Pr, and Nd (Fig. 10.25).

For the Restigouche deposit water-sediment pairs, the flattest patterns are exhibited by borehole MM-88-07 samples. The other samples show variable LREE depletion indicating that the waters are depleted in the LREE (especially Ce, Pr, Nd) relative to the suspended sediments.

10.7 Discussion

One of the critical questions in studies of natural waters is whether REE concentrations are controlled by the source or solubility considerations. Various recent studies of the REE in aqueous systems have shown that both the source and the style of REE-complexation can be variably important depending on the nature of the system.

Rare earth element concentrations in BMC waters are up to 690 μg/L, which is higher than REE abundances in groundwaters from the Carnmenellis Granite which reached 229 μg/L (Smedley, 1991), but lower than groundwaters associated with a U mine in Brazil where REE contents reached 29,000 μg/L (Miekeley et al., 1992b). The surface waters in this study have concentrations on the same orders of magnitudes as major river waters (Elderfield et al., 1990).

10.7.1 Origin of the REE in BMC groundwaters

One of the more striking features of BMC waters are the differences in REE patterns displayed by groundwaters from the Halfmile Lake and Restigouche deposits. These differences are in sharp contrast to the general similarities in REE abundances and patterns expressed by the surface waters from both deposits. Most of the deeper groundwaters from the Halfmile Lake deposit have flat to LREE enriched patterns normalized to NASC and patterns similar in shape to local felsic rocks (Fig. 10.10, 10.14). In contrast, groundwaters from the

Restigouche deposit have LREE-depleted patterns compared to NASC (Figs. 10.18, 10.22), generally different from the host lithologies. These differences may in part be a function of the generally higher pH values observed for Restigouche deposit groundwaters compared to Halfmile Lake deposit groundwaters (Fig. 10.1). It is well established (Elderfield et al., 1990; Smedley, 1991) that REE solubility is greatly influenced by pH, with REE concentrations increasing with decreasing pH (Fig. 10.2). Adsorption of the REE onto oxide surfaces is enhanced at higher pH, especially for the LREE (Dupré et al., 1996), and therefore with increasing pH the degree of LREE depletion would be expected to increase. In addition, the shallow groundwaters from several holes at the Halfmile Lake deposit are also LREE depleted, but the pattern of LREE depletion is very different to that of the majority of groundwater samples from the Restigouche deposit. The mechanism of removal (or inhibition of mobilization) of the LREE relative to the MREE and HREE is clearly more complex than can be explained on the basis of differences in pH. There is no obvious difference in the pH and Eh values for the shallow versus the deeper groundwaters at the Halfmile Lake deposit. In addition, although Halfmile Lake deposit groundwaters are on average lower in pH than those from the Restigouche deposit, there is a fair degree of overlap (Figs. 10.1, 10.2).

The differences in the chemical behaviour of the REE between the Restigouche and Halfmile Lake deposits may be partly influenced by the adsorption onto oxide and silicate surfaces. However, the colloidal material trapped on filter papers is similar in composition between the two deposits, although less material was retained for analysis from the Halfmile Lake deposit (see Chapter Nine). Most of the colloidal material from both deposits is comprised of K-silicates, quartz, and lesser amounts of Fe and Mg silicates. Fe-Mn oxides were only rarely observed, although Fe-oxide surfaces on silicate minerals is difficult to detect by SEM and XRD. Energy-dispersive spectra of suspended silicates typically gives trace Fe peaks, perhaps reflecting Fe-oxide surfaces (see Chapter Nine). In high sulphate waters from the Restigouche and Stratmat Main Zone deposits, Fe-sulphate minerals are common, and in one sample, alunite may be present. The presence of alumino-sulphate minerals may explain the strange

REE patterns of the Stratmat Main Zone deposit waters (Fig. 10.23). Rare earth element analyses of acid-sulphate waters and associated sinter deposits were reported recently by Lewis et al. (1997), although no patterns similar to these were described. It is possible that this is a function of the higher pH of these BMC waters, enhancing fractionation effects. Accessory minerals observed include pyrite, and more rarely other sulphide minerals (sphalerite, galena), especially from the Restigouche deposit. In one sample from the Restigouche deposit, LREE-phosphate minerals were observed. It is unclear, therefore, how the mineralogy of the colloidal material observed by SEM is directly influencing the REE solubility, although there may be differences related to mineral surface coatings not readily observed by SEM. For some of the suspended sediments, the patterns shown by the coexisting groundwater and the host lithology are similar (e.g. the samples from borehole HN94-65; Fig. 10.25), so that the relationship between the media is unclear. However, for many of the suspended sediments, there is a fractionation compared to the host lithologies, and there is also an LREE fractionation between the sediment and the groundwater. Note also that the suspended sediments from the Restigouche deposit have higher REE abundances than those from the Halfmile Lake deposit, whereas, for the groundwaters, the reverse is generally true. This would suggest that adsorption onto "aquifer" colloidal material is an important control on REE mobility in these groundwaters.

The ultimate source of the REE in natural waters is the lithologies through which the waters travel. The deeper Halfmile Lake deposit groundwaters have REE patterns that are very similar to the patterns of the host metavolcanic and metasedimentary rocks (c.f. Figs. 10.10 and 10.14). This suggests that for these waters the host-rocks exert a dominant influence over the relative concentrations of the REE. For example, negative Eu anomalies are common in the host rocks and groundwaters. The absolute abundances are controlled by the source and the capacity of the water to complex REE. The latter is influenced by pH, Eh, anionic complexes and the mineralogy of the source rocks. However, note that Halfmile Lake deposit groundwaters and stream sediments normalized to unaltered host rocks have positive Eu

anomalies indicating the Eu is preferentially mobilized. In contrast, Restigouche deposit groundwaters for the most part have LREE depleted profiles which are unlike the metavolcanic that host the deposit. There is, therefore, a lack of correlation between the relative REE abundances and the host lithologies for Restigouche deposit groundwaters. It was already shown that groundwaters from these two deposits differ in a number of ways including trace and major element compositions, stable isotopes compositions, and apparent hydraulic conductivities (Chapters Seven, Eleven, and Four, respectively).

The unusual pattern of LREE depletion observed in the shallow groundwaters from boreholes HN87-8, HN94-55, and HN94-82 intersecting the Halfmile Lake deposit is interpreted to be controlled by differences in the styles and degrees of weathering undergone by shallow as compared to deeper lithologies. The uppermost 100-200 meters or so of bedrock at The Halfmile Lake deposit is highly fractured and intensely Fe-oxide stained reflecting the influence of deep, pre-glacial weathering under a much warmer climate than exists at the present time (Boyle, 1996). The shape of the REE patterns in the upper part of borehole HN87-8, with a strong convex-up shape from La through Sm may be explained by comparison with a seep from the Restigouche deposit (sample MLW95-345). This sample was very Fe-oxyhydroxide-rich. The upper parts of the Halfmile Lake deposit were heavily weathered in pre-glacial times (Boyle, 1996) as shown by Fe-oxyhydroxide formation in drill core from the uppermost 100-150 m of the deposit. Thus, some of the oxides may be exhibiting a preference for some of the LREE (Ce, Pr > Nd > La > Sm). Sample MLW95-611 from Heath Steele mine also shows a similar pattern. Given the strong influence of Fe-oxides on the LREE (Elderfield et al., 1990), it is possible that the Fe-oxides are limiting the solubility of the LREE in these waters. The shape of the LREE depletion does not appear to be related to the redox state of these waters as there are no significant Ce depletions relative to La and Pr. The fact that the groundwaters at the Halfmile Lake deposit are similar in major ion composition to surface waters yet different in REE composition indicates that there are fundamental differences in the aqueous chemistry of the subsurface and surface environments. Similar patterns are also

shown for Restigouche deposit boreholes MM-88-06 and MM-88-07. The suspended sediment normalized patterns show LREE depletion for the MM-88-06 waters but flatter patterns for the MM-88-07 waters. The latter suspended sediments were more Fe-rich, consistent with LREE control by Fe-oxyhydroxides.

Elderfield et al. (1990) noted that the HREE's form stronger complexes with ligands in solution than do the LREE's; thus, HREE's will be preferentially released to solution during weathering of source rocks and the LREE's will be preferentially adsorbed at particle surfaces in adsorption/equilibria reactions in rivers. The HREE have been shown experimentally to form stronger solution complexes with carbonate than the LREE's whereas, the LREE are preferentially adsorbed/scavenged by a variety of organic and inorganic substrates in seawater (Byrne and Kim, 1990). Experimental work also suggests that adsorption and scavenging should enrich solutions in Gd relative to Eu (Byrne and Kim, 1990). There are strong correlations between Al and most REE for the borehole waters, and generally weak correlations for the surface waters. Condie (1991) noted that moderate correlations between REE's and Al_2O_3 in shales suggests that clays are important in hosting the REE's in shales. SEM studies of the suspended material in BMC groundwaters shows that this fraction is dominated by silicate phases, suggesting that for some of the groundwaters, the REE patterns are also controlled by clay minerals.

Elderfield et al. (1990) showed that where river waters interact with estuarine waters, salinity increases and REE concentration decreases drastically, probably by flocculation of suspended matter with which the REE are interpreted to largely be associated. However, for saline groundwaters, the REE solubility is less clearly associated with suspended sediment flocculation as a function of increasing salinity as there is no clear pattern of decreasing REE abundance with increasing salinity (Fig. 10.6). Sample salinity clearly has some control over the behaviour of the REE; at low salinity (surface waters and shallow groundwaters), La/Ce is highly variable, indicating that Ce behaves very differently from the other REE under these conditions. For waters with salinities in excess of 1 mg/L Cl, La/Ce is relatively constant and

independent of Cl concentration (Fig. 10.6).

One final major control over the REE in the BMC waters is pH. Although there is only a generally poor (though statistically significant) correlation between SREE and pH for the BMC waters as a whole (Fig. 10.1), groundwaters with low pH tend to have REE patterns which are more like the host lithologies than higher pH waters, in addition to possessing higher overall REE abundances. There is a strong correlation between log(Al) and log(SREE) for Halfmile Lake deposit groundwaters. As Al abundances are strongly controlled by pH (Chapter Seven), this also suggests a strong pH control for the REE in these waters. There may be some pH control over Ce anomaly development and REE fractionation. Surface waters from the Restigouche deposit which drain Mt Vroom (Mt Vroom N, NE, and E streams) as well as streams to the west of the deposit, have generally lower pH than the other streams as well as higher Ce/Ce*, lower La/Yb and Gd/Yb (Fig. 10.16). This suggests that these waters also have less fractionated REE patterns.

10.7.2 Origin of the REE in BMC surface waters

As noted above, the surface waters from the Restigouche and Halfmile Lake deposits are broadly similar in REE abundance and pattern, although Restigouche deposit surface waters commonly have larger negative Ce anomalies. The majority of the surface waters are LREE depleted and many show NASC-normalized depletion in the HREE relative to Gd. Clearly, the surface waters are different from the host lithologies in that they are LREE depleted compared to NASC. In addition, most of the surface waters have significant negative Ce anomalies, a feature lacking in the felsic and mafic volcanic and sedimentary host rocks. Sholkovitz (1995) indicated that the lowest shale-normalized Ce anomaly recorded for river waters was 0.37. However, many of the stream waters in this study have Ce anomalies significantly lower than this, as low as 0.09 (Tables 10.1 and 10.5). These Ce anomaly values approach those of groundwaters from metasediments associated with the Carnmenellis Granite (Smedley, 1991) which have Ce anomalies as low as 0.005 to 0.214. The REE composition of many seeps

analyzed from the Halfmile Lake deposit appear to reflect both solubility and lithological controls. These waters typically lack the negative Ce anomalies observed in the stream waters and have well developed negative Eu anomalies similar to the host lithologies, but the LREE are more depleted than the host rocks, similar to the stream waters.

The development of negative Ce anomalies must be a fairly rapid phenomena given that spring waters, and groundwaters, at the Halfmile Lake deposit lack negative anomalies yet surface waters are uniformly depleted in Ce relative to La and Pr (Figs. 10.7 and 10.15). This is consistent with previous work (Byrne and Kim, 1990) which showed that oxidation of Ce^{3+} is rapid in the presence of MnO_2 (time scale of minutes is suggested by their figure 1). These workers also noted that Ce^{4+} is highly surface reactive compared to trivalent Ce (and the adjacent trivalent LREE). Although negative Ce anomalies have been observed previously in natural waters (Elderfield et al., 1990; Miekeley et al., 1992b; Smedley, 1991), most natural waters apparently have minor to no such anomalies (e.g. Johannesson et al., 1994a; Johannesson et al., 1994b; Johannesson et al., 1996a). It is interesting to note that in her study of REE in groundwaters from Carnmenellis, southwest England, Smedley (1991) found large negative Ce anomalies in groundwaters flowing through metasediments and noted that because these negative anomalies are not observed in river waters, the development of Ce anomalies is unlikely to be dominantly a function of Eh. For the waters analyzed in this study, this is not the case; the stream waters almost uniformly possess negative Ce anomalies, whereas, the groundwaters and many of the seeps and springs typically have weak to no negative Ce anomalies. The negative Ce anomalies in Carnmenellis groundwaters are for the most part similar in magnitude to the surface waters from the Halfmile Lake and Restigouche deposits. Both sets of data have much larger Ce anomalies than those reported by Elderfield et al. (1990) for world rivers. For Halfmile Lake and Restigouche deposit surface waters, the REE have generally poor correlations with Fe, Mn and Co with the notable exception of Ce. This would suggest that although not detectable by standard Eh field measurements, Ce is controlled by changes in the redox state of the waters. This is also suggested by the spatial variations in

Ce/Ce* compared to Fe and Mn (cf Figs. 10.8D, 10.16D and Chapter Five).

The REE patterns of the stream sediments (total dissolution) should reflect both the source material (country rock) and the time integrated contributions from surface waters. That both of these REE reservoirs influence the patterns of the stream sediments in Halfmile Lake deposit is evident by comparing Figs. 10.7, 10.12 and 10.14. Compared to NASC the stream sediments are relatively flat with the LREE concentrations very similar to the HREE concentrations. Stream sediments commonly have small NASC-normalized Eu anomalies (average $[Eu/Eu^*]_{NASC} = 0.895$ at the Halfmile Lake deposit and 0.780 at the Restigouche deposit). These characteristics are also typical of the host lithologies (Fig. 10.14). However, unlike the host rocks, the stream sediments typically have negative Ce anomalies and are enriched in the MREE over the light and heavy REE, two features characteristic of most of the surface waters. In addition, normalized to least altered host lithologies, positive Eu anomalies are ubiquitous amongst stream sediments and for surface waters with Eu sufficiently above detection. However, the negative Ce anomalies in stream sediments are smaller than in the corresponding waters. There are two explanations for this. Part of the reduction in the magnitude of the Ce anomaly is undoubtedly related to the source reservoir (i.e. "dilution" of the anomaly), but some must also be a function of the preferential adsorption and loss from the "dissolved" reservoir compared to the other LREE. The LREE-depleted signature of surface waters indicates that LREE are less soluble than middle and heavy REE, and the negative Ce anomalies suggest that Ce is preferentially lost from the "dissolved" phase. The REE patterns displayed by stream sediment sample MLS94-185 from a groundwater seep is significant. The positive Ce anomaly in the sediment is consistent with rapid loss of Ce from groundwaters once they come into contact with atmospheric oxygen.

10.7.3 Association of REE with suspended matter

Other studies have shown that there is typically a strong correlation between the REE content of waters and pH and a typically poor correlation between ΣREE and Eh (Elderfield et

al., 1990; Smedley, 1991). For the entire BMC dataset, there is a generally poor correlation of ΣREE with pH, although there is a general increase in ΣREE with decreasing pH for the different sample groups in this study (Fig. 10.2A). The poorer correlation in this study of ΣREE with pH may also be due to measurement of dissolved REE whereas in other studies dissolved and colloidally bound REE were measured. It is known that development of colloids is highly pH dependent (Elderfield et al., 1990).

There are variations in the relative capacity of the REEs to form complexes with colloids. Several workers have suggested that the positive slope from the LREE to the HREE (i.e. LREE depletion compared to NASC) is due to the greater solubility of HREE-carbonate complexes compared to LREE-carbonate complexes. However, one of the characteristics of both surface and groundwaters from both deposits is that $[La/Sm]_{NASC}$ and $[Gd/Yb]_{NASC}$ are commonly greater than and less than unity, respectively, producing a convex-up REE profile. If the solubility of the REE is in large part controlled by sorption processes on colloidal material, then it indicates that the MREE have the least affinity for sorption/complexation. In many REE profiles for both Halfmile Lake and Restigouche deposit waters and for almost all the stream sediments, Gd is the most abundant NASC-normalized rare earth element. As discussed below, for most of the waters in this study, the REE primarily occur as the free ionic species Ln^{3+}, rather than as complexes. The development of relative MREE enrichment compared to NASC appears to be a function of speciation. It appears from published studies of REE in natural waters that where carbonate at moderate to high pH or sulphate complexes at low pH dominate the REE speciation (e.g. Johannesson and Lyons, 1994; Johannesson et al., 1994a; Johannesson et al., 1996a), the enrichment in the MREE is not developed. Both experimental work and thermodynamic considerations show that the solubility of the HREE is enhanced by carbonate speciation. In waters where the REE are complexed by carbano or dicarbano species, the NASC-normalized REE patterns are LREE depleted and the HREE ≥ MREE (Johannesson and Lyons, 1994; Johannesson et al., 1994a; Johannesson et al., 1996a). However, in waters where the REE dominantly occur as free ions, MREE enrichment is the most well developed,

e.g., waters in this study, Lake Tyrrell, Australia (Fee et al., 1992), many world rivers (Elderfield et al., 1990) and brines from the Palo Dura Basin (Gosselin et al., 1992). Therefore, in the absence of strong complexing ligands, the MREE are either more easily leached from the source rocks or they are more soluble under the Eh and pH conditions commonly found at both the Halfmile Lake and Restigouche deposits.

10.7.4 Origin of low TDS groundwaters at the Halfmile Lake deposit

The question was posed in previous chapters as to the nature of the low salinities of the deeper groundwaters at the Halfmile Lake deposit. The REE data places some interesting constraints on this problem. The low salinities could be a function of dilution by drilling waters; surface water from the headwaters of the Upper/Lower AB stream was the primary drilling fluid used. Alternatively, the deeper waters could be shallow groundwaters flowing downhole and dominating the chemistry as sampled by the flow-through bailer. However, the problem with both these hypothesis is that the deeper groundwaters have different REE patterns compared to the surface waters. Although the shallow groundwaters commonly have LREE depleted patterns somewhat similar to the surface waters, they are more LREE depleted and lack Ce anomalies which most of the surface waters possess. The changes downhole observed for Halfmile Lake deposit groundwaters is consistent with upward gradients and mixing between deeper groundwaters with relatively flat NASC-normalized REE profiles and a shallow groundwater flow system with LREE-depleted profiles (Figs. 10.10, 10.11A).

10.8 Summary

Rare earth element concentrations are highly variable in waters of the BMC, with higher concentrations typical of waters with higher Fe and lower pH. There are significant differences between surface and groundwaters, and between groundwaters from different areas.

The REE contents of surface waters are broadly similar within and between deposit areas, although there are differences between different streams which reflects differences in pH and

lithology. Surface waters typically possess strong negative Ce anomalies, which are produced by oxidation of Ce^{3+} to Ce^{4+} upon leaving the shallow groundwater environment. Groundwaters are typically more reducing and have smaller to no Ce anomalies.

Deeper groundwaters at Halfmile Lake are characterized by REE patterns that are similar to the host rocks, whereas most groundwaters at the Restigouche deposit have LREE depleted patterns compared to NASC. One of the major reasons for the differences between the groundwaters from Halfmile Lake versus those from the Restigouche deposit may derive from the fact that at the Halfmile Lake deposit the pH is somewhat lower and in addition the activities of possible anionic complexes for the REE are low suggesting that the REE are more controlled by source considerations for these reasons. In contrast, the anionic concentrations at the Restigouche deposit are generally greater suggesting that the distribution of the REE is more controlled by solubility/speciation considerations. Shallow waters at the Halfmile Lake deposit and waters from the Stratmat Main Zone deposit have unusual patterns which reflect either the influence of adsorption onto colloidal minerals or onto fracture zone minerals or different fluid histories compared to groundwaters from the Restigouche deposit.

Table 10.1 REE contents and ratios for Halfmile Lake deposit surface waters

Sample	Location	La	Ce	Pr	Nd	Sm	Eu	Gd	Tb	Dy	Ho	Er	Tm	Yb	Lu	ΣREE	$[La/Ce]_{NASC}$	$[La/Yb]_{NASC}$	$[Gd/Yb]_{NASC}$	$[La/Sm]_{NASC}$	Ce/Ce*
MLW94-100	Upper/Lower AB		0.010	0.002	0.011	0.004		0.003		0.003		0.003		0.002		0.038	0.000	0.000	0.894	0.000	
MLW94-105	Upper/Lower AB	0.007	0.010	0.002	0.012	0.002		0.003		0.004		0.003		0.003		0.046	1.597	0.226	0.596	0.623	0.582
MLW94-108	Upper/Lower AB	0.010	0.016	0.003	0.017	0.004		0.005		0.005	0.001	0.003		0.004		0.068	1.426	0.242	0.745	0.445	0.636
MLW94-112	Upper/Lower AB	0.010	0.016	0.004	0.018	0.004		0.007		0.004	0.001	0.004		0.003		0.071	1.426	0.323	1.391	0.445	0.551
MLW94-122	Upper/Lower AB	0.012	0.022	0.004	0.020	0.004		0.006		0.004	0.001	0.003		0.003		0.079	1.244	0.388	1.192	0.534	0.692
MLW94-185	Upper/Lower AB	0.023	0.012	0.013	0.066	0.019	0.002	0.023	0.003	0.016	0.004	0.011	0.002	0.014	0.002	0.210	4.372	0.159	0.979	0.216	0.151
MLW94-186	Upper/Lower AB	0.019	0.013	0.010	0.056	0.017	0.002	0.020	0.003	0.016	0.004	0.011	0.002	0.012	0.002	0.187	3.334	0.153	0.994	0.199	0.205
MLW94-187	Upper/Lower AB	0.102	0.192	0.034	0.153	0.046	0.006	0.049	0.008	0.052	0.010	0.026	0.004	0.023	0.004	0.709	1.212	0.430	1.270	0.395	0.710
MLW94-188	Upper/Lower AB	0.016	0.022	0.004	0.026	0.008		0.007		0.006	0.002	0.004		0.003		0.098	1.659	0.517	1.391	0.356	0.599
MLW94-190	Upper/Lower AB	0.013	0.034	0.004	0.017	0.006		0.005		0.004	0.001	0.003		0.002		0.089	0.872	0.630	1.490	0.386	1.027
MLW94-191	Upper/Lower AB	0.045	0.118	0.014	0.064	0.016	0.002	0.017	0.003	0.017	0.004	0.009	0.001	0.010	0.002	0.322	0.870	0.436	1.013	0.501	1.024
MLW94-121	Halfmile North	0.016	0.008	0.004	0.024	0.005	0.001	0.006		0.006	0.002	0.003		0.003		0.078	4.563	0.517	1.192	0.570	0.218
MLW94-125	Halfmile North	0.027	0.005	0.007	0.033	0.007	0.002	0.011		0.008	0.001	0.004		0.004		0.109	12.319	0.654	1.639	0.687	0.079
MLW94-127	Halfmile North	0.025	0.007	0.007	0.032	0.007	0.002	0.008	0.001	0.004	0.002	0.006		0.004		0.105	8.147	0.605	1.192	0.636	0.115
MLW94-129	Halfmile North	0.030	0.006	0.009	0.041	0.011	0.003	0.010	0.002	0.009	0.002	0.005		0.005		0.133	11.406	0.581	1.192	0.486	0.080
MLW94-132	Halfmile North	0.023	0.006	0.004	0.025	0.007	0.002	0.007		0.006	0.001	0.003		0.003		0.087	8.745	0.743	1.391	0.585	0.136
MLW94-141	Halfmile North	0.022	0.007	0.005	0.027	0.008	0.002	0.008	0.001	0.005	0.002	0.005		0.003		0.095	7.170	0.710	1.590	0.490	0.145
MLW94-144	Halfmile North	0.024	0.006	0.006	0.039	0.007	0.002	0.011	0.001	0.007	0.002	0.006		0.004		0.115	9.125	0.581	1.639	0.611	0.109
MLW94-152	Confluence			0.002	0.008	0.003		0.003		0.002		0.002				0.020					
MLW94-153	Northeast trib	0.027	0.019	0.008	0.031	0.007	0.002	0.007		0.005	0.002	0.005		0.004		0.117	3.242	0.654	1.043	0.687	0.282
MLW94-215	Northeast trib	0.017	0.014	0.004	0.018	0.005	0.001	0.005		0.003		0.003		0.002		0.072	2.770	0.823	1.490	0.606	0.370
MLW94-221	Northeast trib		0.007	0.001	0.008	0.004				0.003		0.002				0.025					
MLW94-222	Northeast trib	0.015	0.012	0.004	0.020	0.003	0.001	0.005		0.005	0.001	0.003		0.002		0.071	2.852	0.727	1.490	0.891	0.337
MLW94-224	Northeast trib	0.017	0.014	0.005	0.021	0.004	0.001	0.008		0.005	0.001	0.003		0.002		0.081	2.770	0.823	2.385	0.757	0.331
MLW94-227	Northeast trib	0.016	0.011	0.004	0.022	0.005	0.002	0.004		0.004	0.001	0.003		0.003		0.075	3.318	0.517	0.795	0.570	0.299
MLW96-701	Northeast trib	0.005	0.005	0.001	0.005	0.002	0.001	0.002	0.001	0.002	0.001	0.002	0.001	0.002	0.001	0.031	2.281	0.242	0.596	0.445	0.487
MLW94-229	North trib	0.021	0.022	0.006	0.026	0.007	0.002	0.007		0.007	0.001	0.005		0.003		0.107	2.178	0.678	1.391	0.534	0.427
MLW94-230	North trib	0.015	0.014	0.004	0.017	0.005		0.006		0.002	0.001	0.003		0.002		0.069	2.444	0.727	1.788	0.534	0.394
MLW94-263	North trib	0.016	0.024	0.004	0.020	0.003		0.006		0.003		0.002		0.002		0.080	1.521	0.775	1.788	0.950	0.653
MLW94-265	North trib	0.011	0.019	0.003	0.016	0.004		0.003		0.004		0.002		0.002		0.064	1.321	0.533	0.894	0.490	0.720
MLW94-266	North trib	0.010	0.016	0.003	0.016	0.004		0.005		0.003		0.003		0.002		0.062	1.426	0.484	1.490	0.445	0.636
MLW94-267	North trib		0.015	0.001	0.007	0.003		0.003		0.002		0.003		0.002		0.036			0.894		
MLW94-268	North trib	0.012	0.018	0.004	0.016	0.004	0.001	0.006		0.004		0.002		0.002		0.069	1.521	0.581	1.788	0.534	0.566
MLW94-269	North trib				0.002							0.001		0.002		0.005					
MLW94-113	West trib				0.002									0.001		0.003					
MLW94-273	West trib	0.008	0.016	0.003	0.017	0.004		0.003	0.001	0.004	0.001	0.003		0.003		0.063	1.141	0.258	0.596	0.356	0.711
MLW94-275	West trib	0.009	0.044	0.002	0.016	0.004		0.005		0.004		0.003		0.003		0.090	0.467	0.291	0.994	0.401	2.259
MLW94-276	West trib	0.007	0.009	0.003	0.013	0.003		0.005		0.004		0.002		0.004		0.050	1.774	0.170	0.745	0.416	0.428
MLW94-284	Halfmile Lake	0.016	0.029	0.005	0.023	0.007	0.002	0.008	0.001	0.006	0.001	0.003		0.002		0.103	1.259	0.775	2.385	0.407	0.706
MLW94-149	NW Miramichi	0.030	0.047	0.009	0.038	0.011	0.002	0.010	0.001	0.008	0.002	0.006		0.006	0.001	0.171	1.456	0.484	0.994	0.486	0.623

All concentrations in µg/L; blank = below detection

Table 10.2 REE contents and ratios for Halfmile Lake deposit groundwaters

Sample	Location	La	Ce	Pr	Nd	Sm	Eu	Gd	Tb	Dy	Ho	Er	Tm	Yb	Lu	ΣREE	$[La/Ce]_{NASC}$	$[La/Yb]_{NASC}$	$[Gd/Yb]_{NASC}$	$[La/Sm]_{NASC}$	Ce/Ce*
MLW94-154	HN87-08	0.005	0.014	0.002	0.014	0.005		0.007	0.001	0.006	0.001	0.003		0.003		0.061	0.815	0.161	1.391	0.178	0.964
MLW94-156	HN87-08	0.007	0.013	0.002	0.010	0.005		0.005		0.004		0.003		0.003		0.052	1.228	0.226	0.994	0.249	0.757
MLW94-158	HN87-08	0.008	0.013	0.002	0.011	0.006	0.001	0.006	0.001	0.004	0.001	0.003	0.001	0.002	0.001	0.060	1.404	0.388	1.788	0.238	0.708
MLW94-162	HN87-08	0.007	0.014	0.002	0.012	0.004		0.008	0.001	0.006	0.001	0.004		0.004		0.063	1.141	0.170	1.192	0.312	0.815
MLW94-163	HN87-08	0.006	0.010	0.001	0.007	0.004		0.005		0.005		0.002		0.002		0.042	1.369	0.291	1.490	0.267	0.889
MLW94-165	HN87-08	0.010	0.019	0.002	0.014	0.004	0.001	0.008	0.001	0.006	0.001	0.004	0.001	0.003	0.001	0.075	1.201	0.323	1.590	0.445	0.925
MLW94-167	HN87-08	0.038	0.069	0.008	0.032	0.010	0.001	0.014	0.002	0.011	0.002	0.004	0.001	0.005	0.001	0.198	1.256	0.736	1.669	0.677	0.862
MLW94-169	HN87-08	0.066	0.123	0.014	0.061	0.015	0.002	0.017	0.003	0.016	0.003	0.008		0.005		0.333	1.224	1.279	2.027	0.784	0.881
MLW94-171	HN87-08	0.099	0.179	0.022	0.091	0.021	0.004	0.025	0.003	0.022	0.004	0.009	0.002	0.009	0.001	0.491	1.262	1.066	1.656	0.840	0.835
MLW96-674	HN92-40	0.005	0.005	0.001	0.001	0.001	0.001	0.002	0.001	0.001	0.001	0.001	0.001	0.001	0.001	0.023	2.281	0.484	1.192	0.891	0.487
MLW96-699	HN92-40	0.008	0.007	0.001	0.003	0.001	0.001	0.002	0.001	0.002	0.001	0.001	0.001	0.001	0.001	0.031	2.607	0.775	1.192	1.425	0.539
MLW94-202	HN93-50	0.017	0.037	0.004	0.019	0.006		0.006		0.006	0.001	0.003		0.002		0.101	1.048	0.823	1.788	0.505	0.977
MLW95-615	HN93-50	0.006	0.013	0.003	0.028	0.013	0.004	0.025	0.003	0.018	0.004	0.008	0.001	0.004		0.130	1.053	0.145	3.726	0.082	0.667
MLW94-205	HN93-50	0.046	0.088	0.012	0.046	0.010	0.002	0.013	0.001	0.008	0.001	0.004	0.001	0.004	0.001	0.237	1.192	1.114	1.938	0.819	0.816
MLW94-209	HN93-50	0.130	0.238	0.027	0.116	0.031	0.006	0.030	0.004	0.021	0.004	0.011	0.001	0.009	0.002	0.630	1.246	1.399	1.987	0.747	0.875
MLW94-211	HN93-50	0.083	0.156	0.019	0.084	0.022	0.004	0.018	0.003	0.016	0.003	0.008		0.006		0.422	1.214	1.340	1.788	0.672	0.856
MLW94-212	HN93-50	0.074	0.141	0.016	0.073	0.020	0.004	0.019	0.002	0.014	0.002	0.006		0.005		0.376	1.197	1.434	2.265	0.659	0.893
MLW94-172	HN93-55		0.028	0.002	0.013	0.008		0.012	0.002	0.014	0.003	0.005		0.004		0.091	0.000	0.000	1.788	0.000	
MLW94-175	HN93-55	0.006	0.025	0.002	0.015	0.008	0.001	0.013	0.002	0.015	0.002	0.008	0.001	0.004	0.001	0.103	0.548	0.145	1.938	0.134	1.572
MLW94-181	HN93-55	0.005	0.024	0.002	0.012	0.009	0.002	0.012	0.002	0.011	0.002	0.006	0.001	0.005	0.001	0.094	0.475	0.097	1.431	0.099	1.653
MLW94-184	HN93-55		0.025	0.002	0.014	0.012	0.001	0.015	0.003	0.014	0.003	0.005		0.004		0.098	0.000	0.000	2.236	0.000	
MLW95-529	HN94-51	0.012	0.015	0.003	0.013	0.002		0.005		0.004		0.002		0.002		0.058	1.825	0.581	1.490	1.069	0.545
MLW95-613	HN94-51	0.021	0.044	0.007	0.031	0.006	0.001	0.005		0.003	0.001	0.001		0.002		0.122	1.089	1.017	1.490	0.623	0.790
MLW95-533	HN94-51	0.033	0.048	0.007	0.029	0.005		0.004		0.004		0.002		0.002		0.134	1.568	1.598	1.192	1.176	0.688
MLW95-537	HN94-51	0.026	0.039	0.005	0.024	0.006		0.006		0.003		0.002		0.002		0.113	1.521	1.259	1.788	0.772	0.745
MLW96-708	HN94-63	0.126	0.300	0.043	0.171	0.052	0.015	0.058	0.010	0.047	0.008	0.020	0.002	0.018	0.003	0.873	0.958	0.678	1.921	0.432	0.888
MLW94-236	HN94-65	0.010	0.029	0.002	0.008	0.003	0.001	0.002		0.005	0.001	0.003		0.002		0.066	0.787	0.484	0.596	0.594	1.412
MLW94-241	HN94-65	0.012	0.032	0.002	0.006	0.003	0.001	0.005	0.001	0.004	0.001	0.002	0.001	0.001	0.001	0.072	0.855	1.163	2.981	0.713	1.423
MLW95-608	HN94-65	0.120	0.408	0.034	0.169	0.050	0.011	0.060	0.008	0.045	0.009	0.024	0.003	0.023	0.003	0.967	0.671	0.505	1.555	0.428	1.391
MLW94-243	HN94-65	0.015	0.035	0.003	0.012	0.006	0.001	0.003	0.001	0.003	0.001	0.002	0.001	0.002	0.001	0.086	0.978	0.727	0.894	0.445	1.136
MLW94-246	HN94-65	0.146	0.317	0.034	0.137	0.023	0.004	0.020	0.003	0.016	0.004	0.010	0.001	0.009	0.002	0.726	1.051	1.572	1.325	1.131	0.980
MLW94-248	HN94-65	0.055	0.134	0.013	0.044	0.010	0.002	0.012	0.001	0.008	0.002	0.005	0.001	0.004	0.001	0.292	0.936	1.332	1.788	0.980	1.091
MLW94-252	HN94-65	0.231	0.514	0.056	0.218	0.039	0.007	0.028	0.004	0.023	0.004	0.011	0.001	0.010	0.001	1.147	1.025	2.238	1.669	1.055	0.984
MLW96-673	HN94-79	0.005	0.005	0.001	0.001	0.001	0.001	0.002	0.001	0.001	0.001	0.001	0.001	0.001	0.001	0.023	2.281	0.484	1.192	0.891	0.487
MLW96-675	HN94-82	0.039	0.089	0.012	0.081	0.054	0.013	0.101	0.014	0.072	0.012	0.027	0.002	0.010	0.001	0.527	1.000	0.378	6.021	0.129	0.896
MLW94-256	HT55-43	0.404	0.781	0.088	0.352	0.065	0.015	0.051	0.006	0.024	0.004	0.011	0.001	0.011	0.002	1.815	1.180	3.558	2.764	1.107	0.902
MLW94-259	HT55-43	0.040	0.088	0.009	0.046	0.009	0.002	0.008		0.003		0.002		0.002		0.209	1.037	1.938	2.385	0.792	1.010

All concentrations in µg/L; blank = below detection

Table 10.2 REE contents and ratios for Halfmile Lake deposit groundwaters

Sample	Location	La	Ce	Pr	Nd	Sm	Eu	Gd	Tb	Dy	Ho	Er	Tm	Yb	Lu	ΣREE	$[La/Ce]_{NASC}$	$[La/Yb]_{NASC}$	$[Gd/Yb]_{NASC}$	$[La/Sm]_{NASC}$	Ce/Ce*
MLW94-154	HN87-08	0.005	0.014	0.002	0.014	0.005		0.007	0.001	0.006	0.001	0.003		0.003		0.061	0.815	0.161	1.391	0.178	0.964
MLW94-156	HN87-08	0.007	0.013	0.002	0.010	0.005		0.005		0.004		0.003		0.003		0.052	1.228	0.226	0.994	0.249	0.757
MLW94-158	HN87-08	0.008	0.013	0.002	0.011	0.006	0.001	0.006	0.001	0.004	0.001	0.003	0.001	0.002	0.001	0.060	1.404	0.388	1.788	0.238	0.708
MLW94-162	HN87-08	0.007	0.014	0.002	0.012	0.004		0.008	0.001	0.006	0.001	0.004		0.004		0.063	1.141	0.170	1.192	0.312	0.815
MLW94-163	HN87-08	0.006	0.010	0.001	0.007	0.004		0.005		0.005		0.002		0.002		0.042	1.369	0.291	1.490	0.267	0.889
MLW94-165	HN87-08	0.010	0.019	0.002	0.014	0.004	0.001	0.008	0.001	0.006	0.001	0.004	0.001	0.003	0.001	0.075	1.201	0.323	1.590	0.445	0.925
MLW94-167	HN87-08	0.038	0.069	0.008	0.032	0.010	0.001	0.014	0.002	0.011	0.002	0.004	0.001	0.005	0.001	0.198	1.256	0.736	1.669	0.677	0.862
MLW94-169	HN87-08	0.066	0.123	0.014	0.061	0.015	0.002	0.017	0.003	0.016	0.003	0.008		0.005		0.333	1.224	1.279	2.027	0.784	0.881
MLW94-171	HN87-08	0.099	0.179	0.022	0.091	0.021	0.004	0.025	0.003	0.022	0.004	0.009	0.002	0.009	0.001	0.491	1.262	1.066	1.656	0.840	0.835
MLW96-674	HN92-40	0.005	0.005	0.001	0.001	0.001	0.001	0.002	0.001	0.001	0.001	0.001	0.001	0.001	0.001	0.023	2.281	0.484	1.192	0.891	0.487
MLW96-699	HN92-40	0.008	0.007	0.001	0.003	0.001	0.001	0.002	0.001	0.002	0.001	0.001	0.001	0.001	0.001	0.031	2.607	0.775	1.192	1.425	0.539
MLW94-202	HN93-50	0.017	0.037	0.004	0.019	0.006		0.006		0.006	0.001	0.003		0.002		0.101	1.048	0.823	1.788	0.505	0.977
MLW95-615	HN93-50	0.006	0.013	0.003	0.028	0.013	0.004	0.025	0.003	0.018	0.004	0.008	0.001	0.004		0.130	1.053	0.145	3.726	0.082	0.667
MLW94-205	HN93-50	0.046	0.088	0.012	0.046	0.010	0.002	0.013	0.001	0.008	0.001	0.004	0.001	0.004	0.001	0.237	1.192	1.114	1.938	0.819	0.816
MLW94-209	HN93-50	0.130	0.238	0.027	0.116	0.031	0.006	0.030	0.004	0.021	0.004	0.011	0.001	0.009	0.002	0.630	1.246	1.399	1.987	0.747	0.875
MLW94-211	HN93-50	0.083	0.156	0.019	0.084	0.022	0.004	0.018	0.003	0.016	0.003	0.008		0.006		0.422	1.214	1.340	1.788	0.672	0.856
MLW94-212	HN93-50	0.074	0.141	0.016	0.073	0.020	0.004	0.019	0.002	0.014	0.002	0.006		0.005		0.376	1.197	1.434	2.265	0.659	0.893
MLW94-172	HN93-55		0.028	0.002	0.013	0.008		0.012	0.002	0.014	0.003	0.005		0.004		0.091	0.000	0.000	1.788	0.000	
MLW94-175	HN93-55	0.006	0.025	0.002	0.015	0.008	0.001	0.013	0.002	0.015	0.002	0.008	0.001	0.004	0.001	0.103	0.548	0.145	1.938	0.134	1.572
MLW94-181	HN93-55	0.005	0.024	0.002	0.012	0.009	0.002	0.012	0.002	0.011	0.002	0.006	0.001	0.005	0.001	0.094	0.475	0.097	1.431	0.099	1.653
MLW94-184	HN93-55		0.025	0.002	0.014	0.012	0.001	0.015	0.003	0.014	0.003	0.005		0.004		0.098	0.000	0.000	2.236	0.000	
MLW95-529	HN94-51	0.012	0.015	0.003	0.013	0.002		0.005		0.004		0.002		0.002		0.058	1.825	0.581	1.490	1.069	0.545
MLW95-613	HN94-51	0.021	0.044	0.007	0.031	0.006	0.001	0.005		0.003	0.001	0.001		0.002		0.122	1.089	1.017	1.490	0.623	0.790
MLW95-533	HN94-51	0.033	0.048	0.007	0.029	0.005		0.004		0.004		0.002		0.002		0.134	1.568	1.598	1.192	1.176	0.688
MLW95-537	HN94-51	0.026	0.039	0.005	0.024	0.006		0.006		0.003		0.002		0.002		0.113	1.521	1.259	1.788	0.772	0.745
MLW96-708	HN94-63	0.126	0.300	0.043	0.171	0.052	0.015	0.058	0.010	0.047	0.008	0.020	0.002	0.018	0.003	0.873	0.958	0.678	1.921	0.432	0.888
MLW94-236	HN94-65	0.010	0.029	0.002	0.008	0.003	0.001	0.002		0.005	0.001	0.003		0.002		0.066	0.787	0.484	0.596	0.594	1.412
MLW94-241	HN94-65	0.012	0.032	0.002	0.006	0.003	0.001	0.005	0.001	0.004	0.001	0.002	0.001	0.001	0.001	0.072	0.855	1.163	2.981	0.713	1.423
MLW95-608	HN94-65	0.120	0.408	0.034	0.169	0.050	0.011	0.060	0.008	0.045	0.009	0.024	0.003	0.023	0.003	0.967	0.671	0.505	1.555	0.428	1.391
MLW94-243	HN94-65	0.015	0.035	0.003	0.012	0.006	0.001	0.003	0.001	0.003	0.001	0.002	0.001	0.002	0.001	0.086	0.978	0.727	0.894	0.445	1.136
MLW94-246	HN94-65	0.146	0.317	0.034	0.137	0.023	0.004	0.020	0.003	0.016	0.004	0.010	0.001	0.009	0.002	0.726	1.051	1.572	1.325	1.131	0.980
MLW94-248	HN94-65	0.055	0.134	0.013	0.044	0.010	0.002	0.012	0.001	0.008	0.002	0.005	0.001	0.004	0.001	0.292	0.936	1.332	1.788	0.980	1.091
MLW94-252	HN94-65	0.231	0.514	0.056	0.218	0.039	0.007	0.028	0.004	0.023	0.004	0.011	0.001	0.010	0.001	1.147	1.025	2.238	1.669	1.055	0.984
MLW96-673	HN94-79	0.005	0.005	0.001	0.001	0.001	0.001	0.002	0.001	0.001	0.001	0.001	0.001	0.001	0.001	0.023	2.281	0.484	1.192	0.891	0.487
MLW96-675	HN94-82	0.039	0.089	0.012	0.081	0.054	0.013	0.101	0.014	0.072	0.012	0.027	0.002	0.010	0.001	0.527	1.000	0.378	6.021	0.129	0.896
MLW94-256	HT55-43	0.404	0.781	0.088	0.352	0.065	0.015	0.051	0.006	0.024	0.004	0.011	0.001	0.011	0.002	1.815	1.180	3.558	2.764	1.107	0.902
MLW94-259	HT55-43	0.040	0.088	0.009	0.046	0.009	0.002	0.008		0.003		0.002		0.002		0.209	1.037	1.938	2.385	0.792	1.010

All concentrations in µg/L; blank = below detection

Table 10.3 REE contents and ratios for Halfmile Lake deposit stream sediments

Sample #	Stream	La	Ce	Pr	Nd	Sm	Eu	Gd	Tb	Dy	Ho	Er	Tm	Yb	Lu	ΣREE	$[La/Ce]_{NASC}$	$[La/Yb]_{NASC}$	$[Gd/Yb]_{NASC}$	$[La/Sm]_{NASC}$	Ce/Ce*
MLS94-100	Upper/Lower AB	28	69	6.9	29	6.0	1.2	6.2	0.96	5.7	1.2	3.2	0.54	3.5	0.54	161	0.909	0.761	1.048	0.816	1.091
MLS94-101	Upper/Lower AB	28	68	7.3	29	6.7	1.1	6.8	1.1	6.0	1.3	3.6	0.56	3.7	0.54	163	0.946	0.743	1.111	0.750	1.028
MLS94-105	Upper/Lower AB	28	60	6.9	28	6.6	1.0	6.5	1.00	5.6	1.1	3.2	0.51	3.4	0.51	151	1.046	0.795	1.148	0.748	0.949
MLS94-185	Upper/Lower AB	66	260	17	64	17	2.2	16.0	2.7	14.5	2.9	7.8	1.3	8.2	1.2	479	0.575	0.774	1.163	0.707	1.697
MLS94-193	Upper/Lower AB	38	79	9.5	36	7.4	1.3	7.2	1.1	6.2	1.4	3.8	0.61	3.9	0.61	195	1.083	0.931	1.101	0.903	0.912
MLS94-126	Halfmile North	52	95	14	54	12	2.5	13.0	1.9	10.0	2.1	5.9	0.89	5.6	0.88	269	1.249	0.900	1.384	0.772	0.781
MLS94-127	Halfmile North	49	83	13	53	12	2.7	13.5	2.0	11.0	2.4	6.6	0.97	6.1	0.98	255	1.355	0.785	1.330	0.727	0.726
MLS94-130	Halfmile North	36	65	9.0	37	7.9	1.9	8.7	1.3	7.3	1.5	4.1	0.63	4.1	0.61	185	1.263	0.861	1.273	0.812	0.787
MLS94-131	Halfmile North	39	61	9.9	42	9.3	2.1	10.5	1.5	8.0	1.7	4.6	0.71	4.3	0.68	195	1.471	0.879	1.456	0.747	0.671
MLS94-132	Halfmile North	42	90	11	43	9.3	2.0	9.2	1.4	7.8	1.6	4.3	0.68	4.3	0.68	226	1.052	0.935	1.269	0.799	0.939
MLS94-133	Halfmile North	40	60	10	43	9.7	2.2	10.5	1.5	8.3	1.8	4.7	0.72	4.3	0.69	197	1.534	0.912	1.473	0.738	0.648
MLS94-134	Halfmile North	43	67	11	44	9.8	2.2	10.5	1.5	8.1	1.8	4.6	0.75	4.4	0.69	209	1.464	0.947	1.423	0.782	0.671
MLS94-135	Halfmile North	45	69	11	45	9.8	2.3	11.0	1.6	8.2	1.8	4.7	0.74	4.4	0.71	214	1.482	0.980	1.490	0.813	0.674
MLS94-138	Halfmile North	44	72	11	45	9.5	2.1	9.9	1.4	7.7	1.6	4.3	0.68	4.2	0.65	213	1.388	1.003	1.398	0.816	0.712
MLS94-141	Halfmile North	39	70	9.6	39	8.1	1.7	8.6	1.2	6.8	1.5	3.8	0.63	3.8	0.57	194	1.271	0.994	1.349	0.858	0.788
MLS94-142	Halfmile North	37	70	9.6	39	8.3	1.8	8.6	1.3	7.1	1.5	4.1	0.65	4.3	0.64	193	1.206	0.834	1.192	0.794	0.811
MLS94-144	Halfmile North	22	39	5.8	23	5.2	1.3	5.4	0.86	4.7	1.1	2.9	0.46	2.9	0.45	115	1.287	0.748	1.130	0.761	0.752
MLS94-213	Northeast trib	37	69	9.0	35	7.6	1.6	7.2	1.1	5.9	1.3	3.3	0.51	3.3	0.48	181	1.207	1.071	1.301	0.855	0.829
MLS94-215	Northeast trib	41	82	10	41	8.4	1.7	7.9	1.2	6.6	1.4	3.8	0.59	3.7	0.55	209	1.141	1.088	1.282	0.869	0.871
MLS94-217	Northeast trib	33	67	8.2	32	7.0	1.4	6.7	0.98	5.9	1.3	3.4	0.54	3.4	0.48	171	1.107	0.940	1.192	0.827	0.894
MLS94-222	Northeast trib	35	67	8.7	34	7.3	1.5	6.9	1.0	5.7	1.2	3.1	0.49	3.1	0.47	174	1.175	1.078	1.327	0.848	0.845
MLS94-224	Northeast trib	37	71	9.1	35	7.4	1.5	6.6	1.0	6.1	1.3	3.4	0.52	3.3	0.50	183	1.173	1.071	1.192	0.879	0.851
MLS94-227	Northeast trib	34	68	8.7	33	6.9	1.5	6.9	1.1	6.2	1.3	3.5	0.55	3.4	0.51	175	1.149	0.969	1.210	0.878	0.855
MLS96-229	Northeast trib	34	63	8.8	35	6.9	1.3	6.6	0.94	5.9	1.2	3.4	0.47	3.2	0.51	171	1.231	1.029	1.230	0.878	0.793
MLS94-231	Northeast trib	36	73	9.2	36	7.5	1.6	7.1	1.1	6.1	1.2	3.3	0.51	3.3	0.49	186	1.125	1.073	1.302	0.861	0.874
MLS94-232	Northeast trib	36	71	9.1	35	7.2	1.6	7.2	1.1	6.2	1.3	3.4	0.52	3.4	0.50	182	1.149	1.027	1.272	0.878	0.854
MLS94-233	Northeast trib	28	54	7.1	29	5.9	1.5	6.4	0.97	5.7	1.2	3.1	0.47	3.1	0.43	145	1.173	0.873	1.251	0.830	0.834
MLS94-263	North tributary	39	76	9.5	37	7.5	1.6	7.5	1.1	6.7	1.4	3.8	0.57	3.5	0.52	195	1.171	1.079	1.277	0.926	0.862
MLS94-266	North tributary	39	75	9.5	38	7.6	1.6	7.7	1.2	6.8	1.4	3.8	0.59	3.7	0.56	196	1.171	1.022	1.249	0.908	0.854
MLS94-267	North tributary	34	68	8.2	33	6.3	1.3	6.4	0.93	5.7	1.2	3.1	0.48	3.0	0.47	171	1.124	1.082	1.272	0.947	0.894
MLS94-268	North tributary	36	74	9.3	38	7.3	1.4	7.4	1.1	6.2	1.3	3.5	0.53	3.4	0.51	189	1.110	1.041	1.317	0.884	0.881
MLS94-270	North tributary	40	81	10.0	40	7.8	1.6	8.3	1.2	6.9	1.4	3.8	0.60	3.9	0.57	206	1.112	0.981	1.269	0.908	0.890
MLS96-277	North tributary	39	73	9.9	38	7.7	1.4	6.9	1.2	7.1	1.5	4.2	0.59	4.1	0.63	195	1.219	0.921	1.003	0.902	0.809
MLS94-114	West tributary	33	61	7.9	31	6.5	1.3	5.6	0.83	4.5	0.93	2.6	0.39	2.8	0.42	158	1.215	1.145	1.214	0.898	0.832
MLS94-276	West tributary	41	88	10	40	8.1	1.6	7.8	1.2	6.5	1.4	3.7	0.58	3.8	0.61	214	1.050	1.032	1.216	0.896	0.934

All concentrations in ppm.

Table 10.4 REE contents and ratios for Halfmile Lake deposit whole rocks

Sample	La	Ce	Pr	Nd	Sm	Eu	Gd	Tb	Dy	Ho	Er	Tm	Yb	Lu	ΣREE	$[La/Ce]_{NASC}$	$[La/Yb]_{NASC}$	$[Gd/Yb]_{NASC}$	$[La/Sm]_{NASC}$	Ce/Ce^*
ML95-320-65	39	89	10	38	7.8	0.30	7.6	1.4	7.9	1.7	4.7	0.71	4.8	0.66	214	1.000	0.787	0.944	0.891	0.982
ML95-321-65	16	45	4.6	18	4.3	0.11	5.1	0.97	6.3	1.3	3.6	0.51	3.6	0.47	110	0.811	0.431	0.845	0.663	1.142
ML95-322-65	35	74	8.9	34	7.3	0.40	7.1	1.2	7.0	1.4	3.6	0.54	3.6	0.50	185	1.079	0.942	1.176	0.854	0.913
ML95-323-65	5.0	12	1.7	8.1	2.4	0.70	3.1	0.65	4.0	0.84	2.3	0.32	2.3	0.30	44	0.951	0.211	0.804	0.371	0.896
ML95-324-65	5.9	16	2.3	10	3.0	0.97	3.7	0.64	3.9	0.80	2.0	0.27	1.7	0.25	51	0.841	0.336	1.298	0.350	0.946
ML95-325-65	26	57	6.9	25	4.7	0.37	4.2	0.68	4.4	0.93	2.6	0.40	2.8	0.42	136	1.041	0.900	0.894	0.985	0.927
ML95-326-65	29	63	7.4	28	5.8		5.2	0.91	5.5	1.2	3.1	0.48	3.2	0.48	153	1.050	0.878	0.969	0.891	0.937
ML95-326-65b	22	47	5.8	23	5.4	0.63	5.1	0.88	5.4	1.1	2.9	0.42	2.6	0.39	123	1.068	0.820	1.169	0.726	0.906
ML95-328-65	26	57	7.0	28	5.8	0.77	6.0	0.98	5.6	1.1	3.1	0.45	3.1	0.48	145	1.041	0.813	1.154	0.798	0.920
ML95-329-65	40	83	9.8	38	7.1	0.77	6.4	1.1	6.6	1.4	3.9	0.59	4.1	0.56	203	1.099	0.945	0.931	1.004	0.913
ML95-330-65	10	22	2.6	9.9	2.0		1.9	0.32	1.9	0.39	1.1	0.17	1.3	0.20	54	1.037	0.745	0.871	0.891	0.940
ML95-331-65	39	82	10	41	7.9	0.99	6.8	1.1	6.5	1.4	4.1	0.58	4.0	0.55	206	1.085	0.945	1.013	0.879	0.904
ML95-332-65	46	94	11	43	8.2	1.1	6.9	1.1	6.4	1.3	3.7	0.54	3.9	0.56	228	1.116	1.143	1.055	0.999	0.910
ML95-333-65	54	110	14	53	10	0.60	9.6	1.7	9.7	2.0	5.7	0.87	6.0	0.83	278	1.120	0.872	0.954	0.962	0.871
ML95-334-65	21	43	5.3	22	4.5	1.1	4.5	0.76	4.4	0.93	2.6	0.39	2.8	0.39	114	1.114	0.727	0.958	0.831	0.888
ML95-335-65	28	59	7.4	32	7.2	1.3	7.2	1.2	6.8	1.4	4.1	0.61	4.5	0.63	161	1.083	0.603	0.954	0.693	0.893
ML95-336-65	17	36	4.5	19	4.2	1.4	4.3	0.69	3.9	0.84	2.3	0.34	2.5	0.34	97	1.077	0.659	1.025	0.721	0.896
ML95-338-65	29	61	6.9	27	5.6	0.52	5.3	0.83	5.1	1.0	2.9	0.42	3.0	0.42	149	1.085	0.936	1.053	0.922	0.939
ML95-339-65	60	120	14	54	8.8	1.3	7.7	1.4	8.8	1.7	4.7	0.66	4.5	0.61	288	1.141	1.292	1.020	1.214	0.902
ML95-341-65	32	71	8.4	33	6.9	0.52	6.5	1.2	6.9	1.4	3.9	0.57	3.8	0.50	177	1.028	0.816	1.020	0.826	0.943
ML95-342-65	38	78	9.6	37	7.3	0.21	6.8	1.2	7.4	1.5	4.4	0.64	4.4	0.60	197	1.111	0.837	0.921	0.927	0.889
ML95-343-65	28	59	6.8	26	5.7	0.81	6.2	1.1	7.2	1.4	4.2	0.59	4.0	0.51	152	1.083	0.678	0.924	0.875	0.931
ML95-344-65	48	100	12	47	9.3	0.75	9.0	1.5	9.3	1.8	4.9	0.69	4.7	0.63	250	1.095	0.989	1.142	0.919	0.908
ML95-345-65	9.9	23	3.3	16	4.3	1.6	5.0	0.84	5.1	1.1	3.0	0.39	2.8	0.40	77	0.982	0.343	1.065	0.410	0.876
ML95-346-65	16	36	4.2	17	3.8	0.25	3.3	0.53	3.1	0.60	1.7	0.27	1.9	0.29	89	1.014	0.816	1.035	0.750	0.956
ML95-347-65	33	71	8.2	31	6.9	0.44	6.6	1.1	6.6	1.3	3.7	0.55	3.9	0.54	175	1.060	0.820	1.009	0.852	0.940
ML95-348-65	5.6	12	1.6	7.2	1.9	1.1	2.1	0.35	2.2	0.45	1.4	0.19	1.6	0.23	38	1.065	0.339	0.782	0.525	0.873
ML95-349-65	7.4	15	1.7	6.6	1.4	1.4	1.1	0.15	1.0	0.20	0.54	0.08	0.59	0.09	37	1.125	1.215	1.111	0.942	0.921
ML95-358-65	32	65	7.7	29	5.8	2.5	4.4	0.73	4.0	0.81	2.2	0.35	2.5	0.38	157	1.123	1.240	1.049	0.983	0.902

All concentrations in ppm.

Table 10.5 REE contents and ratios for Restigouche deposit surface waters

Sample	Location	La	Ce	Pr	Nd	Sm	Eu	Gd	Tb	Dy	Ho	Er	Tm	Yb	Lu	ΣREE	$[La/Ce]_{NASC}$	$[La/Yb]_{NASC}$	$[Gd/Yb]_{NASC}$	$[La/Sm]_{NASC}$	Ce/Ce^*
MLW95-408	Charlotte Brook	0.015	0.010	0.004	0.023	0.005		0.005		0.003	0.001	0.002		0.001		0.069	3.422	1.453	2.981	0.534	0.281
MLW95-410	Charlotte Brook	0.014	0.011	0.003	0.016	0.006	0.001	0.004	0.001	0.002	0.001	0.003	0.001	0.003	0.001	0.067	2.903	0.452	0.795	0.416	0.370
MLW95-412	Charlotte Brook	0.013	0.009	0.003	0.015	0.005		0.005		0.003		0.003		0.001		0.057	3.295	1.259	2.981	0.463	0.314
MLW95-414	Charlotte Brook	0.015	0.011	0.003	0.017	0.006	0.001	0.005	0.001	0.003	0.001	0.003	0.001	0.002	0.001	0.070	3.111	0.727	1.490	0.445	0.357
MLW95-416	Charlotte Brook	0.014	0.009	0.004	0.017	0.004		0.005		0.005	0.001	0.003		0.001		0.063	3.549	1.356	2.981	0.623	0.262
MLW95-418	Charlotte Brook	0.015	0.011	0.004	0.019	0.006		0.007	0.001	0.006		0.003		0.002		0.074	3.111	0.727	2.087	0.445	0.309
MLW95-421	Charlotte Brook	0.015	0.011	0.004	0.021	0.004		0.005		0.005		0.004		0.002		0.071	3.111	0.727	1.490	0.668	0.309
MLW95-422	Charlotte Brook	0.028	0.043	0.008	0.034	0.007	0.001	0.009	0.001	0.008	0.002	0.004		0.003		0.148	1.485	0.904	1.788	0.713	0.626
MLW95-423	Charlotte Brook	0.013	0.013	0.004	0.018	0.003		0.006		0.004	0.001	0.002		0.001		0.065	2.281	1.259	3.577	0.772	0.393
MLW95-425	Charlotte Brook	0.005		0.001	0.007	0.003		0.002		0.001		0.001				0.020				0.297	
MLW95-427	Charlotte Brook				0.004	0.001										0.005					
MLW95-428	Charlotte Brook	0.005	0.005	0.001	0.002	0.002	0.001	0.002	0.001	0.001	0.001	0.001	0.001	0.001	0.001	0.025	2.281	0.484	1.192	0.445	0.487
MLW95-429	Charlotte Brook				0.004							0.001				0.005					
MLW95-433	Charlotte Brook	0.022	0.026	0.005	0.026	0.006	0.001	0.007		0.005	0.002	0.003		0.003		0.106	1.930	0.710	1.391	0.653	0.540
MLW95-458	Charlotte Brook	0.007		0.002	0.009	0.002		0.003		0.002				0.002		0.027		0.339	0.894	0.623	
MLW95-550	Charlotte Brook			0.001	0.006											0.007					
MLW95-442	Charlotte Brook	0.011	0.008	0.003	0.016	0.004		0.005	0.001	0.006		0.002		0.001		0.057	3.137	1.066	2.981	0.490	0.303
MLW95-432	Charlotte Brook				0.004											0.004					
MLW95-426	Charlotte Brook				0.003											0.003					
MLW95-441	Mt Fowler E				0.004	0.001		0.002								0.007					
MLW96-664	Mt Fowler E	0.005	0.005	0.001	0.004	0.001	0.001	0.003	0.001	0.002	0.001	0.002	0.001	0.001	0.001	0.029	2.281	0.484	1.788	0.891	0.487
MLW96-665	Mt Fowler E	0.005	0.005	0.001	0.005	0.002	0.001	0.004	0.001	0.003	0.001	0.003	0.001	0.002	0.001	0.035	2.281	0.242	1.192	0.445	0.487
MLW96-666	Mt Fowler E	0.005	0.005	0.001	0.004	0.002	0.001	0.002	0.001	0.001	0.001	0.001	0.001	0.001	0.001	0.027	2.281	0.484	1.192	0.445	0.487
MLW96-667	Mt Fowler E	0.009	0.005	0.004	0.019	0.005	0.001	0.007	0.001	0.004	0.001	0.002	0.001	0.003	0.001	0.063	4.106	0.291	1.391	0.321	0.182
MLW96-668	Mt Fowler E	0.005	0.005	0.001	0.004	0.001	0.001	0.002	0.001	0.001	0.001	0.001	0.001	0.001	0.001	0.026	2.281	0.484	1.192	0.891	0.487
MLW95-438	Mt Fowler NE	0.012	0.006	0.002	0.016	0.003		0.005		0.004		0.002		0.002		0.052	4.563	0.581	1.490	0.713	0.267
MLW96-684	Mt Fowler NE	0.006	0.005	0.002	0.009	0.003	0.001	0.003	0.001	0.003	0.001	0.001	0.001	0.002	0.001	0.039	2.738	0.291	0.894	0.356	0.314
MLW96-688	Mt Fowler NE	0.005	0.005	0.001	0.003	0.001	0.001	0.002	0.001	0.001	0.001	0.001	0.001	0.001	0.001	0.025	2.281	0.484	1.192	0.891	0.487
MLW95-446	Mt Fowler SW	0.013	0.009	0.004	0.019	0.003		0.005		0.004	0.001	0.002		0.002		0.062	3.295	0.630	1.490	0.772	0.272
MLW95-447	Mt Fowler SW	0.010	0.006	0.002	0.014	0.002		0.005		0.004		0.002		0.001		0.046	3.802	0.969	2.981	0.891	0.292
MLW95-450	Mt Fowler SW	0.012	0.008	0.003	0.016	0.004		0.005		0.004		0.002		0.002		0.056	3.422	0.581	1.490	0.534	0.290
MLW95-453	Mt Fowler SW	0.016	0.010	0.004	0.022	0.005		0.006		0.007		0.003		0.002		0.075	3.650	0.775	1.788	0.570	0.272
MLW95-456	Mt Fowler SW	0.022	0.021	0.007	0.035	0.010	0.001	0.011	0.001	0.008	0.002	0.005		0.005		0.128	2.390	0.426	1.312	0.392	0.369
MLW96-650	Mt Moser NW	0.014	0.005	0.002	0.008	0.002	0.001	0.002	0.001	0.001	0.001	0.001	0.001	0.001	0.001	0.041	6.388	1.356	1.192	1.247	0.206
MLW96-651	Mt Moser NW	0.013	0.009	0.004	0.025	0.008	0.001	0.009	0.001	0.008	0.001	0.003	0.001	0.003	0.001	0.087	3.295	0.420	1.788	0.289	0.272
MLW96-654	Mt Moser NW	0.024	0.011	0.005	0.025	0.007	0.001	0.010	0.002	0.009	0.001	0.004	0.001	0.002	0.001	0.103	4.977	1.163	2.981	0.611	0.219
MLW96-656	Mt Moser NW	0.022	0.023	0.009	0.043	0.013	0.002	0.016	0.002	0.012	0.002	0.006	0.001	0.005	0.001	0.157	2.182	0.426	1.908	0.301	0.356
MLW96-709	Mt Moser WNW	0.011	0.007	0.004	0.020	0.006	0.001	0.010	0.001	0.007	0.001	0.003	0.001	0.002	0.001	0.075	3.585	0.533	2.981	0.327	0.230
MLW96-628	Mt Vroom E	0.010	0.010	0.003	0.015	0.008	0.001	0.005	0.001	0.003	0.001	0.004	0.001	0.003	0.001	0.066	2.281	0.323	0.994	0.223	0.398
MLW96-631	Mt Vroom E	0.011	0.014	0.005	0.016	0.006	0.001	0.005	0.001	0.006	0.001	0.003	0.001	0.006	0.001	0.077	1.792	0.178	0.497	0.327	0.411
MLW96-635	Mt Vroom E	0.010	0.014	0.003	0.017	0.008	0.002	0.005	0.001	0.005	0.001	0.004	0.001	0.004	0.001	0.076	1.629	0.242	0.745	0.223	0.557
MLW96-637	Mt Vroom E	0.016	0.039	0.006	0.032	0.008	0.002	0.009	0.001	0.011	0.001	0.006	0.001	0.008	0.001	0.141	0.936	0.194	0.671	0.356	0.867
MLW96-638	Mt Vroom E	0.013	0.020	0.005	0.023	0.010	0.002	0.008	0.001	0.006	0.001	0.004	0.001	0.006	0.001	0.101	1.483	0.210	0.795	0.232	0.540
MLW96-641	Mt Vroom E	0.005	0.007	0.001	0.007	0.004	0.001	0.003	0.001	0.005	0.001	0.003	0.001	0.003	0.001	0.043	1.629	0.161	0.596	0.223	0.682
MLW95-457	Mt Vroom NE	0.013	0.010	0.004	0.024	0.008	0.002	0.005		0.005		0.003		0.003		0.077	2.966	0.420	0.994	0.289	0.302
MLW95-464	Mt Vroom NE	0.015	0.009	0.006	0.027	0.007	0.001	0.008		0.004	0.001	0.003		0.004		0.085	3.802	0.363	1.192	0.382	0.207
MLW95-467	Mt Vroom NE	0.035	0.042	0.007	0.054	0.017						0.005				0.160	1.901			0.367	0.584
MLW95-468	Mt Vroom NE	0.022	0.009	0.007	0.040	0.009	0.001	0.008	0.002	0.005	0.001	0.004		0.004		0.112	5.576	0.533	1.192	0.435	0.158
MLW95-470	Mt Vroom NE	0.022	0.009	0.007	0.043	0.008	0.002	0.009	0.001	0.007	0.001	0.003		0.004		0.116	5.576	0.533	1.341	0.490	0.158

Table 10.5 REE contents and ratios for Restigouche deposit surface waters

Sample	Location	La	Ce	Pr	Nd	Sm	Eu	Gd	Tb	Dy	Ho	Er	Tm	Yb	Lu	ΣREE	$[La/Ce]_{NASC}$	$[La/Yb]_{NASC}$	$[Gd/Yb]_{NASC}$	$[La/Sm]_{NASC}$	Ce/Ce*
MLW95-301	Mt Vroom N	0.027	0.009	0.009	0.037	0.011	0.001	0.012	0.001	0.007	0.002	0.004		0.004		0.124	6.844	0.654	1.788	0.437	0.126
MLW95-302	Mt Vroom N	0.029	0.014	0.009	0.042	0.008	0.002	0.012		0.010	0.002	0.005		0.006		0.139	4.725	0.468	1.192	0.646	0.189
MLW95-395	Mt Vroom N	0.022	0.008	0.006	0.026	0.008	0.001	0.007		0.005		0.003		0.003		0.089	6.273	0.710	1.391	0.490	0.152
MLW95-398	Mt Vroom N	0.011		0.003	0.014	0.003		0.004		0.003		0.001		0.001		0.040		1.066	2.385	0.653	
MLW95-401	Mt Vroom N	0.015		0.003	0.019	0.002		0.005	0.001	0.004		0.002		0.002		0.053		0.727	1.490	1.336	
MLW95-403	Mt Vroom N	0.061		0.015	0.072	0.018	0.003	0.017	0.002	0.014	0.003	0.008	0.001	0.006	0.001	0.221		0.985	1.689	0.604	
MLW95-404	Mt Vroom N	0.024	0.006	0.006	0.023	0.005		0.008		0.006	0.001	0.003		0.002		0.084	9.125	1.163	2.385	0.855	0.109
MLW95-405	Mt Vroom N	0.015	0.005	0.005	0.019	0.007		0.009		0.005	0.001	0.002		0.003		0.071	6.844	0.484	1.788	0.382	0.126
MLW95-406	Mt Vroom N	0.017		0.006	0.027	0.005		0.006		0.004	0.001	0.004		0.004		0.074		0.412	0.894	0.606	
MLW96-658	Mt Vroom N	0.024	0.011	0.008	0.032	0.012	0.002	0.008	0.001	0.008	0.002	0.005	0.001	0.006	0.001	0.121	4.977	0.388	0.795	0.356	0.173
MLW96-661	Mt Vroom N	0.041	0.021	0.014	0.058	0.017	0.003	0.016	0.002	0.012	0.003	0.008	0.001	0.008	0.001	0.205	4.454	0.496	1.192	0.430	0.191
MLW96-646	Mt Vroom SE	0.026	0.027	0.011	0.040	0.009	0.002	0.012	0.001	0.010	0.002	0.006	0.001	0.006	0.001	0.154	2.197	0.420	1.192	0.515	0.348
MLW95-319	North stream	0.027	0.014	0.009	0.043	0.013	0.001	0.016	0.002	0.013	0.003	0.006		0.004		0.151	4.400	0.654	2.385	0.370	0.196
MLW95-382	North stream	0.036		0.011	0.051	0.013		0.015	0.002	0.012	0.002	0.005	0.001	0.005		0.153		0.698	1.788	0.493	
MLW95-383	North stream	0.038		0.013	0.067	0.014		0.020	0.002	0.012	0.003	0.006		0.005		0.180		0.736	2.385	0.483	
MLW95-385	North stream	0.033		0.009	0.050	0.013	0.001	0.017	0.002	0.011	0.002	0.005		0.004		0.147		0.799	2.534	0.452	
MLW95-389	North stream	0.023		0.006	0.034	0.006	0.001	0.010	0.001	0.008	0.002	0.004		0.004		0.099		0.557	1.490	0.683	
MLW95-393	North stream	0.010		0.003	0.021	0.006		0.006	0.001	0.004		0.003		0.002		0.056		0.484	1.788	0.297	
MLW96-714	North stream	0.012	0.009	0.004	0.018	0.010	0.001	0.008	0.001	0.009	0.001	0.003	0.001	0.002	0.001	0.080	3.042	0.581	2.385	0.214	0.283
MLW95-345	Seep	0.007	0.008	0.001	0.007	0.015										0.038	1.996			0.083	0.659
MLW95-322	Seep	0.010		0.003	0.020	0.006	0.001	0.009		0.005	0.001	0.003		0.002		0.060		0.484	2.683	0.297	
MLW95-300	Seep	0.850	0.830	0.160	0.750	0.410	0.110									3.110	2.336			0.369	0.490
MLW95-434	Seep	0.084	0.020	0.023	0.110	0.027	0.004	0.033	0.004	0.023	0.006	0.015	0.002	0.010	0.002	0.363	9.581	0.814	1.967	0.554	0.099
MLW96-710	West of deposit	0.074	0.181	0.030	0.117	0.043	0.007	0.031	0.006	0.029	0.006	0.019	0.003	0.018	0.003	0.567	0.933	0.398	1.027	0.307	0.837
MLW96-711	West of deposit	0.010	0.012	0.005	0.020	0.008	0.001	0.006	0.001	0.006	0.001	0.003	0.001	0.002	0.001	0.077	1.901	0.484	1.788	0.223	0.370
MLW96-712	West of deposit	0.009	0.005	0.003	0.014	0.002	0.001	0.002	0.001	0.003	0.001	0.001	0.001	0.001	0.001	0.045	4.106	0.872	1.192	0.802	0.210
MLW96-713	West of deposit	0.005	0.005	0.001	0.005	0.001	0.001	0.002	0.001	0.001	0.001	0.001	0.001	0.001	0.001	0.027	2.281	0.484	1.192	0.891	0.487
MLW95-435	18 Mile Brook	0.035	0.016	0.010	0.045	0.008	0.003	0.012	0.002	0.007	0.002	0.004		0.004		0.148	4.990	0.848	1.788	0.779	0.186
MLW95-444	Portage Lake				0.006	0.002				0.002				0.001		0.011					
MLW95-437	SE Upsalquitch	0.046	0.040	0.015	0.064	0.015	0.003	0.018	0.002	0.014	0.003	0.007		0.006	0.001	0.234	2.623	0.743	1.788	0.546	0.332
MLW95-436	Simpsons Brook	0.026	0.012	0.007	0.036	0.010	0.002	0.010	0.002	0.008	0.002	0.005		0.004		0.124	4.943	0.630	1.490	0.463	0.194
MLW95-443	Simpsons Brook	0.028	0.019	0.008	0.038	0.011	0.002	0.010	0.002	0.010	0.002	0.005		0.005		0.140	3.362	0.543	1.192	0.453	0.277

All concentrations in µg/L; blank = below detection

Table 10.6 REE contents and ratios for Restigouche deposit groundwaters

Sample	Location	La	Ce	Pr	Nd	Sm	Eu	Gd	Tb	Dy	Ho	Er	Tm	Yb	Lu	ΣREE	$[La/Ce]_{NASC}$	$[La/Yb]_{NASC}$	$[Gd/Yb]_{NASC}$	$[La/Sm]_{NASC}$	Ce/Ce*
MLW95-561	B-80-15	0.005	0.006	0.001	0.004	0.003	0.001	0.004	0.001	0.005	0.001	0.002	0.001	0.003	0.001	0.038	1.901	0.161	0.795	0.297	0.584
MLW95-563	B-80-15	0.005	0.005	0.001	0.002	0.001	0.001	0.002	0.001	0.001	0.001	0.002	0.001	0.002	0.001	0.026	2.281	0.242	0.596	0.891	0.487
MLW95-590	B-80-7				0.002					0.002		0.001				0.005					
MLW95-581	B-80-7				0.002					0.001		0.002		0.001		0.006					
MLW95-577	B-80-7				0.002					0.002		0.002		0.002		0.008					
MLW95-587	B-80-7	0.011	0.029	0.005	0.028	0.009	0.002	0.017	0.003	0.015	0.004	0.011	0.001	0.010	0.002	0.147	0.865	0.107	1.013	0.218	0.852
MLW95-543	C4/C5 zone	0.005	0.006	0.001	0.005	0.001	0.001	0.002	0.001	0.003	0.001	0.002	0.001	0.001	0.001	0.031	1.901	0.484	1.192	0.891	0.584
MLW95-544	C4/C5 zone	0.005	0.007	0.001	0.004	0.004	0.001	0.008	0.001	0.009	0.001	0.003	0.001	0.001	0.001	0.047	1.629	0.484	4.769	0.223	0.682
MLW95-365	EH-1	0.040	0.019	0.012	0.059	0.018	0.001	0.027	0.003	0.022	0.005	0.015	0.003	0.015	0.003	0.242	4.803	0.258	1.073	0.396	0.189
MLW95-370	EH-1	0.034	0.028	0.010	0.046	0.018	0.002	0.016	0.003	0.016	0.004	0.011	0.003	0.013	0.002	0.206	2.770	0.253	0.734	0.336	0.331
MLW96-649	MM-88-01	0.009	0.010	0.002	0.010	0.004	0.001	0.003	0.001	0.010	0.002	0.008	0.001	0.005	0.001	0.067	2.053	0.174	0.358	0.401	0.513
MLW96-662	MM-88-01	0.005	0.005	0.001	0.003	0.001	0.001	0.002	0.001	0.003	0.001	0.003	0.001	0.002	0.001	0.030	2.281	0.242	0.596	0.891	0.487
MLW95-358	MM-88-06	0.046	0.082	0.008	0.021	0.004	0.001	0.010	0.001	0.007	0.001	0.003	0.001	0.002	0.001	0.188	1.280	2.228	2.981	2.048	0.931
MLW95-361	MM-88-06	0.031	0.056	0.006	0.016	0.005	0.001	0.007	0.001	0.009	0.001	0.004	0.001	0.002	0.001	0.141	1.263	1.502	2.087	1.104	0.894
MLW95-364	MM-88-06	0.013	0.023	0.001	0.006	0.004	0.001	0.002	0.001	0.004	0.001	0.003	0.001	0.003	0.001	0.064	1.289	0.420	0.397	0.579	1.389
MLW95-315	MM-88-07	0.057	0.058	0.009	0.043	0.010	0.002	0.012	0.002	0.013	0.003	0.008		0.004		0.221	2.242	1.380	1.788	1.015	0.558
MLW95-317	MM-88-07	0.030	0.039	0.005	0.016	0.005	0.001	0.009	0.001	0.007	0.001	0.005	0.001	0.003	0.001	0.124	1.755	0.969	1.788	1.069	0.694
MLW95-556	MM-89-100	0.006	0.008	0.001	0.002	0.001	0.001	0.002	0.001	0.001	0.001	0.001	0.001	0.001	0.001	0.028	1.711	0.581	1.192	1.069	0.711
MLW95-570	MM-89-102	0.016	0.046	0.005	0.025	0.007		0.008	0.001	0.010	0.003	0.009	0.001	0.008	0.001	0.140	0.793	0.194	0.596	0.407	1.120
MLW95-546	MM-89-104	0.005	0.005	0.001	0.002	0.001	0.001	0.002	0.001	0.002	0.001	0.001	0.001	0.001	0.001	0.025	2.281	0.484	1.192	0.891	0.487
MLW95-528	MM-89-106				0.004	0.001										0.005					
MLW95-526	MM-89-106		0.010	0.001	0.005	0.001		0.002		0.002		0.001				0.022					
MLW95-522	MM-89-106		0.006	0.001	0.006	0.002								0.001		0.016					
MLW95-512	MM-89-106		0.008	0.002	0.007	0.003		0.003		0.004		0.003		0.002		0.032			0.894		
MLW95-508	MM-89-106	0.008	0.019	0.004	0.016	0.002	0.001	0.003	0.001	0.007	0.001	0.004		0.004		0.070	0.961	0.194	0.447	0.713	0.732
MLW95-504	MM-89-106	0.008	0.018	0.002	0.010	0.003		0.004		0.005		0.002		0.003		0.055	1.014	0.258	0.795	0.475	0.980
MLW95-503	MM-89-106	0.011	0.016	0.003	0.014	0.003	0.001	0.006		0.005	0.001	0.005		0.002		0.067	1.568	0.533	1.788	0.653	0.607
MLW95-596	MM-89-107		0.007	0.001	0.006	0.001										0.015					
MLW95-595	MM-89-107		0.007		0.003	0.001				0.001						0.012					

All concentrations in µg/L; blank = below detection

Table 10.7 REE contents and ratios for Restigouche deposit stream sediments

Sample	Location	La	Ce	Pr	Nd	Sm	Eu	Gd	Tb	Dy	Ho	Er	Tm	Yb	Lu	ΣREE	$[La/Ce]_{NASC}$	$[La/Yb]_{NASC}$	$[Gd/Yb]_{NASC}$	$[La/Sm]_{NASC}$	Ce/Ce*
MLS95-409	Charlotte Brook	51	91	14	54	12	2.1	12	1.7	9.1	1.9	5.0	0.76	4.6	0.68	258	1.266	1.075	1.507	0.782	0.759
MLS95-427	Charlotte Brook	43	93	12	52	12	2.3	13	1.8	9.5	2.0	5.1	0.76	4.7	0.69	251	1.055	0.896	1.603	0.666	0.892
MLS96-408	Charlotte Brook	52	89	14	56	12	2.1	12	1.7	10	2.0	5.2	0.70	4.7	0.77	262	1.333	1.072	1.522	0.772	0.718
MLS96-409	Charlotte Brook	51	86	13	52	11	1.9	11	1.6	8.9	1.8	4.8	0.68	4.4	0.75	249	1.353	1.123	1.490	0.826	0.727
MLS96-410	Charlotte Brook	48	79	13	51	11	1.9	11	1.6	9.0	1.8	5.0	0.68	4.5	0.73	238	1.386	1.033	1.457	0.777	0.689
MLS96-411	Charlotte Brook	48	73	13	52	12	2.0	12	1.7	9.8	1.9	5.1	0.69	4.6	0.75	237	1.500	1.011	1.555	0.713	0.636
MLS96-412	Charlotte Brook	58	88	15	62	14	2.3	14	1.9	11	2.2	5.7	0.81	5.2	0.84	281	1.504	1.081	1.605	0.738	0.650
MLS96-413	Charlotte Brook	50	77	13	53	12	2.0	12	1.7	9.8	1.9	5.1	0.71	4.7	0.78	244	1.481	1.031	1.522	0.742	0.658
MLS96-414	Charlotte Brook	47	73	13	52	12	2.0	12	1.7	10	2.0	5.4	0.75	4.9	0.79	237	1.469	0.929	1.460	0.698	0.643
MLS96-415	Charlotte Brook	50	78	13	53	11	2.0	12	1.6	9.7	1.9	5.1	0.71	4.7	0.75	243	1.462	1.031	1.522	0.810	0.666
MLS96-416	Charlotte Brook	47	71	13	51	12	2.0	11	1.6	9.4	1.9	5.0	0.69	4.5	0.73	231	1.510	1.012	1.457	0.698	0.626
MLS96-417	Charlotte Brook	50	78	13	54	11	2.0	11	1.6	9.1	1.9	5.0	0.69	4.6	0.75	243	1.462	1.053	1.426	0.810	0.666
MLS96-417a	Charlotte Brook	45	66	12	47	11	1.9	11	1.6	9.3	1.9	5.0	0.68	4.4	0.68	217	1.555	0.991	1.490	0.729	0.619
MLS96-418	Charlotte Brook	51	87	13	52	11	1.9	11	1.7	9.8	2.0	5.5	0.76	5.0	0.80	252	1.337	0.988	1.312	0.826	0.736
MLS96-423	Charlotte Brook	41	68	11	45	9.7	1.3	9.6	1.4	8.7	1.8	4.9	0.68	4.5	0.73	208	1.375	0.883	1.272	0.753	0.697
MLS96-424	Charlotte Brook	39	55	11	46	11	1.9	11	1.5	8.9	1.9	5.0	0.65	4.1	0.68	198	1.618	0.921	1.599	0.632	0.578
MLS96-429	Charlotte Brook	27	54	8.0	32	7.2	1.4	7.5	1.1	6.2	1.3	3.4	0.48	3.3	0.53	153	1.141	0.793	1.355	0.668	0.800
MLS96-430	Charlotte Brook	26	56	7.2	29	6.3	1.3	6.3	0.92	5.4	1.1	3.1	0.44	3.0	0.49	147	1.059	0.840	1.252	0.735	0.891
MLS96-433	Charlotte Brook	19	36	5.6	24	5.5	0.70	5.7	0.79	4.5	0.94	2.6	0.36	2.4	0.41	109	1.204	0.767	1.416	0.615	0.760
MLS96-620	Charlotte Brook	47	80	12	50	11	1.9	11	1.5	8.1	1.6	4.6	0.69	4.4	0.68	234	1.340	1.035	1.490	0.761	0.734
MLS96-621	Charlotte Brook	46	76	12	49	11	1.9	11	1.5	8.3	1.7	4.5	0.69	4.5	0.69	229	1.381	0.990	1.457	0.745	0.705
MLS96-622	Charlotte Brook	47	85	12	49	9.8	1.8	10	1.4	7.8	1.6	4.4	0.66	4.3	0.66	235	1.261	1.059	1.386	0.854	0.780
MLS96-623	Charlotte Brook	49	84	13	53	11	2.0	12	1.6	8.9	1.8	4.9	0.76	4.8	0.74	248	1.331	0.989	1.490	0.793	0.725
MLS96-624	Charlotte Brook	50	77	13	54	12	2.0	12	1.7	9.0	1.8	4.9	0.73	4.4	0.70	243	1.481	1.101	1.626	0.742	0.658
MLS96-625	Charlotte Brook	51	84	13	54	11	2.0	12	1.7	9.2	1.8	5.0	0.74	4.6	0.71	251	1.385	1.074	1.555	0.826	0.711
MLS96-626	Charlotte Brook	52	83	14	55	12	2.0	13	1.8	9.6	1.9	5.2	0.77	4.7	0.75	256	1.429	1.072	1.649	0.772	0.670
MLS96-627	Charlotte Brook	52	88	14	55	12	2.0	13	1.8	9.7	2.0	5.3	0.80	4.9	0.75	261	1.348	1.028	1.582	0.772	0.710
MLS96-441	Mt Fowler E	29	44	8.3	35	8.2	1.2	9.1	1.2	6.8	1.3	3.5	0.45	2.9	0.49	151	1.504	0.969	1.871	0.630	0.618
MLS96-663	Mt Fowler E	15	22	4.4	20	4.9	0.81	6.6	0.89	4.8	1.0	2.8	0.41	2.4	0.40	86	1.555	0.605	1.639	0.545	0.590
MLS96-664	Mt Fowler E	11	20	3.1	15	3.7	0.80	5.5	0.78	4.3	0.96	2.7	0.37	2.3	0.39	71	1.255	0.463	1.426	0.530	0.746
MLS96-665	Mt Fowler E	12	18	4.2	20	5.2	1.1	7.9	1.1	5.6	1.3	3.4	0.49	2.8	0.47	84	1.521	0.415	1.682	0.411	0.552
MLS96-666	Mt Fowler E	41	60	11	45	9.2	1.7	10	1.3	7.2	1.5	4.1	0.62	4.2	0.62	197	1.559	0.946	1.419	0.794	0.615
MLS96-668	Mt Fowler E	53	68	15	63	14	2.5	14	1.9	9.7	1.9	5.0	0.75	4.8	0.76	254	1.778	1.070	1.739	0.674	0.525
MLS96-683	Mt Fowler NE	43	69	12	50	11	2.6	13	1.9	9.8	2.0	5.4	0.81	5.2	0.82	227	1.422	0.801	1.490	0.696	0.662
MLS96-684	Mt Fowler NE	41	68	11	46	11	2.4	12	1.7	9.3	1.8	4.9	0.67	4.6	0.73	215	1.375	0.863	1.555	0.664	0.697
MLS96-685	Mt Fowler NE	41	70	12	48	12	2.4	13	1.8	9.6	1.9	4.9	0.69	4.8	0.75	223	1.336	0.827	1.615	0.609	0.687
MLS96-686	Mt Fowler NE	41	71	11	47	11	2.2	11	1.7	8.8	1.8	4.6	0.66	4.4	0.73	217	1.317	0.903	1.490	0.664	0.728
MLS96-687	Mt Fowler NE	38	75	11	45	10	1.9	11	1.6	8.6	1.7	4.6	0.63	4.3	0.71	214	1.156	0.856	1.525	0.677	0.799
MLS95-447	Mt Fowler SW	56	87	16	65	14	2.3	15	2.2	12	2.4	6.4	0.86	5.2	0.79	283	1.477	1.043	1.720	0.739	0.629
MLS96-446	Mt Fowler SW	56	87	15	62	13	2.1	13	1.8	11	2.1	5.6	0.80	5.2	0.86	275	1.468	1.043	1.490	0.767	0.654
MLS96-448	Mt Fowler SW	56	77	16	67	15	2.3	15	2.2	13	2.5	6.5	0.88	5.7	0.95	280	1.659	0.952	1.569	0.665	0.560
MLS96-450	Mt Fowler SW	54	79	15	66	15	2.3	17	2.2	12	2.5	6.7	0.92	5.8	1.0	279	1.559	0.902	1.747	0.641	0.605
MLS96-451	Mt Fowler SW	60	87	17	71	16	2.4	18	2.3	13	2.6	6.9	0.95	6.2	1.0	304	1.573	0.938	1.731	0.668	0.593
MLS96-452	Mt Fowler SW	60	86	17	72	16	2.5	18	2.5	13	2.7	7.1	0.99	6.0	1.0	305	1.592	0.969	1.788	0.668	0.586
MLS96-453	Mt Fowler SW	59	89	16	68	16	2.2	18	2.5	13	2.6	6.7	0.97	5.8	0.88	301	1.512	0.985	1.850	0.657	0.631
MLS96-454	Mt Fowler SW	56	87	16	67	15	2.2	17	2.4	13	2.5	6.7	0.98	5.9	0.90	293	1.468	0.919	1.718	0.665	0.633
MLS96-455	Mt Fowler SW	56	79	15	67	16	2.4	18	2.5	13	2.5	6.5	0.94	5.8	0.86	286	1.617	0.935	1.850	0.623	0.594
MLS96-456	Mt Fowler SW	65	100	19	85	20	3.2	25	3.3	18	3.5	9.1	1.3	7.9	1.2	362	1.483	0.797	1.887	0.579	0.620
MLS96-651	Mt Moser NW	44	80	12	54	13	2.0	16	2.2	11	2.2	5.5	0.78	4.9	0.74	248	1.255	0.870	1.947	0.603	0.758

Table 10.7 REE contents and ratios for Restigouche deposit stream sediments

Sample	Location	La	Ce	Pr	Nd	Sm	Eu	Gd	Tb	Dy	Ho	Er	Tm	Yb	Lu	ΣREE	$[La/Ce]_{NASC}$	$[La/Yb]_{NASC}$	$[Gd/Yb]_{NASC}$	$[La/Sm]_{NASC}$	Ce/Ce*
MLS96-653	Mt Moser NW	43	85	13	55	14	2.0	17	2.3	12	2.3	5.7	0.83	5.0	0.76	258	1.154	0.833	2.027	0.547	0.783
MLS96-654	Mt Moser NW	43	87	12	52	14	1.8	16	2.3	12	2.3	6.0	0.87	5.2	0.80	255	1.128	0.801	1.834	0.547	0.834
MLS96-657	Mt Moser NW	42	88	12	50	12	2.5	12	1.7	8.8	1.7	4.7	0.75	4.9	0.77	242	1.089	0.830	1.460	0.623	0.854
MLS96-628	Mt Vroom E	130	230	29	110	22	4.2	19	2.6	14	2.8	7.5	1.3	7.7	1.2	581	1.289	1.636	1.471	1.053	0.816
MLS96-629	Mt Vroom E	75	150	19	74	16	3.0	14	2.1	11	2.3	6.2	0.90	5.8	0.99	380	1.141	1.253	1.439	0.835	0.865
MLS96-631	Mt Vroom E	93	180	23	90	18	3.3	15	2.1	12	2.3	6.3	1.0	6.7	0.96	454	1.179	1.345	1.335	0.920	0.848
MLS96-632	Mt Vroom E	58	120	15	58	12	2.4	11	1.6	8.7	1.7	4.7	0.79	5.1	0.80	300	1.103	1.102	1.286	0.861	0.886
MLS96-634	Mt Vroom E	50	100	13	51	11	2.2	10	1.6	9.0	1.8	5.1	0.82	5.4	0.80	262	1.141	0.897	1.104	0.810	0.854
MLS96-635	Mt Vroom E	34	76	9.0	35	7.9	1.5	7.4	1.1	5.9	1.1	3.0	0.49	3.4	0.52	186	1.021	0.969	1.298	0.767	0.946
MLS96-636	Mt Vroom E	70	130	18	70	14	2.7	12	1.6	7.7	1.4	3.7	0.64	4.3	0.70	337	1.228	1.577	1.664	0.891	0.798
MLS96-638	Mt Vroom E	64	140	16	64	14	2.5	12	1.8	9.1	1.8	4.8	0.82	5.5	0.84	337	1.043	1.127	1.301	0.814	0.953
MLS96-641	Mt Vroom E	48	99	12	47	9.8	1.8	8.4	1.2	5.7	1.1	2.9	0.50	3.2	0.51	241	1.106	1.453	1.565	0.872	0.898
MLS96-642	Mt Vroom E	62	130	16	66	15	3.0	14	2.0	11	2.1	5.8	0.98	6.7	1.0	336	1.088	0.896	1.246	0.736	0.899
MLS96-644	Mt Vroom E	30	98	11	47	13	2.9	15	2.2	11	2.2	6.1	1.1	7.5	1.2	248	0.698	0.388	1.192	0.411	1.175
MLS95-398	Mt Vroom N	43	90	11	44	9.3	2.0	9.5	1.4	7.4	1.6	4.3	0.66	4.0	0.60	228	1.090	1.055	1.426	0.828	0.901
MLS95-404	Mt Vroom N	59	125	19	80	20	4.6	22	3.1	16	3.2	8.5	1.3	7.6	1.2	368	1.068	0.746	1.726	0.534	0.828
MLS96-301	Mt Vroom N	54	90	15	60	12	2.4	12	1.6	9.4	1.9	5.4	0.72	4.9	0.76	270	1.369	1.068	1.460	0.802	0.689
MLS96-302	Mt Vroom N	50	82	13	56	12	2.1	11	1.5	9.2	1.8	4.8	0.67	4.4	0.71	249	1.391	1.101	1.490	0.742	0.701
MLS96-395	Mt Vroom N	47	87	13	52	11	2.3	11	1.5	8.7	1.8	4.5	0.65	4.4	0.69	246	1.232	1.035	1.490	0.761	0.767
MLS96-395a	Mt Vroom N	53	91	14	62	14	2.9	13	1.9	11	2.3	5.7	0.81	5.2	0.84	278	1.329	0.987	1.490	0.674	0.728
MLS96-397	Mt Vroom N	46	91	13	54	12	2.6	12	1.7	9.7	2.0	5.3	0.75	4.9	0.81	256	1.153	0.909	1.460	0.683	0.811
MLS96-658	Mt Vroom N	39	76	8.6	32	6.4	1.0	6.1	0.96	5.5	1.1	3.3	0.52	3.3	0.51	184	1.171	1.145	1.102	1.085	0.904
MLS96-661	Mt Vroom N	64	110	22	94	23	5.0	24	3.2	16	3.0	7.5	1.2	7.4	1.2	382	1.327	0.838	1.933	0.496	0.638
MLS96-457	Mt Vroom NE	50	98	14	58	12	2.6	13	1.7	8.9	1.8	5.0	0.83	5.4	0.84	272	1.164	0.897	1.435	0.742	0.807
MLS96-461	Mt Vroom NE	45	95	13	55	13	2.7	13	1.8	9.2	1.8	5.0	0.81	5.4	0.87	262	1.081	0.807	1.435	0.617	0.855
MLS96-462	Mt Vroom NE	56	110	16	64	13	2.8	13	1.9	9.5	1.8	5.1	0.81	5.6	0.85	300	1.161	0.969	1.384	0.767	0.800
MLS96-463	Mt Vroom NE	56	120	16	63	14	2.9	14	2.0	9.9	1.9	5.5	0.89	5.8	0.91	313	1.065	0.935	1.439	0.713	0.873
MLS96-464	Mt Vroom NE	55	110	16	66	15	3.2	15	2.2	11	2.2	6.3	1.0	6.7	1.0	311	1.141	0.795	1.335	0.653	0.808
MLS96-465	Mt Vroom NE	46	100	13	57	13	2.8	13	1.8	9.2	1.9	5.0	0.84	5.6	0.87	270	1.049	0.796	1.384	0.630	0.891
MLS96-466A	Mt Vroom NE	45	95	12	51	11	2.3	11	1.5	7.8	1.5	4.3	0.69	4.6	0.71	248	1.081	0.948	1.426	0.729	0.890
MLS96-466B	Mt Vroom NE	49	100	13	53	11	2.4	11	1.6	8.4	1.6	4.6	0.75	4.9	0.76	262	1.118	0.969	1.338	0.793	0.863
MLS96-468	Mt Vroom NE	47	95	16	73	18	4.2	20	2.6	13	2.5	6.9	1.1	7.4	1.2	308	1.129	0.615	1.611	0.465	0.755
MLS96-469	Mt Vroom NE	54	97	20	93	24	5.4	26	3.1	15	3.0	7.9	1.3	8.8	1.4	360	1.270	0.594	1.761	0.401	0.643
MLS95-389	North Stream	79	105	23	94	25	3.7	33	4.8	25	5.0	12.5	1.7	9.1	1.4	420	1.725	0.846	2.141	0.574	0.540
MLS96-381	North stream	53	86	14	57	12	1.8	13	1.9	11	2.3	6.3	0.82	5.3	0.87	265	1.406	0.969	1.462	0.787	0.688
MLS96-385	North stream	68	90	18	79	17	2.4	21	2.9	17	3.5	9.2	1.2	7.1	1.1	337	1.724	0.928	1.763	0.713	0.560
MLS96-386	North stream	72	100	20	85	20	2.8	23	3.5	20	4.1	11.0	1.3	8.1	1.3	372	1.643	0.861	1.693	0.641	0.574
MLS96-387	North stream	64	87	18	75	18	2.4	21	3.1	18	3.7	9.2	1.2	7.1	1.1	329	1.678	0.873	1.763	0.633	0.558
MLS96-391	North stream	100	100	29	120	33	4.6	41	6.0	34	6.6	16.0	2.0	12.0	1.8	506	2.281	0.807	2.037	0.540	0.404

All concentrations in ppm.

Table 10.8 REE contents and ratios for Restigouche deposit whole rocks

Sample	La	Ce	Pr	Nd	Sm	Eu	Gd	Tb	Dy	Ho	Er	Tm	Yb	Lu	ΣREE	$[La/Ce]_{NASC}$	$[La/Yb]_{NASC}$	$[Gd/Yb]_{NASC}$	$[La/Sm]_{NASC}$	Ce/Ce*
ML95-235	65	140	17	66	12	0.92	10	1.5	9.7	1.9	5.4	0.80	5.2	0.83	336	1.059	1.211	1.146	0.965	0.917
ML95-237	73	150	19	73	14	1.5	11	1.8	10	2.1	5.8	0.89	6.1	0.91	369	1.110	1.159	1.075	0.929	0.877
ML95-240	17	39	5.1	23	5.6	1.5	6.7	1.1	7.0	1.4	3.9	0.56	3.5	0.53	116	0.994	0.471	1.141	0.541	0.912
ML95-241	71	140	18	71	14	1.6	11	1.7	9.1	1.8	4.8	0.73	4.9	0.73	350	1.157	1.404	1.338	0.903	0.853
ML95-250	3.5	7.2	0.84	3.4	0.77	0.05	0.97	0.20	1.2	0.24	0.70	0.11	0.71	0.10	20	1.109	0.478	0.814	0.810	0.915
ML95-253	14	31	4.3	19	4.8	1.7	5.9	0.99	5.8	1.3	3.5	0.52	3.3	0.52	97	1.030	0.411	1.066	0.520	0.870
ML95-255	1.3	2.6	0.3	1.4	0.4	0.02	0.6	0.11	0.59	0.11	0.33	0.05	0.43	0.06	8.3	1.141	0.293	0.873	0.579	0.907
ML95-256	31	68	8.4	31	6.5	0.32	6.1	1.0	6.0	1.3	3.6	0.53	3.5	0.51	168	1.040	0.858	1.039	0.850	0.918
ML95-258	7.6	18	2.2	9.2	2.3	0.21	2.4	0.40	2.1	0.40	1.1	0.16	1.2	0.17	47	0.963	0.614	1.192	0.589	0.959
ML95-259	28	67	8.9	35	6.2	0.42	5.2	0.81	4.8	1.0	2.9	0.43	2.9	0.43	164	0.953	0.935	1.069	0.804	0.924
ML95-260	41	89	11	40	8.1	0.45	6.9	1.1	6.5	1.3	3.7	0.53	3.9	0.57	214	1.051	1.018	1.055	0.902	0.913
ML95-262	31	61	7.0	26	5.4	0.86	5.0	0.82	4.8	0.95	2.7	0.40	2.8	0.40	149	1.159	1.073	1.065	1.023	0.902
ML95-263	39	81	11	38	7.7	1.2	6.3	1.1	6.2	1.2	3.4	0.49	3.5	0.51	201	1.098	1.079	1.073	0.902	0.852
ML95-264	14	32	4.4	20	5.1	1.8	6.1	1.0	6.5	1.4	3.7	0.53	3.8	0.54	101	0.998	0.357	0.957	0.489	0.888
ML95-265	65	140	18	68	14	2.0	13	2.1	13	2.6	7.1	1.1	7.1	1.0	354	1.059	0.887	1.092	0.827	0.891
ML95-266	72	160	21	77	15	0.66	13	2.2	12	2.5	6.4	0.95	6.3	0.94	390	1.027	1.107	1.230	0.855	0.896
ML95-269	82	170	22	81	15	1.5	13	1.8	11	2.2	5.8	0.91	6.3	0.92	413	1.100	1.261	1.230	0.974	0.872
ML95-273a	110	230	29	110	24	1.0	20	3.1	18	3.5	8.9	1.3	8.4	1.2	568	1.091	1.269	1.419	0.816	0.887
ML95-273b	22	48	5.6	22	4.4	0.03	4.2	0.70	4.3	0.95	2.7	0.39	2.4	0.36	118	1.046	0.888	1.043	0.891	0.942
ML95-274	69	140	17	66	12	0.76	9.8	1.5	8.6	1.7	4.4	0.65	4.4	0.64	336	1.124	1.519	1.328	1.024	0.890
ML95-276	32	71	8.7	34	8.6	0.96	9.1	1.6	8.9	1.8	4.4	0.56	3.2	0.44	185	1.028	0.969	1.695	0.663	0.927
ML95-277	110	220	29	110	22	1.2	20	2.9	15	2.9	7.4	1.0	6.3	0.91	549	1.141	1.691	1.893	0.891	0.848
ML95-278	64	140	17	63	13	0.85	12	1.9	10	2.0	5.4	0.79	5.1	0.74	336	1.043	1.216	1.403	0.877	0.924
ML95-279	52	110	14	53	12	0.60	10	1.7	9.1	1.8	4.7	0.68	4.4	0.66	275	1.078	1.145	1.355	0.772	0.888
ML95-280	140	290	35	140	26	1.5	20	2.7	17	3.3	9.1	1.4	10.0	1.5	698	1.101	1.356	1.192	0.959	0.902
ML95-283	94	200	23	84	17	2.2	14	1.8	9.2	1.7	4.3	0.66	4.5	0.70	457	1.072	2.024	1.855	0.985	0.937
ML95-284	53	110	13	50	10	1.6	8.9	1.6	9.3	1.9	5.1	0.74	5.0	0.75	271	1.099	1.027	1.061	0.944	0.913
ML95-285	40	91	11	43	9.0	1.2	8.3	1.4	8.1	1.7	4.7	0.71	4.7	0.72	226	1.003	0.824	1.053	0.792	0.945
ML95-297	1.0	1.9	0.23	1.2	0.38	0.14	0.54	0.10	0.55	0.09	0.21	0.03	0.18	0.03	6.6	1.201	0.538	1.788	0.469	0.863
ML95-298	0.40	0.80	0.10	0.70	0.14	0.05	0.21	0.03	0.19	0.03	0.07				2.7	1.141			0.509	0.871
ML95-299	0.70	1.3	0.17	0.90	0.21	0.34	0.24	0.05	0.26	0.05	0.12		0.10		4.4	1.228	0.678	1.431	0.594	0.821
ML95-300	2.7	5.7	0.73	3.3	0.86	0.26	1.1	0.17	0.77	0.13	0.26	0.03	0.17	0.03	16	1.081	1.539	3.857	0.559	0.884
ML95-321	1.2	2.3	0.24	1.1	0.19	0.06	0.18	0.02	0.16	0.03	0.07		0.06		5.6	1.190	1.938	1.788	1.125	0.933
ML95-322	4.2	8.9	0.97	3.7	0.59	0.44	0.49	0.06	0.30	0.05	0.11		0.12		20	1.077	3.391	2.434	1.268	0.960
ML95-324	8.9	17.0	1.8	6.2	1.2	0.22	0.92	0.10	0.50	0.09	0.16	0.02	0.14	0.02	37	1.194	6.158	3.918	1.321	0.925
ML95-371	10	20	2.3	9.2	1.8	3.5	1.5	0.24	1.6	0.32	0.83	0.13	0.85	0.13	52	1.141	1.140	1.052	0.990	0.908

All concentrations in ppm.

Table 10.9 REE contents and ratios for mine waters

Sample	Location	La	Ce	Pr	Nd	Sm	Eu	Gd	Tb	Dy	Ho	Er	Tm	Yb	Lu	ΣREE	$[La/Ce]_{NASC}$	$[La/Yb]_{NASC}$	$[Gd/Yb]_{NASC}$	$[La/Sm]_{NASC}$	Ce/Ce*
MLW95-492	Brunswick #12	4.65			1.39	3.21	4.13							0.140	0.330	13.85		3.22	0.000	0.258	
MLW95-485	Heath Steele	71.75	144.49	16.42	70.59	16.39	4.66	23.23	3.52	21.70	4.32	12.23	1.37	8.60	1.31	400.58	1.13	0.808	1.61	0.780	0.917
MLW95-486	Heath Steele	183.33	284.40	28.49	112.09	15.91	13.09	22.33	2.69	13.69	2.58	6.74	0.580	3.35	0.650	689.92	1.47	5.30	3.97	2.05	0.857
MLW95-478	Heath Steele				0.001	0.001										0.002					
MLW95-481	Heath Steele				0.001											0.001					
MLW95-475	Heath Steele	0.610	0.380		0.190											1.18	3.66				
MLW95-476	Heath Steele				0.001											0.001					
MLW95-488	Heath Steele	0.007	0.011	0.002	0.009	0.002	0.002					0.002				0.035	1.45			0.623	0.640
MLW95-489	Heath Steele	0.023	0.043	0.006	0.019	0.006	0.009	0.007	0.001	0.009	0.002	0.006		0.005		0.136	1.22	0.446	0.835	0.683	0.797
MLW95-609	Heath Steele	0.008	0.022	0.003	0.013	0.002	0.002	0.004		0.003		0.002				0.059	0.830			0.713	0.978
MLW95-610	Heath Steele	0.006	0.009		0.008	0.002	0.001	0.002		0.002						0.030	1.52			0.534	
MLW95-611	Heath Steele	0.007	0.010	0.001	0.006		0.001			0.001				0.001		0.027	1.60	0.678			0.823
MLW96-694	Stratmat MZ	0.013	0.005	0.001	0.001	0.001	0.001	0.002	0.001	0.001	0.001	0.001	0.001	0.001	0.001	0.031	5.93	1.26	1.19	2.32	0.302
MLW96-695	Stratmat MZ	0.092	0.029	0.002	0.007	0.001	0.001	0.004	0.001	0.005	0.001	0.004	0.001	0.004	0.001	0.153	7.24	2.23	0.596	16.39	0.466
MLW96-697	Stratmat MZ	0.021	0.007	0.001	0.001	0.001	0.001	0.002	0.001	0.001	0.001	0.001	0.001	0.001	0.001	0.041	6.84	2.03	1.19	3.74	0.333
MLW96-702	Stratmat MZ	0.008	0.005	0.001	0.001	0.001	0.001	0.002	0.001	0.001	0.001	0.001	0.001	0.001	0.001	0.026	3.65	0.775	1.19	1.43	0.385
MLW95-482	Wedge Deposit	37.35	100.67	9.97	45.61	11.55	2.14	14.08	2.30	12.45	2.31	5.89	0.690	4.57	0.580	250.16	0.846	0.792	1.84	0.576	1.14
MLW95-491	Wedge Deposit	0.750	1.09	0.110	0.660	0.110	0.100			0.260				0.180		3.26	1.57	0.404		1.21	0.827
MLW95-483	Nepisiguit River	0.072	0.080	0.020	0.090	0.022	0.003	0.025	0.003	0.017	0.004	0.008	0.001	0.007	0.002	0.354	2.05	0.996	2.13	0.583	0.459
MLW95-494	Willett Deposit				0.008	0.003		0.004		0.001		0.002		0.002		0.020			1.19		
MLW95-495	Willett Deposit	0.013		0.003	0.017	0.008	0.002	0.007		0.003	0.001	0.002		0.002		0.058		0.630	2.09	0.289	
MLW95-496	Willett Deposit		0.006		0.005		0.001			0.002		0.001		0.001		0.016					
MLW96-719	Willett Deposit	0.011	0.032	0.004	0.023	0.008	0.002	0.011	0.001	0.012	0.003	0.009	0.001	0.009	0.002	0.128	0.784	0.118	0.729	0.245	1.05
MLW96-720	Willett Deposit	0.007	0.018	0.002	0.012	0.005	0.001	0.006	0.001	0.007	0.002	0.005	0.001	0.005	0.001	0.073	0.887	0.136	0.715	0.249	1.05
MLW96-716	Willett Deposit	0.014	0.033	0.004	0.016	0.005	0.001	0.005	0.001	0.006	0.001	0.004	0.001	0.004	0.001	0.096	0.968	0.339	0.745	0.499	0.960
MLW96-718	Willett Deposit	0.005	0.008	0.001	0.005	0.001	0.001	0.002	0.001	0.002	0.001	0.002	0.001	0.002	0.001	0.033	1.43	0.242	0.596	0.891	0.779

All concentrations in µg/L; blank = below detection

Table 10.10 REE contents and ratios for suspended sediments

Sample	Location	La	Ce	Pr	Nd	Sm	Eu	Gd	Tb	Dy	Ho	Er	Tm	Yb	Lu	ΣREE	$[La/Ce]_{NASC}$	$[La/Yb]_{NASC}$	$[Gd/Yb]_{NASC}$	$[La/Sm]_{NASC}$	Ce/Ce*
											Halfmile Lake deposit										
MLF94-236	HN94-65	28	63	7.0	26	5.6	1.1	5.0	0.77	4.3	0.95	2.6	0.38	2.6	0.39	148	1.014	1.043	1.146	0.891	0.980
MLF94-237	HN94-65	29	67	7.5	28	5.8	1.1	5.0	0.76	4.3	0.90	2.5	0.38	2.5	0.40	155	0.987	1.124	1.192	0.891	0.989
MLF94-238	HN94-65	30	68	7.4	28	6.1	1.2	5.5	0.92	5.5	1.2	3.3	0.46	3.1	0.48	161	1.006	0.938	1.058	0.876	0.994
MLF94-242	HN94-65	30	68	7.8	29	5.9	1.3	5.5	0.94	5.3	1.1	3.2	0.45	2.9	0.45	162	1.006	1.002	1.131	0.906	0.968
MLF94-248	HN94-65	31	69	8.0	30	6.1	1.3	5.2	0.79	4.5	0.94	2.7	0.39	2.7	0.37	163	1.025	1.112	1.148	0.905	0.954
MLF94-249	HN94-65	32	70	8.3	35	6.0	1.4	6.6	1.1	5.9	1.2	3.4	0.47	3.4	0.47	175	1.043	0.912	1.157	0.950	0.936
MLF94-255	HT55-43	17	35	4.1	16	3.0		2.1	0.26	1.4	0.26	0.75	0.11	0.72	0.15	81	1.108	2.287	1.739	1.009	0.913
MLF94-257	HT55-43	14	32	3.7	15	2.9		2.3	0.33	1.7	0.37	1.0	0.14	1.0	0.15	75	0.998	1.356	1.371	0.860	0.968
MLF94-258	HT55-43	30	65	7.7	31	6.5	1.5	5.9	0.70	3.5	0.70	1.6	0.27	1.5	0.27	156	1.053	1.938	2.345	0.822	0.931
MLF94-259	HT55-43	18	42	5.0	20	4.0	1.5	3.2	0.44	2.4	0.50	1.3	0.22	1.5	0.25	100	0.978	1.163	1.272	0.802	0.964
MLF96-696	HN92-40	50	99	11	48	8.8	1.8	5.8	0.84	6.3	1.3	3.1	0.52	4.5	0.72	242	1.152	1.076	0.768	1.012	0.919
											Restigouche deposit										
MLF95-307	MM-88-01	67	73	27	140	41	5.4	81	14.0	81	19.0	57.0	7.4	44.0	6.8	664	2.094	0.148	1.097	0.291	0.374
MLF95-309	MM-88-01	69	79	26	130	38	4.8	75	14.0	74	18.0	50.0	6.8	37.0	5.4	627	1.992	0.181	1.208	0.323	0.406
MLF95-312	MM-88-01	67	86	22	110	28	3.4	58	9.5	50	13.0	35.0	4.5	25.0	3.8	515	1.777	0.260	1.383	0.426	0.488
MLF95-313	MM-88-01	61	83	21	110	28	3.9	56	9.9	52	13.0	35.0	4.8	27.0	4.0	509	1.677	0.219	1.236	0.388	0.505
MLF95-606	MM-88-02	45	99	12	48	9.0		9.1	1.4	7.9	1.6	4.3	0.83	4.7	0.74	244	1.037	0.928	1.154	0.891	0.928
MLF95-361	MM-88-06	28	59	7.1	29	5.3		3.9	0.55	3.3	0.58	1.5	0.20	1.7	0.29	140	1.083	1.596	1.368	0.941	0.911
MLF95-362	MM-88-06	32	73	8.3	33	7.0	0.76	5.1	0.79	4.9	0.94	2.4	0.41	2.3	0.34	171	1.000	1.348	1.322	0.814	0.976
MLF95-364	MM-88-06	33	77	9.0	34	6.8	0.24	4.7	0.72	3.8	0.78	1.9	0.29	2.0	0.25	174	0.978	1.598	1.401	0.864	0.973
MLF95-315	MM-88-07	13	33	4.3	19	4.7	1.2	6.4	1.1	5.0	0.95	2.5	0.33	2.0	0.30	94	0.899	0.630	1.908	0.493	0.961
MLF95-317	MM-88-07	16	37	4.4	18	4.4	1.1	5.9	0.97	4.4	0.82	2.1	0.32	1.7	0.25	97	0.986	0.912	2.069	0.648	0.960
MLF95-318	MM-88-07	15	36	4.4	17	4.2	0.98	5.0	0.83	3.8	0.78	2.2	0.29	1.8	0.27	93	0.951	0.807	1.656	0.636	0.965
MLF95-332	MM-89-106	79	140	20	80	16	1.2	15	1.9	10	2.1	5.6	0.89	5.3	0.84	378	1.287	1.444	1.687	0.879	0.767
MLF95-335	MM-89-106	84	150	22	85	18	1.2	14	2.0	10	2.2	5.9	0.89	5.6	0.86	402	1.278	1.453	1.490	0.831	0.760
MLF95-336	MM-89-106	83	150	21	83	16	1.2	14	1.9	11	2.2	5.3	0.81	5.6	0.80	396	1.262	1.436	1.490	0.924	0.783
MLF95-341	MM-89-106	84	160	22	86	17	1.2	14	1.9	10	2.1	5.2	0.85	5.5	0.83	411	1.198	1.480	1.517	0.880	0.811
MLF95-343	MM-89-106	82	150	21	83	17	1.3	14	2.0	11	2.2	5.7	0.93	5.8	0.90	397	1.247	1.370	1.439	0.859	0.787
MLF95-508	MM-89-106	62	120	17	68	12	0.80	9.8	1.4	8.1	1.6	4.5	0.73	4.6	0.77	311	1.179	1.306	1.270	0.920	0.805
MLF95-354	MM-89-107	130	210	31	130	24	2.6	18	2.3	12	2.5	5.9	0.92	6.5	0.97	577	1.412	1.938	1.651	0.965	0.720
MLF95-355	MM-89-107	38	78	9.1	40	6.7	0.67	5.5	0.65	4.6	0.88	2.4	0.40	2.5	0.33	190	1.111	1.473	1.312	1.010	0.914
MLF95-592	MM-89-107	44	89	11	42	8.4	0.55	7.1	1.2	6.8	1.5	3.9	0.63	4.7	0.69	221	1.128	0.907	0.901	0.933	0.881

All concentrations in ppm.

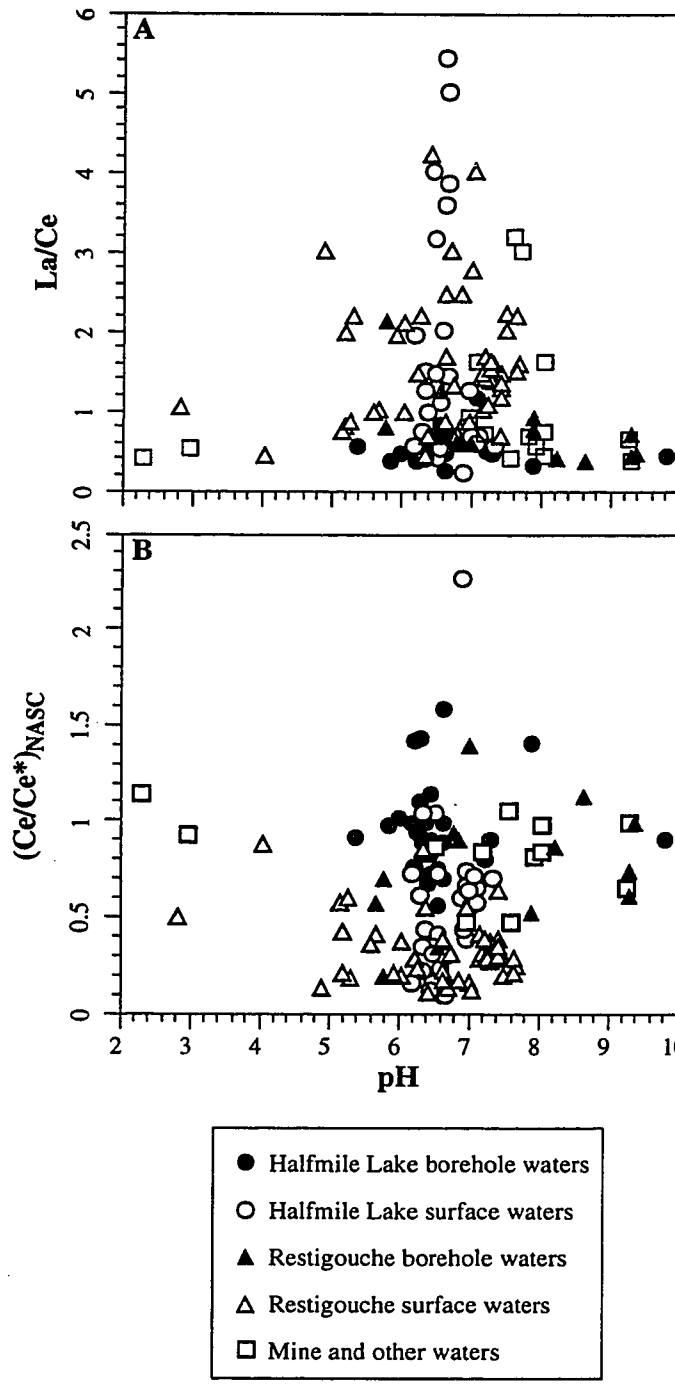


Fig. 10.1 La/Ce and Ce/Ce vs pH for all waters. Note the higher La/Ce and lower Ce/Ce* for surface waters compared to groundwaters. Ce/Ce* is normalized to North American Shale Composite (NASC). Data from Tables 10.1, 10.2, 10.5, 10.6, 10.9.*

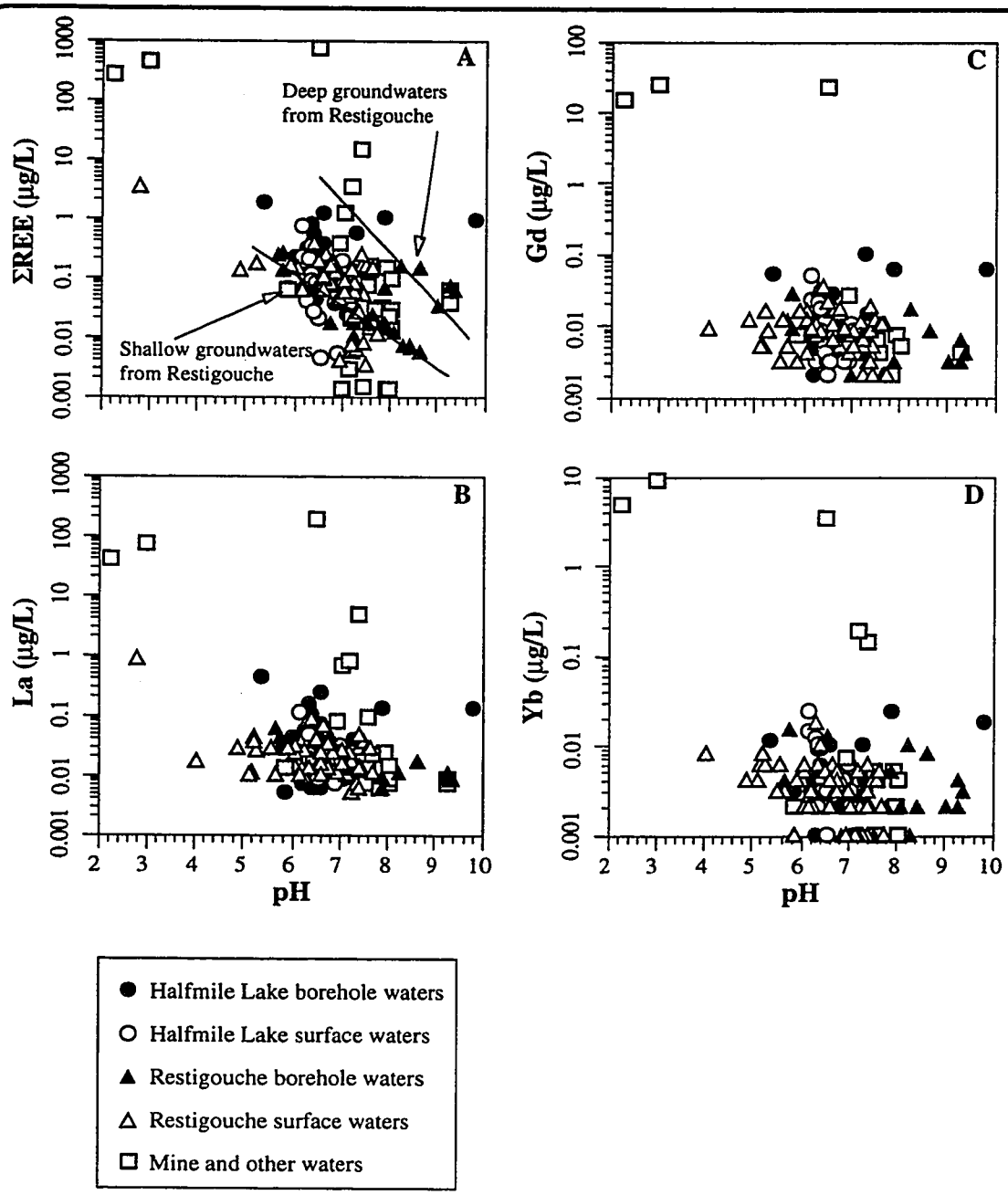


Fig. 10.2 Plots of ΣREE, La, Gd, Yb vs pH for all waters. Note the general decrease in REE parameters with increasing pH, especially for deep versus shallow groundwaters at the Restigouche deposit. Data from Tables 10.1, 10.2, 10.5, 10.6, 10.9.

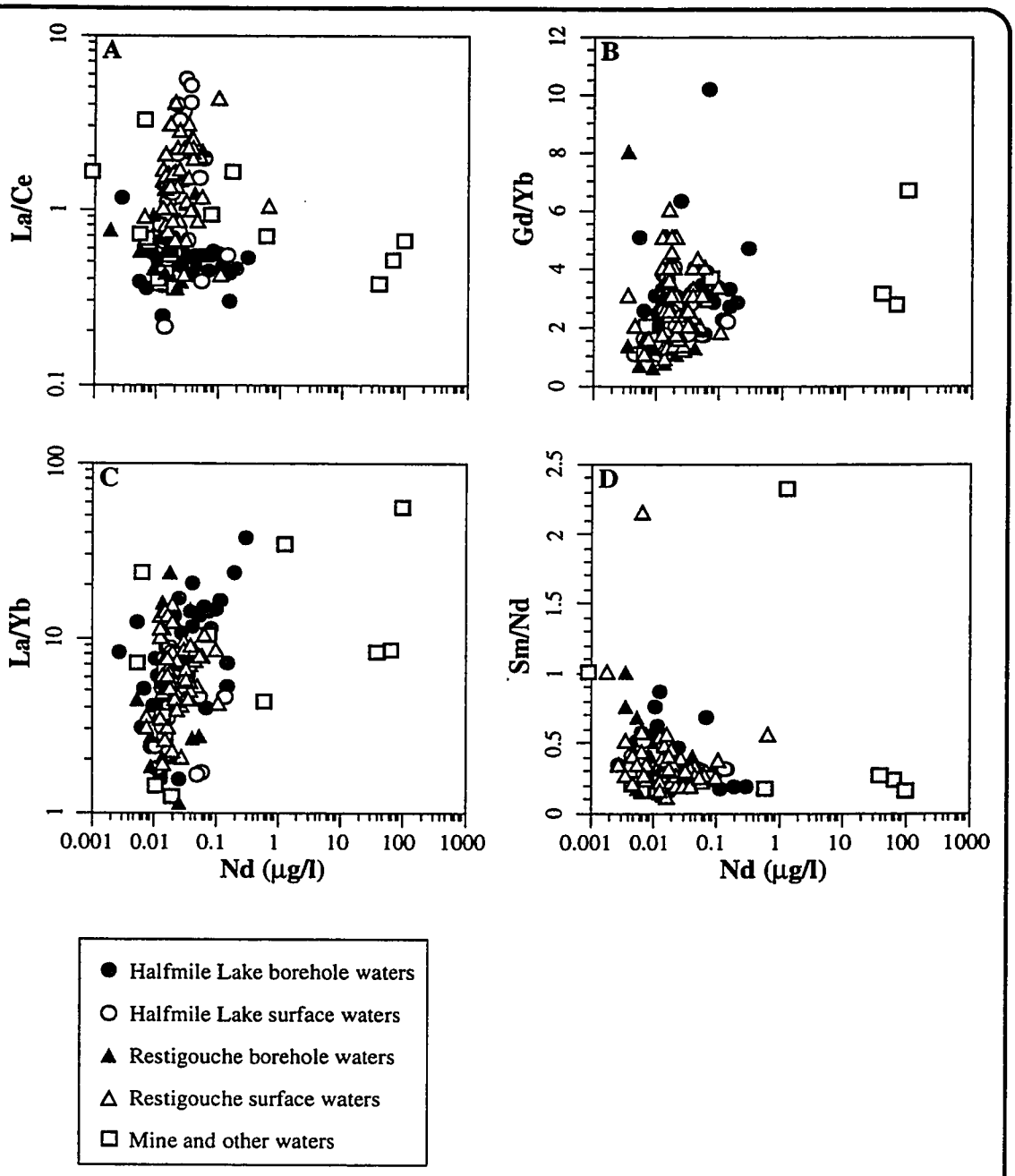


Fig. 10.3 REE inter-element ratios vs Nd contents for all waters. A) La/Ce; B) Gd/Yb; C) La/Yb; D) Sm/Nd. Data from Tables 10.1, 10.2, 10.5, 10.6, 10.9.

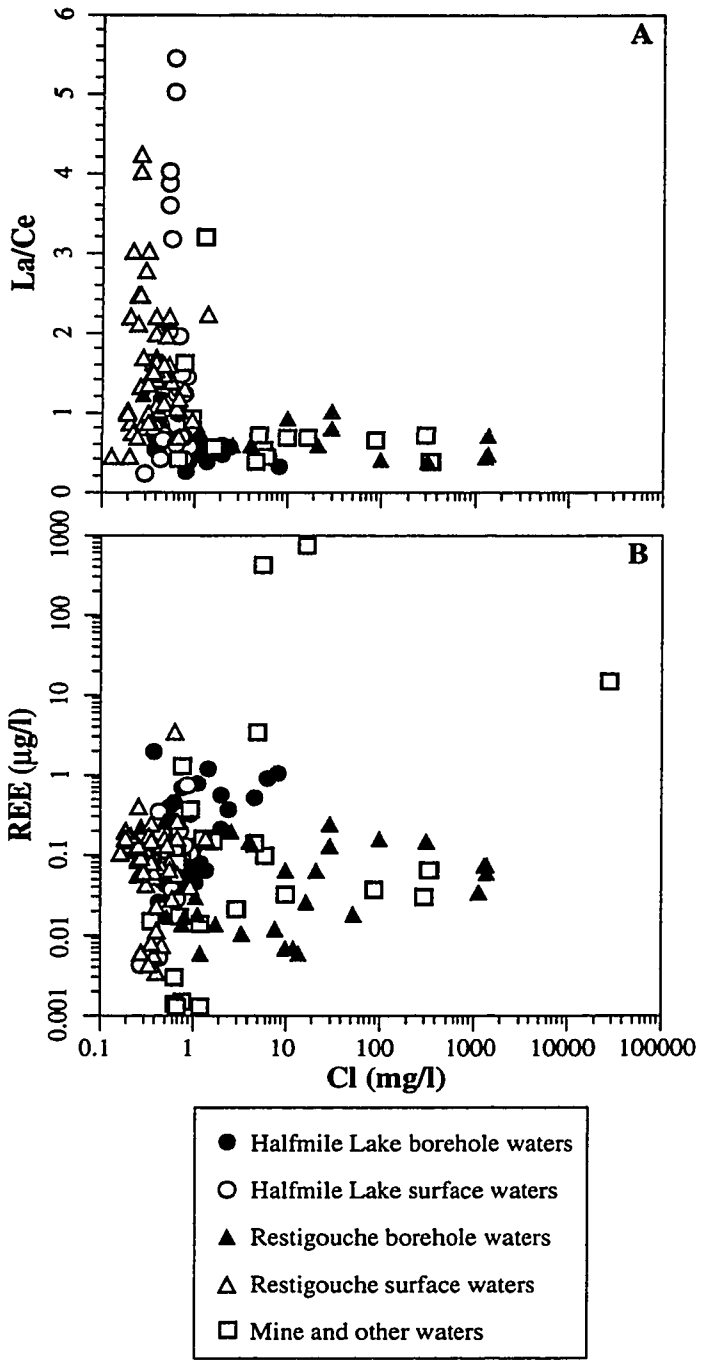


Fig. 10.4 La/Ce vs Cl and ΣREE vs Cl showing variations in REE chemistry with salinity. At low salinity La/Ce is highly variable but is more uniform at higher salinities. Total REE contents do not correlate strongly with salinity. Data from Tables 10.1, 10.2, 10.5, 10.6, 10.9.

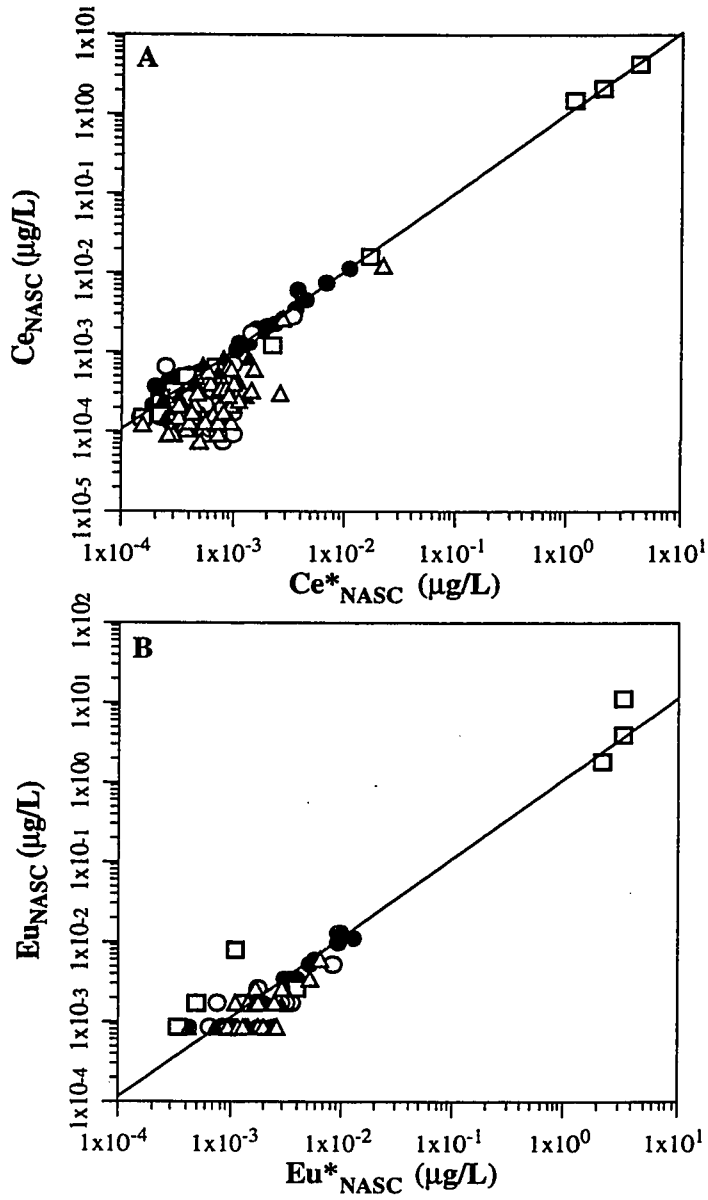


Fig. 10.5 NASC normalized A) Ce vs Ce/Ce and B) Eu vs Eu/Eu*. Note that groundwaters plot close to unity for Ce but surface waters are highly depleted. For Eu, apparent Eu anomalies at low concentrations appear to be an artifact of the detection limit and most samples for which Sm, Eu and Gd data exists are close to unity. Data from Tables 10.1, 10.2, 10.5, 10.6, 10.9.*

- ● Halfmile Lake borehole waters
- ○ Halfmile Lake surface waters
- ▲ Restigouche borehole waters
- △ Restigouche surface waters
- □ Mine and other waters

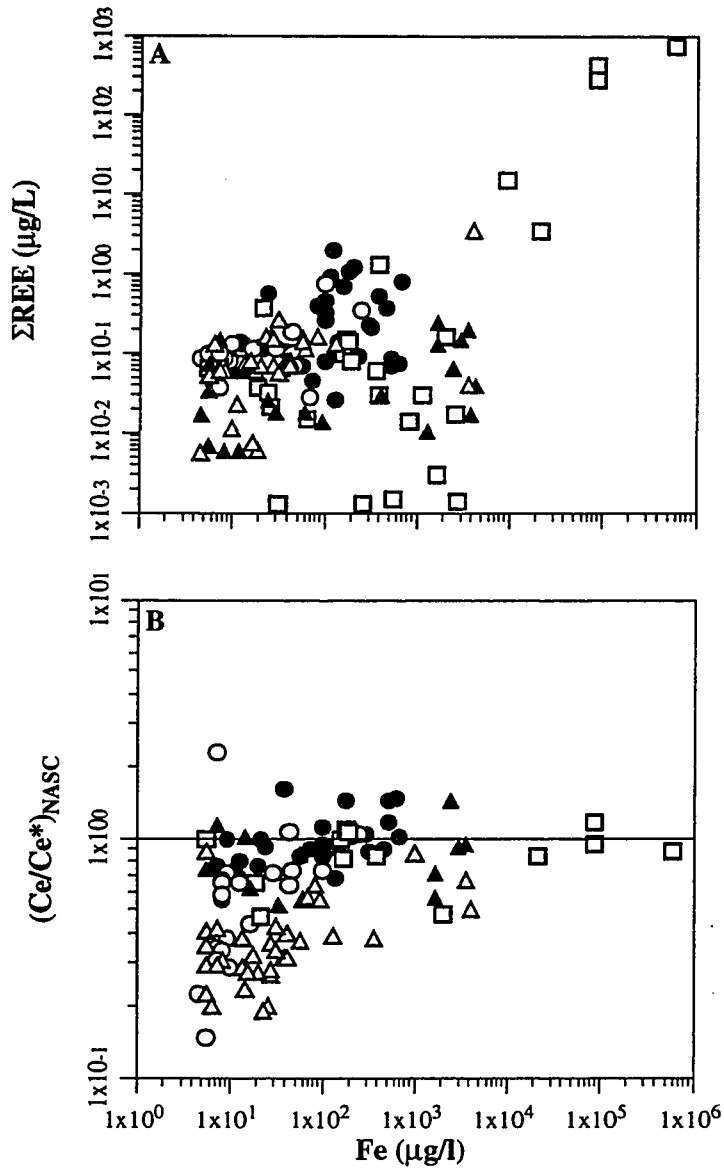


Fig. 10.6 ΣREE and NASC normalized Ce/Ce vs Fe. Note that total REE contents are strongly correlated with total dissolved Fe. The negative Ce anomalies in surface waters are positively correlated with Fe content. Data from Tables 10.1, 10.2, 10.5, 10.6, 10.9.*

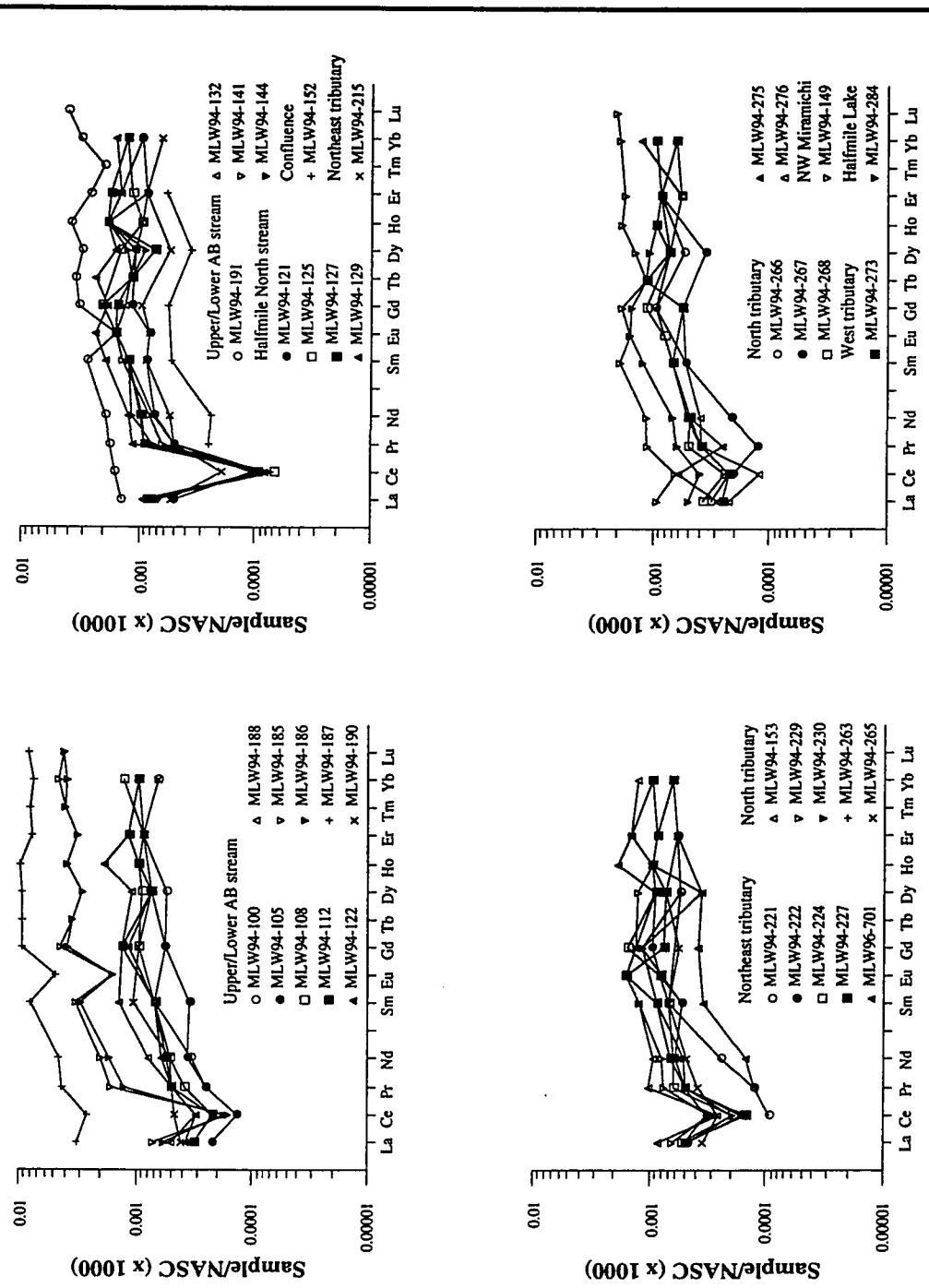


Fig. 10.7 Rare-earth element concentrations of Halfmile Lake surface waters normalized to North American Shale Composite (NASC). Normalizing values are from Haskin et al. (1968) with Dy value from Gromet et al. (1984). Data from Table 10.1.

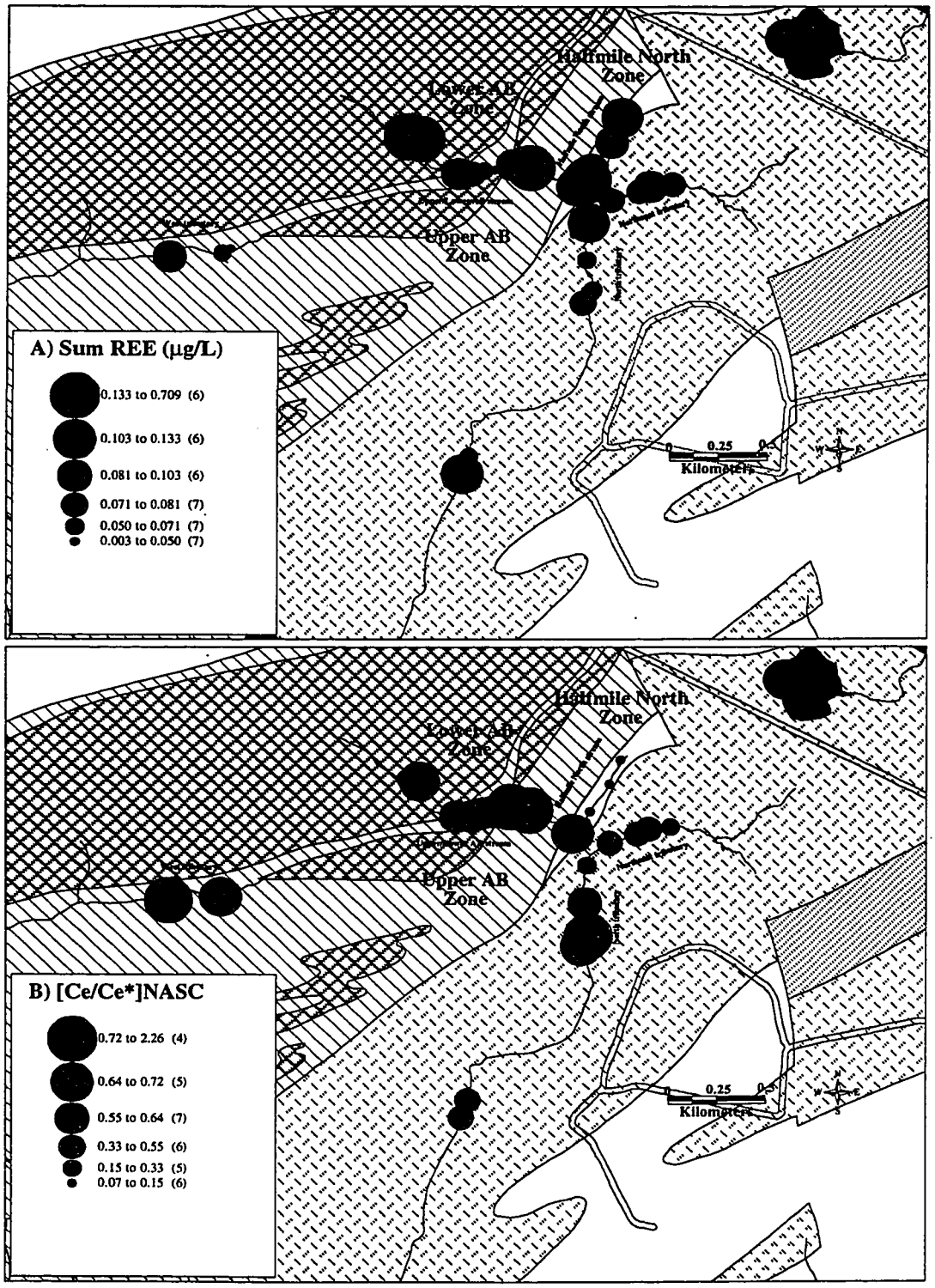


Fig. 10.8 Distribution of REE in Halfmile Lake deposit surface waters

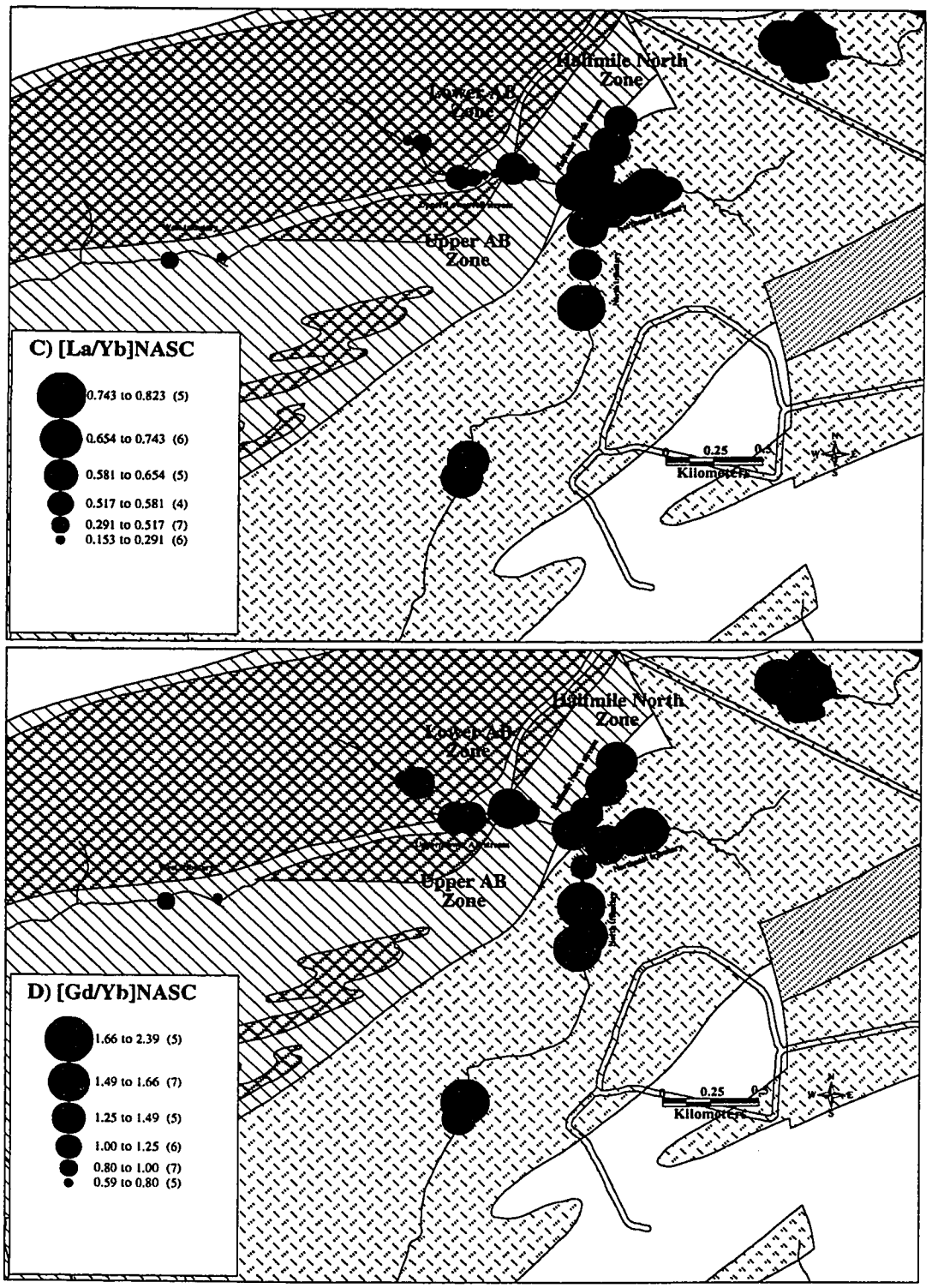


Fig. 10.8 continued.

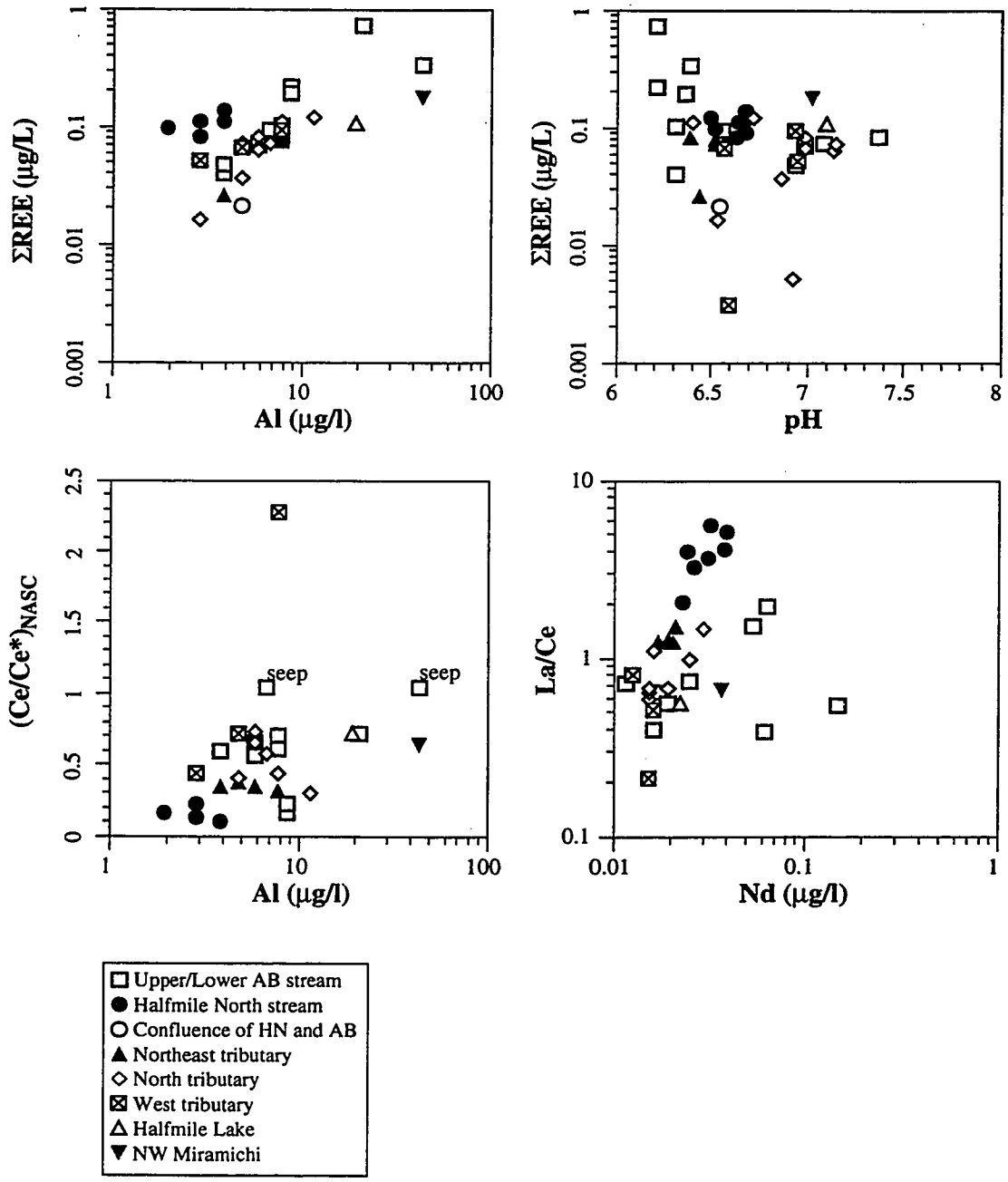


Fig. 10.9 Variations in REE for Halfmile Lake deposit surface waters, subdivided by stream. Data from Tables 10.1.

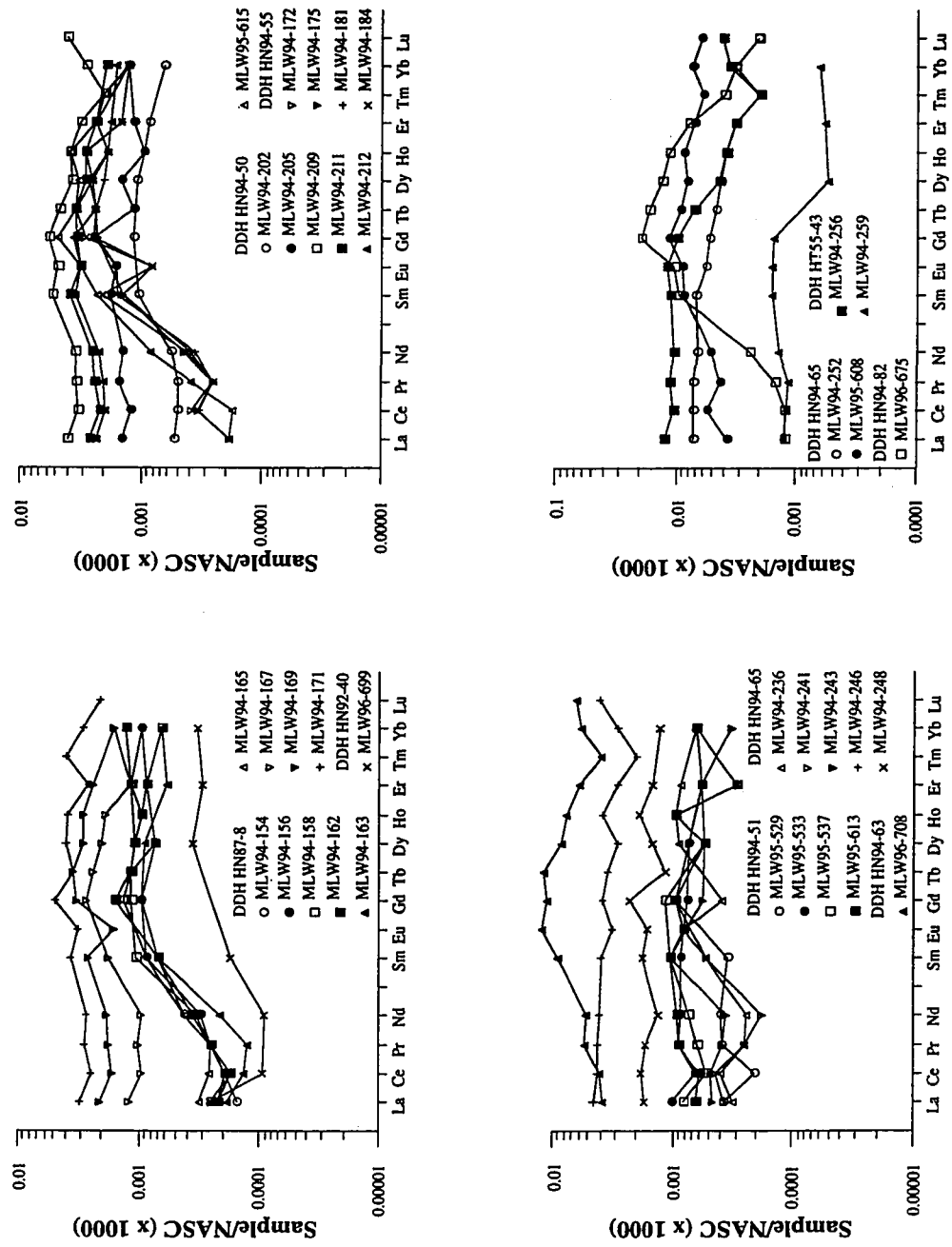


Fig. 10.10 Rare-earth element concentrations of Halfmile Lake borehole waters normalized to North American Shale Composite (NASC). Normalizing values are from Haskin et al. (1968) with Dy value from Gromet et al. (1984). Data from Table 10.2.

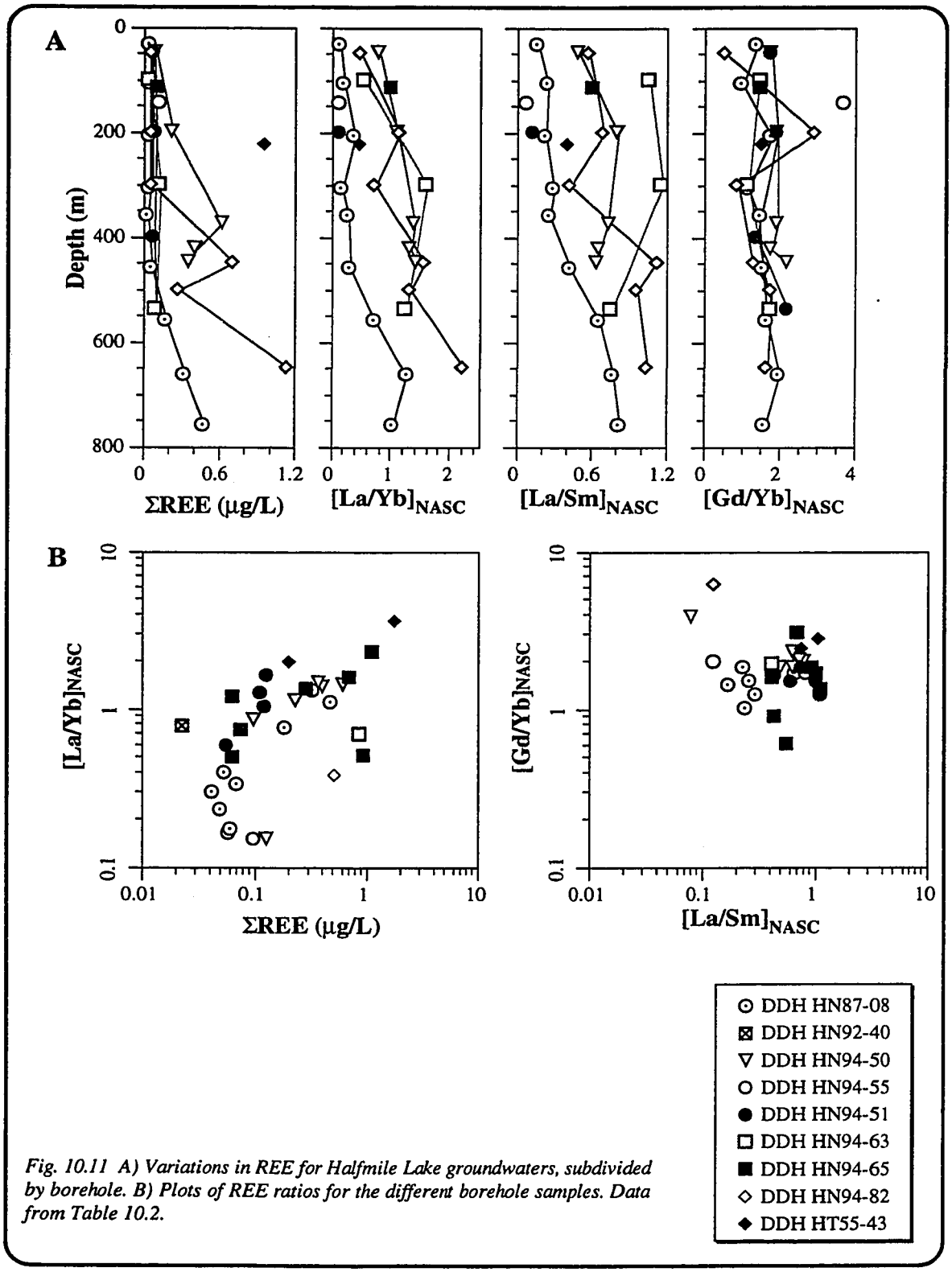


Fig. 10.11 A) Variations in REE for Halfmile Lake groundwaters, subdivided by borehole. B) Plots of REE ratios for the different borehole samples. Data from Table 10.2.

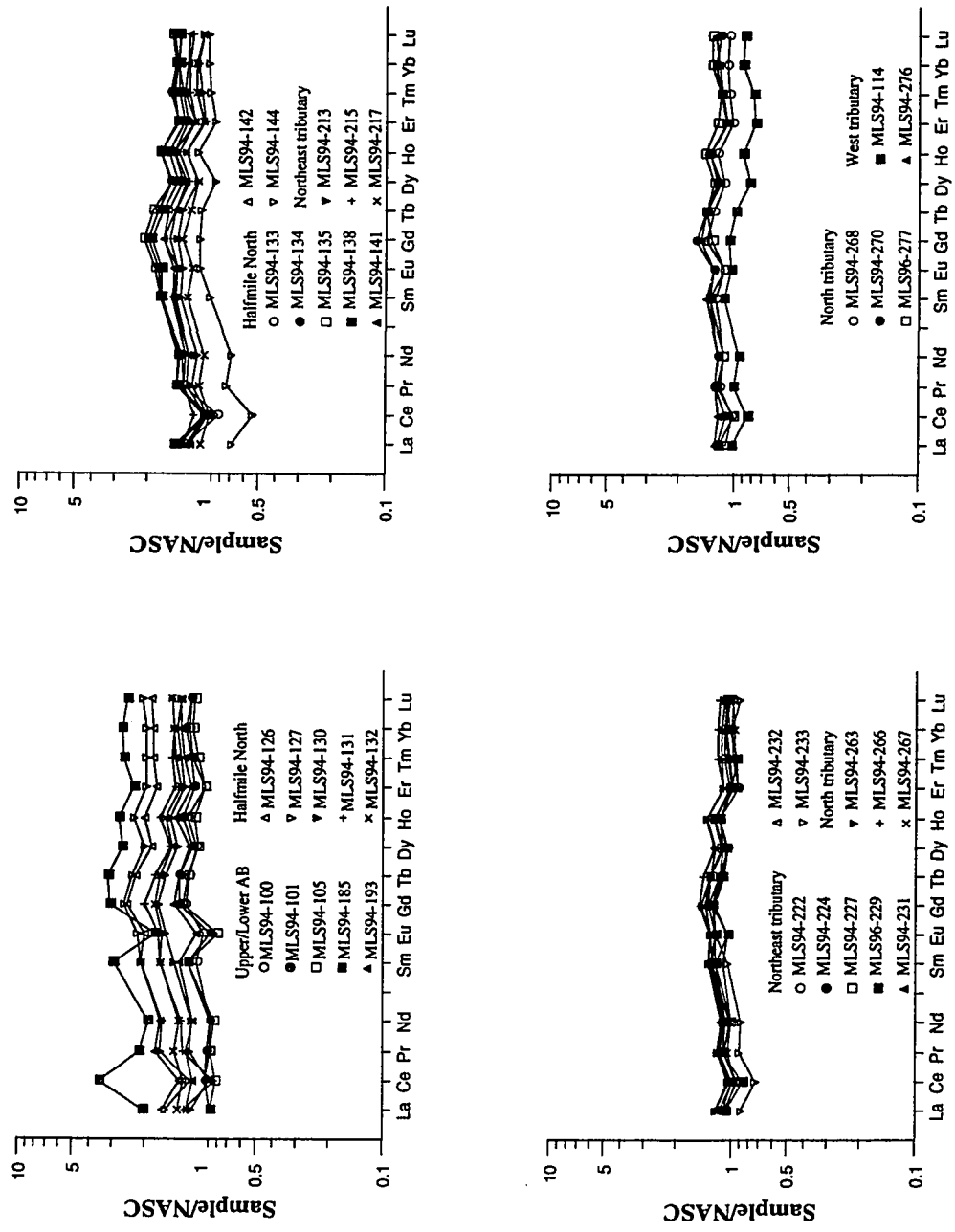


Fig. 10.12 Rare-earth element concentrations of Halfmile Lake deposit stream sediments normalized to North American Shale Composite (NASC). Normalizing values are from Haskin et al. (1968) with Dy value from Gromet et al. (1984). Data from Table 10.3.

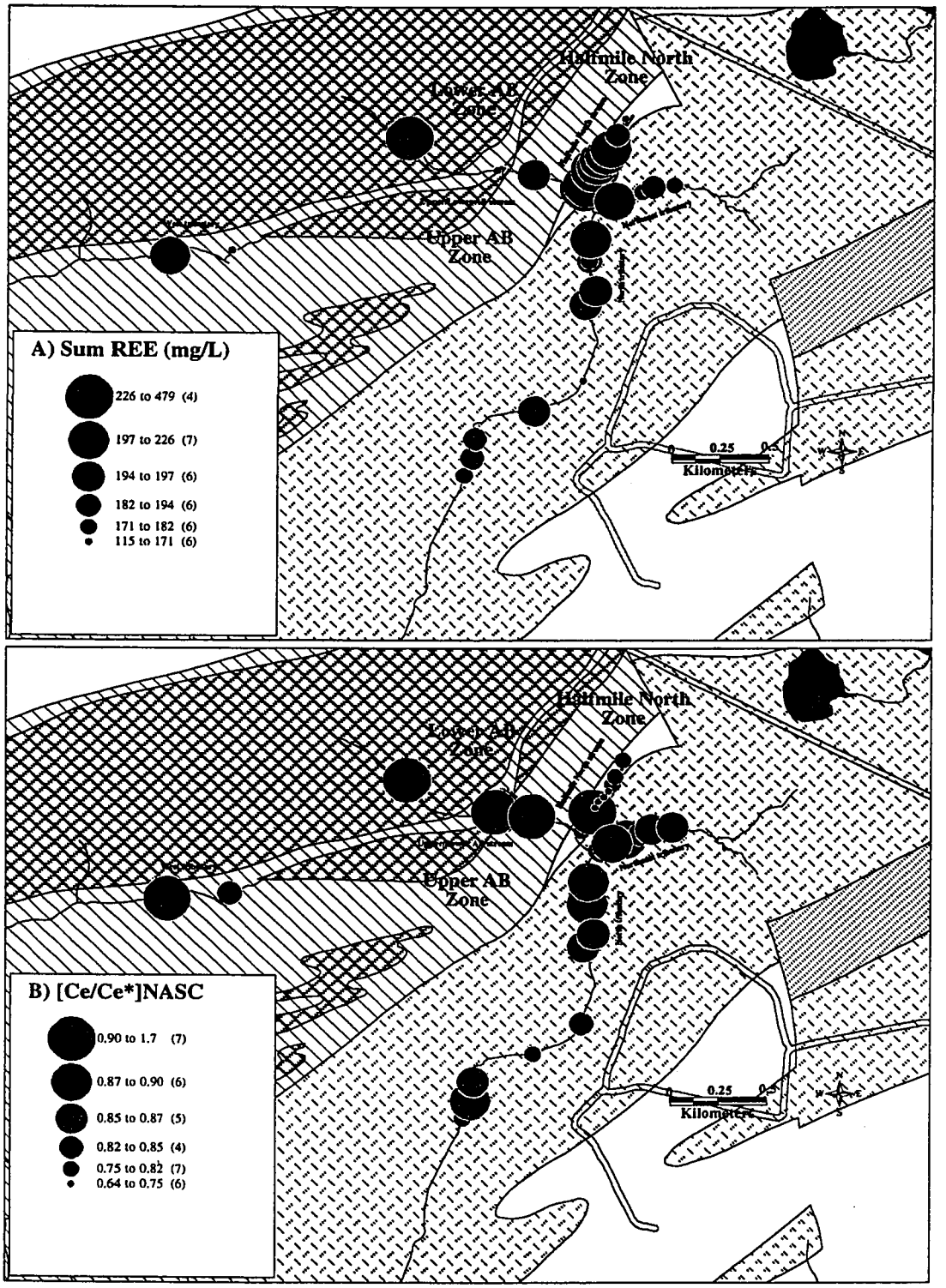


Fig. 10.13 Disibution of REE in Halfmile Lake deposit stream sediments. Data from Table 10.3.

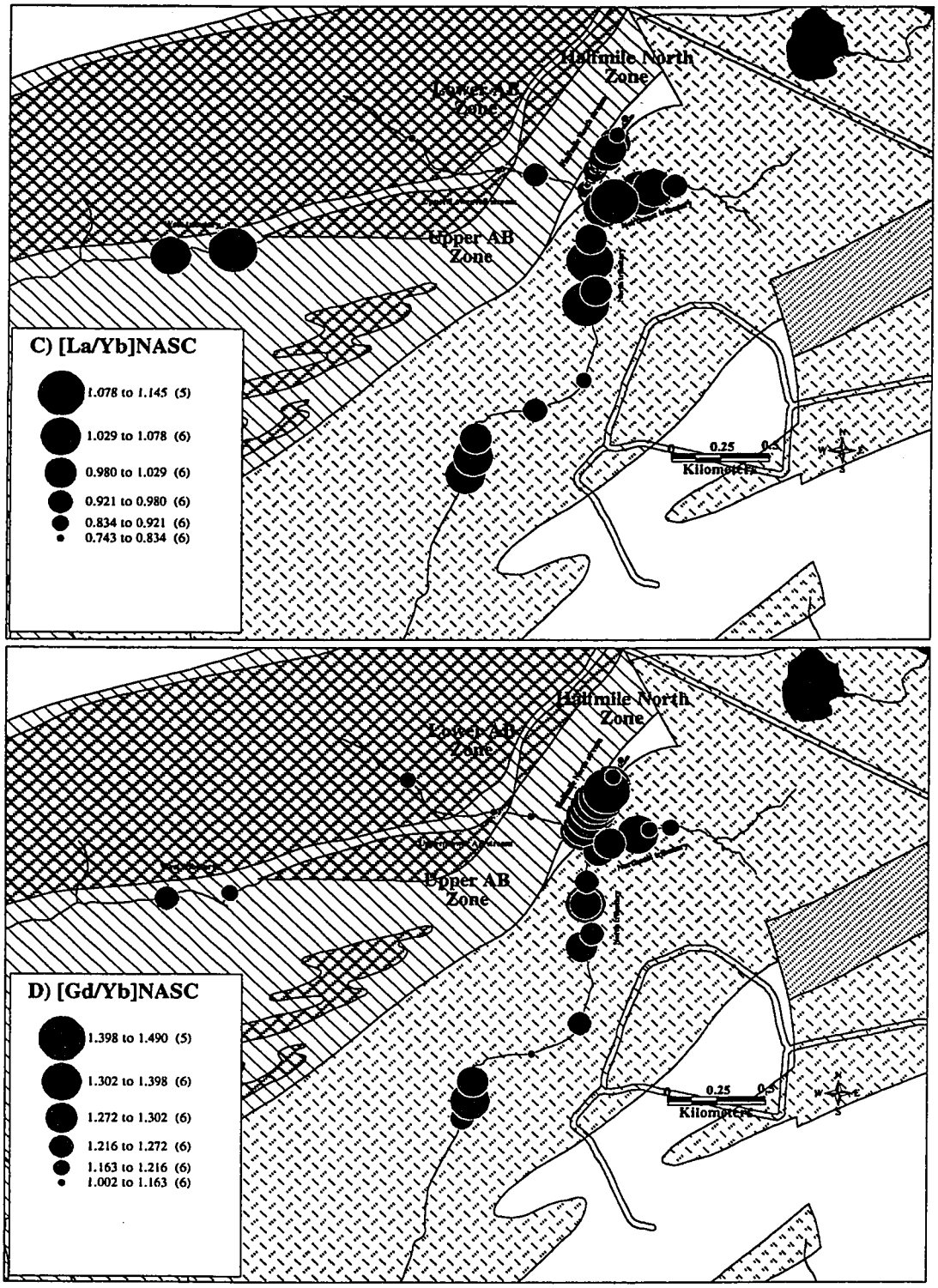


Fig. 10.13 continued.

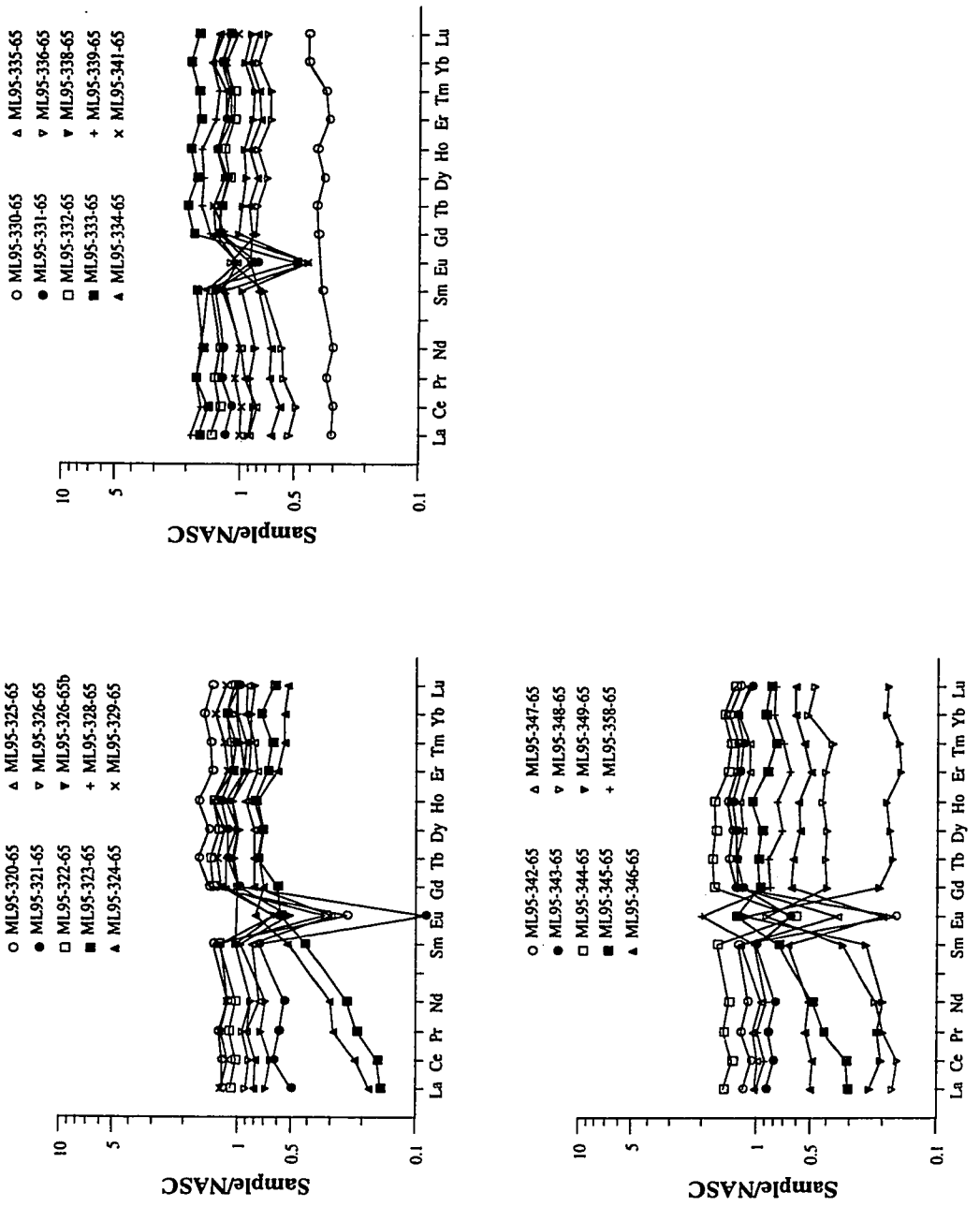


Fig. 10.14 Rare-earth element concentrations of Halfmile Lake lithologies from borehole HN94-65 normalized to North American Shale Composite (NASC). Normalizing values are from Haskin et al. (1968) with Dy value from Gromet et al. (1984). Data from Table 10.4.

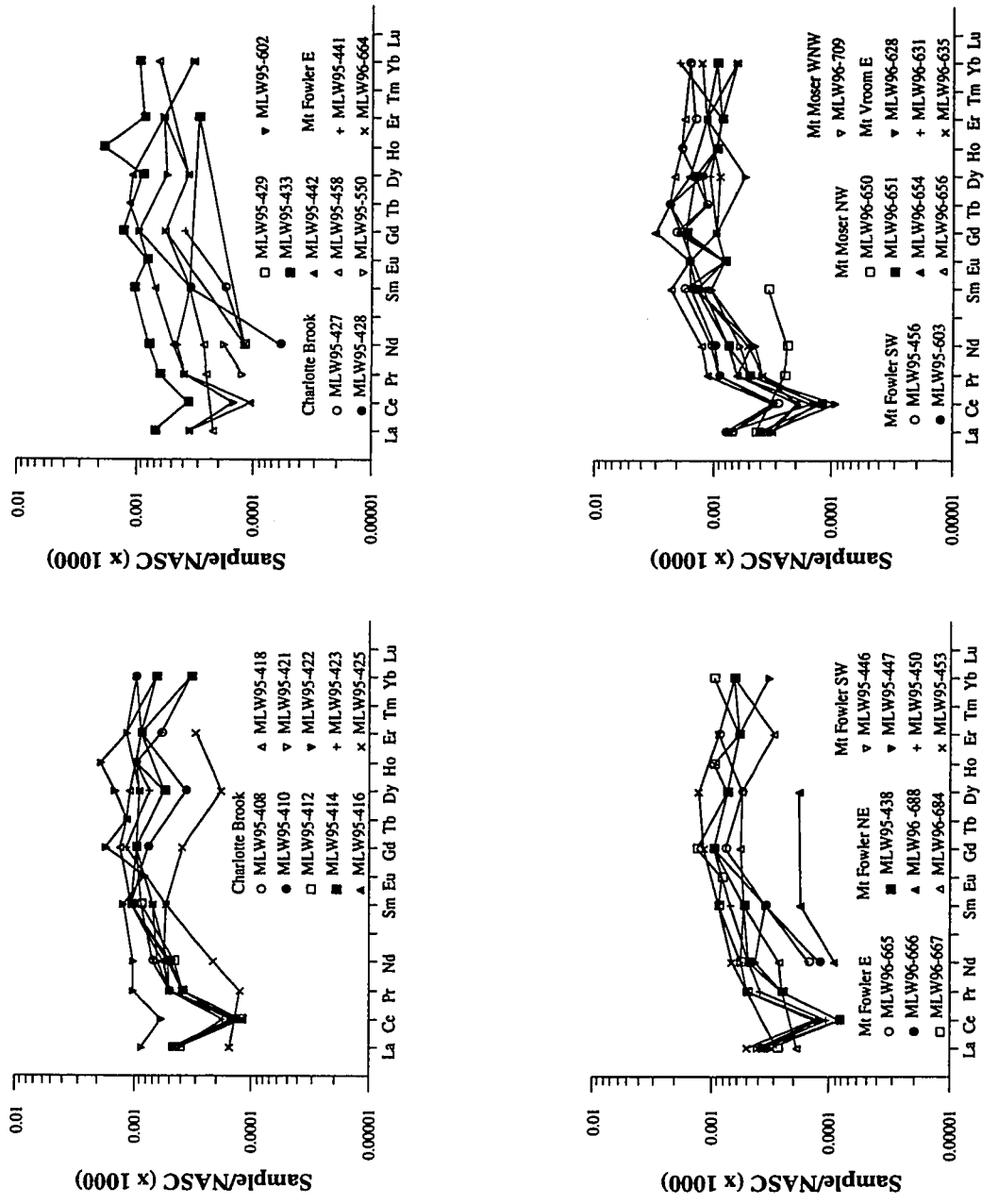


Fig. 10.15 Rare-earth element concentrations of Restigouche deposit surface waters normalized to North American Shale Composite (NASC). Normalizing values are from Haskin et al. (1968) with Dy value from Gromet et al. (1984). Data from Table 10.5.

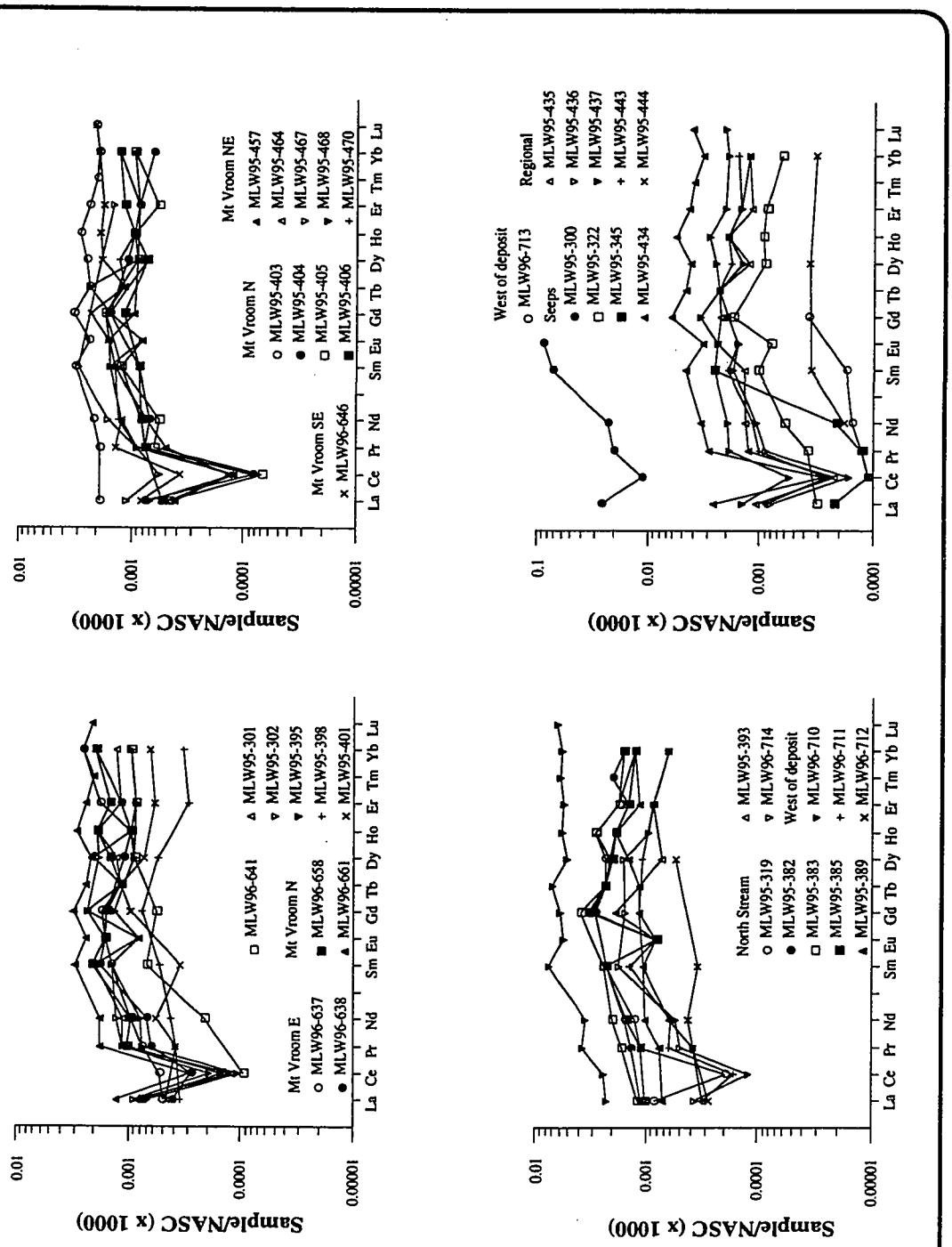


Fig. 10.15 continued.

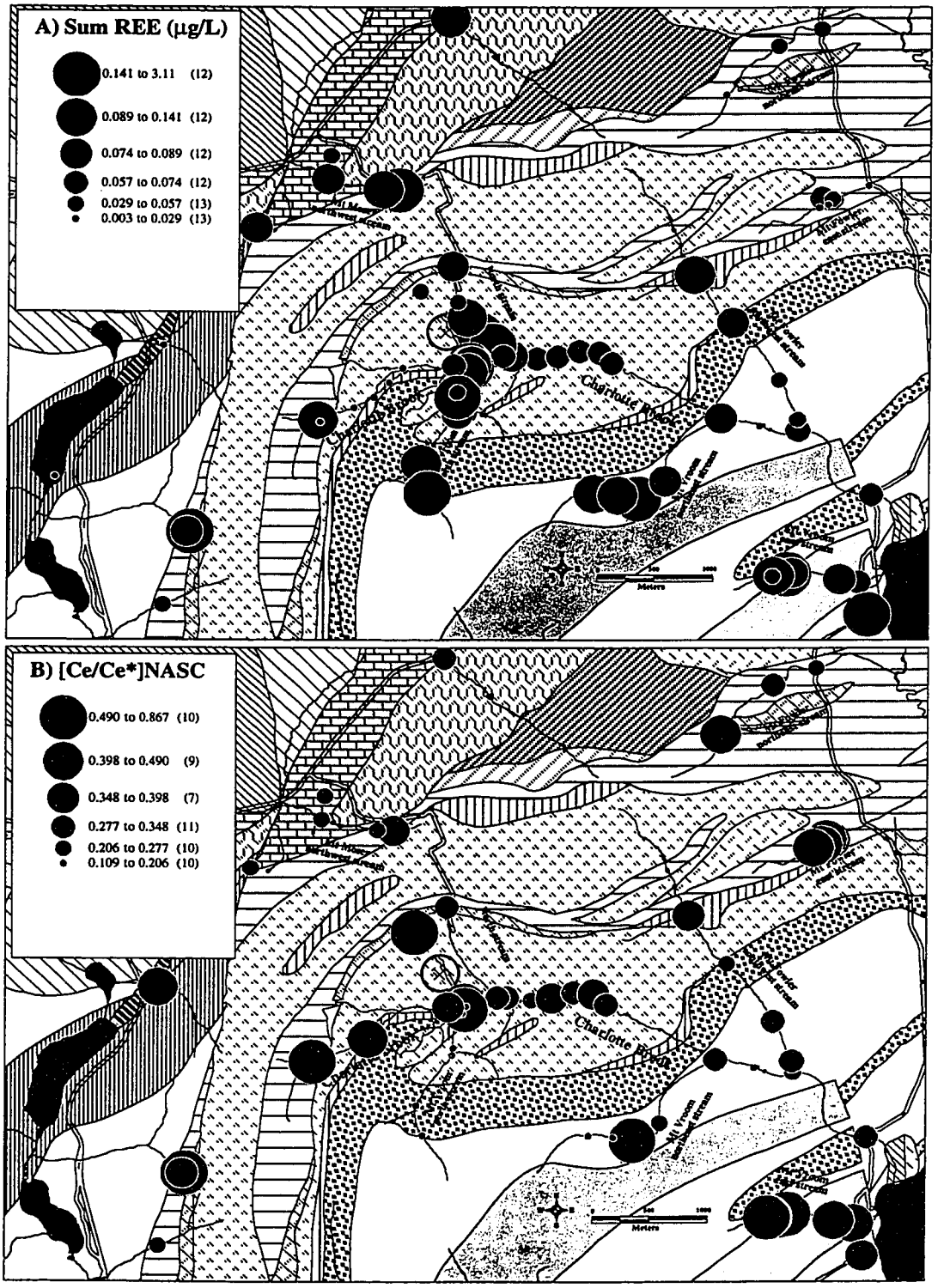


Fig. 10.16 Distribution of REE in Restigouche deposit surface waters. Data from Table 10.5.

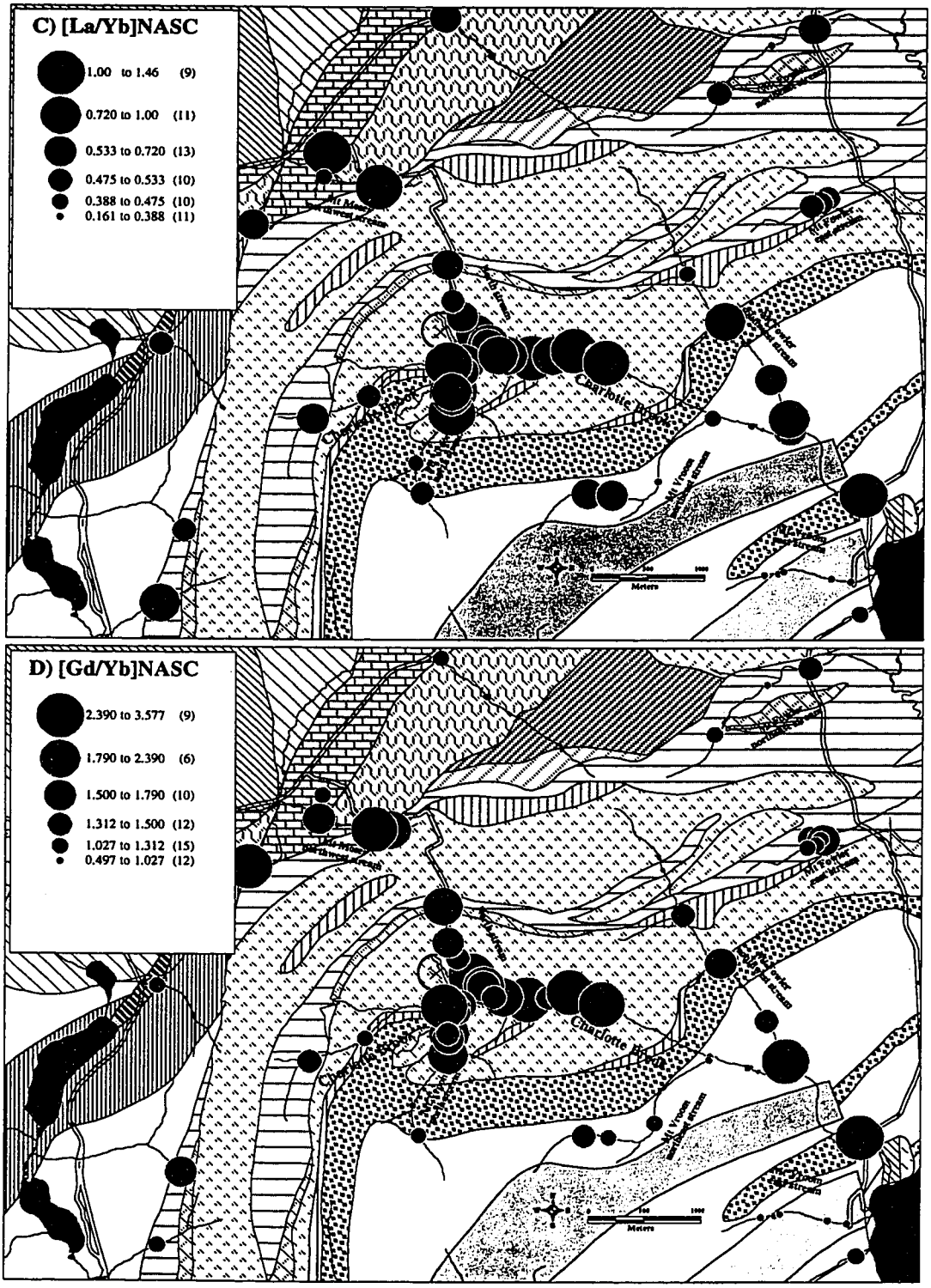


Fig. 10.16 continued.

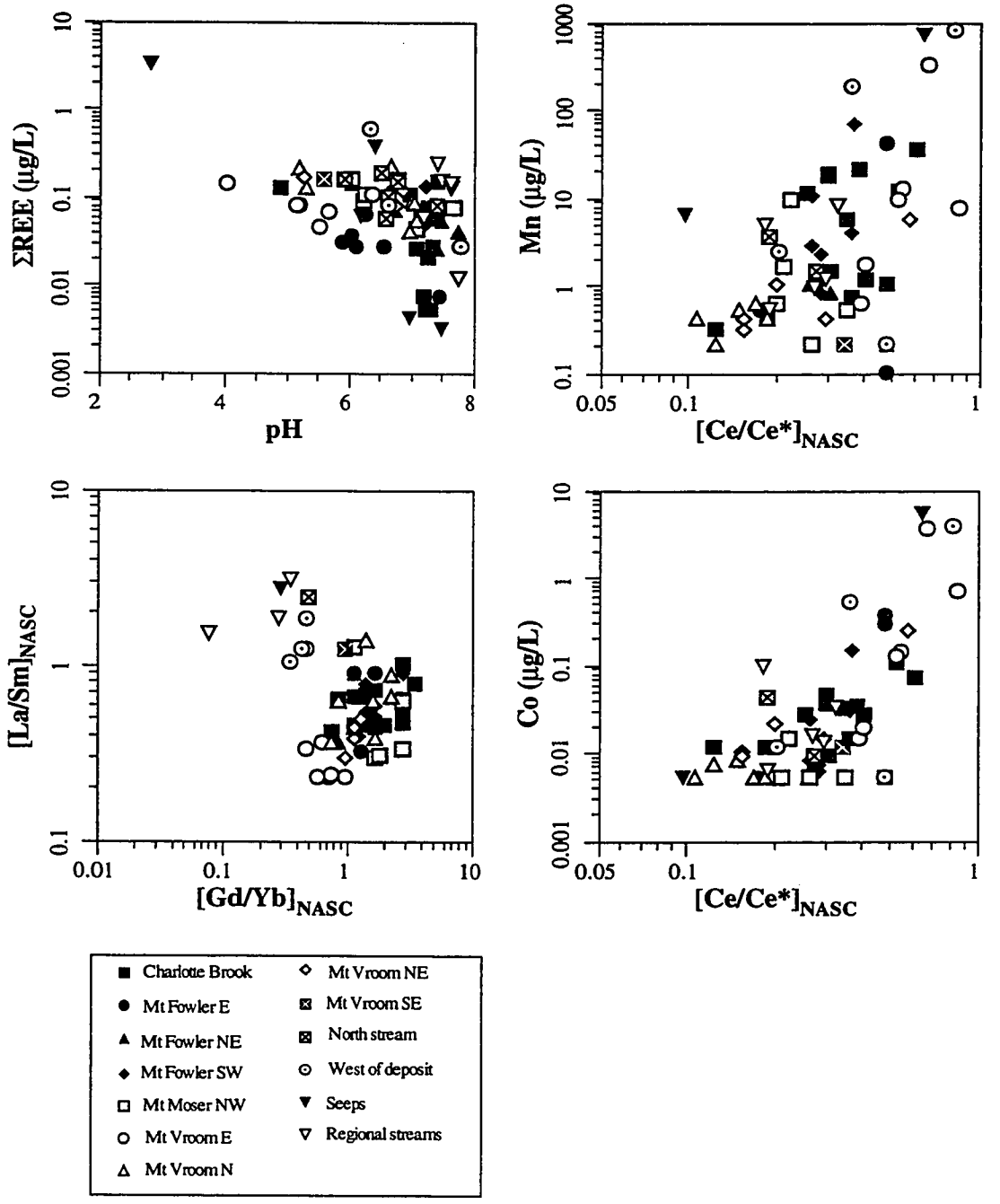


Fig. 10.17 Variations in REE for surface waters from the Restigouche deposit, subdivided by stream. Data from Table 10.5.

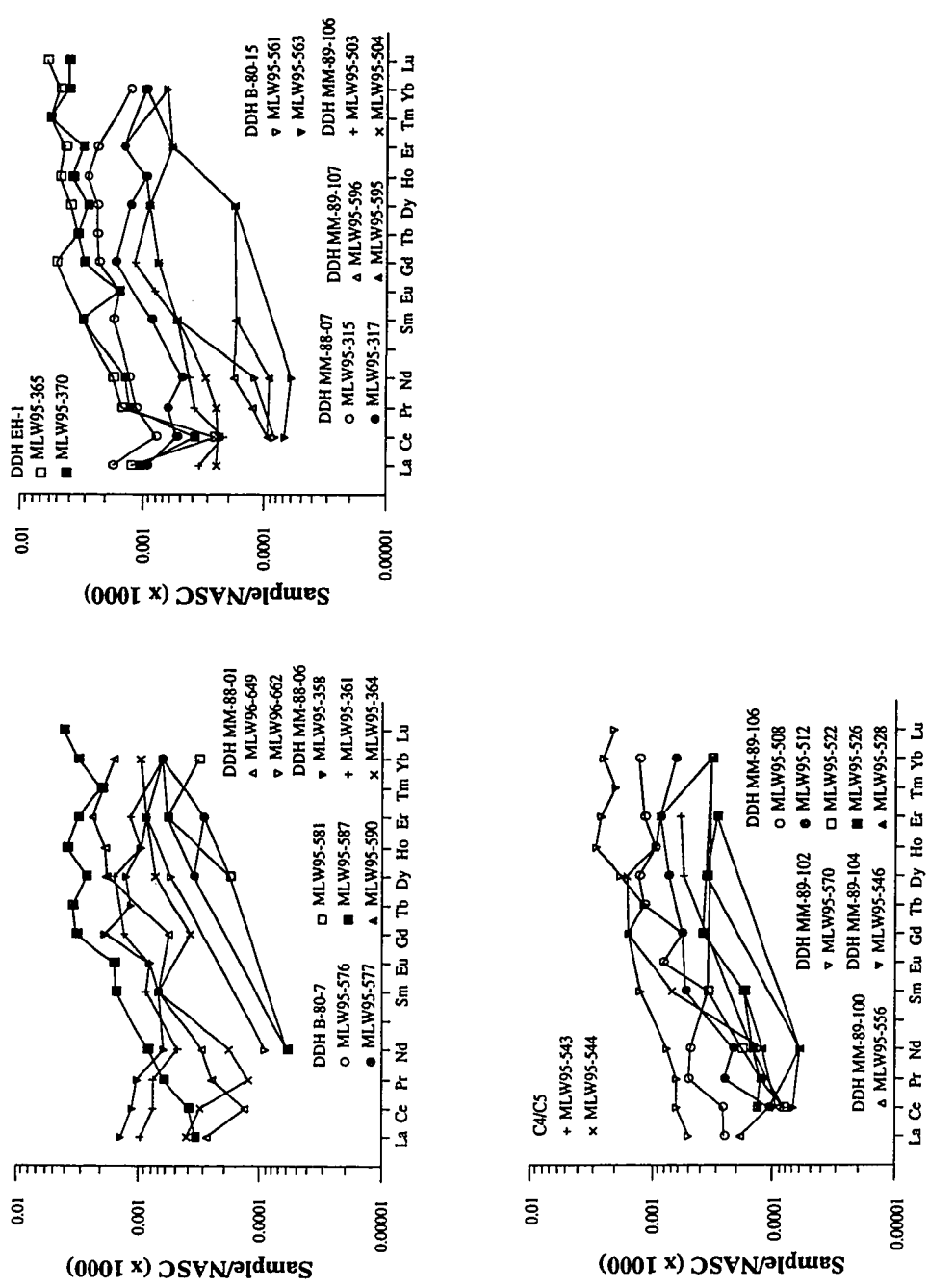


Fig. 10.18 Rare-earth element concentrations of Restigouche deposit borehole waters normalized to North American Shale Composite (NASC). Normalizing values are from Haskin et al. (1968) with Dy value from Gromet et al. (1984). Data from Table 10.6.

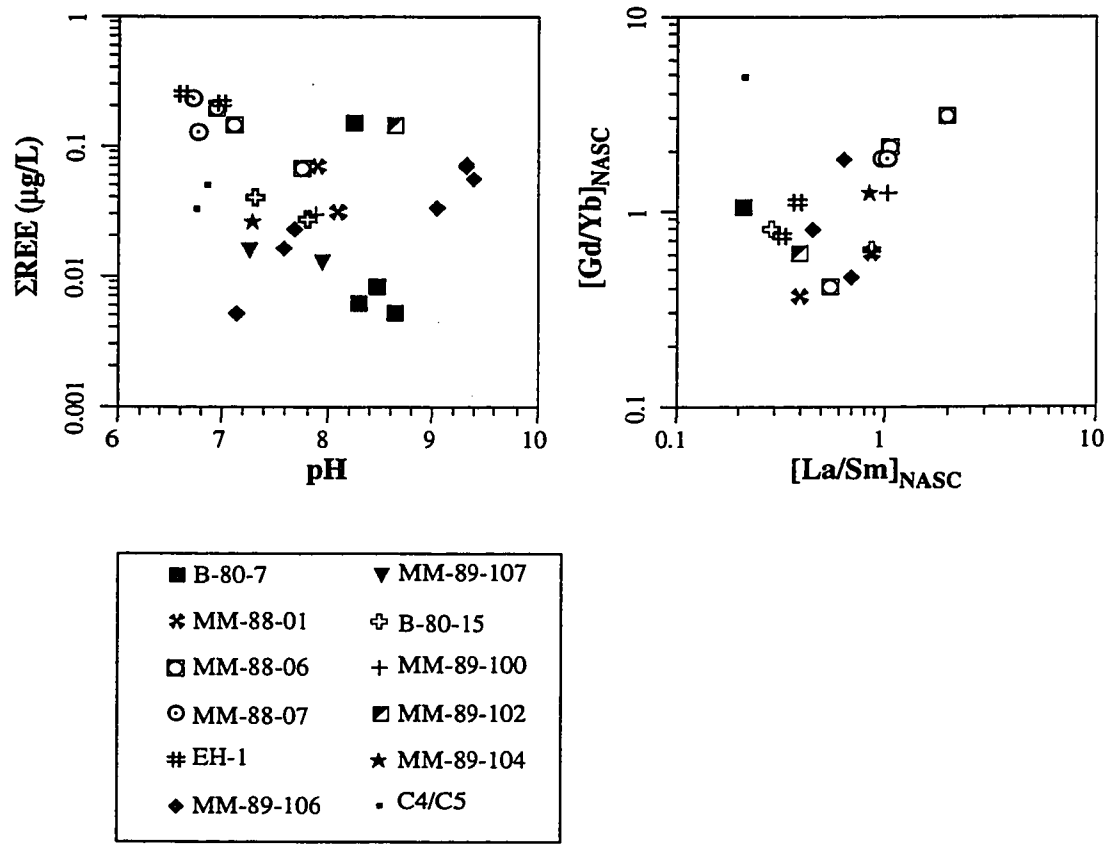


Fig. 10.19 Variations in REE for borehole waters from the Restigouche deposit, subdivided by borehole. Data from Table 10.6.

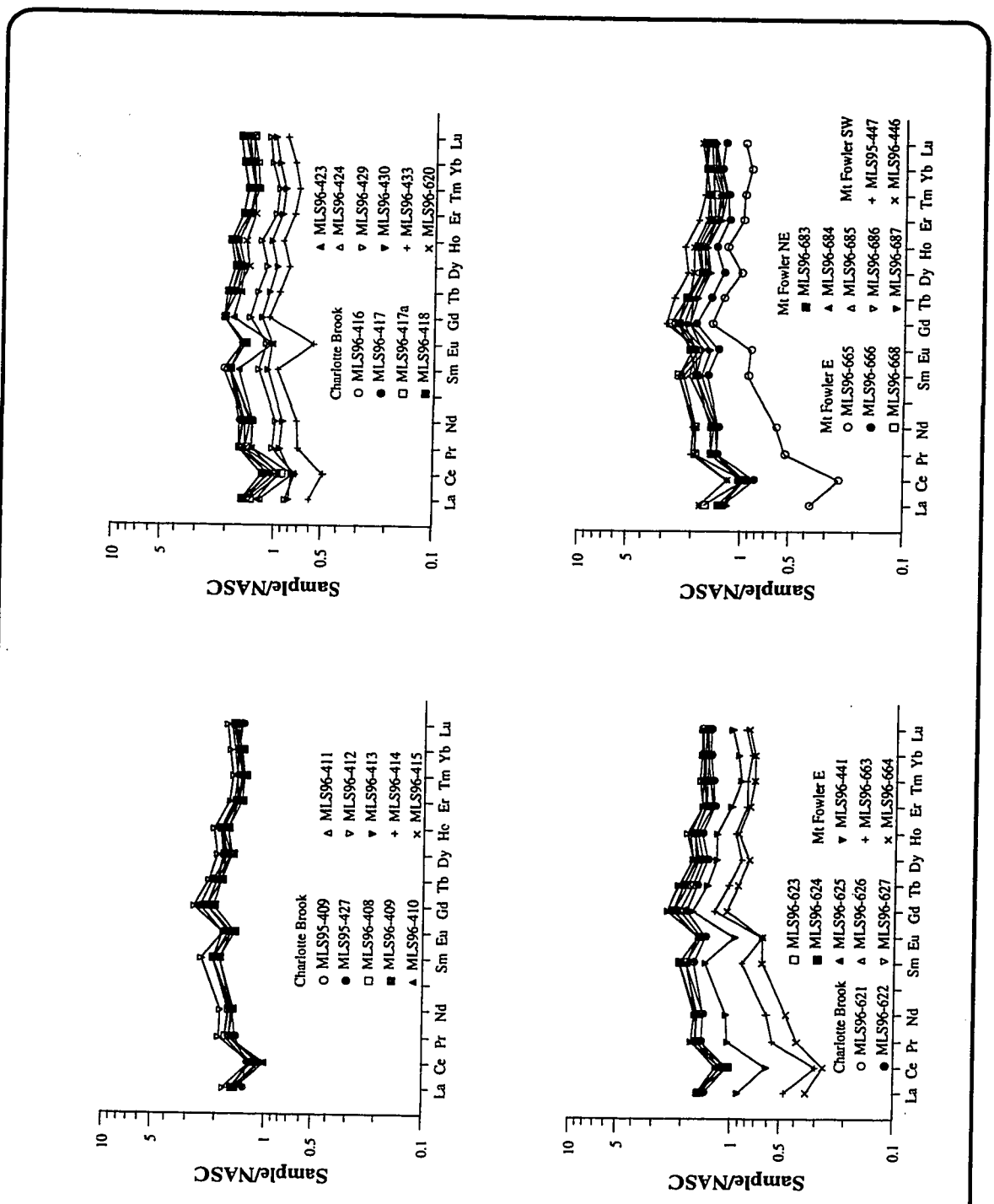


Fig. 10.20 Rare-earth element concentrations of Restigouche deposit stream sediments normalized to North American Shale Composite (NASC). Normalizing values are from Haskin et al. (1968) with Dy value from Gromet et al. (1984). Data from Table 10.7.

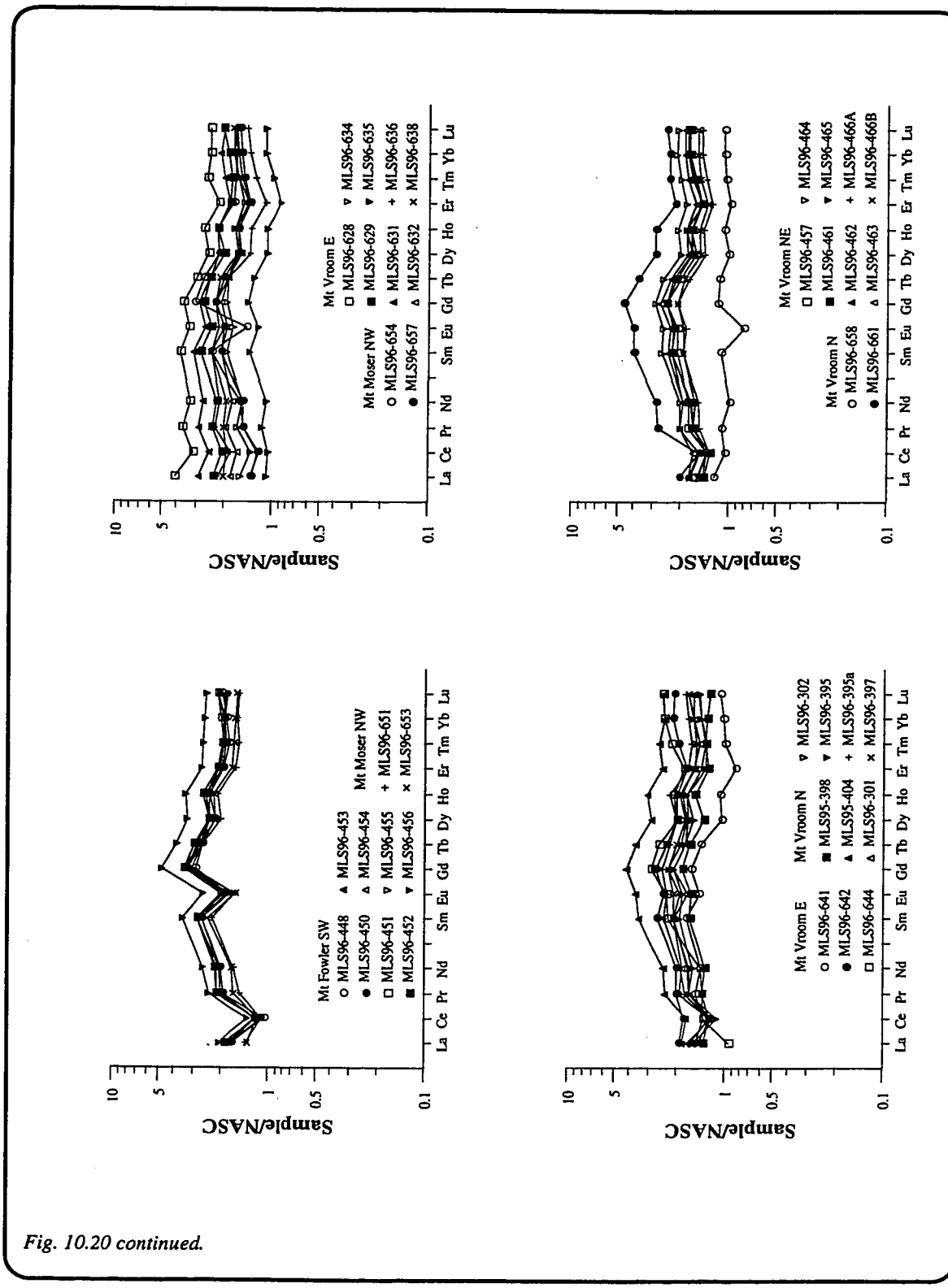


Fig. 10.20 continued.

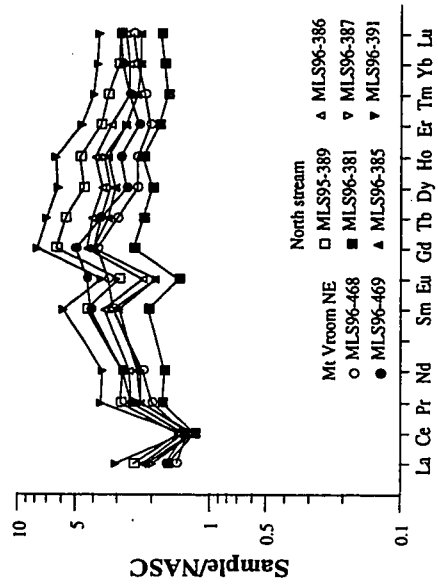


Fig. 10.20 continued.

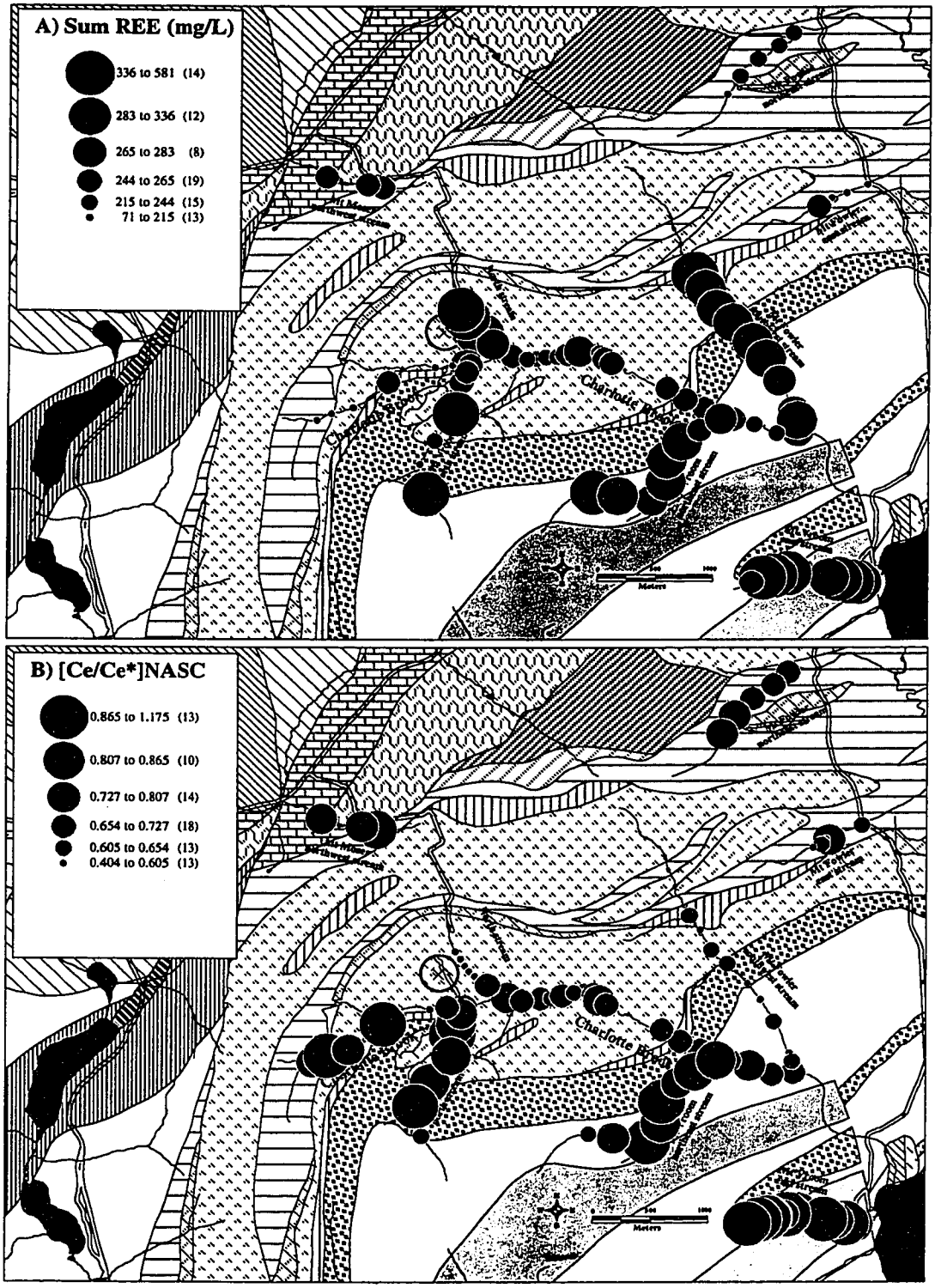


Fig. 10.21 Distribution of REE in Restigouche deposit stream sediments. Data from Table 10.7.

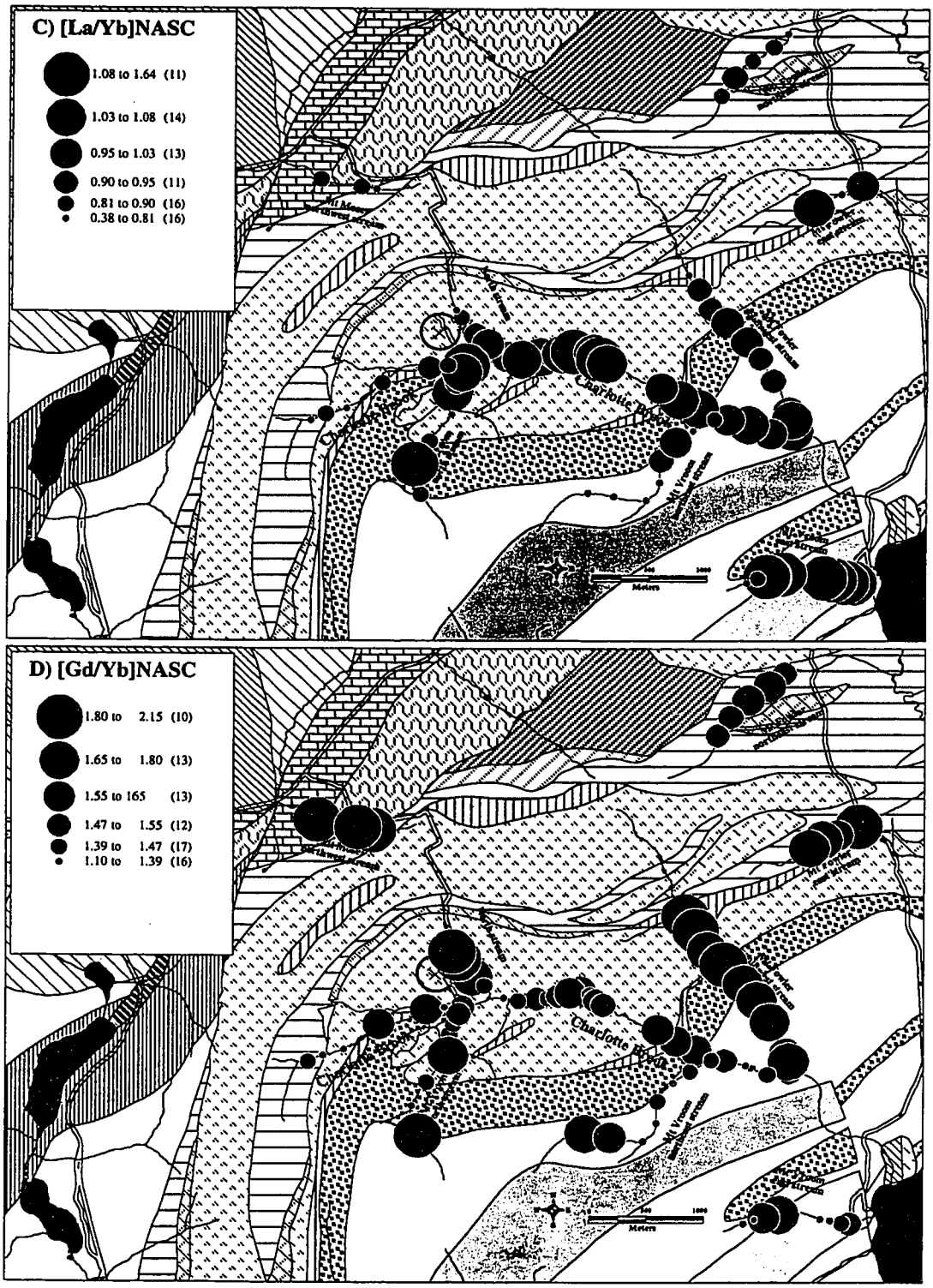


Fig. 10.21 continued.

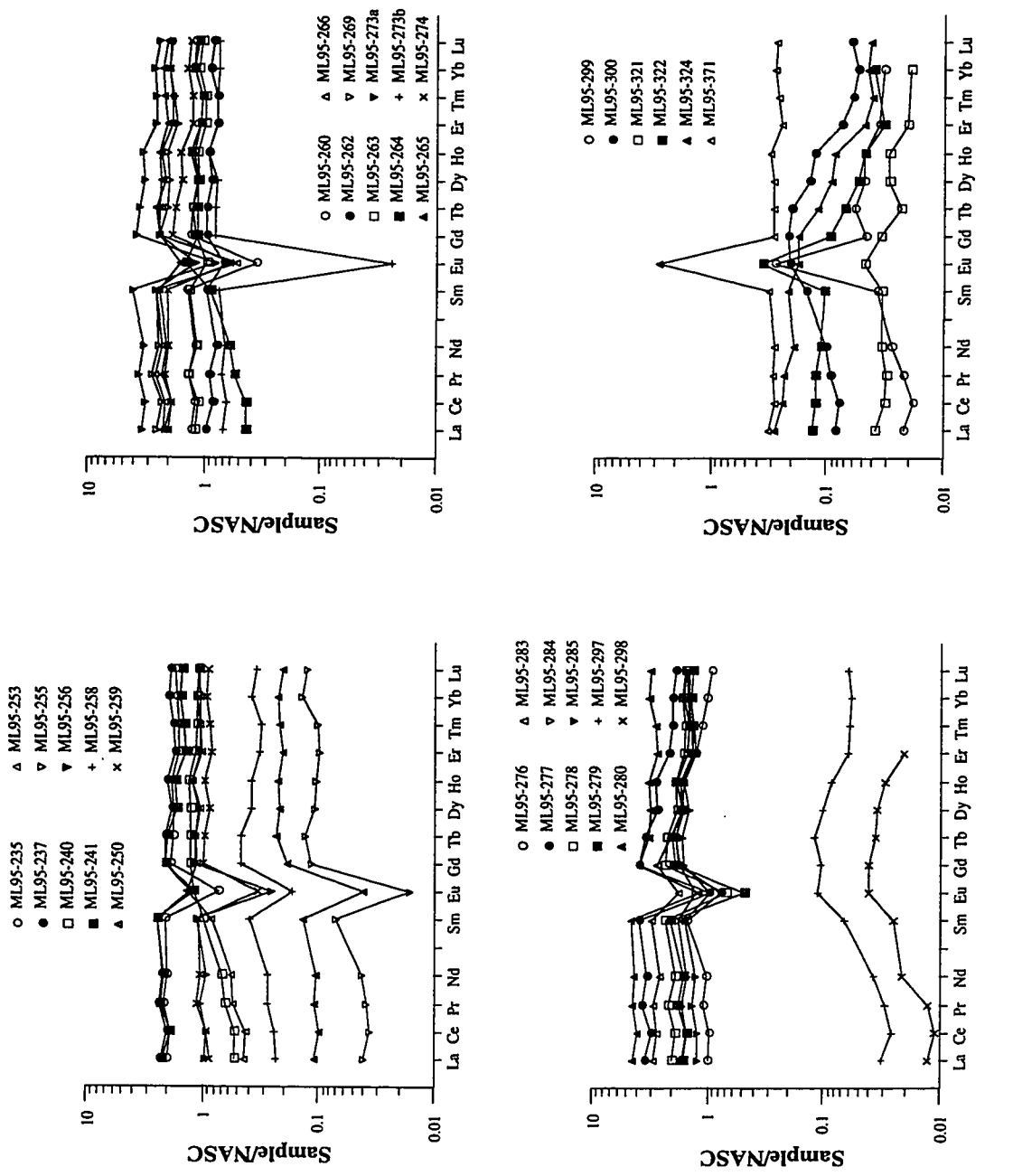


Fig. 10.22 Rare-earth element concentrations of Restigouche deposit lithologies normalized to North American Shale Composite (NASC). Normalizing values are from Haskin et al. (1968) with Dy value from Gromet et al. (1984). Data from Table 10.8.

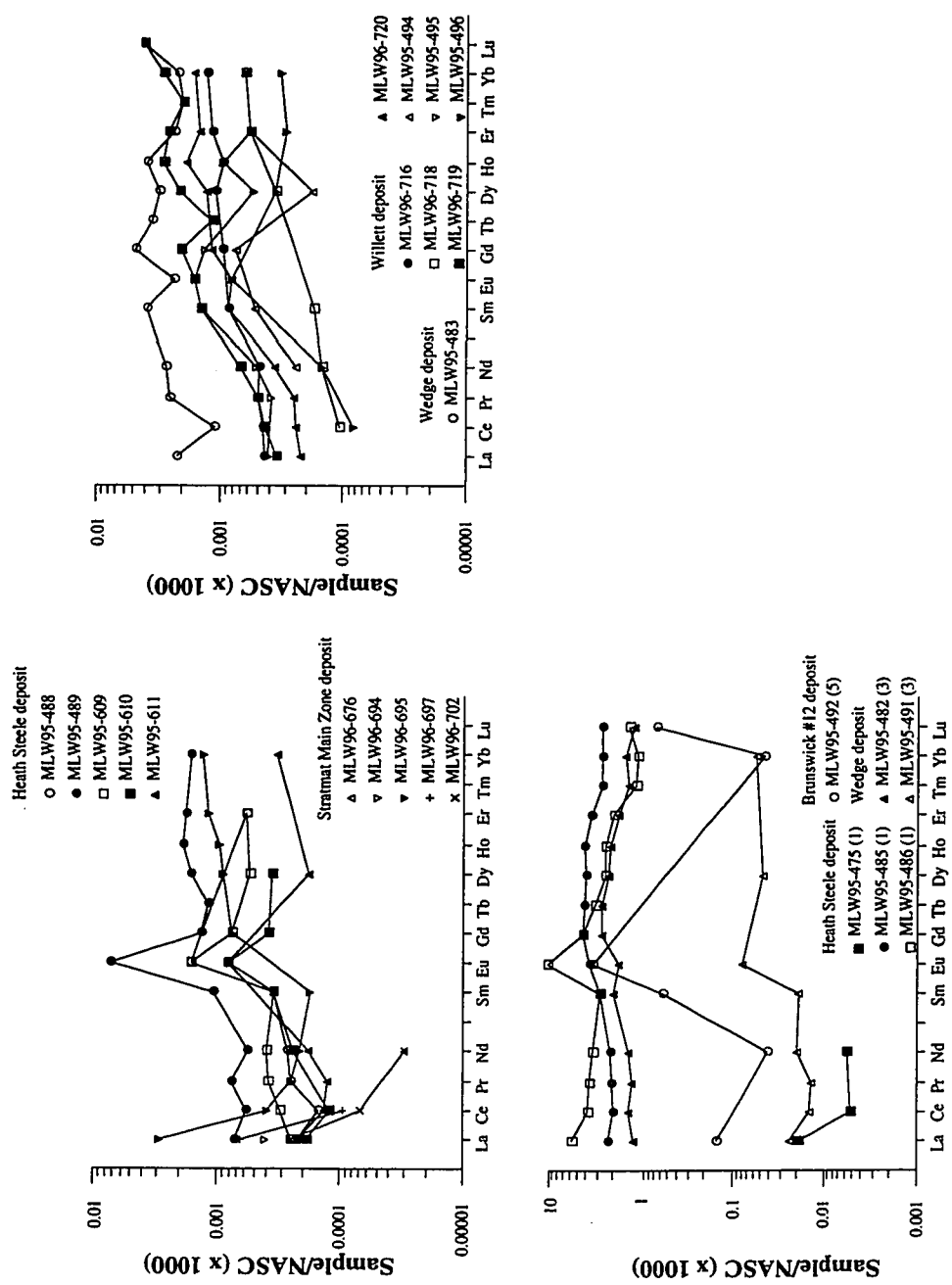


Fig. 10.23 Rare-earth element concentrations of waters from Heath Steele, Stratmat Main Zone, Brunswick #12, Williett and Wedge deposits normalized to North American Shale Composite (NASC). Normalizing values are from Haskin et al. (1968) with Dy value from Gromet et al. (1984). Data from Table 10.9.

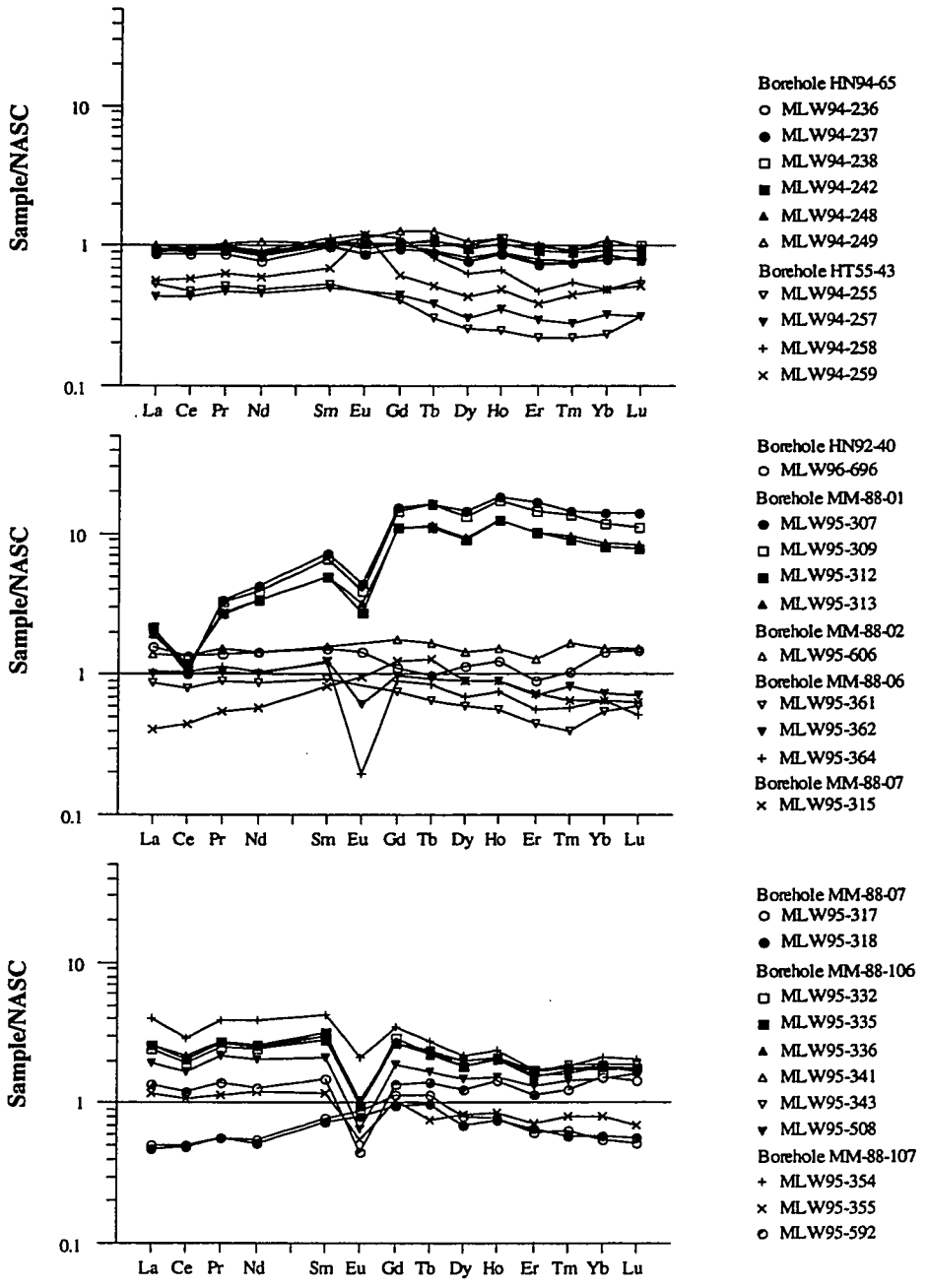


Fig. 10.24 Rare-earth element concentrations of Halfmile Lake and Restigouche deposit borehole suspended sediments normalized to North American Shale Composite (NASC). Normalizing values are from Haskin et al. (1968) with Dy value from Gromet et al. (1984). Data from Table 10.10.

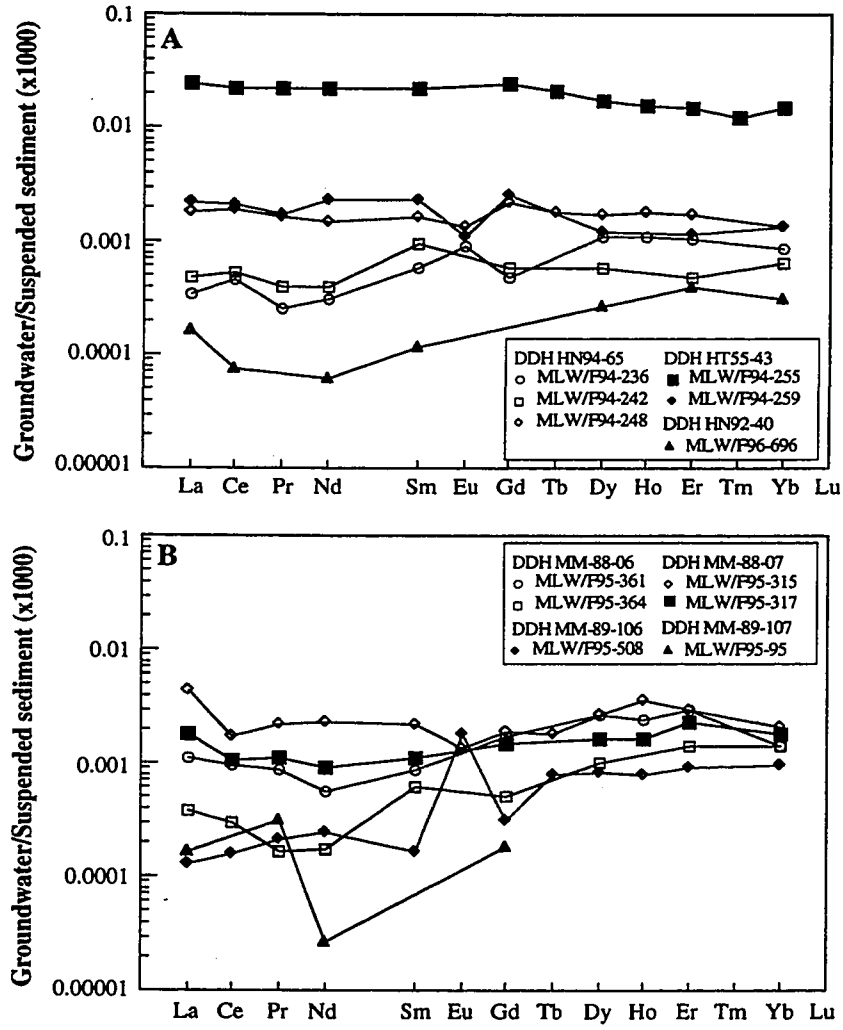


Fig. 10.25 Groundwaters from A) Halfmile Lake deposit and B) Restigouche deposit normalized to the corresponding suspended sediment. Data from Tables 10.2, 10.6, and 10.10.

CHAPTER ELEVEN:
STABLE ISOTOPE GEOCHEMISTRY OF GROUND AND SURFACE WATERS AT THE HALFMILE LAKE AND RESTIGOUCHE DEPOSITS, BATHURST MINING CAMP, NEW BRUNSWICK

11.1 Introduction

Stable isotopes are extremely useful tools in hydrogeology because they allow greater refinement of interpretations of the history of water masses and the dissolved constituents of those water masses (Welhan, 1987). Different isotopes have different utilities in these regards. The stable isotopes of hydrogen and oxygen are useful because they are highly conservative and so allow inferences to be made as to the age, recharge elevation, and infiltration history of precipitation. Fractionations of oxygen and deuterium isotopes due to water-rock reaction, mineral dissolution/precipitation and gas exchange are commonly systematic, generally well-understood and commonly only occur at high temperature and/or very low water/rock ratios. Carbon is a non-conservative element in hydrological systems and the stable isotopes of carbon in ground and surface waters reflect the history and pathways of aqueous carbon. Therefore, the $\delta^{13}C$ of dissolved inorganic carbon (DIC) allows inferences to be made on the style and extent of water-rock reactions (Fritz et al., 1989).

Carbon, oxygen, and hydrogen isotopes have been extensively utilized in hydrogeochemistry, but analyses of boron isotopes is relatively new. Recent advances in ICP-MS (inductively coupled plasma - mass spectrometry) methods have made it possible to measure some isotopes directly, including the B isotopes (e.g. Gregoire, 1990). The behaviour of B lies somewhere between the conservative behaviour of O and H and the non-conservative behaviour of C. The stable isotopes of B are useful because they can provide important constraints on the origin and evolutionary history of groundwater salinity, in particular tracing the source of B, and by inference Br, and Cl (Bottomley et al., 1994; Vengosh et al., 1991; Vengosh et al., 1995).

In this study, over 150 samples of ground and surface waters, and precipitation were analyzed for O and D isotopes. Forty samples of ground and surface waters and twelve samples of vein and fracture carbonate were determined for their carbon isotopic composition. In an attempt to characterize and refine interpretations of the more saline waters collected during this study, a subset of 14 waters, for which B was above detection, were analyzed for their B isotopic composition using ICP-MS. All analytical methods are discussed in Chapter Three. The geochemistry of the surface waters was discussed in Chapter Five and of the groundwaters in Chapters Seven and Eight.

11.2 $\delta^{18}O$ and δD of Precipitation

A small number of precipitation samples were collected during the summer field seasons of 1995 and 1996 (Table 11.1). In addition, the International Atomic Energy Association (IAEA) for several years measured O and D isotopes in precipitation from stations around the world. Two monitoring stations added to their data base occur to the east and west of the study area in St. Agathe, Quebec and Truro, Nova Scotia (Fig. 11.1a; Fritz et al., 1987). These stations were sampled between 1975 and 1983 (www.iaea.org).

Table 11.1 Stable isotope data for BMC precipitation

Sample#	$\delta^{18}O_{VSMOW}$ (‰)	δD_{VSMOW} (‰)	excess d	Date
MLW95-304	-8.56	-55.6	12.88	4 June 1995
MLW95-524	-6.11	-38.9	9.98	24 July 1995
MLW96-647	-9.45	-60.3	15.30	25 June 1996
MLW96-648	-15.26	-106.9	-15.18	27 June 1996
MLW96-670	-9.26	-59.1	14.98	5 July 1996
MLW96-672	-8.11	-47.4	17.48	16 July 1996

Stable isotopes in precipitation are highly variable on an annual scale, reflecting changes in

temperature and sources of the air masses. For example, monthly average $\delta^{18}O_{VSMOW}$ values range from -23.9 to -6.3‰ for St. Agathe and from -20.4 to -5.1‰ for Truro (Figs. 11.1, 11.2). Similarly, δD_{VSMOW} values range from -179 to -36‰ and from 150 to -36‰ for St. Agathe and Truro, respectively. Stable isotope values for precipitation samples collected in this study fall within these ranges and vary from -15.26 to -6.11‰ for $\delta^{18}O_{VSMOW}$ and from -38.9 to 106.9‰ for δD_{VSMOW} (Table 11.1; Fig. 11.1). Sample MLW96-648 is unusual compared to the other precipitation samples in that it has a negative excess deuterium value (Table 11.1). By comparison, only rarely are any of the St. Agathe and Truro station excess deuterium values negative and none are as negative as sample MLW96-648. Excess deuterium is defined as:

$$'d' = \delta D - 8 \cdot \delta^{18}O$$

The St. Agathe data shows greater amplitude for both isotopes, consistent with its location further inland, i.e., greater continentality (Clark and Fritz, 1997). Stable isotopic variations are greater and average compositions lighter for the St. Agathe station than for the Truro station. St. Agathe has an average $\delta^{18}O$ value of -12.77 ± 4.6‰ (n = 80) and δD value of -88.99 ± 35.9‰, whereas, Truro has values of -9.28 ± 3.15‰ (n = 91) and -64.24 ± 23.1‰ for $\delta^{18}O_{VSMOW}$ and δD_{VSMOW}, respectively. In addition, the $\Delta\delta^{18}O_{VSMOW}$ and $\Delta\delta D_{VSMOW}$ between the two monitoring stations for the weighted monthly averages is much greater for winter precipitation than for summer precipitation (Fig. 11.3). Average values for the precipitation collected from the Bathurst Mining Camp (BMC) are slightly more depleted than the June-July data from both Truro and St. Agathe ("BMC precipitation-1"; Fig. 11.3). However, if the very depleted value of sample MLW96-648 is excluded, the average value for BMC precipitation falls between the June weighted average values for Truro and St. Agathe ("BMC precipitation-2"; Fig. 11.3). The variations in the stable isotope data for the two monitoring stations looks regular on a monthly and yearly basis (Fig. 11.2). However, monthly averages mask large fluctuations on a shorter time scale. For example, samples MLW96-647 and MLW96-648 were collected from the same locations during two storm events

two days apart (Table 11.1). The stable isotopic compositions for these two storms are 5.81‰ and 46.6‰ different for $\delta^{18}O_{VSMOW}$ and δD_{VSMOW}, respectively.

Craig (1961) defined the global meteoric water line (GMWL) based on linear regression of $\delta^{18}O$ and δD for worldwide surface waters. The GMWL is defined as:

$$\delta D_{VSMOW} = 8 \cdot \delta^{18}O_{VSMOW} + 10‰$$

The Truro and St. Agathe data can be used to construct more local meteoric water lines which are more appropriate for comparison to the BMC ground and surface water data than the GMWL. The Truro data define a local meteoric water line as:

$$\delta D_{VSMOW} = 7.1 \cdot \delta^{18}O_{VSMOW} + 1.66‰ \ (r^2 = 0.938)$$

Note that this is different from the published slope and intercept quoted by Fritz et al. (1987). The St. Agathe data defines a local meteoric water line that is very close to the GMWL:

$$\delta D_{VSMOW} = 7.75 \cdot \delta^{18}O_{VSMOW} + 9.96‰ \ (r^2 = 0.985)$$

The limited precipitation data collected in this study define a LMWL which is close to the Truro and St. Agathe data (Fig. 11.1):

$$\delta D_{VSMOW} = 7.68 \cdot \delta^{18}O_{VSMOW} + 11.5‰ \ (r^2 = 0.991)$$

The annual variation in $\delta^{18}O_{VSMOW}$ and δD_{VSMOW} in precipitation is very clearly shown for both St. Agathe and Truro (Fig. 11.2). The very strong correlation between stable isotopic composition and vapour temperature (cf Figs. 11.2a and 2b with Fig. 11.2c) illustrates the strong dependency of oxygen and deuterium isotopes on temperature. For the St. Agathe data, the relationship between oxygen isotopes and temperature is defined as:

$$\delta^{18}O_{VSMOW} = 0.349 \cdot T - 14.12 \ (r^2 = 0.874)$$

and for the Truro data as:

$$\delta^{18}O_{VSMOW} = 0.261 \cdot T - 11.03 \ (r^2 = 0.772)$$

However, although these stable isotopes are also commonly influenced by the amount of precipitation (Dansgaard, 1964), in particular in arid regions, there is no correlation between the stable isotopic composition and amount of precipitation for Truro and St. Agathe (Figs. 11.2a, b vs 11.2d).

11.3 $\delta^{18}O$ and δD of Halfmile Lake Deposit Waters

The stable isotopic compositions of both surface and borehole waters from the Halfmile Lake deposit are remarkably uniform (see Figs. 5.1 and 7.1 for surface water and borehole locations, respectively). Surface waters vary between -13.62 and -12.86 for $\delta^{18}O_{VSMOW}$ and -99.8 and -86.1 for δD_{VSMOW} (Table 11.2; Figs. 11.4, 11.5). Groundwaters vary from -13.7 to -13.09 for $\delta^{18}O_{VSMOW}$ and -97.8 and -81.5 for δD_{VSMOW}. Average compositions are essentially identical with average $\delta^{18}O_{VSMOW}$ = -13.32 and -13.42‰ and average δD_{VSMOW} = -90.61 and -90.63‰ for surface and groundwaters, respectively. Sampling of surface waters was carried out to minimize input from direct precipitation, overland flow and throughflow (i.e. in order to sample baseflow). The similarity between the surface and borehole waters indicates that this was successful.

The $\delta^{18}O_{VSMOW}$ isotopic compositions of Halfmile Lake deposit ground and surface water are more depleted than published compilations of groundwaters in Canada (Clark and Fritz, 1997; Fritz et al., 1987), indicating that shallow recharge groundwaters in the Bathurst region should be between -11 and -13‰. Unpublished data for groundwaters closer to Bathurst are within this range (D.R. Boyle, unpublished data 1995; Fig. 11.4). Excess deuterium is high, ranging from 7.7 to 19.8 (average = 15.9) for surface waters and 9.5 to 25.5 (average = 16.7) for groundwaters.

Although the overall variation in stable isotopes is minor, variation in δD_{VSMOW} is greater than for $\delta^{18}O_{VSMOW}$ producing a subtle vertical trend in Figure 11.4. Almost all of the Halfmile Lake waters plot well above the GMWL but closer, on average, to the local meteoric water lines defined by the Truro and St. Agathe precipitation data (Fig. 11.4).

It has previously been noted that groundwaters close to the east and west coasts of Canada typically have stable isotopic compositions close to the annual weighted average of precipitation (Clark and Fritz, 1997; Fritz et al., 1987). The annual weighted averages for Truro and St. Agathe for the years 1975 to 1983 are $\delta^{18}O$ = -9.34‰ and δD = -63.67‰ for Truro, and $\delta^{18}O$ = -12.92‰ and δD = -89.97‰ for St. Agathe. The Halfmile Lake deposit data are lighter, on

average, than both the Truro and St. Agathe weighted averages (Fig. 11.3).

Seeps from the headwaters of the Upper/Lower AB stream are slightly more isotopically depleted than other surface waters and have higher Cl (Fig. 11.6), despite very low TDS values (Chapter Five). The Halfmile North stream has similar elevation range and topography as the Upper/Lower AB and overlaps this latter stream in $\delta^{18}O_{VSMOW}$ and Cl content. In contrast, the Northeast and North tributaries to the NW Miramichi are isotopically heavier than the Halfmile North and Upper/Lower AB streams, consistent with lower elevation (see DEM's in Chapter Four). If the seeps from the headwaters of the Upper/Lower AB stream are ignored, there is a positive correlation between $\delta^{18}O_{VSMOW}$ and Cl content (Fig. 11.6). There are two possible explanations: a) longer more integrated flow paths for the north and northeast streams indicating greater water-rock interaction combined with lower elevation (slight elevation effect) or, B) these lower elevation waters are slightly evaporated causing an increase in salinity and with isotopic composition. The most depleted borehole waters are from the top of the Upper AB zone (borehole HT55-43). The shallowest water in a given borehole is typically slightly depleted in $\delta^{18}O_{VSMOW}$ compared to deeper waters (Table 11.2; Fig. 11.7).

Groundwaters show a slightly more restricted range in $\delta^{18}O_{VSMOW}$ compared to surface waters (Figs. 11.5, 11.6) and trend to higher Cl contents (Fig. 11.6). The groundwaters with the most elevated Cl contents are from boreholes HN87-8 (from which the deepest samples were recovered; up to 760 m) and the packer samples from boreholes HN94-65 and HN94-63 (Fig. 11.6).

Changes in δD_{VSMOW} and $\delta^{18}O_{VSMOW}$ in groundwaters are not always complimentary. For example, in borehole HN87-8, these isotopes show a similar pattern of variation to about 300 m depth, below which the variation in δD_{VSMOW} is antithetical to that in $\delta^{18}O_{VSMOW}$ (Fig. 11.7).

11.4 $\delta^{18}O$ and δD of Restigouche Deposit Waters

Surface and shallow groundwaters at Restigouche are isotopically similar to those from

Halfmile Lake (Figs. 11.3, 11.5) and also plot above the GMWL and are more isotopically depleted than expected for waters from this region (Fig. 11.8). However, local meteoric water lines, defined by Truro, St Agathe, and BMC precipitation data, pass through the Restigouche data (Fig.11.8). There is essentially no isotopic difference between the shallow groundwaters and the surface waters at Restigouche with the exception that the surface waters appear to span a wider range in δD_{VSMOW} at a similar $\delta^{18}O_{VSMOW}$ content compared to the shallow groundwaters (Fig. 11.8; see Figs. 5.12 and 7.13 for surface water and borehole locations, respectively). Surface waters (not including the Portage Lake sample) vary from -13.79 to-13.22‰ for $\delta^{18}O_{VSMOW}$ and from -99.9 to -84.6‰ for δD_{VSMOW} (Table 11.3; Figs, 11.5, 11.8). Shallow groundwaters from boreholes MM-88-01, MM-88-06, MM-88-07, B-80-7, B-80-15, EH-1, MM-89-104, MM-89-107, and MM-89-109 have stable isotopic compositions that vary from -13.62 to -13.21‰ for $\delta^{18}O_{VSMOW}$ and from -98.1 to -89.5‰ for δD_{VSMOW}. The surface waters are isotopically indistinguishable from these shallow groundwaters. The average $\delta^{18}O_{VSMOW}$ and δD_{VSMOW} for surface waters is -13.47‰ and -93.4‰, respectively, and -13.46‰ and -93.8‰ for the shallow groundwaters. Exceptions include shallow groundwaters from the C4/C5 area and from borehole MM-89-100 which are slightly heavier than most shallow groundwaters (Figs. 11.8, 11.9).

The high salinity groundwaters from borehole MM-88-02, the deepest borehole drilled to date at the Restigouche deposit, are the isotopically heaviest of the present study and are on average 2.5 to 3‰ enriched in $\delta^{18}O_{VSMOW}$ compared to the shallow groundwaters (Figs. 11.5, 11.8). Sample MLW96-669 (45 m depth) from borehole MM-88-02 has an intermediate Cl content and has more depleted stable isotope values than the more saline waters deeper in the hole (Figs. 11.8, 11.9). The mid-level (150-250 m depth) brackish groundwaters are also more isotopically enriched than shallow groundwaters but more depleted than waters from borehole MM-88-02. These waters are also intermediate in terms of salinity (Fig. 11.9).

Overall, groundwaters from the Restigouche deposit are highly variable in Cl contents and $\delta^{18}O_{VSMOW}$ values compared to groundwaters from the Halfmile Lake deposit (Fig. 11.5, cf

Figs. 11.6 and 11.9). Shallow groundwaters from the Restigouche deposit with low to moderate Cl contents (approximately < 100 mg/L) generally have $\delta^{18}O_{VSMOW}$ values similar to local surface waters. At higher salinities (generally > 100 mg/L Cl), groundwaters show increasing $\delta^{18}O_{VSMOW}$ values (Fig. 11.9). The groundwaters fall close to a hypothetical two end-member mixing line, although such simple two-component mixing does not account for all of the geochemical differences between the Restigouche deposit groundwaters (Chapters Seven, Twelve).

There are some systematic variations in Cl and $\delta^{18}O_{VSMOW}$ contents for the surface waters at the Restigouche deposit. Upstream from the Restigouche ore body, samples from seeps and a small stream that feed into Charlotte Brook are depleted in $\delta^{18}O_{VSMOW}$ and have low Cl contents (samples MLW95-426, 431 and 432). Sample MLW95-425 is 200 m downstream from where sample MLW95-426 enters Charlotte Brook and is immediately downstream of a beaver dam pond. Sample MLW95-425 has a higher $\delta^{18}O_{VSMOW}$ value than samples upstream, perhaps indicating subtle evaporation effects of the pond. There is no change in the Cl contents however. Downstream from the Restigouche ore body, three samples show increased Cl contents, perhaps indicating influence from the high salinity groundwaters. After the confluence of Charlotte Brook with Mt Vroom NE stream (see Fig. 5.12 for stream locations), Cl contents decrease and $\delta^{18}O_{VSMOW}$ values increase. Although samples from Mt Vroom NE stream higher in the watershed are isotopically more depleted, the sample close to the confluence has a similar isotopic composition as the Charlotte Brook sample downstream from the confluence of the two streams. Seeps (samples MLW95-300, MLW95-322, and MLW95-345) have higher Cl contents but $\delta^{18}O_{VSMOW}$ values are similar to the streams (Fig. 11.9).

Surface water samples from Mt Vroom E and Mt Vroom SE streams have generally higher $\delta^{18}O_{VSMOW}$ values and lower Cl contents than the other surface waters. The exception is a seep on the north bank of Mt Vroom NE stream which has the lowest $\delta^{18}O_{VSMOW}$ value of all the surface waters (Fig. 11.9).

11.5 $\delta^{18}O$ and δD of Groundwaters from the Heath Steele, Brunswick #12, Wedge, Willett, and Stratmat Main Zone Deposits

Groundwaters from the other deposits sampled in this study have a moderately wide range of stable isotopic compositions (Table 11.4; Fig. 11.10), consistent with the diversity in origin and chemistry of these waters (see Chapter Seven). The deepest samples in this study were taken from the Heath Steele and Brunswick #12 deposits (Table 11.4). The Brunswick #12 sample (MLW95-492) has the highest salinity recovered to date from the Bathurst Mining Camp (TDS = 45,751 mg/L). However, these waters are isotopically intermediate between the shallow and deep groundwaters at the Restigouche deposit. All of the mine waters tend to straddle the local meteoric water lines defined by the Truro and St. Agathe precipitation data (Fig. 11.10).

The isotopic and chemical compositions of Heath Steele deposit waters do not vary systematically with depth, a common feature in mine waters from the Canadian and Fennoscandian Shields (e.g. Moser et al., 1989), due to disruption of the hydrological regime from mine excavation. The two shallowest samples from the Heath Steele deposit (samples MLW95-474, 113 m and MLW95-490, 91 m) have $\delta^{18}O_{VSMOW}$ and δD_{VSMOW} values (-12.27 to -12.53‰ and -86.2 to -85.0‰) which are similar to shallow waters from the Stratmat Main Zone deposit borehole S61-19 ($\delta^{18}O_{VSMOW}$ = -12.32 to -12.50‰ and δD_{VSMOW} = -79.4 to -84.0‰). The Stratmat Main Zone deposit and the Heath Steele deposit are geographically close to each other, suggesting there may be a common origin for these waters. However, sample MLW95-490 from 183 m depth in the Heath Steele deposit has lighter isotopic ratios and is isotopically indistinguishable from the shallow groundwaters and surface waters at both the Halfmile Lake and Restigouche deposits (Fig. 11.5). The deepest waters (450 to 840 m depth) from the Heath Steele deposit have the heaviest stable isotope values of the mine waters with $\delta^{18}O_{VSMOW}$ ranging from -11.73 to -11.98‰ and δD_{VSMOW} ranging from -76.9 to -80.7‰ (Table 11.4).

The four samples from the Wedge and Willett deposits are isotopically similar to shallow

groundwaters from the Heath Steele and Stratmat Main Zone deposits (Fig. 11.10). These waters, with $\delta^{18}O_{VSMOW}$ values between 1 and 1.5‰ heavier than recharge waters at the Halfmile Lake and Restigouche deposits, all have low Cl contents and plot below the trend defined by the deeper Heath Steele and Brunswick #12 deposit waters with respect to Cl and $\delta^{18}O_{VSMOW}$ (Fig. 11.10B). These deeper groundwaters show generally increasing salinity with increasing $\delta^{18}O_{VSMOW}$ values, although they do not define a two-component mixing trend (cf Figs. 11.10B and 11.9A).

Waters from the Stratmat Main Zone deposit show changes downhole which mimic changes in chemistry (Chapter Eight) but are fairly restricted, ranging from -12.50 to -11.99‰ for $\delta^{18}O_{VSMOW}$ and -84.3 to -79.4‰ for δD_{VSMOW} (Table 11.4). Oxygen and hydrogen isotopes show a shift to heavier isotopic compositions from the top to the bottom of the ore zone of approximately 0.35 and 4‰, respectively (Fig. 8.8).

11.6 $\delta^{13}C$ of DIC in Ground and Surface Waters

The carbon isotopic composition of dissolved inorganic carbon (DIC) was determined for twenty ground and surface waters from the Restigouche deposit. For the most part, surface waters ($\delta^{13}C_{DIC}$ = -12.57 to -8.36‰, n = 9) overlap the field for shallow groundwaters ($\delta^{13}C_{DIC}$ =-11.32 to -7.30‰, n = 7). A brackish water from the deeper parts of borehole MM-89-106 is slightly heavier than the shallow groundwaters with $\delta^{13}C_{DIC}$ = -6.34‰ (Table 11.5). As with so many other geochemical parameters, the waters from borehole MM-88-02 are anomalous in $\delta^{13}C_{DIC}$ values (Fig. 11.11) with very heavy $\delta^{13}C_{DIC}$ values of +11.98 to +12.48‰ (n = 3). When the bailer samples were recovered from this hole it was noted that the samples effervesced vigorously. In order to test that the high positive values are not the result of degassing-fractionation of CO_2 during transit from depth, one of the samples was initially analyzed and the remaining sample subsequently shaken, allowed to degas and re-analyzed on two successive days. The first re-analysis failed. Despite shaking and degassing, the CO_2 yield was virtually identical to the initial analysis and the $\delta^{13}C_{DIC}$ value was only slightly lower

(11.98 vs 12.21‰) than the initial analysis. This would suggest that degassing of CO_2 was not the cause of the elevated $\delta^{13}C_{DIC}$.

Six packer-sample groundwaters and three surface waters from the Halfmile Lake deposit were analyzed for C isotopes. These waters span a wider compositional range than the Restigouche ground and surface waters, excluding the saline MM-88-02 waters. Halfmile Lake deposit groundwaters range from -14.72 to -5.91‰ $\delta^{13}C_{DIC}$. The three Halfmile Lake surface waters range from -17.89 to -6.03‰ $\delta^{13}C_{DIC}$ (Table 11.5; Fig. 11.11).

For all Halfmile Lake and Restigouche deposit groundwaters there is no relationship between $\delta^{13}C_{DIC}$ and $\delta^{18}O_{VSMOW}$ (Fig. 11.11). In contrast, the carbon and oxygen isotopic composition of the Stratmat Main Zone deposit waters from borehole S61-19 show a strong positive correlation (Fig. 11.11). These waters show a restricted range of $\delta^{13}C_{DIC}$ values from -15.00 to -10.31‰ (Table 11.5). The carbon and oxygen isotopic composition of the Stratmat waters increase through the massive sulphide zone and decrease again below the sulphides and are approximately 3‰ heavier at the bottom of the ore zone compared to the top (Fig. 8.8).

One sample from depth (840 m) at the Heath Steele deposit (sample MLW95-610) yielded a $\delta^{13}C_{DIC}$ value of -5.01‰. A precipitation sample (from the Restigouche deposit) was also analyzed and yielded a $\delta^{13}C_{DIC}$ value of -12.40‰, less than the normal range for atmospheric CO_2 (~ -6 to -8‰; Fig. 11.11).

For Restigouche deposit shallow groundwaters (excluding the deep MM-89-106 and MM-88-02 waters) there is a positive correlation between $\delta^{13}C_{DIC}$ and $1/HCO_3$ (Fig.11.12). Halfmile Lake deposit groundwaters, with the exception of the most depleted sample, show a reverse trend with higher $\delta^{13}C_{DIC}$ values with increasing HCO_3 contents. Surface waters from both deposits show no real correlation between these two parameters. For groundwaters from the Stratmat Main Zone deposit, there is only a very minor variations in DIC contents (HCO_3 = 73.9 to 115.7 mg/L) over the range of $\delta^{13}C_{DIC}$ values in these waters.

The Stratmat Main Zone deposit groundwaters show a strong correlation between HCO_3^-/SO_4^{2-} and $\delta^{13}C_{DIC}$ such that groundwaters from the ore zone with elevated sulphate contents

(Chapter Eight; Fig. 8.4) have the highest $\delta^{13}C_{DIC}$ values (Fig. 11.12B). Groundwaters from the Restigouche deposit with moderate to high sulphate show a similar trend as the Stratmat Main Zone deposit waters, whereas, groundwaters from the Halfmile Lake deposit show an opposite trend. The brackish waters from the bottom of borehole MM-89-106 and from borehole MM-88-02 at the Restigouche deposit have very low to below detection sulphate contents as a consequence of sulphate reduction (Chapter Seven) and so do not plot near the other waters with respect to HCO_3^-/SO_4^{2-} values. There is no real correlation between pH and $\delta^{13}C_{DIC}$ for any of the waters (Fig. 11.13A).

The $\delta^{13}C_{DIC}$ contents of the ground and surface waters varies between values associated with CO_2 produced by C_3 organic matter decomposition and those observed for carbonates at the Restigouche deposit (see Section 11.7 below). No carbonate has been analyzed to date from the BMC that has $\delta^{13}C_{PDB}$ values as heavy as waters from Restigouche deposit borehole MM-88-02.

11.7 Stable Isotopes of Carbonate

11.7.1 Carbonate morphology and paragenesis

Most of the carbonate observed in core from the Restigouche deposit occurs as cross-cutting veins of calcite-ferroan dolomite and siderite. These veins are generally massive in hand sample. Where open vugs occur in carbonate, quartz, and albite veins (Fig. 11.14D), massive carbonate is typically blocky in habit. More rarely, acicular carbonate crystals occur in open vugs and platy carbonate was also observed on some fracture surfaces. Carbonate also occurs as discrete subhedral to anhedral crystals associated with pervasive chlorite and sericite alteration in the stockwork zone underlying the Restigouche massive sulphide deposit (Fig. 11.14C). Graphite was observed in sample ML95-246 where it occurs as sub-cm sized crystals in thick carbonate veins.

The massive carbonate veins typically cross-cut other structures and are commonly associated with late quartz veins. These veins most likely post-date formation of the massive

sulphides. Carbonate associated with sericite and chlorite alteration and interstitial to massive sulphides was most likely part of the hydrothermal system that formed the massive sulphides.

11.7.2 Geochemistry of BMC carbonates

The composition of carbonates was determined semi-quantitatively by SEM methods. Sample ML95-240 contains Mg-rich calcite to ferroan dolomite. Some crystals have Mg ≈ Fe, suggesting that the carbonate compositions approach that of ankerite. Sample ML95-224 has ferroan dolomite and siderite as the dominant carbonate minerals. Although Fe-rich carbonates display variable Mg contents, no magnesite was observed. SEM analyses of sample ML95-259 suggest that in this sample the dominant carbonate is siderite. Typically, massive carbonate crystals are complexly zoned with the zoning due to variations in Mg and Fe contents in ferroan dolomite and to Mg variations in siderite (Fig. 11.14). These compositions are consistent with the results of the carbon isotope measurements with the exception that very little siderite was liberated during evolution of CO_2 by phosphoric acid attack on the carbonates (Table 11.6). In addition, significant CO_2 was liberated during the first two hours of reaction with phosphoric acid, indicating that calcite is a significant carbonate in the Restigouche deposit veins, despite the dearth of unequivocal calcite observed during SEM analyses.

11.7.3 Stable isotopic composition of carbonate minerals and graphite

Carbonate minerals were separated from veins and fractures by micro-drilling in order to avoid contamination from sulphides and silicates (Chapter Three). Carbonate minerals on the surface of a fracture in sample ML95-266 were picked off with the tip of a knife. For most of the carbonate samples a three step process was followed for the generation of CO_2 for isotopic analysis (see Chapter Three). Calcite, dolomite-ankerite, and siderite analyses were generated from the same sample. In all cases, very little gas pressure was generated for the siderite component, although the analyses ran well. Although the dolomite in the veins are Fe-rich, the $\delta^{13}C$ values were calculated assuming a fractionation factor for dolomite. There is a solid

solution between dolomite and ankerite, but given that the fractionation factors for these minerals are fairly close (dolomite = 1.01065 @ 50°C; ankerite = 1.010603 @ 50°C\; Rosenbaum and Sheppard, 1986), no attempt was made to adjust the fractionation factor based on Fe-contents of the dolomite. There is also a solid solution between siderite and magnesite, and there is a large difference in the fractionation factors for the two end-members (siderite = 1.010454 @ 50°C (Rosenbaum, 1993); magnesite = 1.01160 @ 50°C (Perry and Tan, 1972)). However, given the low gas pressures generated during siderite breakdown, and the lack of experimental work to demonstrate how the oxygen isotopic composition varies with variable Fe/Mg within the siderite-magnesite solid solution, the siderite values were calculated based on the fractionation factor for end-member siderite.

Calcite varies between -1.33 and -8.17 ‰ $\delta^{13}C_{VPDB}$, with an average of -5.87‰ (n = 11). Ferroan dolomite typically has lower $\delta^{13}C_{VPDB}$ values, ranging from -4.52 to -11.64‰ with an average of -6.51‰ (n = 9). Siderite has the lightest isotopic values ranging from -5.98 to -10.1 with an average of -7.54 ‰ (n = 8) (Table 11.6). Similarly, the oxygen isotopic composition decreases from calcite to dolomite to siderite, with average $\delta^{18}O_{VSMOW}$ values of 16.82 (11.54 to 20.61‰), 14.87 (6.66 to 20.41‰), and 13.09‰ (11.00 to 15.47‰) respectively (Table 11.6). The carbon and oxygen isotopes form a broad array with positive correlation (r = 0.759) (Fig.11.15). For most samples, the dolomite and calcite stable isotopic compositions of the same sample are similar, but the coexisting siderite typically has lower isotopic values. Sample ML95-244 had two obviously different generations of carbonate vein. The first vein was only analyzed for calcite and gave a considerably heavier isotopic composition ($\delta^{13}C$ = -1.33‰) than the later(?) vein ($\delta^{13}C$ = -4.79‰) despite similar $\delta^{18}O_{VSMOW}$ values (Table 11.6). There is no obvious differences in the isotopic compositions of the fracture, vuggy, and massive vein carbonate (Table 11.6).

Carbonate from the BMC are similar to carbonate from veins and fractures in rocks from the Canadian and Fennoscandian Shields (Frape et al., 1992). BMC carbonates also show a linear trend similar to that for mid-ocean ridge hydrothermal alteration, but are more depleted than

most marine limestones and diagenetic cements (Fig. 11.15B).

Graphite was observed in carbonate veins at the Restigouche deposit (Fig. 11.14). Graphite in these veins is isotopically very light, ranging from -25.56 to -27.79‰ $\delta^{13}C_{VPDB}$ (n = 3; Table 11.6). These values are considerably lighter than graphite from the Patrick Brook Formation which ranges from -13 to -17‰ (Peter and Goodfellow, 1993).

11.7.4 Estimate of the temperature and $\delta^{13}C$ of the carbonate-forming fluid

No fluid inclusion analyses were attempted on these samples. However, an estimate of the temperature of formation is possible by assuming an isotopic composition of the original fluid. Temperatures were calculated using carbonate-water expressions. For the calcite-water system the relationship between the fractionation factor and temperature of the fluid in degrees Kelvin is (Friedman and O'Neil, 1977):

$$1000\text{Ln}\ \alpha_{calcite-water} = 2.78(10^6 T^{-2}) - 2.89$$

For the dolomite-water system (Northrop and Clayton, 1966):

$$1000\text{Ln}\ \alpha_{dolomite-water} = 3.20(10^6 T^{-2}) - 1.50$$

Finally, for the siderite-water system (Carothers et al., 1988):

$$1000\text{Ln}\ \alpha_{siderite-water} = 3.13(10^6 T^{-2}) - 3.50$$

Temperatures were calculated assuming a mineralizing fluid $\delta^{18}O_{VSMOW}$ composition of -1 and 1‰, with the latter value yielding higher temperatures. Oxygen isotopic compositions from mid-ocean ridge vent fluids are typically on the order of 0-2‰, although highly positive values have been calculated based on combined fluid-inclusion and carbonate isotopic compositions from calcite from mid-ocean ridges (Peter et al., 1994). Assuming a fluid of -1‰ ($\delta^{18}O_{VSMOW}$), the derived temperatures range from 65 - 152 °C for calcite, 102 - 199 °C for dolomite (one sample yielded a temperature of 320 °C), and 129-177 °C for siderite (Fig. 11.16A). Dolomite and siderite calculated temperatures are typically 25 - 70 °C higher than calcite temperatures from the same samples. Siderite and dolomite temperatures are similar, within ±20 °C. If it is assumed that the carbonates formed from a meteoric fluid similar to

modern recharge waters at the Halfmile Lake and Restigouche deposits, temperatures as low as 3 - 45 °C (calcite), 30 - 115 °C (dolomite) and 40 - 64 °C (siderite) are derived.

The temperatures derived from the oxygen isotope values of the different carbonate minerals were used in the following expressions to derive the $\delta^{13}C_{VPDB}$ composition of the original fluid. It was assumed that because most of the derived temperatures were close to or exceeded 100°C, the carbonates would have been in equilibrium with CO_2 (Ohmoto, 1972). Therefore, for calcite and siderite (Bottinga, 1969):

$$1000 \text{ Ln } \alpha_{calcite-CO_2/siderite-CO_2} = -8.914/T^3 x10^8 + 8.557/T^2 x10^6 - 18.11/T^3 + 8.27$$

For dolomite (Sheppard and Schwarcz, 1970):

$$1000 \text{ Ln } \alpha_{dolomite-CO_2} = -8.914/T^3 x10^8 + 8.737/T^2 x10^6 - 18.11/T^3 + 8.44$$

For temperatures calculated assuming a fluid $\delta^{18}O$ value of -1‰, a fluid $\delta^{13}C_{VPDB}$ value of -9.5 ± 1.5‰ is derived. This value is similar to the $\delta^{13}C_{VPDB}$ for the DIC of modern groundwaters in the BMC (Table 11.5). If a fluid with a seawater $\delta^{13}C_{VPDB}$ value is assumed, unrealistically high $\delta^{18}O$ values for the fluid are derived at unrealistically high temperatures.

11.8 Boron Isotopes

A small subset of samples from the Halfmile Lake and Restigouche deposits and the Heath Steele and Brunswick #12 mines were selected for boron isotope determination (see Chapter Three for analytical details). Boron isotopes have been used in a limited but increasing number of studies in recent years in order to aid interpretations of the source(s) of groundwater salinity (Bottomley et al., 1994; Moldovanyi et al., 1993; Palmer and Sturichio, 1990; Spivack et al., 1987; Vengosh et al., 1991; Vengosh et al., 1995; Vengosh et al., 1994). There are two stable isotopes of boron, ^{10}B (18.98% of total abundance) and ^{11}B (81.02%). The utility of boron in isotopic work is its high degree of mobility in the secondary environment which, combined with the large mass difference between the two isotopes, result in significant variations in isotopic compositions. Large kinetic isotopic effects exist for ^{10}B and are related to adsorption onto clays, the magnitude being a function of the clay type, solution temperature, and B

concentration.

The boron isotopes and boron abundances determined in this study are presented in Table 11.7. Most samples in this study have B contents below the detection limit of the ICP-ES (16 ppb) technique. However, 61 samples have detectable B and of these, 14 were analyzed for B isotopes (Table 11.7). Boron isotopes for all samples range from -2.5 to 11.1‰ $\delta^{11}B$ with one sample from the Heath Steele deposit at 41.1‰. For comparison, seawater has a $\delta^{11}B$ value of 39‰ (Vengosh et al., 1991; Vengosh et al., 1992). Sample MLW95-492 from the Brunswick #12 deposit has higher salinity than seawater but has a low $\delta^{11}B$ value of 5.9‰. Saline waters from borehole MM-88-02 at the Restigouche deposit have similar salinities (13090 - 13340 mg/L) but range in $\delta^{11}B$ from 5.9 to 11.1‰. The range in $\delta^{11}B$ for these waters is within the analytical error of ± 3‰ (Chapter Three). Boron concentrations for all waters range from 10 to 280 µg/L, much lower than modern seawater (4,600 mg/L). Groundwaters from borehole MM-88-02 at the Restigouche deposit are variable and range from 20 - 280 µg/L for all the waters and from 42 - 260 µg/L for packer samples. Shallow groundwaters and surface waters typically have B contents below detection. In general, boron increases with increasing salinity (Cl concentration; Fig. 11.17). For the 61 samples in Table 11.7, the correlation between Log(Cl) and Log(B) is r = 0.674, which is statistically significant at the 99% confidence level. There is a much better negative correlation between Log(Cl) and Log(B/Cl) of r = -0.915.

The majority of the shallow groundwaters and surface waters have B/Cl and Na/Cl molar ratios greater than seawater (Figs. 11.17). In contrast, the saline waters from Restigouche boreholes MM-88-02 and MM-89-106 and the most saline waters from Heath Steele and Brunswick #12 have lower molar B/Cl and lower or equal molar Na/Cl compared to seawater.

11.9 Discussion

11.9.1 $\delta^{18}O$ and δD relationships between precipitation, surface and ground waters

The stable isotope data allows some constraints to be placed on the timing of infiltration at

the Halfmile Lake and Restigouche deposits. In a study of $\delta^{18}O_{VSMOW}$ and δD_{VSMOW} in precipitation and modern groundwaters across Canada, Fritz et al. (1987) found that although the meteoric water line for Canada as a whole is similar to the global meteoric water line, more localized meteoric water lines are dependent upon temperature, pathway of rain-producing air masses and upon season. For eastern Canada, deuterium excess is typically < 10 in the summer, but > 12 in the winter (12.76 for the Truro station and 15.85 for St. Agatha) (Fritz et al., 1987). The excess deuterium for Halfmile Lake deposits waters varies from 14.38 to 22.78, suggesting that recharge is dominated by winter precipitation. This is supported by the $\delta^{18}O_{VSMOW}$ and δD_{VSMOW} values which are more negative than suggested by regional patterns; the source of winter precipitation is from higher latitudes and air temperatures are colder, resulting in isotopically lighter precipitation compared to summer precipitation (e.g. Rozanski et al., 1993). Regional patterns, such as those given in Fritz et al. (1987; updated in Clark and Fritz 1997), suggest that groundwaters should have $\delta^{18}O_{VSMOW}$ values of around -12‰, whereas, shallow ground waters from the Restigouche deposit and all groundwaters from the Halfmile Lake deposit, in addition to local surface waters are between -13 and -14‰ (Figs. 11.4, 11.5).

It has previously been noted that groundwaters close to the east and west coasts of Canada typically have stable isotopic compositions close to the annual weighted average of precipitation (Clark and Fritz, 1997; Fritz et al., 1987). The annual weighted averages for Truro and St. Agathe for the years 1975 to 1983 is $\delta^{18}O_{VSMOW}$ = -9.34‰ and δD_{VSMOW} = -63.67‰ for Truro and $\delta^{18}O_{VSMOW}$ = -12.92‰ and δD_{VSMOW} = -89.97‰ for St. Agathe (Fig. 11.3). If the shallow groundwaters and surface waters from the Halfmile Lake and Restigouche deposits reflected the weighted average of precipitation, they should have values somewhere between that for Truro and St. Agathe, assuming minimal influence from the Appalachian mountains. The average stable isotopic composition of the Halfmile Lake and Restigouche ground and surface waters (excluding brackish and saline waters from the Restigouche deposit) are lighter than the weighted annual average of precipitation for both the Truro, Nova Scotia and St.

Agathe, Quebec monitoring stations (Fig. 11.3A). In fact, only the monthly weighted averages from the St. Agathe station for December, January, February, and March are significantly lighter than the Halfmile Lake and Restigouche deposit average (Fig. 11.3A). This combined with the generally high excess deuterium values for Halfmile Lake and Restigouche deposit waters, indicates that recharge for these areas is dominated by winter precipitation, recharged during spring runoff.

At both the Halfmile Lake and Restigouche deposits, there is almost no evidence of any of the seasonal variations preserved in the ground or surface waters. The Halfmile Lake deposit surface waters do show a very slight trend to increasing $\delta^{18}O_{VSMOW}$ values suggesting that the slightly heavier stable isotopes are due to greater influence of summer precipitation (Fig. 11.6). The surface waters were sampled during base-flow conditions and largely reflect the stable isotopic composition of the shallow groundwaters. Deeper brackish to saline waters from the Restigouche, Heath Steele and Brunswick #12 deposits, with heavier isotopic values, are interpreted to represent groundwaters recharged under different climates rather than seasonal variations under the present climate (see below).

Seeps at both the Halfmile Lake and Restigouche deposits typically have higher Cl contents than local stream waters but essentially identical $\delta^{18}O_{VSMOW}$ values (Figs. 11.6, 11.9). This suggests that the seeps have longer flow-paths and have undergone greater water-rock interaction compared to the stream waters, but were recharged under the present climatic regime.

11.9.2 Flow path of groundwaters and age constraints

There are three possibilities to account for the spread of stable isotope data for the Restigouche groundwaters. The saline waters in borehole MM-88-02 may be the result of mixing between local meteoric waters and waters with a composition similar to Shield-type brines. There may also be mixing between the different sample groups; the waters from MM-89-106 may represent a mixture of MM-88-02 waters and shallow groundwaters. The third

possibility is that the deeper groundwaters were recharged under a different climatic regime. This is almost certainly true but very difficult to constrain.

From the St. Agathe and Truro precipitation data (see section 11.2) it can be assumed that for the study area the relationship between temperature and $\delta^{18}O_{VSMOW}$ through time would be approximately $T = \Delta\delta^{18}O/0.3$. The saline groundwaters from borehole MM-88-02 at the Restigouche deposit have a $\Delta\delta^{18}O$ of approximately 2.5 to 3‰. This would imply that the MM-88-02 waters were recharged during a time in which the climate was 8 - 10°C warmer than for present day recharge. This temperature change assumes that borehole MM-88-02 groundwaters were recharged under the same conditions as present today (i.e. with recharge dominated by winter precipitation). If recharge were similar to the annually weighted mean at that time, the temperature change would be less extreme. The heavier oxygen isotopes of borehole MM-88-02 waters indicate that they were recharged under warmer climatic conditions. This is in contrast to moderately brackish to saline waters from the Stripa mine (Moser et al., 1989) and other parts of Europe where the saline waters have more depleted stable isotopic compositions, consistent with recharge following the last glaciation. The stable isotopic composition of borehole MM-88-02 waters indicate that they are much older than the last glaciation.

Alternatively, the deeper groundwaters at the Restigouche deposit may be the result of mixing between shallow groundwaters with a more saline end-member groundwater. The mixing hypothesis is somewhat consistent with the $\delta^{18}O$ vs Cl relationships for all Restigouche groundwaters (Fig. 11.9A). The groundwaters all plot on or near a simple binary mixing line between two end-members with compositions of $\delta^{18}O$ = -13.5 ‰, Cl = 0.35 mg/L and $\delta^{18}O$ = -10 ‰, Cl = 14,000 mg/L respectively. Other components of the geochemistry of brackish and saline waters from the Restigouche show that such simple binary mixing cannot account for the range in compositions observed.

Shallow groundwaters from the Heath Steele, Willett, Wedge, and Stratmat Main Zone deposits are isotopically distinct from modern meteoric waters as represented by the shallow

groundwaters and surface waters at the Halfmile Lake and Restigouche deposits. There are two possible explanations. 1) These waters are modern recharge waters but are closer to the annual weighted average of precipitation for northern New Brunswick. 2) These waters may represent older groundwaters that were recharged under a different (warmer) climatic regime. The fact that sample MLW95-490 from 183 m depth in the Heath Steele deposit is isotopically identical to modern recharge waters at the Halfmile Lake and Restigouche deposit would support the second scenario. However, these waters from the Heath Steele, Willett, Wedge, and Stratmat Main Zone deposits all have low Cl contents (Fig. 11.10B; these waters are dominantly Ca-SO_4 and Ca-Fe-SO_4-type waters) suggesting that if they are older waters, they are still much younger than the saline waters from the Brunswick #12 and Restigouche deposits. Supporting the first scenario is the fact that the Wedge and Willett samples are seeps through massive sulphide deposits. In both cases, the likely flow paths are short, consistent with a young age for these waters. Additionally, sample MLW95-490 from the Heath Steele deposit may not be inconsistent with the heavier waters at shallower depth in the deposit. Previous studies have shown that where mines have been opened, the original hydrological environment is commonly perturbed such that more variable stable isotopic compositions are observed. For example, shallow groundwaters at the Stripa mine, Sweden, range from <-14 to >-10‰ in $\delta^{18}O_{VSMOW}$, although deeper groundwaters exhibit much less variability (Moser et al., 1989). Therefore, in mine settings, groundwaters with quite different stable isotopic compositions can occur in close proximity.

Groundwaters of slightly different age are indicated for the groundwaters recovered from borehole S61-19 at the Stratmat Main Zone deposit. As discussed previously (Chapter Eight), groundwaters at the bottom of the ore zone have heavier $\delta^{18}O_{VSMOW}$ and δD_{VSMOW} values coupled with heavier $\delta^{13}C_{VPDB\text{-}DIC}$ values.

11.9.3 Spatial distribution of stable isotopes

Although the study area is only approximately 2° latitude north of the Truro station and

approximately 1° latitude north of the St. Agathe station, it is unlikely that the more negative isotopic values for the Halfmile Lake and Restigouche deposit surface and groundwaters are due to the latitude effect. For continental North America, the latitude effect is approximately equivalent to -0.6‰ per degree change in latitude (Clark and Fritz, 1997). However, compilations of stable isotopic compositions of precipitation and shallow groundwaters across Canada indicate that lines of equal $\delta^{18}O_{VSMOW}$ are essentially north-south for eastern Canada, indicating that shallow groundwaters in the study area should be between the annual weighted average for the Truro and St. Agathe stations (i.e. approximately -12‰). A complicating factor is the Appalachians which cause more negative values due to the altitude effect (see Fig. 4-5 in Clark and Fritz, 1997).

Groundwaters at the Halfmile Lake show very subtle elevation effects. The most depleted groundwaters are from a short borehole (HT55-43) at the top of the Upper AB zone, where the ore deposit crops out.

For surface waters at the Halfmile Lake deposit, samples from the Upper/Lower AB and Halfmile North streams have lighter O and D isotopic values than the northeast and north tributaries to the NW Miramichi River (Fig. 11.6B). This is interpreted to reflect the generally lower elevation of these latter two streams although small amounts of evaporation in beaver dam ponds that occur along both streams cannot be ruled out. If evaporation is occurring, it is not sufficient to be resolved by the combined oxygen and deuterium data.

11.9.4 Origin of antithetical patterns in borehole HN87-08

The downhole variation in stable isotopes for borehole HN87-8 from the Halfmile Lake deposit shows a pattern inconsistent with typical behaviour of stable isotopes. To a depth of around 300 m, changes in the $\delta^{18}O_{VSMOW}$ and δD_{VSMOW} values covary with depth (Fig. 11.7). Below 300 m, changes in the stable isotopes are antithetical (i.e. as the $\delta^{18}O_{VSMOW}$ value increases, the δD_{VSMOW} value decreases and vice versa; Fig. 11.7). The pattern of shifting $\delta^{18}O_{VSMOW}$ and δD_{VSMOW} values downhole is also shown by other geochemical

parameters (see Chapter Seven). In addition, there is a change in the response of the REE below 450 m (Fig. 10.10; Chapter Ten). There are several possible explanations for the antithetical behaviour of the stable isotopes, although none are especially satisfying. Firstly, these groundwaters are low TDS waters, only slightly modified from present recharge waters (e.g. increasing TDS and Cl contents with depth is consistent with increasing water-rock reaction rates with depth; Fig. 11.6). The variations in isotopes and composition could be controlled by adsorption-desorption exchange reactions with clay minerals in the fracture system. This would imply that the waters are out of equilibrium with respect to adsorption reactions, indicating fairly rapid movement and variable input chemistries. The alternative is that the fracture geometry is such that different waters are being sampled at different depths which have all had a different flow path and water-rock reaction history, particularly in terms of stable isotope input. Neither hypothesis is especially appealing. However, the pattern in stable isotopes is very regular which suggests that it is not an artifact of sample handling or analytical error. A third possibility is that there is variable hydration of silicates with depth. Fritz and Frape (1982) showed that hydration of silicates results in heavier deuterium and lighter oxygen isotopes in the residual water for a closed system. For a closed system the isotopic shifts are significant, but for an open system, such as Halfmile Lake, the isotopic effects are likely to be more subtle, if at all observable.

Graham and Johnson (1991) observed similar behaviour in borehole fluids after removal of approximately a million litres from the borehole. They were unable to explain the antithetical behaviour of $\delta^{18}O_{VSMOW}$ and δD_{VSMOW} but noted that the observed response may have been a function of water-rock reactions between drilling fluid clays or secondary minerals within the rock formation (Graham and Johnson, 1991).

11.9.5 Carbon isotopes of DIC

Excluding the isotopically anomalous saline groundwaters from borehole MM-88-02 intersecting the Restigouche deposit, ground and surface waters analyzed in this study have

DIC $\delta^{13}C_{VPDB}$ values that range from -17.89 to -5.01‰ (Table 11.5).

According to Clark and Fritz (1997), the $\delta^{13}C_{VPDB}$ of dissolved inorganic carbon evolves in the following manner. Recharging groundwaters, initially charged with atmospheric CO_2, incorporate carbon from soil zone $CO_{2(g)}$. The $\delta^{13}C$ value of carbon dioxide in the soil zone is controlled to a large extent by the degree of fractionation imparted to atmospheric CO_2 as a result of photosynthetic uptake. For temperate climate forest ecosystems, vegetation which follows the C_3 photosynthetic cycle predominate. The result is that C_3 plants have an average $\delta^{13}C_{VPDB}$ values of around -27‰. Soil zone CO_2 associated with C_3 vegetation is typically around -23‰ $\delta^{13}C$ as a result of CO_2 outgassing following decay of C_3 organic matter (Clark and Fritz, 1997). As recharge waters infiltrate through the soil zone, they dissolve the soil zone CO_2. There is a small isotopic fractionation imparted by this reaction such that $CO_{2(aq)}$ has a $\delta^{13}C$ value of around -24‰. There is a large fractionation associated with the hydration of $CO_{2(aq)}$ to HCO_3^-. As the groundwater evolves to higher pH through weathering processes, the $\delta^{13}C$ of the DIC becomes progressively heavier. Therefore, groundwater with a pH of between 7 and 8 will have a $\delta^{13}C$ value of around -16 to -14‰. Subsequent reactions below the water table modify the carbon isotopic composition of the DIC due to weathering and biochemical reactions that are controlled by temperature, pH, dissolution/precipitation reactions and whether the system is open or closed to atmospheric and soil-zone CO_2 (Clark and Fritz, 1997). For example, subsequent silicate weathering will have little impact on the carbon isotopic composition of the groundwater. However, dissolution of carbonate minerals in the subsurface will alter the isotopic composition of the DIC, the extent of the isotopic shift will depend on the carbon isotopic composition of the carbonate and the extent of the reaction.

As a first approximation, most of the groundwaters and surface waters have $\delta^{13}C_{VPDB}$ values which are between values for soil zone CO_2 and the carbonate minerals that were measured from the Restigouche deposit. For example, calcite, dolomite and siderite from the Restigouche deposit have an average $\delta^{13}C_{VPDB}$ value of around -6.5‰. As was shown in previous chapters (Five and Seven), the dissolved Ca (and Mg to a lesser extent) contents of

shallow groundwaters and surface waters is mainly controlled by carbonate dissolution. Simple mass balance calculations were made (Table 11.8), assuming that all the Ca and Mg in the waters was derived from carbonate dissolution. The $\delta^{13}C$ of the initial fluid was set to -18 and -20‰. These calculations generally produced final $\delta^{13}C$ values which were close (typically to within 0.5‰ or less) to the measured values. Thus, for the shallow groundwaters and surface waters, carbonate dissolution (calcite and dolomite) is interpreted to produce the range of $\delta^{13}C$ values observed. Higher TDS groundwaters commonly have Ca+Mg values which are too low to yield good fits between calculated and observed $\delta^{13}C$ values. The most likely explanation is that Ca and Mg have been removed by cation exchange reactions, producing the downward trend in Ca+Mg with increasing $\delta^{13}C$ (Fig. 11.13C). Much better mass balance results were achieved for these waters by assuming lower initial values of the DIC of recharge waters than was calculated based on the Ca+Mg values. For groundwaters from the Stratmat Main Zone the increase in $\delta^{13}C$ values through the ore zone is consistent with increased carbonate dissolution (increasing Ca+Mg; Fig. 11.13C) and the strong covariation between $\delta^{13}C$ and dissolved sulphate suggests that sulphide oxidation provides additional acidity to enhance carbonate dissolution (Fig. 11.13D).

However, if the only process controlling the variation in $\delta^{13}C_{VPDB}$ for these waters was the relative contributions of soil zone and carbonate carbon, there should be a good correlation between the $\delta^{13}C_{VPDB}$ and HCO_3^- content. In fact, for the data as a whole, there is a poor correlation (Fig. 11.12A). For the Stratmat Main Zone deposit groundwaters $\delta^{13}C_{VPDB}$ increases with increasing HCO_3^- concentrations (Figs. 11.12, 8.8). Similarly, all but one of the Halfmile Lake deposit groundwaters show a similar relationship. Therefore, for these waters, the carbon isotopic composition does appear to be controlled by the two main carbon sources (soil zone CO_2 and carbonate dissolution).

In contrast, the shallow groundwaters from the Restigouche deposit appear to show a trend of increasing HCO_3^- with decreasing $\delta^{13}C_{VPDB}$ values (Fig. 11.12). There are several possible explanations for this. 1) There is no relationship in terms of geochemical evolution for these

waters such that the trend shown in figure 11.12 is fortuitous. 2) There is an additional ^{13}C-depleted source of C for these waters. Taylor and Fox (1996) showed that the addition of biogenic CO_2 within an aquifer explained the $\delta^{13}C_{VPDB}$ systematics of groundwaters from New Zealand. 3) Finally, the trend may represent a mixing line between waters which have been involved in extensive silicate hydrolysis, producing high HCO_3^- but with little perturbation of the $\delta^{13}C_{VPDB}$ and waters which have equilibrated more with carbonate. It is difficult to assess which process is most likely with the available data.

Two surface water samples from the Halfmile Lake deposit are from the same stream, but have very different $\delta^{13}C_{VPDB}$ values. Sample MLW96-678 is from a seep at the headwaters to the Upper/Lower AB stream and has a $\delta^{13}C_{VPDB}$ value of -17.89‰ and a P_{CO_2} of -2.9 whereas, sample MLW96-681 is from the lower end of the stream and has much higher $\delta^{13}C_{VPDB}$ (-6.03‰) and lower P_{CO_2} (-3.5). The P_{CO_2} is essentially identical to that of the atmosphere. The low CO_2 content and relatively heavy carbon isotope value suggest that the Upper/Lower AB stream has undergone CO_2 degassing and equilibration with the atmosphere.

11.9.6 Carbon isotopes of DIC in saline groundwaters

The saline groundwaters from borehole MM-88-02 at the Restigouche deposit are characterized by very heavy $\delta^{13}C_{VPDB}$ values of +11.98 to +12.48‰ (Table 11.5). There are three possible explanations for these very elevated $\delta^{13}C$ values; 1) production of CH_4 through methanogenesis with ^{13}C-enrichment of residual HCO_3, 2) dissolution of ^{13}C-enriched carbonate, and 3) dissolution and precipitation of carbonate with extensive CO_2 degassing (Carothers and Kharaka, 1980).

Carbon dioxide degassing is not considered a viable mechanism to explain the heavy isotopic compositions of the MM-88-02 waters. These waters effervesced vigorously when brought to surface indicating extensive degassing. However, sample MLW95-597/8 was analyzed twice for the same sample bottle. The second analysis followed shaking of the sample and exposure to the atmosphere to allow degassing of any CO_2. There was no significant

difference in gas yields during analysis and the $\delta^{13}C$ values for the two analyses are essentially the same (Table 11.5). This indicates that some other phase degassed during sampling, most likely CH_4.

There is little fractionation imparted to the $\delta^{13}C_{VPDB}$ value of DIC during carbonate dissolution or precipitation. Heavy $\delta^{13}C_{VPDB}$ DIC values can, however, be produced by dissolution of isotopically heavy carbonate. Isotopically heavy carbonate can be produced by contact metamorphism of limestones, methanogenesis during burial producing enriched diagenetic carbonate (Dix et al., 1995), and during ocean anoxia (Baker and Fallick, 1989). However, none of the carbonate analyzed to date in the BMC has $\delta^{13}C_{VPDB}$ values above 0‰ (Peter and Goodfellow, 1993), suggesting that dissolution of isotopically heavy carbonate has not produced the heavy MM-88-02 waters. In fact, the carbonate in the core from borehole MM-88-02 have $\delta^{13}C_{VPDB}$ values between -1.3 and -11.64‰ (average of -6.5‰), indicating that the MM-88-02 waters are most likely allochthonous with respect to the immediate area of the Restigouche deposit. The saline waters may have migrated to their present location recently, perhaps as a result of uplift following deglaciation.

The first hypothesis, that the heavy isotopic composition of the MM-88-02 waters is produced by methanogenesis, is the most likely process. The production of methane through methanogenic reactions can occur by one of three mechanisms: biogenic, abiogenic, and thermogenic. Only biogenic methanogenesis is applicable to the MM-88-02 waters. Both abiogenic (Sherwood Lollar et al., 1993) and thermocatalytic methanogenesis (Dix et al., 1995) operate at relatively high temperatures (not observed for the MM-88-02 waters) and produce increasingly negative $\delta^{13}C_{VPDB}$ values.

There are two principle biologically mediated methanogenic reactions; acetate fermentation (Carothers and Kharaka, 1980),

$$CH_3COO^- + H_2O \rightarrow HCO_3^- + CH_4 \quad (11.1)$$

and CO_2 reduction (Clark and Fritz, 1997),

$$CO_2 + 4H^+ \rightarrow CH_4 + 2H_2O \quad (11.2)$$

In both reactions, light carbon is preferentially metabolized by methanogenic bacteria. The fractionation factor imparted is large and varies as a function of temperature and is approximately 70‰ at 25°C (Bottinga, 1969). During CO_2 reduction, the isotopically lightest C is preferentially converted to methane, enriching the residual DIC pool, which becomes progressively heavier. An important consideration is the sulphate content of the system. During diagenesis, methanogenic bacteria typically become important below the zone of sulphate reduction (Morad et al., 1994). There are four main diagenetic zones, the suboxic, sulphate-reduction, methanogenic, and thermal carboxylic zones (Dix et al., 1995; Morad et al., 1994). Carbon is produced primarily by the oxidation of organic matter in the sulphate-reduction zone by the following reaction (Carothers and Kharaka, 1980):

$$SO_4^{2-} + CH_3COO^- \rightarrow 2HCO_3^- + HS^-$$

This reaction produces light $\delta^{13}C_{DIC}$ values. In Chapter Seven it was shown that the saline MM-88-02 waters had sulphate contents below detection. Therefore, the saline MM-88-02 waters have the following pertinent characteristics: 1) heavy $\delta^{13}C_{DIC}$ values (+12‰), 2) effervescence during recovery from depth, indicating degassing, 3) analytical results suggesting that gas generation was not CO_2, and is interpreted to have been CH_4, 4) SO_4 below detection, and 5) saline compositions suggesting old waters. Taken together, these parameters indicate that the most probable cause for the elevated $\delta^{13}C_{DIC}$ values is methanogenesis.

The $\delta^{13}C_{DIC}$ values for borehole MM-88-02 waters are unusual for groundwaters but certainly not unique. For example, Carothers and Kharaka (1980) presented data for California and Texas oil field brines with $\delta^{13}C_{DIC}$ values as high as +27.8‰. They concluded that these elevated values were produced by methanogenic degradation of acetate (reaction 1) rather than

CO_2 reduction based on increasing HCO_3^- contents with increasing $\delta^{13}C_{DIC}$ values (Carothers and Kharaka, 1980). In contrast, Clark and Fritz (1997) suggested that $\delta^{13}C_{DIC}$ values as high as +31.6‰ in brackish groundwaters from the St. Lawrence Lowlands were produced by CO_2 reduction (reaction 2).

The limited number of samples in this study with heavy carbon isotopes does not allow a determination as to which methanogenic reaction dominates. However, the HCO_3^- contents of the saline MM-88-02 waters are lower than those of brackish waters from the bottom of borehole MM-89-106 at the Restigouche deposit. Sample MLW95-508 from this latter borehole has a moderately heavy $\delta^{13}C_{DIC}$ value of -6.34‰ (Table 11.5). Significantly, the sulphate contents of brackish borehole MM-89-106 waters decrease downhole to values below detection. It is possible, therefore that the low sulphate and relatively heavy carbon indicate the initiation of methanogenic reactions. Indeed, these waters effervesced slightly during recovery from depth. Although these waters have been shown to be unrelated to the MM-88-02 waters in any simple way (Chapters Seven, Twelve), it is tempting to conclude that the higher DIC contents of the brackish waters combined with heavier carbon isotopes in the saline waters indicates that reaction 2 (CO_2 reduction) was the main methanogenic process for the MM-88-02 waters.

It was concluded on the basis of chemical composition and oxygen and hydrogen isotopes that the MM-88-02 waters are old (section 11.9.2). The $\delta^{13}C_{DIC}$ values require that the waters have been isolated from the shallower groundwater system because the DIC contents are sufficiently low and any mixing with modern groundwaters would perturb the carbon isotopic system. Although tritium analyses are required to confirm this, the fact that the shallow groundwaters in the vicinity of MM-88-02 are enriched in SO_4^{2-} and yet the MM-88-02 waters have non-detectable SO_4^{2-} is consistent with minimal mixing with the shallow groundwater system. The apparent upward gradients in MM-88-02 are consistent with this interpretation.

11.9.6 Carbon isotopes of vein and fracture carbonate and graphite

Carbonate (calcite, ferroan dolomite, and siderite) from the Restigouche deposit have $\delta^{13}C_{VPDB}$ values between -1.33 and -11.64‰, although most values are between -4 and -8‰ (the average for all the data is -6.5‰). The $\delta^{18}O_{VSMOW}$ values range from 6.66 to 20.61‰ (Table 11.6). The analyzed carbonates represent massive vein carbonate (the dominant form), acicular carbonate in vugs and on fracture surfaces, and platy carbonate on fracture surfaces (Table 11.6; Fig. 14). There are no obvious differences in the isotopic compositions of the different carbonate types.

The carbon and oxygen isotopic compositions of the Restigouche deposit carbonates fall within the range of values of hydrothermal carbonate from mines in the Canadian and Fennoscandian Shields (Fig. 11.15B) (Frape et al., 1992). In addition, the Restigouche deposit carbonates form a linear array close to that observed for calcite from hydrothermally altered mid-ocean ridge basalt, but have lighter isotopic compositions than diagenetic carbonate and limestone (seawater carbonate)(Fig. 11.15B).

Peter and Goodfellow (1993) reported calcite and siderite isotopic compositions of carbonate from the Brunswick #12 deposit and associated iron formation. They found that $\delta^{13}C_{VPDB}$ values of calcite associated with ore (massive and laminated) ranged from -1 to-6.65‰. These values are similar to the Restigouche deposits carbonates. In contrast, calcite and siderite associated with iron formation (i.e. more distal from the Brunswick #12 deposit) has lighter $\delta^{13}C_{VPDB}$ values, ranging from -8.74 to -16.17‰ (Peter and Goodfellow, 1993).

The $\delta^{13}C_{VPDB}$ values of the Restigouche deposit carbonate are too heavy to have formed from most of the present groundwaters at the Restigouche deposit at their present temperatures. The association of the massive carbonate with late stage hydrothermal quartz veins in the stockwork zone to the deposit suggests that these carbonates formed soon after the main ore forming event. However, the similarity of the isotopic compositions of the acicular and platy carbonate with the massive carbonate suggests either that the acicular/platy carbonate formed from similar fluids as the massive carbonate during the Ordovician or that the massive carbonate has been recrystallized by later fluids which formed the fracture carbonate.

Some inferences as to the nature of the carbonate-forming fluid can be made. It was shown in section 11.7.4 that, assuming a fluid composition close to seawater (i.e., $\delta^{18}O_{VSMOW}$ ~ 0‰), the carbonates formed at temperatures ranging from around 60 to 250 °C. These temperatures are reasonable for hydrothermal carbonate and are similar to fluid inclusion temperatures of carbonate from modern sea-floor hydrothermal systems (Peter et al., 1994; Peter and Shanks, 1992) and from Canadian and Fennoscandian Shield areas (Frape et al., 1992). Assuming that the derived temperatures are correct, the Restigouche deposit carbonates formed from a fluid with a $\delta^{13}C_{VPDB}$ value of -9.5 ± 1.5‰. Such a fluid $\delta^{13}C_{VPDB}$ value would indicate a significant contribution of biogenic CO_2 to the hydrothermal fluid, assuming that the carbonates formed in a hydrothermal system similar to modern sea-floor systems (see Chapter Two). Alternatively, the carbonates may have formed from later meteoric fluids, which typically have $\delta^{13}C_{VPDB}$ values less than seawater.

Whatever the origin of the Restigouche deposit carbonate, there is no evidence from the analyses of the fracture and vein carbonate of any precipitation or replacement of carbonates from isotopically heavy fluids such as those recovered from borehole MM-88-02.

Graphite crystals in massive carbonate veins at the Restigouche deposit are very light isotopically ($\delta^{13}C_{VPDB}$ = -25.6 - 27.8‰), indicative of an organic matter source. These low values further suggest relatively low temperatures of formation of the graphite, consistent with the temperature estimates based on carbonate carbon isotope values.

11.9.7 Constraints on groundwater origin based on $\delta^{11}B$

The boron geochemistry and isotope systematics allows some additional constraints to be placed on the origin of the BMC groundwaters, in particular the more saline waters from the bottom of boreholes MM-89-106 and MM-88-02 at the Restigouche deposit and from the Brunswick #12 deposit. A brief mention needs to be made as to the analytical method used. There are essentially three main methods presently used to measure the isotopes of B; ICP-MS, thermal ionization mass spectrometry (TIMS), and secondary ion mass spectrometry (SIMS).

The advantages and disadvantages of these techniques have recently been reviewed by Aggarwal and Palmer (1995). These authors concluded that the precision obtained by ICP-MS was too poor for this to be a reliable technique for routine B isotope analyses and quoted the precision of ICP-MS as 14‰ (Aggarwal and Palmer, 1995). Others have found that ICP-MS is capable of much more precise analyses. For example, Bottomley et al. (1994) reported a precision of ± 4‰ for Canadian Shield brines and Porteous et al. (1995a; 1995b) reported precision of less than 2‰ for groundwaters from southwest England. In this study, precision during the analytical run was around 3‰, more than sufficient to address differences in the origin of groundwater salinity.

The range in B/Cl suggests that there are at least two end-member type groundwaters in the BMC. One end-member, represented by the saline waters has low B/Cl and Na/Cl, less than seawater for both (Figs. 11.17). The other end-member is represented by the shallow groundwaters at the Restigouche and Halfmile Lake deposits. These waters have high molar Na/Cl and B/Cl suggesting a dominantly terrestrial origin for the B, major cations, and Cl, consistent with the B isotopes. Thus, the B, Na, and Cl chemistry of the BMC groundwaters could be accounted for by mixing between dilute meteoric waters and deeper, older saline groundwaters, at least with respect to Cl, Br and B contents.

For example, Bottomley et al. (1994) looked at the boron isotope composition of saline waters from the Canadian Shield and concluded that the data were consistent with a marine origin for these waters, an interpretation contrary to previous studies (e.g. Frape et al., 1984; Fritz and Frape, 1982; McNutt et al., 1987). The discrimination between marine and non-marine origin is based on the large isotopic fractionation that occurs during adsorption of B onto clays and during the alteration of sea-floor basalts. This fractionation results in seawater being enriched in $\delta^{11}B$ by 40‰ over waters in equilibrium with terrestrial rocks (Spivack et al., 1987).

The MM-88-02 waters have molar Na/Cl and B/Cl that are less than seawater (0.70 - 0.78 vs 0.86). If these waters are modified seawater, it implies both a loss of boron through clay

adsorption and a loss of Na relative to Cl. If the loss of Na is assumed to be due to albitization of Ca-rich feldspar or cation exchange reactions with clay minerals, a 2:1 substitution can be assumed. Thus, the (Na+2Ca)/Cl molar ratio should approximate seawater. This ratio for the MM-88-02 waters varies from 0.80 to 0.90, compared to a seawater value of 0.90. However, the Na/Cl ratio of the Brunswick #12 saline fluid is too low regardless of the addition of the Ca content of the fluid.

Elevated $\delta^{11}B$ is produced by mixing with or derivation from seawater or marine aerosols. In addition, terrestrially derived boron with low isotopic ratios can become increasingly isotopically heavy through low water-rock reactions with adsorption of B onto clays (Vengosh et al., 1991). Vengosh et al. (1991) suggested that elevated $\delta^{11}B$ coupled with Na/Cl < seawater was inconsistent with boron isotopic enrichment due to adsorption processes from a terrestrial source.

Bottomley et al. (1994) showed that for some Canadian Shield groundwaters (Cl ranging from 3.1 to 64,000 mg/L), there was a range in $\delta^{11}B$, B/Cl, and Br/Cl consistent with a marine source, at least for the B, Cl, and Br contents. They postulated that during the Paleozoic, marine incursions resulted in recharge by residual evaporitic brines which have subsequently migrated to their present location at the same time undergoing water-rock reactions to modify the cation contents and cation/Cl ratios. The spread in the $\delta^{11}B$ of the shield brines that they observed was attributed to mixing with less saline meteoric waters (Bottomley et al., 1994). A corollary of this interpretation is that Br and Cl in shield brines are of marine origin rather than due to long time periods of water-rock reaction.

Although the saline waters analyzed for $\delta^{11}B$ in this study span a similar compositional range for B (9 to 31000 mg/L; Table 11.6) as those analyzed by Bottomley et al. (1994) (using the same analytical technique and laboratory), the $\delta^{11}B$ systematics are very different. As discussed (section 11.8), the range in $\delta^{11}B$ for the BMC waters is restricted (-2.5 to 11.1‰, excluding one sample from the Heath Steele deposit) compared to those from the Canadian Shield (Bottomley et al., 1994). The most consistent explanation for the BMC groundwaters is

that the B (and by extension, the Cl and Br) represents a product of water-rock reactions with the host lithologies over long time periods, rather than marine waters. If the BMC waters originated as marine evaporitic waters, the $\delta^{11}B$ values would have to be drastically lowered either by desorption of B from the host rocks, or by dilution by shallow meteoric waters with crustal boron with $\delta^{11}B$ values close to or less than zero.

If the low $\delta^{11}B$ values of the BMC groundwaters were due to B desorption, the B contents of the waters would be expected to be greater than seawater. The B contents of the BMC waters are all considerably lower than seawater (Table 11.6) so that this scenario is unlikely. Most saline waters from the Canadian Shield also have B contents lower than seawater (Bottomley et al., 1994). Similarly, the low $\delta^{11}B$ values cannot realistically be attributed to mixing between an evaporated seawater endmember and shallow meteoric waters. The more saline BMC waters have Cl contents of the same order of magnitude as seawater yet have very low $\delta^{11}B$ values. Mixing by shallow meteoric waters to lower the $\delta^{11}B$ contents would also result in low Cl contents.

Bottomley et al. (1994) suggested that Br, Cl, and B in Canadian Shield brines and sedimentary basin formation waters shared a common origin because of similarities in Cl-Br relationships and because for most of these waters, Br/Cl ratios were greater than for seawater. These workers therefore concluded that the Br, Cl, and B in shield brines was largely allochthonous. However, for BMC waters, although most shallow groundwaters and surface waters have Br/Cl greater than seawater, most of the saline waters, with the exception of sample MLW95-492 from the Brunswick #12 deposit, have Br/Cl < seawater.

Bulk-rock B/Cl ratios are typically much greater than seawater. For example, seawater B/Cl is 0.00024 compared to 0.077 for continental crust, 0.024 for granite, 0.075 for basalt, and 0.56 for shale. With increasing water-rock reaction, increased Cl is leached with respect to B and therefore the B/Cl decreases, ultimately to less than seawater. With increasing water-rock reaction, the B/Cl may also decrease due to B adsorption on clays. The generally higher $\delta^{11}B$ values of the more saline waters may reflect adsorption of B onto aquifer minerals due to lower

water-rock ratios (Vengosh et al., 1994). Thus, shallow recharge groundwaters have low B and Cl due to low contributions from marine aerosols. These recharge waters rapidly acquire the B isotopic signature of the host lithologies. As the degree of water-rock reaction increases, B and Cl contents increase, B/Cl decreases and the $\delta^{11}B$ may increase due to adsorption processes. The shape of the $\delta^{11}B$ vs B and Cl plots could be explained in this way. The B contents and isotopic compositions reach a "steady state" more rapidly than Cl.

The only sample that does not readily fit the discussion so far is sample MLW95-486 from the Heath Steele deposit. This water has a $\delta^{11}B$ of 41‰, which is greater than seawater (Fig. 11.18). There is no obvious reason why this water should be so isotopically heavy compared to the rest of the BMC groundwaters. This water cannot be modified seawater given the very low Br/Cl (0.00032) compared to seawater (0.00158). A tentative explanation is that the elevated B isotopic composition is related to extensive fractionation of B by Fe-oxides. This water was rich in Fe-oxides and was associated with accumulation of Fe-precipitates in the Heath Steele mine, consistent with very high Fe content of the water (650 mg/L). However, the B/Cl of this sample is similar to samples of equivalent Cl (Fig. 11.17).

11.10 Summary

1) Oxygen and deuterium isotopes of surface and shallow groundwaters from both the Halfmile Lake and Restigouche deposits are very uniform (-13 to -14‰ and -85 to -95‰ for $\delta^{18}O_{VSMOW}$ and δD_{VSMOW}, respectively). These values are lighter than predicted for northern New Brunswick and, combined with high excess deuterium, suggest that recharge is dominated by winter precipitation, recharged during spring runoff. The close similarity in stable isotopic composition of surface waters and shallow groundwaters indicates that surface waters were sampled primarily during base flow conditions.

2) Deeper groundwaters from the Restigouche deposit and from the Heath Steele, Brunswick #12, Stratmat Main Zone, and Willett deposits have heavier oxygen and deuterium isotopic compositions than shallow groundwaters indicating recharge under warmer climates.

Restigouche deposit groundwaters can be modelled as mixtures between a saline end-member and shallow recharge waters in terms of Cl contents and stable isotope values. Other geochemical parameters (Chapter Seven) indicate that such simple two-component mixing does not explain the range in groundwater compositions.

3) Carbon isotopic compositions of dissolved inorganic carbon are generally heavy, ranging from -15 to -5‰ $\delta^{13}C_{DIC}$ for most groundwaters and surface waters. Much of the variation in the carbon isotopes is consistent with closed system groundwater evolution involving soil zone CO_2 and fracture zone carbonate minerals. Fracture and vein carbonate minerals at the Restigouche deposit have restricted carbon isotopic compositions of around -5 to -6‰.

4) The carbon isotopic compositions of the saline waters from borehole MM-88-02 at the Restigouche deposit are very heavy (+12‰ $\delta^{13}C_{DIC}$) and indicate fractionation of the DIC due to methanogenesis. This is consistent with the lack of dissolved sulphate in these waters and the observation of degassing during sampling, interpreted to be due to the release of methane.

5) Boron isotopes indicate that the salinity of BMC waters is controlled by variable degrees of water-rock reaction with the host lithologies. Dissolution of non-marine evaporites could also explain the B isotope systematics, but the lack of such deposits in the BMC argues against this source.

Table 11.2. Oxygen and hydrogen stable isotope data for Halfmile Lake deposit waters

Location	Sample #	$\delta^{18}O_{VSMOW}$ (‰)	δD_{VSMOW} (‰)	excess d	Depth (m)
Upper/Lower AB stream	MLW94-111	-13.44	-99.8	7.7	surface
Upper/Lower AB stream	MLW94-112	-13.41	-94.2	13.0	surface
Upper/Lower AB stream	MLW94-148	-13.39	-87.3	19.8	surface
Upper/Lower AB stream	MLW94-185	-13.61	-93.2	15.7	surface
Upper/Lower AB stream	MLW94-186	-13.62	-90.9	18.1	surface
Upper/Lower AB stream	MLW94-191	-13.48	-88.6	19.3	surface
Halfmile North stream	MLW94-122	-13.47	-92.4	15.3	surface
Halfmile North stream	MLW94-124	-13.37	-88.6	18.4	surface
Halfmile North stream	MLW94-127	-13.40	-90.5	16.7	surface
Halfmile North stream	MLW94-128	-13.46	-90.5	17.2	surface
Halfmile North stream	MLW94-142	-13.44	-90.9	16.6	surface
Halfmile North stream	MLW94-144	-13.37	-91.6	15.4	surface
Halfmile North stream	MLW94-194	-13.46	-90.3	17.4	surface
Confluence of 1&2	MLW94-151	-13.13	-89.0	16.0	surface
Confluence of 1&2	MLW94-152	-13.24	-87.4	18.5	surface
Northeast tributary	MLW94-153	-12.95	-86.1	17.5	surface
Northeast tributary	MLW94-214	-13.02	-89.4	14.7	surface
Northeast tributary	MLW94-225	-13.10	-88.3	16.5	surface
North tributary	MLW94-231	-13.12	-91.7	13.2	surface
West tributary	MLW94-113	-13.27	-97.6	8.6	surface
West tributary	MLW94-114	-13.34	-88.0	18.7	surface
Northwest Miramichi R	MLW94-149	-12.86	-87.2	15.7	surface
Artesian bore	MLW94-110	-13.32	-87.6	19.0	surface
HN87-8	MLW94-154	-13.54	-88.3	20.0	36
HN87-8	MLW94-155	-13.46	-88.1	19.6	61
HN87-8	MLW94-156	-13.42	-88.8	18.6	111
HN87-8	MLW94-157	-13.44	-86.9	20.6	160
HN87-8	MLW94-161	-13.47	-87.3	20.5	260
HN87-8	MLW94-162	-13.52	-90.3	17.9	310
HN87-8	MLW94-163	-13.40	-96.0	11.2	360
HN87-8	MLW94-164	-13.48	-92.8	15.0	410
HN87-8	MLW94-165	-13.40	-91.0	16.2	460
HN87-8	MLW94-166	-13.46	-88.7	19.0	510
HN87-8	MLW94-167	-13.47	-89.8	18.0	560
HN87-8	MLW94-168	-13.45	-88.7	18.9	610
HN87-8	MLW94-169	-13.49	-88.0	19.9	664
HN87-8	MLW94-170	-13.44	-89.5	18.0	710
HN87-8	MLW94-171	-13.43	-90.9	16.5	760
HN93-55	MLW94-172	-13.62	-94.0	15.0	50
HN93-55	MLW94-173	-13.58	-91.9	16.7	100
HN93-55	MLW94-174	-13.38	-94.8	12.2	150
HN93-55	MLW94-175	-13.35	-91.8	15.0	200
HN93-55	MLW94-176	-13.38	-88.7	18.3	250
HN93-55	MLW94-177	-13.42	-90.2	17.2	300
HN93-55	MLW94-178	-13.45	-92.0	15.6	350
HN93-55	MLW94-179	-13.41	-97.8	9.5	350
HN93-55	MLW94-184	-13.49	-93.4	14.5	540
HN92-33	MLW94-201	-13.13	-91.1	13.9	200
HN93-50	MLW94-202	-13.52	-88.9	19.2	50
HN93-50	MLW94-203	-13.54	-85.9	22.4	100
HN93-50	MLW94-211	-13.52	-89.7	18.5	425
HN93-50	MLW94-212	-13.50	-94.6	13.4	450
HN94-50	MLW95-615	-13.14	-87.4	17.7	145
HN94-51	MLW95-613	-13.35	-91.5	15.3	117
HN94-65	MLW94-236	-13.48	-92.0	15.9	50
HN94-65	MLW94-246	-13.43	-89.0	18.4	450
HN94-65	MLW94-248	-13.46	-93.3	14.4	500
HN94-65	MLW94-249	-13.09	-93.5	11.2	550
HN94-65	MLW94-252	-13.39	-90.4	16.7	650
HN94-65	MLW95-608	-13.15	-89.1	16.1	223
HN92-40	MLW96-674	-13.21	-91.1	14.6	46
HN94-82	MLW96-675	-13.09	-87.4	17.3	70
HN94-63	MLW96-708	-13.38	-81.5	25.5	450
HT55-43	MLW94-255	-13.70	-97.1	12.5	40
HT55-43	MLW94-259	-13.67	-96.4	13.0	80

Table 11.3. Oxygen and hydrogen stable isotope data for Restigouche deposit waters

Location	Sample #	$\delta^{18}O_{vsmow}$ (‰)	δD_{vsmow} (‰)	excess d	Depth
Charlotte Brook	MLW95-408	-13.49	-97.9	10.02	surface
Charlotte Brook	MLW95-421	-13.45	-93.5	14.10	surface
Charlotte Brook	MLW95-425	-13.48	-90.1	17.74	surface
Charlotte Brook	MLW95-426	-13.62	-89.4	19.56	surface
Charlotte Brook	MLW95-431	-13.64	-95.1	14.02	surface
Charlotte Brook	MLW95-432	-13.72	-96.8	12.96	surface
Charlotte Brook	MLW95-442	-13.48	-98.1	9.74	surface
Charlotte Brook	MLW95-445	-13.34	-84.6	22.12	surface
Charlotte Brook	MLW95-458	-13.49	-91.9	16.02	surface
North stream	MLW95-303	-13.51	-92.2	15.88	surface
North stream	MLW95-381	-13.47	-93.7	14.06	surface
North Stream	MLW95-390	-13.54	-93.9	14.42	surface
North stream	MLW95-549	-13.67	-93.5	15.86	surface
Mt Fowler SW	MLW95-446	-13.39	-92.6	14.52	surface
Mt Fowler NE	MLW95-438	-13.53	-95.3	12.94	surface
Mt Fowler NE	MLW96-684	-13.38	-99.9	7.14	surface
Mt Fowler NE	MLW96-688	-13.38	-94.4	12.64	surface
Mt Fowler E	MLW95-441	-13.68	-91.2	18.24	surface
Mt Fowler E	MLW96-664	-13.50	-91.9	16.10	surface
Mt Fowler E	MLW96-665	-13.47	-89.2	18.56	surface
Mt Fowler E	MLW96-668	-13.47	-96.6	11.16	surface
Mt Vroom NE	MLW95-457	-13.33	-92.9	13.74	surface
Mt Vroom NE	MLW95-465	-13.56	-90.9	17.58	surface
Mt Vroom NE	MLW95-466	-13.57	-98.7	9.86	surface
Mt Vroom E	MLW96-628	-13.31	-93.1	13.38	surface
Mt Vroom E	MLW96-631	-13.3	-93.1	13.30	surface
Mt Vroom E	MLW96-635	-13.29	-90.2	16.12	surface
Mt Vroom E	MLW96-637	-13.4	-90.9	16.30	surface
Mt Vroom E	MLW96-638	-13.44	-89.3	18.22	surface
Mt Vroom E	MLW96-641	-13.79	-96.3	14.02	surface
Mt Vroom N	MLW95-301	-13.45	-93.8	13.80	surface
Mt Vroom N	MLW95-395	-13.57	-96.9	11.66	surface
Mt Vroom N	MLW95-403	-13.46	-95.6	12.08	surface
Mt Vroom N	MLW95-406	-13.47	-92.4	15.36	surface
Mt Vroom N	MLW95-548	-13.46	-99.5	8.18	surface
Mt Vroom N	MLW96-661	-13.30	-86.7	19.70	surface
Mt Vroom SE	MLW96-646	-13.34	-93.4	13.32	surface
Mt Moser NE	MLW96-651	-13.65	-91.1	18.10	surface
Mt Moser N	MLW96-709	-13.27	-92.9	13.26	surface
Seep	MLW95-300	-13.54	-94.7	13.62	surface
Seep	MLW95-322	-13.47	-93.1	14.66	surface
Seep	MLW95-345	-13.24	-96.5	9.42	surface
West of Deposit	MLW96-710	-13.22	-91.5	14.26	surface
West of Deposit	MLW96-711	-13.50	-93.6	14.40	surface
West of Deposit	MLW96-712	-13.41	-93.3	13.98	surface
Simpsons Brook trib	MLW95-443	-13.64	-94.7	14.42	surface
Portage Lake	MLW95-444	-11.83	-82.7	11.94	surface
C4/C5	MLW95-543	-12.58	-86.0	14.64	surface
C4/C5	MLW95-544	-13.35	-92.6	14.20	surface
B-80-15	MLW95-563	-13.21	-92.8	12.88	100
B-80-7	MLW95-577		-90.1	-90.10	209
B-80-7	MLW95-581		-92.0	-92.00	173
B-80-7	MLW95-586	-13.33	-93.1	13.54	142
B-80-7	MLW95-587	-13.41	-91.3	15.98	223
B-80-7	MLW95-590	-13.42	-92.5	14.86	116
EH-1	MLW95-369	-13.49	-98.1	9.82	65
MM-88-01	MLW95-313	-13.45	-94.2	13.40	140
MM-88-01	MLW96-649	-13.58	-95.4	13.24	47
MM-88-01	MLW96-662	-13.44	-97.3	10.22	91
MM-88-02	MLW96-669	-12.40	-77.9	21.30	47
MM-88-02	MLW95-597	-10.89	-71.6	15.52	251
MM-88-02	MLW95-600	-10.82	-66.7	19.86	185
MM-88-02	MLW95-604	-10.79	-69.6	16.72	378
MM-88-02	MLW95-605	-10.80	-68.3	18.10	378
MM-88-02	MLW95-606	-10.76	-71.1	14.98	511
MM-88-06	MLW95-364	-13.58	-93.3	15.34	65
MM-88-07	MLW95-318	-13.46	-92.9	14.78	55
MM-89-100	MLW95-559	-13.00	-87.1	16.90	100
MM-89-102	MLW95-570	-12.94	-86.1	17.42	350
MM-89-104	MLW95-546	-13.36	-91.6	15.28	210
MM-89-106	MLW95-503	-12.42	-87.4	11.96	243
MM-89-106	MLW95-504	-12.53	-86.0	14.24	227
MM-89-106	MLW95-508	-12.63	-91.2	9.84	195
MM-89-106	MLW95-512	-12.67	-87.0	14.36	149
MM-89-106	MLW95-522	-13.56	-95.2	13.28	102
MM-89-106	MLW95-526	-13.67	-95.1	14.26	87
MM-89-106	MLW95-528		-94.1	-94.10	53
MM-89-107	MLW95-595	-13.58	-92.7	15.94	169
MM-89-107	MLW95-596	-13.62	-95.0	13.96	138
MM-89-109	MLW95-547	-13.21	-89.5	16.18	surface

Table 11.4. Oxygen and hydrogen stable isotope data for mine waters

Location	Sample #	$\delta^{18}O_{VSMOW}$ (‰)	δD_{VSMOW} (‰)	excess d	Depth
Brunswick 12	MLW95-492	-11.68	-81.5	11.94	1000
Brunswick 12	MLW95-493	-12.14	-84.6	12.52	1000
Heath Steele	MLW95-474	-12.27	-86.2	11.96	113
Heath Steele	MLW95-479	-12.53	-85.0	15.24	91
Heath Steele	MLW95-485	-12.74	-85.4	16.52	400
Heath Steele	MLW95-486	-11.73	-80.7	13.14	450
Heath Steele	MLW95-490	-13.50	-84.7	23.30	183
Heath Steele	MLW95-609	-11.98	-76.9	18.94	840
Heath Steele	MLW95-611	-11.90	-77.1	18.10	840
Stratmat	MLW96-676	-12.50	-80.8	19.20	26
Stratmat	MLW96-689	-12.38	-83.5	15.54	41
Stratmat	MLW96-690	-12.32	-79.4	19.16	84
Stratmat	MLW96-691	-12.35	-84.0	14.80	85
Stratmat	MLW96-693	-12.36	-81.5	17.38	86
Stratmat	MLW96-694	-12.27	-84.2	13.96	87
Stratmat	MLW96-695	-12.02	-80.2	15.96	88
Stratmat	MLW96-697	-12.00	-81.3	14.70	89
Stratmat	MLW96-702	-11.99	-79.9	16.02	92
Stratmat	MLW96-706	-12.13	-84.3	12.74	103
Wedge	MLW95-482	-12.60	-83.7	17.10	seep
Willett	MLW95-494	-12.46	-89.9	9.78	seep
Willett	MLW95-495	-12.53	-84.3	15.94	seep
Willett	MLW95-496	-12.66	-85.9	15.38	seep

Table 11.5. Carbon isotope values of DIC in surface and groundwaters

Site	Sample #	$\delta^{13}C_{VPDB}$ (‰)	HCO_3 (mg/l)	Notes
		Restigouche		
Mt Fowler NE	MLW96-683	-8.74	56.18	$\delta^{18}O$, δD from MLW96-684
Mt Fowler E	MLW96-663	-9.41	47.21	$\delta^{18}O$, δD from MLW96-664
Mt Fowler E	MLW96-666	-10.13	30.18	$\delta^{18}O$, δD from MLW96-665
Mt Moser NE	MLW96-650	-12.57	99.47	
Mt Moser NE	MLW96-651	-8.36	34.77	
Mt Moser N	MLW96-709	-11.11	51.86	
West of Deposit	MLW96-711	-12.77	8.95	
West of Deposit	MLW96-712	-11.40	34.09	
West of Deposit	MLW96-714	-11.78		
B-80-7	MLW95-586	-11.32	227.70	
B-80-7	MLW95-590	-10.64	152.21	
MM-88-01	MLW96-649	-9.41	79.98	
MM-88-01	MLW96-662	-9.13	114.69	
MM-88-01	MLW96-671	-8.90		
MM-88-02	MLW95-597/8	12.21	130.10	High salinity
MM-88-02	MLW95-597/8	11.98	130.10	Degassed prior to reanalysis
MM-88-02	MLW95-606	12.48	136.91	High salinity
MM-89-104	MLW95-546	-9.29	141.89	
MM-89-106	MLW95-508	-6.34	218.08	Deep
MM-89-106	MLW95-526	-7.30	45.49	Shallow
precipitation	MLW96-670	-12.40	0.00	
		Halfmile Lake		
Upper/Lower AB	MLW96-678	-17.89	6.42	seep; $\delta^{18}O$, δD from MLW94-185
Upper/Lower AB	MLW96-681	-6.03	14.84	$\delta^{18}O$, δD from MLW94-148
Halfmile North stream	MLW96-682	-10.82	26.30	$\delta^{18}O$, δD from MLW94-194
HN94-79	MLW96-673	-7.63	55.67	
HN92-40	MLW96-674	-9.60	38.87	
HN92-40	MLW96-692	-10.45		
HN92-40	MLW96-696	-8.81	53.38	
HN94-82	MLW96-675	-14.72	67.25	
HN94-63	MLW96-708	-5.91	139.97	
		Other waters		
Stratmat	MLW96-676	-14.47	76.16	
Stratmat	MLW96-689	-15.00	80.11	
Stratmat	MLW96-690	-13.55	73.94	
Stratmat	MLW96-693	-13.15	77.86	
Stratmat	MLW96-694	-11.08	90.19	
Stratmat	MLW96-695	-10.73	115.74	
Stratmat	MLW96-697	-10.31	78.89	
Stratmat	MLW96-702	-10.73	97.50	
Stratmat	MLW96-706	-11.79	99.38	
Heath Steele	MLW95-610	-5.01	77.79	$\delta^{18}O$, δD from MLW96-611

Table 11.6. Carbon and oxygen isotope data for fracture and vein carbonate

Borehole (depth m)	Sample #	Mineral	$\delta^{18}O_{VSMOW}$ (‰)	$\delta^{18}O_{VPDB}$ (‰)	$\delta^{13}C_{VPDB}$ (‰)	Notes
MM-88-02 (55)	ML95-245	Calcite	20.61	-10.00	-6.76	Acicular crystals in carbonate vug
MM-88-02 (53)	ML95-246-1	Graphite			-26.81	graphite crystal in carbonate vein
MM-88-02 (53)	ML95-246-1	Graphite			-25.56	graphite crystal in carbonate vein
MM-88-02 (53)	ML95-246-2	Graphite			-27.79	graphite crystal in carbonate vein
MM-88-01 (112)	ML95-224	Calcite	14.73	-15.70	-7.83	
MM-88-01 (112)	ML95-224	Siderite	11.39	-18.94	-10.10	
MM-88-02 (434)	ML95-266	Calcite	13.53	-16.86	-8.03	platy carbonate on fracture surface
MM-88-02 (434)	ML95-266	Calcite	13.78	-16.62	-8.17	repeat
MM-88-02 (434)	ML95-266	Dolomite	12.76	-17.61	-8.10	platy carbonate on fracture surface
MM-88-02 (503)	ML95-269	Calcite	17.31	-13.19	-6.46	
MM-88-02 (503)	ML95-269	Dolomite	18.06	-12.47	-6.23	
MM-88-02 (503)	ML95-269	Siderite	14.94	-15.49	-7.93	
MM-88-02 (52)	ML95-244-1	Calcite	18.94	-11.61	-1.33	vein carbonate
MM-88-02 (52)	ML95-244-2	Calcite	19.93	-10.65	-4.79	vein carbonate
MM-88-02 (52)	ML95-244-2	Dolomite	19.18	-11.37	-4.83	vein carbonate
MM-88-02 (52)	ML95-244-2	Siderite	14.43	-15.99	-7.18	vein carbonate
MM-88-02 (112)	ML95-252	Calcite	19.93	-10.65	-4.79	vein carbonate
MM-88-02 (112)	ML95-252	Dolomite	6.66	-23.52	-11.64	vein carbonate
MM-88-02 (233)	ML95-259	Calcite	11.96	-18.38	-6.52	vein carbonate
MM-88-02 (233)	ML95-259	Dolomite	11.95	-18.39	-6.71	vein carbonate
MM-88-02 (233)	ML95-259	Siderite	11.00	-19.31	-7.71	vein carbonate
MM-88-02 (90)	ML95-290	Calcite	19.79	-10.79	-5.46	idiomorphic vuggy carbonate
MM-88-02 (90)	ML95-290	Dolomite	20.41	-10.18	-4.52	idiomorphic vuggy carbonate
MM-88-02 (90)	ML95-290	Siderite	15.47	-14.98	-6.87	idiomorphic vuggy carbonate
MM-88-02 (50)	ML95-243	Calcite	18.52	-12.02	-4.71	
MM-88-02 (50)	ML95-243	Dolomite	17.75	-12.77	-4.77	
MM-88-02 (50)	ML95-243	Siderite	13.96	-16.44	-7.17	
HN94-65 (630)	ML95-357	Calcite	18.04	-12.48	-3.91	vein carbonate
HN94-65 (630)	ML95-357	Dolomite	14.82	-15.61	-4.77	vein carbonate
HN94-65 (630)	ML95-357	Siderite	12.48	-17.88	-5.98	vein carbonate
HN95-96 (435)	ML95-500	Calcite	11.54	-18.79	-7.55	acicular carbonate on fracture surface
HN95-96 (435)	ML95-500	Dolomite	12.24	-18.11	-7.04	acicular carbonate on fracture surface
HN95-96 (435)	ML95-500	Siderite	11.06	-18.26	-7.39	acicular carbonate on fracture surface

Table 11.7 Elemental and isotopic composition of boron in BMC waters

Sample#	Location	Depth (m)	B (µg/l)	Cl (mg/l)	Ca (µg/l)	Na (µg/l)	B/Cl	$^{11}B/^{10}B$	$\delta^{11}B$ (‰)
				Restigouche					
MLW95-581	B-80-7	173	24	13.6	22000	35000	0.005624	4.052	2.0
MLW95-586	B-80-7	223	35	118	6000	140000	0.000945		
MLW95-587	B-80-7	223	34	112	7100	130000	0.000968	4.068	5.9
MLW95-378	B-80-7	235	17	22.1	23000	49000	0.002452		
MLW96-662	MM-88-01	91	27	8.39	17635	25152	0.010257		
MLW96-671	MM-88-01	93	18	6.96	16380	26945	0.008243		
MLW96-669	MM-88-02	47	83	5923	374994	-20	0.000045		
MLW95-323	MM-88-02	50	240	13000	810000	6380000	0.000059		
MLW95-324	MM-88-02	70	180	13000	810000	6430000	0.000044		
MLW95-325	MM-88-02	100	280	13000	790000	6280000	0.000069		
MLW95-326	MM-88-02	150	20	13000	830000	6530000	0.000005		
MLW95-600	MM-88-02	185	65	13340	800000	6170000	0.000016	4.076	7.9
MLW95-327	MM-88-02	200	180	13000	820000	6430000	0.000044		
MLW95-328	MM-88-02	250	200	13000	770000	6050000	0.000049		
MLW95-597	MM-88-02	251	110	13440	790000	6090000	0.000026		
MLW95-329	MM-88-02	300	190	13000	750000	5970000	0.000047		
MLW95-330	MM-88-02	350	59	13000	820000	6400000	0.000014		
MLW95-604	MM-88-02	378	260	13090	880000	6620000	0.000063	4.089	11.1
MLW95-605	MM-88-02	378	260	13255	820000	6240000	0.000063		
MLW95-331	MM-88-02	400	93	13000	780000	6150000	0.000023		
MLW95-606	MM-88-02	511	42	13255	780000	6200000	0.000010	4.068	5.9
MLW95-344	MM-88-02	540	150	13000	780000	6160000	0.000037		
MLW95-558	MM-89-100	100	26	25.4	19000	46000	0.003262	4.065	5.2
MLW95-564	MM-89-102	50	69	52.3	24000	83000	0.004205		
MLW95-565	MM-89-102	100	35	26.7	16000	46000	0.004178	4.066	5.4
MLW95-566	MM-89-102	150	120	149	8800	180000	0.002567		
MLW95-567	MM-89-102	200	120	133	12000	160000	0.002876		
MLW95-568	MM-89-102	250	130	157	7900	190000	0.002639		
MLW95-569	MM-89-102	300	110	131	14000	160000	0.002676		
MLW95-570	MM-89-102	350	150	351	10000	300000	0.001362	4.044	0.0
MLW95-571	MM-89-102	410	110	200	14000	190000	0.001753		
MLW95-522	MM-89-106	102	10	57.3	8700	38000	0.000556		
MLW95-512	MM-89-106	149	92	1237	11000	780000	0.000237	4.084	9.9
MLW95-508	MM-89-106	195	89	1393	9600	840000	0.000204		
MLW95-504	MM-89-106	227	81	1461	10000	820000	0.000177		
MLW95-503	MM-89-106	243	120	1485	11000	940000	0.000258	4.068	5.9
MLW95-343	MM-89-106	250	27	333	8800	230000	0.000258		
				Halfmile Lake					
MLW94-132	Halfmile North		22	0.56	8000	1200	0.125209		
MLW94-143	Halfmile North		24	0.54	8500	1200	0.141651		
MLW94-153	NE tributary		24	0.89	8100	1900	0.085945		
MLW94-183	HN93-55	500	17	0.84	6400	2900	0.064502	nd	
MLW96-707	HN94-63	400	53	8.96	6247	51695	0.018853		
MLW96-708	HN94-63	450	17	6.83	1825	62681	0.007933		
MLW95-608	HN94-65	223	18	9.24	10000	13000	0.006209	4.034	-2.5
				Mines					
MLW95-492	Brunswick #12	1000	65	30638	4370000	9610000	0.000007	4.068	5.9
MLW95-493	Brunswick #12	1000	91	999	140000	580000	0.000290		
MLW95-609	Heath Steele, C-zone	840	86	378	2200	350000	0.000725		
MLW95-610	Heath Steele, C-zone	840	24	11.1	180000	160000	0.006891	4.089	11.1
MLW95-611	Heath Steele, C-zone	840	80	316	66000	450000	0.000807		
MLW95-486	Heath Steele, B-zone	450	19	18.3	480000	31000	0.003309	4.210	41.0
MLW95-488	Heath Steele, C-zone	185	10	96.4	9800	89000	0.000331		
MLW95-490	Heath Steele, C-zone	185	10	2.23	120000	6900	0.014292		
MLW96-676	Stratmat Main Zone	26	34	1.36	17002	9070	0.079679		
MLW96-694	Stratmat Main Zone	87	17	1.29	75922	48790	0.042001		
MLW96-695	Stratmat Main Zone	88	34	1.44	248895	78533	0.075252		
MLW96-697	Stratmat Main Zone	89	48	0.05	298526	146841	3.059656		
MLW96-702	Stratmat Main Zone	92	37	0.4	145570	107730	0.294811		
MLW96-706	Stratmat Main Zone	103	28	0.72	90719	63384	0.123944		
MLW96-716	Willett Deposit	30	58	6.51	21711	67103	0.028395		
MLW96-717	Willett Deposit	50	56	4.46	20839	69992	0.040018		
MLW96-718	Willett Deposit	100	66	3.18	20384	72534	0.066148		
Seawater			4600	19805	421900	11019500	0.000740		38.4

Seawater chemistry recalculated from Drever (1988). Boron isotopic value for seawater from Vengosh et al. (1991).

Table 11.8 Mass balance calulatations for carbon isotopic compositions of BMC waters

Sample#	pH	HCO_3 mol/L	H_2CO_3 mol/L	CO_3 mol/L	Total DIC mol/L	Mg mol/L	Ca mol/L	DIC_{calc} mol/L	Fluid $\delta^{13}C$ ‰	Fluid $\delta^{13}C$ ‰	Fluid $\delta^{13}C$ ‰	Fluid $\delta^{13}C$ ‰	Meas $\delta^{13}C$ ‰
		1	2	3	4	5	6	7	8	9	10	11	12
Restigouche deposit													
MLW96-683	7.00	9.21E-04	2.66E-04	2.98E-07	1.19E-03	1.15E-04	2.50E-04	8.22E-04	-11.13	-12.07	-8.04	-14.39	-8.74
MLW96-663	6.47	6.37E-04	6.23E-04	6.08E-08	1.26E-03	9.60E-05	3.65E-04	7.99E-04	-12.23	-13.34	-10.01	-16.96	-9.41
MLW96-666	6.61	4.95E-04	3.50E-04	6.52E-08	8.45E-04	6.65E-05	4.30E-04	3.48E-04	-10.37	-11.20	-10.81	-18.86	-10.13
MLW96-650	7.14	1.63E-03	3.41E-04	7.28E-07	1.97E-03	1.10E-04	7.44E-04	1.12E-03	-10.29	-11.30	-7.56	-11.11	-12.57
MLW96-651	6.26	5.70E-04	9.03E-04	3.36E-08	1.47E-03	9.13E-05	2.14E-04	1.17E-03	-13.74	-15.08	-10.03	-17.79	-8.36
MLW96-709	7.73	8.50E-04	4.56E-05	1.48E-06	8.97E-04	1.34E-04	3.28E-04	4.36E-04	-9.40	-10.08	-9.16	-14.92	-11.11
MLW96-711	6.68	1.47E-04	8.84E-05	2.27E-08	2.35E-04	7.64E-05	9.83E-05	6.03E-05	-8.79	-9.37	-14.51	-27.68	-12.77
MLW96-712	7.04	5.59E-04	1.47E-04	1.98E-07	7.06E-04	9.10E-05	1.99E-04	4.16E-04	-10.55	-11.40	-10.42	-17.93	-11.40
MLW95-586	8.23	3.73E-03	6.34E-05	2.05E-05	3.82E-03	1.36E-04	1.50E-04	3.53E-03	-10.32	-12.29	-6.26	-8.00	-11.32
MLW95-590	8.67	2.49E-03	1.54E-05	3.78E-05	2.55E-03	3.13E-04	5.49E-04	1.69E-03	-10.24	-11.05	-6.80	-9.28	-10.64
MLW96-649	7.94	1.31E-03	4.34E-05	3.69E-06	1.36E-03	3.71E-04	5.29E-04	4.58E-04	-8.36	-9.38	-8.04	-12.25	-9.41
MLW96-662	8.12	1.88E-03	4.11E-05	8.02E-06	1.93E-03	3.44E-04	4.40E-04	1.14E-03	-9.92	-10.68	-7.28	-10.44	-9.13
MLW96-671	8.13	1.53E-03	3.27E-05	6.68E-06	1.57E-03	3.23E-04	4.09E-04	8.37E-04	-9.60	-10.31	-7.69	-11.43	-8.90
MLW95-546	7.31	2.33E-03	3.28E-04	1.54E-06	2.66E-03	4.94E-04	6.74E-04	1.49E-03	-10.07	-10.85	-6.91	-9.55	-9.29
MLW95-508	9.33	3.57E-03	4.82E-06	2.47E-04	3.82E-03	1.77E-04	2.40E-04	3.41E-03	-11.35	-12.32	-6.31	-8.12	-6.34
MLW95-526	7.74	7.46E-04	3.91E-05	1.33E-06	7.86E-04	1.15E-04	2.50E-04	4.21E-04	-9.69	-10.42	-9.54	-15.82	-7.30
Halfmile Lake deposit													
MLW96-678	6.47	1.05E-04	1.03E-04	1.00E-08	2.08E-04	1.40E-05	1.83E-05	1.76E-04	-13.13	-14.38	-15.29	-29.54	-17.89
MLW96-681	6.68	2.43E-04	1.47E-03	3.77E-09	1.71E-03	3.10E-05	8.32E-05	1.59E-03	-16.28	-18.01	-13.08	-24.28	-6.03
MLW96-682	6.94	4.31E-04	1.43E-02	1.21E-09	1.47E-02	2.39E-05	2.05E-04	1.45E-02	-17.62	-19.57	-20.95	-19.92	-10.82
MLW96-674	6.95	6.37E-04	2.06E-04	1.84E-07	8.43E-04	7.75E-05	3.81E-04	3.85E-04	-9.50	-10.65	-10.01	-16.96	-9.60
MLW96-673	7.33	9.12E-04	1.23E-04	6.31E-07	1.04E-03	7.57E-05	4.32E-04	5.28E-04	-9.77	-10.50	-8.95	-14.45	-7.63
MLW95-675	7.33	1.10E-03	1.49E-04	7.63E-07	1.25E-03	9.16E-05	4.59E-04	7.01E-04	-10.05	-10.83	-8.46	-13.25	-14.72
MLW95-696	7.09	8.75E-04	2.05E-04	3.48E-07	1.08E-03	1.24E-04	4.84E-04	4.72E-04	-9.56	-10.26	-9.08	-14.73	-8.81
MLW96-708	9.86	2.29E-03	9.13E-07	5.38E-04	2.83E-03	4.98E-06	4.55E-05	2.78E-03	-12.13	-13.22	-6.93	-9.60	-5.91
Stratmat Main Zone deposit													
MLW96-676	7.66	1.25E-03	7.88E-05	1.85E-06	1.33E-03	1.25E-04	4.24E-04	7.80E-04	-10.00	-10.77	-8.16	-12.52	-14.47
MLW96-689	7.79	1.31E-03	6.14E-05	2.62E-06	1.38E-03	7.16E-05	2.96E-04	1.01E-03	-10.65	-11.52	-8.04	-12.24	-15.00
MLW96-690	7.53	1.21E-03	1.03E-04	1.33E-06	1.32E-03	1.45E-04	8.60E-04	3.11E-04	-7.65	-8.06	-8.23	-12.69	-13.55
MLW96-693	7.72	1.28E-03	7.01E-05	2.17E-06	1.35E-03	1.47E-04	8.11E-04	3.90E-04	-8.05	-8.51	-8.10	-12.40	-13.15
MLW96-694	7.87	1.48E-03	5.75E-05	3.55E-06	1.54E-03	1.17E-04	1.89E-03	-4.73E-04	1.11	2.05	-7.77	-11.60	-11.08
MLW96-695	8.05	1.90E-03	4.88E-05	6.89E-06	1.95E-03	4.37E-04	6.21E-03	-4.69E-03	-26.81	-30.17	-7.26	-10.40	-10.73
MLW96-697	7.9	1.29E-03	4.69E-05	3.32E-06	1.34E-03	1.60E-03	7.45E-03	-7.71E-03	-20.62	-23.02	-8.07	-12.32	-10.31
MLW96-702	8.02	1.60E-03	4.40E-05	5.41E-06	1.65E-03	5.56E-04	3.63E-03	-2.54E-03	-40.02	-45.41	-7.60	-11.21	-10.73
MLW96-706	8.02	1.63E-03	4.49E-05	5.52E-06	1.68E-03	3.72E-04	2.26E-03	-9.56E-04	13.47	16.32	-7.56	-11.11	-11.79
Heath Steele deposit													
MLW95-610	7.87	1.27E-03	4.96E-05	3.06E-06	1.33E-03	1.56E-03	4.49E-03	-4.73E-03	-22.80	-25.54	-8.10	-12.40	-5.01

1, measured water HCO_3

2, 3, calculated

4, total DIC of water

5, 6 measured Mg and Ca contents

7, calculated DIC of initial fluid assuming all Ca and Mg is derived from congruent carbonate dissolution.

8, calulated final water $\delta^{13}C$ based on initial fluid value of $\delta^{13}C_{calc}$ = -18‰

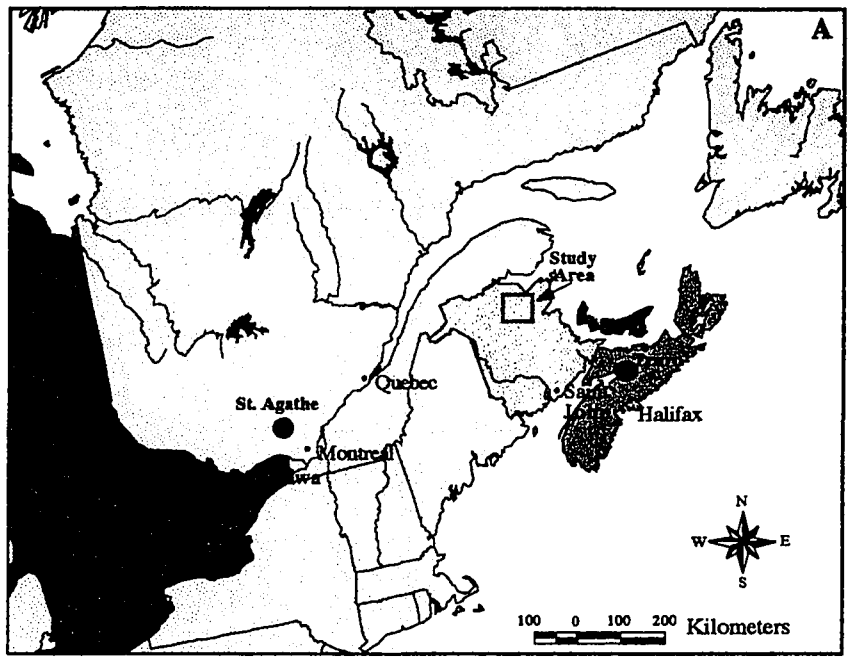
9, calulated final water $\delta^{13}C$ based on initial fluid value of $\delta^{13}C_{calc}$ = -20‰

10, calulated final water $\delta^{13}C$ based on initial fluid value of $\delta^{13}C_{calc}$ = -20‰, DIC = 0.0004 mol/L

11, calulated final water $\delta^{13}C$ based on initial fluid value of $\delta^{13}C_{calc}$ = -20‰, DIC = 0.0008 mol/L

12, mesaured value from Table 11.5

Shaded results indicate close fits



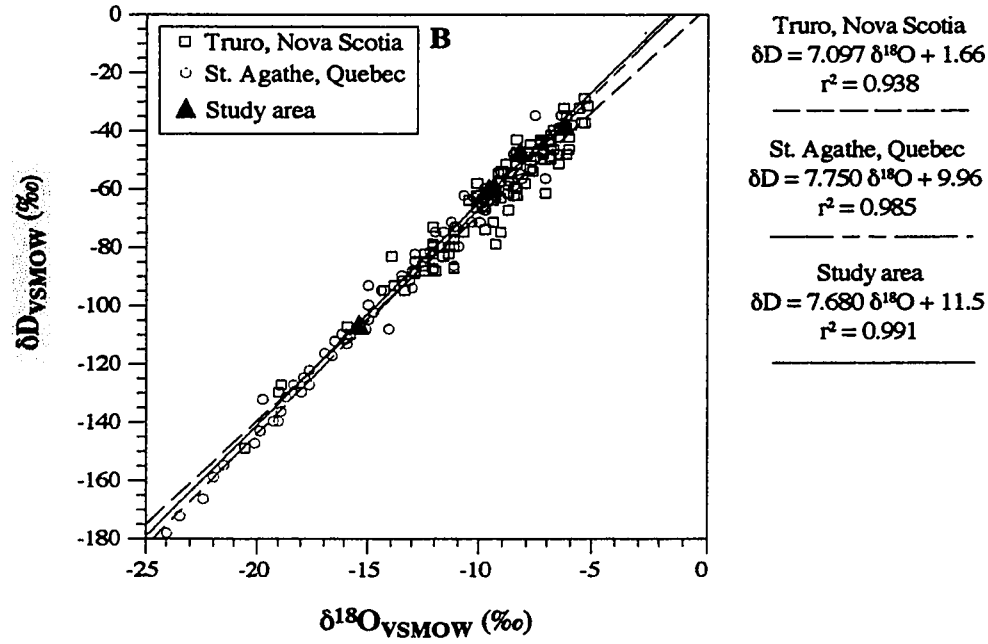


Fig. 11.1 A) Map showing the location of the study area (Bathurst Mining Camp, New Brunswick) with respect to IAEA precipitation monitoring stations at Truro, Nova Scotia and St. Agathe, Quebec. B) IAEA stable isotope data with regression lines representing local meteoric water lines. Also shown are data for precipitation from the study area. IAEA data from www.iaea.com, study area data from Table 11.1.

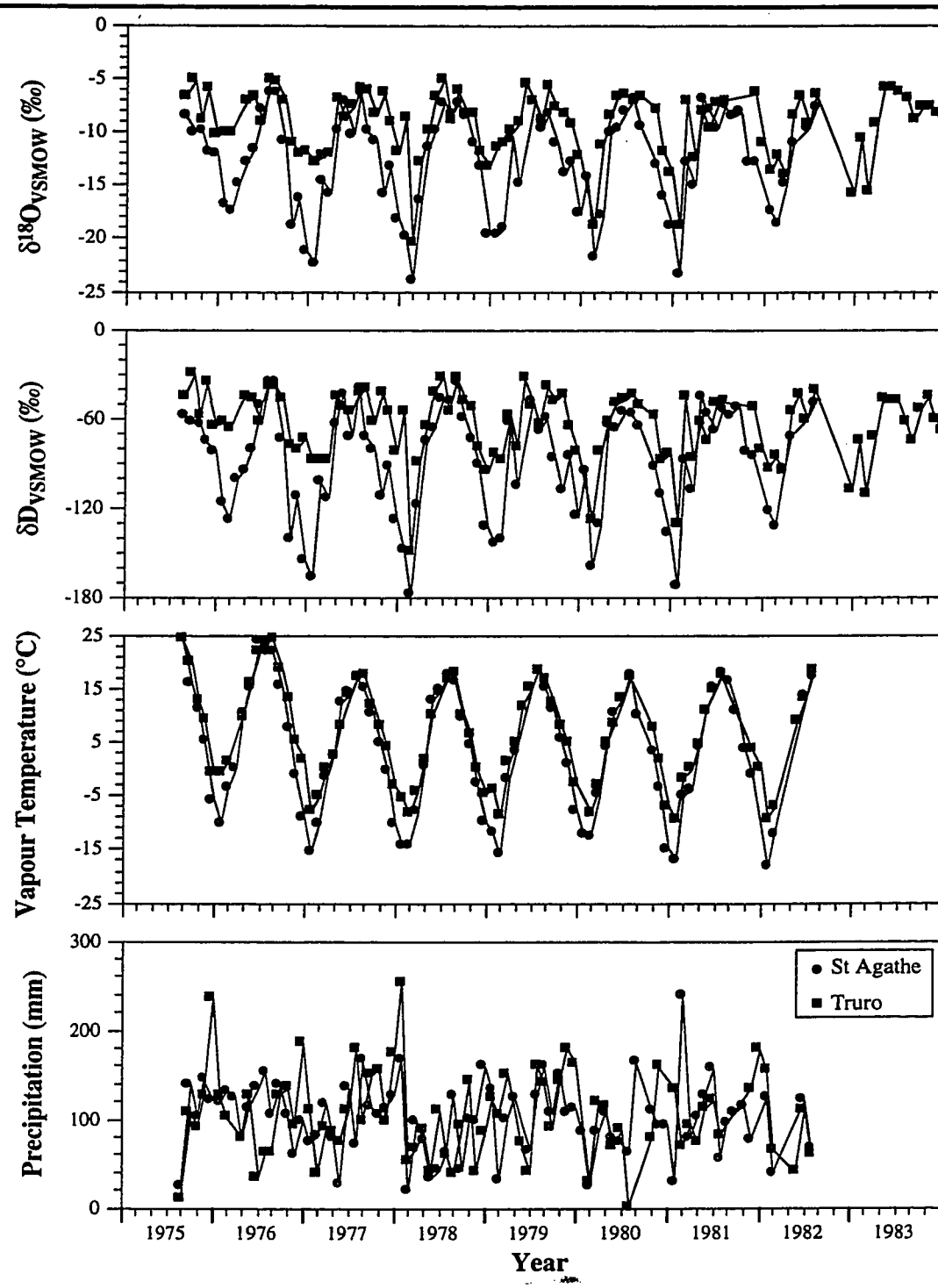


Fig. 11.2. Plots showing the variation in oxygen and deuterium isotopes, vapour temperature and rainfall amount for the St Agathe, Quebec and Truro, Nova Scotia IAEA monitoring sites for the years 1975 - 1983. Data from www.iaea.org.

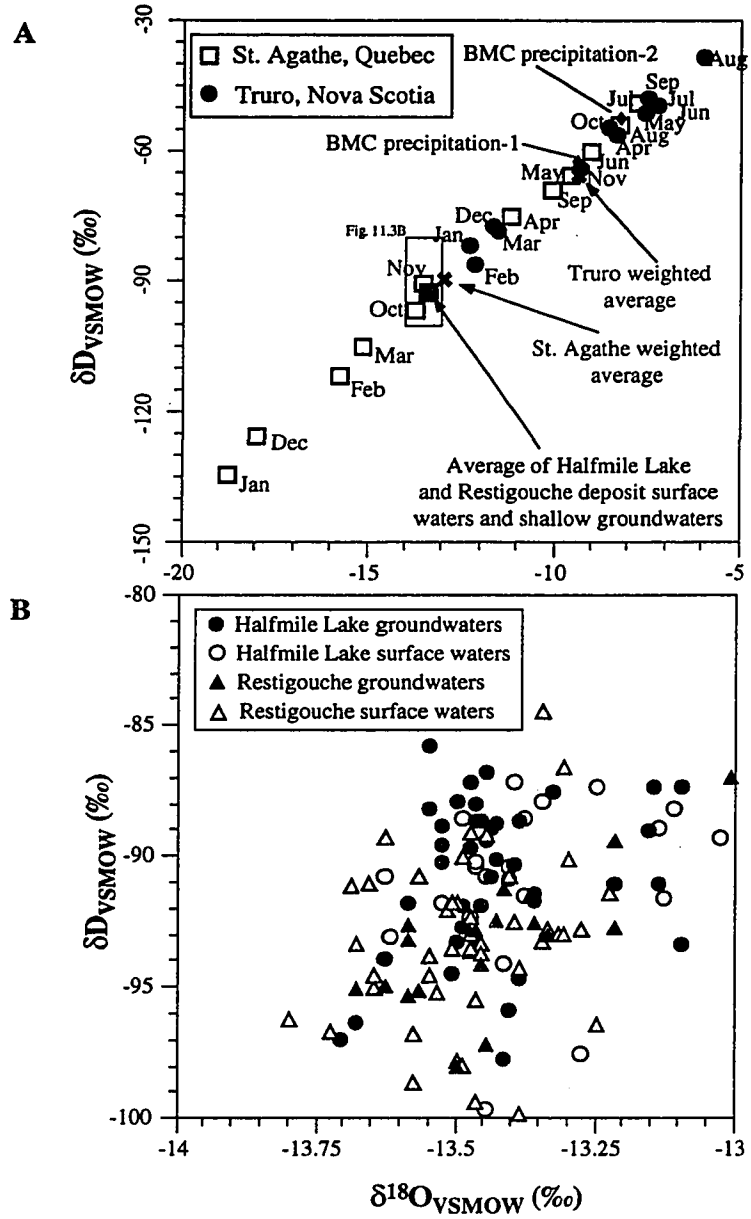


Fig. 11.3. A) Plot of oxygen and deuterium isotopes of monthly mean weighted averages for precipitation from St. Agathe, Quebec and Truro, Nova Scotia. Precipitation data from www.iaea.org. BMC precipitation-1 refers to the average values (not weighted for amount of precipitation) for six precipitation events sampled in June and July of 1995-96 (Table 11.1). BMC precipitation-2 is the average values for the same data excluding the very depleted sample (MLW96-648; Table 11.1). BMC precipitation-2 falls between the June weighted averages for Truro and St. Agathe. Also shown are the weighted average compositions for Truro and St. Agathe precipitation and the average composition of Halfmile Lake deposit surface and groundwaters and Restigouche deposit surface and shallow groundwaters. B) Inset of box in Fig. 11.3A. Plot of oxygen and deuterium isotopes for ground and surface waters from the Halfmile Lake deposit and shallow groundwaters and surface waters from the Restigouche deposit. Data from Tables 11.2 and 11.3.

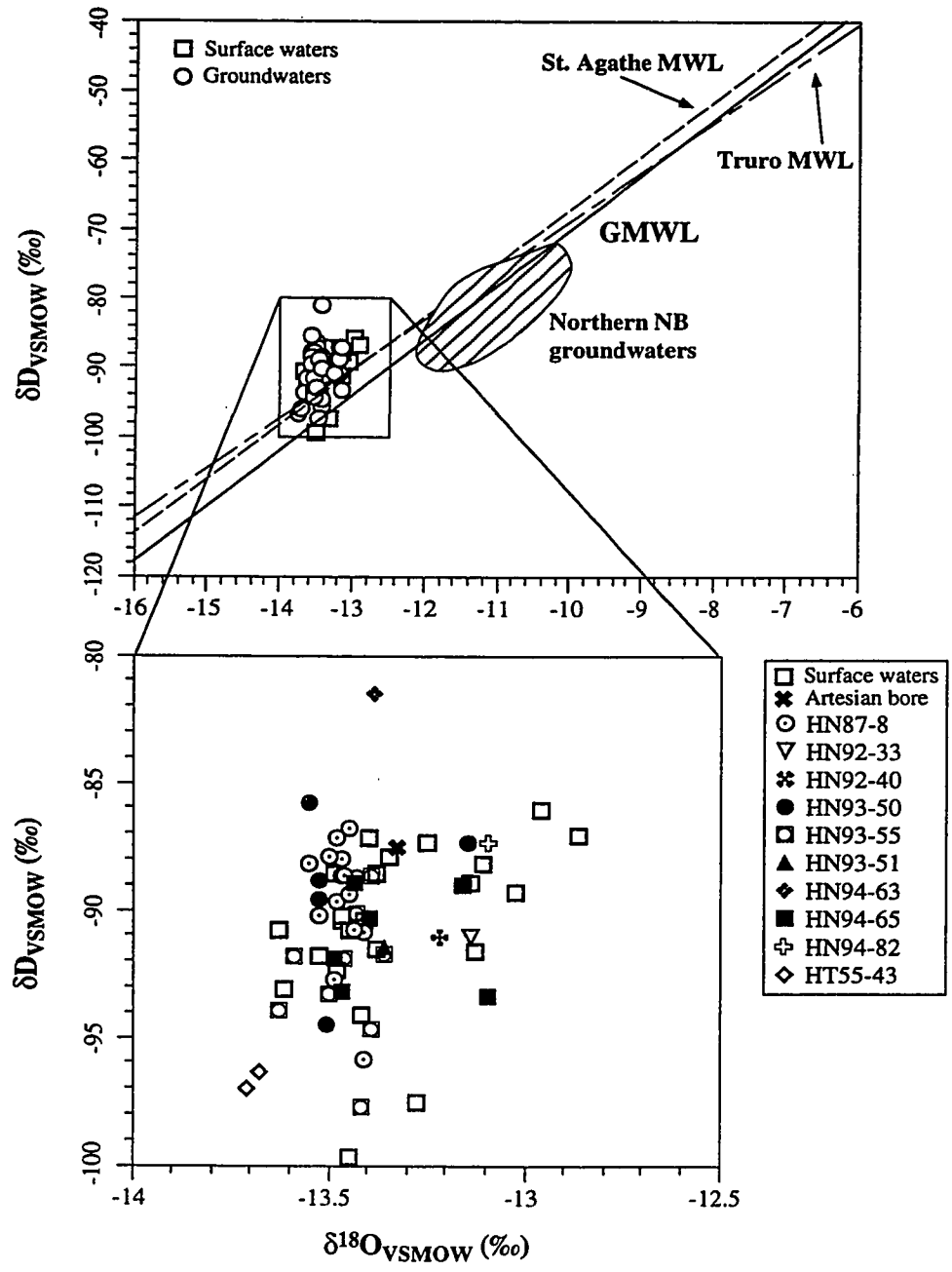


Fig. 11.4 Plot of oxygen and deuterium isotopes for ground and surface waters from Halfmile Lake. Also shown is unpublished data for northern New Brunswick groundwaters (D. R. Boyle, pers. comm.). Waters from Halfmile Lake are very uniform in composition and plot well above the global meteoric water line (GMWL) but closer to meteoric water lines defined by the St Agathe, Quebec and Truro, Nova Scotia precipitation data (www.iaea.org). Surface waters are isotopically very similar to groundwaters (inset). Data from Table 11.2.

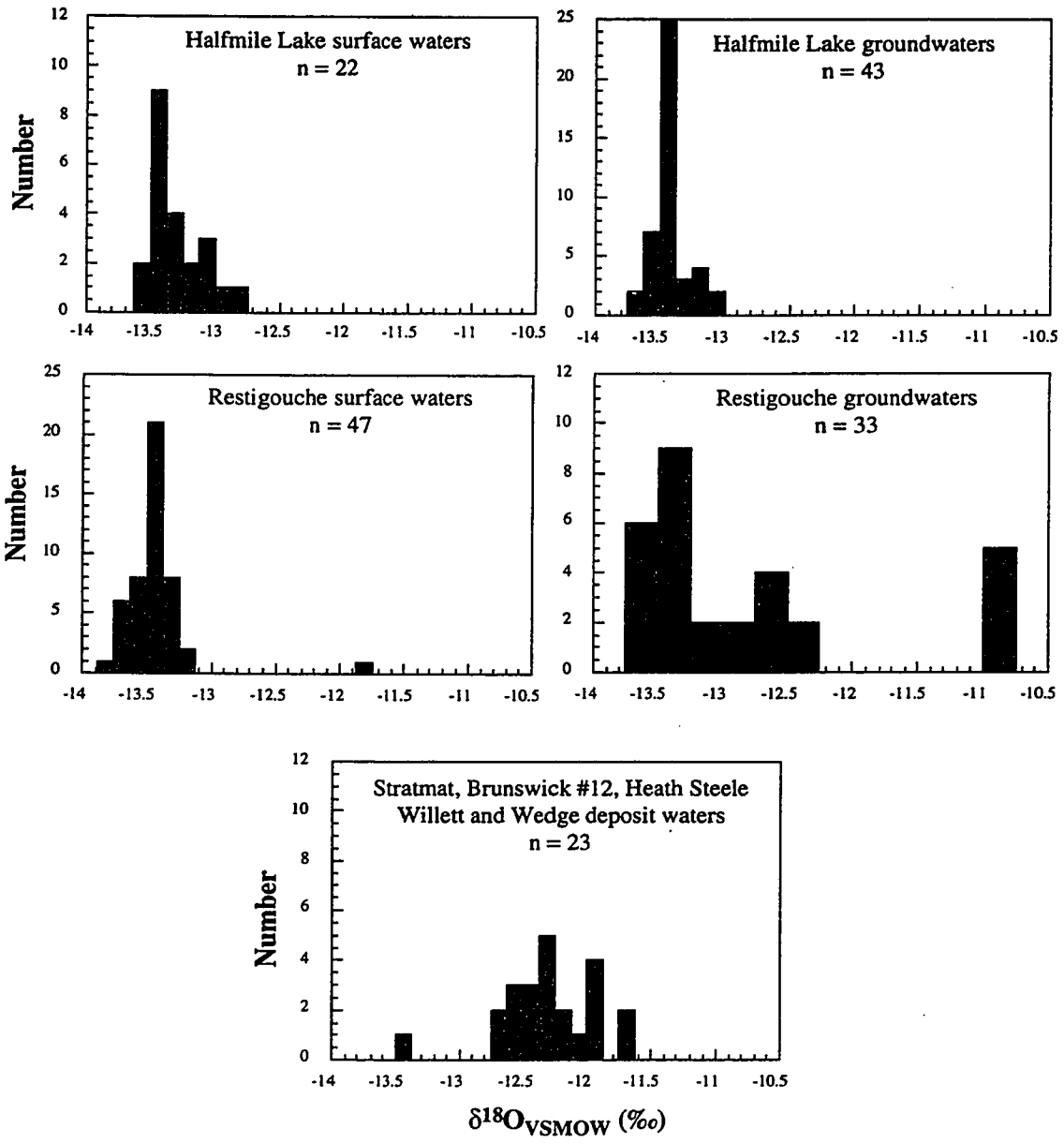


Fig. 11.5 Histograms of $\delta^{18}O_{VSMOW}$ values for surface and groundwaters at the Halfmile Lake, Restigouche, Stratmat, Brunswick #12, Heath Steele, Willett, and Wedge deposits from the Bathurst Mining Camp. Data from Tables 11.2, 11.3, and 11.4.

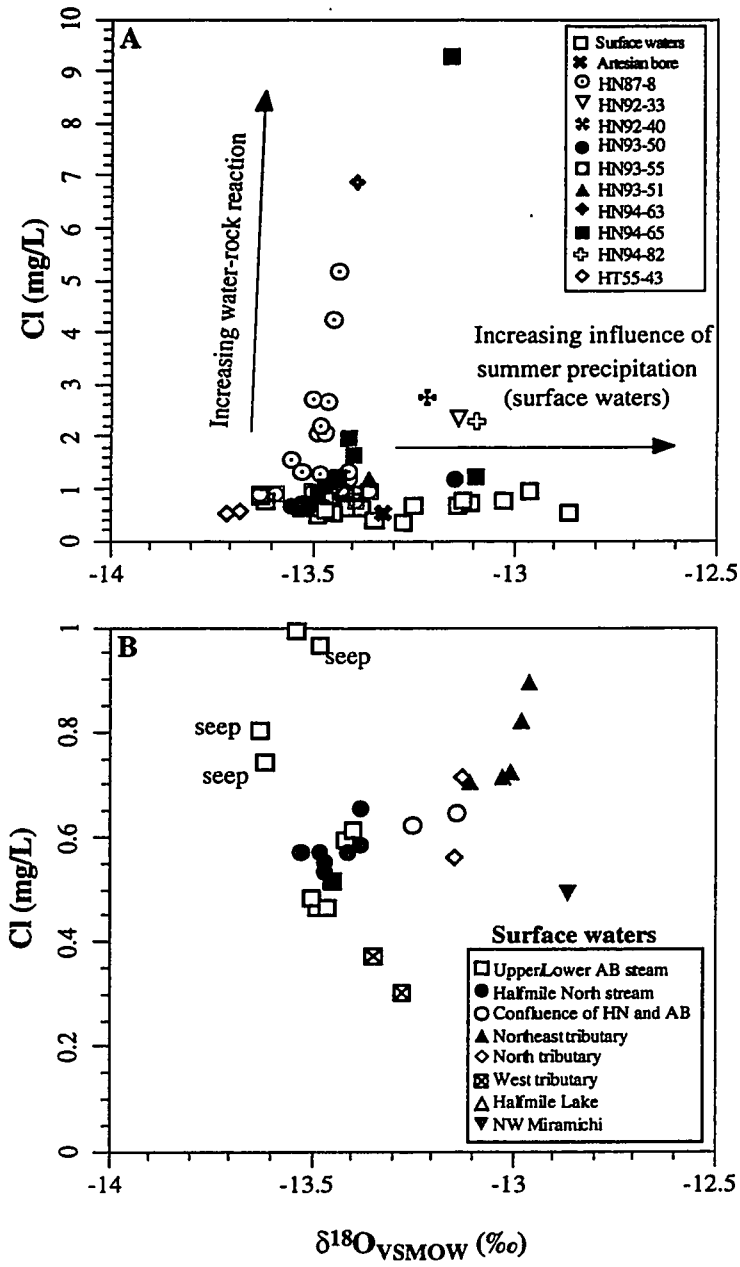


Fig. 11.6 Plot $\delta^{18}O_{VSMOW}$ vs Cl for ground and surface waters from the Halfmile Lake deposit. A) Groundwaters from individual boreholes are compared to each other and to surface waters in general. B) Surface waters subdivided by stream. At Halfmile Lake, surface waters show a subtle trend to higher isotopic compositions. Data from Tables 11.2 and A.3.

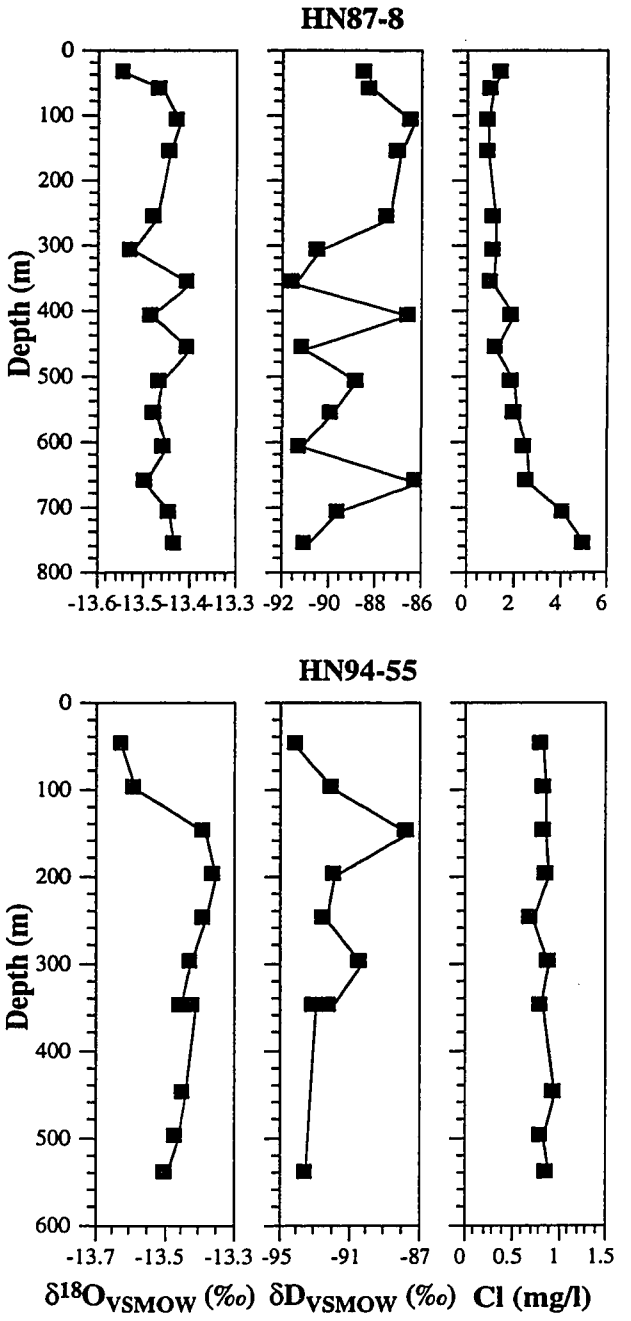


Fig. 11.7. Downhole profiles for groundwaters from boreholes HN87-8 and HN94-55 from the Halfmile Lake deposit. Data from Table 11.2 and A.3.

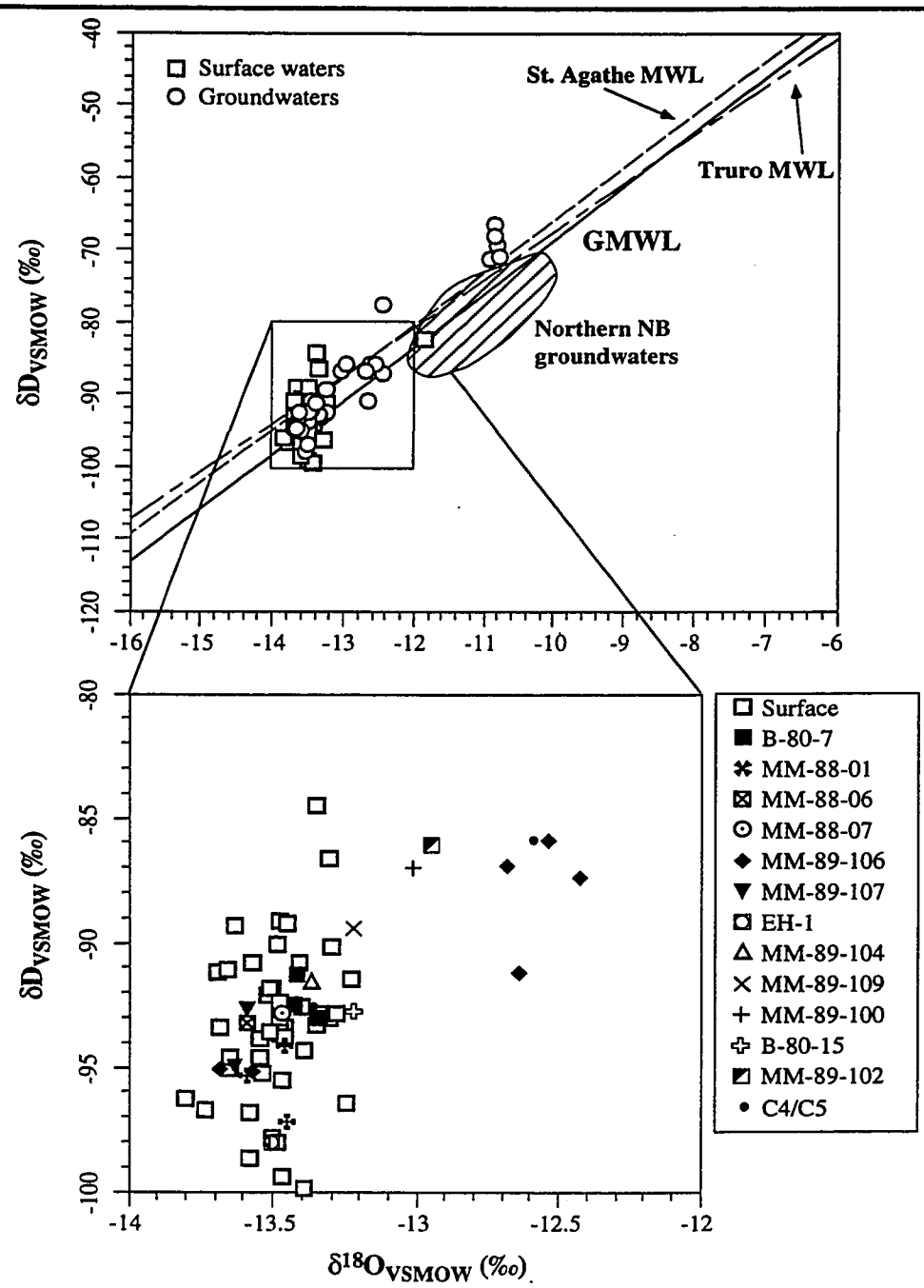


Fig. 11.8. Plot of oxygen and deuterium isotopes for ground and surface waters from the Restigouche deposit. Also shown is unpublished data for northern New Brunswick groundwaters (D. R. Boyle, pers. comm.). Surface waters from the Restigouche deposit are very uniform in composition and generally plot above the global meteoric water line (GMWL) but closer to meteoric water lines defined by the St Agathe, Quebec and Truro, Nova Scotia precipitation data (www.iaea.org). Groundwaters trend to more enriched isotopic compositions compared to groundwaters from the Halfmile Lake deposit (see Figs. 11.4, 11.5). Data from Table 11.3.

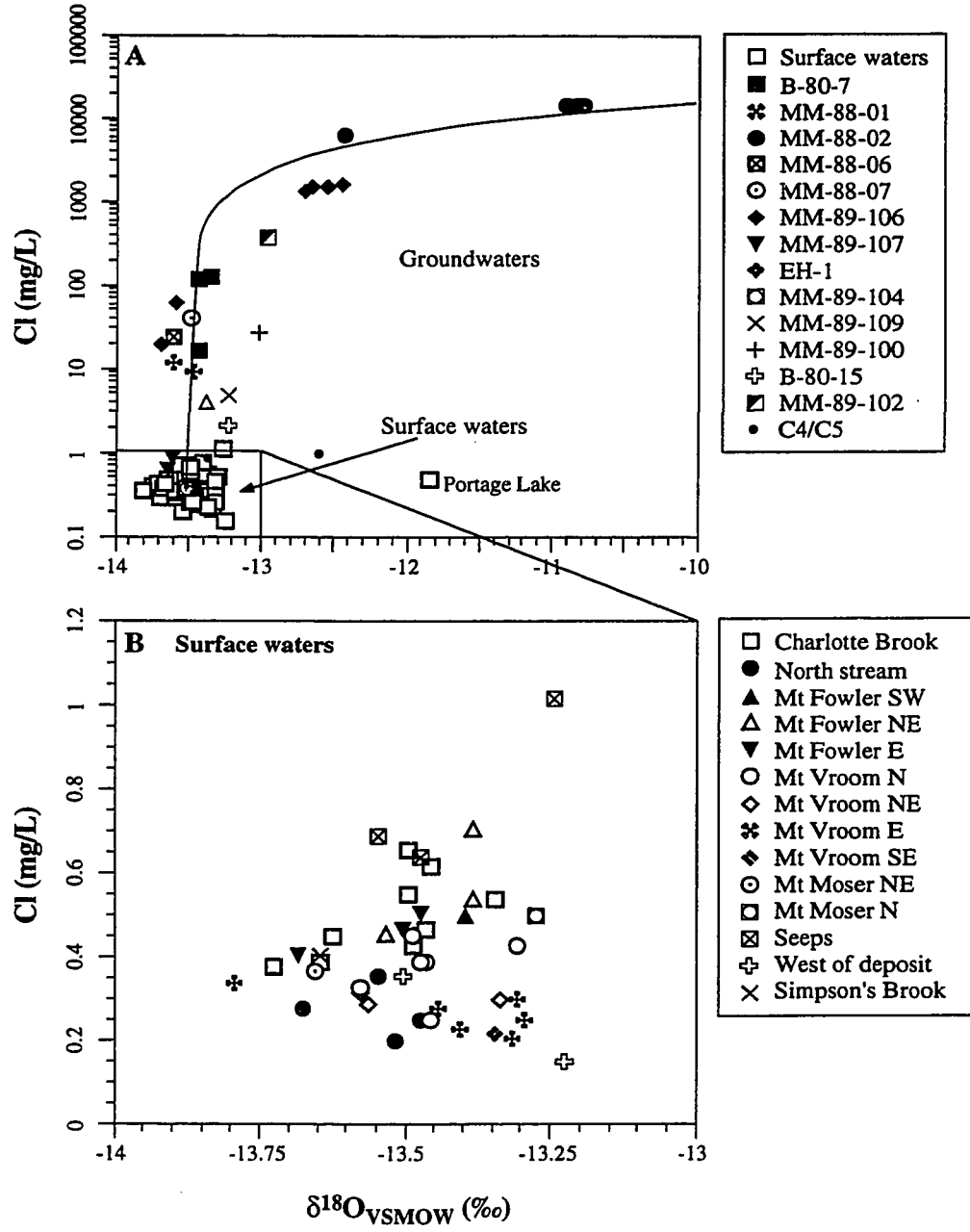


Fig. 11.9 Plot $\delta^{18}O_{VSMOW}$ vs Cl for ground and surface waters from the Restigouche deposit. A) Groundwaters from individual boreholes are compared to each other and to surface waters in general. Also shown is a hypothetical two-component mixing line between Cl = 0.3 mg/L, $\delta^{18}O$ = -13.5‰ and Cl = 14000 mg/L, $\delta^{18}O$ = -10‰. B) Surface waters are compared based on stream segment. Data from Tables 11.3 and B.3.

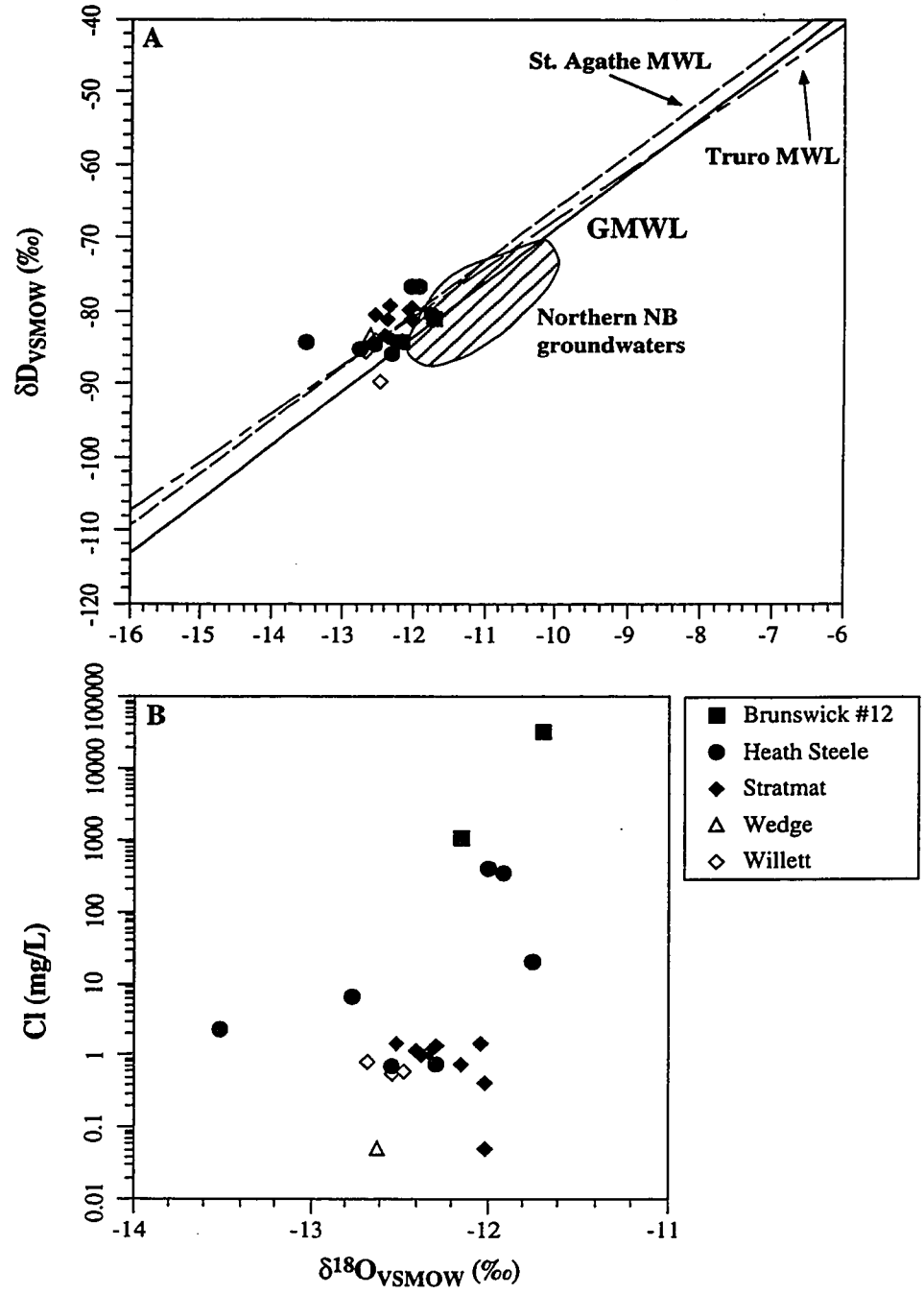


Fig. 11.10. A) Plot of oxygen and deuterium isotopes for groundwaters from the Brunswick #12, Heath Steele, Stratmat, Wedge, and Willett deposits. Also shown is unpublished data for northern New Brunswick groundwaters (D. R. Boyle, pers. comm.), the global meteoric water line (GMWL), and meteoric water lines defined by the St Agathe, Quebec and Truro, Nova Scotia precipitation data (www.iaea.org). B) Cl vs $\delta^{18}O_{VSMOW}$ plot for the same waters. Data from Table 11.4.

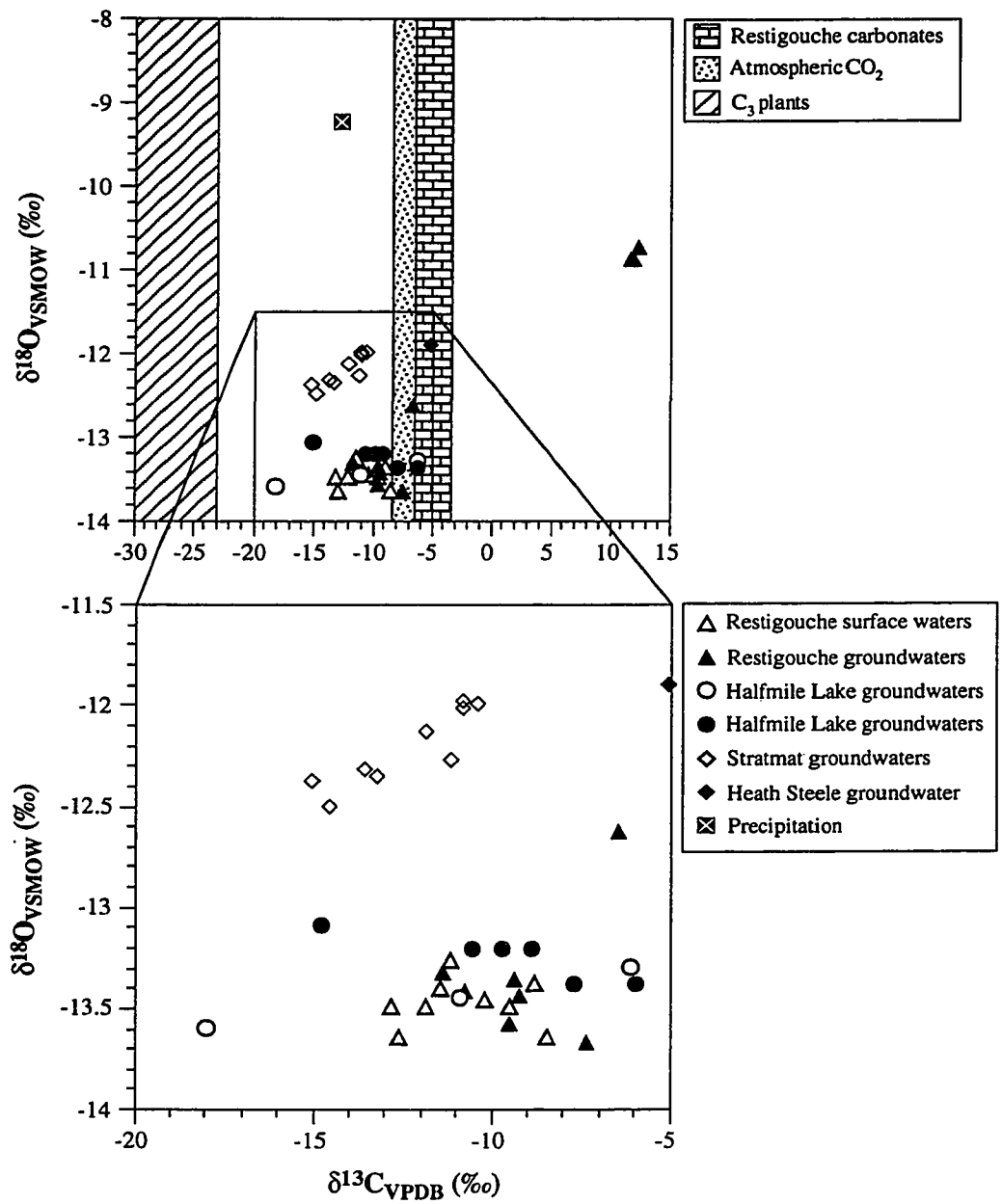


Fig. 11.11 Plots of oxygen and carbon isotopes for ground and surface waters from the Restigouche, Halfmile Lake, Stratmat and Heath Steele deposits (data from Table 11.5). Also shown are the range of carbon isotopic values of C_3 plants and atmospheric CO_2 (from Clark and Fritz, 1997) and of carbonate minerals from veins and fractures at the Restigouche deposit (Table 11.6).

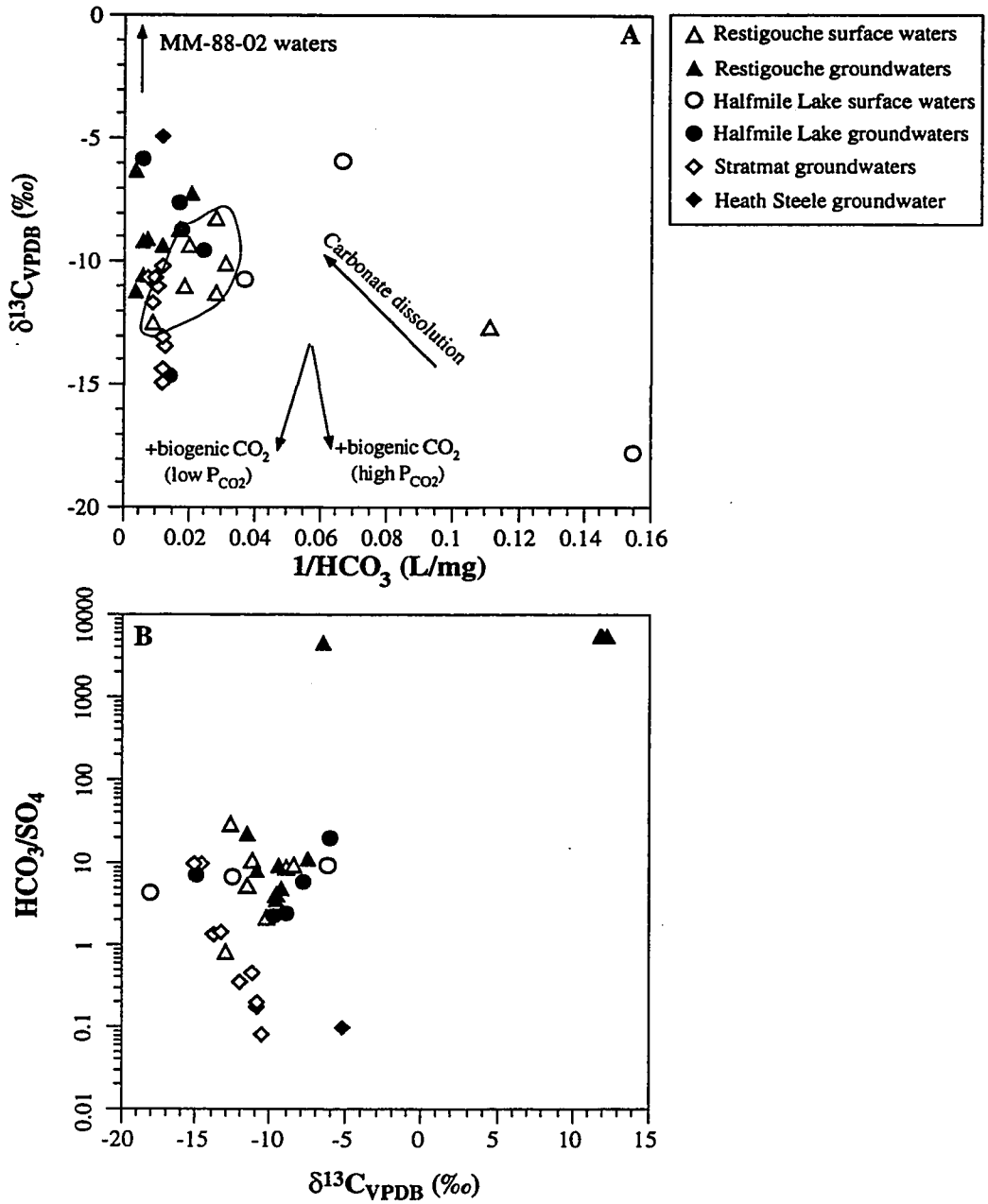


Fig. 11.12 Plots of A) $1/HCO_3$ and B) HCO_3/SO_4 vs $\delta^{13}C_{VPDB}$ for ground and surface waters from the Restigouche, Halfmile Lake, Stratmat and Heath Steele deposits (data from Table 11.5). Also shown are approximate trends for addition of biogenic CO_2 at low and high P_{CO2} (from Taylor and Fox, 1996).

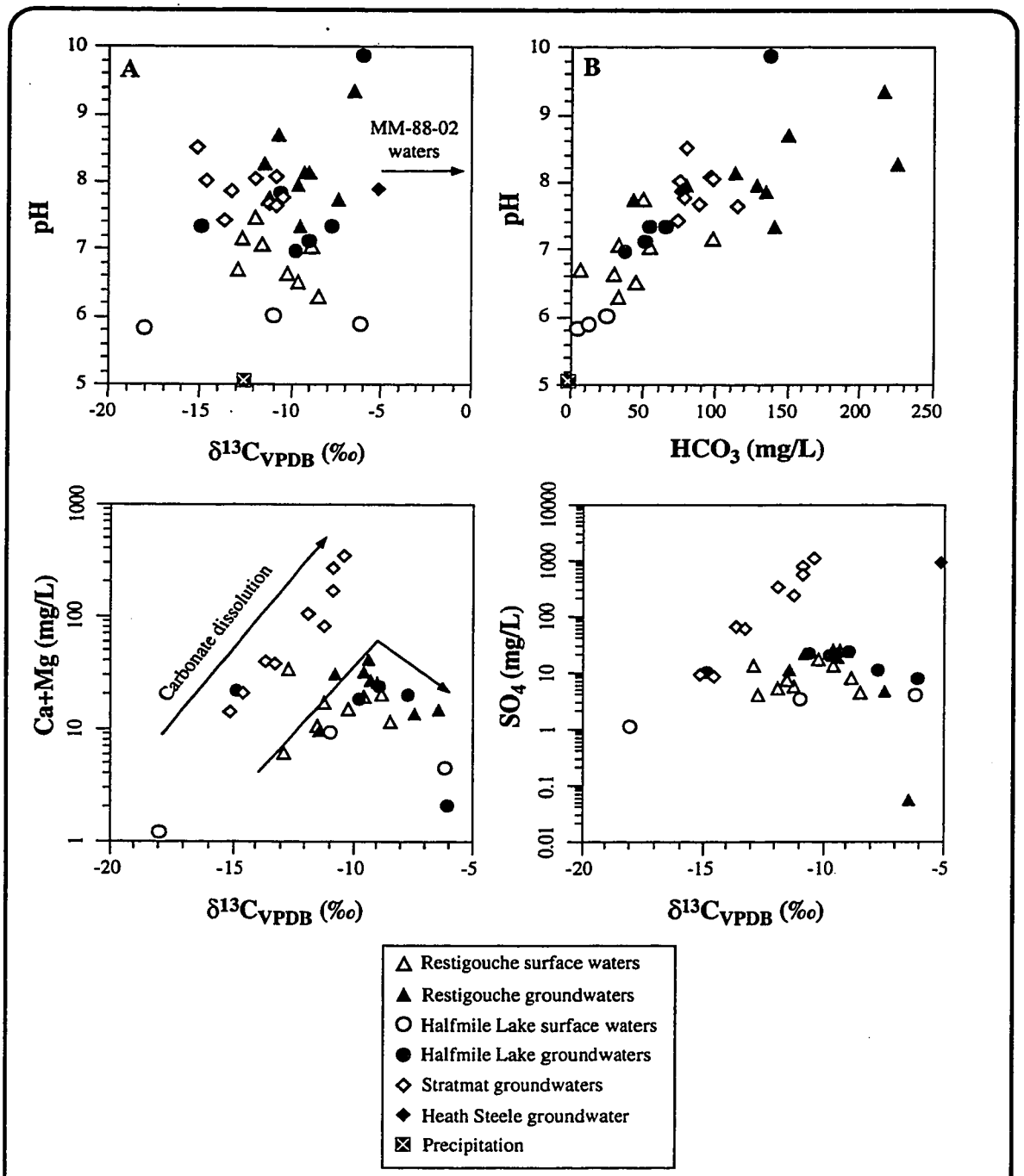


Fig. 11.13 Plots of A) pH vs $\delta^{13}C_{VPDB}$, B) pH vs HCO_3, C) Ca+Mg vs $\delta^{13}C_{VPDB}$ and D) SO_4 vs $\delta^{13}C_{VPDB}$ for ground and surface waters from the Restigouche, Halfmile Lake, Stratmat and Heath Steele deposits (data from Table 11.5).

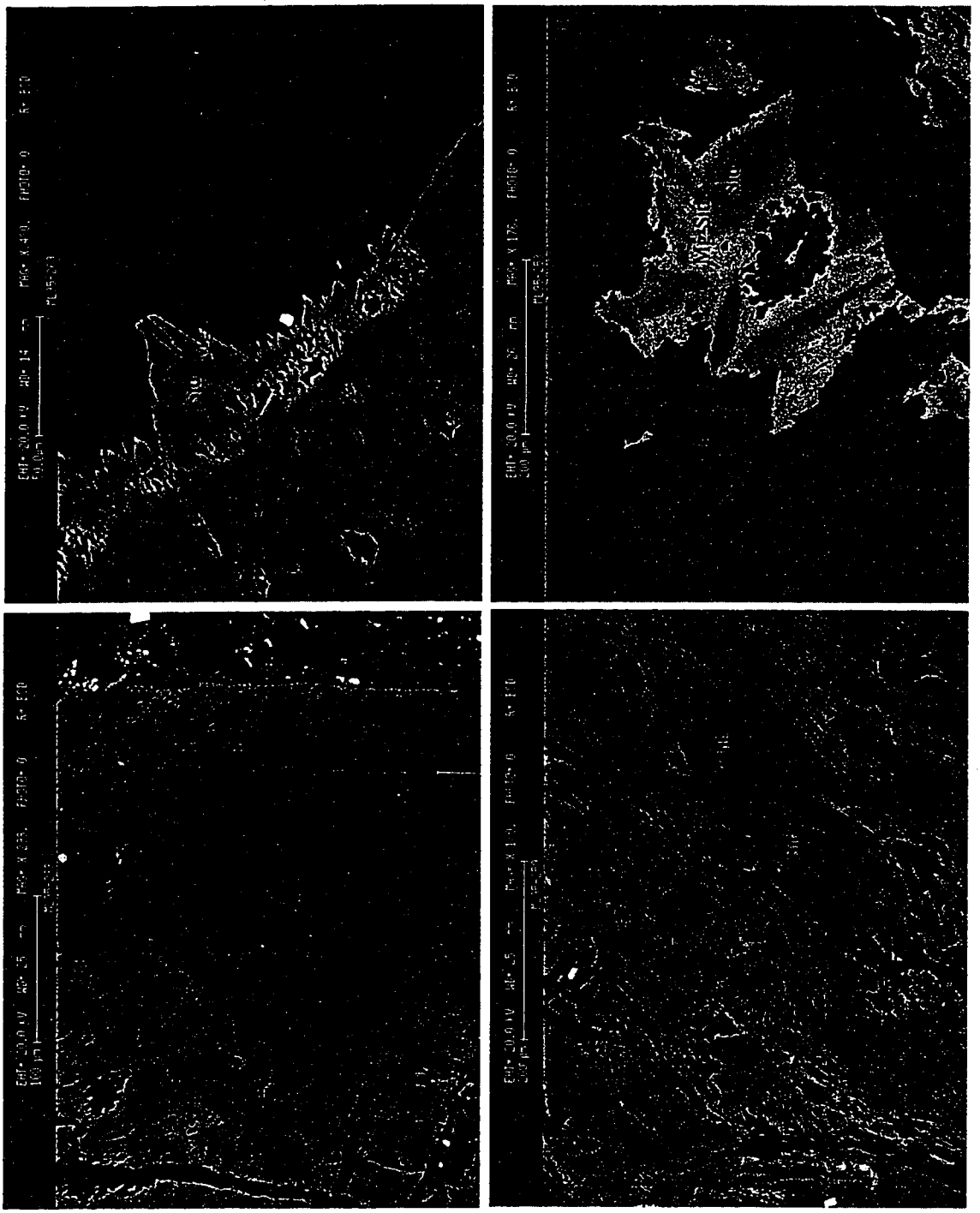


Fig. 11.14 SEM photomicrographs of polished thin section showing carbonate morphology. A) Sample ML95-233. Dolomite (Dol) zones with variable Fe content. Vein cross-cutting sericite (Ser) alteration. B) Sample ML95-269. Calcite (cal) and siderite (Sid) veins. Siderite is zones on variable Mg, calcite zones by variable Mg and fe. C) Sample ML95-259. Siderite (Sid) crystals in chlorite (Chl) and sericite (Ser) alteration. D) Sample ML95-258. Siderite (Sid), zoned by variable Mg, infilling void space with kaolinite (Kao) in albite vein. All samples from the Restigouche deposit.

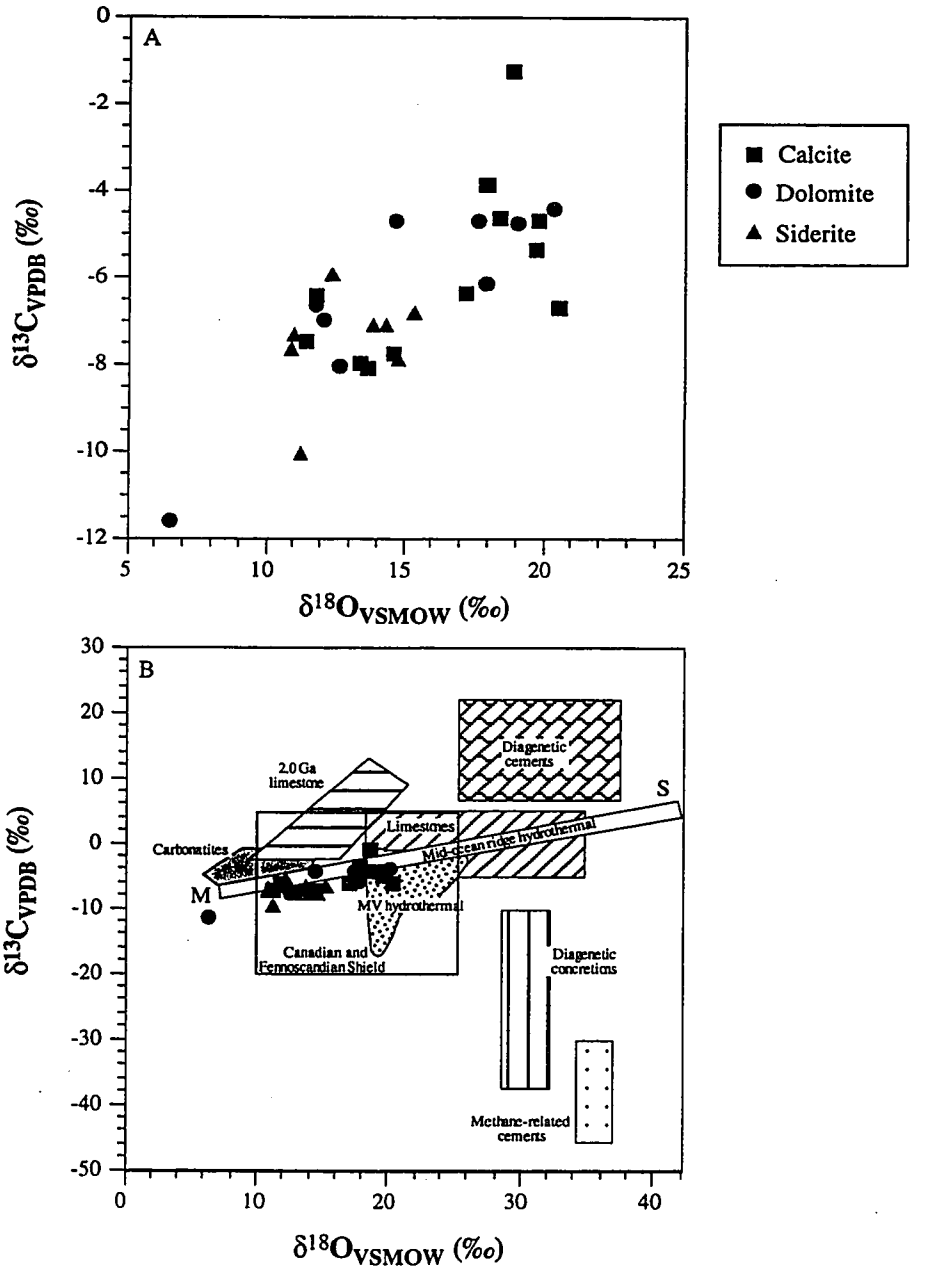


Fig. 11.15 A) Plot $\delta^{13}C_{VPDB}$ vs $\delta^{18}O_{VSMOW}$ for vein and fracture carbonate from the Restigouche and Halfmile Lake deposits. Although SEM data indicated a predominance of ferroan dolomite and siderite, gas pressures during siderite extraction were very low, but generally moderate for calcite extraction (see text for details). Data from Table 11.6. B) Plot $\delta^{13}C_{VPDB}$ vs $\delta^{18}O_{VSMOW}$ of the same carbonate minerals plotted against the fields for carbonates from different environments. Fields modified from Rollinson (1993). M and S represent mantle and seawater carbon end-members for mid-ocean ridge hydrothermal fluids. The open box representing data from Canadian and Fennoscandian Shield areas is based on data from Frape et al. (1992), not including the Stripa Mine, Sweden, where carbonate ranges to very low $\delta^{13}C_{VPDB}$ (-40‰).

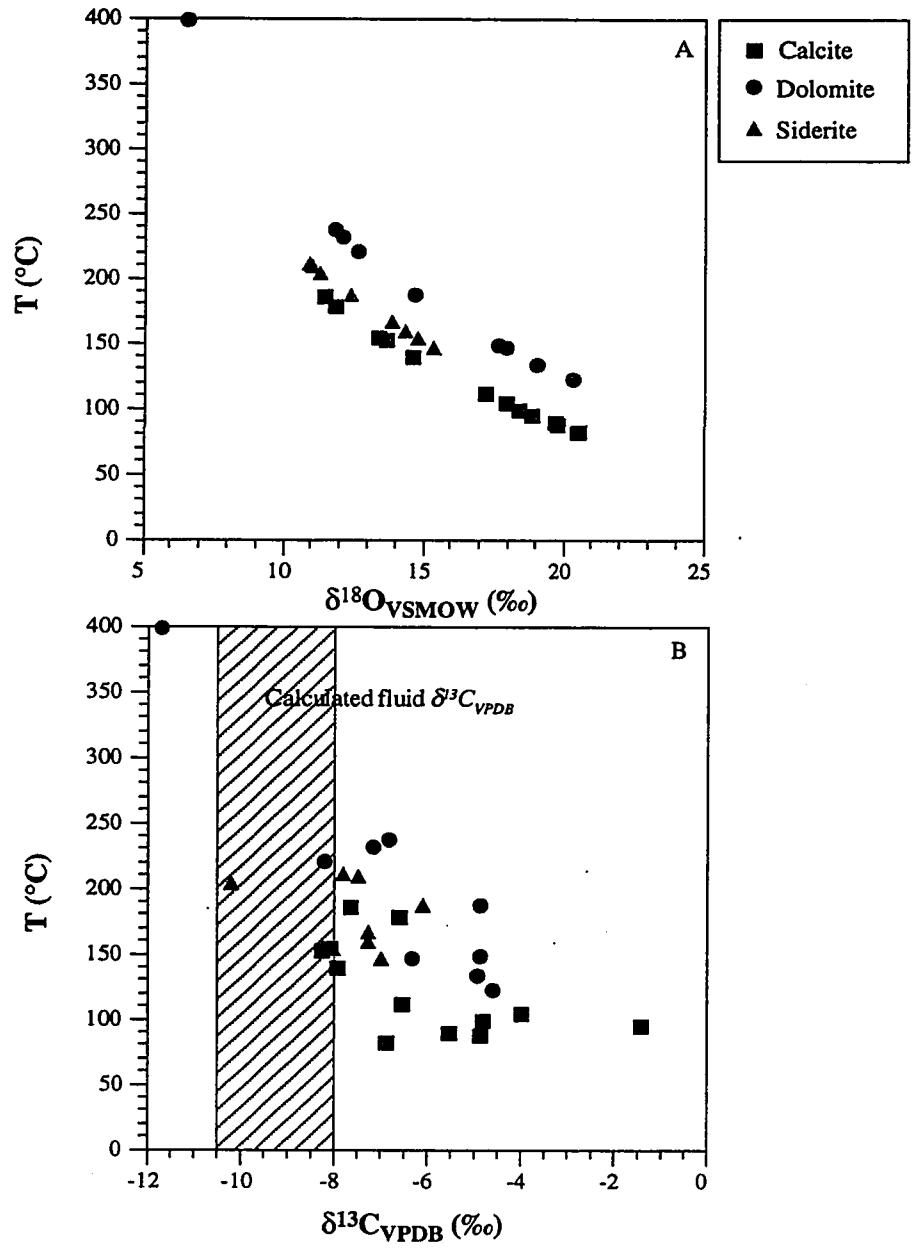


Fig. 11.16 A) Plot $\delta^{18}O_{VSMOW}$ of vein and fracture carbonate from the Restigouche and Halfmile Lake deposits vs calculated temperature of formation assuming a fluid $\delta^{18}O_{VSMOW}$ of -1‰. B) $\delta^{13}C_{VPDB}$ of vein and fracture carbonate vs calculated temperature. Also shown is the $\delta^{13}C_{VPDB}$ of the hydrothermal fluid calculated using the derived temperatures. $\delta^{13}C_{VPDB}$ of the fluid is -9.5±1.5‰ (see text). Data from Table 11.6.

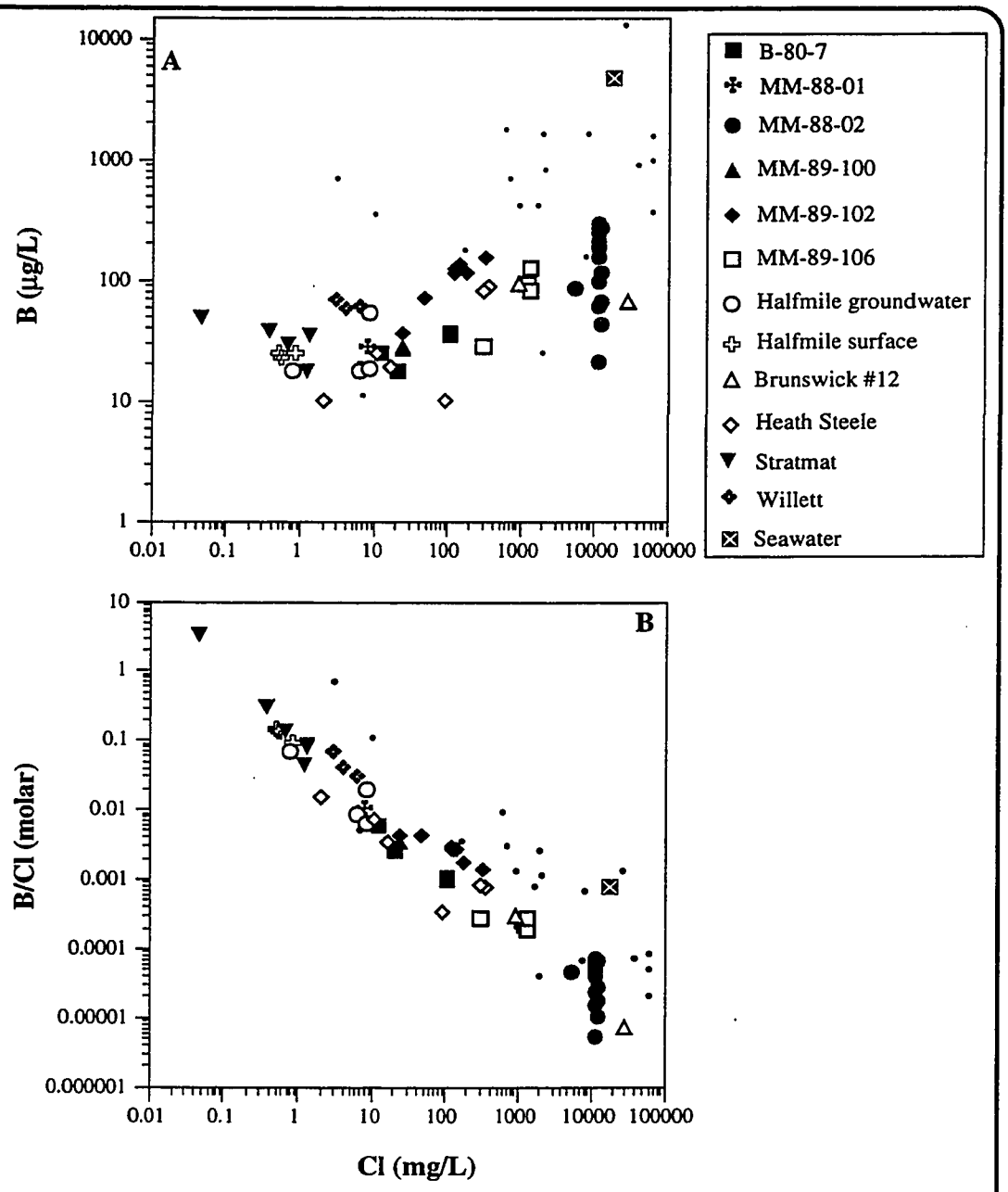


Fig. 11.17 Cl vs A) boron, and B) B/Cl (molar) for ground and surface waters from the study area. Values for seawater are from Vengosh et al. (1991) and Drever (1988). Boron and Cl data from Table 11.7. Small dots represent data from Canadian Shield saline waters (Bottomley et al. 1994).

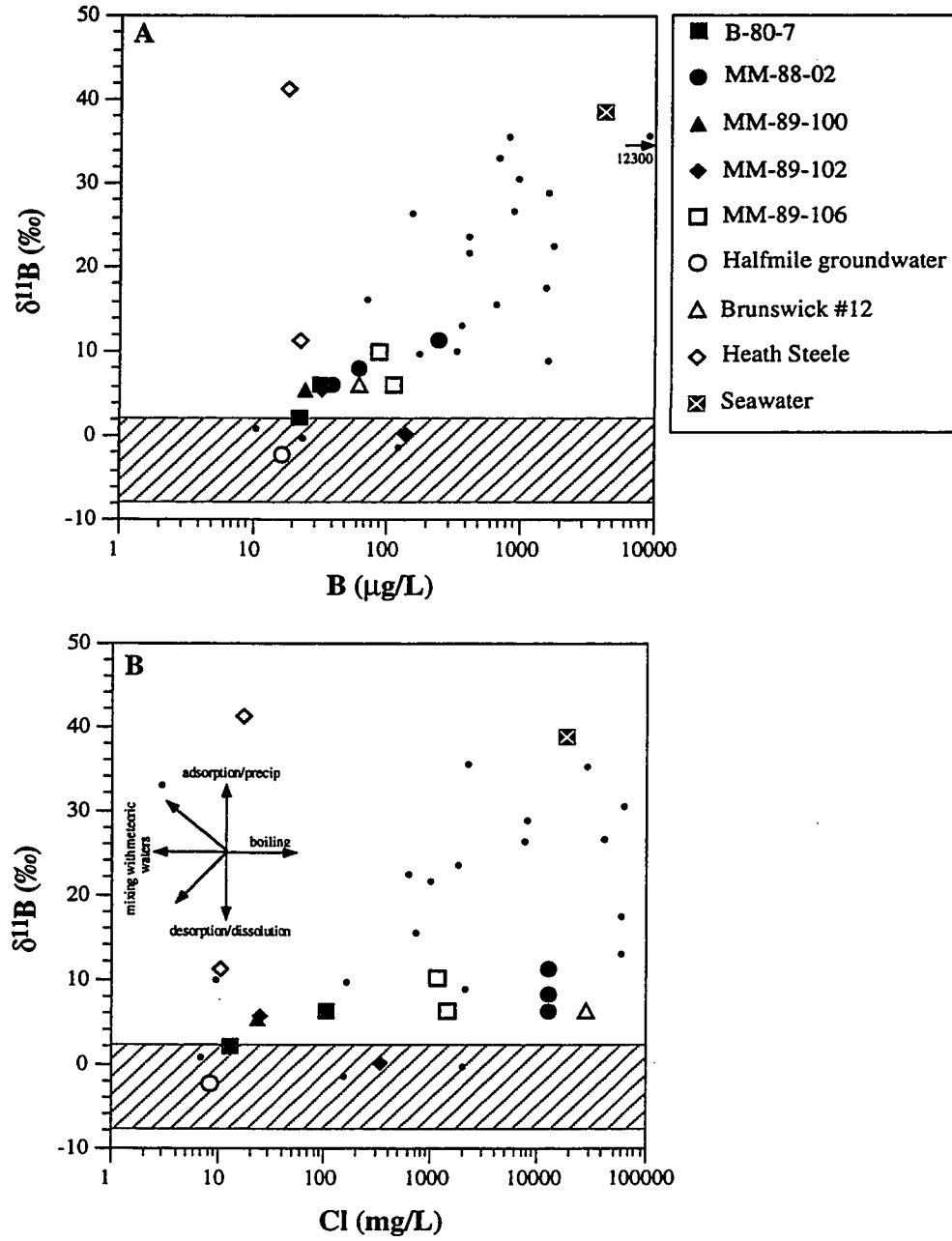


Fig. 11.18 Plot $\delta^{11}B$ vs A) boron, and B) chloride in ground and surface waters from the study area. Values for seawater are from Vengosh et al. (1991) and Drever (1988). Boron data is given in Table 11.7. Shaded region represents average continental crust (Spivak and Edmond 1987). Small dots represent data from Canadian Shield saline waters (Bottomley et al. 1994).

CHAPTER TWELVE:
RADIOGENIC ISOTOPIC COMPOSITION OF GROUND AND SURFACE WATERS, BATHURST MINING CAMP, NEW BRUNSWICK: APPLICATIONS TO WATER-ROCK REACTION AND MINERAL EXPLORATION STUDIES

12.1 Introduction

Radiogenic isotopes are useful in hydrogeochemical studies for understanding the styles and extents of water-rock reactions and, by extension, understanding the mobilization and dispersion of massive sulphide related elements in the secondary environment. The utility of Sr and Pb isotopes derives from the different Rb/Sr, U/Pb and Th/Pb ratios of different minerals such that the isotopic differences between minerals increases with time due to radiogenic decay of ^{87}Rb to ^{87}Sr, ^{238}U to ^{206}Pb, ^{235}U to ^{207}Pb and ^{232}Th to ^{208}Pb. Radiogenic isotopic studies of aqueous systems differ from more traditional studies of whole rock isotopic compositions because different minerals solubilize at different rates due to the kinetic effects of water-rock reactions. Thus, the isotopic composition of ground and surface waters will not necessarily be equivalent to the isotopic composition of the bulk rock, but will more likely reflect the timing and style of water-rock reaction and the mineralogy of the rocks through which the waters have travelled.

Therefore, the purposes of the radiogenic isotope study of ground and surface waters in the Bathurst Camp are as follows:

1) To utilize Sr and Pb isotopes to better constrain reactions between ground and surface waters and the host lithologies. Strontium isotopes have been used in several previous studies of surface waters (e.g. Edmond et al., 1996), groundwaters (Clow et al., 1997; Johnson and DePaolo, 1997) and shield brines and formation waters (Banner et al., 1989; Connolly et al., 1990; Franklyn et al., 1991; McNutt et al., 1990; McNutt et al., 1987). However, Pb isotope studies of natural waters are rare because of low dissolved contents due to the low solubility of

Pb in natural waters. Therefore, Pb isotopic studies have primarily focussed on the suspended load of river waters. For example, Asmeron and Jacobsen (1993) and Allègre et al. (1996) used Pb isotopes of the suspended load of major rivers to estimate the average Pb isotopic composition of the upper continental crust. In this study, the Pb isotopic composition of the dissolved load of selected ground and surface waters from the Bathurst Mining Camp (BMC) was measured.

2) To determine whether Sr isotopes can be used to locate massive sulphide deposits. Massive sulphide deposits in the BMC are commonly associated with spatially extensive halos of hydrothermal minerals, consisting of quartz, sericite and chlorite. Sericite has high Rb/Sr compared to more common rock-forming minerals in the felsic volcanic and volcaniclastic sedimentary host rocks, and should therefore be more radiogenic. Waters interacting with this alteration halo are therefore hypothesized to have more radiogenic $^{87}Sr/^{86}Sr$ than waters interacting with unmineralized bedrock.

3) To characterize the source of Pb anomalies in ground and surface waters by fingerprinting waters using Pb isotopes. Recent studies of tills have shown that Pb isotopes can be used as a vector to massive sulphide deposits (Bell and Franklin, 1993; Lochner, 1996). In the case of the Bathurst Camp, till typically reflects the chemical characteristics of local bedrock due to small glacial dispersion distances (Parkhill and Doiron, 1995) and Pb isotope analyses show a very good correlation between high Pb contents and non-radiogenic Pb typical of sulphide ores (Bell and Franklin, 1993; Lochner, 1996). This relationship is unlikely to hold for waters because Pb can be scavenged by Fe and Mn oxyhydroxides producing "anomalies" due to accumulation of non-ore Pb. Conversely, low Pb levels in waters interacting with massive sulphides may occur as a result the low solubility of Pb. The Pb isotopic composition of ground and surface waters, however, has the potential to more precisely fingerprint the source of dissolved Pb loads and thereby differentiate between mineralized and unmineralized sources.

4) To investigate the utility of analyzing the Nd isotopic composition of dissolved REE in

natural waters. As with Pb, previous studies have focussed on the analysis of Nd isotopes on suspended sediments, primarily to estimate global weathering and river contributions to oceanic elemental budgets (e.g. Allègre et al., 1996). However, Nd isotopic analyses have only rarely been attempted on the "dissolved" REE load of terrestrial waters (e.g. Banner et al., 1989). Of the waters analyzed for REE content in this study (Chapter Ten), seven waters have sufficient Nd to attempt determination of their Nd isotopic composition. Of these seven waters, four were analyzed successfully.

The sampling and analytical methods are presented in Chapter Three. The general geochemical characteristics of the waters discussed in this chapter are discussed in Chapter Five (surface waters) and Chapter Seven (groundwaters).

12.2 Results

12.2.1 Sr isotopic composition of BMC waters

The waters analyzed for the radiogenic isotopes represent a subset of waters from the Restigouche deposit and selected waters from the Heath Steele, Brunswick #12 and Wedge deposits (Table 12.1). These waters were chosen to reflect the range of groundwater compositions encountered in this study.

Surface waters from the Restigouche deposit are moderately radiogenic, with $^{87}Sr/^{86}Sr$ ranging from 0.71324 to 0.71848 for Charlotte Brook, Mt Fowler southwest stream and a stream to the west of the deposit. The seep in the Restigouche deposit gossan has a Sr isotopic value of 0.71599 (Fig. 12.1). The surface waters have moderately high Rb/Sr (0.025 to 0.11) and low Sr contents (6.4 to 32 μg/L) (Figs. 12.1A and 12.2A). One surface water from Mt Fowler east stream is the least radiogenic of all the waters in this study, with a $^{87}Sr/^{86}Sr$ value of 0.70808.

Groundwaters at the Restigouche deposit show similar variability to surface waters in Sr isotopic composition (Fig. 12.1). Shallow groundwaters with high base metal loads recovered from the main ore zone at the Restigouche deposit (boreholes MM-88-01, MM-88-06, and

Table 12.1 Pb and Sr isotopic and abundance results for waters from the Restigouche, Wedge, Heath Steele, and Brunswick #12 deposits

Sample#	Location	$^{206}Pb/^{204}Pb$	$^{207}Pb/^{204}Pb$	$^{208}Pb/^{204}Pb$	Pb	U	U/Pb	$^{87}Sr/^{86}Sr$	Sr	Rb	Rb/Sr
					Waters						
MLW95-300	Seep	18.245	15.666	38.183	4000	0.3	0.0001	0.71599	6.4	0.7	0.1094
MLW95-602	Charlotte Brook	18.182	15.595	38.010	0.409	0.011	0.0269	0.71467	32	0.8	0.0250
MLW95-603	Mt Fowler S	18.316	15.587	38.055	0.131	0.027	0.2061	0.71324	28	0.7	0.0250
MLW95-388	North stream[2]	18.222	15.595	38.016	1.6	0.1	0.0625				
MLW95-467	Mt Vroom NE	18.250	15.643	38.125	2.038	0.007	0.0034				
MLW96-641	Mt Vroom E							0.72167	15	0.5	0.0333
MLW96-664	Mt Fowler E[1]	18.193	15.583	37.980	0.682	0.071	0.1041	0.70808	46	0.5	0.0109
MLW96-711	West of deposit[1]	18.545	15.883	38.710	0.516	0.010	0.0194	0.71848	9	0.6	0.0667
MLW95-586	B-80-7	18.301	15.632	38.134	0.365	0.338	0.926	0.71156	180	1.2	0.0067
MLW95-306	MM-88-01[2]	18.250	15.633	38.113	24	0.1	0.0042	0.71404	100	2.5	0.0250
MLW95-344	MM-88-02[2]	18.258	15.658	38.113	0.2	0.1	0.5	0.71237	88000	28	0.0003
MLW95-601	MM-88-02[2]	*	*	*	0.6	0.1	0.1667	0.71225	89000	27	0.0003
MLW95-606	MM-88-02[2]	*	*	*	0.8	0.1	0.125	0.71223	89000	25	0.0003
MLW95-361	MM-88-06	18.242	15.655	38.141	190	0.028	0.0001	0.71339	43	0.6	0.0140
MLW95-314	MM-88-07[2]	18.262	15.676	38.198	1400	0.1	0.0001	0.71376	69	0.9	0.0130
MLW95-571	MM-89-102							0.71097	360	1.2	0.0033
MLW95-546	MM-89-104	18.220	15.640	38.098	1.735	0.981	0.5654	0.71111	100	1	0.0100
MLW95-504	MM-89-106	18.713	15.815	38.848	0.421	0.989	2.3492	0.71519	580	3.1	0.0053
MLW95-594	MM-89-107	20.203	15.725	40.058	0.248	0.271	1.0927	0.71249	95	0.7	0.0074
MLW95-482	Wedge	18.281	15.658	38.159	72	7	0.0972	0.71490	320	14	0.0438
MLW95-486	Heath Steele							0.71826	2000	35	0.0175
MLW95-610	Heath Steele							0.71932	5000	14	0.0028
MLW95-485	Heath Steele	18.229	15.659	38.130	230	10	0.0435	0.71826	400	4.5	0.0113
MLW95-492	Brunswick #12[2]	18.237	15.671	38.203	3.5	0.1	0.0286	0.72410	880	200	0.2273
					Rocks						
ML95-252	Carbonate	18.303	15.700	38.302				0.708889			
ML95-259	Carbonate	18.262	15.661	38.168				0.714467			
ML95-256	Felsic volcanic	19.661	15.746	39.326	10	4.5	0.4500	0.745397	56	130	2.3214
ML95-262	Dacitic volcanic	19.157	15.724	38.783	8	2.5	0.3125	0.730763	99	100	1.0101
ML95-264	Mafic dyke	18.587	15.676	38.591	5	0.66	0.1320	0.708429	170	3.9	0.0229
ML95-277	Felsic volcanic							0.745655	45	120	2.6667
ML95-285	Felsic volcanic	19.448	15.754	39.806	38	5.5	0.1447	0.739896	50	89	1.7800
ML95-297	Massive sulphide	18.257	15.673	38.197	166000	0.15	0.0000009	0.713662	35	0.5	0.0143
MLS96-664	Stream sediment	17.721	15.576	37.533	52	34	0.6538	0.714138	37	20	0.5405

Water elemental abundances in µg/L; Rock abundances in ppm.

* Insufficient Pb for analysis due to accumulation of salts during sample evaporation.

[1]Low intensity signal for Pb isotopic analysis

[2]U concentration set to half the detection limit where < 0.2 µg/L.

MM-88-07) have $^{87}Sr/^{86}Sr$ values similar to most surface waters, ranging from 0.71339 to 0.71404 (Table 12.1; Fig.12.1). These shallow groundwaters have moderately low Sr contents (43 to 100 μg/L), and Rb/Sr and Sr/Ca similar to the surface waters (Figs. 12.1, 12.2). Shallow groundwaters more distal to the deposit (groundwater MLW95-546 from borehole MM-89-104 and groundwater MLW95-594 from borehole MM-89-107) are less radiogenic than surface waters and groundwaters from the ore zone, with $^{87}Sr/^{86}Sr$ values of 0.71111 and 0.71249, respectively. These waters have similar Sr/Ca and Sr contents as the ore zone groundwaters (95 - 100 μg/L) but somewhat lower Rb/Sr. The more saline waters from the Restigouche deposit are more variable in Sr isotopic composition. Groundwater MLW95-586 from below the ore zone (TDS = 509 mg/L) and groundwater MLW95-571 (borehole MM-89-102; TDS = 693 mg/L) have low Sr isotopic ratios ($^{87}Sr/^{86}Sr$ = 0.71156 and 0.71097, respectively), with the latter having the lowest Sr isotopic ratio of all the groundwaters (Table 12.1). In contrast, the more saline water from borehole MM-89-106 (groundwater MLW95-504, TDS = 2512 mg/L) is more radiogenic, with a $^{87}Sr/^{86}Sr$ value (0.71519) approaching that of the seep water. Finally, the saline waters from borehole MM-88-02 are moderately radiogenic ($^{87}Sr/^{86}Sr$ = 0.71223 - 0.71237) and fall within the field of the brackish waters. The saline waters have much higher Sr contents (180 - 89000 μg/L) and Sr/Ca than the other groundwaters and surface waters and lower Rb/Sr (Figs. 12.1, 12.2).

Five groundwaters were analyzed from other deposits for their Sr isotopic composition, three from the Heath Steele deposit, and one each from the Brunswick #12 and Wedge deposits. The water from the Wedge deposit is moderately radiogenic and is similar to surface waters and shallow groundwaters from the Restigouche deposit with $^{87}Sr/^{86}Sr$ = 0.71490. As discussed previously (see Chapter Seven), this groundwater (MLW95-482) represents shallow groundwater flow through the waste pile at the Wedge deposit and has very low pH and high metal loads. All three waters analyzed from the Heath Steele deposit are more radiogenic than any of the groundwaters from the Restigouche deposit with $^{87}Sr/^{86}Sr$ values ranging from 0.71826 to 0.71932. Despite similar Sr isotopic values, these waters are variable in other

chemical characteristics although all are high-SO_4 waters (see Chapter Seven). The groundwater from the Brunswick #12 deposit (MLW95-492) has the highest salinity of all the waters collected in this study (TDS = 45758 mg/L) and it also has the most radiogenic Sr isotopic signature ($^{87}Sr/^{86}Sr$ = 0.72410) with the highest Rb/Sr and lowest Sr/Ca (Figs. 12.1, 12.2).

Overall, there are two discernible trends between Sr isotopic composition and Rb/Sr (Fig. 12.1A). For shallow groundwaters and surface waters from the Restigouche deposit, the Sr isotopic composition decreases with increasing Sr content, whereas for the mine waters the Sr isotope ratio generally increases with increasing Sr content (Fig. 12.1B). Saline waters from borehole MM-88-02 differ in that they have the highest Sr contents (88000 - 89000 µg/L) but have generally low $^{87}Sr/^{86}Sr$ values and very low Rb/Sr (Fig 12.1). Brackish and saline waters from the Restigouche deposit (boreholes MM-89-102, MM-89-106, B-80-7, and MM-88-02) have higher Sr/Ca and lower Ca/Na than shallow groundwaters, surface waters and mine waters (Fig. 12.2).

The shallow groundwaters and surface waters at the Restigouche deposit have a moderately large range in Sr isotopic composition and have essentially identical $\delta^{18}O_{VSMOW}$ and δD_{VSMOW} values (Fig. 12.2D). More saline waters from the Restigouche deposit and from other mines are distinct in both radiogenic and stable isotopic composition from modern recharge waters. Most brackish to saline waters from the Restigouche deposit are characterized by heavier stable isotopic values and less radiogenic Sr isotopic compositions, whereas, Heath Steele, Wedge, Brunswick #12, and Restigouche deposit groundwater MLW95-504 are characterized by more radiogenic Sr compositions with increasing $\delta^{18}O_{VSMOW}$ (Fig. 12.2D).

12.2.2 Sr isotopic composition of host lithologies

There has been little previous work on Sr isotope analyses of whole rocks or mineral separates for the BMC. Goodfellow and Peter (unpublished data) analyzed several siderite iron formation samples from the Brunswick #12 deposit. The $^{87}Sr/^{86}Sr$ values for these siderite are

moderately radiogenic, ranging from 0.71189 to 0.71508. In this study, five fresh to moderately altered Restigouche host rocks were analyzed (see Table 2.1); three felsic volcanic rocks, a dacitic volcanic rock and a cross-cutting mafic dyke. In addition, two vein carbonates, a massive sulphide, and one stream sediment from Mt Fowler east stream were determined for Sr isotopes (Table 12.1).

The two carbonates are similar to those analyzed by Goodfellow and Peter (unpublished data) in that they range from unradiogenic ($^{87}Sr/^{86}Sr$ = 0.708889) to moderately radiogenic ($^{87}Sr/^{86}Sr$ = 0.714467). The felsic host rocks are the most radiogenic, with $^{87}Sr/^{86}Sr$ values ranging from 0.730763 for the dacite to a high of 0.7456555 for the felsic volcanic rocks (Table 12.1). In contrast, the cross-cutting tholeiitic dyke has the lowest $^{87}Sr/^{86}Sr$ value (0.708429). The massive sulphide (dominantly galena, sphalerite and pyrite) has a moderately radiogenic Sr isotopic composition ($^{87}Sr/^{86}Sr$ = 0.713662) which is similar to the stream sediment from Mt Fowler east stream ($^{87}Sr/^{86}Sr$ = 0.714138).

12.2.3 Pb isotopic composition of BMC waters

A total of eighteen waters were analyzed for the Pb isotopic composition of the "dissolved" load. As discussed in Chapter Seven, Pb has a strong affinity for adsorption onto colloidal surfaces and it is possible that some of the Pb analyzed is not truly dissolved but bound to colloids less than the filter size used (0.45 μm). Most of the waters analyzed fall close to the two-stage Stacey-Kramers evolution curve (Fig. 12.3). The least radiogenic BMC waters and galena (Table 12.2; Thorpe et al. unpublished data) plot close to the age of the host rocks (around 465 - 470 Ma; Chapter Two) on the Stacey-Kramers Pb isotope growth curves for both $^{207}Pb/^{204}Pb$ vs $^{206}Pb/^{204}Pb$ and $^{208}Pb/^{204}Pb$ vs $^{206}Pb/^{204}Pb$ (Fig. 12.3).

Seven surface waters were analyzed from the Restigouche deposit, six stream waters and the seep in the gossan. All the surface waters are non-radiogenic, with the exception of surface water MLW96-711 which had very low intensity Pb signal during analysis. The $^{206}Pb/^{204}Pb$ ratios for the other six surface waters range between 18.182 and 18.316, the $^{207}Pb/^{204}Pb$

ratios from 15.587 to 15.666, and the $^{208}Pb/^{204}Pb$ ratios from 38.010 and 38.183. Surface water MLW96-711 is more radiogenic with values of 18.545, 15.883, and 38.710 for the three Pb isotope ratios, respectively. Lead contents are low in the stream waters (0.13 to 2.04 µg/L), but highly elevated in the seep water (4000 µg/L). In terms of the $^{206}Pb/^{204}Pb$ values, all the stream waters, except surface water MLW96-711, plot in the field of galena from the BMC (Figs. 12.4, 12.5). However, although surface waters MLW95-467 and MLW95-300 also have $^{207}Pb/^{204}Pb$ and $^{208}Pb/^{204}Pb$ ratios similar to BMC galena, the other four surface waters are unusually low in both isotope ratios and plot significantly below the other waters and below BMC galena (Fig. 12.4).

Table 12.2 Pb isotopes in galena from the Bathurst Mining Camp

Deposit	$^{206}Pb/^{204}Pb$	$^{207}Pb/^{204}Pb$	$^{208}Pb/^{204}Pb$
Brunswick No. 12	18.187	15.649	38.100
Brunswick No.6	18.277	15.663	38.219
Austin Brook	18.247	15.658	38.140
Key Anacon	18.247	15.658	38.140
Heath Steele	18.199	15.652	38.124
Stratmat	18.207	15.641	38.116
Wedge	18.275	15.662	38.198
Armstrong "A"	18.287	15.655	38.166
Rocky Turn	18.319	15.668	38.269
Orvan Brook	18.305	15.653	38.195
Caribou	18.276	15.654	38.187
Murray Brook	18.309	15.669	38.219
Halfmile Lake	18.217	15.659	38.152
Chester	18.302	15.659	38.215
Strachans Lake Brook	18.223	15.649	38.119
Canoe Landing Lake	18.243	15.653	38.191
Restigouche	18.241	15.648	38.163
Willett showing	18.295	15.651	38.186
Armstrong "B"	18.298	15.660	38.233
Portage Lakes	18.230	15.647	38.143
Captain	18.279	15.657	38.161

Source: Thorpe et al. (unpublished data).

The groundwaters from the Restigouche deposit are generally non-radiogenic. Groundwaters from boreholes that directly intersect the main ore body have elevated Pb contents, ranging from 24 to 1400 μg/L (Table 12.1). These waters (boreholes MM-88-01, MM-88-06 and MM-88-07) all have values essentially identical to BMC galena (Figs. 12.4, 12.5). Similarly, groundwater MLW95-586 from borehole B-80-7 also has Pb isotopic values close to BMC galena. This is an interesting result because this borehole penetrates the ore zone and this packer groundwater was recovered from 223 m depth, well below the massive sulphides. The Pb content of this groundwater is low (0.42 μg/L) and the fact that it reflects ore-Pb isotopic values may indicate that there is minor galena in the stringer zone below the massive sulphides.

The most saline waters from the Restigouche deposit, from borehole MM-88-02, proved difficult to analyze because of their high salinity. Of the three groundwaters analyzed, only one yielded a Pb isotopic composition. Thick salt accumulations during sample evaporation prevented analysis of the other two groundwaters (Table 12.1). Groundwater MLW95-344, as with the other waters from boreholes intersecting the ore zone, has Pb isotopic values similar to BMC galena. However, the saline waters from borehole MM-88-02 are interpreted to be derived from a major fracture at around 236 m based on downhole geophysical evidence (see Chapter Four). This is well below the massive sulphides in this hole (75-85 m). This groundwater was recovered by flow-through bailer (whereas, MLW95-601 and MLW95-606 are packer groundwaters) making it possible that the standing water column was influenced by Pb derived from the massive sulphides. This cannot be tested until the Pb from the straddle-packer groundwaters can be analyzed.

Groundwater MLW95-546 was recovered from a borehole over 1 km to the west of the main ore body at the Restigouche deposit. This borehole was drilled in 1989 to test a gravity anomaly for potential mineralization at depth. No massive sulphides were recovered from this borehole (Westoll, 1990) although groundwater MLW95-546 has moderate Pb abundance (1.7 μg/L) and a Pb isotopic composition similar to BMC galena (Figs. 12.4, 12.5).

The only groundwaters from the Restigouche deposit with non-ore values are from the two drill holes east of the deposit, boreholes MM-89-106 and MM-89-107. These two groundwaters define a vector towards the ore deposit in that the least radiogenic (MM-89-106) is closer to ore values. Groundwater MLW94-504 (MM-89-106) has values of 18.713 for $^{206}Pb/^{204}Pb$, 15.815 for $^{207}Pb/^{204}Pb$, and 38.848 for $^{208}Pb/^{204}Pb$, whereas groundwater MLW95-594 (MM-89-107) has values of 20.203, 15.725, and 40.058 for the same ratios (Table 12.1). The most radiogenic groundwater, MLW95-594, has Pb isotopic values which fall on similar Pb isotope growth curves as the other Restigouche deposit waters (Fig. 12.3). Groundwater MLW95-504, in contrast, has anomalously high $^{207}Pb/^{204}Pb$ values (Figs. 12.3, 12.4).

The groundwaters from the three past and presently producing mines, Wedge, Heath Steele, and Brunswick #12 all have Pb isotopic compositions similar to BMC galena (Table 12.1; Figs. 12.4, 12.5). These waters have moderate to high Pb contents (3.5 to 230 μg/L) and are highly variable in all other chemical parameters (Chapter Seven).

12.2.4 Pb isotopic composition of host lithologies

A small number of rocks and mineral separates were analyzed to assist in the interpretation of radiogenic isotopes in water (Table 12.1). Four host rocks were determined including two felsic volcanic rocks, a volcanic rock of dacitic composition, and a mafic dyke. In addition, two vein carbonates, one massive sulphide, and an Fe-oxyhydroxide-rich stream sediment were analyzed (Table 12.1).

The four whole rocks from the Restigouche deposit span a wider range in isotopic composition than the tills and granites (Fig. 12.4). The Pb isotopic compositions become increasingly radiogenic from mafic dyke to dacite to felsic volcanic. The most radiogenic whole rock (ML95-285) is close to the most radiogenic groundwater (Fig. 12.4). Generally, carbonate that formed at the same time as the ore deposit would be expected to be radiogenic because U substitutes into the carbonate mineral structure. However, both carbonates (ML95-

252 and ML95-259) are non-radiogenic, with compositions that fall close to and within the range of BMC galena. The massive sulphide has a Pb isotopic composition similar to the carbonates and falls within the range for BMC galena (Fig. 12.4). The massive sulphide is very Pb-rich, containing 16.6 weight % Pb.

Stream sediment MLS96-664 was analyzed in order to test if Fe-oxide-rich sediments in Mt Fowler east stream (see Chapters Five and Six for descriptions of stream waters and stream sediments, respectively) were the products of oxidation of pyritic or massive sulphides in the subsurface. Although surface waters have moderately low Pb and Zn contents, stream sediments have elevated Zn (1600 ppm), but only moderate Pb (56 ppm). This sediment has the least radiogenic Pb isotopic composition of any of the samples analyzed in this study. In fact, to my knowledge, there has been no Pb isotope analysis from the BMC which is this low in radiogenic Pb.

Previous studies using Pb isotopes in the BMC also aid to constrain the variation in Pb isotopes for the host lithologies in the camp. Thorpe et al. (unpublished data, cited in McCutcheon et al., 1993) reported Pb isotopic analyses of galena for a number of the VMS occurrences in the Bathurst Mining Camp (Table 12.2). For all deposits, there is a restricted variation in the Pb isotopic composition (Fig. 12.4). The $^{206}Pb/^{204}Pb$ ratios range between 18.187 and 18.319, the $^{207}Pb/^{204}Pb$ ratios range from 15.641 to 15.669, and the $^{208}Pb/^{204}Pb$ ratios are between 38.100 and 38.269 (Table 12.2).

Plutonic rocks from the BMC are much more radiogenic than BMC galena, with $^{206}Pb/^{204}Pb$ ratios ranging between 18.353 and 18.770, the $^{207}Pb/^{204}Pb$ ratios ranging from 15.675 to 15.709, and the $^{208}Pb/^{204}Pb$ ratios between 38.232 and 38.707 (Whalen et al., in press). Note, however, that the least radiogenic pluton is close to ore values. Samples of till were also collected in order to test the utility of Pb isotopic analyses in mineral exploration in the BMC (Doherty et al., 1997; Hussein, 1996; Lochner, 1996). Till spans much of the compositional range exhibited by the galena and granitoid analyses (Fig. 12.4).

12.2.5 Nd isotopic composition of BMC waters

A small number of Nd isotopic measurements were attempted, and four groundwaters were analyzed successfully (Table 12.3; Fig. 12.6). Analysis of Nd isotopes on the dissolved REE component of natural waters is difficult due to the typically low REE abundances. For example, of more than 200 REE analyses in this study, only six waters had Nd > 0.5 μg/L (see Chapter Ten). Detailed descriptions of the REE in the waters analyzed for Nd isotopes are presented in Chapter Ten. The four groundwaters determined successfully have high REE contents, with ΣREE ranging from 3.1 to 690 μg/L. All four waters are characterized by Ca-SO_4 compositions with elevated Fe (4400 to 650000 μg/L) and base metal (e.g., Zn ranges from 3600 to 340000μg/L) contents. The waters all have low pH (2.33 to 6.56 for field pH and 2.57 to 3.33 for lab pH measurements). The waters, however, differ in REE abundances and REE profiles. Seep water MLW95-300 from the Restigouche deposit has the lowest REE abundances of the four waters and is characterized by a generally flat LREE profile compared

Table 12.3. Nd isotopic and abundance results for BMC waters

Groundwater	Location	$^{143}Nd/^{144}Nd$	error	Nd	Sm	Sm/Nd
MLW95-300	Restigouche	0.512304	0.000030	0.75	0.41	0.5467
MLW95-482	Wedge	0.512296	0.000018	45.61	11.55	0.2532
MLW95-485	Heath Steele	0.512204	0.000014	70.59	16.39	0.2322
MLW95-486	Heath Steele	0.512164	0.000023	112.09	15.91	0.1419

Elemental abundances in μg/L (ICP-MS data; Chapter Ten).

to chondrite (Fig. 12.7). The heavy REE were not detected for this seep. Seep water MLW95-300 is also characterized by a moderately strong negative Ce anomaly. In contrast, the other three groundwaters from the Wedge and Heath Steele deposits (Table 12.3) have elevated REE

contents. Groundwaters MLW95-482 (Wedge) and MLW95-485 (Heath Steele) have convex-up NASC-normalized REE patterns and are strongly LREE enriched with $[La/Sm]_{chon} > 1$ (Fig. 12.7). Groundwater MLW95-486 (Heath Steele) has a strong positive Eu anomaly, similar to massive sulphides from the Halfmile Lake deposit (Chapter Ten).

As a result of these differences in REE patterns, the waters have different Sm/Nd ratios, ranging from 0.5467 to 0.1419 (Table 12.3). Similarly, the waters vary in their Nd isotopic composition with $^{143}Nd/^{144}Nd$ ratios ranging from 0.512304 to 0.512164 (Fig. 12.6). There is a moderate positive correlation between $^{147}Sm/^{144}Nd$ and $^{143}Nd/^{144}Nd$ (Fig. 12.6A) and a negative correlation between $^{143}Nd/^{144}Nd$ and $^{87}Sr/^{86}Sr$ (Fig. 12.6B).

12.2.6 Nd isotopes of host lithologies

As with the Sr and Pb data, a limited number of analyses for Nd isotopes were carried out on whole rocks and mineral separates from the Restigouche deposit (Table 12.4). Samples analyzed include two vein carbonates, a mafic dyke, four felsic volcanic rocks, and an Fe-rich stream sediment. The four felsic rocks have similar Nd isotopic compositions and are non-radiogenic with $^{143}Nd/^{144}Nd$ ranging from 0.512103 to 0.512191 (Fig. 12.6). The mafic dyke is the most radiogenic of the whole rocks, with a $^{143}Nd/^{144}Nd$ vale of 0.512747. The stream sediment is intermediate between the mafic and felsic rocks, implying a contribution from both mafic and felsic rocks (Fig. 12.6). The carbonate veins span a wide range in Nd isotopic composition. Sample ML95-252 is slightly less radiogenic than the mafic dyke, whereas, carbonate ML95-259 is extremely radiogenic, with a $^{143}Nd/^{144}Nd$ value of 0.515347.

With the exception of carbonate from a vein (ML95-259), the other rocks and the four waters form an array between the mafic dyke with radiogenic Nd and non-radiogenic Sr isotopic compositions and the felsic volcanic rocks with radiogenic Sr and non-radiogenic Nd (Fig. 12.6B). The stream sediment and waters fall between these two end-members.

Table 12.4. Nd isotopic and abundance results for Restigouche deposit whole rocks and carbonate

Sample	Type	$^{143}Nd/^{144}Nd$	error	Nd	Sm	Sm/Nd
ML95-252	Carbonate	0.512582	0.000020	11.2	4.62	0.4125
ML95-259	Carbonate	0.515347	0.000016	2.13	4.33	2.035
ML95-256	Felsic volcanic	0.512174	0.000023	31	6.5	0.2097
ML95-262	Dacitic volcanic	0.512191	0.000016	26	5.4	0.2077
ML95-264	Mafic dyke	0.512747	0.000014	20	5.1	0.2550
ML95-277	Felsic volcanic	0.512170	0.000015	110	22	0.2000
ML95-285	Felsic volcanic	0.512103	0.000011	43	9.0	0.2093
MLS96-664	Stream sediment	0.512435	0.000012	15	3.7	0.2467

Elemental abundances in ppm (ICP-MS data; Chapter Two).

12.3 Discussion

12.3.1 Sr isotopes

The primary control over the Sr isotopic composition of a water is the lithology and mineralogy through which the water has flowed, and the time and length of the flow path. In addition, the age of the host rocks is critical given that older rocks will have greater amounts of time to produce ^{87}Sr through ^{87}Rb decay. These factors make it difficult to meaningfully compare the $^{87}Sr/^{86}Sr$ values of BMC waters to other studies, because of variations in the age and composition of host lithologies. However, the Sr isotopic compositions of BMC surface and groundwaters are within the range shown by surface and groundwaters in previous studies (e.g. Bullen et al., 1996; Franklyn et al., 1991; Johnson and DePaolo, 1997; Lent et al., 1997; McArthur et al., 1989; McNutt et al., 1987; Othman et al., 1997; Pande et al., 1994), although most of the BMC waters are higher than the median $^{87}Sr/^{86}Sr$ value for world rivers (Holmden et al., 1997). All of the waters are more radiogenic than modern seawater which has a uniform $^{87}Sr/^{86}Sr$ value of 0.70921 to 0.70924 (Veizer, 1989). The BMC waters are also more radiogenic than middle Ordovician seawater (Veizer, 1989).

The most saline BMC waters (waters from borehole MM-88-02 at the Restigouche deposit

and from the Brunswick #12 deposit) share some geochemical similarities with brines from the Canadian Shield (Chapter Seven). The BMC saline waters fall within the range for brines from the Canadian Shield which vary between 0.707 and 0.755 for $^{87}Sr/^{86}Sr$ (Franklyn et al., 1991; McNutt et al., 1987).

There are several possible trends that can be discerned from the $^{87}Sr/^{86}Sr$ vs Rb/Sr and 1/Sr plots (Fig. 12.1). The surface waters, shallow groundwaters and saline waters from borehole MM-88-02 may define a mixing/evolutionary trend such that with increasing water-rock interaction, Sr content increases and the isotopic ratio is increasingly controlled by the isotopic composition of the most soluble phases in the host rocks. This type of trend was observed previously at the Eye-Dashwa Lakes Pluton (Franklyn et al., 1991), where the deeper saline waters had a common value essentially identical to plagioclase phenocrysts in the host-rock. However, given the quite different trace element ratios, major cation chemistry and stable isotopes between the shallow groundwaters and the saline waters at the Restigouche deposit, it is unlikely that these different waters are in any simple way related. Indeed, it was shown previously (Chapter Seven, Eleven) that major and trace element and stable isotopic considerations preclude simple mixing between shallow groundwaters and a saline end-member, such as the MM-88-02 waters, to produce the range of groundwater compositions recovered from the Restigouche deposit. In particular, the $^{87}Sr/^{86}Sr$ value for the brackish water from the bottom of borehole MM-89-106 (groundwater MLW95-504) is inconsistent with simple mixing between shallow waters and deep saline waters at Restigouche; the Sr isotopic composition of this water is too radiogenic compared to the other Restigouche groundwaters (Fig. 12.1, 12.2). The Sr data for the surface waters and shallow groundwaters may not be a simple mixing relationship, but rather may represent both increasing degrees of water-rock interaction with increasing Sr and lower $^{87}Sr/^{86}Sr$ ratios indicating an increasing component from plagioclase (low Rb/Sr silicate) weathering. In addition, the groundwaters with the lowest $^{87}Sr/^{86}Sr$ ratios are those that are more distal to the orebody; the more radiogenic groundwaters more intimately associated with the orebody may be influenced to a

greater degree by carbonate dissolution and/or K-silicate (high Rb) minerals associated with hydrothermal alteration.

The high $^{87}Sr/^{86}Sr$ but low Sr contents in the shallow groundwaters and surface waters close to the Restigouche ore body most likely represents easily dissolved, weathered materials in the soil/till zone and/or the shallowest portion of the bedrock. At the Restigouche deposit, examination of drill core showed that the uppermost 20-50 meters of bedrock is highly weathered and broken. In addition, although vein and vug carbonate is common lower in the stratigraphy, much of the carbonate has largely been weathered out of the upper part of the section, perhaps indicating that carbonate minerals are dominating the isotopic signature of the shallow groundwaters and surface waters. Carbonate minerals reported here and those analyzed by Peter and Goodfellow (in prep) have $^{87}Sr/^{86}Sr$ values between 0.708889 and 0.71508.

Strontium isotope ratios decrease in Restigouche deposit waters with increasing water-rock reaction, indicating that the waters are increasingly influenced by low-K (and therefore low Rb and low Rb/Sr) mineral(s). The trend shown by the shallow groundwaters and surface waters is similar to Andean rivers and other river waters (Edmond et al., 1996). Edmond et al. (1996) suggested that this trend reflected mixing between waters derived from weathering of carbonate units with high Sr and non-radiogenic $^{87}Sr/^{86}Sr$ with waters derived from silicate weathering with low Sr and high $^{87}Sr/^{86}Sr$. However, for the Restigouche deposit, carbonate close to the ore deposit is more radiogenic than the groundwaters further away from the ore deposit, with the exception of carbonate ML95-252. This carbonate may not be representative of most of the hydrothermal carbonate associated with the ore deposit as it has carbon isotopic compositions that span a wide range compared to other carbonates from the Restigouche deposit (see Chapter Eleven).

There is a moderate positive correlation between $^{87}Sr/^{86}Sr$ and Rb/Sr (Fig.12.1). The most saline waters (MM-88-02 waters and Brunswick #12), are at opposite ends of the spectrum. This indicates that, at least for Sr, they have "seen" very different minerals and/or have mixed

with very different fluids. Thus, it is most likely that there is a trend between the surface waters/shallow groundwaters and the deeper brackish waters (except those from borehole MM-89-106) at the Restigouche deposit, and that the saline waters from borehole MM-88-02 are unrelated to this trend. The low $^{87}Sr/^{86}Sr$ for saline borehole MM-88-02 groundwaters is perhaps suggestive that these waters may have equilibrated with more mafic host rocks than for the other saline waters. This would be consistent with the high Cr, Co, Ni, and Cu values in these groundwaters compared to other groundwaters from the Restigouche deposit. Influence from the mafic sills/dykes would imply that these waters are locally derived, or at least that their Sr isotopic composition is locally derived, or that the sills represent preferential fluid pathways for these saline groundwaters. In fact, the very low $^{87}Sr/^{86}Sr$ coupled with very high Sr concentrations in the MM-88-02 waters indicates that its Sr isotopic composition was derived from dissolution of a low Rb/Sr mineral(s) with high Sr. Although there is extensive development of carbonate veins and fractures in the footwall to the Restigouche deposit (Chapter Eleven), the $\delta^{13}C_{VPDB}$ data is not consistent with carbonate dissolution as the source of the non-radiogenic Sr. The MM-88-02 waters have highly elevated $\delta^{13}C_{VPDB}$ (+12 ‰) indicative of methanogenic reactions, whereas, the local vein carbonates have much lower $\delta^{13}C_{VPDB}$ (most are between -4 and -8 ‰; Table 11.5). The mafic dyke (ML95-264) has the least radiogenic Sr isotopic composition of all the rock samples (Table 12.1) and therefore is the best source of low $^{87}Sr/^{86}Sr$.

For the Brunswick #12 groundwater (MLW95-492), the low Sr contents but radiogenic Sr isotopic signature is not consistent with dissolution of carbonate or plagioclase feldspar. Rather, the Brunswick #12 groundwater is most consistent with dissolution of a high Rb/Sr mineral such as K-feldspar or mica. This also agrees with much higher K/Na for this groundwater compared to other saline waters in the BMC. The low Sr/Ca ratio for this groundwater suggests that mica dissolution exerted a greater influence than K-feldspar dissolution. This could be a reflection of the more intense and extensive alteration halo associated with the Brunswick #12 deposit (Lentz and Goodfellow, 1993a; Lentz and

Goodfellow, 1996) and/or longer, more closed-system, water-rock reactions. In contrast, the brackish water from borehole MM-89-106 at the Restigouche deposit is moderately radiogenic with higher Sr/Ca and very low Ca/Na, suggesting that this water may have equilibrated with a high Rb/Sr mineral which also has high Sr, such as K-feldspar. The felsic volcanic rocks at the Restigouche deposit are more radiogenic than groundwater MLW95-492 from the Brunswick #12 deposit (Fig. 12.1).

Banner et al. (1989) suggested that in-situ growth of ^{87}Sr in saline waters from Missouri is negligible due to the low Rb/Sr of the waters. This is also true for the brackish and saline waters from the Restigouche and Heath Steele deposits which have Rb/Sr « 0.1 (Table 12.1). The notable exception to this is groundwater MLW95-492 from the Brunswick #12 deposit which has Rb/Sr = 0.227. Assuming that the water is the same age as the host lithology, the initial $^{87}Sr/^{86}Sr$ would be 0.71988, compared to the present day $^{87}Sr/^{86}Sr$ of 0.72410 (in the water). By comparison, the saline waters from borehole MM-88-02 have Rb/Sr = 0.0003. Again, assuming that the water is the same age as the host lithology, the initial $^{87}Sr/^{86}Sr$ would be 0.712227, compared to the present day $^{87}Sr/^{86}Sr$ of 0.712233 (groundwater MLW95-606; Table 12.1). Thus, in-situ growth is negligible for all waters except groundwater MLW95-492 if it is very old.

A different trend is also evident from the $^{87}Sr/^{86}Sr$ vs Rb/Sr and $^{87}Sr/^{86}Sr$ vs 1/Sr plots (Fig. 12.1) and $\delta^{18}O_{VSMOW}$ vs $^{87}Sr/^{86}Sr$ plot (Fig. 12.2) for the Heath Steele and Wedge deposit groundwaters. This trend shows increasingly radiogenic Sr with increasing Sr contents, lower Rb/Sr and heavier $\delta^{18}O_{VSMOW}$ values. All four of these groundwaters are Ca-SO_4 to Na-Ca-SO_4-type waters. The trend to higher $^{87}Sr/^{86}Sr$ is consistent with increasing water-rock reactions (producing higher Na/Ca and Sr/Ca; Fig. 12.2). The Wedge deposit groundwater has the shortest flow path of the four groundwaters and has the $^{87}Sr/^{86}Sr$ value closest to that of the surface waters and shallow groundwaters near the Restigouche deposit (Fig. 12.1). Groundwaters MLW95-485 and MLW95-486 are Ca-SO_4 waters with low pH and high base metal loads from moderate depth at the Heath Steele deposit (400-450 m). These

groundwaters have had longer flow paths than the Wedge deposit groundwater and have interacted with a mineral(s) with higher Sr contents and higher $^{87}Sr/^{86}Sr$. The most radiogenic of the Heath Steele groundwaters is probably the most evolved in terms of chemical evolution (Na-SO_4 water) and was recovered from greater depth (840 m).

The Heath Steele and Wedge deposit groundwaters plot along a similar Sr/Ca line as the surface waters and shallow groundwaters from the Restigouche deposit (Fig. 12.2). Unlike the saline and brackish groundwaters from the Restigouche deposit, these groundwaters are undersaturated with respect to carbonate minerals. Therefore it is possible that the isotopic composition of these groundwaters is controlled by dissolution of relatively radiogenic carbonate. Although Rb is typically strongly excluded from carbonate, some studies have reported radiogenic calcite compositions. This may indicate inclusion of some Rb into the carbonate or that the carbonate formed later from fluids which had acquired more radiogenic Sr from the host rocks. One of the carbonates is relatively radiogenic. Siderite from the Brunswick Belt in the BMC ranges in Sr isotopic composition from 0.71189 to 0.71508 which was interpreted by Peter and Goodfellow (in prep.) to reflect precipitation from hydrothermal fluids with Sr derived from Ordovician seawater (Veizer, 1989) and Sr derived from more radiogenic continental crust. Note, however, that these $^{87}Sr/^{86}Sr$ values for BMC siderite are more radiogenic than some of the groundwaters at the Restigouche deposit. These less radiogenic groundwaters have equilibrated with minerals with lower time-integrated Rb/Sr than the continental crustal end-member of the siderites. Given that most of the host lithologies at the Restigouche deposit are felsic volcanic rocks (presumably produced by anatexis of continental crust) or sediments derived from the felsic volcanic rocks, minerals with less radiogenic Sr than the BMC siderite implies that either the continental crust was isotopically heterogeneous during Ordovician times or that the siderite has become more radiogenic with time due to ingrowth of ^{87}Sr from ^{87}Rb decay. Clow et al. (1997) reported calcite with a $^{87}Sr/^{86}Sr$ value of 0.73215 compared to plagioclase in the same rocks with a $^{87}Sr/^{86}Sr$ value of 0.71956. Certainly, the $\delta^{13}C_{VPDB}$ of groundwater MLW95-610 (-6‰) is similar to the

fracture and vein carbonate from the BMC (see Chapter Eleven). Thus, the trend shown by waters associated with the massive sulphide deposits at Wedge, Restigouche and Heath Steele may reflect weathering of sericite, radiogenic carbonate, or a combination of both.

The potential influence of the hydrothermal alteration halo associated with the ore deposit on shallow groundwaters and surface waters suggests that there is potential to use Sr isotopes in mineral exploration. In fact, this was one of the rationales for initiating the radiogenic isotope study of BMC waters. This kind of application was also recently demonstrated for groundwaters near Abra in western Australia (Whitford et al., 1997). Whitford et al. (1997) showed that K-rich alteration halos resulted in ^{87}Sr-rich minerals proximal to the deposits which were reflected by more radiogenic local groundwaters compared to more distal groundwaters. Certainly, sericitic alteration is common around the massive sulphide deposits in the BMC (Lentz and Goodfellow, 1996). Indeed, the groundwaters recovered from the ore zone at the Restigouche deposit (from boreholes MM-88-01, MM-88-06, and MM-88-07) and the seep through the gossan (seep water MLW95-300) are the most radiogenic of the waters collected from the Restigouche deposit (Fig. 12.1). In contrast, groundwaters collected well below the ore zone (groundwater MLW95-586 from borehole B-80-7) or distal from the deposit (boreholes MM-89-102, MM-89-104, and MM-89-107) have less radiogenic Sr isotopic signatures. The Pb isotopic composition of the B-80-7 and MM-89-104 groundwaters suggests that the Pb was derived from BMC-type ore (see section 12.3.2), at odds with the non-radiogenic nature of the Sr isotopic signatures of these waters. However, the contrast in Sr abundance between alteration halo minerals and country rock minerals is much less than is the contrast in Pb abundance between the massive sulphides and country rocks. Therefore, the Sr isotopic composition of a water may be more readily reset by interaction with country rocks away from mineralization.

The Fe-rich stream sediment (MLS96-664) is from the Mt Fowler east stream which drains towards the Upsalquitch River over three kilometers to the east of the main Restigouche deposit. This sediment has Sr isotopic compositions similar to waters close to the Restigouche

deposit and may suggest that the seeps feeding the stream bed, and from which Fe-oxyhydroxides precipitate, are interacting with massive sulphides in the subsurface. This is consistent with elevated Zn contents in the stream sediments and non-radiogenic Pb isotopic compositions (Fig. 12.4). The co-existing water (MLW96-664) is, however, much less radiogenic (Fig. 12.1). Whereas the Sr associated with the stream sediment may be dominantly derived from the seeps, the stream water also includes a contribution of surface water flowing from further upstream. In addition, previous work has shown that dissolved Sr is typically less radiogenic than Sr associated with suspended sediments in large rivers (Allègre et al., 1996). If the Sr in the stream sediment and a stream water are both derived from the stream-bed seep, the dissolved Sr would represent more readily dissolved minerals (carbonate), whereas the Sr in the stream sediment may be more particulate, originating from the erosion of silicate rocks.

12.3.2 Pb isotopes

Most previous studies of Pb isotopes in natural water systems have focussed on the suspended sediment load due to the affinity of Pb for particulate matter (Allègre et al., 1996; Asmerom and Jacobsen, 1993). Few studies have focussed on the "dissolved" Pb component. There is a fundamental difference between the two types of analyses. The suspended load Pb isotopic signature is assumed to reflect the average of the material eroded by that river system (Asmerom and Jacobsen, 1993). In other words, the suspended load reflects to a large extent the mechanically eroded portion of the catchment area. In contrast, the dissolved Pb isotopic composition will reflect the weathered or chemically labile component of the catchment. If all minerals within the catchment underwent equal rates of weathering, the dissolved Pb isotopic composition would closely approximate the suspended load Pb isotopic composition. However, in most cases, the dissolved Pb load will preferentially reflect the most leachable minerals along the flow path of ground or surface waters. The effect may be offset in cases where Pb is not truly dissolved. Some Pb may be associated with colloidal matter < 0.45 μm in size that passes through the filters. Some of this colloidal Pb is likely to be derived from

bedrock erosion and so will reflect the bulk rock Pb isotopic composition, but some of the colloidally bound Pb will represent adsorbed "dissolved" Pb.

The Pb isotopic compositions of groundwaters and surface waters is somewhat easier to explain than was the case for the Sr isotopes. The majority of the waters analyzed in this study have Pb isotopic compositions which are very similar to galena from the Bathurst Mining Camp and much less radiogenic than the country rocks (Fig. 12.4; cf Table 12.1 and 12.2). This indicates that the Pb in these waters is predominantly derived by the oxidation of galena which is consistent with the very elevated Pb contents of some of the groundwaters (up to 4000 μg/L in seep water MLW95-300). The felsic volcanic and metasedimentary country rocks typically have Pb abundances < 50 ppm whereas massive sulphides contain up to several weight % Pb (Chapter Two). Two groundwaters from boreholes MM-89-106 and MM-89-107, which are west of the ore zone, have much more radiogenic Pb values compared to the other waters (Figs. 12.3-12.5). These two groundwaters are also more radiogenic than till samples from the Halfmile Lake deposit (Lochner, 1996) and felsic plutons (Whalen et al. in press) in the BMC. Three felsic volcanic rocks analyzed in this study are also more radiogenic than that measured during previous studies of Pb isotopes in the BMC (Fig. 12.4) but are less radiogenic than groundwater MLW95-594. The most likely explanation for the highly radiogenic Pb values of these groundwaters is that dissolved Pb, as with dissolved Sr, reflects the most labile form of Pb leached by water rather than bulk rock isotope values (differential weathering). For the U-Pb system, the highly radiogenic nature of the MM-89-106/107 waters implies that the Pb content is dominated by mineral phase(s), such as carbonate, which are enriched in U compared to the country rocks that make up the Bathurst Camp. Lead isotope analyses of carbonates of different ages have highly variable $^{206}Pb/^{204}Pb$ and $^{207}Pb/^{204}Pb$ ratios, ranging from less than 20 and 16 respectively to greater than 140 and 35 respectively (e.g. Babinski et al., 1995; Jahn and Simonson, 1995; Russell et al., 1996; Winter and Johnson, 1995). The large range in Pb isotope ratios in carbonates is explained by highly variable U/Pb ratios and, due to the greater solubility of U in oxidizing waters, the degree to

which a system is closed with respect to U loss, and the age of mineral formation (and thus U loss) if the system has not been closed. The discrepancy in the Pb-Pb plots for the groundwaters from boreholes MM-89-106 and MM-89-107 such that the latter groundwater has anomalously low $^{207}Pb/^{204}Pb$ compared to the $^{206}Pb/^{204}Pb$ and $^{208}Pb/^{204}Pb$ compositions could be the result of decoupling of the behaviour of U and Pb in the mineral phase(s) controlling the Pb isotopic compositions of these enriched waters, due to open-system behaviour. In other words, the groundwaters may have interacted with different carbonates with similar Th/Pb ratios but different U/Pb ratios and therefore have different μ values. In this case, groundwater MLW95-594 (MM-89-107) has a lower μ with more radiogenic Pb than groundwater MLW95-504 (Fig. 12.4; Table 12.1). This apparent difference in μ values for these waters indicates that the Pb isotopes are not varying as a simple function of proximity to the ore deposit which would be consistent with the differences in salinities of these waters. The fact that the groundwater from borehole MM-89-106 is less radiogenic yet more saline than the groundwater from borehole MM-89-107 could be explained by a combination of (1) closer proximity to the ore body and therefore a greater contribution of galena Pb, (2) increased influence of plagioclase dissolution (i.e., mixing of more radiogenic shallow groundwater with deeper, plagioclase-equilibrated less-radiogenic groundwaters) such that the influence of carbonate U/Pb ratios is diminished for these waters. This latter interpretation is supported by the Sr isotope values for the groundwaters from borehole MM-89-106 which has more radiogenic Sr than the groundwater from borehole MM-89-107, consistent with the higher Rb/Sr ratios in feldspars compared to carbonate.

An alternative explanation for the anomalous Pb isotopic composition of these two groundwaters is that there is not a common phase controlling their Pb isotopic composition. The reason for the anomalously high $^{207}Pb/^{204}Pb$ value for the MM-89-106 water may be due to dissolution of old phosphate (Cousens, pers com), with high μ (high U/Pb). Note that this water has REE phosphates on the filter paper (see Chapter Nine).

Four of the surface waters have anomalously low $^{207}Pb/^{204}Pb$ and $^{208}Pb/^{204}Pb$ for their

$^{206}Pb/^{204}Pb$ compositions, too consistently low to be explained by analytical error (Fig. 12.4). The only plausible explanation for these low Pb isotopic ratios is that these waters have Pb which was derived from very low U/Pb mineral(s) which have lower μ and higher κ values compared to BMC galena and the rest of the waters. A more mantle-derived Pb mineral would be expected to have lower μ compared to continental crustal materials. The composition of the mafic dykes that cross-cut the Restigouche deposit area of tholeiitic affinity and may provide a source of more mantle-like Pb. Why such a Pb-mineral would be dominating the Pb signature of these surface waters is, however, unclear, especially given the low Pb contents of mafic minerals. An alternative explanation is that these waters have a mixed Pb signature. The stream sediment (stream sediment MLS96-664) from Mt Fowler east stream has a Pb isotopic composition that is less radiogenic than BMC galena. Thus, there may be a contribution from older Pb with lower μ for these surface waters with anomalously low $^{207}Pb/^{204}Pb$ and $^{208}Pb/^{204}Pb$. Note that one of these surface waters is the co-existing stream water to stream sediment MLS96-664 (the Fe-rich sediment).

An interesting question is why the groundwaters from boreholes MM-88-02 and B-80-7 sampled well below the zone of massive sulphides should have Pb isotopic values identical to other samples proximal to ore. One possible explanation is that there is sufficient galena (or other low-μ sulphide minerals) in the stockwork zone below the deposit to impart this signature to these waters. For the MM-88-02 waters, however, the very high Zn loads (Table B.3) suggest that these waters may also have interacted with additional mineralization at greater depth and at some unknown distance from their point of sampling. The fact that Zn contents are still very elevated may limit the distance of transport although this is highly dependent on the speciation of the base metals in these saline fluids (see Chapter Seven). The lack of sulphate in borehole MM-88-02 waters and elevated $\delta^{13}C_{DIC}$ indicates that the Zn is not locally derived by oxidation of he stockwork sulphides.

The two carbonates have Pb isotopic compositions that are close to ore-Pb values for the BMC (Table 12.1; Fig. 12.4). Carbonate typically contains U as a trace element and several

studies have shown that carbonate minerals typically have very radiogenic compositions (e.g. Babinski et al., 1995; Jahn and Simonson, 1995; Russell et al., 1996; Winter and Johnson, 1995). There are two possible explanations for the non-radiogenic character of carbonates ML95-252 and ML95-259. If the carbonate veins formed recently, they would have incorporated Pb derived from oxidation of the Restigouche massive sulphides. However, the morphology and stable isotopic composition of the vein carbonate is not consistent with recent formation. This suggests that the carbonates have low μ.

12.3.3 Pb isotopes in mineral exploration

The utility of hydrogeochemistry in mineral exploration is discussed in full in Chapter Thirteen. In this section, the special case of the use of the Pb-isotopic composition of waters in mineral exploration is discussed. Lead isotopes have been applied to mineral exploration problems for some time (Gulson, 1986). These previous studies have included the use of Pb isotopes in gossan and ironstones (Gulson et al., 1988), Fe and Mn oxides in stream sediments (Gulson et al., 1992), and in glacial till (Bell and Franklin, 1993; Simonetti et al., 1996). This isotopic study of BMC waters was initiated in part to try to extend the use of Pb isotopes in mineral exploration to include natural waters. Toulhoat and Beaucaire (1991) studied the Pb isotope geochemistry of groundwaters as an exploration tool for detecting buried uranium deposits. In that case the utility of the method derived from having groundwaters with anomalously enriched Pb isotope ratios due to extremely high U/Pb ratios in U-rich minerals. For the study of Pb isotopes in a VMS environment, the reverse is the case; ground and surface waters with the least radiogenic isotopes will vector towards the sulphide deposit because galena, the primary source of Pb, has no U and therefore will not have evolved isotopically since the time it formed, unlike U-bearing country rocks. One of the great utilities of Pb isotopes in mineral exploration is that they are generally unaffected by factors such as weathering, mineral precipitation, evaporation, or dilution by meteoric fluids (Whitford et al., 1997). However, although the Pb isotopic composition of the host rocks and massive

sulphides is unfractionated by these processes, differential weathering of minerals by natural waters can produce Pb isotopic values different than the whole rocks (see discussion of groundwaters from boreholes MM-89-106 and MM-89-107 from the Restigouche deposit in the preceding section). The low solubility of Pb in most natural waters means that their Pb isotopic composition shows minimal dispersion compared to other indicator elements and isotopes, and therefore provides excellent target definition (Whitford et al., 1997). For example, Östlund et al. (1995) found that with increasing distance from the source of ore Pb, lake sediments in Sweden were increasingly radiogenic, a relationship similar to that observed for till samples from various mining camps (Bell and Franklin, 1993; Lochner, 1996).

As discussed in the previous section (12.3.2), most of Pb in BMC waters is essentially identical to composition to galena from massive sulphide deposits (Figs. 12.3, 12.4). This indicates that the Pb in these waters is dominantly derived from ore Pb. Clearly, therefore, ground and surface waters which are proximal to a source of massive sulphide mineralization can readily be distinguished from groundwaters distal to mineralization (e.g. groundwaters from borehole MM-89-106 and MM-89-107) on the basis of their Pb isotopes.

Two of the waters used in this study provide test cases for the application of Pb isotopes in this area. Surface water MLW95-467 is from the Mt Vroom NE stream over two km southeast of the Restigouche ore body (see Chapter Five for location). The area drained by this stream was investigated by Teck Corporation in 1967 (Sharpley, 1967) because the underlying rocks are of the same age and composition as the Restigouche deposit. Sharpley (1967) described a fragmental volcanic unit which was interpreted to be correlative with the volcanic rocks underlying the Restigouche deposit. One exploration hole was drilled and only a few small intervals of disseminated pyrite were intersected. There is a small showing 800 m west of Upsalquitch Lake. The showing is comprised of disseminated chalcopyrite, sphalerite, galena, pyrite and pyrrhotite within argillaceous sedimentary units (Brace, 1982). Stream sediment values are anomalous, including those along the Mt Vroom NE stream, although high Mn values suggested that some of the base metal enrichment in the stream sediments was due to

Mn scavenging (Brace, 1982). Stream sediments collected during this study along the Mt Vroom NE stream are not anomalous in Pb (see Chapter Six) although surface water MLW95-467 has a Pb isotopic composition which is indistinguishable from BMC galena (Figs. 12.4, 12.5). Even assuming that Mn and Fe oxides are scavenging and accumulating base metals, the Pb in surface water MLW95-467 most likely was derived from massive sulphides of similar age to the Restigouche deposit. Further exploration efforts in the area may be warranted.

In a similar manner, it is suggested that the area to the west of the Restigouche deposit may have potential for mineralization. Groundwater MLW95-546 was recovered from borehole MM-89-104 located over 1 km west of the main ore body at the Restigouche deposit (see Chapter Seven for borehole location). This borehole was drilled by Marshall Minerals in 1989 but despite a promising gravity anomaly, no massive sulphides were observed (Westoll, 1990). However, groundwater MLW95-546 has moderate Pb abundance (1.7 μg/L) and has Pb isotopic compositions indistinguishable from BMC galena (Figs. 12.4, 12.5). As with the Mt Vroom NE water, the most likely explanation is that a source of non-radiogenic BMC ore occurs relatively close to the borehole.

Bell and Franklin (1993) noted that the linear relationship they observed in the Pb isotopic compositions of till samples defined a secondary isochron rather than a simple mixing between Pb from unrelated sources (i.e., with no age relationship). They based this conclusion on the similarity between the age implied by the secondary isochron and the age of the host lithologies and syngenetic ore deposits. The question is, do the BMC waters also define such an isochron? If not, it does not negate the relationship but rather reflects the fact that waters with radiogenic Pb may have preferentially weathered minerals with different μ values due to solubility considerations rather than the bulk rocks as is the case for the till.

Bell and Franklin (1993) suggested that the technique of using the Pb isotopic composition of till samples is less accurate or useful where the ore deposit is not at or near the surface. For example, in their study of Pb isotopes in glacial till around VMS deposits at Chisel Lake,

Manitoba, they note that the radiogenic Pb in till down-ice from the Chisel North deposit was a reflection of the fact that the deposit did not crop out. In studies of Pb isotopes of glacial till in the BMC, the technique has successfully delineated the Halfmile Lake (Hussein, 1996; Lochner, 1996) and the Restigouche (Doherty et al., 1997) deposits. However, for a mature mining camp such as the BMC, it is likely that most surface and near surface deposits have already been discovered. The real challenge in the BMC is to develop exploration techniques which allow delineation of targets which are more deeply buried. If the Pb isotopic composition of glacial till is as dependent on a deposit being at or near the surface as Bell and Franklin (1993) suggest, then the utility of this method in the BMC may be limited. In contrast, using the Pb isotopic composition of "dissolved" Pb in surface and groundwaters may have more utility, especially where deeper groundwaters are brought to surface via fractures or where access to deeper groundwaters is possible using exploration drill holes or wells. In this study, I have shown that it is technically feasible to routinely measure the Pb isotopic composition of natural waters and that such an analysis can readily reflect the influence of ore-Pb. One major caveat is that alternative sample preparation methods are required for highly saline waters.

There has been no assessment to date of the possible contribution of Pb associated with particulate matter from the Beledune Pb smelter in northern New Brunswick. Due to the low Pb levels in waters, this may be of some concern for the application of Pb isotopes in mineral exploration in the BMC. However, results from studies of till samples from the Halfmile Lake (Lochner, 1996) and Restigouche (Doherty et al., 1997) deposits, would suggest that, at least for till sampling, the effects of anthropogenic Pb from the smelter are negligible. Erel et al. (1990) found that industrial Pb was concentrated in the upper 2 cm of the soil profile in a subalpine watershed in Yosemite National Park, California. Industrial Pb was prevented from reaching deeper aquifers (> 30 cm depth) due to removal by adsorption (Erel et al., 1990). During base flow conditions, the Pb isotopic composition of streams in the watershed primarily reflected values from the deeper (> 30 cm) groundwater, consistent with weathering of natural

rock Pb.

Whitford et al. (1997) suggested that in order to avoid contamination from cased diamond drill holes, uncased percussion or rotary air-blast holes should be used for groundwater sampling of Pb for isotopic analysis. For this study, cased diamond drill holes were the main access for deeper groundwaters (see Chapter Three for field methods). The straddle-packer system allowed the recovery of groundwaters from discrete depths, away from the influence of hole casings. For the groundwaters collected using the flow-through bailer in holes intersecting the Restigouche deposit, the very high Pb contents of the waters makes it highly unlikely that contamination from the casing or drilling fluids was of significance. It seems unlikely that groundwaters with low Pb contents collected using the bailer from boreholes distal to the deposit (e.g. MLW95-546) were contaminated by the casing because these waters have Pb isotopic ratios indistinguishable from galena values. It would be highly fortuitous if the steel used as casing material had the same Pb isotopic value as BMC massive sulphides.

One stream sediment and the related surface water were analyzed (samples MLS96-664 and MLW96-664, respectively). In previous chapters (Five and Six), it was shown that the waters and stream sediments from Mt Fowler east stream are anomalous in that the waters have relatively high SO_4 and the stream sediments are Fe-rich (up to 55 wt% Fe_2O_3) and Zn-rich (up to 1600 ppm). The Zn contents in the Fe-rich sediments are comparable to those in Charlotte Brook, downstream from the main Restigouche ore body. However, the Pb contents of Charlotte Brook stream sediments range up to 1900 ppm, whereas, those in Mt Fowler east stream only range up to 100 ppm. The possibility exists therefore, that the elevated Zn contents are an artifact of scavenging of Zn by Fe-oxyhydroxides by adsorption. Unfortunately, the water had very low Pb contents and the Pb signal during analysis was poor. The data for surface water MLW96-664 should be treated with caution. It is interesting, however, to note that this surface water is the least radiogenic water analyzed. As noted previously, the stream sediment is distinctive in that it is the least radiogenic sample in this study, and is considerably less radiogenic than any previous results from the BMC. Although there is only one sample,

this is an extremely interesting result. If this analysis is correct (and the sample ran well during analysis), it suggests that there is a source of Pb which is older than that which comprises the main BMC ore deposits. Stream sediment MLS96-664 falls on a Stacey-Kramer curve at just around 600 Ma (Fig. 12.3). The implication is that this stream sediment has Pb associated with Fe-oxyhydroxides which was derived from U-free sulphide minerals of Cambrian to latest Precambrian age. Alternatively, the groundwaters that carried the Pb to the site of adsorption and deposition may have interacted with older rocks with low μ and κ values so that there has been very little ingrowth of radiogenic Pb. Given the association of this non-radiogenic Pb with high Zn contents in the stream sediment, it seems more reasonable to suggest that the waters feeding the seeps in Mt Fowler east stream have interacted with sulphide-Pb in the subsurface. Thorpe et al. (1981) noted that Pb isotopic compositions of BMC galena were linearly correlated with very shallow slopes, implying a contribution of Grenville basement to the ores and host volcanic rocks of the BMC. On both $^{207}Pb/^{204}Pb$ vs $^{206}Pb/^{204}Pb$ and $^{208}Pb/^{204}Pb$ vs $^{206}Pb/^{204}Pb$ plots, stream sediment MLS96-664 lies along the projection of regression lines for the BMC galenas. Stream sediment MLS96-664 is therefore interpreted to have a Pb isotopic composition that reflects massive sulphide mineralization in the subsurface. This mineralization is mineralogically different from the main Restigouche deposit based on higher Zn/Pb and higher Ni and Co in the stream sediment in Mt Fowler east stream compared to Charlotte Brook downstream from the Restigouche deposit. The Pb in this postulated subsurface mineralization has a greater contribution of older Pb compared to other deposits in the BMC.

It is interesting to note that in a study of the Pb isotopic composition of suspended loads of several world rivers (Asmerom and Jacobsen, 1993), waters from the Isua Peninsula in Greenland showed anomalously low Pb isotopic compositions, in particular compared to the Nd modal ages for the suspended sediments. Asmerom and Jacobsen (1993) suggested that the anomalously low values might be related to the complex metamorphic history of the lithologies in the Isua catchment or to "unusual isotopic systematics" in the source rocks (Asmerom and

Jacobsen, 1993). An alternative explanation is suggested by the results of this study. Assuming that there is a source of ore-Pb within the Isua catchment, the anomalously low Pb isotopic compositions of the two Isua waters reported by Asmerom and Jacobsen (1993) could reflect a mixed signal between continental crustal Pb and galena Pb. Indeed, Appel et al. (1978) reported Pb isotopic results for galena from the Isua peninsula. The two Isua suspended sediment Pb isotopic values reported by Asmerom and Jacobsen (1993) lie close to a mixing line between the bulk of their waters with continental crustal Pb isotopic values and 3.5 Ga on a two-stage Stacey-Kramer Pb evolution curve, the age of the Isua country rocks and galena.

12.3.4 Pb isotopes in environmental applications

The rationale behind the use of Pb isotopes in natural waters for environmental applications is essentially identical to that of mineral exploration except that instead of attempting to identify potential sources of undiscovered mineralization, the Pb isotopes are used to identify the sources of Pb contamination. For example, Pb derived from leaded gasoline has a very different isotopic signature compared to Pb from BMC ore. In other words, mining related contamination in the BMC can readily be identified if the Pb isotopic composition of a contaminated site is equivalent to BMC galena. If the Pb isotopic composition of Pb contaminant is different, alternative sources of pollution are indicated.

For example, a similar application of Pb isotopes was used by Östlund et al. (1995) who measured the Pb isotopic composition of lake sediments down drainage from the Falun mining area in Sweden. They found that with increasing distance from the source of ore Pb, lake sediments were increasingly radiogenic. Thus, the source of Pb in the lake waters can be identified and traced back to areas of past mining activity.

12.3.5 Nd isotopes

The analytical method for Nd isotope analysis in waters was presented in Chapter Three. Analysis of Nd is difficult and a few comments on the methodology are warranted. In this

study, large volumes of sample were evaporated to preconcentrate the REE, prior to separation of Nd by chromatography. This method caused problems for the most saline groundwaters from borehole MM-88-02 at the Restigouche deposit and the Brunswick #12 deposit groundwater. Preconcentration by evaporation resulted in the formation of thick salts which proved impossible to redissolve. As a result, only four groundwaters had sufficient Nd on the Re filament for isotopic analysis. Banner et al. (1989) also measured Nd isotopes in saline waters although in that study the REE were separated by co-precipitation with $Fe(OH)_3$. Further work is required to improve the analytical protocols for Nd isotopic analyses of dissolved REE.

The four waters do not correspond to a correct age for the host rocks. Regression of all four waters yields an "age" of 77 Ma, based on calculated $^{147}Sm/^{144}Nd$ where (Rock, 1991):

$$^{147}Sm/^{144}Nd = 0.1439 \cdot (Sm/Nd) \cdot (3.69014 + {}^{143}Nd/{}^{144}Nd_{measured})$$

Regressing the three groundwaters with the highest REE contents (and most similar to whole rock REE patterns) yields an "age" of 244 Ma. Therefore, the Nd isotopic compositions of the different groundwaters reflect the time-integrated signature of the mineral or minerals controlling the REE composition of the water. The closer the REE compositions reflect the bulk rock, the closer the regression will be to the true age. Several whole rocks were also analyzed for their Nd isotopic composition. However, the dacitic and felsic volcanic rocks do not have enough variation in Sm/Nd to yield an age. The mafic dyke is tholeiitic in composition and clearly unrelated to the felsic volcanic rocks and therefore cannot be used to derive an age. Although Nd model ages are difficult to interpret, especially for rocks with complex histories, model ages were calculated for the waters and felsic volcanic rocks. The four felsic rocks yield model ages between 940 Ma and 1.2 Ga, suggesting derivation from Grenville (or older) basement. Two of the waters yield similar model ages (1.2 Ga) and have REE patterns very similar to the felsic volcanic rocks (Fig. 12.7).

Although there are only a limited number of analyses, the Nd isotope results of the groundwaters highlight an important point with respect to the solubility of the REE in natural

waters. As discussed previously (Chapter Ten), the REE patterns of the surface waters and the majority of the groundwaters from the Restigouche deposit were primarily controlled by the solubility of the REE whereas many of the groundwaters from the Halfmile Lake deposit had REE profiles which appeared to be controlled mainly by water-rock reactions (Leybourne et al., submitted). Regardless of the control over the REE distribution in a water, if the water was sampling the whole rock the Nd isotopic composition should be similar to the host lithology and consistent with its age. If a given water is preferentially interacting with one or more mineral phases, its derived Nd isotopic composition will reflect the time-integrated value of that mineral(s). For groundwaters MLW95-482 and MLW95-485, the similarity in REE patterns and model ages compared to felsic volcanic rocks suggests that the REE budgets of these groundwaters is rock-dominated.

Alternatively, if a water with a low age was recovering the REE from the bulk rock, this would suggest that the rock through which the water was flowing and which most greatly influenced the REE distribution of that water had undergone extensive alteration at some time after formation. Essentially the Nd isotopic composition of the whole rock would have been "reset" by subsequent alteration. For example, seep water MLW95-300 from the Restigouche deposit has a flat LREE pattern compared to chondrite (Fig. 12.7). This water was collected from a seep flowing through the gossan pile where the Restigouche deposit crops out. Unfortunately, none of the gossans analyzed to date from the Restigouche has similar REE patterns (D.R. Boyle, unpublished data). However, several gossans from the Brunswick #12 deposit have REE patterns very similar to seep water MLW95-300, with similar La/Sm (D.R. Boyle, unpublished data). Although the general shape of the REE patterns of groundwaters MLW95-482, MLW95-485 and MLW95-486 are similar to the host lithologies (Fig. 12.7), the most LREE enriched groundwater, MLW95-486 (from the Heath Steele deposit), has a steeper slope than any of the whole rocks (La/Yb = 55 compared to 5-20 for felsic host rocks; Chapter Ten). However, some gossans from the Heath Steele deposit are likewise LREE-enriched with La/Yb between 48 and 75 (D.R. Boyle, unpublished data).

More detailed study is required on the Nd isotope systematics of natural waters in the BMC to resolve the reason for the low derived ages for groundwaters. Given that both the Sr and Pb isotopes indicate that preferential weathering can play a significant role for these isotopes, the preferred interpretation is that this is also the case for the Nd isotopes. The alternative hypothesis, that the Nd isotopic composition of the water reflects altered source rocks would require fairly rapid changes in the Nd values of the water, given the short spatial extent of potential whole rock materials. This seems unlikely. For example, Banner et al. (1989) reported Nd isotopic compositions of saline waters recovered from springs in Mississippian carbonates and Ordovician sandstone and carbonates from central Missouri. Due to differences of Nd isotopes between waters and host carbonates, Banner et al. (1989) concluded that the groundwaters had attained their Nd (and Sr) isotopes from crustal sources prior to migration through the carbonate host rocks. This implies preservation of the Nd isotopic signature over long time periods and distances. Furthermore, the Nd contents of groundwaters MLW95-482, MLW95-485 and MLW95-486 are high for natural waters (Chapter Ten) making it difficult to rapidly perturb the Nd isotopic compositions.

Stream sediment MLS96-664 has a Nd and Sr isotopic composition which lies between values for the felsic volcanic rocks and the mafic dyke (Fig. 12.6). This suggests that the Sr and Nd in this sediment was derived from both mafic and felsic source rocks which is a reasonable interpretation given that the Mt Fowler east stream flows over Boucher Brook Formation sediments and there are also Mt Brittain Formation felsic volcanic rocks within the catchment (Chapter Six).

12.4 Summary

1) Strontium isotopic compositions of BMC ground and surface waters are variable and more radiogenic than both modern and Ordovician seawater.

2) Most of the waters appear to follow two trends with respect to Sr isotopic compositions. Groundwaters from the Restigouche deposit trend to less radiogenic Sr compositions with

increasing water-rock reaction, probably reflecting increasing contributions of relatively non-radiogenic Sr from plagioclase weathering. Groundwaters interacting with the Restigouche massive sulphides, and the Wedge and Heath Steele deposits appear to trend to more radiogenic Sr isotopic compositions and higher Rb/Sr with increasing depth and water-rock reaction. These relationships are most consistent with increasing contribution of ^{87}Sr from sericite associated with hydrothermal alteration proximal to the massive sulphides, and/or from radiogenic carbonate in the stockwork. The saline waters from borehole MM-88-02 at the Restigouche deposit have very high Sr and relatively non-radiogenic Sr isotopes, most likely indicating equilibration with plagioclase, perhaps associated with mafic dykes that cross-cut the deposit. In contrast, saline waters from the Brunswick #12 deposit have the most radiogenic Sr compositions in the study, suggesting interaction with K-feldspar and/or micas. The brackish water from borehole MM-89-106 is more radiogenic than other saline and brackish groundwaters at the Restigouche deposit. Low Ca/Na and moderately high Sr suggest some influence from K-feldspar weathering.

3) Groundwaters associated with the Restigouche, Wedge and Heath Steele deposits are more radiogenic than those distal to the Restigouche deposit, related to potassic alteration about the deposit, suggesting that there may be some potential for the use of Sr isotopes in waters as an exploration tool.

4) Most waters have non-radiogenic Pb isotopic compositions similar to BMC galena. This indicates that Pb derived from massive sulphide weathering dominates the Pb contents of most of the waters used in this study. Notable exceptions are waters from boreholes MM-89-106 and MM-89-107 from the Restigouche deposit which have Pb which is more radiogenic than the host rocks. Anomalously high $^{207}Pb/^{204}Pb$ in groundwater MLW95-504 from borehole MM-89-106 indicates that the Pb in the water was derived from a high-μ mineral, perhaps phosphate, consistent with the presence of phosphate in the suspended load of this water. Several surface waters have $^{206}Pb/^{204}Pb$ indistinguishable from BMC galena, but have anomalously low $^{207}Pb/^{204}Pb$ and $^{208}Pb/^{204}Pb$, suggesting equilibration with low-μ and low-

κ mineral(s).

5) The Pb isotopic composition of the ground and surface waters indicates that Pb isotopes in waters may be a powerful tool in mineral exploration. Groundwaters can potentially reveal more deeply buried sources of mineralization compared to other techniques which employ Pb isotopes, e.g., Pb isotopic analyses of glacial till and gossans. Two groundwaters distal to the Restigouche deposit have ore-Pb isotopic compositions suggesting as yet undiscovered sources of mineralization.

6) Stream sediment MLS96-664 has the least radiogenic Pb isotopic composition reported to date from the BMC. Combined with high Zn in sediments from this stream, the Pb isotope value is interpreted to reflect massive sulphide mineralization in the subsurface which has a greater contribution of Grenville age Pb compared to other deposits in the BMC.

7) The Nd isotopes of several groundwaters show a wide range in $^{143}Nd/^{144}Nd$, consistent with differences in Sm/Nd and REE patterns. The fact that the Nd isotopic compositions of the waters is different from host rocks and yields incorrect ages indicates that groundwaters are preferentially incorporating the REE from certain minerals rather than from the bulk rock.

8) Data for Sr, Pb and Nd isotopes all indicate that for natural waters, the dissolved loads of these elements have isotopic compositions which reflect differential weathering rather than the bulk rocks through which the waters flow.

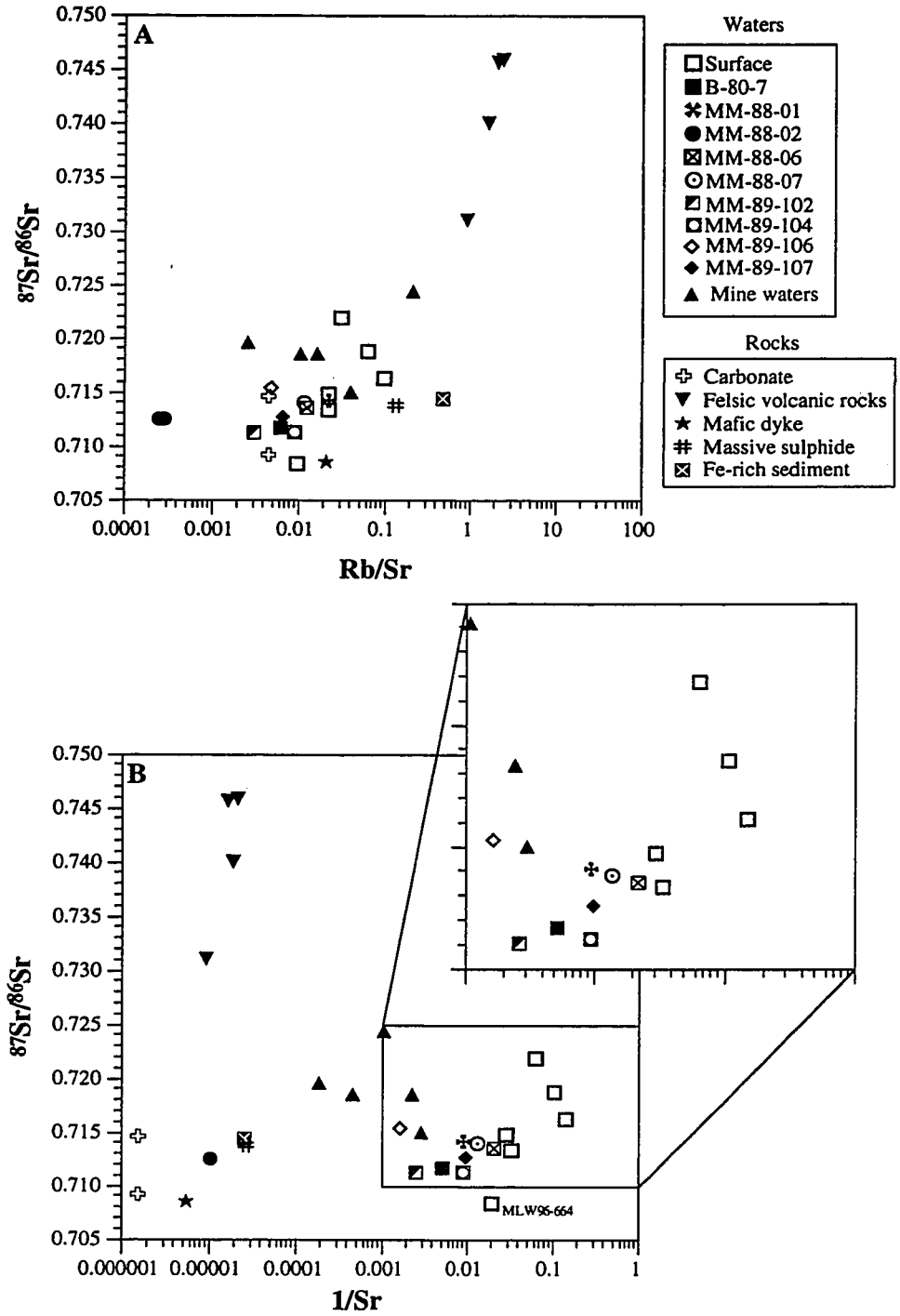


Fig. 12.1 Plots of $^{87}Sr/^{86}Sr$ vs A) Rb/Sr and B) 1/Sr for Restigouche ground and surface waters and host lithologies and mine waters from Heath Steele, Brunswick #12, and Wedge deposits. Data from Table 12.1. Sample MLW96-664 is the surface water collected from the same site as the stream sediment sample.

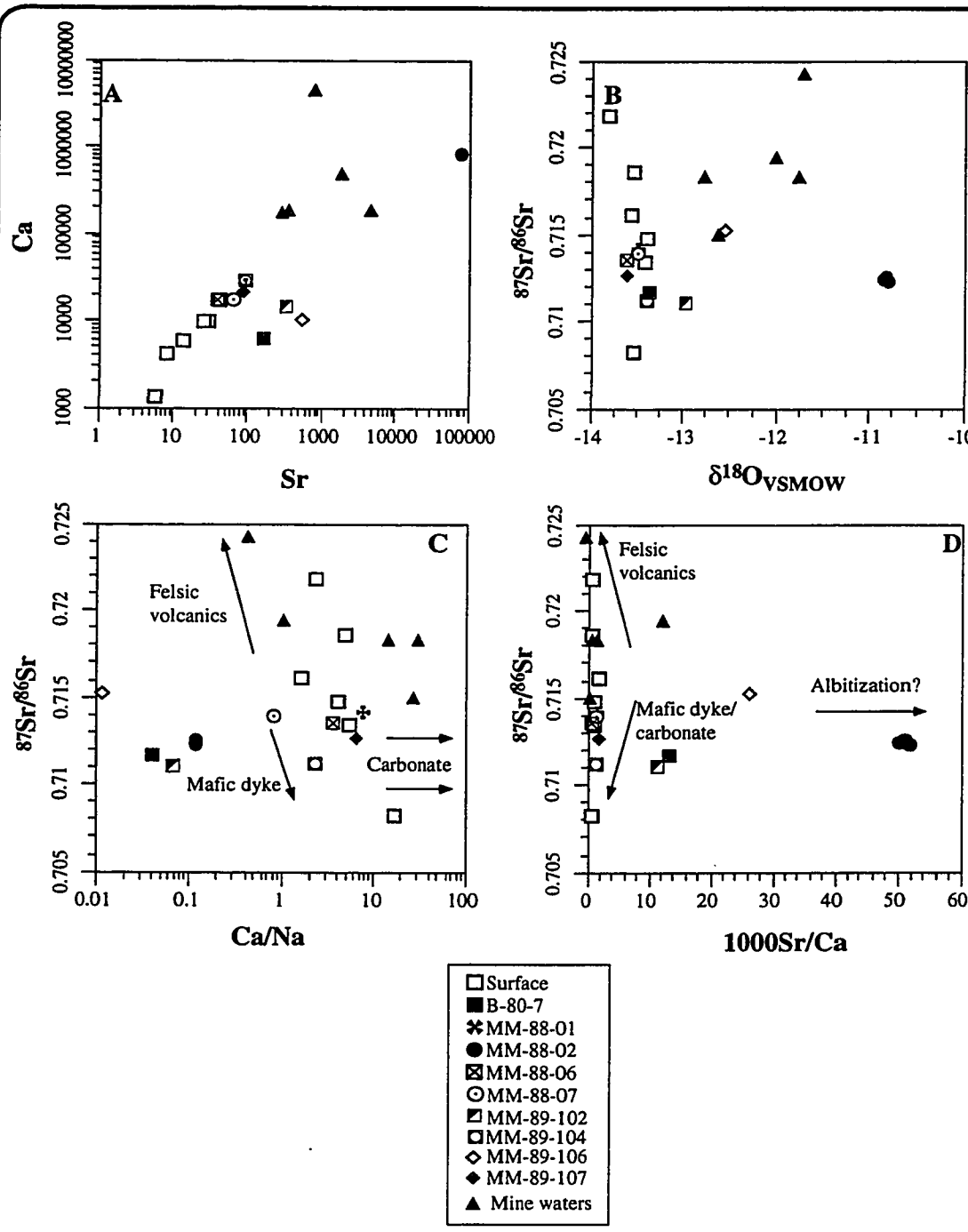


Fig. 12.2 Plots of A) Ca vs Sr; B) $\delta^{18}O_{VSMOW}$ vs $^{87}Sr/^{86}Sr$; C) $^{87}Sr/^{86}S$ vs Ca/Na, and D) $^{87}Sr/^{86}Sr$ vs 1000Sr/Ca for Restigouche ground and surface waters and mine waters from Heath Steele, Brunswick #12, and Wedge deposits. Data from Table 12.1.

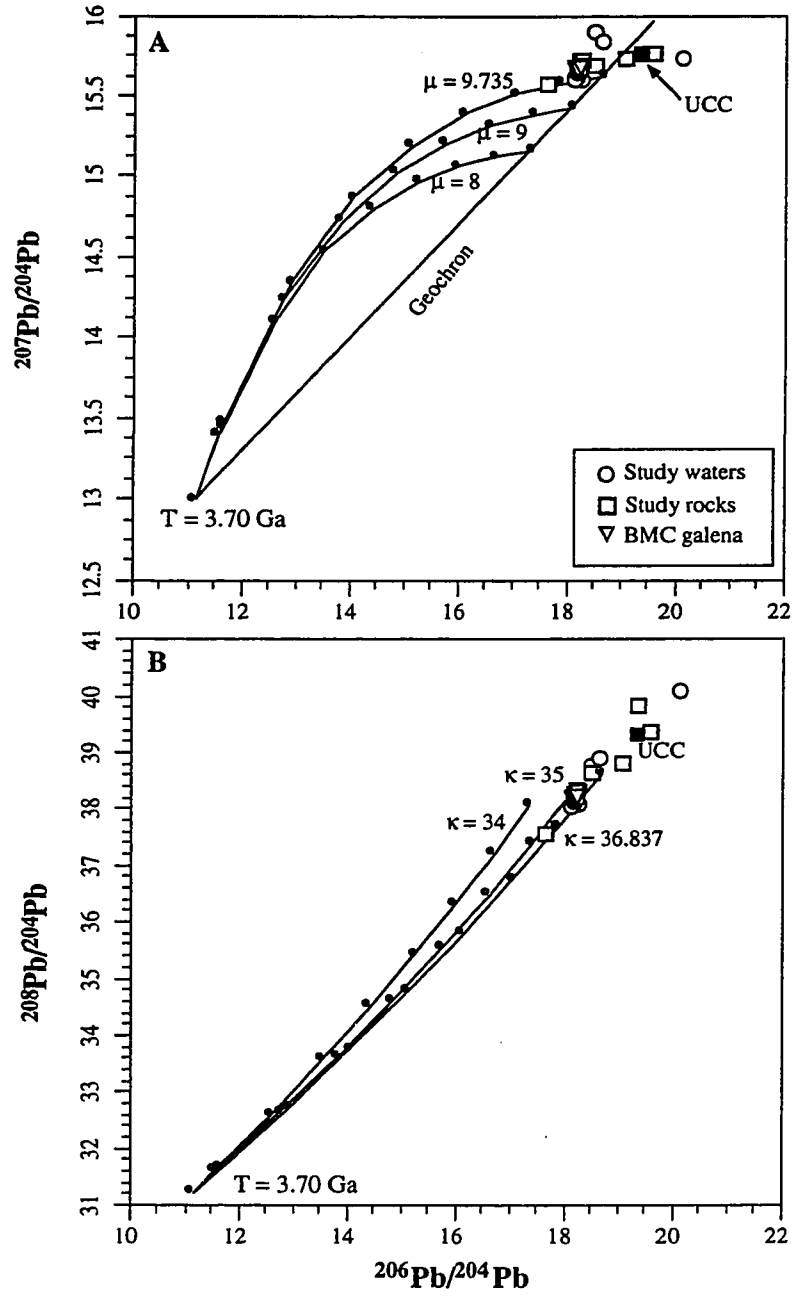


Fig. 12.3 A) Plot of $^{207}Pb/^{204}Pb$ vs $^{206}Pb/^{204}Pb$ for BMC waters and galena. B) Plot of $^{208}Pb/^{204}Pb$ vs $^{206}Pb/^{204}Pb$ for BMC waters and galena. On both figures are also shown Pb-isotope growth curves based on different μ and κ values. Tick marks on growth curves represent 500 Ma intervals. Galena data from Table 12.2 (Thorpe et al. unpublished data) and water data from Table 12.1. Solid squares represent the average upper continental crust (UCC), estimated from Pb isotopic composition of river suspended sediments (Asmerom and Jacobsen 1993).

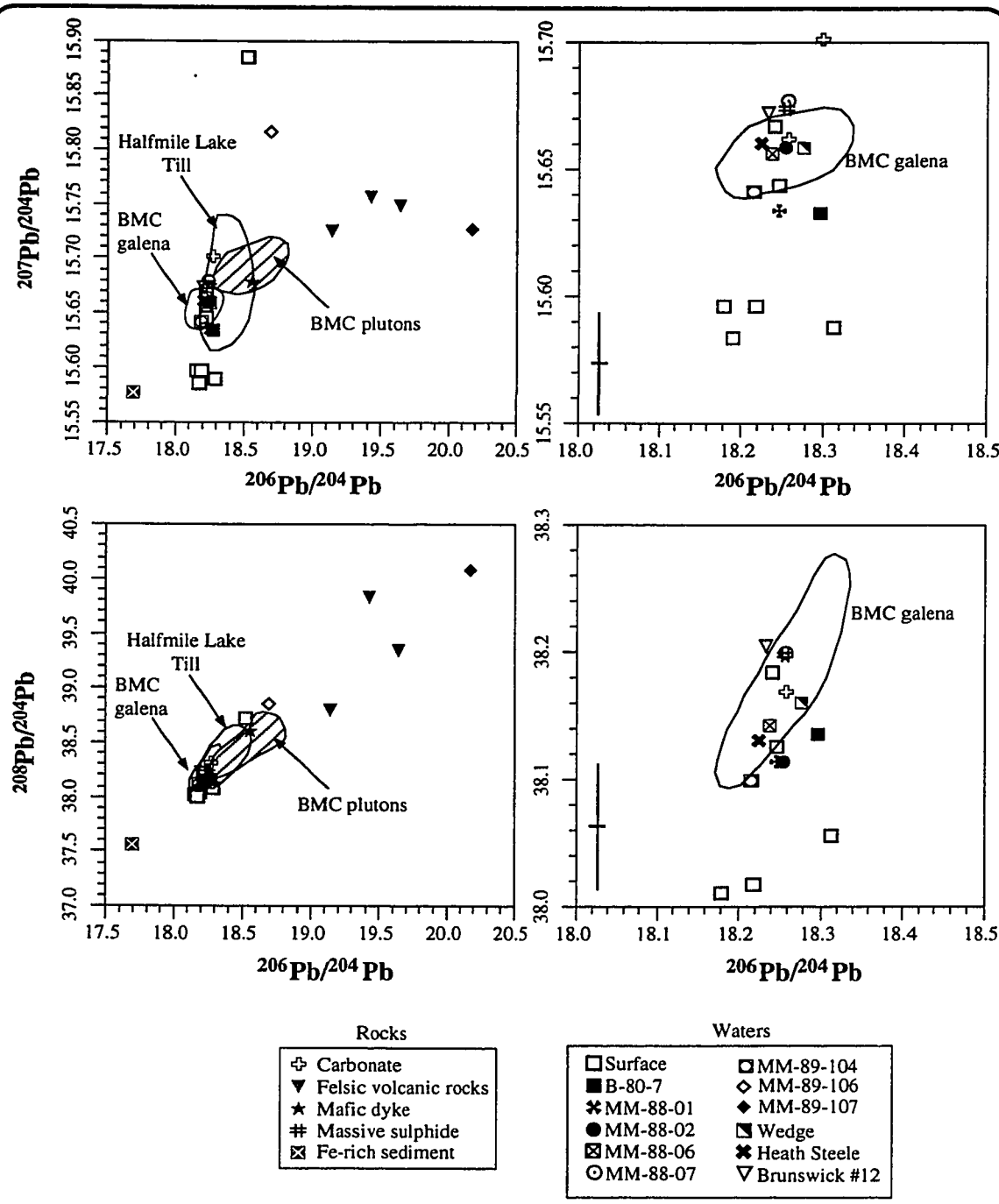


Fig. 12.4 Plots of $^{207}Pb/^{204}Pb$ vs $^{206}Pb/^{204}Pb$ and $^{208}Pb/^{204}Pb$ vs $^{206}Pb/^{204}Pb$ for BMC waters, galena (Thorpe et al. unpublished data), till from Halfmile Lake (Lochner 1996), and Ordovician granitoids from the BMC (Whalen et al., 1998). Data from Table 12.1.

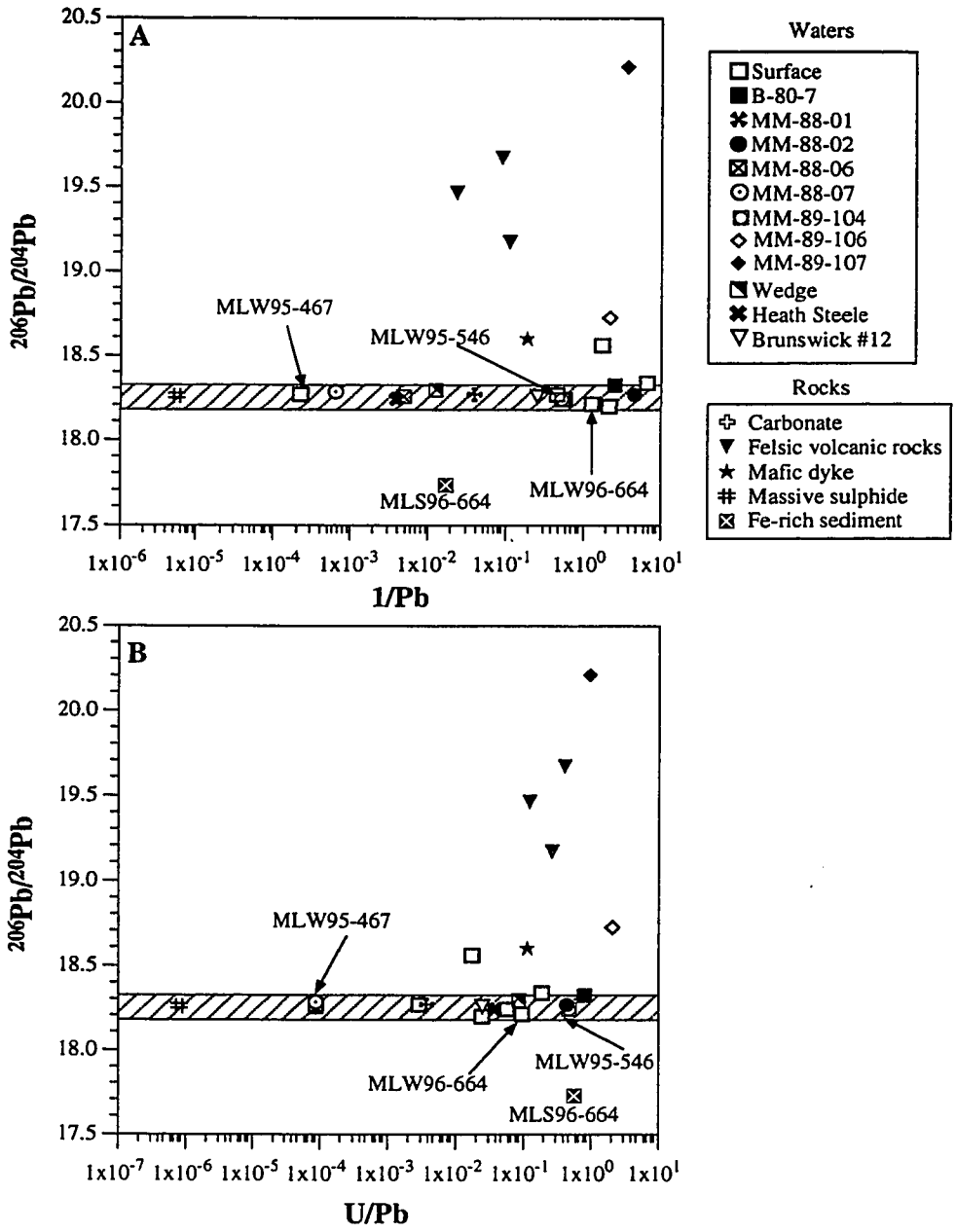


Fig. 12.5 Plots of $^{206}Pb/^{204}Pb$ vs A) 1/Pb and B) U/Pb for BMC waters. The shaded field represents the Pb isotopic composition of BMC galena (Thorpe et al. unpublished data). Note that in A) the rock data is in ppm and the water data in ppb. Water data from Table 12.1.

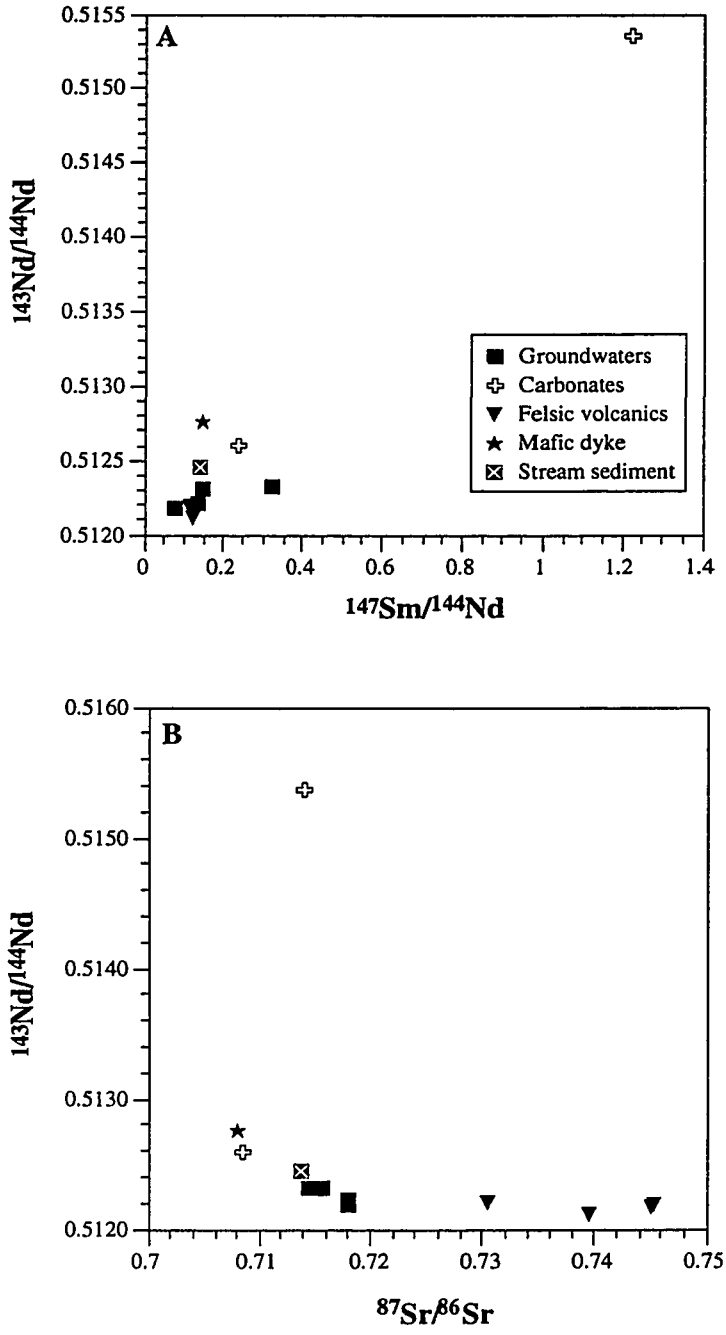


Fig. 12.6 A) $^{143}Nd/^{144}Nd$ vs $^{147}Sm/^{144}Nd$. B) $^{143}Nd/^{144}Nd$ vs $^{87}Sr/^{86}Sr$. Nd and Sr isotope data from Tables 12.3, 12.4 and 12.1.

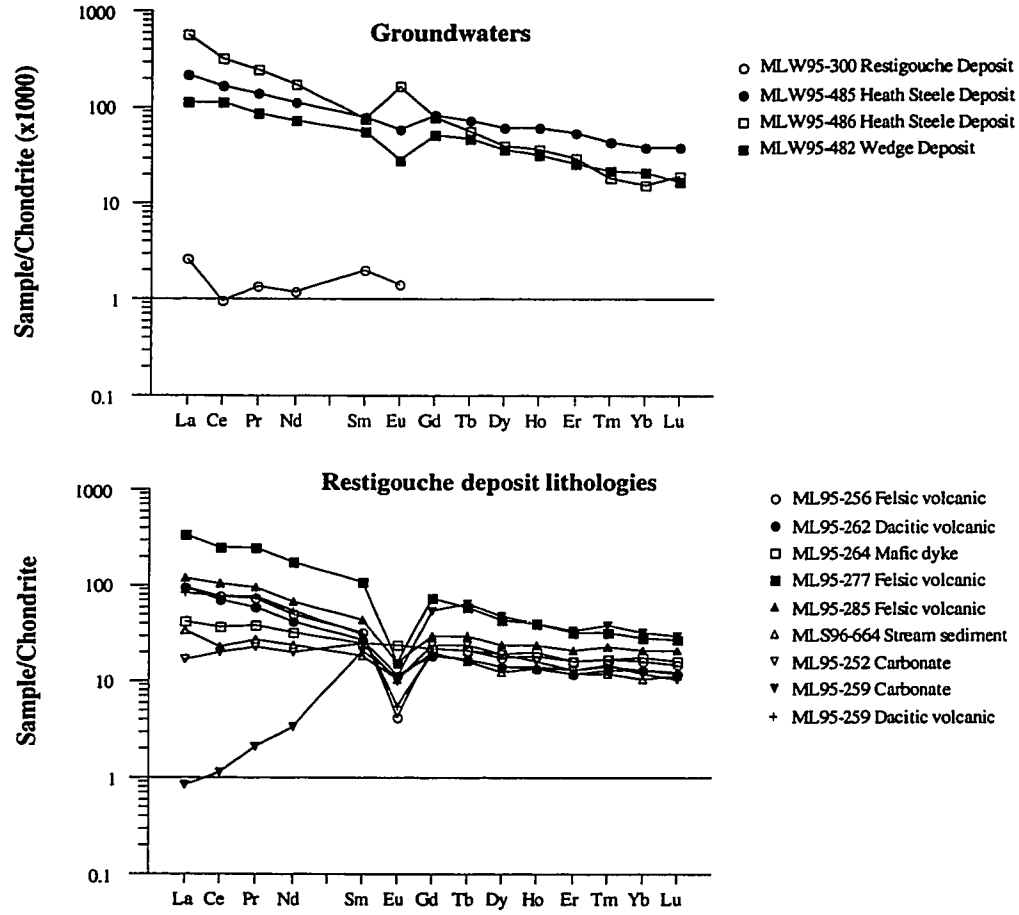


Fig. 12.7 Chondrite-normalized REE profiles for the four groundwaters samples analyzed for Nd isotopes compared to whole rock REE patterns from the Restigouche deposit. Note that samples MLW95-482, MLW95-485, and MLW95-486 have patterns similar to felsic volcanic rocks.

CHAPTER THIRTEEN:
APPLICATION OF HYDROCHEMICAL TECHNIQUES TO MINERAL EXPLORATION IN THE BATHURST MINING CAMP, NEW BRUNSWICK, CANADA

13.1 Introduction

The preceding chapters have described the composition of surface and ground water from the Bathurst Mining Camp (BMC) and how it varies as a function of style, extent and pathway of water-rock interaction, water-water mixing relationships, and adsorption onto solid phases. One of the objectives of this research was to develop new and improved hydrogeochemical methods of in mineral exploration in a mature mining camp such as the BMC. This chapter synthesizes the relevant information presented in the preceding chapters as it relates to mineral exploration including the geochemistry of surface waters (Chapter Five), groundwaters (Chapters Seven, Eight), stream sediments (Chapter Six), stable and radiogenic isotopes (Chapters Eleven, Twelve) and hydrology (Chapter Four).

The BMC is a mature mining camp with several active mines (Brunswick #12, Heath Steele, Caribou and Restigouche deposits), several past producing mines (Wedge, Brunswick #6 and Austin Brook deposits), and over 30 other occurrences (including the Halfmile Lake, Willett and Stratmat Main Zone deposits) (Chapter Two). Most of these deposits, however, occur at the surface and were discovered in the 1950's and 1960's using geochemical and geophysical exploration methods (McCutcheon, 1992). Because groundwaters penetrate deeply into the earth's crust, hydrogeochemistry offers the potential to explore into the third dimension and detect deeply buried mineralization. The utility of hydrogeochemical surveys is not restricted to mineral exploration; stream geochemistry provides data essential for characterizing metal fluxes prior to mine development and for environmental assessment programs. This is an important consideration in the BMC as past and current producing mines were brought into production prior to current, more rigorous environmental guidelines. In some areas, natural

background levels of metals in streams draining sulphide deposits may exceed water quality guidelines (Taufen, 1997) and are therefore important in defining anthropogenic contributions during mining.

The use of natural waters as an exploration tool is not a new concept (e.g. Boyle, 1979; Goodfellow, 1989). However, despite recent reviews (Giblin, 1994; Taufen, 1997), there are comparatively few detailed studies in the literature, although there has been an increase in interest in recent years (e.g. Cidu et al., 1995; Grimes et al., 1995; Ruijin et al., 1994; Wang et al., 1995). Some of the advantages of using natural waters in mineral exploration include their chemical reactivity, physical mobility, relative ease of sampling, uniformity of sample medium and the fact that low background values increase anomaly contrast (Giblin, 1994) as well as the depth of penetration of groundwaters. Ground and surface waters may not be appropriate media for mineral exploration in all conditions, however. Giblin (1994) suggested that catchments with high topographic relief with little or no overburden were more suited to stream sediment methods. In arid environments, surface waters are typically ephemeral and in these conditions groundwaters may provide a suitable medium for exploration (Vriend et al., 1991). Groundwaters are also useful in detecting buried mineralization as they penetrate well into the earth's crust (Giblin, 1994; Grimes et al., 1995). Moon (1995) suggested that natural waters are a generally poor medium for exploration geochemistry because of low detection limits, insolubility of many ore-related metals, variable weathering rates for different minerals, and the risk of contamination during sampling. Recent advances in analytical methods, however, has resulted in the ability to routinely measure trace metals to very low levels (Hall et al., 1995b; Stetzenbach et al., 1994). As shown in this chapter, both surface and groundwaters are successful in delineating massive sulphide deposits in the BMC.

The surface waters sampled in this study include seeps and stream waters, primarily third and fourth order streams (first and second order in some literature) and for the most part these waters represent base flow conditions based on the similarity between the stable isotopes of surface waters and shallow groundwaters. This is an important point because the efficacy of

surface water hydrogeochemical exploration will depend on the extent to which deeper groundwaters are being sampled at the surface. For example, (Ruijin et al., 1994) found that hydrogeochemistry was more effective at delineating mineralization concealed by 30 - 100 meters of basalt flows than more traditional methods such as stream sediment geochemistry.

Rose et al. (1979) suggested that there are six main methods for threshold selection including 1) comparison with literature data, 2) examination of histograms for bimodal or multi-modal populations, 3) statistically, such as choosing the mean plus two or three standard deviations, 4) partitioning of the data into background and anomalous populations based on log-normal probability plots (Sinclair, 1974), 5) spatial associations of anomalous samples, and 6) comparison with orientation surveys. In this study, threshold and background values were chosen based on examination of probability plots and on spatial associations of water and stream sediment compositions about areas of known mineralization at the Halfmile Lake and Restigouche deposits. Statistical methods of threshold selection are less applicable given that a significant proportion of samples were collected close to known mineralization. For many elements in both waters and sediments, several populations are evident based on log-normal probability plots (e.g., Fig. 13.1). In these cases, there are two anomalous populations, and background is interpreted to be all values less than the lower threshold (Table 13.1).

13.2 Results from the Halfmile Lake Deposit

13.2.1 Surface waters

The Halfmile Lake deposit is of moderate size (Adair, 1992), is overturned, and dips steeply to the north and northwest (Chapter Two; Fig. 2.3). The deposit outcrops as a gossan at the top of the Upper AB zone of the deposit. At the Lower AB zone, the massive sulphides are present at depths of up to 1 km (Chapter Two). The surface projection of the massive sulphide and associated stringer-sulphide zone trends west-east at the Upper AB zone and trends to the northeast at the Halfmile North zone (Fig. 13.2). Several streams were sampled at the Halfmile Lake deposit for surface waters and stream sediments (Chapters Six and Five).

The Upper/Lower AB stream drains over the deposit, north of the gossan outcrop. The Halfmile North stream drains to the southeast of the Halfmile North zone, and the West tributary stream drains to the west of the Upper AB zone. The North and Northeast tributary streams drain lithologies more distal to mineralization (Fig. 13.2; see Fig. 4.6).

The major cation and anion compositions of Halfmile Lake deposit surface waters were described previously (Chapter Five). The surface waters are dominantly Ca-HCO_3-type waters and dissolved sulphate is generally low, ranging from 0.57 to 4.64 mg/L (Fig. 13.1). Trace metal abundances are generally low (Appendices A.1.1, A.1.2). Zinc ranges from 0.5 to 15 µg/L, Pb from 0.02 to 0.61 µg/L, Cu from 0.16 to 8.4 µg/L, Cd from 0.01 to 0.11 µg/L, and Co from 0.01 to 0.97 µg/L (Fig. 13.1).

Surface water anomalies are subtle compared to the Restigouche deposit. Sulphate contents are highest along the Upper/Lower AB stream, along the Halfmile North stream and in the North tributary below the confluence with the Upper/Lower AB, Halfmile North, and Northeast tributary streams (Fig. 13.2). Surface water Fe contents are more variable and less obviously related to the known mineralization with elevated values (≥ 90th %ile) associated with the Upper/Lower AB stream and the Northeast tributary stream. Iron contents of Halfmile North stream waters are generally below detection. Of the base metals, Cu and Pb show very scattered values, although there are anomalous values (> 50th %ile) associated with the Upper/Lower AB stream and with the confluence area (Fig. 13.2). In contrast, Zn and Cd are anomalous (> 50th %ile) relative to background along the Upper/Lower AB, West tributary, and Halfmile North streams (Fig. 13.2). Thus, for SO_4, Zn and Cd, anomalous values are associated with surface waters that flow over or drain the immediate area of the deposit, and are generally at background values in the Northeast and North tributaries away from mineralization.

13.2.2 Stream sediments

Base metals in Halfmile Lake deposit stream sediments (average of the two size fractions;

see Chapter Thirteen) are generally low compared to those in Restigouche deposit sediments. The maximum Zn, Pb and Cd contents at the Halfmile Lake deposit are 730, 100 and 2.6 ppm, respectively (Fig. 13.3). Copper contents are generally higher at the Halfmile Lake deposit than at the Restigouche deposit, ranging up to 1000 ppm. Stream sediment background values at the Halfmile Lake deposit are similar to those at the Restigouche deposit for Cd and Pb, but lower for Zn and higher for Cu (Table 13.1). Sediment geochemical data for streams draining the Halfmile Lake deposit area collected as part of regional surveys by the New Brunswick Department of Natural Resources (NBDNR), display values similar to this study (Austria, 1981).

Stream sediments from the West tributary stream, the Halfmile North stream close to the confluence with the Upper/Lower AB stream and the North tributary stream downstream from the confluence contain anomalous Pb contents (> 90th %ile) (Fig. 13.4). Zinc in stream sediments is generally low (most sediments are < 500 ppm), with the exception of sediments from the Halfmile North stream (> 75th %ile) (Fig. 13.4). As noted above, this stream is also anomalous in dissolved Zn. All sediments from the Northeast tributary contain < 200 ppm Zn (< 25th %ile). Cadmium behaves similarly to Zn with the exception of anomalous Cd contents (> 90th %ile) in sediments from the Upper/Lower AB stream. The Halfmile North and West tributary streams have the most anomalous Cu values (> 50th %ile) in the study area (Fig. 13.4), higher than Cu in sediments downstream of the Restigouche deposit. Stream sediment Mo contents range up to 3.6 ppm with the highest values in sediments from the Upper/Lower AB stream (background is < 1.3 ppm). Thus, Zn, Cd, Cu, and Mo are typically anomalous in streams closest to known mineralization (Fig. 13.4).

13.2.3 Groundwaters and suspended sediments

All of the boreholes sampled at the Halfmile Lake deposit are located within the deposit area. Most of the boreholes intersect mineralization with the exception of boreholes HN93-51 and HN93-55 which penetrate stringer-sulphide mineralization but did not intersect massive

sulphides. Borehole HN87-8 did intersect massive sulphides but was blocked at 750 meters, above the stringer and massive sulphide intersections. It is therefore difficult to determine background base metal levels in groundwaters in unmineralized host rocks remote from sulphides. Despite the apparent rapid recharge of oxidizing meteoric waters to considerable depth at the Halfmile Lake deposit (low TDS groundwaters were recovered from 760 m depth; Chapter Seven), groundwater base metal compositions are only slightly higher than local surface waters. This is in contrast to large differences between ground and surface waters at the Restigouche deposit. However, several elements that were below detection in surface waters were detectable in the groundwaters, including As, Mo and Sb. Groundwater Mo contents range from 0.76 to 56 μg/L and are elevated compared to groundwaters from the Restigouche deposit (Table 13.1). Zinc contents are compositionally variable and range from 2 to 1087 μg/L. Zinc measured by both ICP-MS methods shows essentially identical variations including similar inflections on cumulative frequency plots (Fig. 13.5), with background values < 40 μg/L. Lead values range from 0.014 to 9.9 μg/L and Cu from 0.07 to 38 μg/L (Fig. 13.5).

As shown in Chapter Seven, the base metal content of groundwaters show few consistent trends with proximity to sulphide mineralization. However, there are anomalous values associated with different boreholes for different elements (Fig. 13.6). For example, groundwaters with anomalous Sb and As (> 0.2 and 2 μg/L, respectively) occur primarily in boreholes close to the Upper/Lower AB stream (Fig. 13.6). Elevated Cu and Mo (thresholds of 4 and 4.8 μg/L, respectively) occur mostly in deeper boreholes which intersect a greater thickness of footwall stringer alteration (i.e., in boreholes penetrating the Lower AB zone; Fig. 13.6). Elevated Cu values (> 75th %tile) also occur at the top of the Upper AB zone near a gossan outcrop.

Although groundwater metal abundances do not show a clear vertical and spatial association with sulphide mineralization, the suspended sediments show much higher base metal contents close to sulphides. For example, the Pb and Zn in suspended sediments from borehole HN94-65 (which penetrates stringer and massive sulphides at 450 to 480 m depth) are an order of

magnitude higher than in local stream sediments. Zinc contents of some Halfmile Lake deposit suspended sediments are up to three times higher (up to 4000 ppm) than Zn contents of stream sediments downstream from the main Restigouche deposit.

13.3 Results from the Restigouche Deposit

13.3.1 Surface waters

Trace metals show threshold values at different percentiles based on probability plots (Table 13.1). Zinc shows an inflection at the 55th percentile, indicating that Zn values above 3 μg/L are probably anomalous, with a highly anomalous population (Fe-oxyhydroxide-rich seeps) above 18 μg/L (98th %ile; Figs. 13.7, 13.8). The lower threshold is consistent with Zn contents in surface waters from Charlotte Brook upstream and downstream from the main Restigouche deposit (Fig. 13.8). Zinc contents are low upstream from the deposit (with the exception of the headwater sample) with values < 1 μg/L. Surface waters immediately downstream from the deposit have Zn contents of 7 - 8 μg/L (Fig. 13.8) and with increasing distance downstream, Zn contents decrease to around 2 μg/L four kilometers from the Restigouche deposit. Lead shows a much higher threshold value than Zn with the only major inflection at the 95th percentile (1.7 μg/L; Fig. 13.7). A more subtle inflection at the 50th percentile suggests that background values are < 0.55 μg/L. Lead in Charlotte Brook waters display patterns similar to Zn with respect to proximity to the Restigouche deposit (Fig. 13.8). Lead contents are low upstream from the deposit (background values around 0.5 μg/L), increase immediately downstream from the deposit (up to 2.4 μg/L) and ultimately reach background values 2 km from the deposit. Lead values decrease more rapidly than Zn and generally coincide with a rapid decrease in dissolved Fe contents downstream from the deposit. Dissolved Fe in Charlotte Brook shows a sharp peak at the main deposit (up to 90 μg/L) but decreases to background levels (≤ 10 μg/L) one km downstream from mineralization. Copper is generally a poor indicator of proximity to the main Restigouche deposit (Figs. 13.8, 13.9). Most anomalous values occur along the North stream and in streams draining Mt Vroom.

Downstream from the Restigouche deposit in Charlotte Brook, Cu contents are generally low (close to the median value of 0.95 μg/L) and do not display the marked anomalies shown by Fe, Zn and Pb (Fig. 13.8).

Zinc is anomalously high along the North stream (up to 14 μg/L), especially in the headwaters (Fig. 13.9). Surface waters from the North stream are also anomalous in Cd and Cu, and Pb contents are slightly higher than the lower threshold value of 0.55 μg/L (Fig. 13.8). Waters collected closest to the headwaters are associated with transported gossan, 300 meters northeast of the northern extent of the Restigouche deposit.

The Mt Vroom east stream (4 km southeast of the Restigouche deposit) is characterized by elevated Fe and SO_4 values (generally > 75th %ile), but has generally low base metal contents with the exception of the headwaters (Fig. 13.9). The Mt Vroom northeast stream (which joins Charlotte Brook 2 km downstream from the Restigouche deposit) has low SO_4 values (< 50th %ile), and only one sample is significantly anomalous in Pb and Zn (> 75 %tile for Pb). As discussed in Chapter Twelve, the Pb isotopic composition of this water is consistent with derivation from massive sulphide mineralization. Elevated Co (> 75th %ile) in surface waters and stream sediments draining Mt Vroom (northeast and east streams) and in Mt Fowler east stream (4 km to the northeast of the Restigouche deposit) may indicate a different style of mineralization in these areas (e.g., Pb isotopes, Chapter Twelve).

13.3.3 Stream sediments

The composition of stream sediments from the Restigouche deposit is more variable for sulphide-associated elements than sediments from the Halfmile Lake deposit. Cumulative probability plots for Fe, Zn, Pb and Cd show several populations (Fig. 13.10; Table 13.1).

Lead displays two major and one minor populations, with highly anomalous values above 410 ppm (up to 2000 ppm) and background values below 70 ppm (Fig. 13.11). For two kilometers downstream from the Restigouche deposit Pb contents are greater than Zn contents (Fig. 13.11). Maximum Zn contents occur between 500-900 meters downstream from the main

deposit, shifted slightly further downstream compared to the Pb peak (Fig. 13.11). Both Zn and Pb show generally decreasing concentrations beyond one kilometer from the deposit, but do not reach background levels at the limit of this data set (3 km downstream from the deposit; Fig. 13.11). For example, the Charlotte Brook sediment located 3 km downstream from the Restigouche deposit has 1000 ppm Zn, although background Zn levels in this study area are < 500 ppm (Fig. 13.11; Table 13.1). Stream sediments upstream from the main Restigouche deposit have background Zn (< 500 ppm) and Pb (< 70 ppm) contents. Cadmium, In, and Bi show similar patterns to Zn with respect to proximity to the deposit though with more rapid decrease to background values (< 2.2, 0.13 and 1 ppm, respectively) approximately 2 km downstream from the deposit. Copper and Ag display more erratic patterns but still increase with proximity to the deposit (Fig. 13.11).

The very high Pb values are almost an order of magnitude higher than Pb values in stream sediments reported by NBDNRE regional surveys in the Restigouche deposit area. Zinc in stream sediments downstream of the main Restigouche deposit are also elevated compared to the NBDNRE survey but to a lesser extent than Pb (maximum of 1600 ppm Zn versus a maximum of 894 ppm). It is unclear why there should be such a large difference in Pb contents between the two surveys. Assuming similar sampling and analytical methods, this result would imply that the Pb content of stream sediment varies significantly with time and that Pb is both hydromorphically and mechanically transported. Stream sediment from one site downstream from the deposit was sampled in both 1995 and 1996, yielding 1300 ppm Pb in both sediments, and 1000 and 930 ppm Zn.

Zinc and Pb are anomalously high (> 500 and 70 ppm, respectively) in some streams away from the influence of the Restigouche deposit. Zinc is anomalous (up to 1600 ppm) near the top of the North stream and decreases towards Charlotte Brook (200 m east of the Restigouche deposit). Lead contents in the North stream are much lower than in Charlotte Brook where it intersects the Restigouche deposit (Fig. 13.12). Elevated Zn contents (1500 to 1600 ppm) also occur in stream sediments from the Mt Fowler east stream 4 km to the northeast of the

Restigouche deposit. Although these sediments are very Fe-rich (Chapter Four), Zn/Fe ratios are considered too high to have been produced by the preferential adsorption of background Zn onto Fe-oxyhydroxides. These sediments also have the highest Cd contents in the Restigouche deposit study area (Fig. 13.12).

Sediments in streams draining Mt Vroom display low Zn and Pb but elevated Cu and Co contents (up to 280 and 830 ppm, respectively; Fig. 13.12). Several sediments from the Mt Vroom east stream are also anomalous in Ag (up to 2.7 ppm, with a background < 1.3 ppm).

13.3.3 Groundwaters and suspended sediments

Groundwaters were sampled from several boreholes intersecting the main Restigouche deposit, from two boreholes intersecting the C4 and C5 mineralized zones, and from several boreholes located away from the main deposit. Groundwaters proximal to mineralization are characterized by elevated SO_4 (up to 87 mg/L) and base metals with up to 5300 µg/L Zn, 1400 µg/L Pb, 56 µg/L Cu, 5.5 µg/L Cd, 66 µg/L Sb and 120 µg/L As (Fig.13.13). The base metals display multi-modal populations with two threshold values for most sulphide-associated metals, based on probability plots (Fig. 13.13; Table 13.1).

Groundwaters have anomalously high SO_4, Fe, Pb, Zn, As and Sb contents close to the Restigouche massive sulphide outcrop (Figs. 13.14, 13.15). Groundwaters from the C4 and C5 mineralized zones are characterized by high Fe, and have Zn and As values above the 75th percentile. Groundwaters from boreholes away from known mineralization have normalized base metal values which are generally at background levels (Table 13.1; Fig.13.14). Exceptions include Mo which is elevated above background (0.9 µg/L) in boreholes MM-89-106 and MM-89-109 to the east and west of the main deposit, respectively (Fig. 13.14).

Although borehole B-80-7 intersects massive sulphide mineralization at 170 meters depth, the groundwaters from this borehole are have base metal contents generally close to background values (Figs. 13.14, 13.15; Table 13.1). This indicates that the sulphides are below the effective limit of penetration of oxygenated recharge waters. Groundwaters collected

from boreholes in the hanging wall south of the deposit, however, display increasing metal values towards mineralization (Fig.13.14).

The saline groundwaters (borehole MM-88-02) have elevated Fe, Zn and Cu (up to 2800, 1700 and 41 μg/L, respectively; Fig. 13.14). However, the very high TDS contents of these groundwaters indicates that normalized to TDS content metal values would be at background (see discussion).

Lead contents are highest in shallow groundwaters where Restigouche deposit mineralization is close to surface and decrease with depth and with increasing depth of the sulphides (Fig. 13.15), consistent with the limited solubility and mobility of Pb in near-neutral waters. In contrast, Zn contents are high (but Pb contents low) in groundwaters from borehole MM-88-01 which intersects mineralization at greater depth (70 - 80 meters; Fig. 13.15). Arsenic and Sb display similar variation to Pb, indicating either that As- and Sb-bearing phases are only weathered in the very shallow massive sulphides or that As and Sb solubility is limited similar to Pb under conditions of circumneutral pH. These metals may also be removed from solution by adsorption onto Fe-oxyhydroxide phases. Iron contents (apart from the saline waters) are also greatest where the massive sulphides are close to surface (Fig. 13.15).

The metal content of suspended sediments in groundwaters vary as a function of borehole depth, depth of sulphides in boreholes, and lateral proximity to the Restigouche deposit. Boreholes MM-88-06 and MM-88-07 that intersect the shallow parts of the Restigouche deposit have suspended sediments that are highly enriched in Zn and Pb (0.89 to 7.7 and 11.1 to 15.3 weight %, respectively). Cadmium, Tl, Ag and Bi are also elevated in these sediments (see Chapter Nine). This is in contrast to suspended sediments from borehole MM-88-01 located approximately 200 meters from where massive sulphides outcrop at the Restigouche deposit which intersects mineralization at 70 - 80 m depth and contain elevated but less anomalous values of Zn and Pb (2100 to 3400 and 3500 to 6700 ppm, respectively). Distal holes (MM-89-106 and MM-89-107) located 150 and 350 m east of the area of sulphide mineralization have background values Zn and Pb (200 to 1600 and 96 to 430 ppm,

respectively). Zinc and Pb contents of suspended sediments in borehole MM-89-106 increase downhole.

13.4 Geochemistry of Mine waters

In situ oxidation of undisturbed massive sulphides below the water table is presently occurring at the Stratmat Main Zone deposit. Groundwaters within the massive sulphide zone are characterized by very elevated SO_4 compared to groundwaters above and below massive sulphides, and contain an order of magnitude higher SO_4 contents than groundwaters from the Restigouche deposit. Base metal and Fe contents are high in the sulphide zone, consistent with major oxidation of the massive sulphides, although not as elevated as groundwaters in the shallow parts of the Restigouche deposit. However, metals (Fe, Zn and Pb) do not balance the sulphate contents suggesting that they were removed from solution by sorption to Fe-oxyhydroxides. This is consistent with the neutral to alkaline pH conditions of these groundwaters, which promotes cation adsorption.

Groundwaters collected from the Wedge and Heath Steele deposits generally lower pH than Stratmat Main Zone and Restigouche deposit groundwaters with, in some cases, elevated base metal contents (e.g., up to 650,000 µg/L Fe, 340,000 µg/L Zn, 230 µg/L Pb, 17,000 µg/L Cu, 285 µg/L As and 360 µg/L Sb). In these cases, the groundwaters are similar to acid-mine drainage waters which are commonly characterized by very low pH and very high base metal contents (e.g., Al et al., 1994; Alpers et al., 1992).

13.5 Discussion

13.5.1 Surface waters at the Restigouche and Halfmile Lake deposits

Surface waters in streams draining the Restigouche and Halfmile Lake deposits are compositionally different in some respects due to a number of factors that include 1) the orientation of drainage with respect to mineralization, 2) the local hydrology that controls the depth of penetration of oxidizing groundwaters, and 3) the depth and dip of the sulphide

deposits which affects the volume of sulphide exposed to shallow oxidation.

The Halfmile Lake deposit crops out at a topographic high such that the main drainage system is not as intimately associated with mineralization as is the case for the Restigouche deposit. Surface waters at the Halfmile Lake deposit display less coherent anomalies than at the Restigouche deposit. However, SO_4 and Zn values are anomalous for surface waters from the Upper/Lower AB, Halfmile North and West tributary streams that drain areas closest to the surface expression of the Halfmile Lake sulphides (Fig. 13.2). Iron, Pb, and Cu do not display any coherent patterns with respect to proximity to the Halfmile Lake deposit although elevated Pb along the Upper/Lower AB stream coincides with elevated Fe (Fig. 13.2). The Upper/Lower AB stream is discharging along most of its length, as shown by seeps at the headwaters and artesian boreholes further downstream (Chapter Four). The elevated SO_4 and Zn is therefore interpreted to reflect massive sulphide oxidation in the subsurface. Due to the depth of the main Halfmile Lake deposit (Chapter Four), only SO_4 and Zn show consistent anomalies due to their greater mobility compared to Pb and Cu.

Giblin (1994) suggested that a positive correlation between Zn and Mg/Ca would be indicative of derivation of Zn from breakdown of Mg silicate minerals rather than a Zn mineralization, based on Zn substitution for Mg in mineral structures. For the Halfmile Lake deposit, the lowest Mg/Ca ratios occur in the Halfmile North stream which also has the highest overall Zn concentrations (and moderately high Zn; Fig. 13.2). Overall, Zn and Mg/Ca are negatively correlated, although for any one stream, Mg/Ca varies little compared to Zn. The elevated Zn along the Halfmile North stream is interpreted to reflect the greater proximity to surface of the main part of the Halfmile Lake North deposit compared to the Halfmile Lake South orebody (see Chapter Two). There is a large fault that runs parallel to the Halfmile North stream (Fig. 13.2) and it is possible that high Zn in these surface waters may be related to fluid movement along this fault. Surface waters draining the Halfmile North zone have lower Pb contents (Fig. 13.2) than the Upper/Lower AB stream. Iron contents are also low along this stream, suggesting that if the Zn is derived from sulphide oxidation, Fe and Pb have been

removed from solution due to precipitation of Fe-oxyhydroxides in the subsurface, consistent with speciation and mineral saturation calculations (Chapter Two) which indicate that there are no stable Zn, Pb or Cu minerals and that these metals are present primarily as free ions. Zinc in sediments from streams draining the Halfmile Lake deposit are highest along the Halfmile North stream although overall Zn contents of sediments are low compared to the Restigouche deposit (cf, Figs. 13.3, 13.12).

At the Restigouche deposit, Charlotte Brook flows over the deposit body close to where it is exposed at the surface, and there are clear geochemical differences in sulphide-associated elements (Fe, Zn, Pb, and Cd) in surface water compositions downstream of the deposit compared to upstream of the deposit (Fig. 13.8). Decay of Pb contents downstream of the main Restigouche deposit is more rapid than is the case for Zn, and matches the strong decrease in dissolved Fe contents, indicating removal of Pb from solution by adsorption to Fe-oxyhydroxide surfaces. The fact that Charlotte Brook drains the Restigouche deposit close to where it comes to surface means that a larger suite of sulphide-related elements are anomalous downstream of the deposit than was the case for the Halfmile Lake deposit.

Although the sulphide-associated metal anomalies in Charlotte Brook are easily related to known mineralization, there are several other anomalous areas in the Restigouche deposit study area that are distal from the Restigouche deposit. The North stream at the Restigouche deposit has anomalous contents of Zn, Cd, Co, Pb and in the headwaters, Cu (Fig. 13.9) where transported gossan (i.e., hydromorphic) are known to occur (D.R. Boyle, pers. comm.). This area also has anomalous trace metal contents (Co, Cd, Ni, Zn and Cu) in balsam fir and till (Dunn et al., 1996; Parkhill, 1997). Parkhill (1997) has suggested that these anomalies are related to glacial dispersal from the C4 and C5 mineralized zones, which have been interpreted to represent mineralization similar to the Restigouche deposit (Gower, 1996). However, given the transported nature of the gossan at the headwaters of the North stream, combined with elevated Zn relative to Pb in the surface waters and stream sediments (compared to those associated with the main Restigouche deposit) metal anomalies are interpreted to have

originated from groundwater that interacted with buried mineralization. However, Co (and Ni) are not enriched in streams draining the main Restigouche deposit (Fig. 13.9, 13.11) or in massive sulphides (Table 2.1, Chapter Two). For the stream sediments from the North stream the highest values of Zn are in the headwater samples similar to contents downstream from the main Restigouche deposit, but the Pb and Ag values are not elevated compared to Charlotte Brook downstream from the main deposit. This data is most consistent with a hydromorphic origin for the gossans.

Stream sediment from Mt Vroom northeast and Mt Vroom east streams (3 - 4 km southeast of the Restigouche deposit) collected during this study do not display highly anomalous Zn and Pb values similar to sediments close to the main Restigouche deposit. The streams do contain elevated Co, Cu, Ag and Cd but the high contents Fe-oxyhydroxides and ferricrete, and low Fe/metal ratios suggests that these metals may have been scavenged by Fe-oxyhydroxides. Surface waters from these streams have elevated SO_4 and Fe (Mt Fowler east stream) and Co, and scattered Pb, Zn, and Cu anomalies (Fig. 13.9). The Pb isotopic composition of surface water MLW95-467 is consistent with derivation of the dissolved Pb from massive sulphide mineralization (see Chapter Twelve). Thus, although Fe-oxyhydroxide scavenging may be an important process on these streams, there is some hydrogeochemical and Pb isotopic evidence to suggest that there may be massive sulphide mineralization in the subsurface. The large extent of Fe-oxide precipitation in the two streams indicates major Fe-sulphide mineralization in the subsurface.

High sulphate in surface waters from the Mt Fowler east stream 4 km northeast of the Restigouche deposit suggests mineralization may occur in this area (Fig. 13.9). However, base metal contents in these waters are not correspondingly elevated compared to background surface waters (Fig. 13.9). There are two possible explanations for the high sulphate and low base metal contents of the Mt Fowler east surface waters: 1) sulphate is derived from pyrite and/or pyrrhotite oxidation in the subsurface, or 2) other sulphides are also undergoing oxidation but base metals are rapidly removed from solution by adsorption (or co-precipitation)

to Fe-oxyhydroxide surfaces. Sediments in this stream are characterized by high Fe contents reflecting thick accumulation of Fe-oxyhydroxide minerals, and high Zn (up to 1600 ppm) in stream sediments suggests that mineralization in the subsurface is not restricted to Fe-sulphides. Although stream sediment Pb contents are not anomalous (Fig. 13.12), Pb isotope data from a surface water and stream sediment from this stream have very non-radiogenic values suggesting that the Pb was derived from sulphide minerals. The Pb isotopic composition of the stream sediment is less radiogenic than galena from all BMC massive sulphide deposits, suggesting a component of older Pb. This, combined with surface water and stream sediment anomalies in Co, Cd and Ni (Figs. 13.9, 13.12), which differs from the mineralization at the Restigouche deposit, may indicate a different style of sulphide mineralization in the area drained by the Mt Fowler east stream.

13.5.2 BMC surface waters compared to other studies

The composition of waters draining other massive sulphide deposits provides insights into level of metal transport and processes of metal dispersion in surface waters. From the previous discussion, it is evident that although base metal contents in surface waters are generally low, base metal anomalies occur in streams draining the Restigouche deposit (e.g., downstream from the Restigouche deposit, Zn is anomalous at 3 - 8 µg/L). These anomalies are much lower than those associated with the Red Dog, Drenchwater, and Lik deposits in Alaska (Kelley and Taylor, 1997). Surface waters draining the Drenchwater deposit have up to 2600 µg/L Zn, 10 µg/L Pb, 260 µg/L Cu, 26 µg/L As and 270 mg/L Fe. At the Red Dog deposit surface waters have up to 40,400 µg/L Zn, 2,100 µg/L Pb and 396 µg/L Cd. These two deposits are characterized by a lack of carbonate and metal-rich surface waters have generally low pH values (Kelley and Taylor, 1997). In contrast, surface waters draining the more carbonate-rich Lik deposit have metal loads more like those observed at the Halfmile Lake and Restigouche deposits, although Zn contents range up to 2,000 µg/L (Kelley and Taylor, 1997).

Glahder and Asmund (1996) reported on stream waters draining a Zn-Pb Sedex deposit

from northern Greenland. Spring discharge yielded Zn contents of up to 2,445 µg/L although values decreased following peak discharge to levels between 1 to 10 µg/L. A small stream draining sulphate-gossan outcrop had a pH of 2.4 and a Zn content of 155,000 µg/L.

Waters draining mine tailings sites are characterized by generally lower pH values and commonly high base metal loads compared to streams draining massive sulphide deposits in the BMC. For example, Al et al. (1997) reported that pore waters from Kidd Creek deposit tailings contain up to 4,080 mg/L Zn, 2.29 mg/L Pb, 53.6 mg/L Cd and 22,900 mg/L SO_4. Stream draining mines in Wales have values of 480 - 7400 mg/L SO_4, 26.7 - 66.8 mg/L Zn and 48 to 108 mg/L Cu (Fuge et al., 1994). Pore waters from tailings at the Heath Steele deposit have values up to 10,200 mg/L Fe, 24,800 mg/L SO_4, 200 mg/L Zn as well as elevated Ni and Cu (Appleyard and Blowes, 1994). Although such elevated metal and sulphate values are generally restricted to the uppermost parts of tailings, the metal contents are clearly well in excess of those observed in ground and surface waters at the Halfmile Lake, Restigouche and Stratmat Main Zone deposits. Mine tailings stored at the surface increase the exposure of massive sulphides to atmospheric oxygen resulting in sulphide oxidation and the production of low pH and high metal values. The increased surface area of sulphide minerals in tailings facilitates sulphide oxidation and dissolution.

13.5.3 Surface waters in mineral exploration

There have been relatively few studies of hydrogeochemistry in mineral exploration since the uranium exploration boom in the 1970's (Taufen, 1997). However, there has been renewed interest in using waters in mineral exploration due to improvements in analytical techniques. Wang et al. (1995) have described stream waters as the "ideal medium" for mineral exploration of base metal deposits in heavily forested and swampy regions of northeastern China. Streams draining known VMS occurrences are enriched in Cu, Zn, Fe, Mn and SO_4 (Wang et al., 1995). Vandelannoote et al. (1984) showed that high abundances of F, V, Fe, Ni, Cu, Sr, Y, Sb, Ba and I in local surface waters indicated the presence of Zn-Pb mineralization in Brittany.

Ruijin et al. (1994) studied surface water hydrochemistry in areas of northeastern China which are covered in thick (30 - 100 m) sequences of basalt flows and found that elevated contents of dissolved Mo, SO_4, Cu/Ni and Zn/Ni indicated areas of known mineralization that were not evident from stream sediment geochemistry. Cidu et al. (1995) used surface water and suspended sediment to show that dissolved Au, As and Sb contents successfully delineated areas of known Au mineralization in Sardinia, Italy.

The utility of ground and surface waters in mineral exploration is dependent on a number of factors including: 1) geochemical difference between the orebody and immediate host rocks compared with the more regional rock composition, 2) orientation of the deposit and its proximity to surface, 3) whether the hydrology is dominantly recharge or discharge and where recharge is occurring in relation to the deposit, and 4) buffering capacity of the host rocks.

The contrast in the base metal and sulphate contents of ground and surface waters in the BMC between mineralized and unmineralized sources show that hydrochemistry is an effective exploration technique in this camp. Compared to other examples of sulphide oxidation and mine tailings weathering, however, base metal anomalies in BMC surface waters are relatively subtle and commonly spatially localized. This indicates that effective use of hydrogeochemistry in the BMC requires detailed surveys of the type carried out in this study. For routine exploration, a minimum of a sample every 500 meters along a stream is probably required. The results of this study show that anomalous values appropriate for other deposit-types or for VMS deposits in other areas (with different rock types, climate, topography) are not necessarily applicable to the BMC.

The orientation and depth of the massive sulphides, and depth of penetration of O_2-rich recharge waters is critical because base metal loads in ground and surface waters will to a large extent be dependent on the supply of O_2 for sulphide oxidation. Base metal anomalies in ground and surface waters from the Restigouche deposit are elevated compared to the Halfmile Lake deposit in large part because the Restigouche deposit dips shallowly and is close to surface with respect to drainage, whereas the bulk of the Halfmile Lake deposit occurs at

greater depth. Massive sulphide oxidation at the Stratmat Main Zone is enhanced due to groundwater flow through the massive sulphide zone such that DO is constantly supplied by recharging groundwaters (see Chapter Eight).

Although base metal and sulphate contents in Charlotte Brook waters are clearly anomalous downstream from the Restigouche deposit compared to upstream (Fig. 13.8), base metal and sulphate values are much lower than in groundwaters from boreholes (MM-88-06 and MM-88-07) adjacent to Charlotte Brook. The interpretation is that Charlotte Brook was recharging where it crosses the deposit at the time of sampling such that base metal contents and sulphate are lower than expected. It is possible that during spring runoff, base metal and sulphate contents may be more elevated, as in the seep water from the gossan (MLW95-300; Fig. 13.8). The base metal and sulphate contents of Charlotte Brook highlight the importance of the local hydrology which partly controls the potential transfer of the products of massive sulphide oxidation in the subsurface to the secondary environment. Sulphide-associated metals and sulphate may also be lower than expected due to dilution by non-mineralized base flow.

Taufen (1996) discussed the utility of hydrogeochemistry in mineral exploration based on his investigations of metal dispersion in ground and surface waters from mine tailings at the Waite and Amulet deposits in Quebec. He noted that in designing a hydrogeochemical exploration program, it was important to determine the extent of acidic plumes emanating from sulphide oxidation. Samples collected beyond the extent of acidic groundwater plumes would be expected to have low base metal loads due to adsorption and coprecipitation processes associated with increasing pH. Although this is certainly true, the results from the Halfmile Lake, Restigouche and Stratmat Main Zone deposits indicate that massive sulphide oxidation is not necessarily accompanied by large decreases in pH. For example, high base metal loads occur in shallow groundwaters at the Restigouche deposit, yet pH values are still in the 6 - 7 range. Very low pH values of ground and surface waters are commonly associated with acid-mine drainage problems where the high surface area of sulphide minerals, a ready access to atmospheric O_2 and insufficient carbonate minerals for pH buffering result in low pH values.

This is also true for natural oxidation of massive sulphides in the absence of sufficient buffering capacity in the host rocks, e.g., Red Dog and Drenchwater deposits, Alaska (Kelley and Taylor, 1997). Although there are no limestone or dolomite units associated with mineralization in the BMC, vein and fracture zone carbonate appears to be sufficient to buffer sulphide oxidation and maintain circum-neutral pH values at the Restigouche and Stratmat Main Zone deposits. The dispersion of base metals in ground and surface waters is, therefore, likely to be more subtle than is the case for deposits such as Red Dog. The groundwaters collected at the Wedge deposit and from the Heath Steele mine indicate that very high base metal contents can certainly be expected in the BMC where the buffering capacity of the host rocks is exceeded. However, in both these cases, the natural environment has been perturbed during mining.

There are some limitations to the use of hydrogeochemistry in mineral exploration. Because of the generally low base metal contents of natural waters (especially surface waters), consideration must be given to sampling procedures to minimize sample contamination and what filter size to use to remove suspended material. For example, Giblin (1994) suggested that on site filtering in exploration programs should be avoided due to the added risks of sample contamination. She also noted that metal loss by adsorption to container surfaces is minimal for the purposes of exploration. However, filtering on site has the advantage of a standard procedure which combined with sample acidification prevents precipitation of Fe-oxyhydroxides and loss of metals by adsorption. If time and budgets warrant, it may be advantageous to analyze an unfiltered aliquot, in particular for surface waters or groundwaters with a high suspended sediment load. This study has shown, for example, that some groundwaters have high metal contents along with associated high suspended sediment loads. In addition, several recent studies have looked at element partitioning between the truly dissolved loads and colloidal material that is less than the pore size of the filters being used. In this study, of surface waters, this is unlikely to be a major consideration because the suspended sediment load was very minor and the < 0.45 μm load can be considered as the "dissolved"

load in an exploration program. However, in areas where there are large contrasts in suspended and colloidal loads, there is the probability that metals are being fractionated into different media which may affect interpretations as to what is anomalous.

Metal speciation in natural waters is very strongly controlled by pH, and to a lesser extent Eh (Chapter Seven). Results of metal speciation in this study indicate that with increasing pH values, metal CO_3 and HCO_3 complexes become increasingly dominant (Fig. 5.22). At higher pH, there is increased likelihood that Pb and Zn will be stable in solution if they form neutral, stable CO_3 complexes. However, the pH at which these complexes become significant is higher than the typical adsorption edge for these metals on typical clays and amorphous Fe-oxyhydroxides (see Chapter Seven, Fig. 7.43). As a result, there is no correlation between the amount of Pb or Zn present as CO_3 complexes and metal abundance. Mineral saturation calculations for surface waters (Chapter Five) indicate that no base metal mineral phases are stable in these waters. The major control over metal dispersion is therefore related to adsorption to Fe-oxyhydroxide phases (see Chapter Seven for discussion).

Arsenic and Mo occur primarily as oxyanions in natural waters and should be more mobile at higher pH than the base metals. At both the Halfmile Lake and Restigouche deposits, anomalous As contents increased with proximity to massive sulphide mineralization. At the Halfmile Lake deposit, groundwaters have anomalously high Mo contents, compared to surface waters and to groundwaters from the Restigouche deposit. It may well be that As and Mo contents of surface waters would prove a useful exploration tool in the BMC. Unfortunately, the analytical methods used in this study did not have sufficiently low detection limits to measure these elements in surface waters.

Several studies which have investigated the utility of hydrogeochemistry for mineral exploration have suggested that dissolved SO_4 contents act as a good proxy for base metals because SO_4 is not affected by adsorption processes and is therefore more mobile at circumneutral pH (Miller et al., 1991; Miller et al., 1992). In addition, SO_4 is produced as a result of pyrite dissolution wich may be unrelated to Zn-Pb massive sulphide mineralization. At

the Restigouche deposit the base metal contents of Charlotte Brook waters are a much better predictor of proximity to the main deposit (Fig. 13.8). Dissolved sulphate contents of Charlotte Brook downstream from the deposit are lower than many of the other streams, and the SO_4 values are below the 50th percentile (Fig. 13.9A). This is an unexpected result given that shallow groundwaters collected from borehole close to Charlotte Brook have very high SO_4 and base metal loads consistent with significant oxidation of the shallow massive sulphides.

Previous work has suggested that variations in major cations might serve as guides for exploration in hydrogeochemical studies (Giblin, 1994; Giblin and Snelling, 1983). Trace metals are commonly adsorbed to Fe and Mn oxyhydroxides, potentially limiting the extent to which they are transported and therefore limiting dispersion. An early example is the work of Giblin and Snelling (Giblin and Snelling, 1983) who studied the hydrogeochemistry of groundwaters associated with uranium mineralization in the Northern Territories of Australia. They found that although U did not successfully delineate known mineralization, Mg ratios (defined as Mg/(Mg+Ca+Na+K)) were successful due to the chlorite alteration halo associated with U mineralization. At the Halfmile Lake and Restigouche deposits, the major elements most likely to reflect alteration halos about massive sulphide deposits are Mg and K (chlorite and sericite alteration, respectively). However, the abundance of these elements in surface waters is more related to differences in lithology and the restricted solubility of chlorite and sericite than to proximity to known mineralization (see Chapter Five). In most surface waters, Mg contents are largely controlled by carbonate dissolution whereas K contents display little compositional variance, probably due to weathering of feldspars to illite (Chapter Five).

Although hydrogeochemistry is certainly no panacea, the data presented in this study strongly suggests that there is certainly a place for this methodology in mineral exploration in a mature mining camp such as the BMC. However, it is clear from surface water compositions at the Halfmile Lake and Restigouche deposits that background trace metal values are low and that anomalies are subtle compared to deposits elsewhere (e.g. Red Dog deposit).

13.5.4 Groundwaters in mineral exploration

As shown in sections 13.2.3 and 13.3.3 (and Chapters Seven and Eight) groundwaters proximal to massive sulphide mineralization in the BMC have elevated As, SO_4 and base metal (Zn, Pb, Cu, Mo, Sb, Cd) contents at levels considerably higher than local surface waters (Cf, Figs. 13.1, 13.4, 13.7, 13.13). Circumneutral pH values in Halfmile Lake, Restigouche and Stratmat Main Zone deposit groundwaters result in generally restricted mobility of base metals due to adsorption, primarily to Fe-oxyhydroxide minerals, and in rare cases due to precipitation of metal-sulphate minerals (e.g., anglesite in suspended sediments from the Restigouche deposit; Chapter Nine). Thus, groundwaters may be useful in hydrogeochemical exploration because of greater contrast between background and anomalous values of metals in ground and surface waters (e.g., Fig. 13.14).

The use of groundwaters in mineral exploration has received relatively little attention. Grimes et al. (1995) investigated contents of dissolved Au and related elements (As, Sb, W) in groundwaters interacting with Au deposits in Nevada and showed that these elements were anomalous, especially in reducing groundwaters. Grimes and de Carvalho (1994) studied the utility of well water in part of the Neves-Corvo area, part of the Portugese Pyrite Belt, and showed anomalous metal contents proximal to known mineralization.

There are several difficulties in the use of borehole waters in mineral exploration in the BMC, not the least of which is the expense of drilling boreholes. In most parts of the BMC there are insufficient domestic water wells for effective use of groundwater in an exploration program. Drilling typically only occurs after a good exploration target has been identified. However, once drilling has commenced, groundwater composition may be useful in vectoring towards possible new targets and choosing locations for additional drill holes. For example, groundwater (MLW95-546) has generally low base metal contents (Fig. 13.14) but the Pb is non-radiogenic with a Pb isotopic composition similar to massive sulphide deposits in the BMC (Chapter Twelve).

Groundwater exploration is difficult due to the complex nature of subsurface flow systems

in fracture-flow dominated geology. However, metal values in groundwaters from boreholes which intersect the Restigouche deposit clearly delineate massive sulphide mineralization, whereas groundwaters recovered away from mineralization have generally background compositions (Fig. 13.14).

There appears to be an effective depth below which significant sulphide oxidation is not occurring. For example, at the Halfmile Lake deposit, all the boreholes sampled intersect mineralization at depth (> 300 m) and base metal contents are much lower than in Restigouche deposit groundwaters. At the Restigouche deposit, however, groundwaters interacting with sulphides at shallow depths have anomalous base metal and sulphate contents whereas groundwaters from borehole B-80-7 which intersects mineralization at 170 meters are not anomalous (Fig. 13.15). At the Stratmat Main Zone deposit, extensive oxidation of the massive sulphides occurs at 85-90 meters depth (Chapter Eight).

13.5.5 Saline waters from the Restigouche deposit

The saline waters at Restigouche have elevated Zn but have relatively low Pb contents and sulphate contents which are below detection. This raises the question as to the origin of the anomalous Zn. Normalized to TDS, the Zn contents are not anomalous, however. The shallow bore holes which are proximal to the Restigouche deposit have elevated Zn and Pb contents (see Fig. 7.37) and correspondingly high SO_4 consistent with oxidation of the massive sulphide minerals in the Restigouche deposit. However, there is no obvious spatial relationship between the high Zn contents of the MM-88-02 waters and the sulphide zone as the high Zn values occur in groundwaters that were recovered with the straddle-packer at depths well below the deposit. There are several possible explanations for the high Zn contents of the saline waters:

1) the deep saline waters have mixed with more shallow groundwaters with high metal contents resulting from the dissolution of sulphide during oxidation. If this is the case, the low Pb contents could be explained by the low mobility of Pb in natural waters; note the sharp

decrease in Pb contents with depth and distance from the deposit in the shallow borehole waters (Fig. 13.15).

2) the high Zn contents may be unrelated to mineralization. Brines from the Mississippi oil fields contain elevated Zn and Pb concentrations as a result of diagenetic reactions at elevated temperatures (Saunders and Swann, 1990). The high Zn contents may also be due to a combination of Cl and CO_3 complexes (only 25 - 30% of the Zn in these waters is present as free ions) and reducing groundwater conditions which prevents the precipitation of Fe-oxyhydroxides. Fe contents are also high in these waters.

3) these waters may have reacted with mineralization at depth. Borehole MM-88-02 is the deepest hole drilled to date at Restigouche and was drilled to test a gravity anomaly (Westoll, 1990) but further investigation of deeper mineralization was abandoned due to the intersection of thick diabase sills in the hole which were considered adequate to explain the anomalies. The low Pb contents and lack of sulphate suggest that these fluids have migrated some distance from the source of the metals.

As discussed in Chapter Seven, the preferred hypothesis is that the high Zn contents in the MM-88-02 waters reflects further mineralization at depth and at an undefined distance from the Restigouche deposit. These waters also have moderately high Ni, Cr, Cu and Co contents suggesting either a different sulphide mineralogy or that these elements have been concentrated in saline waters from background sources.

The presence of saline waters at the Restigouche deposit has another important implication to mineral exploration. Because of density contrasts, saline waters may remain in situ over long periods of time, effectively limiting the depth to which oxidizing surface waters can penetrate. Thus a deeply buried deposit might be effectively isolated from detection by exploration methods which rely on the hydromorphic transport of the products of sulphide oxidation.

13.5.6 Stream sediments

In this study, stream sediments were determined for total elemental abundances (Chapter

Six). Although many exploration programs employ partial extraction techniques to try and isolate the hydromorphic components from detrital components, total dissolution analysis can be useful in both mineral exploration and environmental surveys. As was shown in Chapter Six (major and trace elements) and Chapter Ten (REE), there is a clear hydromorphic component to the stream sediments, even for the REE which are generally considered to be immobile.

Although only total analyses were used in this study, anomalous metal values are clearly distinguished from background values for the Restigouche deposit (Figs. 13.11, 13.12). Stream sediments from Charlotte Brook downstream from the Restigouche deposit are anomalous in Pb, Zn, In, Bi and Cd and decrease downstream away from the deposit (Fig. 13.11). The abundance of Pb in Charlotte Brook stream sediments downstream from the Restigouche deposit are unusually elevated (up to 2000 ppm). Zinc contents show the least decrease with distance from the deposit. Close to the deposit Zn/Pb ratios are < 1, whereas beyond 2.5 km from the deposit, Zn/Pb ratios are > 1. Copper and Ag show only subtle anomalies, and Co does not vary with proximity to the main sulphide deposit. With increasing distance from the deposit, Pb, Zn, In, Bi and Cd display decreasing abundances.

Stream sediments from the Halfmile Lake deposit have lower metal values and anomalous values are more difficult to distinguish from background streams with the limited data set available. However, as shown in Chapter Six, hydromorphic and detrital contributions of trace metals to stream sediments can be distinguished to a certain extent by comparison with local host rocks. Zinc, Pb, Mo, and Cd show higher abundances in the Halfmile North, the Upper/Lower AB and the West tributary streams close to mineralization. As with the surface waters, comparison of stream sediment compositions between the Halfmile Lake and Restigouche deposits indicates that more deeply buried ore bodies have more subtle surficial geochemical anomalies. Therefore, exploration programs are required to sample in greater detail than regional programs have in the past.

13.5.7 Suspended sediments in VMS exploration

Previous studies of suspended sediment compositions have focussed on surface waters. Seigel (1990), Siegel et al. (1993) and Cidu et al. (1995) showed that stream water suspended sediments could be used to delineate Au and base metal mineralization. Siegel (1990) found that suspended sediment showed more intense anomalies with better contrast with background values when compared to stream sediments (total and partial extraction analyses). Surface waters at both the Halfmile Lake and Restigouche deposits typically were free of suspended sediments during sample filtering (typically 750 to 1000 ml was filtered on site). However, suspended sediments were common in groundwaters collected from the Halfmile Lake and Restigouche deposits using both the flow-through bailer and straddle-packer systems (see Chapter Nine). As discussed previously, base metals reach values similar to the highest values measured for massive sulphides. For example, suspended sediments from the Restigouche deposit have up to 15.3 weight % Pb compared to a maximum of 17.4 weight % Pb for massive sulphides. The major difference between the groundwater suspended sediments compared with stream sediments is that the suspended sediments are generally closer to the source of mineralization, and Eh-pH conditions of the groundwaters with which the suspended sediments are associated may be more conducive to the suspended sediments showing anomalous compositions compared to stream sediments, i.e., the suspended sediments have a greater hydromorphic component. At the Halfmile Lake deposit the main part of the deposit is deeply buried such that surface water and stream sediment anomalies are subdued compared to the Restigouche deposit. Groundwater suspended sediments are anomalous at the Halfmile Lake deposit, showing metal contents in some cases well in excess of stream sediments downstream from the Restigouche deposit. The suspended sediments from the Halfmile Lake deposit are anomalous even though the groundwaters from which they were recovered do not have very high base metal contents compared to the more shallow Restigouche deposit. It was shown in Chapter Nine that although the dominant mineralogy of most of the suspended sediments is consistent with their derivation from the host lithologies (clays, quartz etc), bulk

chemical analyses of the suspended sediments still revealed both detrital and hydromorphic contributions. This suggests that base metals were dissolved in solution following massive sulphide oxidation and subsequently immobilized on the suspended load, primarily by adsorption (and probably co-precipitation). Thus, at both the Halfmile Lake and Restigouche deposits, generally neutral to alkaline pH values result in a strong fractionation of base metals to the suspended sediment phase compared to the dissolved phase.

The Zn/Pb ratios of the suspended sediments may be a useful vector toward massive sulphide mineralization. Suspended sediments in groundwaters close to the Restigouche deposit have ratios < 1 compared with ratios > 1 in sediment from groundwaters remote from mineralization. Similarly, suspended sediments in boreholes HN94-65 and HT55-43 from the Halfmile Lake deposit show decreasing Zn/Pb ratios downhole towards the massive sulphides. This relationship between Zn and Pb is consistent with the greater solubility of Zn compared to Pb due to the preferential adsorption (or co-precipitated) of Pb by suspended sediment. A similar relationship between Pb and Zn is shown for stream sediments from the Restigouche deposit as stream sediments in Charlotte Brook close to the Restigouche deposit have Zn/Pb < 1.

13.6 Summary

1) Surface waters can be routinely analyzed for trace metals to very low detection limits because of recent advances in analytical techniques. This has removed one of the most serious obstacles in the use of natural waters in mineral exploration. Although base metal contents of surface waters at the Halfmile Lake and Restigouche deposits are low compared to other deposits and mine tailings, anomalous Zn, Pb, Fe and Cd are clearly associated with the main Restigouche deposit. The Halfmile Lake deposit is deeper and as a result surface water anomalies are more subtle, although SO_4 and Zn contents increase with proximity to the deposit.

2) Hydrology is an important control over massive sulphide oxidation and development of

hydromorphic anomalies in both groundwater and, therefore, surface environments.

3) Groundwaters show greater base metal abundances and greater contrast between anomalous and background compositions than surface waters, especially at the Restigouche deposit and therefore could be a powerful tool in mineral exploration in the BMC. However, application of this technique is limited due to poor access to boreholes away from areas of known mineralization. Groundwater geochemistry may also be useful in defining exploration targets and in understanding metal dispersion from the site of massive sulphide oxidation to the surface environment.

4) Suspended sediments in groundwaters associated with mineralization have very high metal contents, primarily as a result of circumneutral groundwater pH values, fractionation of the base metals from the aqueous to the suspended sediment phase, and lower dilution by detrital components compared to stream sediments. Suspended sediment geochemistry may be a useful exploration tool to complement ground and surface water hydrogeochemical exploration. In particular, Zn/Pb ratios of suspended sediments decrease with increasing proximity to massive sulphide mineralization.

5) The generally neutral pH values of ground and surface waters at the Halfmile Lake, Restigouche and Stratmat Main Zone deposits results in more subtle base metal anomalies compared to other massive sulphide deposits. As a result, the dispersion trains are generally short making it essential that the sampling be carried out at a detailed scale if it is to be effective in mineral exploration in the BMC. As a result, previous regional geochemical surveys are unlikely to be effective in discovering new deposits in the BMC, particularly if they occur at depth. In order to test the efficacy of hydrogeochemical methods in the BMC based on this work, a large survey was initiated involving a 400 km^2 area. Stream and seep waters and sediments and balsam fir twigs were collected at 500 meter intervals along all stream in the survey area (Leybourne et al., 1997a).

6) Lead isotopes (Chapter Twelve) are a powerful tool in interpreting Pb sources. Although analytical costs are high, Pb isotope analyses may be very useful in follow-up studies to better

distinguish false and real metal anomalies in both surface waters and sediments.

Table 13.1 Anomalous and background values for sulphide-associated elements in waters and sediments

		Halfmile Lake deposit			Restigouche deposit		
		Surface water	Stream sediment	Groundwater	Surface water	Stream sediment	Groundwater
SO_4	Threshold-1	4.1		15	7		41
	Threshold-2	3.2		3	4.3		6
	Background	< 3		< 3	< 3		< 6
Zn	Threshold-1	6.2	350	150	18	1000	300
	Threshold-2	2		40	3	500	48
	Background	< 2	< 350	< 40	< 3	< 500	< 48
Pb	Threshold-1	0.12	68	1	1.7	410	30
	Threshold-2				0.55	70	1
	Background	< 0.12	< 68	< 1	< 0.55	< 70	< 1
Cu	Threshold-1	3.5	550	4	1.9	100	20
	Threshold-2	0.75	150			55	4
	Background	< 0.75	< 150	< 4	< 0.7	<55	< 4
Cd	Threshold-1	0.02	2	0.2	0.02	6	0.25
	Threshold-2					2.2	
	Background	< 0.02	< 2	< 0.2	< 0.02	< 2.2	< 0.25
As	Threshold-1			2			16
	Threshold-2						
	Background			< 2			< 16
Mo	Threshold-1		1.3	9.6		10	1.8
	Threshold-2			4.8		4.9	0.9
	Background		< 1.3	< 4.8		<4.9	< 0.9

Water data in µg/L except SO_4 (mg/L)
Sediment data in ppm

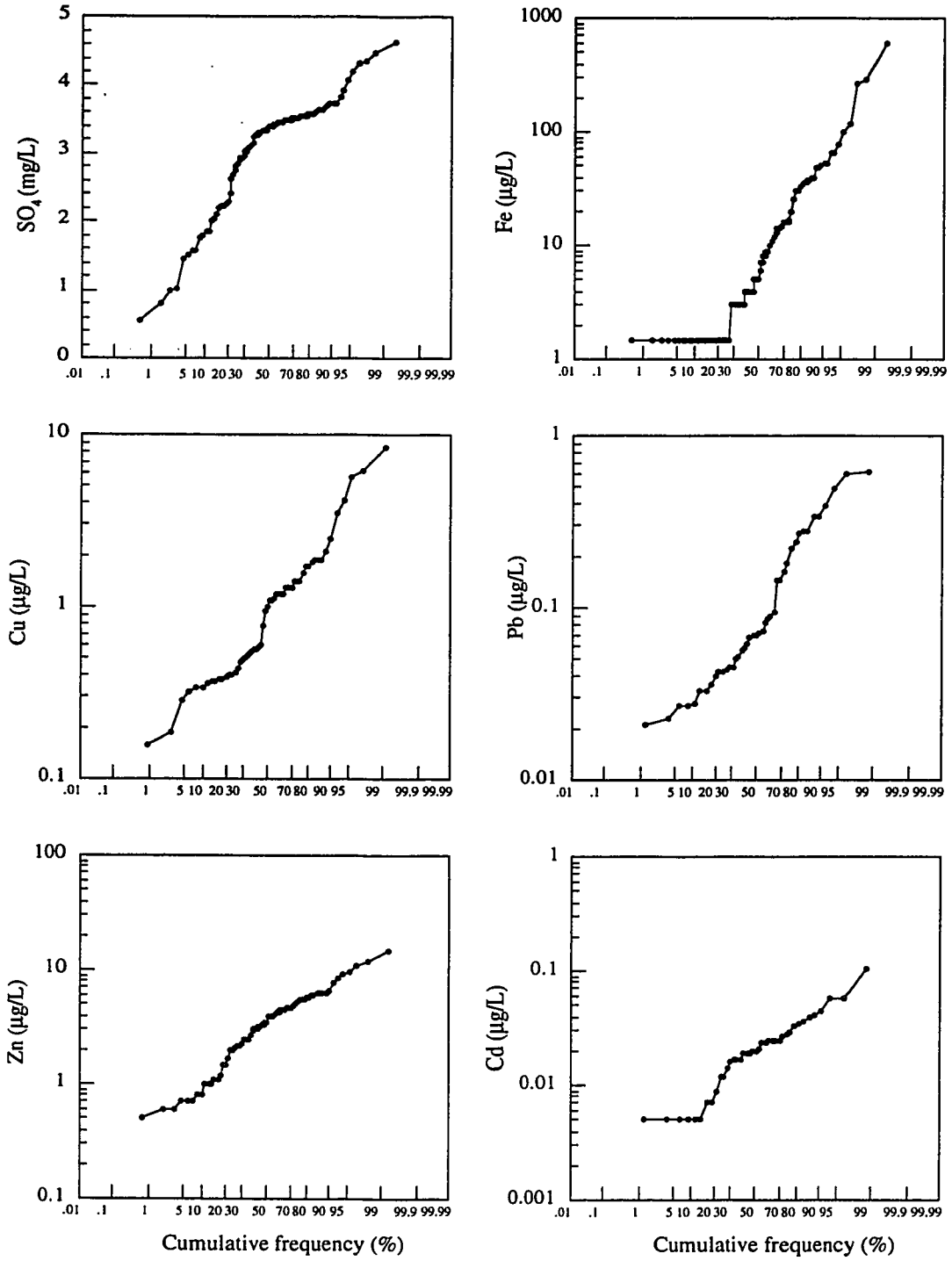


Fig. 13.1 Cumulative probability plots of the main massive sulphide-related elements for Halfmile Lake deposit surface waters.

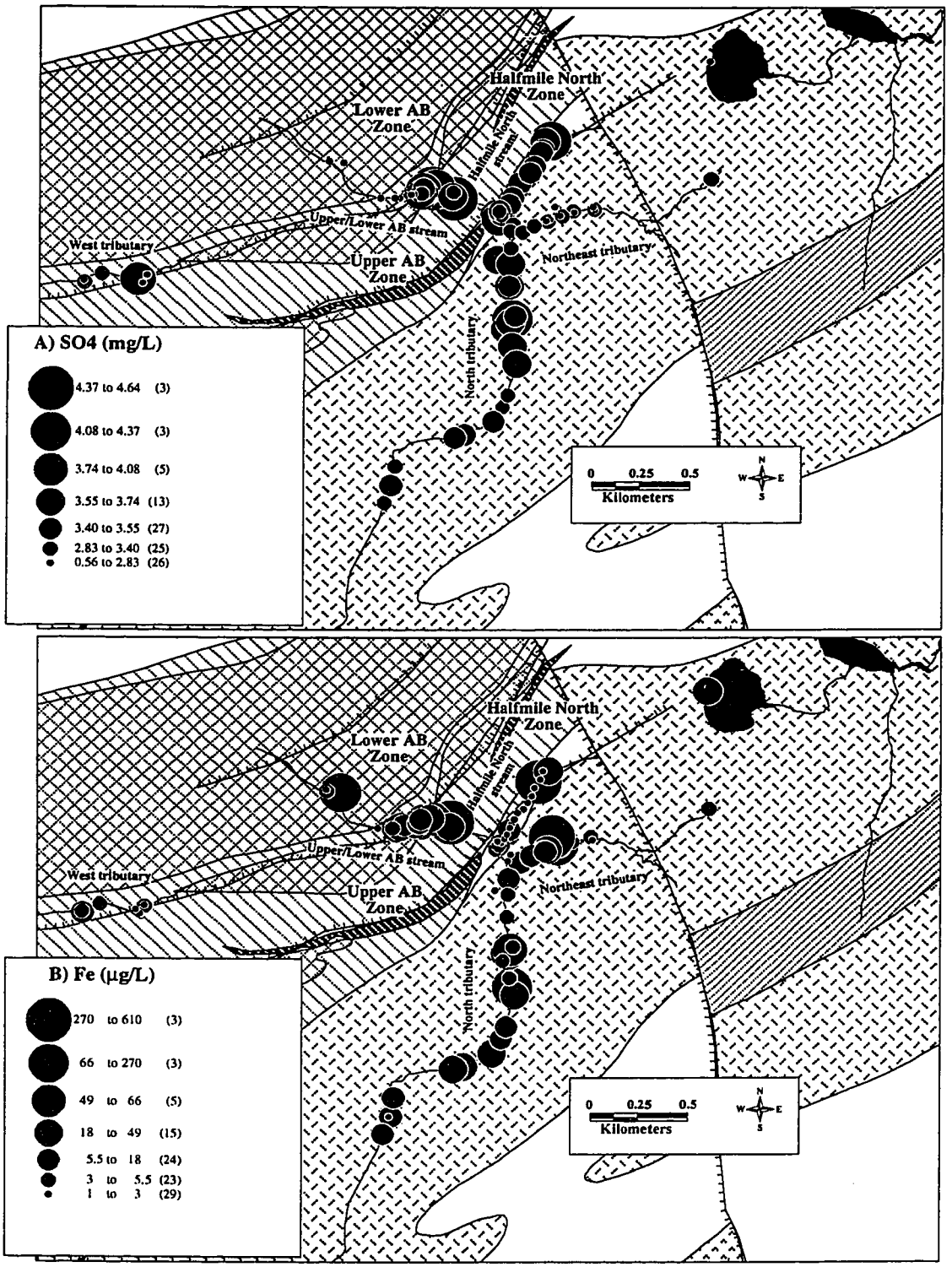


Fig. 13.2 Porportional circle maps of Halfmile Lake deposit surface waters.

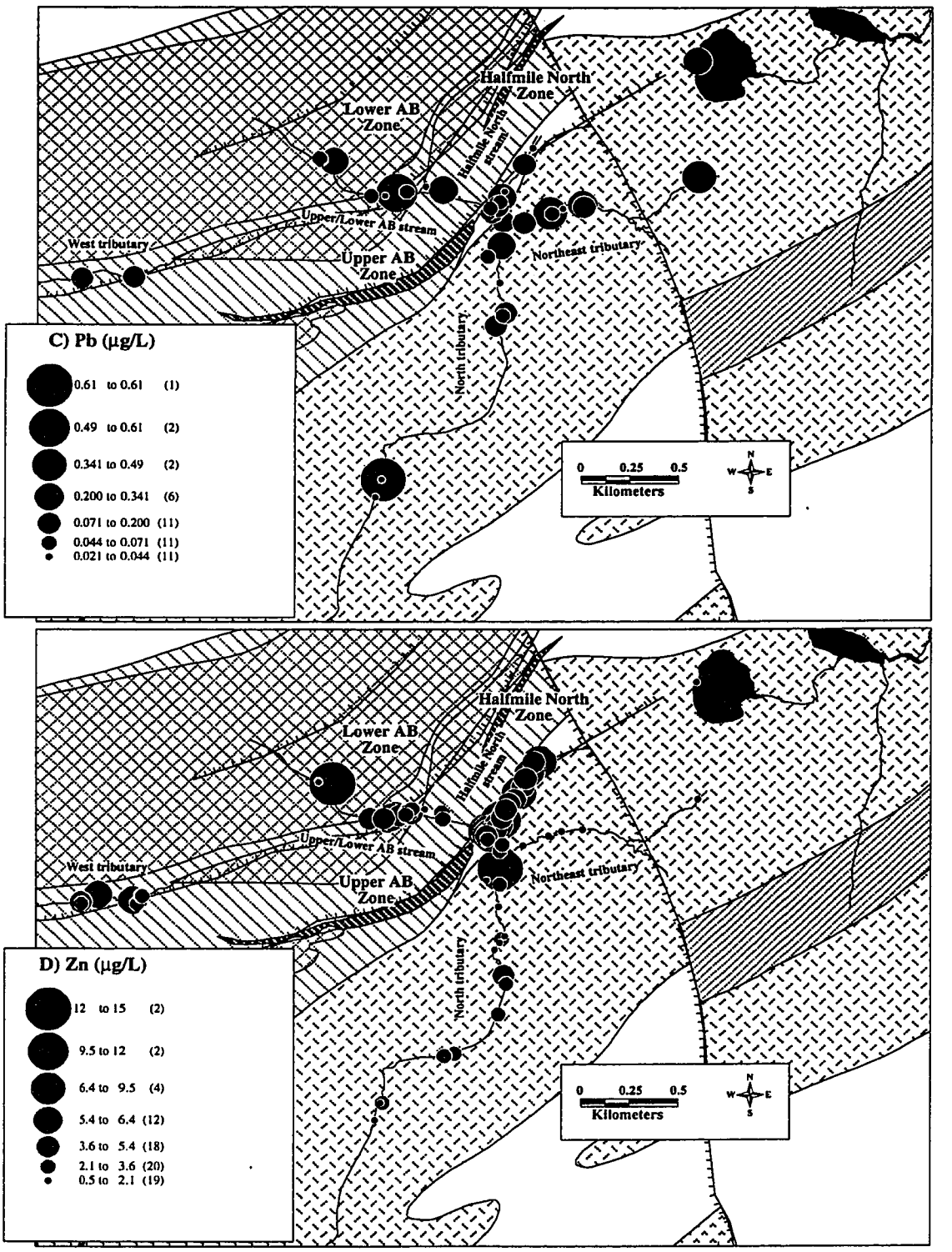


Fig. 13.2 continued.

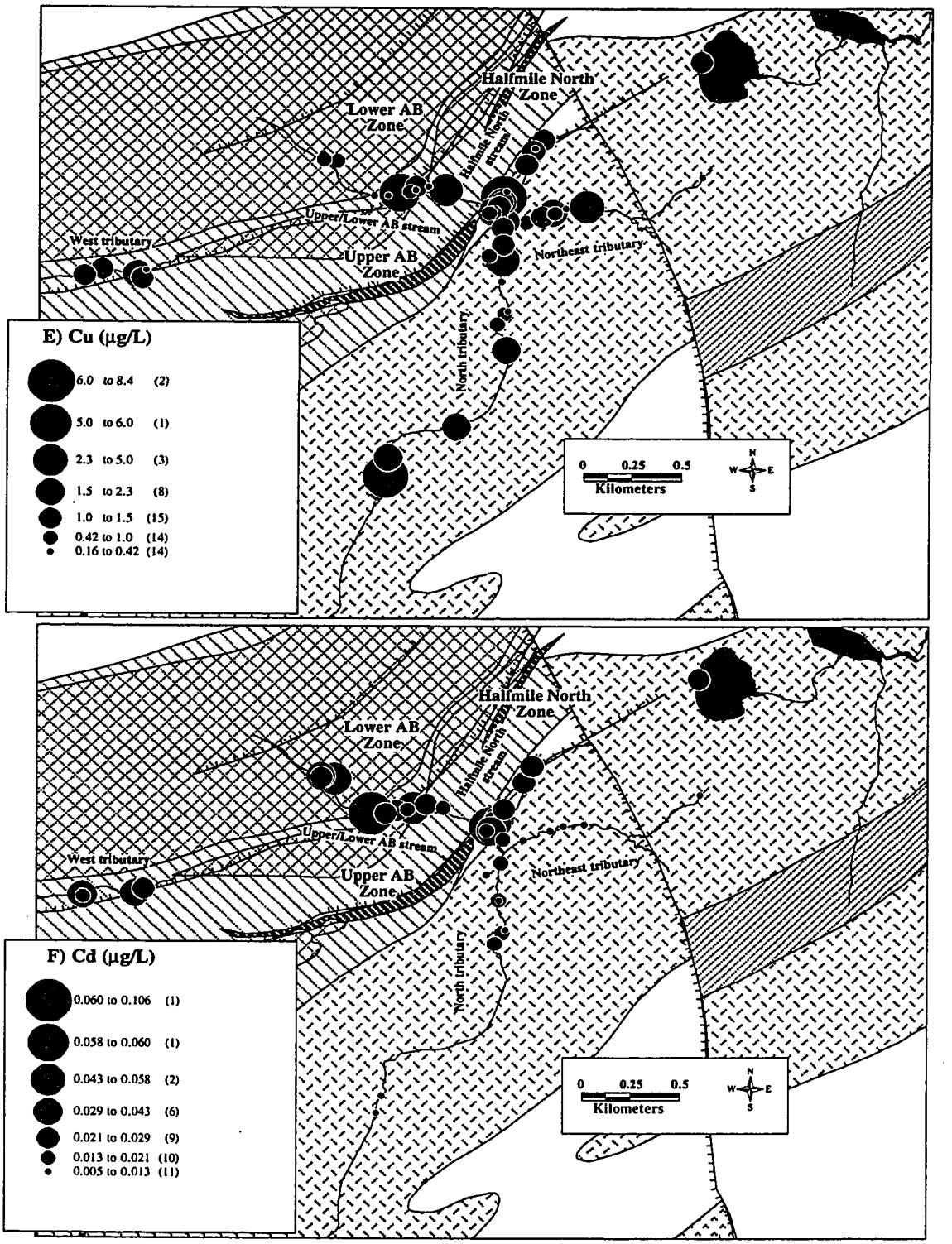


Fig. 13.2 continued.

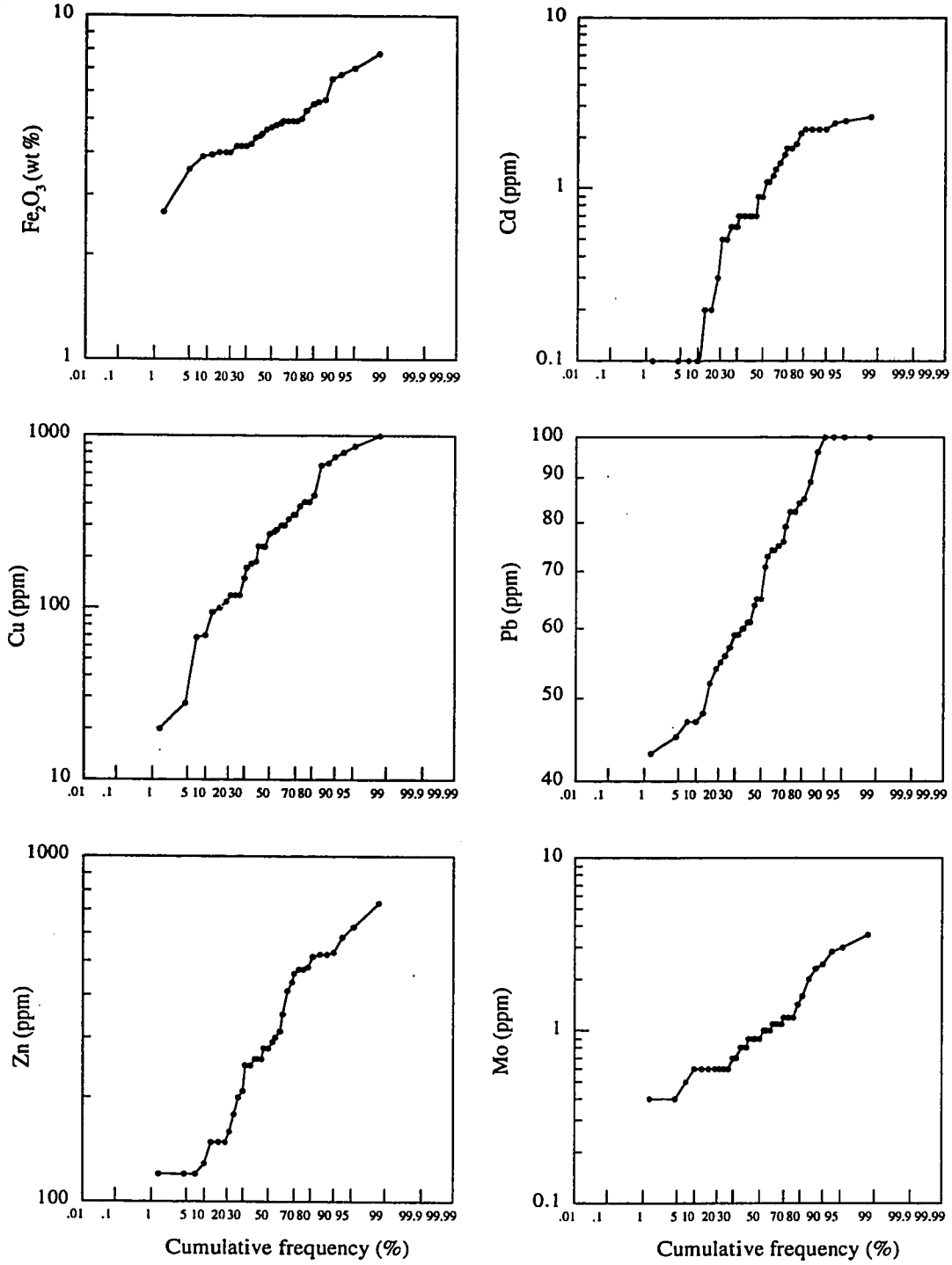


Fig. 13.3 Cumulative probability plots of the main massive sulphide-related elements for Halfmile Lake deposit stream sediments.

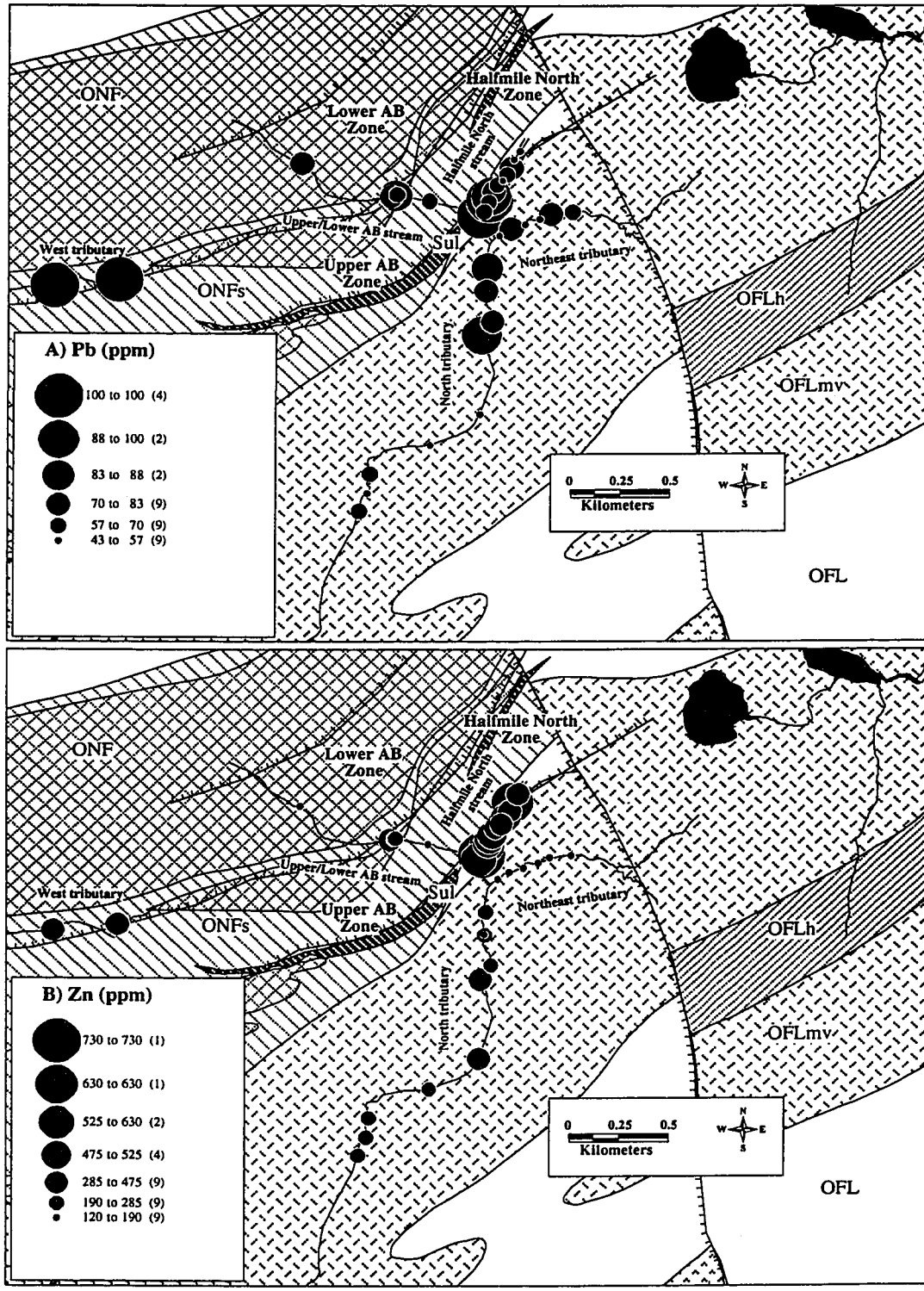


Fig. 13.4 Proportional circle maps of stream sediment compositions from the Halfmile Lake deposit. Geology as in Chapter Two, Sul = surface projection of massive and stringer sulphides.

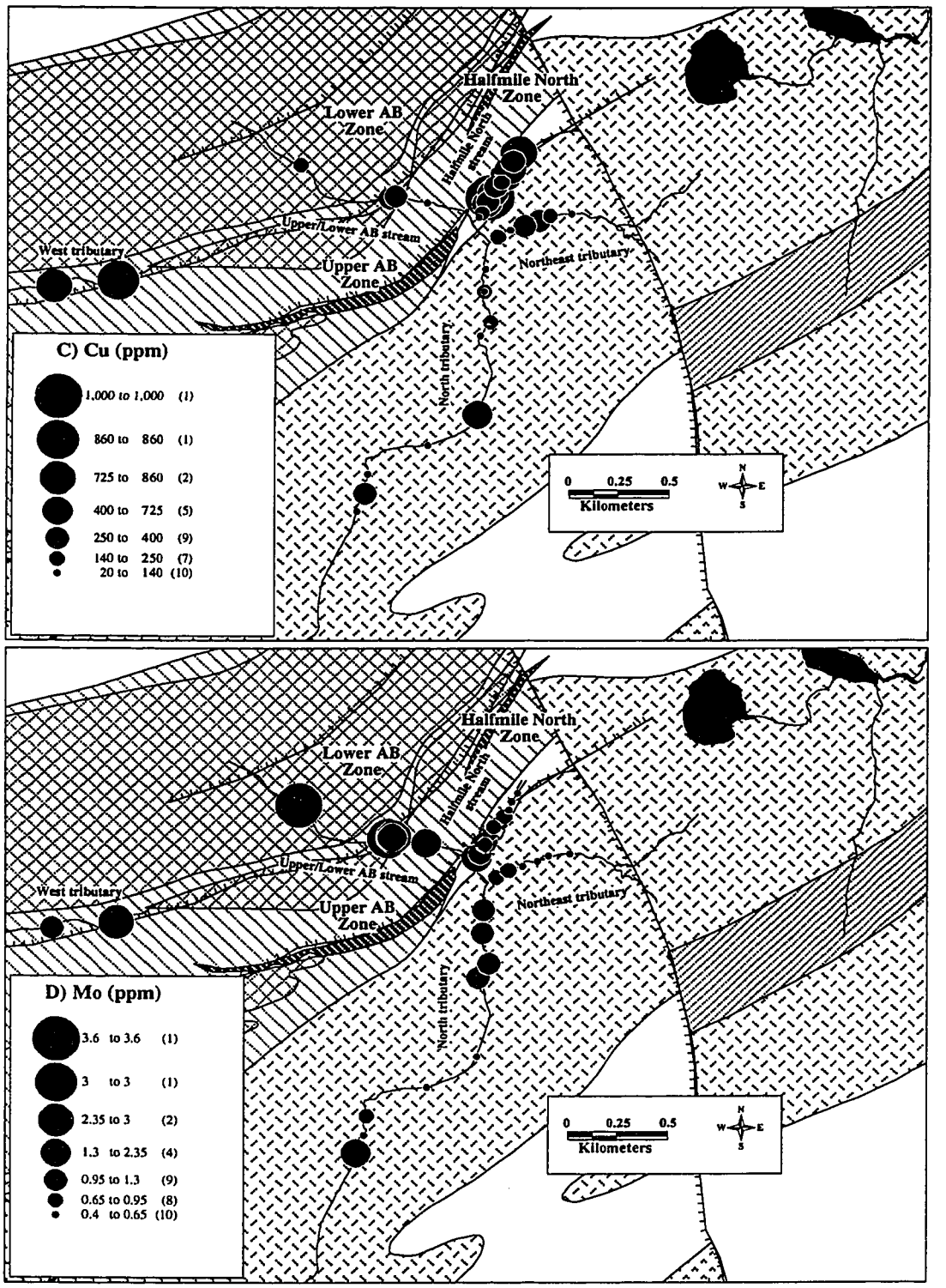


Fig. 13.4 continued.

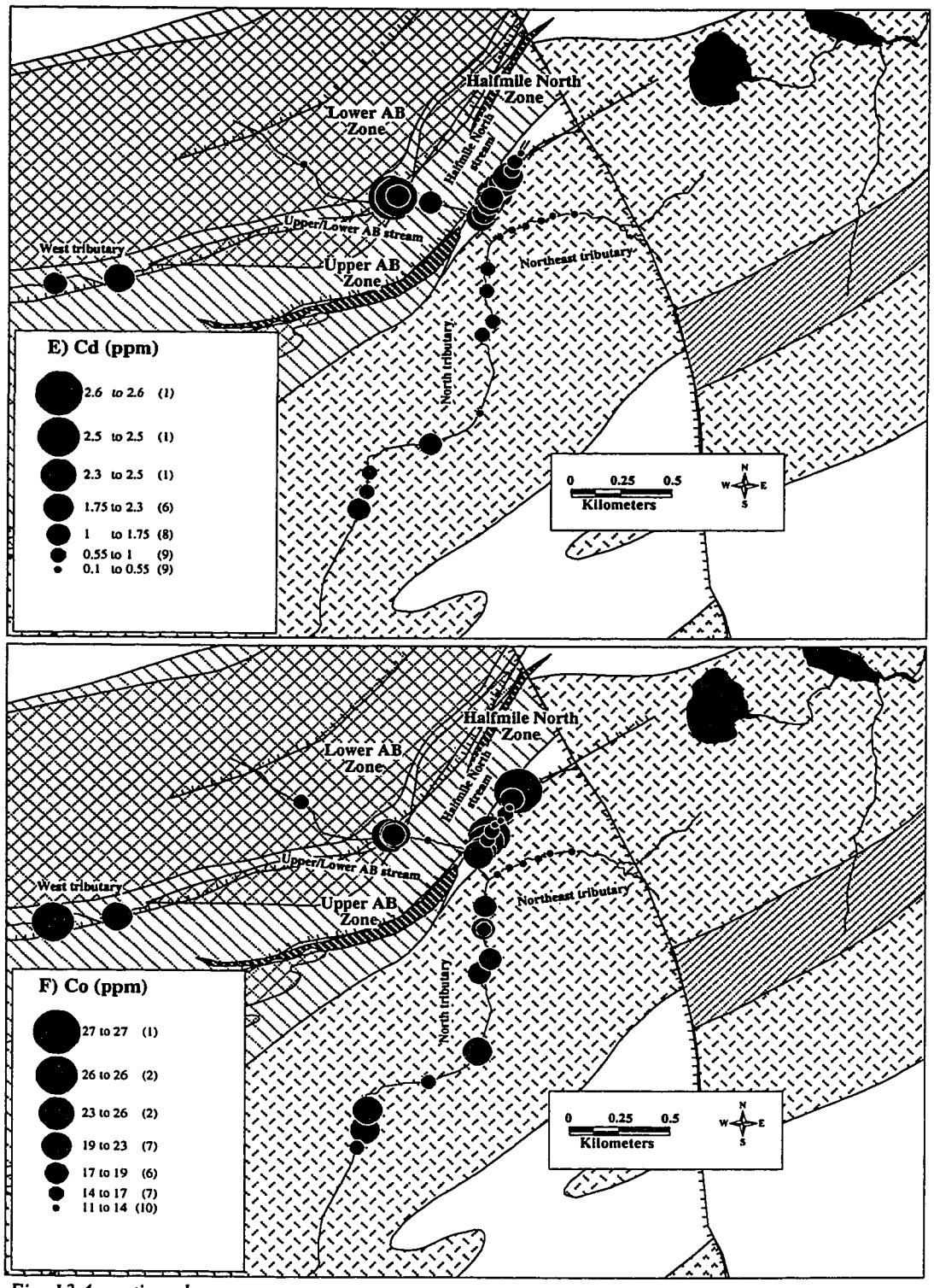


Fig. 13.4 continued.

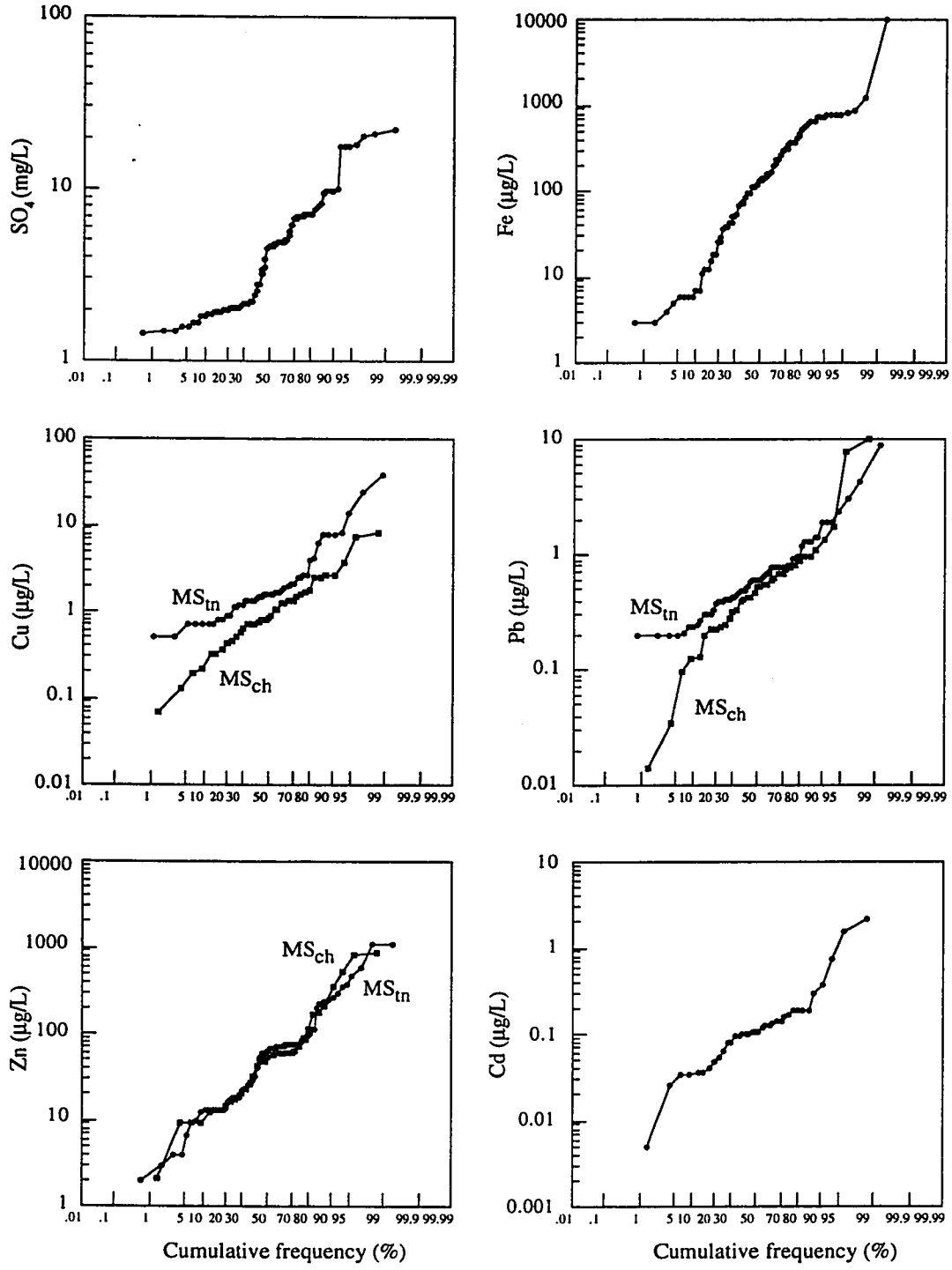


Fig. 13.5 Cumulative probability plots of the main sulphide-associated elements for Halfmile Lake deposit groundwaters. MS_{tn} and MS_{ch} refer to total nebulization and chelation ICP-MS data, respectively.

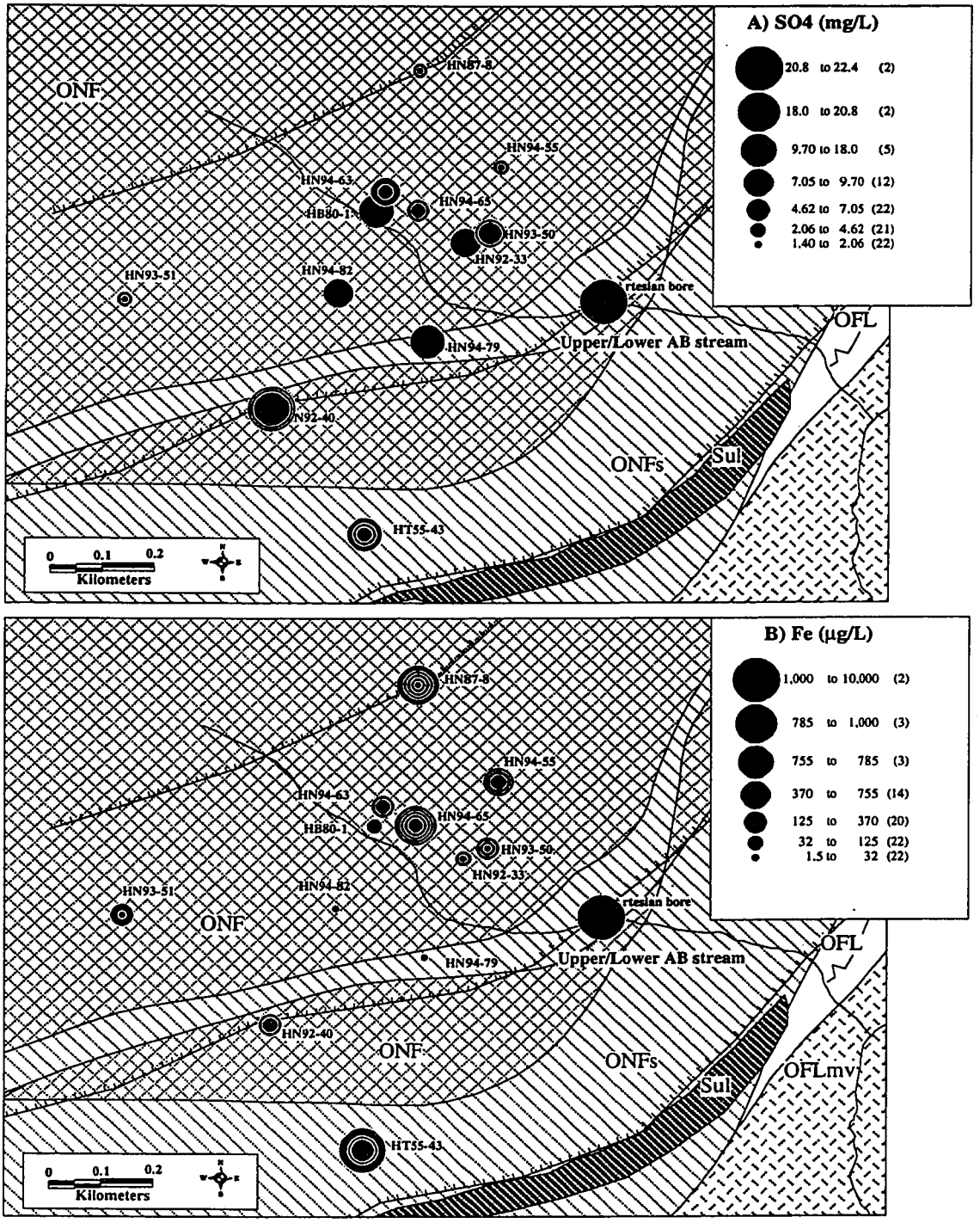


Fig. 13.6 Proportional circle plots of Halfmile Lake deposit groundwater compositions. Geology: ONF, Nepisiguit Falls felsic volcanics; ONFs, Nepisiguit Falls sedimentary rocks; OFL, Flat Landing Brook felsic volcanics; OFLmv, Flat Landing Brook mafic volcanics; Sul, sulphides.

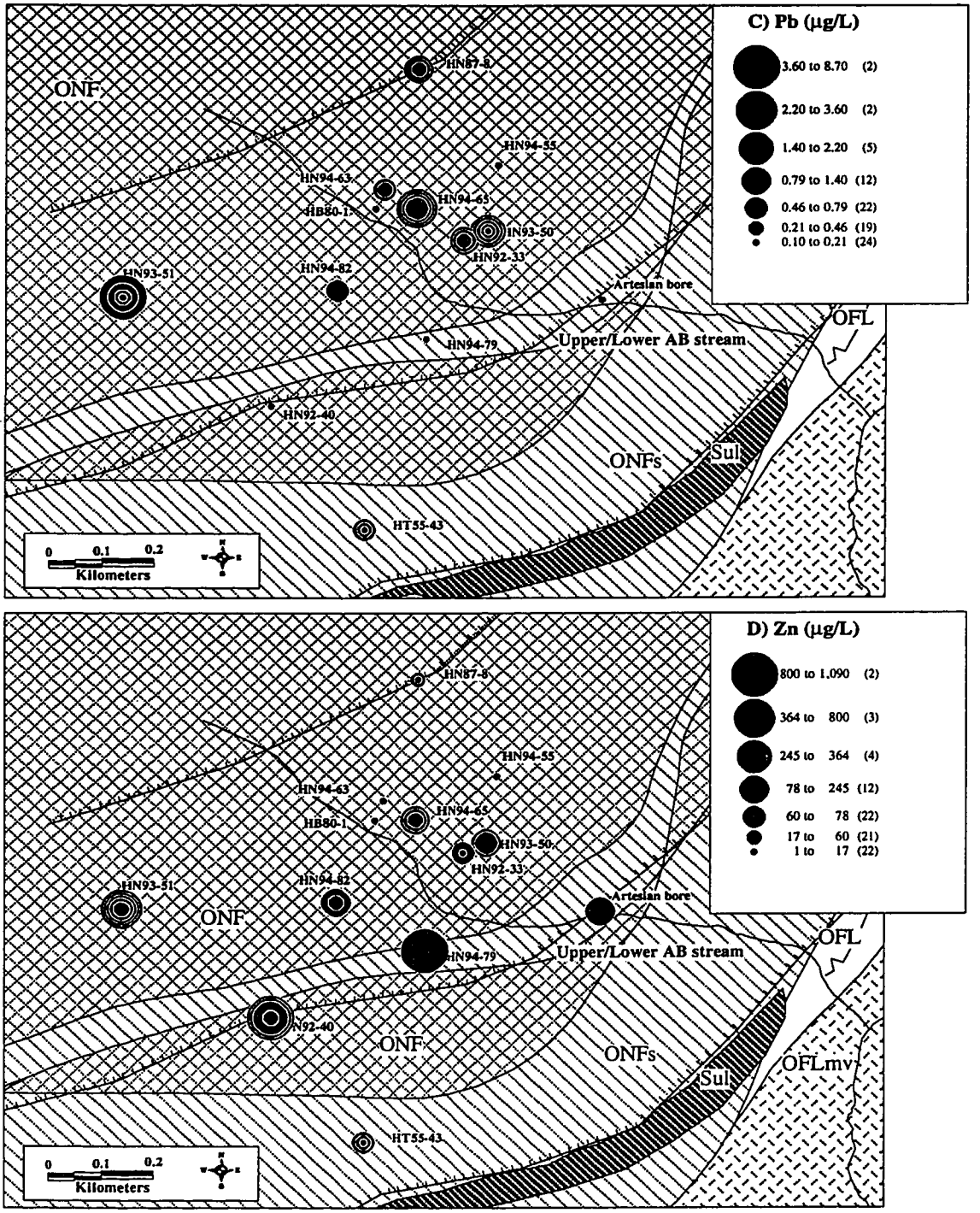


Fig. 13.6 continued.

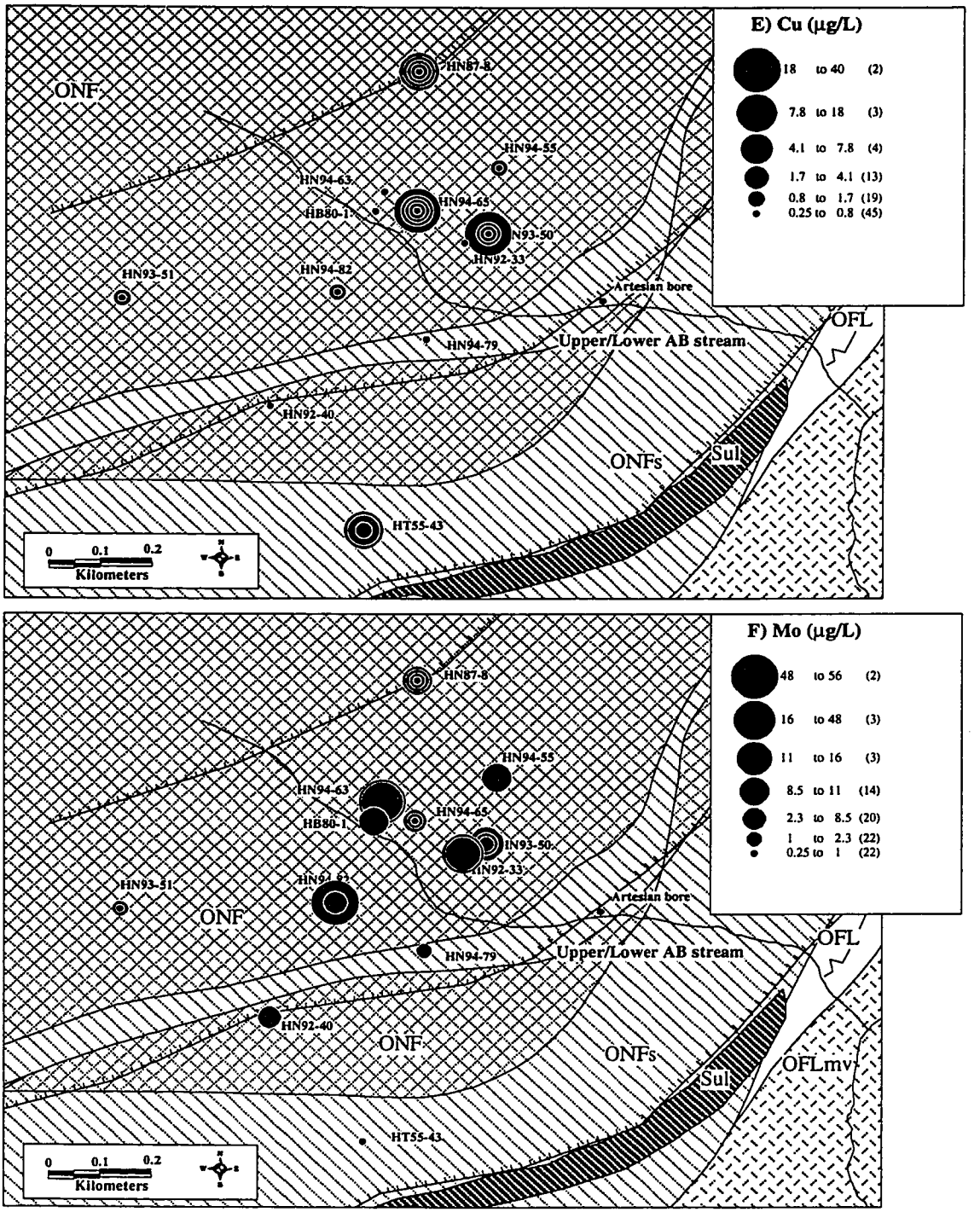


Fig. 13.6 continued.

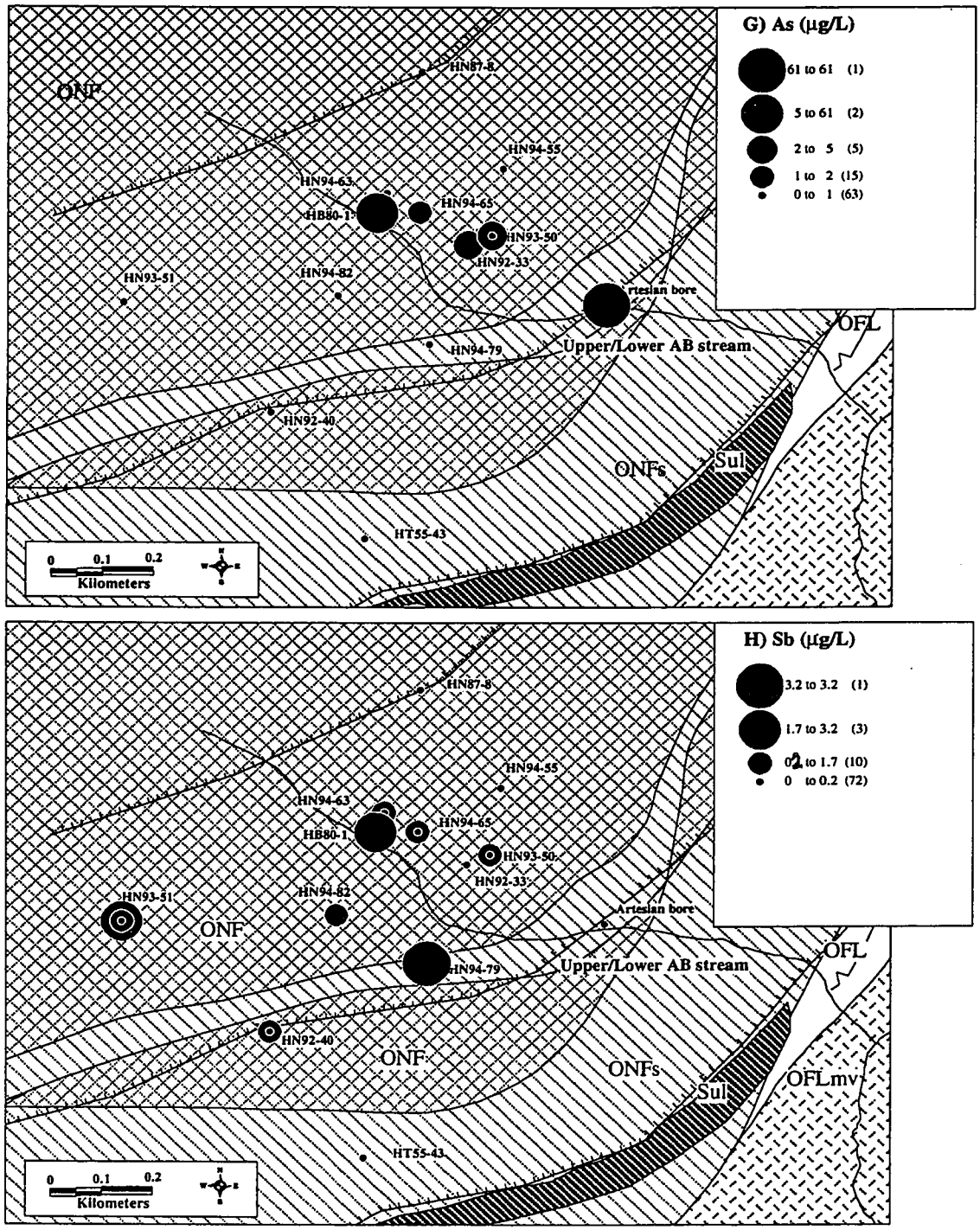


Fig. 13.6 continued.

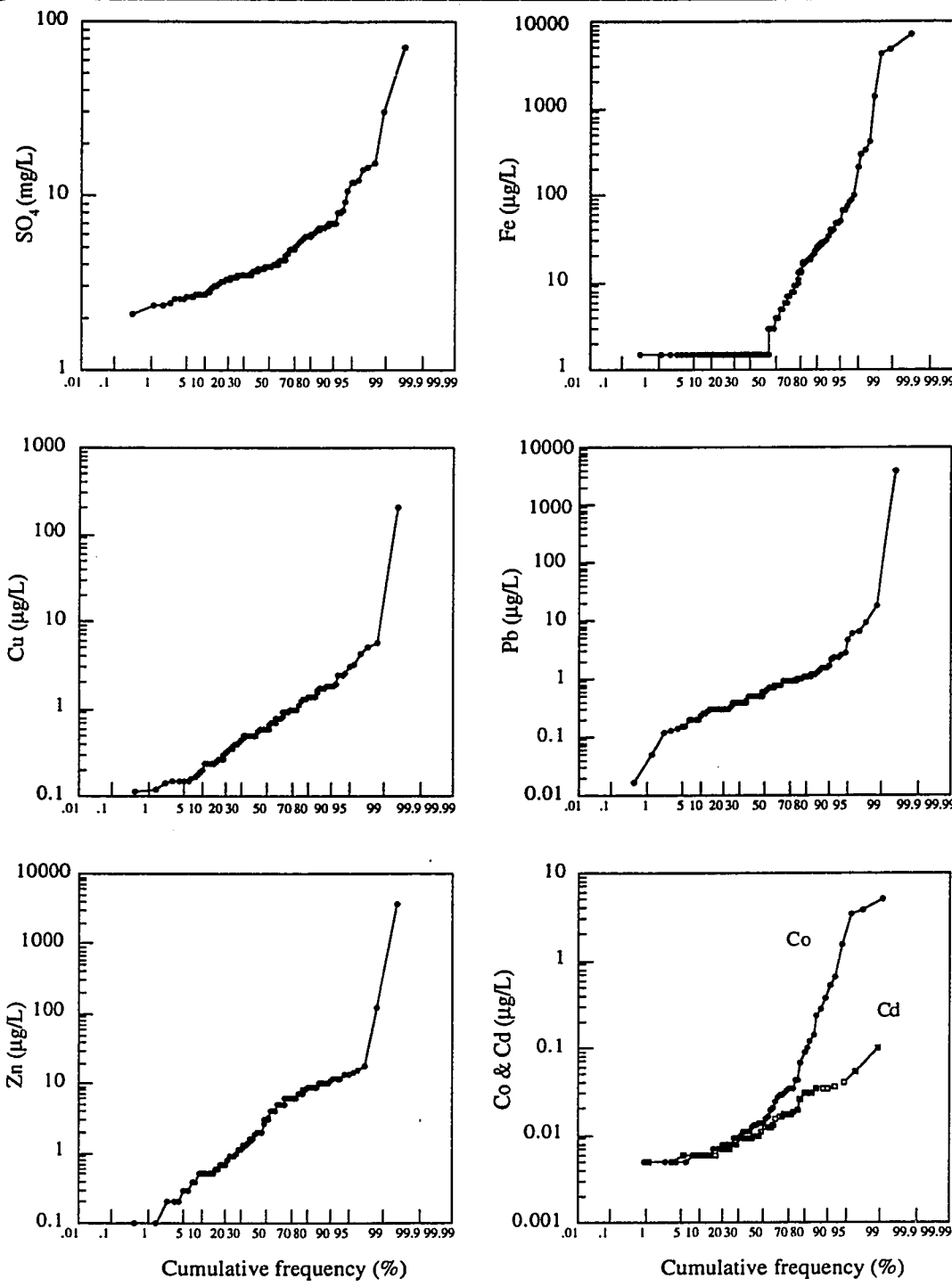


Fig. 13.7 Cumulative probability plots of the main sulphide-associated elements for Restigouche deposit surface waters.

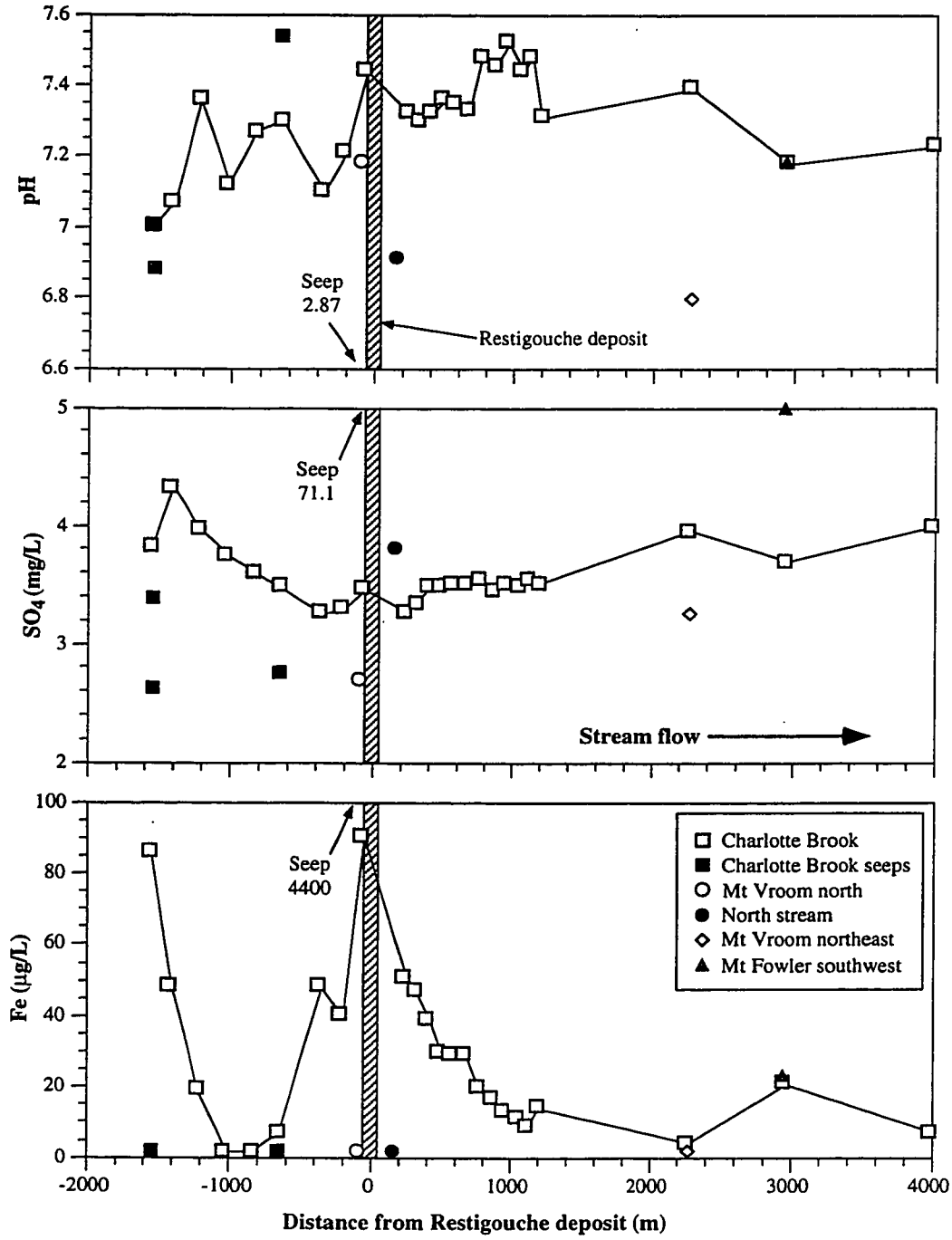


Fig. 13.8 Surface water profiles along Charlotte Brook for selected chemical parameters. Also shown are the last surface waters for tributaries entering Charlotte Brook and SO_4 and metal abundances for the seep in the gossan (MLW95-300).

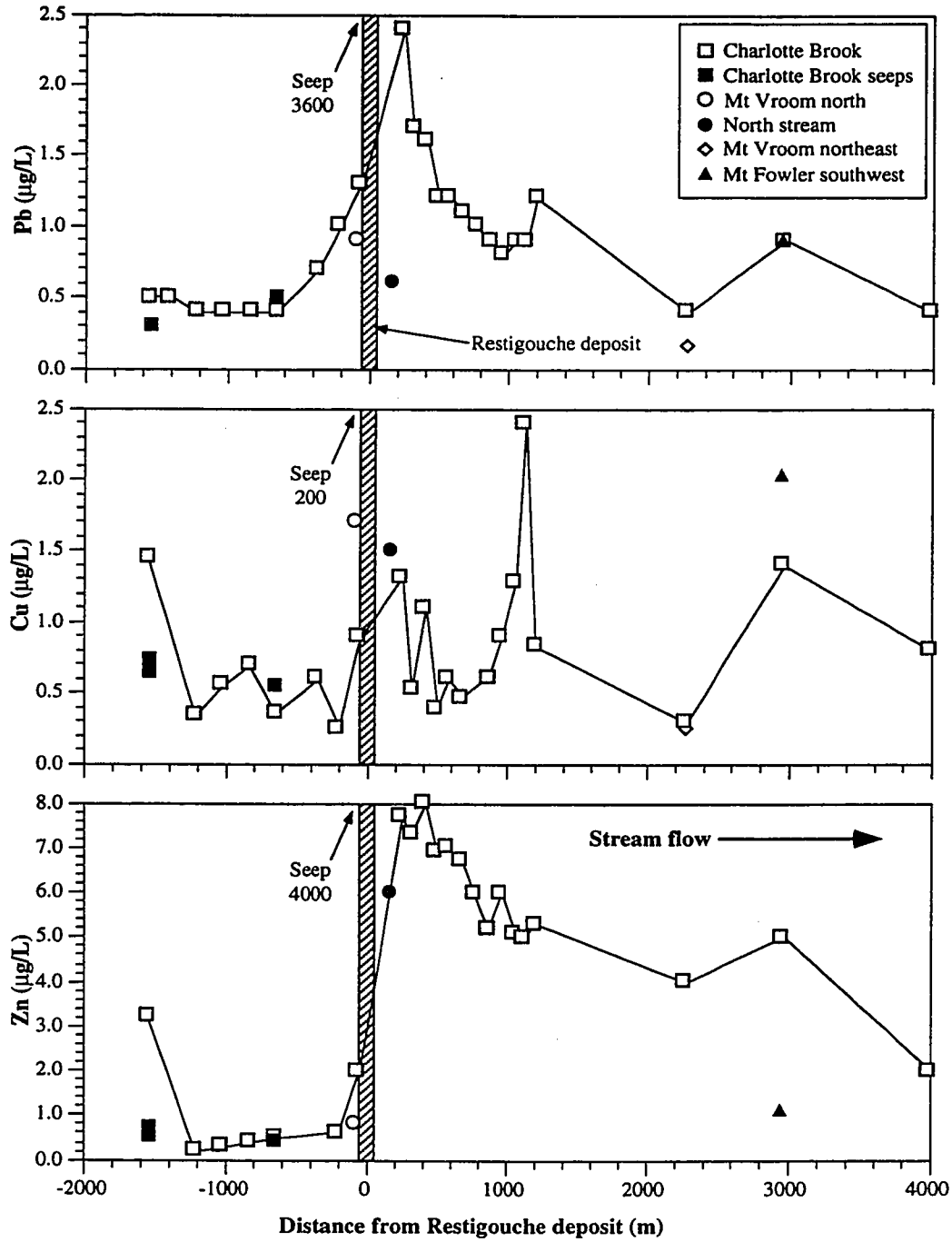


Fig. 13.8 continued.

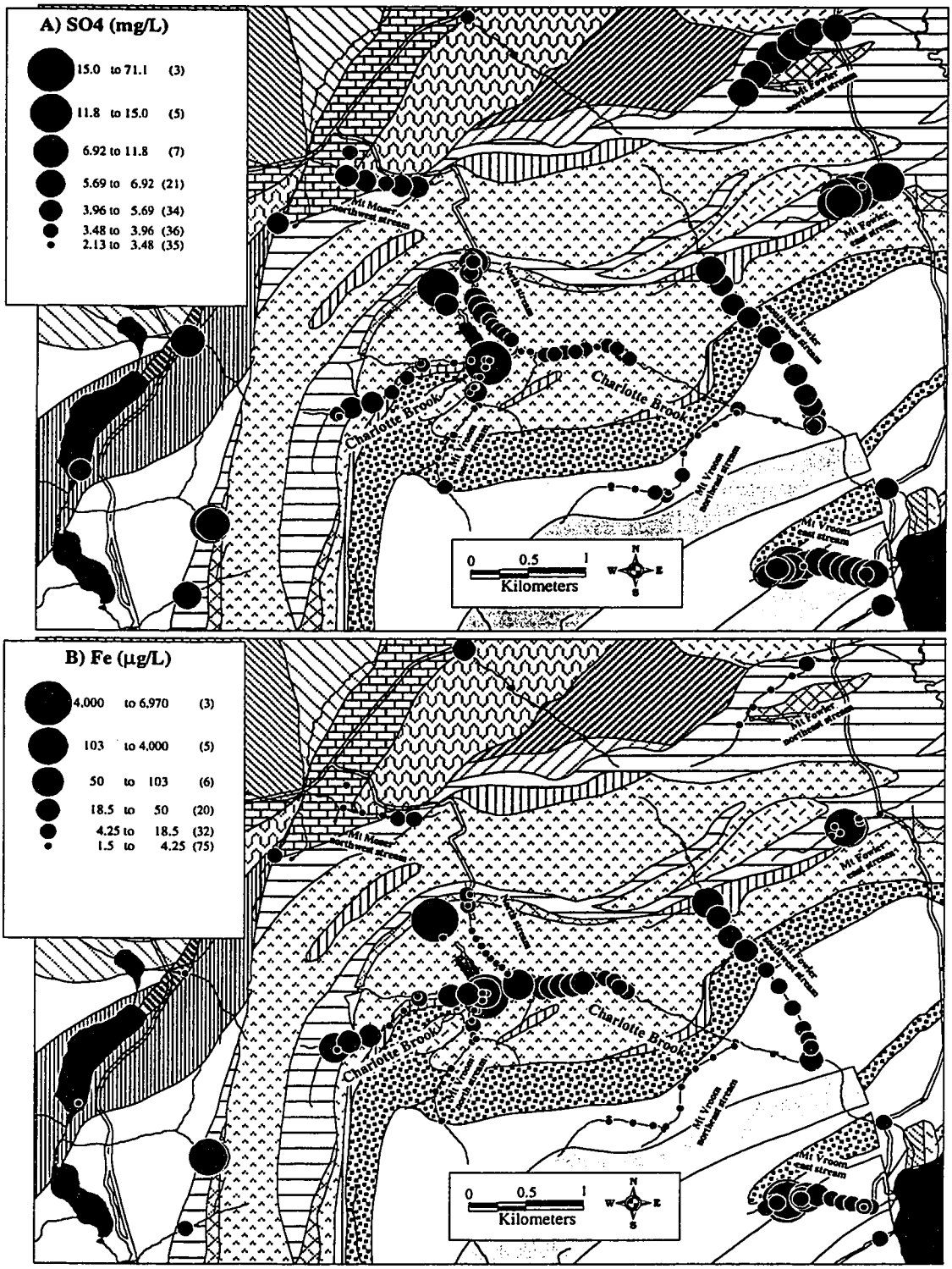


Fig. 13.9 Proportion circle map of Restigouche deposit surface waters.

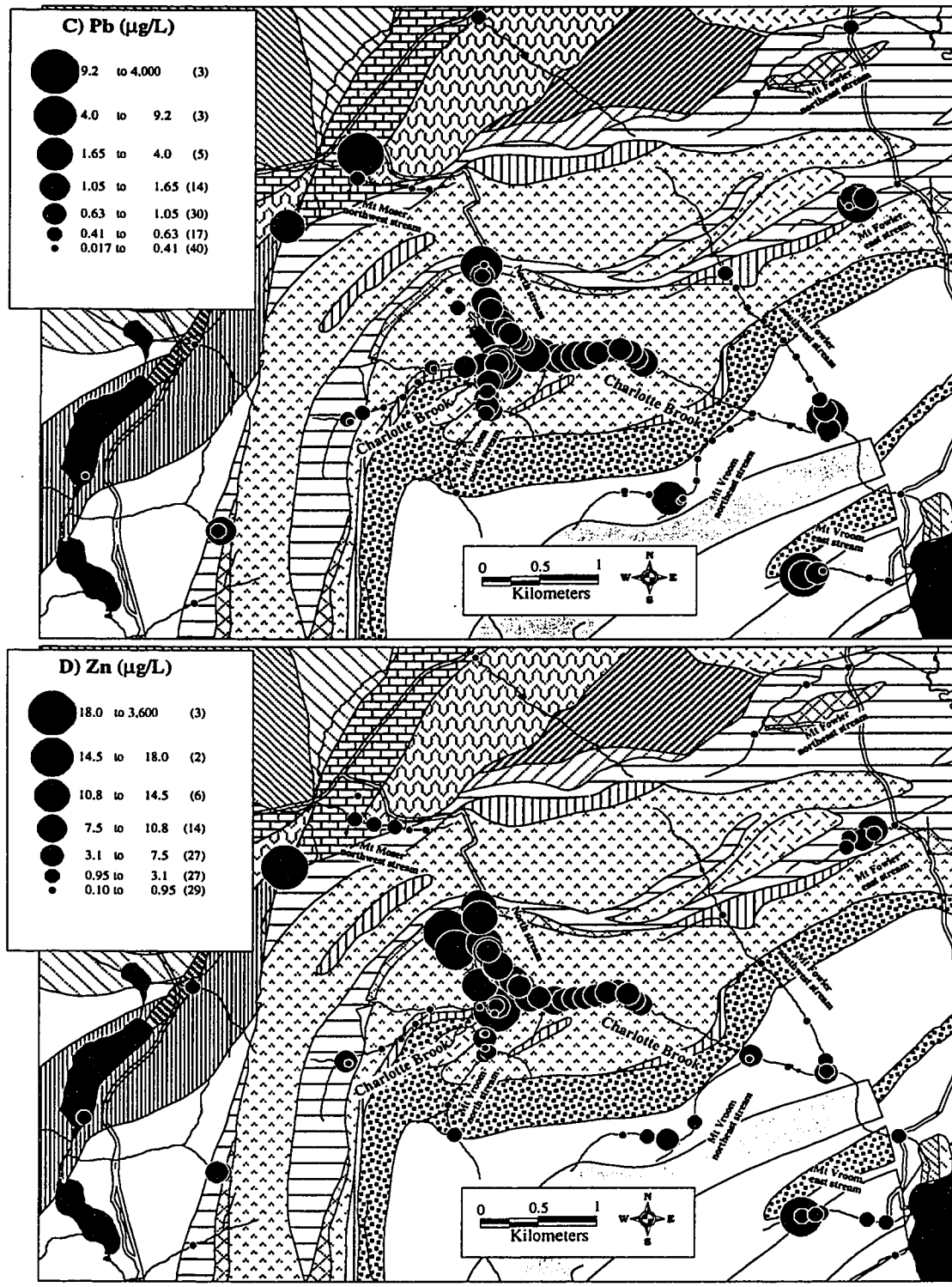


Fig. 13.9 continued.

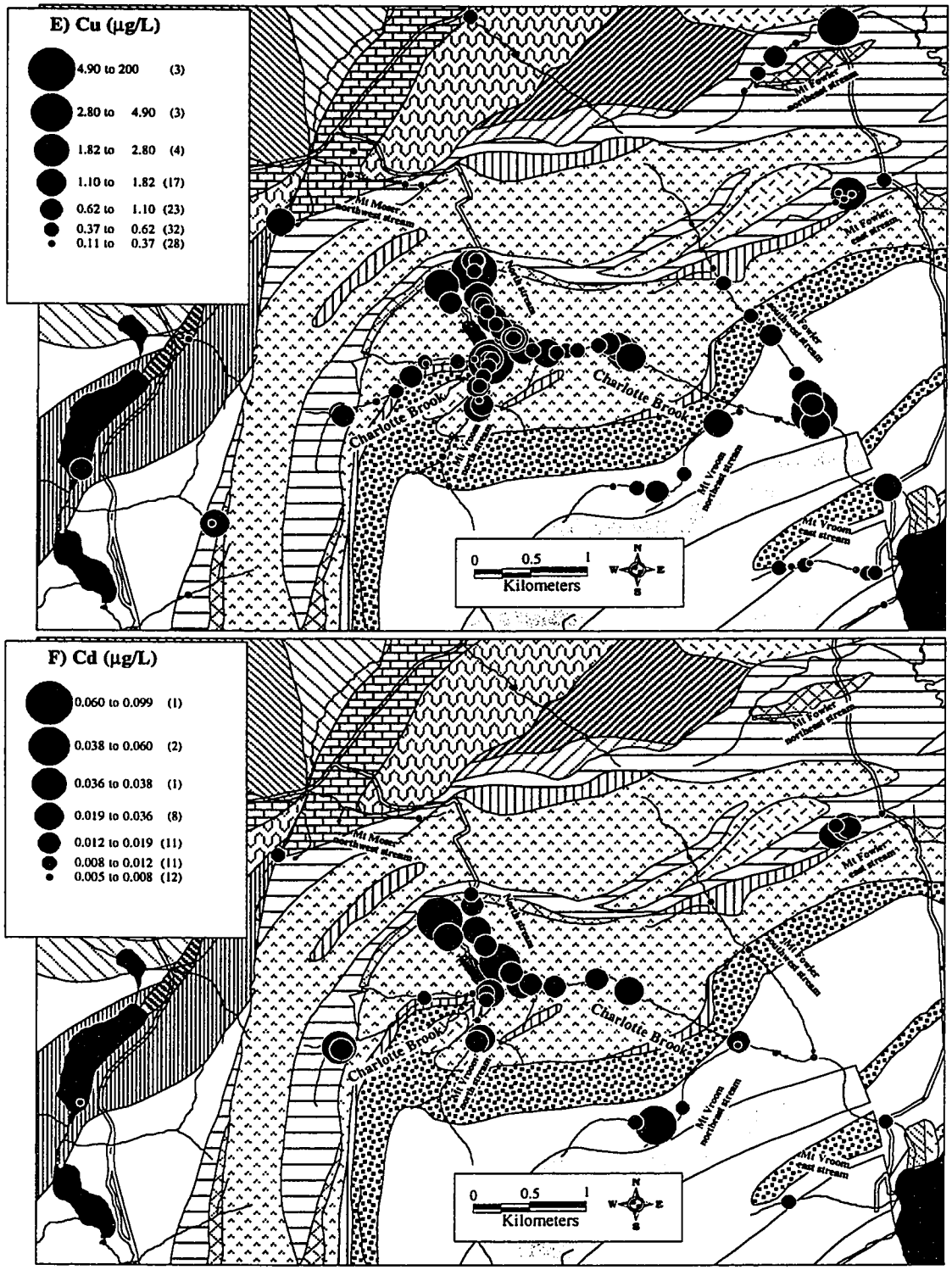


Fig. 13.9 continued.

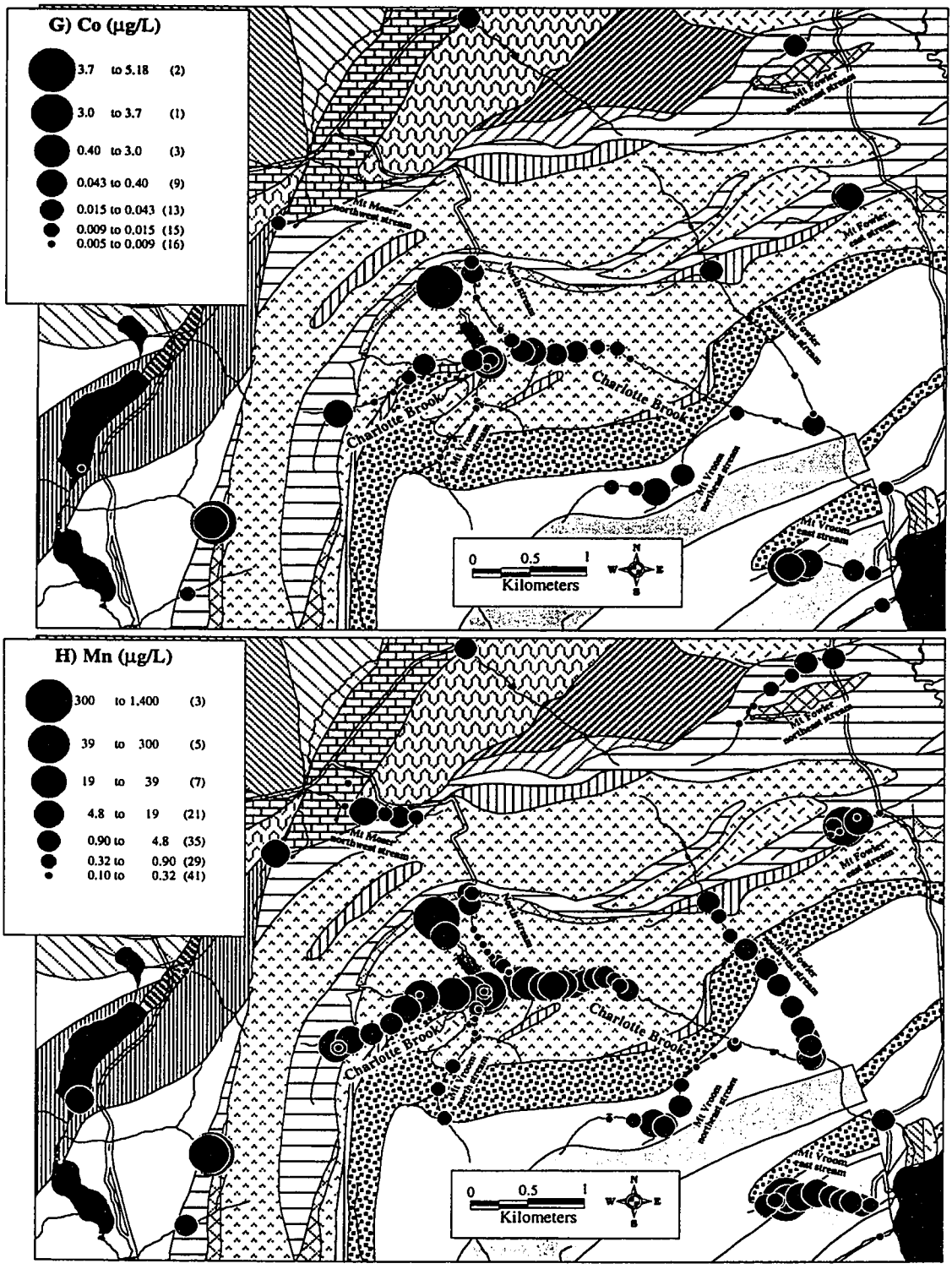


Fig. 13.9 continued.

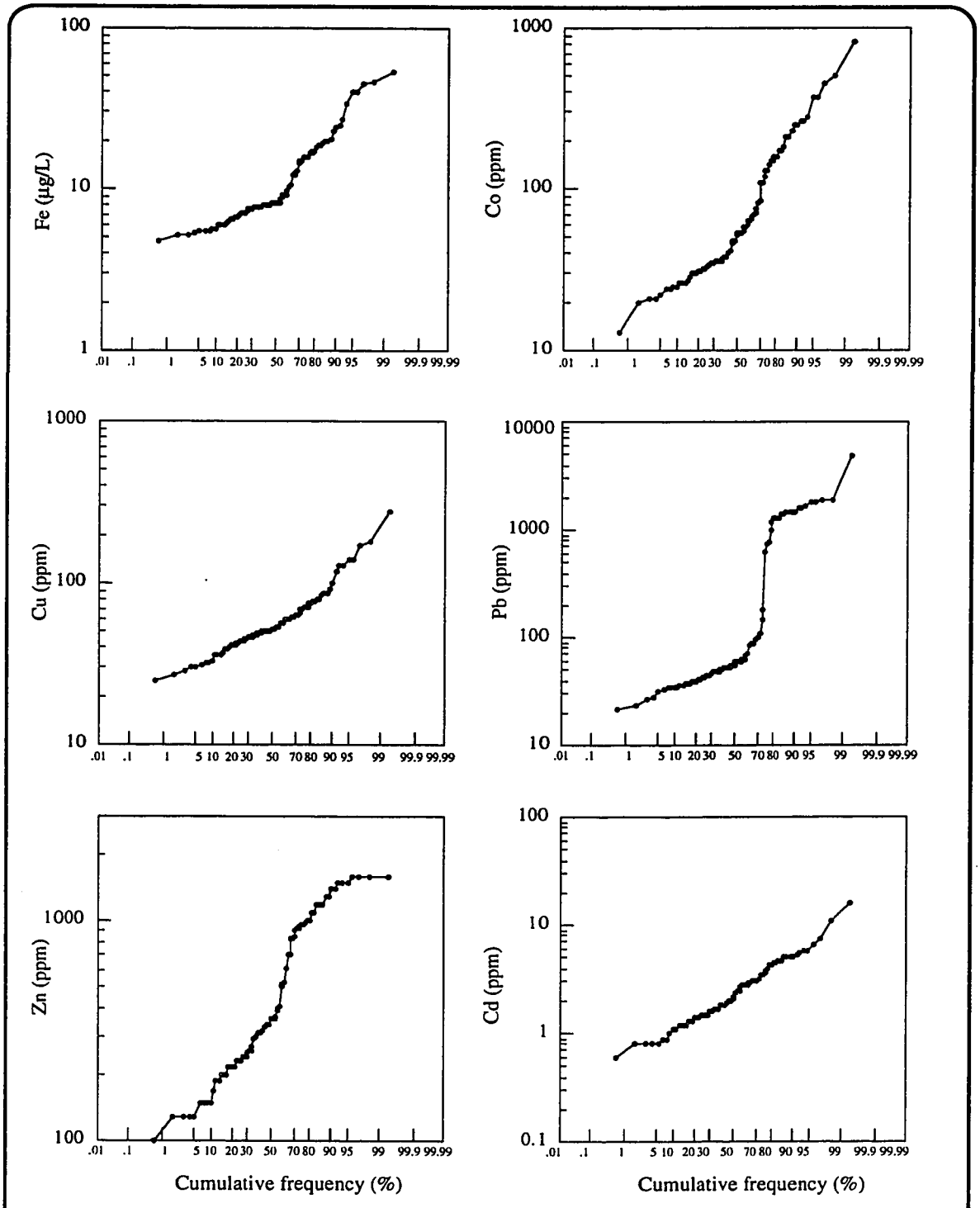


Fig. 13.10 Cumulative probability plots of the main sulphide-associated elements for Restigouche deposit stream sediments.

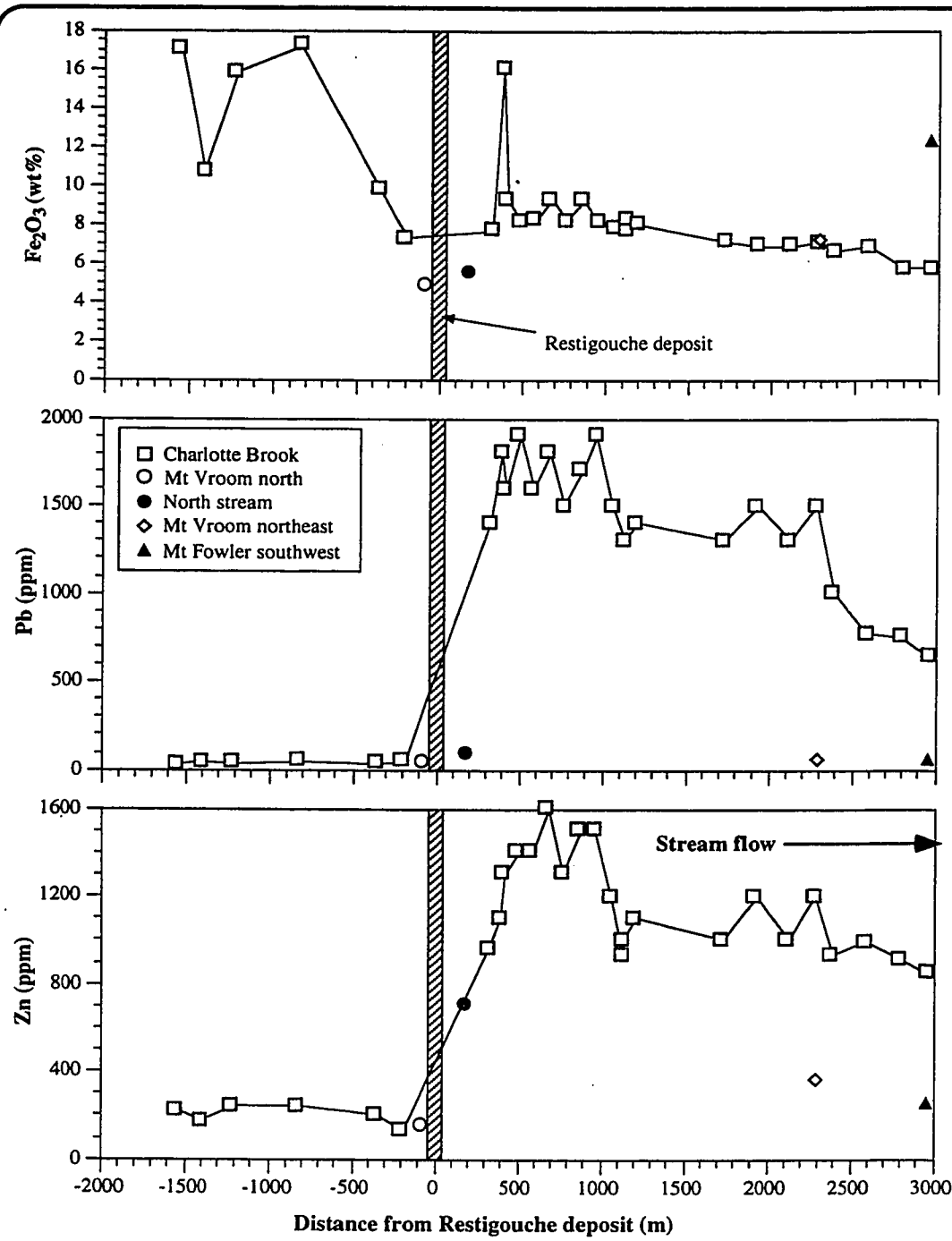


Fig. 13.11 Stream sediment profiles along Charlotte Brook for selected chemical parameters.

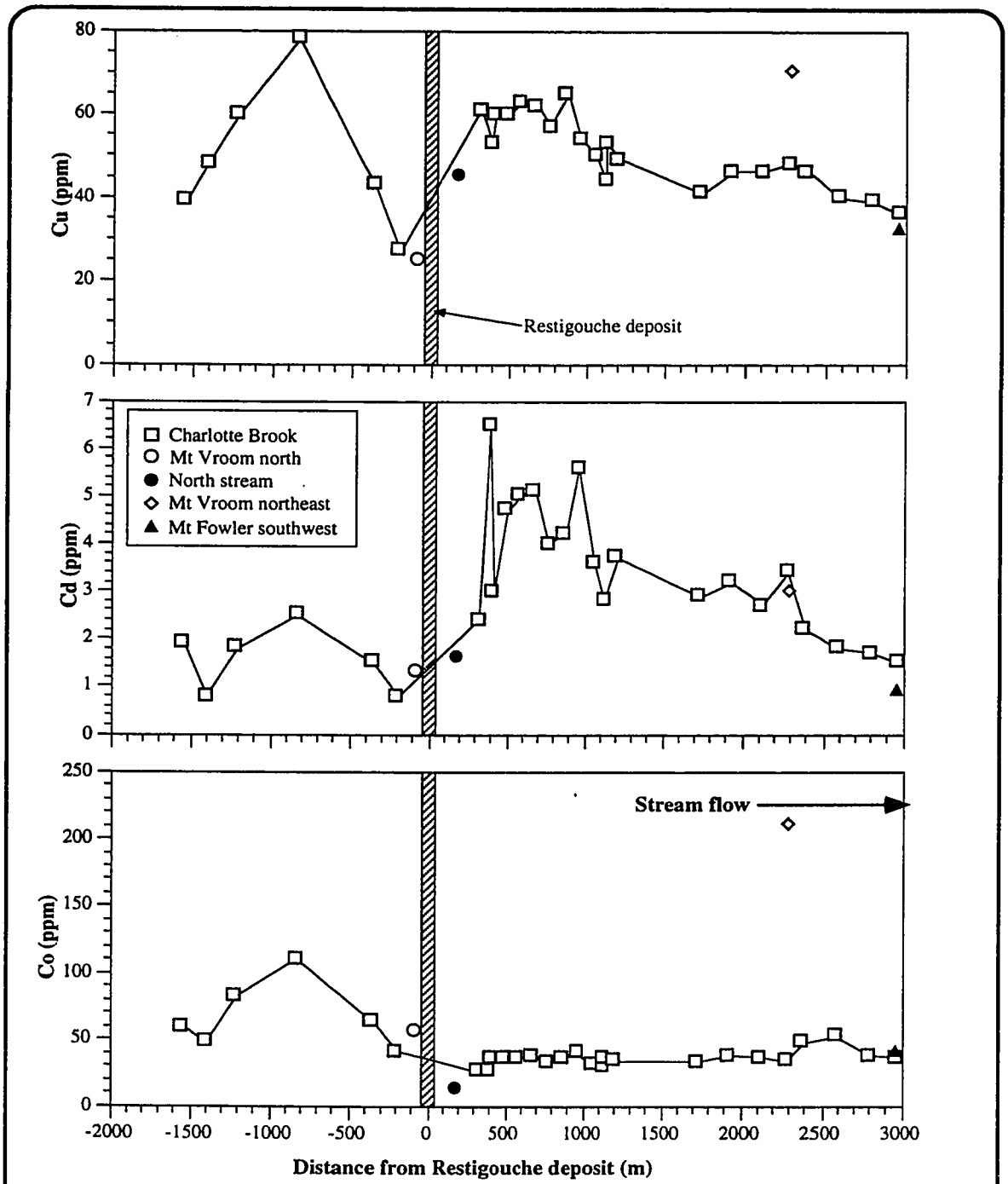


Fig. 13.11 continued.

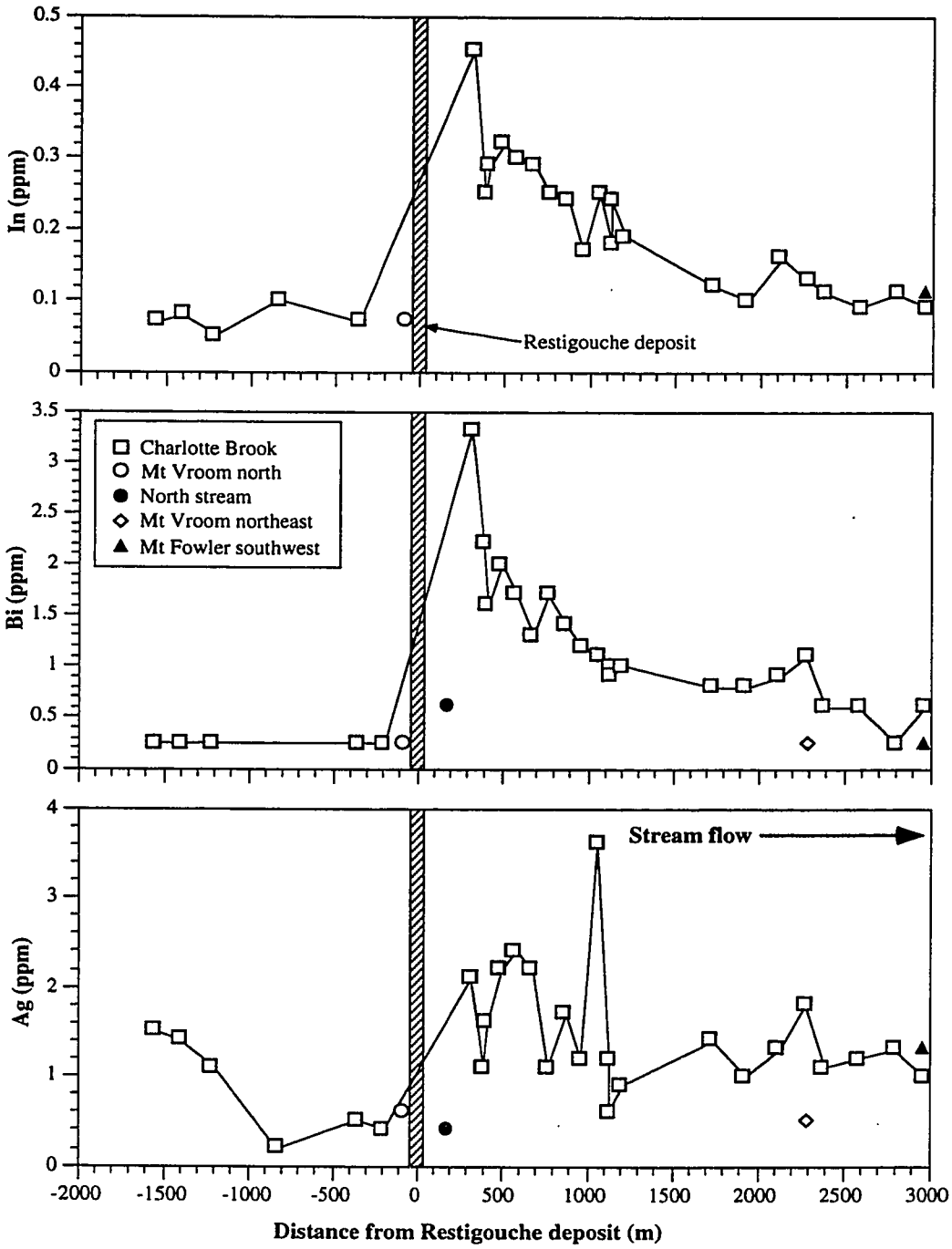


Fig. 13.11 continued.

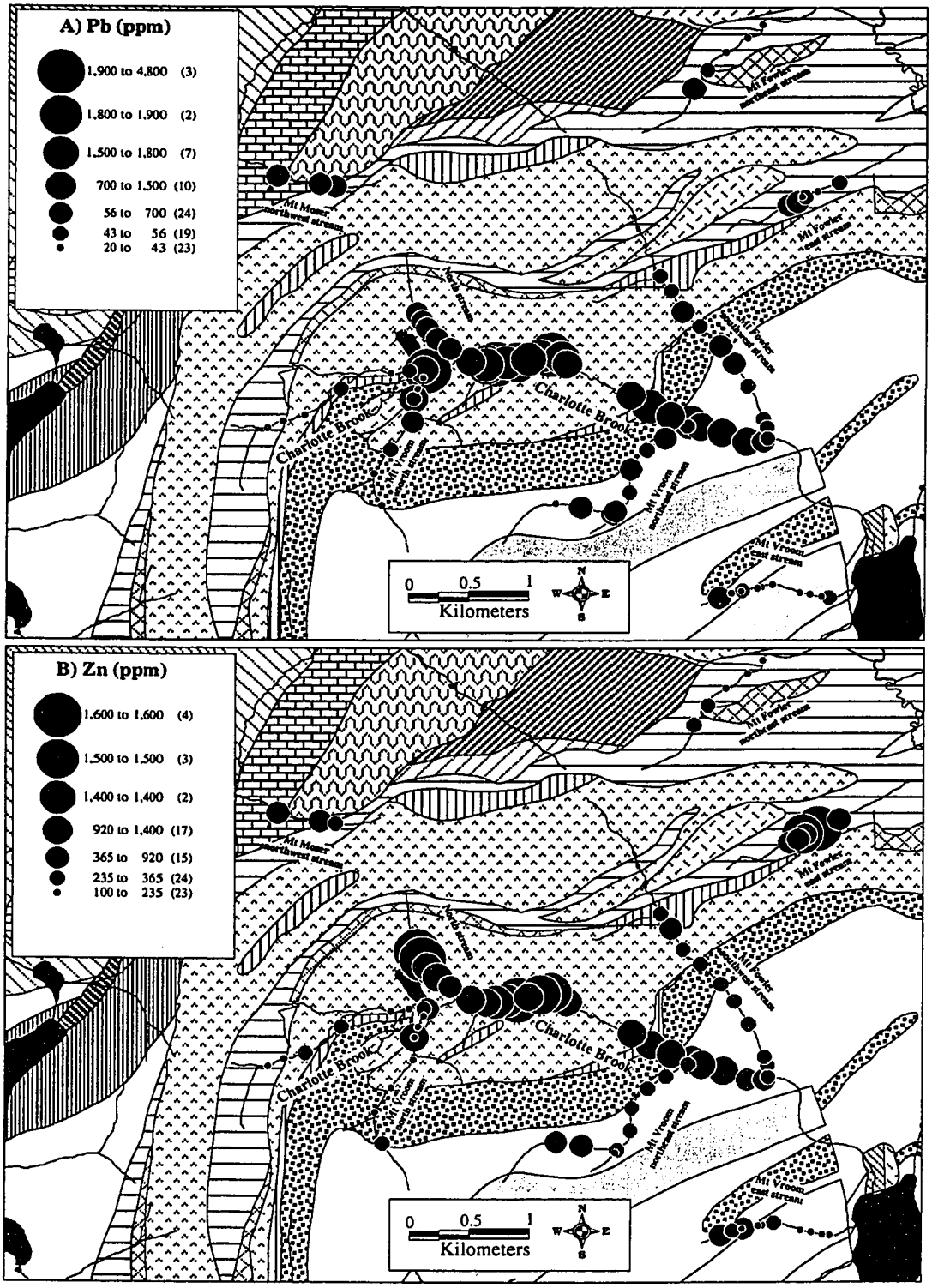


Fig. 13.12 Proportional circle maps of stream sediments compositions from the Restigouche deposit. Geology from Chapter Two.

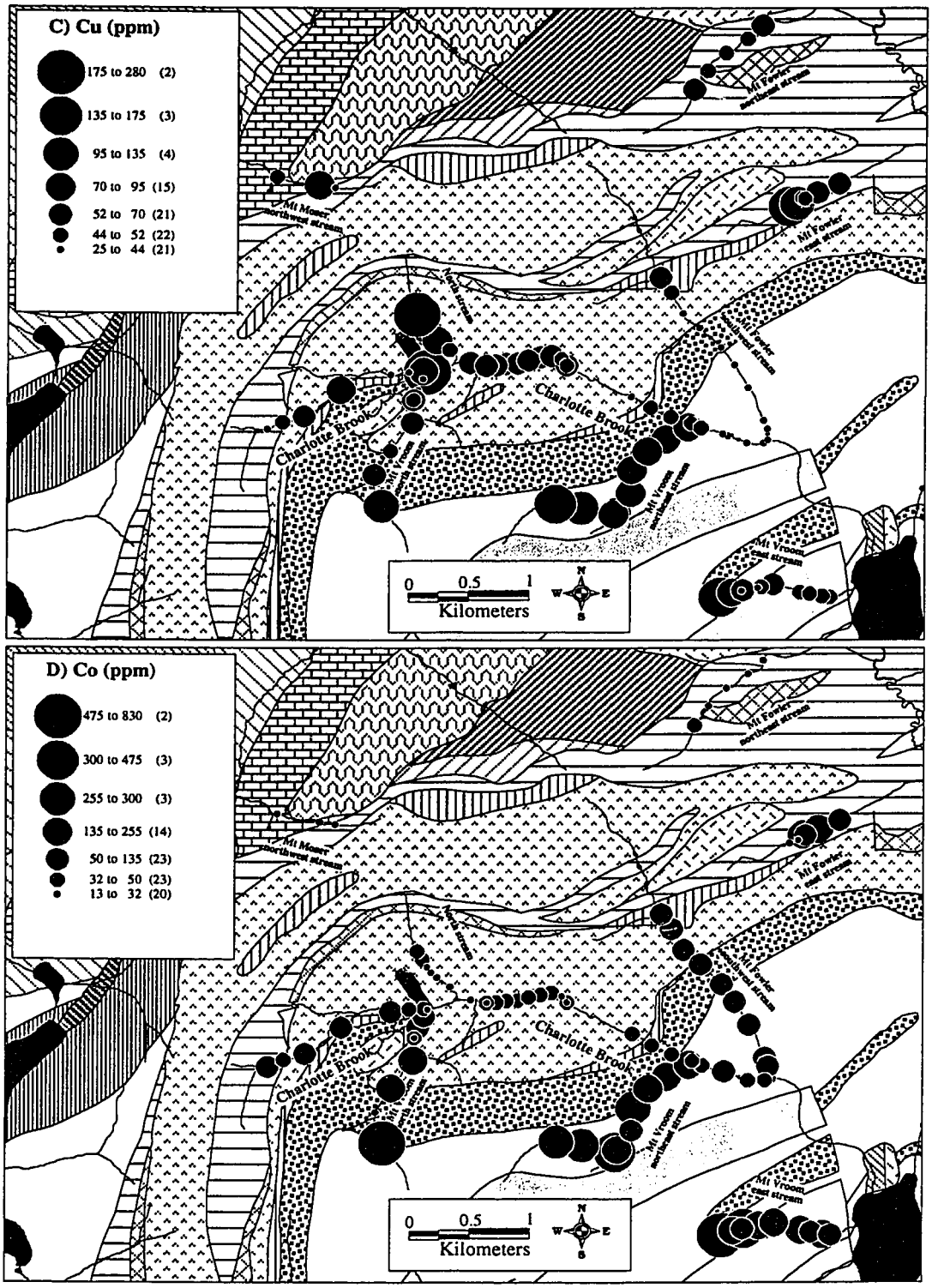


Fig. 13.12 continued.

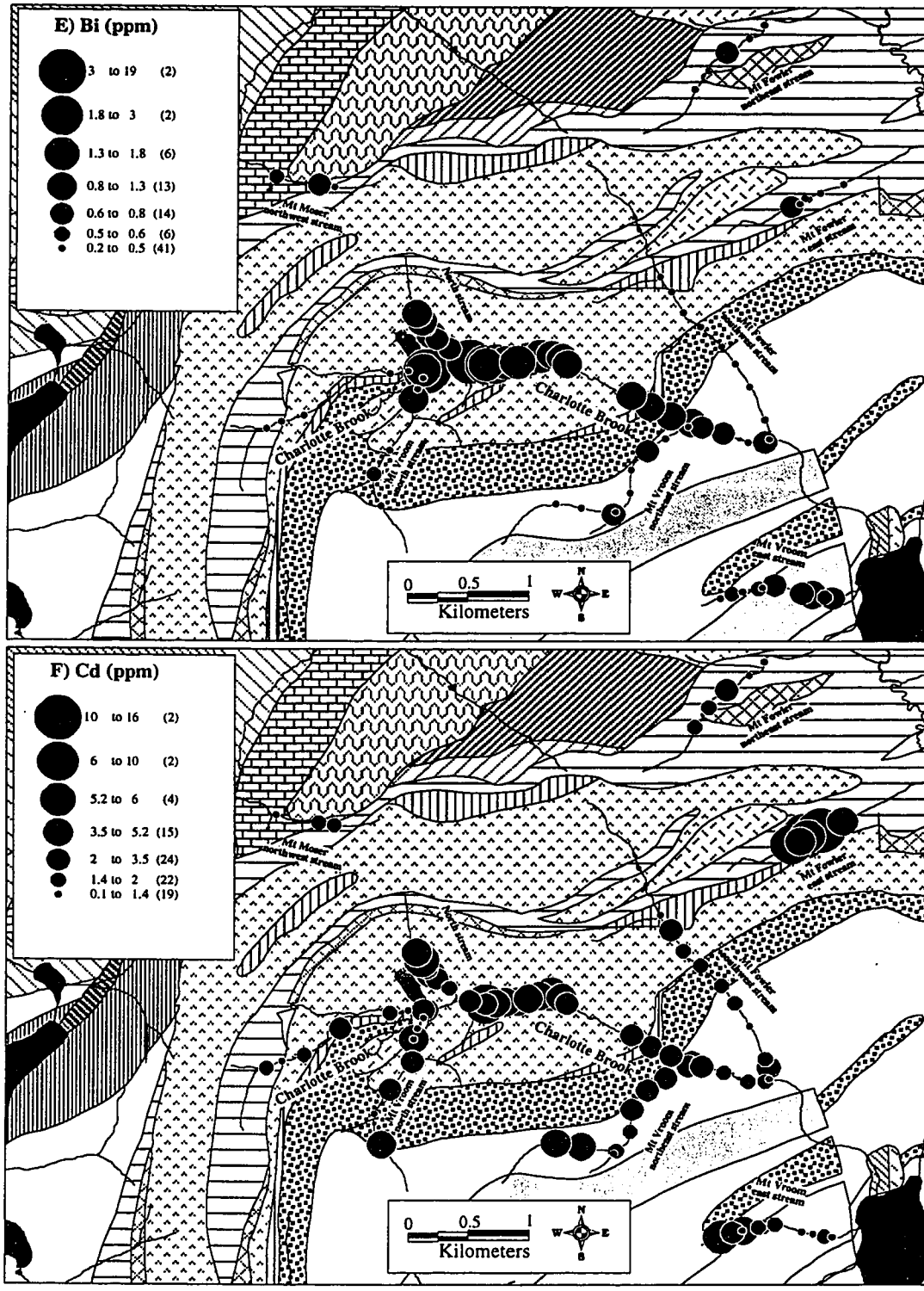


Fig. 13.12 continued.

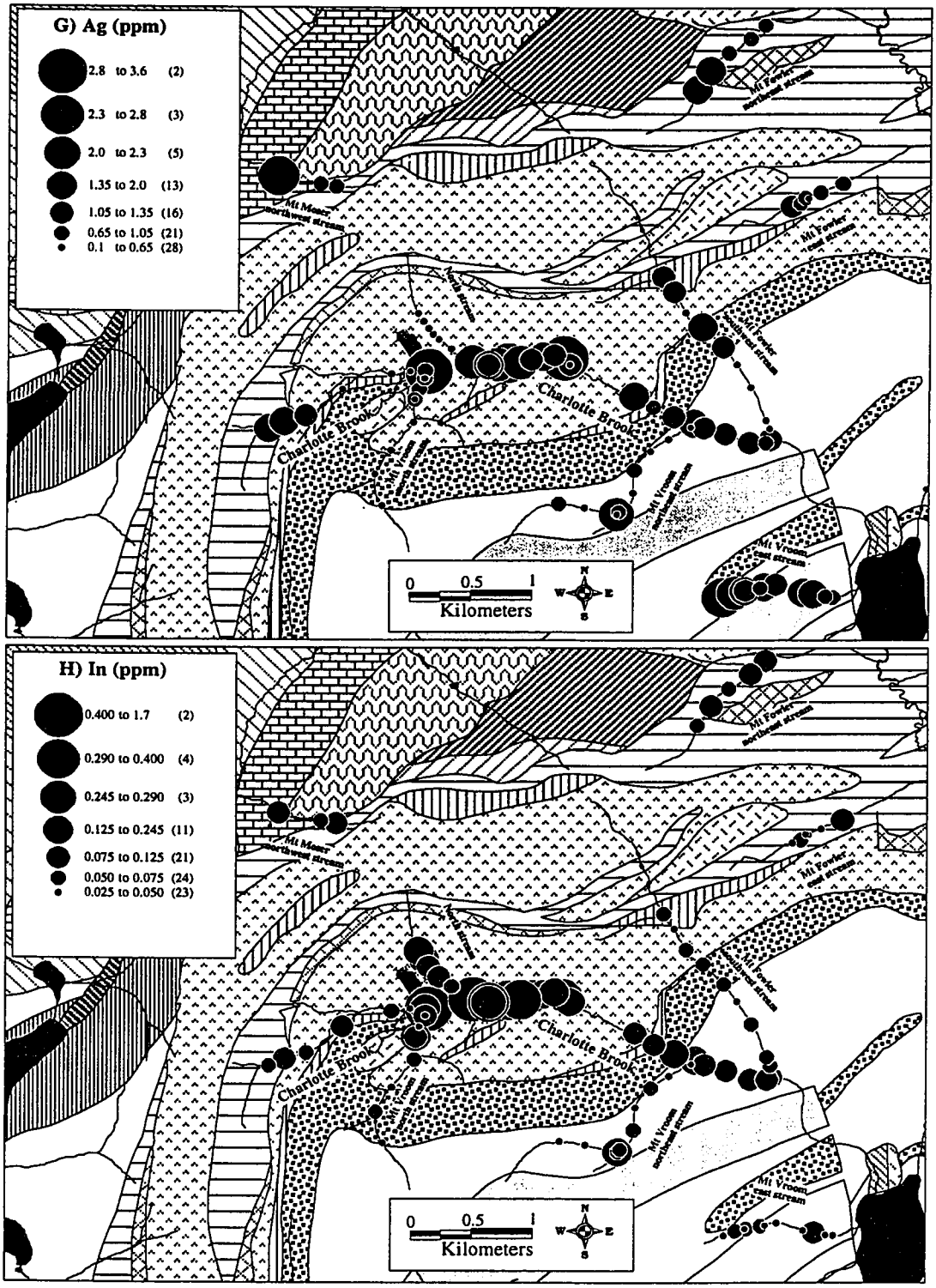


Fig. 13.12 continued.

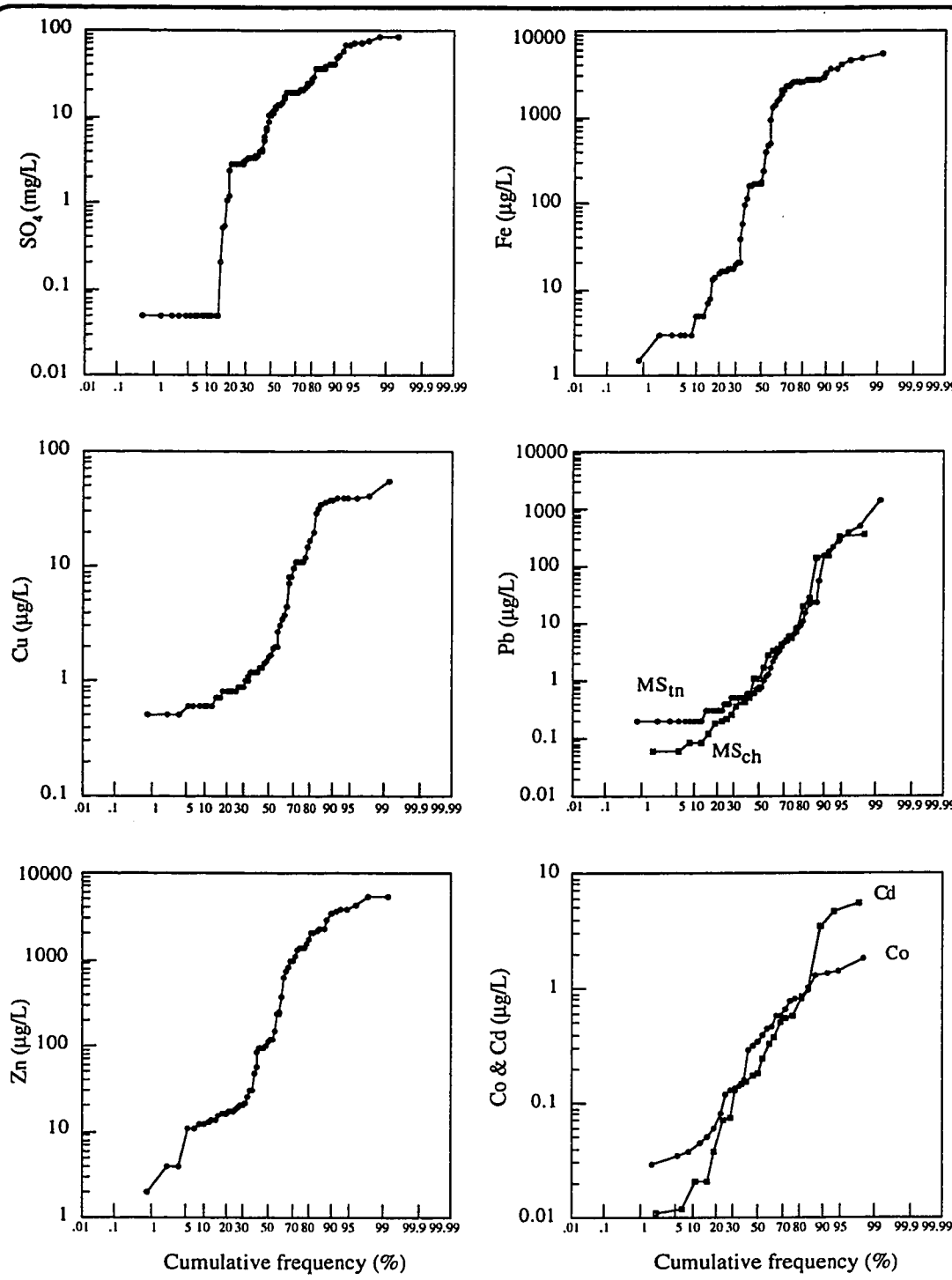


Fig. 13.13 Cumulative probability plots of the main sulphide-associated elements for Restigouche deposit groundwaters. MS_{tn} and MS_{ch} refer to total nebulization and chelation ICP-MS, respectively.

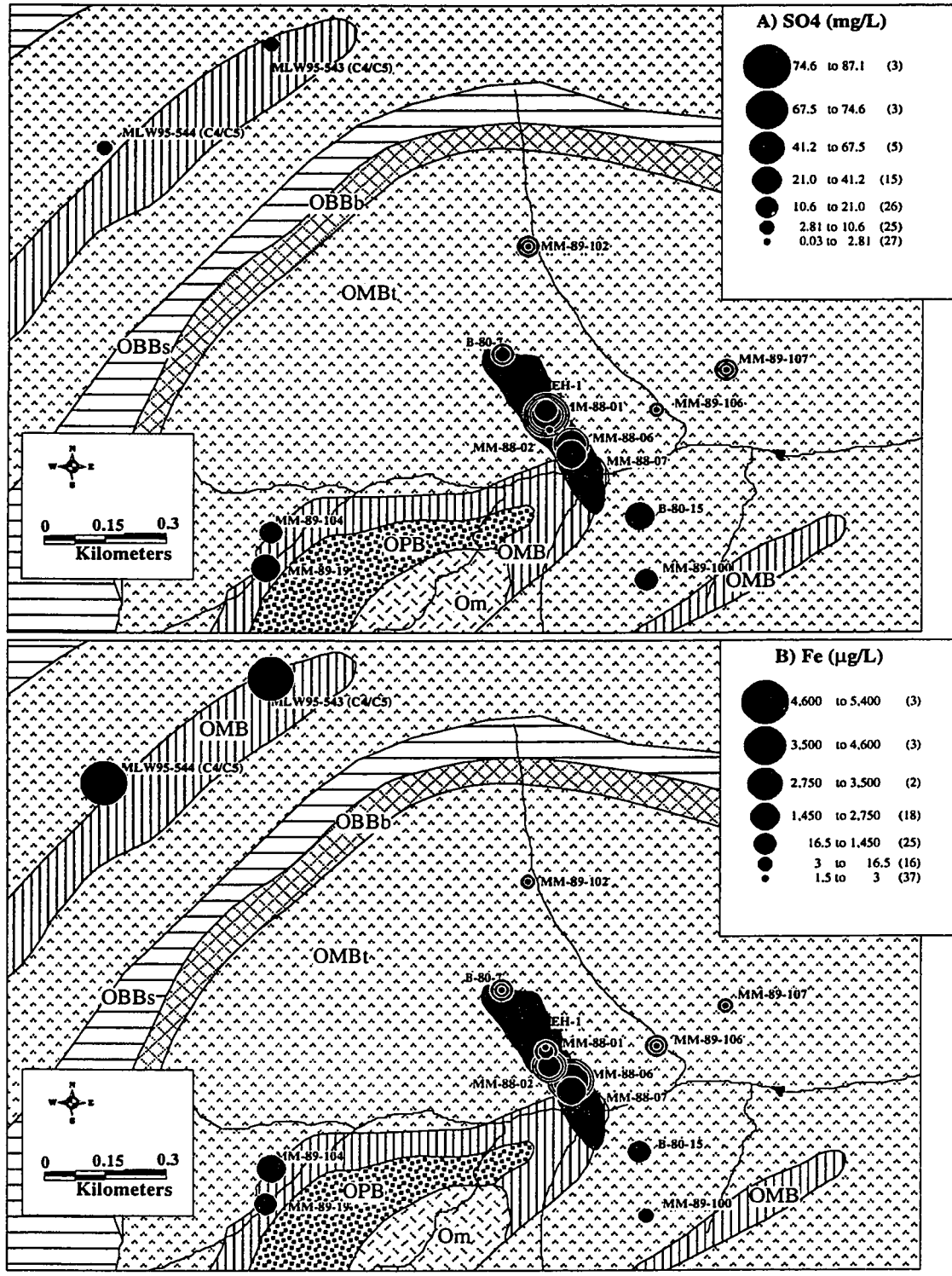


Fig. 13.14 Proportional circle plots of Restigouche deposit groundwater compositions. Geology: OBBs, Eighteen Mile sedimentary rocks; OBBb, Eighteen Mile mafic volcanics; OMBt, Mount Brittain felsic Tuffs; OMB, Mount Brittain rhyolite; OPB, Patrick Brook sedimentary rocks; Om, mafic intrusives. Shaded area is the surface projection of massive sulphides.

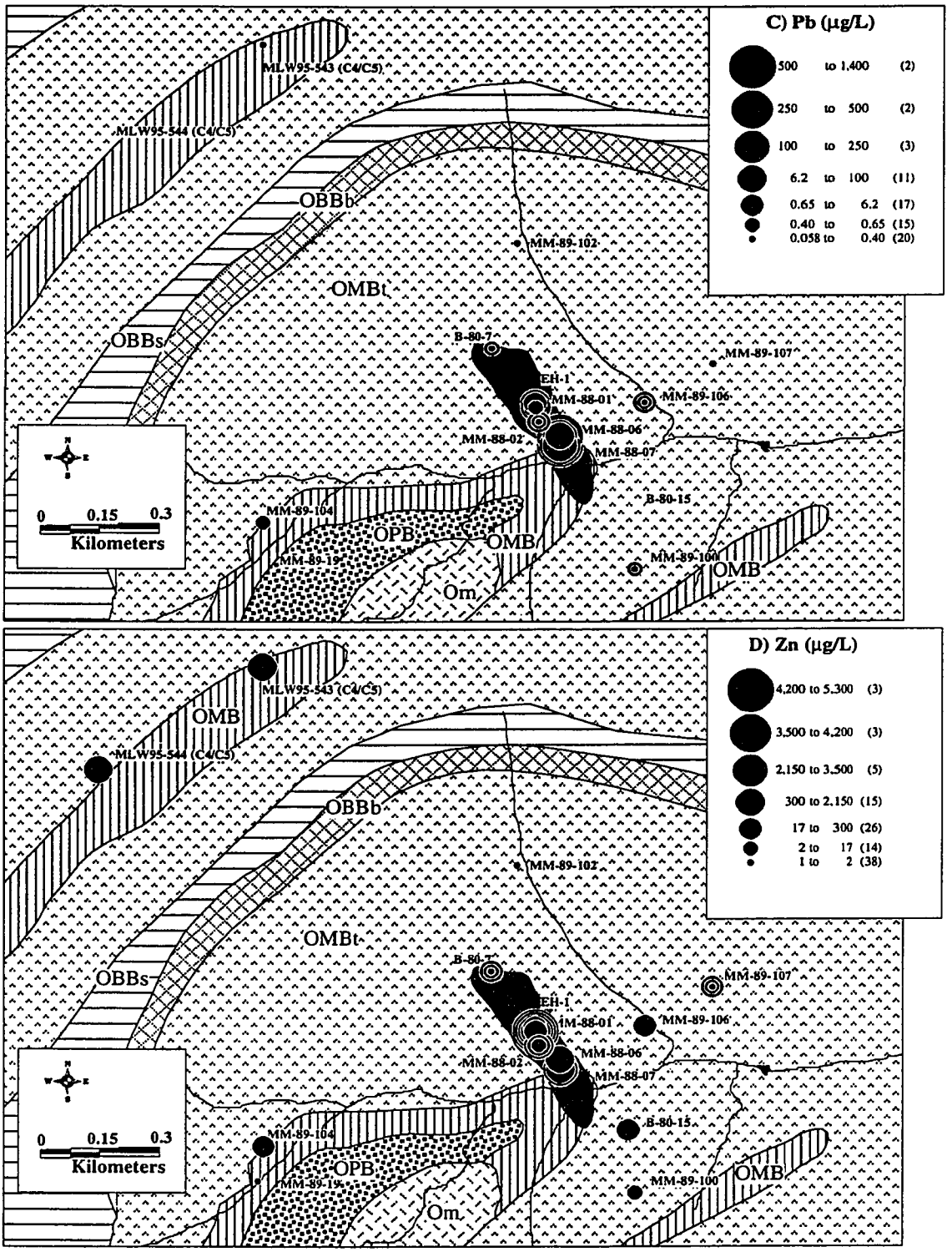


Fig. 13.14 continued.

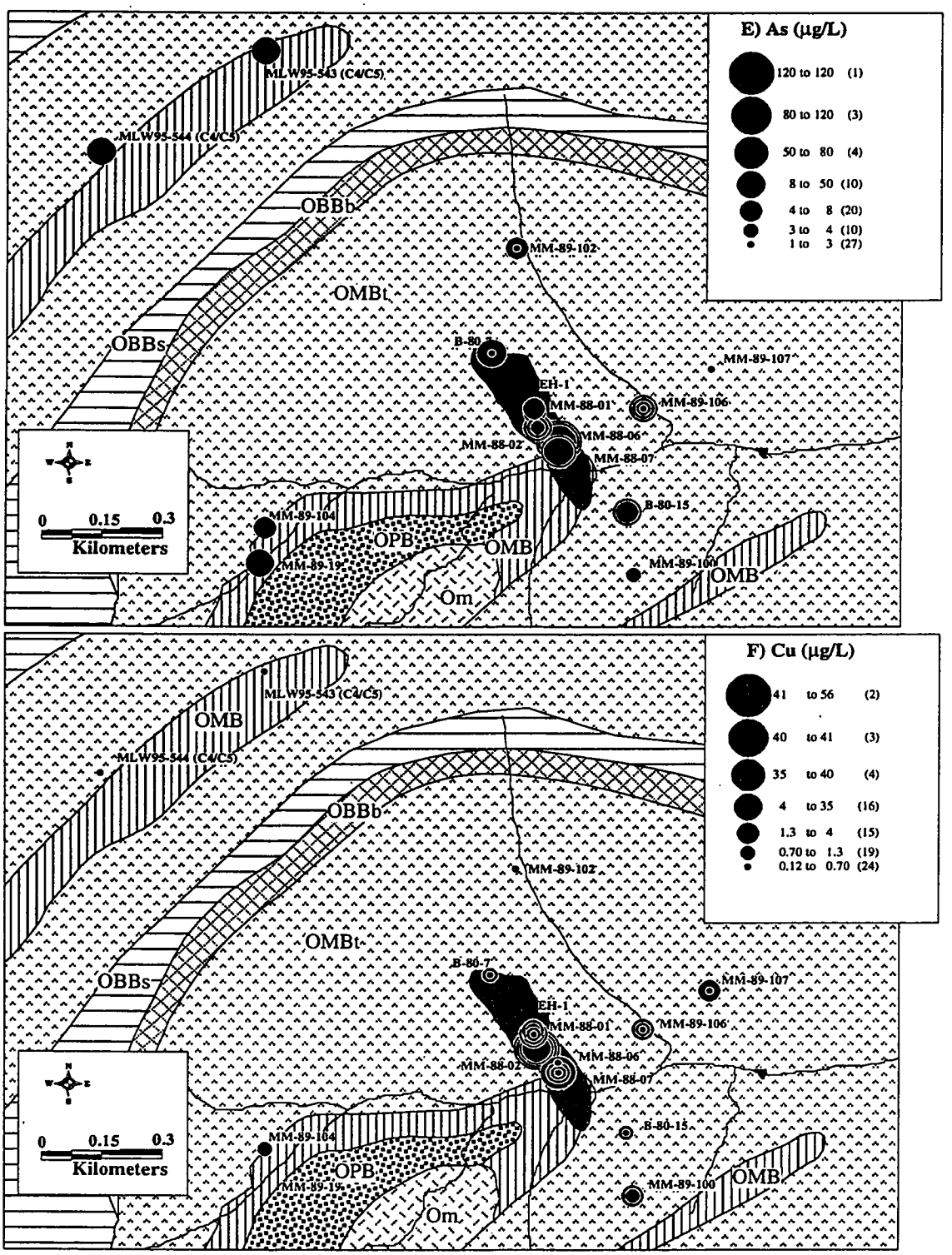


Fig. 13.14 continued.

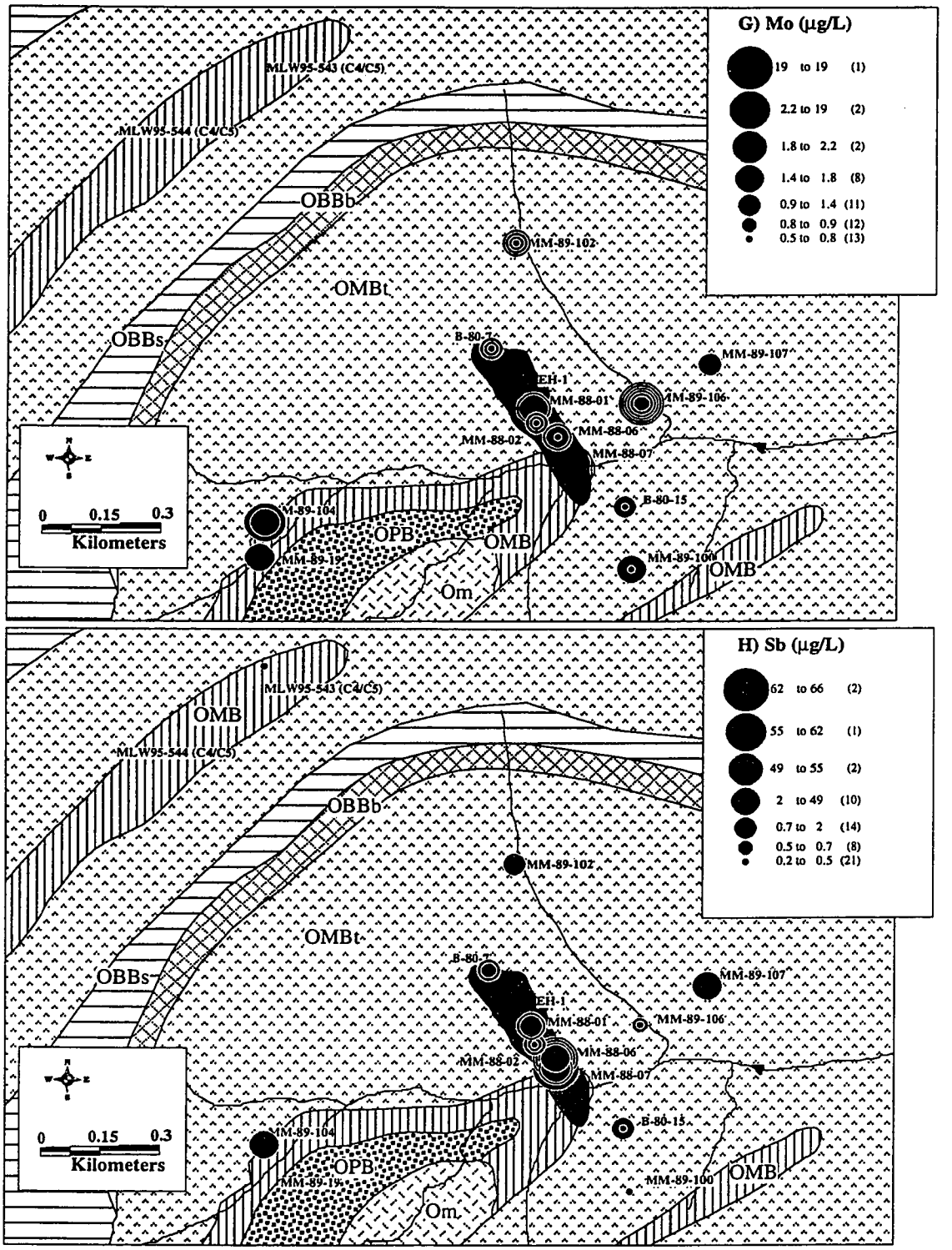


Fig. 13.14 continued.

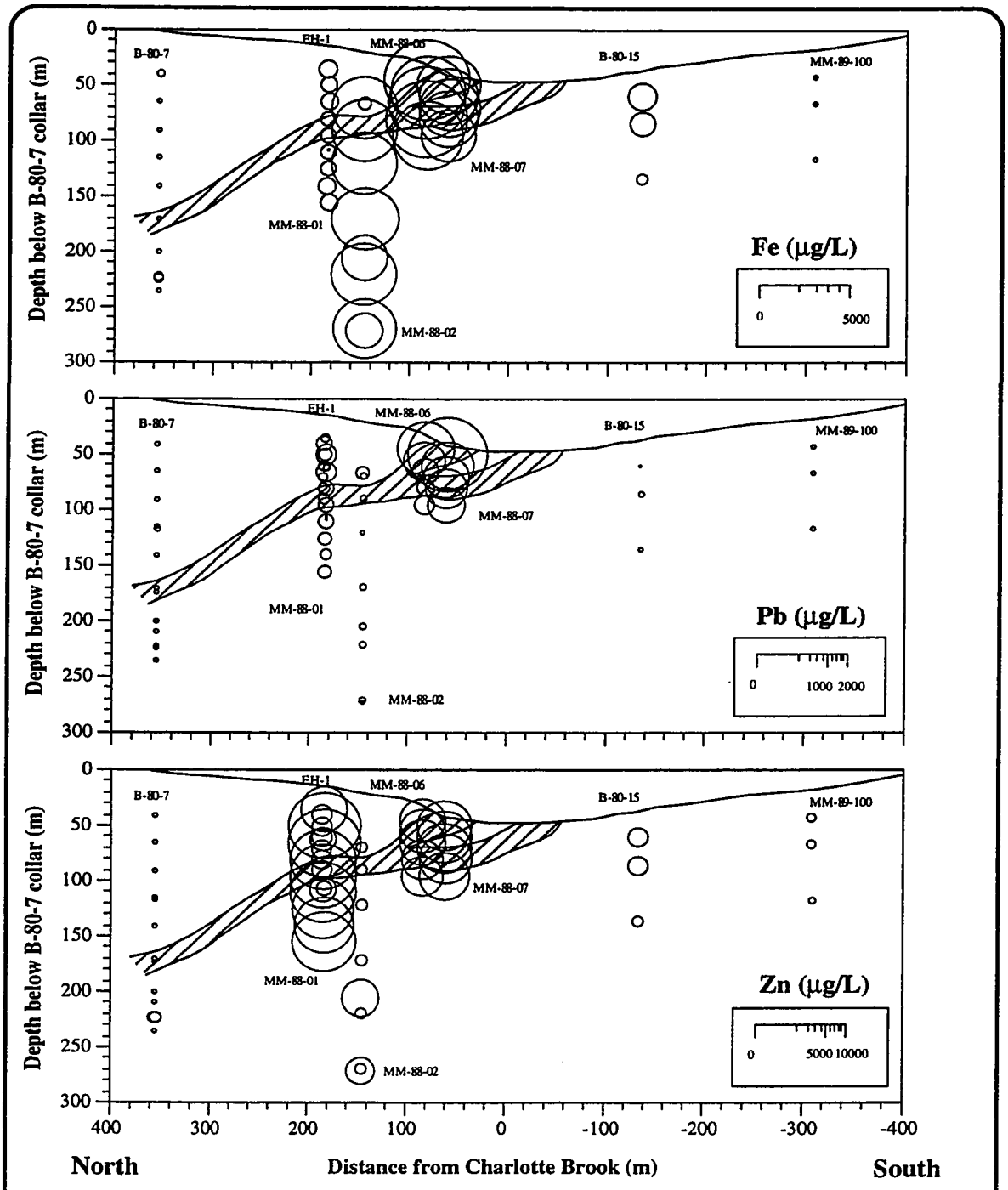


Fig. 13.15 Proportional circle plots of metal contents of borehole waters in the plane of the massive sulphides at the Restigouche deposit. Approximate location of ore zone is shown for reference.

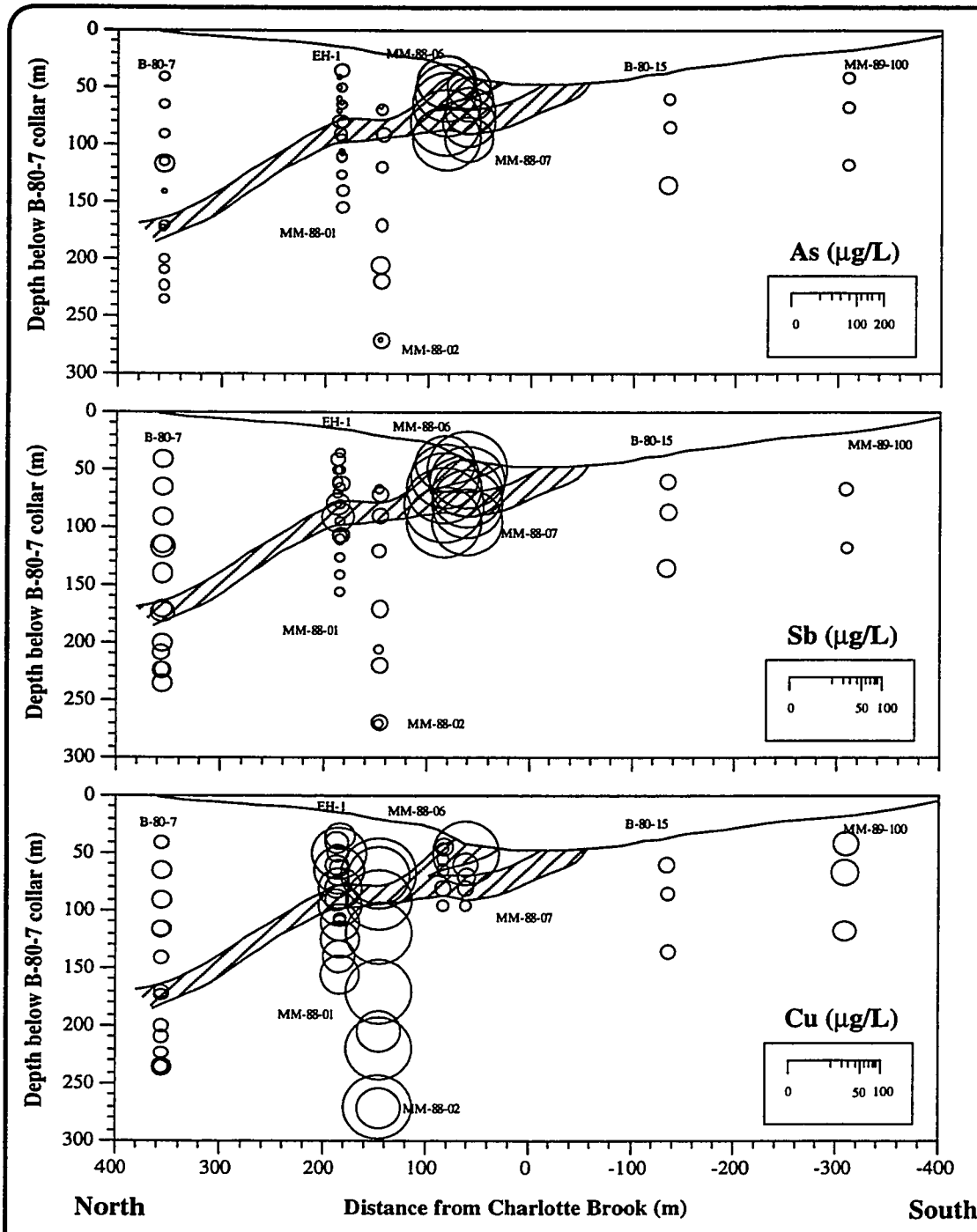


Fig. 13.15 continued.

CHAPTER FOURTEEN: CONCLUSIONS

Chapter Five

Chapter Five focussed on the composition of surface waters from the Halfmile Lake and Restigouche deposits. These waters are dominantly Ca-HCO_3 in composition. Local lithology is the dominant control over surface water composition, although Ca (and Mg) are primarily controlled by dissolution of carbonate in veins and fractures. Surface waters at the Restigouche deposit display larger compositional variability, in particular with respect to pH and SO_4, which is consistent with greater oxidation of sulphide minerals in the near-surface environment compared to the Halfmile Lake deposit. There is no stable isotopic evidence for significant evaporative concentration of major solutes in the surface waters. Surface waters have higher Cl- contents than local precipitation which is interpreted to be the result of rock weathering. The host lithologies and stream sediments have sufficient Cl contents to account for the surface water compositions.

Chapter Six

Stream sediments were collected in conjunction with the surface waters. Stream sediment compositions are fractionated relative to host lithologies consistent with element mobility during weathering and both hydromorphic and detrital contributions are apparent in bulk stream sediment compositions. Many previous studies have normalized suspended sediment loads of rivers to average upper continental crust in order to investigate elemental budgets and riverine contributions to the oceans. Normalization of stream sediments from the Halfmile Lake and Restigouche deposits to upper continental crust display large negative anomalies in mobile elements (Ca, Sr and Na) and smaller anomalies for immobile elements (Nb, Hf) similar to these previous studies. However, these fractionations largely disappear where the Halfmile Lake and Restigouche deposit stream sediments are normalized to local lithologies. This suggests that studies which rely on normalization to a universal standard such as upper

continental crust to make inferences regarding riverine contributions to the oceans and rates of crustal erosion, may be erroneous.

Chapter Seven

The geochemistry of groundwaters from the Halfmile Lake, Restigouche, Brunswick #12, Heath Steele, Wedge and Willett deposits was presented in Chapter Seven. These deposits are hosted in similar lithologies of similar age. The Halfmile Lake deposit is steeply dipping with steep structures (Chapter Four) whereas structures are shallow dipping at the Restigouche deposit and the main sulphide zone is closer to surface. Groundwater flow is dominated by fracture-flow at both the Halfmile Lake and Restigouche deposits, and deposit lithologies, geometry and structures play a fundamental role in determining the hydrology which in turn controls the geochemistry of the groundwaters. The groundwaters recovered from these two deposits are compositionally distinct.

Groundwaters from the Halfmile Lake deposit are dominated by low TDS (< 100 mg/L), Ca-HCO_3 compositions, although deeper groundwaters increase in TDS (< 230 mg/L) and are more evolved Na-HCO_3-type compositions. Although groundwaters were sampled from depths up to 760 meters, no saline waters were observed. The Halfmile Lake deposit groundwaters are interpreted to be modern meteoric waters which are rapidly transmitted to depth along steep structures, consistent with the low TDS and stable isotopic compositions. Any saline groundwaters that may have existed at the Halfmile Lake deposit have been "flushed" from the system.

Groundwaters from the Restigouche deposit range from shallow Ca-HCO_3 and Ca-SO_4 waters and to high TDS Na-Cl waters with increasing depth, in sharp contrast to the Halfmile Lake deposit. Based on groundwater compositions, geochemical modelling and stable isotopes there are several different groundwater systems at the Restigouche deposit. Low TDS Ca-HCO_3-type groundwaters represent shallow-recharge waters with major solute composition controlled by dissolution of carbonate and silicate minerals in the shallow soil zone and upper

parts of the weathered bedrock. Groundwaters with dominantly Ca-SO_4 compositions occur in boreholes which intersect the Restigouche deposit massive sulphide at depths less than 120 meters and are modern recharge waters. The elevated sulphate and sulphide-related metals reflect oxidation of the massive sulphide minerals. There is a deeper groundwater flow system which is characterized by elevated Na and Cl concentrations due to greater water-rock reactions and elevated HCO_3^- due to dissolution of carbonate in the footwall alteration zone to the ore deposit. These groundwaters have much higher TDS contents (up to 2660 mg/L) than the shallow groundwaters. Saline groundwaters (>20,000 mg/L TDS) were recovered from the deepest borehole at the Restigouche deposit.

The Br/Cl ratios of the groundwaters vary from values less than seawater in the saline waters to values much greater than seawater for the shallow groundwaters and surface waters. The shallow groundwaters and surface waters have similar Br/Cl values as those measured in brines from the Canadian Shield. This data suggests either that the saline waters have interacted with non-marine evaporites, or more likely, that Br and Cl are differentially released during water-rock reaction.

The saline waters are interpreted to have been produced by long periods of water-rock reaction. These saline waters have much heavier oxygen and deuterium isotopic compositions indicating recharge under a warmer climatic regime. There is no compelling evidence to support a marine origin for these waters. Elevated Cu, Co, Ni, and Cr contents of the saline waters from borehole MM-88-02 suggest that these waters have interacted with mafic rocks. The mafic dikes which cross-cut the Restigouche deposit may have acted as conduits for flow of these water.

Chapter Eight

A single borehole was sampled with the straddle-packer system at the Stratmat Main Zone deposit to better understand the origin of large negative self potential anomalies and subtle positive thermal anomalies observed through the main massive sulphide zone and to investigate

processes of massive sulphide oxidation below the water table. Groundwaters were sampled systematically downhole and through the sulphide zone and display a rapid increase in TDS in the sulphide zone. The dominant anion is SO_4^{2-}, particularly in the massive sulphides indicating that the primary control over groundwater composition is sulphide oxidation. Geochemical profiles of Fe and base metals through the ore zone are consistent with sulphide oxidation, predominantly at the base of the massive sulphides, with increasing oxidation of Fe^{2+} to Fe^{3+} and precipitation of Fe-oxyhydroxides towards the top of the sulphide zone. Base metals also decrease toward the top of the ore zone due to diffusion and adsorption onto Fe-oxyhydroxides.

The self potential anomaly associated with the ore zone (600 mV anomaly) is interpreted to reflect the development of an electrochemical cell driven by oxidation of massive sulphides at the base of the massive sulphides and reduction of dissolved oxygen at the top of the sulphides. The thermal anomaly is interpreted to be due to greater groundwater flow through the sulphide zone compared to above and below the sulphides and compared to nearby boreholes. Thus, nearby boreholes have no temperature anomaly and have more subdued SP anomalies. The groundwater flow through the sulphides provides a continuous supply of dissolved oxygen to drive the sulphide oxidation reactions. Stable isotope and packer response data are consistent with differential groundwater flow through the massive sulphides, with groundwaters close to the bottom of the sulphides having been recharged under a slightly warmer climatic regime. Carbon isotopes indicate that neutral to alkaline pH values are maintained due to dissolution of carbonate.

Chapter Nine

Groundwaters from the Halfmile Lake and Restigouche deposits commonly had sufficient suspended sediments on the filter papers for mineralogical and geochemical analysis. Suspended sediments recovered from Halfmile Lake deposit groundwaters and those distal from the Restigouche deposit are dominated by quartz and aluminosilicate minerals.

Fe-oxyhydroxides are probably present as surface coatings and amorphous Fe-phases. Suspended sediments from boreholes that intersect the Restigouche deposit massive sulphides consist primarily of Fe, Pb, and Zn sulphate minerals.

The Halfmile Lake deposit suspended sediments are depleted in the mobile elements Cs, Rb, and K compared to the host rocks. Suspended sediments show generally flat patterns normalized to the host lithologies for most other elements but strong enrichments in the hydrothermal suite of elements (Pb, Fe, Co, Zn, Ag, and Eu). The geochemistry of the suspended sediments from the Restigouche deposit shows similar relationships, although the degree of enrichment in metals associated with massive sulphide mineralization is greater. Compared to coexisting groundwaters suspended sediments are relatively enriched in Al, Fe, Pb, and relatively depleted in Ca, Sr, and Mg. Potassium and Rb are generally more strongly fractionated into the suspended sediment phase than other mobile elements, indicating that their abundance in the groundwaters is controlled by secondary silicate phases (e.g., illite).

14.7 Chapter Ten

Rare earth element concentrations are highly variable in waters of the BMC, with higher concentrations typical of waters with higher Fe and lower pH. There are significant differences between surface and groundwaters, and between groundwaters from different areas. The REE contents of surface waters are broadly similar within and between deposit areas, although there are differences between different streams which reflects differences in pH and lithology. Surface waters typically possess strong negative Ce anomalies, which are produced by oxidation of Ce^{3+} to Ce^{4+} upon leaving the shallow groundwater environment. Groundwaters are typically more reducing and have smaller to no Ce anomalies. Seeps commonly have no negative Ce anomaly although adjacent stream waters display strong anomalies, which indicates that the development of negative Ce anomalies in Halfmile Lake and Restigouche deposit surface waters is rapid. Stream sediments also display negative Ce anomalies, but of lower magnitude than surface waters, consistent with rapid oxidation where groundwaters

reach the surface environment.

Deeper groundwaters at Halfmile Lake are characterized by REE patterns that are similar to the host rocks, whereas most groundwaters at the Restigouche deposit have LREE depleted patterns compared to NASC. One of the major reasons for the differences between the groundwaters from Halfmile Lake versus those from the Restigouche deposit may derive from the fact that at the Halfmile Lake deposit the pH is somewhat lower and in addition the activities of possible anionic complexes for the REE are low suggesting that the REE are more controlled by source considerations. In contrast, the anionic concentrations at the Restigouche deposit are generally greater suggesting that the distribution of the REE is more controlled by solubility/speciation considerations. Shallow waters at the Halfmile Lake deposit and waters from the Stratmat Main Zone deposit have unusual patterns which reflect either the influence of adsorption onto colloidal minerals or onto fracture zone minerals or different fluid histories compared to groundwaters from the Restigouche deposit.

14.8 Chapter Eleven

Oxygen and deuterium isotopes of surface and shallow groundwaters from both the Halfmile Lake and Restigouche deposits are very uniform (-13 to -14‰ and -85 to -95‰ for $\delta^{18}O_{VSMOW}$ and δD_{VSMOW}, respectively). These values are lighter than predicted for northern New Brunswick and, combined with high excess deuterium, suggest that recharge is dominated by winter precipitation, recharged during spring runoff. The close similarity in stable isotopic composition of surface waters and shallow groundwaters indicates that surface waters were sampled primarily during base flow conditions. Deeper groundwaters from the Restigouche deposit and from the Heath Steele, Brunswick #12, Stratmat Main Zone, and Willett deposits have heavier oxygen and deuterium isotopic compositions than shallow groundwaters indicating recharge under warmer climates.

Carbon isotopic compositions of dissolved inorganic carbon are generally heavy, ranging from -15 to -5‰ $\delta^{13}C_{DIC}$ for most groundwaters and surface waters. Mass balance modelling

indicates that this range in carbon isotopic composition can be accounted for by closed system groundwater evolution. Recharging groundwaters initially possess $\delta^{13}C_{DIC}$ values of -18 to-20‰ due to equilibration with soil zone CO_2 and the $\delta^{13}C_{DIC}$ evolves to heavier compositions due to dissolution of fracture zone carbonate minerals. Fracture and vein carbonate minerals at the Restigouche deposit have restricted carbon isotopic compositions of around -5 to -6‰.

The carbon isotopic compositions of the saline waters from borehole MM-88-02 at the Restigouche deposit are very heavy (+12‰ $\delta^{13}C_{DIC}$) and cannot be modelled by carbonate dissolution. These heavy carbon isotope values are most consistent with fractionation of the DIC due to methanogenesis. This interpretation is supported by the lack of dissolved sulphate in these waters and the observation of degassing during sampling, interpreted to be due to the release of methane.

Boron isotopes indicate that the salinity of BMC waters is controlled by variable degrees of water-rock reaction with the host lithologies, which is consistent with Br/Cl ratios (Chapter Seven).

14.9 Chapter Twelve

Most of the waters appear to follow two trends with respect to Sr isotopic compositions. Groundwaters from the Restigouche deposit trend to less radiogenic Sr compositions with increasing water-rock reaction, probably reflecting increasing contributions of relatively non-radiogenic Sr from plagioclase weathering. Groundwaters interacting with the Restigouche massive sulphides, and the Wedge and Heath Steele deposits appear to trend to more radiogenic Sr isotopic compositions and higher Rb/Sr with increasing depth and water-rock reaction. These relationships are most consistent with increasing contribution of ^{87}Sr from sericite associated with hydrothermal alteration proximal to the massive sulphides, and/or from radiogenic carbonate in the stockwork. The saline waters from borehole MM-88-02 at the Restigouche deposit have very high Sr and relatively non-radiogenic Sr isotopes, most likely indicating equilibration with plagioclase, perhaps associated with mafic dykes that cross-cut the

deposit. In contrast, saline waters from the Brunswick #12 deposit have the most radiogenic Sr compositions in the study, suggesting interaction with K-feldspar and/or micas. The brackish water from borehole MM-89-106 is more radiogenic than other saline and brackish groundwaters at the Restigouche deposit. Low Ca/Na and moderately high Sr suggest some influence from K-feldspar weathering.

Groundwaters associated with the Restigouche, Wedge and Heath Steele deposits are more radiogenic than those distal to the Restigouche deposit, suggesting that there may be some potential for the use of Sr isotopes in waters as an exploration tool.

Most waters have non-radiogenic Pb isotopic compositions similar to BMC galena. This indicates that Pb derived from massive sulphide weathering dominates the Pb contents of most of the waters used in this study. Notable exceptions are waters from boreholes MM-89-106 and MM-89-107 from the Restigouche deposit which have Pb which is more radiogenic than the host rocks. Anomalously high $^{207}Pb/^{204}Pb$ in groundwater MLW95-504 from borehole MM-89-106 indicates that the Pb in the water was derived from a high-μ mineral, perhaps phosphate, consistent with the presence of phosphate in the suspended load of this water. Several surface waters have $^{206}Pb/^{204}Pb$ indistinguishable from BMC galena, but have anomalously low $^{207}Pb/^{204}Pb$ and $^{208}Pb/^{204}Pb$, suggesting equilibration with low-μ and low-κ mineral(s).

The Pb isotopic composition of the ground and surface waters indicates that Pb isotopes in waters may be a powerful tool in mineral exploration. Groundwaters can potentially reveal more deeply buried sources of mineralization compared to other techniques which employ Pb isotopes, e.g., Pb isotopic analyses of glacial till and gossans. Two groundwaters distal to the Restigouche deposit have ore-Pb isotopic compositions suggesting as yet undiscovered sources of mineralization.

Stream sediment MLS96-664 has the least radiogenic Pb isotopic composition reported to date from the BMC. Combined with high Zn, Ni and Co in sediments from this stream, the Pb isotope value is interpreted to reflect massive sulphide mineralization in the subsurface which

has a greater contribution of Grenville age Pb compared to other deposits in the BMC.

The Nd isotopes of several groundwaters show a wide range in $^{143}Nd/^{144}Nd$, consistent with differences in Sm/Nd and REE patterns. The fact that the Nd isotopic compositions of the waters is different from host rocks and yields incorrect ages indicates that groundwaters are preferentially incorporating the REE from certain minerals rather than from the bulk rock.

14.10 Chapter Thirteen

Geochemical modelling in combination with Pb isotopic compositions indicates that massive sulphides at the Restigouche, Halfmile Lake and Stratmat Main Zone deposits are undergoing variable degrees of oxidation with subsequent hydromorphic transport of sulphide-associated metals (Zn, Cd, Pb, Cu, Fe). This suggests that the composition of natural waters may be useful in mineral exploration in the Bathurst Mining Camp. Surface waters can be routinely analyzed for trace metals to very low detection limits because of recent advances in analytical techniques which has removed one of the most serious obstacles in the use of natural waters in mineral exploration.

Although base metal contents of surface waters at the Halfmile Lake and Restigouche deposits are low compared to other deposits and mine tailings, anomalous values are clearly associated with the Restigouche sulphide deposit. The Halfmile Lake deposit is deeper and as a result surface water anomalies are more subtle, although SO_4 and Zn contents are highest closest to the deposit.

Groundwaters show greater base metal abundances and greater contrast between anomalous and background compositions, especially at the Restigouche deposit and therefore could be a powerful tool in mineral exploration in the BMC. However, application of this technique is limited due to poor access to boreholes away from areas of known mineralization. Groundwater geochemistry may also be useful in defining exploration targets. Suspended sediments from groundwaters associated with mineralization have very high metal contents, primarily as a result of circumneutral groundwater pH values and fractionation of the base

metals from the aqueous to the suspended sediment phase. At the Halfmile Lake deposit, suspended sediments have higher metal contents than waters or stream sediments. Thus, suspended sediment geochemistry may be a useful exploration tool to complement ground and surface water hydrogeochemical exploration. In particular, Zn/Pb ratios of suspended sediments decrease with increasing proximity to massive sulphide mineralization.

BIBLIOGRAPHY

Adair R. N. (1992) Stratigraphy, structure, and geochemistry of the Halfmile Lake massive-sulfide deposit, New Brunswick. *Exploration and Mining Geology* 1, 151-166.

Aggarwal J. K. and Palmer M. R. (1995) Boron isotope analysis: a review. *Analyst* 120, 1301-1307.

Al T. A., Blowes D. W., and Jambor J. L. (1994) A geochemical study of the main tailings impoundment at the Falconbridge Limited, Kidd Creek Division metallurgical site, Timmins, Ontario. In *Short Course Handbook on Environmental Geochemistry of Sulfide Mine-Wastes*, Vol. 22 (ed. J. L. Jambor and D. W. Blowes), pp. 333-364. Mineralogical Association of Canada.

Al T. A., Blowes D. W., Martin C. J., Cabri L. J., and Jambor J. L. (1997) Aqueous geochemistry and analysis of pyrite surfaces in sulfide-rich mine tailings. *Geochimica et Cosmochimica Acta* 61, 2353-2366.

Allègre C. J., Dupré B., Négrel P., and Gaillardet J. (1996) Sr-Nd-Pb isotope systematics in Amazon and Congo River systems: Constraints on erosion processes. *Chemical Geology* 131, 93-112.

Alpers C. N., Blowes D. W., Nordstrom D. K., and Jambor J. L. (1994) Secondary minerals and acid mine-water chemistry. In *Short Course Handbook on Environmental Geochemistry of Sulfide Mine-Wastes*, Vol. 22 (ed. J. L. Jambor and D. W. Blowes), pp. 247-270. Mineralogical Association of Canada.

Alpers C. N., Nordstrom D. K., and Burchard J. M. (1992) Compilation and interpretation of water-quality and discharge data for acidic mine waters at Iron Mountain, Shasta County, California, 1940-91. *Water Resources Investigations.*

Anderson P. R. and Christensen T. H. (1988) Distribution coefficients of Cd, Co, Ni, and Zn in soils. *Journal of Soil Science* 39, 15-22.

Andrew R. L. (1980) Supergene alteration and gossan textures of base metal ores in southern Africa. *Minerals Science and Engineering* 12, 193-215.

Appel P. W. V., Moorbath S., and Taylor P. N. (1978) Least radiogenic terrestrial lead from Isua, West Greenland. *Nature* 272, 524-526.

Appleyard E. C. and Blowes D. W. (1994) Applications of mass-balance calculations to weathered sulfide mine tailings. In *Environmental Geochemistry of Sulfide Oxidation* (ed. C. N. Alpers and D. W. Blowes), pp. 516-534.

Asmerom Y. and Jacobsen S. B. (1993) The Pb isotopic evolution of the earth: inferences from river water suspended loads. *Earth and Planetary Science Letters* 115, 245-256.

Austria V. (1981) Stream and spring sediment geochemistry maps, California Lake west (21O/8W). *Department of Natural Resources and Energy, Mineral Resources and Energy Division* Open File 81-45.

Azcue J. M. and Nriagu J. O. (1995) Impact of abandoned mine tailings on the arsenic concentrations in Moira Lake, Ontario. *Journal of Geochemical Exploration* 52, 81-89.

Babinski M., Chemale F.-J., and Van Schmus W. R. (1995) The Pb/Pb age of the Minas Supergroup carbonate rocks, Quadrilátero Ferrífero, Brazil. *Precambrian Research* 72, 235-245.

Baker A. J. and Fallick A. E. (1989) Heavy carbon in two-billion-year-old marbles from Lofoten-Vesteralen, Norway; implications for the Precambrian carbon cycle. *Geochimica et Cosmochimica Acta* 53(5), 1111-1115.

Baker E. T., Feely R. A., Mottl M. J., Sansone F. T., Wheat C. G., Resing J. A., and Lupton J. E. (1994) Hydrothermal Plumes Along the East Pacific Rise, 8 degrees 40' to 11 degrees 50'N - Plume Distribution and Relationship to the Apparent Magmatic Budget. *Earth Planet Sci Lett* 128(1-2), 1-17.

Ball J. W. and Nordstrom D. K. (1991) *Users manual for WATEQ4F with revised thermodynamic database and test cases for calculating speciation of major, trace, and redox elements in natural waters.* USGS Open-File Report 91-183.

Banner J. L., Wasserburg G. J., Dobson P. F., Carpenter A. B., and Moore C. H. (1989) Isotopic and trace element constraints on the origin and evolution of saline groundwaters

from central Missouri. *Geochimica et Cosmochimica Acta* 53, 383-398.

Barrie C. Q. (1982) Summary Report Restigouche Property N.T.S. 21O/7E and 10E. Billiton Canada Limited.

Barrow N. J., Gerth J., and Bruemmer G. W. (1989) Reaction kinetics of the adsorption and desorption of nickel, zinc and cadmium by goethite; II, Modelling the extent and rate of reaction. *Journal of Soil Science* 40(2), 437-450.

Bau M. and Dulski P. (1996) Anthropogenic origin of positive gadolinium anomalies in river waters. *Earth and Planetary Science Letters* 143, 245-255.

Bell K. and Franklin J. M. (1993) Application of lead isotopes to mineral exploration in glaciated areas. *Geology* 21, 1143-1146.

Belland M. (1991) Letter to the Editor. *Canadian Mining Journal*, 9.

Benjamin M. M. and Leckie J. O. (1981a) Competative adsorption of Cd, Cu, Zn, and Pb on amorphoud iron oxyhydroxide. *Journal of Colloid and Interface Science* 83, 410-419.

Benjamin M. M. and Leckie J. O. (1981b) Multiple-site adsorption of Cd, Cu, Zn, and Pb on amorphous iron oxyhydroxide. *Journal of Colloid and Interface Science* 79, 209-221.

Berner E. K. and Berner R. A. (1987) *The Global Water Cycle*. Prentice-Hall.

Bethke C. M. (1994) The Geochemist's Workbench. University of Illinois.

Bethke C. M. (1996) *Geochemical Reaction Modeling: Concepts and Applications*. Oxford University Press.

Bigham J. M., Schwertmann U., Carlson L., and Murad E. (1990) A poorly crystallized oxyhydroxysulfate of iron formed by bacterial oxidation of Fe(II) in acid mine waters. *Geochimica et Cosmochimica Acta* 54(10), 2743-2758.

Billett M. F., Lowe J. A. H., Black K. E., and Cresser M. S. (1996) The influence of parent material on small-scale spatial changes in streamwater chemistry in Scottish upland catchments. *Journal of Hydrology* 187, 311-331.

Blain C. F. (1977) Sulphide weathering and the evaluation of gossans in mineral exploration. *Minerals Science and Engineering* 9, 119-150.

Blain C. F. and Brotherton R. L. (1975) Self-potentials in relation to oxidation of nickel-sulphide bodies within semi-arid climatic terrains. *Transactions of the Institution of Mining and Metallurgy* 84, B123-B127.

Blowes D. W., Jambor J. L., Cherry J. A., and Reardon E. J. (1990) The occurrence and potential importance of cemented layers in base-metal mine tailings impoundments. *Anonymous. Geological Association of Canada; Mineralogical Association of Canada; annual meeting; program with abstracts Association Geologique du Canada; Association Mineralogique du Canada; reunion annuelle; programme et resumes. Program with Abstracts Geological Association of Canada; Mineralogical Association of Canada; Canadian Geophysical Union, Joint Annual Meeting* 15, 12.

Blowes D. W. and Ptacek C. J. (1994) Acid-neutralization mechanisms in inactive mine tailings. In *Short Course Handbook on Environmental Geochemistry of Sulfide Mine-Wastes*, Vol. 22 (ed. J. L. Jambor and D. W. Blowes), pp. 271-292. Mineralogical Association of Canada.

Bölviken B. and Logn Ö. (1974) An electrochemical model for element distribution around sulphide bodies. Geochemical Exploration 1974 Developments in Economic Geology, 1, 631-648.

Bonham-Carter G. F. (1993) *Geographic Information Systems for Geoscientists: Modelling with GIS*. Pergamon.

Bottinga Y. (1969) Calculated fractionation factors for carbon and hydrogen isotopic exchange in the system calcite-carbon dioxide-graphite, methane-hydrogen-water vapor. *Geochim. Cosmochim. Acta* 33, 49-64.

Bottomley D. J. (1984) Origins of some arseniferous groundwaters in Nova Scotia and New Brunswick, Canada. *Journal of Hydrology* 69, 223-257.

Bottomley D. J., Gregoire D. C., and Raven K. G. (1994) Saline groundwaters and brines in the Canadian Shield: geochemical and isotopic evidence for a residual evaporite brine component. *Geochimica et Cosmochimica Acta* 58, 1483-1498.

Bottomley D. J., Ross J. D., and Graham B. W. (1984) A borehole methodology for hydrogeochemical investigations in fractured rock. *Water Resources Research* 20, 1277-1300.

Bowell R. J. and Bruce I. (1995) Geochemistry of iron ochres and mine waters from Levant Mine, Cornwall. *Applied Geochemistry* 10, 237-250.

Bowell R. J., Morley N. H., and Din V. K. (1994) Arsenic speciation in soil porewaters from the Ashanti Mine, Ghana. *Applied Geochemistry* 9, 15-22.

Boyle D. R. (1979) The dispersion of uranium in the vicinity of Miocene 'basal type' uranium occurrences in Lassie Lake area, South-central British Columbia. In *Current research; Part A.*, Vol. 79-1a, pp. 349-356. Geological Survey of Canada.

Boyle D. R. (1995) Geochemistry and genesis of the Murray Brook precious metal gossan deposit, Bathurst Mining Camp, New Brunswick. *Exploration and Mining Geology* 4(4), 341-363.

Boyle D. R. (1996) Supergene base metals and precious metals. In *Geology of Canadian Mineral Deposit Types*, Vol. Geology of Canada, no. 8 (ed. O. R. Eckstrand, W. D. Sinclair, and R. I. Thorpe), pp. 92-108. Geological Survey of Canada.

Boyle R. W., Hornbrook E. H. W., Allan R. J., Dyck W., and Smith A. V. (1971) Hydrogeochemical methods applications in the Canadian Shield. *Canadian Institute of Mining and Metallurgy Bulletin* 64, 60-71.

Boyle R. W., Tupper W. M., Lynch J., Friedrich G., Ziauddin M., Shafiqullah M., Carter M., and Bygrave K. (1966) *Geochemistry of Pb, Zn, Cu, As, Sb, Mo, Sn, W, Ag, Ni, Co, Cr, Ba, and Mn in the waters and stream sediments of the Bathurst-Jacquet River District, New Brunswick.* Geological Survey of Canada. Ottawa, ON, Canada. Pages: 50.

Brace T. D. (1982) Report of Work, Restigouche South Property, Restigouche and Northumberland Counties, New Brunswick. Teck Exploration Ltd.

Bullen T. D., Krabbenhoft D. P., and Kendall C. (1996) Kinetic and mineralogic controls on the evolution of groundwater chemistry and $^{87}Sr/^{86}Sr$ in a sandy silicate aquifer, northern

Wisconsin, USA. *Geochimica et Cosmochimica Acta* 60, 1807-1821.

Byrne R. H. and Kim K.-H. (1990) Rare earth element scavenging in seawater. *Geochim. Cosmochim. Acta* 54(10), 2645-2656.

Byrne R. H. and Liu X. (1996) Metal speciation assessments in natural waters: Comment on "Rare earth element complexation behaviour in circumneutral pH ground waters: Assessing the role of carbonate and phosphate ions" by Kevin H. Johannesson, Klaus J. Stetzenbach. Vernon F. Hodge and W. Berry Lyons. *Earth and Planetary Science Letters* 145, 135-137.

Caissie D., Pollock T. L., and Cunjak R. A. (1996) Variation in stream water chemistry and hydrograph separation in a small drainage basin. *Journal of Hydrology* 178, 137-157.

Cameron E. M. (1977) Geochemical dispersion in lake waters and sediments from massive sulphide mineralization, Agricola Lake, Northwest Territories. *Journal of Geochemical Exploration* 7, 327-348.

Canada E. (1991) Hydat surface water and sediment data, CD-ROM Version 4.0. *Surveys and Information Systems Branch, Environment Canada.*

Carmichael I. S. E. and Eugster H. P. (1987) Thermodynamic Modeling of Geological Materials: Minerals, Fluids and Melts, Vol. 17 (ed. P. H. Ribbe), pp. 499. Mineralogical Society of America.

Carothers W. W., Adami L. H., and Resenbaur R. J. (1988) Experimental oxygen isotope fractionation between siderite-water and phosphoric acid liberated CO_2-siderite. *Geochimica et Cosmochimica Acta* 52, 2445-2450.

Carothers W. W. and Kharaka Y. K. (1980) Stable carbon isotopes of HCO_3^- in oil-field waters—implications for the origin of CO_2. *Geochimica et Cosmochimica Acta* 44, 323-332.

Chen W., Tan S. K., and Tay J. H. (1996) Distribution, fractional composition and release of sediment-bound heavy metals in tropical reservoirs. *Water, Air, and Soil Pollution* 92, 273-287.

Chuan M. C., Shu G. Y., and Liu J. C. (1996) Solubility of heavy metals in a contaminated

soil: effects of redox potential and pH. *Water, Air, and Soil Pollution* 90, 543-556.

Cidu R., Fanfani L., Shand P., Edmunds W. M., Dack L. V. t., and Gijbels R. (1995) Hydrogeochemical exploration for gold in the Osilo area, Sardinia, Italy. *Applied Geochemistry* 10(5), 517-529.

Clark I. D. and Fritz P. (1997) *Environmental Isotopes in Hydrogeology*. Lewis Publishers.

Clow D. W., Mast M. A., Bullen T. D., and Turk J. T. (1997) Strontium 87/strontium 86 as a tracer of mineral weathering reactions and calcium sources in an alpine/subalpine watershed, Loch Vale, Colorado. *Water Resources Research* 33, 1335-1351.

Condie K. C. (1991) Another look at rare earth elements in shales. *Geochim. Cosmochim. Acta* 55, 2527-2531.

Connolly C. A., Walter L. M., Baadsgaard H., and Longstaffe F. J. (1990) Origin and evolution of formation waters, Alberta Basin, Western Canada Sedimentary Basin. II. Isotope systematics and water mixing. *Applied Geochemistry* 5, 397-413.

Coston J. A., Fuller C. C., and Davis J. A. (1995) Pb^{2+} and Zn^{2+} adsorption by a natural aluminum- and iron-bearing surface coating on an aquifer sand. *Geochimica et Cosmochimica Acta* 59, 3535-3547.

Cousens B. L. (1996) Magmatic evolution of Quaternary mafic magmas at Long Valley Caldera and the Devils Postpile, California: Effects of crustal contamination on lithospheric mantle-derived melts. *Journal of Geophysical Research* 101, 27,673-27,689.

Craig H. (1961) Isotopic variations in meteoric waters. *Science* 133, 1702-1703.

Curtis P. J. and Walker P. (1994) Release of metals from a Cd-contaminated streambed in response to experimental acidification and neutralization. *Water Resources Research* 30, 3449-3454.

Cwynar L. C., Levesque A. J., Mayle F. E., and Walker I. (1994) Wisconsinan late-glacial environmental change in New Brunswick; a regional synthesis. In *North Atlantic Seaboard Programme IGCP-253; Climate changes in areas adjacent to the North Atlantic during the last glacial-interglacial transition.*, Vol. 9; 2 (ed. J. J. Lowe), pp. 161-164. John Wiley and

Sons for the Quaternary Research Association.

Dansgaard W. (1964) Stable isotopes in precipitation. Tellus 16, 436-468.

Davis J. A. and Kent D. B. (1990) Surface complexation modeling in aqueous geochemistry. In *Mineral-water interface geochemistry.*, Vol. 23 (ed. M. F. Hochella, Jr. and A. F. White), pp. 177-260. Mineralogical Society of America.

Davisson M. L. and Criss R. E. (1996) Na-Ca-Cl relations in basinal brines. *Geochimica et Cosmochimica Acta* 60, 2743-2752.

Dechow E. W. C. (1960) Geology, sulfur isotopes, and the origin of the Heath Steele ore deposits, Newcastle, N.B., Canada. Econ. Geol. 55, 539-556.

de Roo J. A. and van Staal C. R. (1991) The structure of the Half Mile Lake region, Bathurst Camp, New Brunswick. *Current Research, Part D, Geological Survey of Canada* Paper 91-1D, 179-186.

de Roo J. A., Williams P. F., and Moreton C. (1991) Structure and evolution of the Heath Steele base metal sulfide orebodies, Bathurst camp, New Brunswick, Canada. *Economic Geology* 86, 927-943.

Degueldre C., Grauer R., laube A., Oess A., and Silby H. (1996a) Colloid properties in granitic groundwater systems. II: Stability and transport study. *Applied Geochemistry* 11, 697-710.

Degueldre C., Pfeiffer H.-R., Alexander W., Wernli B., and Bruetsch R. (1996b) Colloid properties in granitic groundwater systems. I: Sampling and characterization. *Applied Geochemistry* 11, 677-695.

Deveaux J. L., Arnold G. W., and Csabai J. (1988) Report of work, Project 4215/4217, Stratmat Group. New Brunswick Department of Natural Resources and Energy, Mineral and Energy Division, Assessment File 473864.

Dix G. R., Thomson M. L., Longstaffe F. J., and McNutt R. H. (1995) Systematic decrease of high $\delta^{13}C$ values with burial in late Archean (2.8 Ga) diagenetic dolomite: evidence for methanogenesis from the Crixás Greenstone Belt, Brazil. *Precambrian Research* 70, 253-

28.

Doherty W., Gregoire D. C., Goodfellow W. D., Firard I., and Lightfoot P. C. (1997) Determination of lead isotope ratios by ICP Mass Spectrometry: Application to base metal exploration in the Bathurst Mining Camp. *Ottawa '97, Joint Annual Meeting of the Geological Association of Canada/Mineralogical Association of Canada*, A-39.

Drever J. I. (1988) *The geochemistry of natural waters*. Prentice-Hall.

Dunn C. E., Parkhill M. A., and Balma R. G. (1996) Geochemical study around the Restigouche deposit, Bathurst Mining Camp, New Brunswick, in Carroll, B.M.W. (ed) New Brunswick Department of Natural Resources and Energy, Minerals and Energy Division, Information Circular (IC) 96-131-32.

Dupré B., Gaillerdet J., Rousseau D., and Allègre C. J. (1996) Major and trace elements of river-borne material: the Congo Basin. *Geochimica et Cosmochimica Acta* 60, 1301-1321.

Earle S. A. M. and Drever G. L. (1983) Hydrogeochemical exploration for uranium within the Athabasca Basin, northern Saskatchewan. *Journal of Geochemical Exploration* 19, 57-73.

Edmond J. M., Palmer M. R., Measures C. I., Brown E. T., and Huh Y. (1996) Fluvial geochemistry of the eastern slope of the northeastern Andes and its foredeep in the drainage of the Orinoco in Columbia and Venezuela. *Geochimica et Cosmochimica Acta* 60, 2949-2976.

Eggleston C. M. and Stumm W. (1993) Scanning tunneling microscopy of Cr(III) chemisorbed on α-Fe_2O_3 (001) surfaces from aqueous solution: direct observation of surface mobility and clustering. *Geochimica et Cosmochimica Acta* 57, 4843-4850.

Elderfield H., Upstill-Goddard R., and Sholkovitz E. R. (1990) The rare earth elements in rivers, estuaries, and coastal seas and their significance to the composition of ocean waters. *Geochimica et Cosmochimica Acta* 54, 971-991.

Erel Y., Patterson C. C., Scott M. J., and Morgan J. J. (1990) Transport of industrial lead in snow through soil to stream water and groundwater. *Chemical Geology* 85, 383-392.

Farrah H., Hatton D., and Pickering W. F. (1980) The affinity of metal ions for clay surfaces.

Chemical Geology 28, 1-2.

Fee J. A., Gaudette H. E., Lyons W. B., and Long D. T. (1992) Rare-earth element distribution in Lake Tyrrell groundwaters, Victoria, Australia. In *The Geochemistry of Acid Groundwater Systems. Chemical Geology*, Vol. 96 (ed. W. B. Lyons, D. T. Long, A. L. Herczeg, and M. E. G. E. Hines), pp. 67-93.

Feely R. A., Gendron J. F., Baker E. T., and Lebon G. T. (1994) Hydrothermal Plumes Along the East Pacific Rise, 8 degrees 40' to 11 degrees 50'N - Particle Distribution and Composition. *Earth and Planet ary ScienceLetters* 128(1-2), 19-36.

Fouquet Y., von Stackelberg U., Charlou J. L., Donval J. P., Erzinger J., Foucher J. P., Herzig P., Muhe P., Soakai S., Wiedicke M., and Whitechurch H. (1991a) Hydrothermal activity and metallogenesis in the Lau back-arc basin. *Nature* 349, 778-781.

Fouquet Y., von Stackelberg U., Charlou J. L., Donval J. P., Foucher J. P., Erzinger J., Herzig P., Wiedicke M., Soakai S., and Whitechurch H. (1991b) Hydrothermal activity in the Lau back-arc basin: sulfides and water chemistry. *Geology* 19, 303-306.

Franklyn M. T., McNutt R. H., Kamineni D. C., Gascoyne M., and Frape S. K. (1991) Groundwater $^{87}Sr/^{86}Sr$ values in the Eye-Dashwa Lakes pluton, Canada: evidence for plagioclase-water reaction. *Chemical Geology* 86, 111-122.

Frape S. K., Blyth A. R., Jones M. G., Blomqvist R., Tullborg E.-L., McNutt R. H., McDermott F., and Ivanovich M. (1992) A comparison of calcite fracture mineralogy and geochemistry for the Canadian and Fennoscandian Shields. In *Proceedings of the 7th International Symposium on Water-Rock Interaction; Volume 1, Low Temperature Environments.*, Vol. 7 (ed. Y. K. Kharaka and A. S. Maest), pp. 787-791. International Association of Geochemistry and Cosmochemistry and Alberta Research Council, Sub-Group on Water-Rock Interaction.

Frape S. K., Fritz P., and McNutt R. H. (1984) Water-rock interaction and chemistry of groundwaters from the Canadian Shield. *Geochimica et Cosmochimica Acta* 48, 1617-1627.

Friedman I. and O'Neil J. R. (1977) *Compilation of stable isotope fractionation factors of geochemical interest.*

Fritz P., Drimmie R. J., Frape S. K., and O'Shea K. (1987) The isotopic composition of precipitation and groundwater in Canada. In *Isotopic Techniques in Water Resources Development, Symp. 299, March, 1987* (ed. I. A. E. Agency), pp. 539-550.

Fritz P., Fontes J.-C., Frape S. K., Louvat D., Michelot J.-L., and Balderer W. (1989) The isotope geochemistry of carbon in groundwater at Stripa. *Geochimica et Cosmochimica Acta* 53, 1765-1775.

Fritz P. and Frape S. K. (1982) Saline groundwaters in the Canadian Shield - a first overview. *Chemical Geology* 36, 179-190.

Fritz P., Frape S. K., Drimmie R. J., Appleyard E. C., and Hattori K. (1994) Sulfate in brines in the crystalline rocks of the Canadian shield. *Geochimica et Cosmochimica Acta* 58, 57-65.

Fuge R., Pearce F. M., Pearce N. J. G., and Perkins W. T. (1994) Acid mine drainage in Wales and influence of ochre precipitation on water chemistry. In *Environmental Geochemistry of Sulfide Oxidation* (ed. C. N. Alpers and D. W. Blowes), pp. 261-274.

Fyffe L., McCutcheon S. R., and Wilson R. A. (1996) The Miramichi-Tetagouche boundary and its relationship to the Patrick brook Formation, 12.

Fyffe L. R., Forbes W. H., and Riva J. (1983) Graptolites from the Benton area of west-central New Brunswick and their regional significance. *Maritime Sediments and Atlantic Geology* 19, 117-125.

Gaillardet J., Dupré B., and Allégre C. J. (1995) A global geochemical mass budget applied to the Congo Basin rivers: Erosion rates and continental crust composition. .

Gaillardet J., Dupré B., Allègre C. J., and Négrel P. (1997) Chemical and physical denudation in the Amazon River Basin. *Chemical Geology* 142, 141-173.

Garrels R. M. and Christ C. L. (1965) *Solutions, Minerals and Equilibria.* Harper & Row.

Garrels R. M. and Thompson M. E. (1960) Oxidation of pyrite by iron sulfate solutions.

American Journal of Science 258-A, 57-67.

Gascoyne M. (1997) Evolution of redox conditions and groundwater composition in recharge-discharge environments on the Canadian Shield. *Hydrogeology Journal* 5, 4-18.

Gascoyne M., Davison C. C., Ross J. D., and Pearson R. (1987) Saline groundwaters and brines in plutons in the Canadian Shield. In *Saline water and gases in crystalline rocks*, Vol. Geological Association of Canada Special Paper 33 (ed. P. Fritz and S. K. Frape), pp. 53-68.

Gavrieli I., Starinsky A., Spiro B., Aizenshtat Z., and Nielsen H. (1995) Mechanisms of sulfate removal from subsurface calcium chloride brines: Heletz-Kokhav oilfields, Isreal. *Geochimica et Cosmochimica Acta* 59, 3525-3533.

Giblin A. (1994) Natural waters as sample media in drainage geochemistry. In *Handbook of Exploration Geochemistry*, Vol. 6 (ed. G. J. S. Govett), pp. 269-303. Elsevier Science.

Giblin A. M. (1980) The role of clay adsorption in genesis of uranium ores. In *Uranium in the Pine Creek Geosyncline; proceedings of the International uranium symposium on the Pine Creek Geosyncline.*, Vol. Sti/pub/555 (ed. J. Ferguson and A. B. Goleby), pp. 521-529. International Atomic Energy Agency.

Giblin A. M. and Snelling A. A. (1983) Application of hydrogeochemistry to uranium exploration in the Pine Creek geosyncline, Northern Territory, Australia. *Journal of Geochemical Exploration* 19, 33-55.

Glahder C. and Asmund G. (1996) Natural Zn elevations in arctic water bodies, 811-817.

Gómez P., Turrero M. J., Moulin V., and Magonthier M. C. (1992) Characterization of natural colloids in groundwaters of El Berrocal, Spain. In *Proceedings of the 7th International Symposium on Water-Rock Interaction; Volume 1, Low Temperature Environments.*, Vol. 7 (ed. Y. K. Kharaka and A. S. Maest), pp. 797-800. International Association of Geochemistry and Cosmochemistry and Alberta Research Council, Sub-Group on Water-Rock Interaction.

Goodfellow W. D. (1975) Rock geochemical exploration and ore genesis at Brunswick No. 12

deposit. Ph.D. Thesis, University of New Brunswick, Fredericton.

Goodfellow W. D. (1983) Stream sediment and water geochemistry of the Howard's Pass (XY) Zn-Pb deposit and Nor Zn-Pb-Ba occurrence, Selwyn Basin and Northwest Territories. *Geological Survey of Canada Open File Report 845*, 12 + appendices.

Goodfellow W. D. (1989) Interpretation of stream geochemistry leading to the discovery of a secondary zinc deposit, Pelly River, Nahanni map area, Yukon. *Current Research* Part E, Geological Survey of Canada, Paper 89-1E, 31-50.

Goodfellow W. D. (1995) EXTECH-II: A new multidisciplinary, integrated and collaborative project on the development and testing of exploration methods and technology in the Bathurst Mining Camp, New Brunswick. *Exploration and Mining Geology* **4**, 327-329.

Goodfellow W. D. and participants E.-I. (1996) The EXTECH-II project in the Bathurst mining camp: New concepts on the genesis and methods for the detection of massive sulphide deposits. *Mineral Colloquium 1996.*

Goodfellow W. D. and Peter J. M. (1996) Sulphur isotope composition of the Brunswick #12 massive sulphide deposit, Bathurst Mining Camp, New Brunswick: implications for ambient environment, sulphur source, and ore genesis. *Canadian Journal of Earth Sciences* 33, 231-251.

Goodman B. A. (1986) Adsorption of metal ions and complexes on aluminosilicate minerals. In *Geochemical processes at mineral surfaces.*, Vol. 323 (ed. J. A. Davis and K. F. Hayes), pp. 342-361. American Chemical Society.

Goodyear K. L., Ramsey M. H., Thornton I., and Rosenbaum M. S. (1996) Source identification of Pb-Zn contamination in the Allen Basin, Cornwall, S.W. England. *Applied Geochemistry* 11, 61-68.

Gosselin D. C., Smith M. R., Lepel E. A., and Laul J. C. (1992) Rare earth elements in chloride-rich groundwater, Palo Duro Basin, Texas, USA. *Geochimica et Cosmochimica Acta* 56, 1495-1505.

Govett G. J. S., Goodfellow W. D., and Whitehead R. E. (1976) Experimental aqueous

dispersion of elements around sulfides. *Economic Geology* 71(5), 925-940.

Gower S. J. (1995) Geology of the Portage Brook area (NTS 21 0/O7h and part of 21 0/10a), Restigouche and Northumberland Counties, New Brunswick. New Brunswick Department of Natural Resources and Energy, Minerals and Energy Division, Plate 95-26.

Gower S. J. (1996) Geology, lithogeochemistry and mineral occurrences in the Portage Brook area, northwestern Bathurst Mining Camp, New Brunswick (NTS 21 O/7h, part of 21 O/10a). In *Current Research 1995*, Vol. Mineral Resources Report 96-1 (ed. B. M. W. Carroll), pp. 13-43. New Brunswick Department of Natural Resources and Energy, Minerals and Energy Division.

Graham D. L. and Johnson V. G. (1991) Effects of fluid rotary drilling on hydrochemical sampling results from deep boreholes in fractured Columbia River Basalt. *Journal of Hydrology* 128, 171-212.

Gregoire D. C. (1990) Determination of boron in fresh and saline waters by inductively-coupled plasma mass spectrometry. *Journal of Analytical Atomic Spectroscopy* 5, 623-626.

Grimes D. J. and de Carvalho D. (1994) Geochemical exploration studies in the Portuguese pyrite belt. In *Advances in research on mineral resources, 1994.* (ed. B. R. Berger), pp. 53-77. U. S. Geological Survey.

Grimes D. J., Ficklin W. H., Meier A. L., and McHugh J. B. (1995) Anomalous gold, antimony, arsenic, and tungsten in ground water and alluvium around disseminated gold deposits along the Getchell Trend, Humboldt County, Nevada. *Journal of Geochemical Exploration* 52, 351-371.

Gromet L. P., Dymek R. F., Haskin L. A., and Korotev R. L. (1984) The "North American shale composite": its compilation, major and trace element characteristics. *Geochim. Cosmochim. Acta* **48**, 2469-2482.

Group R. C. (1996) Restigouche Mine Development Groundwater Monioring Program. Prepared for: East West Caribou Mining Limited.

Gulson B. L. (1986) *Lead Isotopes in Mineral Exploration*. Elsevier.

Gulson B. L., Church S. E., Mizon K. J., and Meier A. L. (1992) Lead isotopes in iron and manganese oxide coatings and their use as an exploration guide for concealed mineralization. *Applied Geochemistry* 7, 495-511.

Gulson B. L., Large R. R., and Porritt P. M. (1988) Gold exploration using lead isotopes at Tennant Creek, Australia. *Applied Geochemistry* 3, 243-254.

Hall G. E. M., Vaive J. E., and McConnell J. W. (1995b) Development and application of a sensitive and rapid analytical method to determine the rare-earth elements in surface waters. *Chemical Geology* 120, 91-109.

Hamilton A. (1992) Geology of the Stratmat Boundary and Heath Steele N-5 zones, Bathurst Camp, New Brunswick. *Exploration and Mining Geology* 1, 131-135.

Hamilton A. and Wilson R. A. (1997) Part 1. The Heath Steele deposits. In *Geology and massive sulphides of the Bathurst Camp, New Brunswick* (ed. S. R. McCutcheon), pp. 16-28. Geological Association of Canada - Mineralogical Association of Canada, Joint Annual Meeting, Ottawa '97, Field Trip B7, Guidebook.

Harley D. N. (1977) Geology of the Half Mile Lake Zn-Pb-Cu Deposit, New Brunswick. M.Sc., The university of Western Ontario.

Harley D. N. (1979) A mineralized resurgent caldera complex in the Bathurst-Newcastle mining district, New Brunswick, Canada. *Econ. Geol.* 74, 786-796.

Haskin L. A., Haskin M. A., Frey F. A., and Wildeman T. R. (1968) Relative and absolute terrestrial abundances of the rare earths. In *Origin and Distribution of the Elements, 1.* (ed. L. H. Ahrens), pp. 889-911. Pergamon Press.

Hochella M. F., Jr. (1990) Atomic structure, microtopography, composition, and reactivity of mineral surfaces. In *Mineral-water interface geochemistry.*, Vol. 23 (ed. M. F. Hochella, Jr. and A. F. White), pp. 87-132. Mineralogical Society of America.

Hodge V. F., Johannesson K. H., and Stetzenbach K. J. (1996) Rhenium, molybdenum, and uranium in groundwater from the southern Great Basin, USA: evidence for conservative behaviour. *Geochimica et Cosmochimica Acta* 60, 3197-3214.

Hofmann A. W. (1988) Chemical differentiation of the Earth: the relationship between mantle, continental crust, and oceanic crust. *Earth. Planet. Sci. Lett.* 90, 297-314.

Holmden C., Creaser R. A., and Muehlenbachs K. (1997) Paleosalinities in ancient brackish water systems determined by $^{87}Sr/^{86}Sr$ ratios in carbonate fossils: A case study from the Western Canada Sedimentary Basin. *Geochimica et Cosmochimica Acta* **61**, 2105-2118.

Honeyman B. D. and Leckie J. O. (1986) Macroscopic partitioning coefficients for metal ion adsorption; proton stoichiometry at variable pH and adsorption density. In *Geochemical processes at mineral surfaces.*, Vol. 323 (ed. J. A. Davis and K. F. Hayes), pp. 162-190. American Chemical Society.

Hovdan H. and Bølviken B. (1985) Sulphide self potentials in relation to oxygen content in drill-hole water. *Geoexploration* 23, 387-394.

Hussein A. A. (1996) Application of Pb isotopes to mineral exploration using glacial till of the Halfmile Lake area, Bathurst, New Brunswick, Caleton University.

Jahn B. and Simonson B. M. (1995) Carbonate Pb-Pb ages of the Wittenoom Formation and Carawine Dolomite, Hamersley Basin, Western Australia (with implications for their correlation with the Transvaal Dolomite of South Africa). *Precambrian Research* 72, 247-261.

Jambor J. L. (1994) Mineralogy of sulfide-rich tailings and their oxidation products. In *Short Course Handbook on Environmental Geochemistry of Sulfide Mine-Wastes*, Vol. 22 (ed. J. L. Jambor and D. W. Blowes), pp. 59-102. Mineralogical Association of Canada.

Johannesson K. H. and Lyons W. B. (1994) The rare earth element geochemistry of Mono Lake water and the importance of carbonate complexing. *Limnology and Oceanography* 39, 1141-1154.

Johannesson K. H., Lyons W. B., and Bird D. A. (1994a) Rare earth element concentrations and speciation in alkaline lakes from the western U.S.A. *Geophysical Researh Letters* 21, 773-776.

Johannesson K. H., Lyons W. B., Fee J. H., Gaudette H. E., and McArthur J. M. (1994b)

Geochemical processes affecting the acidic groundwaters of Lake Gilmore, Yilgarn Block, Western Australia: a preliminary study using neodymium, samarium, and dysprosium. *Journal of Hydrology* 154, 271-289.

Johannesson K. H., Stetzenbach K. J., and Hodge V. F. (1997) Rare earth elements as geochemical tracers of regional groundwater mixing. *Geochimica et Cosmochimica Acta* 61, 3605-3618.

Johannesson K. H., Stetzenbach K. J., Hodge V. F., and Lyons W. B. (1996a) Rare earth element complexation behaviour in circumneutral pH groundwaters: Assessing the role of carbonate and phosphate ions. *Earth and Planetary Science Letters* 139, 305-319.

Johannesson K. H., Stetzenbach K. J., Hodge V. F., and Lyons W. B. (1996b) Reply to comment on the paper "Rare earth element complexation behaviour in circumneutral pH groundwaters: Assessing the role of carbonate and phosphate ions". *Earth and Planeary Science Letters* 145, 139-141.

Johannesson K. H., Stetzenbach K. J., Kreamer D. K., and Hodge V. F. (1996c) Multivariate statistical analysis of arsenic and selenium concentrations in groundwaters from south-central Nevada and Death Valley, California. *Journal of Hydrology* 178, 181-204.

Johnson T. M. and DePaolo D. J. (1997) Rapid exchange effects on isotopic ratios in groundwater systems 2. Flow investigation using Sr isotope ratios. *Water Resources Research* 33, 197-209.

Kamineni D. C. (1987) Halogen-bearing minerals in plutonic rocks: A possible source of chlorine in saline groundwater in the Canadian Shield. In *Saline Water and Gases in Crystalline Rocks*, Vol. 33 (ed. P. Fritz and S. K. Frape), pp. 69-79. Geological Association of Canada Special Paper.

Kamineni D. C., Gascoyne M., Melnyk T. W., Frape S. K., and Blomqvist R. (1992) Cl and Br in mafic and ultramafic rocks: Significance for the origin of salinity in groundwater. In *Proceedings of the 7th International Symposium on Water-Rock Interaction; Volume 1, Low Temperature Environments.*, Vol. 7 (ed. Y. K. Kharaka and A. S. Maest), pp. 801-

804. International Association of Geochemistry and Cosmochemistry and Alberta Research Council, Sub-Group on Water-Rock Interaction.

Kelley K. D. and Taylor C. D. (1997) Environmental geochemistry of shale-hosted Ag-Pb-Zn massive sulfide deposits in northwest Alaska: natural background concentrations of metals in water from mineralized areas. *Applied Geochemistry* 12, 397-409.

Kesler S. E., Appold M. S., Martini A. M., Walter L. M., Huston T. J., and Kyle J. R. (1995) Na-Cl-Br systematics of mineralizing brines in Mississippi Valley-type deposits. *Geology* 23, 641-644.

Kilty K. T. (1984) On the origin and interpretation of self-potential anomalies. *Geophysical Prospecting* 32, 51-62.

Klinkhammer G., German C. R., Elderfield H., Greaves M. J., and Mitra A. (1994a) Rare earth elements in hydrothermal fluids and plume particulates by inductively coupled plasma mass spectrometry. *Marine Chemistry* 45, 179-186.

Klinkhammer G. P., Elderfield H., Edmond J. M., and Mitra A. (1994b) Geochemical implications of rare earth element patterns in hydrothermal fluids from mid-ocean ridges. *Geochimica et Cosmochimica Acta* 58, 5105-5113.

Knauth L. P. (1988) Origin and mixing history of brines, Palo Duro Basin, Texas, U.S.A. *Applied Geochemistry* 3, 455-474.

Lasaga A. C. (1990) Atomic treatment of mineral-water surface reactions. In *Mineral-Water Interface Geochemistry* (ed. M. F. J. Hochella and A. F. White), pp. 17-85. Mineralogical Society of America.

LeBlanc S. (1989) Massive sulphide-associated gold: Brunswick No. 12 mine, Bathurst, New Brunswick. Hons. B.Sc., University of New Brunswick.

Lent R. M., Gaudette H. E., and Lyons W. B. (1997) Strontium isotopic geochemistry of the Devils Lake drainage system, North Dakota: a preliminary study and potential paleoclimatic implications. *Journal of Paleolimnology* 17, 147-154.

Lentz D. R. (1996) Recent advances in lithogeochemical exploration for massive-sulphide

deposits in volcano-sedimentary environments: petrogenetic, chemostratigraphic, and alteration aspects with examples from the Bathurst camp, New Brunswick. In *Current Research 1996*, Vol. Mineral; Resource Report 96-1 (ed. B. M. W. Carroll), pp. 73-119. New Brunswick Department of Natural Resources and Energy, Minerals and Energy Division.

Lentz D. R. and Goodfellow W. D. (1992a) Re-evaluation of the petrochemistry of felsic volcanic and volcaniclastic rocks near the Brunswick No. 6 and 12 massive sulphide deposits, Bathurst Mining Camp, New Brunswick. *Current Research, Part E; Geological Survey of Canada* Paper 92-1E, 343-350.

Lentz D. R. and Goodfellow W. D. (1992b) Re-evaluation of the petrology and depositional environment of felsic volcanic and related rocks in the vicinity of the Brunswick No. 12 massive sulphide deposit, Bathurst Mining Camp, New Brunswick. *Current Research, Part E; Geological Survey of Canada* Paper 92-1E, 333-342.

Lentz D. R. and Goodfellow W. D. (1993a) Geochemistry of the stringer sulphide zone in the Discovery Hole at the Brunswick No. 12 massive sulphide deposit, Bathurst, New Brunswick. *Current Research, Part E; Geological Survey of Canada* Paper 93-1E, 259-269.

Lentz D. R. and Goodfellow W. D. (1993b) Mineralogy and petrology of the stringer sulphide zone in the Discovery Hole at the Brunswick No. 12 massive sulphide deposit, Bathurst, New Brunswick. *Current Research, Part E; Geological Survey of Canada* Paper 93-1E, 249-258.

Lentz D. R. and Goodfellow W. D. (1993c) Petrology and mass-balance constraints on the origin of quartz-augen schist associated with the Brunswick massive sulfide deposits, Bathurst, New Brunswick. *Canadian Mineralogist* 31, 877-903.

Lentz D. R. and Goodfellow W. D. (1994) Petrology and geochemistry of altered volcanic and sedimentary rocks associated with the FAB stringer sulphide zone, Bathurst, New Brunswick. *Current Research, 1994-D; Geological Survey of Canada*, 123-133.

Lentz D. R. and Goodfellow W. D. (1996) Intense silicification of footwall sedimentary rocks

in the stockwork alteration zone beneath the Brunswick no. 12 massive sulphide deposit, Bathurst, New Brunswick. *Canadian Journal of Earth Sciences* 33, 284-302.

Lentz D. R. and Gregoire C. (1995) Petrology and mass-balance constraints on major-, trace-, and rare-earth-element mobility in porphyry-greisen alteration associated with the epizonal True Hill granite, southwestern New Brunswick. *Journal of Geochemical Exploration* 52, 303-331.

Lewis A. J., Palmer M. R., Sturchio N. C., and Kemp A. J. (1997) The rare earth element geochemistry of acid-sulphate and acid-sulphate-chloride geothermal systems from Yellowstone National Park, Wyoming, USA. *Geochimica et Cosmochimica Acta* 61, 695-706.

Leybourne M. I., Boyle D. R., Goodfellow W. D., Dunn C. D., Turcotte C., Gilliss M., and Allaby G. (1997a) Detailed hydrogeochemical, stream sediment and biogeochemical mineral exploration program in the Murray Brook-Restigouche area, Bathurst Mining Camp, New Brunswick. *Abstracts/Résumés - 1997, 22nd Annual review of Activities.*

Leybourne M. I., Goodfellow W. D., and Boyle D. R. (1995a) Chemical composition of ground and surface waters at the Halfmile Lake deposit, Bathurst Mining Camp, northern New Brunswick - EXTECH II. In *Current Research1994. New Brunswick Department of Natural Resources and Energy, Minerals and Energy Division, Miscellaneous Report 18* (ed. S. A. A. Merlini), pp. 113-126.

Leybourne M. I., Goodfellow W. D., and Boyle D. R. (1995b) Hydrochemistry of ground and surface waters at the Restigouche and Halfmile Lake deposits, Bathurst Mining Camp, New Brunswick. *Abstracts/Résumés - 1995, twentieth Annual review of Activities.*, 26.

Leybourne M. I., Goodfellow W. D., and Boyle D. R. (1995c) Hydrogeochemistry and hydrology of groundwaters associated with the Halfmile Lake Deposit, Bathurst mining camp, New Brunswick. *Geological Survey of Canada Forum.*

Leybourne M. I., Goodfellow W. D., and Boyle D. R. (1996a) Chemical and stable isotopic composition of ground and surface waters from the Restigouche Zn-Pb massive sulphide

deposit, Bathurst Mining Camp, northern New Brunswick - EXTECH II. *Current Research, Part E; Geological Survey of Canada* Paper 1996-1E., 243-254.

Leybourne M. I., Goodfellow W. D., and Boyle D. R. (1996b) Contrasting chemical and isotopic compositions of groundwaters from the Halfmile Lake and Restigouche Zn-Pb deposits, Bathurst Mining Camp, N.B., Canada. *Geological Society of America Annual Meeting,.*

Leybourne M. I., Goodfellow W. D., and Boyle D. R. (1996c) Hydrochemistry of ground and surface waters at Restigouche and Halfmile Lake Deposits, Bathurst Mining Camp, Northeastern N.B. *Geological Survey of Canada, 1996 Minerals Colloquium.*

Leybourne M. I., Goodfellow W. D., and Boyle D. R. (1997b) Hydrochemical exploration in the Bathurst Mining Camp, northern New Brunswick: Results from the Restigouche and Halfmile Lake Zn-Pb deposits. *GAC-MAC Ottawa '97.*

Leybourne M. I., Goodfellow W. D., and Boyle D. R. (1997c) Hydrogeochemical and isotopic evidence for multicomponent mixing of groundwaters and oxidation of the Restigouche Zn-Pb massive sulphide deposit, Bathurst Mining Camp, New Brunswick. *Abstracts/Résumés - 1997, 22nd Annual review of Activities.*

Leybourne M. I., Goodfellow W. D., and Boyle D. R. (1997d) Hydrology, hydrochemistry and stable isotopic compositions of ground and surface waters from the Restigouche and Halfmile Lake Zn-Pb massive sulphide deposits, Bathurst Mining Camp, northern New Brunswick. *GAC-MAC Ottawa '97.*

Leybourne M. I., Goodfellow W. D., and Boyle D. R. (1997e) Variable Geochemical Responses to Water-Rock Interactions at Two Undisturbed Zn-Pb Massive Sulphide Deposits, Bathurst Mining Camp, N.B., Canada. *Abstracts/Résumés - 1997, 22nd Annual review of Activities.*

Leybourne M. I., Goodfellow W. D., and Boyle D. R. (1997f) Variable geochemical responses to water-rock interactions at two undisturbed Zn-Pb massive sulphide deposits, Bathurst Mining Camp, N.B., Canada. *4th International Symposium on Environmental*

Geochemistry (ISEG).

Leybourne M. I., Goodfellow W. D., and Boyle D. R. (submitted-a) Variable geochemical responses to water-rock interactions at two undisturbed Zn-Pb massive sulphide deposits, Bathurst Mining Camp, N.B., Canada. *Journal of Geochemical Exploration.*

Leybourne M. I., Goodfellow W. D., Boyle D. R., and Hall G. M. (submitted-b) Rapid development of negative Ce anomalies in surface waters and contrasting REE patterns in groundwaters associated with Zn-Pb massive sulphide deposits. *Applied Geochemistry.*

Leybourne M. I., Mwenifumbo J. C., Goodfellow W. D., and Boyle D. R. (submitted-c) Hydrogeochemical and geophysical evidence for in situ oxidation of an undisturbed massive sulphide deposit and development of self-potential anomalies, Stratmat Main Zone, New Brunswick. *Geochimica et Cosmochimica Acta.*

Lochner C. G. (1996) Pb isotopes and abundances in vertical profiles of glacial till, Halfmile Lake VMS Deposit, Bathurst Camp, New Brunswick. M.Sc., Carleton University.

Long D. T., Fegan N. E., Lyons W. B., Hines M. E., Macumber P. G., and Giblin A. M. (1992) Geochemistry of acid brines: Lake Tyrrell, Victoria, Australia. In *The Geochemistry of Acid Groundwater Systems. Chemical Geology*, Vol. 96 (ed. W. B. Lyons, D. T. Long, A. L. Herczeg, and M. E. G. E. Hines), pp. 33-52.

Luff W., Goodfellow W. D., and Juras S. (1992) Evidence for a feeder pipe and associated alteration at the Brunswick No. 12 massive sulphide deposit. *Exploration and Mining Geology* 1, 167-185.

Luff W. M., Lentz D. R., and McCutcheon S. R. (1997) Day 2. The Brunswick No. 12, Brunswick No. 6 and Austin Brook deposits. In *Geology and massive sulphides of the Bathurst Camp, New Brunswick* (ed. S. R. McCutcheon), pp. 40-63. Geological Association of Canada - Mineralogical Association of Canada, Joint Annual Meeting, Ottawa '97, Field Trip B7, Guidebook.

Maest A. S. (1996) Divining the past: the limitations of current methods for determining baseline water quality at mine sites. *Geological Society of America 1996 Annual Meeting.*

Mast M. A., Drever J. I., and Baron J. (1990) Chemical weathering in the Loch Vale watershed, Rocky Mountain National Park, Colorado. *Water Resources Research* 26, 2971-2978.

McAllister A. L. (1960) Massive sulphide deposits in New Brunswick. In *Symposium on the occurrence of massive sulphide deposits in Canada.* Canadian Institute of Mining and Metallurgy. Montreal, PQ, Canada.

McArthur J. M., Turner J., Lyons W. B., and Thirlwall M. F. (1989) Salt sources and water-rock interaction on the Yilgarn Block, Australia; isotopic and major element tracers. *Applied Geochemistry* 4(1), 79-92.

McCutcheon S. R. (1992) Base-metal deposits of the Bathurst-Newcastle district: characteristics and depositional models. *Exploration and Mining Geology* 1, 105-119.

McCutcheon S. R., Langton J. P., van Staal C. R., and Lentz D. R. (1993) Stratigraphy, tectonic setting and massive sulphide deposits of the Bathurst Mining Camp, northern New Brunswick. In *Guidebook to the Metallogeny of the Bathurst Camp*, Vol. Trip #4 of Bathurst '93: 3rd Annual Field Conference, Geological Society of CIM (ed. S. R. McCutcheon and D. R. Lentz), pp. 1-39.

McCutcheon S. R. and Lentz D. R. (1993) Application of Recent Geological Concepts to Exploration in the Northern Appakachians. Guidebook to the Metallogeny of the Bathurst Camp [Field Trip #4]. Canadian Institute of Mining, Metallurgy and Petroleum.

McCutcheon S. R. C. (1997) *Geology and massive sulphides of the Bathurst Camp, New Brunswick.* Geological Association of Canada – Mineralogical Association of Canada, Joint Annual Meeting, Ottawa '97, Field Trip B7, Guidebook.

McNutt R. H., Frape S. K., Fritz P., Jones M. G., and MacDonald I. M. (1990) The $^{87}Sr/^{86}Sr$ values of Canadian Shield brines and fracture minerals with applications to groundwater mixing, fracture history, and geochronology. *Geochimica et Cosmochimica Acta* 54, 205-215.

McNutt R. H., Gascoyne M., and Kamineni D. C. (1987) $^{87}Sr/^{86}Sr$ values in groundwaters of

the East Bull Lake pluton, Superior Province, Ontario, Canada. *Applied Geochemistry* 2, 93-101.

Melchior D. C. and Bassett R. L. (1990) Chemical Modeling of Aqueous Systems II, Vol. 416, pp. 556. American Chemical Society.

Memon B. A. (1995) Quantitative analysis of springs. *Environmental Geology* 26, 111-120.

Miekeley N., Coutiho de Jesus H., Porto da Silveira C. L., and Degueldre C. (1992a) Chemical and physical characterization of suspended particles and colloids in waters from the Osamu Utsumi mine and Morro do Ferro analogue study sites, Poços de Caldas, Brazil. *Journal of Geochemical Exploration* 45, 409-437.

Miekeley N., Coutinho de Jesus H., Porto da Silveira C. L., Linsalata P., and Morse R. (1992b) Rare earth elements in groundwaters from the Osamu Utsumi mine and Morro do Ferro analogue study sites, Poços de Caldas, Brazil. *Journal of Geochemical Exploration* 45, 365-387.

Miller W. R., Ficklin W. H., and Learned R. E. (1982) Hydrogeochemical prospecting for porphyry copper deposits in the tropical-marine climate of Puerto Rico. *Journal of Geochemical Exploration* 16, 217-233.

Miller W. R., Ficklin W. H., and McHugh J. B. (1991) Hydrogeochemical exploration in areas of thin glacial overburden, northeastern Minnesota. In *USGS research on mineral resources, 1991; program and abstracts.* (ed. E. E. Good, J. F. Slack, and R. K. Kotra), pp. 55-60. U. S. Geological Survey.

Miller W. R., Ficklin W. H., and McHugh J. B. (1992) Geochemical exploration for copper-nickel deposits in the cool-humid climate of northeastern Minnesota. *Journal of Geochemical Exploration* 42, 327-344.

Millero F. J., Sotolongo S., and Izaguirre M. (1987) The oxidation kinetics of Fe(II) in seawater.*Geochimica et Cosmochimica Acta* 51, 793-801.

Moldovanyi E. P., Walter L. M., and Land L. S. (1993) Strontium, boron, oxygen and hydrogen isotope geochemistry of brines from basal strata of the Gulf Coast sedimentary

basin, USA. *Geochimica et Cosmochimica Acta* 57, 2083-2099.

Moon C. J. (1995) Exploration geochemistry. In *Introduction to Mineral Exploration.* (ed. A. M. Evans), pp. 138-160. Blackwell Science.

Morad S., Ismail H. N. B., Deros L. F., Alaasm I. S., and Serrhini N. E. (1994) Diagenesis and formation water chemistry of Triassic reservoir sandstones from southern Tunisia. *Sedimentology* 41(6), 1253-1272.

Moser H., Wolf M., Fritz P., Fontes J.-C., Florkowski T., and Payne B. R. (1989) Deuterium, oxygen-18, and tritium in Stripa groundwater. *Geochimica et Cosmochimica Acta* 53, 1757-1763.

Moses C. O. and Herman J. S. (1991) Pyrite oxidation at circumneutral pH. *Geochimica et Cosmochimica Acta* 55, 471-482.

Muller B. and Sigg L. (1992) Adsorption of lead (II) on the goethite surface: voltammetric evaluation of surface complexation parameters. *Journal of Colloid and Interface Science* 148, 517-532.

Mwenifumbo C. J. (1991) Field evaluation of electrodes for drillhole self potential measurements. In *Proceedings of the 4th International IGLS/KEGS Symposium on Borehole Geophysics for Minerals, Geotechnical and Groundwater Applications*, pp. 179-189.

Mwenifumbo C. J. (1993) Temperature logging in mineral exploration. *Journal of applied geophysics* 30, 297-313.

Mwenifumbo C. J. and Killeen P. G. (1995) Preliminary results of geophysical logging in exploration holes at the Halfmile Lake massive sulphide deposit, New Brunswick. In *Current Research 1994*, Vol. New Brunswick Department of Natural Resources and Energy, Minerals and Energy Division, Miscellaneous Report 18 (ed. S. A. A. Merlini), pp. 157-163.

Nativ R. (1996) The brine underlying the Oak Ridge Reservation, Tennessee, USA: Characterization, genesis, and environmental implications. *Geochimica et Cosmochimica*

Acta 60, 787-801.

Négrel P., Allègre C. J., Dupré B., and Lewin E. (1993) Erosion sources determined by inversion of major and trace element ratios and strontium isotopic ratios in river water: The Congo Basin case. *Earth and Planetary Science Letters* 120, 59-76.

Nicholson R. V. (1994) Iron-sulfide oxidation mechanisms: laboratory studies. In *Short Course Handbook on Environmental Geochemistry of Sulfide Mine-Wastes*, Vol. 22 (ed. J. L. Jambor and D. W. Blowes), pp. 163-184. Mineralogical Association of Canada.

Nordstrom D. K., Ball J. W., Donahoe R. J., and Whittemore D. (1989a) Groundwater chemistry and water-rock interactions at Stripa. *Geochimica et Cosmochimica Acta* 53, 1727-1740.

Nordstrom D. K., Lindblom S., Donahoe R. J., and Barton C. C. (1989b) Fluid inclusions in the Stripa granite and their possible influence on the groundwater chemistry. *Geochimica et Cosmochimica Acta* 53, 1741-1755.

Nordstrom D. K., Olsson T., Carlsson L., and Fritz P. (1989c) Introduction to the hydrogeochemical investigations within the International Stripa Project. *Geochimica et Cosmochimica Acta* 53, 1717-1726.

Northrup D. A. and Clayton R. N. (1966) Oxygen isotope fractionation in systems containing dolomite. Jour. Geol. 74, 174-196.

Ohmoto H. (1972) Systematics of sulfur and carbon isotopes in hydrothermal ore deposits. *Economic Geology* 67, 551-579.

Östlund P., Torssander P., Mörth C.-M., and Claesson S. (1995) Lead and sulphur isotope dilution during dispersion from the Falun mining area. *Journal of Geochemical Exploration* 52, 91-95.

Othman D. B., Luck J.-M., and Tournod M.-G. (1997) Geochemistry and water dynamics: application to short time-scale flood phenomena in a small Mediterranean catchment I. Alkalis, alkali-earths and Sr isotopes. *Chemical Geology* 140, 9-28.

Pajari G. E., Jr., Rast N., and Stringer P. (1977) Paleozoic volcanicity along the Bathurst-

Dalhousie geotraverse, New Brunswick, and its relations to structure. In *Volcanic Regimes in Canada*, Vol. Special Paper 16 (ed. W. R. A. Baragar, L. C. Coleman, and J. M. Hall), pp. 111-124. Geological Association of Canada.

Paktunc A. D. (1990) Geochemical constraints on the tectonic setting of the mafic rocks of the Bathurst Camp, Appalachian Orogen. *Can. Jour. Earth Sci.* 27, 1182-1193.

Palmer M. R. and Edmond J. M. (1993) Uranium in river water. *Geochimica et Cosmochimica Acta* 57, 4947-4955.

Palmer M. R. and Sturichio N. C. (1990) The boron isotope systematics of the Yellowstone National Park (Wyoming) hydrothermal system: A reconnaissance. *Geochimica et Cosmochimica Acta* 54, 2811-2815.

Pande K., Sarin M. M., Trivedi J. R., Krishnaswami S., and Sharma K. K. (1994) The Indus river system (India-Pakistan): Major-ion chemistry, uranium and strontium isotopes. *Chemical Geology* 116, 245-259.

Parkhill M. A. (1997) Surficial geology and till geochemistry in northern New Brunswick: aummary of EXTECH-II projects and current database. In *Current Research 1996*, Vol. Mineral Resources Report 97-4 (ed. B. M. W. Carroll), pp. 201-223. New Brunswick Department of Natural Resources and Energy, Minerals and Energy Division.

Parkhill M. A. and Doiron A. (1995) Quaternary geology and glacial dispersal of sulphides at the Half Mile Lake and Restigouche deposits, Bathurst Mining Camp, Northern New Brunswick - EXTECH-II. In *Geoscience Research 1994*, Vol. Miscellaneous report 15 (ed. J. P. Langton), pp. 45-58. New Brunswick Department of Natural Resources and Energy, Minerals and Energy Division.

Parkhurst D. L. (1995) User's guide to PHREEQC—a computer program for speciation, reaction-path, advective-transport, and inverse geochemical calculations. U.S. Geological Survey.

Parks G. A. (1990) Surface energy and adsorption at mineral/ water interfaces; an introduction. In *Mineral-water interface geochemistry.*, Vol. 23 (ed. M. F. Hochella, Jr. and A. F.

White), pp. 133-175. Mineralogical Society of America.

Perry E. C. and Tan F. C. (1972) Significance of oxygen and carbon isotope variations in early Precambrian cherts and carbonate rocks of southern Africa. *Geological Society of America Bulletin* 83, 647-664.

Peter J. M. and Goodfellow W. D. (1993) Bulk and stable sulphur and carbon isotope geochemistry of hydrothermal sediments associated with the Brunswick No. 12 deposit, northern New Brunswick. In *Current Research*, Vol. 93-1 (ed. S. A. Abbott), pp. 154-169. New Brunswick Department of Natural Resources and Energy, Mineral Resources, Information Circular.

Peter J. M. and Goodfellow W. D. (1996) Mineralogy, bulk and rare earth element geochemistry of massive sulphide-associated hydrothermal sediments of the Brunswick Horizon, Bathurst Mining Camp, New Brunswick. *Canadian Journal of Earth Sciences* 33, 252-283.

Peter J. M., Goodfellow W. D., and Leybourne M. I. (1994) Fluid inclusion petrography and microthermometry of the Middle Valley hydrothermal system, northern Juan de Fuca Ridge. In *Proceedings of the Ocean Drilling Program, Scientific Results*, Vol. 139. Ocean Drilling Program.

Peter J. M. and Shanks W. C., III. (1992) Sulfur, carbon, and oxygen isotope variations in submarine hydrothermal deposits of Guaymas Basin, Gulf of California, USA. *Geochimica et Cosmochimica Acta* 56, 2025-2040.

Plummer L. N., Prestemon E. C., and Parkhurst D. L. (1995) *An interactive code (NETPATH) for modeling net geochemical reactions along a flow path-version 2.0.* U.S. Geological Survey Water Resources Investigations Report.

Porteous N. C., Mather J. D., and Walsh J. N. (1995a) Determination of boron isotopic ratios using ICP-MS and its application to groundwater studies. In *Water-Rock Interaction* (ed. Kharaka and Chudaev).

Porteous N. C., Walsh J. N., and Jarvis K. E. (1995b) Measurement of boron isotope ratios

in groundwater studies. *Analyst* 120, 1397-1400.

Pratt A. R., Nesbitt H. W., and Mycroft J. R. (1996) The increased reactivity of pyrrhotite and magnetite phases in sulphide mine tailings. *Journal of Geochemical Exploration* 56, 1-11.

Rast N., Kennedy M. J., and Blackwood R. F. (1976) Comparison of some tectonostratigraphic zones in the Appalachians of Newfoundland and New Brunswick. *Canadian Journal of Earth Sciences* 13, 868-875.

Rice R. J. and van Staal C. R. (1992) Sedimentological studies in the Ordovician Miramichi, Tetagouche and Fournier Groups in the Bathurst camp and the Belledune-Elmtree inlier, northern New Brunswick. In *Current Research*, Vol. Part D, Paper 92-1D. Geological Survey of Canada.

Richard P., Shimizu N., and Allègre C. J. (1976) $^{143}Nd/^{146}Nd$, a natural tracer: an application to oceanic basalts. *Earth and Planetary Science Letters* **31**, 269-278.

Ritchie A. I. M. (1994) Sulfide oxidation mechanisms: controls and rates of oxygen transport. In *Short Course Handbook on Environmental Geochemistry of Sulfide Mine-Wastes*, Vol. 22 (ed. J. L. Jambor and D. W. Blowes), pp. 201-246. Mineralogical Association of Canada.

Rock N. (1991) IsoCalc. Gary Carroll and the University of Western Australia.

Rogers N. and van Staal C. R. (1995) Distribution and origin of felsic volcanic rocks, Tetagouche Group, Bathurst Mining Camp, New Brunswick. *Abstracts/Résumés - 1995, twentieth Annual review of Activities.*, 7.

Rogers N., Wodicka N., McNicoll V., and van Staal C. R. (in press) U-Pb zircon ages of Tetagouche Group felsic volcanic rocks, northern New Brunswick. In *Radiogenic Age and Isotopic Studies: Report 11*, Vol. Bulletin 72. Geological Survey of Canada.

Rollinson H. R. (1993) *Using Geochemical Data: Evaluation, Presentation, Interpretation*. Longman Scientific and Technical.

Rose A. W., Hawkes H. E., and Webb J. S. (1979) *Geochemistry in Mineral Exploration*. Academic Press.

Rose D. G. and Johnson S. C. (1990) New Brunswick computerized mineral occurrence database. New Brunswick department of Natural Resources and Energy, Mineral Resources Division.

Rosenbaum J. M. (1993) Mantle phlogopite: a significant lead repository? *Chemical Geology* 106, 475-483.

Rosenbaum J. and Sheppard S. M. F. (1986) An isotopic study of siderites, dolomites and ankerites at high temperatures. Geochim. Cosmochim. Acta 50, 1147-1150.

Rozanski K., Araguas-Araguas L., and Gonfiantini R. (1993) Isotopic patterns in modern global precipitation. In *Continental Isotope Indicators of Climate*, pp. 1-36. AGU Monograph 78.

Ruijin J., Tianxiang R., Hua Z., Shengming M., and Mu K. (1994) Orientation hydrogeochemical survey of the Liudaogou Cu-Mo mineralized zone in a basalt-covered area, northeastern China. *Journal of Geochemical Exploration* 51, 79-91.

Runnells D. D. and Lahermo P. W. (1984) Workshop 3: hydrochemistry in mineral exploration. *Journal of Geochemical Exploration* 21, 129-131.

Russell J., Chadwick B., Rao B. K., and Vasudev V. N. (1996) Whole rock Pb/Pb isotopic ages of Late Archaean limestones, Karnataka, India. *Precambrian Research* 78, 261-272.

Sato M. and Mooney H. M. (1960) The electrochemical mechanism of sulphide self potentials. *Geophysics* 25, 226-249.

Saunders J. A. and Swann C. T. (1990) Trace-metal content of Mississippi oil field brines. *Journal of Geochemical Exploration* 37, 171-183.

Scholten J. C., Stoffers P., Walter P., and Plüfer W. (1991) Evidence for episodic hydrothermal activity in the Red Sea from the composition and formation of hydrothermal sediments, Thetis Deep. *Tectonophysics* 190, 109-118.

Sen Z. (1995) *Applied Hydrogeology for Scientists and Engineers*. CRC Press.

Sharpley F. J. (1967) Exploration Report, Restigouche Group "G", Restigouche County, New Brunswick for Teck Corporation.

Sheppard S. M. F. and Schwarcz H. P. (1970) Fractionation of carbon and oxygen isotopes and magnesium between coexisting metamorphic calcite and dolomite. *Contributions to Mineralogy and Pettrology* 26, 161-198.

Sherwood Lollar B., Frape S. K., Weise S. M., Fritz P., Macko S. A., and Welhan J. A. (1993) Abiogenic methanogenesis in crystalline rocks. *Geochimica et Cosmochimica Acta* 57, 5087-5097.

Sholkovitz E. R. (1995) The aquatic chemistry of rare earth elements in rivers and estuaries. *Aquatic Geochemistry* 1, 1-34.

Simonetti A., Bell K., and Hall G. E. M. (1996) Pb isotopic ratios and elemental abundances for selective leachates from near-surface till: implications for mineral exploration. *Applied Geochemistry* 11, 721-734.

Smedley P. L. (1991) The geochemistry of rare earth elements in groundwater from the Carnmenellis area, southwest England. *Geochimica et Cosmochimica Acta* 55, 2767-2779.

Smith E. E., Svanks K., and Schumate K. (1968) Sulfide to sulfate reaction studies. *Proceedings of the Second Symposium on Coal Mine Drainage Research*, 1-11.

Smith J. K. (1985) A geological study of the Brunswick No. 12 massive sulfide deposit, Bathurst, N.B., with emphasis on the geochemistry of the associated rock types. B.Sc. thesis, Mount Allison University.

Spivack A. J. and Edmond J. M. (1987) Boron isotope exchange between seawater and the oceanic crust. *Geochim. Cosmochim. Acta* 51, 1033-1043.

Spivack A. J., Palmer M. R., and Edmond J. M. (1987) The sedimentary cycle of the boron isotopes. 51, 1939-1949.

Sposito G. (1983) The chemical forms of trace metals in soils. In *Applied environmental geochemistry.* (ed. I. Thornton), pp. 123-170. Acad. Press.

Stallard R. F. and Edmond J. M. (1983) Geochemistry of the Amazon; 2, The influence of geology and weathering environment on the dissolved load. *Journal of Geophysical Research* 88(14), 9671-9688.

Stanton R. L. (1959) Mineralogical features and possible mode of emplacement of the Brunswick Mining and Smelting orebodies, Gloucester County, New Brunswick. In *Gill, J. E., chm., Symposium on the genesis of massive sulphide deposits.* Canadian Institute of Mining and Metallurgy. Montreal, PQ, Canada.

Stanton R. L. (1960) General features of the conformable "pyritic" orebodies--Part 2, Mineralogy. *Canadian Mining and Metallurgical Bulletin (Canadian Institute of Mining and Metallurgy)* 53(574), 66-74.

Stetzenbach K. J., Amano M., Kreamer D. K., and Hodge V. F. (1994) Testing the limits of ICP-MS: determination of trace elements in ground water at the parts-per-trillion level. *Ground Water* 32, 976-985.

Sullivan K. A. and Aller R. C. (1996) Diagenetic cycling of arsenic in Amazon shelf sediments. Geochimica et Cosmochimica Acta 60, 1465-1477.

Sullivan R. W. and van Staal C. R. (1990) Age of metarhyolite from the Tetagouche Group, Bathurst, New Brunswick, from U-Pb isochron analyses of zircons enriched in common lead. In *Radiogenic Age and Isotopic Studies, Report 3*, Vol. Paper 89-2, pp. 109-117. Geological Survey of Canada.

Swartz C. H., Ulery A. L., and Gschwend P. M. (1997) An AEM-TEM study of nanometer-scale mineral associations in an aquifer sand: Implications for colloid mobilization. *Geochimica et Cosmochimica Acta* 61, 707-718.

Symons D. T. A., Lewchuk M. T., and Boyle D. R. (1996) Pliocene-Pleistocene genesis for the Murray Brook and Heath Steele Au-Ag gossan ore deposits, New Brunswick, from paleomagnetism. *Canadian Journal of Earth Sciences* 33(1), 1-11.

Taufen P. M. (1996) A geochemical study of groundwaters and stream waters at two mineralized sites in the Noranda District, Quebec; application to mineral prospecting, mine development, and environmental remediation. Doctoral, Colorado School of Mines. Golden, CO, United States.

Taufen P. M. (1997) Ground waters and surface waters in exploration geochemical surveys. In

Proceedings of Exploration 97: Fourth Decennial International Conference on Mineral Exploration (ed. A. G. Gubins), pp. 271-284.

Taylor C. B. and Fox V. J. (1996) An isotopic study of dissolved inorganic carbon in thecatchment of the Waimakariri River and deep ground water of the North Canturbury Plains, New Zealand. *Journal of Hydrology* 186, 161-190.

Taylor S. R. and McLennan S. M. (1985) *The Continental Crust: its Composition and Evolution.* Blackwell Scientific Publications.

Thornber M. R. (1975) Supergene alteration of sulphides, I. A chemical model based on massive nickel sulphide deposits at Kambalda, Western Australia. *Chemical Geology* 15, 1-14.

Thornton I. (1996) Impacts of mining on the environment; some local, regional and global issues. *Applied Geochemistry* 11, 355-361.

Thorpe R. I., Franklin J. M., and Sangster D. F. (1981) Evolution of lead in massive sulphide ores of Bathurst District, New Brunswick, Canada. *Trans. Inst. Min. Metall.* 90B, 55-56.

Toulhoat P. and Beaucaire C. (1991) Comparison between lead isotopes $^{234}U/^{238}U$ activity ratio and saturation index in hydrogeochemical exploration for concealed uranium deposits. *Journal of Geochemical Exploration* 41, 181-196.

van Staal C. R. (1987) Tectonic setting of the Tetagouche Group in northern New Brunswick: implications for plate tectonic models of the northern Appalachians. *Canadian Journal of Earth Science* 24, 1329-1351.

van Staal C. R. (1990) Evidence for a post-Taconic blueschist suture in northern New Brunswick, Canada. *Geology* 18, 1073-1077.

van Staal C. R. and Fyffe L. (1991a) The New Brunswick Dunnage and Gander Zones. In *The Appalachian/Caledonian Orogen of Canada and Greenland, Decade of North American Geology*, Vol. F-1 (ed. H. c.-o. Williams).

van Staal C. R. and Fyffe L. R. (1991b) Dunnage and Gander Zones, New Brunswick: Canadian Appalachian Region. *New Brunswick Department of Natural Resources and*

Energy, Mineral Resources, Geoscience Report 91-2, 39.

van Staal C. R., Fyffe L. R., Langton J. P., and McCutcheon S. R. (1992) The Ordovician Tetagouche Group, Bathurst Camp, northern New Brunswick, Canada: history, tectonic setting, and distribution of massive-sulfide deposits. *Exploration and Mining Geology* 1, 93-103.

van Staal C. R. and Luff W. M. (1990) The Brunswick No. 12 and No. 6 mines, Brunswick Mining and Smelting Corporation Limited. In *Field Guide to Massive Sulphide Deposits in Northern New Brunswick* (ed. L. R. Fyffe), pp. 72-83. Minerals and Energy Division, Department of Natural Resource and Energy, New Brunswick.

van Staal C. R. and Williams P. F. (1986) Structure, origin, and concentration of the Brunswick No. 6 and 12 ore bodies. *Economic Geology* 79, 1669-1692.

van Staal C. R., Winchester J. A., and Bedard J. H. (1991) Geochemical variations in Middle Ordovician volcanic rocks of the northern Miramichi Highlands and their tectonic significance. *Can. Jour. Earth Sci.* 28, 1031-1049.

Vandelannoote R., Blommaert W., Sadurski A., Van T' Dack L., Gijbels R., Van Grieken R., Bosch B., Rochon J., Sarcia C., and Sureau J. F. (1984) Trace-elemental anomalies in surface water near a small lead-zinc mineralization at Menez-Albot (Brittany, France). *Journal of Geochemical Exploration* 20, 33-46.

Veizer J. (1989) Strontium isotopes in seawater through time. *Annual Reviews Earth and Planetary Science Letters* 17, 141-167.

Vengosh A., Chivas A. R., McCulloch M. T., Starinsky A., and Kolodny Y. (1991) Boron isotope geochemistry of Australian salt lakes. *Geochimica et Cosmochimica Acta* 55, 2591-2606.

Vengosh A., Chivas A. R., Starinsky A., Kolodny Y., Baozhen Z., and Pengxi Z. (1995) Chemical and boron isotope compositions of non-marine brines from the Qaidam Basin, Qinghai, China. *Chemical Geology* 120, 135-154.

Vengosh A., Starinsky A., and Chivas A. R. (1994) Boron isotopes in Heletz-Kokhav oilfield

brines, the Coastal Plain, Isreal. *Isreal Journal of Earth Sciences* 43, 231-237.

Vengosh A., Starinsky A., Kolodny Y., Chivas A. R., and Raab M. (1992) Boron isotope variations during fractional evaporation of sea water: New constraints on the marine vs. nonmarine debate. *Geology* 20, 799-802.

Viers J., Dupré B., Polvé M., Schott D., J.-L., and Braun J.-J. (1997) Chemical weathering in the drainage basin of a tropical watershed (Nsimi-Zoetele site, Cameroon): comparison between organic-poor and organic-rich waters. *Chemical Geology* 140, 181-206.

Vriend S. P., Dekkers M. J., Janssen M. A., and Commandeur J. (1991) Well sediments: a medium for geochemical prospecting, an example from the Nisa region, Portugal. *Journal of Geochemical Exploration* 41, 151-167.

Waite T. D., Davis J. A., Payne T. E., Waychunas G. A., and Xu N. (1994) Uranium(VI) adsorption to ferrihydrite: application of a surface complexation model. *Geochimica et Cosmochimica Acta* 58, 5465-5478.

Walker J. A. and McCutcheon S. R. (1996) Geology of the Wedge massive sulphide deposit (NTS 21O/8E), Bathurst Mining Camp, New Brunswick. In *New Brunswick Department of Natural Resources and Energy, Minerals and Energy Division*, Vol. Mineral Resources Report 96-1 (ed. B. M. W. Carroll), pp. 155-177.

Walker J. A. and McCutcheon S. R. (1996) Geology of the Wedge massive sulphide deposit (NTS 21O/8E), Bathurst Mining Camp, New Brunswick. In *New Brunswick Department of Natural Resources and Energy, Minerals and Energy Division*, Vol. Mineral Resources Report 96-1 (ed. B. M. W. Carroll), pp. 155-177.

Wang M., Ren T., Liu Y., and Liu S. (1995) Stream water, an ideal medium for rapidly locating polymetallic mineralization in forest-swamp terrain; a case study in the Da Hinggan Mts., northern Heilongjiang, China. In *Geochemical exploration 1993.*, Vol. 55; 1-3 (ed. Y. T. Maurice and X. Xie), pp. 257-264. Elsevier.

Wayne D. M., Warwick J. J., Lechler P. J., Gill G. A., and Lyons W. B. (1996) Mercury contamination in the Carson River, Nevada: a preliminary study of the impact of mine

wastes. *Water, Air, and Soil Pollution* 92, 391-408.

Welhan J. A. (1987) Stable isotope hydrology. In *Short Course in Stable Isotope Geochemistry of Low Temperature Fluids*, Vol. 13 (ed. T. K. Kyser), pp. 129-162. Mineralogical Association of Canada.

Wen L.-S., Santschi P. H., and Tang D. (1997) Interactions between radioactively labeled colloids and natural particles: evidence for colloidal pumping. *Geochimica et Cosmochimica Acta* 61, 2867-2878.

Westoll N. D. S. (1990) Report on exploration diamond drilling, Restigouche Property, Restigouche County, New Brunswick. Marshall Minerals Corp. New Brunswick Department of Natural Resources and Energy, Mineral and Energy Division, Assessment File 473864.

Whalen J. B., Rogers N., van Staal C. R., Longstaffe F. J., Jenner G. A., and Winchester J. A. (1998) Geochemical and isotopic (Nd, O) data from Ordovician felsic plutons and volcanic rocks of the Miramichi Highlands: petrogenetic and metallogenetic implications for the Bathurst Mining Camp. *Canadian Journal of Earth Sciences* **35**, 237-252.

Whitehead R. E. S. and Goodfellow W. D. (1978) Geochemistry of volcanic rocks from the Tetagouche Group, Bathurst, New Brunswick, Canada. *Canadian Journal of Earth Sciences* 15, 207-219.

Whitford D., Andrew A., Carr G., and Giblin A. (1997) Multi-isotopic studies of groundwaters: exploration for concealed mineralization. *Exploration and Mining Research News* 7, 5-7.

Williams H. (1979) Appalachian Orogen in Canada. *Canadian Journal of Earth Sciences* 16, 792-807.

Wilson R. A. (1993) Geology of the Heath Steele - Halfmile Lake area, Northumberland County, New Brunswick (part of NTS 21 O/8). New Brunswick Department of Natural Resources and Energy, Mineral Resources.

Wilson S. E., Walker I. R., Mott R. J., and Smol J. P. (1993) Climatic and limnological

changes associated with the Younger Dryas in Atlantic Canada. *Climate Dynamics* 8(4), 177-187.

Wilson T. P. and Long D. T. (1993) Geochemistry and isotope chemistry of Michigan brines: Devonian formations. *Applied Geochemistry* 8, 81-100.

Winter B. L. and Johnson C. M. (1995) U-Pb dating of a carbonate subaerial exposure event. *Earth and Planetary Science Letters* 131, 177-187.

Wolery T. J. (1992a) *EQ3/6, a software package for geochemical modeling of aqueous systems: package overview and installation guide (version 7.0).* UCRL--MA-110662-PT-I, Lawrence Livermore National Laboratory.

Wolery T. J. (1992b) *EQ3NR, a computer program for geochemical aqueous speciation-solubility calculations: package overview and installation guide (version 7.0).* UCRL--MA-110662-PT-I, Lawrence Livermore National Laboratory.

Wood S. A. (1990) The aqueos geochemistry of the rare-earth elements and yttrium 1. Review of available low-temperature data for inorganic complexes and the inorganic REE speciation of natural waters. *Chemical Geology* 82, 159-186.

Zierenberg R. A. and Shanks W. C., III. (1988) Isotopic studies of epigenetic features in metalliferous sediment, Atlantis II Deep, Red Sea. *Canadian Mineralogist* 26, 737-753.